COMMISSION OF THE EUROPEAN COMMUNITIES

EURATOM

RADIATION PROTECTION

PROGRAMME

PROGRESS REPORT

1985-89

Volume 1

EUR 13268 DE/EN/FR

I N H A L T S V E R Z E I C H N I S

T A B L E O F C O N T E N T S

T A B L E D E S M A T I E R E S

V O L U M E I

* Bericht noch nicht verfügbar
Report not yet available
Rapport pas encore disponible

** Tätigkeitsbericht
Progress report
Rapport annuel

*** Vertrag verlängert für 1990-1991
Contract prolonged in 1990-1991
Contrat prolongé en 1990-1991

McKinlay, A.	NRPB Chilton	BI6-016-UK	
Menzel, H.G./Grillmaier, R.E.	Univ. Homburg	BI6-010-D	
Norris, A.C./Haque, A.K.M.M.	Polytech.South Bank London	BI6-025-UK	
Portal, G.	CEA-CEN Fontenay-aux-Roses	BI6-020-F	
Rechenmann, R.V.	Univ. Strasbourg	BI6-021-F	
Siffert, P.	CNR Strasbourg	BI6-304-F	**
Uggerhoj, E.	Univ. Aarhus	BI6-303-DK	**
Watt, D.E.	Univ. St. Andrews	BI6-024-UK	
EURADOS (Dennis, J.A.)	TNO Rijswijk	BI6-026-NL	***
ICRU (Allisy, A.)	Bethesda	BI6-027-US	
ICRU (Allisy, A.)	Bethesda	BI6-217-US	

B. Verhalten und Kontrolle der Radionuklide in der Umwelt
Behaviour and control of radionuclides in the environment
Comportement et contrôle des radionucléides dans l'environnement

Aarkrog, A.	RISØ Nat. Lab. Roskilde	BI6-030-DK	
Apostolakis, C./ Papanicolaou, E.P.	NRC Demokritos Athens	BI6-293-GR	**
Bell, J.N.B./Minski, M.J.	Imperial College London	BI6-032-UK	
Bonka, H.	RWTH Aachen	BI6-033-D	
Bunnenberg, C.	Nieders. Inst. Rad. Hannover	BI6-041-D	
Coughtrey, P.J.	ANS Epsom	BI6-194-UK	
Cremers, A.	Univ. Leuven	BI6-035-B	
Cunningham, J.D.	NEB Dublin	BI6-218-IRL	
Damiani, V.	ENEA-CRE Santa Teresa	BI6-034-I	
Decallonne, J.	Univ. Louvain-la-Neuve	BI6-042-B	
Derwent, R.G.	UKAEA Harwell	BI6-046-UK	
Duursma, E.K.	NIOZ Den Burg	BI6-199-NL	
Frissel, M.J.	RIVM Bilthoven	BI6-036-NL	
Führ, F.	KFA Jülich	BI6-053-D	
Führ, F.	KFA Jülich	BI6-189-D	
Galvao, J.P.	LNETI Sacavem	BI6-198-P	
Grauby, A.	CEA-CEN Cadarache	BI6-037-F	
Grauby, A.	CEA-CEN Cadarache	BI6-325-F	**
Hamilton, E.I.	NERC Swindon	BI6-038-UK	
Heal, O.W.	NERC Swindon	BI6-233-UK	
Heaton, B.	Univ. Aberdeen	BI6-318-UK	
Heip, C.	Delta Instituut Yerseke	BI6-191-NL	
Hoppenheit, M.	Bio. Anst. Helgol. Hamburg	BI6-039-D	
Kirchmann, R.	Fac. Sc. Agronom. Gembloux	BI6-327-B	**
Martin, J.M.	Inst. Biogéochimie Montrouge	BI6-234-F	
McAulay, I.R.	Trinity College Dublin	BI6-043-IRL	
Mingot Buades, F.	CIEMAT Madrid	BI6-195-E	
Moser, H.	GSF Neuherberg	BI6-056-D	
Pentreath, R.J.	MAFF Lowestoft	BI6-200-UK	
Pieri, J.	Univ. Nantes	BI6-047-F	
Roed, J.	RISØ Nat. Lab. Roskilde	BI6-326-DK	**
Silva, S.	Univ. Sacro Cuore Milano	BI6-329-I	**
Stather, J.W./Fry, F.A.	NRPB Chilton	BI6-048-UK	
Vandecasteele, C.	CEN-SCK Mol	BI6-040-B	

V O L U M E I I

Gössner, W./Kellerer, A.M./ Spiess, H.	GSF Neuherberg/Univ. Würzburg/Univ. München	BI6-083-D	***	1
Gössner, W./Kellerer, A.M./ Spiess, H.	GSF Neuherberg/Univ. Würzburg/Univ. München	BI6-221-D	***	1
Hagen, U.	GSF Neuherberg	BI6-085-D		1
Healey, T.	BNL-CEGB Berkeley	BI6-095-UK		1
Janowski, M.	CEN-SCK Mol	BI6-090-B		1
Kaldor, J.	IARC Lyon	BI6-319-F	**	1
Kjeldgaard, N.O.	Univ. Aarhus	BI6-086-DK		1
Lohman, P.H.M.	Univ. Leiden	BI6-202-NL		1
Malone, J.F.	St. James Hospital Dublin	BI6-093-IRL		1
Morgan, A.	UKAEA Harwell	BI6-235-UK		1
Mothersill, C.	St. Luke's Hospital Dublin	BI6-092-IRL		1
Parmentier, N.	CEA-IPSN Fontenay-aux-Roses	BI6-101-F		1
Planel , H.	Univ. Toulouse	BI6-201-F		1
Ramsden, D.	UKAEA Winfrith	BI6-102-UK		1
Rommelaere, J.	Univ. Bruxelles	BI6-178-B		1
Rossi, G.B.	Ist. Sup. Sanità Roma	BI6-103-I		1
Stahlhofen, W.	GSF Frankfurt	BI6-236-D		1
Stather, J.W.	NRPB Chilton	BI6-089-UK	***	1
Strom, R.	Univ. "La Sapienza" Roma	BI6-196-I		1
Tallone Lombardi, L.	Univ. Milano	BI6-177-I		1
Taylor, D.M.	KFK Karlsruhe	BI6-091-D		1
Tipton, K.F./Mothersill, C.	Trinity College Dublin	BI6-184-IRL		1
Vanderborght, O.	SCK-CEN Mol	BI6-094-B		1
van der Eb, A.J.	Univ. Leiden	BI6-185-NL		1
Williams, E.D.	Welsh Nat. Sch. Med. Cardiff	BI6-097-UK		1
Zurcher, C.	TNO Rijswijk	BI6-212-NL		1
EULEP (Maisin, J.R.)	UCL Bruxelles	BI6-099-D	***	1

V O L U M E I I I

E. Genetische Wirkungen ionisierender Strahlen
Genetic effects of ionizing radiation
Effets génétiques des rayonnements ionisants 1

Baan, R.A.	TNO Rijswijk	BI6-148-NL		1
Barendsen, G.W.	Univ. Amsterdam	BI6-330-NL		1
Bianchi, M.	Univ. Milano	BI6-204-I		1
Bootsma, D.	Univ. Rotterdam	BI6-141-NL		1
Bridges, B.A.	MRC Brighton	BI6-142-UK		2
Bryant, P.E.	Univ. St. Andrews	BI6-294-UK		2
Cattanach, B.M.	MRC Harwell	BI6-143-UK	***	2
Cortes-Benavides, F.	Univ. Sevilla	BI6-311-E		2
Devoret, R.	CNRS Gif-sur-Yvette	BI6-145-F		2
Dutrillaux, B.	Institut Curie Paris	BI6-147-F		2
Dutrillaux, B.	CEA-IPSN Fontenay-aux-Roses	BI6-149-F		2
Ehling, U.H.	GSF Neuherberg	BI6-156-D	***	2
Elli, R.	Univ."La Sapienza" Roma	BI6-205-I		2
Evans, H.J.	MRC Edinburgh	BI6-157-UK		2

Jensen, O.M.	Inst. Cancer Ep. København	BI6-333-DK	***
Jonassen, N.	Univ. Lyngby	BI6-113-DK	
Kessler, G.	KFK Karlsruhe	BI6-128-D	***
Kollas, J.	NRC Demokritos Athens	BI6-114-GR	***
Lochard, J.	CEPN Fontenay-aux-Roses	BI6-105-F	
Lochard, J.	CEPN Fontenay-aux-Roses	BI6-207-F	
Madelaine, G.	CEA-CEN Fontenay-aux-Roses	BI6-115-F	
McLaughlin, J.P.	Univ. College Dublin	BI6-117-IRL	
Mikkelsen, T.	RISØ Nat. Lab. Roskilde	BI6-296-DK	
Morlat, G./Anguenot, F.	CEDHYS Paris	BI6-121-F	
O'Riordan, M.C./Fry, F.A.	NRPB Chilton	BI6-118-UK	
Parmentier, N.	CEA-IPSN Fontenay-aux-Roses	BI6-119-F	
Porstendörfer, J.	Univ. Göttingen	BI6-130-D	
Quindos Poncela, L.S.	Univ. Santander	BI6-314-E	***
Roed, J.	RISØ Nat. Lab. Roskilde	BI6-107-DK	
Siemssen, R.H.	Univ. Groningen	BI6-120-NL	
Siemssen, R.H.	Univ. Groningen	BI6-210-NL	
Stather, J.W.	NRPB Chilton	BI6-116-UK	***
Stather, J.W.	NRPB Chilton	BI6-213-UK	***
Uzzan, G.	CEA-IPSN Fontenay-aux-Roses	BI6-122-F	***
Sub Contract : Delpoux, M.	Univ. Toulouse	SC-003-F	
van Kaick, G.	DKFZ Heidelberg	BI6-298-D	***
ICRP (Smith, H.)	Chilton	BI6-124-UK	
Broerse, J.J./Zoetelief, J.	TNO Rijswijk	BI6-138-NL	
Donato, L.	Univ. Pisa	BI6-139-I	
Fagnani, F.	CAATS-INSERM Font.-aux-Roses	BI6-132-F	***
Faulkner, K.	General Hospital Newcastle	BI6-315-UK	
Fendel, H.	Univ. München	BI6-211-D	***
Galvao, J.	LNETI Sacavem	BI6-299-P	**
Hoeschen, D.	PTB Braunschweig	BI6-316-D	**
Jacobi, W./Drexler, G.	GSF Neuherberg	BI6-133-D	
Jessen, K.A.	Univ. Hospital Aarhus	BI6-317-DK	**
Malone, J.F.	St. James Hospital Dublin	BI6-134-IRL	
McKinlay, A.	NRPB Chilton	BI6-135-UK	
Padovani, R.	Ospedale S. Maria Mis. Udine	BI6-136-I	***
Schmidt, T.	Univ. Erlangen-Nürnberg	BI6-137-D	
Taylor, C.J.	Christie Hospital Manchester	BI6-140-UK	
Vano Carruana, E.	Univ. Madrid	BI6-214-E	***

IV. Koordinierungstätigkeit
Coordination activities
Activités de coordination

V. Auswahl einiger auf Veranlassung der Kommission erschienener Veröffentlichungen
Selection of publications issued on the initiative of the Commission
Choix de publications éditées à l'initiative de la Commission

VI. Verzeichnis der Forschungsgruppenleiter
List of research group leaders
Index des chefs de groupe de recherche

I

EINLEITUNG

INTRODUCTION

INTRODUCTION

Vorwort

DE

Das Strahlenschutzprogramm, das 1989 zu Ende ging, war das sechste Forschungs- und Ausbildungsprogramm, das unter dem EURATOM-Vertrag der Kommission der Europäischen Gemeinschaften (KEG) seit 1960 durchgeführt wurde. In den 3 vorliegenden Bänden werden die wissenschaftlichen Ergebnisse des Zeitraums 1985-1989 dargestellt.

Dieses Gemeinschaftsprogramm spielt bei den europäischen Forschungsaktivitäten auf dem Gebiet des Strahlenschutzes eine wesentliche Rolle, indem es eine Reihe von Forschungsgebieten behandelt, denen besonders hohe Priorität eingeräumt worden ist, und indem es wissenschaftliche Zusammenarbeit der verschiedenen nationalen Forschungsinstitutionen fördert, sodass eine optimale Nutzung der begrenzt verfügbaren apparativen Mittel und des vorhandenen personellen Potentials gewährleistet wird. Innerhalb der umfangreichen Strahlenschutzforschung erhielten folgende spezifische Gebiete Vorrang: Dosimetrie von Personen und gemischten Strahlenfeldern, Entwicklung biophysikalischer Modelle, Rolle der Speziation beim Transfer und Verhalten der Radionuklide in der Umwelt, Reparatur von Schädigungen der DNA, Zelltransformation, Risiken von Radon, Anwendung des ALARA Prinzips, Reduzierung der Patientendosis in der diagnostischen Radiologie und Management von Nuklearunfällen sowie Gegenmassnahmen. Das Strahlenschutzprogramm der Kommission hat zudem die Aufgabe, neu auftretende Probleme zu identifizieren und Lösungen auszuarbeiten, insbesondere wenn sie den Strahlenschutz auf Gemeinschaftsebene betreffen. Nach dem Reaktorunfall in Tschernobyl 1986 nahm das Programm Sonderaktionen in zehn verschiedenen multinationalen Vorhaben in Angriff, die Probleme im Zusammenhang mit der weitreichenden radiokativen Kontaminanierung betrafen. Die Ergebnisse dieser zehn Forschungsvorhaben werden zu einem späteren Zeitpunkt veröffentlicht werden. Die gesamten Aktivitäten des Programms werden in enger Zusammenarbeit mit den verordnungspolitischen Aufgaben der KEG im Strahlenschutz durchgeführt.

Im Rahmen des abgelaufenen Fünfjahresprogramms sind rund 250 Studiengruppen, Workshops, Seminare und Symposia organisiert worden, die die Zusammenarbeit zwischen den Wissenschaftlern in den Mitgliedstaaten, die in früheren Programmen aufgebaut wurde, weiter verstärkt haben. Weitere Zusammenarbeit mit

Wissenschaftlern in den Vereinigten Staaten von Amerika und in Kanada wurde durch die "Absichtserklärungen" eingeleitet, die die Kommission mit dem US Department of Energy und der Atomic Energy of Canada Ltd. abgeschlossen hat. Diese Absichtserklärungen führten zu einer zunehmenden Koordinierung der Forschungsprogramme auf der Ebene des Vertragsmanagements und ermöglichten die gemeinsame Durchführung mehrerer Tagungen. Dadurch wurden Wissenschaftler diesseits und jenseits des Ozeans regelmäßig zum Austausch von Ideen und Ergebnissen zusammengeführt.

Wie in früheren Programmen wurden die Forschungen auf der Grundlage von Kostenteilungsverträgen mit nationalen Forschungsinstitutionen und Universitäten in Mitgliedstaaten durchgeführt. Während der Laufzeit des Programms sind zwei neue Länder, Spanien und Portugal, der Gemeinschaft beigetreten, und ihre Strahlenschutzforschung wurde aktiv in das Gemeinschaftsprogramm integriert. Im Jahre 1987 wurde die Verantwortung für die Durchführung des Programms von der Direktion Biologie, Strahlenschutz und Medizin auf die Direktion Nuklearforschung und Entwicklung, die dann in die Direktion Forschung über nukleare Sicherheit umbenannt wurde, übertragen. Ein Budget von 58 Mio Ecu wurde dem Programm für die Jahre 1985-1989 zugewiesen. Ungefähr 340 Forschungsvorhaben, an denen etwa 500 vollzeitlich beschäftigte Wissenschaftler von allen wesentlichen Strahlenschutzforschungsinstituten in der Gemeinschaft beteiligt waren, führten zur Veröffentlichung von etwa 4000 wissenschaftlichen Arbeiten; die meisten davon sind in diesem Endbericht aufgeführt.

Eine Bewertung des Programms durch ein Gremium unabhängiger Sachverständiger (Report EUR 12145 EN, 1989) betonte die Ausgewogenheit, Produktivität und Vollständigkeit des Programms. Die Bewertung folgerte, dass das Programm "einen solch hohen Entwicklungsstand erreicht hat, dass es den Respekt anderer großer Programme in der Welt...." gewonnen hat und dass "es ihm gelungen ist, die meisten, erfahrenen Wissenschaftler auf diesem Gebiet an der Gemeinschaftsforschung zu beteiligen und so auf diese Weise ein allgemein koordiniertes Programm in Europa erzielt werden konnte".

Ein neues Programm mit einem Budget von 21.2 Mio Ecu wurde für den Zeitraum 1990-1991 begonnen, womit die Fortführung eines integrierten europäischen

Strahlenschutzprogramms gesichert ist. Dies schließt das spezielle Problem der Weiterbildung junger Wissenschaftler im Strahlenschutz ein, die erforderlich ist, um die Fachkenntnisse auf diesem Gebiet in Europa zu erhalten.

Die Forschungsvorhaben sind in diesen 3 Bänden eingehender beschrieben als es früher der Fall war. Diejenigen Leser, die einen Überblick über die Hauptergebnisse wünschen, seien auf die "Synopsis of the Results of the 1985-1989 Programme" hingewiesen, die Ende 1990 veröffentlicht werden wird.

S. Finzi
Direktor GD XII-D
Forschung über nukleare Sicherheit

G.B. Gerber
Abteilungsleiter GD XII-D-3
Strahlenschutzforschung

E. Bennett
Direktor GD XI-A
Nukleare Sicherheit, Auswirkungen der Industrie auf die Umwelt und Bevölkerungsschutz

The Radiation Protection Programme, completed in 1989, was the sixth multi-annual research and training programme carried out under the Euratom Treaty of the Commission of the European Communities (CEC) since 1960. The results reported in these 3 volumes provide a comprehensive account of the scientific progress made during the period 1985-1989.

This Community Programme plays a major role in the European research activities in radiation protection by emphasising a number of high priority research areas and by strengthening collaboration between the various national research organisations to achieve an optimal exploitation of the limited institutional and manpower resources. Within the broad field of radiation protection research, priority has been given to specific topics, eg personnel and mixed field dosimetry, biophysical modelling, the role of speciation in the transfer and control of radionuclides in the environment, repair of DNA damage, cell transformation, radon risks, application of the ALARA principle, reduction of patient exposure in diagnostic radiology and management of nuclear accidents as well as remedial actions. The Commission's Programme has also the task of identifying and responding to new problems as they arise, especially when they have implications for radiation protection throughout the whole Community. In 1986, following the reactor accident at Chernobyl, the Programme launched a special action to cover, in 10 different multi-national projects, the urgent research issues highlighted by the widespread radioactive contamination. The results of these 10 research projects will be reported in a separate publication. In all these activities the Programme retained a close collaboration with the Commission's regulatory and legislative undertakings in radiation protection.

The 1985-1989 Radiation Protection Programme has organised about 250 study groups, workshops, seminars and symposia which have increased the co-operation between scientists from the Member States already established in previous Community programmes. Further co-operation with scientists in the United States of America and in Canada has been stimulated by the Memoranda of Understanding made between the Commission and the US Department of Energy and the

Commission and the Atomic Energy of Canada Ltd. These Memoranda of Understanding have led to increased co-ordination of research programmes at the contract management level and have allowed several of the scientific meetings to be co-sponsored. In this way, scientists from both continents were regularly brought together to exchange ideas and results in radiation protection research.

The Programme was implemented by shared-costs contracts with national research organisations and universities in the Member States, as in previous programmes. In the course of the Programme, two new Member States, Spain and Portugal, joined the Community and the radiation protection research in these countries was actively dovetailed into the Programme. In 1987 the responsibility for the management of the Programme was transferred from the Biology, Radiation Protection and Medical Research Directorate to the Directorate for Nuclear Research and Development which has become the Directorate for Nuclear Safety Research. A budget of 58 MEcu was allocated to the programme for the period 1985-1989. Some 340 projects involving 400 full time scientists from all the major radiation protection research organisations in the Community produced nearly 4,000 publications, most of which are listed in this final report.

An evaluation made by a panel of independent experts (Report EUR 12145 EN, 1989) stressed the maturity, productivity and the comprehensiveness of the programme. The evaluation concludes that the Programme "has reached a level of sophistication that ensures its respect from other major programmes in the world" and "has succeeded in involving most of the knowledgeable scientists in this field in the European Community, thus creating an overall co-ordinated programme for Europe".

A new Programme has been started for the years 1990-1991 with a budget of 21.2 MEcu. This will ensure a continuation of this integrated European research Programme. A specific item on the training of young scientists in radiation protection research is included in order to ensure the maintenance of expertise in Europe.

Detailed descriptions are presented in these 3 volumes for each project in a more comprehensive way than was done previously. Those readers who wish to have an

abridged version of the main achievements are referred to the Synopsis of the Results of the 1985-1989 Programme which will be published at the end of 1990.

S. Finzi
Director DG XII.D
Nuclear Safety Research

G.B. Gerber
Head of Unit DG XII-D-3
Radiation Protection Research

E. Bennett
Director DG XI.A
Nuclear Safety, Industry and
Environment, Civil Protection

Le programme Radioprotection qui a pris fin en 1989 était le sixième programme de recherche pluriannuel exécuté depuis 1960 sous le couvert du Traité Euratom de la Commission des Communautés Européennes. Les résultats communiqués dans ces trois volumes donnent un aperçu complet des principales réalisations scientifiques obtenues durant la période 1985-1989.

Ce programme communautaire joue un rôle prépondérant dans les activités de recherche sur la radioprotection en Europe en mettant l'accent sur les domaines de recherche jugés prioritaires et en renforçant la collaboration entre les différentes institutions nationales de recherche afin d'utiliser de manière optimale les ressources disponibles tant sur le plan institutionnel qu'humain. Parmi le vaste éventail des recherches en radioprotection, des domaines spécifiques ont reçu la priorité; parmi ceux-ci citons la dosimétrie personnelle et dans un champ mixte, la modélisation biophysique, le rôle de la spéciation dans le transfert et le contrôle des radionucléides dans l'environnement, la réparation des lésions de l'ADN, la transformation cellulaire, les risques liés au radon, l'application du principe ALARA, la réduction de l'exposition du patient lors d'examens radiologiques et la gestion des accidents nucléaires ainsi que les actions correctives. Le programme de la Commission a aussi la tâche d'identifier les nouveaux problèmes et d'y répondre dès qu'ils surviennent, particulièrement lorsqu'ils ont des implications en radioprotection au niveau de toute la Communauté. En 1986, suite à l'accident survenu au réacteur de Tchernobyl, le programme a lancé une action spéciale pour couvrir, au moyen de dix projets multinationaux, les besoins urgents de recherche mis en évidence par la contamination radioactive sur de très grandes surfaces. Les résultats de ces dix programmes de recherche seront communiqués dans une publication séparée. Dans toutes ces activités le programme a maintenu une étroite collaboration avec les actions réglementaires et législatives de la Commission.

Le programme radioprotection 1985-1989 a organisé environ 250 groupes d'études, symposia, ateliers et séminaires, ce qui a permis d'accroître la coopération qui existait déjà dans les programmes communautaires précédents entre les scientifiques des Etats Membres. Une coopération accrue avec les scientifiques des Etats-Unis

d'Amérique et du Canada a été stimulée par les accords d'association établis entre la Commission et le Département américain de l'Energie (USDOE) et entre la Commission et la Société de l'Energie atomique du Canada (AECL). Ces accords d'association ont abouti à un accroissement de la coordination des programmes de recherche au niveau de la gestion des contrats et ont permis de soutenir financièrement plusieurs réunions scientifiques communes. En conséquence des scientifiques des deux continents ont pu se rencontrer régulièrement pour échanger des idées et des résultats dans le domaine de la recherche en radioprotection.

La mise en oeuvre du programme s'est faite, comme pour les programmes précédents, au moyen de contrats à frais partagés avec des organismes de recherche nationaux et des universités des divers Etats Membres. Durant le programme, deux nouveaux Etats Membres, l'Espagne et le Portugal, ont rejoint la Communauté et ces deux pays se sont intégrés activement dans le programme. En 1987, la responsabilité de la gestion du programme a été transférée de la Direction "Biologie, Radioprotection et Recherche Médicale" à la Direction "Recherche et Développement nucléaire" qui est devenue la Direction "Recherche Sécurité Nucléaire".

Un budget de 58 MECU a été attribué au programme pour la période 1985-1989. Environ 340 projets de recherche faisant appel à la collaboration active à temps plein de quelque 500 scientifiques des principales institutions de recherche en radioprotection de la Communauté ont donné lieu à la publication de près de 4.000 documents scientifiques dont la plupart sont cités dans ce rapport final.
Une évaluation menée par un groupe d'experts indépendants (EUR 12145 EN, 1989) a souligné la maturité, la productivité et la cohérence du programme. Cette évaluation a conclu que le programme " a atteint un niveau de perfectionnement qui lui assure le respect des autres programmes importants de par le monde, lequel a atteint son but en impliquant la plupart des scientifiques compétents dans ce domaine dans la communauté européenne, créant ainsi un programme global de coordination pour l'Europe".

Un nouveau programme a démarré pour les années 1990-1991, avec un budget de 21.2 MECU. Ceci assurera une continuation de ce programme complet de recherche européen. Un point spécifique sur l'éducation et la formation de jeunes scientifiques dans le domaine de la recherche en radioprotection a été inclus en vue d'assurer le

maintien de la compétence en Europe.

Des descriptions détaillées sont fournies ici pour chaque projet de manière plus complète que ce qui a été fait précédemment. Les lecteurs souhaitant une version abrégée des réalisations les plus importantes sont priés de se référer au "Synopsis" des résultats du programme 1985-1989 qui seront publiés en 1990.

S. Finzi
Directeur DG XII-D
Recherche sécurité nucléaire

G. Gerber
Chef de l'Unité DG XII-D-3
Radioprotection

E. Bennett
Directeur DG XI-A
Sécurité nucléaire, impact de l'industrie sur l'environnement et protection civile

II

Mitglieder und Experten 1989

Beratender Verwaltungs- und Koordinierungsausschuss "STRAHLENSCHUTZ"

Members and experts 1989

Management and Coordination Advisory Committee "RADIATION PROTECTION"

Membres et experts 1989

Comité consultatif en matière de Gestion et de Coordination "RADIOPROTECTION"

Mitglieder und Experten 1989
Beratender Verwaltungs- und Koordinierungsausschuss "STRAHLENSCHUTZ"

Members and experts 1989
Management and Coordination Advisory Committee "RADIATION PROTECTION"

Membres et experts 1989
Comité consultatif en matière de Gestion et de Coordination "RADIOPROTECTION"

BELGIQUE - BELGIE

S. HALLEZ °
N. HENRY °
R. KIRCHMANN
O. VANDERBORGHT

BUNDESREPUBLIK DEUTSCHLAND

W. GÖSSNER °
A.M. KELLERER
H.H. LANDFERMANN °

DANMARK

H.L. GJØRUP °
K.A. JESSEN
N.O. KJELDGAARD °

ELLINIKI DIMOKRATIA

D. MAINTAS °
E.G. SIDERIS °

ESPANA

L. ARRANZ
J.L. BUTRAGUENO CASADO
E. IRANZO
F. MINGOT BUADES °
B. SANCHEZ MURIAS °

FRANCE

L. FITOUSSI °
H. JAMMET
B. JAMPSIN
J. LAFUMA °
H. METIVIER

IRELAND

T. COLGAN
J.D. CUNNINGHAM ° (Chairman)
C.P. O'TOOLE °

ITALIA

A. CIGNA ° (Chairman)
V. COVELLI
F. GIORCELLI °
F. MORSELLI °

LUXEMBOURG

P. KAYSER °

NEDERLAND

B. BOSNJAKOVIC °
M.J. FRISSEL °
P.H.M. LOHMAN
A.T. NATARAJAN
D.W. VAN BEKKUM

PORTUGAL

M. BRITES SANTOS PATRICIO °
E. MENDES MAGALHAES
J. PISTACCHINI GALVAO °

UNITED KINGDOM

G.E. ADAMS
J.A. DENNIS °
A. EGGLETON
D.T. GOODHEAD
H. WALKER °

° Member

COMMISSION

H. ERISKAT
G. GERBER
J.M. MOUSNY
H. SCHIBILLA : Secretariat

III

FORSCHUNGSTÄTIGKEIT STRAHLENSCHUTZ

RESEARCH IN RADIATION PROTECTION

RECHERCHE EN RADIOPROTECTION

III A

STRAHLENDOSIMETRIE UND IHRE INTERPRETATION

RADIATION DOSIMETRY AND ITS INTERPRETATION

DOSIMETRIE DES RAYONNEMENTS ET SON INTERPRETATION

RADIATION PROTECTION PROGRAMME
Final Report

Contractor:

Contract no.: BI6-A-292-F

Association pour le Développement
de la Physique Atomique, ADPA
118, route de Narbonne
F-31062 Toulouse Cedex

Head(s) of research team(s) [name(s) and address(es)]:

Prof. D. Blanc
Centre de Physique Atomique
Université Paul Sabatier
118, route de Narbonne
F-31062 Toulouse Cedex

Telephone number: 61-556857

Title of the research contract:

Development of a general method allowing the complete modellisation of proportional counters.

List of projects:

1. Development of a general method allowing the complete modellisation of proportional counters.

Title of the project n° : B16-A-292-F

Development of a general method allowing the complete modelling of proportional counters

Head of project :

P. Ségur, Directeur de Recherche au C.N.R.S.

Scientific Staff :

I. Pérès, Allocataire du M.R.S.T.
M.C. Bordage, Chargée de Recherche au C.N.R.S.

I. Objectives of the project :

Our purpose is to carry out a systematic modelling of the motion of ions and electrons in a cylindrical proportional counter. This modelling will be useful to improve our basic knowledge of this type of detector. This better knowledge will allow us to determine the optimum geometrical, electrical and physical parameters in order to achieve a miniaturization of the counters especially intended for microdosimetric purposes (Rossi type counters for example). In this case, the determination of the optimum gain is very important and this can be done with the calculation of the various transport parameters.

II. Objectives for reporting period :

Transport parameters which characterize the electron motion in the counter (drift velocity, diffusion coefficients, ionization coefficients) will be calculated in equilibrium and non-equilibrium situations. These calculations will be made in tissue-equivalent gases, for which few data (electron-molecule cross sections for example) are available in the literature at the moment. These transport parameters will be used to carry out the macroscopic modelling of the motion of ions and electrons in the counter.

III Progress achieved :

1-Methodology

Since the order of magnitude of the minimum voltage applied and the energy resolution of a proportional counter are directly related to the value of the gas gain, its accurate determination is of paramount importance to estimate the best operating mode of the counter. However, many factors may change the theoretically expected value of the gain causing poor prediction of the optimum operating mode. Irregularities at the surface of the anode and its contamination by polymerized particles (due to the decomposition of the gas under the action of high energy ionizing radiation) are known to significantly decrease the gain. These two phenomena are irreversible and may only be suppressed by periodically changing the central wire of the counter and the filling gas. Another important phenomenon which has been found to decrease the gain (and change the energy position of the voltage pulse) is the space charge effect due mainly to the creation of positive ions in the vicinity of the anode wire. This space charge causes a change in the electric field within the detector to a value different from the field resulting from the applied potential between the central wire and the (grounded) external cylinder, thus changing the gas amplification factor for any subsequent event which occurs before the space charge has drifted to the cathode. This gain shift may appear, not only for high applied voltages but also, consecutively to the existence of very strong ionizing events or the occurrence of high count rates.

The rigourous calculation of the space charge field in a proportional counter must be made by simultaneously solving the continuity equations for electrons and ions and the Poisson equation. The continuity equations are macroscopic equations obtained by integrating the Boltzmann equation over the velocity space. They describe the space and time variations of the densities of various charged species. These equations depend on three macroscopic parameters that must be determined in a first step. They are the drift velocities, the diffusion coefficients and the ionization coefficient. Drift velocities and diffusion coefficients must be known for electrons and ions. Ionization coefficients are only needed for electrons but partial ionization coefficients, corresponding to every positive ion produced by dissociation, are also needed.

It is known that when the pressure is high enough and/or the variation of the electric field on the scale of an electron (or an ion) mean free path is low, it may be assumed that these parameters depend only on the ratio E/N (or E/p, E electric field, N density of the neutral background gas, p pressure). This assumption means that electrons or ions are considered to be in equilibrium with the electric field, that is to say that the average energy gained from this field is exactly balanced by the loss of energy due to collisions with the neutral background gas. The variation as a function of E/N of these macroscopic parameters (drift velocities, diffusion coefficients and ionization coefficients) must then be determined through measurements in uniform field geometry experiments, or by calculations with the help of the Boltzmann equation.

The fast variation of the electric field near the anode wire in cylindrical counters causes the equilibrium assumption to be doubtful, and we may wonder if the real (non equilibrium) values of the swarm parameters are very different from the corresponding equilibrium values.

In order to answer this question, it is necessary to solve the Boltzmann equation in equilibrium and non-equilibrium situations. This is what we did during the first year of this work.

Our work was divided into four parts :

a) Determination of electron molecule cross sections for many different gases;

b) Numerical solution of the Boltzmann equation and determination of swarm parameters in equilibrium situations;

c) Numerical solution of the Boltzmann equation in non-equilibrium situations using the Monte Carlo method.

d) Numerical solution of the macroscopic equations (using the results obtained in b) and c)), and determination of the onset of space charge field.

2- Results

Electron-molecule cross sections

The necessary and difficult starting point of all our calculations is the determination of the electron molecule cross sections. Although it is outside of our scope here to go fully into the details of this subject, we think it first necessary to say a few words about the difficulties in the determination of cross sections in view of application to the modelling of proportional counters.

Usually, in weakly ionized gases, electrons have low energies (below 100 eV), so the main problem is the determination of low energy cross sections for all the processes. Since the energy of electrons is low, it is assumed that the influence of the cross section angular distribution is negligible and that the only important cross sections are the total or momentum transfer cross sections. This assumption (which gives good results in most traditional situations) means that all the cross sections used are considered to be isotropic. Furthermore, the determination of these cross sections generally corresponds to energies below four or five hundred electron volts. In a proportional counter, at low pressure, the value of the ratio E/p may be very large at the anode (greater than 5000 V cm^{-1} $Torr^{-1}$). If the equilibrium values of α/p are to be calculated, this must be done from low to very high values of E/p and it is obvious that, for these values, the energy of the electrons will be very high, above 500 eV. It is then necessary to extend the traditional set of cross sections to very high energy values.

Figure 1 shows the methane cross sections we determined. The low energy part of these cross sections is obtained from the experimental and theoretical data available. Their magnitude is modified in order for the swarm parameters (drift velocity, diffusion coefficients, ionization coefficients) calculated with this set of cross sections to be consistent with the corresponding experimental values. In this way, we make the calculated values of the first ionization coefficient very similar to the experimental data. The high energy part of the cross sections (energies higher than 100 eV) is determined using the Bethe theory (dissociation and ionization cross sections) and by assuming that the atoms in the molecule are separate scattering centers (elastic cross sections).

Similar sets of cross sections have been obtained for argon, nitrogen and carbon dioxide.

Equilibrium values of the first ionization coefficient

The variation with E/p of the equilibrium first ionization coefficient, calculated with the help of our cross sections, is given in figure 2 for argon and methane and for

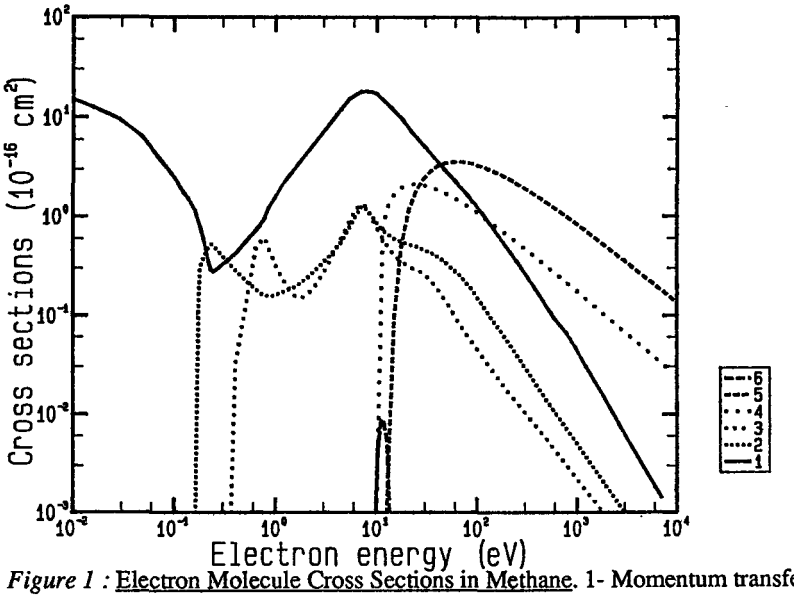

Figure 1 : Electron Molecule Cross Sections in Methane. 1- Momentum transfer cross section, 2- Vibrational cross section (ν_2-ν_4 modes), 3- Vibrational cross sections (ν_1-ν_3 modes), 4-Dissociation cross section, 5-Ionization cross section, 6-Attachment cross section.

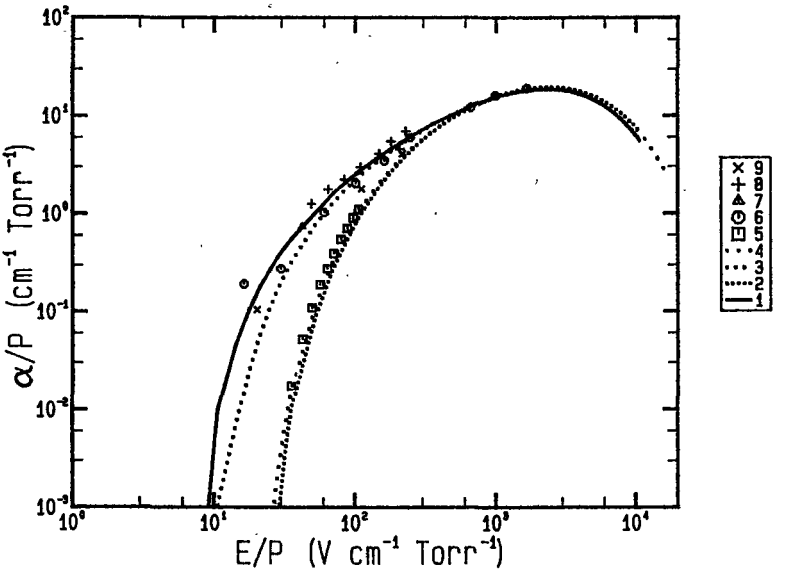

Figure 2 : Variation as a function of E/p of the equilibrium first ionization coefficient. 1 - Argon, 2 - Argon-methane mixture (Argon 90%), 3 - Argon-methane mixture (Argon 10%), 4 - Methane. Symbols correspond to experimental data.

two different argon-methane mixtures. Experimental data are also plotted when available. We see that, for low E/p values, α/p is much higher in pure argon and that it decreases when the percentage of CH_4 increases. On the other hand, for high E/p, the order of magnitude of all the ionization coefficients is very similar. The reason for these modifications in the behaviour of the various curves is that, when E/p is low, the values of the ionization coefficients depend on the mean energy losses of the electrons. Since (as we can see in figure 1) there are important vibrational processes in CH_4, the mean energy losses are stronger in CH_4 than in argon, the mean energy of electrons and thus the ionization coefficient are lower. Conversely, for high energies, vibrational processes play no role and the ionization coefficient is controlled by ionization cross sections. Since these cross sections are very similar in CH_4 and argon, the values of α/p calculated have the same order of magnitude. However the equilibrium value of the gain is higher in argon than in CH_4.

Although argon-methane mixtures are generally not used for microdosimetry purposes, we decided to do these calculations because a great number of gain measurements are available in the literature for these mixtures and so it is possible to compare the results.

Equilibrium values of α/p for CH_4, N_2, CO_2 and a tissue equivalent gas (64.4% CH_4, 32.4% CO_2 and 3.2% N_2) are given in figure 3. Between 100 and 1000 V cm^{-1} $Torr^{-1}$, the first ionization coefficient in the tissue equivalent gas closely follows α/p in CH_4 because CH_4 is the most abundant gas in the mixture and the values of α/p in CO_2 are of the same order of magnitude as those of CH_4. Above 1000 V cm^{-1} $Torr^{-1}$, α/p is controlled by CO_2 more than by CH_4. Note that due to its low proportion, nitrogen plays a minor role in the magnitude of α/p of the tissue equivalent gas.

To calculate the spatial distribution of the positive ion density (which is obtained by solving the corresponding continuity equations) variation of the production rates of the various ionized species must be known. In noble gases, only one type of ion is created. In molecular gases, since molecules dissociate very quickly under electron impact, several different ionic species may appear. Whereas the cross sections for dissociation can be measured and are generally well known, the production rates cannot easily be measured and can only be determined only by calculation. Figure 4 gives (together with the electron attachment coefficient) the E/N variation of the reduced partial ionization coefficients that we calculated for the various positive ions created in CH_4 by dissociation under electron impact. It must be emphasized that the feasability of the macroscopic study of the motion of electrons and ions in the proportional counter is closely related to the accurate knowledge of these coefficients.

Non-equilibrium values of the first ionization coefficient

To calculate the non-equilibrium values of α/p, the dimensions of the counter must be specified. The radius of the cathode was kept constant and equal to 1.8 cm, but different anode radii, different pressures and different voltages were used. All the calculations are very lengthy and were only done in methane.

The results that can be obtained from the calculations are the spatial variations of α/p. However, since the calculations were done in various conditions, it is very difficult to compare the different results if we only plot α/p as a function of the position. The best way, noting that different positions may correspond to the same values of E/p, is to plot all the results as a function of E/p. In figure 5 we give the whole set of results obtained for different anode radii and pressures. The corresponding equilibrium values are also

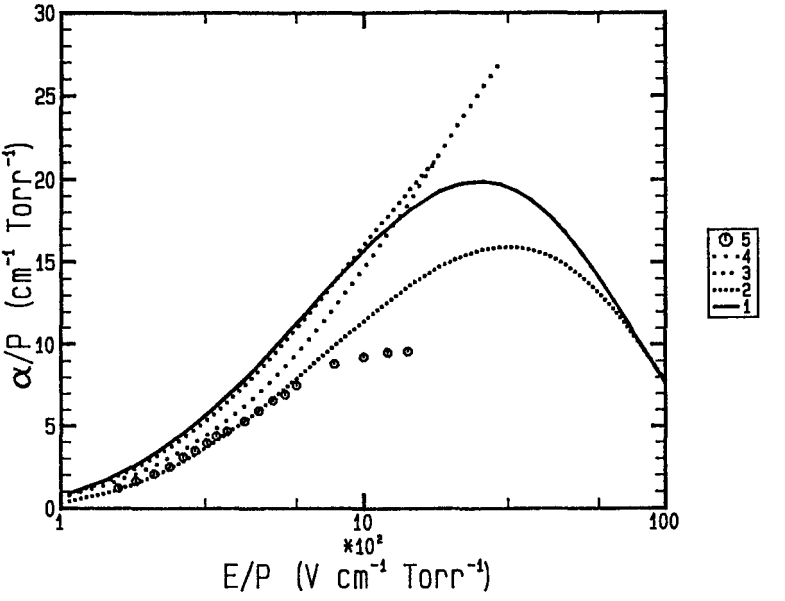

Figure 3 : Variation as a function of E/p of the equilibrium first ionization coefficient. The results are given for methane (1), nitrogen (2), carbon dioxyde (4), and a tissue equivalent gas (64.4% CH_4, 32.4% CO_2 and 3.2% N_2) (3). Symbols correspond to experimental data in nitrogen.

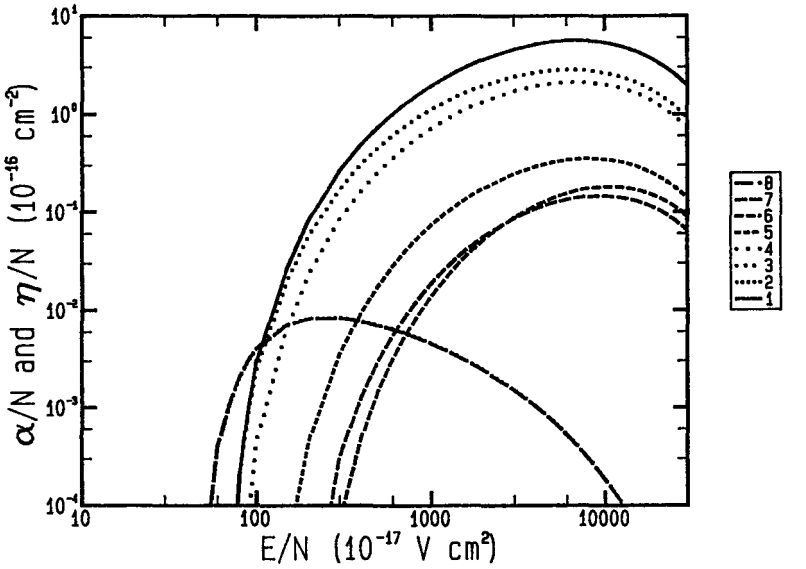

Figure 4 : Variation of partial ionization coefficients, total ionization coefficient and attachment coefficient in methane as a function of E/N. (1), Total ionization coefficient; (2)-(7), Partial ionization coefficients, (2), (3), CH_4^+ ions, (4), CH_3^+ ions, (5), CH_2^+ ions, (6), CH^+ ions, (7), H^+ ions; (8), Attachment coefficient.

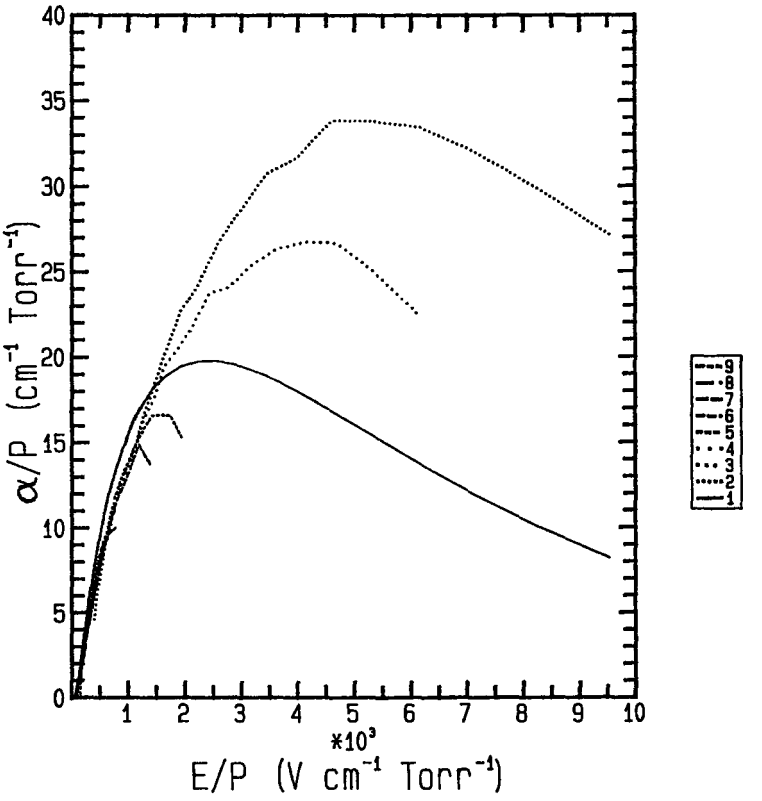

Figure 5 : Variation as a function of E/p of the non equilibrium and equilibrium values of the first ionization coefficient. The non equilibrium results correspond to different pressure-anode radius products. V = 500 Volts. (1), (3), (5), (7), equilibrium; (2), p=5 Torr, r_a = 12.5 μm, (4), p=5 Torr, r_a = 25 μm, (6), p=5 Torr, r_a = 100 μm, (8), p=40 Torr, r_a = 12.5 μm, (9),p=5 Torr, r_a = 500 μm.

plotted. The curve with the smallest anode radius-pressure product (curve 1, p = 5 Torr and r_a = 12.5 μ m) seems, at first glance, to include all the other curves corresponding to higher values of the product p r_a. Every curve has a part common with curve 1 for low values of E/p, but they show a different behaviour for the higher E/P values. In this region, the growth of α/p is first slowed down (compared to the growth of curve 1) and then followed by a decrease. This peculiar behaviour is increased for low values of the p r_a product.

We may furthermore note that, in the part common to all the curves, the non equilibrium values are lower than the equilibrium values. When E/p grows above 2000 V cm^{-1} $Torr^{-1}$, the equilibrium values of α/p decrease faster than the non-equilibrium values and the situation is inverted.

The non-equilibrium α/p curve is lower than the equilibrium curve (below 2000 V cm^{-1} $Torr^{-1}$), because the distribution function of electrons in this region cannot attain equilibrium. The increase in the electric field is so fast that electrons (which undergo many more collisions when the electric field is low) are not able to follow its variation; they present a delay and their mean energy is lower than the energy they would have in a constant electric field.

This phenomenon is a typical field gradient effect. To our knowledge, this is the first time it has been demonstrated from calculation. It has recently been postulated, on experimental grounds, by Beingessner et alii [1].

This non-equilibrium effect cannot explain the change in the growth of α/p for high E/p values. Another process is involved in the increase of the ionization coefficient. This process is made clear in figures 6 and 7 where the spatial variation of the electron density in the counter is plotted as a function of the polar angle θ and for two different values of p r_a. Figure 6 corresponds to p = 5 Torr and r_a = 12.5 μm. This is a case where, since the pressure is low and the wire radius small, electrons may circle the anode. It can be seen from the figure that this is actually the case, the density of electrons being almost constant with the angle. The situation is very different in figure 7 corresponding to p = 40 Torr and r_a = 100 μm. Unlike the previous situation, the angular variation of electron density is very strong and only a small number of electrons were able to turn around the wire.

Figures 6 and 7 show that the increase in the non-equilibrium values of the ionization coefficient is due to the fact that electrons may turn around the anode. Clearly this effect is enhanced with the decrease of pressure or/and anode radius. This can readily be seen in figure 5.

The wire effect mentioned above can only increase the ionization coefficient. The decrease in α/p which is observed at the end of every curve is caused by a wall effect. The anode wire being assumed to absorb electrons perfectly, there is a lack of electrons leaving the walls. It follows that since, near the anode, most of the electrons move forward, there is a strong increase in the mean velocity W, the backward component in W being almost negligible. As a consequence, the ionization coefficient decreases in the vicinity of the wire.

The above results show that the ionization coefficient does not depend on E/p (or on E/N) and it can be shown that it depends on the pressure-distance product (p r) and also on certain parameter K (= $V/\log(r_b/r_a)$) (V being the voltage applied). Comparisons made between calculated and measured values of the gain, must take into account the above results, i.e. they must be made for the same values of these two quantities. Figure 8 gives the variation as a function of E/N of the reduced ionization coefficient α/N for

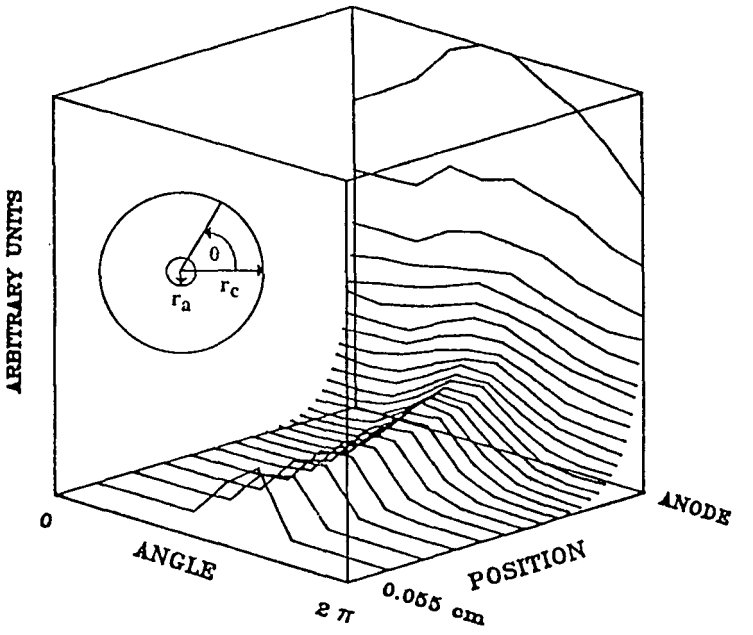

Figure 6 : Variation of the electron density as a function of the position and the polar angle θ. p = 5 Torr, r_a = 12.5 μm, V = 500 Volts.

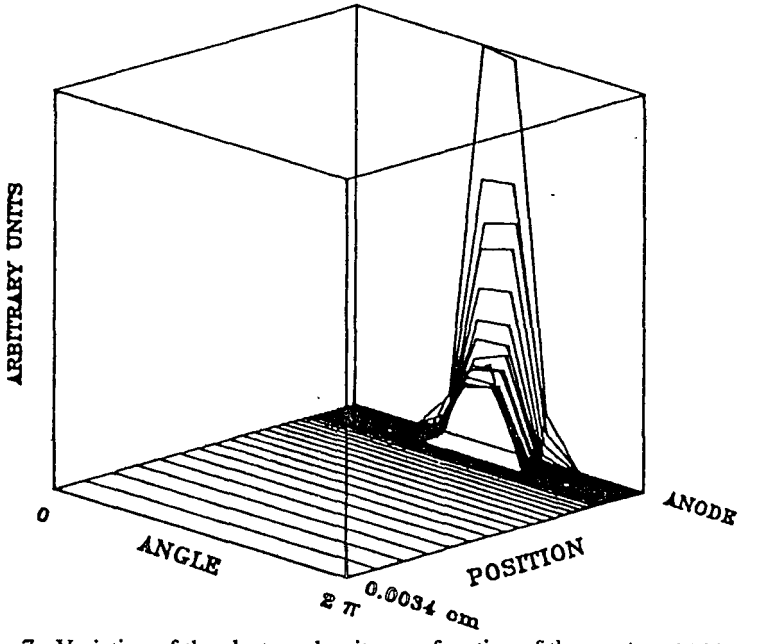

Figure 7 : Variation of the electron density as a function of the position and the polar angle θ. p = 40 Torr, r_a = 100 μm, V = 500 Volts.

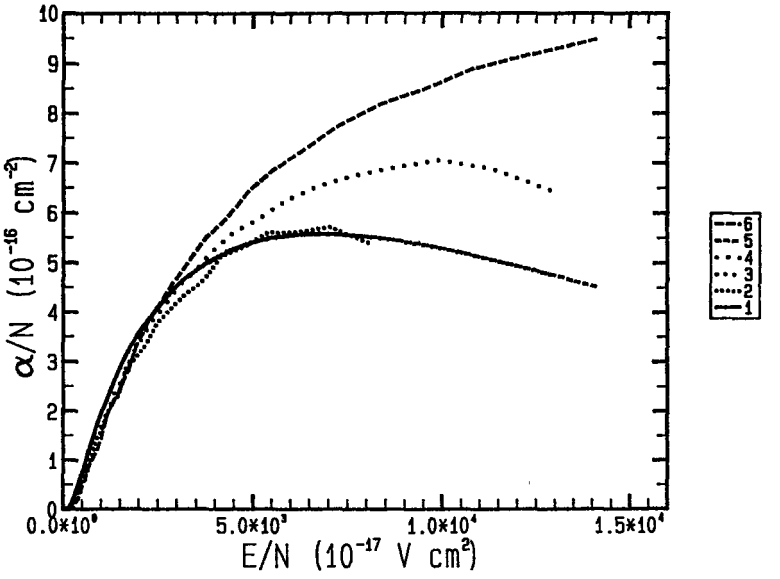

Figure 8 : Comparison between equilibrium and non equilibrium values of α/N for three different voltages; gas methane, p = 10 Torr, r_a = 25 μm, r_c = 1.8 cm., (1), (3), (5), equilibrium; (2), V=500 Volts, (4), V=800 Volts, (6), V=1000 Volts.

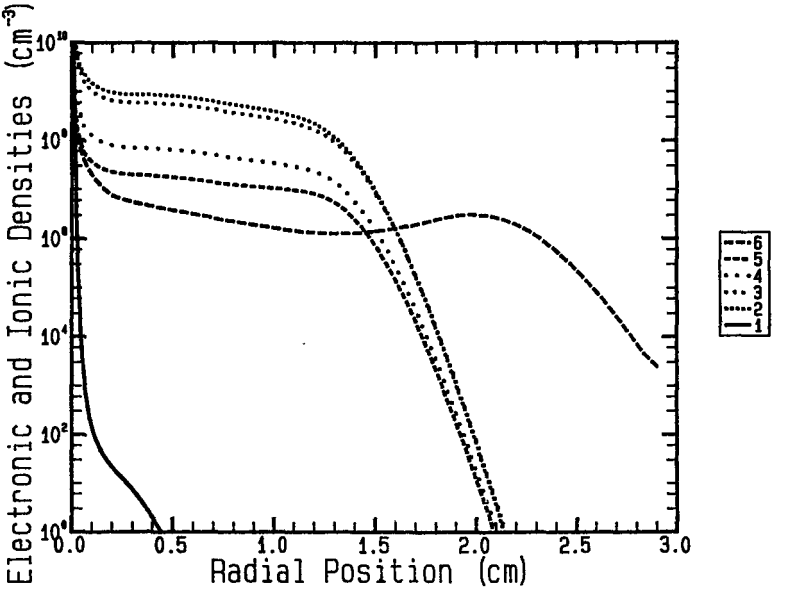

Figure 9 : Space variation of electron and ion densities in methane; V = 4000 volts; r_a = 100 μm; r_c = 3 cm; p = 65 Torr; L = 40 cm; 10000 initial electrons, t=3.8 10^{-8} s, (1), electrons, (2), CH_4^+ ions, (3), CH_3^+ ions, (4), CH_2^+ ions, (5), CH^+ ions, (6), H^+ ions.

three different values of the applied voltage corresponding to three different values of K. Differences between these three curves are clearly seen.

Determination of the space charge field :

In the present work, the calculations were done by assuming that electrons and ions are in equilibrium with the electric field. It follows that all the macroscopic parameters (drift velocity, diffusion coefficients and ionization coefficients) depend on position and time through the space and time variation of the electric field. In the case of electrons, the data used for these parameters come from our calculations (see above).

Furthermore, it is assumed that the space charge distribution is cylindrically symmetric and that its longitudinal extension is equal to the length of the counter. In these conditions, all the above equations are unidimensional and only depend on the radial variable r. The validity of these assumptions is related to the spatial distribution of the initial incoming particles (X-rays, β-rays). They must be located inside a cylindrical ring having the same length as the counter; the radial extension is arbitrarily chosen. It is clear that this distribution is realistic for incoming X-rays, but not for β-rays or α particles.

Note that attachment of electrons to neutral molecules, recombination between electrons and ions and other secondary processes such as photoionization and secondary emission from the electrodes are neglected.

Spatial variations in electron and ion densities are given in figure 9 for methane at 3.8 10^{-7} s. In this case, most of the electrons are collected and most of the charged species are ions. Due to differences in partial ionization coefficients of ions and their mobilities, the spatial distribution of the various ionic species are different. Most ions (CH_4^+, CH_3^+, CH_2^+, CH^+) are located in the almost same region, the heaviest being the most numerous. The reason is that, for these four species, the order of magnitude of mobilities is almost the same and that a molecule can be more easily dissociated into a heavy ion than into a light one. This also explains the space distribution of H^+ ions which are less numerous; as their mobility is higher than that of other species, they have already reached the cathode.

We have seen that most electrons and ions are created by ionization in a region close to the anode wire and since electrons are very quickly collected (in a time of the order of 10^{-9} s), the ionic space charge (which depends on the mobility of ions in the gas) remains in the gap for a long time (about 10^{-3} s). If the ion density is high enough, a resulting space charge field opposite to the initial electric field is created. Since the voltage applied is maintained constant, its effect is to decrease the anode field and increase the cathode field. When most of the electrons have been collected, the shape of the electric field is similar to that in figure10 (here the electric field corresponds to the densities shown in figure 9) where a minimum close to the anode can be observed. The ions move towards the cathode with time and this minimum may be expected to follow the motion of the ions.

The gas amplification coefficient G is defined as the ratio between the total number of electrons created by ionization inside the counter and the initial number of electrons deposited by the incoming radiation. When the initial electrostatic field is not perturbed by charged particles, G is exactly equal to the integral along the cylinder radius of the ionization coefficient α. When the space charge field cannot be neglected, G can no longer be calculated by integrating α and another method of calculation for G must be found.

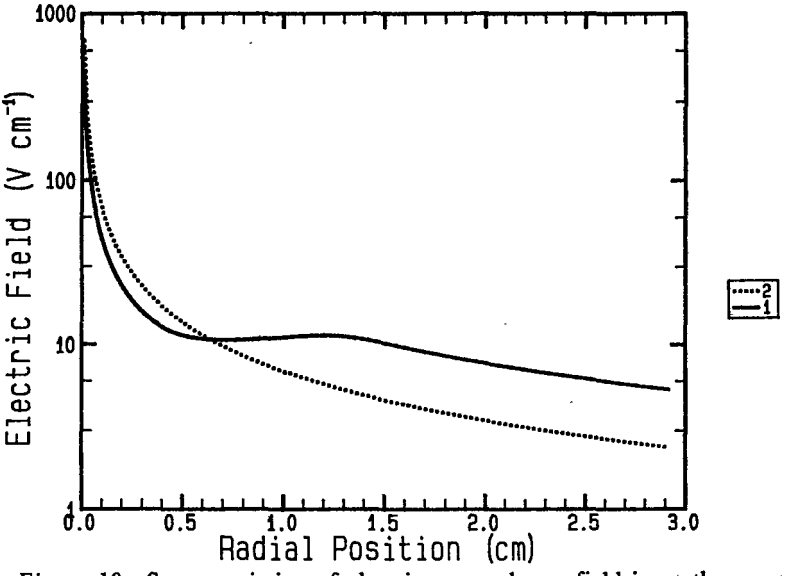

Figure 10 : Space variation of electric space charge field in methane; same conditions as in figure 9.

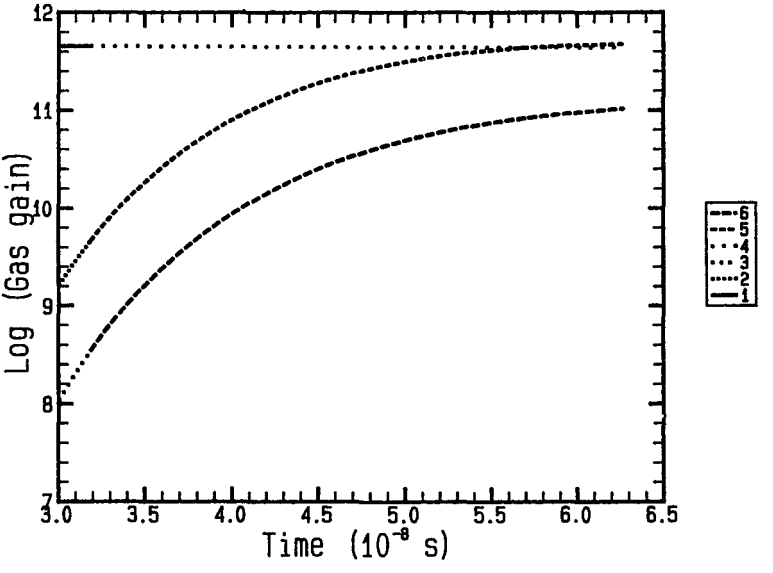

Figure 11 : Comparisons between the results obtained with the three different methods used for the calculation of the gas gain. (1),(4), direct integration of α; (2),(5), electron anodic flux integration; (3), (6), total induced current; V = 2040 volts; r_a = 100 µm; r_c = 3 cm; p = 65 Torr; L = 40 cm; 720 initial electrons.

The total number of electrons produced by ionization is equal to the time integration of the electron flux at the anode, multiplied by the anode area: this suggests how G can be calculated. The second way is found by integrating the current induced on the electrodes by charged particles moving inside the counter.

The electronic flux integration method (referenced as (1) in figures 11 and 12) allows a very fast calculation of G since electrons are quickly collected. On the other hand, the second one, based on induced current estimation (referenced as (2)) requires a very long computation time. The reason is that, to obtain the gain value, it would be necessary to wait until all charges, electrons and ions are collected at the electrodes. Figure 11 shows that, without space charge effects, our first method of calculation gives the same gain value as the direct integration of α. In figure 12, however, which corresponds to a situation where the space charge is high, we see that there are large differences between the G values calculated by integration of α, and those obtained by our two methods.

Note that, in all the works of other authors related to the estimation of space charge effects, the gain is calculated by direct α integration. We can see that this method introduces large errors in the determination of G if the space charge field becomes large.

3-Discussion

In our opinion, the objective planned for this reporting period has been fulfilled since we have not only done equilibrium calculations of the ionization coefficient (and of all the swarm parameters), but we have also been able to study the importance of the non-equilibrium behaviours of electrons in this type of geometry. Furthermore, the modelling of the kinetics of ions and electrons in a cylindrical proportional counter allowed us, not only to be able to accurately follow the space and time evolutions of ionic and electronic densities when a space charge field is present, but, also to determine the onset of the appearance of this charge space field and to calculate the various parameters playing an important role in the variation of the gas gain (non-equilibrium of electrons, space charge fields, etc.).

We shown that, at low pressure, large gain may be obtained as a consequency of the non-equilibrium electrons rotating around the central wire. Clearly, this result is of paramount importance in microdosimetry.

References

1 - Beingessner P., Carnegie R.K. and Hargrove C.K., *An Extended Parametrization of gas Amplification In Proportional Wire Chambers,* Nucl. Instr. and Meth. **A260**, 210-226 (1987).

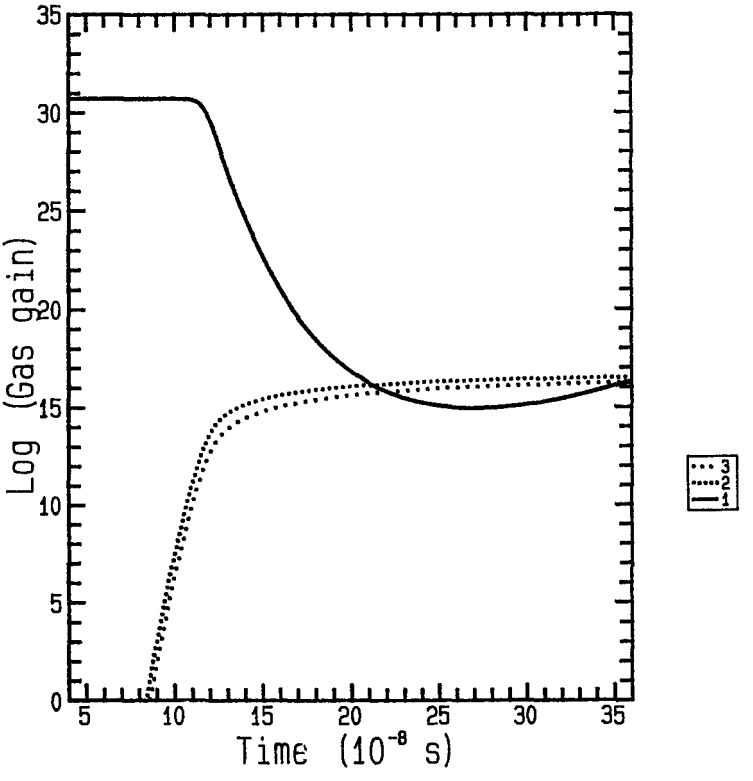

Figure 12 : Comparisons between the results obtained with the three different methods used for the calculation of the gas gain. (1), direct integration of α; (2), electron anodic flux integration; (3), total induced current; same conditions as in figure 9.

IV - Other Research group collaborating actively on this project :

J. Barthe, G. Portal

Commissariat à l'Energie Atomique,
S.I.D.R.,
B.P. n°6
92265, Fontenay aux Roses CEDEX

V - Publications :

Publications in Scientific Reviews :

P. Ségur, I. Pérès, J. P. Boeuf and M. C. Bordage, *Microscopic Calculation of Gas Gain in Cylindrical Proportional Counters,* Radiat. Prot. Dosim. (in press).

P. Ségur, I. Pérès, J. P. Boeuf and J. Barthe, *Modelling of the electron and ion kinetics in cylindrical proportional counters,* Radiat. Prot. Dosim. (in press).

Meetings and International Conferences (Invited Papers) :

P. Ségur, I. Pérès, *Microscopic Calculation of Gas Gain in Cylindrical Proportional Counters,* Implementation of Dose Equivalent Meters based on Microdosimetric techniques in Radiation Protection, Schloss Elmau, RFA, 18-20 Octobre 1988.

P. Ségur, *Modelling of the electron and ion kinetics in cylindrical proportional counters,* Xth Symposium on Microdosimetry, Rome, 1989.

P. Ségur et M. C. Bordage, *Recent Advances in the Solution of the Boltzmann Equation for the Motion of Electrons in a Weakly Ionized Gas,* XIX° Conference on Phenomena in Ionized Gases, Belgrade, 1989.

Meetings and International Conference :

M. Terrissol, M. C. Bordage, V. Caudrelier, P. Ségur, *Cross-sections for 0.025 eV-1 keV electrons and 10 eV-1 keV photons;* Atomic and Molecular Data for Radiotherapy, Proceedings of an advisory group meeting organized by the International Atomic Energy Agency and held in Vienna, 13-16 June, 1988, IAEA-TECDOC-506 (1989).

I. Pérès, P. Ségur and J. P. Boeuf, *Numerical Modelling of Space Charge Effect in Cylindrical Proportional Counters*, Proceedings of the XIX° ICPIG, July 1989, Belgrade.

M. C. Bordage, P. Ségur and I. Pérès, *Calculation of Ionization coefficient at high E/N values in helium, argon and methane*, Proceedings of the XIX° ICPIG, July 1989, Belgrade.

RADIATION PROTECTION PROGRAMME
Final Report

Contractor:

Centre de Physique Atomique
Université Paul Sabatier
118, route de Narbonne
F-31062 Toulouse Cédex

Contract no.: BI6-A-180-F

Head(s) of research team(s) [name(s) and address(es)]:

Prof. D. Blanc
Centre de Physique Atomique
Université Paul Sabatier
118, route de Narbonne
F-31062 Toulouse Cédex

Dr. M. Terrissol
Centre de Physique Atomique
Université Paul Sabatier
118, route de Narbonne
F-31062 Toulouse Cédex

Telephone number:

Title of the research contract:

Simulation of low-energy electron transport as a function of time. Application to microdosimetry and radiobiology.

List of projects:

1. Electron transport calculations, considering interaction transfer energies and the related radiation species and their temporal development with application to biophysical models of radiation action.

Title of project no. :

Electron transport calculations, considering interaction transfer energies and the related radiation species and their temporal development with application to biophysical models of radiation action.

Head of project :

M. TERRISSOL

Scientific staff :

M. TERRISSOL, A. SAIFI, M. ROCH

I. Objectives of the project :

The aim of the research is to obtain spatial and time function distribution (10^{-16} to 1 second) of all chemical species involved within the slowing down of electrons and photons in biological material for energies up to 30 keV.

II. Objectives for the reporting period :

Final report.

III. Progress achieved :

1- Introduction

In order to supply the radiobiologist with realistic data, the goal pf this work was to obtain the space and time evolution of each chemical species created or set in motion during the slowing-down of electrons and photons in biologic media. To get that evolution in liquid water, we have elaborated three Monte-Carlo type codes, chained together. For low energy photons (few eV to 10 keV) we have developed methods to calculate differential and total cross-sections for molecular gazes and used them in transport codes.

2- Chemical species evolution model.

To simulate all the events starting with the initial energy deposition in liquid water and followed until a chemical equilibrium is reached, we have built a model using three stages corresponding to three correlated programs.

2-1 Physical step.

The first program simulates the physical stage of the energy deposition by the incident particle and allows to obtain the inchoative distribution of all events occurring with times less than 10^{-15} second. The model is described in (1). During this very fast step, the appeared species are H, OH, H_2O, OH^+, H^+, H_2O^* and subexcitation electrons with energies less than 7.4 eV.

2-2 Physico-chemical step.

During the physico-chemical step (10^{-15} s to 10^{-12} s), the subexcitation electrons are transported with the use of cross-sections measured in amorphous ice (2),(3), and species are created following semi-empirical rules. During this step, primary species are quickly transformed in molecular and radicalar products. The subexcitation electrons lose their energy during many elastic collision, rotational or vibrational excitation of the H_2O molecules before their recombination or their thermalization, becoming aqueous electrons : e^-_{aq}. At the end of this second stage, the involved species are e^-_{aq} , H, OH, H_2O_2, H^+_{aq}, H_2. The parameters used to simulate this step are semi-empirical, but we continuously try to ameliore this partially unknown stage.

2-3 Chemical step.

The high reactive species created during the second stage will now diffuse and react between them and the medium: it's the chemical stage from 10^{-12} to 10^{-6} second. To obtain

all desired distributions we must solve the differential system:

$$\frac{\partial C_i}{\partial t} = D_i \nabla^2 C_i - \Sigma_j k_{ij} C_i C_j + \Sigma_{lj \neq i} k_{lj} C_l C_j$$

where the C_i, the concentrations of species i, are a function of space and time, D_i are the diffusion constants and k_{ij} the rate of reaction between species i and j. In the case of pure irradiated water, we have 11 species and about 27 possible reactions. To simulate this chemical stage we use a Monte-Carlo type time-step model : during a small interval of time ΔT, the species are assumed to diffuse randomly accordling to the Smoluchowski law:

$$F_i(r) = \frac{r^2}{D_i \Delta T \sqrt{4\pi D_i \Delta T}} \exp\left(\frac{-r^2}{4D_i \Delta T}\right)$$

When all species have diffused, the program selects the pairs species with a distance less or equal to the interaction distance a_{ij}, calculated with the Debye equation :

$$a_{ij} = \frac{k_{ij}}{4\pi D_{ij} N} \left[\frac{Q}{e^Q - 1}\right]$$

$$Q = Z_i Z_j \frac{e^2}{a_{ij} \varepsilon KT}$$

N : Avogadro number $\quad D_{ij} : D_i + D_j$

ε : dielectric constant $\quad$ K : Boltzmann constant

T : absolute temperature

Among the selected pairs, the reactions are taken into account beginning with the smallest distance. Then another time step is injected, all species diffuse, all pairs distances are newly calculated and the process is repeated steadily up to 10^{-6} second.

2-3-1 *Logarithmic time step.*

We begin the calculations with $\Delta T = 10^{-12}$ second. During that interval time, the mean diffusion distance is of the molecular radius order. For ΔT longer, the mean diffusion distance are too large and species can go nearby, but the program does not see their reaction. For ΔT smaller, the diffusion distances are very small, and it's necessary to inject several ΔT to move species enough to observe a new reaction. When the time increase, the probability that two selected species react together discrease. Then we have adopted a logarithmic variation of ΔT to spare computer time, based on the Smoluchowski law and related to that probability.

2-3-2 *Clusters.*

To spare more computer time we have built a program which splits, as many times as

necessary, the space distribution of species into "clusters". A cluster is a group of species able to react during a time Tc (a multiple of ΔT). The distances between all the species of one cluster with all other species of the track are greater than Lc, a length chosen so that the probability for any species to diffuse during the time Tc over a distance between 0 and Lc, be very close to 1 (we have taken 0.999990). So it's quite impossible that a reaction occurs between species of two different clusters during time Tc, and clusters are then assumed to be independent during that time . At the end of each period Tc, a new cluster's distribution is calculated and injected. With clusters, the computer time for tracks with more than 500 species is often divided by a 4 to 8 factor.

The physico-chemical and this chemical steps are fully described in the thesis of A.Beaudré (4).

3- Results.

3-1 Main result.

We have applied our set of programs to the simulation of species evolution created by electrons with initial energies ranging from 50 eV to 10 keV. For pure liquid water, a data set in a four coordinates system (t, x, y, z) is then obtained for each species : e^-_{aq}, $OH^\cdot$, $H^\cdot$, H_3O^+, H_2O_2,OH^-, H_2 ,HO_2 between 10^{-15} s and 1 second. On fig.1 are represented these space and time evolutions for one 10 keV electron slowing-down in liquid water, chosen randomly. To clarify the plot, projections have been done on a plane and all chemical species are represented as a dot. N is the total number of radiolytics species present. We have noticed that at times about 10^{-6} s nearly all the tracks obtained for different initial electrons lie in a cylindrical tube; their initial shape (at 10^{-15} s) is no longer discernible. From 10^{-5} s and up the shape is more and more spherical.

3-2 Thermalization times and distances.

During the physico-chemical step our code is able to obtain results on thermalization time and distance distributions. On fig.2, thermalization distance distributions for 0.2 and 7 eV are plotted and compared with useful theoretic functions (5) :

modified exponential $$D(r_{th}) = \frac{r^2_{th}}{2b^3} \exp\left(-\frac{r_{th}}{b}\right)$$

Gaussian $$D(r_{th}) = \frac{4\, r^2_{th}}{\sqrt{\pi}\, b^3} \exp\left(-\frac{r^2_{th}}{b^2}\right)$$

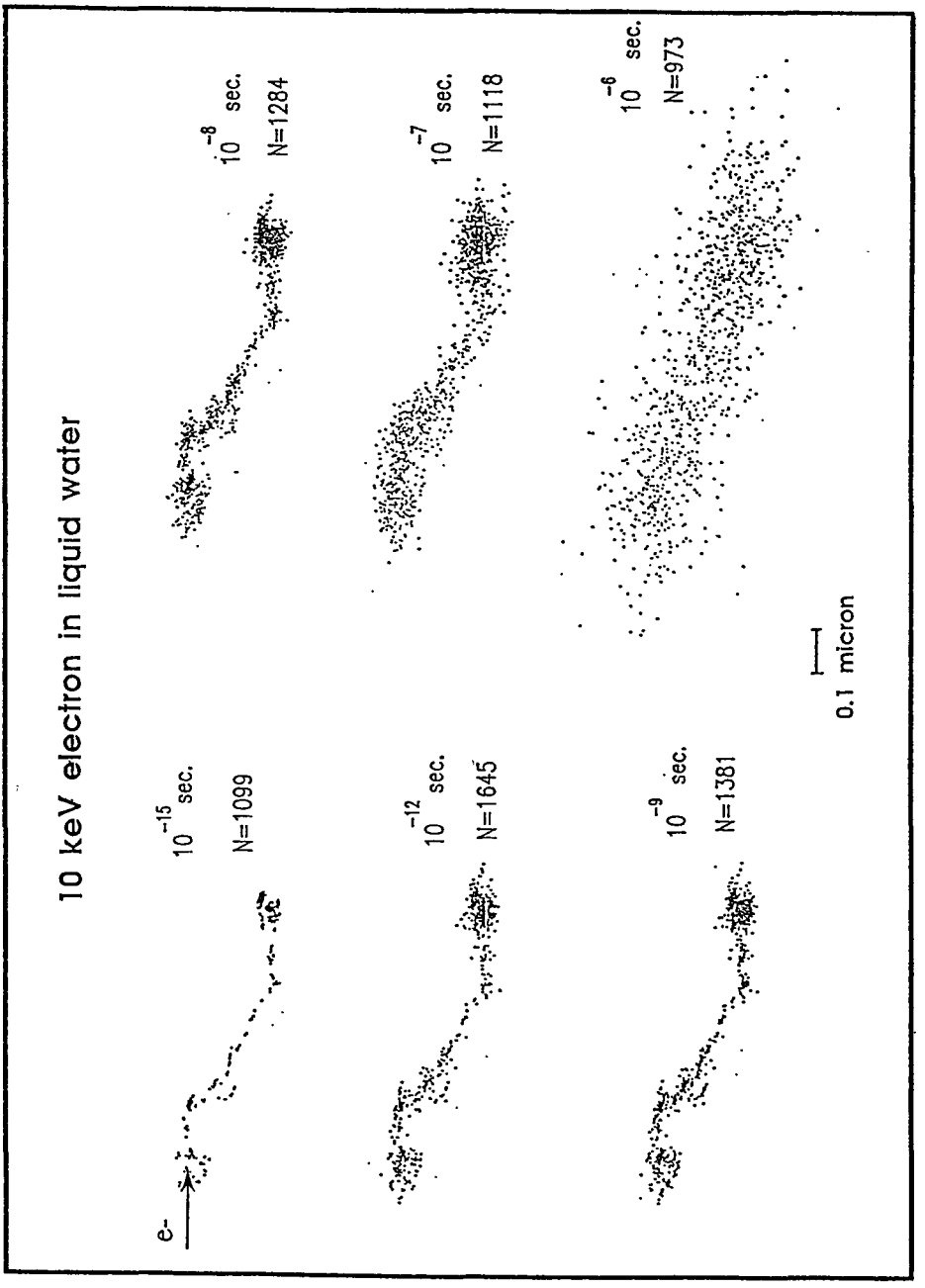

Fig - 1 : Development of one electron track in space and time. Each dot represent one species. N is the number of species present at considered time.

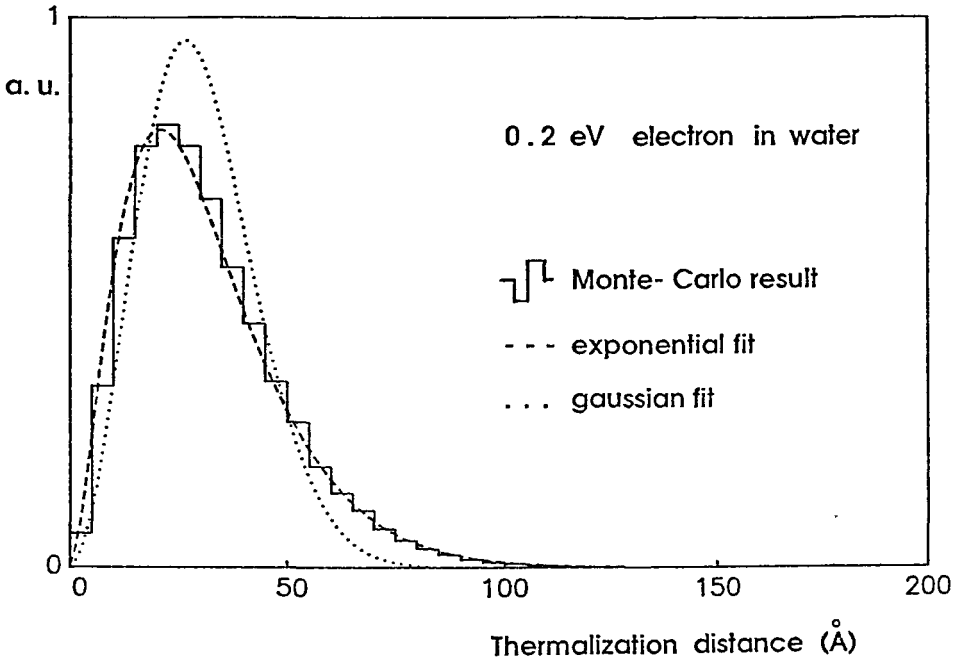

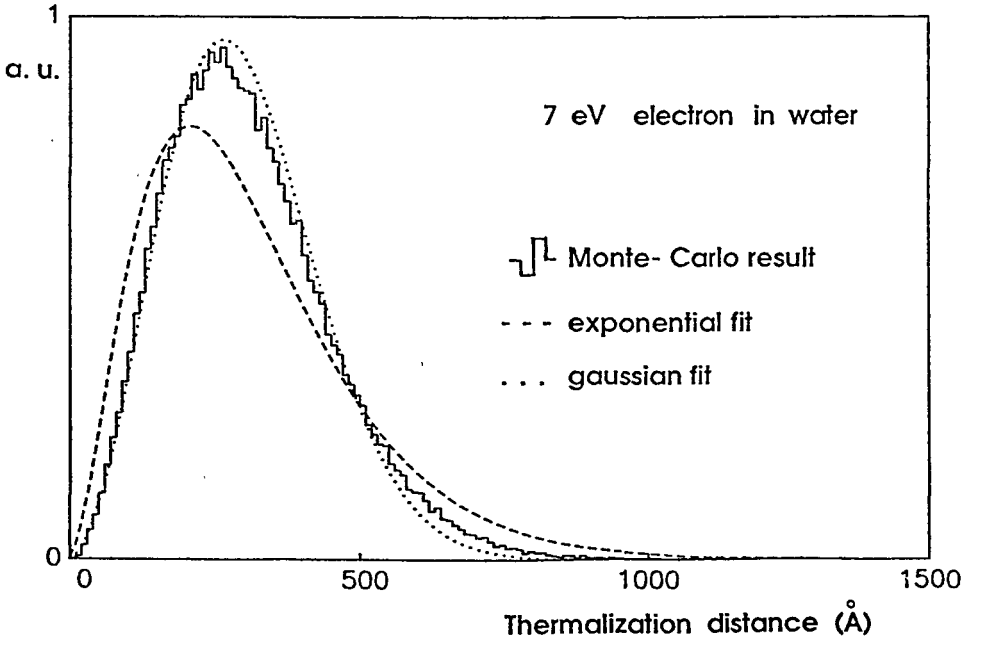

Fig - 2 : Distributions of thermalization distances for subexcitation electron in water.

with the thermalization distance r_{th} and b an adjustable parameter.We find that the modified exponential function fits well (98% confidence with Kolmogorov test) for energies about 0.2 eV(with b= 10.6 Å for 0.2 eV), while the Gaussian one, fits (92% confidence) for the greatest subexcitation electron energies, about 7 eV(with b=272.2 Å for 7 eV). There is not a single function valid for the whole energy range 0.025 - 7.4 eV. The results are somewhat in agreement with the results of Goulet (6), but the mean thermalization distances are found a little higher than that of Bolch (7).

3-3 G-Values

Just as an example, we show on fig.3 G-values for a 10 keV electron in pure liquid water. These results are obtained after integration over space, of the distributions (t, x, y, z). We may notice that the data represent only one electron and are statistical results for 100 different but independent tracks, so, values for times close to 10^{-3} s must be taken carefully because they do not represent the continuous species background yield during irradiation. A discussion and comparison with other works can be found in (4). We are now beginning studies as a function of the dose rate, and these data will be completed and improved.

3-4 Adding solutes.

The model readily permits the addition of different solutes able to react with the irradiated system species. To see for instance the influence of the solved oxygen we add O_2 in the initial system and additional chemical reactions concerned with O_2, O_2^- , HO_2 and HO_2^-. On fig.4 we have G-value for e^-_{aq} for three partial pressures of O_2 . We have noticed between 10^{-9} and 10^{-6} the disappearing of e^-_{aq} and $H\cdot$, and creation of O_2^- and HO_2 between 10^{-7} and 10^{-6} second. There is no perceptible effect on $OH\cdot$ G-value.

3-5 Applications and developments.

The main interest of our model is its great easiness of adaptation, not only on the method, but on the application side. It is easy to change such cross-section or diffusion coefficient or to add a particular chemical reaction. For instance we have recently begun the study of species space and time distributions created by inside Auger emitters. We are able now to apply our codes to more realistic biologic investigations.

Aside we are developping a method to solve numerically the differential chemical system (see § 2-3), using a Thomas three-diagonal-matrix-algorithm suggested by Patankar. Four coordinates species concentrations (x,y,z,t) are discretised in space and time. When the time increase, the digital dimensions of the system become prohibitive, and results can only be obtained in special cases and limited times, 10^{-6} second for instance. Results are in good agreement with the above Monte Carlo model .

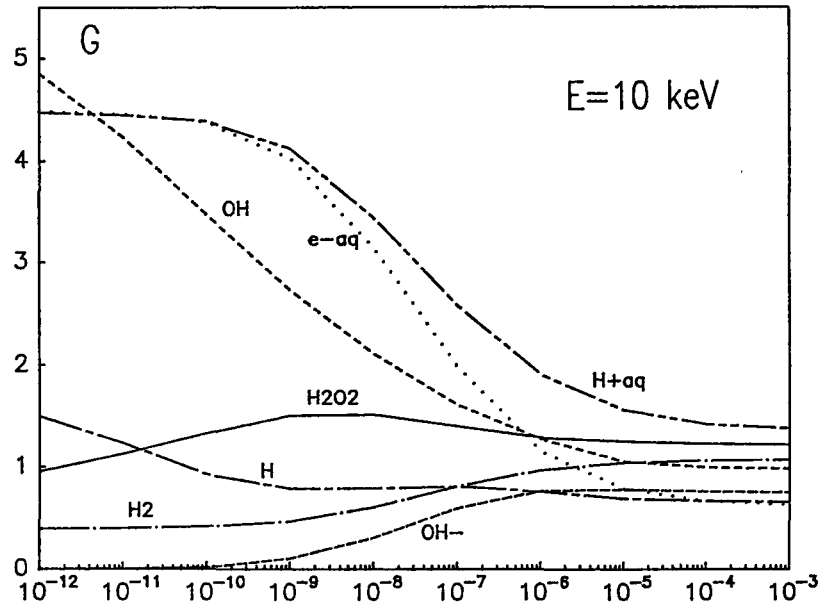

Fig - 3 : Variation with time of G-values for 10 keV electron in water.

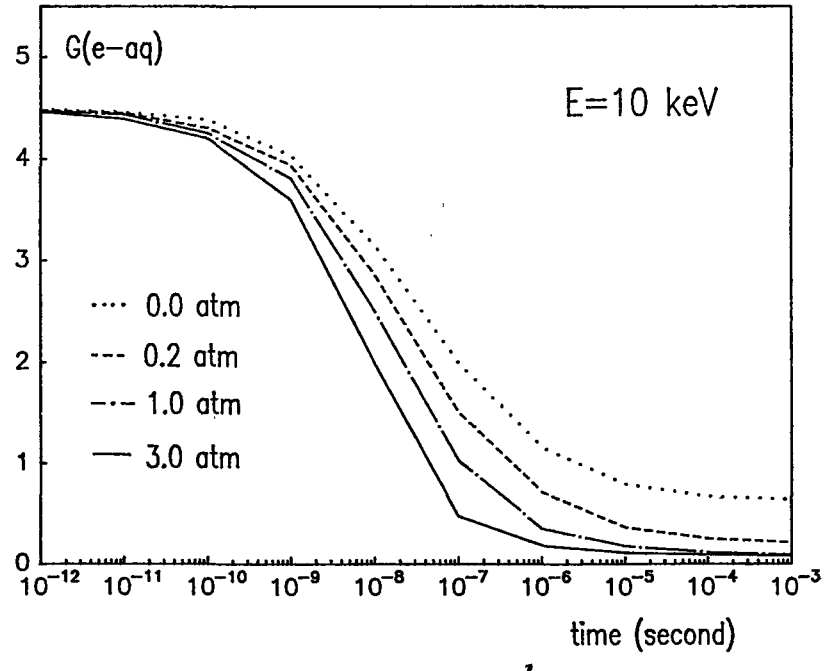

Fig - 4 : Variation with time of e^-_{aq} G-value for 10 keV electron in water for different O_2 partial pressure.

4- Low energy photons.

For low energy photons, we are able to simulate their transport down to about 10 eV in molecular gases (H_2O, CH_4, CO_2 and N_2) and in mixtures of them (tissue equivalent-gas for instance). First of all we need the knowledge of differential and total molecular orbital cross-sections of all interactions.

4-1 Molecular cross-sections.

In the considered energy range (30 kev - 10 eV), classical interaction events are accompanied with complementary effects modifying the cross-sections.

4-1-1 *Photoelectric scattering.*

For the photoelectric effect and for energies near the ionizations thresholds, we used the differential cross-section given by RABALAIS. The complexity of molecular system make photoionization theory difficult to elaborate. We have taken into account several mechanisms that goes with each molecule. For total cross-sections, we have nevertheless adopted the semi-empirical summation theory of GELIUS, which allows to obtain each molecular orbital cross-section as a weighted sum of the corresponding atomic orbital cross-sections intervening in the molecule : the cross-section of one level is the sum of all atomic contributions to this level and that the intensity is proportional to the product of the cross-section by the electronic density.

4-1-2 *Coherent and incoherent scattering.*

For coherent and incoherent scattering, modifications were brought to the differential cross-sections. We corrected the THOMSON formula with the atomic structure factor and the KLEIN-NISHINA formula with the incoherent scattering function.

4-1-3 *Cross-section values.*

There is a good agreement between found experimental results and our calculations, even at low energy and we used as far as possible all the available experimental data to calibrate our results. Total cross-sections obtained for the H_2O, CO_2, CH_4 and N_2 molecules can be seen on the last 1988 progress report and in (8).

4-2 Transport code.

We have then elaborated a model which simulate the photon transport in several molecular media and mixtures of molecular gazes. The secondaries electrons set in motion are transported and the chemical species evolution simulated as explain above. For

mixtures, to avoid excessive computer time, but to nevertheless obtain relevant results, we have settled up a little theoretical code only based on the molecular cross-section knowledge, allowing to find values very close to those obtained with the full Monte-Carlo program. Various results can be found in (8).

5- Conclusion.

We are able to apply our set of programs to the simulation of species evolution created by electrons with initial energies ranging from 50 eV to 10 keV. We obtain the space and time distributions of the radicals and the molecular products coming from the water radiolysis between 10^{-15} and 1 second : e^-_{aq}, OH, H, H_3O^+, H_2O_2,OH-, H_2 ,HO_2. These basic data may then be used to do radiophysical, radiotherapic, microdosimetric or radiobiological applications or investigations.

6- Bibliography.

1- Terrissol, M. *Méthode de simulation du transport des électrons d'énergies comprises entre 10 eV et 30 keV.* Thèse de Doctorat ès-sciences, Université Paul Sabatier, Toulouse, France, n° 839 (1978),.

2- Michaud,M. and Sanche,L. *Total cross-section for slow electron (1-20 eV) scattering in solid H_2O.* Phys. Rev. A 36, 4672-4683 (1987).

3- Michaud,M. and Sanche,L. *Absolute vibrational excitation cross-sections for slow electron (1-18 eV) scattering in solid H_2O.* Phys. Rev. A **36**, 4684-4699 (1987).

4- Beaudré,A. *Simulation spatio-temporelle des processus radiolytiques induits dans l'eau par des électrons.* Thèse Université Paul Sabatier, Toulouse, France, n° 371 (1988).

5- Casanovas,J., Guelfucci,J.P. and Terrissol,M. *Determination of the ionization quantum yield and thermalization distance of photoelectrrons created by v.u.v. photoionization in pure liquid alkanes and tetramethylsilane.* Radiat. Phys. Chem. 32(3) 361-373 (1988).

6- Goulet,T. and Jay-Gerin,J.P. *Thermalization distances and times for subexcitation electrons in solid water.* J. Phys. Chem. 92(24) 6871-6874 (1988).

7- Bolch,W.E.,Turner,J.E.,Yoshida,H., Bruce Jacobson,K., Hamm,R.N.,Wright,H., Ritchie,R.H. and Klots,C.E. *Monte-Carlo simulation of indirect damage to biomolecules irradiated in aqueous solution.* ORNL-TM-10851 (1988).

8- Caudrelier, V. *Simulation par la méthode Monte Carlo du transport des photons de 30 keV à quelques eV dans des gaz moléculaires.* Thèse de l'Université Paul Sabatier, Toulouse, France, n° 467 (1989)

IV. Objectives for the next reporting period :

Final report. Work continue now for the new radiation protection program.

V. Other research groups collaborating actively on this project [names and addresses] :

VI. Publications :

BEAUDRE A and TERRISSOL M, " Simulation de l'évolution spatiale des réactions et des produits de radiolyse de l'eau entre 10^{-15} et 10^{-6} seconde. " Proceedings of the XXVème Congrès de la Societé Française des Physiciens d'Hopital, Université Paul Sabatier TOULOUSE , pp 239-247 (1986).

M. TERRISSOL, A. BEAUDRE, V. CAUDRELIER :" Simulation of spatial and temporal evolution of chemical species created by electrons and photons in liquid water." 8th International Congress of Radiation Research, Edimbourg , Taylor & Francis Ed. p.48, 1987.

J. CASANOVAS, J.P. GUELFUCCI, M. TERRISSOL :" Determination of the ionization quantum yield and thermalization distance of photoelectrons created by v.u.v. photoionisation in pure liquid alkanes and tetramethylsilane." Radiat.Phys. Chemistry, vol. 32,n°3, pp. 361-373, 1988.

V. CAUDRELIER et M. TERRISSOL : " Les sections efficaces de quelques eV à 30 keV. " Compte rendus du 27ème Congrès de la Société Française des Physiciens d'Hôpitaux,Centre Jean Perrin, Clermont-Ferrand, Juin 1988. Résumé dans le Journal Européen de Radiothérapie, vol 3, 1988, Masson Ed.

A. BEAUDRE : " Simulation spatio-temporelle sur ordinateur des processus radiolytiques induits dans l'eau par des électrons. " Thèse n° 371, Doctorat de l' Université Paul Sabatier, Toulouse 1988.

V. CAUDRELIER : " Simulation par la méthode Monte Carlo du transport des photons de 30 keV à quelques eV dans des gaz moléculaires. Thèse de l'Université Paul Sabatier, Toulouse, France, n° 467 (1989)

M. TERRISSOL, M.C. BORDAGE, V. CAUDRELIER, P. SEGUR :" Cross-sections for 0.025 eV - 1 keV electrons and 10 eV - 1 keV photons." In " Atomic and molecular data for radiotherapy" Publication IAEA-TECDOC-506, pp 218-232, Vienne 1989.

A. BEAUDRE, M. TERRISSOL :" Simulation des processus radiolytiques induits dans l'eau par des électrons." Comptes rendus des Journées d'Etudes sur la Chimie sous Rayonnement, Marly le Roi, 1988.

V. CAUDRELIER, M. TERRISSOL : " Les sections efficaces photoniques de quelques eV à 30 keV." Compte rendus du XXVII ème Congrès de la S.F.P.H. , Centre Jean Perrin,CLERMONT-FERRAND, 1988.

M. TERRISSOL and A. BEAUDRE : " Simulation of space and time evolution of radiolytics species induced by electrons in water " Tenth Symposium on Microdosimetry, Rome, 1989, Published in Radiation Protection Dosimetry.

RADIATION PROTECTION PROGRAMME
Final Report

Contractor:

Contract no.: BI6-A-002-NL

Radiobiological Institute TNO
Division for Health Research
Lange Kleiweg, 151
NL-2280 HV Rijswijk

Head(s) of research team(s) [name(s) and address(es)]:

Dr. J.J. Broerse
Radiobiological Institute TNO
Division for Health Research
Lange Kleiweg, 151
NL-2280 HV Rijswijk

Dr. J. Zoetelief
Radiobiological Institute TNO
Division for Health Research
Lange Kleiweg, 151
NL-2280 HV Rijswijk

Telephone number: 15-13.69.40

Title of the research contract:

Neutron dosimetry instrumentation for radiation protection and radiobiology.

List of projects:

1. Neutron dosimetry instrumentation for radiation protection and radiobiology.

Title of the project no.:

Neutron dosimetry instrumentation for radiation protection and radiobiology

Head(s) of project:

Prof.dr. J.J. Broerse and Dr. J. Zoetelief

Scientific staff:

Prof.dr. J.J. Broerse, A.C. Engels, Dr. J. Zoetelief

I. Objectives of the project:

Studies on neutron dosimetry are required for radiation protection as well as for radiobiological investigations of mechanisms relevant for risk assessments. In radiation protection dosimetry there is still a need for the development of sensitive detectors with a response proportional to dose equivalent for a wide range of radiation qualities. For the interpretation of biological results, obtained with various types of radiation, it is essential that dosimetry systems provide information on radiation quality in addition to accurate and precise dose values. The practical implementation of high-pressure ionization chambers for these purposes will be investigated.

II. Objectives for the reporting period:

The experimental studies with the TE and Al high pressure ionization chambers employing CH_4, C_2H_4, TE gas and Ar will be continued for 0.5 MeV neutrons. The analysis of the pressure dependence of the reading, ion recombination and cavity size effects will be continued. This analysis will partly be performed in cooperation with the National Institute of Standards and Technology at Gaithersburg, USA. The experimental studies of the high-pressure ionization chamber system will mainly be performed under conditions relevant for radiation protection practice.

III. Progress achieved:

Thimble type tissue-equivalent (TE) and aluminium (Al) high-pressure ionization chambers have been constructed with a sensitive volume of about 1 cm^3 (Zoetelief et al., Proc. Fourth Symp. on Neutron Dosimetry, EUR 7448, Vol. II, pp. 315-326, 1981). The responses of these chambers operated at gas pressures of up to 10 MPa have been investigated with various gases (e.g., TE gases, Ar, CH_4, C_2H_4 and CO_2) for ^{137}Cs gamma rays and monoenergetic neutrons. Measurements with the chambers at different pressures were performed at various values of the collecting potential. The maximum applied collecting potential of 600 V corresponds to a field strength of 2.9 kV/cm.

When the pressure increases, the relative reading (defined here as the ionization chamber reading at pressure p and a collecting potential of 600 V relative to that at 0.1 MPa and 600 V) of ionization chambers increases due to an increasing mass of the gas in the cavity. The increase of mass of the gas in the cavity causes an increase in the ionization produced in the cavity by charged particles produced in the wall and the gas, which can be limited by the ranges of the secondaries; in addition, the probability of interaction of neutrons and/or photons with the gas increases. With increasing gas pressure in the cavity of an ionization chamber, the initial ion recombination increases. This causes a decrease in the relative reading dependent on the neutron energy and the filling gas employed and limits the increase in the relative reading with increasing pressure.

Studies for both chambers operated with different filling gases are aimed at obtaining sensitive photon dosemeters and total absorbed dosemeters for a range of neutron energies, i.e., 0.9 to 15 MeV. For photon dosemeters it is also essential that the system has a low relative neutron sensitivity, k_U. Concerning k_U, investigations were also made for conventional (i.e. operated at pressures of around 0.1 MPa) Mg/Ar ionization chambers partly initiated by an unexpectedly high k_U value of the Al high pressure chamber filled with Ar at 0.1 MPa.

For radiation protection purposes, it is essential that a dosimetry system is capable of providing information on radiation quality. The pressure dependence of the (relative) reading is dependent on neutron energy, wall material of the chamber and filling gas. The adequacy of the use of the pressure dependence of the relative reading for assessment of radiation quality is investigated with different filling gases in the Al and TE high pressure ionization chambers. Another method to obtain information on radiation quality is based on the dependence of initial ion recombination on neutron energy by measurement of the reading at various values of the collecting potential. Since initial recombination is also dependent on the filling gas and the gas pressure, measurements were made for various gases and gas pressures.

In general, mixed field dosimetry is based on the validity of the Bragg-Gray principle, relating the absorbed dose in the gas of the chamber to the absorbed dose in the chamber wall material.

One of the requirements for fulfilling the Bragg-Gray conditions is that the ranges of the secondaries produced by the neutrons are large compared to the cavity dimensions (infinitesimal cavity). When the pressure of the filling gas is increased, the ranges will decrease and this can be applied to study the influence of cavity size.
With increasing gas pressure initial recombination increases considerably. The data obtained at high pressures can be analyzed in terms of different ion recombination theories to provide more insight in the validity of existing models.

Studies to obtain sensitive photon dosemeter with small k_U

Studies for 0.9 MeV neutrons with Ar as filling gas had shown that the Al high-pressure chamber provides a system with a very small relative neutron sensitivity, i.e., less than 0.001 (Zoetelief et al., 1985). In general, however, k_U will increase with increasing neutron energy. Therefore, measurements were made with both high-pressure ionization chambers for ^{137}Cs gamma rays and 15 MeV neutrons. Pure Ar was used as filling gas in comparison with 90 per cent Ar mixed with methane and Ar mixed with 0.5 per cent acethylene. The addition of methane is of interest since at high pressures this hydrogen rich gas might increase the amount of charged particles produced in the gas. The addition of acethylene could provide through the Jesse effect (see, e.g., ICRU, 1979) a more sensitive dosimetry system when the increase in ion recombination remains small.
It was concluded that for ^{137}Cs gamma rays for pressures up to about 5 MPa the relative readings of all gases show a similar dependence upon pressure. At higher pressures (e.g., 8 MPa) the relative reading with Ar + 0.5 per cent C_2H_2 is significantly smaller than that of the two other gases indicating a higher contribution from initial recombination. At about 8 MPa the recombination is smallest for Ar, intermediate for 90 per cent Ar + 10 per cent CH_4 and largest for Ar + 0.5 per cent C_2H_2, respectively. At 0.1 MPa the highest absolute reading was observed for Ar + 0.5 per cent C_2H_2, i.e., about 19 per cent higher that that with Ar. This indicates that at 8 MPa the highest reading per unit of dose is found for Ar + 0.5 per cent C_2H_2.
For d+T neutrons, up to about 4 MPa the relative readings with Ar and 90 per cent Ar + 10 per cent CH_4 are about the same for the same pressure. At higher pressures the readings with the gas mixture become lower than that with pure Ar. At 8 MPa the ratio of the relative readings with the two gases is 1.23 for the Al chamber. This ratio is in the order of magnitude of the difference in recombination for the two gases, indicating that the contribution to the reading of charged particles created in the gas is relatively small.
Initially, at 0.1 and 8 MPa k_U values of 0.38 and 0.21 were estimated. These values were unexpectedly high since in general at 0.1 MPa a k_U value of about 0.16 is found for conventional Mg or Al/Ar chambers for d+T neutrons. Additional experiments with the Al high

pressure ionization chamber with Ar resulted in k_U values of the Al/Ar high pressure chamber for d(1)+T neutrons of 0.14 at 0.1 MPa and 0.055 at 8 MPa. The value at 0.1 MPa is in good agreement with the values given generally reported for conventional Al/Ar or Mg/Ar chambers. For 90 per cent Ar + 10 per cent CH_4 a k_U value of 0.037 for d(1)+T neutrons is derived at 8 MPa gas in the Al high pressure chamber. This indicates that by addition of impurities to Ar the k_U value for d(1)+T neutrons at high pressures can be reduced.

Ethene showed for photons a large initial recombination (Zoetelief et al., 1985). It might have been expected that the ion recombination for neutrons in ethene would result in a very small reading, thus providing a neutron insensitive detector. However, the readings for 2.1, 5.3 and 15 MeV neutrons with ethene indicated a considerable neutron sensitivity.

The dependence of the relative reading on gas pressure with Ar in the TE and Al chambers for 2.1 MeV neutrons is qualitatively similar to that for 0.9 MeV neutrons, mainly due to photons and can be used to derive the photon component of the total absorbed dose (Zoetelief et al., 1988).

Relative neutron sensitivity, k_U, of Mg/Ar chambers used as photon dosemeters in mixed fields.

To try to resolve the problems of the discrepancies in the k_U values of the Al/Ar high-pressure chamber, investigations were made on the characteristics of Mg/Ar ionization chambers (also representative for Al/Ar chambers) which are commonly used as gamma-ray dosimeters in mixed neutron-photon fields.

For conventional Mg/Ar chambers, studies were performed on the dependence of the chamber reading on gas flow rate, wall thickness and charge collection as well as on k_U values (Zoetelief et al., 1986).

The dependence of the reading of Mg or Al ionization chambers on Ar flow rate shows an unexpected maximum at flow rates between about 15 and 25 $cm^3\ min^{-1}$, which might be caused by the Jesse effect (Zoetelief et al., 1986). A possible solution might be the use of a gas mixture of Ar with a few per cent of a suitable hydrogen-free gas. In addition, relatively long preflushing periods are required for Mg/Ar chambers before stable readings are found, which may be related to air adsorption to the rather rough Mg surface.

The relative neutron sensitivity, k_U, of different Mg/Ar chambers of the same design can show different values in the same neutron field (see Zoetelief et al., 1986) which gives an additional uncertainty in the determination of the relative photon contribution to the total dose.

Recently, (Schlegel-Bickmann, Brede, Guldbakke, Lewis and Zoetelief) studies were made on Exradin M2 Mg/Ar ionization chambers for 5, 8, 15 and 19 MeV neutrons. Several problems were identified: different chambers of the same design show different polarity effects; there appeared to be two pairs of chambers with different mean k_U values.

Only at 19 MeV there is agreement in k_U between all four chambers studied; the response of a Mg/Ar chamber increases steadily with increasing wall thickness in the 8 MeV and 15 MeV neutron fields and this may effect absolute k_U values.

It can be concluded that users should apply both negative and positive bias for measurements and take the mean result. If their chambers are used for fields with energies below 19 MeV it is recommended that the responses are compared with either a GM counter or a Mg/Ar chamber that has been used in a standard field to select an appropriate set of k_U values. Further studies are required to solve the problems identified.

Total dosemeter aimed at high sensitivity

From initial studies with the TE high pressure chamber it appeared that Ar was the most appropriate gas among the investigated ones to obtain a sensitive dosimetry system for ^{137}Cs gamma rays and 15 MeV neutrons, but not for 0.9 MeV neutrons. Studies of the relative reading as a function of pressure of several filling gases were therefore extended to 2.1, 5.3 and in part to 15 MeV neutrons. The results are given in Figures 1 and 2 for 2.1 and 5.3 MeV neutrons, respectively.

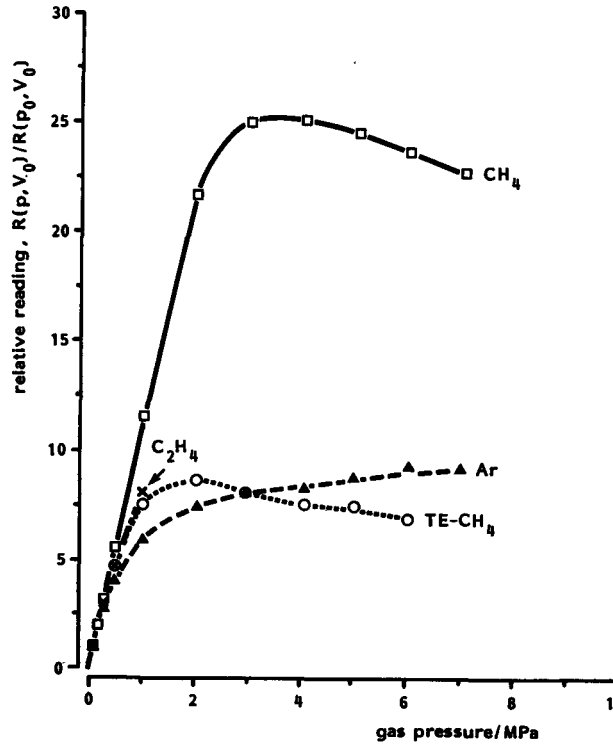

Figure 1. Relative reading of the TE high-pressure chamber as a function of the pressure of various gases for 2.1 MeV neutrons.

The use of methane as filling gas provides the most sensitive system except for 15 MeV neutrons, where with Ar as filling gas, the relative reading is highest at pressures in excess of 1 MPa. For lower energy neutrons, i.e., 0.9 and 2.1 MeV the relative reading for all gases except Ar shows a maximum; for 0.9 MeV neutrons and the use of CH_4 at approximately 2 MPa. This limits the pressure to be used for obtaining a sensitive dosimetry system. At 2 MPA the relative readings with CH_4 are approximately 16, 23, 18 and 16 for 0.9, 2.1, 5.3 and 15 MeV neutrons, respectively.

Determination of radiation quality

Information on radiation quality can be obtained from the pressure dependence of the reading as well as from initial ion recombination.

A parameter which can be used to relate the pressure dependence of the relative reading to radiation quality might be the ratio of the values at two pressures, e.g. at 2 and 4 MPa which is dependent on neutron energy. The suitability of such a parameter has to be investigated in more detail when measurements are made for a larger range of neutron energies.

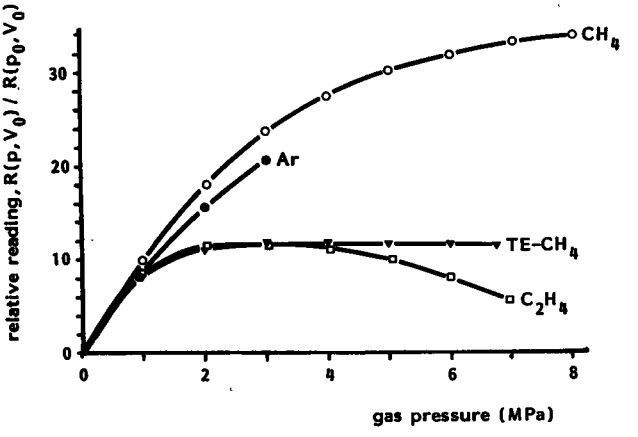

Figure 2. Relative reading of the TE high pressure chamber as a function of the pressure of various gases for 5.3 MeV neutrons.

For lower energy neutrons employing CH_4 as filling gas (below 2.1. MeV) the pressures at which the maxima occur as well as the ratio of the maximum relative readings with the Al and TE chamber can be used to assess radiation quality (Zoetelief et al., 1988).

Probably, the most suitable parameter for the determination of radiation quality is related to the reading, R, at different collecting potentials. The recombination parameter R(500V)/R(100V) is dependent on neutron energy for all filling gases at elevated pressures as shown e.g. at a pressure of 1 MPa in Table 1.

Table 1: Ion recombination in several gases for the TE chamber at several neutron energies.

	R(500V)/R(100V) at about 1 MPa			
gas	0.9 MeV	2.1 MeV	5.3 MeV	15 MeV
Ar	1.15	1.13	1.06	1.05
TE-CH_4	2.26	1.56	1.42	1.29
CH_4	1.60	1.42	1.21	1.13
C_2H_4	--	1.60	1.39	1.28

- The strongest dependence of the recombination parameter on neutron energy is observed for TE and C_2H_4. The use of CH_4 seems also suitable for using the recombination parameters to assess radiation quality and provides the most sensitive dosimetry system.

Cavity size effects

When ion recombination is small and the production of secondary charged particles in the gas is considerable the relative reading increases more rapidly than the pressure. This phenomenon is observed for CH_4 with both the TE and Al high pressure chamber for 0.9 MeV neutrons (Zoetelief et al., 1985) and 2.1 MeV neutrons (see Figure 1 and Zoetelief et al., 1988). This indicates that the cavity size is becoming important. For 5.3 (see, Figure 2) and 15 MeV neutrons this is not observed indicating a considerable smaller contribution to the ionization from charged particles produced in the gas.

The relative reading with Ar in the TE chamber for 0.9 and 2.1 MeV neutrons shows an initial a rapid increase with pressure and subsequently a slower, approximately linear increase (see, Figure 1 for 2.1 MeV neutrons). The range of the most energetic protons produced by 2.1 MeV neutrons is about 8.0 cm in argon at atmospheric pressure. The cavity diameter of the chamber is 0.8 cm and the central electrode diameter is 0.4 cm. Consequently, at higher pressures (in excess of 1 to 2 MPa), it is expected that all protons produced in the chamber wall are stopped in the gas and that a further increase in the pressure will not increase the reading due to protons created in the wall (and central electrode). The neutron cross section of Ar is quite small. Therefore, the approximately linear increase in the relative reading as a function of pressure observed in excess of about 2 MPa has to be attributed mainly to the photons in the mixed field. The relative reading of the Al chamber filled with Ar for 2.1 MeV neutrons shows an almost linear increase mainly due to the photon contribution of the beam. The relative readings as a function of the pressure of Ar in the TE and Al high-pressure chambers can be used to assess the photon component (Zoetelief et al., 1988).

Assuming that the reading at 0.1 MPa in the Al chamber filled with CH_4 is completely due to secondary charged particles created in the gas, it is estimated for the TE chamber with CH_4 gas

that at the contributions to the total ionization of secondary charged particles created in the wall are about 0.47 and 0.77 for 0.9 and 2.1 MeV neutrons, respectively (Zoetelief et al., 1988).

Analysis of ion recombinations and cavity size effects

The analysis of ion recombination, e.g., in terms of columnar (Jaffé) or cluster (Kara-Michailova/Lea) theories is seriously hampered by the absence of data for the saturation conditions (i.e., negligible ion recombination). In both theories, a large number of parameters is required such as ion mobilities which are also dependent on pressure for which data are not available from other sources. The measurement conditions are usually not close to saturation, which implies an uncertain extrapolation to saturation conditions.

Recently (see, e.g., Coyne et al., 1990), experience was obtained with calculation of ion yield and cavity size effects with the NIST-code for calculation of microdosimetric spectra (see, e.g., Caswell, Radiat. Res. **27**, 92-107, 1966; Caswell and Coyne, Proc. 6th Symp. Microdosim. EUR-6064, Vol . II, 1159-1171, 1978). The code was recently installed at our institute and has to be modified with the aim of getting information on cavity size effects for larger cavities relevant for high-pressure chambers.

Conclusions

- To obtain a sensitive photon dosemeter, the Al high-pressure chamber operated at 8 MPa of Ar or 90 per cent Ar + 10 per cent CH_4 with k_U values of 0.055 and 0.037, respectively, for d+T neutrons should be used.
- The use of ethene which seemed promising on the basis of results for photons is not suitable to obtain a photon dosemeter.
- The photon component of the 0.9 and 2.1 MeV mixed fields could be determined on the basis of the pressure dependence of the reading of both chambers filled with Ar.
- Conventional Mg(or Al)/Ar ionization chambers show various problems related to dependence of reading on gas flow rate, polarity effect, dependence of the reading on wall thickness and different k_U values for different chambers of the same design.
- The use of methane in the TE high-pressure chamber appears to provide the most suitable detector among the investigated gas-chamber combinations for total dose determination in neutron photon fields for neutron energies from 0.9 to 15 MeV. At 2 MPa, the relative readings are approximately 16, 23, 18 and 16 for 0.9, 2.1, 5.3 and 15 MeV neutrons, respectively.
- Ion recombination in CH_4 inside the TE high-pressure chamber at elevated pressures seems most promising for assessment of radiation quality, although also the pressure dependence of the reading can be employed for this purpose. Extension of the measurements to lower and higher neutron energies are required to make a decision on the most practical method

for a field instrument.

- Calculations of cavity size effects, most likely on the basis of the NIST-code to be modified for large cavities, is of great interest for comparison with experimental results on the influence of cavity size as well as for analysis of ion-recombination.

IV. Other research group(s) collaborating actively on this project [name(s) and address(es)]:

- Dr. J.J. Coyne, National Institute of Standards and Technology, Gaithersburg, MD 20899, USA.
- Dr. N. Golnik, Institute of Atomic Energy, Swierk, Poland.
- Dr. D. Schlegel-Bickmann, Physikalisch Technische Bundesanstalt (PTB), Braunschweig, FRG.
- Dr. V.E. Lewis, National Physical Laboratory (NPL), Teddington, UK.

V. Publications:

- J. Zoetelief, A.C. Engels, C.J. Bouts, J.J. Broerse and L.A. Hennen, 1985. In: Proc. Fifth Symp. on Neutron Dosimetry, eds. H. Schraube, G. Burger and J. Booz, EUR 9762, Commission of the European Communities, Luxembourg, p. 705.
- J.J. Broerse, J.T. Lyman, and J. Zoetelief, 1985. In: The Dosimetry of Ionizing Radiation, eds. K.R. Kase, B.E. Bjärngard and F.H. Attix, Academic Press, New York, pp. 230-281.
- J. Zoetelief, D. Schlegel-Bickmann, H. Schraube and G. Dietze, 1986. Phys. Med. Biol. **31**, 1339-1351.
- J. Zoetelief, N. Golnik and J.J. Broerse, 1988. Studies of high-pressure ionization chambers in neutron and photon fields. Proc. Sixth Symp. on Neutron Dosimetry. Radiation Protection Dosimetry **23**, 451-454.
- J.J. Coyne, R.S. Caswell, J. Zoetelief and B.R.L. Siebert. Improved calculations of microdosimetric spectra for low energy neutrons (submitted for publication).

RADIATION PROTECTION PROGRAMME
Final Report

Contractor:

H.H. Wills Physics Laboratory
University of Bristol
Tyndall Avenue
GB Bristol BS8 1TL

Contract no.: BI6-A-006-UK

Head(s) of research team(s) [name(s) and address(es)]:

Prof. R.G. Chambers
H.H. Wills Physics Laboratory
University of Bristol
Tyndall Avenue
GB Bristol BS8 1TL

Dr. D.L. Henshaw
H.H. Wills Physics Laboratory
University of Bristol
Tyndall Avenue
GB Bristol BS8 1TL

Telephone number: 272-241.61

Title of the research contract:

A programme of study to examine the microdistribution of alpha-emitting radionuclides in man and the development of fast neutron spectrometry and dosimetry.

List of projects:

1. The microdistribution of alpha-active nuclides in the human lung.
2. A study of the uptake and burial of alpha-radionuclides in human bone.
3. The provision of facilities for the assay of occupationally exposed plutonium in lung, liver and skeleton.

Title of the project no.:

B16-006-UK (1)
The microdistribution of α-active nuclides in the human lung.

Head(s) of project:

Dr D L Henshaw
Professor J E Enderby

Scientific staff:

Dr D L Henshaw
Dr A P Fews

I. Objectives of the project:

This project extends existing research in this laboratory using quantitative analysis of CR-39 (TASTRAK) α-particle autoradiographs. The lung burden of α-activity from particulate matter will be studied for the general population. Application of the analysis techniques will enable the abundance of the principal α-active nuclides at each site and the identity of individual particles with multiple activity to be determined. The aim will be to use this information to elucidate the deposition, retention and clearance patterns of different α-emitting particles in association with their physical size and chemical form. In particular, the patterns of retention in both lymph nodes and tracheobronchial wall can be determined enabling proper microdosimetric calculations to be made.

II. Objectives for the reporting period:

The CEC funding for this project specified that this should be restricted to development of further techniques. Therefore, the research has concentrated on one aspect of natural α-radioactivity in the human lung. The observation of a higher activity at the visceral pleura compared to a few millimetres away in the lung parenchyma is of particular interest as it indicates a natural clearance route in healthy lung. The aim will be to study this effect in more detail be analysing autoradiographs from all five lobes in 16 lung cases.

111. Progress achieved:

Methodology. We report here our detailed work on retention of α-active particulates at the visceral pleura which has exploited our techniques of inferring particle size from small point clusters of α-activity on the plastic autoradiographs.

Autoradiographs from the lung periphery have been analysed in detail from 16 autopsy cases all taken from the Bristol area. Nine of these cases had a known smoking history and seven were non-smokers. In each case a slice of tissue taken from the lung periphery of each of the five lobes and mounted against two sheets of TASTRAK nuclear track detector. One plastic sampled the visceral pleura and the other the parenchymal tissue a few millimetres away. An area of at least 6.25 cm^2 on each of the processed plastic autoradiographs has been scanned by a manual microscope observer. The data provided by the measurements have been described in detail in previous reports and elsewhere[1]. Briefly, the count density of α-activity recorded on the plastic may be converted to tissue activity per unit mass. Given sufficient statistics, the relative number of point double, triple and higher order decays observed on the plastic may be used to calculate the mean activity of individual α-emitting particles in tissue. Particle size may be inferred from the knowledge that these point clusters of activity indicate the presence of uranium and thorium-bearing minerals naturally inhaled and retained in the lung.

Results. In all 16 cases, activity values have been analysed for the right upper, right middle and left lower lobes. For the remaining lobes the data are partially analysed. All cases show some form of enhanced activity at the visceral pleura. There is no difference between smokers and non-smokers. The effect is most marked in the right upper and left lower lobes. An example of the excess activity in the visceral pleura for the right upper lobe is shown in figure 1. Table 1 shows the activity values for all lobes averaged over all cases.

Although the overall data show insufficient statistics to enable the fractional activity from point multiples to be determined throughout all tissue sites, the quantity has been calculated for the activity seen on the autoradiographs. The results are summarised in table 2 and show that the activity from multiple point decays is itself in excess at the visceral pleura. The particle size derived from the multiple activity is in the range 1 - 5 μm.

One case; No. 35, an 88 year-old female, shows a particularly high excess activity at the visceral pleura, up to 10 times higher in some lobes. Here the activity at the pleura is characterised by numerous point clusters, approximately 30 over the scanned area of one plate, each cluster containing up to 20 tracks. The results are summarised in table 3.

Table 1 Average Activities of Alpha Emitters in $Bq.kg^{-1}$ at the Visceral Pleura compared to the Parenchyma averaged over 16 cases.

Lobe	Parenchyma	Visceral Pleura	Activity Ratio
Right Upper	0.78 +/- 0.14	1.37 +/- 0.23	1.76 +/- 0.43
Right Middle	0.41 +/- 0.12	0.45 +/- 0.12	1.09 +/- 0.43
Right Lower	0.54[1]	0.46[2]	-
Left Upper	0.44[3]	0.47[4]	-
Left Lower	0.31 +/- 0.06	0.58 +/- 0.12	1.86 +/- 0.50

Table 2 Ratio of Multiple to Total Alpha Activity on Autoradiographs at the Visceral Pleura and Neighbouring Parenchyma averaged over 16 cases.

Lobe	Parenchyma	Visceral Pleura	Ratio
Right Upper	0.040 +/- 0.015	0.074 +/- 0.018	1.85 +/- 0.83
Right Middle	0.121 +/- 0.031	0.153 +/- 0.031	1.26 +/- 0.41
Right Lower	0.16[1]	0.063[2]	-
Left Upper	0.083[3]	0.100[4]	-
Left Lower	0.068 +/- 0.014	0.118 +/- 0.023	1.74 +/- 0.49

[1]4 cases only; [2]6 cases ; [3]4 cases; [4]6 cases

Table 3 Average Activity values at the visceral pleura compared to the parenchyma for an 88 year-old female, case 35.

Lobe	Parenchyma	Visceral Pleura	Ratio
Right Upper	1.28 +/- 0.13	1.56 +/- 0.07	1.22 +/- 0.14
Right Middle	0.17 +/- 0.02	0.73 +/- 0.05	4.29 +/- 0.08
Right Lower	0.23 +/- 0.03	2.36 +/- 0.09	10.3 +/- 1.4
Left Upper	0.15 +-/ 0.02	1.63 +/- 0.07	10.9 +/- 1.0
Left Lower	0.12 +/- 0.02	0.69 +/- 0.05	5.75 +/- 1.0

Discussion

This work has explicitly shown that in addition to the single particle activity, the activity from multiple point decays is itself in excess at the visceral pleura. The multiple activity emanates from small grains of uranium and thorium-bearing minerals. As indicated above, this implies that particles in the size range 1-5μm are preferentially retained at the visceral pleura. This indicates, as with the known behaviour of asbestos, that particles deposited higher up in the lung are transported by macrophages to the lung periphery into the pleural region and into the lymphatics, this being a natural lung clearance mechanism by which comparatively large particles reach the pleura. The results here illustrate the use of naturally inhaled radioactive particles to map the clearance of particulate matter in normal healthy lung.

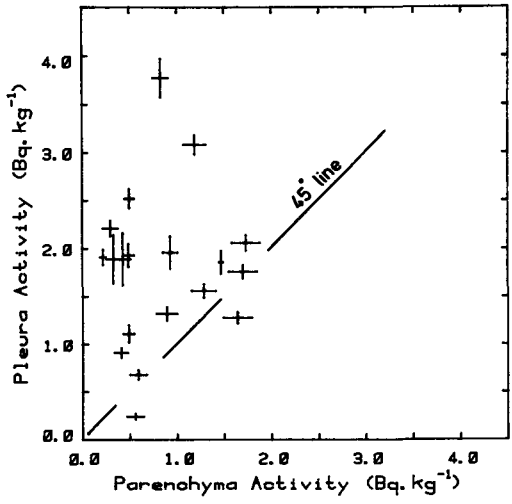

Fig. 1.

IV. Other research group(s) collaborating actively on this project [name(s) and address(es)]:

None.

V. Publications:

(1) "Microdistribution of alpha-active nuclides near the visceral pleura in the human lung." D L Henshaw, R, Maharaj, and Janet Allen. Proceedings of the Second International Workshop on Deposition and Clearance of Aerosols in the Human Respiratory Tract, Sept 18 - 20, 1986, Salzburg, Austria; published by Facultas Universitatsverlag 1987 ISBN 3-85076-232-7.

Title of the project no.:

B16-006-UK (2)
A study of the uptake and burial of alpha-radionuclides in human bone.

Head(s) of project:

Dr D L Henshaw
Professor J E Enderby

Scientific staff:

Dr D L Henshaw, Dr A Worley and Mr P H Randle

I. Objectives of the project:

In recent years new and sophisticated techniques for low-level α-particle autoradiography in CR-39 (TASTRAK) nuclear track detector have been developed in this laboratory. These techniques allow quantitative analysis of α-emitting particles in human tissue. The present study aims to use these techniques to fill important gaps in the scientific knowledge by providing a quantitative description of α-radionuclide uptake in human bone as a function of age, for the general population exposed to natural levels of activity. The work will include wherever possible parallel determinations of the α-radionuclide levels present in the liver which should provide new information on the rate of translocation to the skeleton in man.

II. Objectives for the reporting period:

The aim will be to analyse natural levels of α-radioactivity in a large set of autopsy bone samples to determine dose values to bone marrow.

111. Progress achieved:

MATERIALS AND METHODS

Introduction. During the course of the contract a considerable number of autopsy bone samples have been analysed representing the natural burden of alpha-emitting radionuclides. Under various stages of analysis are samples of vertebrae, rib and part of the skull taken from 131 autopsy cases. Seventeen whole femurs and seven whole vertebral columns are also under analysis. Later in the contract studies have begun of fetal transfer of alpha-radioactivity and of calculations of the radiation dose to red bone marrow from domestic radon exposure. The first part of this report will discuss the analysis of a particular set of autopsy bone samples obtained from adults and children who were former residents of West Cumbria. At Bristol total alpha-activity was determined in unconcentrated samples using TASTRAK plastic track detector. Separately, samples were assayed radiochemically for plutonium at the National Radiological Protection Board (UK). The second part of the report will discuss fetal transfer of alpha-radioactivity and calculations of radon dose to red bone marrow.

Tissue collection and preparation Autopsy samples from eleven cases were obtained from West Cumbria and the Newcastle area. These were divided between four adults and seven children under the age of 16 years, as summarised in Table 1.

Table 1. Summary if cases analysed

Case	Age/Sex	Residence
Adults		
N1	64M	Oxfordshire
N2	82F	West Cumbria
N3	65F	..
N4	22M	..

Children

X7	14M	Newcastle
X8A	15	West Cumbria
X8B	15M	..
X9	9	..
X10	<1	..
X11	sb*	..
X12	4M	..

* still born

A total of 30 sites were examined. These ranged from sections of femoral bone taken from the distal, mid-shaft and proximal regions, to sections of rib, sternum and vertebrae; in the child cases samples of liver and lung were also obtained. The samples were cut into sections at least 2 mm thick and stored at -20°C for periods ranging up to 289 days against CR-39 (TASTRAK) plastic, made in our laboratory. The plastic was pre-etched to reveal background α–particle tracks as described elsewhere[1]. In total 43 α–autoradiographs were produced. In the present work no attempt was made to separate the contribution of ^{210}Po by bodily intake to that from ingrowth from ^{210}Pb. All but one of the samples were mounted within two weeks of death. After exposure, the position of the bone section on the plastic was recorded photographically in both colour and black and white and the plastic then etched at 75°C in 6.25N NaOH. The track response of the plastic was calibrated using the procedures described elsewhere[2,3]. The etch time for the autoradiographs was chosen to etch a ^{210}Po α particle (5.3 MeV, range = 37.2 μm) just beyond the end of its range and was obtained for each TASTRAK manufacturing batch by calibration during the etch using a separate plastic exposed to a ^{252}Cf α–source[3]. All etch times were close to 5.5h. On the final autoradiographs the transition between tracks being etched out and not etched out occurred at a range of 39 μm. The autoradiographs were scanned manually for α-particle tracks under x250 magnification over an area of up to 36cm^2. The XY coordinates, together with the position of any point double, triple, or higher order multiple decays, were recorded. These were superimposed on a full size print from the black and white negative. The colour transparency was used to study detailed features of the sample. On eight of the autoradiographs, from adult cases, the parameters of each individual track under the bone section were measured under x400 magnification. In parallel with the manual measurements, the autoradiographs were analysed by fully automated image analysis, using the system developed in this laboratory[3,4].

Analysis The analysis procedures have been discussed in detail elsewhere[1-4]. The important features will be summarised here.

Activity per unit mass of wet bone. Activity values recorded on the autoradiographs in tracks.cm^{-2} can be converted to sample activity in Bq.kg^{-1} from the mean tissue thickness sampled by the plastic on the assumption of a uniform particle emission with height above the plastic. In the present work this has been calculated for the etch conditions employed and has a value of 7.34μm on the assumption that the majority α emitter present is ^{210}Po. The sample activity is then given by:

$$\text{Activity in Bq.kg}^{-1} = \frac{N \times 11.95}{T} \qquad \text{.....(1)}$$

where N is the number of observed α particle tracks per cm^2 on the plastic end and T the exposure time in days.

Minimum resolvable activity. For a given exposure period we can define a minimum detectable activity in tissue A_{min} which is two standard deviations above background. Assuming Poissonian fluctuations in the track count this is given by:

$$A_{min} = \frac{2\{1 + (1 + ab)^{1/2}\}}{am} \qquad \text{.....(2)}$$

where a is the area scanned in cm^2 on the plastic and m the slope of the relation between the track count and activity. The latter is given by 11.95/T. A_{min}, therefore, depends not only on the background count but also on the area scanned and exposure time. A value may be calculated for each sample: some typical values are given in Table 2. In this work a mean background count of 3.0 tracks.cm^{-2} was measured. This was determined from scans of control plastics mounted in Perspex frames and stored in the same Polythene bag and stored for the same time as the sample

Table 2. Some values of A_{min}

Area (cm^2)	Background (tracks.cm^{-2})	Exposure time	A_{min} (Bq.kg^{-1})
25	3	2y	0.013
10	3	1y	0.043
6	4	1y	0.066
6	6	6 mon	0.160

^{226}Ra activity. Whenever ^{222}Rn is produced in a sample from the decay of ^{226}Ra it can diffuse through the sample and into the plastic itself prior to decay. The diffusion of radon in tissue and TASTRAK has been extensively investigated in this laboratory. At the sample storage temperature of -20°C the mean diffusion distance for ^{222}Rn in tissue is 100 μm. The presence of radon in a sample is readily identified by the observation of characteristic point double or triple decays where two or three of the point decays from ^{222}Rn and its short-lived daughter nuclei ^{218}Po and ^{214}Po are recorded in the plastic. In general, the plastic may record either one, two, or all three of the three point multiples decays and has associated sampling thickness for these events P(3,1), P(3,2) and P(3,3) μm. These quantities are functions both of the mean radon diffusion distance and the plastic track response under the etch conditions employed and are calculated explicitly for each set of samples analysed. In order to determine the total amount of ^{222}Rn recorded by the plastic, the number of single tracks on the plastic S' that in fact originate from radon point multiple decays must first be calculated. This is given by:

$$S' = \frac{P(3,1)}{P(3,2) + P(3,3)} \times M \qquad .....(3)$$

where, in this work, for a diffusion distance of 100 μm, P(3,1) = 28.5, P(3,2) = 5.7, and P(3,3) = 0.59 μm, and M is the sum of the number of characteristic double and triple events. The total number of radon and hence radium decays is therefore S' + M = 5.53 x M. Assuming that the ^{222}Ra activity is equal to the ^{222}Rn activity then the former is given by:

$$\text{Activity on Bq.kg}^{-1} = \frac{M \times 13.9}{T} \qquad .....(4)$$

For the production of ^{220}Rn from the decay of ^{224}Ra in the ^{232}Th decay chain, the thoron diffusion distance is ~1/80th of that for ^{222}Rn. The corresponding sampling probabilities, however, yield a similar ratio to that in Equation 3 above. Thus, Equations 1 and 4 have to be applied to the separate numbers of derived true single and multiple events respectively.

Alpha particle range spectra The number of tracks recorded in the plastic with length between L and L + dL is given by:

$$N(L)dL = \left\{ \int_{(\delta)} \int_{(R)} (1/2)\sin(\delta)\cos(\delta) g_1(h) g_2(R) dR d\delta \right\} dL \qquad .....(5)$$

where $g_1(h)$ is the emissivity between height h and dh above the plastic surface where $h = (R - L)\sin(\delta)$, and $g_2(R)dR$ the number of α particles emitted with range between R and R + dR.

If constant emissivity with height above the plastic is assumes, so that $g_1(h) = k$, say, then for a given α particle range R, Equation 5 may be integrated over dip angles δ from which we have

$$N(L)dL = \frac{k(1+\cos(2\delta_c))dL}{8}$$

where δ_c is the cut-off dip angle for track detection and is about 10° for the plastic used in this work. This shows that for a given single species α source uniformly distributed with depth in the sample, the range spectrum observed in TASTRAK will be flat up to the maximum α-particle range. For a combination of α-emitting nuclides present, the range spectrum will be step-shaped with the height of each step proportional to the activity concentration for the given nuclide. In practice, there is a minimum track length cut-off that can be determined by the length below which the etched track is spherical under the etch conditions employed.

RESULTS

An example of the distribution of α-activity is shown in Figure 1. The black and white photograph, upper, shows the bone section taken across a vertebra from the lower lumbar region of a 64 year-old male, case N1. The plot, lower, shows the corresponding activity. Each point represents one α-particle track and each cross a point multiple decay. The unexpected feature of this example is that most of the activity appears outside the tissue region. In Figure 1, the presence of background tracks is precluded by the stringent procedures involved in the pre-etch technique: all detected tracks fall within the calculated limits for the etch conditions employed. Outside the bone area, the activity is partly attributed to soft tissue and partly to associated fluids surrounding the bone itself and the inevitable spreading of these fluids over the plastic surface during mounting. The smeared fluids are clearly visible on the colour transparency of the autoradiograph.

In the above case, the activity undoubtedly arises from the sample itself. Also, the vast majority of activity is in the form of single tracks and not point multiples characteristic of radon and short-lived daughter nuclei. This

indicates that the proportion of radium present in the sample is small. The majority of the activity is presumed to be from the decay of ^{210}Po. This is supported by the spectral measurements, and is consistent with that expected from the radiochemical data. Within the bone region the activity of the sample is 1.71 $Bq.kg^{-1}$.

All autoradiographs show similar features to the above examples in that the activity exists outside as well as inside the bone section.

We conclude from these observations that ^{210}Po has no affinity for bone. It is clearly present in the bone itself, in marrow and in the surrounding tissue. The majority is presumed to derive from the decay of the ^{210}Pb in bone which, owing to its apparent non-affinity for bone, is free to wander into neighbouring tissue. Its presence in marrow is most important, for it implies a significant α-dose to bone marrow, far higher than has previously been assumed.

A second feature of the recorded activity is the small number of point multiple α-tracks. The number is considerably less than that seen in autoradiographs of lung tissue. Those seen, however, show similar structure to those found in lung and their form is in most cases characteristic of the presence of radon and therefore radium.

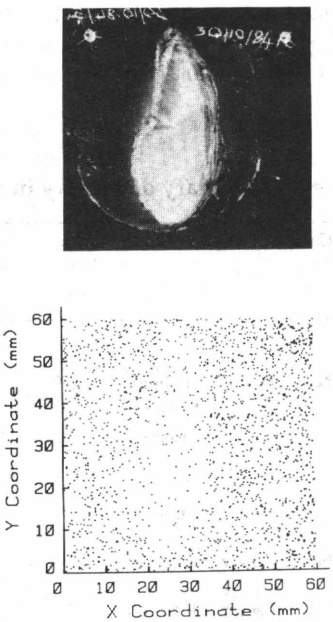

Fig. 1

The recorded activity confined to the bone area itself on the autoradiograph has been converted to sample activity in $Bq.kg^{-1}$. ^{210}Po and ^{226}Ra α-activity values have been calculated and the results are given in Table 3. The average ^{210}Po activity is 1.46 ± 0.13 $Bq.kg^{-1}$ and for ^{226}Ra 0.040 ± 0.014 $Bq.kg^{-1}$. The ^{210}Po values agree well with published radiochemical data[3,4] but in the current sample, the ^{226}Ra values are rather lower than those expected[5,6]. A detailed discussion of the plutonium measurements determined radiochemically at NRPB may be found elsewhere[7]. The average value was below 0.020 $Bq.kg^{-1}$ contributing less than 1% to the total activity present.

The measurements of individual track parameters have been converted to particle range in the plastic. The range spectra from the autoradiographs confirm that the activity over the autoradiographs is consistent with that from a thick source compared with the α-particle range. This confirms that the conversion of track count to tissue activity is a valid procedure.

For the child cases, the storage time for all of these autoradiographs was 192 days which, coupled with the lower activity present, has resulted in a much reduced activity on the plastic. In bone, the average ^{210}Po activity is 0.33 ± 0.04 $Bq.kg^{-1}$. The average plutonium values were below 0.002 $Bq.kg^{-1}$ and, as in adult bone, contribute less than 1% to the total activity.

Table 3. Summary of activity in bone sections

No.	Case	Region	Storage time (days)	Sample area (cm^{-2})	Number of tracks in sample					Activity ($Bq.kg^{-1}$)	
					Total	S	D	T	M	^{210}Po	^{226}Ra
1	N1	Femur: Proximal	289	17.1	943	933	5	-	-	2.14±0.07	0.014±0.006
2	"	Mid-shaft	"	8.8	455	412	10	3	2(1)	1.82±0.10	0.071±0.020
3	"	Distal	"	15.4	567	557	5	-	-	1.38±0.06	0.016±0.007
4	"	Vertebra (1)	"	9.8	440	418	7	1	1(2)	1.65±0.09	0.039±0.014
5	"	(2)	"	9.1	234	215	3	1	2(3)	0.86±0.07	0.021±0.011
6	N2	Femur: Mid-shaft	240	8.2	268	221	16	5	-	1.20±0.09	0.149±0.032
7	N3	Femur: Mid-shaft	"	9.0	199	193	3	-	-	0.92±0.08	0.019±0.011
8	N4	Femur: Mid-shaft (1)	"	6.4	223	219	2	-	-	1.56±0.12	0.018±0.013
9	"	Femur: Mid-shaft (2)	"	6.1	216	214	1	-	-	1.60±0.12	0.010±0.010

Notes: (i) S = single. D = double, T = triple, M = >3 tracks
(ii) (1)Two clusters one of 6 and one of 8 tracks.
(iii) (2)One cluster of 5 tracks.
(iv) (3)Two clusters each of 5 tracks.
(v) The average ^{210}Po and ^{226}Ra activities are 1.46 ± 0.13 $Bq.kg^{-1}$ and 0.040 ±0.014 $Bq.kg^{-1}$, respectively: errors quoted are those in the mean.

Table 4. Activity values in Bq.kg^{-1}

Region	^{210}Po	^{226}Ra	Pu[1]
Adult's bones	1.46 ± 0.13	0.040 ± 0.014	<0.01
Children's bones	0.33 ± 0.04	0.024 ± 0.007	<0.002
Children's liver	0.11 ± 0.02	0.010 ± 0.003	-
Children's lungs	0.11 ± 0.03	0.028 ± 0.003	-

Table 5. Dose values

	Red marrow		Endosteal cells	
	(μGy.y^{-1})	(μSv.y^{-1})	(μGy.y^{-1})	(μSv.y^{-1})
Adult's bones				
^{210}Po	39	780	39	780
^{226}Ra[2]	8.8×10^{-1}	1.8×10^{-2}	1.3×10^{-2}	2.6×10^{-1}
Children's bones				
^{210}Po	8.8	176	8.8	176
^{226}Ra	7.2×10^{-1}	1.4×10^{-2}	8.2×10^{-3}	1.6×10^{-1}
Black Committee[3]				
^{210}Po	0.29	5.8	-	-
^{210}Pb (High LET)	1.53	30.6	-	-
^{226}Ra	0.68	13.6	-	-
Total high LET	2.50	50.0	-	-

Notes (i) [1]Popplewell *et al* [7]

(ii) [2]In the case of ^{226}Ra the dose values have been calculated using the factors derived by Spiers[11].

(iii) [3]See References 8, 9 and 10.

DISCUSSION

On the assumption that the activity values calculated above apply to red marrow and also to the endosteal cells lining bone surfaces, the consequent

dose values to these regions are given in table 5. These are compared with that in the Report of the Independent Advisory Group into the investigation of the possible increased incidence of cancer in West Cumbria and with the evidence supplied to that Group. For red marrow, the α-dose from ^{210}Po is 780 and 176 $\mu Sv.y^{-1}$ in adults and children respectively. These values are considerably higher than that assumed by the Report and supporting evidence.

Measurements in Separated Marrow

Central to the interpretation of the above data is the assumption that activity over the marrow region on the autoradiographs genuinely refers to activity within marrow *in-vivo*. Following the above observations several samples of separated marrow have been mounted against TASTRAK and stored for 1 year. All of these samples were obtained from the Bristol area. The activity measurements in separated marrow yield dose values of approximately 160 $\mu Sv.y^{-1}$. These values are still well above what was assumed in the Black Report and further detailed studies in marrow are in progress.

Fetal Transfer of Alpha-radionuclides

A new project has commenced to study fetal transfer of α-radioactivity at natural exposure levels and will continue under the new contract supplied by CEC. First results from this study are available.

Under appropriate ethical committee approval fetal tissues samples from 39 cases are currently under analysis. The cases range in age from 20 weeks to still born. Samples of liver, vertebra, spleen and where possible corresponding placenta and cord blood are stored against TASTRAK plastic track detector for at least one year. The cases under study include three from West Cumberland Hospital, Whitehaven taken from West Cumbria catchment area.

The results of early measurements from four cases from the Bristol area are summarised below.

Summary of Preliminary Alpha-radioactivity Values in Autopsy Fetal Tissues and Placenta in $\mu Sv.y^{-1}$

Case	Placenta	Umbilical Cord	Liver	Spinal Column	Spleen
S2	17+/-5	52 +/-8	36 +/-6	-	-
S3	10 +/-4	40 +/-7	7.8 +/-3	171 +/-12	-
S6	29 +/-6	62 +/-9	-	128 +/-12	-
S8	23 +/-4	-	8.1 +/-4	229 +/-35	42 +/-12

^{210}Po forms the majority of activity present but in the spinal column there appears to be a significant contribution from ^{226}Ra. The higher activity in the spinal column is unexpected but mirrors the postnatal uptake of α-radionuclides by the skeleton. It is assumed though not established at this stage, that the majority of ^{210}Po in the fetus is supported by ^{210}Pb, representing the transfer of maternal lead to the fetus.

The project aims to determine fetal transfer factors for ^{120}Pb, ^{210}Po and ^{226}Ra, being the principal long-lived radionuclides of interest to the transfer of radon short-lived daughters. Such information is required as input data to fetal dosimetry from maternal radon exposure during pregnancy. Overall the aim is to provide fetal dosimetry as a function of fetal age.

Of fundamental interest is the fetal dose contribution of maternal resorption of both ^{210}Pb and ^{226}Ra. A substantial contribution from ^{210}Pb resorption would have implications for the maternal accumulated radon exposure in the home.

For the placental studies, samples are being obtained as a function of maternal age and smoking history. If reliable fetal transfer factors can be found then measurements in placenta alone can be used as a measure of fetal dose from natural long-lived α-emitters.

Radon Dose to Red Bone Marrow

We have recently performed[12] calculations of radiation dose to red bone marrow and the fetus from radon and daughter products, taking into account previously unconsidered factors, chief of which are: (i) red bone marrow contains fat cells in varying proportions depending upon skeletal location and age and in which radon is 16 times more soluble than in the surrounding marrow. The diameter of these cells is typically 100-150 micrometres[7,8]. Consequently, alpha-particle decays from radon and its short-lived daughter nuclei polonium-214 and polonium-218 within the fat cell deliver some of their energy to surrounding marrow and hence to the haemopoietic cells; (ii) room air contains not pure radon but also radon daughters which may enter the bloodstream leading to an additional daughter contribution to the dose to marrow as evidenced by observations of enhanced radioactivity in the blood of Spa workers.

We have recently updated our calculations and the resulting doses to marrow for adults, children and the fetus, exposed to given radon levels in room air, are summarised in table I. The values quoted use a quality factor for the alpha-particle of 20 as used by ICRP. That the doses to adult and child marrow are similar is largely coincidental. In the case of children an important effect

is their higher radon daughter deposition rate but lower bone marrow fat content compared with adults. At the average radon level in the UK of 20 $Bq.m^{-3}$ a dose range is given. This reflects uncertainties in the transport of radon short-lived daughters within the body. For radon concentrations of 400 and 1000 $Bq.m^{-3}$ an average dose to marrow is given. Note that the increase of marrow dose with radon exposure is non-linear owing to the ingrowth of ^{210}Po in bone[13]. These doses should be seen against a background dose from low LET radiation: gamma rays and cosmic rays, of approximately 1000 $\mu Sv.y^{-1}$. Thus, for example, we calculate that children and adults living in houses at or above the National Radiological Protection Board's (NRPB) recently announced new Action Limit of 200 $Bq.m^{-3}$ radon exposure[14] receive a radon-derived dose to marrow similar to or in excess of that from low LET radiation.

This result implies that domestic radon exposure could be a causative factor in leukaemia induction and urgent investigations are underway to test this hypothesis.

Table I Doses to red marrow and the fetus from radon and its daughter products ($\mu Sv.y^{-1}$) assuming an alpha-particle quality factor of 20.

	Radon Exposure ($Bq.m^{-3}$)		
	20	400	1,000
Adult	80-100	2,360	6,920
Child age 10	60-110	2,370	6,310
Fetus	15-45	990	2220

REFERENCES

1. Henshaw. D. L., Fews. A. P., and Webster, D. J. *A Technique for High-sensitivity Alpha Autoradiography of Bronchial Epithelium Tissue.* Phys. Med. Biol. **24**.(6), 1227-1242 (1979).

2. Fews. A. P. and Henshaw. D. L. *Alpha-particle Autoradiography in CR-39: A Technique for Quantitative Assessment of Alpha-emitters in Biological Tissue.* Phys. Med. Biol. **28**, 459-474(1983).

3. Hatzialekou. U. and Henshaw. D. L. *Automated Image Analysis of Alpha-particle Autoradiographs of Human Bone.* Nucl. Instrum. Methods **263**. 504-514(1988).

4. Fews. A. P. *Fully Automated Image Analysis of Alpha Particle and Proton Etched Tracks in CR-39.* Nucl. Tracks **12**. (1-6). 221-225 (1986).

5. Fisenne. I. M., Keller. H. W. and Harley. H. H. *Worldwide Measurement of ^{226}Ra in Human Bone: Estimate of Skeletal α-dose.* Health Phys. **40** 163-171(1981).

6. Walton. A., Kologrivov. R. and Kulp. J. L. *The Concentration and Distribution of Radium in the Normal Human Skeleton.* Health Phys. **1**. 409 (1959).

7. Popplewell. D. S., Ham. G. T., Dodd. N. J. and Shuttler. D. D. *Plutonium and ^{137}Cs in Autopsy Tissues in Great Britain.* Sci. Total Environ. **70** 321-334 (1988).

8. *Investigation of the Possible Increased Incidence of Cancer in West Cumbria.* Report of the Independent Advisory Group. Chairman: Sir Douglas Black (HMSO) (1984).

9. ICRP. *Limits for Intakes of Radionuclides by Workers.* Publication 30. Part 1. Ann. ICRP 2(3/4) (Oxford: Pergamon Press) (1979).

10. Stather. J. W., Wrixon. A. D. and Simmonds. J. R. *The Risks of Leukaemia and other Cancers in Seascale from Radiation Exposure.* NRPB-R171 (HMSO) (1984).

11. Spiers. F. W. *Radionuclides and Bone - from ^{226}Ra to ^{90}Sr.* Br. J. Radiol. **47**. 833-844 (1974).

12. Richardson. R. B., Etough. J. P. and Henshaw. D. L. *The Contribution of Radon Exposure to the Radiation Dose Received by the Red Bone Marrow and the Fetus.* UK Association for Radiation Research Meeting 20-22 Sept 1989, Bristol. UK.

13. Blanchard. R. L., Archer. V. E. and Saccomanno. G. *Blood and Skeletal Levels of ^{210}Pb - ^{210}Po as a Measure of Exposure to Inhaled Radon Daughter Products.* 1969 Health Physics, Vol. 16 p585-596.

14. Documents of the NRPB Vol. 1 No. 1 1990 HMSO.

IV. Other research group(s) collaborating actively on this project [name(s) and address(es)]:

NRPB

V. Publications:

1. Henshaw. D. L., Hatzialekou. U. and Randle. P. H. *Analysis of Alpha Particle Autoradiographs of Bone Samples from Adults and Children in the UK at Natural levels of Exposure.* Rad. Prot. Dos. Vol. 22 No. 4 pp. 231-242 (1988).

2. Richardson. R. B., Etough. J. P. and Henshaw. D. L. *The Contribution of Radon Exposure to the Radiation Dose Received by the Red Bone Marrow and the Fetus.* UK Association for Radiation Research Meeting 20-22 Sept 1989, Bristol. UK.

Title of the project no.:

B16-006-UK (3)

The Provision of facilities for the assay of occupationally exposed plutonium in lung, liver and the skeleton.

Head(s) of project:

Dr D L Henshaw
Professor J E Enderby

Scientific staff:

DR D L Henshaw

I. Objectives of the project:

Much of this work will involve the analysis of α-activity by TASTRAK autoradiography in autopsy samples for litigation purposes. Therefore, the measurements obtained will not in general be available for publication.

The objective of the project, vis-a-vis the CEC funding provided, is to construct new laboratory facilities and in due course gain approval by the Health and Safety Executive (UK) for this work. The analyses should use techniques proven in the related research at Bristol or uptake of α-radionuclides by man.

II. Objectives for the reporting period:

The objective was to analyse such cases as became available through the National Radiological Protection Board (UK) where existing collaboration exists. Work should commence on a purpose-built laboratory in the Physics Department at Bristol University.

III. Progress achieved:

During the course of the contract tissue samples from three cases involving occupational exposure have been carried out. At present the results of these analyses are not available for publication. As part of this and our other tissue analysis work, a purpose built tissue preparation laboratory has been constructed in the Physics Department of Bristol University. This contains a biological safety cabinet so that unfixed human tissue may be processed in a manner conforming to the "Code of Practice for the Prevention of Infection in Clinical Laboratories and Post-mortem Rooms (UK)".

The majority of the funding provided by CEC has been used on our contract to study the distribution of alpha-radionuclides in the human skeleton at natural exposure levels.

IV. Other research group(s) collaborating actively on this project [name(s) and address(es)]:

Analysis of occupationally exposed samples has not featured largely in this study and further funding from the CEC for this work has not been sought.

V. Publications:

National Radiological Protection Board, Harwell, U K.

RADIATION PROTECTION PROGRAMME
Final Report

Contractor:

Com.Naz.per la Ricerca e per lo
Sviluppo dell'Energia Nucleare e
delle Energie Alternative, ENEA
Viale Regina Margherita, 125
I-00198 Roma

Contract no.: BI6-A-004-I

Head(s) of research team(s) [name(s) and address(es)]:

Prof. M. Coppola
Div.Fisica e Scienze Biomed.
ENEA, CRE Casaccia
Casella Postale 2400
I-00100 Roma

Telephone number: 6-30.48.39.64

Title of the research contract:

Study of radiobiological effects at low doses.

List of projects:

1. Study of radiobiological effects at low doses.

Title of the project no.:

Study of radiobiological effects at low doses

Head(s) of project:

Dr. Vincenzo Covelli

Scientific staff:

Prof. M. Coppola, Dr. V. Di Majo, Dr. S. Rebessi

I. Objectives of the project:

Study of the biological effectiveness of low doses of different radiation qualities for various modes of irradiation and suitable endpoints (life-shortening and tumor induction) in experimental animals.

A. Analysis of results obtained from large experimental series on mouse populations whole-body irradiated with low doses of neutrons and X rays (single and fractionated), for the study of dose-effect relationships for tumor induction in different organs at risk.

B. Study of in-vivo risk of transformation per cell by an experimental model system based on transplant of irradiated cell suspensions into syngeneic hosts.

C. Study of neoplastic transformation of mouse embryo cells in vitro.

II. Objectives for the reporting period:

III. Progress achieved:

1. Studies of dose-response relationships for radiation carcinogenesis after single and fractionated neutron doses

An experiment on female BC3Fl mice irradiated with two different radiation qualities was carried out. The study was focused on tumor incidence (age-adjusted), life span shortening, and time to tumor appearance. Complete observation of survival and late pathology was carried out on over 2000 BC3F1 female mice, which had been irradiated with single doses of either 1.5 MeV neutrons, produced by a Van de Graaff accelerator (0.5 to 16 cGy), or 250 kVp X rays (HVL=1.5 mm Cu) (4 to 256 cGy), and followed until spontaneous death.

Data of mean survival time appear to be consistent with a linear decrease with the dose, without threshold, for both fast neutrons and X rays, although the effect was too small to be significant at the lower doses, i.e., below 8 cGy and 64 cGy, respectively. The ratio of the fitted linear slopes was 12.3±1.8.

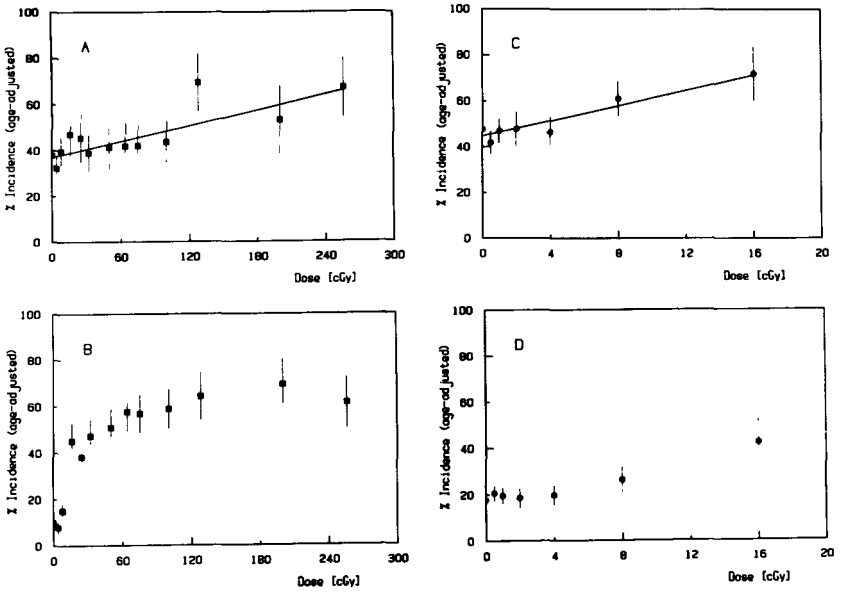

Fig. 1. Percentage incidence of solid tumors induced in mice by X rays (A) and fast neutrons (C). Plots B and D are for ovarian tumor induction after X-ray and neutron irradiation, respectively.

Mortality rates for specific causes of death were examined using a Weibull-type time dependence, and the relative risks at the various doses were calculated accordingly. This calculation indicated that the risk of death with ovarian tumors is already appreciably increased below 0.1 Gy for both neutrons and X rays. For other solid tumors the minimum doses of this experiment producing a significant increase of the risk are 8 cGy and 64 cGy, respectively.

These findings were consistent with the analysis of the final tumor age-adjusted incidence, which showed that for ovarian tumors the dose-response curve presents a steep rise starting between 5 and 10 cGy for both neutrons and X rays (Fig. 1). For other solid tumors, the incidence was significantly increased above that in the control, starting from the doses of 8 cGy and 128 cGy, respectively. This was also confirmed by the results of a statistical analysis, testing the existence of a positive trend of tumor incidence with the dose.

As an extension of our previous study of ovarian tumor induction, a new experimental series has been planned using appropriately designed lead shieldings to X-irradiate only one ovary per animal, in order to investigate the radiosensitivity of this organ under reduced hormonal unbalance.

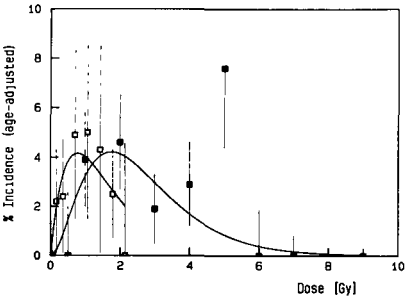

Fig. 2. Myeloid leukemia after whole-body exposure to 250 kVp X rays (■) and fission neutrons (□).

In parallel, the analysis of lymphoma and myeloid leukemia incidence data in about 3000 BC3F1 male mice irradiated at Casaccia with single acute doses of X rays and fission neutrons has shown some interesting aspects regarding the shape of the dose-effect relationships. For malignant lymphoma, which is expressed with a very high spontaneous incidence, the data are well described assuming for X rays a quadratic-dose induction model and for fission neutrons a linear model, corrected by exponential cell inactivation acting on both the spontaneous and the radia-

tion-induced components. The best fitting value for the inactivation probability per unit dose was 0.70±0.04 Gy^{-1} and 1.0±0.5 Gy^{-1} for X rays and fission neutrons, respectively. These values are in agreement with those expected from the hematopoietic cell survival. This agrees with the hypothesis that such cells are responsible for the lymphomas. As far as induction of myeloid leukemia by radiation is concerned, the BC3F1 mouse used in these experiments appears to be a suitable model system, as no myeloid leukemia was observed in 600 unirradiated controls. In irradiated $BC3F_1$ mice myeloid leukemia is a rare event, nevertheless, the dose-response curves are very similar in shape to those already reported for CBA/H and RF/Un mice. Also for this tumor, the induction appears to be linear for fission neutrons and quadratic for X rays, with an exponential correction for cell inactivation (Fig. 2).

We have also shown that liver tumors can be induced in mice with very different spontaneous incidences (CBA/Cne: 67%, BC3F1: 11%). Based on these findings, we have enlarged the analysis to include the influence of radiation quality, namely X rays and fission neutrons, on the induction of such tumors in BC3F1 mice. For both radiation qualities the final incidence appeared to increase with the dose in a broad dose range (0-1.43 Gy and 0-7 Gy for fission neutrons and X rays, respectively). A statistical method, developed by Peto et al., has indicated that the increase is significant not only in these dose ranges, but also in the lower dose intervals (0-0.36 Gy and 0-2 Gy for fission neutrons and X rays, respectively). The values of age-adjusted incidence as a function of dose have been well fitted using a linear model in the neutron dose range of 0 to 1.43 Gy. For X rays the fit quality is not very good, unless a threshold dose of 1 Gy is introduced.

Recently, a new experiment has been undertaken to study the carcinogenic effect of fractionated doses of fission neutrons in BC3F1 male mice. This study is of a special importance in the framework of radiation protection, as it allows the in-vivo investigation of the influence of dose fractionation on late somatic effects.

Complete observation of survival and late pathology was planned to be carried out on a population of about 2000 mice, irradiated with fractionated doses of fission neutrons produced by the RVS TAPIRO reactor of ENEA Casaccia, and followed until spontaneous death. Nine different mouse groups were given 5 equal daily dose fractions of 0.5 to 14.2 cGy, for total doses from 2.5 to 70 cGy, at a dose rate of 0.4 cGy/min. A similar fractionated dose irradiation was carried out using X rays, for total doses from 25 to 300 cGy.

By the end of 1989 almost all animals have come to death, and the analysis of survival and of the incidence of solid tumors, lymphomas and leukemias, as well as of other non-neoplastic diseases, observed at death, has been initiated.

2. Studies of in-vivo and in-vitro transformation per surviving cell

Considerable attention was given to the study of the mechanisms of tumor induction at the cellular level, in order to obtain an estimation of the risk of neoplastic transformation per cell in vivo. For this, a technique was set up consisting in the transplantation of irradiated and enzymatically dissociated cell suspensions of epithelial tissue into syngeneic hosts [5], and observation of the nodules which appear in the transplantation sites. This system allows the determination of the surviving fraction and the observation of long-term dysplastic and/or neoplastic lesions at the transplantation site.

This method was used for a quantitative in-vivo study of cell survival and risk of transformation in the harderian gland on CBA/Cne mice after X-ray irradiation. A fit of the multi-target single-hit model to the experimental survival data yielded for D_0 the value 1.83 Gy and for the extrapolation number the value 7.23. The dose-response curve for lesions observed in the grafted sites was compared with that for lesions observed in glands irradiated in situ. The risk of transformation per surviving cell was estimated both for dysplastic lesions and for tumors. The results approximated a dose-squared relationship in both cases, suggesting a common induction mechanism at the cellular level (Fig. 3).

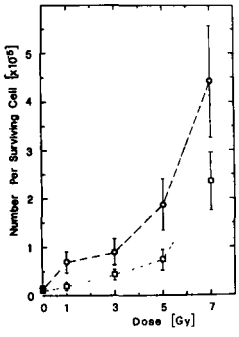

Fig. 3. Number of primary harderian gland tumors (□) and severe dysplasia (○) in transplantation nodules per surviving cell, after X rays.

The same experiment has shown that myeloid leukemia is present at all doses with a maximum at about 3 Gy and with a dose dependence which confirms the important results reported by Mole (1983), in particular, the high efficiency of

the CBA/Cne mouse as a sensitive experimental model system for studying radiation induced leukemia.

The transplantation technique used for studies of harderian gland tumors was also applied to the in-vivo study of hepatocyte survival and the risk of neoplastic transformation per surviving cell in the mouse. The survival curve of CBA/Cne mouse hepatocytes obtained in this way had a D_0 of 3.08 Gy and an extrapolation number of 1. The age-adjusted number of hepatocellular tumors induced by X rays (250 kVp, 1.5 mm Cu HVL) in two mouse strains, namely CBA/Cne and BC3Fl, was divided by the corresponding average number of surviving cells. The resulting ratios are presented in Fig. 4. The data for CBA/Cne mice are consistent with a linear-quadratic dose effect relationship, while for BC3Fl mice a simply quadratic expression, provides a better fit to the experimental points.

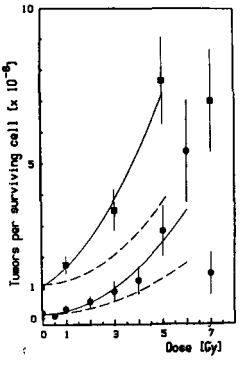

Fig. 4. Number of hepatocellular tumors per surviving cell as a function of X-ray doses for CBA/Cne (■) and BC3F1 (●) mice.

Recent results of the dose-rate influence on in-vitro neoplastic transformation have fostered further experimental work at our laboratory to compare the transforming effectiveness of equal doses delivered to C3H10T1/2 cells following either acute or fractionated irradiation protocols. The results of these experiments confirm that the neutron dose fractionation does not influence significantly the survival compared to acute irradiation. In addition, the dose-response curve for cell transformation is not markedly changed when passing from acute to fractionated doses, and the change, if any, goes towards a decreased effectiveness for the fractionated irradiation mode.

3. Late somatic effects of total lymphoid irradiation (TLI)

Late somatic effects of total lymphoid irradiation have been investigated in BC3F1 mice using a fractionated protocol (TLI). A similar protocol is utilized in medicine for the treatment of patients with lymphoma or which have to undergo organ transplantation. In particular, using a mouse population with a high natural lymphoma incidence, it was intended to investigate whether the expected depression of this tumor following irradiation is associated with the appearance of other tumor types or a life span shortening. A total X-ray dose of 34 Gy was distributed in 17 daily fractions. The results indicate the presence of a relevant incidence of malignant skin cancers, which appear to be the most likely cause of life shortening of the treated mice together with kidney degenerative disease (see Table).

Table. Survival and incidence of neoplastic and non-neoplastic diseases at spontaneous death in BC3F1 mice after TLI.

					Solid tumors					
	No of mice	*Mean survival time ± SD (days)*	*Nephro-sclerosis*	*Malignant lymphoma*[a]	*Lung*	*Liver*	*Skin*	*Soft tissues*	*Others*[b]	*Total*
Control	88	887 ± 189	7 (8)	43 (49)	5 (6)	12 (14)	1 (1)	4 (5)	4 (5)	26 (30)
Irradiated	68	673 ± 144*	26 (38)*	4 (6)	3 (4)	13 (19)	18 (26)*	5 (7)	6 (9)	45 (66)*

a FCC-lymphoma, mixed cell type.
b Adrenal, kidney, stomach, bone, and vascular tumors.
* $P<0.001$ in the Mann-Whitney U-test for comparison of survival times, and in the χ^2 test for comparison of frequencies.

In the framework of the research activities concerning the late effects of total lymphoid irradiation (TLI), we have also started the analysis of the data from one experiment in which the lymphatic tissue of BC3F1 mice was exposed to single acute X-ray doses (0.5 to 9 Gy). The preliminary results indicate a different shape of the dose-response relationships for the different tissues exposed. In particular, they show a bell-shaped relationship for malignant lymphoma, while, within the solid tumors observed, skin cancers are induced only at doses greater than 2 Gy. This might suggest the presence of a threshold dose below which the treatment with TLI could be used in therapy without appreciable risk of inducing skin cancers. Nevertheless, the presence of solid tumors and degenerative diseases of the kidney seems to play a role in causing life-span shortening, although it is difficult to ascertain the relative importance of each class of disease.

4. Other issues

A minor portion of the available time was spent to finalize some work already undertaken towards the end of the previous contractual term. This included the analysis of data relative to the study of radiation damage induced in the murine eye-lens by various radiation qualities, and further progress in the study of chromosomal aberrations produced in human lymphocites by radiation and/or other noxious agents. Part of the results indicate that the relative frequency of acentrics to dicentrics can be differently influenced by the type of treatment.

IV. Other research group(s) collaborating actively on this project [name(s) and address(es)]:

V. Publications:

1) Di Majo, V., Coppola, M., Rebessi, S., Bassani, B., Alati, T., Saran, A., Bangrazi, C., Covelli, V. Dose-response for harderian gland tumors in the CBA mouse. Third Sardinian International Meeting on Agents and Processes in Chemical Carcinogenesis, Cagliari, 1985.

2) Di Majo, V., Coppola, M., Rebessi, S., Bassani, B., Alati, T., Saran, A., Bangrazi, C., Covelli, V. Relazione dose-risposta per i tumori radioindotti nella ghiandola harderiana del topo CBA. Atti del Congresso Nazionale della Società Italiana di Radiobiologia (AIRB) e della Società Italiana per le Ricerche sulle Radiazioni (SIRR), pp. 95-96, Milano, 1985.

3) Bertoncello, G., Coppola, M., Staffa, A. Efficacia biologica di radiazioni ionizzanti per l'induzione di danno al cristallino del topo. Atti del Congresso Nazionale della AIRB e della SIRR, pp. 301-303, Milano, 1985.

4) Coppola, M., Vulpis, N., Bertoncello, G. Influenza del tipo di agente nocivo sulla frequenza relativa di aberrazioni cromosomiche nei linfociti umani. Atti del Congresso Nazionale della AIRB e della SIRR, pp. 81-83, Milano, 1985.

5) Di Majo, V., Coppola, M., Rebessi, S., Bassani, B., Alati, T., Saran, A., Bangrazi, C., Covelli, V. Dose-response relationship of radiation-induced harderian gland tumors and myeloid leukemia of the CBA/Cne mouse. JNCI 76, 955-966, 1986.

6) Di Majo, V., Coppola, M., Rebessi, S., Bassani, B., Alati, T., Saran, A., Bangrazi, C., Covelli, V. Radiation induced mouse liver neoplasms and hepatocyte survival. JNCI 77, 933-939, 1986.

7) Coppola, M., Vulpis, N., Bertoncello, G. Relative frequency of acentrics to dicentrics caused by radiation and by chemical action on human lymphocytes. Mutation Research 174, 75-78, 1986.

8) Di Majo, V., Coppola, M., Rebessi, S., Bassani, B., Alati, T., Saran, A., Bangrazi, C. , Covelli, V. Radiation hepatocyte survival and liver tumor induction in the mouse. Int. J. Radiat. Biol. 51, 749, 1987.

9) Coppola, M., Bertoncello, G. Neutron RBE at low doses: micronuclei formation in the murine eye-lens epithelium. Int. J. Radiat. Biol. 51, 914-915, 1987.

10) Di Majo, V., Coppola, M., Rebessi, S., Saran, A., Alati, T., Covelli, V. Radiation epithelial cell survival and tumor induction in the mouse. In: Proceedings of the 8th International Congress of Radiation Research, Edinburg (Fielden, E.M., Fowler, J.F., Hendry, J.H., Scott, D., eds.), vol. 1, p. 193, Taylor & Francis, 1987.

11) Covelli, V., Coppola, M., Di Majo, V., Bassani, B., Rebessi, S. Dose-response curves for carcinogenesis at low doses of neutrons. In: Proceedings of the 8th International Congress of Radiation Research, Edinburg (Fielden, E.M., Fowler, J.F., Hendry, J.H., Scott, D., eds.), vol. 1, p. 208, Taylor & Francis, 1987.

12) Covelli, V., Coppola, M., Di Majo, V., Rebessi, S., Bassani, B. Relazione dose-effetto per l'induzione di tumori dell'ovaio del topo alle basse dosi. In: Abstracts of IV Convegno Nazionale SIRR, S. Teresa, Lerici, p. 29, 1987

13) Di Majo, V., Coppola, M., Rebessi, S., Covelli, V. Efficacia biologica relativa per effetti somatici tardivi nel topo. In: Abstracts of IV Convegno Nazionale SIRR, S. Teresa, Lerici, p. 30, 1987.

14) Covelli, V., Coppola, M., Di Majo, V. Rischio di trasformazione neoplastica a livello cellulare. In: Radiazioni e Tumori, Atti VIII Congresso Nazionale AIRM, pp. 55-66, Ischia, 1989.

15) Coppola, M. Aspetti radiobiologici rilevanti ai fini della radioprotezione. Sicurezza e Protezione 15, 78-92, 1987.

16) Coppola, M., Covelli, V., Di Majo, V., Rebessi, S. Study of dose-response relationships for late somatic effects of low neutron doses. In: Neutron Dosimetry, Proceedings of the Sixth Symposium on Neutron Dosimetry (H. Schraube, G. Burger, J. Booz, eds.). Radiation Protection Dosimetry 23, nos 1-4, 69-72, 1988.

17) Covelli, V., Coppola, M., Di Majo, V., Rebessi, S., Bassani, B. Tumor induction and life shortening in BC3F1 female mice at low doses of fast neutrons and X rays. Radiat. Res. 113, 362-374, 1988.

18) Di Majo, V., Covelli, V., Coppola, M., Rebessi, S., Bangrazi, C., Bassani, B. Long-term effects in mice after Total Lymphoid Irradiation. 79th Annual Meeting of the American Association for Cancer Research. Cancer Res, New Orleans, Louisiana,1988.

19) Covelli, V., Di Majo, V., Coppola, M., Rebessi, S., Bangrazi, C., Doria, G. Late somatic effecs in mice after total lymphoid irradiation (TLI). Radiat. Res. 116, 503-510, 1988.

20) Di Majo, V., Covelli, V., Coppola, M., Rebessi, S., Bangrazi, C. Depression of malignant lymphoma in BC3F1/Cne mice following Total Lymphoid Irradiation (TLI). International Meeting on physical, biological and clinical aspects of total body irradiation, Den Haag, The Netherlands, 1988.

21) Covelli, V., Coppola, M., Di Majo, V. Current studies on experimental radiation carcinogenesis. In: Radiation Protection: Advances in Yugoslavia and Italy. Proceedings of the II Yugoslav-Italian Symposium, Udine, Italy, 1988.

22) Covelli, V., Di Majo, V., Coppola, M., Rebessi, S. Development of malignancy in mice after Total Lymphoid Irradiation (TLI). European Society for Radiation Biology, 21st Annual Meeting, Tel Aviv, Israel, 1988.

23) Covelli, V., Coppola, M., Di Majo, V., Rebessi, S. Experimental models for radiation carcinogenesis. In: Low dose radiation - biological bases of risk assessment. 14th L.H. Gray Conference, Oxford, U.K., 1988.

24) Covelli, V., Di Majo, V., Coppola, M., Rebessi, S. The shape of the dose-response relationship for myeloid leukemia and malignant lymphoma in $BC3F_1$ mice. Radiat. Res. 119, 553-561, 1989.

25) Coppola, M., Covelli, V., Di Majo, V., Rebessi, S. Induction of myeloid leukemia and malignant lymphoma by X rays and fission neutrons in $BC3F_1$ mice. E.S.R.B. 22nd Annual Meeting, Brussels, Sept. 1989.

26) Rebessi, S., Coppola, M., Covelli, V., Di Majo, V. Induzione di tumori epatici in topi $BC3F_1$ da radiazioni di diversa qualità. V Convegno Nazionale S.I.R.R., Roma, Ottobre 1989.

27) Coppola, M., Covelli, V., Di Majo, V., Rebessi, S. Leucemia mieloide e linfomi maligni in topi $BC3F_1$ irraggiati con raggi X e neutroni di fissione. V Convegno Nazionale S.I.R.R., Roma, Ottobre 1989.

28) Saran, A., Pazzaglia, S., Coppola, M., Rebessi, S., Di Majo, V., Garavini, M., Covelli, V. Trasformazione neoplastica di cellule C3H10T1/2 da raggi X e neutroni di fissione. V Convegno Nazionale S.I.R.R., Roma, Ottobre 1989.

RADIATION PROTECTION PROGRAMME
Final Report

Contractor:

Istituto Nazionale di
Fisica Nucleare
Sede Centrale INFN
Casella Postale 56
I-00044 Frascati / Roma

Contract no.: BI6-A-193-I

Head(s) of research team(s) [name(s) and address(es)]:

Prof. P. Dalpiaz
Laboratori Nazionali dell'
INFN di Legnaro
Via Romea 4
I-35020 Legnaro (Padova)

Dr. P. Colautti
Laboratori Nazionali dell'
INFN di Legnaro
Via Romea 4
I-35020 Legnaro (Padova)

Telephone number: 049/641.200

Title of the research contract:

Stochastic variables in the energy deposit and their meaning in the hazard of neutrons.

List of projects:

1. Stochastic variables in the energy deposit and their meaning in the hazard of neutrons.

Title of the project no.: BI6-A-193-I

Stochastic variables in the energy deposit and their meaning in the hazard of neutrons.

Head(s) of project:

Dr. P. Colautti

Scientific staff:

P. Colautti
G. Talpo
G. Torni elli

I. Objectives of the project:

The project concerns with the study of the stochastic variable "y" (lineal energy) at simulated diameter less than 1 μm.
Objective of the project is to investigate the possibility to manufacture a spherical tissue-equivalent proportional counter able to work properly at pressures as low as possible in order to simulate tissue diameters less than 1 μm.

II. Objectives for the reporting period:

The experimenta set-up to measure the avalanche characteristics of a cylindrical TEPC at low pressure had to be assembled and first measurements had to be done.

III. Progress achieved:

INTRODUCTION

From the beginning microdosimetry has dealt with measurements of absorbed energy in volumes as small as possible. The extension of experimental microdosimetry into the nanometer region constitutes the major remaining challenge.

In the ordinary use of a tissue-equivalent proportional counter (TEPC) one can observe that decreasing the gas counter pressure the resolution of the calibration α-peak worsenes. Different causes produce this effect: an increase of the deposited energy fluctuation due to the small quantity of released energy, an increase of the relative variance of the avalanche and eventually an enlargment of the avalanche region which makes TEPC to work in condition of no-proportionality. This last phenomenon destroys the physical meaning of the experimental spectra then its quantitative description is introductory to the discussion about the lowest tissue-equivalent diameter which a TEPC is able to simulate.

METHODOLOGY

The basic idea is to send a collimated ion beam into a cylindrical detector along an equipotential straight line. The changes in the pulse height spectra, which are collected at different radial distances from the anode, will point out the entrance of the beam into the avalanche region, supposing that the beam cross section is ideally zero and no ion recombination processes take place.

The gain G of a cylindrical gas proportional counter is indeed given by the general expression

$$\ln G = \int_{r_a}^{r_c} \alpha dr$$

where α is the Townsend's first ionization coefficient, r_a and r_c are the anode and cathode radius respectively. If the sensitive volume of the detector is divisible in a drift and in an avalanche region then the gain of a multiplication process can be separated into two integrals and so:

$$\ln G = \int_{r_a}^{r_1} \alpha dr$$

where r_1 is the limit between the drift region in which $\alpha \cong 0$ and the avalanche region. Because the pulse height is proportional to the product of the energy released in the sensitive volume by gain, it should remain constant from r_c to r_1 by moving an ideal parallel-to-anode beam from the cathode to the detector axis and then it should decrease monotonically.

A cylindrical TEPC was obtained drilling a cylindrical cavity in a block of A-150 plastic, the two openings were closed by two disks of *makor* (a machinable glass ceramic made by CORNING -USA-) which carry anode wire and guard tubes. Two slits of 1 mm in thickness run parallely from the anode to the cathode, they allow the ion beam to enter the cylinder, cross the detector, cross a collimator with a 1 mm hole and eventually to impinge the solid state detector. Only the proportional counter pulses in coincidence with the solid state detector pulses are collected, this assures that the pulses come from particles traversing longitudinally the cylindrical detector at radial distances determined with the precision of ± 0.5 mm (figure 1).

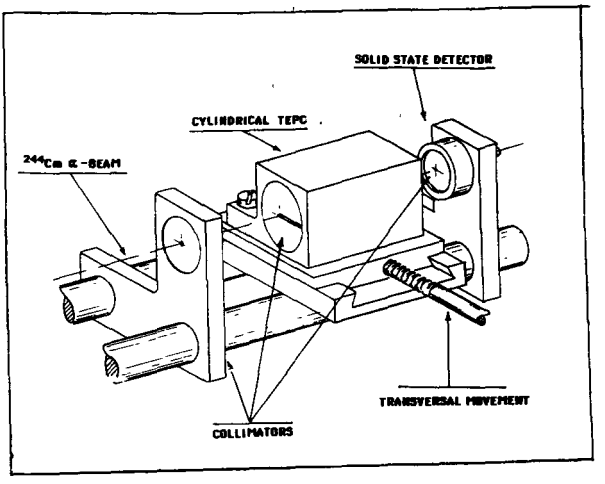

Figure 1

Guard-tubes of 1.5 mm in diameter stick out from *makor* disks for 10 mm internally into the cylinder and then they define a cylindrical TEPC 25 mm long and 20.4 mm in diameter. Two sets of measurements were performed, with a 10 μm and with a 50 μm gold-plated tungsten wire as anode respectively.

All the apparatus was put in a vacuum chamber which was filled with the propane-based tissue-equivalent mixture. Lengths from 0.1 to 0.4 μm were simulated by varying the gas pressure from 227 to 909 Pa; the pressure was controlled with an analogical absolute meter (Wallace and Tiernan), which has an accuracy of 8 Pa, and a digital absolute gauge (MKS Baratron 222 B), which has an accuracy better than 2 Pa. In all the measurements the gas pressure constancy was better than 1%.

As ion probe a ^{244}Cm α-source has been first used. In this arrangement there was no window between the source and the detector, the α-particle energy at the entrance of the sensitive volume was decreased by increasing the gas pressure; this decrease ranged from 9.9 to 39.8 KeV that implied a dE/dx changed of less than 1%.

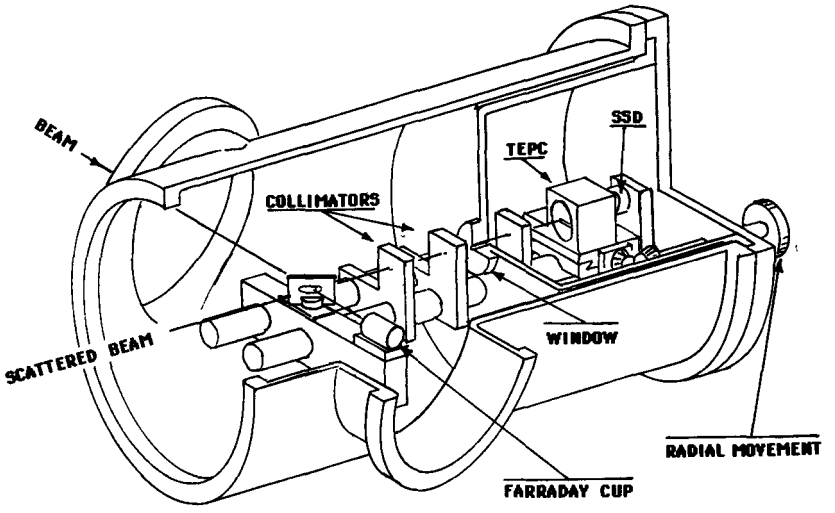

Figure 2

When a light ion beam accelerated by the the Legnaro Laboratories' 7MV-Van der Graaff is used, the primary beam is scattered to 90 degree from a thin gold layer of 150 mgm/cm^2 in order to decrease the particles flux and then enters the measure chamber through an alluminated mylar window of 1.3 μgm/cm^2 of thickness, see figure 2.

RESULTS

α MEASUREMENTS

Pulse height spectra were collected for simulated lengths of 0.4, 0.3, 0.2, 0.1 μm and for different radial positions of the α-beam. The peak positions have been plotted versus the distance R of the beam from the anode. The peak position, that is the most probable value of the pulse height distribution, seems indeed to be the meaningful parameter in this experiment. In figure 3a the results were obtained with an anode wire of 10 μm; in figure 3b the same measurements have been repeated with a 50 μm wire.

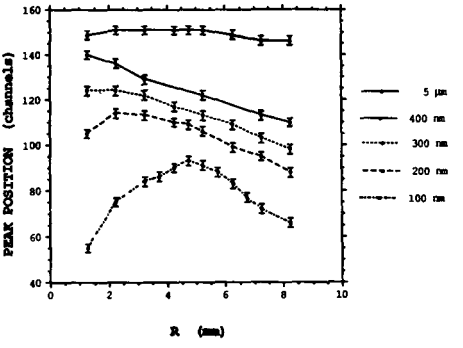

Figure 3a

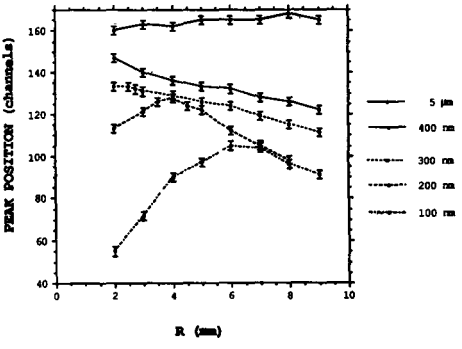

Figure 3b

In both sets of measurements the anode was at positive voltage of 400 volts and the cathode earthed. The amplification of the electronic chain was constant and controlled with a precision pulser BNC Model PB-4. The data at the simulated length of 5 μm were collected to check the thickness uniformity of the sensitive volume, the values were properly reduced in order to allow for an easy reading of the figures. For every experimental point several trials were performed to reduce the statistical uncertainty of the peak position to less than 2 channels.

The curves in figure 3a-b show maxima at small simulated lengths and monotonical decreases at bigger lengths, that is at higher pressures, as the beam approaches the counter wall. This decrease is due to the δ-ray escape on the wall.We came to this conclusion by comparison of the experimental data with calculated absorbed energy spectra of 5.8 MeV α-particles in water vapor cylinders of the same lengths as those ones simulated in the measurements and of radius varying from 25 to150 nm. The reduction of the radius simulates the physical situation of the α-beam approaching the TEPC wall.

Because of this δ-ray effect the entrance of the α-beam in the avalanche region, as it approaches the anode, pruduces a maximum in the peak-position to radial-distance plots. The maximum is clearly visible in the 200 nm and 100 nm curves.

The experimental results do not show any plateau which can easily be interpreted as a drift region; nevertheless the monotonical decrease of the pulse-height peak when the α-beam approaches the detector wall is consistent with a δ-ray escape, as can be deduced from the calculations, and it also points out a detector region where the multiplication effects are not relevant. On the other hand, positions are visible where the electrical signal increases as the α-beam departs from the anode, showing that they are inside the avalanche region. The maxima point out only these two conflicting effects. However the corresponding values of the reduced electrical field are closed to each other thus demonstrating that they are univocally related to the drift-to-avalanche limit.

However this kind of probe cannot determine with precision the equipotential line at which the avalanche starts because of the high yield of long-range δ-rays. At gas pressures as low as necessary to simulate less than

1 μm lengths, the δ-rays cloud makes the probe size larger than that defined by the collimators.

These experimental findings suggest the use of slow ion probes for measuring the avalanche limit, in order to have a very short-range δ-ray production and so maintain the real size of the probe inside the collimator opening.

^{15}N MEASUREMENTS

A ^{15}N beam of 6.42 MeV of energy has been used in a first run of measurements to produce the same set of data but with low high energy δ-ray yield. The TEPC was equipped with a 10 μm wire.
Just behind the mylar window the scattered nitrogen beam has got 5.15±0.35 MeV of energy and then it has to cross 85 mm of tissue-equivalent gas before entering the TEPC sensitive volume. Depending on the gas pressure the ion energy at the entrance of the TEPC changes from 4.77 to 3.61 MeV as we change the simulated length from 100 to 400 nanometers, the energy released in the detector changes consequently from 111.7±8.0 KeV to 453±14 KeV.

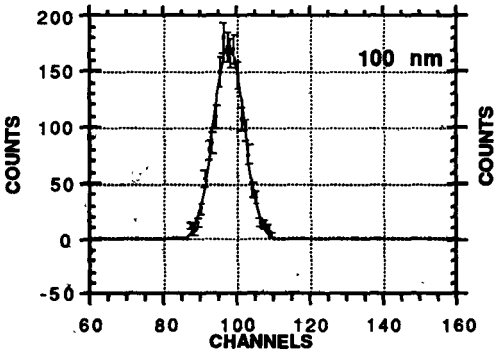

Figure 4a

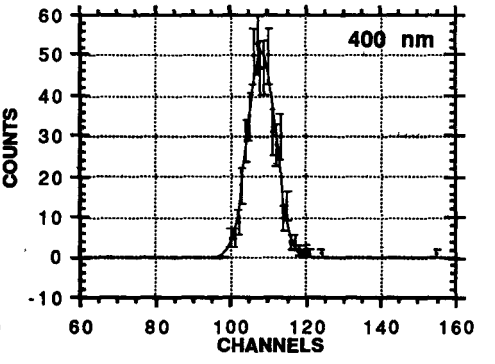

Figure 4b

In figure 4a-b two experimental spectra are showed. Data have been collected at 100 nm and 400 nm out of the avalanche region. In both the cases a gaussian curve fits well the experimental data. Since we can disregard energy escape the absolute TEPC gain can be evaluated by taking an average W-value of 35 eV.

Figure 5a shows the detector gain with respect to R, which is the beam distance from th anode. Now the plateau of the drift region is clearly visible and in consequence its limit r_1. Only at 100 nm of simulation a small δ-ray escape seems to be still present. In figure 5b the data are plotted versus the reduced electrical field.

Another finding of the figures 5a-b is higher gains at lower pressures, this depends both on a bigger avalanche region and on an increase of α-value at low pressures. Remembering that the Townsend's first ionisation coefficient is:

$$\alpha = \frac{1 \cdot dG}{G \cdot dr}$$

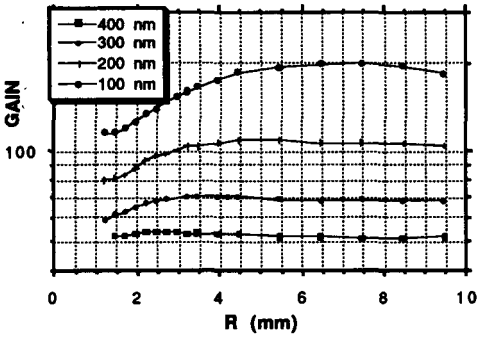

Figure 5a

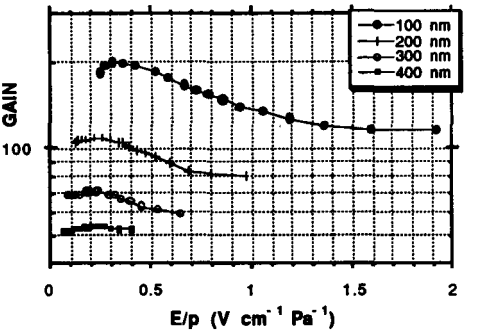

Figure 5b

the figure 6 shows the experimental reduced α-coefficients (α/p) versus the reduced electrical field (E/p) for different simulated diameters namely for different pressures. Two findings are clear: a big increase of the reduced

ionisation coefficient at low pressure and that all the curves reach a maximum and then decrease.

P. Segur et al. (*Microscopic Calculations of the Gas Gain in Cylindrical Proportional Counters* in Rad.Prot.Dos., 29, 23-30, 1989) found similar findings in their Monte Carlo calculations which they explained to be related to non-equilibrium conditions due to low pressures and very thin anode wires.

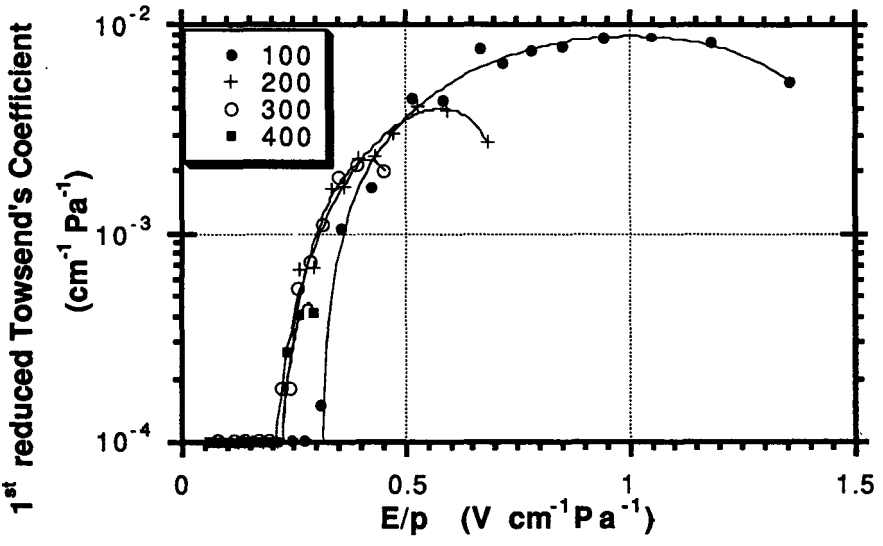

Figure 6

CONCLUSIONS

The research project concerned the study of the stochastic variable "y" (lineal energy) at simulated diameters less than 1 μm. The first part of the project aimed to investigate the gain and resolution characteristics of a

TEPC at very low pressures in order to determine the minimum simulable diameter. The second part of the project aimed to measure calibrated neutron spectra in order to study the variations in the y-spectra at simulated diameters less than 1 μm.

The complex behaviour of a TEPC when low pressure and thin wires are used forced us to dedicate much effort in the first part of the project which cannot be considered concluded yet. If not all the aimes of the research have been reached it depends on the very interesting and original results which have been obtained in the TEPC operating at low pressure and which deserve further studies.

IV. Other research group(s) collaborating actively on this project [name(s) and address(es)]:

Dr. G. Leuthold and Dr. H. Schraube
Institut für Strahlenschutz GSF - München - FRG

Dr. D. E. Watt
Physics Department of the St. Andrews University - U.K.

V. Publications:

P. Colautti, G. Leuthold, G. Talpo, G. Tornielli
" Parallel-to-Anode Ion Probe in a Cylindrical TEPC at Simulated Lenghts Less than 1 μm "

Radiation Protection Dosimetry, to be published 1990.

RADIATION PROTECTION PROGRAMME
Final Report

Contractor:

Université de Limoges
Allée André Maurois
F-87060 Limoges Cédex

Contract no.: BI6-A-192-F

Head(s) of research team(s) [name(s) and address(es)]:

Dr. J.L. Decossas
L.E.P.O.F.I.
123, rue Albert Thomas
F-87060 Limoges Cédex

Dr. J.C. Vareille
L.E.P.O.F.I.
123, rue Albert Thomas
F-87060 Limoges Cédex

Telephone number: 55.45.74.51/55

Title of the research contract:

Study and realization of a high performance personal neutron dosemeter.

List of projects:

1. Study and realization of a high performance personal neutron dosemeter.

Title of the project no.: B 16 - A - 192 F

Study and realization of a high performance personal neutron dosemeter

Head(s) of project:

Dr. J.L. DECOSSAS
Dr. J.C. VAREILLE

Scientific staff:

Drs.DECOSSAS, MAKOVICKA, VAREILLE

I. Objectives of the project:

Calculation of dosemeter responses for neutrons, realization of a composite radiator detector system based on CR 39 and experimental test of the developed dosemeter

II. Objectives for the reporting period:

Cf. ci-dessus

III. Progress achieved:

Le système dont traite cette étude est destiné à réaliser la détection des neutrons thermiques intrermédiaires et rapides dans le cadre de la radioprotection des personnels. Nous présentons les différentes étapes de sa conception et concluons par une ouverture vers d'autres systèmes, à base de capteur électronique, qui tirent parti des études menées dans le cadre de ce contrat.

I - METHODOLOGIE - PRINCIPE DU DISPOSITIF

1 - Constitution

Le détecteur solide de traces utilisé est du CR 39 qui a montré au cours de ces dernières années la meilleure sensibilité aux particules chargées. En général, il s'agit de CR 39 fourni par Pershore, mais des comparaisons ont été également menées avec un DST de la même famille fourni par ESSILOR et noté ici CAD.

La structure de base du dosimètre est décrite sur la figure 1. Elle repose sur la méthode différentielle qui consiste à irradier deux plages d'un détecteur, l'une précédée d'un convertisseur (neutron-particules chargées), l'autre non et à retrancher les réponses. Nous verrons par la suite l'intérêt de cette méthode tant au niveau du bruit de fond que de la contribution des atomes lourds de recul. Le convertisseur est constitué de polyéthylène implanté au bore 10, mettant à profit :

- la réaction (n, p) pour les neutrons rapides, elle génère un flux de protons enregistrés par le DST
- la réaction ^{10}B (n, α) ^{7}Li pour les neutrons thermiques et intermédiaires (pour ces derniers intervention de l'albédo). Elle conduit à un flux de particules α (énergie égale à 1,47 MeV pour 94 % d'entre elles) et des ions ^{7}Li d'énergie voisine de 0,9 MeV ; les émissions dans les deux cas pouvant être supposées isotropes.

Nous allons voir que les études théorique et expérimentale permettent de réaliser un convertisseur dont l'efficacité effective est sensiblement constante quand l'énergie des neutrons varie.

2 - Traitement des DST

Notre objectif était de maîtriser pleinement les convertisseurs utilisés, en

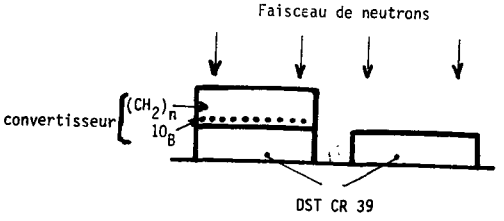

Figure 1 : Schéma de principe du dosimètre

particulier de déterminer précisément les flux de particules émises ; il nous fallait donc prendre en considération toutes les traces révélables et c'est pourquoi la révélation chimique simple a été utilisée : NaOH 6,25 N, 60° C.

Après révélation les détecteurs sont lus au microscope optique soit manuellement (pour toutes les vérifications des calculs) soit par un système de traitement automatique d'image.

II - RESULTATS

A - Etude sous neutrons rapides

1 - Etude théorique du convertisseur

Pour déterminer les caractéristiques du flux de protons issus du convertisseur $(CH_2)_n$ un programme de calcul a été élaboré qui fait appel à la méthode de Monte-Carlo. Notre travail repose sur les lois, données et conditions suivantes :

- lois classiques de la diffusion élastique
- les sections efficaces d'interactions "neutron - H/C/O/N/" fournies par le Centre de Compilation des Données Neutroniques du Commissariat à l'Energie Atomique (CEA - France)
- les pertes d'énergie des particules chargées d'après Steward (thèse Berkeley, 1968)
- une épaisseur de convertisseur très faible devant ses dimensions transversales (surface 1 cm^2).

Une série de 6 programmes PNEMORG (Passage de Neutrons à Travers des Milieux ORGaniques) a été mise au point. Dans ces conditions les distributions énergétique et angulaire des protons issus du convertisseur sont parfaitement connues comme l'illustrent les figures 2, 3, 4, dans le cas de faisceaux monoénergétiques ou

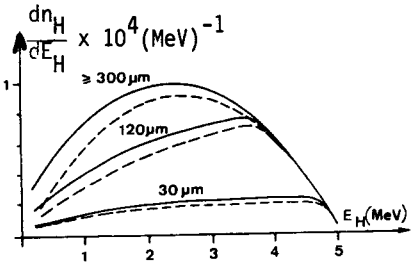

Fig. 2 : Spectres énergétiques dH_H/dE_H des protons générés par des neutrons (E_n = 5 MeV) d'incidence normale dans un convertisseur d'épaisseur variable
Pour un neutron incident : --------- méthode Monte Carlo
_____ méthode analytique

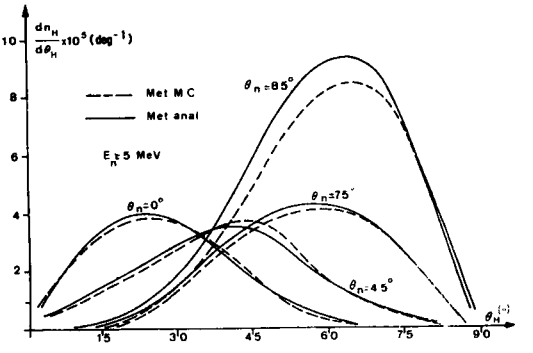

Fig. 3 : Spectres angulaires des protons émis pour quatre valeurs d'incidence neutronique θ_n (E_n=5 MeV)
------- méthode Monte Carlo
_____ méthode analytique

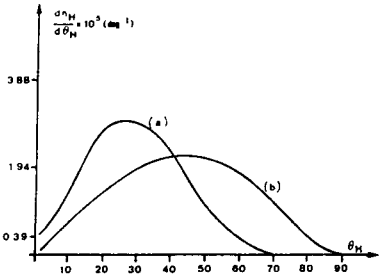

Fig. 4 : Spectre angulaire de protons émis sous irradiation d'une source d'Am-Be
a - incidence normale b - incidence aléatoire

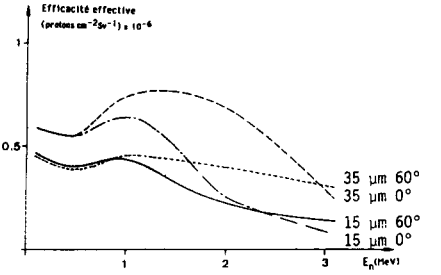

Fig. 5 : Efficacité dosimétrique effective pour des convertisseurs de 15 à 35 µm de $(CH_2)_n$ pour des incidences θ = 0° et 60° entre 0.2 et 3 MeV

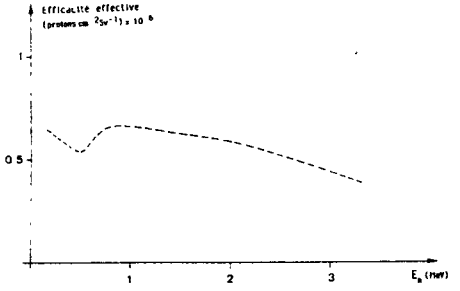

Fig. 6 : Efficacité dosimétrique effective pour un convertisseur de 35 µm $(CH_2)_n$ sous incidence isotrope des neutrons d'énergie 0,2 - 3 MeV

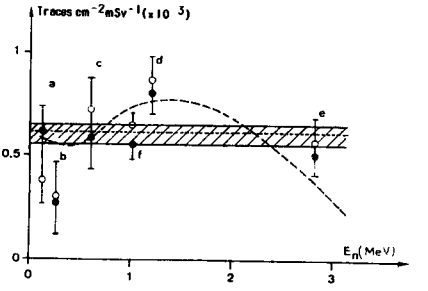

Fig. 7 : Résultats obtenus par la méthode différentielle (traces cm^{-2} mSv^{-1}) comparés à l'efficacité effective calculée du convertisseur (-----) de 35 µm
Points expérimentaux O CR 39 (Pershore) - ● CAD ESSILOR

polyénergétiques, d'incidence normale ou isotrope.

Il faut souligner qu'il s'agit là d'une somme de données utilisables quelle que soit la nature du détecteur utilisé après le convertisseur.

2 - Efficacité dosimétrique du dispositif $(CH_2)_n$ - CR 39

L'étude théorique de la sensibilité d'un dosimètre suppose d'une part que l'on applique les méthodes précédentes de calcul à l'épaisseur de détecteur éliminée par l'attaque chimique, d'autre part que l'on introduise pour les protons provenant du détecteur et du convertisseur, les caractéristiques du développement chimique et de l'observation au microscope optique, de façon à déterminer le nombre de protons enregistrés. Enfin, le calcul de la sensibilité dosimétrique implique l'étude de la variation du facteur de conversion d'équivalent de dose en fonction de l'énergie et de l'angle d'incidence des neutrons. Les valeurs retenues pour notre étude sont celles recommandées par l'ICRU 39. En ce qui concerne les incidences obliques ou isotrope nous avons déduit l'équivalent de dose, à 1 cm de profondeur, dans un fantôme ICRU, des résultats de CHEN et CHILTON (Radiation Research, 78, 335-370 (1977)).

Dans ces conditions, nous avons pu calculer dans différentes situations l'influence de l'épaisseur du convertisseur, de l'énergie et de l'angle d'incidence des neutrons comme l'illustrent les figures 5 et 6. On constate que l'épaisseur du convertisseur joue de façon considérable sur la dépendance énergétique de l'efficacité alors que la dépendance angulaire est plus faible. On montre que sous irradiation isotrope, dans le domaine d'énergie 0,2 MeV - 3 MeV, l'épaisseur optimale de polyéthylène est de 35 µm dans ce cas où les caractéristiques de détection du CR 39 sont prises en compte.

3 - Contribution des atomes lourds de recul

Cette contribution apparaît facilement si l'on compare les valeurs calculées et mesurées du nombre de protons enregistrés dans un DST CR 39 placé dans un flux de neutrons d'incidence normale, sans convertisseur. Il n'y a alors à prendre en compte que les protons générés dans le DST. Les résultats sont résumés dans le tableau n° 1.Vers les faibles valeurs d'énergie des neutrons, on constate que la valeur calculée N est supérieure à celle expérimentale N_e, ce qui s'explique par l'existence d'un seuil énergétique d'enregistrement des protons par le CR 39. Par contre au-delà de 0,5 MeV les valeurs expérimentales sont supérieures à N ce que nous avons expliqué et vérifié par

la contribution des atomes de recul (carbone et oxygène). A partir des données sur la diffusion élastique des carbone et oxygène sous faisceaux de neutrons, et en introduisant les limitations expérimentales de détection de ces ions par le CR 39 (énergie limite et angle limite d'enregistrement) nous avons mis au point un programme de calcul qui donne la contribution des atomes lourds de recul.

E_n (MeV)	0,13	0,2	0,5	0,57	1	1,5	2	2,8	3,4
N x 10^7	520	650	640	650	300	630	470	200	130
N_e x 10^7	340	380	870	820	780	1360	1050	850	1580

Tableau n° 1 : Comparaison entre le nombre N calculé de protons générés et enregistrables dans le CR 39 et le nombre N_e de traces obtenues

L'expérience confirme avec une bonne approximation ces calculs, comme le montre le tableau n° 2.

Energie Mev	0,57	1	1,5	2	2,8	3,5
Nombre de traces de C x 10^7	28	210	362	310	520	639
Nombre de traces d'O x 10^7	0	246	141	120	120	299
Nombre de traces de protons x 10^7	650	300	630	470	200	120
Nombre total de traces calculé	678	756	1133	900	843	1068
Nombre expérimental	820	780	1360	1050	850	1580

Tableau n° 2 : Irradiation par des neutrons d'incidence normale à différentes énergies
Les nombres donnés sont rapportés à un neutron.

En conclusion, dans la réponse d'un DST inclus dans un dosimètre apparaissent les traces des protons issus du convertisseur et de la couche de CR 39 enlevée lors de la révélation, mais aussi celles des atomes de recul carbone, oxygène générés dans la couche déjà citée. Les atomes lourds de recul créés dans le convertisseur ne contribuent pas à la réponse finale car ils possèdent une énergie trop faible pour émerger du convertisseur et être enregistrés.

4 - Contrôle expérimental des résulats acquis

Dans certains cas afin de nous affranchir de la contribution propre du détecteur à la réponse totale, et partiellement des perturbations introduites par le bruit de fond du CR 39, nous avons utilisé la méthode différentielle telle qu'elle a été décrite au paragraphe I. Elle permet d'accéder aux traces enregistrées dues aux protons issus du convertisseur seul. C'est ce nombre que nous avons calculé systématiquement en introduisant la limitation angulaire du CR 39 :

$$\sin \theta_L = 0{\cdot}85 \exp (- 0.236\, E_H)$$

où E_H est l'énergie du proton à détecter.

a - Efficacité effective en fonction de l'énergie

La figure 7 donne l'efficacité effective E_e en fonction de l'énergie, les résultats théoriques sous forme de courbe d'une part, et d'autre part, les différents points expérimentaux dans le cas d'une incidence normale. L'épaisseur du convertisseur retenue est celle de 35 µm qui, dans nos conditions, assure la meilleure indépendance de E_e en fonction de l'énergie. On constate une assez bonne concordance entre les calculs et les mesures ; l'écart étant plus important aux faibles énergies pour lesquelles une amélioration pourrait être obtenue avec un temps de révélation mieux adapté.

Il faut souligner sur ces résultats la comparaison à laquelle nous nous sommes livrés entre deux types de détecteur CR 39 et CAD. Leurs réponses sont en bonne concordance bien qu'il ait été nécessaire, pour réduire son bruit de fond, de procéder à une attaque chimique préliminaire sur le CAD (1 h dans un mélange 60 % éthanol 40° C NaOH 6,25 N à 70° C).

b - E_e en fonction de l'angle d'incidence θ_n des neutrons

Ce problème est important car la radioprotection des personnels a à prendre en compte des situations avec des incidences neutroniques variables. La courbe de la figure 8 donne l'évolution de E_e en fonction de θ_n pour des neutrons d'énergie 3 MeV, dans le cas du convertisseur d'épaisseur 35 µm. A partir de ces résultats on a pu simuler la réponse à une irradiation isotrope pour obtenir

$$E_{e_i} = 357 \text{ traces} \pm 64 \text{ traces cm}^{-2}$$

alors que les calculs conduisent à 400 traces cm^{-2}.

c - Influence de l'épaisseur du convertisseur

Pour l'étudier on utilise la réponse totale du DST, sans appliquer la méthode différentielle. On obtient les courbes de la figure 9, tracées pour différents θ_n sur

lesquelles les flèches représentent les valeurs calculées. Une concordance satisfaisante existe là aussi.

d - Spectres énergétiques des protons issus du convertisseur

Grâce au dispositif électronique qui est cité dans la suite, nous avons pu vérifier les spectres déterminés par les programmes PNEMORG. L'allure des spectres de la figure 10 est à rapprocher de celle des spectres de la figure 2.

5 - Tests dans différents champs de neutrons du dispositif

La méthode de comptage par système automatique a été appliquée à des tests systématiques du dispositif avec utilisation de la méthode différentielle. Un exemple de résultats est donné figure 11 desquels on peut tirer les valeurs du tableau n° 3 qui présente une comparaison avec les valeurs calculées.

Epaisseur de polyéthylène	20	35	150
Efficacité effective théorique (6) (protons/cm^2/mSv)	222	360	1230
Efficacité effective expérimentale (protons/cm^2/mSv)	178	357,5	1357

Tableau n° 3 : Efficacités théoriques et expérimentales des dosimètres pour différentes épaisseurs de polyéthylène, E_n = 3,3 MeV

En conclusion, on met en évidence, avec les neutrons rapides, une bonne concordance entre les mesures et calculs effectués sur les convertisseurs utilisés avec des détecteurs solides de traces. Bien sûr, dans les résultats expérimentaux on relève la contrainte du bruit de fond qui limite la mesure aux faibles équivalents de dose ; ce phénomène est d'autant plus délicat qu'une attaque chimique simple est utilisée qui conduit à des traces de protons de faibles dimensions.

B - Etude sous neutrons thermiques

Comme cela a déjà été indiqué le convertisseur est réalisé par implantation de bore 10 dans du polyèthylène. Cette opération s'effectue sur l'accélérateur d'ions HVEE 400 kV du laboratoire. Pour assurer une faible profondeur d'implantation (réduction de l'absorption des ions émis) l'énergie des ions bore a été choisie égale à 50 keV

(pénétration de 0,3 μm). Le nombre d'atomes implantés doit conduire à un nombre d'ions α et Li entrainant une densité de traces révélées au voisinage de 500 traces cm^{-2} mSv^{-1} si l'on désire assurer la même efficacité que celle obtenue pour les neutrons rapides. Dans nos calculs, la limitation angulaire θ_L pour l'enregistrement des particules α et des ions Li a été prise à 75°, compte-tenu du mode de révélation chimique. Dans ces conditions, la densité d'implantation devrait se situer à 1,6 10^{15} atomes de bore cm^{-2}. Nous avons testé plusieurs convertisseurs dont les densités d'implantation varient de 10^{14} à 2 10^{15} atomes de bore cm^{-2}.

Les résultats obtenus sur deux sites [(Harwell U.K.) et Cadarache (France)] avec deux types de convertisseur implanté (métal ou polyéhtylène) sont présentés sur la figure 12.

III - DISCUSSION - CONCLUSION

Les calculs effectués sur un convertisseur en polyéthylène bombardé par des neutrons rapides ont permis de connaître les spectres énergétiques et angulaires des protons émis de façon à optimiser ses caractéristiques. Ces données sont disponibles quel que soit le type du détecteur utilisé. Nous les avons exploitées dans ce contrat en utilisant un détecteur CR 39 qui possède des limitations d'enregistrement énergétique et angulaire. En injectant ces dernières dans nos calculs, on arrive à déterminer les sensibilités dosimétriques (nombre de traces cm^{-2} mSv^{-1}) dont la vérification expérimentale a été menée à bien avec un accord satisfaisant.

Pour les neutrons thermiques et intermédiaires un convertisseur implanté au bore 10 a été calculé et testé de façon à donner une sensibilité dosimétrique voisine de celle utilisée aux neutrons rapides. Cela permet, pour obtenir l'équivalent de dose dans un champ neutronique, de n'effectuer qu'un comptage de traces puisque le facteur de conversion d'équivalent de dose a été pris en compte dans l'optimisation des caractéristiques du convertisseur. Par contre, il faut souligner que la révélation chimique des DST, qui a l'avantage de permettre une bonne vérification des valeurs calculées quand elle s'accompagne de comptages statistiques manuels est délicate à exploiter en routine avec un traitement d'images. En effet, les traces (en révélation chimique simple) sont de dimensions faibles et un bruit de fond existe qui introduit des écarts considérables. L'usage que nous avons fait de la méthode différentielle est apparu intéressant dans le cadre d'une étude de base qui compare théorie et expérience. Mais l'utilisation en routine demanderait l'exploitation en parallèle de deux échantillons, ce qui alourdirait le dépouillement déjà fastidieux de ces dosimètres à DST qui, de plus,

n'autorisent qu'un contrôle a posteriori des doses reçues. Enfin, les détecteurs solides de traces peuvent apparaître, à bien des égards, comme désuets à l'ère de l'électronique.

Nous avons été ainsi amenés à nous interroger sur l'utilisation de nos convertisseurs calculés et testés avec des détecteurs semi-conducteurs dans une configuration différentielle. On peut alors comparer la réponse du système à DST à celle du "capteur électronique" comme l'illustre la figure 13. On constate grâce aux valeurs reprises dans le tableau n° 4 que le dispositif électronique présente une meilleure sensibilité que le dispositif à DST.

Epaisseur du convertisseur de $(CH_2)_n$ en µm	20	35	150
Efficacité effective théorique pour les DST (protons $cm^{-2}.mSv^{-1}$)	222	360	1250
Efficacité effective expérimentale pour les DST (protons $cm^{-2}.mSv^{-1}$)	195	357,5	1357
Efficacité effective expérimentale pour les diodes (protons $cm^{-2}.mSv^{-1}$)	469,5	909	1798
Efficacité intrinsèque théorique (protons $cm^{-2}.mSv^{-1}$)	598	918	2000

Tableau n° 4 : Valeurs comparées des efficacités obtenues en théorie, avec les DST et à l'aide des diodes

Cependant, le détecteur semi-conducteur et le configuration du capteur électronique doivent être améliorés et optimisés avant le passage à un système intégré utilisable en radioprotection individuelle. Cela doit faire l'objet de travaux à venir.

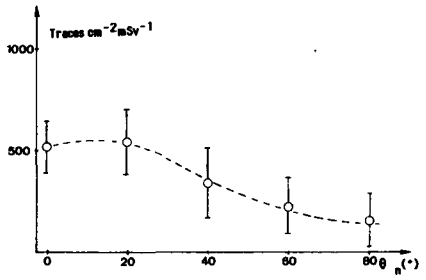

Fig. 8 : Efficacité effective en fonction de l'incidence des neutrons (E_n = 3,4 MeV) détecteur CAD convertisseur d'épaisseur 35 µm

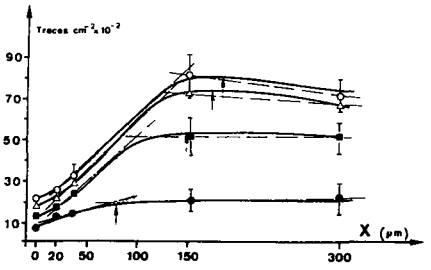

Fig. 9 : Réponse d'un détecteur CR 39 en fonction de l'épaisseur x du radiateur en $(CH_2)_n$ (E_n : 3,4 MeV, 11,49 mSv, lecture "manuelle" microscope optique ; ↑ valeurs théoriques
O:θ_n=0°, ●:θ_n = 40° Δ:θ_n=20° ●:θ_n=80°

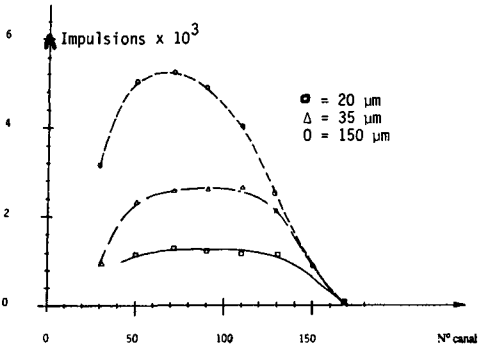

Fig. 10 : Spectres énergétiques des protons générés par les neutrons (E_n = 3,3 MeV) d'incidence normale et détectés par les diodes pour des épaisseurs de convertisseurs variables. Chaque point correspond à une moyenne effectuée sur plusieurs mesures. Résultats exprimés pour un équivalent de dose de 10 mSv

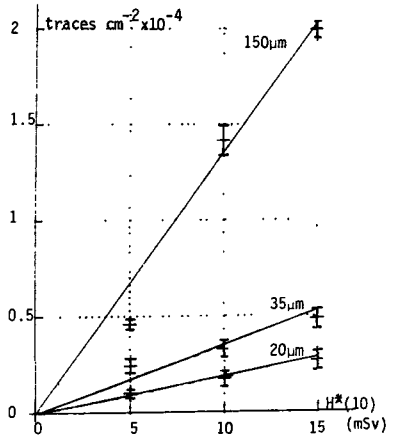

Fig. 11:Efficacité effective des dosimètres (mesure differentielle) en fonction de l'équivalent de dose à 3,3 MeV pour 3 épaisseurs de radiateur

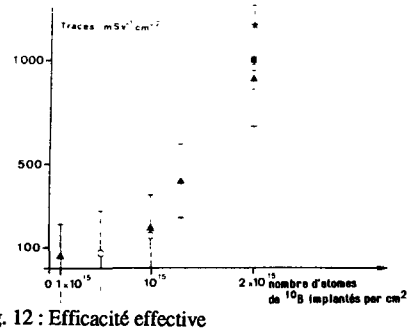

Fig. 12 : Efficacité effective
Irradiations à Cadarache
CAD ESSILOR Δ - implantation dans du métal (Fe)
O - implantation dans $(CH_2)_n$ de 35 µm
Irradiations à Harwell
CAD ESSILOR * - implantation dans $(CH_2)_n$ 35 µm
CR 39 PERSHORE - implantation dans $(CH_2)_n$ 35µm

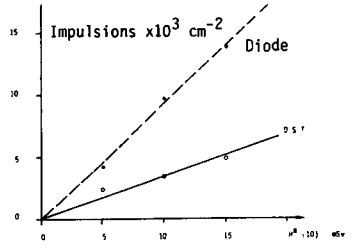

Fig. 13 : Comparaison des efficacités effectives obtenues à l'aide des dosimètres à DST et à diodes
(convertisseur de 35 µm d'épaisseur)

IV. Other research group(s) collaborating actively on this project [name(s) and address(es)]:

Irradiations within the neutron joint irradiations of the CENDOS-EURADOS (n° 5)

Collaboration with the SIDR CEA (Fontenay-aux-Roses - Cadarache)

V. Publications:

1 - Study of a polyethylene - CR 39 fast neutron dosemeter
Part I : Characteristics of proton fluxes emitted by a polyethylene radiator
L. MAKOVICKA, S. SADAKA, J.C. VAREILLE, J.L. DECOSSAS, J.L. TEYSSIER
Rad. Prot. Dos., 16, 4, 273-279 (1986)

Part II : Dosimetric efficiency of the device
S. SADAKA, L. MAKOVICKA, J.C. VAREILLE, J.L. DECOSSAS, J.L. TEYSSIER
Rad. Prot. Dos., 16, 4, 281-287 (1986)

Contribution of heavy recoils to the response of a damage track neutron dosemeter
S. SADAKA, L. MAKOVICKA, J.C. VAREILLE and J.L. DECOSSAS
Rad. Prot. Dos., 18, 4, 215-220 (1987)

Experimental study of the dosimetric efficiency of a radiator-CR 39 fast neutron dosemeter
L. MAKOVICKA, J.L. DECOSSAS and J.C. VAREILLE
Rad. Prot. Dos., 20, 1/2, 63-66 (1987)

Detection of the thermal neutrons by CR 39 using a boron implanted convecter
L. MAKOVICKA, B. BARELAUD, J.L. DECOSSAS and J.C. VAREILLE
Rad.Prot. Dos., 23, 1/4, 191-194 (1988)

2 - Contribution à la dosimétrie neutron gamma - Etude d'un ensemble radiateur-détecteur type CR 39
L. MAKOVICKA, Thèse d'état n° 17-87, Limoges, 1987

Experimental results of CENDOS neutron irradiations
J.L. DECOSSAS, J.C. VAREILLE, L. MAKOVICKA
KFK 4305 EURADOS CENDOS report 1987-01

DEA Physique Radiologique
Didier PAUL - juin 1988 - Toulouse

Results of background survey
J.L. DECOSSAS, L. MAKOVICKA, D. PAUL, J.C. VAREILLE
Report EURADOS CENDOS PAS FIBI DOSI (1989)

RADIATION PROTECTION PROGRAMME
Final Report

Contractor:

Contract no.: BI6-A-005-F

Commissariat à l'Energie
Atomique, CEA
CEN de Grenoble
85 X
F-38041 Grenoble Cédex

Head(s) of research team(s) [name(s) and address(es)]:

Mme S. Descours
Serv.de Prot.contre les Rayonn.
CEA, CEN de Grenoble
85 X
F-38041 Grenoble Cédex

Telephone number: 76-88.33.96

Title of the research contract:

Study of a transfer dosemeter for the determination of dose in tissue close to beta-radiation sources

List of projects:

1. Study of a transfer dosemeter for the determination of dose in tissue close to beta-radiation sources.

Title of the project no.:

Study of a transfer dosemeter for the determination of dose in tissue close to beta radiation sources.

Head(s) of project:

Y. HERBAUT

Scientific staff:

J.B. LEROUX

I. Objectives of the project:

. Evaluation of the uncertainties in beta absorded doses measured with currently used extremity dosemeters.
. Use of an extrapolation chamber as a reference detector and TSEE or ultra thin TL dosemeters as transfer instruments.

II. Objectives for the reporting period:

III. Progress achieved:

1/ Extrapolation chambers

The reference detector, in a beta irradiation field calibrated by PTB consists of a FWT extrapolation chamber, connected to a keithley electrometer model 642 with a measuring limit of 10^{-17} A. The data are stored in a Apple II microcomputer (basic language) during a first period, and now in a HP Vectra computer (turbo pascal language /1/) ; the uncertainties on temperature, pression, the feedback capacitor, the stopping power ratio and the average energy per ion pair are taken into account in the beta software, for the determination of the tissue dose and its accuracy (the standard deviation is multiplied by a safety factor equal to 3, as recommended by LMRI, the French Primary Laboratory). Two similar ionization chambers, type FWT-EIC1, with an entrance window of graphite coated mylar foil 0,83 $mg.cm^{-2}$ thick or a 7 $mg.cm^{-2}$ A 150 TE material absorber were used. Their ratio gives the corresponding transmission factor T :

For ^{90}Sr + ^{90}Y T = 1,036 ± 1,8 %
So we can reach the transmission factor T' between a 7 mg/cm^2 mylar entrance window and a 7 mg/cm^2 ET one for the same radionuclide :

T' = 0,98 ± 1,8 %

For one of these chambers, the cavity can be filled with a methan based tissue equivalent gas (GET) ; so we can reach the product Stg.Wg, where :

. S_{tg} is the ratio of average mass collision stopping powers, in the case of beta spectrum, for tissue and TE gas.
. W_g is the average energy required to produce an ion pair by beta particles in the gas.

For the ^{90}Sr + ^{90}Y source, and GET, we obtained $S_{tg}.W_{g/e}$ = 28.41 ± 2 % J/C

Four beta irradiation beams are calibrated by PTB : ^{90}Sr + ^{90}Y without flattening filters at three distances, ^{90}Sr + ^{90}Y with flattening filters, ^{204}TL with flattening filters, ^{147}Pm with flattening filters.
The computation of the areas S of the collecting volumes for the two ionization chambers was carried out in two ways :

. in ^{60}Co calibrated beams, under electronic equilibrium conditions.

. by the J. BOHM'S method (/2/).

The values obtained by the two manners are in good agreement ; for instance, we have S = 0,836 cm^2 ± 1,9 % for the 7 $mg.cm^{-2}$ entrance window extrapolation chamber. This determination has been confirmed in the first irradiation beam of a Büchler facility calibrated by PTB : ^{90}Sr + ^{90}Y without flattening filters at 11, 30, 50 cm source detector distances.

If we put $R = \frac{(\dot{D}_t)m}{(\dot{D}t)r}$

where

. $(\mathring{D}t)m$ is the absorbed dose rate measured by the 7 $mg.cm^{-2}$ ET FWT chamber.

.$(\mathring{D}t)r$ is the reference absorded dose rate in tissue, at a 7 $mg.cm^{-2}$ depth under the skin surface, given by PTB.

We have :

d_{cm}	R ± ΔR
11	1.02 ± 0.04
30	0.99 ± 0.04
50	1.0 ± 0.036

Values of R for a 90(Sr + Y) source

The Laboratory participated to an intercomparison for ^{204}TL, organised by LMRI ; the difference between our results and the reference value is equal to 9 % (/3/). Actually no explanation has been found.
We can also operate with a beta irradiation facility built by CEA/FAR/DPT (France) using large diameter beta sources (active diameter = 42 mm) according to set 1 of ISO recommendations (/4/) and calibrated (with and without flattening filters) by LMRI (France).
Moreover we have measured absorbed dose rates in tissue $D_{7,t}$ close to beta sources with the 7 $mg.cm^{-2}$ ET FWT extrapolation chamber (in the last column, we compute values using the $1/d^2$ law) :

Source to detector distances in cm	Tissue dose rate $\mathring{D}_{7,t}$ measured with an extrapolation chamber in $Gy.h^{-1}$	Values of dose rates in $Gy.h^{-1}$ calculated with the $1/d^2$ law
11 (distance of calibration)	1.72	1.72
5	8.3	8.32
3	20.4	23.12
1.5	89.2	92.50

Values of $\mathring{D}_{7,t}$ for the ^{90}Sr + ^{90}Y PTB source and several distances (reference date : 14/09/89)

Source to detector distances in cm	Tissue dose rate $\mathring{D}_{7,t}$ measured with an extrapolation chamber in $Gy.h^{-1}$	Values of doses rates in $Gy.h^{-1}$ calculated with the $1/d^2$ law
30 (distance of calibration)	0.048	0.048
10	0.52	0.43
5	1.91	1.73

Values of $\mathring{D}_{7,t}$ for the ^{204}Tl extended source without flattening filters, calibrated by LMRI (reference date : 14/12/89)

Figure 1 shows for the ^{204}Tl extended source and a 10 cm distance between source and detector, the measured ionization current I plotted versus the apparent cavity depth y of the chamber.

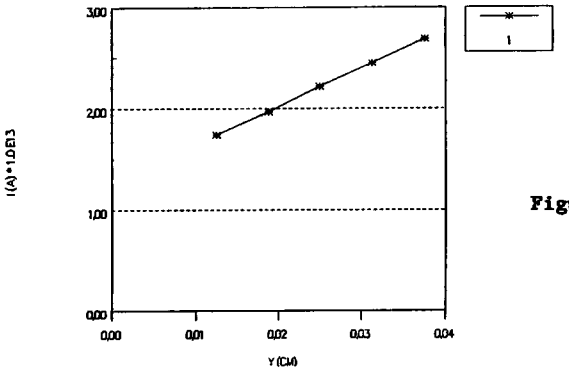

Figure 1

2/ Beta dosimetry using thermoluminescence and thermally stimulated exoelectron emission

2.1 TL dosemeters

TL dosemeters, each calibrated, are Fli 7 thin layers from Teledyne. Their geometrical characteristics are 12,7 mm in diameter and a thickness of 130 µm. The calibration source is the ^{60}Co source under electronic equilibrium, the Buchler ^{90}Sr + ^{90}Y radioactive source without filter at a 11 cm distance, or the Buchler ^{204}TI one with its own filter, according ISO recommendations giving, for 5/10/1979, a tissue dose rate $\mathring{D}_{7,t}$ of 821.1 $\mu Gy.h^{-1}$ at a 30 cm distance under a 7 $mg.cm^{-2}$ tissue depth, which allows to compute the relative response R' of these disks.

Source	R'
^{60}Co	1
^{90}Sr + ^{90}Y	1 ± 0.07
^{204}Tl with its filter	0.92 ± 0.08

Two measurements, for each dosemeter, are performed with the Toledo 654 reader :

. the first one L1 giving an information related to the irradiation.
. the second one L2 for the background of the sample.

So the difference L1-L2 is proportional to D_7.
The broad TL^{204} source ($\varnothing$ = 42 mm), calibrated by LMRI, at 30 cm, with its ISO filter exhibits a ratio $D_{7,c}/D_{7,Fli}$ equal to 1.01. ($D_{7,c}$ is the measurement done with the 7 $mg.cm^{-2}$ FWT extrapolation chamber, $D_{7,Fli}$ the mean value of four results of Fli disks covered by a 7 $mg.cm^{-2}$ A 150 film laying on a 20 mm perpex phantom).
Experiments were also carried out with these disks at small distances from the radioactive source. In the next table, we show the values obtained, for the PTB ^{90}Sr + ^{90}Y source, (reference date : 14/09/89) and we compare the results with the extrapolation chamber measurements (see extrapolation chamber paragraph) (r is the ratio of extrapolation chamber values and disks ones).

Source to detector distance in cm	Tissue dose $\dot{D}_{7,t}$ in $Gy.h^{-1}$ measured with disks	r
11 (calibration distance)	1.67 (reference value)	/
5	7.66	1.08
3	19.50	1.05
1.5	92.81	0.96

The same in gatehred for the extended ^{204}Tl source, without flattening filters in the following table (reference date : 14/12/89)

Source to detector distance in cm	Tissue dose $\mathring{D}_{7,t}$ in $Gy.h^{-1}$ measured with disks	r
30	calibration value 0.048	/
10	0.50	1.04
5	1.84	1.04

2.2 TSEE dosemeters

TSEE BeO thin film dosemeters, each calibrated, consist of a thin film about 100 µm thick, on a graphite substrate of 1 mm. Detectors of 12,7 mm in diameter were used. They have been developed in recent years by the Battelle Institute in Frankfurst and the University of Giessen (/5/) and bought to the firm NRW of Dortmund. The TSEE read out consists of a window less methan gas flow multineedle counter associated with a pulse counter built by the Digitec firm. This device has been realized by M. PETEL (/6/). The parameters, witch have been varied, were high voltage, gas flow rate, amplification gain, discriminator level. The high voltage applied in 2.35 kV and the flow gas rate 20 $l.h^{-1}$. The integration interval is between 200° C and 600° C, the lowest integration limit being reached with a linear rate of $7°C.s^{-1}$, and the final temperature with a rate of $3°\ C.s^{-1}$.
Two measurements were done for each sample :

. a B1 information in relation with the irradiation.

. a B2 information for the noise of the BeO dosemeter.

So the difference B1-B2 is proportional to the tissue dose under a fixed depth.

Figure 2 shows dose response (in the range 25 10^{-5} Gy to 5 10^{-3} Gy) for ^{90}Sr + ^{90}Y irradiation, a 2.35 kV high voltage and a 20 $l.h^{-1}$ methan flow rate.

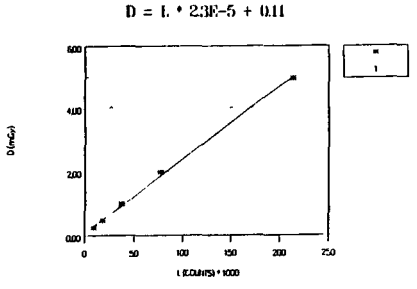

Figure 2

The dosimetric detectors, embedded in a plexiglass box (for electronic equilibrium) and covered either by a 7 $mg.cm^{-2}$ film of black vinyl or a 6 $mg.cm^{-2}$ film of Makrofol are irradiated by Co^{60} with a tissue dose under a 7 $mg.cm^{-2}$ tissue depth of 0.02 Gy ± 2 %.
We have studied the dispersion of a 30 dosemeter set (± 125 %), the long term reproductibility (± 18 %), the short term stability (± 28 %) (/7/).
These detectors, because of the quoted relative errors, seem not to be able to be employed in radioprotection for skin dosimetry at the present time.

3 - Conclusion

The extrapolation chamber is a suitable instrument for beta dosimetry ; the smallest distance between the two electrodes is independant of the source - entrance window distance but it seems very sensitive to their parallelism. The $1/d^2$ law for short source-detector distances (greater than 1.5 cm) gives rough results (with a relative error smaller than ± 30 %) - Nevertheless this device in not practical.
We have carried out experiments with Fli dosemeters (e = 0.13 mm) and TSEE ones. Fli disks work well at small distances from the ^{90}Sr + ^{90}Y and ^{204}Tl radioactive sources.
TSEE BeO dosemeters, because of their dispersion ,seem not to be able at this moment to be employed in radioprotection of low LET particles.
Experiments must be completed with the Vinten extremity dosemeter and the radionuclide ^{147}Pm.

4 - REFERENCES

/1/ Pons Frédéric : Mémoire de stage (1989).

/2/ Böhm J. : Instruction manual : extrapolation chamber for the measurement of the absorbed dose rate to tissue for beta radiation - PTW Freiburg (W Germany).

/3/ Herbaut Y. and Leroux J. B. : Note intérieure SPR/88.147.

/4/ ISO 6980 : Rayonnements béta de référence pour l'étalonnage des dosimètres et débitmètres et la détermination de leur réponse en fonction de l'énergie béta (1984).

/5/ C. U. Wieters et al. : Electron Dosimetry with thermally stimulated exoelectron emission (TSEE) phys. Med. Biol. 1984 - Vol 29 n° 9 (1097-1107).

/6/ M. Petel et al. : Multineedle counter with cathodic focusing (MNCF) used for TSEE dosimetry. RPD vol.4 3/4 (171-173).

/7/ J. B. Leroux : Study of TSEE dosemeters their stability and reproductibility.
Note intérieure 89.281.

RADIATION PROTECTION PROGRAMME

Progress Report

1989

Contractor:

Physikalisch-Technische
Bundesanstalt (PTB)
Bundesallee 100
D-3300 Braunschweig

Contract no.: BI6-A-012-D

Head(s) of research team(s) [name(s) and address(es)]:

Prof.Dr. G. Dietze
PTB
Bundesallee 100
D-3300 Braunschweig

Prof.Dr. R. Jahr
PTB
Bundesallee 100
D-3300 Braunschweig

Telephone number: 5926500

Title of the research contract:

Investigation and development of neutron spectrometers and investigation and implementation of dose equivalent quantities.

List of projects:

1. Development of neutron spectrometers for radiation protection practice.
2. Realization of dose equivalent quantities for photons and neutrons using microdosimetric methods.
3. Investigation of dose equivalent quantities for individual dosimetry

Title of the project no.: 1

Development of neutron spectrometers for radiation protection practice

Head(s) of project:

Dr. M. Cosack (up to 31.12.87), Dr. H. Klein (from 1.1.88), Dr. K. Knauf

Scientific staff:

A. Alevra, Dr. M. Matzke, A. Plewnia, Dr. B.R.L. Siebert

I. Objectives of the project:

Development and investigation of neutron spectrometers for use in real radiation fields

a) Development of a well-specified and reproducible multisphere system (Bonner spheres). Experimental determination of the response of Bonner spheres in monoenergetic neutron fields with the aim of establishing a response matrix by intercomparison with calculated responses.

b) Development of a neutron spectrometer using proton recoil proportional counters and an NE213 scintillation detector. Investigation of these systems in monoenergetic neutron fields and in fields with broad energy spectra.

II. Objectives for the reporting period:

- Design, assembly and characterization of the various spectrometers to be applied in radiation protection practice.
- Calibration of the detector responses with monoenergetic neutrons.
- Test of the unfolding procedures which are necessary for all spectrometers, by means of measurements in well known fields.
- Measurements in unknown fields with all detector systems available and applicable.

III. Progress achieved:

1. INTRODUCTION

Neutron spectrometers to be used in radiation protection practice /1/ must cover a wide dynamic energy range (thermal to some tens of MeV) and should have an isotropic response and a neutron detection efficiency large enough for the investigation of neutron fields causing a dose equivalent below 100 µSv/h. As spectrometry is generally performed in mixed fields with photon fluences up to a factor of 100 higher than neutron fluences, the spectrometers must either be insensitive to photons or capable of discriminating between neutron and photon-induced events. Finally, extreme environmental conditions (temperature, humidity etc.) must to some extent be considered.

Three different types of spectrometers have been designed, assembled and specified at the PTB, namely:

- a set of Bonner spheres (BS) with small ^{3}He-proportional counters as the central detector for the entire energy range but with a limited energy resolution,
- NE213 liquid scintillation detectors for proton recoil spectrometry in the energy range above 0,5 MeV and
- spherical proportional counters with various gas fillings (H_2, CH_4) for proton recoil spectrometry in the energy range from 10 (50) keV up to 1 (2) MeV.

The completely characterized systems were for the first time used simultaneously to determine the spectral flux density and dose equivalent rate at the national fission material depot.

2. BONNER SPHERES

Design. At PTB /2/ a set of 14 BS with diameters from 5.08 cm to 45.72 cm was manufactured using polyethylene with a density of 0.946 g/cm^3. Two types of ^{3}He-filled proportional counters are used as central detectors. A small cylindrical central detector of type 0.5NH1/1K from LCC Thomson-CSF France, can be placed in all 14 BS constituting the "F" BS set, while a larger spherical central detector of type SP90 of Centronic Ltd UK, can be used only in 12 BS with diameters from 7.62 cm to 45.72 cm and constitutes the "C" BS set. Inserts made of polyethylene of the same

density allow an almost spherical symmetry to be achieved for each central detector-BS combination without interrupting the HV supply of the detector.

Calibration with monoenergetic neutrons. The experiments were carried out in the low-scatter experimental hall of the PTB's 3.5 MV Van-de-Graaff accelerator. In two series of measurements /3,4/ the reactions $^{65}Cu(p,n)$, $^{45}Sc(p,n)$, $^{7}Li(p,n)$, T(p,n), D(d,n) and T(d,n) were used to produce monoenergetic neutrons of 12 energies : 1.21 keV, 8.15 keV, 27.4 keV, 71 keV, 144 keV, 250 keV, 425 keV, 565 keV, 1.2 MeV, 2.5 MeV, 5.0 MeV and 14.8 MeV. The neutron fluence was determined using a DePangher long counter, a proton recoil proportional counter, or a proton recoil telescope. Four different monitors were used as transfer instruments for the neutron fluence. The shadow-cone technique was applied to determine the room and inscatter contribution to the sphere readings. Deadtime, air attenuation and source-detector geometry corrections were taken into account. The influence of neutrons scattered from the BS under calibration into monitors was investigated /5/ and corrected. The fluence measurement results and the experimentally obtained BS responses were both corrected for target neutron scattering in the target backing and mounting. Typical uncertainties in the measured responses are 3 % to 4 %, but in the keV region or for low value responses the uncertainties increase up to 10 %.

Calibration with thermal neutrons. The measurements were performed /6/ at the thermal column facility of NPL, Teddington, UK. Gold foil activation was used for fluence determinations, and a fission chamber was used as monitor. Bare detectors and BS's with diameters up to 25.4 cm were exposed in the thermal flux free and under cadmium cover. The difference in readings is due to neutrons with energies below the cadmium cut-off whose spectrum is well known.

Establishment of fluence response matrices. To complete the experimental data it was necessary to use calculated fluence responses for the BS sets under study. From the most recently computed responses we have used those of D.J. Thomas /7/, which refer to a BS system very similar to our "C" set. The shapes calculated by Thomas were used in least-squares fits to all "C" and most of the "F" experimental data. Fit factors varying slowly and smoothly with the BS diameters were obtained, but values between 2 and 4 for the reduced chi-square showed only limited compatibility

between calculated and measured responses. In order to evaluate the calibrations with thermal neutrons the fitted responses were extrapolated down to 0.001 eV and then folded with the known spectral distribution of the thermal field. The calculated responses for various BS of the "C" or "F" sets were about 80 % to 120 % higher than the experimental ones. The discrepancy is removed by smooth reductions of the fitted and extrapolated responses between 0.001 eV and 100 eV. As an example, the response matrix for the PTB-"F" BS set is shown in Fig. 1.

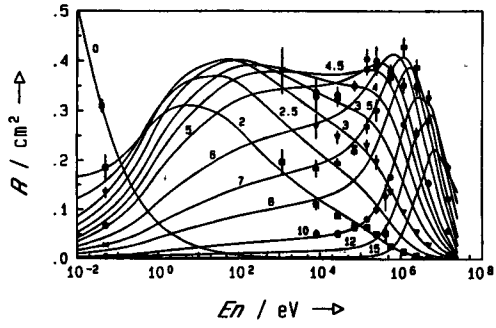

Fig. 1. The neutron fluence response $R(E_n)$ of the PTB-"F" set of Bonner spheres. The indices designate the sphere diameters in inches. The index "0" designates the bare detector. In a few cases the experimental points to which the curves were fitted are shown. E_n = neutron energy

Few-channel unfolding of BS data from measurements. A European intercomparison of computer codes /8/ has indicated that the spectral result of a few-channel unfolding are significantly influenced by the choice of a guess spectrum or a set of basic spectra. Among the codes in use at PTB, the iterative algorithm of SAND II was taken to develop a procedure which allows a quick check of various guess spectra to be made. A guess spectrum whose shape remains practically unaltered during several hundred iterations, and which produces a solution which is stable for various combinations of BS, is considered to be acceptable.

3. NE213 LIQUID SCINTILLATION SPECTROMETER

Set-up: Three detector systems with different neutron detection efficiencies were assembled at PTB. Commercially available liquid scintillators (Nuclear Enterprise, BA-1 type NE213), 12.9, 43.4 and 411.6 cm^3 in volume, were fitted to fast photo-tubes (VALVO types XP 2020

and 2041). A double resistor chain and an LED gain stabilizer developed at PTB /9/ guarantee reliable measurements even at high count rates (up to 10^5 counts/s) and for a wide range of environmental temperatures (10 to 35 °C). The discrimination of photon and neutron-induced events is performed by means of the charge integration method /10/ (LINK model 5010) which separates neutron-induced events from photon-induced events a hundred times more intensive without significant losses of recoil protons with energies larger than 0.6 MeV.

Calibration: The properties of the detector systems had to be carefully investigated. The light output function of the recoil protons was determined by means of time-of-flight spectrometry in wide energy neutron spectra from ^{9}Be + d (13 MeV) reactions. Multiparameter data processing enabled the response spectra to be analysed for monoenergetic neutrons between 0.5 and 15 MeV, corresponding to properly set time-of-flight windows. The almost linear light output function for electrons derived from Compton spectra /11/ always served as a reference.
The precise light output functions are required as input data of the NRESP code developed at the PTB for Monte Carlo simulations of the neutron response spectra /12/. The spectra calculated for monoenergetic neutrons, folded with the appropriate pulse height resolution and normalized for the fluence at the center of the detector, were used to determine neutron fluences in the energy range from 1.2 to 14.8 MeV (fig. 2). Excellent agreement (within ± 3 %) was achieved for the fluence values measured with a proton recoil telescope /13/.

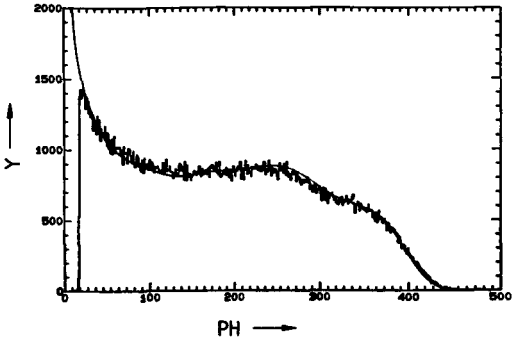

Fig. 2: Experimental pulse height spectrum Y(PH) of the liquid scintillation spectrometer (histogram) for monoenergetic neutrons of 2.5 MeV compared with the corresponding Monte Carlo simulated response function (line).

Unfolding: The calculated response functions formed the response matrix needed for the unfolding of the pulse height spectra. Besides handling the data input and output the matrix inversion code FERDOR /14/ was

modified to enable the measured pulse height spectra to be analysed for any experimental threshold without extrapolation. Reasonable agreement was achieved for the spectral neutron fluences derived either from time-of-flight measurements or from the simultaneously measured pulse height spectrum by unfolding /15/.
All the calibration measurements were performed in directional fields of point sources. Monte Carlo calculations of the angular dependence of the fluence response showed almost isotropic response for irradiation from the forward hemisphere. For irradiation through the phototube and the light guide a significant, energy dependent attenuation of the neutron fluence has to be taken into account, but this concerns only a small solid angle.

4. PROTON RECOIL PROPORTIONAL COUNTERS

The neutron energy range below 2 MeV can be covered by proportional counters filled with H_2 or a hydrogenous gas like CH_4 or a mixture of H_2 + Ar. The upper energy limit results from the increasing recoil proton range, and depends on the counter size and the stopping power of the filling gas. The ultimate lower limit is about 1 keV, set by the deterioration of the proton energy resolution. The practical lower limit, however, is higher, due to problems with the separation of the neutron and γ-induced pulses. The entire energy range can only be spanned by measurements covering smaller energy segments. The counters used for each segment differ in the nature of the filling and the gas amplification. Regions of overlap allow the spectral segments to be merged into a single spectrum.
Set-up: Spherical counters of the Benjamin type SP2 are in use, and these are filled at the PTB with H_2 up to a pressure of 1 MPa. The filling procedure, the electronic arrangement, measurements and related problems are described in detail elsewhere /16, 17/.
The discrimination between γ and neutron-induced events which is necessary in the lower energy range (below some tens of keV), is performed by pulse-shape discrimination taking advantage of the differing pulse rise times due to differing track lengths of electrons and protons of the same energy /18/. A signal related to the rate of rise is obtained by differentiation of the pulse before it reaches its maximum value and

by subsequent normalization to the maximum. The pulses are sorted in a pulse height analyser according to two parameters, the energy and the relative rate of rise. Subsequently, the actual separation is done by a computer /16/. The separation process proves increasingly difficult the lower the particle energy. The practical lower limit depends on the ratio of the γ to neutron-flux density. For the measurements in the fission material depot /19/ the lower limit was approximately 50 keV, but when the spectra of filtered reactor neutrons are studied thresholds below 10 keV were achieved.

Calibration: The counters are calibrated by exposing them to iron-filtered reactor neutrons. The neutron spectrum unfolded from the measurement shows a series of distinct lines. The transmission function of the filter can be calculated on the base of a cross section library and shows groups of narrow lines. The function can be adapted to the measured spectrum very well after folding with a Gaussian and using the standard deviation as a fit parameter. Comparing the measured spectrum (depending on the channel number) with the fitted one (depending on the energy) produces an excellent energy calibration.

Unfolding: For high-energy neutrons outside the particular energy segment covered by the measurement the response function was derived from the Snidow and Warren algorithm /20/ which only takes the wall effects into account. In the case of lower energies the electrical effect was also allowed for by assuming the response function to be trapezoidal (Fig. 3) with a slope as shown in Fig. 5 of ref. 21.

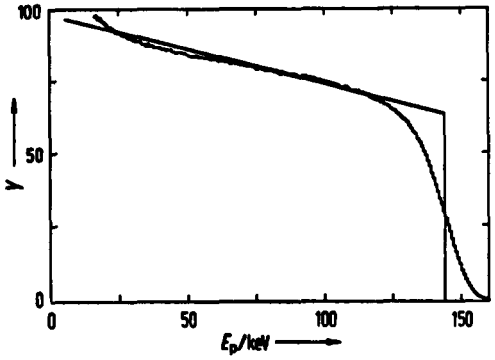

Fig.3: Experimental response $Y(E_p)$ of a spherical counter (histogram) to the 144 keV neutrons of a Si + Ti filter in a reactor beam tube compared with the calculated response function used for unfolding (line). E_p = proton energy

Prior to unfolding the neutron spectrum in a segment, the downscatter spectrum (i.e. the pulses due to neutrons with energies exceeding the upper energy limit of the segment) must be subtracted from the pulse height distribution. The downscatter spectrum is calculated by means of the response matrix and the spectrum originating in measurements above the limit. The difference pulse height spectrum is smoothed before the neutron spectrum is extracted. In carrying out the unfolding process the proton energy resolution of the counter is disregarded. Thus the response matrix is triangular and the unfolding is reduced to a simple recursion, i.e. a simple stripping algorithm. This procedure entails the counter resolution being projected into the neutron spectrum.

5 APPLICATIONS

Benchmark measurements in a well-known field of a ^{252}Cf fission source.
Both PTB BS sets ("C" and "F") and the NE213-scintillation spectrometer took part in these measurements at NPL Teddington /22/. Again, the shadow-cone technique was used to measure the net spectrum. The neutron emission rate of the ^{252}Cf source was precisely (± 1%) determined in a manganese bath. BS responses calculated by folding the fission spectrum of ^{252}Cf with our response matrices agree with the measured data within ± 3 %. For the NE213-scintillation spectrometer, the unfolded spectral fluence agrees above 1.0 MeV both in shape and absolute scale with the spectrum calculated for the calibrated neutron source strength (Fig. 4). The discrepancy between the experimental threshold (≈ 0.6 MeV) and a neutron energy of about 1 MeV is due to the particular n/γ-discrimination used at low pulse height.

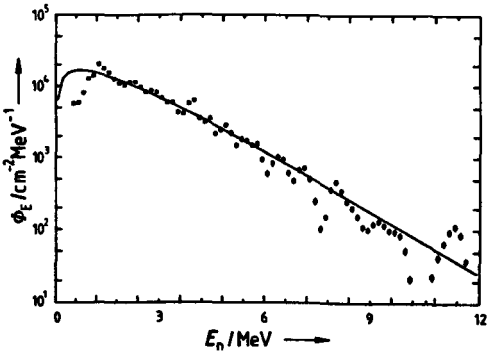

Fig. 4: Spectral neutron fluence $\Phi_E(E_n)$ as unfolded from the pulse height spectrum measured with the liquid scintillation spectrometer for a bare Cf 252 source (points) in comparison with the spectral fluence expected for the well known source strength (line). E_n = neutron energy

Benchmark measurements in a partly-known field of a moderated ^{252}Cf source. These measurements were also performed at NPL at a distance of 150 cm from the source. The source strength was not given but the spectral distribution can be assumed to be that recommended by ISO. Fig. 5 shows results obtained with the PTB-"C" set using the bare counter, Cd-covered bare counter, and all BS up to 38.1 cm (15") in diameter. The 6 solution spectra shown are obtained with various guess spectra. The ISO spectrum is confirmed by these results, but a thermal and/or a slowing-down contribution below the cadmium cut-off seems to be present in the large experimental hall. The solution spectrum results in an integral fluence rate of 174 $cm^{-2}s^{-1}$, a dose equivalent rate of 53.7 μSv/h and a mean fluence-to-dose equivalent conversion factor of 85.73 $pSv \cdot cm^2$, which represents 93.6 % of the ICRP 21 recommended value for a moderated ^{252}Cf spectrum, in qualitative agreement with the suggested contribution below the cadmium cut-off.

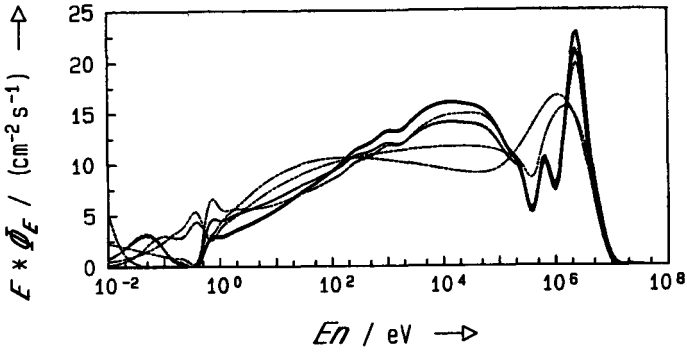

Fig. 5. Six solution spectra obtained using different guess spectra by unfolding the "C"-BS data measured in a D_2O-moderated ^{252}Cf neutron field. The thick line shows the ISO recommended spectrum.

Measurements in a completely unknown neutron field. All three spectrometric techniques were used for measurements in the fission material depot of the Federal Republic of Germany /19/. The measurements were performed and unfolded independently for each spectrometer. Only in the case of unfolding the proportional counter data the downscatter spectrum was calculated using the information given by the NE213 liquid scintillation spectrometer. The spectral results from all three techniques are shown in Fig. 6. The full curve covering the whole range is due to the BS spectrometer, the histogram above 1 MeV is due to the

NE213 scintillation spectrometer while the histogram below 1 MeV resulted from the measurement with the hydrogen-filled proportional counter. The good agreement between the three spectra is also confirmed by the integral results for the fluence and the dose-equivalent rates /19/.

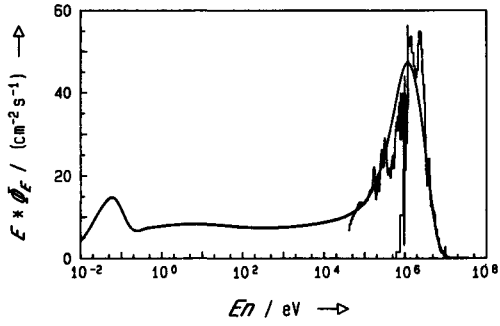

Fig. 6. The spectral neutron fluence rate at the national fission material depot, as obtained with three different spectrometric techniques. BS: thick full line; NE213: histogram over 1 MeV; Pr.C.: histogram under 1 MeV; E_n = neutron energy

6 CONCLUSIONS

Within the framework of this project various neutron spectrometers designed for application in radiation protection practice were carefully investigated. The experimental calibration of the response of four sets of Bonner spheres (2 x PTB, GSF, NPL) required most of the effort. Three series of measurements were necessary at PTB and NPL in order to cover the entire energy range from thermal to ~ 15 MeV neutrons. The experimental data could not be explained by simple ANISN calculations. Preliminary and more realistic Monte Carlo simulations describe these data much better. Systematic calculations are in progress. In the meantime, properly modified ANISN calculations fitting the experimental data have been used to calculate the response matrix needed for the few-channel unfolding procedure. While the spectral neutron fluence derived from few channel BS data exhibits large uncertainties and depends heavely on the a priori information required in some unfolding procedures, the integral data such as fluence or dose equivalent are determined with reasonable uncertainties ($\leq$ 10 %).

The proton recoil spectrometers cover the energy range most important for dosimetry, as the fluence to dose equivalent conversion factor increases by a factor of 10 - 20 for neutron energies above 10 keV. However, the application of the small spherical proportional counters is limited by

their neutron detection efficiency, while its sensitivity to photon radiation may be the drawback of the liquid scintillation spectrometer, even if fast n/γ discrimination circuits are available.
The spectrometers will be used in combination depending on the environmental conditions and the particular properties of the fields to be investigated.

7 References

/1/ W. Cross, H. Ing
Neutron spectroscopy. In: The Dosimetry of Ionizing Radiation, Eds. V.R: Kase, B. Bjorngard, F. K. Attix, Academic Press, New York, 1987, Vol. II, p. 91 - 157

/2/ A. V. Alevra: to be published (1990).

/3/ A. V. Alevra, M. Cosack, J. B. Hunt, D. J. Thomas and H. Schraube: Radiat. Prot. Dosim. 23 (1988) 293

/4/ A. V. Alevra, M. Cosack, J. B. Hunt, D. J. Thomas and H. Schraube: to be published (1990).

/5/ A. V. Alevra: to be published (1990).

/6/ D. J. Thomas, J. B. Hunt, H. Schraube and A. V. Alevra: to be published (1990).

/7/ D. J. Thomas: Private communication. NPL, Teddington, U.K. (1989).

/8/ A. V. Alevra, B. R. L. Siebert, A. Aroua, M. Buxerolle, M. Grecescu, M. Matzke, M. Mourgues, C. A. Perks, H. Schraube, D. J. Thomas, and H. L. Zaborowski: Laboratory Report PTB-7.22-90-1, Braunschweig (1990)

/9/ H.J. Barrenscheen, H. Klein; to be published

/10/ J.M. Adams, G. White; Nucl. Instrum. Meth. 156 (1978) 459

/11/ G. Dietze, H. Klein; Nucl. Instrum. Meth. 193 (1982) 549

/12/ G. Dietze, H. Klein; PTB Report ND-22 (1982)

/13/ H. Schuhmacher, S. Guldbakke, H. Klein, H. Strzelczyk to be published

/14/ W.P. Burrus, V.V. Verbinski; Nucl. Instrum. Meth. 67 (1969) 181

/15/ L.J. Antunes, B. Börker, H. Klein, G. Bulski
In: Nuclear Data for Basic and Applied Science, Vol. I, Gordon and Breach Science Publishers, New York (1986) 577

/16/ K. Knauf and J. Wittstock, PTB-Report FMRB-114 (1987)

/17/ K. Knauf, A. Plewnia, H. Schumny, J. Wittstock, to be published

/18/ E. F. Bennet, Rev. Sci. Instrum. 33 (1962) 1153

/19/ K. Knauf, A. Alevra, H. Klein, J. Wittstock; PTB-Mitt. 99 (1989) 101

/20/ N. L. Snidow, H. D. Warren, Nucl. Instrum Meth. 51 (1967) 109

/21/ I. R. Brearly, A. Bore, N. Evans, M. S. Scott, Nucl. Instrum Meth. 192 (1982) 439

/22/ J. B. Hunt, B. R. More, D. J. Thomas, H. Schraube, A. V. Alevra and H. Klein: to be published (1990).

IV. Other research group(s) collaborating actively on this project [name(s) and address(es)]:

Dr. J. B. Hunt, Dr. D. Thomas
Div. of Radiation Science and Acoustics
NPL, Teddington, UK

Dr. H. Schraube
Inst. für Strahlenschutz
GSF, Neuherberg, FRG

V. Publications:

1. In scientific journals:

/1/ A. V. Alevra, M. Cosack, J. B. Hunt, D. J. Thomas and H. Schraube:
Experimental Determination of the Reponse of four Bonner Sphere Sets to Monoenergetic Neutrons.
Radiat. Prot. Dosim. 23 (1988) pp 293 - 296

/2/ K. Knauf, A. V. Alevra, H. Klein, J. Wittstock:
Neutronenspektrometrie im Strahlenschutz.
PTB-Mitteilungen 99/2 (1989) pp 101 - 106

/3/ A. V. Alevra, M. Cosack, J. B. Hunt, D. J. Thomas and H. Schraube:
Experimental Determination of the Reponse of four Bonner Sphere Sets to Monoenergetic Neutrons (II). to be published.

/4/ D. J. Thomas, J. B. Hunt, H. Schraube and A. V. Alevra:
Experimental Determination of the Reponse of four Bonner Sphere Sets to Thermal Neutrons. to be published.

/5/ J. B. Hunt, B. R. More, D. J. Thomas, H. Schraube, A. V. Alevra and H. Klein:
Benchmark Measurements with 252Cf and Heavy Water Moderated 252Cf Sources using four Bonner Sphere Systems and an NE213 Spectrometer.
to be published.

2. In PTB reports:

/1/ A. V. Alevra and Siebert, B.R.L.: Influence of Neutron Spectra and Fluence Response Data on the Determination of Dose Equivalent with Bonner Spheres.
PTB-Report ND-28, Braunschweig (1986).

/2/ A. V. Alevra, B. R. L. Siebert, A. Aroua, M. Buxerolle, M. Grecescu, M. Matzke, M. Mourgues, C. A. Perks, H. Schraube, D. J.Thomas and H. L. Zaborowski: Unfolding Bonner Sphere Data: a European Intercomparison of Computer Codes. Laboratory Report PTB-7.22-90-1, Braunschweig (1990).

/3/ A. V. Alevra: EVALDA - a FORTRAN 77 Code to Evaluate Data from Calibration Measurements with Neutron Sensitive Spherical Devices.
to be published (1990).

/4/ A. V. Alevra: The PTB Bonner Sphere Systems.
to be published (1990).

/5/ K. Knauf and J. Wittstock: Neutron Spectrometry with Proton Recoil Proportional Counters at the Research and Measurement Reactor Braunschweig - Status of the Technique -
PTB-Report FMRB-114 Braunschweig (1987)

/6/ K. Knauf, A. Plewnia, H. Schumny and J. Wittstock:
Neutron Spectrometry with Proton Recoil Proportional Counters at the Research and Measurement Reactor Braunschweig - Progress Report -
to be published (1990)

Title of the project no.: 2

Realisation of dose equivalent quantities for photons and neutrons using microdosimetric methods

Head(s) of project:

Dr. W.G. Alberts

Dr. G. Dietze

Scientific staff:

Dr. H.J. Brede, Dr. E. Dietz, Dr. S. Guldbakke, H. Kluge, Dr. H. Lesiecki, Dr. U.J. Schrewe, Dr. H. Schuhmacher, Dr. B. Siebert

I. Objectives of the project:

Investigation of tissue-equivalent low-pressure proportional counters (TEPC) for determining dose equivalent quantities. Development of a transfer instrument based on a TEPC. Measurement of dose equivalent in tissue-equivalent spheres. Intercomparison of instruments for practical radiation protection dosimetry based on tissue-equivalent proportional counters in well-defined monoenergetic and broad neutron fields.

II. Objectives for the reporting period:

Completion of the transportable multiparameter system and its employment to complete investigations concerning neutron and photon dose separation in monoenergetic neutron fields based on time-of-flight techniques. Measurement of kerma factors in neutron fields of energies above 30 MeV by separating neutron components of lower energy by their difference in velocity.

III. Progress achieved:

1. INTRODUCTION

The operational dose-equivalent quantities to be measured for area monitoring in radiation protection are defined in phantoms. Determination of these quantities is usually performed by instruments which primarily measure different quantities, e. g. photon air kerma or neutron fluence. Tissue-equivalent proportional counters (TEPC) offer one more step towards measuring dose equivalent by evaluating single-event energy deposition of secondary particles produced by both photon and neutron radiation. Although their principles of measurement are more closely related to the definition of dose equivalent than those of other "dosemeters", there are distinct differences and limitations [1].

The aim of the project reported on here was therefore an investigation of the fundamental aspects of dose-equivalent determination with TEPCs. This investigation comprised intercomparison measurements of existing TEPC-based instruments in reference radiation fields as well as detailed studies of important TEPC properties such as their calibration and timing properties for the discrimination of neutrons and photons. The latter aspect is of importance for investigations in phantoms where neutron-induced photons represent a major contribution to dose equivalent.

2. INVESTIGATIONS OF PROTOTYPE TEPC AREA MONITORS

An intercomparison of nine prototypes of TEPC based area monitors was jointly organized by EURADOS Committee 1 and PTB and carried out in two steps in 1986 and in 1987 in various reference fields, using the reactor and accelerator facilities of PTB. Thermal neutrons and monoenergetic neutrons with nominal energies of 24.5 keV, 73 keV, 144 keV, 570 keV, 1.2 MeV, 5.0 MeV and 14.8 MeV were employed. In addition measurements were made at a D_2O moderated ^{252}Cf source and a ^{60}Co gamma ray source. Details of the radiation fields have been published [2-5].

Reference values for kerma in ICRU muscle, K, were calculated using fluence-to-kerma conversion factors [6] and for ambient dose equivalent, H*(10), using fluence-to-dose equivalent conversion factors [7]. The TEPC readings of absorbed dose and dose equivalent were divided by K and H*(10), respectively, to yield the kerma response and the dose equivalent response. Particular effort was required to determine the contribution of contaminating neutrons and of photons to the readings of the TEPCs. The corresponding investigations included measurements with a ^3He spectrometer for the reactor-produced 24.5 keV beam [5], measurements with moderator-type neutron detectors for the ^{252}Cf field [2], calculations with a Monte

Carlo code for the accelerator-produced neutron fields [4] and measurements of the photon kerma with a GM counter in all radiation fields [2,5].

The primary aim of the intercomparison was to determine the neutron energy dependence of the dose equivalent and the kerma responses and to study the influence of counter geometry, data processing and evaluation procedures on these responses. Moreover, the intention was to investigate calibration procedures, to study the ability of the instruments to determine neutron and photon dose equivalent simultaneously and to study the sensitivity [3] of the instruments.

A rather large energy gap remains between thermal energies and 24 keV for the data gained during the intercomparison. However, data in this energy range are of particular importance because the differences in the detector designs play a dominant role here and neutron energy spectra behind shieldings often contain significant contributions of neutrons in the low-energy range. In collaboration with the Universität des Saarlandes and the National Institute for Standards and Technology (NIST) additional measurements with TEPCs were performed in the filtered neutron beams with energies of 2 and 24 keV at the NIST research reactor. As expected from an earlier comparison of the beams [8] the contribution from beam contamination to the TEPC reading in the NIST beams was significantly smaller than in the corresponding PTB beams. Particular emphasis was put on investigations of the influence of three different parameters of the detector design on the dose equivalent response: the wall thickness, the simulated diameter and the detector size [9].

The dose equivalent response, R_H, measured in the intercomparison, is shown in Fig. 1. Although a general trend is observed - a reduction of neutron energy leads to a decrease of R_H and R_H is below 1 for nearly all energies - significant differences can be found, in particular for low neutron energies. The response varies by a factor of 3 to 20 for the TEPC systems. The dose equivalent responses of the different systems for the broad neutron energy spectrum of the $^{252}Cf(D_2O)$ radiation were in much better agreement than those for monoenergetic neutrons.

A detailed analysis of the results, which included the microdosimetric spectra provided by several of the systems and the measurements performed at NIST, clarified the reasons for the differences, making possible recommendations for further improvements of the systems [9,10].

The various parameters of the detector design exert influence in different neutron energy regions: (1) an increase in the wall thickness increases R_H for energies below 50 keV, but decreases R_H for energies between 50 keV and 1 MeV, (2) an increase of the detector size increases R_H for energies below

20 keV and (3) a decrease in the simulated diameter increases R_H for energies between about 10 keV and 500 keV.

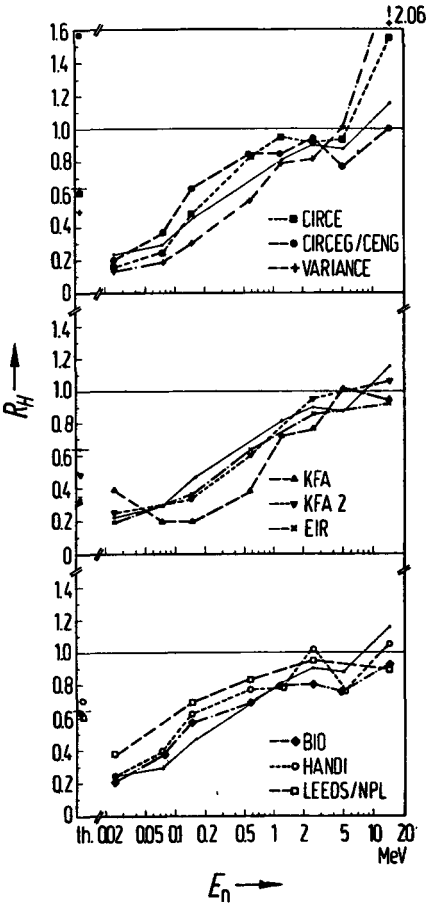

FIGURE 1
Measured ambient dose equivalent response, R_H, as a function of neutron energy, E_n, for all participating systems. The connecting lines between the measured data together with the average response of all TEPC-based systems (solid line) serve as eye guides. Results for thermal neutrons are included at the left-hand side.

The sensitivity depends in a complex way on the radiation field and the counter geometry. This is due to the fact that the statistical uncertainty depends on the pulse rate as well as the pulse-height distribution. By choosing the appropriate detector size and wall thickness TEPCs can be made as sensitive as conventional moderator-based dosemeters (Table 1).

System	$^{252}Cf(D_2O)$ T (min:s)	^{60}Co T (min:s)
VARIANCE	0:60	0:02
LEEDS/NPL	1:19	0:02
KFA	3:21	0:05
KFA2	2:93	0:04
BIO	5:91	0:12
LEAKE	1:05	-

Table 1: Measurement time, T, needed to achieve a relative statistical uncertainty of 20% of the dose equivalent reading in a $^{252}Cf(D_2O)$ and a ^{60}Co radiation field of 20 µSv/h. The TEPC systems are ordered with decreasing detector size. A conventional dose equivalent meter (LEAKE) is included for comparison.

The conventional calibration procedures in terms of lineal energy or absorbed dose lead to a calibration in terms of kerma. Calibration in a neutron beam in terms of ambient dose equivalent improves the dose-equivalent response. As measurements in the $^{252}Cf(D_2O)$ source were included in the intercomparison, it was possible to "post-calibrate" all systems in terms of H*(10). The results are shown in Fig. 2 for three of the systems. The resulting improvement can be observed by comparing with Fig. 1.

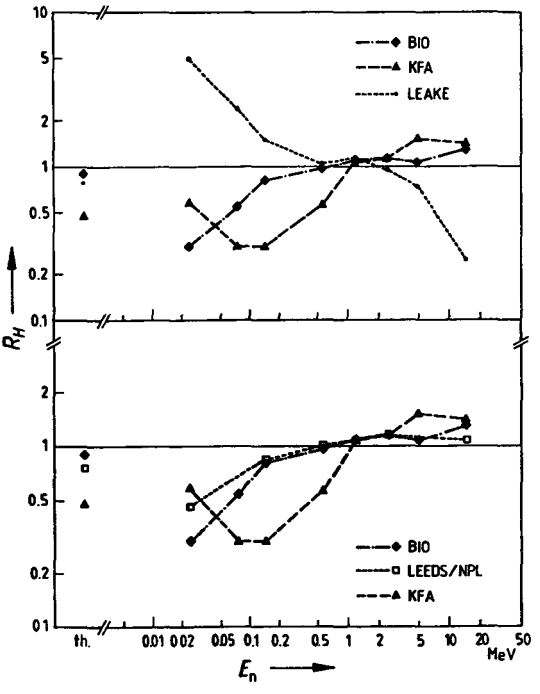

FIGURE 2
Ambient dose equivalent response, R_H, as a function of neutron energy, E_n, for different systems after "post-calibration" (see text). TOP: BIO (thin-walled TEPC), KFA (thick-walled TEPC) and LEAKE (moderator-type dose equivalent meter). BOTTOM: BIO, KFA and LEEDS/NPL (large thin-walled TEPC). The connecting lines between the measured data serve as eye guides. Results for thermal neutrons are included at the left-hand side.

3. IMPROVEMENTS OF THE CALIBRATION WITH α PARTICLES

Among the various methods for the calibration of TEPCs the so-called single-event calibration method [11] is based on built-in α-particle sources. Nearly monoenergetic α particles cross the detector cavity along trajectories of approximately full chord length. Usually, the centroid of the peak which corresponds to their energy loss is used for the calibration in lineal energy, y. Provided that the geometrical data and the α-particle energy are well known, the energy deposit in the detector can be calculated with the theoretical stopping power data of the detector gas. Major contributions to the uncertainty for this method are:

1) The various theoretical stopping power data of tissue-equivalent materials, particularly for gases, are diverse.

2) The α-particle energy is smaller than the nominal source energy, due to self absorption in the source layer.

3) Misalignments of the α-particle source are possible.

Energy loss and scattering in the detector wall around the bore hole result in particles which enter the detector with a broad energy distribution and cross the cavity on various trajectories. These events are observed above the calibration peak with an upper cut-off corresponding to α particles which are slowed down to energies around the Bragg maximum and which cross the cavity with the maximum path length. The energy loss in the cavity for those particles corresponding to the edge can be calculated. Its value is independent of the actual α-ray source energy and of the quality of the source and detector arrangement. Therefore, the uncertainty of the cut-off energies contains fewer systematic contributions than the energy loss of the unscattered particles from the source.

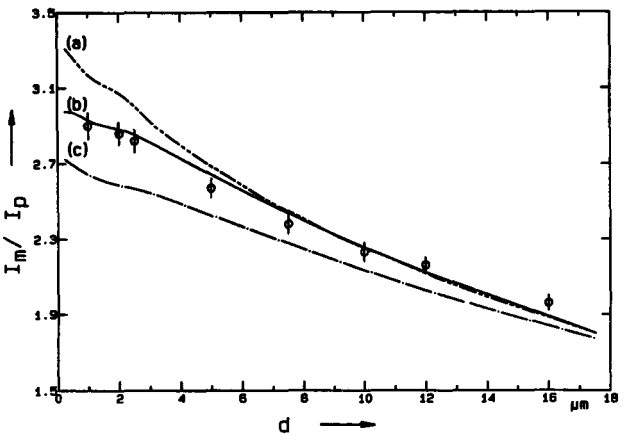

FIGURE 3
Comparison of the experimental ratio of "edge-to-peak" pulse heights, I_m/I_p, for various TE gas pressures in the cavity expressed in units of simulated diameter, d, and the ratios calculated from different stopping power data: (a) Oldenburg and Booz [14], (b) Ziegler [13], (c) SPAR-code [15].

With calibrated ^{244}Cm α-ray sources, spectra were measured for various gas pressures and the experimental edge-to-peak ratios were compared with calculated ratios [12]. This comparison is a sensitive test for the quality of various stopping power predictions around the Bragg maximum. The calculated ratios deviate up to 30%, particularly for low gas pressures (Fig. 3). The best agreement was obtained with the stopping power formulae of Ziegler [13] and the future use of these data is recommended for the calibration of TEPCs.

Very often, commercially available detectors are sealed, although it would be of importance to prove the nominal α-ray energy or the quality of the source-detector arrangement. The comparison of the experimental edge-to-peak ratios of the α-ray spectra with theoretical ratios calculated with the best-suited stopping power data [13] offers a practical tool for quality assurance of the detector.

4. THE USE OF TOF TECHNIQUES WITH TEPC

The TEPC spectra measured in mixed neutron-photon fields can in principle be used to determine the individual dose fractions of different radiation components. The possibility of attributing parts of a spectrum according to the different primary radiation is based on the fact that different secondary particles are produced (namely leptons and hadrons), which have a distinct linear ionization density along the flight path. Various methods of separating the partial doses on the basis of the y spectrum only are described in literature. However, all these methods become more inaccurate with an increasing portion of neutrons of low energy. This is important because in radiation protection practice, mixed fields with strong low-energy neutron components are very frequent. Therefore the TEPC response was investigated separately for photons and neutrons in various monoenergetic neutron fields and also in a field with a broad neutron-energy distribution.

A direct separation of photon and neutron events was achieved by using their difference in time-of-flight (TOF). This technique requires pulsed radiation fields, realised with a pulsed charged-particle beam, and a good timing resolution capacity of the detector. The commercial TEPC have a poor, pulse-height dependent timing resolution capacity. This could be partly compensated for with a special multi-parameter detection system and by optimising the gas composition [16,17]. Figure 4 illustrates how photon and neutron events can be separated.

Ten mixed fields of photons and nearly monoenergetic neutrons of energies between 0.012 and 1.2 MeV produced in the low-scattering area of PTB's accelerator facility were investigated [18,19]. As a result, the photon component could be subtracted with n/γ-separation on the basis of TOF techniques. The resulting dose distributions, y d(y), of pure, monenergetic neutrons are all similar in shape. They are most uniform at lower lineal energies, particularly in the region which overlaps with photon events, whereas differences in incident neutron energy and in energy width are of influence only at higher lineal energies. For lineal energies between the experimental threshold of about 100 eV/µm and 10-20 keV/µm the logarithm of the dose distribution is proportional to the logarithm of y, and the slope

is almost independent of the neutron energy and not influenced by a finite energy width.

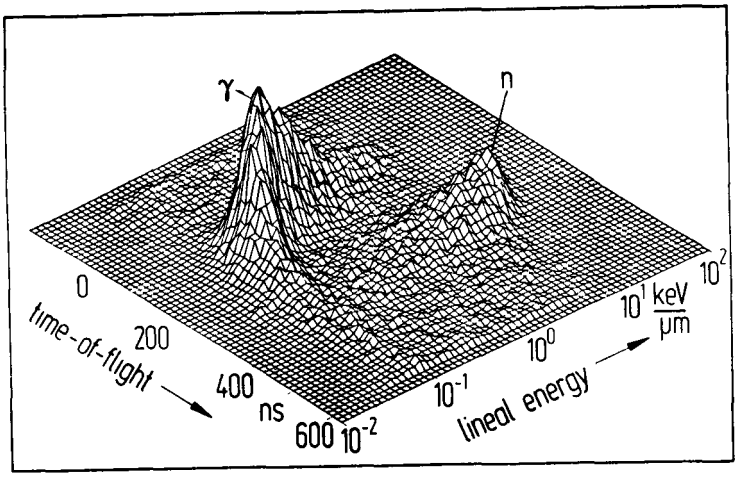

FIGURE 4
The frequency distribution, f(y), plotted as y f(y) versus TOF and the lineal energy, y, is shown for a radiation field with a neutron energy of 35 keV. The regions related to prompt photons (γ) and prompt neutrons (n) from the target are indicated. The random events outside the prompt peaks are caused by room background of photons and scattered neutrons.

By averaging the slopes determined for the different neutron energies investigated, a mean value of 1.6 ± 0.1 was obtained. The measured y distributions of monoenergetic neutrons were also compared with calculated ion yield spectra [20]. These spectra showed, in the same lineal-energy interval as the experimental ones, the same proportionality and energy dependence of the slope.

The same technique was applied for measurements in an intense neutron field produced by bombarding a thick Be target with deuterons with an energy of 13.4 MeV. The neutron spectrum obtained is very broad, covering an energy range between 0.5 and 18 MeV [21,22]. The frequency distribution in two-dimensional representation and the dose distributions separated into the components from prompt photons and neutrons from the target are shown in Figure 5.

The n/γ-separation techniques applied in the wide-spectrum neutron field of the Be + d reaction confirm the simple linear relation of the logarithm of the dose distribution and the logarithm of the lineal energy. On the basis of this result it is possible to propose a method for separating combined dose distribution to obtain partial dose fractions, which method can be

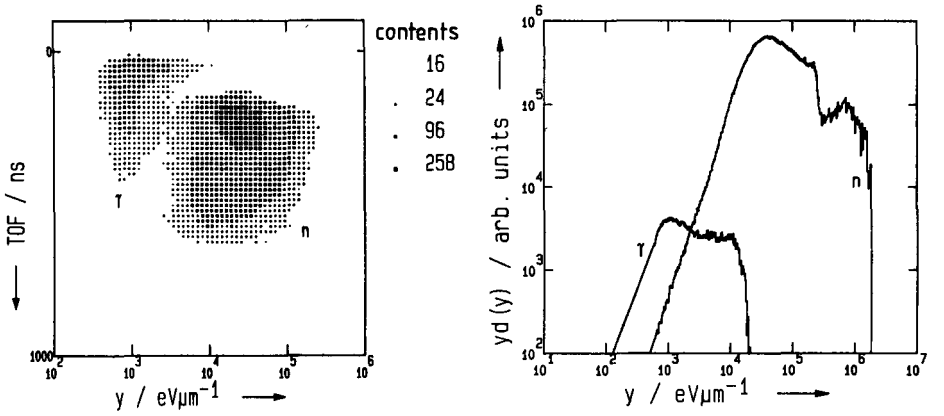

FIGURE 5
Left: The event frequency, y f(y), as function of TOF (flight path 6m) and the lineal energy, y. The regions related to prompt photons (γ) and prompt neutron (n) are indicated. Right: The dose distributions, y d(y), versus the lineal energy, y, separated according to photon and neutron events.

applied without TOF techniques: the neutron and photon dose fractions can be derived by extrapolating the neutron distributions to lower lineal energies assuming the linear relation and a fixed slope of 1.6. As an alternative in unknown neutron fields, the slope can be determined empirically by fitting a straight line to the distribution (in logarithmic representation) between about 10 and 50 keV/μm.

5. CONCLUDING REMARKS

The investigations described in the previous chapters lay the basis for further development towards the realisation of operational dose equivalent quantities in mixed neutron and photon fields. This development requires extensive calculational support.

The combination of neutron transport calculations and energy deposition calculations is required for the theoretical simulation of dosemeters such as TEPCs because the measured energy deposition spectrum and such derived quantities as absorbed dose or dose equivalent are influenced by the neutron scattering in the detector wall and adjacent material.

The code of Caswell and Coyne [20] installed at PTB enables the calculation of neutron-induced secondary charged particles and their energy deposition

in spherical cavities. Recently a Monte Carlo code for neutron and photon transport calculations (MCNP) was also installed at PTB. First results were obtained by calculating the spectral neutron fluence in the wall and the gas of a TEPC in various irradiation geometries and by taking these results as input data for the Caswell/Coyne code to calculate the energy deposition spectra.

Together with the above calculations the TOF technique, employed for neutron-photon separation at low and high energies, should now enable the study of the combination of TEPC and phantom. This technique can also be utilised to investigate the possibility of measuring dose equivalent at high neutron energies (E_n > 30 MeV). Initial results have been obtained from measurements performed at the monoenergetic neutron beam facility at PSI Villigen (collaboration with Universität des Saarlandes, UCL Louvain-la-Neuve and University Basel); they show considerable low-energy neutron contributions which could be corrected for by using the TOF technique.

REFERENCES

[1] Dietze, G., Menzel, H.G., Schuhmacher, H.: Determination of Dose Equivalent with Tissue-Equivalent Proportional Counters. Radiat. Prot. Dosim. 28 (1989), S. 33-36.

[2] Dietze, G., Guldbakke, S., Kluge, H. and Schmitz, Th.: Intercomparison of Radiation Protection Instruments Based on Microdosimetric Principles. PTB-Report ND-29 (1986).

[3] Dietze, G., Booz, J., Edwards, A.A., Guldbakke, S., Kluge, H., Leroux, J.B., Lindborg, L., Menzel, H.G., Nguyen, V.D., Schmitz, Th. and Schuhmacher, H.: Intercomparison of Dose Equivalent Meters Based on Microdosimetric Techniques. Radiat. Prot. Dosim. 23, 227-234 (1988).

[4] Dietze, G., Edwards, A.A., Guldbakke, S., Kluge, H., Leroux, J.B., Lindborg, L., Menzel, H.G., Nguyen, V.D., Schmitz, Th. and Schuhmacher, H.: Investigation of Radiation Protection Instruments Based on Tissue-Equivalent Proportional Counters. Results of a Eurados Intercomparison. EUR 11867 (Luxembourg: CEC) (1988).

[5] Alberts, W.G., Dietz, E., Guldbakke, S., Kluge, H. and Schuhmacher, H.: Radiation Protection Instruments Based on Tissue-Equivalent Proportional Counters: Part II of an International Intercomparison. PTB Report PTB-FMRB-117, Physikalisch-Technische Bundesanstalt, Braunschweig (1988).

[6] Caswell, R.S., Coyne, J.J. and Randolph, M.L.: Kerma Factors for Neutron Energies below 30 MeV. Radiat. Res. 83, 217-254 (1980).

[7] Wagner, S.R., Grosswendt, B., Harvey, J.R., Mill, A.J., Selbach, H.-J. and Siebert, B.R.L.: Unified Conversion Functions fir the New ICRU Operational Radiation Protection Quantities. Radiat. Prot. Dosim. 12, 231-235 (1985).

[8] Alberts, W.G. and Schwartz, R.B.: Comparison of Filtered Neutron Beams at the NBS and PTB Reactors by Calibrating a Spherical Rem Meter.

Proc. 5th Symp. on Neutron Dosimetry, EUR 9762 (Luxembourg: CEC) pp. 629-636 (1985).

[9] Schuhmacher, H., Menzel, H.G., Kunz, A., Coyne, J.J. and Schwartz, R.B.: The Dose Equivalent Response of Tissue-Equivalent Proportional Counters to Low-Energy Neutrons, Radiat. Prot. Dosim. in press.

[10] Menzel, H.G., Lindborg, L., Schmitz, Th., Schuhmacher, H. and Waker, A.J.: Intercomparison of Dose Equivalent Meters Based on Microdosimetric Techniques: Datailed Analysis and Conclusions. Radiat. Prot. Dosim. in press.

[11] Dietze, G., Menzel, H.G. and Bühler, G.: Calibration of tissue-equivalent proportional counters used as radiation protection dosemeters. Radiat. Prot. Dosim. 9, 245-250 (1984).

[12] Schrewe, U. J., Brede, H. J., Pihet, P. and Menzel, H.G.: On the Calibration of Tissue-Equivalent Proportional Counters With Built-In α Particle Sources, Radiat. Prot. Dosim. 23, 249-252 (1988).

[13] Ziegler, J. F.: Helium Stopping Powers and Ranges in all elements. Vol. 4, Pergamon Press, New York, Toronto, Oxford, Sydney, Frankfurt, Paris (1977).

[14] Oldenburg, U. and Booz, J.: Mass Stopping Power and Pathlength of Neutron Produced Recoils in Tissue and Tissue Equivalent Materials, I. Neutron Energy < 6 MeV, Report No. EUR 4786 e (1972).

[15] Armstrong, T. W. and Chandler, K. C.: Stopping Powers and Ranges for Muons, Charged Pions, Protons, and Heavy Ions. Nucl. Instrum. Meth. 113, 313 (1973).

[16] Schrewe, U. J., Brede, H. J. and Dietze, G.: Dosimetry in Mixed Neutron-Photon Fields with Tissue-Equivalent Proportional Counters. Radiat. Prot. Dosim., in press.

[17] Schrewe, U. J. and Langner, F.: A Multi-Parameter Data Acquisition System For Microdosimetric Detectors Including Time-Resolving Measurements. PTB-Report, in preparation.

[18] Schrewe, U. J., Brede, H. J. and Dietze, G.: Investigation of Tissue-Equivalent Proportional Counters in Mixed Neutron-Photon Fields also Applying Time-of-Flight Techniques. Radiat. Prot. Dosim. 23, 239-243 (1988).

[19] Schrewe, U. J., Schuhmacher, H., Brede, H. J. and Dietze, G.: Determination of Photon Neutron Dose Fractions with Tissue-Equivalent Proportional Counters. Radiat. Prot. Dosim., in press.

[20] Coyne, J. J. and Caswell, R. S.: Microdosimetric Energy Deposition Spectra and Their Averages for Bin-Averaged and Energy-Distributed Neutron Spectra. Proc. 7th Symp. on Microdosimetry, eds. J. Booz, H. G. Ebert and H. D. Hartfield, EUR 7147, 689-696, (1980).

[21] Brede, H. J., Dietze, G., Schrewe, U. J., Tancu, F. and Wen, C.: Investigation of Intense Neutron Fields. Radiat. Prot. Dosim. 23, 301-304 (1988).

[22] Brede, H. J., Dietze, G., Kudo, K., Schrewe, U. J., Tancu, F. and Wen, C.: Neutron Yields from Thick Be Targets Bombarded With Deuterons or Protons. Nucl. Instr. and Meth. A274, 332-344 (1989).

IV. Other research group(s) collaborating actively on this project [name(s) and address(es)]:

- H. G. Menzel, Inst. für Biophysik der Univ. des Saarlandes, D-6650 Homburg
- EURADOS Committee 1 ("Dose equivalent meters based on microdosimetric techniques")
- J. J. Coyne, R. B. Schwartz, National Institute for Standards and Technology, Gaithersburg, MD
- R. Henneck, Inst. für Pysik der Univ., CH-4056 Basel
- J. P. Meulders, Inst. de Physique Nucleaire, Université Catholique Louvain-la-Neuve, B-1343 Louvain-la-Neuve.

V. Publications:

1. Schuhmacher, H., Alberts, W.G., Menzel, H.G. and Buehler, G.: Dosimetry of Low-Energy Neutrons Using Low-Pressure Proportional Counters. Radiat. Res. 111, 1-13 (1987).
2. Dietze, G., Guldbakke, S., Kluge, H. and Schmitz, Th.: Intercomparison of Radiation Protection Instruments Based on Microdosimetric Principles. PTB-Report ND-29 (1986).
3. Schuhmacher, H., Menzel, H.G. and Kluge, H.: Dosimetry of a bare and a D_2O-moderated Cf252 source using low-pressure proportional counters. Radiat. Prot. Dosim. 19, 103-109 (1987).
4. Dietze, G., Booz, J., Edwards, A.A., Guldbakke, S., Kluge, H., Leroux, J.B., Lindborg, L., Menzel, H.G., Nguyen, V.D., Schmitz, Th. and Schuhmacher, H.: Intercomparison of Dose Equivalent Meters Based on Microdosimetric Techniques. Radiat. Prot. Dosim. 23, 227-234 (1988).
5. Schrewe, U. J., Brede, H. J., Pihet, P. and Menzel, H.G.: On the Calibration of Tissue-Equivalent Proportional Counters With Built-In α Particle Sources, Radiat. Prot. Dosim. 23, 249-252 (1988).
6. Schrewe, U. J., Brede, H. J. and Dietze, G.: Investigation of Tissue-Equivalent Proportional Counters in Mixed Neutron-Photon Fields also Applying Time-of-Flight Techniques. Radiat. Prot. Dosim. 23, 239-243 (1988).
7. Alberts, W.G., Dietz, E., Guldbakke, S., Kluge, H. and Schuhmacher, H.: Radiation Protection Instruments Based on Tissue-Equivalent Proportional Counters: Part II of an International Intercomparison. PTB Report PTB-FMRB-117, Physikalisch-Technische Bundesanstalt, Braunschweig (1988).
8. Alberts, W.G.; Dietz, E.; Guldbakke, S.; Kluge, H. and Schuhmacher, H.: International Intercomparison of TEPC systems used for Radiation Protection. Radiat. Prot. Dosimetry (1989), in press.
9. Pihet, P.; Menzel, H.G.; Alberts, W.G. and Kluge, H.: Response of tissue equivalent proportional counters to low and intermediate energy neutrons using modified TE-^{3}He gas mixtures. Radiat. Prot. Dosimetry (1989), in press.

10. Menzel, H.G., Lindborg, L., Schmitz, Th., Schuhmacher, H. and Waker, A.J.: Intercomparison of Dose Equivalent Meters Based on Microdosimetric Techniques: Datailed Analysis and Conclusions. Radiat. Prot. Dosim., in press.

11. Schrewe, U. J., Brede, H. J. and Dietze, G.: Dosimetry in Mixed Neutron-Photon Fields with Tissue-Equivalent Proportional Counters. Radiat. Prot. Dosim., in press.

12. Dietze, G., Edwards, A.A., Guldbakke, S., Kluge, H., Leroux, J.B., Lindborg, L., Menzel, H.G., Nguyen, V.D., Schmitz, Th. and Schuhmacher, H.: Investigation of Radiation Protection Instruments Based on Tissue-Equivalent Proportional Counters. Results of a Eurados Intercomparison. EUR 11876 (Luxembourg: CEC) (1988).

13. Menzel, H.G., Dietze, G., Schuhmacher, H.: Practical Determination of Dose Equivalent Using Low-Pressure Tissue-Equivalent Proportional Counters. Radiation Protection Practice, Vol. I, 308-311 (1988) (Pergamon Press, Sydney).

14. Dietze, G., Menzel, H.G., Schuhmacher, H.: Determination of Dose Equivalent with Tissue-Equivalent Proportional Counters. Radiat. Prot. Dosim. 28 (1989), S. 33-36.

15. Brede, H. J., Dietze, G., Kudo, K., Schrewe, U. J., Tancu, F. and Wen, C.: Neutron Yields from Thick Be Targets Bombarded With Deuterons or Protons. Nucl. Instr. and Meth. A274, 332-344 (1989).

16. Schrewe, U. J., Schuhmacher, H., Brede, H. J. and Dietze, G.: Determination of Photon Neutron Dose Fractions with Tissue-Equivalent Proportional Counters. Radiat. Prot. Dosim., in press.

17. Schuhmacher, H., Menzel, H.G., Kunz, A., Coyne, J.J. and Schwartz, R.B.: The Dose Equivalent Response of Tissue-Equivalent Proportional Counters to Low-Energy Neutrons, Radiat. Prot. Dosim., in press.

Internal Report:

1. Schrewe, U. J. and Langner, F.: A Multi-Parameter Data Acquisition System For Microdosimetric Detectors Including Time-Resolving Measurements. PTB-Report, in preparation.

Title of the project no.: 3

INVESTIGATION OF DOSE EQUIVALENT QUANTITIES FOR INDIVIDUAL DOSIMETRY

Head(s) of project:

B R L Siebert

Scientific staff:

Prof. Dr. W.G. Alberts, B.W Bauer, Dr. E. Dietz, Dr. S. Guldbakke, R. Hollnagel, Prof. Dr. R. Jahr, H. Kluge

I. Objectives of the project:

Experimental and theoretical examination of individual dosemeters. Investigation of procedures for calibration and evaluation of individual dosemeters in order to achieve compliance with the system of dose limitation for radiation protection. Investigation and intercomparison of appropriate quantities for individual dosimetry (choice of phantoms and measurement positions).

II. Objectives for the reporting period:

1. Supplementary measurements, especially using bare and D_2O-moderated ^{252}Cf sources.
2. Completion and application of a Monte Carlo programme for predicting theresponse of dosemeters on phantoms if their fluence response in free air is known.
3. Summary report on the experimental results.
4. Theoretical interpretation of the results and discussion of appropriate quantities for individual dosimetry in neutron fields.

III. Progress achieved:

INTRODUCTION

Dose equivalent (DE) quantities for the assessment of individual radiation exposure are defined in the human body whereas DE-meters are worn on the body to estimate one of these DE quantities for external irradiation. The primarily limiting quantity for radiation protection dosimetry is the *effective* DE, H_E [1]; it is a weighted mean of DE in various organs and is related to risk within a system of dose limitations. H_E is defined for all kinds of external and internal irradiation.

This project is devoted to practical problems with individual monitoring for external irradiation with neutrons. In routine radiation protection practice neutrons occur less frequent than photons. However, on account of the properties of neutrons (e.g. the strong dependence of kerma and quality factor on the spectrum) one may in general apply radiation concepts derived for neutrons to photon dosimetry, but not necessarily vice versa.

The ICRU recommends[2] for individual monitoring for strongly penetrating radiation the *Individual Dose Equivalent, Penetrating*, $H_p(d)$, which is defined as the DE below a specified point on the body at a depth d that is appropriate for strongly penetrating radiation. The recommended depth is $d = 10$ mm.

In practice phantoms are used to define operational DE quantities and to calibrate DE-meters. Different design aims may be pursued for phantoms for defining and for calibrating. The MIRD-V phantom in its original or further developed form is used for H_E. A detailed discussion may by found e.g. in [3,4]. The soft-tissue ICRU sphere serves as phantom for defining operational DE quantities [2,5,6], however, other phantoms, such as a soft-tissue slab are also being discussed. The choice of phantoms for calibrating is still under discussion. In one concept, it is proposed to select a phantom which simulates the influence of the body on the DE-meter reading in an appropriate approximation; another concept requires a phantom which serves for defining an operational DE quantity and for calibrating an individual monitor at the same time.

An extensive discussion of these concepts, pure and in mixed forms, took place in two seminars [7,8] on the implementation of the newly introduced ICRU quantities [2]. The new quantities for individual monitoring, however, still pose conceptual and practical problems. The conceptual problems are due to the pecularities of human beeings, as to geometry, composition and structure, and the human behaviour in the environment [9], i.e. the varying exposure conditions of workers in the field. The practical problems concern the implementation which requires agreed upon calibration procedures and conversion factors.

Within this project work was spent on contributing to agreed upon conversion factors and the influence of phantom shape and material on calibration procedures was studied in detail experimentally and theoretically. Mainly thermoluminescence albedo dosemeters have been selected for our experimental studies as they are widely used in routine practice. The Monte Carlo method has been used for the theoretical studies.

CHOICE OF PHANTOMS.

The discussion on phantoms can be guided by using the concept of *independence-of-shape approximation* (ISA) [10,11] which is schematically representated in Figure 1 for normally incident neutrons. The basic

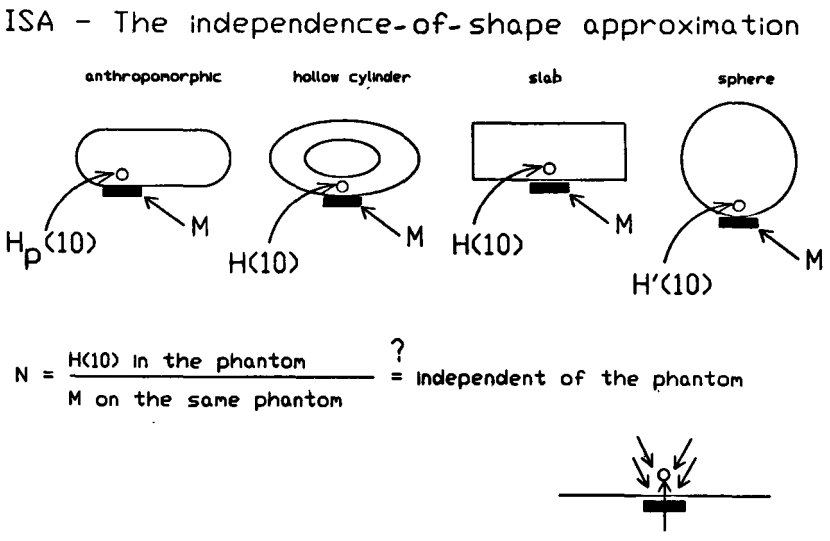

Figure 1. Schematic view of the Independence-of-Shape Approximation. The insert in the lower right corner depicts the irradiation of dosemeters in AP geometry

idea is that $H(10)$ and the reading of a DE-meter vary for any given reasonable phantom in such a way that the calibration factor is nearly unaffected by the choice of the phantom. In this concept a distinction between phantoms for defining and calibrating is not required. For practical radiation protection within the system of dose limitations one may tolerate deviations of -30% and +50%. In practice the material of the phantom for calibration and for defining DE are different, as DE is always defined in standard soft-tissue, whereas the calibration phantoms consists of polyethylene. $H(10)$ has been also computed for phantoms consisting of polyethylen, here, however, an infinitesimal sphere consisting of soft-

tissue about the point of reference has been assumed in the calculation. The DE calculated in this manner serves to understand material dependent neutron transport.

In a generalized way ISA is understood to encompass the case of practical relevance where DE is defined in a soft-tissue phantom and the calibration is performed on a phantom consisting of polyethylene or other practicable materials.

The choice of phantoms for the experimental studies was guided by the intention to supply data to all aspects of the above mentioned discussion. Many types of neutron detectors used as monitors in individual dosimetry utilize or are influenced by the albedo, i.e back scatter, from the wearer. An appropriate calibration procedure should account for this effect, which is quite important for TLDs[12]. Apart from resonances in cross sections, e.g. ^{16}O at 1 MeV, materials with approximately the same hydrogen content produce similar albedo when irradiated from the frontal half-space. Polyethylene was therefore selected as it is easily available and well suited for shaping different phantoms without the need for complicated containments.

As ICRU suggested the sphere not only as phantom for *defining* DE but also for *calibrating*, a polyethylene sphere of 30 cm in diameter has been selected; this phantom is termed SPP. For the routine calibration *practice* a slab is often preferred. Therefore a polyethylene slab, of 40 cm in width and height and 15 cm in thickness has also been added; this phantom is termed SLP. Finally, as a more *anthropomorphic* phantom a hollow ellptical polyethylene cylinder of 70 cm in height and with outer and inner semiaxes of 20 cm and 10 cm, and 8 cm and 4 cm, respectively, has been created; this phantom is termed CYP.

The sphere is not a suitable phantom for irradiations from the back. Phantoms sufficiently anthropomorphic with respect to both, material and shape, are then needed to obtain reliable results for such irradiation geometries. The hollow elliptical cylinder may be used as an appproximation to study such irradiation geometries.

For the theoretical study phantoms consisting of ICRU soft-tissue have been added: the sphere itself (SPI), the slab (SLI), the cylinder (CYI) and an additional hollow elliptical cylinder of 70 cm in height and with outer and inner semiaxes of 20 cm and 10 cm, and 8 cm and 7 cm, respectively. This phantom is termed CAI, and is considered as simple substitute for the MIRD V phantom within the context of the present study.

EXPERIMENTAL RESULTS

Experimental studies of three albedo dosemeter systems supplied by CEN (Fontenay-aux-Roses: FR), KfK (Karlsruhe: KR) and PTB (Braunschweig: BR) have been performed.

The dosemeters were irradiated free in air and attached to the phantoms SPP, SLP and CYP. In addition to AP (anterior-posterior) and PA (posterior-anterior), irradiation geometries under 30^0, 60^0 and 90^0 were implemented. The slab phantom SLP has been only used in AP geometry.

The PTB Research and Measurement Reactor Braunschweig (FMRB) provided thermal, 2 keV (scandium filter), 24 keV (iron filter) and 144 keV (silicon filter) neutrons. The PTB Van-de-Graaff accelerator was used to produce monoenergetic neutron fields at higher energies: 144 keV, 250 keV and 570 keV using the reaction Li(p,n); 1.2 MeV and 2.5 MeV using the reaction T(p,n); and 5.0 MeV using the reaction D(d,n). Furthermore, reference radiations from a bare and a D_2O moderated ^{252}Cf source were provided. These fields encompass all ISO energies from thermal up to 5 MeV.

Table 1 **Summary on Experimental Results of R_Φ for Albedo Neutron Dosemeters and Intercomparison with Calculated Ratios of R_Φ on CYP and SLP to R_Φ on SPP for Normally Incident Neutrons.**

E_N	th.	2 keV	24 keV	144 keV	250 keV	570 keV	1.2 MeV	2.5 MeV	5 MeV
R_Φ(SPP) *									
KR/pSvcm^2	*38.3*	*166*	*130*	*110*	*131*	*68*	*55*	*38*	*24*
FR/KR	6.7	0.96	0.95	0.78	0.71	0.76	0.78	0.72	0.96
BR/KR	0.72	0.75	0.70	0.72	0.61	0.75	0.71	0.70	0.79
R_Φ(CYP)/R_Φ(SPP)									
KR	1.07	1.11	1.17	1.16	1.11	1.16	1.47	1.46	1.32
FR	1.15	1.17	1.12	1.32	1.39	1.24	1.01	1.10	0.89
BR	1.08	1.02	1.20	1.27	1.29	1.20	1.15	1.29	1.20
MC	1.03	1.07	1.08	1.11	1.10	1.16	1.17	1.14	1.13
R_Φ(SLP)/R_Φ(SPP)									
KR	1.02	1.19	1.27	1.20	1.35	1.29	1.51	1.49	1.38
FR	1.11	1.11	1.11	1.34	1.22	1.39	1.12	1.29	1.34
BR	1.08	1.07	1.31	1.33	1.28	1.32	1.36	1.51	1.48
MC	1.03	1.09	1.10	1.13	1.13	1.19	1.22	1.23	1.33
R_Φ(Free in Air) *									
KR/pSvcm^2	*16.7*	*50*	*15*	*8*	*18*	*4*	-	-	-
FR/KR	12	0.72	0.79	1.04	0.99	0.59	-	-	-
BR/KR	0.73	0.63	0.67	0.78	0.69	0.59	-	-	-

KR, FR and BR — experimental results from KfK, Karlsruhe, CEN, Fontenay-aux-Roses, and PTB, Braunschweig, respectively.

MC — Monte-Carlo results [23] for a simplified albedo dosemeter.

*) Fluence response for albedo dosemeters, R_Φ, on SPP or free in air.

KR — Absolute fluence response, in terms of pSvcm^2, reading in terms of pSv obtained with a calibration factor using ^{60}Co exposure. Absolute values are indicated by *italics*.

FR/KR, BR/KR — Ratios of fluence responses on SPP for FR and BR to those for KR

Preliminary results have been published earlier [13]. A full presentation of all measured data, which include irradiations under different angles of incidence can be found in a separate report [14], which also describes the irradiation facilities in sufficient detail. A detailed analysis of the results for the BR dosemeter is given in an additional report [15]. The latter report discusses also irradiation of the PTB dosemeter on an Alderson phantom. Using a bare ^{252}Cf source the influence of phantom shape on the dosemeter reading has been studied using the above mentioned and additional phantoms [16].

The results for AP irradiation are shown in Table 1. The influence of the phantoms for AP irraddition is shown by tabulating the ratio of R_Φ on CYP or SLP to R_Φ on SPP.

If order to achieve better basic data for the calculation at higher energies α-paricle cross sections on carbon have been measured, using the response of a liquid scintillator [17].

CALCULATIONAL AND THEORETICAL RESULTS

The strong energy dependence of albedo dosemeters (TLD) affords the use of additional dosemeters if measurements in neutron fields with unknown spectrum are to be performed. One possiblity is to use etched track (TED) dosemeters for this purpose. Calculations [18] of the response of pairs of a TLD and a TED on the ICRU-Phantom (SPI) showed that the energy variation of the DE response in the energy region from thermal up to 14 MeV of such a pair of dosemeters can be kept within one order of magnitude.

In critical working environments, where doses near the investigation threshold could occur, it may be necessary to take into account the angular distribution of the neutron field and to wear more than one dosemeter. By calculating the response of a system of two albedo Dosemeters worn on chest and back in various directionally distributed neutron fields [19] it could be shown that the angular dependence of the effective DE response in monoenergetic fields energy region from 1 eV up to 14 MeV can be reduced to ± 43% and even better in more realistic fields such as a D_2O moderated ^{252}Cf fission neutron field, namely to ± 10%.

The influence of phantoms on the response of TEDs is less prominent but by no means negligible, as could be shown by calculations[20]. In a numerical study of the influence of phantom material and shape on the calibration of individual dosemeters for neutrons [21] the trend found in experiments could be by and large reproduced. An analogous study, however, using the MIRD V phantom [22] revealed some phantom effects, too. An additional numerical study includes the computation of $H(10)$ in various phantoms [23]. Calculated ratios for R_Φ for a simplified albedo dosemeter on CYP or SLP to R_Φ on SPP are shwon in Table 1. Additional results concerning the total neutron fluences on the surface of the phantoms, $\Phi(0)$, and in 10 mm depth,

Table 2 **Computational study of phantom influences on a simplified albedo dosemeter.**

Absolute values are indicated by *italics* and given for SPI
The units given pertain only to values for SPI

PHANTOM		SPI	SPP/SPI	SLP/SPI	CAI/SPI	SPI	SPP/SPI	SLP/SPI	CAI/SPI
E_N			25.3 meV				2 keV		
$\Phi(10)$		*2.483*	.77	.74	.97	*2.848*	1.01	1.02	.98
h(10)	/pSvcm^2	*4.48*	.75	.72	.97	*2.30*	1.02	.98	.92
$\Phi(0)$		*1.646*	1.00	1.01	1.01	*1.362*	1.00	1.03	1.01
R_Φ	/cm^2	*.643*	1.00	1.03	1.02	*.216*	1.02	1.11	1.05
E_N			24 keV				144 keV		
$\Phi(10)$		*2.776*	1.03	1.04	.98	*2.544*	1.06	1.10	1.04
h(10)	/pSvcm^2	*11.96*	.82	.84	.98	*92*	.87	.88	1.04
$\Phi(0)$		*1.372*	1.01	1.03	1.01	*1.337*	1.01	1.03	1.00
R_Φ	/cm^2	*.152*	1.02	1.12	1.00	*.105*	1.05	1.19	.96
E_N			250 keV				570 keV		
$\Phi(10)$		*2.472*	1.00	1.07	.95	*2.142*	1.06	1.14	.98
h(10)	/pScvm^2	*150*	.88	.89	.96	*241*	.93	.96	1.03
$\Phi(0)$		*1.322*	1.00	1.02	.99	*1.278*	.99	1.02	.99
R_Φ	/cm^2	*.108*	1.02	1.15	.91	*.067*	1.01	1.20	.89
E_N			1.0 MeV				1.2 MeV		
$\Phi(10)$		*2.164*	.98	1.03	.96	*1.909*	1.05	1.13	1.00
h(10)	/pSvcm^2	*369*	.86	.88	.96	*329*	.98	.98	1.03
$\Phi(0)$		*1.371*	.90	.92	.98	*1.252*	.97	1.00	.98
R_Φ	/cm^2	*.052*	1.00	1.19	.84	*.045*	1.03	1.26	.85
E_N			2.5 MeV				5.0 MeV		
$\Phi(10)$		*1.594*	1.15	1.20	.97	*1.500*	.99	1.14	.90
h(10)	/pSvcm^2	*331*	1.07	1.06	1.02	*405*	.97	1.06	.96
$\Phi(0)$		*1.158*	1.02	1.04	.98	*1.123*	1.01	1.03	.98
R_Φ	/cm^2	*.027*	1.11	1.37	.81	*.015*	1.15	1.53	.86

QUANTITIES:

E_N Incident neutron Energy

$\Phi(10)$ Total neutron fluence in 10 mm depth per incident neutron fluence.

h(10) Dose equivalent per incident fluence. The DE in SPP, CYP and SLP has been computed in an infinitesimal sphere in 10 mm depth consisting of ICRU-soft tissue. The contribution from secondary photons is excluded.

$\Phi(0)$ Total neutron fluence on the surface per incident neutrom fluence.

R_Φ Response of TLD-chip containing ^{6}Li and 0.89 mm thick and shielded with Cd against thermal neutrons on the side facing the neutron source.

$\Phi(10)$, and R_Φ for the simplified albedo dosemeter and the DE in 10 mm depth, H(10) are given in Table 2. The simplified albedo dosemeter is simulated by calculating the fluence fraction reacting with ^{6}Li in a 0.89 mm thick LiF chip, which is shielded to the incident thermal neutrons with a Cd layer. The influence of the different phantoms is demonstrated by the corresponding ratios as indicated in the first row of the table.

In order to supply aggreed upon fluence to DE conversion factors for individual neutron dosimetry calculation for H_E have been performed [4] and

a procedure for standardising the relationship between the directional DE [2] and neutron fluence has been proposed [6].

Finally, theoretical work was published, in which operational quantities and calibration procedures for individual monitoring in terms of H_E and the new ICRU DE quantities have been proposed [24,25].

DISSCUSSION OF RESULTS.

The albedo neutron dosemeter is well suited to study the concept of ISA as its reading depends quite strong on the albedo neutrons emanating from the phantom. This can bee seen in Table 1 by intercomparing the response on phantoms to the response free in air (cf. Table 1). The difference in fluence response can be explained by the different construction and/or evaluation procedures. The large difference between R_Φ for FR with respect to R_Φ for KR and BR for thermal neutrons is caused by differences in design: The FR albedo dosemeter is not shielded against incident thermal neutrons. The differences between R_Φ for KR and BR are explained by different procedures of integrating the glow curves. Despite of the variance of single albedo dosemeter measurements the expected trends are observable. More details may be found in the above mentioned report [14]. The extent to which ISA is a valid approximation can also be seen in Table 1. The Monte Carlo results [23] pertains to a first order approximation to the dosemeter consisting of a bare chip of ^{6}LiF. In real dosemeters one expects some moderation of the incident neutrons by the constructional material. This effect enhances the experimental ratios. In addition, in real dosemeters thermal neutrons are affected by intrigue design. Considering the simplified approach the agreement between experiments and calculations is satisfying and justifies to draw conclusions from the Monte Carlo results.

Apart from the difference due to material $H(10)$ does not depend significantly on the shape of the phantom, except for CAI at 2 keV (cf. Table 2). This is also true when considering SLI and CYI [23] which are not shown here. The calculations do not include the contributions from secondary photons. Their contribution is only of importance at energies up to 24 keV (≈ 10%), it peaks at 2 keV with ≈ 30%. This contribution is approximatively proportional to a weighted average of $\Phi(0)$ and $\Phi(10)$, which at low energies do not depend significantly on the shape of the phantom. Therefore the inclusion of secondary photons would not change the ratios of $H(10)$ significantly.

The physical explanation of the insensitivity of $H(10)$ with respect to phantom shape is given by the dependence of the cross section density, the kerma factor and the quality factor for neutrons on energy. For thermal neutrons $\Phi(10)$ is dominated by scattered neutons and the thermal equilibrium does not depend much on shape details at the surface. With increasing neutron energy $\Phi(10)$ is influenced by this shape. Here, however,

the contribution of the unscattered neutrons becomes more and more important, at 5 Mev this fraction amounts to ≈ 50%. The kerma and quality factor at high energies increase the relative importance of the unscatterered fraction. Therefore the difference due to shape effects in the scattered fraction is "washed out".

The situation at the surface, i.e. for the albedo dosemeters is quite different. The contribution to $\Phi(0)$ by the incident neutrons increases of course with increasing energy, too. Here, however, due to the $^1/_v$ cross section of $^6Li(n,\alpha)$, the scattered fraction (albedo) contributes increasingly to the dosemeter reading. The shape of the surface has, apart from thermal neutrons , strong influence on the scattered neutrons. The curvature of the surface determines the amount of mass which contributes to the albedo. For this reason the ratio of the readings on SPP and CYP does depend on the angle of incidence of the primary neutrons. For an angle of incidence of 90^0,i.e. LAT, the readings on SPP are generally higher than on CYP. This is shown in [13,14,15] but of no concern here, as this report is devoted to the problem of routine calibrations using AP geometry.

At very high energies the phantom CAI produces smaller values of $\Phi(10)$ and $\Phi(0)$. This is due to the "lung" which simulated as a simple void.

The data given in Table 2 allow to juge the quality of ISA. Considering the phantom SPI as phantom for defining and as anthropomorhic, i.e. simulating the body of an exposed person, calibration on SLP would lead to an underestimation from 1.03^{-1} for thermal neutrons up to 1.53^{-1} for 5 MeV, i.e. by the inverse of the corresponding ratios specified for R_Φ for SLP/SPI. However, for energies where the albedo dosemeter may be meaningfully used this correction amounts to less than 20%. If the phantom CAI were considered as phantom for defining, then the ratio of R_Φ for SLP/CAI could be used as correction factor. Up to 144 keV these corection factors are almost idendical with the first mentioned ones.

In summary, as far as albedo dosemeters are used one can safely rely on ISA. This allows to select a polyethylene slab as calibration phantom. It is interesting to note the ISA is valid, not due to a homologous influence of phantom shape on DE and dosemeter response, but rather due to acceptably small variations of the dosemeter reading (c.f. Table 2). These findings are also true for Monte Carlo simulated idealised fluence , kerma and dose equivalent meters [23].

CONCLUSIONS

Routine radiation protection encounters usually doses way below the investigation threshold. Wearing one dosemeter is then sufficient and the influence of spectral and angular distribution may be accounted for by using appropriate calibration factors and positions for wearing the dosemeter. For these routine cases a calibration with neutron fields such

as thermal or the D_2O moderated ^{252}Cf source and using the simple AP irradiation geometry is felt to be sufficiently safe.

The results obtained for neutron albedo dosmeters are in compliance with ISA for such routine applications. This should influence the intense discussion on calibration practice still underway in literature: it gives room for several basic concepts, as their implementation leads to interpretational but not physical differences. The interpretational differences, however, can be quite important in view of juridical and metrological problems.

The data presented may serve to derive appropriate correction factors for phantom shape and material for both, the dosemeter reading and the DE quantity used, if this should be desirable in the context of a specific calibration concept. These calculated factors can be termed reliable as demonstrated by intercomparing some of the calculations with experiments.

In case of non-routine applications, i.e. in environments where the investigation threshold might be exceeded, ISA may be not sufficient. Here a careful analysis of the distribution of the field in energy and angle is required and additional experimental and theoretical work needed.

The dependence of dosemeter readings on phantom shape and material has also been found for photon radiation experimentally [26] and in calculations [27]. These results are also in compliance with ISA.

In summary ISA is a valid concept for practical calibration and routine radiation protection.

ACKNOWLEDGMENT

The helpful assistance by the technical staff at the irradiation facilities and the central computer of PTB is acknowledged.

REFERENCES

1.) International Commission on Radiological Protection (ICRP): *Recommendations of the International Commission on Radiological Protection.* ICRP Report 26, Annals of the ICRP (1977)

2.) International Commission on Radiation Units and Measurements. *Determination of Dose Equivalents Resulting from External Radiation Sources.* ICRU Report 39 (Bethesda,MD(USA):ICRU Public.) (1985)

3.) Egbert, S.D.: *Anthropomorphic Phantoms.* Transactions of the American and European Nuclear Society, TANSAO 57 (1988), p. 216-217

4.) Hollnagel, R.A.: *Effective Dose Equivalent and Organ Doses for Neutrons from Thermal to 14 MeV.* acepted for publication in Rad.Prot.Dosim.

5.) Alberts, W.G.: *Calibration of Individual Monitors Using the New ICRU Quantities.* Rad.Prot.Dosim. 27 (1989) p. 245-249

6.) Siebert, B.R.L.; Morhart, A.: *A Proposed Procedure for Standardising the Relationship between the Directional Dose Equivalent and Neutron Fluence.* Rad.Prot.Dosim. 28 (1989) p. 47-51

7.) Booz, J.; Dietze, G. (Editors): *Radiation Protection Quantities for External Exposure.* Radiat.Prot.Dosim. 12 No.2 (1985)

8.) Dietze, G.; Booz, J.:(Editors): *Implementation of Dose-Equivalent Operational Quantities into Radiation Protection Practice.* Rad.Prot.Dosim. 28 No.1-2 (1989)

9.) Wagner, S.R.:*Personal Dosimetry and the New Quantities in Radiation Protection.*

10.) Harder, D., Göttingen (FRG): priv. communication (1989) and in epilogue to ref.7, p. 229 - 230

11.) Alberts, W.G.; Dietze, G.:: *Practical Calibration of Neutron Area and Individual Monitors.* Rad.Prot.Dosim. **12** (1985) p. 163-166

12.) Hollnagel, R.; Jahr, R.; Siebert, B.R.L.: *Estimation by Means of Albedo Fluence Calculations of the Response of Individual Neutron Dosemeters Fixed to Phantoms.* Proc. 5th Int. Symp. on Neutron Dosimetry. EUR 9762 (Luxemburg:CEC) (1985) p. 123-132

13.) Bauer, B.W., Alberts, W.G.; Burgkhardt, B.; Guldbakke, S.; Medioni, R.; Piesch, E.; Portal, G.; Siebert, B.R.L.: *Energy and Angle Dependence of and Phantom Influence on Readings of Neutron Individual Dosemeters: First Results of Experiments.* Rad.Prot.Dosim. **28** (1989) p. 115-119

14.) Bauer, B.W., Alberts, W.G.; Burgkhardt, B.; Dietz, E.; Guldbakke, S.; Jahr, R.; Kluge, H.; Medioni, R.; Piesch, E.; Portal, G.; Siebert, B.R.L.: *Experimental Investigation of Neutron Individual Dosemeters with respect to the Influences of Neutron Energy, Angle of Incidence and Phantom Shape: Experimental Procedure and Summary of Results.* In preparation as external PTB Report

15.) Bauer, B.W., Alberts, W.G.; Luszik-Bhadra M.; Siebert, B.R.L.: *Experimental Investigation of Response of an Albedo Neutron Individual Dosemeters with respect to the Influences of Neutron Energy, Angle of Incidence and the Use of Phantoms. Shape: Detailed Analysis of Results for the Albedo Neutron Dosemeter used at PTB.* In preparation as external PTB Report

16.) Alberts, W.G.: *Response of an Albedo Neutron Dosemeter to ^{252}Cf Neutrons on Various Phantoms.* Rad.Prot.Dosim. **22** (1988) p. 183-186

17.) Brede, H.J.; Dietze, G.; Klein, H.; Schölermann , H.: *Determination of Neutron Induced α-particle Cross Sections on Carbon Using the Response of a Liquid Scintillation Detector.* (accepted for publication in Nucl.Sci. and Eng.)

18.) Siebert, B.R.L.; Hollnagel, R.; Jahr, R.: *Calculated Dose Equivalent Responses of Albedo and Track Etch Individual Neutron Dosemeters on the ICRU-Phantom.* In: Twenty Years Experience in Radiation Protection: Compacts of 4th Europ. Congr. and 13th Regional Congr. of the Intern. Radiat. Prot. Association. (IRPA) , Salzburg 1986. (Seibersdorf:Österr. Verb. f.Strahlenschutz, 1988, p 563-567)

19.) Jahr, R.;Hollnagel, R.; Siebert, B.R.L. *Response of a System of two Albedo Dosemeters Worn on Chest and Back in Various Directionally Distributed Neutron Fields.* Rad.Prot.Dosim. **23** (1988) p. 139-142

20.) Hollnagel, R.; Jahr, R.; Siebert, B.R.L.:*The Influence of Phantoms on the Response of Etched Track Detectors.* Rad.Prot.Dosim. **20** (1987) p. 25-29

21.) Bauer, B.W., Hollnagel, R.; Siebert B.R.L.: *Numerical Study of the Influence of Phantom Material and Shape on the Calibration of Individual Dosemeters for Neutrons* Rad.Prot.Dosim. **23** (1988) p. 207-210

22.) Hollnagel R.; Alberts W.G.: *Reading of Personal Neutron Dosemeters on the MIRD phantom.* (accepted for publication in Rad.Prot.Dosim.)

23.) Siebert, B.R.L.; Alberts, W.G. ; Bauer, B.W.: *Computational Study of Phantoms for Indidvidual Neutron Dosimetry.* In preparation as external PTB Report

24.) Jahr, R.; Siebert, B.R.L.; Alberts, W.G.: *Operational Quantities and Calibration Procedures for Individual Monitoring.* Rad.Prot.Dosim. **28** (1989) p. 33-36

25.) Siebert, B.R.L. Jahr, R.: *Calibration of Indivdual Neutron Monitors in Terms of H_E and the New ICRU Dose Equivalent Quantities.* Same as (3) : TANSAO **57** (1988), p. 221

26.) Selbach, H.J.; Hohlfeld, K.; Kramer, H.M.: *Calibration of Personal Dosemeters for X and Gamma Radiation in Front of Different Phantoms.* Rad.Prot.Dosim. **28** (1989) p. 69-72

27.) Bartlett, D.T.; Francis, T.M.; Dimbylow, P.J. *Methodology for the Calibration of Photon Personal Dosemeters: Calculation od Phantom Backscatter and Depth Dose Distributions.* Rad.Prot.Dosim. **27** (1989) p. 231-244

IV. Other research group(s) collaborating actively on this project [name(s) and address(es)]:

G. Portal, CEN, Fontenay-aux-Roses, France

E. Piesch, KfK, Postfach 3640, Karlsruhe, Germany

V. Publications:

1.) Siebert, B.R.L.; Hollnagel, R.; Jahr, R.:
Calculated Dose Equivalent Responses of Albedo and Track Etch Individual Neutron Dosemeters on the ICRU-Phantom.
In: Twenty Years Experience in Radiat. Protection: Compacts of 4th Europ. Congr. and 13th Regional Congr. of the Int. Radiat. Prot. Ass. (IRPA) , Salzburg 1986. (Seibersdorf: Österr. Verband für Strahlenschutz, 1988, p. 563-567)

2.) Hollnagel, R.; Jahr, R.; Siebert, B.R.L.:
The Influence of Phantoms on the Response of Etched Track Detectors.
Rad.Prot.Dosim. 20 (1987) p. 25-29

3.) Bauer, B.W., Hollnagel, R.; Siebert B.R.L.:
Numerical Study of the Influence of Phantom Material and Shape on the Calibration of Individual Dosemeters for Neutrons.
Rad.Prot.Dosim. 23 (1988) p. 207-210

4.) Jahr, R.;Hollnagel, R.; Siebert, B.R.L.:
Response of a System of Two Albedo Dosemeters Worn on Chest and Back in Various Directionally Distributed Neutron Fields.
Rad.Prot.Dosim. 23 (1988) p. 139-142

5.) Bauer, B.W., Alberts, W.G.; Burgkhardt, B.; Guldbakke, S.; Medioni, R.; Piesch, E.; Portal, G.;Siebert, B.R.L.:
Energy and Angle Dependence of and Phantom Influence on Readings of Neutron Individual Dosemeters: First Results of Experiments.
Rad.Prot.Dosim. 28 (1989) p. 115-119

6.) Siebert, B.R.L.; Morhart, A.:
A Proposed Procedure for Standardising the Relationship between the Directional Dose Equivalent and Neutron Fluence.
Rad.Prot.Dosim. 28 (1989) p. 47-51

7.) Jahr, R.; Siebert, B.R.L.; Alberts, W.G.:
Operational Quantities and Calibration Procedures for Individual Monitoring.
Rad.Prot.Dosim. 28 (1989) p. 33-36

8.) Alberts, W.G.:
Response of an Albedo Neutron Dosemeter to ^{252}Cf Neutrons on Various Phantoms.
Rad.Prot.Dosim. 22 (1988) p. 183-186

9.) Jahr, R.; Hollnagel, R.; Siebert, B.R.L.:
Computational Indivdual Dosimetry at the PTB.
In: Proc. 2nd Conf. on Radiat. Prot. and Dosimetry, Orlando, Florida (USA), 1988. Oak Ridge Nat. Lab. 1988 (ORNL/TM-10971), p. 75-84

10.) Siebert, B.R.L. Jahr, R.:
Calibration of Indivdual Neutron Monitors in Terms of H_E and the New ICRU Dose Equivalent Quantities.
Procedings of the American and European Nuclear Society, TANSAO 57 (1988), p. 221

11.) Hollnagel, R.A.:
Effective Dose Equivalent and Organ Doses for Neutrons from Thermal to 14 MeV.
(accepted for publication in Rad.Prot.Dosim.)

12.) Hollnagel R.; Alberts W.G.:
Reading of Personal Neutron Dosemeters on the MIRD phantom.
(accepted for publication in Rad.Prot.Dosim.)

13.) Bauer, B.W., Alberts, W.G.; Burgkhardt, B.; Dietz, E.; Guldbakke, S.; Jahr, R.; Kluge, H.; Medioni, R.; Piesch, E.; Portal, G.; Siebert, B.R.L.:
Experimental Investigation of Neutron Individual Dosemeters with Respect to the Influences of Neutron Energy, Angle of Incidence and Phantom Shape: Experimental Procedure and Summary of Results.
(In preparation as external PTB Report)

14.) Bauer, B.W., Alberts, W.G.; Luszik-Bhadra M.; Siebert, B.R.L.:
Experimental Investigation of Neutron Individual Dosemeters with Respect to the Influences of Neutron Energy, Angle of Incidence, and the Use of Phantom Shape: Detailed Analysis of Results for the Albedo Neutron Dosemeter used at PTB.
(In preparation as external PTB Report)

15.) Siebert, B.R.L.; Alberts, W.G.; Bauer, B.W.:
Computational Study of Phantoms for Inididvidual Neutron Dosimetry.
(In preparation as external PTB Report)

16.) Brede, H.J.; Dietze, G.; Klein, H.; Schölermann, H.:
Determination of Neutron Induced α-particle Cross Sections on Carbon Using the Response of a Liquid Scintillation Detector.
(accepted for publication in Nucl.Sci. and Eng.)

RADIATION PROTECTION PROGRAMME
Final Report

Contractor:

Contract no.: BI6-A-007-D

Kernforschungsanlage Jülich GmbH
Postfach 1913
D-5170 Jülich 1

Head(s) of research team(s) [name(s) and address(es)]:

Prof.Dr. L.E. Feinendegen
Institut für Medizin
Kernforschungsanlage Jülich
Postfach 1913
D-5170 Jülich 1

Telephone number: 2461-61.64.43

Title of the research contract:

Application of microdosimetric methods to radiation protection.

List of projects:

1. Implementation of a low-pressure proportional counter for use as a diagnostic working area and environmental dosemeter of high sensitivity and high dynamic range in LET.
2. Magnitude and meaning of local dose profiles around single decays of incorporated radionuclides in radiation protection.

Title of the project no.: 1

Implementation of a low-pressure proportional counter for use as a diagnostic working area and enviromental dosemeter of high sensitivity and high dynamic range in LET

Head(s) of project:

L.E. Feinendegen

Scientific staff:

L.E. Feinendegen, J.Booz, Th. Schmitz
K. Morstin (Univ. Krakow), A. Dydejczyk (Univ. Krakau), S. Mukherjee (Univ. Calcutta)

I. Objectives of the project:

- Adaption of the KFA counter to practical requirements
- Developement of a simple external calibration method for the KFA counter
- Collection of information on dose equivalent distributions of neutron/gamma fields at working areas with the KFA counter

II. Objectives for the reporting period:

- Further improvement of the dose-equivalent response of the KFA counter
- Collection of information with the KFA counter on dose-equivalent distributions of neutron/gamma fields at simulated realistic radiation protection fields and at working areas, e.g. at Cadarache and the accelerator and reactor facilities of the Crakow University

III. Progress achieved:

Low pressure tissue equivalent proportional counters (TEPC) allow the measurement of energy deposition spectra for tissue equivalent targets (simulated diameters) down to 1 μm in mixed neutron gamma radiation fields. From these distributions, values of the absorbed dose or dose rate in tissue can be assessed as well as the mean quality of the radiation field at the position of the counters sensitive site. This information is necessary to derive dose equivalent, the quantity used in radiation protection as an indication for the biological implications of radiation exposure. Due to the measurement of spectra, a TEPC can in addition give information on fractions of absorbed dose and dose equivalent due to low and high radiation quality. For the reasons given, low pressure proportional counters are well suited for use in radiation protection.

The objectives of this project were

- to optimize the proportional counter with respect to it's wall thickness that it's reading matches ambient dose equivalent, $H^*(10)$, as close as possible in the neutron energy range between thermal and 20 MeV and for photons above 30 keV. Ambient dose equivalent is the operational quantity recommended by the ICRU for use in enviromental radiation protection dosimetry for penetrating radiation

- to develope a practical instrument for use in radiation protection

- to test and optimize the performance of the developed instrument

- to participate in an intercomparison of several proportional counter based instruments.

The result is the KFA counter. It consists of

- a proportional counter with a total wall thickness of 15 mm; the sensitive volume is cylindrical with equal diameter and hight of 7 cm

- an amplifying system with nonlinear gain characteristic

- a portable PC for data acquisition and evaluation.

A further result emerging from the study of the optimal counter response is a program system which simulates measurements with proportional counters. Its features are

- PC based, fast operation
- easy to use
- several counter materials and constructional parameters can be choosen.

The KFA counter is frequently in use for measurements around working places and in radiation beams used for biological experiments. The latter application is now becoming increasingly interesting within the framework of the concept of biological response functions described in the second project.

Optimization of the Counter Response

Ambient dose equivalent, $H^*(10)$, is defined in 1 cm depth in the ICRU sphere, an ICRU-muscle tissue sphere of 30 cm in diameter. Therefore, the value of $H^*(10)$ is influenced by the scattering properties of the ICRU sphere and by the transport of the primary radiation in the material. Ussually low pressure proportional counters (e.g. Rossi counters) apply a 'thin' wall of about 3 mm, which is sufficiently thick to provide charged particle equilibrium. Therefore, the point of reference of the counter is in 3 mm depth in tissue, against 10 mm in case of $H^*(10)$. In addition, the mass of the ICRU sphere is 14 kg, whereas the mass of a Rossi counter is 50 g, assuming an internal diameter of 6.35 cm (2.5").

The aim of the optimization was to determine the wall thickness for the proportional counter for which the fluctuations of the ambient dose equivalent response (ratio of the detector reading, H_y, to ambient dose equivalent, $H^*(10)$) is minimal in the energy range between thermal and 20 MeV. The investigations were performed with the help of computer simulations. These included the transport of radiation through the detector wall (ANISN) and the calculation of energy imparted and ionisation events in the counter's sensitive volume (NESLES & STARTERS). Figure 1 shows as an example the counter response to neutrons of different energies as a function of the total counter wall thickness. From these results it emerges that a minimal fluctuation of the counter ambient dose equivalent response is achieved if a wall thickness of 15 mm is used.

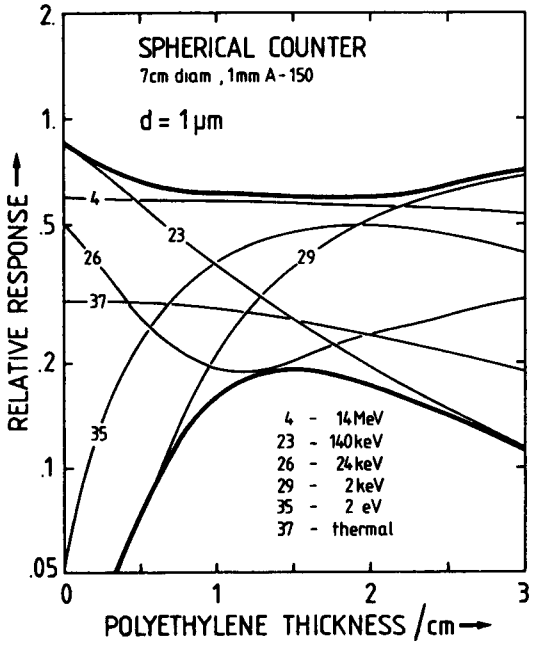

Figure 1: *Ambient dose equivalent response of a spherical counter with 7 cm diameter versus polyethylene cap thickness. Different curves correspond to different incident neutron energies*

Photon and Neutron Responses[+]

Figure 2 displays the experimentally determined responses of the KFA counters KFA1[*] (20 mm wall thickness) and KFA2 (15 mm wall thickness) in terms of $H^*(10)$ for photon irradiation. The responses are better than 0.8 for incident photon energies above 30 keV; the influence of the different wall thicknesses is negligible.

+ The measurements in the monoenergetic neutron fields and at the heavy water moderated ^{252}Cf source, referred to in the next two chapters, were performed during intercomparison measurements at the PTB Braunschweig. The intercomparison was organized by the EURADOS Commitee 1.

* KFA1 was the first prototype of the KFA counter. The wall thickness of 20 mm was choosen prior to the optimization.

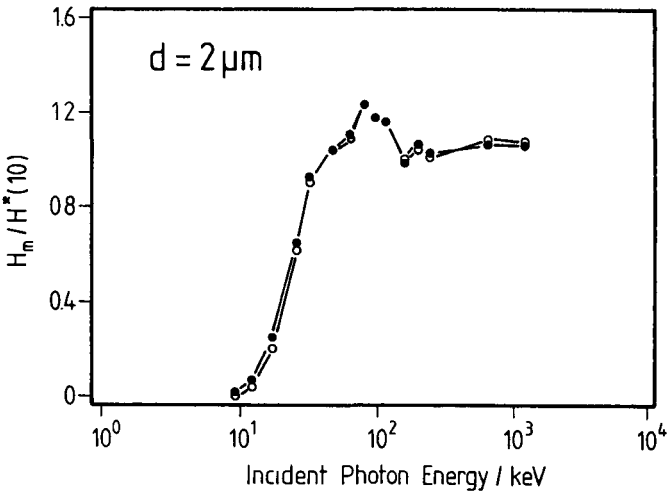

Figure 2: *Ambient dose equivalent response of KFA1 (open circles, 20 mm wall thickness) and KFA2 (closed circles, 15 mm wall thickness) as a function of incident photon energy*

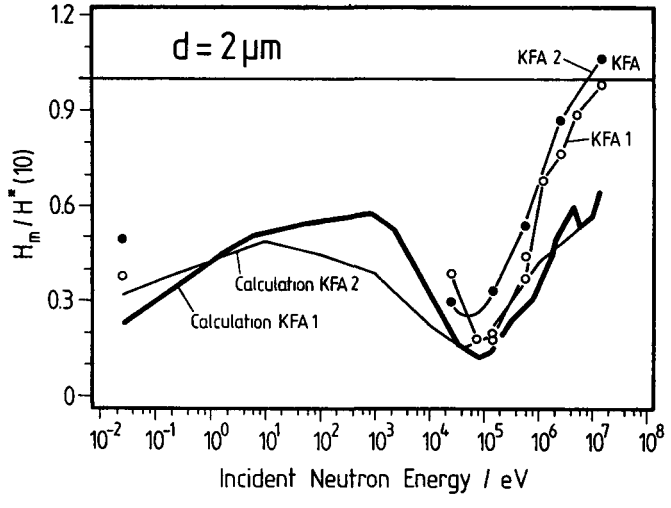

Figure 3: *Ambient dose equivalent response of KFA1 (20 mm wall thickness) and KFA2 (15 mm wall thickness) versus incident neutron energy. The solid lines represent results of calculations, the symbols results of experiments*

Figure 3 presents the responses of KFA1 and KFA2 with respect to $H^*(10)$ for neutron irradiation. The lines indicate results of calculations, the symbols those of experiments.

The theoretical results show that the reponses of counters with wall thicknesses of 15 mm and 20 mm decrease between 15 MeV and 100 keV incident neutron energy. Below 100 keV, the responses increase until they reach a local maximum at about 1 keV and 10 eV for respectively 20 mm and 15 mm wall thickness. For even lower energies, the reponses decrease slightly until thermal neutron energies are reached. The results also show that the overall response of a counter with 15 mm wall thickness is flatter than the one of a counter with 20 mm wall thickness, i.e., the ratio of the maximal and minimal response is lower in the case of 15 mm wall thickness. In particular, the response of a 15 mm wall counter is better than for a 20 mm wall counter for thermal energies and between 100 keV and 15 MeV neutron energies.

The experimental results confirm the calculated reponses but are generally higher.

Sensitivity of KFA2

Figure 4 displays the measurement time needed to achieve a statistical precision of 20 % of the dose equivalent reading in a field of 20 μm/h as a function of the incident neutron energy. The measurement times vary between about 10 min and 2 min.

For photon irradiations between 30 keV and 1.25 MeV mean energy, the corresponding measurement times are below 1 min.

Calibration of KFA2

The KFA counter is calibrated with respect to lineal energy, y. For this purpose a ^{60}Co source is mounted on the counter surface. The measured distribution is evaluated with respect to pulse height and compared to a calibrated ^{60}Co spectrum, which is contained in the database of the calibration program. From the comparison, the calibration factor to convert pulse height into lineal energy is achieved.

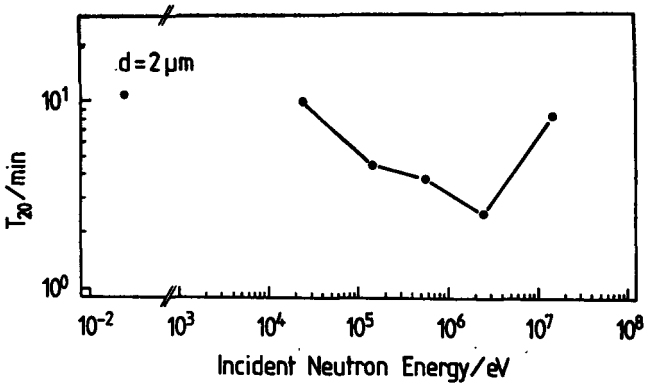

Figure 4: *Sensitivity of KFA2 (15 mm wall thickness) versus incident neutron energy. Shown is the measurement time, which is needed to achieve a statistical uncertainty of not more than 20 % in a field of 20 µSv/h.*

Judgement of the Response of KFA2

Ambient dose equivalent, $H^*(10)$, is the recommended operational quantity for the dosimetry of penetrating radiation in the enviroment, whereas effective dose equivalent, H_e, is the limiting quantity. It is our opinion that ambient dose equivalent may be underestimated by the reading of a radiation protection instrument, but effective dose equivalent must not be underestimated in any circumstance.

The KFA counter underestimates $H^*(10)$ by up to a factor of about 3 for monoenergetic neutrons around 100 keV. Effective dose equivalent is underestmated by the KFA counter in the energy range between 100 keV and about 2 keV. This underestimation can be excluded, if an additional weighting factor is used in the evaluation of dose equivalent. Figure 5 shows an example. The measured dose distributions are wheighted above a lineal energy of 7 keV/µm with a factor of 1.5. Below this threshhold no additional wheighting is performed. The threshhold value was choosen, because it allows reasonably well the discrimination between fractions of absorbed dose due to low (below the threshhold) and high (above the threshhold) radiation qualities.

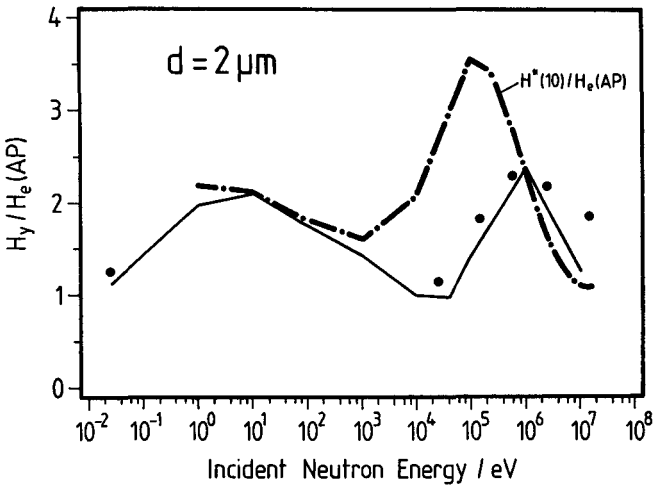

Figure 5: *Effective dose equivalent response of KFA2 (15 mm wall thickness) as a function of neutron energy. The experimental results are indicated as solid circles. For the evaluation of the experimental data, the measured dose distributions were weighted with an additional step function to ashure that the reponse is always greater than 1 (for explanation please see text). The solid line indicates theoretical results with a constant additional weighting of a factor of 2. The dash dotted line shows the ratio between ambient dose equivalent and effective dose equivalent.*

The simple weighting of the dose distribution ashures that effective dose equivalent is not underetimated in the neutron energy range between thermal and 20 MeV.

Furthermore, in practical radiation protection, broad neutron fields are encountered. Measurement in a heavy water moderated ^{252}Cf source, which is recommended by ISO for calibrating neutron dosimetry devices, show that in broad fields the underestimation of ambient dose equivalent is significantely lower than in the case of monoenergetic neutrons. With the additional weighting described above, a mean response of 0.9 (0.7 without weighting) was achieved for three different field qualities in front of such a source at the PTB Braunschweig.

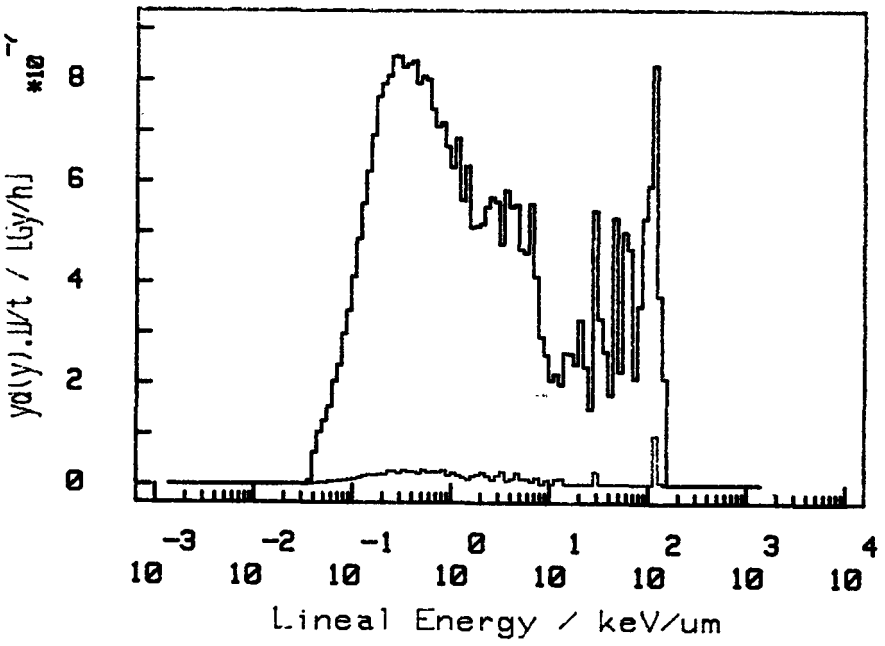

Figure 6: *Dose distributions versus lineal energy measured with the KFA counter in two offices above a d->t neutron generator normalized to dose rate. One measurement (thick line) was perfomed in a room direcly above the generator, the second (thin line) in a room ajacent to the first. In the first case, only a normal sealing shields the neutron generator, whereas in the second case, the generator is shielded by a thick concrete wall.*

Practical Application

Figure 6 shows dose distributions measured in rooms above an operating d->t neutron generator. The first measurement (thick line) was perfomed in a room direcly above the generator, the second (thin line) in a room ajacent to the first. The distributions are normalized to dose rate. In the first case, only a normal sealing shields the neutron generator and a strong neutron induced component appears in the spectrum above 10 keV/μm. In the second case, a thick wall shields the generator. There is only a minor neutron induced part in the spectrum and the dose rate is lower by a factor of 40. The dose equivalent rate is in this case lower by a factor of 43.

IV. Other research group(s) collaborating actively on this project [name(s) and address(es)]:

- Members of EURADOS Committee I on "Dose equivalent meters based on microdosimertic techniques"

- G. Portal, CEA Fontenay-aux-Roses

V. Publications:

1985

Booz, J., Kawecka, B., Morstin, K.
The Influence of Neutron Transport Phenomena on KERMA, Absorbed Dose and Energy Deposition Spectra
Proc. Fifth Symposium on Neutron Dosimetry, (CEC, Luxembourg) EUR 9762, pp. 227-235 (1985).

Morstin, K.
On some Symmetries that may Influence Radiation Protection Regulations
Radiat. Res. 102, pp.399-403 (1985).

Morstin, K., Booz, J.
A Radiation Protection Operational Quantity that is Isotropic and CAN be Measured
Radiat. Prot. Dosim. 12, pp.113-117 (1985).

Morstin, K., Kawecka, B., Booz, J.
What is New in the ICRU Sphere?
Proc. Fifth Symposium on Neutron Dosimetry, (CEC, Luxembourg) EUR 9762, pp. 227-235 (1985).

Morstin, K., Kawecka, B., Booz, J.
Combined Primary and Secondary Particle Transport Calculations of Microdosimetric Distributions in Tissue and Tissue Substitutes
Radiat. Prot. Dosim. 13, No.1-4 pp. 103-110

Schmitz, Th., Smit, Th., Morstin, K., Müller, K.D., Booz,J.
Construction and First Application of a TEPC Dose Equivalent Meter for Area Monitoring
Radiat. Prot. Dosim. 13, pp. 335-339 (1985).

1986

Dietze, G., Guldbakke, S., Kluge, H., Schmitz, Th.
Intercomparison of Radiation Protection Instruments Based on Microdosimetric Principles
PTB Report, PTB-ND-29, (1986)

Humm, J.L., Booz,J
An Anomaly in the Performance of Spherical Proportional Counters for Microdosimerty
Radiat. Prot. Dosim., Vol. 15, pp. 9-14 (1986)

Schmitz, Th., Smit, Th., Morstin, K.,Müller, K.D., Booz J.
Investigations on the Performance of a TEPC Dose-Equivalent Meter for Area Monitoring
Poster Presentation during the 4^{th} European Congress, 13^{th} Regional Congress of IRPA, Salzburg 15.9-19.9 1986

1987

J. Booz and L.E.Feinendegen
Application of Microdosimetry
Radiation Research; Proceedings of the 8^{th} International Congress of Radiation Research, Vol 2. Taylor and Francis (London), pp. 331-337 (1987)

Dietze, G., Guldbakke, S., Kluge, H., Schmitz, Th.
Intercomparison of Radiation Protection Instruments Based on Microdosimetric Principles
Report PTB-ND-29 (1986)

Morstin, K., Dydejczyk, A., Booz, J.
High Energy Neutron Interactions with Tissues and Tissue Substitutes
Nuclear and Atomic Data for Radiotherapy and Related Radiobiology, pp. 239-262 (IAEA, Wien, 1987).

1988

Booz, J.
Microdosimetric Applications in Radiation Biology
7th Annual Meeting of the European Society for Therapeutic Radiology and Oncology, ESTRO, Den Haag, 2-8 September 1988.

Morstin, K., Dydejczyk, A., Booz, J.
Nuclear Model Calculations for High Energy Neutron Dosimetry
Radiat. Prot. Dosim. 23, No. 1-4 pp. 35-39 (1988)

Morstin, K., Dydejczyk, A., Booz, J.
Nuclear Model Calculations for High Energy Neutron Dosimetry
Radiat. Prot. Dosim. 23, No.1/4 pp. 35-39 (1988)

Dietze, G., Booz, J., Edwards, A.A., Guldbakke, S., Kluge, H., Leroux, J.B., Lindborg, L., Menzel, H.G., Nguyen, V.D., Schmitz, Th., Schumacher, H.
Intercomparison of Dose Equivalent Meters Based on Microdosimetric Techniques
Radiat. Prot. Dosim. 23, No. 1-4 pp. 227-234 (1988)

Schmitz, Th., Morstin, K., Booz, J.
Performance of a Dose Equivalent Meter for Area Monitoring
Radiat. Prot. Dosim. 23, No. 1-4 pp. 235-238 (1988)

Dietze, G., Edwards, A.A., Guldbakke, S, Kluge, H., Leroux, J.B., Lindborg, L., Menzel, H.G., Nguyen, V.D., Schmitz, Th., Schumacher, H.
Investigation of Radiation Protection Instruments Based on Tissue-Equivalent Proportional Counters. Results of an Intercomparison
Commission of the European Communities, (CEC,Luxembourg) EUR 11867 (1988)

1989

Schmitz, Th., Smit, Th., Booz, J., Feinendegen, L.E.
Data Processing for Measuring Dose Equivalent with a TEPC
IAEA-SR-136, pp. 358-365. (1989)

Bednarek, B., Olko, P., Booz, J.
Double Peak Effect in Microdosimetric Proportional Counters and it's Interpretation
Nucl. Instr. Meth. Phys. Res. A274, pp. 349-358 (1989)

Booz, J., Olko, P., Schmitz, Th., Feinendegen, L.E., Morstin, K.
The KFA Counter - Its Photon and Neutron Responses, Sensitivity, Performance, and its Potential for Future Developement
Workshop on Implementation of Dose Equivalent Meters Based on Microdosimetric Techniques in Radiation Protection, Schloß Elmau, 18-20 Oktober 1988
Radiat. Prot. Dosim. (in press)

Schmitz, Th., Booz, J.
Measurements of the Gas-Amplification Coefficient in a TEPC
Workshop on Implementation of Dose Equivalent Meters Based on Microdosimetric Techniques in Radiation Protection, Schloß Elmau, 18-20 Oktober 1988
Radiat. Prot. Dosim. (in press)

Schmitz, Th., Kramer, H.M., Booz, J.
Assessment of the Photon Response of a TEPC as a Contribution to Implementing Operational Quantities for Dose Equivalent in Radiation Protection
Workshop on Implementation of Dose Equivalent Meters Based on Microdosimetric Techniques in Radiation Protection, Schloß Elmau, 18-20 Oktober 1988
Radiat. Prot. Dosim. (in press)

Menzel, H.G., Lindborg, L., Schmitz, Th., Schuhmacher, H., Waker, A.J.
Intercomparison of Dose Equivalent Meters Based on Microdosimetric Techniques : Detailed Analyses and Conclusions
Workshop on Implementation of Dose Equivalent Meters Based on Microdosimetric Techniques in Radiation Protection, Schloß Elmau, 18-20 Oktober 1988
Radiat. Prot. Dosim. (in press)

Title of the project no.: 2

Magnitude and meaning of local dose profiles around single decays of incorporated radionuclides in radiation protection

Head(s) of project:

L.E. Feinendegen

Scientific staff:

L.E. Feinendegen, J.Booz, P. Olko

I. Objectives of the project:

- Assesment of energy deposition distributions and local dose profiles around single decays of incorporated radionuclides and other radiation sources
- Implications for radiation protection limits of incorporated radionuclides
- Understanding of the underlying radiation mechanisms

II. Objectives for the reporting period:

- Application of the developed analytical functions for the description of ionization distributions from charged particles to various radiation modalities.
- Further development of the methodology for the evaluation of biological response functions
- Quantification of radiation quality with the help of biological response functions.

In the biological effectiveness of incorporated Auger emitters, as well as of low energy X-rays and external heavy ion irradiations, the creation of high local energy densities within critical targets in tissue may play an important role. For example, radiobiological experiments with ^{125}I, incorporated specifically into the DNA of cells have demonstrated the high radiation toxicity of this Auger emitter. Thererfore, the correlation was studied between energy depostion spectra caused by such radiations in target volumes of some nanometer up to several micrometer and observed biological effects. Furtheron, implications of these studies for radiation protection and for the understanding of mechanisms of radiation action were addressed. The results of the work fall into the categories

- Basic microdosimetric data
- Biological response functions
- Implications for radiation protection

Basic microdosimetric data

In the case of Auger emitters, Dirac-Fock calculations of energy levels in combination with the Monte Carlo simulation technique were used to derive the electron number and energy spectra. This information was then used to calculate dose profiles around single decays of Auger emitters as well as corresponding microdosimetric distributions. Figures 1 and 2 show results of these calculations for ^{125}I, the isotope studied most intensively up to now due to its significants for nuclear medicine and radiation biology (^{125}I shows high radiation toxicity and is therefore potentially interesting for radiation therapy).

The mean electron spectrum for iodine (Figure 1) shows the high density and frequency at low electron energies (below 10 keV). These electrons are believed to be responsible for the high biological toxicity of this radionuclide.

The dose profile in Figure 2 reveals the important contribution of the ionisation potential of the charged nucleus created during the decay especially for target diameters below 100 nm. This ionization potential is assumed to be deposited at the site of the decaying ion. For comparison, the result of the same calculation is shown, when the electron spectrum is used as input, which is given by ICRP in its Publication No. 38, 1983. With respect to investigations of the biological effectiveness of ^{125}I incorporated specifically into DNA, a target Volume of 20 nm diameter was assumed. For such a Volume, the energy deposited by electrons is 0.96 keV. To this value the ionisation

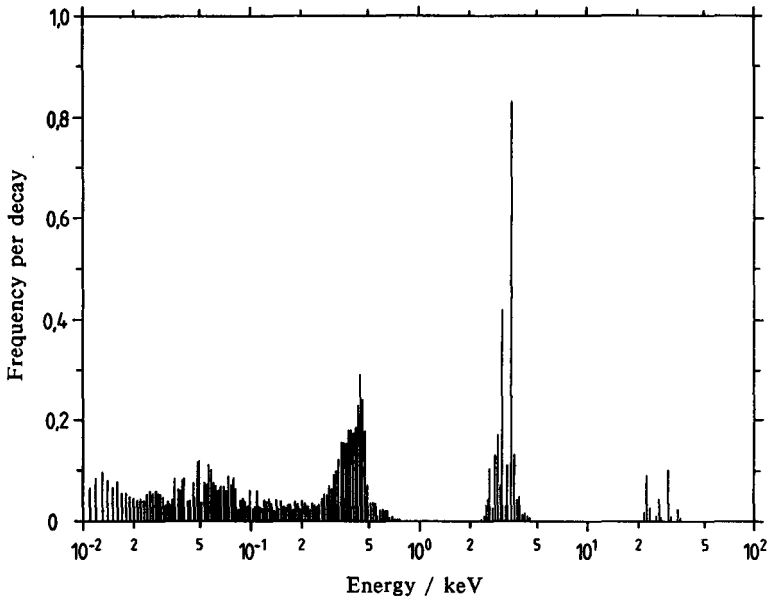

Figure 1 : Mean β particle spectrum of an ^{125}I decay.

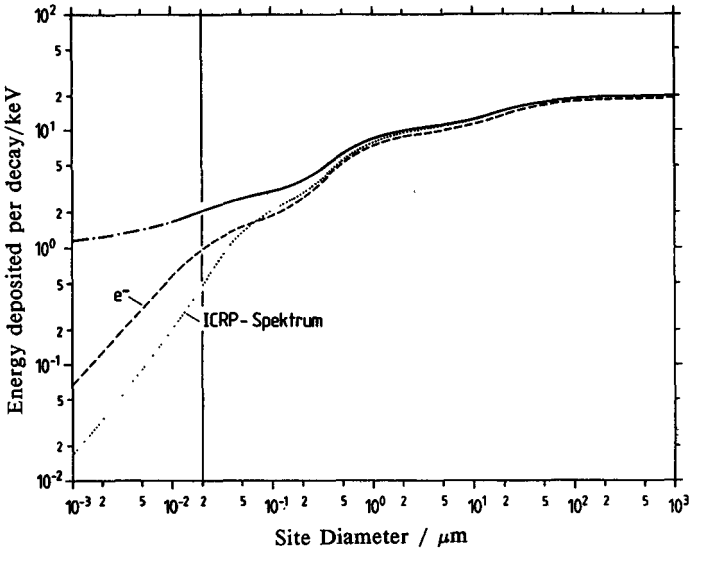

Figure 2: Mean deposited energy per ^{125}I decay as a function of target size. Solid line: Auger electrons plus ionization potential; dashed line: Auger electrons only; dotted line: energy deposition calculated according to the mean electron spectrum given by ICRP (ICRP, 1983).

potential of 1.07 keV has to be added, so that the total energy deposition becomes 2.03 keV.

The microdosimetric characterisation of ^{125}I gave a frequency mean lineal energy, y_F, of 270 keV/μm for a critical target size of 20 nm and of below 2 keV/μm outside this volume. Setting y_F equal to LET, the value for 20 nm site size belongs to the high LET range.

To study the radiation action of external radiation in biological matter, the advanced Monte-Carlo codes MOCA8 and MOCA14 (author: H.G. Paretzke, GSF Neuherberg) were adapted for simulating track structures of electrons (MOCA8) and heavy charged particles (MOCA14) in water vapour.

The results of the calculations with MOCA14 for protons and apha particles were used to develop an analytical function to desrcibe energy deposition spectra in spherical volumes of diameters of some nanometers up to several micrometers. The derived functions allow for the possibilities of ion events (particles crossing the site), delta events (depostion of energy in the target through secondary electrons created by particles passing by outside) and for the straggling of energy depostion for the ion events. Based on the track structure simulations, a complete set of parameters has been derived to describe energy deposition spectra for different types of ions (from protons to oxygen ions) between 0.3 MeV/amu and 10 MeV/amu in sites between 1 nm and 1000 nm.

The code MOCA8 was used to simulated electron tracks in water vapour. It was applied in conncetion with the code Phoel II, which generates primary electron spectra from interactions of photons in different materials, to calculate microdosimetric distributions for X-rays of energies up to 300 kVp. The limitation to this energy range of photons is due to the fact that MOCA8 can process electrons only up to energies of 100 keV.

Biological Response Functions

The main assumption in the concept of biological response functions is that there exists a function which relates energy deposited in the target to the probability of the biological effect in the target. It wass not not the aim to measure directly such a function. Results of typical radiobiological experiments are mean values which reflect an average response of individual cells in a large population affected by different energy deposition events. It is, however, possible to unfold this function from experiments with several radiation modalities, covering the range of energy deposited of interest.

An input data set used to unfolding biological response functions consists of coefficients, α, which express initial slopes of dose-response curves, for given radiation modalities. It also consists of microdosimetric distributions, f(y), characterising radiation qualities and being specific for radiation modalities and size of targets. Initial slopes of dose-response curves were collected either from literature directly or evaluated on the basis of data taken from literature. Microdosimetric distributions were calculated for experiments with photons and ions. These distributions and initial slopes were used to unfold biological response functions.

The unfolding technique used was based on a discrete interval method because it is rather independent from assumed models of biological action of radiation. After several tests and itercomparisons performed with different unfolding programs, the code SAND-II was modified and applied. This program was developed to unfold a set of integral equations resulting from neutron spectrum measurements with activation foils. Particular problems in activation foil analysis are somewhat different from those in radiobiology, e.g. the shapes and the coverage of microdosimetric distributions are not necessarily similar to those represented by neutron cross sections. SAND's algorithm has, however, the advantages that it is simple and easily to control, always gives positive solutions, is time-efficient and can be performed on small computers.

Biological response functions (BRF) were unfolded for DNA dsb for site diameters of 20 nm. The choice of the target diameter was somewhat arbitrary. 20 nm corresponds approximately to the diameter of the nucleosome fiber, which seems to be the basic structure formed by DNA throughout most of the time in the cell cycle.

Figure 3 presents unfolded biological response functions for experiments of Christensen et al. [1972] with ΦX-174 bacteriophages (bold line with dashed lines denoting 1 SD) and of Ritter et al. [1977] with Hamster cells (bold dashed-dotted line with dotted lines denoting 1 SD). The quality of unfolding was tested with the χ^2 test. For both functions high probabilities (P=0.999 and P=0.9999) were derived. The calculated maximum probability (cross section), σ_ϵ, for ΦX-174 is 5.58 $10^{-15}m^2$, which corresponds to a diameter of about 80 nm. The maximum cross section, σ_ϵ, calculated for Chinese hamster cells was 1.38 $10^{-8}m^2$ which is about 200 times higher than the geometrical cross section of the mammalian cell nucleus (64 μm^2). Therefore, an ion crossing the cell nucleus with lineal energy greater than 1000 keV/μm can produce, at maximum, about 200 non-rejoining DNA breaks in the cell nucleus. For energy deposition around 100 keV/μm the number of breaks is, on the average, about 20.

Once a BRF is available it can be used to calculate the frequency of DNA dsb after irradiations with arbitrary radiation modalities. For these purposes the response function R(y) for DNA breaks in Chinese hamster cells (Figure 3) was used as an universal response function. First, the microdosimetric distributions, corresponding to radiation modalities from different experiments, were calculated. Then, these distributions were folded with the

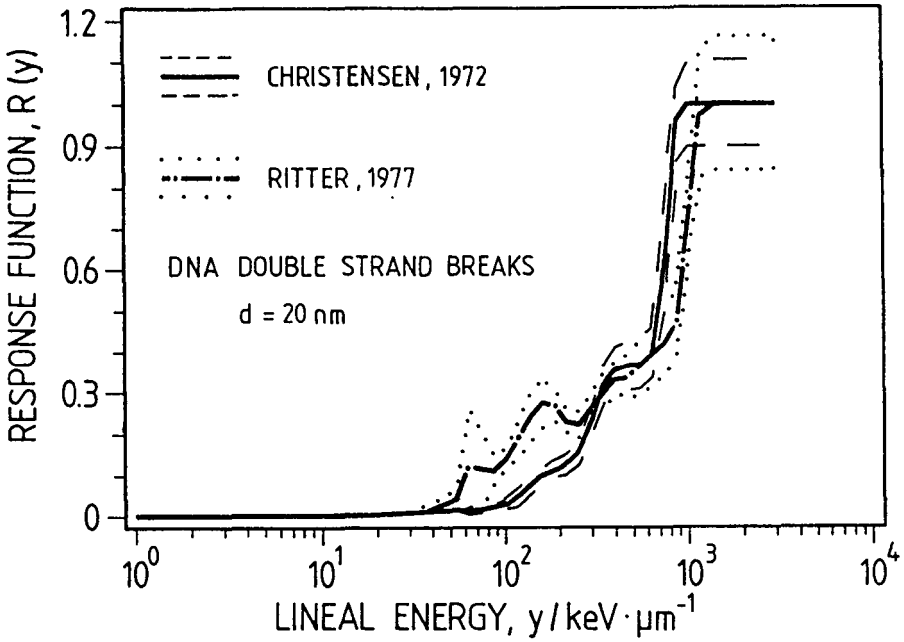

Figure 3: Biological response functions for DNA dsb unfolded for the experiments of [Christensen et al., 1972] and [Ritter et al., 1977].

R(y) in order to calculate the frequencies of DNA breaks. The ratio of the frequency of DNA breaks, α_n, induced by a given radiation and the frequency of breaks for 250 kVp X-rays, α_X, is called here RBE_{DNA}

Figures 4 show the correlation between the relative efficiency in producing a given biological effect, e.g. cell killing, mutation etc., (RBE_0) and the efficiency in producing DNA breaks in these cells (RBE_{DNA}) by the same radiations. The analysis is performed for the set of cellular experiments of Skarsgard et al. [1967] and Cox et al. [1977a]. Lines representing direct proportionality (at 45°) and quadratic dependence (at 63°) between the relative efficiencies of DNA breaks and the investigated end-points are plotted to guide the eyes. The linear or quadratic dependence of cellular effects on frequency of DNA double-strand breaks can suggest the different basic mechanisms leading to biological effects on cellular level.

The closest correlation between the frequency of DNA double-strand breaks and the corresponding cellular effect can be observed for HF-19 mutations and abnormal methaphasis in $CH2B_2$ cells. The maximum RBE_{DNA} is of about 6 what reflects the DNA breakage data applied to unfolding. This corresponds to the well-known experimental

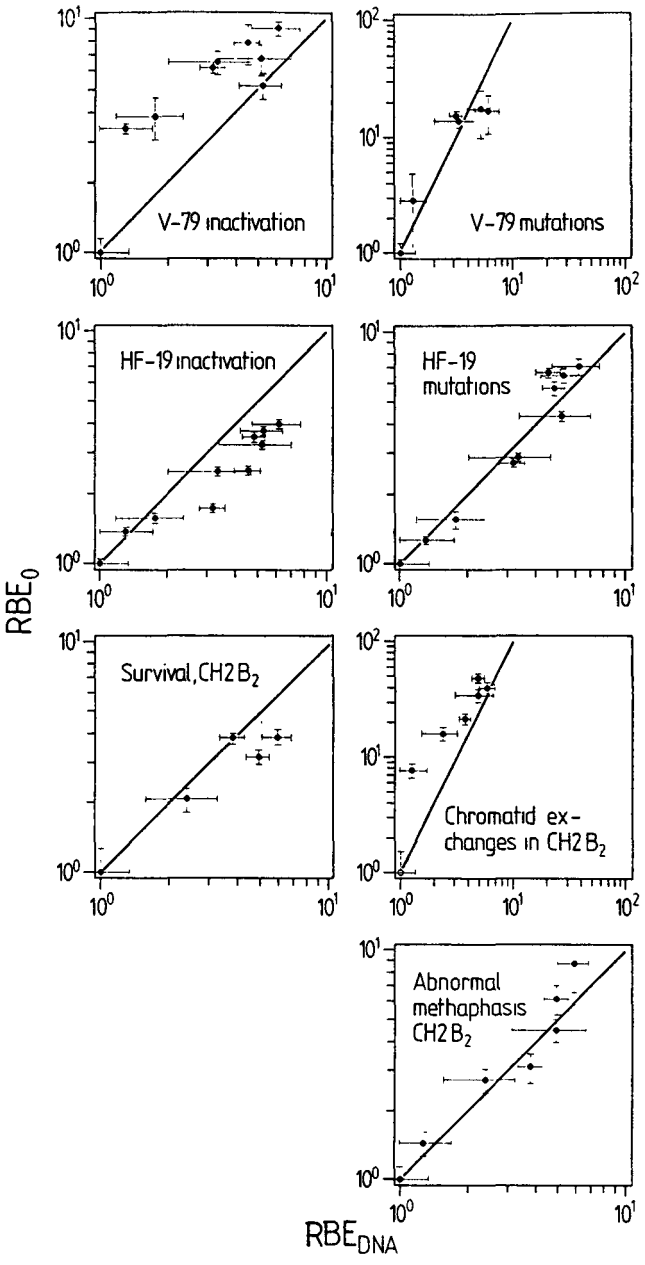

Figure 4: *Relative efficiency in inducing an effect on cellular level (RBE_0) versus efficiency in producing DNA breaks (RBE_{DNA}). The cellular data concern experiments of [Skarsgard et al., 1967] and [Cox et al., 1977a]*

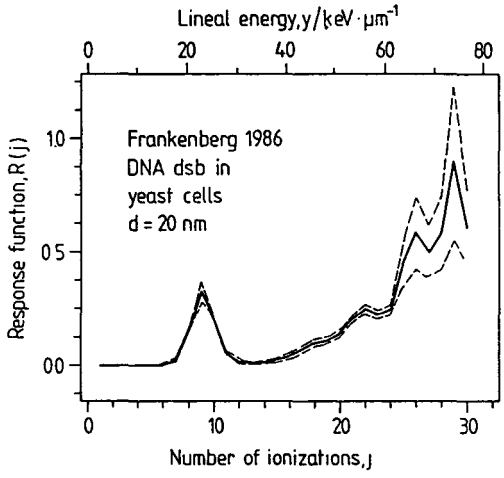

Figure 5: *Preliminary results of unfolding the biological response function for DNA dsb induced in yeast cells by soft X-rays [Frankenberg et al., 1986]. Due to the lack of microdosimetric distributions for Co-60 gamma rays, the distribution for 250 kVp X-rays was used. The dashed lines show the 1 SD of the unfolded function.*

---

observation, that even for very densly ionizing radiations, the RBE for production of DNA breaks is much smaller than the RBE for most cellular end-points and for tissues, which for some end-points for neutrons exhibit an RBE greater than 100.

It is a well documented hypothesis that DNA breaks are the primary lesions leading to most of the biological alterations in living organisms. It should be, however, kept in mind that these lesions only initiate a long chain of biochemical processes, leading to very different effects in the variety of systems. Therefore it should not be surprising that the efficiency of radiation to produce DNA double strand breaks and the efficiency to produce a given effect are not the same, even if the primary lesion is in the DNA. Energy deposition in the site is an important but certainly not the only factor which determinates radiation quality. There is experimental evidence that in addition to direct action on the DNA, an indirect action due to low-LET radiations occurs, e.g. due to the production of long-range radicals.

Investigating biological response in terms of energy deposited in the site does not always give reasonable results. Figure 5 presents the unfolded BRF for DNA dsb in yeast cells [Frankenberg et al., 1986]. Cells were irradiated with 0.3, 1.5 keV and Co-60 photons. In this analysis, instead of microdosimetric distributions for Co-60, which are unavailable for nanometer-size sites, the distribution for 250 kVp X-rays was used. The unfolded function exhibits a sharp peak around 8 to 10 ionizations (20 keV/μm) which corresponds to lineal energies produced by 0.3 keV photons in 20 nm targets. The response function is an integral probability function; with increasing energy deposited the probability of an effect cannot decrease. Therefore, the observed sharp peak is an indication that the published value of absorbed dose within the cell nucleus is either incorrect or does not correctly represent absorbed dose in DNA.

Applications for radiation protection

The consequences of the observed high LET behavior of ^{125}I incorporated into DNA with regard to dose limitations has been investigated. The Annual Limit on Intake (ALI) has been recalculated according to the ICRP regulations. For a homogenious distribution of ^{125}I nuclides in the critical organ thyroid and on the present quality factor of Q = 20, it should not be necessary to reduce the present ALI-values of 1 MBg for ingestion and 2 MBg for inhalation. However, in the case of a specific DNA incorporation, e.g. by injection of ^{125}IUdR, the ALI should be reduced to 70 kBq. Even with a quality factor of Q = 40 for the deposited energy in the model target, the preliminary analysis gives no indication for consequences with regard to dose limitations for ingestion or inhalation. However, for specific DNA-incorporation, the ALI would need to be further reduced to 30 kBq. A quality factor of 40 is suggested by the analysis of biological data relevant for radiation protection, e.g. chromosome aberrations, mutation and malignat transformation.

The practical aspect of investigating biological response functions for radiation protection is to contribute to the determination of radiation quality for different radiations. The quality functions were calculated for chromosome aberrations in human lymphocytes. Figure 6 compares the unfolded functions (bold lines) with the quality function (ICRU-40) recommended by a task group of the International Commission of Radiation Units and Measurements and the proposal of Zaider and Brenner. The results show that for lineal energies below 10 keV/um, unfolded functions cannot be determined unequivocally and the final shape of the quality factor critically depends on e.g. different techniques of smoothing and or initial guess functions. The present results cannot confirm the recommendations given in the ICRU Report No. 40. This problem will be further investigated.

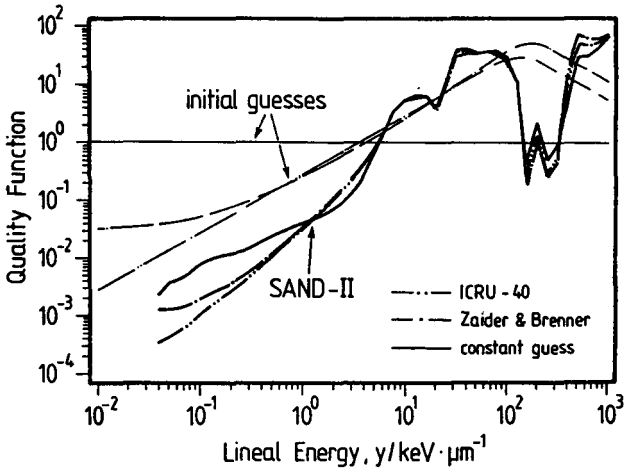

Figure 6: Quality function for experiments with chromosome abberations in human lymphocytes. The thin lines denote different initial guess functions, the bold lines the corresponding unfolded quality functions.

Refernces

Christensen, R.C., Tobias, C.A., Taylor, W.D. (1972) *Heavy-ion-induced single-and double-strand breaks in X-174 replicative form DNA.* Int. J. Radiat. Biol. **22**, 457-477

Cox, R., Thacker, J., Goodhead, D.T. and Munson, R.J. (1977a) *Mutation and inactivation of mammalian cells by various ionizing radiations* Nature **267**, 425-427

Frankenberg, D., Goodhead, D.T., Frankenberg-Schwager, M., Harbich, R., Bance, D.A. and Wilkinson, R.E. (1986) *Effectiveness of 1.5 keV aluminium K and 0.3 keV carbon K characteristic X-rays at inducing DNA double-strand breaks in yeast cells.* Int. J. Radiat. Biol. **50**, No.4, 727-741

Ritter, M.A., Cleaver, J.E. and Tobias, C.A. (1977) *High-LET radiations induce a large proportion of non-rejoning DNA breaks.* Nature 266,653-655

Skarsgard, L.D., Kihlam, B.A., Parkr, L., Pujara, C.M. and Richardson, S. *Survival, chromosome abnormalities, nd recovery in heavy ion- and x-irradaited mammalian cells* Radiat. Res. Suppl. 7, 208-221 (1967)

IV. Other research group(s) collaborating actively on this project [name(s) and address(es)]:

- H. G. Paretzke, GSF Neuherberg

- D.T. Goodhead, MRC Harwell

V. Publications:

1985

Feinendegen, L.E., Booz, J., Bond, V.P., Sondhaus, C.A.
Microdosimetric Approach to the Analysis of Cell Response at Low Dose and Low Dose Rate
Radiat. Prot. Dosim 13, No. 1-4 pp. 299-306 (1985)

1986

Morstin, K., Dydejczek, A., Booz, J.
Implications of Some New Formulations of Quality Factor
Radiat. Prot. Dosim. 12, No. 4 pp. 319-323 (1986)

1987

Booz, J.
Applications of Microdosimetry
Proc. of the 8th ICRR, Edingburgh, Vol. 2 Fielden, E.M. et al., pp. 331-337 (1987)

Booz, J., Paretzke, H.G., Pomplun, E., Olko, P.
Auger Electron Cascades, Charge Potential and Microdosimetry of I-125
Radiat. Env. Biophys. 26, pp. 151-162 (1987)

Pomplun, E., Booz, J., Dydejczek, A., Feinendegen, L.E.
A Microdosimetric Interpretation of the Radiobiological Effectiveness of I-125 and the Problem of Quality Factor
Radiat. Env. Biophys. 26, pp. 181-188 (1987)

Pomplun, E., Booz, J., Charlton, D.E.
A Monte Carlo Simulation of Auger Cascades
Radiat. Res. 111, pp. 533-552 (1987)

Charlton, D.E., Pomplun, E., Booz, J.
Some Consequences of the Auger Effect: Fluorescence Yield, Charge Potential and Energy Imparted
Radiat. Res. 111, pp. 553-564 (1987)

1988

Olko, P., Booz, J., Paretzke, H.G., Wilson, W.E.
Energy Deposition in Nanometer Sites Based on Track Structure Calculations
Proceedings of the IAEA Group Meeting on Atomic and Molecular Data for Radiotherapy, Wien, (in press).

Booz, J., Feinendegen, L.E.
A Microdosimetric Understanding of Low-Dose Radiation Effects
Int. J. Radiat. Biol. 53, S. 13-21 (1988)

Bond, V.P., Feinendegen, L.E., Booz, J.
What is a "Low Dose" of Radiation ?
Int. J. Radiat. Biol. 53, S. 1-12 (1988)

Feinendegen, L.E., Bond, V.P., Booz, J., Mühlensiepen, H.
Biochemical and Cellular Mechanisms of Low-Dose Effects
Int. J. Radiat. Biol. 53, S. 23-37 (1988)

Feinendegen, L.E., Booz, J., Bond. V.P.
Empirical Approaches to Developement of Biophysical Models; Biophysical Aspects
XXI Radiobiological and Chemical Physics Contractor's Meeting, Los Alamos, 11-12 Mai 1988.

Booz, J., Feinendegen, L.E., Olko, P., Bond, V.P.
Empirical Approaches to Developement of Biophysical Models; Differentiation of Cellular Responses to Specific and Non-Specific Effects
XXI Radiobiological and Chemical Physics Contractor's Meeting, Los Alamos, 11-12 Mai 1988.

Olko, P., Booz, J., Paretzke, H., Wilson, W.E.
Energy Deposition in the Nanometer Sites Based on the Track Structure Calculations
IAEA group meeting on atomic and molecular data for radiotherapy, Wien, 13-16 Juni 1988

Olko, P., Schmitz, Th., Booz, J.
Energy Deposition and Ionization Yields of Photon Radiation in Sites of DNA Dimensions
21st annual meeting of European Soc. of Radiation Biology, Tel Aviv, 24-30 October 1988.

1989

Olko, P., Booz, J.
Energy Deposition by Protons and Alpha Particles in Sperical sites of Nanometer to Micrometer Diameter
Radiat. Env. Biophys. (in press).

Olko, P., Schmitz, Th., Morstin, K., Dydejczyk, A., Booz, J.
Microdosimetric Distributions for Photons
Radiat. Prot. Dosim. 29, No. 1-2 pp. 105-108 (1989).

RADIATION PROTECTION PROGRAMME
Final Report

Contractor:

Universidad Autonoma de Barcelona
Serv. de Fisica de las Radiaciones
E-08193 Bellaterra, Barcelona

Contract no.: BI6-A-232-E

Head(s) of research team(s) [name(s) and address(es)]:

Prof. F. Fernandez Moreno
Departamento de Fisica
Univ. Autonoma de Barcelona
E-08193 Bellaterra, Barcelona

Telephone number: 3/6920200 1659

Title of the research contract:

Heating by laser of thermoluminescence dosimeters; application to the measurement of low energy beta rays.

List of projects:

1. Heating by laser of thermoluminescence dosimeters, application to the measurement of low energy beta rays.

TITLE OF THE PROJECT Nº: B-16-A-232-E

LASER HEATING OF THERMOLUMINESCENT DOSEMETERS: APPLICATION TO THE MEASUREMENT OF LOW ENERGY BETA PARTICLES

HEAD OF PROJECT:

Profesor Francisco Fernández Moreno
Departamento de Física
Universidad Autónoma de Barcelona
E-08193 Bellaterra, Barcelona.

SCIENTIFIC STAFF:

Francisco Fernández Moreno
Alejo Vidal Quadras
Carmen Baixeras Divar

I. OBJECTIVES OF THE PROJECT:

- Reading of the thermoluminescent dosemeters by laser heating: Application to beta dosimetry.
- Setting up of a Valladas thermoluminiscence reading system.
- Manufacturing of our own $CaSO_4$:Dy and dosemeters.
- Study of the response of our dosemeters as a function of the energy, powder grain size and layer thickness.
- Comparison of our results with those obtained by other workers.

III. PROGRESS ACHIEVED:

1. Methodology:

The memory phenomenon in thermoluminiscence materials, exposed to ionizing radiation, is well know. Reading of the recorded information is carried out by means of controlled heating, in order to register the light emission from the dosemeter. This heating may be carried out by several methods. In this project we are using both laser and conventional heating, what has allowed us to do a very complete study of the fabricated dosemeters. In this work we have used a conventional thermoluminiscence reader, together with a software package that has been set up for this work.

2. Results:

2.1 Presentation of the conventional reader

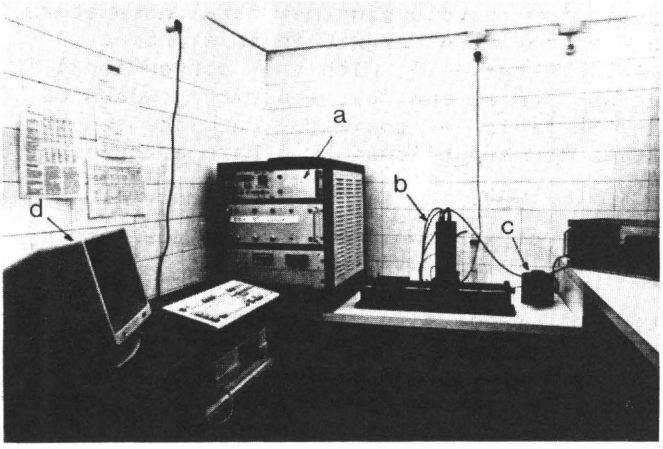

Figure 1.- Configuration of the reader.
a) Command unit.
b) Measuring device.
c) Irradiation system.
d) Data processing uint.

The thermoluminiscence reader used is Valladas type and was built in the C.R.N. of Strasbourg (France). We have carried out a complete calibration of all thermal parameters with the aim of optimizing the usage of the Tl reader.

2.2 Software development

In order to completely optimize the Tl reader it has been necessary to develop two program packages. One of them is completly designed to collect data from the Tl reader system and contains the TLGRAF and TLGROW codes. The other one is designed for data processing and contains a program package called PAK.

A counter (ORTEC 871) has been recently incorporated to the reader system. This counter is controlled by the code TLGRAF, wchich permits the counting of the emitted photons from the dosemeter for a fixed temperature interval.

Due to the conception of this system, a great flexibility is expected, in particular in front of a laser heating device, less versatile as many relevant TL thermal parameters cannot be controlled with the same efficiency than a conventional system. It is of great interest to have both TL reading systems for developping new beta dosemeters, as both instruments are complementary within this project.

A first test (1) with the conventional TL reading system has been carried out by measuring powders of $CaSO_4$:Dy, well know in the field of dosimetry, and the results obtained agree well with those published by others authors.

2.3 Manufacturing of our own $CaSO_4$:Dy and dosemeters

The practical limitation in developping a new generation of readers is the production of suitable and well matched dosemeters.

We have developped a facility to produce the large amount of $CaSO_4$:Dy powder required in the preparation and optimization of the dosemeter, adapted to beta dosimetry and radiation mapping.

We have used a method similar to the one suggested by Yamashita (2) for the thermoluminescent material preparation. First, a mixture of dehydrated $CaSO_4$:Dy with 1% per mol doping agent (Dy_2O_3) is dissolved in a concentrated solution of sulphuric acid. The destillation of this solution produces the crystallisation of the $CaSO_4$. Crystals are washed with destilled water and heated to 900°C in order to eliminate

impurities and to improve the dopant diffusion. The crystals so obtained are crushed and sieved to select the grain size in order to make different types of dosemeters.

In order to prepare the thermoluminescent dosemeter, crystals of a given grain size are mixed with a especial resin. The mixture is deposited over a base of different materials and dryed by annealing at 250°C during 1 hour.

Using this procedure we have obtained, thermoluminescent dosemeters with the following charecteristics:

Base thickness: 50 μm kapton; 250 μm stainless steel.
Layer thickness: 50 μm to 250 μm.
Detector size: 7 mm diameter discs. (20x20) cm^2 plates.

Our activity is first devoted to the test of irradiated dosemeters using a conventional reader. Future work will include laser reading of dosemeters.

2.4 Response of our dosemeters

Conventional dosemeters have been unable to fulfill the requirements for beta dosimetyry, so it is important to fully characterize our dosemeters. In this section we discuss the resuls obtained with our dosemeters regarding to their homogeneity and reproductivity.

Homogeneity

Various TL dosemeters developped for low penetrating radiation have been tested. Figure 2 shows the homogeneity of dosemeters (40 μm < grain sise < 50 μm) irradiated to 0.4 cGy with a $^{90}Sr/^{90}Y$ source. Observed fluctuations lie between 3% and 7%, in good agreement with values obtained for the same dosemeters with a laser reader (3).

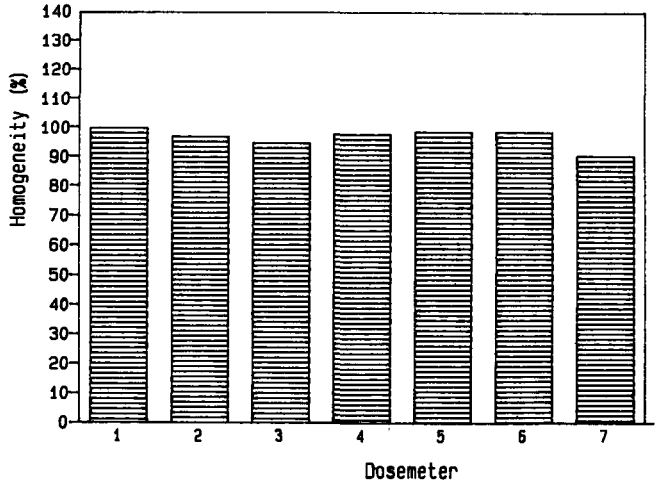

Figure 2.- Homogeneity test of TL dosemeter (40μm < grain size < 50μm) irradiated to 0.4 cGy with a $^{90}Sr/^{90}Y$ source.

Reproductivity

In Figure 3 we present the reproductivity results obtained for three different thermal processes and for a set of seven dosemeters having grain size between 40 μm and 50 μm. For increasing grain size, it is easier for the detector grains to grow loose, specially for temperatures higher than 500°C. This fact is a limitation to the thermal process that can be used and suggest a change in the preparation method for dosemeters with grain size bigger than 100 μm. The resuls show a total variation of 3%

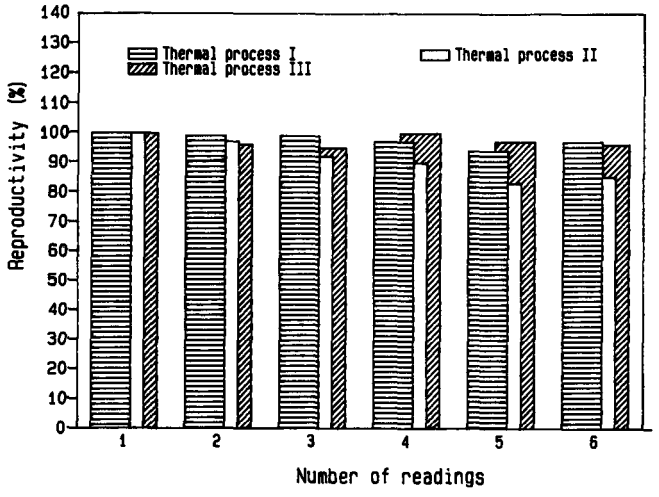

Figure 3.- Reproductivity test of TL dosemeter ($40\mu m$ < grain size < $50\mu m$) for three thermal processes:

Thermal process I : 1 hour at 350°C + 3.30 hours at 400°C

Thermal process II : 1 hour at 350°C + 7 hours at 400°C

Thermal process III : 1 hour at 350°C + 13.30 hours at 400°C irradiated to 0.4 cGy with a $^{90}Sr/^{90}Y$.

Energy dependence with grain size

The tests are conducted on various dosemeters using different grain sizes: 40-50 μm, 70-100 μm, 100-125 μm, 125-160 μm and 160-200 μm. In our measurements, we have used the same irradiation level (0.2 cGy) for the three conventional sorces: $^{90}Sr/^{90}Y$, ^{204}Tl and ^{147}Pm. The results were in good agreement with those obtained with different beta source. The sensitivity is the usual parameter to measure the quality of the detector in beta dosimetry. For a given dosemeter and dose, the sensitivity, S, is the ratio of the TL signal to the mass. A good detector should present a flat response as the energy changes from 100 KeV to 10 MeV. The variation of the sensitivity with the energy of the beta radiation is representative of the efficiency of the dosemeter. In general, considering the usually available sources, one takes the ratio S_{Pm}/S_{Sr-Y} as a measure of the quality of the beta response of a given dosemeter.

The sensitivity is presented in Figure 4. As expected, the sensitivity increases with the beta energy. The grain size dependence is only related to the dosemeter composition.

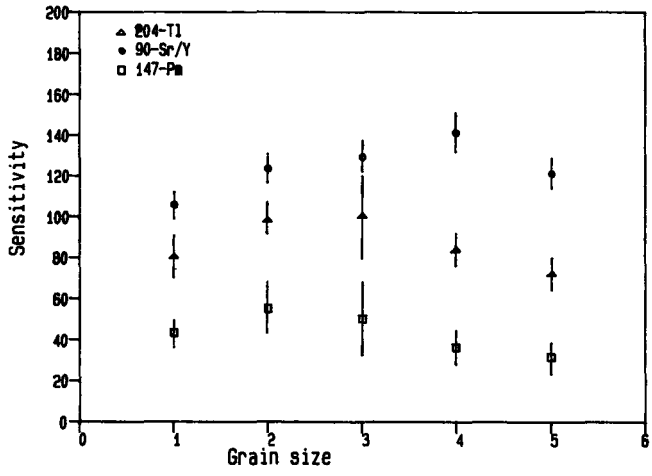

Figure 4.- Sensitivity vs. grain size (1: 40–50 μm, 2: 70–100 μm, 3: 100–125 μm, 4: 125–160 μ, 5: 160–200 μm) for TL dosemeter irradiated to 0.2 cGy with $^{90}Sr/^{90}Y$, ^{204}Tl and ^{147}Pm sources.

The same kind of results have been obtained elsewhere with laser reading. Our experiments show a S_{Pm}/S_{Sr-Y} ratio in the range of 25 to 45 percent. Typical pellets dosemeters present sensitivity ratios S_{Pm}/S_{Sr-Y} below 10 percent (4).

Regarding the sensitivity, the use of a thin dosemeter approaches the ideal case. Nevertheless, the TL signal loss associated to the loss of mass cannot be disregarded. Furthermore, extracting the light of very thin crystals leads to loss of efficiency. These remarks may contribute to explain the behaviour of the sensitivity as the grain size and preparation change.

Energy dependence with the layer thickness

The tests are carried out using dosemeters made of different layer thicknesses of a 40–50 μm grain size powder. A dose level of 0.1 cGy was obtained by irradiation with $^{90}Sr/^{90}Y$, ^{204}Tl and ^{147}Pm at C.E.A. in Fontenay-aux-Roses. The results are presented in Table I.

TABLE I

layer thickness	Ratio $^{147}Pm/^{90}(Sr+Y)$ Laser reader	Ratio $^{147}Pm/^{90}(Sr+Y)$ Conventional reader
50 μm	0.50	0.43
100 μm	0.38	0.40
150 μm	0.30	0.40
200 μm	0.27	0.45

The main value of the sensitivity for the conventional reader is of 0.42 ± 0.03. This is, not unexpectelly, is shown to be independent of the larger thickness, as our reader integrates the signal. However, the observed laser reader sensitivity diminishes significantly with layer thickness, due possibly to the different heating system used.

3. Discussion:

Before this study was started, the Centre d'Electronique de Montpellier achieved a unique experience in Eorope mastering laser heating for thermoluminescent dosemeters. As it was previously mentioned, some aspects of this technique should be solved in order to develop the procedure. In particular, developpment of adapted dosemeters and control of laser heating.

A remarkable progress was achieved in laser heating control during this study. Present conditions allow us to read plates as large as 20x20 cm^2. Calcium sulphate powder was used in order to gain experience and as a starting point to develope future materials in particular tissue equivalent. It should be emphasized the contribution of Montpellier in the preparation of powders and dosemeters.

The preparation of a large amounts of thin dosemeters is now well controlled in our laboratory. In the present configuration $CaSO_4$:Dy (grain size between 50 and 200 μm) is layed on a base (50 to 250 μm), tipically of kapton or stainless steel. The sample size ranges from 1 cm^2 up to (20x20) cm^2.

The homogeneity, as well as the reproductivity, from sample to sample is in the range of 5% Regarding the sensitivity, our experiment shows a S_{Pm}/S_{Br-Y} ratio as good as 45%, close to the best ever reported for plain TL materials.

Using the same technique, a batch of LiF (TLD 100) and $Li_2B_4O_7$:Mn (TLD 800) dosemeters have been made and tested. Mean quality of those dosemeters did not gave us an improvement of previous results. This situation should improve as much as effort will be given to this subject.

4. References:

1. Luguera, E. Postgraduate Research Project: Puesta a punto de un lector de termoluminiscencia para dosimetría beta. Universidad Autónoma de Barcelona, Spain 1989.

2. Yamashita, T., Nada, N., Onishi, H. and Kitamura S. Calcium sulphate phosphor actived by rare earth. CONF-680920. Int Proc. Conf. on Luminiscence Dosimetry, Gallinburg 1988.

3. Zangaro R. These•Etude et aplication du sulphate de calcium en cartographie de radiation ionisante. Université des Sciences Techniques du Languedoc, France 1988.

4. Driscoll, C.M.H., Francis, T.M. and Richards, D.J. The response of thermoluminiscent materials to beta radiation. Radiat. Prot. Dosim. 9 293-305(1984).

IV. OTHERS RESEARCH GROUPS COLLABORATING ACTIVELY ON THIS PROJECT:

Centre d'Electronique de Montpellier
Université des Sciences et Techniques du Languedoc
Place Eugene Bataillon, F- 34060 Montpellier Cedex
Professeur Jean Gasiot

CEA.CEN/ STEP-STID, BP 6, F-9226o Fontenay-aux-Roses
Dr. G. Portal

V. PUBLICATIONS:

Thin $CaSo_4$:Dy for beta Dosimetry, grain size and energy dependence. To be published in Radiat. Prot. Dosim.

Dosimetria beta por termoluminiscencia. Proc. of III Congreso Nacional de Protección Radiológica.Spain 1989

Puesta a punto de un lector de termoluminiscencia para dosimetria beta. Postgraduate Research Project,Barcelona 1989.

RADIATION PROTECTION PROGRAMME

Progress Report

1989

Contractor: Contract no.: BI6-A-302-I

II Univ. Degli Studi di Roma
"Tor Vergata"
Via O. Raimondo
I-00173 Roma

Head(s) of research team(s) [name(s) and address(es)]:

Prof. C. Franconi
Dipart. di Medicina Interna
II Univ. Degli Studi di Roma
Via O. Raimondo
I-00173 Roma

Telephone number: 06-6131170

Title of the research contract:

Development of high sensitivity spectrometric alpha emitter detector for use in monitoring of environment and radio protection.

List of projects:

1. Development of high sensitivity spectrometric alpha emitter detector for use in monitoring of environment and radio protection.

Title of the project no.:

Development of high sensitivity spectrometric alpha emitter detector for use in monitoring of environment and radio protection.

Head(s) of project:

Prof. C. Franconi - Dipartimento di medicina Interna - II Università degli Studi di Roma - Via O. Raimondo - 00173 Roma - Tel.(06)6131170.

Scientific staff:

Dr. A. Magrini, Dr. G. Izzo, Prof. K.V. Ettinger, Dr. M. Guerrisi, Dr. E. M. Staderini.

I. Objectives of the project:

Design, development and evaluation of a high sensitivity alpha particle detector, suitable both for the monitoring of presence of alpha emitters in the air as well as those deposited on the filter paper. the design of the instrument, based on the principle of multiwire an assay of a continuous carrier strip.

II. Objectives for the reporting period:

The main objective was establishment of the overall concept of the alpha emitter spectrometric detector. The particular objectives were: 1. Design of the structure of multiwire proportional counter based on the analysis of electric fields inside the structure.
2. Design and construction of the low noise preamplifier protected from damage by overloads, sparks and other discharges, inherent in the planned use of the device.
3. Design of the vacuum system as well as the gas filling line.

III. Progress achieved:

The key element in the project is the multiwire proportional counter itself. Selection of the design and its optimization were the first tasks in the project.

The efficiency of charge collection in counters of this type depends on the intensity of an electric field at the periphery i.e. in the vicinity of the cathode wires. In the multianode systems there are also "dead spaces" and their location and extent were checked for each considered design in order to minimize their effect on the operation of the counter.

The effect of low or even null field intensity volumes leads to an effective counting volume that is smaller than the geometrical volume and has some effect on the resolution. On the other hand the uniformity of gas multiplication depends upon the electric field close to the anode wire.

Two methods were applied to the design of electric fields in the counter. The first method was based on conformal transformations and yelded approximate values of field and potential lines in a periodic structure of infinite length. this method was implemented by means of a general mapping program, written in FORTRAN and permitted a quick evaluation of the proposed structures. the information from the conformal mapping did not provide, however means for evaluating the effects of finiteness of the counter structure. For practical reasons the ratio of anode wire spacing to their length for the considered designs was of an order of 8 - 10 and the ratio of length to width of the whole counter was in the range of 2 - 3. With such geometry the resulting field distributions and shapes of equipotential surfaces obtained by conformal mapping were considered approximate.

The more accurate, but also more costly in terms of computing effort were field and potential distributions evaluated by means of a finite elements program, following the method of Waligorski ("Design of Finite Multiwire Proportional Counter" Report of the Inst.Nucl.Phys., Cracow 1979).

The chosen design of the counter is so called plane parallel structure inside a rectengular metallic box. The space inside the counter is divided into the drift space and collection space. The collection space is delineated by the cathode wires. The sample deposited on a filter paper is placed in a volume between the walls of the counter and the collection space and thus the operation of the counter should not be affected by the presence of a dielectric. The field distributions were calculated for a 2, 3, 4 and 5 anode wire systems.

The second part of the program for the first year of project was the selection of the most satisfying electronic circuit for the amplification, integration and discrimination of signals from the proportional counter. A number of commercially available microcircuits were evaluated and so far the most suitable is RL-724 charge sensitive preamplifier manufactured by REL-LABS Inc. in Hicksville NY. The circuit is made using hybrid technology and is provided with an integral input protection. It has a very low equivalent noise of about 300 eV and is suitable for source capacitences of up to 100 pF. The integral linearity of the device is better than 0,05%, which is more than adequate for beta and alpha spectroscopy in a broad range of energies. The individual anodes of the proportional counter will be joined together (about 18 pF each) so that a single hybrid amplifier suffices for all of them. It is hoped that all the anode wires can be connected in parallel, by virtue of contiguos segments being used, taken from the same manufacturer's spool.

The preamplifier is located on a printed circuit board inside the proportional counter box. The same board supports the set of anopde wires. It was decided, that the discriminating and shaping electronics will utilize NIM modules. It is likely that at a later stage these modules will be replaced

by custom designed circuits, once their requirements are experimentally found.
During the reporting period the vacuum and gas filling systems were assembled, with manual controls at this stage, in anticipation of the testing of the designs for the counter.
It was not possible to proceed with the full testing of the input protection devices for the preamplifier, because realistic tests of this type require an assembled and working system. However, the manufacturer's data and the estimates of maximum voltages as well as maximum charges released accidentally, indicate that the chosen preamplifier should operate reliably even if the connecting cables are discharged accidentally through the input.

IV. Objectives for the next reporting period:

In the second part of the project the chamber will be assembled with all the parts of the proportional multiwire counter and connected to the pumping as well as the gas filling system. The operation of the chamber will be tested with samples of U, Th and Am deposited on filter paper. Attention will be paid to optimize both the sensitivity and resolution. In addition to argon-methane mixtures argon alone will be tried as the counting gas. Software for spectrum analysis, setting up and isotope identification will be written and tested.

V. Other research group(s) collaborating actively on this project [name(s) and address(es)]:

VI. Publications:

RADIATION PROTECTION PROGRAMME
Final Report

Contractor:

Contract no.: BI6-A-018-UK

National Radiological
Protection Board, NRPB
Chilton, Didcot
GB Oxon OX11 ORQ

Head(s) of research team(s) [name(s) and address(es)]:

Miss F.A. Fry
Environm. Measurements Dept.
NRPB
Chilton, Didcot
GB Oxon OX11 ORQ

Telephone number: 235-83.16.00

Title of the research contract:

The development of realistic phantoms to assist in the interpretation of *in vivo* measurement of low-energy photon-emitting radionuclides in bone.

List of projects:

1. Production of skull and chest phantoms suitable for the calibration of detectors for the measurement of 241-Am, 210-Pb and 90-Sr in bone.

Title of the project no.: 1

Production of skull and chest phantoms suitable for the calibration of detectors for the measurement of ^{241}Am, ^{210}Pb and ^{90}Sr in bone.

Head(s) of project: F A Fry

Scientific staff:

M R Bailey, A Birchall, N J Dodd, M D Dorrian, G Etherington, N Green, J D Harrison, J R H Smith

I. Objectives of the project:

The objective of this project is to provide phantoms which can be used to calibrate detectors for in vivo measurement of low-energy photon-emitting radionuclides in bone.

II. Objectives for the reporting period:

To obtain information on the initial skeletal distribution of bone-surface seeking radionuclides in man, from measurements on subjects injected with ^{88}Y and ^{239}Np.

To obtain phantoms suitable for the calibration of detectors used for in-vivo measurement of low-energy photon-emitting radionuclides in bone.

To improve methods of assessing intakes and body content of bone-seeking radionuclides, by developing an improved model of plutonium biokinetics for assessing systemic uptake of plutonium from excretion measurements.

III. Progress achieved:

1. Methodology

(i) Measurements of the distribution of bone-seeking radionuclides

Opportunities to measure the initial distribution of bone-seeking radionuclides in man arose from the administration of ^{88}Y ($t_{\frac{1}{2}}$ 107 d) and ^{239}Np ($t_{\frac{1}{2}}$ 2.4 d) to volunteers in studies of radionuclide biokinetics conducted at NRPB. Both radionuclides were administered by intravenous injection of 0.5 ml of 0.9% sodium chloride solution to which the radionuclide had been added as the citrate at pH 7.

Longitudinal scans of the body, and measurements of whole body, head, liver and bladder activity were carried out using 150 mm diameter cylindrical NaI(Tl) detectors in the NRPB low-background enclosure. Scans were made using a vertical ring of four detectors centred on the subject, who lay on a sliding bed. The detectors were fitted with side-shields and 40 mm x 150 mm slit collimators to reduce interference from activity elsewhere in the body. Measurements were made at 9 positions, 200 mm apart. For position 1 the centre of the detector ring was aligned with the centre of the head, 110 mm from the crown. Whole body activity was measured using five detectors positioned above and below the subject to give uniform response. Activity in the head was measured using a ring of four detectors fitted with side-shields. Liver and bladder activity were each measured with a single collimated detector.

Two subjects were injected with 4 kBq ^{88}Y. Longitudinal scans of subject A were made at 2 hours, 22 days and 84 days after injection. As redistribution of the activity in the body occurred predominately between the first two measurements, scans of subject B were performed at 5, 25 and 49 hours, and at 4, 7, 9, 15, 24, 29, 53 and 178 days. Two phantoms were constructed for calibration. Each consisted of 10 polythene containers, filled with ^{88}Y solution, which when assembled gave dimensions approximating to those of ICRP Reference Man. For one the activity was partitioned according to bone volume and for the other

according to bone surface-area. The latter was calculated from the work of Durbin and Schmidt (Health Phys. 49:623-661, 1985), who estimated the initial distribution of americium in the human skeleton from concentrations measured in the bones of Cynomolgous monkeys killed soon after injection with ^{241}Am, combined with the mass distribution of human skeletons.

Subjects C and D were injected with 4 kBq and 2.5 kBq ^{239}Np respectively. Scans were made on subject C at 1 and 3 days after injection, and on subject D at 1 day. A scan was made of a ^{239}Np phantom in which activity was distributed according to bone surface-area.

These initial distributions of activity in bone were compared with the distribution found from the post-autopsy measurements of United States Transuranic Registry (USTR) case 102 (H.E.Palmer et al. Health Phys. 49:577-586, 1985), who is thought to have incurred most of his intake of ^{241}Am through a wound 25 years before death. A scan of the skeleton had been performed using collimated dual-phosphor detectors. Only measurements at 200 mm intervals starting at 100 mm from the crown of the head (corresponding to position 1) were used here.

(ii) Bone phantoms

Phantoms of the head, knee and elbow were identified as being most useful for calibrating measurements of total skeletal activity. As the skull contains a large mass of bone which is almost independent of body size, is remote from other organs containing activity, and has little overlying tissue to attenuate photons, it is in most cases the best measurement site. For each radionuclide a matched pair of head phantoms is required, one with all exterior surfaces of the skull labelled and the other with interior surfaces labelled. Calibrations can then take account of variations in skull thickness and distribution of activity within the skull. Estimates of total skeletal activity can be improved by measurement of more than one region, and a particular site may be excluded by the presence of a contaminated wound. The knee and elbow are suitable, although both contain a much smaller bone mass than the

skull, and the fraction of skeletal activity in the knee is subject to variation due to bone remodelling. Thorax phantoms are required in addition, in order to make allowance for activity in the bones of the chest when measuring activity in the lungs and liver.

Enquiries established that there was considerable interest at several other UK institutions (AWE Aldermaston, BNFL Sellafield, and the UKAEA establishments at Dounreay, Winfrith and Harwell) in having a full set of ^{241}Am-labelled bone phantoms permanently available. Since such phantoms are only needed intermittently at any one facility, it was agreed that a joint purchase be made from New York University Medical Center (NYU), of a set of two skull phantoms, one thorax, one arm and one leg. Extensive discussions, co-ordinated by NRPB, were held to agree arrangements for sharing its use, and the following specification:

(a) An average chest wall thickness of 30 mm for the thorax phantom.
(b) An activity distribution within each phantom similar to that of previous ^{241}Am phantoms, and that found in USTR ^{241}Am total body autopsy cases.
(c) Activities (skull 5 kBq (each), thorax 10 kBq, leg 2.3 kBq, arm 0.75 kBq) chosen to give adequate count rates while avoiding dead-time problems. Fabrication techniques do not permit the activities of the arm and leg phantoms to be selected precisely in advance, although they are known afterwards. The relative activities of the different components of the phantom approximately conform to the expected distribution of activity in a subject.

The NRPB will be custodian of the ^{241}Am phantom. It has independently ordered a pair of ^{210}Pb-labelled skulls. All the phantoms have now been constructed and delivery is expected in February 1990.

(iii) Biokinetic model for plutonium

Because of the low yields and energies of photons emitted in the decay of plutonium isotopes, they cannot be measured directly in the

human body at levels corresponding to annual limits on intake. Evaluation of intakes may have to rely on air sampling or excreta monitoring or on a combination of techniques. A major problem with interpreting excreta measurements is the lack of a satisfactory biokinetic model. Models developed for calculating doses from intakes do not represent excretion sufficiently accurately, while mechanistic models which do so are too complicated for routine practical use.

Existing models and relevant information on plutonium biokinetics in man were reviewed. A model (Figure 1) was developed that is simple, but soundly based biologically, and which adequately represents the retention in body tissues and urinary and faecal excretion rates of plutonium following systemic uptake in man. All compartments are linked by first order kinetics. The parameters of the bone compartments were obtained by reducing a complex metabolic model of bone surface-seeking radionuclides to a simpler yet mathematically equivalent system. The remaining parameters were derived from observed urine and faecal rates of plutonium measured in man in the study conducted by Langham. The model's predictions of the organ distribution of plutonium were shown to be consistent with recent measurements of activity in organs of deceased plutonium workers made by the USTR.

2. Results

To compare results of the longitudinal scans, normalised net count rates, D_i, were calculated:

$$D_i = C_i \times 100 \; / \; \Sigma_i \, C_i$$

where C_i is the net count measured at position i. The distribution of ^{88}Y changed steadily over the first four days, after which it remained approximately constant, reflecting uptake to bone from body fluids. The only organ other than the skeleton that still contained a significant fraction (5% - 11%) of whole body activity was the liver. The calculated contribution from activity in the liver was subtracted from longitudinal scans made after four days, to give the expected response

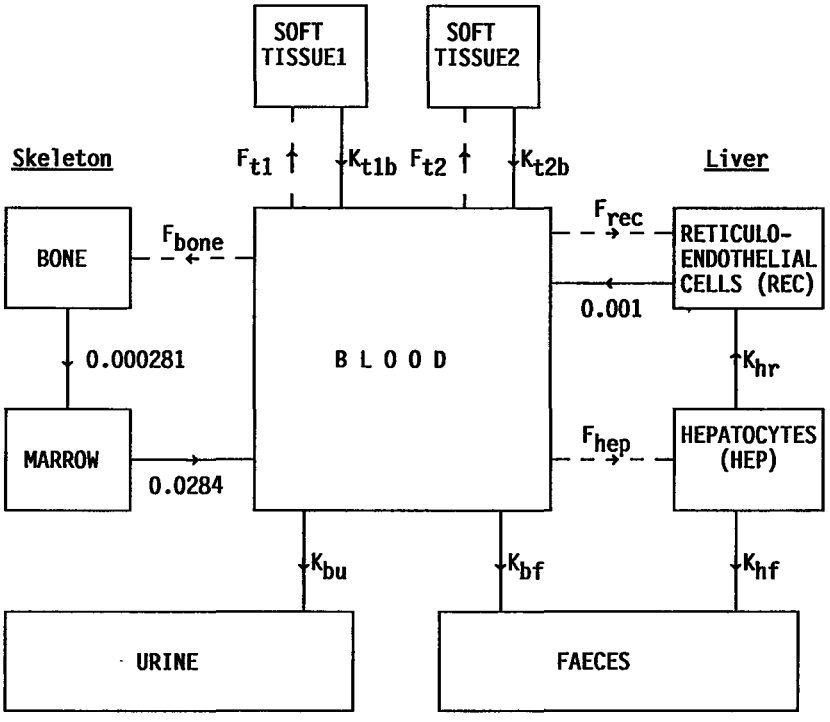

Parameter	Description	Rate(d^{-1}) or fraction	Half life (d)
F_{bone}	initial fraction to bone	23%	—
F_{rec}	initial fraction to REC	12%	—
F_{hep}	initial fraction to HEP	11%	—
F_{t1}	initial fraction to tissue 1	25%	—
F_{t2}	initial fraction to tissue 2	29%	—
K_{bu}	blood to urine	0.0242	28.6
K_{bf}	blood to faeces	0.000951	729
K_{hf}	HEP (liver) to faeces	0.0339	20.4
K_{hr}	HEP (liver) to REC (liver)	0.291	2.39
K_{t1b}	tissue 1 to blood	0.138	5.01
K_{t2b}	tissue 2 to blood	0.0228	30.4

Figure 1: Biokinetic model for plutonium in man

to the activity in bone. The average of the results so obtained for subject B is shown in Figure 2. There is quite good agreement with the scan of the phantom containing activity partitioned according to the estimated bone-surface distribution; much better than the bone-volume distribution.

Relatively limited information on the redistribution of ^{239}Np was obtained, because of its short half-life, but it suggested a similar pattern of behaviour to that of ^{88}Y. Activity in soft tissues may contribute significantly to the ^{239}Np scans (Figures 3 and 4), as they were made within a few days of injection. As for ^{88}Y, there is reasonable agreement with scans of the bone-surface distribution phantom (Figure 3), which improves as contributions from activity in soft tissue are reduced (Figure 4).

In comparison, the scan of USTR case 102 is much closer to that of the bone volume distribution phantom (Figure 5). Activity is noticeably high at the leg joints, evidence of its redistribution by bone remodelling, enhanced by vigorous exercise. The activity in the upper thorax is low in comparison to other USTR cases and it has been suggested that may be a result of a malignant melanoma that the subject suffered on his back (T.P Lynch et al., J. Radiol. Prot. 8:67-76, 1988).

The ^{88}Y activity in the head was estimated to be 17.0% and 18.5% of the whole body activity for subjects A and B respectively. For ^{239}Np, this fraction was somewhat higher, being 26% and 28% for subjects C and D respectively. These results are in reasonable agreement with that expected on the basis of bone surface-area distribution (17%).

3. Discussion

Comparison of longitudinal scans of subjects intravenously injected with ^{88}Y or ^{239}Np, with those of the phantoms confirmed that the initial uptake by the skeleton was broadly consistent with the estimated bone surface-area distribution. It is planned to deconvolute the longitudinal scans using the spatial response of the detection system to give a better estimate of the actual distribution of activity in each

FIGURE 2 LONGITUDINAL SCANS OF Y-88

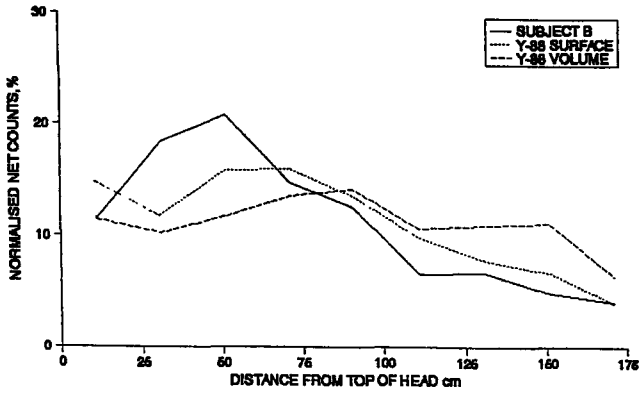

FIGURE 3 LONGITUDINAL SCANS OF Np-239

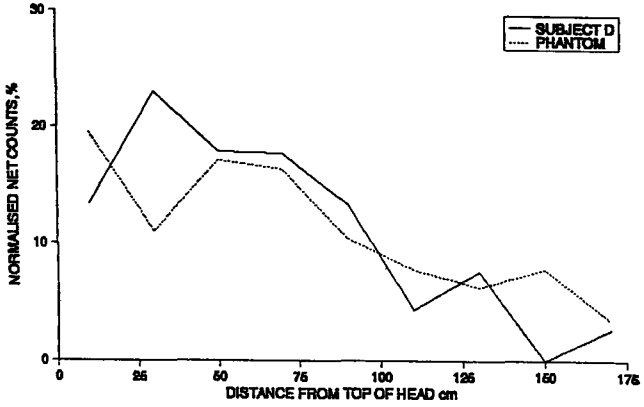

FIGURE 4 CHANGE IN Np-239 DISTRIBUTION IN SUBJECT C,BETWEEN 1 AND 3 DAYS AFTER INJECTION

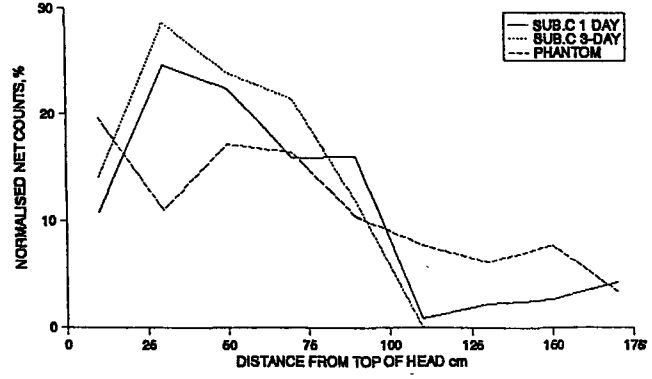

FIGURE 5 A COMPARISON OF USTR CASE 102; SUBJECT B AND Y-88 BONE VOLUME PHANTOM

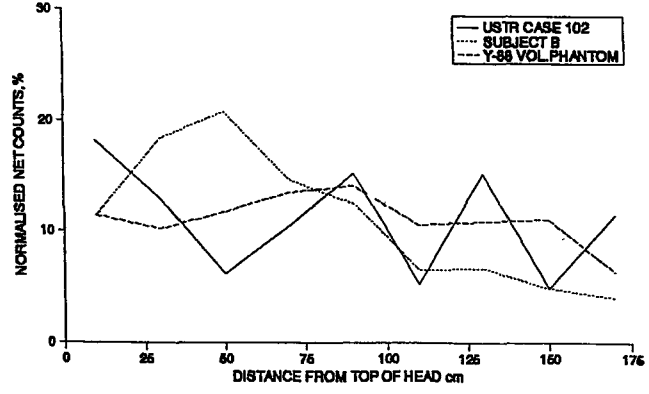

subject. Comparison with USTR case 102 suggests that in time bone remodelling will result in an activity distribution which is closer to the bone volume distribution. This redistribution may be affected by the pattern of intake, physical exercise and medical history of the subject. Differences between the scans of the subjects and phantoms were greatest in the region of the head, neck and upper thorax. This was attributed to the dimensions of the phantom being only approximately anthropomorphic in this region, and to the use of a large thorax component containing uniformly distributed activity. Such discrepancies illustrate the need for truly anthropomorphic phantoms for bone-seeking radionuclides.

To meet the aims of this project, it was originally intended that the NRPB should itself construct realistic bone phantoms for calibrating measurements of low-energy photon emitters such as ^{241}Am, ^{210}Pb and ^{90}Sr. However, recent legislation in India and the United Kingdom has severely decreased the availability of human bones, and no source of good quality specimens dimensionally close to the European norm could be found. The possibility of purchasing bone phantoms from New York University Medical Center (NYU) arose, for the first time, early in 1989. NYU has considerable experience of manufacturing bone phantoms, having previously constructed ^{241}Am phantoms of the thorax, skull and limbs, as well as skull phantoms labelled with a range of radionuclides. Calibration of its ^{241}Am phantoms has been verified by post-mortem analysis of ^{241}Am activity in a human skeleton obtained through the USTR. Purchasing from NYU was considered preferable to independent manufacture, since it would not only overcome the problems in obtaining suitable material, but would also provide a greater degree of standardisation with phantoms in use in the United States. As the phantoms could be used to measure cases varying from an acute, recent intake to a chronic, historic intake it was considered more important that the distribution and calibration of activities in the phantoms should be well documented, than that they exactly match the distribution found in any specific case.

IV. Other research group(s) collaborating actively on this project [name(s) and address(es)]:

V. Publications:

1. G Etherington, M R Bailey, M-D Dorrian and A Hodgson (1989) A study of the biokinetics of intravenously administered yttrium-88 in man. Radiation Protection - Theory and Practice. Proc. 4th Int. Symp. of the Society for Radiological Protection, Malvern, 4-9 June 1989, (IOP, Bristol) 445-448.

2 G Etherington, M R Bailey, M-D Dorrian and A Hodgson (1989) The biokinetics of intravenously administered yttrium-88 in man. Radiological Protection Bulletin No 105 September 1989 pp. 16-19.

3 A Birchall (1989) Uncertainty in bioassay determination of plutonium intakes. NRPB Memorandum M-207 (in press).

RADIATION PROTECTION PROGRAMME

Progress Report

1989

Contractor: Contract no.: BI6-A-306-I

Department of Physics
Rome University "La Sapienza"
Ple. A. Moro 2
I-00185 Roma

Head(s) of research team(s) [name(s) and address(es)]:

Dr. C. Furetta
Dept.of Physics, Group FIME
Rome University "La Sapienza"
Ple. A. Moro 2
I-00185 Roma

Telephone number: 6-49913459

Title of the research contract:

Development of an universal personal dosimeter using semiconductor sensors for mixed radiation fields.

List of projects:

1. Development of an universal personal dosimeter using semiconductor sensors for mixed radiation fields.

Title of the project no.:

DEVELOPMENT OF AN UNIVERSAL PERSONAL DOSIMETER USING SEMICONDUCTOR SENSORS FOR MIXED RADIATION FIELDS.

Head(s) of project:

Dr. C. FURETTA, Dept. of Physics, Group FIME
Rome University "La Sapienza"
P.le A. Moro, 2 - I-00185 ROMA

Scientific staff: Prof. C. Bacci, Dr. C. Furetta and Prof. B. Rispoli
Dept. of Physics, Rome University "La Sapienza"

I. Objectives of the project:

The objective of the project is to develop a pocket sized personal dosimeter using semiconductor materials. This dosimeter will be able to give a reading as close as possible to the dose equivalence in radiation fields existing around reactors, accelerators, X-ray , etc. Furthermore, the pocket dosimeter will give a flat energy response according to the most recent ICRP recommendations.

II. Objectives for the reporting period:

The program consisted of measuring the response of a certain number of Si-detectors received from Dr. Siffert in Strasbourg. They were exposed to different types of photons from radioactive sources like Am-241, Cs-137 and Co-60 as well as from heavily filtered X-rays.

III. Progress achieved:

METHODOLOGY

Nine Si-detectors (surface barrier type) have been tested zith different types of photons and heavily filtered X-rays. The specifications of the detectors are given in Table 1.

The procedure for all photon measurements in the calibration laboratory where the following:

a. Mount detector directly to front end of preamplifier using BNC-DNC or BNC-SMA adaptor.
b. Irradiation were made in the collimated beams of Americium, Cesium, Cobalt and also with X-rays from Stabilipan. Different intensities were obtained by changing distance for the sources and tube current for the X-ray machine.
c. Using ORTEC scaler/timer system count for at least 5 sampling periods of 1,10 or 100 seconds at each distance. Calculate mean countrate and standard deviation. Count background for at least 3 periods of 100 seconds.

This procedure was followed closely during all measurements.

The amplifier system used for the photon measurements consisted in a NIM pre-amplifier located close to the detector in the irradiation room. It was connected via 20 m coax cable to a main amplifier with RC-shaping placed in the control room. The preamplifier was a M124 ORTEC or a NB-21 from Harshaw.

The following block diagram shows the amplifier system with a setup for electronic calibration (Fig. 1).

It was foreseen to expose each detector in radiation field of Am-241 (60 KeV), Cs-137 (662 KeV) and Co-60 (1.25 MeV).

The detectors and preamplifier assembly were mounted on a special support in the calibration bench and alligned with a laser beam.

The detectors were exposed without any build-up material in front of the windows and also without phantoms. Exposures were made at a number of distances etween 0.5 and 3 meters.

The same calibration bench was also used for exposure of the detectors to X-rays. All X-ray irradiations were made with the detector in the reference distance, which is at a distance of 2.718 m from the target centre.

RESULTS

At first a detailed test of a large area Si-detector (4173) both in the protection level calibration system (low levels) and in the calibration bench has been done.

The results are given in tables 2 and 3 as an example of the measurements carried out on all detectors (see enclosed reprint RP-CD/89-02).

The efficiency of each detector has been plotted as a function of energy. Fig. 2 shows the results.

Block diagram of Amplifier System.

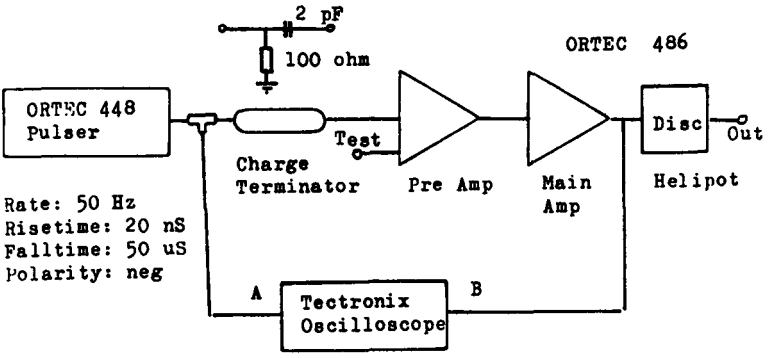

Fig. 1

Table 1. Characteristics of Solid State Detectors calibrated with X- and Gamma-Radiation.

Ref. No.	Serial No.	Type	Area (mm^2)	Thickness (um)	Resistivity (ohmcm)	Bias (V)	Resolution (kev)
S1	4173	Si - AB	500	100	1000	+45	50
S2	4179	Si - AB	500	100	1000	+45	50
S3	4180	Si - AB	500	100	1000	+45	50
S4	4344	Si - TM	500 ?	300	9000	+45	
S5	1(1)	Si - AM	50		150	+45	13
S6	2(1)	Si - AM	50		1500	+45	21
S7	3(1)	Si - AM	50		2000	+45	11.6
S8	4(6)	Si - AM	50		3000	+45	14
S9	5(4)	Si - AM	50		7000	+45	18

Table 2

PHOTON CALIBRATION OF SOLID STATE DETECTORS AT CERN.

Detector: STRASBOURG DETECTOR NO. 4173 NO. S1
Preamplifier: NB-21 Amp. Gain (coarse): 16
Bias Voltage: +45V Discriminator (E): 3.0
Date: 310889 Resolving Time (uS): 2.5

Exposure in collimated beams and cal. system:

Source No.	Dist. (m)	Doserate (uSv/h)	Mean Countrate Brutto (CPS)		Effeciency (cts/uSv)	
AM-2619	0.5	1252	71.2	2.6	205	
	1.0	312	9.92	1.2	114	104
	1.5	138	3.53	0.12	92	
	2.0	77.6	2.22	0.32	103	
	2.5	49.5	1.46	0.5	106	
CS-2045	1.0	111294	80436		3257	
	1.5	49434	40003		3237	3249
	2.0	27790	23508		3235	15
	2.5	17775	15500		3266	
CO-1665	1.0	26758	18020		2539	
	1.5	11862	7754		2400	2474
	2.0	6655	4470		2445	
	2.5	4249	2945		2513	
CO-151	0.867	300	354.1	7.6	4253	
	1.132	200	230.4	4.3	4149	
	1.732	100	112.4	1.8	4048	
	1.976	80	85.9	3.0	3865	3833
	2.589	50	49.3	2.7	3551	329
	3.449	30	29.3	1.9	3511	
	4.315	20	19.2	1.4	3456	
CS-2621	0.77	1500	1491.1	8.7	3592	
	1.084	1000	972.0	9.4	3508	3432
	1.801	500	467.8	4.2	3372	149
	2.525	300	271.1	5.8	3255	
CS-631	0.985	300	284.5	7.5	3417	
	1.421	200	184.7	1.5	3327	3182
	2.420	100	87.2	4.8	3140	184
	3.872	50	41.9	2.6	3020	
	5.360	30	25.1	1.6	3007	
CS-477	1.155	30	27.6	0.9	3317	3190
	2.972	10	8.3	1.0	2999	168
	4.832	5	4.5	0.4	3254	
RA-168	0.907	500	465.4		3355	
	1.174	300	270.3		3246	3213
	1.442	200	177.6		3198	111
	2.052	100	89.4		3219	
	2.926	50	42.3		3046	
RA-44	1.280	50	43.12		3105	
	1.658	30	25.9		3096	3012
	2.039	20	17.21		3076	111
	2.907	10	8.16		2894	
	4.160	5	4.13		2887	
AM-521	0.866	10	0.38		94	94
	1.230	5	0.25		93.6	1
NONE		BG	0.122	0.015		

Table 3
PHOTON CALIBRATION OF SOLID STATE DETECTORS AT CERN.

Detector: STRASBOURG SI-DETECTOR 5 CM2 NO. 4173
Preamplifier: NB-21 Amp. Gain (coarse): 64
Bias Voltage: +45V Discriminator (E): 1.40
Date: 110985 Resolving Time (uS): 2.5

Exposure in collimated beams:

Source No.	Dist. (m)	Doserate (uSv/h)	Mean Countrate Brutto (CPS)		Effeciency (cts/uSv)
AM-2619	0.5	1252	108	2	311
	1.0	312	18.1	1.6	209
	1.5	138	7.6	1.3	198.3
	2.0	77.6	3.6	0.5	167
	2.5	49.5	2.2	0.4	160
	2.95	35.4	1.7	0.3	173
CS-2045	1.0	111210	85279	288	3509
	1.5	49397	41866	121	3408
	2.0	27769	24827	155	3432
	2.5	17761	16174	180	3416
	2.95	12749	11742	131	3416
CO-1665	1.0	26642	18849	117	2673
	1.5	11811	8281	51	2577
	2.0	6627	4746	33	2609
	2.5	4230	3160	17	2711
	2.95	3031	2339	11	2794
None	-	BG	0.2	0.08	-

Exposure to X-rays at 2.718 m distance.

Spectrum	I(Tube) (mA)	Mon. (V)	Doserate (uSv/h)	Mean Countrate (CPS)		Effeciency (cts/uSv)
A100	4	0.40	840	179	4	767
	10	0.87	1827	319	9	629
	20	2.10	4410	735	17	601
A200	4	1.55	3255	1110	14	1231
	10	2.92	6132	2205	19	1302
	20	5.80	12180	4131	35	1234

Remarks: Nonlinearity at short distances from AM-2619 might be due to influence of noise or pile-up.

Source:	AM-241	A-100	A-200	CS-137	CO-60
E(keV):	60	89	161	662	1250
Mean Eff:	167	666	1256	3436	2673
Std.Dev.:	7	89	40	42	86

Unit: cts/uSv (Photon Dose Equivalent). DET. NO. S1

A number of measurements were also made with alpha-sources. It was essentially tests of FWHM made with an Am-241 alpha source in vacuum and measurements leakage current as function of bias voltage. The results from this are presented in Fig.3 .

DISCUSSION

The photon energy response curves from a pead starting point for a discussion. One can observe that the curves have a shape approximately as expected for Silicium with higher sensitivities for the lower energies, where photoelectron absorption is dominant. Moreover, the detector noise is very low.

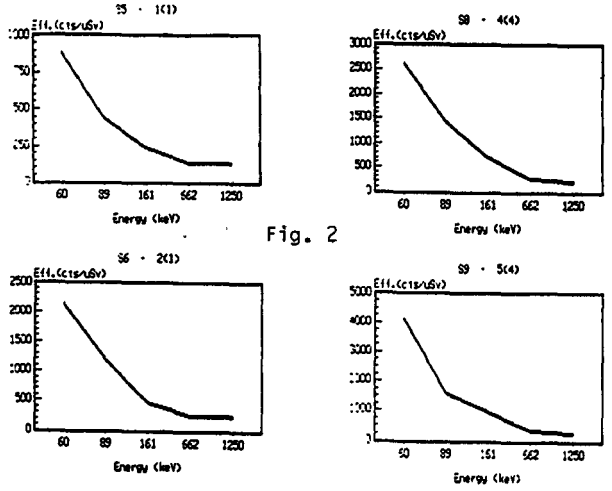

Fig. 2

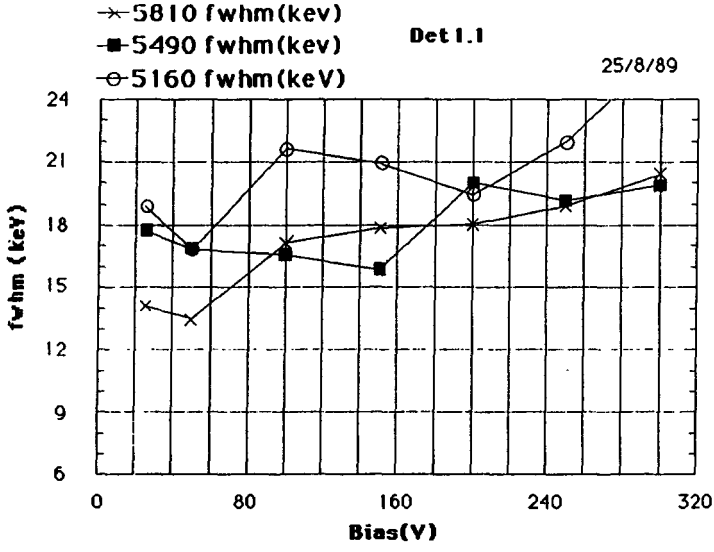

Fig. 3 FWHM as function of Bias Voltage for Si- Detector S5 (1(1))

IV. Objectives for the next reporting period:

To optimalize the detectors in both structure and size.
To study the response to thermal and fast neutrons.
To study the detectors behaviour in various environmental conditions (R.H. from 40% to 95%; temperatures from 20°C to 60°C).

V. Other research group(s) collaborating actively on this project [name(s) and address(es)]:

DENMARK: Institute of Physics University Aarhus;
FRANCE: Centre National de la Recherche Scientifique, Service Central de Securité, Centre de Recherches Nucleaires, Strasbourg;
GERMANY: Physikalisch Technische Bundesanstalt, Braunschweig;
CERN: European Organization for Nuclear Research, Geneva.

VI. Publications:

R.C. Raffnsoe, C. Furetta, C. Bacci - Photon sensitivity of solid state detectors - RP-CD/89-02, Calibration Report.

RADIATION PROTECTION PROGRAMME
Final Report

Contractor: Contract no.: BI6-A-231-F

Université des Sciences et
Techniques du Languedoc (USTL)
U.S.T.L.
Place Eugène Bataillon
F-34060 Montpellier Cédex

Head(s) of research team(s) [name(s) and address(es)]:

Dr. J. Gasiot
Ctre. d'Electr.de Montpellier
U.S.T.L.
Place Eugène Bataillon
F-34060 Montpellier

Telephone number: 67/52 56 33

Title of the research contract:

Heating by laser of thermoluminescence dosimeters; application to the measurement of low energy beta rays.

List of projects:

1. Heating by laser of thermoluminescence dosimeters; application to the measurement of low energy beta rays.

Title of the project no.: **CONVENTION N° B 16* 231-F**

**CHAUFFAGE PAR LASER
DE DOSIMETRES THERMOLUMINESCENTS.
APPLICATION A LA MESURE DES BETAS DE FAIBLE ENERGIE.**

Head(s) of project:

Professeur Jean Gasiot, Equipe Dosimétrie,
Centre d'Electronique de Montpellier,
Université des Sciences et Techniques du Languedoc, Case 083,
Place Eugène Bataillon, F-34 060 Montpellier Cedex.

Scientific staff:

Jean Gasiot
Jean-Pierre Charles

I. Objectives of the project:

Application à la dosimétrie béta du chauffage de dosimètres thermoluminescents par laser.

II. Objectives for the reporting period:

Lecture des dosimètres thermoluminescents par chauffage laser:
Application à la dosimétrie β:

* Utilisation du $CaSO_4$: Dy comme matériau thermoluminescent;
* Réalisation des dosimètres très fins;
* Lecture et amélioration;
* Positionnement des résultats par rapport aux autres équipes.

III. Progress achieved:

1. Methodology

La thermoluminescence est l'une des méthodes physiques des plus employées en dosimétrie des rayonnements ionisants et l'on cherche constamment à en améliorer les performances en particulier par l'introduction de nouveaux procédés de chauffage. L'utilisation d'un laser nous permet aujourd'hui de faire progresser la méthode de façon décisive, non seulement en améliorant l'efficacité des lectures, mais aussi le temps de lecture qui est réduit d'un facteur 1000 environ, cette technique ouvre un nouveau champ d'applications en cartographie de dose par thermoluminescence. Nous savons que l'intensité lumineuse est d'autant plus élevée que la vitesse de chauffage est plus grande.

La réduction des temps de lecture est considérable, il se situe aux alentours de 10 ms. La technique laser, du fait de sa spécificité introduit de nouvelles contraintes par rapport à un chauffage conventionnel. Sa rapidité nécessite la mise au point de dosimètres adaptés, ils doivent être suffisamment fins afin de permettre un chauffage rapide ne permettant pas l'installation d'un gradient de température important dont la présence serait préjudiciable à la qualité de la lecture de doses. Nous avons mis au point des capteurs particulièrement bien adaptés à notre mode de chauffage, ils sont, du fait de leur faible épaisseur, particulièrement intéressants en dosimétrie des radiations faiblement pénétrantes.

2. Résultats.

2.1 Préparation des matériaux: Nos besoins en poudres thermoluminescentes adaptées à la réalisation de dosimètres performants chauffés par laser nous ont conduit à préparer du sulfate de Calcium:

* Ce matériau peut être préparé facilement au laboratoire, ce qui permet un approvisionnement abondant de poudres de qualité. Ceci a facilité la mise au point des dosimètres individuels et des plaques de grandes tailles dédiées à la cartographie de doses.
* Sa sensibilité est remarquable.
* Son absorption importante à 10 μm permet un chauffage par laser CO_2 efficace.

Pour la préparation des poudres, nous utilisons une méthode similaire à celle proposée par Yamashita, cette opération comporte quatre étapes:

- En premier lieu, on mélange du $CaSO4:2H2O$ avec le dopant (le plus souvent sous forme d'oxyde) dans de l'acide sulfurique concentré.
- On procède ensuite à un chauffage qui assure la dissolution du sulfate puis la distillation, d'abord de l'eau, puis de l'acide conduisant à la formation de cristaux de sulfate.
- Ensuite on effectue un lavage à l'eau distillée, suivi d'un recuit au voisinage de 900°C pendant une heure environ ce qui permet d'éliminer les impuretés et de diffuser le dopant.
- Enfin, interviennent toutes les opérations de broyage et de tamisage.

Nous avons utilisé deux sulfates d'origines différentes (Merck et Prolabo pour analyses). Les poudres obtenues à partir de ces deux produits ne

présentent pas au niveau de la thermoluminescence de différences notables ceci est vrai au niveau du fading, de la reproductibilité ainsi que de la sensibilité. Pour ce qui est des autres matériaux, LiF.. utilisés pour la réalisation de dosimètres, ils ont été achetés dans le commerce.

2.2 Technique de fabrication des dosimètres: Après avoir testé plusieurs méthodes dépôt, par décantation, par couchage, et par inclusion dans du PTFE (teflon) par exemple, nous avons retenu la méthode de couchage par sérigraphie, elle nous a permis d'obtenir les meilleurs résultats sur des supports de verre ou de kapton.

Nous utilisons les supports de Kapton, ils sont légers et pratiques d'emploi. Leur tenue en température est excellente malgré une absorption très importante au voisinage de 10,6 µm (230 cm^{-1}) leur absorption dans le visible (316 cm^{-1} à 500 nm).

Caractéristiques typiques des dosimètres: Ces derniers sont réalisés à partir de $CaSO_4$: Dy:

Support: Kapton, épaisseur 50 micron (11,2 mg. cm^{-2});
Granulomètrie: entre 25 et 50 µm ;
Densité de dépôt: 6,8 mg. cm^{-2};
Homogénéité: dispersion inférieure à 5% ;
Recuit: à 240°C pendant 2 heures

2.3 Irradiations :

Les résultats présentés ici ont été obtenus avec nos dosimètres irradiés par divers types de sources:

- Les tests de reproductibilié, sensibilité, dynamique du signal par chauffage laser sont obtenus en utilisant une source Rayons X dentaire (50 KeV), pour une irradiation uniforme, la dispersion des mesures de thermoluminescence sur une plaque est en général inférieure à 5% pour des doses de quelques milligray.
- L'essentiel des irradiations beta ont été réalisées par le CEA, soit à Grenoble (SPR/GMI), soit à Fontenay aux Roses (CEN/STEP-STID).
- Afin de disposer rapidement d'irradiations béta, nous avons aussi été conduits à mettre en place au laboratoire des sources de ^{147}Pm, ^{204}Tl et $^{90}Sr/Y$. Elles sont opérationnelles depuis quelques semaines.

2.4 Présentation du lecteur Laser:

Le lecteur utilise un laser CO_2 (10,6 µm) pour le chauffage. Pour le faisceau laser IR, une lentille de germanium permet de faire varier le diamètre du faisceau entre 300 µm et 2 mm. La détection de la thermoluminescence, qui correspond à une émission de lumière visible, est assurée par un photomultiplicateur de grande sensibilité couplé à une chaine de comptage de photons. Un micro-ordinateur assure la gestion de toutes les données recueillies lors des lectures ainsi que la commande des différentes parties du lecteur. Les conditions de lecture typiques sont les suivantes:

Puissance laser: 3,6 Watt (variation de 5% environ sur une journée);
Temps d'exposition: entre 40 et 80 ms
Diamètre du faisceau laser: 1 mm;
Etalonnage statique:ELS(source lumineuse): 3350 coups. $canal^{-1}$. s^{-1};
Bruit de fond: 32 coups. $canal^{-1}$. s^{-1}.

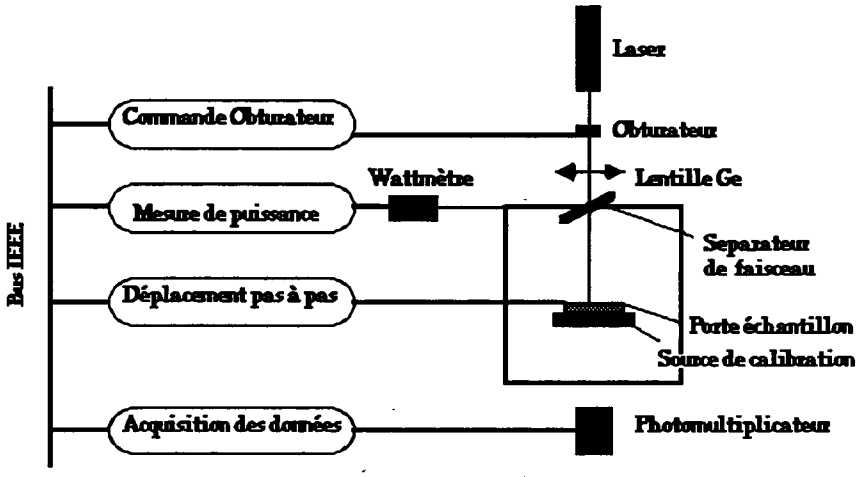

FIGURE I: **Schéma synoptique du lecteur**

2-5 Résultats :

L'interprétation d'un signal de thermoluminescence en termes de dose est souvent très difficile. Ce signal présente une très forte dépendance en fonction de l'énergie et de l'angle d'incidence du rayonnement béta en cours d'irradiation; par ailleurs, les dimensions et la nature du dosimètre influent sur la réponse. Les dosimètres commercialisés pour la dosimétrie béta ont des épaisseurs variant entre 44 $mg.cm^{-2}$ (0,2 mm de PTFE) et 200 $mg.cm^{-2}$ (0,9 mm Pellet). De nombreuses équipes ont contribué à l'optimisation des dosimètres: l'essentiel des travaux porte sur la mise au point de capteurs de faible épaisseur, ce qui réduit leur dépendance en énergie. Une autre méthode qui permet de réduire l'épaisseur effective consiste à inclure du graphite dans le dosimètre.

Linéarité : Le signal de thermoluminescence, STL est linéaire pour les doses, comprises entre 100 et 800 mRad. Pour cette expérience, notre niveau de bruit est assez élevé, cela est lié au mode de lecture qui, dans ce cas, est loin d'être optimisé. Pour les irradiations ^{147}Pm, il a été difficile d'obtenir les doses souhaitées par suite du très faible débit des sources, par ailleurs le calcul des doses est délicat, il doit tenir compte de la géométrie et des conditions atmosphériques (pression atmosphérique ainsi que le degré d'humidité). Les résultats obtenus sont donnés dans la figure II. Dans la figure suivante (Figure III), nos résultats sont comparés à quelques valeurs typiques présentées dans la littérature.

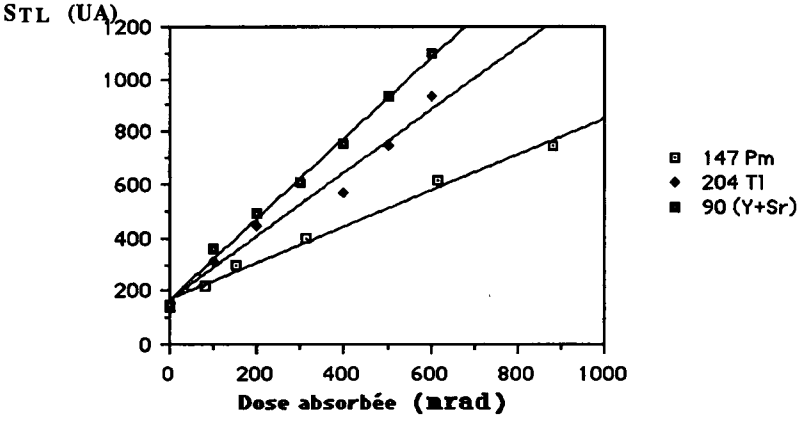

Figure II : Réponse, STL(UA) en fonction de la dose de dosimètres thermoluminescents de sulfate de calcium dysprosium préparés à Montpellier.

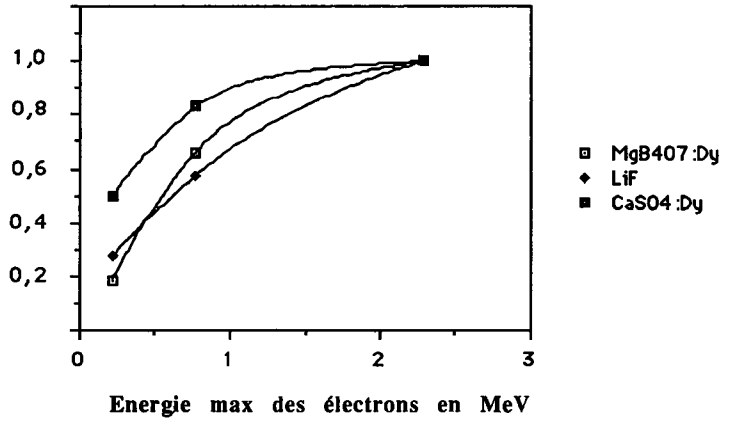

Figure III : Réponse relative R des dosimètres thermoluminescents à des électrons de différentes énergies.
$R = TL(^{a}X)/TL(^{90}(Sr+Y))$
Les sources utilisées, ^{a}X, sont par ordre croissant d'énergie, le ^{147}Pm, le ^{204}Tl et le $^{90}(Sr+Y)$. Le 100 % est la réponse à une irradiation $^{90}(Sr+Y)$.

Les résultats des figures 2 et 3 sont otenus avec des dosimètres qui se présentent sous forme de dépôts fins, ils sont développés spécialement pour la mesure des doses peau (entre 5 et 10 mgcm-2). Les LiF (7,2 mgcm^{-2}) ont été fabriqués par G. URCHIN de l'Institue of Isotopes of the Hungarian Academy of Sciences. Les MgB4O7: Dy (8,4 mgcm^{-2}) sont developpés par M. PROKIC du Boris Kidric Institue (Yugoslavia). Les CaSO4: Dy (9,2 mgcm^{-2}) sont ceux préparés à Montpellier. Les résultats obtenus sur nos dosimètres sont un peu meilleurs que ceux présentés par les autres groupes. Il serait possible d'améliorer encore le rapport des signaux (^{147}Pm/^{90}(Sr+Y)) à mieux que 0,5 en utilisant pour le dépôt un métériau plus léger.

Réponse du dosimètre en fonction de l'épaisseur du dépôt: Afin de tester la réponse de nos dosimètres en fonction des épaisseurs de dépôts, nous avons préparé 4 familles de dosimètres ayant les caractéristiques suivantes:

1er dépôt: épaisseur 50 µm (6 mg.cm^{-2});
2eme dépôt: épaisseur 99 µm (11,9 mg.cm^{-2});
3eme dépôt: épaisseur 149µm (17,9 mg.cm^{-2});
4eme dépôt: épaisseur 200 µm (24,02 mg.cm^{-2});

La dose est de 100 mRad, les résultats obtenus sont reportés dans le tableau I. La décroissance du signal mesuré en fonction de l'épaisseur semble due en partie au fait que les mesures de thermoluminescence sont effectuées sur la lumière qui émerge du support de kapton par la face arrière.

Epaisseurs des dépôts (micron)	Rapport R (^{147}Pm/ ^{90}(Sr+Y))
50	0,50
100	0,38
150	0,30
200	0,27

Tableau I : Réponse relative, R, des dosimètres thermoluminescents en fonction de l'épaisseur des dépôts avec une source de ^{147}Pm. Les lectures ont été effectuées par chauffage laser.

Reproductibilité et dépendance énergétique en fonction de la taille des grains: Nous avons préparé spécialement une série de dosimètres avec diverses tailles de grains variables, sur des supports en inox (250µm). Les mesures de reproductibilité sont effectuées sur des dosimètres irradiés à 0,2cG, avec une source ^{90}(Sr+Y), lues sur un lecteur conventionnel et en faisant intervenir trois types de recuits:

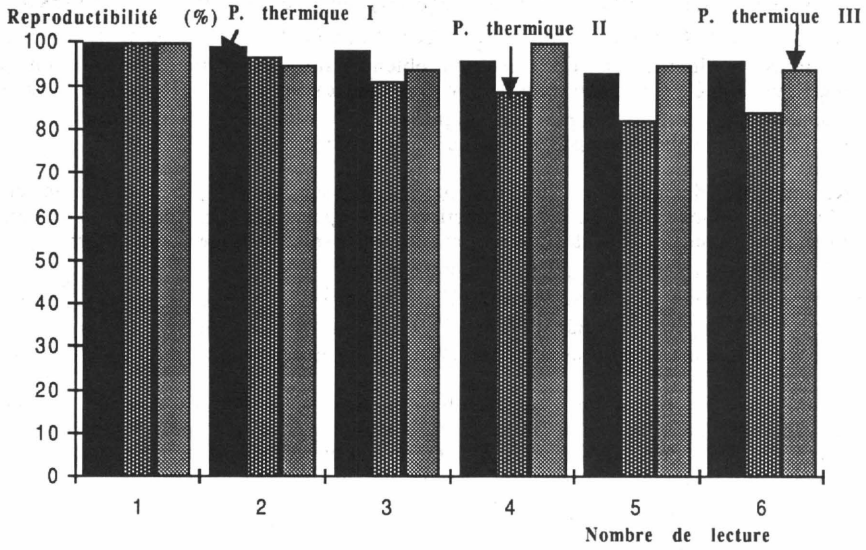

Figure IV : Mesure de la reproductibilité en fonction du nombre de lectures pour trois traitements thermiques avant irradiation.

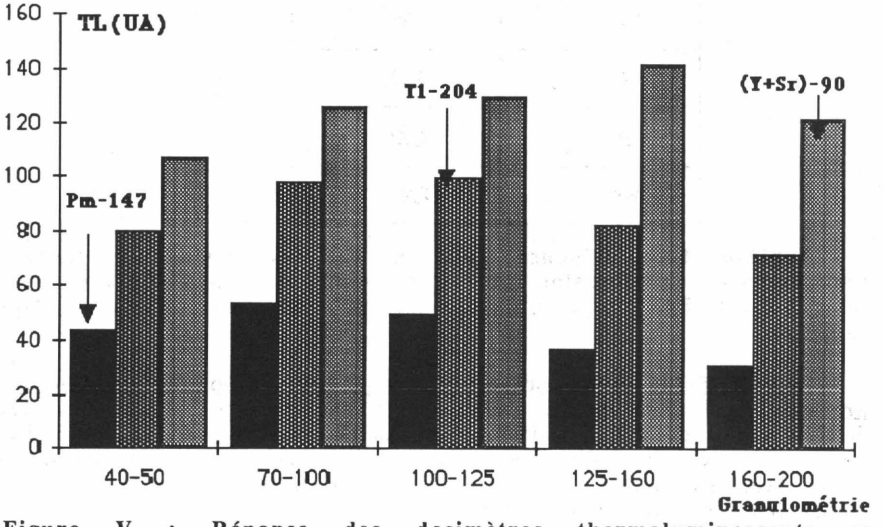

Figure V : Réponse des dosimètres thermoluminescents en fonction de l'énergie des électrons et pour des dosimètres préparés à partir de poudres de granulométrie différentes.

* Le 1er: un chauffage à 350°C (1h) suivi d'un chauffage à 400°C (3,3h);
* Le 2eme: un chauffage à 350°C (1h) suivi d'un chauffageà 400°C (7h);
* Le 3eme: un chauffage à 350°C (1h) suivi d'un chauffage à 400°C (13,3h).

La figure V montre la dépendance du signal de thermoluminescence en fonction de l'énergie des béta pour diverses tailles de grains.
Nous pouvons estimer que le meilleur résultat est obtenu par les dosimètres préparés à partir d'une granulométrie entre 40 et 50 µm. Le rapport des TL ($^{147}Pm/^{90}Sr$) est voisin de 0,45.

3- Discussion et positionnement:

Avant le début de cette étude le Centre d'Electronique de Montpellier avait acquis une expérience unique en Europe dans le domaine du chauffage par laser des dosimètres thermoluminescents. Comme nous l'avions indiqué, il restait cependant quelques points à régler afin de permettre le développement de cette technique complexe et prometteuse : la mise au point de dosimètres adaptés, le développement de l'expérience et à un degrè moindre, le contrôle du chauffage faisaient partie de ces points restant à améliorer. La recherche d'une solution adaptée à la dosimétrie béta, but de la présente convention, a constitué une étape dans le développement de cette technique.

Au cours de cette étude nous avons fait des progrès considérables dans la préparation des dosimètres, le contrôle du chauffage par laser, enfin le lecteur a recu des améliorations importantes qui nous permettent même de lire des plaques de grande taille (20x20 cm^2). L'apport de Barcelone a été déterminant dans le domaine du test des dosimètres. La préparation de poudres de sulfate de calcium a été un point de passage obligé. Ce matériau est comme nous l'avons justifié par ailleurs le meilleur choix dans la phase transitoire de mise au point. Il nous est maintenant possible d'aborder avec succès la préparation de dosimètres à base de matériaux tissus équivalents. Les essais réalisés dans ce sens n'ont pas connu le succès escompté car nous ne disposions pas de poudres de qualité suffisante pour assurer une préparation de bons dosimètres. Nos lecteurs de dosimètres ont beaucoup progressé, restent quelques améliorations au niveau de la collection de lumière. Nous venons de mettre en place à Montpellier une série de sources béta, ^{147}Pm, ^{204}Tl et $^{90}(Sr+Y)$, elles nous permettent de disposer, d'un moyen d'irradiation pour des test rapides.

La réponse de détecteurs spécifiques développés pour répondre aux contraintes d'un chauffage rapide permet de mesurer un rapport des signaux pour le sulfate de calcium ($^{147}Pm/^{90}Sr$) voisin de 0,5. Nous avons fabriqué de la même façon, des dosimètres à base du LiF (TLD100) et du $Li_2B_4O_7$: Mn (TLD800), qui sont tissus-équivalents. La qualité très moyenne de ces dépôts ne nous a pas permis, comme escompté, d'améliorer les résultats. Cette situation transitoire devrait pouvoir évoluer dans la mesure où nous concentrons nos efforts dans ce domaine.

IV. Other research group(s) collaborating actively on this project [name(s) and address(es)]:

Laboratorio de Fisica de las Radiaciones, Dept. de Fisica, Universitad Autonoma de Barcelona, Bellaterra (Barcelona), Pr. F. Fernandez

The irradiations were performed by :
CEA - CEN/STEP-STID, BP 6, F-92 260 Fontenay-aux-Roses, Dr. G. Portal
CEA - Service de Protection contre les Rayonnements, SPR/GMI, CEG, F-38 041 Grenoble CEDEX,
Dr. Y. Herbaut

V. Publications:

THIN CaSO4: FOR BETA DOSIMETRY. GRAIN SIZE AND ENERGY DEPENDENCE.

E. Leguera, F. Fernàndez, J. Planas,
Fisica de les Radiacions.
Universitat Auonoma de Barcelona.
E-08193 Bellaterra (Barcelona). Spain.

K. Ed Dahabi; G. Bruguier, M. Daoud, J. Gasiot.
C.E.M. C.N.R.S. UA 391
Université des Sciences et Techniques du Languedoc
F-34095 Montpellier Cedex 5. France.

Submitted for publication at the 9th International Conference on solid state dosimetry (Vienna'89)

RADIATION PROTECTION PROGRAMME

Progress Report

1989

Contractor:

European Organisation for
Nuclear Research (CERN)
CH-1211 Genève 23

Contract no.: BI6-A-307-CH

Head(s) of research team(s) [name(s) and address(es)]:

Dr. K. Goebel
CERN
Div. TIS/RP
CH-1211 Genève 23

Telephone number: 022-832159

Title of the research contract:

Development of an universal personal dosimeter using semiconductor sensors for mixed radiation fields.

List of projects:

1. Development of an universal personal dosimeter using semiconductor sensors for mixed radiation fields.

Title of the project no.: Development of an universal personal dosemeter using semiconductor sensors for mixed radiation fields.
Project No. BI6-A-307-CH

Head(s) of project: Dr. K.Goebel
CERN Div. TIS/RP
CH-1211 Geneve 23

Scientific staff: R.C.Raffnsoe
CERN Div. TIS/RP
CH-1211 Geneve 23

I. Objectives of the project:

The objective is to develop a pocket-sized personal dosemeter with dose-equivalent response. The instrument is intended to be used by persons working in areas near accelerators, reactors and other sources of radiation, which produces both gamma-radiation and neutrons of widely varying energies. The detector system in the dosemeter is composed of a set of solid-state detectors (Si, CdTe or GdO) with or without polythene radiators, - each chosen to cover their part of the radiation spectrum.

II. Objectives for the reporting period:

Contribution of CERN during the first part of the project was to provide facilities for measuring the photon response of some batches of Silicon Detectors. The purpose was to choose optimum parameters like thickness, resistivity, bias etc and the work included development of equipment and methods for measuring photon response over a wide range of energies.

III. Progress achieved:

The first batches of Si-detectors were received from CNRS, Strasbpurg in July 1989 and our measurements took place in September after end of the holiday period.

The first part of the work consisted in building supports and other hardware for exposing the detectors in our calibration facilities with best possible accuracy and reproducibility. It was here particularly important to obtain lowest possible influence of scatter. The amplifier system was built from conventional NIM electronics with a low-noise preamplifier placed next to the detector in the irradiation room and with main amplifier, bias supply and analyser etc in an adjacent control room. The procedure for setting up and measurement was made in a simple and standardized way to allow similar tests being made in the other laboratories participating in the project with their own electronics. Read-out was in most cases done with an integral discriminator and a scaler-timer system.

Each detector was exposed in collimated beams of AM-241 (60 keV), CS-137 (662 keV) and CO-60 (1.25 MeV) and at two different settings of an X-ray machine (A100 and A200 spectra). The intensity was varied by placing the detectors at a number of source-detector distances between 0.5 and 3 meters.

The results of measuring first batch (Detectors S5 to S9) allows plotting effeciency as a function of resistivity as shown on the graph below.

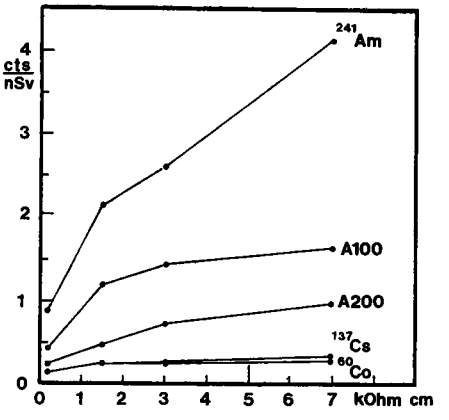

The photon effeciency is given in cts/nSv and there is one curve for each of the five photon energies. The A100 and A200 spectra gives mean energies of 89 and 161 keV, respectively. The Silicium detectors had all a thickness of 300 μm and a surface area of 50 mm^2. They were exposed with a PVC protection cap in order to exclude light but without filters for shaping the energy response. The sensitivity is therefore much larger at low photon energies.

The Cesium sensitivity is uniform over a large range of doserates and only affected at high intensities by the amplifier resolving time (2.5 - 3 uS) for which compensation could be made. One of the larger detectors was exposed to doserates from 5 μSv/h to more than 100 mSv/h and showed a uniform sensitivity of 3.2 cts/nSv. This type had, however, a much larger noise level, which made it less useful for measurement of low energy photons. The reason for this was that the discriminator level had to be set high to cut the noise and this eliminated also counts produced by Americium 60 keV X-rays.

The CNRS detectors were similarly compared with a number of other solid state detector types used at CERN. The work in this first part of the project serves thus for establishing a standard method for tests and an appreciation of the problem. The objective for the photon detector in the pocket dosemeter is to obtain a flat energy response from 50 keV to above 2 MeV and the idea is to get this by using a single Si-diode with a suitable filter or to employ a simple form of pulse height analyser with 4 or 8 channels. Numerous new measurements have to be made with other batches of detectors before the proper one can be chosen.

The irradiation facilities and experimental equipment was available at CERN, but we did unfortunately not possess a modern MCA in the calibration laboratory. This equipment will be indispensable for the neutron measurements and we will try to borrow a unit. We find it a bit disappointing that the EEC-funds put to our disposition cannot be used for purchase of instrumentation.

IV. Objectives for the next reporting period: The program for the first 6 months of 1990 will include continued tests of photon response on a new batch of detectors as well as measurements of fast neutron response as function of polythene radiator thickness. The influence of bias voltage on sensitivity and noise level is to be investigated in detail and the response of GdO to thermal neutrons will be examined. The GdO foil will be mounted on a Si photodiode. The influence of backscatter from standard phantoms will be measured with some of the detectors.

V. Other research group(s) collaborating actively on this project [name(s) and address(es)]:

CRN/PHASE	Strasbourg	Dr. Siffert
Univ. Aarhus	Aarhus (DK)	Dr. E.Uggerhoj
Univ. Rome	Rome (I)	Dr. C.Furetta
PTB	Braunschweig (RFA)	Dr. Kramer

VI. Publications: RP-CD/89-02 Internal Report
PHOTON SENSITIVITY OF SOLID STATE DETECTORS
R.C.Raffnsoe 3.10.89

RADIATION PROTECTION PROGRAMME
Final Report

Contractor:

Contract no.: BI6-A-009-UK

Medical Research Council
20 Park Crescent
GB London W1N 4AL

Head(s) of research team(s) [name(s) and address(es)]:

Dr. D.T. Goodhead
MRC Radiobiological Unit
Cell and Molecular Biology Div.
Harwell, Didcot
GB Oxon OX11 ORD

Telephone number: 235-83.43.93

Title of the research contract:

Biophysical studies of relations between radiation dose, quality and biological effect.

List of projects:

1. Analysis of physical properties of diverse radiations in relation to their observed biological effectiveness.
2. Development of radiation sources and dosimetric techniques for radiobiological studies at low and high dose-rate.

Title of the project no.: 1

Analyses of physical properties of diverse radiations in relation to their observed biological effectiveness.

Head(s) of project:

D.T. Goodhead

Scientific staff:

D.T. Goodhead
H. Nikjoo
D.E. Charlton
J. Thacker
D.L. Stevens

I. Objectives of the project:

This project is to generate and analyse relevant physical and biological data and to deduce the implications for radiation protection. The specific aims are:

(a) Calculation and comparison of local energy deposition by radiations of different qualities in target structures of varying size and shape including simple models of biological macromolecules such as the DNA duplex and higher order DNA structure.

(b) Undertaking of in vitro biological experiments to supplement and extend the data already available on the biological effectiveness of diverse radiations in inducing relevant cellular effects.

(c) Comparison of physical properties of radiation energy deposition with observed biological effectiveness, so as to identify regions of volume and energy which do, or do not, correlate with biological effectiveness.

II. Objectives for the reporting period:

As above

III. Progress achieved:

INTRODUCTION

The general strategy of this project is (1) to generate, from track structure calculations, a wide and consistent data-base of information on the microscopic (nanometre upwards) patterns of energy deposition by diverse radiations, (2) to investigate experimentally the radiobiological properties of analytical radiations of well-defined track structure (supported by development of sources and dosimetric techniques in Project 2) in a variety of biological systems and (3) to compare these data, plus others from the literature, to seek particular properties of radiation tracks which may be most relevant to the biological consequences and thereby to place constraints on possible mechanisms of action.

1 METHODOLOGY

Methods used in the project included the following:

1.1 Computations from track structure

The Monte-Carlo track structure codes MOCA8b and MOCA14 of Paretzke and Wilson were used to generate statistically representative large numbers of slowing down tracks of monoenergetic electrons (MOCA8b) or monoenergetic segments of protons or α-particles (MOCA14). These codes produce a full history, including energy deposition and spatial coordinates of all ionisations and excitations, of the primary and secondary particles of each track as it passes through water vapour, adjusted to density of liquid water. Tracks were also generated to correspond to irradiation with selected monoenergetic ultrasoft X-rays, including the processes of photon absorption and emission and full slowing-down of the one or more primary electrons and their secondaries. For this purpose complex input data tables were formulated for absorption of given X-ray energies in the elements of mammalian cells [18].

Cylindrical target volumes were then superimposed randomly on the above tracks to determine the frequency distributions of energy deposition by a wide variety of well-defined radiations in a wide range of target dimensions from 0.5 nm upwards and including dimensions corresponding approximately to known DNA-related structures such as the DNA double-helix, nucleosomes and elementary chromatin fibre. In order to achieve statistically stable results within acceptable computer times different scoring methods were developed to suit different types of tracks and computers (Norsk Data ND500 and Cray XMP supercomputer). In each case, the axes of the final target cylinders were defined by μ-random cords through a virtual volume enclosing all or part of a track. The virtual volumes were cylinders enclosing proton and α-particle segments [1,2], spheres enclosing low energy electrons and ultrasoft X-ray tracks up to about 3 keV [16,18] and spheres enclosing subsamples of higher energy electron or X-ray tracks [18]. The scoring codes contained numerous internal consistency checks, including comparison of the different methods. The final data were produced in the form of frequency distributions of magnitude of energy deposition in the cylindrical targets, normalized either to unity or to absolute frequencies per target per Gy to the medium. In this latter form they can be compared directly with experimental radiobiological data.

Additional codes allowed analysis of energy deposition around Auger-emitting radionuclides, which required inclusion of the stochastics of the decay and de-excitation processes themselves [8,10], high-resolution analyses of the patterns of energy deposition within individual components of the DNA helix so as to simulate the production of single- and double-strand breaks (ssb and dsb) by various radiations [24] and analysis of the dose contribution versus electron energy for local energy deposition in electron radiations [38].

1.2 Experiments on biological effects of radiations

A variety of radiations were used, selected either for their analytical value as well-defined probes of radiation action or as conventional reference radiations. Developments of the radiation techniques are described in Project 2. The main radiations used were monoenergetic C_K (0.28 keV) and Al_K (1.5 keV) ultrasoft X-rays from a transmission-target discharge source [5,7] or by proton bombardment of solid targets on our Cockcroft-Walton accelerator [6], monoenergetic slow α-particles of 3.24 MeV (± 0.22 MeV hwhh) at high and low dose rates from ^{238}Pu [4,12,15,20], cyclotron-produced monoenergetic α-particles of 30 and 35 MeV and protons of corresponding LET (1.2 and 1.4 MeV) [46-51], 24 keV epithermal neutrons by Fe-S filtration on a Harwell Laboratories reactor [22] and reference radiations of 250 kV X-rays and ^{60}Co γ-rays. These selected radiations each had track-structure properties of particular interest, namely short electron tracks comparable to DNA and chromatin dimensions (ultrasoft X-rays), higher-LET tracks of short length (epithermal neutrons), well-defined narrow tracks of high-LET (124 keV μm^{-1}) in the region of maximum biological effectiveness (slow α-particles), or tracks of identical (intermediate) LET (20-23 keV μm^{-1}) but different microscopic structures (cyclotron protons and α-particles).

Biological systems, mostly in vitro, were selected for quantitative accuracy with the required radiations, particular genetic aspects of radiation damage observable at the cellular or sub-cellular level or relevance to particular mechanistic questions. These systems included clonal survival assays of standard Chinese hamster cell lines V79 and CHO and their series of radiation-sensitive mutants irs (Jones et al.) and xrs (Jeggo), respectively, to investigate effects of radiation quality [4], of $10T\frac{1}{2}$ mouse cells (dose-rate effects for high-LET α-particles) [12] and of V79, BHK (Syrian hamster) and HF19 (human fibroblast) cells for comparison with chromosome damage by ultrasoft X-rays and α-particles [5,7,20]. Chromosome aberration assays included scoring of dicentric (and other) aberrations at metaphase after V79 cells were irradiated in plateau phase with C_K ultrasoft X-rays (to investigate formation of exchange aberrations by these very short tracks)[7]; of chromosome and chromatid aberrations in 7 parts of the cell cycle (including 5 sub-phases of S) of assynchronous BHK cells irradiated with C_K X-rays (using the replication banding/sub-phasing method of Savage et al. to investigate the efficiency of very short tracks before, during and after DNA replication) [5]; of breaks in prematurely condensed chromosomes (PCC) immediately after irradiation of plateau phase HF19 human fibroblasts with high-LET α-particles (to investigate the effect of radiation quality on this earliest observable chromosome damage) [20]; and of sister chromatid exchanges (SCE), as well as chromosome aberrations and micronuclei, in human lymphocytes irradiated (before stimulation) with α-particles or epithermal neutrons (to investigate the induction of SCE by radiations of high-LET, uniquely)

[15,22]. Induction of transformed foci of 10T½ mouse cells were assayed after irradiation with 3.2 MeV α-particles at high and low dose rates to seek dose-rate effects with these high-LET particles [40]. A variety of these mammalian cell assays, as well as others including DNA dsb and mutation induction, were included in a four-laboratory collaboration to compare the effectiveness of protons and α-particles of identical LETs (at 20 and 23 keV μm^{-1}) in inducing a wide variety of biological effects in different cell types [46-51].

Repair-proficient (211*B) and repair-deficient (rad 54-3/rad 54-3, at the conditional temperature of 36^0C) strains of yeast were assayed for induction of dsb (by neutral sucrose sedimentation) and cell survival after irradiation with C_K and Al_K ultrasoft X-rays and ^{60}Co γ-rays [6]. Yeast offers particular advantages for accurate determination of dsb, and for defined cell sizes in ultrasoft X-ray irradiations.

The effects of high-LET 3.2 MeV α-particles on haemopoetic stem cells in CBA/H mouse were measured by in vitro irradiation of marrow followed either by CFUs assays in recipient mice or by haemopoetic repopulation, and cytogenetic sampling, in oblated recipient mice. The CFUs assay was also used to observe the effect of irradiation of mouse marrow, in vitro, with 24 keV epithermal neutrons.

2. RESULTS

2.1 Computations from track structure

A consistent data-base has now been established for absolute and relative frequency distributions of energy deposition in microscopic cylindrical target volumes in water irradiation with a wide variety of different radiations. Full sets of data have been compiled in tabulated form as they have been completed [2,16] and samples of these have been presented in graphical form for comparisons and inferences [1-3,9,11,16-19,23,24,27-30]. Two full compilations are complete to date. The first is for segments of monoenergetic protons (at intervals of energy from 0.3 to 4.0 MeV) and α-particles (at intervals of energy from 1.2 to 20 MeV) [2]. These cover the main energy regions of radiobiological interest, except at the lower end which is determined by the validity of the present MOCA14 code. Dimensions of the cylindrical targets were varied from diameters (d) of 1 nm to 500 nm and lengths of d/2 to 8d. The larger diameters were not included for cases when a simple LET/chord length approximation gave similar results. For most applications the LET approximation (presented as a universal table in the monograph) will be adequate for larger diameters, but the track structure computations clearly show the inadequacy of LET as a microscopic description for the smaller diameters. Cylinders may serve as a useful simple approximation to real biological structures, including DNA (~ 2 nm diameter, and length of choice), nucleosomes (~ 10 nm diameter and 5 nm length) and elementary chromatin fibre (25-30 nm diameter, and length of choice). The tabulations show many interesting features, including: very large stochastic variations of energy deposition by a given particle (for example, ranging from a few eV up to several thousand eV in a nucleosome-sized target for slow α-particles); very large differences in distributions between different particle energies and types; clear 'overkill effects' with increasing stopping power for particular target sizes and energy depositions; and little increase in magnitudes of energy

deposition once the target length is more than a few times its diameter.

The second completed tabulation is for the complete slowing-down tracks of monoenergetic ultrasoft X-rays, of energies 0.28 keV (C_K), 1.49 keV (Al_K), 4.51 keV (Ti_K) and 8.05 keV (Cu_K), following photo-electric absorption in material of the elemental composition of mammalian soft tissue [16]. Cylinder diameters were varied from 1 to 100 nm and lengths from d/2 to 8d or more. LET provides a very poor approximation for photon and electron radiations in general. These distributions clearly show, inter alia, the special features of low-energy electrons in being able to deposit substantial amounts of energy in small targets. Associated calculations have shown that a large proportion (30-50%) of the energy deposited by all 'low-LET' radiations is via secondary electrons of similarly low energy [27,38].

Scoring and data compilation for frequencies of energy deposition in cylindrical targets, of dimensions as above, by complete slowing-down tracks of monoenergetic electrons from 0.1 to 100 keV are almost completed. These show very little variation for initial energies of $\gtrsim$ 40 keV. 100 keV is the upper energy limit for the application of code MOCA8b but it seems unlikely that the distributions would be much different above this energy. The lowest-energy electrons show the same general feature as ultrasoft X-rays. Methods are being developed to combine these electron distributions according to the primary electron spectra of selected hard X-ray irradiations in order to add hard X-rays also to the data-base of frequencies of energy deposition. The computations show that for none of the radiations do multiple-track effects make a significant contribution to energy deposition in these DNA targets except at very large doses (>> 100 Gy) [19].

Additional scoring was carried out for energy depositon by K-shell ultrasoft X-rays from elements of atomic number 4 to 20 to see if there might be irregularities in the smooth progression of frequencies versus X-ray energy which might then warrant experimental investigation of the radiobiological consequences [53]. For simplicity, all photon absorptions were assumed to take place in oxygen atoms. Although there were some hints of discontinuity, confirmation of their magnitude and potential as probes of radiobiological mechanisms would require extensive further scoring with greater statistics and for photon absorptions in all elements of tissue.

Computation of frequencies and magnitudes of energy deposition in cylinders and spherical volumes containing, or near to, Auger-electron-emitting radionuclides (^{125}I and ^{51}Cr) showed very large stochastic variations in energy deposition, that these decays are likely to deposit very large concentrations of energy in their immediate locality, but not even a few nanometres away, and that a decay of ^{125}I within DNA is liable to be much more damaging than even the passage of a slow α-particle [8,10].

Consideration was also given to the internal structure of the energy depositions within DNA for a variety of radiations. Using Charlton and Humm's model of DNA single-strand breakage matched to experimental data for breakage by ^{125}I, the expected absolute numbers of ssb and dsb were computed from track structure simulations for 0.28 and 1.5 keV ultrasoft X-rays, 20 keV electrons, and protons and α-particles of LETs from about

15 to 200 keV μm^{-1} [24]. With their assumption that breaks are due to direct energy depositions of $\gtrsim$ 17.5 eV in the sugar-phosphate moieties of of DNA the calculated absolute numbers of ssb agreed well with experimental data in the literature. The calculated values for dsb were mostly about a factor 2 greater than experimental values but the relative values for the different radiations agreed well.

2.2 Experiments on biological effects of radiation

A brief summary of the main observations made during the contract is as follows, starting first with the effects of ultrasoft X-rays and then considering α-particles, epithermal neutrons and protons.

Because of the high dose-rate of ultrasoft X-rays produced by our accelerated-proton source (Project 2), it was possible to carry out a series of yeast experiments in collaboration with Frankenberg et al. Results showed dose-response curves (dsb induction or log survival) which were linear and gave RBEs (relative to γ-rays) of 2.4 (Al_K) and 2.6 (C_K) for cell inactivation in strain 54-3 and 2.2 (Al_K) and 3.8 (C_K) for induction of dsb in strain 211*B [6]. Therefore it seems that the high RBE of ultrasoft X-rays for cellular effects, as seen in most mammalian-cell experiments, is also present at the DNA level. Since the dimensions of unattached living yeast cells can be accurately measured, these results are free of some of the difficulties associated with mammalian cell ultrasoft X-ray experiments.

Despite the fact that the electron tracks from C_K ultrasoft X-ray have ranges of only $\lesssim$ 7 nm, a few times the diameter of DNA, they were found to be efficient at inducing complete exchange aberrations, and inactivation, in plateau phase V79 cells [7]. In assynchronous BHK cells it was found that C_K X-rays produced aberrations efficiently in pre-S, S and post-S cells despite the differences in DNA conformation [5]. Both these results suggest that exchange aberrations can be produced either by radiation damage to only a single chromatid or to the DNA from separate chromatids when they are virtually in contact. Preliminary results with Al_K ultrasoft X-ray irradiation of an irs radiosensitive mutant of V79 cells suggest that its relative sensitivity (ratio to wild type) is slightly reduced compared to γ-rays.

A major series of ultrasoft X-ray cell-inactivation experiments were carried out by Raju et al. at Los Alamos with us as collaborators. These experiments confirmed our previously-found high RBEs with V79 cells, and the increase with decreasing X-ray energy, established that the relative variation of sensitivity through the cell cycle was similar to hard X-rays, and that the OER slightly and progessively reduced with decreasing energy of ultrasoft X-rays [13]. This trend of decreasing OER was found also for $10T\frac{1}{2}$ cells [21]. But the most dramatic finding of their series of experiments with 5 different cell lines, including AG1522 [25], CHO-10B and HS-23 [26] was that RBEs can apparently be as small as about 1 (even for C_K X-rays) or up values of 4 or greater. These values correlate with cell thickness (as measured after fixation, embedding and sectioning) but also very nearly with radiosensitivity (to hard X-rays). Compilation of these ultrasoft X-ray data, together with all others in the world, shows excellent experimental agreement between laboratories but a major puzzle in understanding the full significance of the results in terms of radiobiological mechanisms of action [29]. A limited number of

alternative explanations have been identified, mostly open to experimental verification, and it seems clear that resolution of the puzzle will provide valuable new mechanistic insight not previously anticipated on crucial differences in intrinsic radiosensitivity and/or spatial distribution of intracellular target material [29].

A number of experiments with slow α-particles from our ^{238}Pu irradiator have sought dose-rate effects in the light of reports of enhanced effectiveness of low dose rate fission neutrons for cell transformation of 10T½ cells. Similar observations with α-particles would allow considerable scope for analytic experimentation into the mechanisms. Collaborative experiments with Roberts et al. have to date found no significant dose-rate effects for inactivation [12] or transformation [40] of 10T½ cells by α-particles. Induction of inactivation and chromosome aberrations in plateau-phase V79 cells shows a small dose-rate effect in the conventional direction (ie, reduced effectiveness at low dose-rate); these data await full statistical analysis.

Cellular responses to different magnitudes of local energy deposition can be probed with slow α-particles compared to low-LET, and other, radiations. It was found that the RBE of 3.2 MeV α-particles was much smaller for the radiosensitive xrs-mutants than for the normal CHO parent cells [4]. This is similar to earlier results with ataxia-telangiectasia human cells. Experiments have continued with three radiosensitive irs mutants of V79 cells, isolated in our laboratory by Jones and Thacker. All three are more sensitive to α-particles than the parent cells but, again, the RBEs are reduced. The survival data and associated measurements are now sufficiently accurate to allow detailed analyses of the sensitivity in terms of particle track structure and DNA repair capabilities.

The PCC technique allows observation of early subcellular damage intermediate in scale between DNA breaks and metaphase chromosome aberrations. Induction of PCC breaks by 3.2 MeV α-particles in non-cycling HF19 human fibroblasts was found to increase linearly with dose and to have an RBE relative to hard X-rays of 2.16 ± 0.13 [20]. This is considerably smaller than the RBEs reported for chromosome aberrations and is nearer to the values reported for dsb. The numbers of PCC are intermediate between the numbers of dsb and chromosome aberrations.

Another class of DNA damage may be revealed by SCE. It has been generally found that X-ray irradiation of unstimulated human lymphocytes is unable to induce this damage but Savage and Holloway discovered in our laboratory that it is induced by 42 MeV d-Be neutrons and we have now shown that it is induced also by 3.2 MeV α-particles [15] and 24 keV epithermal neutrons [22]. It appears that all these high-LET radiations are able to produce a qualitatively different class of initial damage, compared to X-rays, and that this should be related to characteristic features of their track structure. In these experiments it was found also that the 24 keV neutrons are efficient at inducing exchange aberrations in accordance with the relatively high-LET, but despite the relatively short track lengths, of their recoil protons [22].

Irradiation of mouse marrow in vitro has suggested that haemopoetic stem cells have a very low probability of surviving the passage of a single high-LET α-particle. This is indicated by a CFUs dose-response

curve which is similar to that expected if the only surviving cells were those which, by statistical chance, had not been hit by an α-particle. In agreement with this, the blood lymphocytes arising from marrow repopulation of oblated mice carry very little cytogenetic damage. Irradiation of marrow in vitro with 24 keV epithermal neutrons followed by the CFUs assay shows, however, that cells can survive with internal damage from relatively high-LET particles.

A comprehensive series of collaborative experiments, involving 4 laboratories, was carried out [47] to confirm and test the generality of the report of Belli et al. that protons in the region of 20-30 keV μm^{-1} have substantially greater biological effectiveness than α-particles of the corresponding LET. This finding has substantial implications for the mechanistic importance of relatively subtle differences in track structure and for understanding the effects on neutrons. Results of these experiments are still undergoing analysis but they have qualitatively confirmed Belli's observation for inactivation of V79 cells [46,48], shown that the effect is of similar magnitude for inactivation of 2 strains of HeLa cells [49], is smaller or absent for inactivation and transformation of 10T½ cells [51], is considerably larger for mutation (compared to inactivation) of V79 cells [50] and is not detectable for dsb-induction which shows little variation over a wide range of radiation qualities. Other data, including chromosome aberrations in V79 cells, are still pending.

4 DISCUSSION

In accordance with the general and specific objectives of the contract, (1) an extensive and consistent data-base has been computed for microscopic patterns of energy deposition by diverse radiations including α-particles, protons, ultrasoft X-rays, electrons and some radionuclides [1-3,8-11,16-19,23,24,27-29], (2) experimental data have been obtained on the biological effectiveness of diverse radiations, selected for their value as mechanistic probes, in inducing relevant subcellular and cellular effects [4-7,12,13,15,19-22,25,26,46-51] and (3) comparison has been made of these physical and biological properties of the radiations so as to identify regions of local volume and energy deposition which do, or do not, correlate with biological effectiveness and to place theoretical and experimental constraints on possible biological mechanisms of radiation action [3,5-12,14,17,19,21,24,27-30]. Effort has concentrated on low-energy electrons (including ultrasoft X-rays) because of their major presence in all low-LET radiations, slow α-particles because of their practical relevance from radon and other radionuclides, and slow protons because of their relevance from fission neutrons. All of these, and epithermal neutrons, also have particular value as mechanistic probes. Some notable features which emerged from these analyses are summarized below.

It was found that all radiations studied by track structure computations were able to produce appreciable numbers (~ 10^3 Gy^{-1} per mammalian cell) of direct energy deposition events in DNA (and also in its higher order structures) and that various features of the frequency distributions of energy deposition correlated well with different aspects of the relative effectiveness of the radiations in producing particular biological effects [19,27,30]. The absolute numbers of direct energy

depositions of $\gtrsim$ 100 eV in DNA were similar to the absolute numbers of measured dsb, and initial yields of ssb and dsb could be modelled by assuming direct action only [24]. Electron-producing radiations, and particularly low-energy electrons and ultrasoft X-rays, are efficient at depositing energy of about 100 eV in DNA (by electron track-ends), and observed differences in intrinsic radiosensitivity and ultrasoft-X-ray RBE may be a consequence of how different cell types respond to the spectrum of events smaller and larger than this [19,29]. High-LET radiations produced appreciable numbers of larger events in DNA and nucleosomes and it seems likely that these should be less modifiable, by cellular repair, dose-rate, or growth conditions, as was experimentally observed for cellular effects [4,12]. The relatively large RBEs of slow α-particles for final cellular effects such as aberrations and inactivation, compared to the smaller RBEs seen for initial DNA and chromosome damage [20,24], may well be due to a qualitative difference from these larger depositions. DNA-incorporated Auger-radionuclides are likely to be more efficient than even slow α-particles in producing such large events [8,10].

Another notable feature of the track structures of high-LET radiations is their ability to make moderate numbers (a few per Gy per cell) of uniquely large energy depositions in DNA, nucleosomes and chromatin such as cannot be made by any track from low-LET radiations. This allows for qualitatively unique initial damage and possibly unique biological consequences. An example of this may be SCE-induction in human lymphocytes by fast and epithermal neutrons and by α-particles but apparently not at all by X-rays [15,22]. This gives an effective RBE of infinity, consistent with the track structure calculations which indicate that relative effectiveness for initial damage can have values from less than unity to infinity depending on the class of damage [23,27,30].

A set of working hypotheses have emerged from the analyses of this project whereby the microscopic damage from radiations is considered in 4 broad classes in or near DNA-related targets [3,19,27,30]: sparse ionisations/excitations (suggested as of little cellular relevance), moderate clusters of ionisations/excitations depositing about 100 eV in DNA (characteristic of low-LET radiation effects and associated with dsb), large clusters depositing about 400 eV in nucleosome-size targets (characteristic of high-LET effects) and very large clusters, perhaps depositing $\gtrsim$ 800 eV in nucleosomes (responsible for damage unique to high-LET radiations).

Other implications suggested by the analyses include that the integrity of only a small fraction (~ 2-4%) of a mammalian cell's genome may be critical for its survival [3,11,31,33]; mutation and transformation of cells in vitro can be brought about by damage to target regions which are somewhat larger than the functional sequence of the gene (for mutation) or much larger (for transformation) [11,33]; the probability of a mammalian cell surviving the passage of a slow α-particle, and therefore being able to carry viable genetic damage, can vary from very large values (eg, > 80% for flattened 10T½ cells [12]) to very small values (eg, mouse haemopoetic stem cells) depending on the cell geometry [11,12] and the cell type; parameters and concepts of various existing models of radiation, and their implications, are open to reevaluation and reinterpretation with the track-structure-scoring data [3,9,11,14,17, 28,30].

IV. Other research group(s) collaborating actively on this project [name(s) and address(es)]:

J.S. Bedford, Colorado State University, Fort Collins, U.S.A.
M. Belli, Instituto Superiore di Sanitá, Rome, Italy.
D.E. Charlon, Physics Department, Corcordia University, Canada.
D. Frankenberg, GSF, Frankfurt, W. Germany.
J.H. Humm, Div. Exper. Path. & Therap., MRC RBU, Chilton, U.K.
E. Jones, St. Bartholomew's Medical College, London, U.K.
S. Lorimore, Div. Radiat. Oncogenesis, MRC RBU, Chilton, U.K.
A. Mill, CEGB Berkeley Nuclear Laboratories, Berkeley, U.K.
H.G. Paretzke, GSF, Neuherberg, W. Germany.
M.R. Raju, Life Sciences Division, Los Alamos National Laboratory, U.S.A.
C.J. Roberts, U.K.A.E.A. Harwell Laboratories, Didcot, U.K.
W.E. Wilson, Pacific Northwest Laboratories, Richland, U.S.A.

V. Publications:

Full Papers and Monographs

[1] D.E. Charlton, D.T. Goodhead, W.E. Wilson and H.G. Paretzke, "The deposition of energy in small cylindrical targets by high LET radiations." Radiat. Prot. Dosim. 13, 253-258 (1985).

[2] D.E. Charlton, D.T. Goodhead, W.E. Wilson and H.G. Paretzke, "Energy deposition in cylindrical volumes: (a) Protons, energy 0.3 MeV to 4.0 MeV, (b) Alpha-particles, energy 1.2 MeV to 20.0 MeV." MRC RBU Monograph 85/1, (MRC Radiobiology Unit, Chilton, Didcot, OX11 0RD, UK) (1985).

[3] D.T. Goodhead and D.E. Charlton, "Analysis of high-LET radiation effects in terms of local energy deposition." Radiat. Prot. Dosim. 13, 253-258 (1985).

[4] J. Thacker and A. Stretch, "Response of 4 X-ray sensitive CHO cell mutants to different radiations and to irradiation conditions promoting cellular recovery." Mutation Res. 146, 99-108 (1985).

[5] R.E. Wilkinson, D.T. Goodhead and J. Thacker, "Induction of chromosome aberrations by very short tracks at different stages of the cell cycle." Radiat. Prot. Dosim. 13, 161-165 (1985).

[6] D. Frankenburg, D.T. Goodhead, M. Frankenberg-Schwager, R. Harbich, D.A. Bance and R.E. Wilkinson, "Effectiveness of 1.5 keV aluminium and 0.3 keV carbon X-rays to induce DNA double-strand breaks in yeast cells." Int. J. Radiat. Biol. 50, 727-741 (1986).

[7] J. Thacker, R.E. Wilkinson and D.T. Goodhead, "The induction of chromosome exchange aberrations by carbon ultrasoft X-rays in V79 hamster cells." Int. J. Radiat. Biol. 49, 645-656 (1986).

[8] D.E. Charlton, "Atomic data required for the calculation of local energy deposition near isotopes decaying by electron capture or internal conversion." In: Nuclear and Atomic Data for Radiotherapy and Related Radiobiology, STI/PUB/741 (IAEA, Vienna), pp.27-35 (1987).

[9] D.T. Goodhead, "Physical basis for biological effect". In: Nuclear and Atomic Data for Radiotherapy and Related Radiobiology, STI/PUB/741 (IAEA, Vienna), pp.37-53 (1987).

[10] D.E. Charlton, "The range of high LET effects from ^{125}I decays." Radiat. Res. 107, 163-171 (1986).

[11] D.T. Goodhead, "Relationship of microdosimetric techniques to applications in biological systems." In: Dosimetry of Ionizing Radiation, Vol.2, eds. K.R. Kase, B.E. Bjarngard and F.H. Attix

(Academic Press, New York), pp.1-89 (1987).
[12] C.J. Roberts and D.T. Goodhead, "The effects of ^{238}Pu α-particles on the mouse fibroblast cell line C3H 10T½: Characterization of source and RBE for cell survival." Int. J. Radiat. Biol. 52, 871-882 (1987).
[13] M.R. Raju, S.G. Carpenter, J.J. Chmielewski, M.E. Schillaci, M.E. Wilder, J.P. Freyer, N.F. Johnson, P.L. Schor, R.J. Sebring and D.T. Goodhead, "Radiobiology of ultrasoft X-rays: I. Cultured hamster cells (V79)." Radiat. Res. 110, 396-412 (1987).
[14] D.T. Goodhead, "Biophysical models of radiation action." In: Radiation Research, Proceedings of the 8th Int. Congr. of Radiation Research, Edinburgh, July 1987 (Taylor and Francis, London), Vol.2, pp.306-311 (1987).
[15] Z.S. Aghamohammadi, D.T. Goodhead and J.R.K. Savage, "Induction of sister chromatid exchanges (SCE) in G_0 lymphocytes by plutonium-238 α-particles." Int. J. Radiat. Biol. 53, 909-915 (1988).
[16] H. Nikjoo, D.T. Goodhead, D.E. Charlton and H.G. Paretzke, "Energy deposition by C, Al, Ti and Cu X-rays in cylindrical volumes within mammalian cells." MRC RBU Monograph 88/1, (MRC Radiobiology Unit, Chilton, Didcot, OX11 0RD, UK) (1988).
[17] D.T. Goodhead, "Spatial and temporal distribution of energy and possible implications for radiation protection." Health Phys. 55, 231-240 (1988).
[18] H. Nikjoo, D.T. Goodhead and D.E. Charlton, "Energy deposition in small cylindrical targets by ultrasoft X-rays." Phys. Med. Biol. 34, 691-705 (1989).
[19] D.T. Goodhead and H. Nikjoo, "Track structure analysis of ultrasoft X-rays compared to high- and low-LET radiations." Int. J. Radiat. Biol. 55, 513-529 (1989).
[20] J.S. Bedford and D.T. Goodhead, "Breakage of human interphase chromosomes by alpha-particles and X-rays." Int. J. Radiat. Biol. 55, 211-216 (1989).
[21] M.E. Schillaci, S. Carpenter, M.R. Raju, R.J. Sebring, M.E. Wilder and D.T. Goodhead, "Radiobiology of ultrasoft X-rays. II. Cultured C3H mouse cells (10T½)." Radiat. Res. 118, 83-92 (1989).
[22] Z.S. Aghamohammadi, D.T. Goodhead and J.R.K. Savage, "Production of chromosome exchange aberrations, micronuclei and sister chromatid exchanges by 24 keV epithermal neutrons in human G_0 lymphocytes." Mut. Res. 211, 225-230 (1989).
[23] H. Nikjoo and D.T. Goodhead, "The relative biological effectiveness achievable by high- and low-LET radiations." In: Low Dose Radiation: Biological Bases of Risk Assessment. Eds. K.F. Baverstock and J.W. Stather (Taylor and Francis, London), pp.491-502 (1989).
[24] D.E. Charlton, H. Nikjoo and J.L. Humm, "Calculation of initial yields of single- and double-strand breaks in cell nuclei from electrons, protons and alpha-particles." Int. J. Radiat. Biol. 56, 1-19 (1989).
[25] M.N. Cornforth, M.E. Schillaci, D.T. Goodhead, S.G. Carpenter, M.E. Wilder, R.J. Sebring and M.R. Raju, "Radiobiology of ultrasoft X-rays. III. Normal human fibroblasts and the significance of terminal track structure in cell inactivation." Radiat. Res. 119, 511-522 (1989).
[26] S.G. Carpenter, M.N. Cornforth, W.F. Harvey, M.R. Raju, M.E. Schillaci, M.E. Wilder and D.T. Goodhead, "Radiobiology of ultrasoft X-rays. IV. Flat and round shaped hamster cells (CHO-10B, HS-23)." Radiat. Res. 119, 523-533 (1989).

[27] D.T. Goodhead, "The initial physical damage produced by ionizing radiations." Int. J. Radiat. Biol. 56, 623-634 (1989).
[28] D.T. Goodhead, "Relationship of radiation track structure to biological effect: A re-interpretation of the parameters of the Katz model." Nucl. Tracks Radiat. Meas., Int. J. Radiat. Appl. Instrum. Part D (in press).
[29] D.T. Goodhead and H. Nikjoo, "Current status of ultrasoft X-rays and track-structure analysis as tools for testing and developing biophysical models of radiation action." Radiat. Prot. Dosim. (in press).
[30] D.T. Goodhead, "Radiation effects in living cells." Canadian J. Phys. (in press).

Short communications

[31] D.T. Goodhead and D.E. Charlton, "Critical properties of radiation at low doses." In: Abstracts of papers for the Thirty-Third Annual Meeting of the Radiation Research Society (Radiation Research Society, USA), p.121 (1985).
[32] D.T. Goodhead, "Radiation biology of aberrations." Int. J. Radiat. Biol. 48, 448 (1985).
[33] D.T. Goodhead, "Biophysical analysis of radiation-induced cell transformation." Int. J. Radiat. Biol. 49, 521-522 (1986).
[34] D. Frankenburg, M. Frankenburg-Schwager and D.T. Goodhead, "RBE-values of 1.5 keV aluminium K and 0.3 keV carbon K characteristic X-rays for the induction of DNA double strand breaks in yeast cells." In: Abstracts of papers for the Forty-Fourth Annual Meeting of the Radiation Research Society (Radiation Research Society, USA) p.59 (1986).
[35] D.T. Goodhead, D.E. Charlton and H. Nikjoo, "Physical constraints for critical biological damage." Ibid., p.109 (1986).
[36] M.R. Raju, S. Carpenter, J. Chmielewsky, M.E. Schillaci, M.E. Wilder and D.T. Goodhead, "Radiobiology of ultrasoft X-rays." Ibid., p.86 (1986).
[37] M.R. Raju, S. Carpenter, M. Cornforth, M. Schillaci and D.T. Goodhead, "Cell killing by ultrasoft X-rays." In: Abstracts of Papers for Thirty-Fifth Annual Meeting of the Radiation Research Society, (Radiat. Res. Society, Philadelphia), p.31 (1987).
[38] H. Nikjoo and D.T. Goodhead, "Physical and biological consequences of high- and low-LET radiations in biological targets." In: Radiation Research, Proc. 8th Int. Congr. of Radiation Research, Edinburgh, July 1987 (Taylor and Francis, London), Vol.1, p.80 (1987).
[39] H. Nikjoo and D.T. Goodhead, "Energy deposition in small size targets by high and low LET radiations." Ibid., Vol.1, p.87 (1987).
[40] C.J. Roberts, D.T. Goodhead, G.R. Morgan and P.D. Holt, "Transformation of C3H 10T½ with ^{238}Pu alpha particles." Ibid., Vol.1, p.182 (1987).
[41] J.S. Bedford and D.T. Goodhead, "Breakage of human interphase chromosomes by alpha particles." Ibid., Vol.1, p.226 (1987).
[42] D.T. Goodhead, J.R.K. Savage and Z.S. Aghamohammadi, "Do high-LET radiations have infinite RBE for induction of sister chromatid exchanges (SCE) in human lymphocytes." In: Abstracts of Papers for Thirty-Sixth Annual Meeting of the Radiation Research Society, (Radiat. Res. Society, Philadelphia) p.141 (1988)
[43] D.T. Goodhead, "The radiobiology of short-track particles." In: Abstracts of Papers for Thirty-Seventh Annual Meeting of the

Radiation Research Society, (Radiat. Res. Society, Philadelphia), p.58 (1989).
[44] H. Nikjoo and D.T. Goodhead, "Properties of initial biophysical damage due to high and low LET radiations." Ibid., p.120 (1989).
[45] M.R. Raju, S. Carpenter, W.C. Inkret, M.E. Schillaci, K. Thompson and D.T. Goodhead. "Cell inactivation by alpha-particles." Ibid., p.201 (1989).
[46] M. Belli, A.N. Ganesh, D.T. Goodhead, F. Ianzini, G. Simone, D.L. Stevens, A. Stretch, M.A. Tabocchini and R.E. Wilkinson, "Comparison of the biological effectiveness of protons and alpha particles with the same LET." Int. J. Radiat. Biol. (in press).
[47] D.T. Goodhead and M. Belli, "Direct comparison of biological effectiveness of LET-matched protons and α-particles - rationale and experimental design." Int. J. Radiat. Biol. (in press).
[48] D.L. Stevens, D. Bance, M. Belli, A.N. Ganesh, D.T. Goodhead, F. Ianzini, G. Simone, A. Stretch, M.A. Tabocchini and R.E. Wilkinson, "Inactivation of V79 cells by alpha-particles and protons of the same LET." Int. J. Radiat. Biol. (in press).
[49] A.J. Mill, L.A. Allen, S.C. Hall and D.T. Goodhead, "Inactivation of HeLa and HeLa S3 cells by protons and alpha-particles having the same LET." Int. J. Radiat. Biol. (in press).
[50] M. Belli, D.T. Goodhead, F. Ianzini, G. Simone and M.A. Tabocchini, "Biological effectiveness of protons and alpha-particles on mutation induction at the HGPRT locus in V79 Chinese hamster cells." Int. J. Radiat. Biol. (in press).
[51] S.C. Hall, L.A. Allen, A.J. Mill, D.T. Goodhead and C.J. Roberts, "A direct comparison between protons and alpha particles of the same LET: Survival and transformation studies with C3H 10T½ cells." Int. J. Radiat. Biol. (in press).

Title of the project no.: 2

Development of radiation sources and dosimetric techniques for radiobiological studies at low and high dose-rate

Head(s) of project:

D.T. Goodhead

Scientific staff:

D.T. Goodhead
H. Nikjoo
D.L. Stevens

I. Objectives of the project:

This project is to develop experimental techniques and methodologies of special radiation sources for quantitative investigation of relevant biological effects and their interpretation. The specific aims are the investigation and optimization of conditions of production of ultrasoft, and intermediate energy, X-rays, especially by proton bombardment. This should include assessment of a variety of monoenergetic beams which can be produced, their accurate measurement and their applicability to investigate problems in radiation biology and biochemistry.

II. Objectives for the reporting period:

As above

III. Progress achieved:

INTRODUCTION

In accordance with the objectives of this project, a variety of different experimental technologies and methodologies were developed so that special radiation sources could be applied for quantitative investigation of relevant biological effects in cellular systems. These were largely in support of Project 1. Most development was for ultrasoft X-rays, because these are a useful mechanistic probe of intracellular mechanisms of radiation action and show the specific effects of the low-energy electrons which form a major component in all low-LET irradiations. Other development was for slow α-particles, because these are a useful probe of the mechanisms of action of well-defined high-LET radiations and they show the specific effects of the α-particles from natural (e.g. radon) and artificial (e.g. plutonium and americium) radionuclides. Further development was also required for higher energy α-particles, and lower-energy protons (such as are produced by fission neutrons) of corresponding LET, to allow direct comparison of the effects of these particles.

This report will sequentially consider developments relating to each of these radiations in turn.

1. ULTRASOFT X-RAYS

Before the start of this contract we had undertaken a considerable number of investigations of the biological effectiveness of ultrasoft X-rays, first with Al_K (1.5 keV) and then with C_K (0.28 keV) and Ti_K (4.5 keV) characteristic X-rays (see [29] for references). These had been entirely with X-rays from a cold-cathode discharge tube and the irradiations had been physically quantified in terms of absorbed dose, as determined by fixed-volume ionization chambers, on the incident surface of the monolayer cells. Radiobiological interpretation required also biological assumptions as to the distribution of critical target material within the cells. The present project sought, inter alia, to test and extend all aspects of the production, characterization, dosimetry, versatility, applicability and interpretation of the ultrasoft X-rays so as to validate the earlier results, improve their accuracy and extend them.

1.1 Ultrasoft X-ray dosimetry and beam characterization

Dosimetry: Because of the unique physical and biological properties of ultrasoft X-rays, it was highly desirable to check by independent means the method of dosimetric quantification. This was first carried out in collaboration with Los Alamos National Laboratory, whose Physics Division has a highly sophisticated ultrasoft X-ray calibration laboratory for diagnostic instruments related to nuclear fusion. Therefore, we installed an MRC cold-cathode discharge tube at Los Alamos. Using their standard quantification method of photon-flux counting with gas-flow proportional counters, good agreement (within 7%) was obtained compared with ionization chamber determination of the X-ray flux (or absorbed dose) [52]. There are a minimum of common assumptions or parameters between these two methods.

Subsequently, in our own laboratory, three different styles of ionization chamber have been compared for routine dosimetry, and for special applications, with ultrasoft X-rays. These were the MRC (Chilton) fixed-volume chambers (with Al- or C-foil windows, as appropriate) as were used for all our earlier radiobiology, a Far West Technology extrapolation chamber (EIC-1) with modified window assembly [52] and double-windowed fixed-volume chambers designed and constructed at GSF, Frankfurt. All these chambers were used to measure the dose-rates of C_K (0.3 keV) and Al_K (1.5 keV) X-ray beams produced by proton-bombardment on our Cockcroft-Walton accelerator (see below). All three styles of chamber, including design variations within each, gave consistent results.

Each chamber design has its own advantages and disadvantages. The MRC chambers have particular advantages of small size and simple operation (but with very fragile windows), the GSF chambers have particular advantages of robustness and simple operation. Conventional methods of sensitivity (or volume) calibration with a standard γ-ray source are not suitable for the Far West Technology or the GSF chambers because of the inability to establish charged-particle equilibrium with high-energy photons. However, their regularly-shaped volumes can be obtained by direct calculation.

Interlaboratory comparisons of ultrasoft X-ray dosimetry can also be made, indirectly, by comparing the results of radiobiological results when similar monoenergetic X-ray irradiations were made on similar mammalian cell lines. Such comparisons add further confidence to the reliability of the physical dosimetry [29]. Data are available showing the survival curves, and RBEs, of V79 hamster cells irradiated with Al_K (or similar energy) X-rays in 5 different laboratories in the world (MRC and Gray Laboratory in the UK, and Los Alamos, Columbia and Wisconsin in the USA) using different sources (two cold-cathode sources, two hot-filament sources and a synchrotron, respectively) and different dosimetric methods. Corresponding data for C_K X-rays are available from two laboratories (MRC and Los Alamos). In all cases there is good agreement between laboratories and this provides further validation of the dosimetry as well as confirmation of our original results. Good agreement has also been found for inactivation of yeast cells by C_K X-rays in two laboratories (MRC and GSF).

Beam characterization: Application of the ultrasoft X-ray beams, and meaningful interpretation of the results, also requires good knowledge of other properties of the beams as used, including spectral purity at the irradiation position and uniformity of intensity over the irradiation area. Useful, complementary, methods for characterization of spectral purity were found to be attenuation measurements with a variety of absorbing materials and pulse-height spectra in a gas-flow proportional counter. The Manson Model 01 proportional counter was very suitable and gave line-widths very near to the theoretical minimum for counter statistics. Comparable accuracy was not achieved with an L.E. Pink Engineering EP110 Variable Geometry Proportional Counter. The dosimetry method which we developed for the Far West Technology extrapolation chamber provided information on deviations from expected spectral composition [52].

Methods available for determining beam uniformity include small area ionization chambers, small aperture proportional counters and photographic

film. All these methods were found to be successful and useful, each having particular advantages and disadvantages [52].

1.2 Production of ultrasoft X-rays

Proton bombardment: Our early ultrasoft X-ray experiments were carried out entirely with C_K, Al_K and Ti_K X-rays from a cold-cathode discharge source with a transmission target. For both C and Ti there were significant limitations on target life and dose-rate. Bremsstrahlung-contamination was lower than can usually be obtained with hot-filament sources. We showed that all these properties can be improved by producing the X-rays by proton-bombardment of solid targets. A versatile source was provided by constructing an ultrasoft X-ray beam line on our Cockcroft-Walton proton accelerator, so that large-area samples could be irradiated with high purity ultrasoft X-rays at a high dose rate comparable to what might be practically achievable on synchrotrons. For example, with proton bombardment currents of 450-630 μA and energies 600-640 kV onto an Al or C target, dose rates of 10-24 Gy min^{-1} or 8-12 Gy min^{-1}, respectively, were obtained over a sample area, in air, of 30 mm diameter. The bremsstrahlung contamination was << 1% and the intensity was uniform to better than 10% over the sample area. The particular parameters provided the high doses required for experiments with yeast [6].

Two factors of importance which emerged in the design of this beam line was the need to include in the X-ray flight-path sufficient filtration to eliminate scattered protons from the target and also any C_K X-rays which may be produced by in vacuo contamination of a non-C target. Protons elastically scattered at up to almost the full primary energy must be prevented from reaching any X-ray monitor and also from reaching the position of the biological sample to be irradiated. This can be readily achieved by suitable choice of windows, absorbers and flight path gas but for any given configuration it does set an upper limit to the primary proton energy (and hence the ultrasoft X-ray dose rate) which can be used. Contamination C X-rays are of no relevance in a C_K X-ray beam and they can be reality filtered from an Al_K X-ray beam, but they may seriously limit the practical availability of lower-energy beams such as B_K and N_K [53,54].

We have collaborated with Jones and Smith in their measurements, on the Van der Graaff accelerator at St. Bartholomew's Medical College, of X-ray production as a function of incident and emission angles for proton bombardment at energies of 500 keV. Targets investigated were B, C, two grades of Al, Si/C, Si/N, Au (M-shell X-rays) and TiB_2 [53,54]. By identifying production rates, optimum angles and effects of C contamination, this study provides valuable information for the design of radiobiologically useful beams of proton-induced ultrasoft X-rays.

α-particle bombardment: Experiments have commenced to investigate the production of ultrasoft X-rays by bombardment of solid targets with slow α-particles from radionuclide sources to determine whether this might provide a convenient and stable source of X-rays for radiobiological experiments. Bremsstrahlung contamination should be particularly low because an α-particle has no dipole moment; therefore bremsstrahlung should be produced only be the delta-rays.

Preliminary results suggest that a practically useful source is unlikely to be achieved by this method. However, full evaluation is not yet complete.

Laser bombardment: To extend the types of radiobiological investigations which can be undertaken with ultrasoft X-rays, we collaborated with the Rutherford Laboratory in evaluating the production of ultrasoft X-rays by bombardment of solid targets with a high-intensity laser. A single pulse from the laser can form a transient X-ray-emitting plasma characteristic of the target material and the plasma temperature. Such methods allow production of very short, high-intensity pulses of ultrasoft X-rays and therefore fast time-resolved studies of early radiation processes, including very fast cellular repair. The physical and biological properties were determined of ultrasoft X-rays produced by bombardment of a steel target with 0.3 J/pulse of light from a KrF laser [55]. The mean energy of the X-rays was approximately 0.85 keV (Fe_L) and they were found to have similar biological effectiveness (per unit absorbed dose at the incident surface of the cells) for killing of V79 hamster cells as has been found for C_K X-rays. With this laser and experimental design the dose rate at the cells was about $2x10^{-2}$ Gy/pulse, and X-ray pulse duration was 5-10 ns; the required doses were achievable by repeating pulses at 5 Hz onto a rotating steel target. Single-pulse irradiations should become possible with a higher-powered laser.

Comparison of sources: Comparative studies suggest that the source of choice for most radiobiological studies with K characteristic ultrasoft X-rays is proton bombardment, especially in view of the low bremsstrahlung contamination, long target lives, high dose rates and large field areas which can be achieved. The beams are suitable not only for mammalian cell radiobiology but also microbial radiobiology, and biochemical and radiation chemistry systems. Practical performance can be comparable to that of synchrotrons which usually suffer from the disadvantages of much more stringent time, vacuum and manpower problems. However, synchrotrons are unique in their ability to produce tunable monoenergetic beams of energies between the characteristic atomic lines; this advantage may be overriding for some radiobiological studies, for example, where closely adjacent energies across absorption edges are required or when matched attenuations at different energies are required. Cold-cathode electron-bombardment still retains advantages of simplicity, with reasonable intensity, for selected targets (including aluminium) and the ability to produce L-characteristic X-rays without the presence of K X-rays. Hot-filament sources extend the choice of targets and intensity, at some cost of complexity and beam purity. Laser-bombardment sources provide X-rays which are not monoenergetic but are available in precisely timed repetitive or single, high-intensity pulses.

1.3 First International Workshop on Ultrasoft X-ray Radiobiology

We organised this meeting in Oxfordshire, for 17 and 18 July 1987 to be adjacent in time to 8th International Congress of Radiation Research in Edinburgh. It was attended by more than 40 people from 6 countries and 4 continents, who represented about 14 different research groups including all of those active in ultrasoft X-ray radiobiology at that time. As intended, the meeting concentrated on the diverse technical problems associated with both the physics and the biology of the application of ultrasoft X-rays to investigative radiobiology. It also served to

introduce many of the groups to each other for the first time. It is hoped that the Second Workshop will be held in North America in July 1991, near to the time of the 9th ICRR in Toronto, especially since there have been important scientific advances since 1987 and more research groups have entered the field.

1.4 Dimensional measurements of cells

The major uncertainty in detailed mechanistic interpretation of the radiobiological effectiveness of ultrasoft X-rays, especially for the lowest energy C_K X-rays, arises from the rapid attenuation of these X-rays through a single attached cell. Physical absorbed dose at the incident surface of the cell can be accurately measured and specified as above and attenuation with depth can be calculated accurately. However, description of the radiobiologically relevant dose, as an average or at a point in the cell, requires biological information, or assumptions, on the thickness of the cell and the intra-cellular locations or distribution of relevant target material [29]. The hamster cells as used in the above experiments were apparently relatively thick (4-7 μm), and the collaborative experiments carried out at Los Alamos on different cell lines did not reveal the simple dependence with cell thickness which might have been expected for exponential attenuation through a uniform distribution of target material in the cell nucleus [13,21,25,26]. Thinner cells, such at 10T½ mouse and AG1522 human cells, showed substantially reduced RBEs of ultrasoft X-rays when evaluated in this way. Coincidentally, the thickness of the particular cell lines used correlates with their resistance to penetrating low-LET radiations, such as γ-rays, so it is at present not clear whether the apparent reduction in RBE with reducing cell thickness is really due primarily to assumptions for dose-overaging or whether it is reflecting a true mechanistic association with cell sensitivity. For example, if a particular cell type is more sensitive because it responds to smaller very local intra-track concentrations of energy deposition, then it would be expected to have a reduced RBE of ultrasoft X-rays relative to standard low-LET radiations [35,21,29]. This expectation follows clearly from the track structure analyses described in Project 1. On the other hand, explaining the apparent reduction in RBE predominantly in terms of attenuation and distribution of target material can reconcile much of the data for the various cell types only by making very strange assumptions as to the distribution of target material [29]. It would be quite unable to reconcile the similar, although reduced, RBE/cell-line trend in the data seen for the higher-energy ultrasoft X-rays (Ti_K and Cu_K) for which attenuation effects are negligible [29].

It has become of central importance to ultrasoft X-ray radiobiology to understand this RBE/cell-line conundrum. Solving it should provide additional new and valuable mechanistic information not previously anticipated. In particular, insight should be provided on crucial differences between the intrinisic radiosensitivity of different cells and/or on the spatial distributions of the critical intracellular target material. In order to approach these problems with precision, it became essential to carry out accurate population measurements of the thickness profiles of attached living cells under the exact conditions of irradiation with ultrasoft X-rays, and also of internal shapes and positions of the cell nuclei. Fixation, embedding and subsequent measurements by optical or electron microscopy provide precise information

on cell and nuclear dimensions in these embedded sections, but they leave open the question of possible distortion by the preparation procedures.

We have investigated various methods of making such measurements with optical microscopy directly on the unperturbed living cells, including phase-contract, bright-field with vital stain, Namarski interference contrast and laser confocal microscopy. Most of these were found to be inadequate with the notable exception of laser confocal microscopy.

After preliminary developments and trials, we installed a Biorad MRC-500 laser confocal microscope and are optimizing techniques for precise measurement of the required dimensions of living cells with minimum perturbation of the samples. A systematic comparison has been undertaken of the distributions of thickness of a population of V79 cells obtained when measured by electron microscopy (with fixation and embedding) and by confocal microscopy on living cells [56]. For the latter measurements the extracellular growth medium was fluorescently stained and all microscopy of a sample completed within 10 minutes. Horizontal optical sections at 0.5 μm intervals through the cells were digitally stored for subsequent analysis. Measurement and analysis shows that for V79 cells, under the particular growth conditions used, there was not more than about 10% shrinkage of cell thickness in the electron microscopy preparations [56]. Further systematic comparisons of this type will be undertaken with different cell types and growth conditions. Methods are also being optimized for measurement of other cellular dimensions, including nuclear projected area, with the confocal microscope.

Conclusions to date from this work are: firstly, the laser confocal microscope does, indeed and for the first time, allow accurate measurements of cell thickness on unperturbed living cells; and secondly, for the one conditon investigated in detail to date, electron microscope preparation causes only small shrinkage.

It should be mentioned that for irradiation of yeast cells with ultrasoft X-rays a different irradiation configuration had to be developed. For almost all our mammalian cell experiments the cells were irradiated flattened and well-attached to the Hostaphan or Melinex plastic base of a sample dish; the X-rays were incident through the plastic, thereby giving a precisely defined incident position of the cell surface. The yeast cells do not attach to plastic so a holder had to be developed to irradiate them as round cells sandwiched between a filter and a plastic film through which the X-rays were incident; low temperature (5^0C), high humidity and aeration were maintained during irradiation [6]. The dimensions of these round cells could easily be measured by bright-field optical microscopy. The fact that large RBEs for ultrasoft X-rays were found in this experimental systems provided further confidence that the high RBEs obtained in mammalian systems were not due to artefacts in the early measurement of cell thickness.

2. PU-238 α-PARTICLE IRRADIATOR

Project 1 required irradiation of mammalian cells under a variety of conditions with low-energy α-particles to investigate radiation effects when the LET is in the region of maximum RBE for most systems. This is in

the region of 100-200 keV μm^{-1}. For this purpose an α-particle irradiator was constructed with a 2 cm source disc of 36 mCi of ^{238}Pu in a He-flushed chamber. The α-particles emerged from this chamber as an appoximately parallel beam through a Hostaphan window, and after a 3 mm air path they enter through the Hostaphan base of a sample dish. 10 such dishes can be irradiated 'simultaneously' mounted in a wheel passing above the source window. The energies of the α-particles entering the cells can be varied from zero to about 4 MeV, and the dose-rate can be varied from $< 10^{-5}$ Gy min^{-1} to > 2 Gy min^{-1} with essentially no change in the quality of the beam (mean energy and line width) by means of internal apertures and external radial sector plates. The entire irradiator is in a temperature-controlled, insulated cabinet so that the cells can be maintained at any required temperature from ambient to about 50^0C, with continuous gas supplies to the sample dishes.

The most commonly used configuration to date has been with α-particles incident on the cells with a mean energy of 3.24 MeV and an energy spread of 0.22 MeV half-width at half-height. This purity compares very favourable with α-particle irradiators developed in other laboratories and it has considerably greater versatility than most. With this particular configuration, attached monolayers of cells are irradiated uniformly with track segments of α-particles of incident LET 122 keV μm^{-1}. [4,12,20,22,57].

Methods were developed also for irradiating unattached mammalian cells in suspension in very thin layers of liquid. This method allowed approximated uniform irradiation of human lymphocytes [15] and suspensions of mouse marrow.

CR39 plastic track-etch methods were adapted as in independent means of dosimetric comparison, a routine indicator of beam purity and particle direction and of complete irradiation of the suspension samples. Primary dosimetry was with fixed-volume and extrapolation ionization chambers, and energy measurments were with silicon detectors.

In summary this α-particle irradiator has proved to be very convenient and highly versatile for track-segment irradiation of mammalian cells of different types and under different conditions, including high and low dose rates with controlled temperature and gas environment.

3. VARIABLE-ENERGY CYCLOTRON

As described in Project 1 it was required to irradiate mammalian cells with protons and α-particles of identical LET-values of 20 and 23 keV μm^{-1} to investigate the consequences of subtle differences in track structure between these particles. Particularly efficient irradiation methods were required because of the need to irradiate large numbers of samples of different cell types (to generalize the results) within a few months (because of the active international collaboration of 4 laboratories) with 4 different beams (each to be repeated) within 8 morning shifts on the accelerator (to be within the available budget for this work). The irradiations were carried out on the Variable Energy Cyclotron of the United Kingdom Atomic Energy Authority, Harwell, generally using the beam line, monitoring, dosimetric and irradiation systems that we had developed and used in the 1970s to investigate LET dependence of mutation induction in mammalian cells. Some additional

systems were added, including the use of CR39 track-etch detectors for independent confirmation of dosimetry and field uniformity. In addition, convenient tabulations were generated of stopping powers and ranges of protons, deuterons and α-particles in water and all components of the beam lines [57]. These tabulations were essential for planning and execution of the cyclotron experiments [46-51].

IV. Other research group(s) collaborating actively on this project [name(s) and address(es)]:

D.Frankenburg, GSF, Frankfurt, W.Germany.
M.Hoshi, Research Institute for Nuclear Medicine, Hiroshima University, Hiroshima, Japan.
F.O'Neill, Rutherford Appleton Laboratory, Chilton, U.K.
M.R.Raju, Life Sciences Division, Los Alamos National Laboratory, U.S.A.
A.F.Smith and E.Jones, St. Bartholomew's Medical College, London, U.K.
S.Townsend, AMTS Division, MRC Radiobiology Unit, Chilton, U.K.
N.White, Zoology Department, Oxford University, Oxford, U.K.

V. Publications:

Full Papers and Monographs

[52] M. Hoshi, D.T. Goodhead, D.J. Brenner, D.A. Bance, J.J. Chmielewski, M.A. Paciotti, J.N. Bradbury, "Dosimetry comparison and characterisation of an Al K ultrasoft X-ray beam from an MRC cold-cathode source." Phys. Med. Biol. 30, 1029-1041 (1985).

[53] E.A. Jones, "The production and use of proton-induced ultrasoft X-rays." Ph.D. Thesis, University of London (1988).

[54] E.A. Jones, F.A. Smith, D.T. Goodhead and J. Oriel, "Some optimum conditions for proton induced ultrasoft X-ray production." Phys. Med. Biol. 33, 1385-1397 (1988).

[55] F. O'Neill, I.C.E. Turcu, G.J. Tallents, J. Dickerson, T. Lindsay, D.T. Goodhead, A. Stretch, C.W. Wharton and R.A. Meldrum, "A repetitive laser-plasma X-ray source for radiobiology research." Proc. 2nd Int. Congress on Optical Science and Engineering, Paris, 24-28 April 1989 (in press).

[56] K.M.S. Townsend, A. Stretch, D.L. Stevens and D.T. Goodhead, "Thickness measurements on V79-4 cells. A comparison between laser scanning confocal microscopy and electron microscopy." (Submitted).

[57] D.L. Stevens, H. Nikjoo and D.T. Goodhead, "Stopping powers and ranges of protons, deuterons and alpha-particles in selected materials. Part I Protons, Energy = 10 keV to 20 MeV. Part 2 Deuterons, Energy = 10 keV to 20 MeV. Part 3 Alpha-particles, Energy = 1 MeV to 50 MeV." MRC RBU Monograph 89/1 (Parts 1-3) (MRC Radiobiology Unit, Chilton, Didcot OX11 0RD, UK) (1989).

Short communications

[58] M.E. Schillaci, S.G. Carpenter, M.N. Cornforth, M.R. Raju, R.J. Sebring, M.E. Wilder and D.T. Goodhead, "RBE dependence on cell thickness using ultrasoft X-rays." In: Radiation Research, Proc. 8th Int. Congr. of Radiation Research, Edinburgh, July 1987 (Taylor and Francis, London), Vol.1, p.182 (1987).

RADIATION PROTECTION PROGRAMME
Final Report

Contractor:

Division of Radiation Science
and Acoustics
National Physical Laboratory
Queens Road
GB Teddington, Middx TW11 OLW

Contract no.: BI6-A-003-UK

Head(s) of research team(s) [name(s) and address(es)]:

Dr. J.B. Hunt
Div.of Rad.Science and Acoust.
National Physical Laboratory
Queens Road
GB Teddington, Middx TW11 OLW

Telephone number: 1-943-6853

Title of the research contract:

Development and investigation of a reproducible multisphere system for radiation protection purposes, and its use to correct personnel dosemeter measurements.

List of projects:

1. Development and investigation of a reproducible multisphere system for radiation protection purposes, and its use to correct personnel dosemeter measurements.

Title of the project no.: BI6-A-003-UK

Development and investigation of a reproducible multisphere system for radiation protection purposes, and its use to correct personnel dosemeter measurements.

Head(s) of project:

Dr J B Hunt (to 14.11.89) Dr D J Thomas (from 15.11.89)

Scientific staff:

D J Thomas, A G Bardell and B R More

I. Objectives of the project:

The development and characterisation of a well specified, reproducible, multisphere system (Bonner spheres), for use in stray neutron fields. Determination of the sphere response functions by a combination of computational and experimental techniques. Investigations of spectrum unfolding methods. Use of the system to investigate dose equivalent values and instrument responses in stray neutron fields, and to investigate correction factors for area survey instruments and personal dosemeters.

II. Objectives for the reporting period:

- Design and construction of the system.
- Calibration of the spheres in monoenergetic neutron fields for the range of energies where this is possible.
- Calculations of the response functions to allow interpolation between measured values and extrapolation to regions where experimental calibration is not possible.
- Investigation of the most suitable spectrum unfolding code.
- Validation of the response functions in known broad-range fields.
- Use of the spectrometer in stray neutron fields.

III. Progress achieved:

1. INTRODUCTION

Multisphere systems (Bonner spheres) have been used for many years to derive coarse spectrometric information about neutron fields[1]. They have a number of attractive features: namely that they cover the full energy range of interest (thermal to 20 MeV), they have an effectively isotropic response, and are reasonably simple to set up and use. The chief disadvantage is poor energy resolution; however, depending on the application, good resolution may not be essential. Moreover, even in situations where high resolution is needed, and more elaborate spectrometers have to be used, multispheres are often employed to cover energy ranges inaccessible to the other instruments.

The most common central detector to date has been a LiI scintillator, although this does suffer problems from its photon response. A number of response function calculations have been published for systems with such a detector, and some experimental calibrations have also been made[1]. To date, however, no attempt has been made, for any type of central detector, to tie together the experimental and calculational approaches to derive a best possible set of response functions using all the information from both approaches. It is important to know the uncertainty on these response functions since they contribute significantly to the uncertainty in the final derived spectrum. Finally, in using multispheres, it is necessary to investigate very carefully the unfolding procedure and the code used to perform this task.

2. SYSTEM DESIGN

The system designed and built at NPL consists of nine polyethylene spheres of diameters from 7.62 cm (3") to 38.1 cm (15"). (Historically multispheres have been labelled in terms of their diameters in inches). A ^{3}He proportional counter (Centronic Ltd, type SP90) was chosen as the central detector since this type of counter is less sensitive to photons than a LiI crystal. It has a spherical neutron sensitive volume of about 32 mm diameter, is filled with ^{3}He to about 200 kPa, and has proved reliable.

The design of the spheres ensures that the detector can be transfered between spheres without disconnecting the high voltage supply. Conventional NIM electronics are employed, the discriminator level in the pulse counting system being set by using a multichannel analyser to view the spectrum of events in the detector.

Calculations have indicated[1] that the shapes of the response functions are strongly dependent on polyethylene density, and material of the same density was specified for all spheres. Subsequent analysis, however, showed some variation (from about 0.93 to 0.96 g cm^{-3}), and this was taken into account when calculating response functions.

3. EXPERIMENTAL MEASUREMENTS

3.1 Calibrations with monoenergetic neutrons

The sphere responses to monoenergetic neutron fluences were determined under low-scatter conditions at PTB Braunschweig, FRG. Charged particle beams from the 3.5 MV Van de Graaff accelerator were used to produce monoenergetic neutrons via the reactions $^{65}Cu(p,n)$, $^{45}Sc(p,n)$, $^{7}Li(p,n)$, T(p,n), D(d,n), and T(d,n) providing neutrons of energy 1.2 keV, 8.2 keV, 27.4 keV, 71 keV, 144 keV, 250 keV, 565 keV, 1.2 MeV, 2.5 MeV, 5.0 MeV and 14.8 MeV. Measurements were performed in 1986[2], and 1987[3]. Repeat measurements performed in 1987 as a consistency check exhibited good agreement.

Neutron fluences were determined using a DePangher long counter, a proton recoil proportional counter, or a proton recoil telescope, depending on the neutron energy. Overall, five different fluence monitor systems were employed depending on the particular reaction. These were: the charged particle current on the neutron producing target, a $^{10}BF_3$ counter in a polyethelene moderator, a similar detector surrounded by stearin, a ^{3}He proportional counter in a small polyethelene moderator, and a long counter.

The shadow cone technique was used to correct for room and air inscatter contributions. Other corrections included those for dead-time, air attenuation, and the presence of contaminant lower energy neutrons produced by scattering in the targets. The effects of scatter between the spheres and the monitors were also investigated and corrections applied. Overall uncertainties in the calibrations varied from about 4% in the most favourable cases, 71 keV to 5 MeV, to about 10% in the most unfavourable, 1.2 keV, where there was a significant subtraction for contaminant neutrons from the ^{65}Cu targets. All uncertainties throughout the report are quoted at an estimated one standard deviation.

3.2 Calibrations with thermal neutrons

Neutrons from the column of the standard thermal fluence facility at NPL[4] were used to provide a thermal calibration for all spheres up to the 10". The diameter of the column precluded measurements on the two larger spheres. Fluences were measured using the standard gold foil activation technique with a ^{235}U fission counter as monitor[5].

Measurements were performed on the spheres both bare and fully enclosed in 1 mm thick cadmium. The difference between these two measurements gave the response to neutrons in the sub-cadmium region of the spectrum where the distribution consists of a thermal Maxwellian peak, at an estimated temperature of 316 K, and a small (3%) epithermal component between the peak and the cadmium cut-off energy of 0.51 eV[6].

Overall uncertainties in the calibrations ranged from about 3% for the small spheres, due mainly to the uncertainty in the fluence measurement, to about 7% for the largest sphere. The biggest contribution to the uncertainty for the larger spheres arises from the large (up to 73%) subtraction for the measurements made under cadmium.

3.3 Measurement of the amount of ^{3}He in the SP90 counter

Calculation of the sphere responses requires the amount of ^{3}He in the central thermal neutron detector to be known. Only an approximate figure is given by the manufacturers, and some degree of variation is to be expected between actual counters.

Because the cross section for the $^{3}He(n,p)T$ reaction is known in the thermal region, being well represented by a 1/v shape, the amount of ^{3}He present can be determined from a measurement of the counter response in a known thermal neutron fluence. Allowances need to be made for the enclosing steel shell of the counter, and for self-shielding effects[5].

The results for the counter of the NPL sphere set gave an effective pressure of (179 ± 7) kPa assuming a spherical active volume of diameter 32 mm. Results for other SP90 counters gave results which exhibited a standard deviation of about 3% around the mean (for 5 counters), with a maximum difference between any two counters of about 7%.

4. CALCULATION OF RESPONSE FUNCTIONS

A number of multisphere response function calculations have been published[1], however, almost all have been for a LiI central detector. Two methods have been used: either a Monte Carlo simulation, or a discrete ordinates calculation (the S_n method). Both have their advantages and disadvantages. The S_n method is fast, but lacks flexibility in handling complex geometrical shapes. The Monte Carlo technique does allow complex geometry effects to be investigated, but very considerable computing time is required to calculate the full response function at all energies. Since the sphere and detector combination is, except for the stem of the detector, spherically symmetric, the S_n method was adopted in this case.

The calculations were performed with the computer code ANISN[7], using the adjoint mode. This allows the full response function to be calculated in a single run of the program[8]. Cross sections were obtained from the UKCTRI library[9] where the data are given in 46 energy bins ranging from 10^{-3}eV to 14.2 MeV. The calculated response functions are expressed in terms of these 46 energy bins.

The calculations were performed initially assuming 0.94 g cm^{-3} for the polyethelene density, and 4.5×10^{19} atoms cm^{-3} for the ^{3}He number density. However, ANISN was also run with slightly altered values for these parameters yielding information on the sensitivity to these densities, from which response functions can be derived for any polythene density or ^{3}He number density reasonably close to the original values. These data were used to derive calculated response functions for the NPL and PTB multisphere sets which differ somewhat in densities. This approach to correcting for density variations is only feasible because ANISN calculates the full response function in one run, and prohibitively long computing times are not involved. Tables of the results are available from NPL for the SP90 counter bare, and with spheres ranging in diameter from 7.62 cm to 38.1 cm.

5. RESPONSE ADJUSTMENT

Having obtained a calculated estimate of the response functions, and experimental calibrations, the problem arises of how to make full use of all this data to arrive at a best estimate of the response functions and

their uncertainties based on all the available information. The problem is completely analogous to that of using multispheres to adjust a neutron spectrum where there is some *a priori* information e.g. from a neutron transport calculation. In this case the multisphere measurements adjust the *a priori* spectrum and reduce the uncertainties - the small sphere data adjusting the low energy end of the spectrum, and the large sphere data the high energy end etc. Deriving response functions when there is calculated and experimental data is exactly analogous in that the calibrations can be used to adjust the calculated estimates. The analogous quantities are given below, those on the left being for spectrum adjustment and those on the right for response function adjustment.

Calculated *a priori* spectrum	-	a calculated response function
Measured multisphere responses	-	measured calibration data
Multisphere response functions	-	a function which is 1 for the bin at the calibration energy, 0 elsewhere.

The adjustment must be performed for each response function separately, and can be carried out with the code used for spectrum unfolding.

A calibration only affects one bin of the response function; but the responses for adjacent bins must vary smoothly with energy and they should not be altered completely independently. This correlation between responses in the bins over a limited energy region can be expressed mathematically by introducing covariance terms between the uncertainties in the responses for these bins. The process thus requires the response function adjustment to be performed with an unfolding code, such as STAY'SL[10], which can handle these covariances. The main problem is the present unavailability of uncertainty values from the calculation. Ideally the program which calculates the response function should also provide uncertainties for the responses in each bin, and also an estimate of the correlations between these responses. These correlations arise because the same cross section set is used for all the calculations.

In the absence of these data, uncertainties in the response values for individual bins were estimated from considerations of the cross section uncertainties and the differences between calculated and experimentally measured values. Covariance terms were introduced, in a somewhat ad hoc way, to provide short range correlations between a few adjacent bins thus ensuring that any adjustment based on measurement was not excessively localised but extended over nearby bins.

Figure 1 gives an example of a typical adjustment. The calibrations and calculations agree well in the keV to MeV region. No normalisation of the calculated curves was needed for spheres up to the 5" although some

initial overall normalisation was introduced for the larger spheres; the normalisation factor increasing monatonically to about 1.13 for the largest sphere. In the thermal region calculation and experiment do not generally agree and the final adjusted responses correspond essentially to the measured values. The difference between calculation and experiment is about a factor of 2 for the 3" sphere, but decreases to about 46% for the 10" sphere. The calculation for the bare SP90 counter, however, gave excellent agreement with the measurements. No explanation has yet been found for the poor results of ANISN for small spheres at thermal energies.

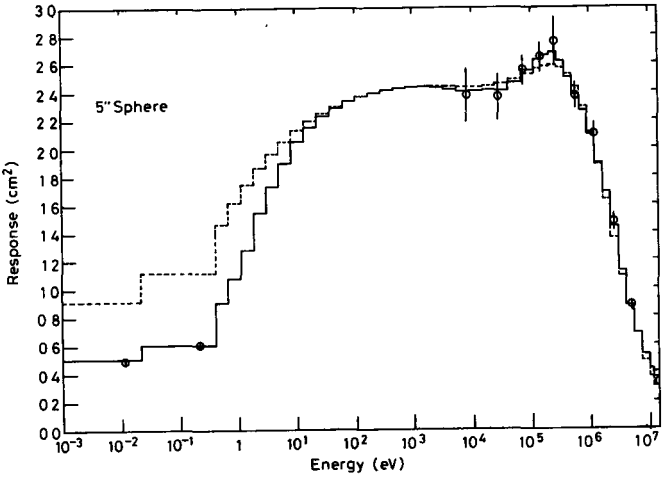

Figure 1 Response function of the 5" Bonner sphere The dashed line represents the calculated response, the points the measured data, and the solid line the final adjusted response function

The above approach gives a best estimate of the response function consistent with all the data, and also, because STAY'SL adjusts the covariances, provides an estimate of the final covariance uncertainty matrix. This information is required if STAY'SL is to be used for unfolding spectra.

6. SPECTRUM UNFOLDING

The equations for multisphere spectrum unfolding with m spheres are:

$$c_i = \sum_{j=1}^{n} r_{ij} \phi_j \qquad \text{for } i = 1, \ldots m \qquad (1)$$

where c_i is the count rate for sphere i in a spectrum with n bins and

fluence $\emptyset_j$ per bin. The response function for the i^{th} sphere is r_{ij}, with j = 1,.... n. The solution required is for $\emptyset_j$, given measurements of c_i and estimates of the response functions. If j > i there is no exact mathematical solution, even if the r_{ij} values are known exactly. The approach taken in STAY'SL, however, involves expanding equations (1) in a Taylor series about an expansion point. Manipulating the expressions[10] gives an equation of the conventional least-squares form, involving all the quantities c_i, r_{ij}, and $\emptyset_j$ as variables, with uncertainties. The design matrix, however, only involves values of r_{ij} and $\emptyset_j$ at the expansion point. The equations can be solved exactly without the need for an iterative technique. This makes the program very quick to run.

The penalty for this approach is that all quantitites, including an *a priori* estimate of the spectrum, need to be available with uncertainties. However, the approach can still be used, even in cases where there is no real prior information, provided large enough uncertainties are assigned to the guess spectrum used. A few preliminary runs with a variety of guess spectra can quickly identify a reasonably appropriate one.

STAY'SL was used by NPL in a recent European intercomparison of unfolding codes[11] and gave results which were amongst the best. The intercomparison showed that the unfolded spectra were, considering the limitations of the system, quite reasonable, and the derived total fluence and dose equivalent values were surprisingly good. STAY'SL has now been adopted as the program to be used at NPL and has been employed to analyse measurements performed at nuclear installations in the UK.

7. BENCHMARK MEASUREMENTS IN WELL KNOWN FIELDS

As a test of the derived response functions a set of measurements with the complete sphere set were performed at NPL in two well known broad range neutron fields[12]. The first was that of a bare ^{252}Cf fission source. Measurements were corrected for room and air in-scatter effects using the shadow cone technique, and further corrections were made for air out-scatter and dead-times. The corrected sphere count rates were then compared with those obtained by folding the response functions with the ^{252}Cf spectrum recommended by ISO[13]. Agreement between measurement and calculation was good, differences averaging about 5% with a bias

indicating that the response functions were on average slightly high. Since the neutron emission rate of the ^{252}Cf source was known precisely from manganese bath measurements this was a test of the absolute magnitudes as well as the shapes of the response functions. Subsequent re-analysis of target scattering effects for the monoenergetic calibrations at PTB indicate the need for reductions of a few percent to the response functions, thus improving the fit to the ^{252}Cf data. Revised response functions will be produced in due course.

The second broad range field used was that of a ^{252}Cf source moderated by a 30 cm diameter sphere of heavy-water encased in a 1 mm cadmium shell. Measurements were performed at a fixed distance of 1.5 m from the centre of the source. Shadow cone correction techniques were not possible because of the large physical size of the moderator. Instead the bare and cadmium covered SP90 detector measurements were used to estimate the thermal neutron contribution at the measurement position; produced in this case by room and air scattering effects. This thermal component was then added to the heavy-water moderated ^{252}Cf spectrum recommended by ISO[13], which has no neutrons below the cadmium cut-off energy. The resulting spectrum was then folded over the response functions and the predicted count rates compared with the measured ones. Since the absolute output from the heavy-water moderator is not known precisely, normalisation of the overall spectrum was allowed but with no change in the spectrum shape. The agreement was again good, differences being about 3% on average.

Finally STAY'SL was used to adjust the heavy-water moderated spectrum shape in response to the sphere measurements. The program altered the spectrum very little, but did reduce (by a few percent) the uncollided ^{252}Cf peak at the high energy end of the spectrum. This is probably a further indication that the response functions are a few percent too high over this energy region, rather than a true indication of problems with the ISO spectrum.

8. MEASUREMENTS IN STRAY NEUTRON FIELDS

The multisphere set has been used to perform measurements in unknown spectra at 3 locations in the UK. The results are not yet freely

available. Figure 2, however, shows results of measurements made in the vicinity of a nuclear power reactor. The significant feature is the low energy of the neutrons - there being no evidence of any above about 1 MeV. This is very significant information for interpreting dosemeter and area survey meter readings in this field. It should be noted that no other spectrometry system would measure any but a small fraction of this distribution.

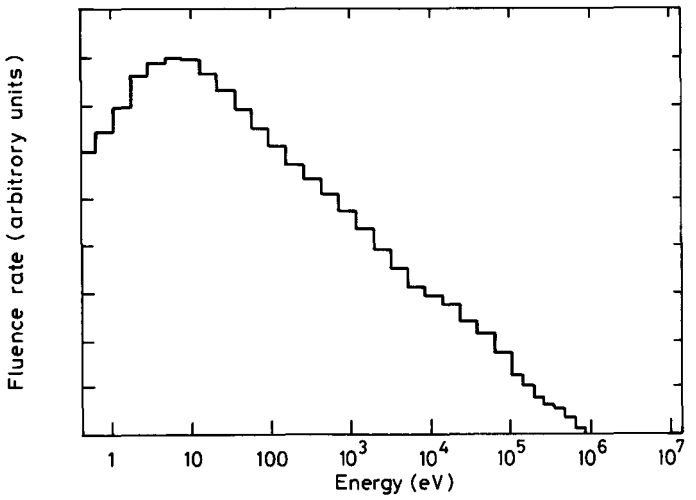

Figure 2 The measured distribution of neutron fluence rate in the vicinity of a reactor in the UK

9. CONCLUSIONS AND DISCUSSION

A new multisphere spectrometry system has been established. Extensive measurements of the sphere responses in monoenergetic fields have been combined with calculations to provide reliable response functions. The suitability of the spectrum unfolding code was investigated, and measurements performed in stray neutron fields.

Comparison of experimental calibrations, and calculations performed with the program ANISN reveal good agreement in the keV to MeV region, but poor agreement for the small spheres at thermal energies. This is difficult to understand since the spheres are moderating devices and the thermal cross sections are used not only for calculating the thermal response of the small spheres, but also in calculating the responses of all spheres at all energies. More sophisticated Monte Carlo codes may perform better, and promising initial results have been obtained[14] with

the Winfrith code McBEND. These results do show, however, that the presence of the SP90 detector stem, which can not be allowed for using ANISN, has little effect.

Future improvements to the system will include using the ^{252}Cf source measurements to further improve the response functions. This can be achieved using the techniques outlined in section 5.

REFERENCES

1. M Awschalom and R S Sanna; Radiat. Prot. Dosim. 10 (1985) 89-101.

2. A V Alevra, M Cosack, J B Hunt, D J Thomas and H Schraube; Radiat. Prot. Dosim. 23 (1988) 293-296.

3. A V Alevra, M Cosack, J B Hunt, D J Thomas and H Schraube; to be published.

4. T B Ryves and E B Paul; Journal of Nucl. Energy 22 (1968) 759-775.

5. D J Thomas, J B Hunt, H Schraube and A V Alevra; to be published.

6. D J Thomas and N Soochak; NPL Report RS(Ext)104 (July 1988).

7. W W Engles; A User's Manual for ANISN, Union Carbide Corporation Nuclear Division Report K-1693, Oak Ridge, Tennessee (1967).

8. N E Hertel and J W Davidson; Nucl. Instr. and Meth. in Phys. Research A238 (1985) 509-516.

9. T D Beynon and N P Taylor; The UKCTRI Data Library: 46 Group Neutron Cross Sections for Fusion Reactor Calculations, University of Birmingham, Department of Physics, Paper No. 79-02.

10. F G Perey; Least-Squares Dosimetry Unfolding: The Program STAY'SL, Oak Ridge National Laboratory Report ORNL/TM-6062, ENDF-254.

11. A V Alevra et al.; Unfolding Bonner Sphere Data: a European Intercomparison of Computer Codes, Laboratory Report PTB-7.22-90-1, Braunschweig (1990).

12. J B Hunt, B R More, D J Thomas, H Schraube, A V Alevra and H Klein; to be published.

13. ISO International Standard ISO 8529.

14. G A Wright; AEA Technology Winfrith, Private communication.

IV. Other research group(s) collaborating actively on this project [name(s) and address(es)]:

Dr M Cosack, Dr H Klein, and Dr A V Alevra,
Physikalisch-Technische Bundesanstalt,
Bundesallee 100, D-3300 Braunschweig, FRG

Dr H Schraube,
Inst. für Strahlenschutz,
GSF, Neuherberg, Munich, FRG

V. Publications:

1. In scientific journals:

1. A V Alevra, M Cosack, J B Hunt, D J Thomas and H Schraube; *Experimental Determination of the Response of four Bonner Sphere Sets to Monoenergetic Neutrons,* Radiat. Prot. Dosim. 23(1988)293-296.

2. A V Alevra, M Cosack, J B Hunt, D J Thomas and H Schraube; *Experimental Determination of theResponse of four Bonner Sphere Sets to Monoenergetic Neutrons (II),* to be published.

3. D J Thomas, J B Hunt, H Schraube, and A V Alevra; *Experimental Determination of the Response of four Bonner sphere Sets to Thermal Neutrons,* to be published.

4. J B Hunt, B R More, D J Thomas, H Schraube, A V Alevra, and H Klein; *Benchmark Measurements with ^{252}Cf and Heavy Water Moderated ^{252}Cf Sources using four Bonner Sphere Systems and an NE213 Spectrometer,* to be published.

2. In reports:

1. D J Thomas and N Soochak; *Determination of the ^{3}He number density for the proportional counter used in the NPL Bonner sphere system,* NPL Report RS(EXT)104 July 1988

2. D J Thomas; *NPL contribution to a EURADOS Working Committee 4 intercomparison of unfolding codes for Bonner sphere data,* NPL Report RS(EXT)112 December 1988

3. A V Alevra, B R L Siebert, A Aroua, M Buxerolle, M Grecescu, M Matzke, M Mourgues, C A Perks, H Schraube, D J Thomas, and H L Zaborowski; *Unfolding Bonner Sphere Data: a European Intercomparison of Computer Codes,* Laboratory Report PTB-7.22-90-1, Braunschweig, 1990.

4. D J Thomas; *Response function calculations for a Bonner sphere set with a ^{3}He central thermal detector,* to be published.

RADIATION PROTECTION PROGRAMME
Final Report

Contractor:

Gesellschaft für Strahlen- und Umweltforschung mbH
GSF
Ingolstädter Landstr. 1
D-8042 Neuherberg

Contract no.: BI6-A-172-D

Head(s) of research team(s) [name(s) and address(es)]:

Prof. W. Jacobi
Institut für Strahlenschutz
GSF
Ingolstädter Landstr. 1
D-8042 Neuherberg b. München

Dr. G. Burger
Institut für Strahlenschutz
GSF
Ingolstädter Landstr. 1
D-8042 Neuherberg b. München

Telephone number: 89-31.87.22.25

Title of the research contract:

Radiation exposure analysis and biological dosimetry.

List of projects:

1. Exposure analysis for occupationally, medically and accidentally exposed persons (with emphasis on neutron irradiation).
2. Microdosimetry and biological dosimetry.

Title of the project no.: 1

Exposure Analysis for Occupationally, Medically and Accidentally Exposed Persons (with Emphasis on Neutron Irradiation)

Head(s) of project:

A. Wittmann

Scientific staff: G. Burger, G. Leuthold,
H. Wiechell*, A. Morhart*, H. Schraube*

*part time involvement

I. Objectives of the project:

One of the major problems in exposure analysis is the link of measurements in radiation protection to the operational or primary limited quantities.
The group has concentrated in this respect on two items:

- Evaluation of instruments and methods for ambient and personal neutron monitoring.
- Theoretical determination of fluence-to-dose conversion functions for relevant dosimetric quantities, as defined in international recommendations and regulations.

II. Objectives for the reporting period:

The following more specific objectives have been coped with during the period 1985-1989.

1. Working place field analysis and dose assessment.
2. Development of tools for easy three-dimensional modelling of real man.
3. Calculation of quality factors for neutron exposure of soft tissue.
4. Performance of transport calculations in anthropomorphic phantoms and the ICRU-sphere to establish a complete set of relevant fluence-to-dose conversion functions in neutron radiation protection.

III. Progress achieved:

1. Working place field analysis and dose assessment.

1.1 Performance of multisphere measurements in reactor environments, compilation of typical spectra from other sources and dosimetric analysis of these data:

The response functions of practically applied instruments differ from those of recommended operational quantities. The latter differ from that of the primary limited one, the effective dose eqivalent H_E. To check the relevance of these differences in radiation protection a set of 76 stray and leakage spectra of neutrons has been compiled. 31 are indirectly determined by own multisphere measurements in the experimental hall of a swimming pool research reactor. For all spectra and several assumed exposure conditions (A-P and isotropic radiation incidence) various quantities relevant in radiation protection have been determined. This concerns the effective dose equivalent H_E, the ambient dose equivalent H*(10), as defined in the ICRU-sphere, and finally the expected reading of albedo dosemeters, some Bonner spheres and of a standard Anderson & Braun rem counter /12, 15, 16, 19, 20/.

The results are as follows:

- The ratios of the responses of the rem counter and the 12" Bonner sphere (C_{12}) to H*(10) don't show any relation to the shape of the spectrum. The standard deviations of these ratios are 0.13 (rem counter) and 0.15 (12" sphere). So H*(10) can be measured by these instruments with an uncertainty (2 SD) of 30% approximately.
- The albedo dosemeter can be used reasonably for personal monitoring only when it is calibrated in situ in working environments by means of Bonner sphere measurements.
- The ratios $H^*(10)/H_E$ are strongly, but not systematically dependent on the spectra. In worst cases the ratio exceeds 5. In all cases the ratio is greater than 1. The averaged values are 1.5 for a parallel uniform A-P field and 3.0 for an isotropic radiation field.

It is concluded that it is possible to measure H*(10) with conventional instruments with reasonable accuracy, but H*(10) is highly overestimating the effective dose equivalent.

1.2 Performance of calibration and intercomparison studies.

The group was operating a secondary standard laboratory with poor scatter neutron calibration facilities equipped with radionuclide sources and a 3 MeV ion accelerator /4, 7, 8/. Several small scale intercomparison studies have been performed partly under the auspices of EURADOS-CENDOS /1, 9, 13/. For the special calibration of Albedo dosimeters a D_2O-moderated Cf-252-source was established. The leakage spectra of the device for several moderator diameters were calculated in a joint effort by members of EURADOS working group IV: Numerical Dosimetry. The results were evaluated in a standardized manner (Fig. 1), and the spectra used for the calculation of responses of several neutron monitoring devices and of operational and primary limited quantities relevant in radiation protection /6, 7, 18/.

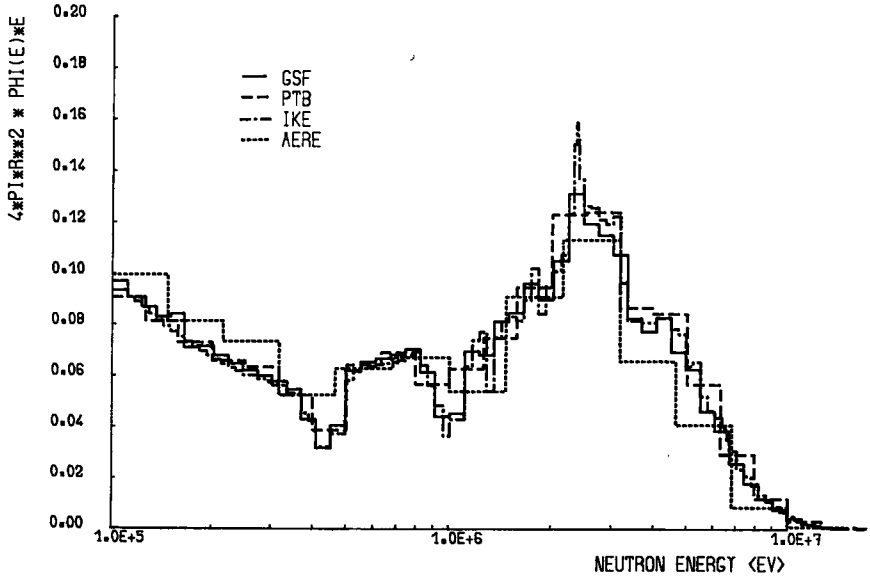

Fig. 1: High energy part of the Cf-252 spectrum leaking out of a 30 cm diameter heavy water sphere at the moderator surface. Intercomparison of calculations by A. Morhart, Neuherberg/Munich, B. Siebert, Braunschweig, G. Hehn, Stuttgart, and K.G. Harrison, Harwell (within EURADOS Working Group IV: Numerical Dosimetry)

2. Development of tools for easy three-dimensional modelling of real man.

A programme package available (MOVIE-BYU) had to be further developed and improved to perform reasonable threedimensional surface reconstructions from serial tomographic images based on a grid model. It was applied to whole body tomograms of infant leukemia patients (jointly with B16-133-D), to check the validity of assumptions when shrinking the adult mathematical anthropomorphic phantom to a child phantom in establishing a phantom 'family' for radiation transport calculations. Special emphasis was laid on processing of magnetic resonance images to provide easier access to whole body tomography of volunteer adults. Now there is a system available with the possibility of real time reconstructions using more than 150 tomograms for one processed volume based on a voxel model /3, 10, 21, 22/.

3. Calculation of quality factors for neutron exposure of soft tissue

The quality factor as function of neutron energy was calculated for different proposals /14, 17, 23/.

a) ICRP 51, the old quality factor times two
b) ICRU 40, the quality factor in terms of lineal energy y. The quantity y was calculated with Coyne's program for a sphere of 1 micron diameter.

To retain the formulation of the quality factor in terms of LET, three new proposals were made. They all have the following characteristics: The quality factor remains 1 up to some level L_o, increases to a value of 30 at 100 keV/micron and declines beyond 100 keV/micron proportional to 1/sqrt(L). In the old formulation and ICRP 51 recommendation the quality factor remains constant for high LET particles. As the influence of these particles is therefore lower in the new proposals, the protons play a major role. The value L_o becomes crucial as it influences the fast protons for which one would like to end up with a quality factor of one. L_o-values of 3.5, 10, and 25 keV/micron were assumed. Table 1 summarizes the proposals based upon which the total quality factor for neutrons was derived (Fig. 2). The results provide hints for the decision making on the revision of

Table 1: Quality factors for which organ doses, effective dose equivalent in the phantom and directional dose equivalents in the ICRU-sphere are available.

◇ ICRU 16 : (old quality factor)

□ ICRP 51 : (old quality factor for neutrons component times two)

△ ICRU 40 : (Q(y))

▽ Q(L) = (Kellerer)

1	L < 3.5 keV/micron
0.3 L	else
300/sqrt(L)	L >100 keV/micron

◁ Q(L) = (Drexler)

1	L < 25 keV/micron
5.8 sqrt(L)-28	else
300/sqrt(L)	L >100 keV/micron

○ Q(L) = (compromise)

1	L < 10 keV/micron
.32 L - 2.2	else
300/sqrt(L)	L >100 keV/micron

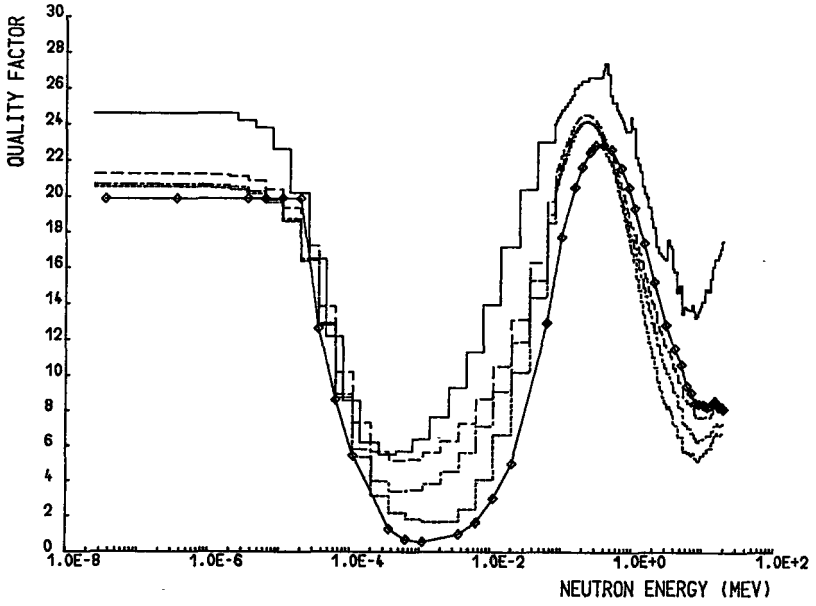

Fig. 2: Quality factor as a function of neutron energy for several proposals. ICRU 51 (solid line), ICRU 40 (solid line with symbols), Kellerer (dashed), Drexler (dotted), compromise (dash-dotted)

the quality factor. A compromise value of L_o = 10 keV/micron seems now to be under discussion.

4. Performance of transport calculations in anthropomorphic phantoms and the ICRU-sphere to establish a complete set of relevant fluence-todose conversion functions in neutron radiation protection.

Introduction:
Existing calculations of organ doses in anthropomorphic phantoms were based on the CHORD-approximation and for the male phantom on the Monte Carlo code SAM-CE /2, 11/. Continued investigations concerned
- the improvements in the SAM-code and calculation of the female phantom
- the possible improvement of the CHORD-method by including the scatter profile around a mathematical ray (pencil beam) into the computations

Calculations:
For both male and female adult phantoms SAM-CE calculations have been repeated for AP, PA and LAT-exposure geometry in the energy range of 1 eV to 14 MeV. All relevant organs, including those in the 'remainder' have been considered. The dose in the latter is defined as the mass weighted mean of the average doses in stomach, small and large intestine, liver and pancreas. All calculations were performed for the five formulations of quality factor as a function of neutron energy. In general the dose equivalent based on the new quality factor assumptions is higher with increasing tendency at higher neutron energies. The exception is the ICRP 51 proposal, where high LET-particles have a constant quality factor. As a consequence the curves show a shoulder, especially for A-P radiation geometry. The calculations were performed for four irradiation geometries in the phantom. Fig. 3 shows the effective dose equivalent H_E in the phantom for the ICRU 40 quality factor proposal.

The calculations of the dose equivalents in the ICRU-sphere include five irradiation geometries /5, 14/. In order to compare the several proposals of the quality factors and their influence on neutron dose equivalents in the phantom and the sphere, the effective quality

factor, i.e. the ratio of dose equivalent to kerma, resp. kerma-equivalent inside the receptor was evaluated. This was done for the phantom organs and their weighted sum leading to H_E and for 10 mm depth in the sphere for A-P radiation geometry. The influences of the L_O-value in the quality factor can be seen very clearly. For the highest L_O-value (L_O = 25 keV/micron) the new effective quality factor is lower than the old one. Fig. 4 shows the effective quality factor as function of neutron energy for 10 mm depth in the sphere. The symbols refer to those in Table 1.

Recently there were new proposals for the revision of risk data and hence modified organ weighting factors for deriving H_E.The new calculations still based on the old quality factor show that the ratios of the new effective dose equivalents to the old one vary about + 10% over the whole energy range and are of minor relevance in radiation protection. New calculations were also performed for all relevant dosimetric quantities for 45 compiled neutron spectra. (See also chapter 1). The ratios of H_E based on ICRU 40 to the old one vary between 1.2 and 1.6 for all environmental spectra /23/.

As the Monte Carlo calculations are very time consuming, effect was put into the improvement of the CHORD-method. The main shortcomings of the method can obviously be overcome by including the scatter component around each mathematical ray (pencil beam profile) into the superposition routine. This can easily be done in homogeneous material, surface effects at tissue borders can, however, not be taken into account. Depending on the resolution of the pencil beam profile, the calculation times were about 10 times that of the Ray-CHORD method. The programme was therefore not yet applied for whole body exposure situations, seems however extremely suitable for partial body exposure problems.

The data sets derived over the past 5 years constitute the basis of recommendations on neutron conversion functions in ICRP-Publication 51 'Data for Use in Protection Against External Radiation', March 87, ICRU-Report 39, 'Determination of Dose Equivalents Resulting from External Radiation Sources', Feb. 1985 and ICRU-Peport 43, Determination of Dose Equivalents Resulting from External Radiation Sources: Part 2, Dec. 1988. The data on the several recent quality factor proposals, including their influence on organ doses and operational dose quantities have been delivered to an ICRP-committee on the revision of the quality factor and constitute the basis for new recommendations.

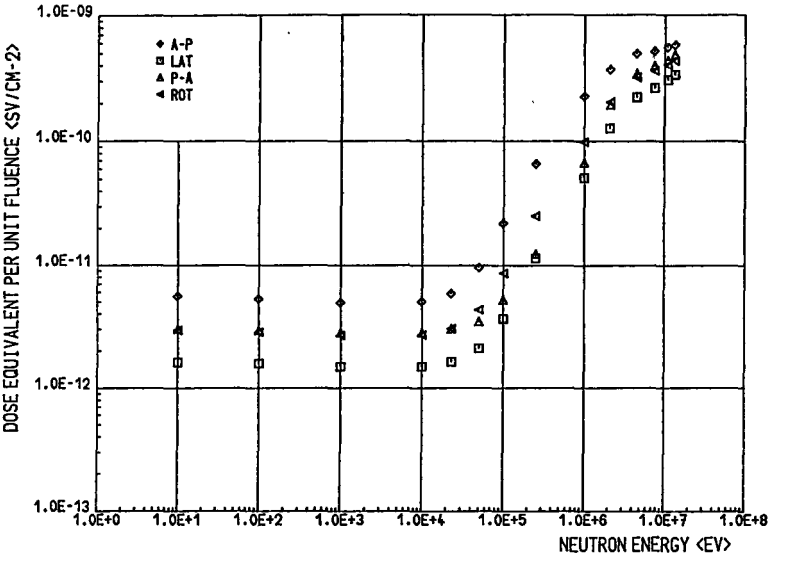

Fig. 3: Effective dose equivalent H_E in the phantom for four irradiation geometries. Quality factor according to ICRU 40.

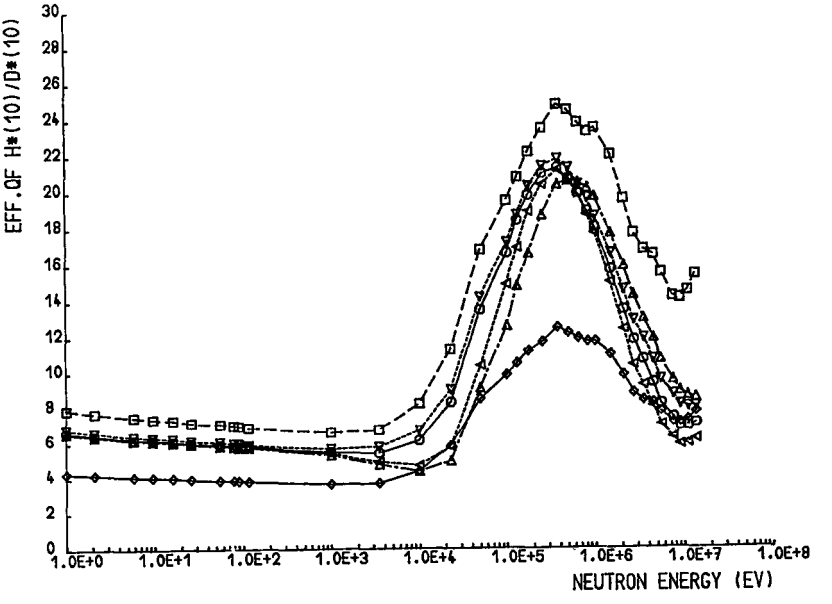

Fig. 4: Effective quality factor (dose equivalent/kerma) as a function of neutron energy for the effective dose equivalent in the phantom. A-P irradiation geometry. Symbols refer to the quality factors listed in Table 1.

IV. Other research group(s) collaborating actively on this project [name(s) and address(es)]:

Dr. G. Dietze, PTB, Braunschweig, FRG
Dr. G. Drexler, GSF, Neuherberg, FRG
Dr. J.B. Hunt, NPL, Teddington, GB
Dr. K. Pfändner, TU Munich, FRG
Dr. R.B. Schwartz, NBS, Washington, USA
Dr. B. Siebert, PTB, Braunschweig, FRG
Dr. R.E. Swaja, ORNL, Oak Ridge, USA
Dr. J. Zoetelief, TNO, Rijswijk, NL

V. Publications:

1. Publications in scientific journals, monographs etc.

(1) Alevra, A.V., Cosack, M., Hunt, J.B., Thomas, D.J., Schraube, H.: Experimental determination of the response of four Bonner sphere sets to monoenergetic neutrons. Radiat. Prot. Dosimetry 23, 293-296 (1988)

(2) Burger, G., Morhart, A., Wittmann, A.: The Conceptual Basis of Neutron Radiation Protection. Proc. Fifth Symposium on Neutron Dosimetry in Biology and Medicine (eds. Schraube, H., Burger, G., Booz, J.) EUR 9762, Vol. 1, 71-83 (1985)

(3) Burger, G., Rodenacker, K., Wittmann, A., Buchinger, G., Pfändner, K., Deimling, M.: Die bildanalytische Verarbeitung und Generierung von MR-Bildern. In: NMR in der Medizin (Hrsg. F. Nüsslin, H. Weidhausen), Urban & Schwarzenberg, München, 111-119 (1986)

(4) Burger, G., Schwartz, R.B.: Guidelines on calibration of neutron measuring devices. International Atomic Energy Agency, Vienna, Technical Reports Series no. 285, 1988

(5) Morhart, A., Burger, G.: Specified Dose Eqivalent Quantities for Neutrons in the ICRU-sphere and their Applicability. Radiat. Prot. Dosimetry 12, No. 2, 107-111 (1985)

(6) Schraube, H.: Multisphere measurements at a heavy water moderated Cf-252 fission source. Proc. Fifth Symposium on Neutron Dosimetry in Biology and Medicine (Eds. Schraube, H., Burger, G., Booz, J.) EUR 9762, Vol. 1, 583-593 (1985)

(7) Schraube, H.: Sources of neutrons, characteristic fields and spectra. Radiat. Prot. Dosimetry 20/1-2, 9-17 (1987)

(8) Schraube, H., Chartier, J.L., Cosack, M., Delafield, H.J., Hunt, J.B., Schwartz, R.B.: Calibration procedures for determining the radiation response characteristics of neutron measuring devices used for radiation protection. Radiat. Prot. Dosimetry 23, 217-221 (1988)

(9) Schraube, H., Swaja, R.E.: Characteristics of individual neutron monitors in the view of international intercomparisons. Proc. International Conference on Radiation Dosimetry and Safety, Taipei, Taiwan, 81-91 (1987)

(10) Williams, G., Zankl, M., Abmayr, W., Veit, R., Drexler, G.: The calculation of dose from external photon exposures using reference and realistic human phantoms and Monte Carlo methods. Phys. Med.. Biol. 31, 4449-4452 (1986)

(11) Wittmann, A., Morhart, A., Burger, G.: Organ doses and effective dose equivalent. Radiat. Prot. Dosimetry 12, Nr. 2, 101-106 (1985)

(12) Wittmann, A., Burger, G., Kollerbaur, J., Schraube, H.: Neutron occupational exposure and radiological protection. Proc., Fifth Symposium on Neutron Dosimetry in Biology and Medicine (Eds. Schraube, H., Burger, G., Booz, J.), EUR 9762, Vol 1: 157-168 (1985)

(13) Zoetelief, J., Schlegel-Bickmann, D., Schraube, H., Dietze, G.: Characteristics of Mg/Ar ionization chambers used as gamma-ray dosimeters in mixed neutron-photon fields. Phys. Med. Biol. 31, 1339-1351 (1986)

2. Short Communications, theses, internal reports etc.

(14) Burger, G., Leuthold, G., Morhart, A., Wittmann, A.: Neutron conversion functions and their accuracy. Abstract, 6th Symposium on Neutron Dosimetry, Neuherberg, 1987 (to be published 1990)

(15) Burger, G., Morhart, A., Schraube, H., Schießl, W., Wittmann, A.: Der Neutronen-Konverter am FRM als Standardquelle für Dosimetrie, Internal Report, GSF-Munich (1985)

(16) Kollerbaur, J., Burger, G., Schraube, H., Wittmann, A.: Neutronenexpositionsanalyse in Reaktoren. Internal Report, GSF-Munich, (Feb. 1985)

(17) Leuthold, G., Burger, G.: The quality factor for neutrons. Internal Report, GSF-Munich, (Dec. 1989) (to be published 1990)

(18) Morhart, A., Burger, G.: Ergebnisse von Neutronentransportrechnungen zur Bestimmung von Entkommspektren und Dosiskonversionsfaktoren für Cf-252 Quellen in kugelförmigen Wassermoderatoren. Internal Report, GSF-Munich, (Dec. 1985)

(19) Morhart, A., Burger, G., Schraube, H., Schießl, W., Wittmann, A.: Berechnungsergebnisse für die Energiespektren und Äquivalentdosis-Konversionsfaktoren am Neutronenkonverterstrahl der FRM. Internal Report, GSF-Munich, (Oct. 1985)

(20) Schraube, H.: Analyse von Neutronenfeldern in Kernkraftwerken. Internal Report, GSF-Munich, (Feb. 1986)

(21) Wagner, H.: Entwicklung von Programmen zur mathematischen Morphologie für das VICOM Bildanalysesystem unter Berücksichtigung der VICOM Rechenwerke. Thesis, FH Munich (1986)

(22) Wiechell, R. Erkennung und Darstellung von morphologischen Merkmalen aus räumlichen Bildsequenzen am Beispiel histologischer Serienschnitte. Thesis, Univ. Heidelberg, Heilbronn (1986)

(23) Wittmann, A., Morhart, A., Leuthold, G., Burger, G.: Organ doses and the effective dose equivalent derived in adult antropomorphic phantoms for neutron exposure. Part 1: Basic data and method. Part II: Tables and graphs. Internal Reports, GSF-Munich 1989/1990 (to be published)

Title of the project no.: 2

Microdosimetry and Biological Dosimetry

Head(s) of project:

G. Burger

Scientific staff: G. Burger, G. Leuthold, M. Makarewicz (until 1986), M. Aubele (since 1986), K. Rodenacker*, A. Chaudhuri*, U. Jütting*, A. Voss*, M. Heymann*

*part time involvement

I. Objectives of the project:

The objective of the project is an improved understanding of biological efficiency of radiation. A first step is the understanding of the physical stages of radiation interaction and particle transport. It provides the theoretical basis for the calculation of radiation response of dosimeters. Of central interest is the event and energy distribution in model targets of biological relevance based upon charged particle track structure. Experimental studies on cytometric biological dosimetry are of immediate relevance for radiation protection monitoring and serve as a radiobiological link to the microdosimetric studies.

II. Objectives for the reporting period:

The following more specific objectives have been coped with throughout (during) the period 1985-1989.

1. Calculation of energy depositions in spherical cavities based upon modified continuous-slowing-down models for the charged particles and on Monte Carlo calculation for the primary radiation.
2. Monte Carlo simulations of track structure of protons and heavier charged particles and analysis of energy deposition and event distribution in small cavities (nanometer region).
3. Investigations on imaging cytometry and application of this technology for providing new endpoints in biological monitoring.

III. Progress achieved:

1. Calculation of energy depositions in spherical cavities based upon modified continuous-slowing-down models for the charged particles and on Monte Carlo calculation for the primary radiation.

Rationale:

Improved performance and analysis of radiobiological experiments with neutrons require accurate experimental dosimetry and microdosimetry. This necessitates continuously improved calculations of ion chamber responses as well as event size distributions in proportional counters.

Basic data compilations:

W values for protons, alpha and heavy particles in TE (methane) gas and CO_2 have been re-evaluated. Corresponding stopping powers were newly calculated, because those compiled in ICRU 36 seemed to be unreliable. Secondary particle spectra were calculated by means of a code from Caswell and Coyne. For TE gas the derived W_n values are somewhat lower than those of Goodman and Coyne up to about 13 MeV. The difference is usually less than 0.6%, except in the energy region of 0.1-0.2 MeV, where it rises to 1.1%. An overall uncertainty of 3% has been estimated. W_n for CO_2 gas increases steeply with decreasing neutron energy. An overall uncertainty of 5-6% is assumed. A great uncertainty is expected with respect to neutron cross-sections, particularly for carbon, and with respect to the W function for C ions, especially at higher energies /7, 11, 18, 19/.

For TE/TE chambers the gas-to-wall conversion factor r varies with cavity size within 2-3%. However, variations up to 6% are possible. Therefore, in precise neutron dosimetry the size dependency of r should be considered. The above statements are based on the data for 0.01, 0.1, 1 and 10 cm^3 cavities, as well as for infinitesimal and infinite ones. Maximal variations may be slightly higher for W_n, and substantially higher for r, if a full range of cavity sizes would be considered. At least for the 1 cm^3 chamber and for neutron energies above 12 MeV one may use the easily calculable values of W_n for gas and of r for the Bragg-Gray chamber. Cavities extremal in size (infitesimal, infinite) do not determine extreme values either for absorbed dose or for specific ionization inside a cavity. They give asymptotic values only /17/.

Chamber calculations:

Using the reevaluated basic data neutron sensitivities of TE/TE and C/CO_2-ionization chambers have been calculated as a function of neutron energy and for several chamber sizes. Fig. 1 shows k_T for a TE/TE chamber. The calculations have been performed by means of an analytical approach similar to that of Rubach. Based upon recent available experimental data also the spectral neutron sensitivity of a 1 cm^3 airfilled TE chamber was assessed by valid approximations /2, 7, 21/.

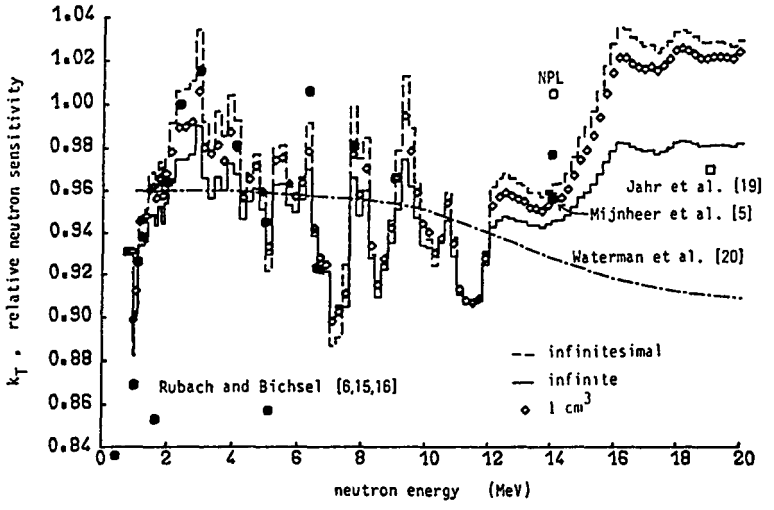

Fig. 1: Relative sensitivity k_T of TE/TE ionization chambers

In order to check the applicability of such chambers for phantom measurements in calibration studies with Cf-252 sources, as well as for radiation biology and therapy dosimetry in a reactor beam and for 15 MeV, neutrons transport calculations have been performed inside a water phantom and the local chamber sensitivities have been calculated. Within the geometrical limits of the fission beam, the local average neutron energy varies between 0.94 and 1.6 MeV. k_T for the TE/air chamber varies in the range of 0.73 to about 0.85 necessitating suitable corrections. k_T for the TE/TE chamber is practically constant (k_T = 0.96 + 0.002). k_u of a C/CO_2-chamber varies from 0.08 to 0.09. For 15 MeV neutron beams k_T for the TE/TE-chamber is practically constant, for the TE/air chamber the variation is between 0.83-0.98 with the lower values near the beam edge.

2. Monte Carlo simulations of track structure of protons and heavier charged particles and analysis of energy deposition and event distribution in small cavities (nanometer region).

Monte-Carlo program and cross sections:
Simulation of charged particle tracks by the Monte-Carlo method is based upon a complete evaluated set of interaction cross-section of the ions and the secondary electrons. Those for proton interaction were extended up to 15 MeV using single and double differential ionisation cross-section given by Senger. The energy range for ion-track simulation reaches now from 0.2 MeV/amu up to 15 MeV/amu. The simulation of primary interaction of alpha particles is based upon proton data properly scaled according to the effective charge.

Energy deposition in experimentally simulated targets of minimum size:
Recently energy deposition distributions were calculated for the diametral passage of 0.25 - 1 MeV/amu alpha-particles through spherical volumes with 50 - 400 nm diameter. At 50 nm assymmetric distributions were found due to straggling effects. Energy deposition distributions for 5.8 MeV alpha particle in small cylindrical targets (Z = 100 - 400 nm, R = 25 - 200 nm) were calculated. These calculations were in collaboration with the University of Padua to give theoretical spectra for the comparison with measurements in a small proportional counter /8, 9/.

Ion track sampling by the proximity function:
The proximity function defined by Kellerer gives the possibility of analysing the particle track without referring to a specified target. As an ion track can be considered as a linear sequence of ion interactions and a surrounding region formed by the secondary electron interactions, the proximity function can be defined for different structural components of the particle track. These include the ion interaction core (i), the individual delta-ray track (e) and interactions between them (ie,ee). An important one is the component (e) which describes the energy deposition events within the same secondary electron track. With increasing ion energy the proximity function is dominated at small distances by this electron component, which is rather independent of the ion energy in contrast to LET. This result demonstrates the important role of event clusters in the track of delta-rays. Fig. 2 shows the

Components of the track

1. Proton interaction only (i)
2. Ion-electron event correlation (i-e)
3. Different secondary electron tracks (e-e) "Intertrack"
4. Electron events within the same electron track (e) "Intratrack"

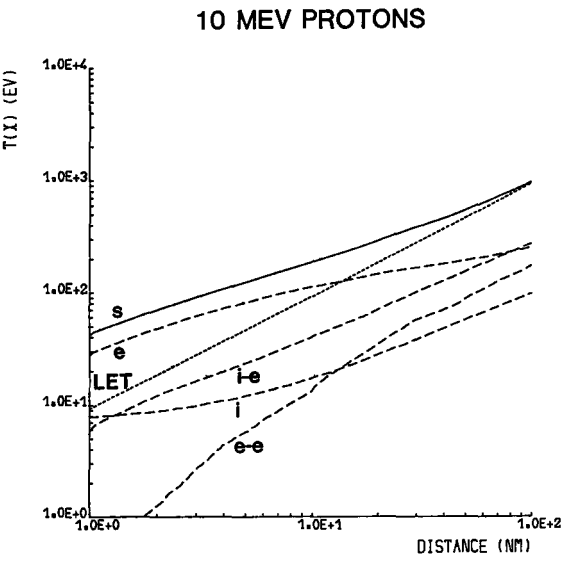

Fig.2 Proximity functions for 10 MeV protons: 4 components, total proximity function (s) and LET-approximation (dotted)

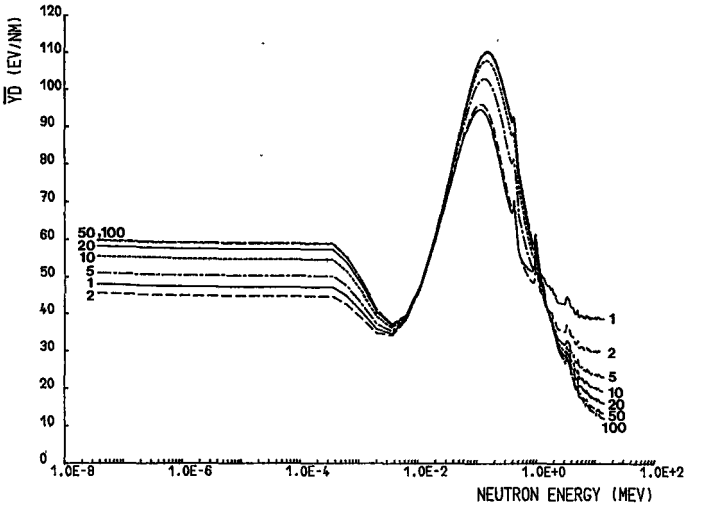

Fig.3 $\overline{y}_D$ values plotted against neutron energy for target diameters from 1 to 100 nm

proximity function of 10 MeV protons. Note the dominance of the delta-ray component (e) for small target sizes.

Calculation of y_D:
The dose mean lineal energy y_D is an important quantity in microdosimetry and analytical radiobiology. y_D was calculated by use of the proximity function without the explicit knowledge of the lineal energy distribution. The calculations of y_D in spherical targets show, of course, the same effect as described above. With increasing proton energy (above 1 MeV) the energy deposition clusters from delta-rays are most important, and the LET-approximation leads to an underestimation of y_D. On the other hand below 1 MeV the LET-approximation overestimates y_D due to the delta-ray escape effect. These findings are most pronounced at small target sizes at the nanometer level /12, 13, 14, 16/.

Generally, the following relations on ion energy and target diameters are found: At high ion energies the track ends of secondary electrons dominate the energy deposition pattern. This leads to an underestimation of y_D when estimated by the LET-approximation. At lower energies the delta-ray escape gives y_D values which are lower than those derived by LET. This holds for protons and alpha particles at different energy levels, depending on the stopping power of the ion.

y_D-values were also calculated from radial dose profiles around proton tracks. The radial dose profile was calculated by averaging the energy deposited in simulated tracks within cylindrical shells around the track core. The y_D-values of the "amorphous" track model show a different behaviour as function of target diameter. For small target diameters a big underestimation of energy deposition results, due to the averaging of the non-homogeneous event pattern.

In order to derive y_D for neutrons, firstly the slowing down spectra of secondary charged particles after neutron irradiation were calculated by a program of Caswell and Coyne. y_D was then calculated for these spectra, implying that all particles are assumed to be crossers which seems to be a reasonable approximation in the energy range above 0.2 MeV/amu and small target sizes. Below this value no track structure calculations can be performed due to the lack of interaction cross sec-

tions. This holds generally for all heavy recoils. For protons and alpha particles below 0.2 MeV/amu the track structure results for y_D have been reasonably extrapolated, for the heavy recoils the LET-approximation for y_D was used. Fig.3 shows y_D as a function of neutron energy for target sizes of 1 - 100 nm when the complete slowing down spectra are used. The approximations mentioned allow to assume that the curves are not realistic around the dip between neutron energies of 10^{-4} to 10^{-1} MeV. Here the very low energetic recoil protons play the major role which are no longer crossers at least in targets above 50 nm diameter. At high neutron energies and small target sizes there is a big increase of y_D due to the role of secondary electron track and clusters.

3. Investigations on imaging cytometry and application of this new technology for providing new endpoints in biological monitoring.

Rationale:

For biological radiation monitoring only two cytogenetic techniques have been established in the past. The more elaborate one is the measurement of chromosome aberrations, the second one the detection of micronuclei. Both techniques suffer essentially from lack of sensitivity to be used routinely for biological monitoring of radiation workers or members of the public overexposed operationally or accidentally with doses not too far beyond the legally set limits /3/.

Material and Methods:

To check the principal feasibility of such an approach methodological studies have been performed in several model cell systems. They include rat erythroblasts from bone marrow samples and peripheral lymphocytes, as well as spermatides and spermatozoa from testes and epididymes of irradiated mice.

The animals were irradiated at various times before sampling. Doses ranged from 0.25 up to 15 Gy. Smears were made on glass slides following various preparation protocols, and Feulgen stained. Measurements were performed by automated TV-microscopy. The wave length of the light was about 550 nm. TV-images were digitized with nominal grey value resolution of 8 bit and pixel distances of 0.25 micron. The images are gene-

rally preprocessed and transformed, the complete nuclei and the contrasted chromatin regions segmented and up to 60 photometric, morphologic and textural features extracted /4, 5, 6/. Generally 100-300 cells are measured per specimen and two specimens prepared per animal, dose and time after exposure.

Measurements:

- Rat erythroblasts

  In a preliminary study erythroblasts were investigated as a model system for the acute noncumulative expression of radiation damage. Adult Sprague Dawley rats received Cs whole body irradiation of 1 Gy and were sacrificed, 1, 5 and 24 hrs later. Bone marrow smears were prepared and Giemsa-stained. On these smears 300 erythroblasts per slide were located for storage of coordinates and were allocated to morphological compartments. Subsequently, the Giemsa dye was removed and a Feulgen staining performed, and the cells were measured /20/.

  As already demonstrated earlier with human erythroblasts, the four compartments could be efficiently reclassified by the computer. A discrimination of control versus irradiated cells was only possible 1 h after irradiation and was restricted to the basophilic, polychromatic and orthochromatic erythroblast compartments. Proerythroblasts, the fastest proliferating compartment did not show any difference at any time, while the difference of the non-proliferating orthochromatic erythroblasts was as much as that of the other proliferative compartments. The cytometric effects were significant the results could, however, not be validated as the project was terminated.

- Mouse sperm and blood

  Based upon reports in the beginning of the 80's on the possibility of morphometric sperm assays a study was started on mouse sperm damage expression and kinetics /1/.

  In a first experiment NMRI mice testes were irradiated by collimated x-rays at dose levels from 0.25 Gy up to 15 Gy. One set of mice received single doses, another split doses with a time lapse of 8 h in between. One animal was available per dose and up to 250 elongated spermatids were measured per animal. Testicular biopsies have been

analysed and DNA-content and shape parameters have been calculated. Fig. 4 shows dose effect curves for the fraction of sperm with DNA greater than 1.5c for a single and a split dose experiment. Note the low sensitivity of the ploidy assay. Additionally several shape parameters have been calculated. They proved to be of higher sensitivity, but show large variances due to the unavoidable mixture of spermatids and spermatozoa of varying degree of maturation and shape expression in testes. To eliminate the problem of biased visual selection of mature sperm in testes biopsies, further investigations were performed with mature spermatozoa collected directly from epididymes. Additionally conventional blood smears were taken to investigate the radiation effect upon lymphocytes. Sperm and blood sampling was performed 21 days post radiatio (dpr), 35 dpr, and on controls. Conventional smears were produced on glass slides, fixated and Feulgen stained.

Multivariate linear discriminant analysis (LDA) was performed for the three cell classes: Control, 21 dpr, 35 dpr. The results demonstrated marked differences in sperm and lymphocytes between irradiated animals and controls. Additionally in the sperm head analysis 2 sets of features were applied: shape and densitometric. The differences 35 dpr concerned predominantly shape parameters, those 21 dpr predominantly staining density distribution parameters.

Lymphocyte measurements in conventional blood smears showed poor reproducibility. The problems are likely due to non-stoichiometric dye-binding in the non-homogeneous cell layers. Therefore in a new experiment the preparation technique was improved by using suspension techniques. Blood samples were taken in this case from irradiated 101*C3H-mice (2 Gy) 1, 3, 5, 14, and 21 dpr. In a six-class-LDA the pooled lymphocytes from each sampling group and the controls could be correctly reclassified by 53.1%. The distances of the mean of each cell pool from irradiated mice to the control in the multidimensional space of selected features (Mahalanobis distances) showed a curve peaking in between 6-20 days. Fig. 5 shows the dose effect curve for measurements on spermatozoa 35 dpr as the result of a multiple linear regression analysis. Two features were applied. The first, most important one, is describing shape based upon a Fourier analysis of the circumference.

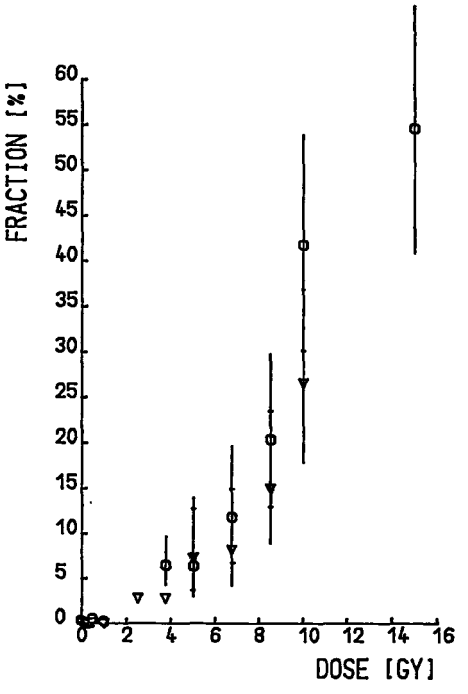

Fig. 4: Dose effect curves for the fraction of nonhaploid sperm in murine testes biopsies 21 days after collimated irradiation of gonads.

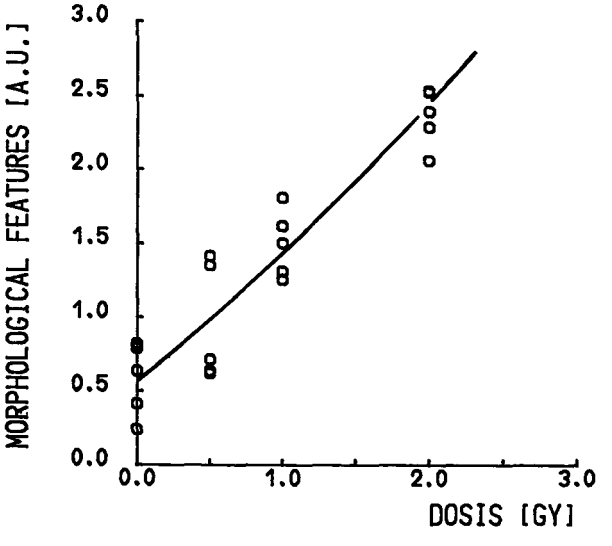

Fig. 5: Dose effect curves for a combination of cytometric features for murine spermatozoa 35 days after whole body irradiation.

IV. Other research group(s) collaborating actively on this project [name(s) and address(es)]:

Dr. H. Bichsel, Seattle, USA

Dr. P. Colautti, INFN, Leguaro, I

Dr. J. Coyne, NBS, Washington, USA

Dr. P. Dörmer, GSF, Munich, FRG

Dr. B. Senger, INSERM, Strasbourg, F

V. Publications:

1. Publications in scientific journals, monographs etc.

(1) Aubele, M., Jütting, U., Rodenacker, K., Gais, P., Burger, G., Hacker- Klom, U.: Quantitative evaluation of radiation-induced changes in sperm morphology and chromatin distribution. Cytometry, in press (1990)

(2) Bichsel, H., Makarewicz, M.: Comments about a 'new' TE gas. Letter to the Editor. Phys. Med. Biol. 30 (11), 1257-1260 (1985)

(3) Burger, G.: Assessment of body doses from measured values of indicators: Neutrons. In: Biological Indicators for Radiation Dose Assessment (Eds.: A. Kaul et al.) bga Schriften 2/86, MMV, Munich, 164-172 (1986)

(4) Burger, G.: Image analysis cytometry: an overview. Proc. Corso in CITOMETRIA 1988. Genova, Italy: Istituto Nazionale per la Ricerca sul Cancro, 99-104 (1988)

(5) Burger, G., Jütting, U.: Specimen classification in cytometry: An intercomparison of various means of decision making. Pattern Recognition in Practice II (Eds.: E.S. Gelsema, L.N. Kanal), Amsterdam, New York, Oxford, North Holland Publ. Comp., 509-519 (1985)

(6) Burger, G., Rodenacker, K., Jütting, U., Gais, P., Schenck, U.: Morphological markers in cytology. Acta Stereologica, 4/2, 243-248 (1986)

(7) Burger, G., Makarewicz, M.: Average energy to produce an ion pair in gases (W-values) and related quantities of relevance in neutron dosimetry. In: Nuclear and Atomic Data for Radiotherapy and Related Radiobiology. Vienna: IAEA, 225-238 (1987)

(8) Colautti, P., Cutaia, M., Makarewicz, M., Schraube, H., Talpo, G., Tornielli, G.: Neutron microdosimetry in simulated volumes less than 1 micrometer in diameter. Radiat. Prot. Dosimetry 13, 117-121 (1985)

(9) Colautti, P., Leuthold, G., Talpo, G., Tornielli, G.: Longitudinal ion probe in a cylindrical TEPC at simulated lengths less than 1 micrometer. Radiat. Prot. Dosimetry (in press) (1990)

(10) Combecher, D., Kollerbaur, J.: The measurement of electron spectra in the track of protons in water vapour. Radiat. Prot. Dosimetry 13 (1-4), 23-26 (1985)

(11) Huber, R., Combecher, D., Burger, G.: Measurement of average energy required to produce an ion pair (W-value) for low-energy ions in several gases. Radiation Research 101, 237-251 (1985)

(12) Leuthold, G., Burger, G.: Dose mean lineal energy for neutrons. Radiat. Prot. Dosimetry (in press) (1990)

(13) Leuthold, G., Burger, G.: Dose mean lineal energy for computer simulated proton tracks. Proc. 5th Symp. on Neutron Dosimetry in Biology and Medicine (Eds.: Schraube, H. et al) 1, 245-253 (1985)

(14) Leuthold, G., Burger, G.: Dose mean lineal energy for fast neutrons in small spherical targets. Radiat. Prot. Dosimetry 23, 49-51 (1988)

(15) Leuthold, G., Burger, G.: Mathematical simulation of proton tracks in water vapour and their microdosimetric analysis. Radiat. Environ. Biophys. 27, 177-187 (1988)

(16) Leuthold, G., Burger, G.: Structure and microdosimetric classification of computer simulated ion tracks. Radiat. Prot. Dosimetry 13 (1-4), 37-40 (1985)

(17) Makarewicz, M., Burger, G.: Dose dependence on cavity size: A contribution to cavity theory. Radiat. Prot. Dosimetry 13 (1-4), 369-371 (1985)

(18) Makarewicz, M., Burger, G.: W_n for methane-based TE-gas and carbon dioxide and W_n and gas-to-wall dose conversion factors for TE/TE cavities. Proc. Fifth symposium on Neutron Dosimetry in Biology and Medicine (Eds.: Schraube, H. et al) 1, 257-283 (1985)

(19) Makarewicz, M., Burger, G., Bichsel, H.: On the stopping power for tissue-equivalent gaseous ionisation devices used in neutron dosimetry. Phys. Med. Biol. 3 (3), 281-284 (1986)

2. Short Communications, theses, internal reports etc.

(20) Dörmer, P., Abmayr, W., Burger, G.: Image analysis of erythroblast nuclei in rats after irradiation with 1 Gy in vivo. Abstract in Proc. Intern. Symposium on Clinical Cytometry and Histometry, Elmau, Germany (1987)

(21) Makarewicz, M., Burger, G., Morhart, A.: Calculation of neutron sensitivity for tissue equivalent and C/CO_2 chambers. Abstract in 6th Symposium on Neutron Dosimetry, Neuherberg, Germany, Oct. 1987 and Internal Report, GSF-Munich (Feb. 1988).

RADIATION PROTECTION PROGRAMME
Final Report

Contractor:

Gesellschaft für Strahlen-
und Umweltforschung mbH
GSF
Ingolstädter Landstr. 1
D-8042 Neuherberg

Contract no.: BI6-A-011-D

Head(s) of research team(s) [name(s) and address(es)]:

Prof. Dr. W. Jacobi
Institut für Strahlenschutz
GSF
Ingolstädter Landstr. 1
D-8042 Neuherberg b. München

Dr. H.G. Paretzke
Institut für Strahlenschutz
GSF
Ingolstädter Landstr. 1
D-8042 Neuherberg b. München

Telephone number: 89-31.87.22.25

Title of the research contract:

Track structure calculations.

List of projects:

1. Track structure calculations for radiation risk estimation.

Title of the project no.: 1

TRACK STRUCTURE CALCULATIONS FOR RADIATION RISK ESTIMATION

Head(s) of project:

H.G. Paretzke and W. Jacobi

Scientific staff:

H.G. Paretzke, W. Weinzierl, K. Long,
S. Henß, W. Jacobi

I. Objectives of the project:

Track structures of charged particles describing the primary locations of relevant molecular changes produced by irradiation will be calculated for complex, heterogeneous, condensed targets (cells, etc.) and evaluated with respect to the characteristics determining their biological consequences (e.g. DNA damage, cellular damage). The radiation fields considered include internal emitters, external photon fields and HZE-particles. To this purpose the existing Monte Carlo-Computer programs for particle transport simulation have to be modified with respect to the physical cross section data base, the geometrical scoring routines and the methods of classification of results.

II. Objectives for the reporting period:

- To finalize work on and describe all interaction cross-sections needed in this project taking shortcomings into account which cannot be resolved presently (due to the lack of adequate experiments and theories).
- To extend the HZE-cross-sections to the parameter range used in radiobiological experiments at GSI and Bevelac for the interpretation of the experimental data obtained there.
- To use the alpha-particle and electron code to estimate the potential hazard from incorporated "warm" and "hot" particles emitted from the Chernobyl reactor.

III. Progress achieved:

1. Methodology

In order to tackle the objectives of this project, different tasks had to be performed:

a) to extend the energy ranges of particles that could be considered in the Monte Carlo Programme from 1 eV - 30 MeV for electrons and 1 keV and to 1 GeV/amu for heavy charged particles,
b) to produce a cross section set for photon track structure calculations from 1 eV to 10 MeV,
c) to introduce complex geometry routine to permit scoring in structured, heterogeneous targets (e.g. micro-dosimeters, biological cells and tissues),
d) to extend all cross sections from a previous application to gas phase targets to the condensed phase (e.g. tissues),
e) to apply the code to explain radiation biological data, in addition, the variable "time" (dose-rate effects) and fast biochemical reactions had to be introduced.

These tasks were mainly solved by analysis of literature data, comprehensive own calculations and adaptions of cross sections and the development and testing of the multi-purpose charged particle track structure code PARTRAC, which is written in FORTRAN 77 and which runs now under the Operating system UNIX on a fast parallel computer (INTEL IPSC/2).

2. Results

The results for the double differential cross sections for electron interaction with a water molecule, a cluster of water molecules and liquid water have been presented elsewhere (ref. 15). Here we give a brief summary of the new results. Fig. 1 shows the double differential cross section for a 200 eV electron incident on a water molecule, and central molecule of a cluster of 5 molecules, as a function of secondary electron energy, where both electrons are counted as secondary because they can not be distinguished from each other. The results show

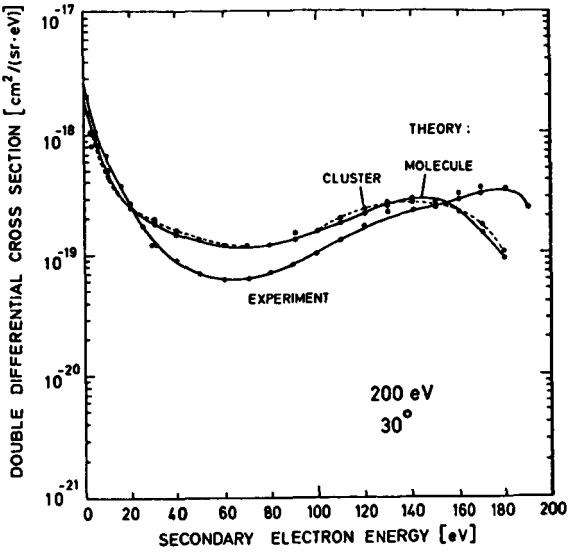

Fig. 1 Double differential cross section for electron scattering from a water molecule and the central molecule of a cluster of 5 water molecules for an incident energy of 200 eV and an angle of 30° together with experimental results for the water molecule.

reasonable agreement between theory and experiment and a small but finite difference between the cluster and the molecule. The main source of disagreement probably comes about because of a too simple treatment of exchange. The angular dependence of the double differential cross section also agrees reasonably well with experiments. At 500 eV agreement between experiment and theory is good.

In the case of protons extensive calculations have been carried out (ref. 23) (16 angles and 50 secondary electron energies at each of 5 incident proton energies: 150 keV, 300 keV, 500 keV, 1000 keV, and 1500 keV). At each of these energies the single differential cross has also been calculated. Finally the total cross section for ionization has been calculated as a function of the incident energy. In Fig. 2 the double differential cross section for an incident proton energy of 300 keV is shown as a function of the secondary electron energy, for a water molecule, and the central molecule of a cluster of 5 water mole-

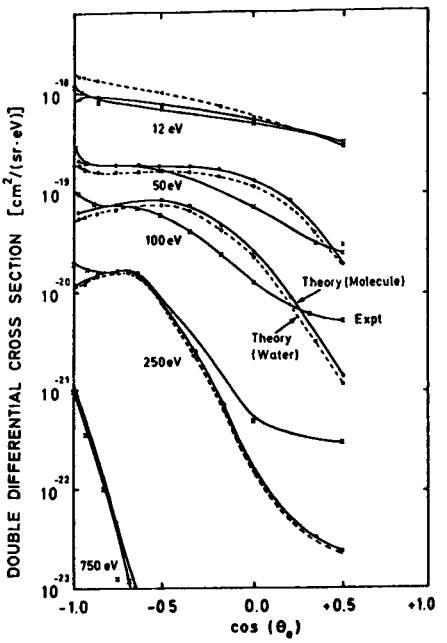

Fig. 2 Double differential cross section for secondary electron emission due to proton impact from water molecule and water at a proton energy of 300 keV, at various secondary electron energies as a function of the angle of emission.

cules. This shows that the agreement between experiment and theory is reasonably good except at large angles. Here a better continuum wavefunction needs to be used and a way of doing this has been developed. At increasingly higher energies the agreement becomes very good. As can be seen there are significant differences between the double differential cross sections for the water cluster and a water molecule. The difference is a function of both the secondary electron energy and the angle of emission. In Fig. 3 the total cross section for secondary electron emission is plotted as a function of incident energy both for the molecule x and the cluster (central molecule), [redacted], and also shown are the experimental results (denoted by a dot). The agreement is excellent and shows the somewhat lower cross section for 'water' which corresponds to the observed lower energy loss per unit path length for water. Single differential cross sections also agree very well with experimental results except at 150 keV where the agreement is still good.

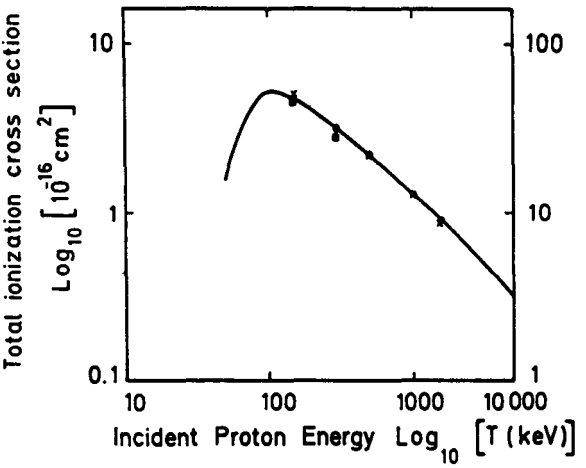

Fig.3 Total ionization cross section for secondary electron emission due to proton impact as a function of incident energy for a water molecule, x; water, ▮; (central molecule of a cluster) as compared to experimental results, solid line.

The very extensive calculations carried out in this work were only made possible by the use of a parallel supercomputer. Further significant increases (> 10) in the computing power available in the near future should enable even more accurate calculations especially at large angles and enable calculations to be carried out at lower energies.

Further on, the energy differential secondary electron ejection cross sections for 15 target materials (including liquid water, DNA, and polymers and gases used in experimental microdosimetry) and the projectiles proton and alpha-particles have been calculated approximately by the empirical method proposed by M.E. Rudd (Phys. Rev. A38, 6129-6137, 1988); classical assumption were made regarding the angular distributions. The target materials considered comprise water, H_2, He, Ar, O_2, and polymeric biomolecules. These energy dependent cross sections will now be used in the ion-track structure code PARTRAC.

Various sets of literature date on photon scattering cross sections were evaluated, checked for consistency with other integral data and the data chosen were prepared in a tabular form adequate for fast

computation and minimum storage requirements. The photon scattering cross sections for all relevant materials, energies and types of interaction (differential in angle and target shell) are now available in a form optimized for speed of computation and memory space needed.

Complex geometry computer routines were developed and tested by comparison of computed results for the location of points deterministically migrating on straight lines through the bodies (within/without) with analytical solutions. The complex geometry algorithms describing now 20 different simulated bodies are accurate enough for the intended purpose; in some cases the speed of computation has still to be improved. Fig. 4 gives as an example electron tracks in spherical ellipsoid and a sphere simulating a cell and its nucleus respectively. For various

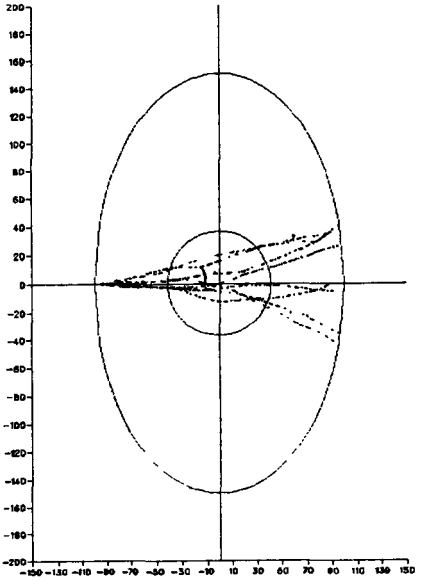

Fig. 4 Simulated tracks of 10 electrons of 100 keV in a simulated cell.

primary charged particles the statistical density distributions for energy deposited and number of ionizations produced in small target volumes as a function of eccentricity were calculated (fig. 5). It was found that close to the surface of a target the LET-approximation could lead to wrong estimates of these distributions.

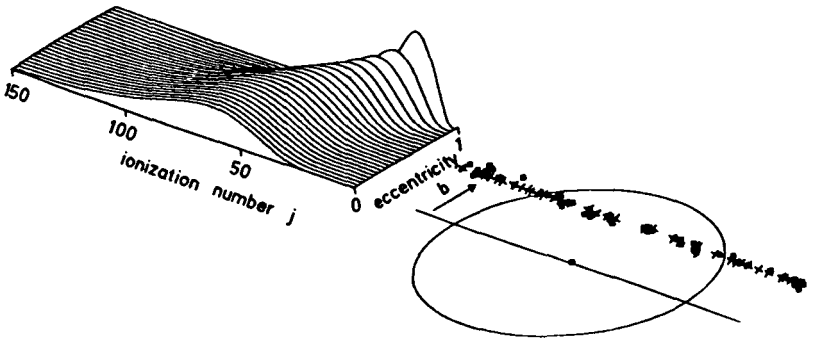

Fig. 5 Number of produced ion pairs in a small sphere by 1 MeV protons as a function of eccentricity.

Also photon track structure calculations can now be made, e.g. to permit comparison with proportional counter experiments. Fig. 6 shows such an intercomparison for incident 12 keV photons, which shows excellent agreement at larger lineal energy values. The discrepancy at lower y - values might be due to noise problems in the measerements.

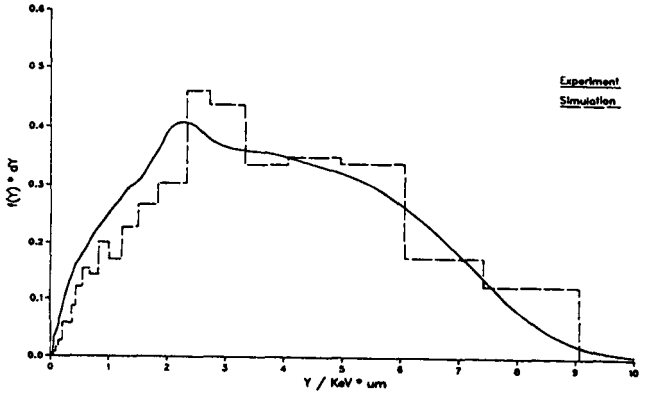

Fig. 6 Comparison of measured calculated spectra of lineal energy for 12 keV photons in a proportional counter.

The code PARTRAC was further extended to permit simulation of the fate of new chemical species in a biological cell. With this extended version first calculations were performed as to the relative contributions of direct and indirect effects on the induction of double strand breaks in a DNA-molecule (Fig. 7).

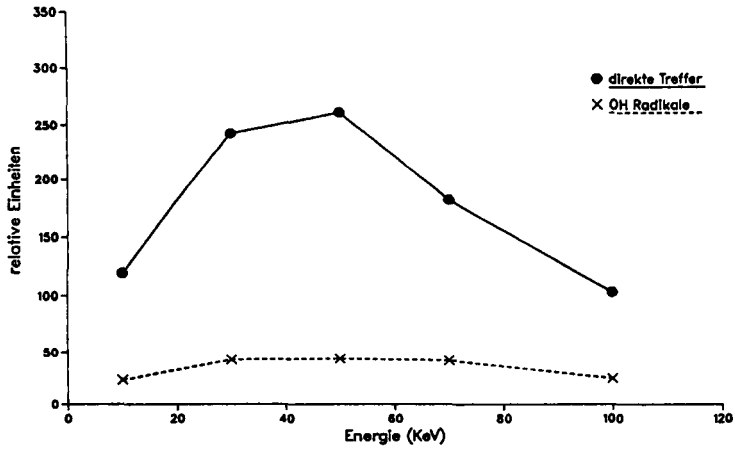

Fig. 7 Calculated contributions to double strand break formation by direct (•) and indirect effects (x) by fast electron impact.

Intercomparisons of calculated results for various sets of potentially classifying track structure quantities with experimental cell inactivation data indicate that, a), there are basic differences in the biological natures of primary relevant events produced in mammalian cells by irradiation with high and low LET-radiations, and, b), that it is necessary to consider for classification both the microstructure of clusters within cell nuclei and the total number of clusters exceeding certain sizes within the same nucleus.

Finally, the electron transport code was also used to calculate energy deposition frequencies in volumes of cellular dimensions for the decay of I-125. 10 000 electron energy spectra derived by J. Booz et al., KFA Jülich were used as start spectra, and two scoring geometries were used. First, the decays were assumed to occur in the centre of

concentric spheres with 16 radii from 0.1 nm to 10 μm and the frequency spectra of imparted energy were scored in each sphere; this simulates e.g. the situation for an Iodine atom decaying within the DNA molecule. Secondly, a homogeneous distribution of decaying nuclides within a 10 μm diameter sphere was assumed and the frequency spectra of imparted energy within this large sphere and within a concentric 1 μm diameter sphere were scored retaining the spatial information of the start location; this simulated the irradiation of the DNA-volume from a homogenous Iodine distribution in tissue.

These data were also used to derive first and second moments of these spectra and other microdosimetric quantities useful for the interpretation of radiobiological data obtained with I-125.

3. Discussion

The implementation of the photon interaction cross sections has been completed now.

The theory developed for the derivation of electron and other charged particle inelastic scattering cross sections show the right trends with increasing target density. However, the absolute values do not yet agree well with all reliable experimental data (e.g. on binding energies measured in ESCA-work), and means to improve this agreement have to be looked for. From the results presented above it can be seen that calculations of the cross sections for the gaseous and condensed phases have been carried out at energies above 200 eV for electrons and 200 keV for protons. The results show that the difference between the gaseous and condensed phase are less than 25 % in this region. At lower energies it is necessary to proceed to tackle two further problems. The wavefunctions of the incoming and outgoing particles and of the emitted secondary electron need to be much more complicated and one needs to calculate higher order terms in the Born approximation as the charged particle can then interact several times with the scattering region at lower energies. Further the electronic states and excitations in the condensed phase need to be calculated more accurately as smaller energy differences become important and other processes start to contribute to

the energy loss, such as phonons, excitons etc., and not just electronic excitation. The low energy cross sections of electrons are particularly important as the majority of secondary electrons which are created by the primary charged particle have energies of less than 100 eV.

It is also important to be able to calculate the cross section for the production of OH-radicals due to electron impact on liquid water. In order to tackle these problems one would need to develop a very good descripton of the electronic and dynamical properties of liquid water together with a good theory of the collective modes of the system and possibly of their decay.

The complex geometry computer routines appear to work well; more realistic bodies simulating DNA coiled around histones should now be developed.

Further work is needed to improve radiological classification schemes particularly taking energy migration along affected molecules into account. A feasible approach for characterization of charged particle tracks as regards their radiobiological effectiveness by more than one quantity has to be developed; apparently combined effects on three different structural levels are determining this effectiveness. Nevertheless, it can be concluded that the track structure code PARTRAC, which has been developed in the framework of this project, can be expected to be a very useful tool in these investigations.

IV. Other research group(s) collaborating actively on this project [name(s) and address(es)]:

Physical aspects: Dr. Booz (KFA Jülich) and other members of EURADOS-committee 1, Prof. Blanc (Univ. Toulouse), Prof. Sigmund (Univ. Odense), Prof. Hatano (Inst. of Technology, Tokyo), Dr. Toburen (Battelle, Richland), Dr. Inokuti (Argonne National Laboratory, USA), Dr. Turner (Oak Ridge National Laboratory), Dr. Diercksen (Max-Planck-Institut, Garching).

Biological aspects: Drs. Dennis, Lloyd (NRPB, Chilton), Drs. Broerse, Barendsen (TNO, Rijswijk), Dr. Goodhead, (MRC, Chilton), Dr. Lafuma CEA, Fontenay-aux-Roses), Prof. Hall (Columbia Univ., N.Y.)

V. Publications:

1. Jacobi, W., Paretzke, H.G.:
Risk Assessment for Indoor Exposure to Radon Daughters.
Sci. Tot. Environm. 45 (1985) 551-562

2. Charlton, D.E., Goodhead, D.T., Wilson, W.E., Paretzke, H.G.:
The Deposition of Energy in Small Cylindrical Targets by High LET Radiations.
Rad. Prot. Dos. 13 (1985) 123-125

3. Paretzke, H.G., Turner, J.E., Hamm, R.N., Wright, H.A., Ritchie, R.H.:
Calculated Yields and Fluctuations for Electron Degradation in Liquid Water and Water Vapor.
J. Chem. Phys. 84 (1986) 3182-3188

4. Paretzke, H.G.:
Physical Events of Heavy Ion Interactions with Matter.
Adv. Space Res. 6, 67-73 (1986)

5. Paretzke, H.G.:
Simulation von Elektronenspuren im Energiebereich 0,01 bis 10 keV in Wasserdampf.
Technische Universität, München (1987)

6. Paretzke, H.G.:
Radiation Track Structure Theory.
Chapt. 3 in: Kinetics of Nonhomogeneous Processes, G. Freeman, Ed., J. Wiley & Sons, N.Y., S. 89-170 (1987)

7. Booz, J., Paretzke, H.G., Pomplun, E., Olko, P.:
Auger-Electron Cascades, Charge Potential and Microdosimetry of Iodine-125.

8. Wilson, W.E., Paretzke, H.G.:
An Analytical Model for Ionization Distributions Produced in Nanometer Volumes by Recoil Protons.
Rad. Prot. Dos. 23, 45-48 (1988)

9. Wilson, W.E., Metting, N.F., Paretzke, H.G.:
Microdosimetric Aspects of 0.3 to 20 MeV Proton Tracks, I. Crossers.
Radiat. Res. 115, 389-402 (1988)

10. Paretzke, H.G.:
Problems in Theoretical Track Structure Research for Heavy Charged Particles.
in: Quantitative Mathematical Models in Radiation Biology, J. Kiefer (Ed.), Springer-Verlag, Heidelberg, S. 49-56 (1988)

11. Paretzke, H.G.:
Energy Deposition at the Molecular and Cellular Levels.
In: Mechanisms of Radiation Interaction with DNA: Potential Implication for Radiation Protection, U.S. Dept. of Energy, Nat. Techn. Inform. Sevice, Springfield, 39-47 (1988)

12. Olko, P., Booz, J., Paretzke, H.G., Wilson, W.E.:
Energy Deposition in Nanometer Sites Based on Track Structure Calculations.
"Atomic and Molecular Data for Radiotherapy", Intern. Atomic Energy Agency, Vienna, TECDOC-506, p. 105-116, 1988

13. Paretzke, H.G.:
Pysical Events in the Track Structure of Heavy Ions and their Relation to Alterations of Biomolecules.
Adv. Space Res. 9, 15-20 (1989)

14. Paretzke, H.G.:
Physical Aspects of Radiation Quality.
Proc. 14th Gray Conference "Low Dose Radiation - Biological Bases of Risk Assessment", Francis + Taylor, Oxford, p. 514-522, 1989

15. Long, K.A., Paretzke, H.G., Müller-Plathe, F., Diercksen, G.H.F.:
Calculation of Double Differential Cross Sections for the Interaction of Electrons with a Water Molecule, Clusters of Water Molecules and Liquid Water.
J. Chem. Phys. 91, 1569-1577 (1989)

16. Nikjoo, H., Goodhead, D.T., Charlton, D.E., Paretzke, H.G.:
Energy Deposition of Ultrasoft X-Rays in Cylindrical Volumes.
Medical Research Council, Radiobiology Unit, Monograph 88/1, Chilton, England, 1989.

17. Nikjoo, H., Goodhead, D.T., Charlton, D.E., Paretzke, H.G.:
Energy Deposition in Small Cylindrical Targets by Ultrasoft X-Rays.
Phys. Med. Biol. 34, 696-705 (1989)

18. Paretzke, H.G.:
Extrapolation from Radiogenic Cell Transformation to Human Cancer Risks.
in: Cell Transformation and Radiation-induced Cancer, K.H. Chadwick C. Seymour, and B. Barnhart, Eds., Adam Hilger, Bristol and New York, 387-399 1989

19. Nikjoo, H., Goodhead, D.T., Charlton, D.E., Paretzke, H.G.:
Energy Deposition of Monoenergetic Electrons in Cylindrical Volumes.
Medical Research Council, Radiobiology Unit, Monograph, submitted for Publication, Chilton, England

20. Nikjoo, H., Goodhead, D.T., Charlton, D.E., Paretzke, H.G.:
Energy Deposition in Small Cylindrical Targets by Monoenergetic Electrons.
Submitted for publication

21. Paretzke, H.G., Turner, J.E., Hamm, R.N., Wright, H.A.:
Spatial Distributions of Inelastic Events Produced by Electrons in Gaseous and Liquid Water.
Submitted to Radiat. Res.

22. Paretzke, H.G.:
Radiation Physics: Stochastic Deposition of Energy.
Submitted to Can. J. Phys.

23. Long, K., Paretzke, H.G.: Comparison of Cross Sections for Secondary Electron Emission by Protons from a Water Molecules and Clusters of Water Molecules.
Submitted to J. Chem. Phys.

RADIATION PROTECTION PROGRAMME
Final Report

Contractor:

Julius-Maximilians-Universität
Würzburg
Institut für Med. Strahlenkunde
Sanderring 2
D-8700 Würzburg

Contract no.: BI6-A-013-D

Head(s) of research team(s) [name(s) and address(es)]:

Prof. Dr. A.M. Kellerer
Institut für Med.Strahlenkunde
Universität Würzburg
Versbacher Str. 5
D-8700 Würzburg

Telephone number: 931-201.38.36

Title of the research contract:

Development of the twin detector method and of microdosimetric concepts and methods for radiation protection.

List of projects:

1. Implementation of the twin detector method and computational studies.
2. Mathematical and numerical studies in microdosimetry.
3. Microdosimetry of heavy ion beams at the UNILAC.

Title of the project no.:

Implementation of the Twin Detector Method and Computational Studies

Head(s) of project:

Prof.Dr.Albrecht M.Kellerer

Scientific staff:

Dr.J.Breckow, Dr.H.Roos, J.Chen, A.Philipp, H.Friede

I. Objectives of the project:

The objective of the project was the further development of the variance-covariance method (Kellerer and Rossi, Radiat.Res.97, 237, 1984) which permits the determination of microdosimetric parameters in radiation fields of fluctuating intensity. A pair of detectors (the twin-detector) is exposed to the same radiation field and registers the energy imparted within each of the detectors simultaneously. The difference between the variance (due to the fluctuations of energy imparted) and the covariance (due to the dose-rate fluctuations of the radiation field) determines the intrinsic microdosimetric fluctuations depending only on radiation quality, i.e. the inherent properties of the radiation.

II. Objectives for the reporting period:

III. Progress achieved:

The theoretical basis of the twin detector method is the variance-covariance method which was developed in earlier work sponsored by the European Community (Kellerer and Rossi, Radiat.Res.97,237,1984). The twin detectors, a pair of microdosimetric detectors, are exposed to the same radiation field, and the energy imparted within each of the detectors is registered simultaneously. The variance of the microdosimetric fluctuations, reflecting radiation quality, is determined as the difference between variance and covariance of the energy imparted within the detectors. Fluctuations of dose rate and disturbances from various sources contribute to the covariance and are eliminated, provided they affect the signals of both detectors simultaneously and with the same amplitude.

The instrumentation which has been developed during the reporting period utilizes a tissue equivalent twin detector that consists of two regular cylindrical proportional counters. The height of the sensitive volume (20mm) is defined by guard tubes. The diameter of the guard tubes is not much greater than the diameter of the central wire, hence their influence on the electric field within the sensitive volume is negligible and field tubes become unnecessary. Both detectors are linked to the same negative high voltage source; it is connected to the outer cylinder of the detectors. They are also supplied by one common gas flow system that regulates the gas density; methane based tissue equivalent gas is used. The detector currents are integrated in the feed-back capacitors of the electrometer operational amplifiers. The voltages of the two capacitors are concurrently digitized, with frequencies up to 10^4 s^{-1} (corresponding to a minimum sampling interval of 100μs), and the results are stored on a PC.

The electrometer circuit has a compensation function to clamp the central wire of the detector to zero potential. Integration of the detector currents has, in comparison to direct current measurements, the advantage of higher sensitivity, but it makes it necessary to discharge the integration capacitors periodically. The discharge is achieved by computer activated relay contacts. For calibration of the detectors and of the signal processing a collimated Am-241 α-ray source, integrated in the detector shell, with known energy - and LET spectrum, is used.

In a series of experiments the special possibilities and inherent advantages of the variahce-covariance method have been examined and quantitatively assessed. Measurements were performed with a low dose rate ^{241}Am source. The main component of the ^{241}Am-photon spectrum is the 60 keV peak (the α-radiation is absorbed within the source coverage). As a reference scale the single-event spectrum was determined by recording the pulse-height distribution of one detector in conventional pulse technique; from the pulse-height distribution the weighted mean of specific energy was calculated. The results of variance-covariance measurements in constant photon fields agreed well with the reference data over a wide range of dose increments per sampling interval between 1nGy and 1μGy. The maximum dose of 1μGy and the maximum sampling frequency of 10kHz correspond to a dose rate of 10mGy/s. On the other extreme measurements of 1nGy/s are feasible. One concludes that the instrumentation is applicable in a range of 7 orders of magnitude in dose rate, starting from a few energy deposition events per second and reaching to about one tenth of the dose rate of a typical therapeutic γ-irradiation source. The time required for recording the data for evaluation of the relevant parameters is a few minutes.

The main advantage of the variance-covariance method, compared to the variance method, is its applicability in time-varying radiation fields. To assess its potential the method was employed under conditions where the correlated variations contributed a substantial part of the variance. The distance between the twin detector and a ^{137}Cs source was periodically varied by a motor driven device. The contribution to the variance by the changing dose rate was increased from zero, for a constant field, to about 90% of the total variance. The values of lineal energy derived from these series of measurements were sufficiently constant over this range of dose-rate variations.

The dependence of lineal energy on site size was examined in a constant field of ^{137}Cs-γ rays. In these measurements the diameter of the simulated volume was varied between 67nm and 6.7µm. The data were compared to the results obtained earlier by other authors with different experimental techniques. The comparison yielded differences of up to 50% to the other data; the results were close to the data of Dvorak with maximum deviations less than 10%.

The twin detector method is insensitive to noise superimposed to the signals of both detectors simultaneously and with equal amplitude. If the dose rates in both detectors are exactly equal the influence of the noise is completely eliminated. In pratice there are always slight dose rate differences between the detectors. Numerical analyses and experimental studies demonstrated in this case that the values of lineal energy obtained by the two detectors are influenced in opposite direction; averaging the results from the two detectors can, therefore, substantially eliminate the influence of the noise.

IV. Other research group(s) collaborating actively on this project [name(s) and address(es)]:

Radiation Research Laboratories of Columbia University, New York, (Drs. H.H.Rossi, P. Kliauga and M. Zaider).

Radiophysical Laboratory, Aarhus Kommunehospital, (Dr. K. A. Jessen)

National Institute Radiation Protection, Stockholm (Dr. L. Lindborg)

V. Publications:

Breckow, J., Wenning, A., Roos, H.
The Variance-Covariance Method Experimental Realisation and Tentative Applications. IMSK 86/110.

Breckow, J., Wenning, A., Roos, H., Kellerer, A.M.
The Variance-Covariance Method: Microdosimetry in Time-Varying Low Dose-Rate Radiation Fields.
Radiat.Environ.Biophys.27, 247-259, 1988.

Chen, J, Breckow, J., Roos, H. and Kellerer A.M.
Further Development of the Variance-Covariance Method.
Proc.of the 10th Symposium of Microdosimetry Rome, May 1989, in press, Rad.Prot.Dosimetry.

Philipp A., Monte-Carlo Simulations of Photon Tracks in Water.
Internal Report IMSK 122/89.

Title of the project no.:

Mathematical and Numerical Studies in Microdosimetry

Head(s) of project:

Prof.Dr.Albrecht M.Kellerer

Scientific staff:

Dr.J.Breckow, Dr.H.Roos, J.Chen, A.Philipp, H.Friede

I. Objectives of the project:

The development of microdosimetry in recent years has been greatly influenced by the new methods of the simulation of charged particle tracks. This has led to various extensions of microdosimetric concepts. However, there is still insufficient connection to work performed in stochastic geometry and stereology. To introduce mathematical methods developed in other fields into microdosimetry was a main objective of the program. Application of microdosimetric concepts to radiobiology was a second objective.

II. Objectives for the reporting period:

III. Progress achieved:

The microdosimetric quantities energy imparted, lineal energy, and specific energy are defined with reference to certain volumes, but are quantified in terms of frequency distributions of possible values without regard to spatial interrelations. Computer simulations of the patterns of energy deposits seem, therefore, only loosely related to the microdosimetric distributions. In a more general formulation we have treated the specific energy and the related microdosimetric quantities as point functions; in this way it has become possible to deal with the spatial distribution of their random values and not merely with the frequency of different values. A further extension of the formalism admits reference regions of vanishing size; the inchoate distribution of energy deposits is then the limit case of specific energy. The new definitions are closely related to Matheron's concept of the regularization of a spatial variable; this is a convolution process that permits a flexible mathematical treatment. One resulting possibility is the definition of specific energy with reference not to the conventional geometry of a sphere or a cylinder but to a disperse region of support. This extension provides distributions of specific energy that are relevant to diffusion or transport processes and it can help to free biophysical models from a one-sided fixation on the concept of geometric targets. The formalism has been applied also to the definition of the proximity functions and the related spatial autocorrelation functions.

The generalized formulation of microdosimetry has clarified the linkages between the spatial distribution of energy deposits, their proximity function, and the specific energy. The role of the proximity function suggests that it may replace, for various purposes, the inchoate distribution. The Fourier transform of the proximity function is the product of the Fourier

transform of the inchoate distribution with its conjugate. This operation causes the loss of phase information, and the reconstruction problem - the reconstruction of the inchoate distribution from its proximity function - can, therefore, not be resolved by a mere deconvolution. For any finite point pattern one can, however, show that its proximity function permits - in principle - the reconstruction. Numerical examples with 2-dimensional patterns of up two 30 points have consistently led to unique solutions, apart from reflections. While there is a finite algorithm, it is readily seen that the number of steps becomes excessive when the number of points in the pattern increases. The reconstruction problem can, thus, be solved in principle but not strictly in practice.

A more general approach must thus be based on numerical optimization. The algorithm starts with an assumed initial point pattern and utilizes a suitable measure for the difference between its proximity function and that of the original pattern. Minimizing this difference could lead to an identification of the original pattern. Usually, however, one obtains convergence only for patterns with a moderate number of points. Improved optimization methods have been developed and they provide rapid solutions that correspond very close to any proximity function although they do not in general agree to the original patterns. The 'microdosimetric equivalence' of patterns with the same, or nearly the same, proximity functions will require further studies.

The mathematical methods and results from the microdosimetric investigations have found a number of interesting applications in other fields. Of particular interest are relations between the Minkowsky functionals of Boolean schemes (random configurations of geometric objects) for automatic

particle counting, with applications e.g. in cell or bacterial counting. A further example for the broad applicability of the results of the microdosimetric studies is the exact solution that has been obtained for the errors in volume or surface determinations by systematic sectioning, a common sterological procedure.

IV. Other research group(s) collaborating actively on this project [name(s) and address(es)]:

Columbia University, New York, (Drs.H.H.Rossi, Dr.M.Zaider)

Gesellschaft für Strahlen- und Umweltforschung, (GSF, Neuherberg), Institut für Strahlenschutz

V. Publications:

Kellerer, A.M.
Models of Cellular Radiation Action
In: 'Kinetics of Nonhomogeneous Processes' (Gordon R.Freeman, Ed.), 305-375, J.Wiley & Sons, New York, 1987.

Kellerer, A.M.
Fundamentals of Microdosimetry.
In: 'The Dosimetry of Ionizing Radiation', (K.R.Kase et al., Eds.), Vol.1, 77-162. Academic Press, New York, 1985.

Kellerer, A.M.
The New Operational Quantities for Radiation Protection.
Radiat.Protection Dosimetry 12, 79-81 ,1985.

Kellerer, A.M.
Fundamentals of Dosimetry and Microdosimetry and the Relative Biological Effectiveness of Ionizing Radiations.
In: 'Epidemiology and Quantitation of Environmental Risk in Humans from Radiation and Other Agents' (A.Castellani, Ed.), Vol.96, 123-140, Plenum Press, New York, 1985.

Kellerer, A.M.
The Variance of a Poisson Process of Domains.
J.Appl.Prob.23, 307-321, 1986.

Kellerer, A.M.
Concepts of Geometric Probability for Application in Radiobiology.
IMSK 86/106.

Roos, H., Kellerer, A.M.
An Alpha Irradiation Device for Cell Studies. IMSK 86/108.

Kellerer, A.M.
Exact Formulae for the Precision of Systematic Sampling.
J.Microscopy 153, 285-300, 1989.

Kellerer, A.M.
A Generalized Formulation of Microdosimetric Quantities.
Proc.of the 10th Symposium of Microdosimetry Rome, May 1989, in press,
Rad.Prot.Dosismetry.

Rossi, H.H., Kellerer, A.M.
Intermediate Dosimetric Quantities, submitted for publication.

Breckow, J., Friede, H., Hahn, K., Roos, H. and Kellerer, A.M.
The Reconstruction Problem in Microdosimetry.
Proc.of the 10th Symposium of Microdosimetry Rome, May 1989, in press,
Rad.Prot.Dosimetry.

Roos, H., Kellerer, A.M.
Design Criteria and Performance Parameters of an α-Irradiation Device
for Cell Studies.
Phys.Med.Biol.34, 1823-1832, 1989.

Title of the project no.:

Microdosimetry of Heavy Ion Beams at the UNILAC

Head(s) of project:

Prof. Dr. Albrecht M. Kellerer

Scientific staff:

Dr. M. Laßmann, Dr. H. Roos, Dr. J. Breckow

I. Objectives of the project:

The project was aimed at microdosimetric studies with heavy ion beams of the linear accelerator UNILAC of the GSI (Gesellschaft für Schwerionenforschung, Darmstadt). While a variety of radiobiological projects are being performed with the heavy ion beams, there has been a lack of microdosimetric studies on heavy ions. Such studies are required to supplement and to verify computational results obtained from simulated particle tracks.

II. Objectives for the reporting period:

III. Progress achieved:

A variety of radiobiological investigations has been performed with heavy-ion beams; nevertheless there is lack of microdosimetric studies with heavy ions. Experimental microdosimetric data are restricted to energies below about 2MeV/u. For higher energies up to 20MeV/u there is even a lack in the experimental collision-cross sections which are required for Monte-Carlo simulations.

Measurements with proton beams have therefore been performed in the energy range from 4MeV to 11MeV in nitrogen to evaluate the distribution of absorbed dose in a plane perpendicular to the beam axis, i.e. the lateral dose distribution. The data are required to check Monte-Carlo codes based on theoretical cross sections.

The lateral distribution of energy deposition in nitrogen was measured by observation of the intensity of the emitted fluorescent light in single photon counting technique. Two transitions are observed, the first negative system at a wave length of 391.4nm and the second positive system at 337.1nm. The excitation-cross section of the first negative system is, for energies in excess of 25eV, proportional to the total ionization-cross section and therefore it is possible to evaluate the number of ion pairs formed from the observation of this transition. The transition at 337.1nm is excited nearly exclusively by low energy electrons and therefore is suited to judge qualitatively their contribution to the electron fluence.

The main advantage of this method is, apart from the high spatial resolution, that it avoids the disturbance of the radiation field that can not be eliminated if charged particle detectors are used. The necessity of a correction for collision quenching is a disadvantage of the method; the

achieveable accuracy is limited primarily by the accuracy of the cross sections for collision quenching.

The experimental system is based on equipment and experiences of Ibach and colleagues at the GSF who have earlier performed corresponding measurements with proton energies below 2MeV.

The response of the photon-detection system at 391.4nm was determined by calibration measurements with a narrow collimated electron beam of various energies between 1keV and 12keV; the response at 337.1nm was then calculated utilizing the known wave-length dependence of the transmission of the optical system.

As a 'by-product' of the calibration measurements lateral distributions of absorbed dose in narrow, unidirectional and monoenergetic electron beams have been evaluated from the measured light intensity profiles. Compared to the earlier results of other authors the spatial resolution is increased and the measurements are extended to larger radial distances. Our data are in general agreement with the results obtained from measurements in air by Grün. The differences appear to be due to the better spatial resolution of our instrumentation.

To derive the lateral emission density from the measured data and then the lateral distribution of absorbed dose the Abel-inversion of the data is required; this was achieved by a optimisation method utilizing the generalized reduced gradient algorithm (GRGA). If the Abel-inversion is determined this way, it is possible to introduce constraints for the solution; in our case nothing but a monotonous decrease of the emission density with increasing lateral distance was postulated.

For the measurements with proton beams the tandem-accelerator at the Physics Department of the University of Erlangen was used. The proton energy was varied between 4MeV and 11MeV. In these experiments the advantages of light-emission measurements are apparent; the lateral distances that were examined extended from about 1nm up to about 4µm at 11 MeV, and the emission density changes approximately 8 orders of magnitude.

In a rough approximation absorbed dose is often assumed to decrease proportional to the inverse square of the lateral distance. The experiments show that this approximation is suitable only for medium distances from the track core; at larger distances absorbed dose decreases faster.

Comparison of the emission densities at 391.4nm and at 337.1nm indicates that in close approximation to the beam axes, the contribution of low-energy electrons is increasing, whereas this contribution is constant at larger distances. At small distances there are low-energy electrons ejected by protons and in addition low-energy eletrons liberated by electron-electron collisions; at larger distances only the latter contribution is present. This interpretation is in line with the electron measurements where the contribution of low-energy electrons is constant within the whole radiation field.

The experimental results were compared with results, obtained by Monte-Carlo simulations. The transport code was based on a program developed by Zaider and Brenner for the simultation of proton tracks in water. In its original version the code is restricted to proton energies below 1.5MeV. The reason for the restriction is the utilization of experimental cross sections that were not available for higher energies. The applicability of

the code was extended to energies up to 20MeV primarily by implementation of the binary-encounter approximation of Rudd et al. for calculating the emission of secondary electrons. By appropriate scaling the results for water can be transferred to nitrogen. Comparison between experiment and simulation at 8MeV yielded excellent agreement of the lateral distributions of absorbed dose.

In a comparison of experimental data obtained with different techniques the results of Mills et al. exhibited in the vicinity of the track core considerably more narrow lateral distributions than the results of our study. A tentative explanation could be that the measurement of ionization corresponds to a higher effective cut-off energy than our light measurement. Energy transport by low energy electrons, not visible in ionization measurements, could account for the broader distributions, we have determined.

IV. Other research group(s) collaborating actively on this project [name(s) and address(es)]:

Gesellschaft für Strahlen- und Umweltforschung, (GSF, Neuherberg), Institut für Strahlenschutz,

Physikalisches Institut der Universität Würzburg,

Gesellschaft für Schwerionenforschung (GSI), Darmstadt.

V. Publications:

Laßmann, M.
Messung der räumlichen Lumineszenzverteilung zweier optischer Übergänge des molekularen Stickstoffes um die Bahn geladener Teilchen.
Thesis, University Würzburg, 1989.

RADIATION PROTECTION PROGRAMME

Progress Report

1989

Contractor: Contract no.: BI6-A-305-D

Physikalisch Technische
Bundesanstalt
Bundesallee 100
D-3300 Braunschweig

Head(s) of research team(s) [name(s) and address(es)]:

Dr. H.M. Kramer
Physikalisch Technische
Bundesanstalt
Bundesallee 100
D-3300 Braunschweig

Telephone number: 0531-5926410

Title of the research contract:

Development of an universal personal dosimeter using semiconductor sensors for mixed radiation fields.

List of projects:

1. The investigation of the radiological properties of the dosemeter in photon and neutron reference fields.
2. The extension of the useful energy range for photons down to about 20 keV.

Title of the project no.:

Development of a universal personal dosimeter using semiconductor sensores for mixed radiations

Head(s) of project:

Dr. H. M. Kramer
Physikalisch-Technische Bundesanstalt, Braunschweig

Scientific staff:

Dipl.-Phys. D. Schäffler, Dr. H. M. Kramer, Dr. H.-J. Selbach, Dr. L. Büermann

I. Objectives of the project:

Development and optimization of semiconducting detector system to be used in a personal dosemeter. A configuration of up to three different Si-diodes, each equipped with different compensation filters, should be estalished, allowing photon dosemeasurements in an eneregy range between about 20 keV and at least up to 1,3 MeV.

II. Objectives for the reporting period:

Systematic investigation of the relevant parameters determining the response and its energy dependence of the Si-diodes.

III. Progress achieved:

In the reporting period a total of seven Si-diodes were examined systematically in view of their radiological properties. The diodes varied in their cross sectional area, the thickness of their depletion layer (50 to 300 µm) and their conductivity. The response of the diodes was investigated without and with a series of filters consisting of the materials Al, Cu, Sn, Pb and a rare earth mixture. In order to draw a maximum amount of information out of the measurements a pulse height spectrum was recorded for any given combination of radiation quality, diode type and filter. A total of about 500 such spectra have been recorded. These spectra have been stored in a computer and can easily be accessed in the future in case a more promising algorithm for the evaluation is to be examined.

Figure 1 shows a typical example of such spectra for a heavily filtered radiation with 80 kV tube voltage and for the radiation of Cs 137. The pulse height spectra were analysed in a number of different ways in order to develop an algorithm, which employed in an individual monitor will provide the best possible dosemeter performance.

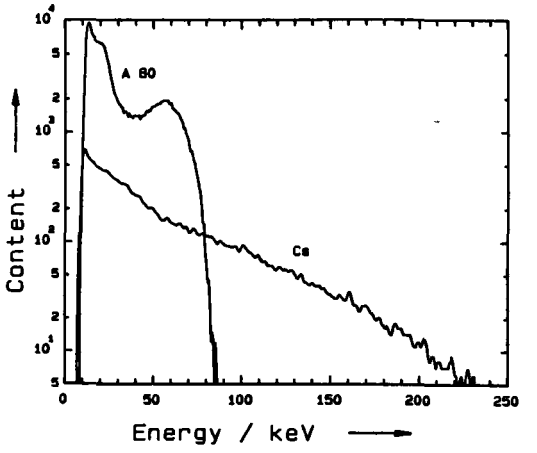

PULSE HEIGHT SPECTRA FOR A HEAVILY FILTERED RADIATION WITH 80 kV TUBE VOLTAGE (A80) AND FOR THE RADIATION OF CS 137

The simplest approach was to calculate the integral over the pulse height spectra as a function of the position of a lower level discriminator. By positioning this discriminator to a level corresponding to an energy of about 80 keV an acceptably flat energy dependence of response was obtained, however at the obvious price that there was no response to radiation with energies below that threshold.

The next method of analysis investigated was termed 'few channel analyser'. For this algorithm the pulse height spectra were subdivided into up to 10 subregions. The sum of events in each subregion was multiplied with a factor chosen in such a way that a linear combination resulted in a response which was sufficiently independant of energy. With this method quite acceptable results in view of an energy inde-pendent response were obtained. A more detailed investigation showed however certain disadvantages in view of a dose rate dependence. For higher dose rates the combination of diode and electronics produced a certain 'pile up', i.e. two pulses occurring in a time interval shorter than the inte-gration time are interpreted as one single event. As the weighting factors for the subdivisions corrsponding to the upper energy region are numerically much greater than those for the lower energy region the response increases substantially with increasing 'pile up' as caused by an increasing dose rate. As the 'few channel analyser' method is potentially a very elegant one further studies to overcome the drawback outlined above will be conducted.

While the two methods of analysis of the pulse height spectra described above were predominantly used for the bare detectors without any compensating filter the third approach was based on the use of such filters. Up to now the combination of a diode having a depletion layer thickness of about 150 µm with a lead filter of 0,12 mm thickness produced the widest useful energy range. **Figure 2** gives the response of this detector with respect to ambient dose equivalent H* (10). It can be seen that an energy range from about 23 keV to 660 keV is covered with a variation of response within ± 30% relative to that at 660 keV. From the shape of the curve in figure 2 it can be inferred that the useful energy range will go below 20 keV.

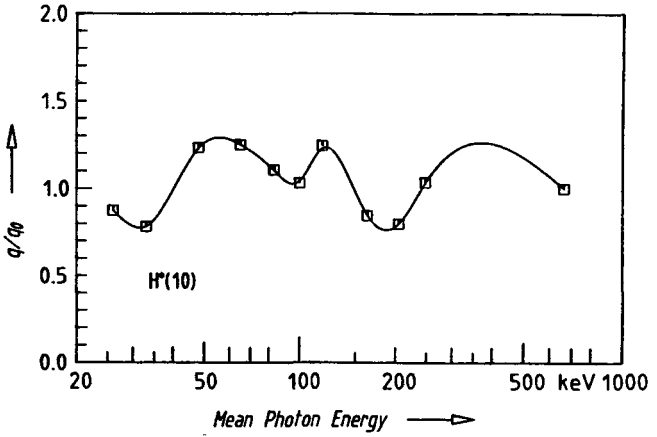

ENERGY DEPENDENCE OF RESPONSE OF THE DETECTOR WITH RESPECT TO AMBIENT DOSE EQUIVALENT

IV. Objectives for the next reporting period:

Finalize details of the optimized configuration in view of number of detectors, their area and thickness of depletion area, material and thickness of compensating filters, optimized algorithm to convert the measured pulse rate (s) into a doserate.

V. Other research group(s) collaborating actively on this project [name(s) and address(es)]:

CNRS, Straßbourg
Inst. Phys., University of Aarhus
Inst. Phys., University of Rome
CERN, Div. IIS, Geneva

VI. Publications:

Results to be published during 1990

RADIATION PROTECTION PROGRAMME
Final Report

Contractor: Contract no.: BI6-A-008-NL

Rijksinstituut voor Volksgezondheid
en Milieuhygiëne (RIVM)
P.O.Box 1
NL-3720 BA Bilthoven

Head(s) of research team(s) [name(s) and address(es)]:

Dr. H.P. Leenhouts
Laboratory for Radiation Res.
RIVM
P.O.Box 1
NL-3720 BA Bilthoven

Telephone number: 030-743016

Title of the research contract:

Comparative risk assessment of radiation and other mutagenic agents. Low dose relative risk of different ionizing radiations and comparison with UV radiation.

List of projects:

1. Comparative risk assessment of radiation and other mutagenic agents. Low dose relative risk of different ionizing radiations and comparison with UV radiation.

Title of the project no.:

Comparative risk assessment of radiation and other mutagenic agents: Low-dose relative risk of different ionizing radiations and comparison with UV radiation

Head(s) of project:

H.P. Leenhouts

Scientific staff:

B. Bouwens
K.H. Chadwick
H.P. Leenhouts
M.J.M. Pruppers
E. Wijngaard

I. Objectives of the project:

The aim of the project is to develop a comprehensive conceptual approach to permit a comparative risk assessment of the cellular effectiveness of different radiations and other mutagenic agents on the basis of the mechanisms of action. To that purpose, calculations of the radiation quality dependence of the linear term of the dose relationship will be made, and both experimentally and theoretically the similarities and differences between ionizing radiation and UV will be investigated in a consideration of the quadratic term of the dose relationship.

II. Objectives for the reporting period:

- Development and improvement of a track structure model in liquid water to calculate radiation effectiveness of X rays, gamma rays, electrons, ions and neutrons.
- Application of the track model to demonstrate the behaviour of the linear term of the radiobiological dose-effect relationship for different ionizing radiations.
- Development of a stationary cellular system to directly compare the effects on survival of the repair of sublethal and potentially lethal damage following UV radiation and gamma rays.

Introduction

III. Progress achieved:

The assessment of risks from low doses of ionizing radiation relies on information from a number of different research areas including the understanding of the action of radiation at the cellular level, which can be gained from the development of biophysical models.

The model studied here is based on the assumption that the crucial molecular lesions induced by radiation are DNA double strand breaks, and that these breaks are responsible for cell killing, chromosomal aberrations and mutations. The number N of DNA double strand breaks induced by a dose D of radiation can be derived as:

$$N = \alpha D + \beta D^2 \qquad (1)$$

where α is the probability per cell per unit dose that a double strand break is induced by the passage of one ionizing particle, and β is the probability per cell per unit dose squared that two independently induced single strand breaks are associated both spatially and temporally that they form a double strand break.

The work presented here is concerned with the investigation of the two coefficients 'α' and 'β' of the equation (1) to determine the validity of the dose-effect relationship defined by equation (1) taking into account the influence of radiation quality, dose fractionation and repair processes on the cellular response. The work has not been concerned with the actual correlation of the molecular damage, DNA double strand breaks, with the cellular effect, but recent work of Radford [1], Prise et al. [2], Murray et al. [3] and Dikomey [4] do provide support for the association between DNA double strand breaks and cell killing, at least for sparsely ionizing radiation.

Investigation of the α-coefficient through track structure calculations.

The α-coefficient is dependent on the induction of DNA double-strand breaks by one ionizing particle. The induction of DNA double strand breaks in the passage of one ionizing particle clearly depends on the spatial distribution of energy deposition events in the particle track. For an effect two events in the track must occur close to each of the two strands of the DNA helix to cause a double strand break. Intuitively, more densely ionizing radiation is expected to be more efficient in producing a double strand break than sparsely ionizing radiation. In fact the question can be posed whether sparsely ionizing radiation is at all capable of producing a DNA double-strand break in the passage of one ionizing particle, and this question is strongly related to the relative biological effectiveness (RBE) of different radiations at low doses.

The calculation of the efficiencies of different types of ionizing radiation depends on the availability of a mathematical description of the spatial distribution of energy deposition events in a particle track at nanometer dimensions bearing in mind the nanometer dimensions and double helix structure of the DNA molecule. In an earlier contract (BIO-E-478-83-NL) an attempt was made to calculate radiation efficiencies. In the present contract it has been necessary to improve the model considerably to make it more flexible and uniformly applicable for all types and energies of ionizing radiation.

The model describes radiation track structure in water at the nanometer scale in three dimensions, which provides the possibility of calculating the probability that a track interacts with a structured 'target' to produce an effect. A characteristic of the model is that it provides a uniform description of tracks for both electrons and ions of all energies,

based on the physical principles of radiation interaction with matter, and thus permits the calculation of radiation effects for X-rays, γ-rays, electrons, ions and neutrons.

In general, tracks are characterized by the stopping power, the radial dimension of energy deposition around a track and the mean energy lost in each interaction of the track with the water. These parameters are clearly dependent on the energy of the ionizing particle and have been calculated considering basic physical phenomena in the radiation interaction process. The calculated stopping power can be compared with experimental data for liquid water. In fig. 1 experimental data for electrons and protons are shown and compared with the calculated stopping powers for electrons, protons and different ions, and in fig. 2 the average energy loss per event and the average track radius are shown as a function of particle energy. These parameters provide a spatial description of primary radiation events caused by the passage of the ionizing particle.

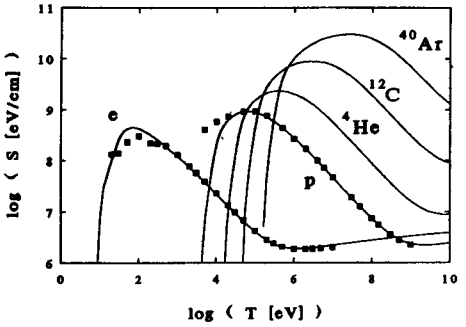

Figure 1. The calculated stopping power for electrons, protons and ions in water compared with experimental data for electrons and protons.

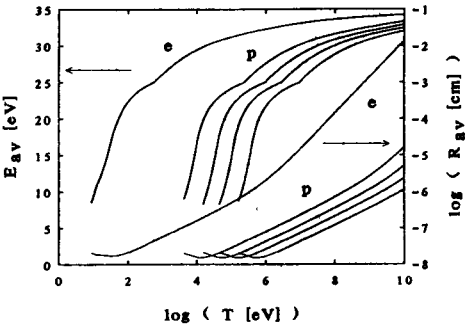

Figure 2. The average energy loss per interaction event and the average track radius as a function of energy for electrons, protons and ions calculated from the track structure model.

The primary particle track and all the secondary particle tracks it generates are divided into small energy segments in which the stopping powers, the average energy loss per interaction and the average track radius are assumed to be constant. Starting at the highest energy segment of the primary particle the spectrum of secondary particles and their contribution to dose is calculated using the excitation spectrum of water and this procedure is repeated for all lower energies of the primary particle. The same calculations are made for all the secondary particles generated, so that starting from a primary particle spectrum in a repetitive and cumulative calculation the total slowing down spectrum can be determined.

The track model can be used to calculate radiation effectiveness by using the structure of the 'target' and the distribution of primary events in the particle track. For example, for a single hit detector it is assumed that a radiation track contributes to the radiation effect with probability f_1 if a radiation event occurs in a sphere with radius r_t around the target. For a more structured 'target', such as DNA, the calculation is more complicated: a particle is assumed to contribute to the α-coefficient of DNA double strand break induction if the particle crosses the 'first' strand at a distance r_t and produces an event with probability f_1, and in

addition crosses the 'second' strand at a distance r_t and produces another event with probability f_1 as well. The radiation effect is calculated for each energy segment of the primary and secondary tracks of the radiation type and finally, the effectiveness of the considered radiation is calculated as the dose weighted average of the effectiveness of all energy segments of the tracks involved. The interaction parameters f_1 and r_t can be determined by comparing experimental data with calculations.

Examples of calculations are shown in fig. 3 and 4 for single-hit detectors and DNA double-strand breaks, respectively. The calculations have been made for electrons and various ions with a wide range of energies and demonstrate a family of curves with a characteristic dependence on stopping powere for each primary particle. This shows that the effectiveness of radiation is not uniquely related to stopping power. The experimental data for the relative response of an alanine detector to different radiations is included in figure 3 illustrating a good agreement with the calculations made at the values of f_1 and r_t quoted in the figure. In fig. 4 the triangles indicate the calculated response expected for different ions with equal velocity (4 MeV per atomic mass unit). These triangles form an envelope on the family of curves and show the typical humped form of radiation effectiveness which is found in cellular radiobiology and also for the induction of DNA double-strand breaks [5].

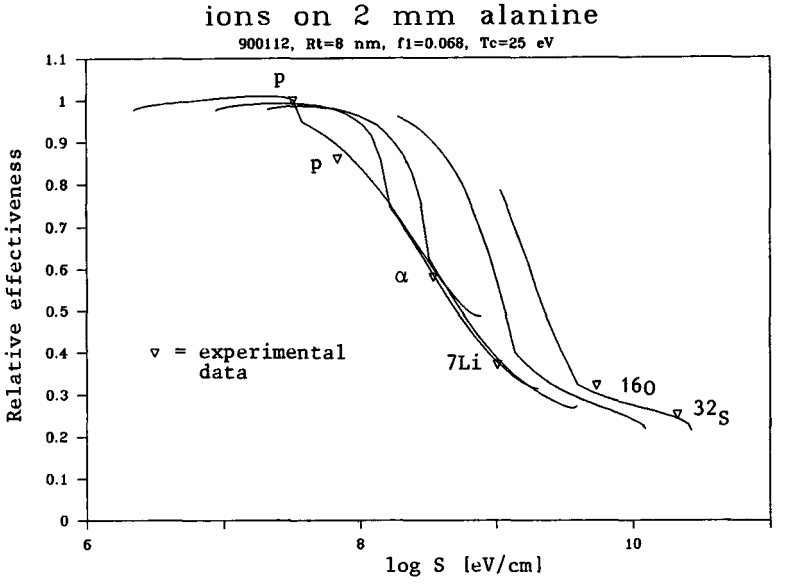

Figure 3. The relative response of a single-hit detector predicted for different radiations as a function of stopping power calculated using r_t = 8 nm and f_1 = 0.068.

Using the same set of parameters the response for X-rays and mono-energetic neutrons as a function of energy has been calculated and reveals an increasing effectiveness with decreasing X-ray energy below 10 keV down to 270 eV and a maximum effectiveness for neutrons at approximately 300 keV. The results show that for each radiation type the effectiveness for the induction of DNA double-strand breaks is always greater than zero, which indicates that, if DNA double-strand breaks are the crucial lesions in radiation biology, a positive α-coefficient is predicted even for

sparsely ionizing radiation so that at low doses the effect will be proportional to dose through the origin.

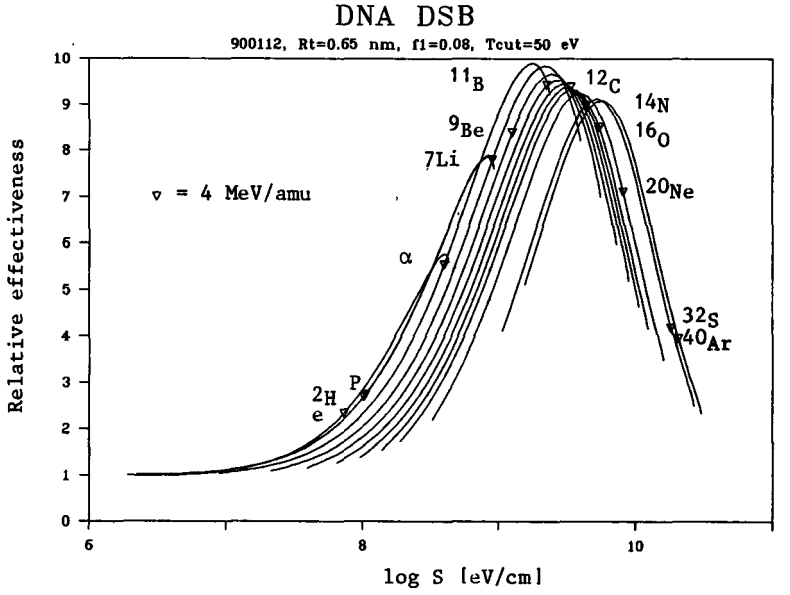

Figure 4. The relative radiation effect for the induction of DNA double-strand breaks for different radiations as a function of stopping power calculated using the track structure model with r_t = 0.65 nm and f_1 = 0.08; the response of different ions having the same velocity is indicated with triangles.

Investigation of the β-coefficient.

The β-coefficient was investigated by comparing the effects of γ-rays and UV radiation on cell killing and by analysing γ-ray fractionation effects.

a. Comparison of γ-rays and UV.

For γ-rays cell survival S can be derived as a function of dose D if it is assumed that each DNA double-strand break has a probability p of causing cell death, as:

$$S = \exp[-pN] = \exp[-p(\alpha D + \beta D^2)] \quad (2)$$

If stationary cells are allowed to repair after irradiation the number of double-strand breaks will be reduced, but not all the breaks will be repaired perfectly so that after repair the number of double-strand breaks will be gN, where $0 < g < 1$, and 'delayed' survival S_d is:

$$S_d = \exp[-pgN] = \exp[-pg(\alpha D + \beta D^2)] \quad (3)$$

If stationary cells are treated with two equal doses, D_1 and D_2, with a time interval between fractions which allows complete repair of single-strand breaks then survival after fractionation S_f is:

$$S_f = \exp[-p(N_1 + N_2)] = \exp[-p(\alpha(D_1 + D_2) + \beta(D_1^2 + D_2^2))] \quad (4)$$

If $D = D_1 + D_2$, comparison of equations (2) and (4) reveals a sparing effect of fractionation and $S_f > S$ (see [6] for more detail).

For UV radiation frank strand breaks are not induced, but single-strand lesions in the DNA are induced and in analogy with the model for ionizing radiation it is proposed that a combination of two single-strand lesions can form a potentially lethal lesion (see [7]). This model has been combined with a suggestion by Park and Cleaver [8] that two pyrimidine dimer lesions, one on either side of a replication terminus, could block the convergence of replication forks and form a potentially lethal lesion. The most important implication of this is that 'paired dimer' lesions are only recognized as such when DNA replication occurs. The individual dimers can be repaired during and after irradiation up to the following S-phase. Thus, the number of paired dimer lesions N_d induced by an exposure X is:

$$N_d = \epsilon X^2 \tag{5}$$

where ϵ is the probability per cell per unit exposure squared that two independently induced dimers form a paired dimer lesion. Cell survival is:

$$S = \exp [-pN_d] = \exp [-p\epsilon X^2] \tag{6}$$

If stationary cells are allowed to repair after exposure the number of dimers and thus the number of 'paired dimer' lesions will be reduced. Dimer repair can be complete and perfect, thus if f is the proportion of dimers not repaired before DNA replication, 'delayed' survival S_d is

$$S_d = \exp[-pf^2\epsilon X^2] \tag{7}$$

and as $f \to 0$ given sufficient time, survival may eventually become 100 %, and the cells will not indicate any effect of UV exposure.

If stationary cells are treated with two equal exposures, there will be more repair of the dimers induced by the first exposure than of those induced by the second exposure, i.e. $f_1 < f_2$. Survival after fractionation S_f is:

$$S_f = \exp[-p\epsilon(f_1X_1+f_2X_2)^2]$$

$$= \exp[-p\epsilon(f_1^2 X_1^2 + 2f_1f_2X_1X_2 + f_2^2 X_2^2)]. \tag{8}$$

If $X = X_1 + X_2 = 2 X_1$ then survival of cells given an exposure X at the time of the first fraction and plated after the second fraction, i.e. with repair factor f_1, is:

$$S = \exp[-pf_1^2 \epsilon X^2] = \exp[-p\ 4f_1^2\ \epsilon X_1^2]. \tag{9}$$

Comparison of equations (8) and (9) reveals that in this case the survival after fractionation is less than the survival after the single exposure.

Thus, the model predictions indicate that both the β-coefficient for ionizing radiation and the ϵ-coefficient for UV are basically two-hit components, but that because of the different nature of the lesions the consequence of post-irradiation repair and fractionation will be different for the two types of radiation.

These predictions of the model have been investigated experimentally. In all experiments CHO-K1 cells have been used either in stationary phase or in exponential growth. The cells have been cultured according to the methods described by Nelson et al. [9]. In general, the survival of CHO cells after γ-ray and UV exposure could be analysed according to equations (2) and (5), respectively. For example, figure 5 shows survival after UV exposure analysed with equation (5).

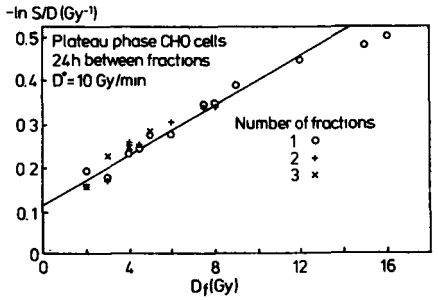

Fig. 7a. The analysis of γ-ray fractionation experiments in stationary CHO cells with a 24 h fraction interval analysed according to equation (12).

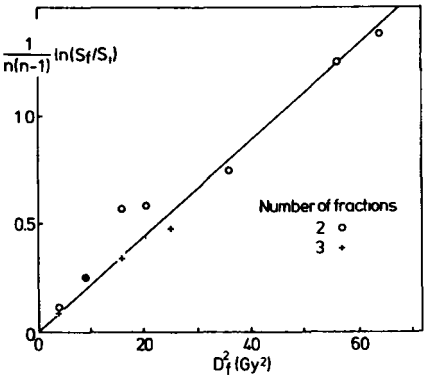

Fig. 7b. The analysis of the same data analysed according to equation (14).

Discussion and conclusions.

It is well known that a linear-quadratic dose relationship provides a good description of cellular radiobiology effects such as cell killing and chromosomal aberrations. What is less well known is whether the linear-quadratic relationship represents a truly two-hit nature of the radiation effect or is merely an approximation of a more complicated process. In this contract the two-hit nature of the effect has been investigated using the assumption that the DNA double strand break is the crucial lesion for which there has recently been some experimental support [1-4].

Calculations of the linear component, the α-coefficient, of the dose-effect relationship using the track structure model and assuming that the DNA double-strand helix is the molecular target indicate that the well known humped response of cellular effects as a function of radiation quality can be qualitatively described by the model. This implies that two simultaneous energy deposition events along the path of an ionizing particle and close to each of the strands of the DNA can cause a biological effect. The calculations also show that even for sparsely ionizing radiation this double energy deposition process is possible and this implies that sparsely ionizing radiation will have a linear component of the dose-effect relationship at low doses.

The calculations also show that each specific primary radiation type has its own specific effectiveness versus stopping power relationship which implies that the biological effect is not only dependent on the stopping power but also on the radial distribution of energy deposition events around the particle tracks, that is, different types of radiation with the same stopping power will have different biological effectiveness.

The experimental data investigating the quadratic or β-coefficient of the dose-effect relationship using fractionation, delayed plating and a comparison with 254 nm UV radiation have been shown to be compatible with the theoretical predictions implying that the β-coefficient is indeed a two-hit or two-event effect. The experiments and analyses indicate that repair between fractions and repair after irradiation can modify the dose-effect relationships but that these modifications are also in accordance with the theoretical predictions. The comparison with UV exposure

These figures demonstrate experimental results which are in accordance with the predictions of the model for the two-hit nature of the γ-ray and UV radiation interaction with the biological cell.

b. γ-ray fractionation.

Equation (3) predicts that survival S_f after two equal dose fractions D_f with complete repair between fractions is

$$S_f = \exp[\ -p\ 2(\alpha D_f + \beta D_f^2)] \tag{10}$$

This equation can be generalized for survival S_f after n equal dose fractions D_f with complete repair between fractions as

$$S_f = \exp[\ -p\ n(\alpha\ D_f + \beta\ D_f^2)] \tag{11}$$

As $nD_f = D$, the total dose, this equation reduces to

$$\frac{-\ln\ S_f}{D} = p\alpha + p\beta D_f \tag{12}$$

for all values of n and D_f. Thus equation (12) provides a generalized analysis of dose fractionation experiments, so that all the data can be used to determine $p\alpha$ and $p\beta$, the coefficients governing cell survival.

An alternative analysis which arizes from a comparison of equations (10) and (11) is that

$$\frac{S_f}{S'} = \exp\ [\ p\ \beta\ D_f^2\ (n^2 - n)] \tag{13}$$

i.e.

$$\frac{1}{n(n-1)}\ \ln\ (\frac{S_f}{S}) = p\ \beta\ D_f^2 \tag{14}$$

and this equation provides a generalized analysis of dose fractionation experiments so that all the data can be used to derive $p\beta$. The model equations assume that the radiation sensitivity of the cells does not change during the experiment.

Stationary CHO-K1 cells have been irradiated with γ-rays using different fractionation regimes, where a fraction interval of 24 h allowed complete repair of sub-lethal damage between fractions and a delay of 24 h after the last dose fraction was used to avoid any confusion of the results by different repair levels of potentially lethal damage. The results presented according to the analyses suggested by equations (12) and (14) are shown in figures 7a and b, respectively. The data all congregate along a straight line in accordance with the equations.

Previous fractionation experiments using fraction intervals of 3 and 5 h had indicated an incomplete repair of sub-lethal damage between fractions and had permitted an estimate of the repair rate of the sub-lethal damage of 0.30 h^{-1}. An independent experiment using two equal dose fractions with different times between fractions indicated a repair rate of 0.28 h^{-1}.

All the data of the fractionation experiments, that have been designed specifically to investigate the two hit component, satisfy the mathematical predictions made by the model. It can be concluded that the experiments support the assumption that the β-coefficient of the linear-quadratic equation is a true two-hit component, at least for sparsely ionizing radiation, stationary CHO cells, doses up to 16 Gy and cell survival down to 0.01 %. It should be emphasized that the experiments do not provide any indication of the nature of the lesions which are involved in the two-hit component of the equation, but the calculations and the model used are compatible with DNA double-strand breaks as the crucial lesions.

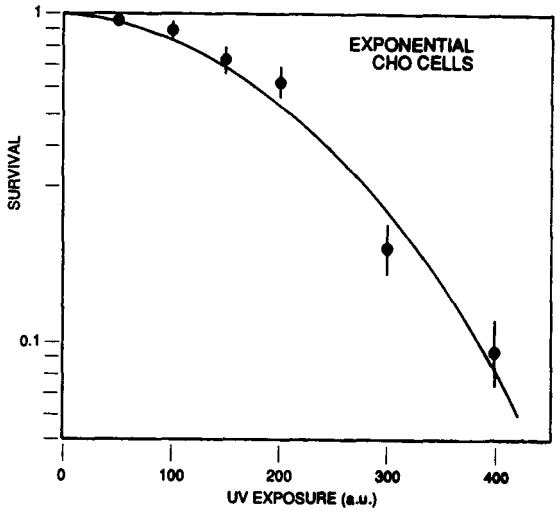

Figure 5. The survival of CHO cells after UV exposure analysed using a pure quadratic dose-effect relationship.

Fig. 6a presents the survival of stationary CHO cells with immediate and delayed plating at 24 and 48 h after γ-irradiation demonstrating the repair of potentially lethal damage over the first 24 h, but no extra repair at 48 h. This is contrasted with the case after UV exposure which is presented in fig 6b. The results show that, after UV, continuing repair of the potentially lethal lesions up to 72 h is evident.

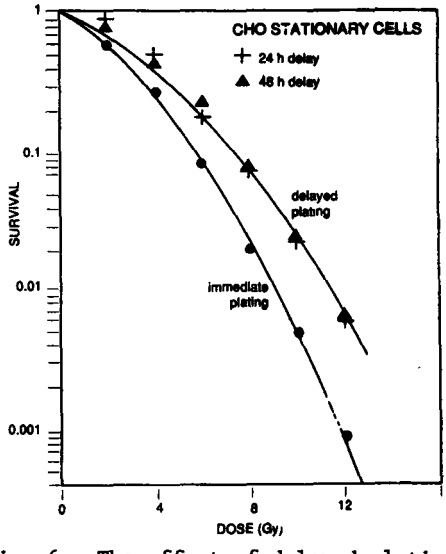

Fig. 6a. The effect of delayed plating of 24 and 48 h on the effect of γ-ray cell killing in stationary cells.

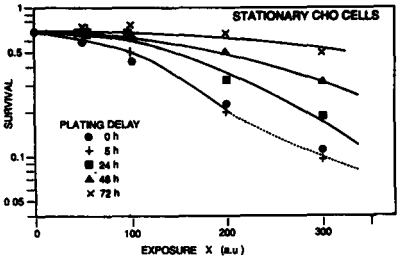

Fig. 6b. The effect of delayed plating of 24, 48 and 72 h on the effect of UV exposure on cell killing in stationary cells demonstrating continued repair.

illustrates that while the effect of both types of radiation can be described by a two-hit or two-event type of damage, the nature of the lesions and the recognition of these lesions by the cell alter the way in which the cell responds to the lesions and how repair processes modify this response.

In conclusion, the results of the contract support the idea that the linear-quadratic dose relationship does reflect a two-hit ot two-event type of radiation effect. The track structure calculations of the linear term indicate that the DNA double-strand break could be the crucial lesion and that the two simultaneous events should occur close to each strand of the DNA molecule in a single track. The experimental data indicate that the quadratic term arizes from the combination of two time independently induced events the role of which can be modified by repair but these data do not provide any information on the nature of the radiation induced lesions. Future research should concentrate on determining the sensitivity of the track structure model to changes in the parameters used in the fitting of the calculations to experimental data and to understanding the physical, chemical and biological implications of these changes. Cellular experiments should aim to compare the different repair processes which modify the radiation effect with the effect of different wavelength UV exposures and to investigate the potential interaction between UV and γ-rays and study how this might alter the low-dose response of cells to ionizing radiation.

References.

1. Radford,I.R. 1986. Int.J.Radiat.Biol. 49, 611-620.
2. Prise,K.M., Davies,S. and Michael,B.D. 1987. Int.J.Radiat.Biol. 52, 893-902.
3. Murray,D., Prager,A. and Milas,L. 1989. Radiat.Res. 120, 154-163.
4. Dikomey,E. 1982. Int.J.Radiat.Biol. 41, 603-614.
5. Ritter,M.A., Cleaver,J.E. and Tobias,C.A. 1977. Nature 266, 653-655.
6. Chadwick,K.H. and Leenhouts,H.P. 1981. The Molecular Theory of Radiation Biology (Springer Verlag, Heidelberg).
7. Chadwick,K.H. and Leenhouts,H.P. 1983. Phys.Med.Biol. 28, 1369-1383.
8. Park,F.D. and Cleaver,J.E. 1979. Proc.Natl.Acad.Sci.USA 76, 3927-3931.

IV. Other research group(s) collaborating actively on this project [name(s) and address(es)]:

Drs. J.M. Nelson and L.A. Braby. Pacific Northwest Laboratory, Richland, USA

Drs. A. Cebulska-Wasilewska and M. Waligorski. Institute for Nuclear Physics, Krakow, Poland

V. Publications:

1. Publications in scientific journals

1.1 Leenhouts, H.P. and Stoutjesdijk, J.F.
The use of reference levels in the dose limitation procedure.
The Science of the Total Environment 45 (1985) 585-592

1.2 Chadwick, K.H. and Leenhouts, H.P.
The dependence on radiation quality of the repair of potentially lethal damage. Proc. 9th Microdosimetry Symposium.
Radiation Protect. Dosim. 13 (1985) 275-279

1.3 Leenhouts, H.P. and Chadwick, K.H.
Radiation energy deposition in water: calculation of DNA damage and its association with RBE. Proc. 9th Microdosimetry Symposium
Radiation Protect. Dosim. 13 (1985) 267-270

1.4 Chadwick, K.H. and W.F. Oosterheert
Dosimetry concepts and measurements in radiation processing.
Int. J. Appl. Radiat. Isotop. 37 (1986) 47-52

1.5 Leenhouts, H.P.
Wetenschappelijke uitgangspunten van de stralingshygiëne.
Presented at 25th Anniversary Symposium of the Dutch Radiation Protection Society, NVS Publikatie No. 7. (1986) 1-23

1.6 Leenhouts, H.P., Sijsma, M.J., Cebulska-Wasilewska, A. and Chadwick, K.H.
The combined effect of DBE and X-rays on the induction of somatic mutations in Tradescantia.
Int. J. Radiat. Biology 49 (1986) 109-119

1.7 Leenhouts, H.P., Stoutjesdijk, J.F., Köster, H.W., Mattern, F.C.M. and Frissel, M.J.
De gevolgen van het reactorongeval te Tsjernobyl voor Nederland.
Tijdschrift voor Milieukunde 1 (1986) 107-111

1.8 Chadwick, K.H. and Leenhouts, H.P.
DNA damage and chromosome aberrations.
Radiation Carcinogenesis and DNA Alterations (eds. Burns, F.J., Upton, A.C., Silini, G.) Plenum Publ. Corp. N.Y. (1986) 245-264

1.9 Chadwick, K.H. and Leenhouts, H.P.
Chromosome break-points, somatic mutation and oncogene activation: some comments.
Radiation Carcinogenesis and DNA Alterations (eds. Burns, F.J., Upton, A.C. and Silini, G.) Plenum Publ. Corp. N.Y. (1986) 265-276

1.10 Leenhouts, H.P. and Chadwick, K.H.
The yield of chromosomal aberrations and its correlation with other biological endpoints.
Radiation Carcinogenesis and DNA Alterations (eds. Burns, F.J., Upton, A.C. and Silini, G.) Plenum Publ. Corp. N.Y. (1986) 277-291

1.11 Leenhouts, H.P. and Chadwick, K.H.
Fundamental aspects of the dose effect relationship for ultraviolet radiation.
Human exposure to ultraviolet radiation: Risks and regulations (eds. Passchier, W.F. and Bosnjakovic, B.F.M.) Elsevier, Amsterdam (1987) 21-25

1.12 Chadwick, K.H., Leenhouts, H.P., Wijngaard, E. and Sijsma, M.J.
DNA double-strand breaks and their relation to cytotoxicity.
Quantitative Mathematical Models in Radiation Biology (ed. Kiefer, J.) Springer Verlag, Heidelberg (1988) 147-158

1.13 Chadwick, K.H.
Dosimetry concepts in food irradiation for the gamma irradiation of food.
Proc. of Health Impact, Identification, and Dosimetry of Irradiated Foods (eds. Bögl, K.W., Regulla, D.F. and Suess, M.J.) Publ. BGA ISH Heft 125 (1988) 400-404

1.14 Frissel, M.J., Blaauboer, R.O., Köster, H.W., Leenhouts, H.P., Vaas, L.H. and Stoutjesdijk, J.F.
Radioactive contamination of food and the intake by man.
Radiat. Phys. Chem. Vol. 34, no. 2 (1989) 327-336

1.15 Leenhouts, H.P. and Chadwick, K.H.
Recessive malignant genes, radiation induced cell transformation and animal carcinogenesis.
Cell transformation and radiation-induced cancer (eds. Chadwick, K.H., Seymour, C. and Barnhart, B.) Adam Hilger, Bristol and New York (1989)

1.16 Miller, A. and Chadwick, K.H.
Dosimetry for the approval of the food irradiation process.
Radiat. Phys. Chem. 34 (1989) 999-1004

1.17 McLaughlin, W.L., Boyd, A.W., Chadwick, K.H., McDonald, J.C. and Miller, A.
Dosimetry for Radiation Processing
Taylor and Francis, London (1989)

1.18 Leenhouts, H.P. and Chadwick, K.H.
The molecular basis of stochastic and non-stochastic effects.
Health Physics 57, suppl. 1 (1989) 343-348

1.19 Leenhouts, H.P. and Chadwick, K.H.
Comparison of the dose-effect relationship for UV radiation and ionizing radiation.
Proceedings Second U.S.-Dutch expert workshop on UV-B: measurements, exposure and effects, 11-13 December 1989

2. Short communications

2.1 Leenhouts, H.P. and Chadwick, K.H.
Track structure and single hit detectors.
Radiation Research, Proc. 8th Int. Congress Radiation Research. Taylor and Francis, London, (1987) vol. 1 p.84 (Abstract)

2.2 Leenhouts, H.P. and Chadwick, K.H.
On the common nature of the cytotoxic lesion.
Radiation Research, Proc. 8th Int. Congress Radiation Research. Taylor and Francis, London, (1987) vol. 1 p. 63 (Abstract)

2.3 Leenhouts, H.P. and Chadwick, K.H.
Radiobiological arguments for a linear dose-effect relationship of stochastic effects at low doses.
Radiation Protection Practice (Proc. of 7th IRPA Congress) Volume III (Pergamon Press, New York) (1988) 1215-1218

2.4 Chadwick, K.H., Leenhouts, H.P., Wijngaard, E. and Sijsma, M.J.
DNA double-strand breaks and their relation to cytotoxicity.
Radiation Environm. Biophysics 27 (1988) 211 (Abstract)

2.5 Leenhouts, H.P., Chadwick, K.H., Wijngaard, E. and Sijsma, M.J.
Fundamentele aspecten van de werking van gammastraling en ultraviolette straling.
Berichten uit het RIVM, 1988, Volksgezondheidsreeks VR 89/05 (1989) 320-323

2.6 Pruppers, M.J.M., Leenhouts, H.P. and Chadwick, K.H.
A track structure model for the spatial energy deposition of ionizing radiation.
Book of Abstracts Tenth Symposium on Microdosimetry, Rome (1989) 68-69 (Abstract)

2.7 Leenhouts, H.P., Pruppers, M.J.M. and Chadwick, K.H.
Track structure, target structure and radiation effectiveness.
Book of Abstracts Tenth Symposium on Microdosimetry, Rome (1989) 100-102

RADIATION PROTECTION PROGRAMME
Final Report

Contractor:

Com.Naz.per la Ricerca e per lo
Sviluppo dell'Energia Nucleare e
delle Energie Alternative, ENEA
Viale Regina Margherita 125
I-00198 Roma

Contract no.: BI6-A-023-I

Head(s) of research team(s) [name(s) and address(es)]:

Dr. L. Lembo
ENEA - Lab. Applicazioni di
Dosimetria
Via Mazzini 2
I-40138 Bologna

Telephone number: 051-498350

Title of the research contract:

Track-structure detectors for neutron and alpha dosimetry.

List of projects:

1. Neutron dosimetry by damage track detector: advantages and limitations.
2. Applied personal dosimetry by chemical etched CR-39 dosimeters.
3. The assessment of low concentration of alpha emitting radionuclides.

Title of the project no.:

1. Neutron dosimetry by damage track detector: Advantages and limitations

Head(s) of project:

L. Tommasino

Scientific staff:

L. Tommasino, G. Torri

I. Objectives of the project:

The solutions of many problems in neutron dosimetry (respectively for personnel, area and environmental monitoring) may be achieved through the optimization of the electrochemical etching parameters such as Electric Fields, Temperature and Frequency. The major scope of this project is to demonstrate how it is possible to obtain any desired neutron-dosemeter response through a proper choice of the parameters of the electrochemical etching of CR-39 detectors.

II. Objectives for the reporting period:

Analysis of the response of CR-39 dosemeter electrochemically etched under different electric fields. Further investigations on the advantages of the two-steps etching made respectively of chemical and purely electrical processes. The optimization of the two steps-etching for the improvement of the signal-to-noise ratio of Cr-39 detectors.

III. Progress achieved:

1. METODOLOGY.

The most attractive characteristic of the electrochemical etching-ECE is the possibility to choose several combinations of the ECE parameters to obtain a large variety of different responses to neutrons. A systematic approach has been undertaken to investigate individual ECE parameters with the scope to provide guidelines for the optimization of these etching procedures. In particular the response of the electrochemical etched CR-39 detector has been studied at different electric fields.
Furthermore for a better understanding of ECE parameters, the electrochemical etching has been studied in two distinct steps made respectively of chemical etching and purely electrical phenomena.
With this two-steps etching the formation of tracks is obtained by chemical etching, while the tree initiation and propagation is obtained by electrical processes. Under these etching procedures, all the tracks (formed by chemical etching) start treeing together at the beginning of the electrical processes and have equal opportunity to propagate. Under these conditions, track spots with relatively uniform diameters are obtained, thus providing excellent characteristics for track counting and discrimination. Because of these attractive characteristics of the spot size distribution, systematic investigations have been undertaken with CR-39 foils irradiated to neutrons with different energies.
For these investigations, the chemical etching step has been obtained by 6N KOH solution in water at 60°C for 3 hours, while the electrical processes have been achieved with the application of an electric field of 30kV/cm RMS and 2kHz at 25°C for 5 hours using the same above etchant.

2. RESULTS

The response of CR-39 detectors to neutrons (by way of proton recoils) changes drastically in the energy range between 10 keV up to 500 keV when electric fields from 50 kV/cm to 20 kV/cm are used.
The left-hand side of Figure 1 shows different detector responses obtained by using different electric fields under otherwise identical electrochemical etching processes. These results show promise for the solution of the complex problem of neutron dosimetry and/or spectrometry in that energy range (10 keV-100 keV) where most of the conventional systems are no more reliable.

Unfortunately when the electric field is increased, there is also an increase in the background.
The results obtained with the two-steps etching of CR-39 are shown on the right-hand-side of Fig.1.
In this case, the CR-39 detector response versus the neutron energy is reported for different chemical etching times of 1,1.5, 2 and 5 hours.
In these two-steps etching processes, the track formation occurs during the chemical pre-etching while the successive electro-etching does not alter the already formed tracks, but simply produces electrical spots at their tips. Since the tracks start trecing together, the electrical spots have the same opportunity to grow so that overlapping in almost impossible. Excellent conditions for automated spot counting are thus obtained because of the uniform spot diameters and negligible overlapping. By contrast, with the results obtained with purely electrochemical etched CR-39 (left-hand-side of Fig. 1), the two-steps etching processes make it possible to alter drastically the high energy part of the detector response.
This two-steps etching procedure presents the following registration characteristics:

a. Electrical spots with uniform size;
b. Possibility to differentiate background-spots from those induced by tracks;
c. Possibility of observing chemically-etched tracks even after electrical processes;
d. Forbidden overlapping.

In spite of the many efforts made in the past, little success has been reported in the production of consistently low background material. At this stage the possibility to use the etching process and counting procedure capable of differentiating background from neutron-induced recoil tracks is the most attractive. Fig. 2 shows the track size distribution respectively for the background sample and those irradiated with neutrons of different energies. Efforts have been made to obtain these different track-size distribution under the same conditions, such as the same illumination, the same total number of tracks-spots analyzed in samples with approximately same track density (typically 500 tracks/cm^2) with the exception of the background track density being only 105 tracks/cm^2.
It apppears clear from Fig. 2 that the distribution of the brackground spot-size is different from those due to neutron induced recoil tracks. Furthermore, as we have anticipated, the distribution of spot-size does not depend strongly on the neutron energy.
These results make it possible to discriminate the background from the neutron-induced tracks, which discrimination can be obtained simply by:

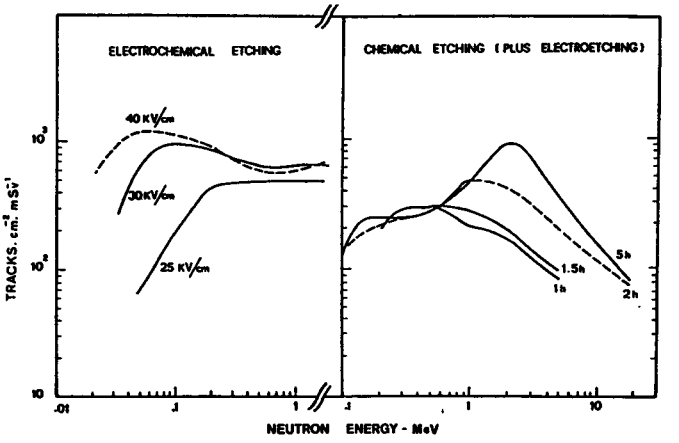

FIG. 1 CR-39 detector responses obtained using different chemical and electrochemical etching processes.

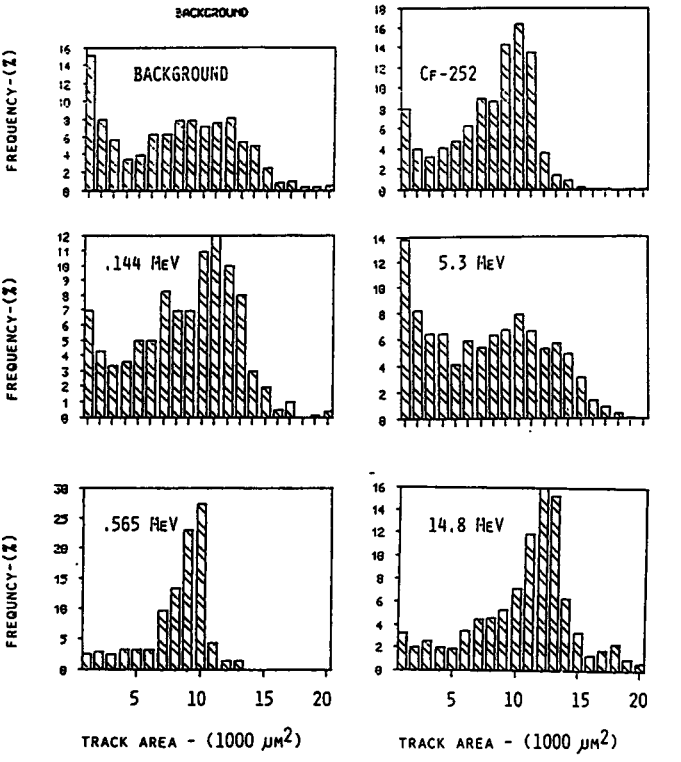

Fig. 2. Track size distribution for the background sample and those irradiated with different neutron energies.

- selecting a proper shape factor using a pre-selected value of the form factor, f, where $f = (4\pi S)/p^2$ with S the pit area and p its perimeter,
- choosing a treshold value for the spot-size for track counting.

3. DISCUSSIONS

The advantages of the electrochemical etching processes appear clear from the so many CR-39 detector responses which have been gathered in the whole contract period.

Actually the most attractive characteristics of these etching processes is the possibility of obtaining any desired neutron detector response by choosing among a large variety of different combinations of parameters such as temperature, electric field and frequency. Such parameters are easy to vary using microprocessor controlled equipment and, in addition to drastically changing the neutron detector response, they provide means of reducing the background. In summary, by a proper choice and control of the ECE parameters for CR-39 it is possible to obtain:

a) Large and uniform track spot size from about 10 keV to 15 MeV.
b) Flat energy response in the entire energy range of interest.
c. Neutron energy response with different thresholds.
d. Identification of recoil tracks according to their energy and time for track formation.
e. Reasonably low background.

To conclude, it is the ability to control the etching procedure with an external apparatus that could considerably expand to usefulness of ECE processes.

IV. Other research group(s) collaborating actively on this project [name(s) and address(es)]:

R.V. Griffith - Lawrence Laboratory - USA
W.G. Cross - Chalk River Nuclear laboratory - CANADA
S. Djeffal - Commissariat aux Energies Nouvelles - ALGERIE

V. Publications:

1. G. Espinosa, J.I. Calzarri, I. Camboa, L. Tommasino and R.V. Griffith - Digital image counting system for nuclear track detectors. Nucl. Track Vol. 12, 235 (1986)
2. L. Tommasino - Recent trends in radioprotection dosimetry - Promising solutions for personal neutron dosimetry. Nuclear Instruments and Methods - A 255, 293 - 297 (1987)
3. G. Zapparoli, L. Tommasino, S. Djeffal and A. Maiorana - Additional results with electrochemically etched CR-39 neutron dosimeters. Nuclear Tracks, 12, 675-678, 1986
4. D. Azimi-Garakani, L. Tommasino and G. Torri - Further investigations an electrochemically etched CR-39 neutron detectors. Nuclear Tracks Radiat. Meas. 15, 309-312, 1988
5. L. Tommasino - Future developments in etched track detectors for neutron dosimetry - Rad. Prot. Dos. 20, 121-124 (1987)

Title of the project no.:

Project N. 2 - Applied Personal Dosimetry by Chemical Etched CR-39 Dosimeters

Head(s) of project:

L.Lembo

Scientific staff:

L. Lembo, O.Civolani, M. Beozzo

I. Objectives of the project:

Development of a CR-39 Neutron Personal Dosimeter for Large Dosimetry Service.

II. Objectives for the reporting period:

Determination of the energy response of CR-39 neutron detectors etched with different electrochemical etching conditions. Investigations on the possibilities to overcome the inconvenience of the large variantions of background track density.

III. Progress achieved:

Introduction

The main aim of this research project has been the study and development of a personal neutron dosemeter based on the use of solid state nuclear track detectors(SSNTD's).

The research work was initially devoted to investigation of the neutron response of CR-39 detectors chemically etched. Due to its simplicity and low cost this technique is of great interest for applications to routine personnel dosimetry. However the results obtained with this etching method showed two limitations : first the neutron energy threshold is rather high above approximately 100-200 keV and second, neutron-induced tracks have very small size compared to those present in unirradiated material and even when using a very sophsticated automatic image analyser it is difficult to get a sufficiently reliable evaluation of neutron induced-tracks. Some improvements were obtained using the optical microscope with incident light from optical fibres on the edge of the detector. In this way the tracks are seen by the microscope as bright points. However, even in these conditions track evaluations were still affected by large uncertainties, mainly due to the bad quality of the commercially available CR-39 materials. To overcome this inconveniennce, a facility was built to manufacture, in controlled laboratory conditions, small samples of CR-39 polymer starting from commercial CR-39 monomers and reducing their impurity concentrations (1). No significant background improvements were achieved with the polymers produced in this way so it was decided to change the etching conditions by investigating and developing a technique based on a combination of chemical and electrochemical etching of CR-39 detectors.

Results.

A special facility for simultaneous electrochemical etching of a large number of CR-39 detectors was designed and developed (2) . It is mainly composed of 4 lucite cells, each containing 24 detectors, inserted in an alluminium holder placed inside an oven maintained at 60 °C. The whole etching cycle is automatically performed through a computer system which allows the cells to be filled with KOH 6 N solution and the H.V. power supply to be controlled. The detectors , 4x4 cm^2 in dimension and 600 μm thick, are electrochemically etched on the back side with respect to the incident neutrons for 8 hours at 60 Hz and for 25 minutes at 2000 Hz with an electric field of 35 kV/cm, then chemically etched for 15 minutes . The tracks are counted using a simple, cheap image commercial analyser.

The neutron energy response of the CR-39 detectors etched in these conditions was tested during the Eurados-Cendos neutron intercomparison organized in 1987. The results showed a sufficiently good energy response up to 14 meV , with an energy threshold detection of less than 100 keV.

In 1988 this technique was introduced in our neutron personnel dosimetry Service for about 10000 users, replacing the nuclear emulsions previously employed. However, the data obtained in operational conditions exhibited extremely large variations of background tracks, much higher than those observed in laboratory conditions, with a corresponding minimun detectable dose equivalent higher than one mSv.

The last period of this project was then devoted to investigating the possibility of overcoming this inconvenience, mentioned also by other laboratories involved in this research field. Background reduction can be obtained either by improving etching conditions and/or quality of the CR-39 polymer. As far as the quality of commercially available material is concerned, a systematic investigation

has been perfomed to evaluate the background characteristics of various CR-39 polymers manufactured by different factories and stored in different laboratory conditions. This activity has also been a part of a large survey of background in CR-39 detectors organized by Eurados-Cendos at European level (3). In accordance with the etching conditions used by NRPB's laboratories, the electric field employed during electrochemical etching was greatly reduced.

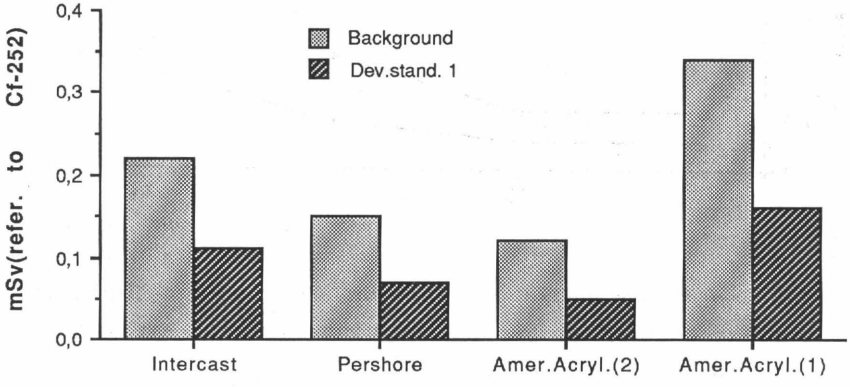

Fig.1 - Average background and standard deviation of some commercialy available CR-39 polymers. Electro-chemical etching performed using an electric field of 25 kV/cm.

Fig.1 shows the background values of CR-39 polymers produced by different companies, obtained by reducing the electric field of the previously described etching cycle to 25 kV/cm. In these conditions the minimun detectable dose equivalent, considered as three times the background standard deviation and referred to Cf-252 neutrons , ranges between 0.2 and 0.6 mSv, depending on the CR-39 material considered. The background dependence on the electric field of the etching cycle is reported in Fig. 2. These results show how at low electric field there is an almost flat

region , while a strong background increase starts above 28 kV/cm.

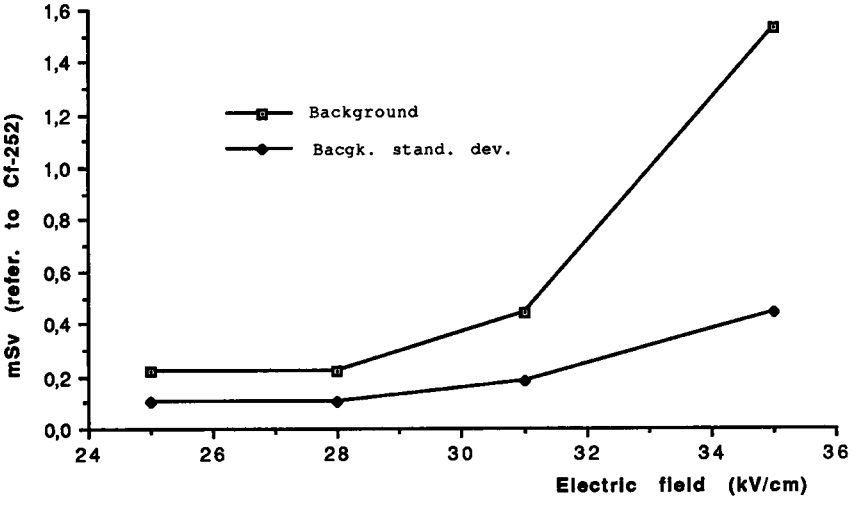

Fig.2 - Background dependence on the electric field used during the electrochemical etching cycle of American Acrylics CR-39 polymers.

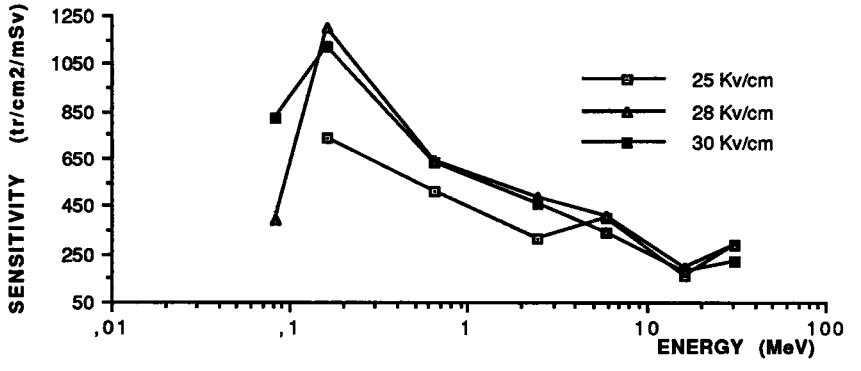

Fig.3 - Cr-39 neutron energy dependence for different electric field values used during the electrochemical etching cycle At 27.8 MeV additional CR-39 converter 6 mm thick has been used.

On the other hand , the neutron energy response is strictly related to the electric field used to etch the CR-39 detectors, as shown in fig. 3. This figure summarizes the data obtained during the Eurados Cendos neutron intercomparison organized in 1989. Considering both the results of figs. 2 and 3 , an electric field value of 28 kV/cm should be used to achieve the best results , which corresponds to an energy threshold of about 75 keV and a minimun detectable dose equivalent equal to 0.3 mSv. Neutron sensitivity for Cf-252 is equal to (391 ± 39) cm^{-2} mSv^{-1}.

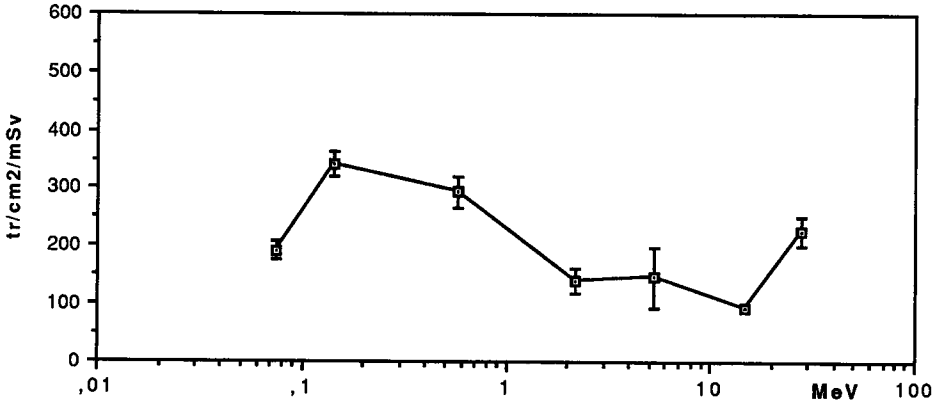

Fig.4 - Cr-39 neutron energy dependence obtained with a chemical pre-etching of 0.5 h followed by an electrochemical etching for 2 h at 28 kV/cm and 2000 Hz.

Finally a more recent attempt to further improve the CR-39 background has been performed by making a chemical pre-etching before the electrochemical one. The preliminary results of this technique , under investigation also in other laboratories, seems to give promising results. Fig. 4 shows data obtained in our laboratory using CR-39 chemically pre-etched for 0.5 h with a 6N KOH solution at 60 °C and then electrochemically etched with the same solution for 2 h

at 28 kV/cm and 2000 Hz. Though the improvement in background track density, equal to (25 ± 12) cm^{-2} with a neutron sensitivity of (139 ± 21) cm^{-2} mSv^{-1} for Cf252, was limited , the energy response was better and more flat from 70 keV to 14 MeV. In this condition the minimum detectable dose equivalent for Cf-252 is equal to 0.25 mSv.

More investigations in this direction are under way in order to confirm these results and possibly achieve further imporvements.

References.

(1) L.Lembo et al. " Improvement on CR-39 Manufacturing for Neutron Dosimetry Applications", Nuclear Tracks, Vol. 12,Nos 1-6,pp. 633-636,1986.

(2) L.Lembo "Personal Neutron Dosimetry Using Track Detectors", Nuclear Tracks Rad.Meas., Vol. 15, Nos 1-4,pp. 473-481,1988.

(3) "Results of a Survey of Backgounds of etched track neutron Dosimeters Organized by Eurados-Cendos in 1988", Edited by Enea (Italy), Report Pas-Fibi-Dosi(89)1, 1989

IV. Other research group(s) collaborating actively on this project [name(s) and address(es)]:

NRPB, Harweel (UK)
Istituto di Fisica,University of Bologna (Italy)
Laboratori Nazionali di Legnaro- INFN Padova (Italy)
PINSTECH-SSNTD Laboratory (Pakistan)

V. Publications:

L.Lembo et al. " Improvement on CR-39 Manufacturing for Neutron Dosimetry Applications", Nuclear Tracks, Vol. 12,Nos 1-6,pp. 633-636,1986.

L.Lembo and O. Civolani " Summary of the Results Obtained by Enea-Bologna in Joint European-US-Canadian Neutron Dosimeter Irradiations". Eurados-Cendos Report KfK (Germany) 4305, 1987-01, 1987.

L.Lembo "Personal Neutron Dosimetry Using Track Detectors", Nuclear Tracks Rad.Meas., Vol. 15, Nos 1-4,pp. 473-481,1988.

"Results of a Survey of Backgrounds of Etched Track Neutron Dosimeters Organized by Eurados-Cendos in 1988", Enea (Italy) Eurados-Cendos Report, Pas-Fibi-Dosi(89)1, 1989

L.Lembo et al. " Miglioramenti conseguiti nella dosimetria dei neutroni con rivelatori a tracce", National Congres of Italian Radiation Protection Association (AIRP), Verona 13-15 Sept. 1989.

Title of the project no.:

3. The assessment of low concentrations of alpha emitting radionuclides.

Head(s) of project:

Tommasino, Torri

Scientific staff:

F. Breur, G. Santori, G. Sciocchetti, L. Tommasino, G. Torri.

I. Objectives of the project:

Development and applications of new detectors based on track-structure properties for the assessment of low concentrations of natural and man-made alpha emitting radionuclides in man and his environment.

II. Objectives for the reporting period:

A. Man-made alpha emitters
Assessment of low concentrations of plutonium necessary for the New Derived Investigation Level by spark counting large areas of cellulose nitrate detectors.

B. Natural alpha emitters - Radon
Short-term radon measurements in dwellings using cellulose nitrate detectors.

III. Progress achieved:

1. METHODOLOGY.

The registration of alppha particles by damage track detectors is often considered not sufficiently sensitive, since it is assumed that tracks can only be counted under the microscope and that the typical area scanned is less than 20 square mm.

Actually it is the simplicity of scanning large detector areas by the spark counter which makes this technique unique for the assessment of sufficiently low concentrations of alpha emitters such as uranium, plutonium and radon.

Assuming valid the Poisson statistics, the lower limit of detection-LLD can be related to the area of the detector counted, S, as in the following:

$$LLD = \frac{4.6\sqrt{\rho S}}{\varepsilon S} \qquad (1)$$

where ρ is the background track density and ε the track registration efficiency per unit of exposure.

According to the equation (1), if the detector area counted is increased by a factor of one hundred the LLD_2 decreases a factor of ten. Since detector areas up to hundreds of cm^2 can be easily counted by the spark counter, sufficiently low limits of detection can be easily obtained with this techniques. The advantages of the spark counter for alpha particle detection apply also to the registration of fission fragments when the same counting technique is used.

The signal-to-noise ratio can also be increased drastically using two plastic foils for counting coincidence sparks. In this case the background can be reduced by a factor of 10^4 as it has been demonstrated for the spark counting of neutron induced fissions. In brief, when compared with microscope counting, the sensitivity wich can be achieved by snark counting can be up to one million times higher.

2. RESULTS

A. Man-made alpha-emitters-Plutonium

According to the ICRP 30, new Derived Investigation Level-D.I.L. of plutonium in urine are suggested, which can be even two orders of magnitude lower than the value (7.4 mBq/l) which is used at present.

With these new Derived Investigation Levels, both an improved chemical procedure for plutonium separation and an alpha detector with sufficiently high sensitivity are needed.

Among all the existing detectors only damage track detectors have appeared convenient for these applications. However, CR-39 chemically etched has not proved to the suitable for the counting of such low track densities (about 10 tracks/cm^2) encoutered in these measurements, even when using the most advanced automatic systems available at present.

The assessment of alpha emitters with sufficient sensitivity for the new Derived Investigarion Levels can be easily obtained with Spark-Conted LR-115.

For these latter measurements, the sample, once chemically treated, is first electrodeposited on a stainless-steel disk, then covered by a 10-micron thick polycarbonate degrader (needed to optimize the detector response) and finally placed against a strippable LR-115 film. After the exposure the LR-115 film is etched, stripped from the polyester backing and spark counted.

When compared with conventional detectors only spark counting presents a sufficiently low limit od detection as illustrated in Fig.1.

The left-hand-side of this figure reports respectively the current investigation level (indicated by old DIL) and the new DIL's (in unit of Bq per day, which in practice is equivalent to unit of Bq per litre) for the inhalation of the class W and Class Y of plutonium. For each class, the minimum value is obtained assuming a 30-days sampling time, while the maximum value corresponds to a sampling time of 180 days.

The right-hand-side of the figure reports the lower detection limits of both the electronic counters and the LR-115 detectors for two different exposure periods. It can be easily seen that sufficiently low detection limits adequate for the new DIL's can only be obtained by spark counted LR-115 foils. These results have been obtained under the assumption that the only contribution to the background is that due to the detector itself.

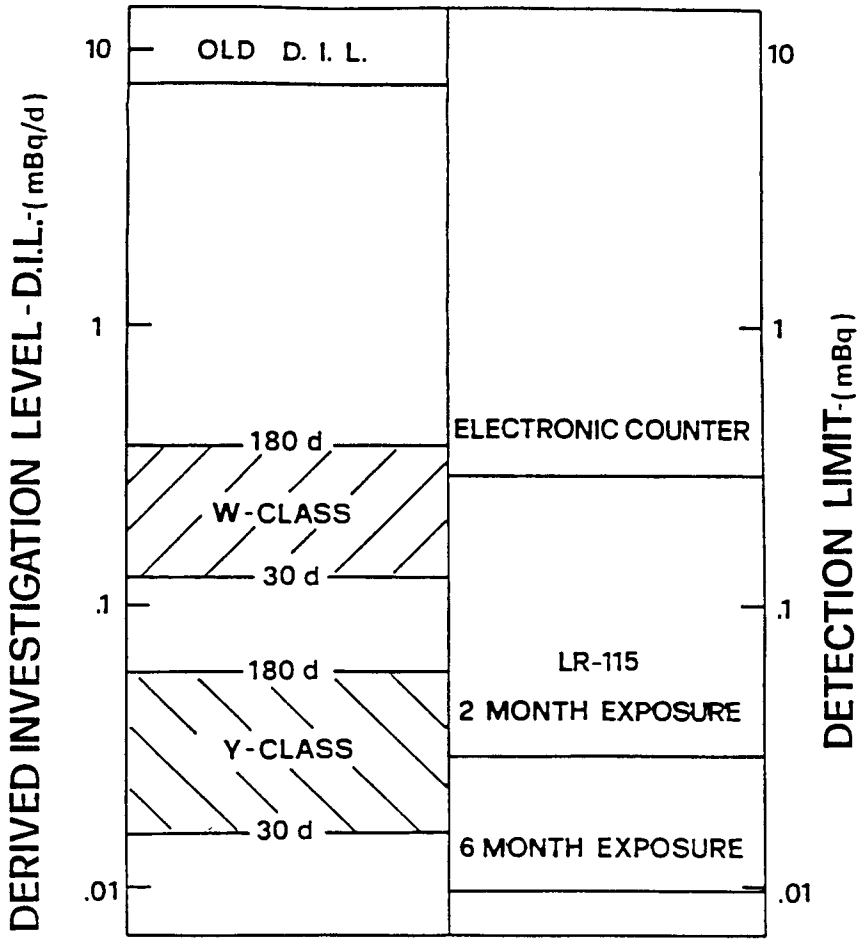

FIG. 1 Derived Investigation Levels for Pu-239 and Lower Detection Limits of electronic counters and spark counted LR-115 foils.

B. Natural alpha emitters - Radon

Passive gas radon monitoring devices based on damage track detectors are very attractive for their ability to integrate over long periods of time (months to years).

Unfortunately the above radon gas samplers are not sufficiently sensitive for short-term epoxure periods. For these applicatons the diffusion barrier charcool adsorption collector-DBCA is used, in spite of its limitations such as poor integration characteristics and response highly dependent on temperature and humdity.

These shortcomings can be easily overcome by using large-area detectors.

With these considerations in mind, a new gas radon sampling device for short-term exposure periods (typically one week) has been developed as shown in fig. 2.

This radon monitor device is simply made of an entire LR-115 foil enclosed in one envelope. Half of the foil is protected by a plastic cover thick enough to stop all the radon daughters, thus providing the "blank". The remaining bare part is used for the detection of the radon and its daughters. Incidentally bare LR-115 detectors have a response directly proportional to the radon concentration with little dependence on the plate-out and the equilibrium factor.

When compared with the Diffusion barrier Charcool Adsorption Collector method, the spark-counted bare LR-115 foil is an excellent integrator of radon exposures with a response, which in addition to being little dependent on temperature and humidity, is sufficiently sensitive and accurate.

The overall advantageous characteristics of the envelope-type sampler for indoor-radon can be summarized as in the following:

- High sensitivity and accuracy for short-term indoor exposures
- Extreme simplicity of counting large detector areas
- Possibility to turn on and off the detector simply by closing and opening the envelope containing the detector
- Unique possibility of having a "blank" detector
- Fast sampling time with no diffusion time required for the radon to enter the detector environment.

3. DISCUSSIONS.

The assessment of sufficiently low concentrations of man-made and natural alpha emitters can be successfully obtained by damage track detectors.

With these passive registration techniques it is possible to integrate over long period of exposure-time so that the intrinsic background of the detector can become negligible.
The possibility to scan large detector areas by the spark counter makes it possible to obtain sufficiently high sensitivity both for short-term-radon measurements and for the assessment of plutonium concentrations in urine lower than the New Derived Investigation Levels.
With the spark counter, the scanning of up square meters of detector areas becomes a simple task so that unique sensitivity can be easily achieved.
From the experience accumulated in this research contract, it appears possible that the signal-to-noise ratio can also be increased drastically using two plastic foils for counting coincidence sparks (as already demonstrated for neutron-induced fission-fragment track-holes).
In this case the background can be easily reduced by a factor of 10^4 or even more.
The combinations of such different unique characteristics as the possibility to integrate over long period of time, the simplicity of scanning an square meter detector area and the possibility to achieve coincidence counting make it possible to obtain alpha measurements with any desired or unlimited sensitivity

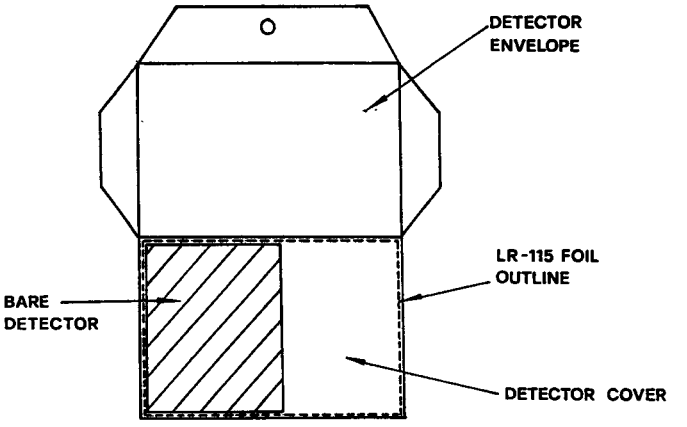

FIG. 2 Envelope-type radon gas detector.

IV. Other research group(s) collaborating actively on this project [name(s) and address(es)]:

1. O.C. Oppon - Ghana Atomic Commission - Ghana
2. D. Azimi Garakani - Teheran University - Iran
3. D.E. Cherouati - Commissariat aux Energies Nouvelles - Algerie

V. Publications:

1. Tommasino L., Cherouati D. E., Seidei J.L. and Monnin M. - A plastic bag sampler for passive radon monitoring. Nuclear Tracks 12: 661, 1986.
2. Tommasino L., Cherouati D.E., and Raponi f. - Improvements in spark replica counter and the breakdon counter. Nuclear Tracks 12: 275, 1986.
3. Azimi-Garakani D., Flores B., Piermattei S., Susanna A.F., Seidel J.L., Tommasino L., and Torri G. - Radon gas sampler for indoor and soil measurements and its applications. Radiat. Prot. Dos. 24: 269, 1988.
4. Torri G. - The plastic bag radon monitor and survey results - Paper presented at the International Workshop on Radon Monitoring in Radioprotection, Environmental Monitoring and Earth Sciences, Trieste, Italy, April 4-13, 1989.
5. Tommasino L. - Assessment of natural and man-made alpha emitting radionuclides - Nucl. Tracks and Rad. Meas. 15: 555, 1988.
6. Torri G., Azimi-Garakani D., Oppon O.C., Piermattei S., Susanna A.F., Seidel J., Tommasino L., and Ardanese L. - Measurements of soil and indoor radon in Italy. Nucl. tracks and Rad. Meas. 15: 637, 1988.

RADIATION PROTECTION PROGRAMME
Final Report

Contractor:

National Radiological
Protection Board, NRPB
Chilton, Didcot
GB Oxon OX11 ORQ

Contract no.: BI6-A-016-UK

Head(s) of research team(s) [name(s) and address(es)]:

Dr. A.F. McKinlay
National Radiological
Protection Board, NRPB
Chilton, Didcot
GB Oxon OX11 ORQ

Telephone number: 235-83.16.00

Title of the research contract:

Calculation of doses from external radiation.

List of projects:

1. Calculation of doses from external radiation.

Title of the project no.: 1

Calculation of Organ Doses from External Photon Irradiation

Head(s) of project:

Dr P J Dimbylow

Scientific staff:

Dr D G Jones

I. Objectives of the project:

To calculate organ doses and effective dose equivalent in various situations of practical dosimetric importance. Calculations will also be undertaken to assist in the understanding of experimental measurements.

II. Objectives for the reporting period:

This is the final report and covers all the previously reported work together with the extension to the work on doses arising from an infinite plane source buried under a layer of soil.

III. Progress achieved:

The work falls under three headings:

1) A comparison of organ doses and personal dosemeter readings under different photon irradiation conditions.

2) The identification of radiation fields that give rise to large differences between effective dose equivalent and dosemeter reading.

3) Calculations of kerma in air, organ doses and dosemeter readings for a particular field configuration.

1) Organ doses from external photon fields

A computer program was written to calculate organ doses arising from external photon irradiation. The program was based on Monte Carlo methods and followed the transport of photons through the body taking into account photoelectric interactions, coherent (Rayleigh) and incoherent (Compton) scattering and pair production. The energy range covered was from 5 keV to 10 MeV. The transport of ejected or scattered electrons was not considered as their track-lengths will be small compared with organ sizes for incident energies of most interest. The mathematical description of the body and organs was based on the adult hermaphrodite phantom derived by Cristy (1980) from the earlier MIRD5 phantom of Snyder et al at ORNL.

In the first set of calculations, the doses to the organs were determined for isotropic irradiation of the phantom for a range of energies from 10 keV to several MeV. This was a collaboration with G Williams at GSF.

For the second, more extensive set of calculations the phantom was irradiated by parallel beams of photons from selected directions, and the calculated effective dose equivalent was compared with the response of an idealised dosemeter placed on the phantom. This was done for AP, PA and lateral directions and for a complete rotation about the phantom in a

horizontal plane. The range of energies used was from 10 keV to 10 MeV. The values of H_E per unit kerma in air for the four geometries as a function of energy are given in table 1.

The dosemeter was located on the midline of the anterior of the body 14 cm above the bottom of the trunk. It consisted of a small disk of tissue equivalent material and the dose response was calculated by treating it as a thin absorber surrounded by sufficient material for it to be in electronic equilibrium, but not enough material to appreciably attenuate the photon flux. The effect of any photons backscattered from the phantom was included in the response.

The relationship between H_E and dosemeter reading is shown in figure 1. Some of the calculations were also repeated with a 1 cm thick tissue equivalent absorber placed on top of the dosemeter to more accurately simulate a real dosemeter, but this had little effect above a few tens of keV.

The relationships between H_E and kerma in air and between some selected organ doses and kerma in air were compared for A-P irradiation with the corresponding values in an extensive set of results published by G Williams et al (1985) at GSF. The latter results were based on separate male and female phantoms.

Expressing the differences as a percentage of the maximum value within the energy range, the two sets of results for the skeleton agreed within 3%, those for H_E, active marrow and lungs agreed to within 7%, those for gonads to within 8%, and those for breasts and thyroid to within about 13%. The largest differences occurred in the case of skin where the differences were up to 21% for energies below 30 keV, but much lower above this level when they dropped to 4%.

The differences for the breasts may reflect the fact that the breast size is about 50 percent larger in the GSF female phantom than in the Cristy adult hermaphrodite. The results for the smaller organs like the thyroid and the gonads are affected by the necessarily poorer statistical accuracy.

2) A consideration of the radiation fields that arise in practice

The comparison of dosemeter and organ dose calculations showed that the larger differences occurred with energies below a few hundred keV. In practice, there should be little difficulty in providing adequate shielding for photons of this energy, so that the main problem would arise with secondary radiation from higher energy photons. To investigate this a series of calculations were performed to determine the energy spectra of photons either transmitted through various materials or scattered off them. Some results for calcium carbonate, representing an inexpensive shielding material e.g. concrete or soil, are shown in figure 2. It can be seen that by far the most important source of these lower energy photons was due to reflection from the material (albedo).

3) Dose calculations applied to a particular radiation field

Work on the comparison of personal dosemeter readings with organ doses and effective dose equivalent was extended to photon irradiation from an extended plane source, as would arise for example in a fallout situation.

The problem was suggested by G Williams (formerly of GSF) as a benchmark calculation at a EURADOS working group meeting, and consisted essentially of two parts:

a) To calculate the air kerma at 1 m above ground due to an infinite plane Cs-137 source located in the soil. The soil composition was to be that used in a GSF publication (Jacob et al. 1986).

b) To use the angular and energy distribution of the kerma to calculate the dose rate to the organs of a man standing in the field.

A program was written to calculate the mean kerma as a function of energy and angle, and an earlier program was modified to calculate the organ doses for each of a set of angular intervals. The source depth was set at 3 mm to enable direct comparison with the results published by GSF (Jacob et al. 1988), and the organ doses were calculated for both the

male and female GSF mathematical phantoms to give a composite effective dose equivalent.

The total air kerma was found to be identical to the GSF value (Jacob et al. 1986) of 5.70E-16 Gy/sec per unit areal activity where areal activity is expressed as the number of source photons emitted per second from each square metre of the plane source. The effective dose equivalent was 4.08 ± .03E-16 Sv per photon per square metre compared with the GSF figure of 4.4E-16 (Jacob et al. 1988). Most of the individual organ doses agreed with the GSF values to within 10%, and all but two to within 20%. The exceptions were the adrenals at 21% lower, and the skeleton which was 22% higher. Some of the differences may arise because the present method treats the angular dependence of kerma by splitting direction space into a number of equal solid angles and then calculating the dose response for each segment. Whereas, the GSF method uses data from 6 irradiation geometries and interpolates between them.

The effective dose equivalents for the separate male and female phantoms were 3.79 ± .04E-16 and 4.13 ± .05E-16 Sv per photon per square metre respectively. These values were compared with the doses recorded by an idealised dosemeter located on the midline of the anterior of the body 14 cm above the bottom of the trunk. The dosemeter on the male phantom gave 4.0 ± 0.2E-16, and that on the female 4.9 ± 0.3E-16 Sv per photon per square metre i.e. differences of 6% and 19% respectively, but in the male case of no statistical significance.

Work was continued to resolve some of the larger organ dose differences, and a further comparison was made with GSF results to check an earlier step in the calculation, namely the kerma in air at 1 metre height above the ground. This was done for a series of monoenergetic sources with energies from 40 keV to 5 MeV and at depths up to 30 cm. The results of the comparison are given in table 2 and show good agreement for this stage of the calculation.

A similar type of comparison was carried out with G Hehn (IKE) at the behest of EURADOS using different soil types and using radionuclides rather than monoenergetic sources. In general the agreement was good,

but there were some exceptions, possibly associated with the source specifications which need to be resolved.

4) Discussion

The calculation of H_E and personal dosemeter reading in various fields shows that serious errors can arise in interpreting dosemeter readings, even where the irradiating field is a broad one. The most obvious case is at the middle energies around a few hundred keV where the body can partially shield the dosemeter, but the photons are still sufficiently energetic to deposit appreciable doses in the internal organs. Under these conditions area monitoring might prove a better safeguard.

The work on the calculation of organ doses due to an infinite plane source under a layer of soil is continuing. There is good agreement between ourselves and GSF over the kerma rate in air above the source for a wide range of energies and source depths, and there is also good agreement on the value of H_E in the case of a Cs_137 source, but there remain appreciable (20%) differences in the doses to a few parts of the body.

References

1) Cristy M. Mathematical Phantoms Representing Children of Various Ages for Use in Estimates of Internal Dose. ORNL/NUREG/TM-367 (1980).

2) Kramer R, Zankl M, Williams G and Drexler G. The Calculation of Dose from External Photon Exposures using Reference Human Phantoms and Monte-Carlo Methods. Part I. The Male (Adam) and Female (Eva) Adult Mathematical Phantoms. GSF Bericht S-885 (1982).

3) Williams G, Zankl M, Eckerl H and Drexler G. The Calculation of Dose from External Photon Exposures using Reference Human Phantoms and Monte Carlo Methods. Part II: Organ doses from occupational exposures. GSF-Bericht S-1079 (1985).

4) Jacob P and Paretzke H G. Gamma-Ray Exposure from Contaminated Soil. Nucl. Sci. Eng., 93, 248-261 (1986).

5) Jacob P, Paretzke H G, Rosenbaum H and Zankl M. Organ Doses from Radionuclides on the Ground. Part 1. Simple Time Dependences. Health Phys. 54, No. 6, 617-633 (1988).

TABLE 1

EFFECTIVE DOSE EQUIVALENT

EXPRESSED AS DOSE PER UNIT KERMA IN AIR

ANTERIOR-POSTERIOR			POSTERIOR-ANTERIOR		
E(keV)	Sv/Gy	ERROR(%)	E(keV)	Sv/Gy	ERROR(%)
10	4.25E-03	1.8	10	1.70E-04	0.1
15	4.71E-02	0.9	15	3.31E-03	0.2
30	4.42E-01	0.8	30	1.63E-01	0.2
50	1.10E+00	0.7	50	7.01E-01	0.8
70	1.37E+00	0.9	70	9.91E-01	0.9
85	1.43E+00	0.7	85	1.07E+00	0.8
100	1.40E+00	0.8	100	1.05E+00	0.8
150	1.25E+00	0.9	150	9.84E-01	0.8
300	1.10E+00	1.0	300	8.95E-01	1.1
600	1.04E+00	1.4	600	8.89E-01	1.3
1000	1.03E+00	1.4	1000	8.78E-01	1.3
3000	1.01E+00	2.3	3000	9.30E-01	2.4
6000	1.01E+00	3.6	6000	9.84E-01	2.1
10000	1.04E+00	2.8	10000	9.62E-01	2.4

LATERAL			ROTATION(2PI)		
E(keV)	Sv/Gy	ERROR(%)	E(keV)	Sv/Gy	ERROR(%)
10	9.84E-04	1.4	10	1.69E-03	2.4
15	8.34E-03	0.5	15	1.84E-02	1.1
30	1.10E-01	0.5	30	2.20E-01	1.0
50	4.18E-01	0.5	50	6.55E-01	0.8
70	5.93E-01	0.5	70	8.79E-01	0.8
85	6.46E-01	0.5	85	9.29E-01	0.8
100	6.52E-01	0.6	100	9.36E-01	0.9
150	6.33E-01	0.6	150	8.80E-01	1.2
300	6.18E-01	0.7	300	8.10E-01	0.9
600	6.59E-01	1.0	600	8.08E-01	1.1
1000	6.98E-01	0.9	1000	8.34E-01	1.5
3000	8.40E-01	1.1	3000	9.14E-01	2.2
6000	8.77E-01	1.5	6000	9.35E-01	2.0
10000	8.97E-01	1.3	10000	9.54E-01	1.8

TABLE 2

A COMPARISON OF NRPB AND GSF VALUES FOR AIR KERMA RATE
(GY/YR PER PHOTON/SEC/SQ.CM.)-GSF VALUES IN BRACKETS
AS A FUNCTION OF ENERGY AND DEPTH IN SOIL

DEPTH (cm)	40 keV	50 keV	100 keV	200 keV
0.1	2.01(2.20)E-5	2.01(2.13)E-5	3.01(3.14)E-5	6.57(6.63)E-5
0.3	1.28(1.37)E-5	1.44(1.52)E-5	2.52(2.59)E-5	5.43(5.54)E-5
1.0	4.90(5.25)E-6	7.19(7.66)E-6	1.74(1.80)E-5	3.90(4.00)E-5
3.0	6.45(7.17)E-7	1.81(1.97)E-6	9.01(9.28)E-6	2.30(2.30)E-5
10.0	1.73(2.13)E-9	2.95(3.50)E-8	1.36(1.43)E-6	5.95(6.00)E-6
30.0	-	-	7.91(8.26)E-9	1.55(1.57)E-7

DEPTH (cm)	662 keV	1000 keV	5000 keV
0.1	2.16(2.21)E-4	3.13(3.18)E-4	1.03(1.10)E-3
0.3	1.81(1.80)E-5	2.57(2.61)E-4	8.71(9.16)E-4
1.0	1.28(1.30)E-4	1.83(1.89)E-4	6.45(6.79)E-4
3.0	7.85(7.89)E-5	1.16(1.16)E-4	4.24(4.56)E-4
10.0	2.71(2.76)E-5	4.28(4.37)E-5	1.99(2.14)E-4
30.0	2.51(2.46)E-6	4.91(5.25)E-6	5.18(5.58)E-5

FIG. 1 DOSEMETER READING / H_E
BASED ON MALE & FEMALE ORGANS
PARALLEL BEAM IRRADIATION

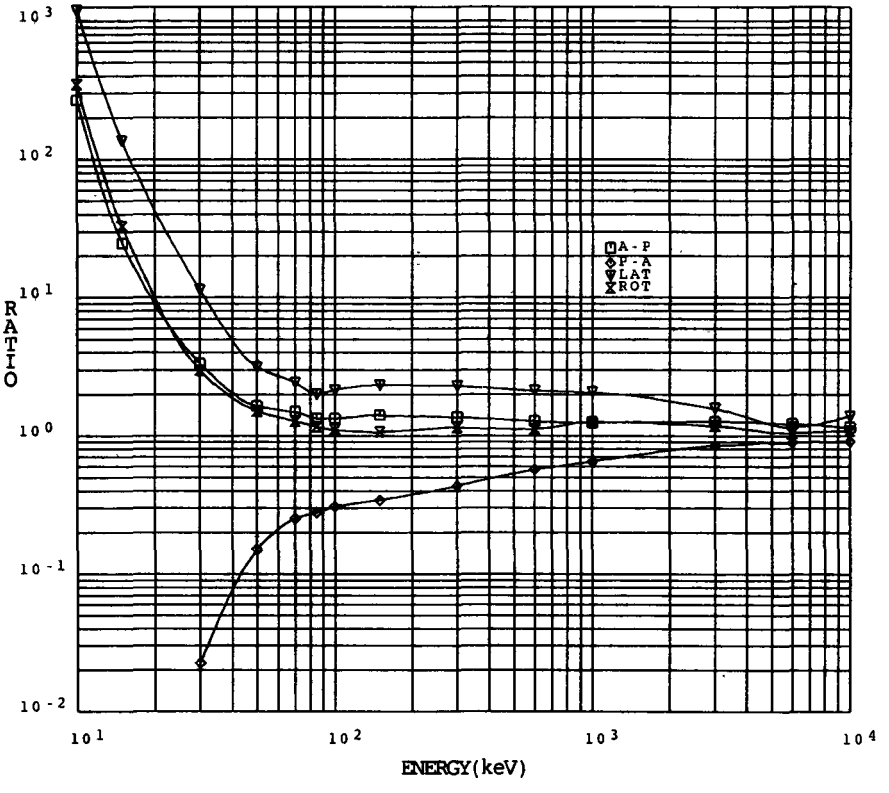

FIG. 2 ALBEDO & TRANSMITTED FLUXES
INCIDENT ENERGY 1 MeV
MATERIAL - CALCIUM CARBONATE 50 GM/CM^2

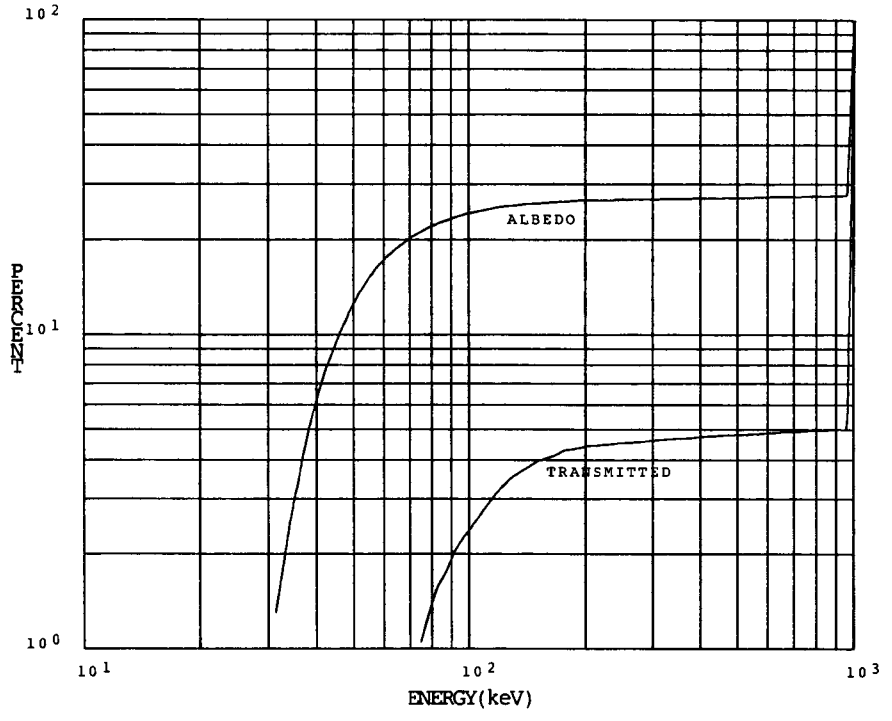

ENERGY SPECTRUM

CUMULATIVE FREQUENCY v. ENERGY

IV. Other research group(s) collaborating actively on this project [name(s) and address(es)]:

None

V. Publications:

None

RADIATION PROTECTION PROGRAMME
Final Report

Contractor:

Universität des Saarlandes
St.Johanner Stadtwald
D-6600 Saarbrücken

Contract no.: BI6-A-010-D

Head(s) of research team(s) [name(s) and address(es)]:

Dr. H.G. Menzel
Universität des Saarlandes
Boris Rajewsky Institut
D-6650 Homburg (Saar)

Prof. Dr. R. Grillmaier
Universität des Saarlandes
Boris Rajewsky Institut
D-6650 Homburg (Saar)

Telephone number: 6841-16.62.02

Title of the research contract:

Dosimetric research and radiation protection dosimetry with proportional counters and physical and biological accident dosimetry.

List of projects:

1. Basic physical data for the dosimetry and radiation protection dosimetry of neutrons and photons with low pressure proportional counters.
2. Investigation of practical aspects of employing microdosimetric counters as dose equivalent meters.

Title of the project no.: 1

Basic physical data for the dosimetry and radiation protection dosimetry of neutrons and photons with low pressure proportional counters.

Head(s) of project: H.G. Menzel

Scientific staff: Bühler, G., Dahmen, P.,
Folkerts, K.H., Kunz, A.,
Pihet, P., Schuhmacher, H.

I. Objectives of the project:

The accuracy and precision achievable in dosimetry of external ionising radiation depends on the availability of adequate basic physical data. Examples for required improvements are neutron interaction data (cross sections, secondary charged particles) and dosimetric data (kerma factors) for different elements and materials and neutron energies above 14 MeV. The ability af low pressure proportional counters to measure absorbed dose with relatively low uncertainty and simultaneously ionisation yield events due to single primary interactions are used to determine required interaction and dosimetric data for neutrons and photons with widely varying energies.

II. Objectives for the reporting period:

To carry out measurements with low pressure proportional counters (PC) with walls made of A-150 and graphite in monoenergetic neutrons beams between 14 and 20 MeV at PTB (Braunschweig). To performe combined pulse height and time-of-flight measurements with these PC's in beams of quasi monoenergetic neutrons (20 - 70 MeV) in combination with neutron fluence measurements performed by PTB, Braunschweig, and relative spectral fluence measurements performed by UCL (Louvain-la-Neuve). To evaluate ionisation yield spectra and kerma factors for A-150 and carbon for these energies. To compare the results with theoretical data based on nuclear model calculations.

III. Progress achieved:

SUMMARY :

Significant progress was achieved in the method of applying low pressure proportional counters (PC) for the determination of basic physical data required in neutron and photon radiation dosimetry. The overall experimental uncertainty was reduced considerably by the introduction of new, and the combination of several, calibration procedures and by improvements in the evaluation procedure by combining measurements using PC's with walls made of different materials. The timing resolution of PC's was optimized with regard to the counting gas mixtures. In collaboration with the Physikalisch Technische Bundesanstalt (PTB, Braunschweig, FRG) time-of-flight techniques were applied with these optimised PC's to separate events of different neutron energies. The range of application of tissue-equivalent proportional counters (TEPC) was enlarged by applying counting gas mixtures containing small amounts of ^{3}He gas combined with the variation of the counter wall thickness. This method was employed to study the attenuation and thermalization of low energy neutrons in hydrogenous material and the influence of theses processes on absorbed dose and dose equivalent.

The principal suitability of PC's to measure absorbed dose and kerma for low neutron energies was investigated in measurements with monoenergetic neutrons in the range from thermal neutrons to 144 keV neutrons (at the PTB). Absorbed dose measurements of high accuracy for various irradiation geometries were also performed at the bare and D_2O-moderated ^{252}Cf reference sources of the PTB.

A main objective of the contractual period was to determine kerma factors and fractional kerma for various secondary particles in different materials for monoenergetic fast neutrons in the energy range 14 - 20 MeV (at the PTB) and 20 - 70 MeV (at the Paul Scherrer Institute, PSI, Villigen, Switzerland). In order to achieve the desired accuracy in the evaluation of the measurements using cavity chamber principles, new approaches to evaluate effective W-values and gas-to-wall absorbed dose conversion factors were developed. This work was of particular importance for the non-homogeneous counters, i.e. the counters with walls made of carbon and other non-hydrogenous materials.

The applicability of cavity chambers of different materials to determine absorbed dose for photons was investigated with PC's in the radiation fields of nearly monoenergetic gamma-rays nuclide sources (in the energy range 140 keV - 1.2 MeV).

The objectives of the contractual period have been largely achieved. The emphasis in the kerma measurements has been slightly shifted from using many different materials to improving the experimental method. Remaining problems which require further work include : - to extend the comparison of experimental and theoretical results by including neutron transport into the energy deposition calculation (low energy neutrons) and by enlarging the range of calculation to at least 60 MeV; - the measurement of kerma factors at high neutron energies have

to be optimized by appropriate combination of different techniques (recoil proton telescope, TOF spectrometry, TOF techniques as applied with PC's in collaboration with PTB-Braunschweig and UCL-Louvain) and to be extended to other materials, in particular to oxygen.

METHODS :

Ionisation yield spectra and kerma in mono-energetic neutron and photon fields were measured using low pressure proportional counters (PC) of 12.7 mm inner diameter with walls made of A-150 tissue-substitute plastic (TEPC), carbon (CPC), aluminium, magnesium and iron. The counter wall thickness was 2.54 mm for the TEPC and CPC, and 1.27 mm for the other counters. When necessary additional caps in the wall material were used in order to achieve charged particle equilibrium. For the experiments with low energy neutrons, TE caps of up to 32.5 mm thickness were used in order to investigate the influence of neutron transport on absorbed dose and dose equivalent. These measurements were performed using PC's with 12.7 mm and 59.3 mm inner diameters.

The counters were filled with propane based TE gas mixture at pressures resulting in a mass per area ranging from $1x10^{-4}$ to $5x10^{-4}$ $g.cm^{-2}$ along the cavity diameter (simulated diameters from 1 to 5 μm respectively). Different gas mixtures were used in order to solve specific problems.

In order to improve the time resolution of PC's measurements were performed with photons and with neutrons of varying energies using counters with different sizes and filled with propane, isobutane-based TE gas or pure isobutane. The best time resolution was obtained with pure isobutane and the smallest counter. This research enabled the application of time-of-flight (TOF) techniques with PC's. This method was developed in collaboration with PTB and applied at PSI in order to separate the contribution of low neutron energy contaminants in the quasi mono-energetic neutron beams used (from 20 to 70 MeV) (Menzel et al., 1988). The dual parameter data acquisition system of the PTB was used in order to provide detailed analysis of the correlated pulse height and TOF spectra (U. Schrewe et al., Rad. Prot. Dosim., 23, 239, 1988).

Measurements at low neutron energies were performed using the normal TE gas mixture and gas mixtures modified by addition of small amounts of ^3He. These measurements were initially aimed at the compensation of the too low TEPC dose equivalent response in the low and intermediate neutron energy range. The method takes advantage of the moderation and thermalisation of low energy neutrons in the counter wall, the large cross-section and the large kinetic energy released for the $^3He(n,p)^3H$ reaction for thermal neutrons. It enabled quantitative assessments to be made of neutron thermalisation in the counter wall (Pihet et al., 1989).

PC-measurements were evaluated in terms of absorbed dose distributions in the microdosimetric quantity lineal energy, y. The kerma in the wall material was evaluated from the total absorbed dose as derived from the integral of the spectra measured under condition of charged particle equilibrium. Furthermore

quantitative information, in terms of fractional kerma, for the components of the secondary radiation released by neutrons was derived from the measured ionisation yield spectra. The accuracy achievable for kerma measurements with PC's is determined by the uncertainty on the calibration of the PC's in lineal energy and on the conversion factors required for the application of the cavity chamber principles.

The calibration procedure of the proportional counters was improved by combining three independent techniques. The calibration of the pulse height in units of lineal energy (y in $keV.\mu m^{-1}$) was obtained by using the spectrum of collimated alpha particles produced by an internal ^{244}Cm source. This method is however associated with considerable uncertainties (Schrewe et al., 1988). For each counter used it was improved by performing a calibration in absorbed dose using the reference standard ^{60}Co source of the PTB. Furthermore, for neutron measurements with TEPC and CPC, the sharp cut off of the pulse height for protons and alpha particles released by neutrons were used as internal calibration values. Stopping power and range tables required to calculate the maximum energy loss by the particles in the cavity were critically evaluated (Schrewe et al., 1988; Pihet and Menzel, 1989). The Andersen and Ziegler fitting formulae (Pergamon Press, 1977) were adopted.

The knowledge of appropriate average W-values and gas-to-wall conversion factors is required to evaluate the absorbed dose in the gas from the ionisation spectra and the value of the absorbed dose in the material of the detecor wall. The unavoidable inhomogeneity of wall and gas for carbon and metal counters requires a choice to be made for a suitable gas mixture. The gas-to-wall conversion factors differ significantly from unity for these counters. Earlier measurements showed that for non-hydrogenous PC's filled with TE gas mixtures at pressures corresponding to a simulated diameter of 1 m the contribution of recoil protons to absorbed dose is negligibly small. TE gas mixtures have better counting gas properties than hydrogen free gases.

Gas-to-wall dose conversion factors ($r_{m,g}$) at a given neutron energy are determined by the ratio of the average stopping powers between wall and gas for the secondary charged particles and by the contribution of these particles to the total absorbed dose. For the aluminium and magnesium PC's used in the neutron energy range 14 - 19 MeV, a method was proposed which is based on the approximate separation of the dose contributions for the different secondary radiation components from the measured ionisation spectra (Bühler et al., 1986). The mean energy of the secondary particles were estimated from the reaction kinematics. A similar approach was adopted to evaluate TEPC and CPC measurements in the neutron energy range from 5 to 60 MeV (Pihet and Menzel, 1989). The method was improved by comparing the spectra measured with both TEPC and CPC exposed in the same conditions. Accounting for the contribution of carbon in A-150 plastic (78 % by weight), the CPC spectra were fitted above 150 $keV.\mu m^{-1}$ to the corresponding TEPC spectra (Menzel et al., 1988). This comparison enabled a direct evaluation of $r_{m,g}$ for the CPC from the difference

between the two spectra. It also improved the discrimination of recoil protons and heavier particles in the ionisation spectra measured with TEPC. Calculated ionisation spectra contributed towards improved separation of the different overlapping components in the measured spectra and to take the contribution of neutron interactions with the gas in the cavity into account. At neutron energies below 20 MeV ionisation yield calculations for idealized PC's, e.g. C-wall filled with "C-gas", were used as an alternative approach.

Similar methods were applied to evaluate average W-values for the secondaries released by neutrons for TEPC and CPC (Pihet and Menzel, 1989). These investigations included a critical evaluation of published W-values.

RESULTS :

Measurements in low energy neutron fields. TEPC measurements were performed at the Physikalisch Technische Bundesanstalt (PTB, Braunschweig, FRG) with neutrons of thermal energies, 2 keV, 24.5 keV and 144 keV produced at the filtered neutron beams of the Research and Measurement Reactor (FMRB) (Schuhmacher et al., 1987a). These experiments were aimed at investigating the suitability of TEPC for dosimetry in the low neutron energy range because these low energies raise specific problems. The non negligible contribution of secondaries produced in the gas was assessed by performing additional measurements with CPC (Figure 1). The attenuation of the neutron fluence in the counter wall was accounted for by theoretical investigations, i.e. from capture cross section data and neutron transport calculation. Furthermore the high neutron energy contamination in the filtered beams was taken into account by applying difference filter methods. Additional measurements were recently performed at these energies in improved filtration conditions at the National Institute for Science and Technology (NIST, previously NBS, Washington DC, USA). Their evaluation is in progress.

The measurements performed have shown that the proportional counter method represents an excellent tool to obtain relevant data on the interaction of low energy neutrons with materials employed in neutron dosimetry. This is due to the capability of PC's to provide simultaneously : (1) the ionisation yield spectra of the secondary charged particles; and (2) the total absorbed dose in the wall material from the integral of the spectra. The ionisation yield spectra in particular provided quantitative information on the effect of short range secondaries produced in the cavity which contribute significantly to the total absorbed dose. Combined TEPC-CPC measurements showed that the fraction of absorbed dose attributed to interactions with the gas (simulated diameter 1 μm) was 12, 90 and 50 % for thermal, 24.5 keV and 144 keV neutrons respectively (Figure 1). The corrections to account for the average W-values associated to the short range recoil protons released were evaluated by using different simulated diameter and by comparing the maximum energy deposition corresponding to the neutron energy with the maximum detected in the ionisation yield spectra (Figure 1). Published ionisation spectra calculations were found in good agreement with the

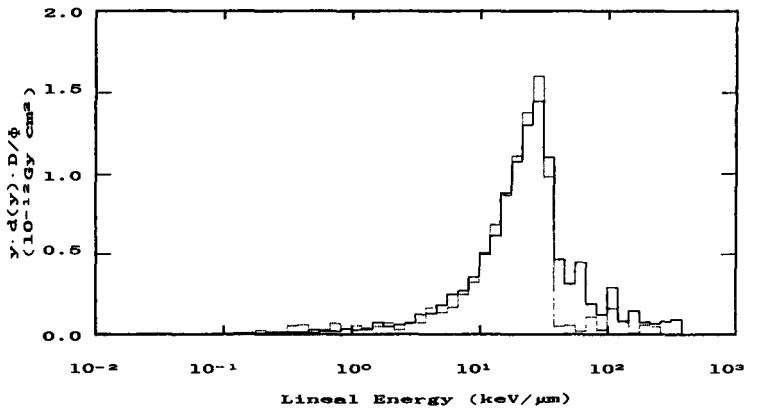

Figure 1. Absorbed dose distributions in lineal energy measured using a TEPC (full line) and a CPC (dotted line) for 24.5 keV neutrons (difference spectra) (from Schuhmacher et al., 1987a). The figure showes three problems encountered at these low neutron energies illustrating the suitability of the PC method : (1) the high (90 %) contribution of neutron interactions with gas in the cavity represented by the CPC distribution; (2) the maximum lineal energy for the short range recoil protons higher (x1.3) than the expected value from the maximum energy deposition of 24.5 keV enabling assessments to be made of the average W values for low energy protons; and (3) the remaining high energy contamination above the proton peak.

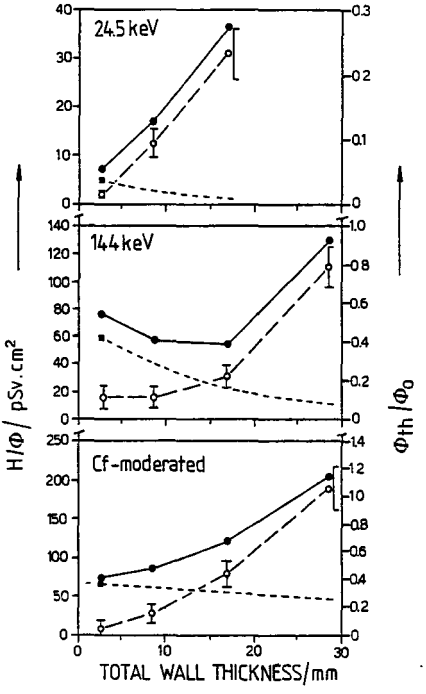

Figure 2.
Dose equivalent per unit fluence attenuation curves (left scale) measured with TEPC filled with normal TE gas (dashed lines) and with the gas mixture containing 1 % of ^{3}He (closed symbols) for different neutron fields. The difference between the curves is due to neutron capture reactions with ^{3}He for thermal neutrons. At low neutron energy the fluence of thermal neutrons increases rapidely with wall thickness as showed by the curves for the fluence of thermalized neutrons in the detector wall with respect to the fluence of primary neutrons (open symbols, right scale). These curves were established using the dose equivalent response of the TEPC with 1 % ^{3}He measured in primary thermal beams as calibration value. From Pihet et al., 1989.

Neutron energy (MeV)	TEPC $(W)_N$ (eV)	TEPC $(r_{m,g})_N$	CPC $(W)_N$ (eV)	CPC $(r_{m,g})_N$	$\frac{K_C}{K_{A-150}}$
5.0	30.2	1.003	38.2	0.585	0.159
13.9	30.1	0.992	32.1	0.811	0.265
15.0	30.1	0.989	31.7	0.796	0.296
17.0	30.0	0.992	31.3	0.809	0.343
19.0	29.8	0.992	30.6	0.836	0.405
27.8	29.8	0.995	30.3	0.830	0.372
39.7	29.7	0.997	30.0	0.840	0.448
60.3	29.6	0.997	29.7	0.851	0.537
d(14)+Be	29.8	0.999	31.7	0.806	0.150
d(0.25)+T	30.1	0.992	31.9	0.784	0.284
p(62)+Be	29.8	0.996	30.0	0.845	0.467

Table 1. Results of kerma measurements for fast neutrons in A-150 plastic and in carbon obtained with TEPC and CPC, both filled with TE gas (Menzel et al., Phys. Med. Biol., 29, 1537-1554, 1984; Bühler et al., 1985ab; Menzel et al., 1988). The kerma values as a function of neutron energy were derived from the integral of the measured spectra after applying the related average W-values and gas-to-wall conversion factors into account. These dose conversion factors were evaluated using the information contained in the ionisation spectra for the dose components of the secondary radiations and published basic physical data, W values and stopping powers (Pihet and Menzel, 1989). From Pihet and Menzel, in press.

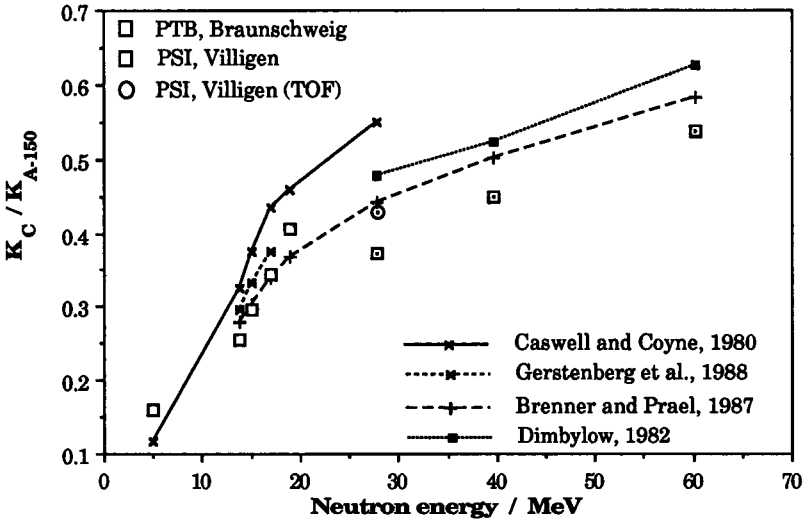

Figure 3. Kerma ratios in carbon and in A-150 plastic as function of neutron energy obtained from TEPC and CPC measurements (Table 1). The experimental values are compared to the results of theoretical investigations using different nuclear model calculations. For neutron energy above 20 MeV the experimental values require additional correction in order to take the contamination of neutrons with lower energy into account. A solution to this problem was found by applying TOF techniques with PC's. The first result evaluated for 28 MeV neutrons is indicated showing a better agreement between the corrected and calculated values. Modified from Pihet, 1989.

measured distributions. Kerma factors, i.e. kerma per unit neutron fluence, in A-150 TE plastic were determined at each neutron energy. The results agreed with theoretical values by Caswell et al. (Rad. Res., 83, 217-254, 1980) within the stated overall uncertainties. However the results obtained at PTB for 2 keV and 24.5 keV neutrons were associated with large uncertainties due to considerable contribution of high energy neutron contaminants (Figure 1).

At the same neutron energies measurements with TEPC with 59.3 mm inner diameter (similar to those used for area monitoring in radiation protection) were performed by using additional TE caps with up to 32.5 mm thicknesses and in a cylindrical water phantom (Schuhmacher et al., 1985b ; Pihet et al., 1989). Dose equivalent quantities are indeed defined in a phantom and absorbed dose and dose equivalent critically depend on the irradiation geometry at low neutron energies. This problem is generally investigated using neutron transport and energy deposition calculations. The measurements performed, evaluated in terms of the lineal energy spectra normalised to absorbed dose and dose equivalent per unit neutron fluence, provided relevant tests for comparison with the results of theoretical investigations (Figure 2).

Neutron transport in the detector wall at low energy consists of fluence attenuation and thermalisation processes. In order to quantitatively assess these combined effects the measurements were repeated in the same beams but using 12.7 mm TEPC's filled with TE gas mixtures containing 0.1, 0.5 and 1 % of ^{3}He and exposed with TE caps up to 26 mm thicknesses (Pihet et al., 1989). The result of measurements performed with primary thermal neutrons (1% ^{3}He) gave an increment of dose equivalent per fluence of 150 $pSv.cm^2$ attributed to capture reactions of thermal neutrons with ^{3}He. This value could be used to calibrate the contribution of neutron thermalisation in the counter wall and surrounding medium for the other radiation fields (Figure 2).

Similar measurements and evaluation, i.e. combined TEPC and CPC measurements, using different cap thicknesses and modified ^{3}He-TE gas mixtures, were performed in the field of a bare and D_2O moderated ^{252}Cf source (Schuhmacher et al., 1987b; Pihet et al., 1989). In particular the capability of PC's to enable the separation of the photon and neutron dose components was investigated with regard to the wall thickness. The excellent agreement (within 1 up to maximum 5 %) between the measured values of absorbed dose (related to neutron fluence) and the values of calculated mean fluence to kerma conversion factors indicates the accuracy achievable for absorbed dose determination with TEPC's.

Kerma measurements with PC's for fast neutrons. PC measurements were performed with mono-energetic neutrons with energies between 5 and 20 MeV were produced by the reaction $T(d,n)^{4}He$ at the low scattering accelerator facility of the PTB (Bühler et al., 1985ab; Bühler et al., 1986; Menzel, 1987) . These measurements completed under improved experimental conditions earlier experiments. The energy range up to 60 MeV could be investigated by using quasi-monoenergetic neutron beams produced at the PSI by bombarding a thin

beryllium target with protons of 30, 43 and 64 MeV (neutron energies of 28, 40 and 60 MeV, respectively) (Menzel et al., 1988a).

Kerma measurements were concentrated on A-150 TE plastic and in carbon materials due to the particular importance of these materials for neutron dosimetry. For the neutron beams produced at PTB the spectral fluence, the fluence contribution of scattered neutrons in the experimental hall and the contamination of background neutrons produced in the target system were accurately determined. For these "well-defined" neutron fields the evaluation of the results was carried out in terms of kerma factors, i.e. kerma per unit neutron fluence at the nominal energies. At PSI, the spectra were normalized to the charge of the proton beam incident on the target. Fluence measurements are currently carried out in these beams by the PTB. Instead of kerma per-unit-fluence the results were therefore evaluated first in terms of kerma ratios in carbon and in A-150 plastic, $K_C/K_{A\text{-}150}$.

The overall uncertainty of absorbed dose measurements was reduced to the order of 5 % for TEPC and 8-10 % for CPC. This improvement was achieved by improving the calibration techniques and by determining appropriate average W-values and gas-to-wall dose conversion factors for the charged secondaries released as a function of neutron energy (Table 1). Uncertainties on these factors were decreased by using the stopping powers given by Andersen and Ziegler (Pergamon Press, 1977) and the accurate W values for protons and alpha particles by Thomas and Burke (Phys. Med. Biol., 1985).

Table 1 summarizes the results in terms of $K_C/K_{A\text{-}150}$ ratio currently obtained at PTB and PSI after revision using the dose conversion factors recently evaluated. Figure 3 compares these values with those calculated by Caswell et al. (Rad. Res., 83, 217-254, 1980), Brenner (Phys. Med. Biol., 29, 437-441, 1983) and Dimbylow (Phys. Med. Biol., 27, 989-1001, 1982). This comparison showed large discrepancies in particular with the calculations by Caswell et al. in the neutron energy range between 15 and 19 MeV for which neutron cross sections and reaction kinematics for non-elastic processes are known with considerable uncertainties. A better agreement is observed with the values recently revised by Gerstenberg (Rad. Prot. Dosim., 23, 41-44, 1988). The experimental values are however in good agreement with the calculations by Brenner based on different nuclear models. Accurate TEPC-CPC-fluence measurements were recently repeated in this critical energy interval by bins of 0.5 MeV in order to reduce the experimental uncertainties. The values found at PSI between 20 and 70 MeV, the first experimental data obtained at these high energies, were found to be systematically lower than the values by Brenner. This deviation may be explained by a contamination of the radiation field with neutrons of lower energies. Combined PC-TOF techniques were developed in close collaboration with PTB in order to solve this problem. According to preliminary evaluations, the first corrected value obtained for neutrons of 28 MeV (Figure 3) is in better agreement with the calculated values by Brenner illustrating the suitability of this approach.

Kerma factors were determined using PC's in aluminium and in magnesium for neutrons with energies of 13.9, 15.0, 17.0 and 19.0 MeV produced at PTB. These materials are used for the construction of ionisation chambers with electrically conductive walls applied in neutron dosimetry. The kerma factors obtained up to 17 MeV were in good agreement with the theoretical values obtained by Caswell et al. (Rad. Res., 83, 217-254, 1980) and by Dimbylow (Phys. Med. Biol., 27, 989-1001, 1982). At 19 MeV the results were found higher than the values by Caswell, in good agreement with those by Dimbylow.

Measurements in monoenergetic photon fields. Lineal energy spectra were measured in identical conditions for photons with energies of 140, 660 and 1250 keV from nuclide sources using PC's with walls made of A-150 plastic, carbon, aluminium and iron and simulated diameters ranging from 1 to 5 μm (Dahmen et al., 1989). The analysis of the normalised lineal energy distributions showed that the maximum lineal energy is independent of photon energy with TEPC. The spectra measured with CPC were very similar to those with TEPC. However, the maximum lineal energy increased significantly for metal counters. This effect was observed for all photon energies and for simulated diameter up to 5 μm. The comparison of the spectra normalised to particle fluence were also achieved using a suitable approximation procedure. The spectra revealed differences between different counters in the range from 0.01 to 0.5 $keV.\mu m^{-1}$. These differences were interprated as attributed partly to modifications in the slowing down spectra of the electrons entering the cavity but also to wall effects, in particular re-entry effect related to back-scattered electrons as supported by theroretical investigations.

DISCUSSION :

The measurements performed at neutron energies below 500 keV showed the applicability of TEPC for accurate determination of a absorbed dose at low neutron energy. Specific problems related to secondaries with range less the simulated diameter were investigated by analysing the shape of the dose distributions and by comparing the spectra measured with TEPC and CPC. The uncertainty on absorbed dose remains mainly determined by the uncertainty on W values for the low-energy secondaries. Although the shape of the lineal energy spectra enabled appropriate corrections for W-values to be evaluated, progress in the comparison of calculated and measured energy deposition spectra are expected to reduce further the uncertainty on absorbed dose.

TEPC measurements performed with variable wall thicknesses show to be a powerful tool to study the influence of the attenuation and the moderation of low energy neutrons on measurements of absorbed dose and dose equivalent in phantoms. A method was developed based on measurements with TEPC's filled with TE gas mixtures containing small amounts of ^3He. This method gave additional information on the fluence of neutrons thermalized in the detector wall as a function of neutron energy and wall thickness. The data collected provided suitable tests for comparison with the results of neutron transport calculations.

The measurements performed at low neutron energy were systematically repeated in californium reference sources showing the accuracy level achievable with TEPC for determination of absorbed dose in neutron fields with broad energy spectra. It was shown that TEPC enable accurate separation of the neutron and photon dose components taking the energy spectra into account. These investigations demonstrated the suitability of TEPC as standard instruments for calibration purposes.

PC measurements performed in different materials, in particular in carbon and in A-150 plastic, for fast neutrons in the energy range from 5 to 60 MeV showed that PC's can be used to measure absorbed dose and kerma for these penetrating radiations with relatively low uncertainties applying the cavity chamber principles. A method based on the approximation of the secondary radiation dose components from the measured spectra was proposed as a pragmatic approach to evaluate appropriate dose conversion factors with regard to neutron energy, composition of wall and gas. This method presents an alternative solution compared with the more common approach of secondary charged particles and related energy deposition calculations. It was applied successfully for high energy neutrons for which till now no data existed. An evaluation of published stopping power and W values contributed to identify the needs for further research in order to reduce the uncertainty on absorbed dose with gas cavity detectors.

Ionisation yield spectra measured for fast neutrons were compared, in the neutron energy range between 14 and 20 MeV, to the spectra calculated using the analytical code by Caswell et al. based on the ENDF/B cross section data. These detailed investigations showed the suitability of PC measurements to improve the obviously inadequate knowledge of kerma factors and basic interaction data for high energy neutrons. The analysis was concentrated on the spectra measured in carbon in which alpha particle producing reactions play an important role. Special attention was given to the (n,n'3α) reaction which is inadequately treated in the calculations still extensively used in neutron dosimetry. Between 15 MeV and 17 MeV this lead to discrepancies of up to 50 % in partial kerma factors in carbon for this reaction between calculated and measured data. Above 20 MeV neutron energy, additional (neutron fluence, spectral fluence, PC-TOF spectra) data are required to reduce the experimental uncertainties and to enable comparisons with theoretical investigations.

Taking advantage of the experience gained in measurements with neutrons the applicability of PC's for kerma measurements in photon fields for different materials was tested. The spectra measured with photons of 140, 660 and 1250 keV using metal PC's presented unexpected differences compared to the spectra measured with TEPC and CPC indicating the possible influence of re-entry effect related to electron backscattering. This observation showed the limitations of the Bragg-Gray cavity principles for absorbed dose measurements with photons using gas cavity detectors with walls made of electrically conductive materials. More detailed calculations of the ionisation yield spectra based on track structure calculations are required to improve the analysis of the results.

IV. Other research group(s) collaborating actively on this project [name(s) and addres(es)] :

Physikalisch-Technische Bundesanstalt (PTB), Group Neutronendosimetrie (Drs. G. Dietze and H. Brede) Braunschweig, FRG
National Institute for Science and Technology (NIST), Center for Radiation Research (Drs. J.J. Coyne and R.S. Caswell), Washington, D.C., U.S.A.
Universität Basel (Dr. R. Henneck) and Paul Scherrer Institute, PSI, Villigen, Switzerland.
Université Catholique de Louvain, UCL, Unité de Radiobiologie et de Radioprotection (Prof. A. Wambersie), Bruxelles, and Unité de Physique Nucleaire (Prof. J.P. Meulders), Louvain-la-Neuve, Belgium.
International Atomic Energy Agency, IAEA, Nuclear Data Section, (Dr. K. Okamoto), Vienna, Austria.

V. Publications :

1.

Bühler, G., Menzel, H.G., Schuhmacher, H. and Guldbakke, S. Dosimetric studies with non-hydrogenous proportional counters in well defined high energy neutron fields. Proc. 5th Symp. on Neutron Dosimetry (H. Schraube, G. Burger, J. Booz, Eds.), EUR 9762, 3O9-32O (1985a).

Schuhmacher, H., Menzel, H.G., and Coyne, J.J.,Critical evaluation of neutron kerma factors using theoretical and experimental ionisation yield spectra, Proc. 5th Symp. on Neutron Dosimetry (H. Schraube, G. Burger, J. Booz, Eds.),EUR 9762, 213-223 (1985a).

Schuhmacher, H., Menzel, H.G., Bühler, G. and Alberts, W.G. Experimental basis for optimisation of the wall thickness of microdosimetric counters. Proc. 9th Symp. on Microdosimetry, Toulouse, 1985 (J.A. Dennis, J.J. Booz and B. Bauer, Eds.), CEC, EUR 9644, Radiat. Prot. Dosim., 13, 341-345 (1985b).

Bühler, G., Menzel, H.G., Schuhmacher, H. and Dietze, G., Neutron interaction data in carbon derived from measured and calculated ionisation yield spectra. Proc. 9th Symp. on Microdosimetry, Toulouse, 1985 (J.A. Dennis, J.J. Booz and B. Bauer, Eds.), CEC, EUR 9644, Radiat. Prot. Dosim., 13, 13 - 17 (1985b).

Bühler, G., Menzel, H.G., Schuhmacher, H., Dietze, G. and Guldbakke, S., Neutron kerma factors for magnesium and aluminium measured with low pressure proportional counters. Phys. Med. Biol., 31, 6, 6O1 - 611 (1986).

Menzel, H.G. and Schuhmacher, H., Fast neutron interaction data from measurements with low pressure proportional counters. Proc. of the Int. Conf. on Fast Neutron Physics, Dubrovnik (D. Miljanic et al., eds.), 14O (1986).

Schuhmacher, H., Alberts, W.G., Menzel, H.G. and Bühler, G. Dosimetry of low energy neutrons using low-pressure proportional counters. Rad. Res., 111, 1-13 (1987a).

Menzel, H.G., Fast neutron and pion interaction data from low pressure proportional counter measurements. In Nuclear and Atomic Data for Radiotherapy and Related Radiobiology, Proc. of an Advisory Group Meeting organized by the International Atomic Energy Agency, Rijswijk, Sept. 1985, 265 - 284 (1987).

Brenner, D.J., Zaider, M., Coyne, J.J., Menzel, H.G. and Prael, R.E., Evaulation of nonelastic neutron cross sections in carbon above 14 MeV. Nucl. Sci. Eng., 95, 311 - 315 (1987).

Schuhmacher, H., Menzel, H.G. and Kluge, H. Dosimetry of a bare and a D_2O-moderated ^{252}Cf source using low pressure proportional counters. Rad. Prot. Dosim., 19, 2, 103 - 109, (1987b).

Menzel, H.G., Pihet, P., Folkerts, K.H., Grillmaier, R.E., Dosimetry research using low pressure proportional counters for neutrons with energies up to 60 MeV. Proc. 6th Symp. on Neutron Dosimetry, München, 1987 (H. Schraube, G. Burger, J. Booz, Eds.), CEC, EUR 11663, Radiat. Prot. Dosim., 23, 389 - 392, (1988a).

Menzel, H.G., The use of low pressure proportional counters in neutron dosimetry. In Ionizing Radiation: Protection and Dosimetry (G. Paic, ed.), CRC Press Boca Raton, 187 - 216 (1988b).

Schrewe, U.J., Brede, H., Pihet, P., Menzel, H.G., Improvements on the calibration of tissue-equivalent proportional counters with built-in a-particle sources. Proc. 6th Symp. on Neutron Dosimetry, München, 1987 (H. Schraube, G. Burger, J. Booz, Eds.), CEC, EUR 11663, Rad. Prot. Dosim., 23, 249- 252 (1988).

Pihet P. and Menzel, H.G. Atomic data required in accurate measurements of kerma for neutrons with low pressure proportional counters. Proc. Advisory Group Meeting - Atomic and Molecular Data for Radiotherapy, Vienna, 1988, IAEA-TECDOC-506, 91-105 (1989).

Pihet, P., Menzel, H.G., Alberts, W.G. and Kluge, H. Response of tissue-equivalent proportional counters to low and intermediate energy neutrons using a modified Te-^{3}He gas mixtures. IN Proc. Workshop on Implementation of dose equivalent meters based on microdosimetric techniques in radiation protection,Schloss Elmau (FGR), 1988 (H.G. Menzel, H.G. Paretzke and J.J. Booz, eds.), Rad. Prot. Dosim., 29, 113-118 (1989).

Dahmen, P., Menzel, H.G., Grillmaier, R.E. Dosimetry of photons with low pressure proportional counters. In Proc. Workshop on Implementation of dose equivalent meters based on microdosimetric techniques in radiation protection, Schloss Elmau (FGR), 1988 (H.G. Menzel, H.G. Paretzke and J.J. Booz, eds.), Rad. Prot. Dosim., 29, 81-85 (1989).

Schuhmacher, H., Kunz, A., Menzel, H.G., Coyne, J.J. and Schwartz, R.B. The dose equivalent response of tissue equivalent proportional counters to low energy neutrons. Proc. 10th Symp. on Microdosimetry, Rome, 1989. Rad. Prot. Dosim. (in press).

2.

Bühler, G., Anwendung mikrodosimetrischer Methoden für die Dosimetrie und Messung von Ionisationsverteilungen mit metallischen Proportionalzählern für Neutronen zwischen 13.9. MeV und 19 Mev Energie. Thesis, Universität des Saarlandes, Saarbrücken, (1985).

Dahmen P., Untersuchungen mit Niederdruck-Proportionalzählern über den Einfluss verschiedener Wandmaterialien und die Energiedepositionsspektren und die Anwendbarkeit des Bragg-Gray-Prinzips für y-Strahlen. Diplomarbeit, Universität des Saarlandes, Saarbrücken (1988).

Pihet, P., Etude microdosimetrique de faisceaux de neutrons de haute energie. Applications dosimetriques et radiobiologiques, Thesis, Louvain-la-Neuve (1989).

Pihet, P. and Menzel, H.G. Kerma ratio in carbon and in A-150 TE Plastic for neutrons from 5 to 60 MeV measured with low pressure proportional counters. In Proc. International Workshop on particle therapy, Essen 1988. Strahlentherapie (abstract)(in press.).

Title of the project no.: 2

Investigation of practical aspects of employing microdosimetric counters as dose equivalent meters

Head(s) of project: H.G. Menzel

Scientific staff: Bühler,G.,Dahmen,P.,
Folkerts,K.H.,Kunz,A.,
Pihet, P., Schuhmacher, H.

I. Objectives of the project:

Radiation protection dosemeters based on tissue equivalent proportional counters (TEPC) have been shown to have very good energy response for neutrons in terms of operational quantities such as $H^*(10)$ and to possess diagnostic capabilities for mixed radiations. The construction of a portable area monitor based on a TEPC will be completed and the instrument will be tested in calibrated neutron and mixed radiation fields and in radiation environments of practical importance. The construction will be optimised with regard to the requirements of operational health physics and with regard to its dose equivalent response.

II. Objectives for the reporting period:

To carry out further measurements with the portable prototype TEPC area dosemeter in radiation environments of practical interest. To implement the established optimisation procedures with regard to calibration, operation, neutron-photon discrimination in the hardware and software of the area dosemeter. To complete the study of the influence of ^{3}He-gas additions and wall thickness on the dose equivalent response. To build several identical TEPC area dosemeters to be used by operational health physic at different institutes.

III. Progress achieved:

SUMMARY :

The work in this project was concentrated on the construction and implementation of a portable area monitor based on tissue-equivalent proportional counters (TEPC) suitable for routine application in operational radiation protection. The suitability of the newly developed system ("HANDI") was tested in reference neutron and photon fields and in radiation environments of practical importance by comparison with our standard laboratory equipment for experimental microdosimetry ("BIO"), and with different TEPC instruments developed by other laboratories. This collaboration was coordinated by EURADOS Committee 1. In particular, our laboratory was actively involved in the intercomparison of TEPC dose equivalent meters organised by EURADOS and Physikalisch Technische Bundesanstalt PTB (Braunschweig, FRG) and its evaluation. In addition separate and more detailed experiments were performed in the same reference fields with the aim to provide a basis for further improvement of the dose equivalent response of TEPC's at low neutron energies.

A prototype of our area monitor "HANDI" became operational at approximately the middle of the contractual period. A second version using improved analog and digital electronics developed by CAD techniques was finished towards the end of the project and consists of a portable battery powered instrument suitable for semi-industrial production. The relatively simple mode of operation enables the instrument to be used for routine operational health physics work. The two produced versions showed the anticipated technical and physical performance. In particular, no significant decrease in accuracy or loss in diagnostic capacity was observed if compared to the laboratory equipment.

Measurements with the HANDI system, and partly with BIO, were performed at medical irradiation facilities, high energy accelerators, a nuclear power reactor and a nuclear fuel processing industrial plant. In some cases comparisons could be made with other neutron dose equivalent meters. These measurements documented the principal suitability of the HANDI system for operational applications and provided evidence for the usefulness of the diagnostic information only available from TEPC area monitors in particular instruments equiped with spectra storage capabilities such as HANDI.

Detailed and comprehensive measurements with TEPC's in reference photon and neutron fields at PTB and at National Institute for Science and Technology (NIST, formely NBS, Washington DC, USA) provided useful data on radiation transport and interaction processes in the counter wall and gas. The resulting quantitative understanding of the detector response showed that the too low dose equivalent response at low neutron energies can be substantially improved and was used to investigate the feasibility of a TEPC to be used as a reference or transfer instrument.

The original objectives of the project have been achieved. The operational version of our portable area monitor provides the basis for further improvement in

order to construct a truly hand-held system. This step forward however implies that the detector itself is incorporated within the electronic package. This objective was delayed in order to enable the final design of the counter accounting for optimum parameters with regard to dose equivalent response. This optimisation became possible from the basic data accumulated during the contractual period. Furthermore the capability of the present version for further miniaturisation of the electronic will enable the reduction of size, power consumption and therefore weight to maintain and improve the practical suitability of the final instrument for routine application in radiation protection. It will also include technical improvements resulting from the practical experience gained with the existing versions at several different institutes.

METHODS :

Measurements with low pressure tissue equivalent proportional counters (TEPC) were performed in the environment of different accelerators and at nuclear facilities using a counter made of A-150 tissue substitute plastic with an inner diameter of 59 mm and a wall thickness of 2.5 mm. The counter was filled with propane based TE gas at a pressure resulting in a simulated tissue diameter of 2 µm. Measurements with this counter were performed using our microdosimetric laboratory system (named "BIO") and our microprocessor based portable area monitor "HANDI" (Homburg Area Neutron Dosimetry Instruments). The laboratory system used conventional analog electronics based on three linear amplifiers and linear analog-to-digital (ADC) converters (3k channels) operating simultaneously to cover a range in lineal energy (y) from 10^{-2} to 10^{4} keV.µm^{-1} after redistribution of the linear subspectra on a logarithmic scale in y by software. For the system HANDI a quasi-logarithmic ADC (16 channels) was developed to cover a similar lineal energy range and to enable the construction of a portable and autonom survey instrument (Kunz et al., 1989).

The development of the prototype version of the HANDI system initiated during the previous research programme was completed by constructing analog-digital electronics specifically designed to develop a portable equipment. Based on the experience gained with the first version a second and improved instrument has been constructed by designing newly all electronic components using CAD-techniques in order to be able to build a hand-held instrument with low power consumption and small physical size. To date the area monitor is equiped with commercially available TEPC's with 59 mm inner diameter.

Although the TEPC dose equivalent response is good for neutrons with sufficiently high energy, the dose equivalent readings for neutrons below a few hundred keV are considerably too low. Several parameters (thickness and mass of the wall, composition of wall and gas, simulated diameter, software) may be varied in order to improve the TEPC response in the low and intermediate neutron energy range. The influence of the counter wall thickness on the TEPC response was assessed by using counters with additional caps of different thicknesses (up to 32 mm) in neutron fields of different energies produced at the PTB

(Schuhmacher et al., 1985). As an alternative and complementary approach TEPC's filled with counting gas mixtures containing small amounts (0.1, 0.5 and 1 %) of ^{3}He were used in the same fields in order to evaluate the increase of the TEPC response due to the moderation of low energy neutrons in the counter wall and to the large cross section of the ^{3}He(n,p)^{3}H reaction for thermal neutrons (Pihet et al., 1989). Furthermore measurements performed by combining the two techniques of using ^{3}He-gas mixtures and variable wall thicknesses enabled a quantitative assessment to be made of the influence of the competing processes attenuation and thermalization on absorbed dose and dose equivalent as a function of neutron energy. So far these experiments were only performed with small TEPC's (12.7 mm in diameter) and the laboratory system BIO.

TEPC measurements were performed around the pulsed radiation fields of medical electron accelerators (Schuhmacher and Kraus, 1986). The time structure of these pulsed beams can lead to problems due to the necessity of the TEPC method to analyse single events. At too high photon dose rates pulse pile-up may occur which leads to an increase in quality factor and thus dose equivalent. For these experiments therefore small TEPC's with 12.7 mm inner diameter were used in order to decrease the count rates for a given dose rate and to minimize pile-up of events.

TEPC measurements with BIO and HANDI systems were evaluated in terms of the dose distributions in lineal energy d(y) and when possible related to the neutron fluence. The absorbed dose was derived from the integral of the spectra. The dose equivalent was obtained using the conventional method using the approximation of the quality factor $Q(L_\infty)$ defined by the ICRP (ICRP Publication 21, 1973) by a function Q(y) where L_∞ is set numerically equal to y (Menzel et al., 1988). The integral of the weighted dose distribution Q(y).d(y) provided the mean quality factor for the field. For calibrated fields, the TEPC dose equivalent response was evaluated as the ratio of the measured dose equivalent with respect to the reference ambient dose equivalent $H^*(10)$. Neutron-gamma discrimination was achieved by two different methods depending on the photon energy spectra present in the mixed fields.

RESULTS :

Technical development. The portable, battery powered, TEPC area monitor HANDI has been developed (Kunz et al., 1989). The operational version currently achieved is integrated in a 19 inch rack with a total weight (without detector) of 6 kg including 2.5 kg for the NiCd battery pack. The instrument consists of a complete data acquisition and analysis system and includes a miniaturized adjustable high voltage supply. The maximum total power consumption is 5 W.

The analog part of the portable system consists of a low noise charge preamplifier (Radeka,Proc. Symp. Nuclear Electronics, 1968) and two newly designed linear amplifiers with gain ratio of 1 to 100. These amplifiers use a common pole-zero stage and pulse forming stages based on two poles low-pass

filters. The pulse height analysis system has been specifically designed to perform fast pulse processing over a large dynamic range by developing a quasi-logarithmic ADC to cover up to 4 orders of magnitude with 16 channels. This ADC is based on a flash converter with 16 fast comparators operating in parallel and with a non-linear quantization characteristic determined by a resistor network. A single board computer (SBC) microprocessor associated to a 4k memory buffer achieves the on-line evaluation of the data (absorbed dose and dose equivalent rates, time, count rate) and their display in real time. The SBC memory stores the accumulated 16-channels dose spectra to be read out over a RS 232 serial line.

Comparative measurements in various reference fields and practical radiation environments were performed with the HANDI system and with our conventional microdosimetric laboratory system BIO (Folkerts et al., 1988). An example is given in Figure 1. Considering all measurements currently performed at the facilities visited an agreement better than 20 % was observed between the two systems showing the suitability of the 16-channels method adopted in HANDI with no significant loss of accuracy. Thus the reduced pulse height resolution in HANDI does not significantly influence the evaluation of radiation quality parameters and maintains the diagnostic capabilities of the instrument. In particular HANDI enables neutron-gamma discrimination to be performed with appropriate software adjustments in order to take the photon energy distributions observed in the specific mixed radiation field into account (Kunz et al., 1989).

Measurements in calibrated radiation fields. Both HANDI and BIO measuring systems were used within the two intercomparisons of seven TEPC area dosemeters carried by EURADOS Committee 1 in the calibrated fields produced at the PTB (Dietze et al., 1988; Menzel et al., 1989). The measurements were performed with neutrons of thermal energies up to 144 keV produced at the filtered neutron beams of the reactor and for monoenergetic neutrons with energy ranging from 0.073 MeV up to 14.8 MeV produced by the accelerator. They were also performed in the fields of ^{60}Co photons and of D_2O moderated ^{252}Cf reference sources. Details of the intercomparisons and the results obtained may be found in several PTB reports, in a CEC Report (Report EUR 11867 EN, 1988) and in the proceedings of a Workshop held at Schloss Elmau, FRG (Rad. Prot. Dosim., Vol. 29, 1989).

The results of the intercomparison confirmed the agreement between BIO and HANDI systems. The ratio of their dose equivalent readings at all energies was 0.94 with a standard deviation of 0.07. For absorbed dose the ratio was 1.01 with the same standard deviation. With regard to either absorbed dose or dose equivalent rate, the intercomparison showed similar variation of the responses as a function of neutron energy for all TEPC area monitors with a characteristic decrease of the response with decreasing neutron energy in particular below 500 keV. Comparing the responses of the different instruments significant differences were observed which can be attributed to different calibration procedures and counter geometries. These differences, however, resulted in a standard deviation of less than 10 %.

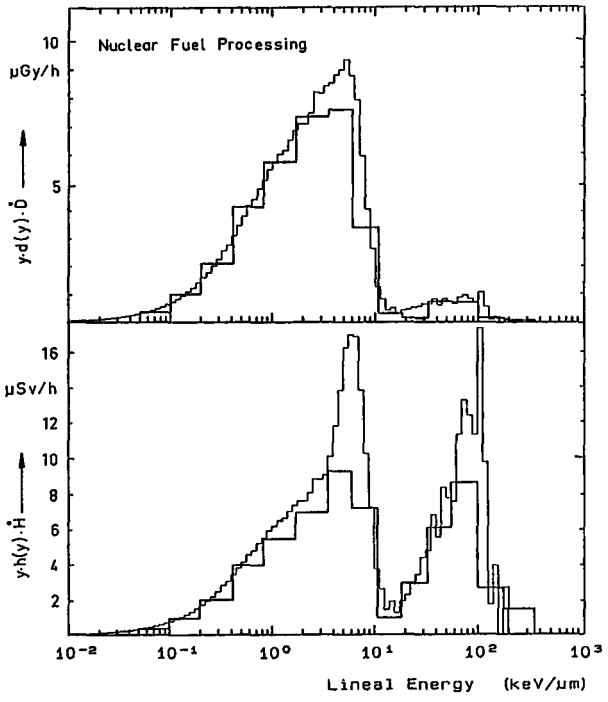

Figure 1.
Comparison of absorbed dose (top) and dose equivalent (bottom) distributions in lineal energy measured with BIO laboratory system (thin line) and HANDI area monitor (thick line) at a nuclear fuel processing plant (UO_2+PuO_2). The spectra are normalised to absorbed dose rate and dose equivalent rate respectively. They show a high photon dose component discriminated from the neutron component at the level of 10 keV.μm^{-1}. From Kunz et al., 1989.

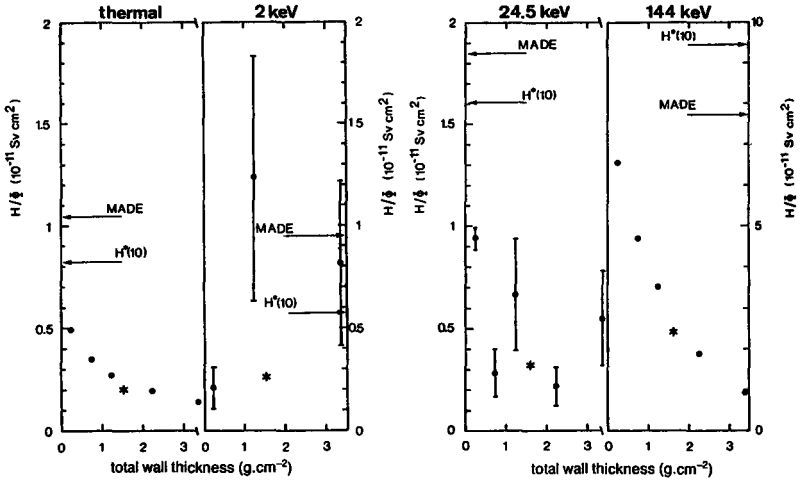

Figure 2. Dose equivalent per unit neutron fluence attenuation curves for low energy neutrons derived from the lineal energy spectra measured with a TEPC (59 mm inner diameter, BIO system) exposed with additional cap thicknesses. Error bars denote 1 SD of the statistical uncertainty. Reference values for MADE and H*(10) operational dose equivalent quantities and calculated response (star) are indicated for comparison. From Schuhmacher et al., 1985.

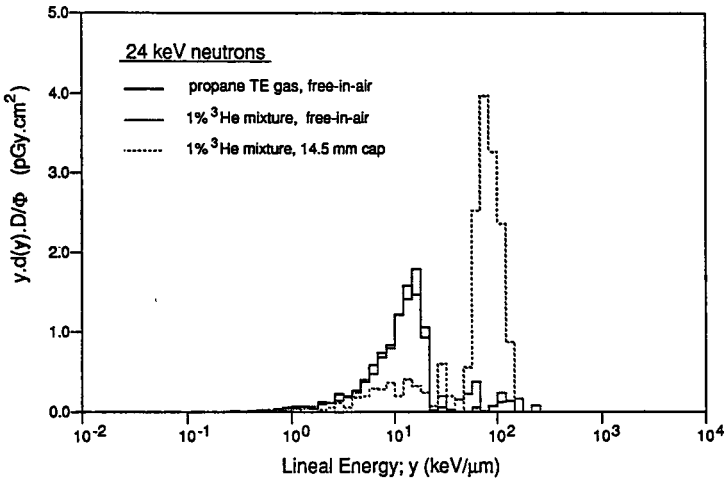

Figure 3. Fluence normalised dose distributions of lineal energy measured for 24.5 keV neutrons with TEPC's (12.7 mm inner diameter, BIO system) by using normal TE gas and modified ^{3}He-TE gas mixtures, and with different wall thicknesses. The peak corresponding to neutron capture reaction events by thermal neutrons with ^{3}He is seen at about 100 keV.μm^{-1}. From Pihet et al., 1989.

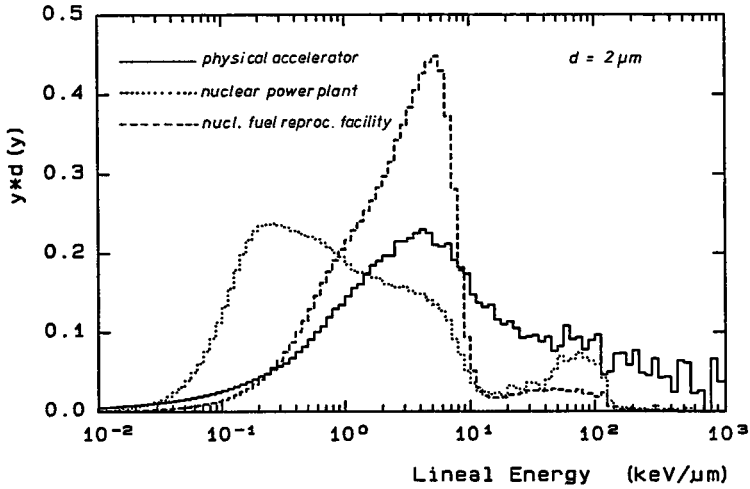

Figure 4. Variation of radiation quality observed in the environment of different facilities. Large differences in the relative neutron and photon dose components are seen. The spectra provide additional information about the neutron and photon energy spectra present in the mixed fields. These measurements were performed using the BIO system. Similar measurements are currently carried out with the newly developed HANDI portable area monitor (Figure 1). From Folkerts et al., 1988.

The intercomparison showed clearly that the capability of the dosemeters to store and display the energy deposition spectra is an important advantage for the interpretation of the data. As an example the comparison of the spectra measured by the KFA (Jülich) system (reference) and by our HANDI revealed that the differences in response at low neutron energies is explained by differences in attenuation of the primary neutrons and in the degree of thermalization of neutrons due to differences in counter wall thickness (20 or 15 mm KFA, 2.5 mm for HANDI).

The too low dose equivalent response of TEPC's in the low and intermediate neutron energy range is related to the short range of the recoil protons compared to the size of the simulated volume and by the transport of the neutrons in the detector wall (Menzel, 1985). In addition to the measurements performed within the EURADOS intercomparisons, two detailed investigations were performed in the same beams in order to study these effects and to find the optimum parameters of TEPC with regard to dose equivalent response (Schuhmacher et al., 1985; Pihet et al., 1989).

Measurements were performed in the low energy neutron fields of the reactor at the PTB using PC's with additional caps of different thicknesses. These experiments provided useful data expressed in terms of dose equivalent per unit fluence attenuation curves (Figure 2) and the related spectra. The results were found in excellent agreement with those of published neutron transport calculations (Kawecka et al., Rad. Prot. Dosim., 9, 203-206,1984) and confirmed that the wall thickness is a suitable parameter to influence the TEPC response at low and intermediate neutron energy. The data, however, showed that there does not exist a wall thickness which would result in a optimum dose equivalent reading at all energies. Our study led to the conclusion that for neutron spectra likely to be encountered in practice a counter of not more than 5 mm wall thickness will be the best choice.

An improved solution was investigated using a complementary approach. The measurements were repeated for the same fields with PC's filled with gas mixtures containing ^{3}He combined with variable wall thicknesses. The effect of adding ^{3}He to the counting gas mixture is illustrated in Figure 3 for 24.5 keV neutrons. The peak due to the proton recoils of the neutron capture reaction with ^{3}He is clearly seen. This results not only in a higher absorbed dose but also in a higher quality factor and therefore in a large influence on the dose equivalent response. The figure shows also the large effect of adding ^{3}He and increasing the wall thickness in the same time. As an example, for the measurements shown in the figure (24.5 keV neutrons), the dose equivalent response increases by factor of 1.5 for the counters filled with 1 % ^{3}He-gas with 2.5 mm total wall thickness and by a factor of 3.3 for a wall thickness of 8.5 mm compared with the counter filled with normal TE gas and 2.5 mm wall thickness. The results showed that the principle of separation of the neutron and photon dose components is not influenced by small amounts of ^{3}He for the fields investigated.

A detailed study of the bare and moderated ^{252}Cf reference source of the PTB was performed using different TEPC's, cap thicknesses and gas mixtures as

described above (Schuhmacher et al., 1987; Pihet et al., 1989). An excellent agreement was observed between measured values for absorbed dose and calculated fluence-to-kerma conversion factors. The results confirmed the conclusion drawn on the basis of the measurements for monoenergetic neutrons that thin walled counters are suitable for broad neutron energy spectra. Small addition of ^{3}He did not significantly modify the response for thin counters, however it increased the response by about 10-20 % with somewhat thicker walls (about 8-9 mm total wall thickness). Some measurements were performed in front and within a phantom. Attention was given to an accurate separation of the neutron and photon dose components with a quantitative assessment for the relative contribution of primary photons and of secondary photons produced in the phantom and the counter wall.

Measurement in practical radiation environments. TEPC measurements with BIO and HANDI systems were performed in practical radiation environments encountered in radiation protection. They include : medical electron accelerators (15 MV X-rays) (Schuhmacher and Krauss, 1986) and 25 MV X-rays; high energy accelerators (PSI, Villigen; UCL, Louvain-la-Neuve) (Menzel et al., 1986; Folkerts et al., 1988); neutron therapy facilities (Pihet et al., 1987; Vynckier et al., 1988; Sabattier et al., 1989); a nuclear power plant and a fuel processing industry (Folkerts et al., 1988; Kunz et al., 1989). The results of these measurements were expressed in terms of dose equivalent rate and related lineal energy spectra (Figures 1,4).

The spectra measured with TEPC's showed large variations of radiation quality in the vicinity of neutron and photon producing radiation sources and showed the suitability of the instrument to detect and analyse these variations (Figure 4). The variation of radiation quality often is mainly due to variations in the relative photon and neutron components without large variations in the neutron quality factor. At some facilites, however, in particular in the environment of high energy particle accelerators and in nuclear fuel processing but also at some nuclear power plants, significant variation of the neutron quality factor for different locations and work places has been observed.

The use of software for the evaluation of quality factors and dose equivalent in the TEPC method enables also different quality functions Q(y) to be applied and tested. For example, if the function proposed in ICRU 40 is compared to the Q(y) based on ICRP 21 considerable differences in the quality factors for monoenergetic neutrons and for photons are obtained. However, for mixed radiations the differences are not very pronounced.

The diagnostic capacity of TEPC based instrument was used in order to analyse in more details local variations of radiation quality. Measurements performed in the treatment rooms, mazes and control rooms at therapy irradiation facilities showed the influence of the shielding material used and the geometrical arrangement on dose equivalent and radiation quality. At a nuclear fuel processing plants (UO_2+PuO_2), measurements in working areas and storage rooms enabled the identification of neutron components from spontaneous fission and (α,n)

reactions. The spectra provided also information on the energy of photons present in the fields. This led to the use of different methods of separation for the neutron and photon components based either on the comparison with pure photon spectra (suitable in nuclear power plants, Figure 4) or the selection of a lineal energy treshold (suitable nuclear fuel processing, Figures 1 and 4).

An important aspect of the measurements in radiation environments of practical interest is the comparison with results obtained by other methods, in particular with the widely used moderator type neutron dose equivalent meter ("rem-counter"). Such an instrument was also included in the EURADOS intercomparison. In general, good agreement was found between TEPC and rem-counters for broad neutron spectra not extending to too high energies as encountered e.g. behind shieldings at reactors or other facilities. In presence of a high energy neutron component, as present in the environment of high energy accelerators, large differences of factors up to three were observed. This has to be attributed to the very low dose equivalent response of rem-counters at energies above 5-10 MeV. The difference is also significant if a large monoenergetic component is contained in the neutron energy spectrum as found behind shielding consisting predominantly of steel. The TEPC appears to offer advantages over rem-counters not only because of the flatter dose equivalent response but also because it reveals radiation quality differences and variations at work places.

The comparison with the results obtained by the multisphere system DINEUTRON showed in general much larger discrepancies.

DISCUSSION :

The portable TEPC area monitor HANDI designed and built by our laboratory fulfils most of the requirements of a routine survey instrument without significant losses in accuracy and diagnostic information if compared to a full scale laboratory equipment. The currently used version is a hand-held instrument (weight 6 kg) which is fully battery operated (40 hours operation time). The actual design insures minimum operator control and easy handling for routine use by persons working in the field of operational radiation protection. It displays in real time dose equivalent (rate) and absorbed dose (rate). Optimally the photon dose component and the quality factor can be read out. For additional diagnostics the lineal energy spectrum accumulated since the last reset is available via an interface. The instrument uses dedicated CAD designed electronic circuits suitable for semi-industrial production. The application of SMD techniques will further reduce the size and weight of the electronic components to about 25 %. A new single board computer in CMOS technique will provide considerable improvements with regard to the required hardware and power consumption which will be reduced by a factor of 2. This will provide either longer operating time or reduced weight due to the reduction in weight of the batteries.

The currently used HANDI version appears sufficiently progressed to be used by physicists involved in radiation protection dosimetry without any specific experience in the TEPC technique. Several models of this version (up to 10) are

being built in our laboratories to be used in institutes where neutron and mixed radiations are encountered. There will be a close co-operation with these institutes in order to incorporate experiences gained in routine applications into the design and construction of the final version.

TEPC area monitors have specific properties not available in other dose equivalent meters which may be of advantage in general or in particular tasks. The use of the digital electronics and software to evaluate the various quantities allows modifications to be easily introduced either because of official changes in conversion factors or quality factors or because of desired changes in response or operation (e.g. introduction of dose rate alarm). The detailed diagnostic information available (neutron and photon dose component, quality factors, lineal energy spectra) extends the range of applicability. These applications can include investigation of shielding effects, interpretation of complex and high energy radiation fields as encountered at particle accelerators or in space dosimetry and the use as a transfer or reference instrument.

The suitability of a TEPC area monitor, and in particular of our HANDI system, for routine use in operational area monitoring depends also on the following criteria:

Sensitivity : The statistical uncertainty in the determination of dose equivalent with a TEPC depends on both, the count rate and the pulse height distribution and therefore is a complex function of radiation quality and other parameters such as counter geometry. In the field of D_2O moderated ^{252}CF source and for a dose equivalent rate of 20 $\mu Sv h^{-1}$ with over 59 mm diameter counter a statistical uncertainty of 20 % would be achieved after approximatly 6 min as compared to 1 min of a rem-counter of the LEAKE type is used. However, increase of the counter diameter by a factor of 2 decreases required time by a factor of 4. Thus it can be concluded that TEPCs can be made sufficiently sensitive for all operational conditions of practical interest.

Energy dependence of dose equivalent response : Although the dose equivalent response curve for existing TEPCs is flatter than that of any other neutron dose equivalent meter there is a marked and undesired decrease for neutron energies less than several 100 keV. Optimisation of the response in this energy range has been started but is not yet completed. An original solution was assessed and tested in reference fields based on adding up to several percent of ^3He to the counting gas. Other parameters to be optimized are geometry of counter (wall thickness, size), material composition of wall and counter gas, effective cavity size and evaluation algorithm. On the base of available results it appears feasible to achieve a response of $\pm$ 50 % in the energy range between thermal neutrons and 20-50 MeV.

Cost : The commercial feasibility of TEPC based area monitors is still not known. It will depend on the range of application (conventional area monitoring, survey and investigation, reference and transfer instrument) and the size of the market. It will also depend on whether improved precision will be required in future due to modifications in dose limits and quality factors.

IV. Other research group(s) collaborating actively on this project [name(s) and address(es)]:

Physikalisch-Technische Bundesanstalt (PTB),Gr. Neutronendosimetrie (Dr. G. Dietze), Gr. Metrologie der Reaktorneutronen (Dr. W. Alberts), Braunschweig, FRG
Deutsches Krebsforschungszentrum (DKFZ),Abt. Strahlen-schutz und Dosimetrie (Dr.G.Hartmann), Heidelberg, FRG
Université Catholique de Louvain, UCL, Unité de Radio-biologie et de Radioprotection (Prof. A. Wambersie), Bruxelles, Belgium
National Physical Laboratory (Drs. J. Hunt and A.J. Waker), Teddington and University of Leeds, U.K.
EURADOS Committee 1
Neutron Therapy Facility, CHRO-CNRS (Dr. R. Sabattier),Orléans, France
Paul Scherrer Institute, PSI, (Dr. F. Cartier), Villigen, Switzerland

V. Publications:

1.

Menzel, H.G., Practical implementation of microdosimetric counters in radiation protection. Proc. 5th Symp. on Neutron Dosimetry, Munich, 1984 (H. Schraube, G. Burger, J. Booz, Eds.), CEC, EUR 9762, 287 - 3O5 (1985).

Schuhmacher, H., Menzel, H.G., Bühler, G. and Alberts, W.G., Experimental basis for optimisation of the wall thickness of microdosimetric counters in radiation protection. Proc. 9th Symp. on Microdosimetry, Toulouse, 1985 (J.A. Dennis, J.J. Booz and B. Bauer, Eds.), CEC, EUR 9644, Radiat. Prot. Dosim., 13, 341 - 345 (1985).

Schuhmacher, H. and Krauss, O., Area monitoring of photons and neutrons from medical electron accelerators using tissue-equivalent proportional counters. Radiat. Prot. Dosim., 14, 325 - 327 (1986).

Menzel, H.G., Schuhmacher, H. and Cartier, F., Radiation protection dosimetry of neutrons and photons at a high energy accelerator using a low pressure proportional counter. IN Proc. of 4th European Congress and 13th Regional Congress of the International Radiation Protection Association. Austrian Association for Radiation Protection, 597 - 6O2 (1986).

Menzel, H.G., Applications of microdosimetry in radiation protection. In Radiation Research, Proc. 8th Int. Congress of Radiation Research, Edinburgh, 1987 (Fielden E.M., Fowler J.F., Hendry J.H., Scott D., eds.), 345 - 350 (Taylor and Francis, London) (1987).

Schuhmacher, H., Menzel, H.G., Kluge, H., Dosimetry of a bare and a D_2O moderated ^{252}Cf source using low pressure proportional counters. Radiat. Prot. Dosim., 19, 1O3-1O9 (1987).

Menzel, H.G., Dietze, G., Schuhmacher, H., Practical determination of dose equivalent using low pressure proportional counters, in "Radiation Protection Practice", Proc. of. 7th Int. Congress of the Int. Radiation Protection Association, Sydney, April 1988, S. 308 - 311, Pergamon Press (1988).

Folkerts, K.H., Menzel, H.G., Schuhmacher, H., Arend, E., TEPC radiation protection dosimetry in the environment of accelerators and at nuclear facilities. Proc. 6th Symp. on Neutron Dosimetry, München, 1987 (H. Schraube, G. Burger, J. Booz, Eds), CEC, EUR 11663, Radiat. Prot. Dosim. 23, 261 - 264 (1988).

Vynckier, S., Sabattier, R., Kunz, A., Menzel, H.G., Wambersie, A., Determination of dose equivalent and the quality factor in the environment of clinical neutron beams. Proc. 6th Symp. on Neutron Dosimetry, München, 1987 (H. Schraube, G. Burger, J. Booz, Eds), CEC, EUR 11663, Radiat. Prot. Dosim. 23, 269 - 272 (1988).

Dietze, G., Booz, J., Edwards, A.A., Guldbakke, S., Kluge, H., Leroux, J.B., Lindborg, L., Menzel, H.G., Nguyen, V.D., Schmitz, Th., Schuhmacher, H., Intercomparison of dose equivalent meters based on microdosimetric techniques. Proc. 6th Symp. on Neutron Dosimetry, München, 1987 (H. Schraube, G. Burger, J. Booz, Eds), CEC, EUR 11663, Radiat. Prot. Dosim. 23, 227 - 234 (1988).

Pihet, P., Menzel, H.G., Alberts, W.G. and Kluge, H., Response of tissue-equivalent proportional counters to low and intermediate energy neutrons using a modified TE-^{3}He-gas mixtures. In Proc. Workshop on Implementation of dose equivalent meters based on microdosimetric techniques in radiation protection, Schloss Elmau (FRG), 1988 (H.G. Menzel, H.G. Paretzke and J.J. Booz, eds.), Rad. Prot. Dosim. ,29, 113 -118 (1989).

Kunz, A., Menzel, H.G., Arend, E., Schuhmacher, H. and Grillmaier, R.E., Practical experience with a prototype TEPC area monitor. In Proc. Workshop on Implementation of dose equivalent meters based on microdosimetric techniques in Radiation Protection, Schloss Elmau (FRG), 1988 (H.G. Menzel, H.G. Paretzke and J.J. Booz, eds.), Rad. Prot. Dosim. ,29, 99 -104 (1989).

Menzel, H.G., Lindborg L., Schmitz, Th., Schuhmacher, H. and Waker, A.J., Intercomparison of dose equivalent meters based on microdosimetric techniques in Radiation Protection. In Proc. Workshop on Implementation of dose equivalent meters based on microdisimetric techniques in Radiation Protection, Schloss Elmau (FRG) (H.G. Menzel, H.G. Paretzke and J.J. Booz, eds.), 1988, Rad. Prot. Dosim. ,29, 55 - 68 (1989).

Sabattier, R., Pihet, P., Bajard, J.C., Noale, M., Menzel, H.G. and Breteau, N., Radioprotection à L'Unité de neutronthérapie d'Orléans. Radiation Protection GEDIM, 24, 123-132 (1989).

Schuhmacher, H., Kunz, A., Menzel, H.G., Coyne, J.J. and Schwartz, R.B. The dose equivalent response of tissue equivalent proportional counters to low energy neutrons. Proc. 10th Symp. on Microdosimetry, Rome, 1989. Rad. Prot. Dosim. (in press).

2.

Pihet, P., Meulders, J.P., Marquebreucq, S., Menzel, H.G., Wambersie, A., Dose equivalent determined by tissue-equivalent proportional counters in the environment of the neutron therapy facility at Louvain-la-Neuve, Brit. Journ. Radiol., 60, 311 (1987) (abstract).

Menzel, H.G., A study of the National Physical Laboratory microdosimetry research programme in collaboration with the University of Leeds, NPL Report RS (EXT) 93 (1987).

Dietze, G., Edwards, A.A., Guldbakke, S., Kluge, H., Leroux, J.B., Lindborg, L., Menzel, H.G., Nguyen, V.D., Schmitz, Th. and Schuhmacher, H., Investigation of radiation protection instruments based on tissue-equivalent proportional counters. Results of a Eurados intercomparison. Commission of the European Communities, CEC Report EUR 1 1867 EN (1988).

RADIATION PROTECTION PROGRAMME
Final Report

Contractor:

Polytechnic of the South Bank
Borough Road
GB London SE1 0AA

Contract no.: BI6-A-025-UK

Head(s) of research team(s) [name(s) and address(es)]:

Dr. A.C. Norris
Dept of Phys.Sc.& Techn.
Polytechnic of the South Bank
Borough Road
GB London SE1 0AA

Dr. A.K.M.M. Haque
Dept of Phys.Sc.& Techn.
Polytechnic of the South Bank
Borough Road
GB London SE1 0AA

Telephone number: 1-928.89.89

Title of the research contract:

Computation of the radiation dose due to the daughter products of radon deposited in the lung.

List of projects:

1. Computation of the radiation dose due to the daughter products of radon deposited in the lung.

Title of the project no.: BI6-A-025-UK

Computation of the radiation dose due to the daughter products of radon deposited in the lung

Head(s) of project:

DR A K M M HAQUE

Scientific staff:

Dr I A M Al-Affan
Research Fellow

I. Objectives of the project:

Human exposure to radon and its daughter products,even in normal living and working conditions,could amount to a substantial proportion of the total exposure to natural radiation. A comprehensive computation of the radiation dose to the lungs would be valuable in view of the new information on aerosols,lung parameters,stopping power etc..

II. Objectives for the reporting period:

The objectives of the research project over the period, 1985-1989, were to compute first the radiation dose in details following the deposition of the daughter products of radon in the lungs; to compare extensively our dose calculation results with those of other authors; to carry out microdosimetric study of the energy deposition distribution in the sensitive targets; finally, to estimate the lung cancer risk on the basis of oncogenic transformation following alpha particle irradiation of mammalian cells,and by epidemiological studies of lung cancer deaths.

III.

1. Introduction

It has been confirmed in recent years that the radiation dose following inhalation of radon and its daughters products contribute about 50% of the total annual dose to the general public from natural and man-made sources. Although the risk of lung cancer due to radon and its daughters has been studied since the end of the last century, particularly in uranium mines, the risk cannot at present be accurately evaluated. This is attributed to several factors, physical as well as chemical and biological, which contribute to the uncertainty in dose calculations and risk assessment.

However, the study of the hazard due to radon and its decay products has been extended in recent years to dwellings due to the discovery of high radon concentrations in the dwellings of many countries and due to changes in living conditions. The awareness of radon hazard in dwellings has been reflected in the Radiation Protection Programmes of the CEC. The efforts have taken different directions in order to improve the risk assessment. For example, there has been extensive epidemiological studies of the workers in underground mines on the association of human lung cancer with exposure to radon and its decay products. These case-control studies have in recent years been extended to dwellings.

The other direction in which there has been considerable activity is the calculation of the dose based on more accurate information on the alpha particle stopping power in tissue-equivalent materials, detailed information on aerosol size distribution, activity median diameter, deposition of the activity in the respiratory tracts etc. In addition, recent studies have shown that the secretory cells lining the airways could be just as important as the basal cells as tumour induction sites. This fact has led to a significant change in the philosophy of lung dosimetry, in that a new awareness has developed for the need for a detailed dose calculation in the sub-regions of the lung.

The aims of the research reported here were to compute first the radiation dose due to the decay products of radon deposited in the lung, to compare in details our results with the work of other authors and finally to estimate the risk on the basis of oncogenic transformation following alpha particle irradiation of mammalian cells.

The work has included:

i) Refinement of the dose calculation with improved data on lung models, aerosol parameters, deposition and clearance mechanisms.

ii) Formulation of the phase effect and the straggling of energy loss,and their influence on the dose calculations.

iii) Extensive analysis of results and comparison with the calculations of previous authors.

iv) Microdosimetric study of the energy deposition distribution in the sensitive target of interest (ie. lung cell nucleus).

v) Lung cancer induction model employing the information on lung cells, their radiosensitivity and distribution.

vi) Monte Carlo simulation of the dosimetry of the lung.

It is to be noticed that during the present CEC programme, attention and efforts have increased in order to understand better the problem of radon (NCRP 1984 Rep. 78, ICRP 1987 Rep. 50 and BEIR IV, 1988). In the following the details of the progress made during the present contract will be presented in outline.

2. Calculations of absorbed dose

The radiation dose to the airways is assumed to be due to alpha particles from RaA and RaC' only (because they are the only alpha emitters with short half-lives). The dose is obtained by summing the energy deposited in a $1\mu m$ diameter sphere of tissue in the condensed state, at different depths from the mucus-tissue interface. The calculations were carried out mainly using the Weibel model, although some limited comparisons have been made with the Yeh and Schum morphometry.

The energy deposited in the spherical volume has been calculated in terms of equilibrium activity (the activity attaining a constant value for each of RaA, RaB, and RaC) mixed uniformly with a $15\mu m$ thick mucus.

The main factors affecting the lung dose calculation are as follows.

2.1 Diffusion coefficent of the unattached daughters

The unattached daughter products may not be a single chemical species, but depending on the conditions, may be hydrated or react chemically with oxygen or other gases of the atmosphere. Hence, Prostendorfer and Mercer (Atmos. Env. 12, 2223, 1978) suggested D to be 0.085 cm^2s^{-1}, whereas Knutson et al (Hlth. Phys. 45, 445, 1983) and Harley and Pasternack (Hlth. Phys. 42, 789, 1982) considered it to lie in the range 0.0025–0.005cm^2 s^{-1}. Haque and Al-affan (BNES, 171, 1987) have recommended D to be 0.03 cm^2s^{-1} for unattached RaA and 0.004 cm^2s^{-1} for unattached RaB and RaC, on the basis of the experimental work of Raghunath and Kotrappa (J. Aerosol. Soc., 10, 133, 1979) by taking into account the average life and growth of the daughter products. Figure 1 shows the effect of the chosen D value on the dose calculated as a function of airway generation number. The choice of the maximum value for D instead of the minimum will enhance the dose by as much as a factor of 2 in generations 1–5 and by a factor of 0.75–1 in generations 6–16. The diffusion coefficient, D, is therefore an important parameter for lung dose calculation and should be chosen carefully. The two D values recommended for RaA and RaB by Haque and Al-affan have the same effect as that of an average D = 0.015 cm^2s^{-1} which has been suggested by ICRP (Rep. 24) based on the average size of the daughter products.

2.2 Aerosol size distribution

The activity median diameter (AMD) of the attached aerosol may vary naturally between different environments and also with additional sources of aerosols.

Figure 2 shows the effect of three AMDs on calculated doses; for example, a value of 0.12μm, common for city atmospheres, 0.18μm for country atmospheres and 0.06μm when additional sources such as smoke, stoves, etc. are present. The effect of the lowest AMD will be to produce a dose twice that of 0.18μm over the whole of the lung.

2.3 Room conditions

Several variables related to different atmospheres and ventilation rates have been collated, as shown in Table 1. Figure 3 shows for LC1, low ventilation, that the dose rate is high in generations 3–8, while medium ventilation, LC2, gives lower dose rates because of lower concentration of uncharged daughter products (see Table 1). Introducting smoke or an additional source of aerosols to LC2 will produce higher does rates, especially in generations 7–16.

2.4 Breathing rate

This factor is determined by whether the person is resting, corresponding to a flow rate of 10.5 l min^{-1}, carrying out moderate work, with a flow rate of 21 l min^{-1}, or carrying out heavy work, with a flow rate of 31.5 l min^{-1}. The above values correspond to 15 breaths per minute and tidal volumes of 0.75, 1.45 and 2.15 l, respectively. The 0.05 l of air entering the trachea is considered to contain no particles. Figure 4 shows the effect of flow rate on the dose calculated as a function of generation number.

2.5 Morphometry of the lung

Figure 5 shows a comparison of the dose rates for the Weibel, and Yeh and Schum (whole lung) models for LC2. The Weibel model gives higher dose rates for generations 1–13. This is attributed to narrower and longer airways in the Weibel model.

2.6 Physical dosimetry

In the recent past, experimental values of the stopping power and ranges of alpha particles from radon and its daughters were available for tissue equivalent gases, which did not stimulate the condensed phase of tissue. Lately, however, stopping power and range data for liquid water and tissue-equivalent materials have become available. Figure 6 shows the effect of physical state [ie. ratio = dose rate (vapour)/dose rate (liquid)] as a function of the depth in tissue. As can be seen, the influence of this factor is evident, in comparison with others, only at the end of the range of alpha particles. Also, the ratio is approximately constant for generations 0–16.

TABLE 1

Characteristics of three living conditions (LC). LC1 and LC2 are for rooms with natural aerosols. In LC3 additional aerosols from cigarette smoke, cooking or a stove are introduced. f_A and f_B are the percentage of free ions of RaA and RaB respectively.

	LC1	LC2	LC3
AMD	0.12	0.12	0.06
Ventilation rate	$V < 0.3$ h^{-1}	$0.3 < V < 1$ h^{-1}	$0.3 < V < 1$ h^{-1}
F	0.28	0.25	0.39
f_p	0.12	0.09	0.05
f_A	0.3	0.22	0.15
f_B	0.13	0.03	0.03
Concentration of aerosol particles (cm^{-3})	5×10^3	10^4	4×10^4

TABLE 2

Values of constants used to calculate doses shown in Figs 1–6

Diffusion coefficient (D) for unattached RaA = 0.03cm^{2}s^{-1}
Diffusion coefficient (D) for unattached RaB = 0.004cm^{2}s^{-1}
Mucus thickness = 15 μm
Activity Median Diameter (AMD) = 0.12 μm
Tidal volume (V_T) = 0.75 l
Flow rate = 10.5 l min^{-1}
Breathing rate = 15 min^{-1}
Living condition (LC2) of medium ventilation is assumed ($0.3 < V < 1$h^{-1})
Concentration of Rn = 23 Bq m^{-3}
Alpha stopping powers and ranges are for water
Airway diameters and lengths are for Weibel model
Dose rate is for a depth of 22μm in tissue

TABLE 3

Annual dose due to Rn-222 activity of 23 Bq m^{-3} for smoking and non-smoking living conditions as a function of generation number *G* and depth in tissue. LC1 is considered as a bedroom; time spent, one-third of the day. The rest of the day spent in non-smoking (LC2) and smoking (LC3) environment.

Depth (μm)	*G*	Annual dose (mGy $year^{-1}$)	
		Non-smoking	smoking
1	0	2.9	3.8
	5	4.3	4.6
	16	1.8	2.7
20	0	1.2	1.6
	5	1.8	2.0
	16	0.9	1.4

3. Microdosimetry of Inhaled Radon Daughters

The calculation of the average absorbed dose outlined in Section 2 may be considered of limited value for the consideration of cell damage in terms of transformation when the frequency of energy deposition is more important.

Microdosimetry is proving to be a valuable tool in the study of the mechanisms of cell damage by different types of radiation (ICRU, 1983, Rep. 36; 1986 Rep. 40). This is specially true for the cases when the cells survive after irradiation. Here the stochastic parameters, lineal energy, y and specific energy, z, have to replace the non-stochastic parameters LET and the absorbed dose, D.

In the present work an analytical method has been developed to calculate the microdosimetric spectra of alpha particles emitted by the radon decay products deposited on the mucus surface in the lung airways. In each case, the contribution of the near and far wall was computed separately. Figure 7 shows the total number of events as a function of the energy deposited by 6 MeV (RaA) and 7.7 MeV (RaC') alpha particles for the airway of diameter 3500 μm.

The non-stochastic parameters, namely, the frequency mean in lineal energy, $\overline{y}_F$, dose mean in lineal energy, $\overline{y}_D$, for RaA and RaC' alphas are given in table 4 for the diameter 18000, 3500 and 600 μm. Although $\overline{y}_F$, and $\overline{y}_D$ could be useful for the evaluation of the radiation quality, the energy distribution is considered more important when the effect of radiation are being assessed.

Table 4 $\bar{y}_F$ and $\bar{y}_D$ for alpha particles from RaA and RaC′

Rn daughter	Airway diameter μm	$\bar{y}_F$ kev μm^{-1}	$\bar{y}_D$ kev μm^{-1}
RaA	18000	121	150
	3500	111	136
	600	110	133
RaC′	18000	91	113
	3500	87	107
	600	86	106

4. Assessment of Lung Cell Transformation due to Radon Daughters

A dosimetric model has been developed to estimate lung cell transformation following inhalation of radon daughters. The information on survival fraction, S, from experiments in vitro, the calculated total fraction of cells hit by alpha particles, N_{tot}, at a particular radon concentration, the life-span of stem cells, t, the fraction of transformed cells, T_1, during 1 year and the lung growth from birth to adulthood, have been incorporated to estimate the cumulative fraction of transformed cells, T(A) at age A, given by:

$$T(A) = [T(A-1) + (T(A-1) + T_1)R(A)]\ [1-K_T T(A-1)]$$

where R(A) is the total fraction of the lung cells to be generated each year, and K_T is the total fraction of the lung cells killed each year.

The number of cells renewed each year depends on the fraction of cells dying each year from causes other than radiation, and the number of new cells added to the airway between ages 0 and 25 years.

For a radon concentration of 50 Bq m^{-3}, the fraction of cell nuclei hit, N_{tot}, during one year is 1 x 10^{-2}, 3 x 10^{-3}, 3 x 10^{-4} and 0 for RaA alphas, and 2×10^{-3}, 6×10^{-3}, 2×10^{-3}, 3 x 10^{-4} for RaC′ alphas, at depths 0, 20, 40 and 60 μm, respectively. The average specific energy $\bar{z}_D$ for a cell nucleus of dia. 7 μm calculated for the above depths are 0.54, 0.68, 1 and 0 Gy for RaA alphas, and 0.4, 0.5, 0.65 and 0.93 Gy for RaC′ alphas, respectively.

Incorporating the above values for alpha particle doses at different depths, with the fraction of cells traversed, the transformation rate, T_1, during 1 year, has been calculated using the results of Hieber et al (Int J. Rad, Biol., 52, 859, 1987). The values of T_1 are 2.8, 1.6, 1.1 and 1 per 10^6 for RaA, and 3, 1.9, 1.4, and 1.1 per 10^6 for RaC′ for the above depths.

The fraction of cell nuclei traversed by two alpha particles has been found to be less than 2% of that traversed by a single alpha particle.

The cumulative fraction of the transformed cells, T(A), has been plotted as a function of radon concentration for cumulative exposure over 40 and 70 years in fig. 8. It can be seen that for an exposure time of 70 years the values of T(A) are approximately 6 and 0.2 per cent for radon concentrations of 100 and 50 Bq/m^3, respectively; these are 0.1 and 0.01 per cent for an exposure for 40 years. It is concluded from the above that the effect of radon alone is very small for low concentration and for a clean environment.

5. Epidemiololgy of Lung Cancer Deaths

The ICRP Task Group (1987, Rep. 50) has analysed lung cancer risk from indoor exposure to radon daughters, the coefficients having derived applying a proportional hazard model. Cigarette smoking is still the major source of lung cancer, but a significant fraction of the observed lung cancer frequency is considered to be due to exposure to radon daughters.

A limited epidemiological study of female lung cancer deaths has been carried out by us using OPCS figures during 1951–60 in Devon and Cornwall. Assuming that cigarette smoking is not an important cause of lung cancer in females in the fifties, the excess deaths due to radon exposure alone is compatible with the risk of 60/year/WLM/million; the baseline risk due to causes other than radon is 40/year/million. The average radon concentration in the two above countries are 74 and 110 Bq/m^3, according to NRPB survey of 1987.

We have also examined the total lung cancer deaths of males and females in Devon and Cornwall during 1961–70 and 1971–1985 using ICRP derivation of the attributable excess lifetime risk as a function of indoor exposure to radon for the mixed population of smokers and non-smokers.

This work is being continued for the whole country on the basis of more extensive radon surveys.

6. Monte Carlo Calculation

The aim of this work is to evaluate the fraction of lung cell nucleus hit by alpha particles emitted by radon daughter products and to compare with that obtained by the analytical method. The technique consists of generating randomly all possible angles of emission of alpha particles, and calculating their pathlengths and residual energies. Chord lengths of alpha particles interacting with the cell nucleus have also been generated randomly. Preliminary results confirm those obtained by the analytical method.

Conclusion:

The possible lung cancer risk associated with indoor exposure to radon daughter products has led to world-wide interest in quantifying the hazard. At present, the estimation of risk is based on epidemiological studies of miners alone. To address the effect of radon daughters in homes and work places, risk estimates of long term exposure at low levels of radiation are required. Better dosimetric modelling,

radiobiology of human lung cells and epidemiology in domestic environment will lead to better estimates of the risk.

Far improved dosimetric modelling, more accurate knowledge of the frequency and location of basal, secretory etc. cells is essential; the thickness of the mucus layer is very relevant together with the effect of smoking on its thickness. Furthermore, there is scanty information on the variation in size or frequency of the airways within the general population. The domestic environment, its extensive characterisation, experimental values of F and f_p - their dependence on ventilation and presence of other aerosol sources, influences greatly the dose calculation. Comparative dosimetry in domestic and mine settings will be important.

At present, the transformation work is being carried out in mammalian cells in vitro. Human lung tissue cell culture should be tried, and when established should be irradiated and monitored for lung tumour markers. The results obtained with the new tissue culture needs to be compared with the already established transformation assay system C3H10T$_{\frac{1}{2}}$ for the same dose range and dose rates to assess its suitability.

Continued epidemiology of miners and epidemiology in the domestic environment, more information on the interaction between cigarette smoking and radon will lead to better estimates of the risk.

Finally, there is the interesting question of whether radon is implicated in the aetiology of other cancers. It has been implicated in acute myloid leukaemia, in melanomas, kidney cancers etc.

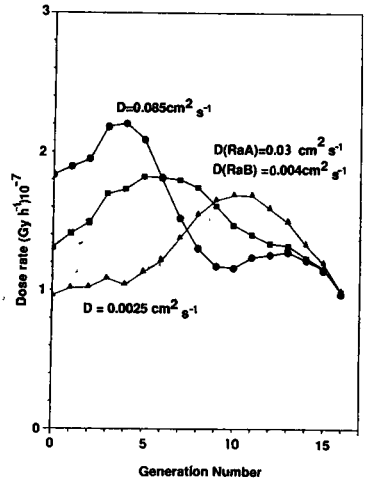

Fig. 1. The effect of unattached decay products.

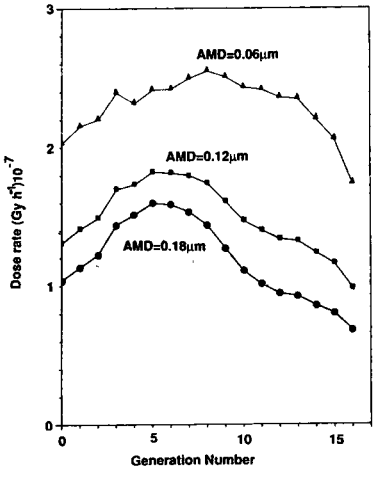

Fig. 2. The effect of activity median diameter (AMD).

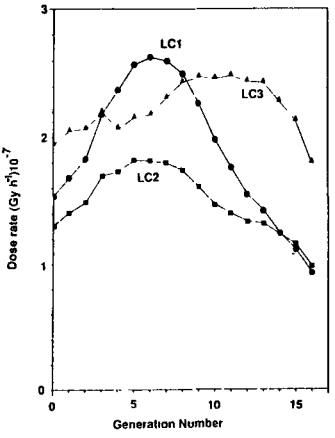

Fig. 3. The effect of ventilation.

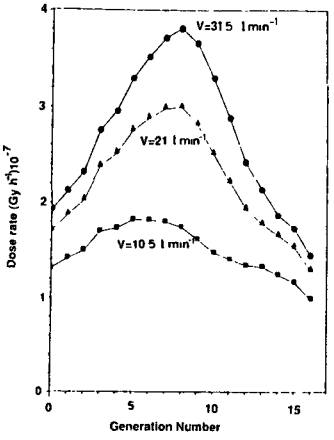

Fig. 4. The effect of flow rate.

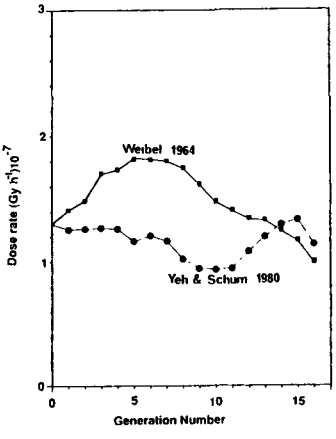

Fig. 5. The effect of lung Morphometry.

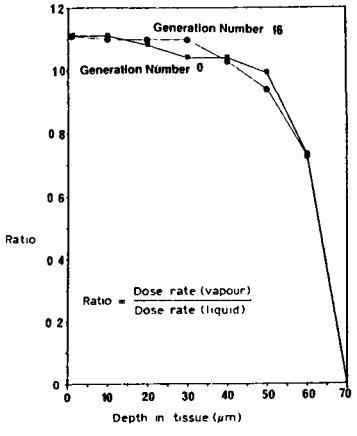

Fig. 6. The effect of Physical state of the medium.

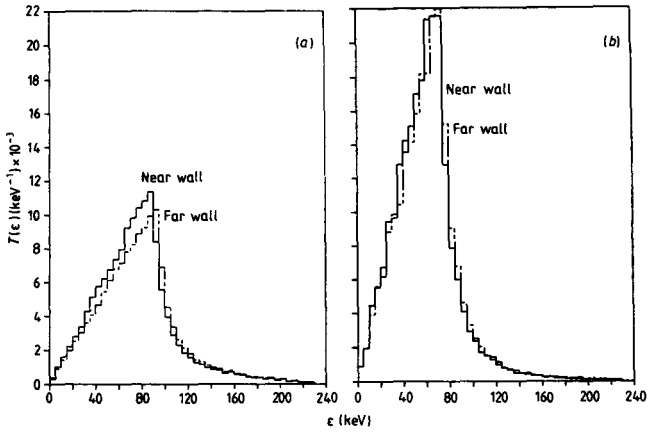

Fig. 7. Energy deposition event spectra in a tissue sphere 1 um in diameter, for alpha particles emitted from (a) RaA and (b) RaC'.

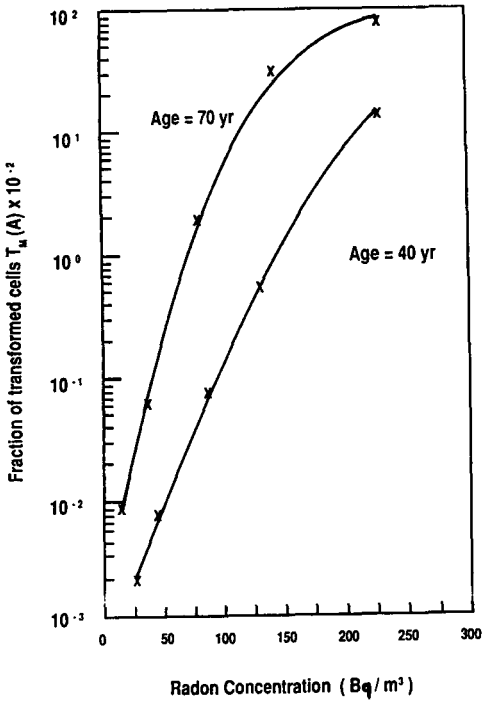

Fig. 8. The fraction of transformed cells vs. radon concentration for cumulative exposure over 40 and 70 years.

IV. Other research group(s) collaborating actively on this project [name(s) and address(es)]:

Prof. D M Taylor	University of Heidelberg
Dr J Miles	NRPB UK

V. Publications:

Haque A K M M and Al-Affan I A M, Influence of the physical state and straggling on the computation of the radiation dose due to radon daughters deposited in the lung, Physics Med Biol 32 1001 1987.

Haque A K M M and Al-Affan I A M, Radiation dose to the lungs due to inhalation of alpha emitters, BNES, London,1987,171 pp.

Haque A K M M and Al-Affan I A M, Main factors affecting the calculation of radiation dose to the lung from inhalation of radon daughters, The Sc Total Environ ,74 279 1988.

Al-Affan I A M and Haque A K M M,Local energy deposited for alpha particles emitted from inhaled radon daughters, Physics Med Biol, 34 97 1989.

Al-Affan I A M and Haque A K M M, Transformation of lung cells from inhalation of radon daughters in dwellings: A preliminary study, Int J Rad Biol, 56 413 1989.

Haque A K M M and Al-Affan I A M, Exposure to high environmental radon concentration in the UK- Lung cancer risk? 14th L H Gray Conf Oxford September 11-15 1988.

Al-Affan I A M and Haque A K M M, Lung cell transformation efficiency by alpha particles from radon daughters,Assoc for Rad Research,Autumn Meet September 19-22,1989,Bristol UK.

RADIATION PROTECTION PROGRAMME
Final Report

Contractor:

Commissariat à l'Energie
Atomique, CEA
CEN de Fontenay-aux-Roses
B.P.N° 6
F-92260 Fontenay-aux-Roses

Contract no.: BI6-A-020-F

Head(s) of research team(s) [name(s) and address(es)]:

Dr. G. Portal
IPSN/DPT/SIDR
CEA - CEN, Fontenay-aux-Roses
B.P.N° 6
F-92260 Fontenay-aux-Roses

Telephone number: 46.54.72.28

Title of the research contract:

Neutron individual and area dosimetry, realization of neutron calibration sources, beta-particle dosimetry, accident dosimetry of clothes.

List of projects:

1. Estimation of mean electron energy.
2. Thermoluminescence and exoelectron dosimetry in tissue of cotton.
3. Dosimetry on natural and synthetic tissue by ESR.
4. Realization of an "operational" spectrometry unit for neutrons.
5. Study and realization of an individual dosimeter based on photographic emulsions.
6. Area and individual dosimetry with proportional counters.

Title of the project no.: 1

Estimation of mean electron energy.

Head(s) of project:

M. PETEL and J. BARTHE

Scientific staff:

J.C. CHAPUIS and L. LE CORRE

I. Objectives of the project:

The method is based on the use of a single dosemeter which can be read either simultaneously or consecutively by radiothermoluminesence (RTL) and thermally stimulated exoelectron emission (TSEE). The difference between the responses obtained using these two techniques arises from differences between optical transmission through a depth of a few hundred micrometers in the case of RTL and electron transmission from a depth of between 1 and 10nm from the detector surface in the case of TSEE.

II. Objectives for the reporting period:

The objectives for the present reporting period are multifold :

1/ Use of composite material dosemeters : films, ceramics, beryllium oxide, lithium fluoride,

2/ Testing of the mixed head reader,

3/ Investigations of the effects of variable mean energy in mixed energy beams.

III. Progress achieved:

1. Introduction

The investigations carried out in the framework of this contract are aimed at improving skin dosimetry for persons working, for example, in glove boxes. The difficulties encountered in evaluating skin doses are essentially related to determining the beta radiations energy and hence their penetration powers; as an example whereas 10 keV beta radiation penetrates only 2 μm in biological tissue and is therefore does not present any danger (except for the eyes), 2 MeV beta radiation (Yttrium-90) penetrates up to one centimeter. In order to provide a meaningful dosimetry, it is therefore necessary to know the mean energy of the radiation in addition to the skin dose.

2. Method employed

Exoelectron emission is the most suitable method presently available for measuring such doses. At energies above a few keV, this method depends little on either incident energy or on the angle of the incident radiation up to an angle of 60 degrees with respect to the normal to the surface. However this method only gives information about surface skin dose and does not provide any information about depth dose.

In order to obtain the complementary information required, a detector, whose yield varies as a monotonic function of energy over a range extending from a few keV up to a few MeV is used. Thermoluminescence (TL) dosimetry was chosen for these measurements ; in TL dosimetry the yield increases with beta energy as a result of build up in the dosemeter material.

TSEE and TL information is obtained, either from different materials, or, from the same material read simultaneously or consecutively. Either a mixed readout head device or a detector possessing two thermally separated traps is used.

3. Materials and glow curves

Figures 1 shows typical TSEE and TL glow curve shapes for LiF pellets: Na,Dy from Desmarquest (France). Figure 2 shows TSEE glow curves of a thin layer of BeO deposited on graphite from MPA (FRG). Figures 3a and 3b show the TSEE and TL glow curve of sintered BeO from Beryllium Oxide Consolidated Corporation (UK). The TL sensitivity of BeO pellets is low in comparison with LiF; the detection threshold is about 5 mGy and the reproducibility mediocre (± 10%).

In the case of BeO pellets the cycle used to thermally stimulate the samples destabilizes the TSEE or TL response (depending on which method is used). The results obtained with the most recent batches of both BeO (BeO Consolidated...) and Brush Beryllia (USA) have demonstrated that it is virtually impossible to make a comprise.

Various heat treatments have been employed :

- under vacuum, in an atmosphere of nitrogen, argon or air,
- varying the temperature in the 500°C to 1100°C range,
- using different annealing times (1/2 hour to 24 hours).

It was not found possible with any combination of these parameters to obtain better results.

4. Experimental equipment

A system with a double headed reader is used : one of the heads consists of a multineedle counter adapted for measurements on weakly conducting samples (configuration and amplitude of the electrical field, drift range...), the other head consists of an optical detection unit (comprised of one or several filters, a photomultiplier, a cooling circuit, a shutter...).

As only very low light intensities are produced, pulse counting techniques have been employed. Measurements are therefore carried out under stacking conditions: under such conditions the linearity with the luminous flux is only assured for constant amplitude spectrum pulses; this conditions are only verified for very low intensity fluxes. The upper cut-off frequency is close to 10 MHz, the background noise inherent to the system a few Hz in the absence of black body emission.

The mixed head device poses many problems, the main problems being the much higher frequency of the exoelectrons in comparison with that of the photons and the persistance effects from the anodic sheatch on the different electrodes of the counter.

The irradiations were carried out with a "Buchler" irradiator constructed and standardized by the PTB (FRG). Doses are delivered through various appropiate filters at a distance of 30 cm. Temperature, humidity and atmospheric pressure are taken into consideration throughout the irradiations; this is particularly true for Pm-137 irradiations. Figure 4 shows the shapes of the energy spectra corresponding to the 3 sources used.

5. Principal results and discussion

One of the most interesting results obtained using exoemission techniques is the very low amount of variation in response with the energy of the incident beta radiation and with the angle of incidence.

Figure 5a shows the TSEE response, for different mean energies (obtained from "Buchler" sources) of a dosemeter consisting of a thin layer of BeO on a graphite substrate.

Figure 5b shows how the TL response of LiF : Na, Dy varies as a function of the mean energy obtained under the same conditions for exoemission. The detector, here was covered with a polyethylene film, 60 μm thick to simulate H(0.07) conditions.

Figure 6 shows the TSEE response, for different mean energies and different incidence angles.

It is observed experimentally that the responses obtained are very dependent on irradiation conditions, the nature of the substrate and sample holder, and of the phantom used, etc....).

The best results were obtained with a BeO/C-LiF couple, both dosemeters being particularly sensitive and reproducible.

Figure 7 shows the response of this pair of dosemeters to mean energies in the 60 to 600 keV range. A low energy response threshold due to absorption by the 60 μm compensation film is not. Attention is also drawn to the fact that exoemissive dosemeters are sufficiently sensitive to beta radiation from tritium to allow a correct evaluation to be made of doses in excess of about 100 μGy.

6. Conclusions

The work, performed in the framework of this contract, has demonstrated the feasiblity of developing an operational beta dosimetry based on exoemissive detectors. A combined BeO/LiF detector gave very good results, for both dose measurements and mean energy estimations are concerned; the latter being determined with greater accuracy for low energies as a result of characteristic build up at low energies.

Measurement accuracy for both the TL and TSEE is of the order of 5% for measurements in the dose range considered (1 mGy). The mean uncertainty in the energy estimation is larger ≈ 20% between 300 and 700 keV. When doses greater than 10 mGy are considered the error decreases to ≈ 10%. Emphasis is drawn to the fact that both TL and TSEE responses vary significantly with the immediate environment of the dosemeters; this factor must be take into consideration if meaningful results are to be obtained.

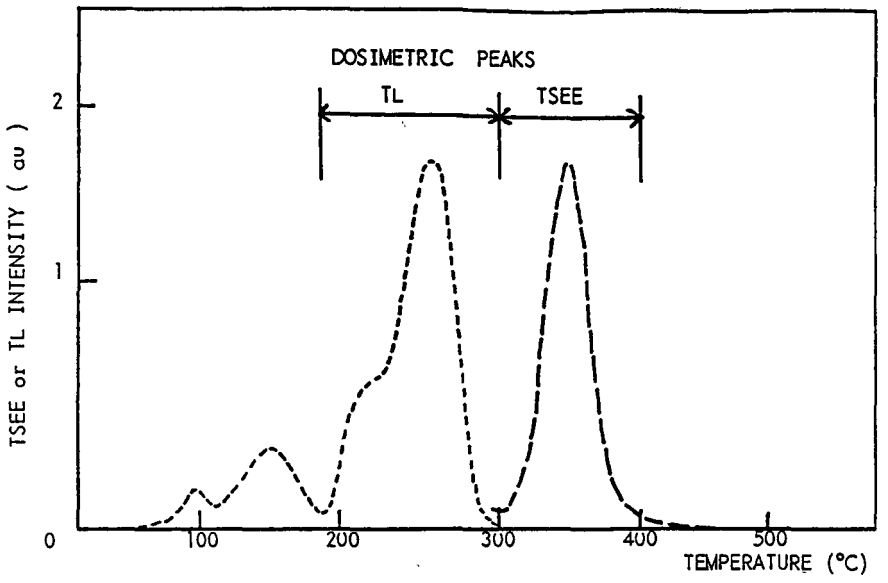

Figure 1 : TSEE and TL glow curves of LiF : Na, Dy pellets.

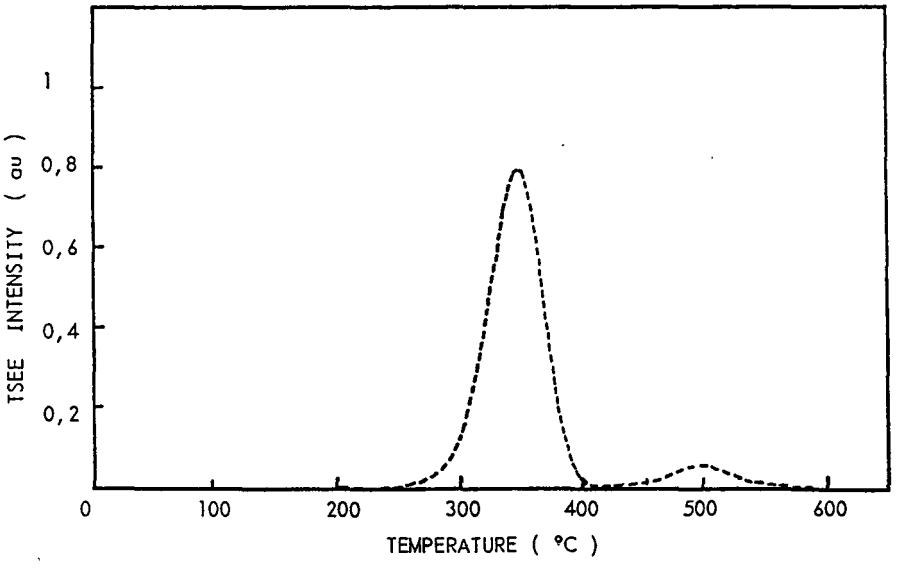

Figure 2 : TSEE glow curve of BeO thin film.

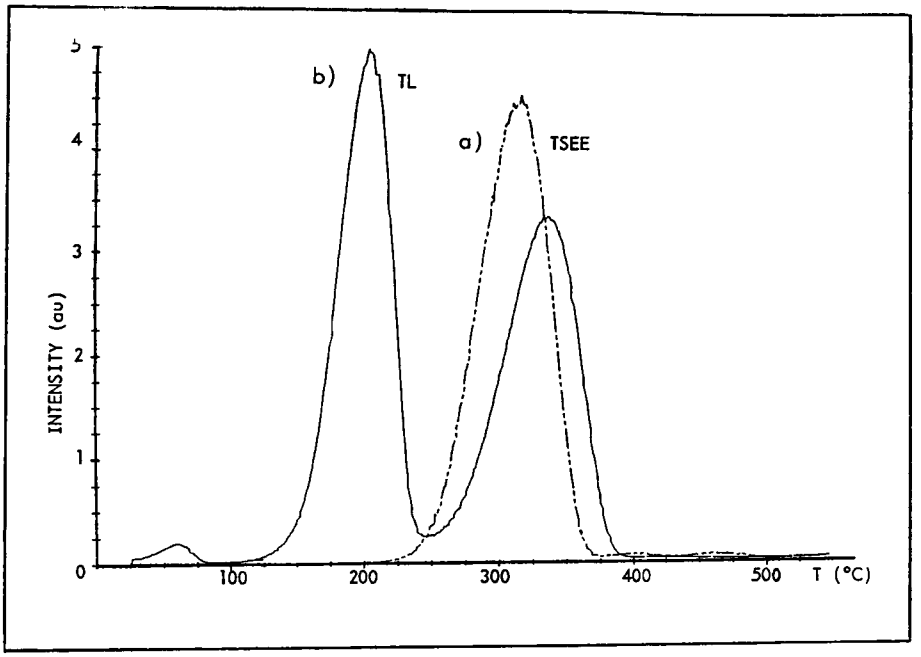

Figure 3 : TSEE and TL glow curves of BeO Consolidated Corporation pellets.

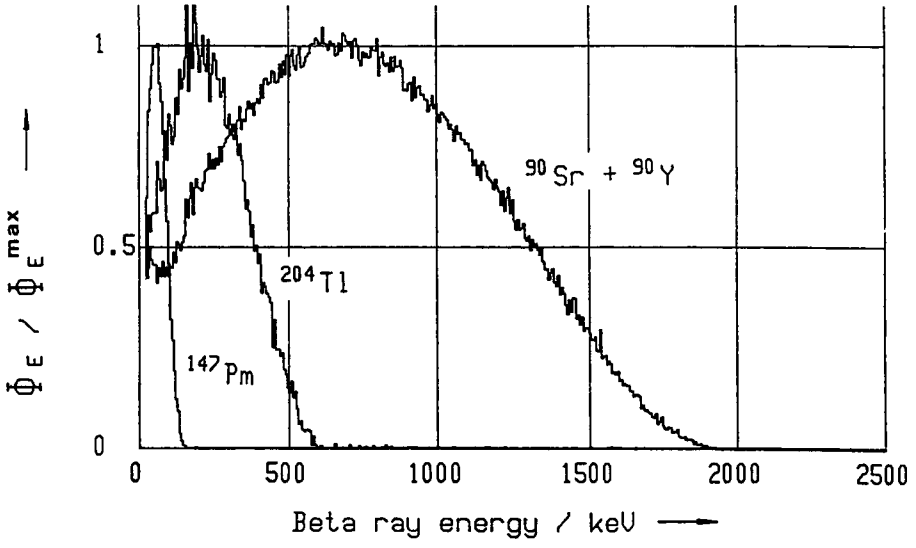

Figure 4 : Energy spectrum of used beta sources (PTB).

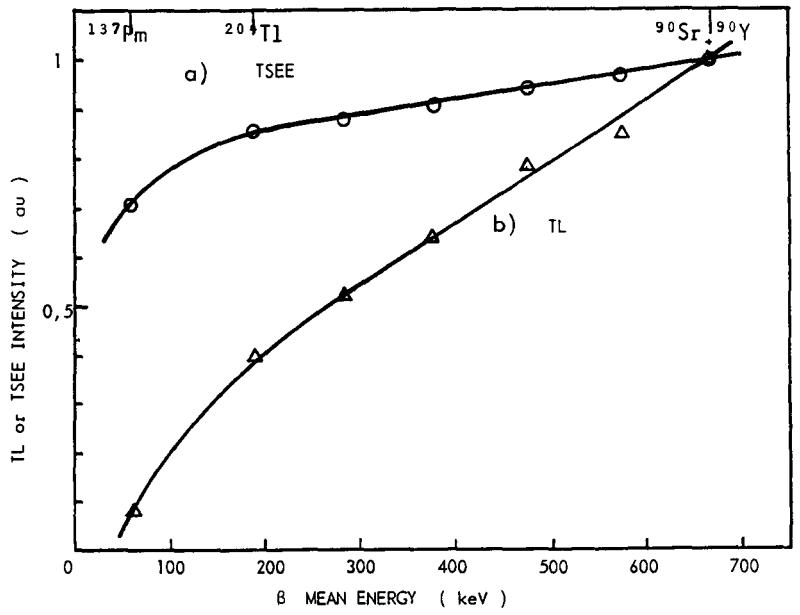

Figure 5 : TSEE (BeO thin film) and TL (LiF:Na,Dy) dosemeter responses versus beta mean energy.

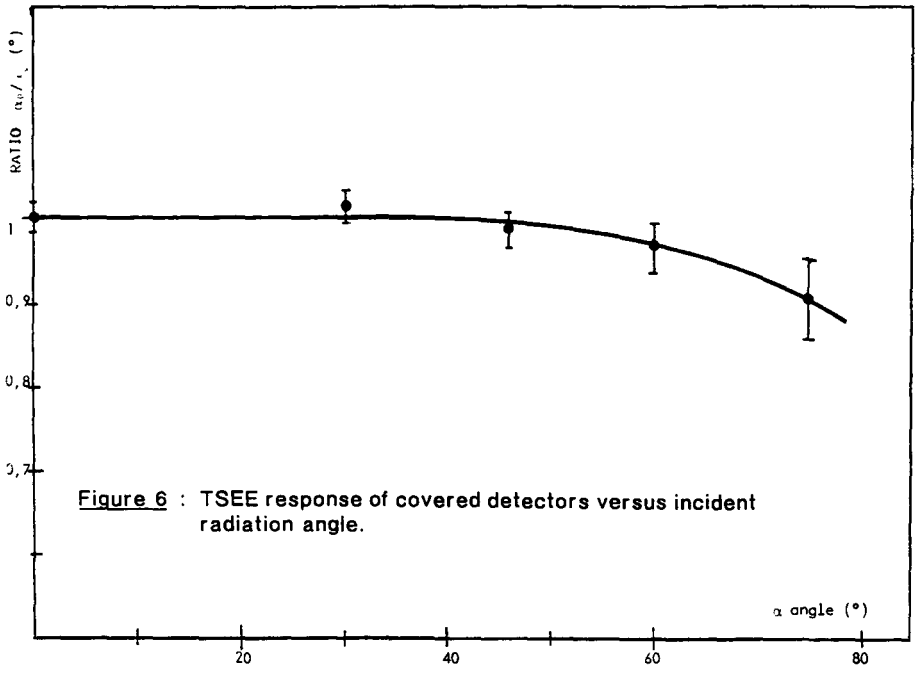

Figure 6 : TSEE response of covered detectors versus incident radiation angle.

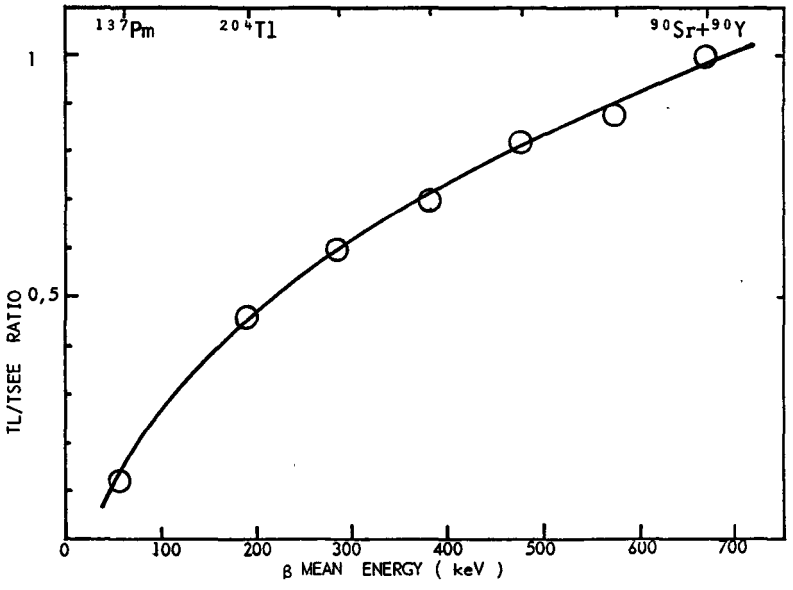

Figure 7 : TL/TSEE response ratio of coupled dosimetric detectors versus beta mean energy.

IV. Other research group(s) collaborating actively on this project [name(s) and address(es)]:

Professor A. SCHARMANN
I Physikalische Institut des Universitat Giessen
Heinrich, Buff-Ring 16
6300 GIESSEN - FRG -

V. Publications:

W. KRIEGSEIS, M. PETEL, A. SCHARMANN, C.U. WIETERS:
Potentials of TSEE Beta-Rays Dosimetry of Beta Particles and Low Energy X-Rays.
Saclay, 7-9 October, 1985.
Radiation Protect. Dosimetry. Vol 14, n°2 (1986) pp 151-156

M. PETEL, G. COMBY, J. QUIDORT, J. BARTHE:
"A marketable multineedle Counter with cathode Focusing for TSEE investigation". IXth Polish Seminar on Exoelectron Emission and Related Phenomena,
(3-7 May 1985) Karpacs (Pologne). Editors B. Sujak and K. Gieroszynska
Acta Universitatis Wratislawiensis (1985) pp 161.

M. PETEL, W. KRIEGSEIS, A. SCHARMANN, C.U. WIETERS:
"Dependence of the TSEE response of Beta-rayed BeO Thin film Dosemeters on the Thickness of Polycarbonate foils".
8th International Symposium on Exoelectron Emission and Applications
(August 25-30, 1985) Osaka (Japon).
Japanese journal of applied physics, Vol 24 (1985) Sup. 24-4 pp 257-258

G. HOLZAPFEL, J. LESZ, M. PETEL and A. SCHARMANN
"Energy Response of Hot-Pressed Thin Layer Detectors to Photon and Electrons Irradiations".
Proc. of the VII Int. Conf. or Sol. State Dosimetry.
Rad. Prot. Dosim. 17 (1/4) (1986) pp. 71-76.

W. KRIEGSEIS, M. PETEL, G. PORTAL, A. SCHARMANN and C.U. WIETERS
"Skin Dose Determination with the TSEE of BeO thin Film Detectors".
Proc. of the VII Int. Conf. or Sol. State Dosimetry.
Rad. Prot. Dosim. 17 (1/4) (1986) pp. 97-98.

M. PETEL and J. BARTHE
"Measurement of the Mean Energy of Soft Betas Using Thermoluminescence and thermally stimulated Exoelectron Emission".
Proc. of the VII Int. Conf. or Sol. State Dosimetry.
Rad. Prot. Dosim. 17 (1/4) (1986) pp. 93-96.

W. KRIEGSEIS, M. PETEL and A. SCHARMANN
"Response of BeO thin film dosemeters to beta irradiation".
9th International Symposium on Exoelectron Emission and Applications.
WROCLAW Pologne, October 3-8 (1988).

M. PETEL, J. BARTHE and G. PORTAL
"A new computerized TSEE Reader".
9th International Symposium on Exoelectron Emission and Applications.
WROCLAW Pologne, October 3-8 (1988).

M. PETEL, J. BARTHE, W. KRIEGSEIS, G. PORTAL, A. SCHARMANN and G. SIRIEX
"Fast reader for thermostimulated exoelectron dosemeters used for beta ray dosimetry".
9th Int. Conf. on Solid State Dosimetry, Vienna, Nov. 6-10, 1989 (to be published).

M. PETEL, J.L. CHARTIER, C. ITIE, H. KESSLER, W. KRIEGSEIS and
A. SCHARMANN
"Dependence of the TSEE of beta-Rayed BeO thin film detectors".
9th Int. Conf. on Solid State Dosimetry, Vienna, Nov. 6-10, 1989 (to be published).

Title of the project no.: 2

Thermoluminescence and exoelectron dosimetry in tissue of cotton.

Head(s) of project:

J. BARTHE

Scientific staff:

C. HICKMAN, C. LAUREANA

I. Objectives of the project:

The aim of this work is to develop a method to determine the dose received by a person accidentally irradiated with γ radiation, but not wearing a dosemeter. The clothing worn is used to estimate the dose. Clothing is made of natural or synthetic fibers very nearly equivalent to biological tissues. Two complementary research activities have been pursued:

- dosimetry by low temperature thermoluminescence after phototransfer, only the clothing fabric, itself, being used.
- dosimety of specially adapted textile fabrics doped with a radiothermoluminescent product.

The various procedures and methododologies corresponding to both approaches have been defined.

II. Objectives for the reporting period:

The main objective for this last contractual period is the definition of a complete dosimetry system including textile fabric manufacture at a pre-industrial stage, optimization of operational procedures and the first steps towards the simulation of a gamma irradiation accident.

Studies of the definition of the characteristics of the pre-industrial stage have not yet been completed; some work in this direction is envisaged during 1990 ; particular emphasis will be given to the manufacture of special clothing fabric using commonly employed techniques.

III. Progress achieved:

Work undertaken in the framework of studies concerning the fabrication of working clothing is nearing completion as far as basic research, dosimetry and technological investigations are concerned. Present studies are aimed at verifying whether industial fabrication methods can produce clothing fabric having the same characteristics as fabrics prepared on a laboratory scale.

Initially several solutions were conidered, however, it rapidly became clear that only solutions involving the depositing of a radiothermoluminescent product in the structure of a textile fabric gave satisfactory results ; the use of undoped fabrics as dosemeters did not lead to any encouraging results.

Two methods have been considered: thermoluminescence (TL) and thermostimulated exoelectron emission (TSEE) ; both these methods were applied to fabrics doped with an inexpensive easily available radiosensitive product: alumina. Different aluminas manufactured by Desmarquest (Evreux, France) were tested.

The following experimental equipment was implicated in these studies:

1) a TL reader system operating between 77 K and 600 K,

2) a TSEE reader system provided with a multianode counter very insensitive to the surface electrical conductivity of textile fabrics.

1. Fundamental studies on alumina

Prior to undertaking studies on textile fabrics loaded with alumina (5-20 μm and 44 μm) Desmarquest investigated the possible methods of carrying out TL and TSEE measurements at positive temperatures or at low temperatures after phototransfer. Some experiments were carried out on the intrinsic fading of alumina; the thermal fading of alumina has been extensively studied elsewhere, however, the studies performed here relate

specially to optically induced fading and to the effects of UV from ambiant lighting and sunlight.

1.1. Thermoluminescence

Figures 1 and 2 give glow curves for alumina in the 77 K to 650 K temperature range together with the emission spectra of the corresponding peaks.

In order to avoid any deterioration of the textile substrate during in situ TL measurements, low temperature phototransfer techniques were employed. A very schematic representation of the principles of this method is given in figure 3. The amplitude of the TL signal obtained after phototransfer depends on the UV exposure sequence as seen in figure 4. Figure 5 reveals that a room temperature annealing modifies the response of some of the peaks: the E peak is the most stable and the C peak the least stable.

1.2. Exoelectron emission

TSEE studies were carried out in parallel with the TL measurements as it was observed that with TL, the colour of the substrate sometimes changed during readout (depending on readout conditions), thus altering the signal; this phenomenon does not occur with TSEE. Figure 6 shows the shapes of the corresponding TSEE spectra.

As in the case of TL, phototransfer occurs. The principles behind this phenomenon are indicated in figure 7. Figure 8 shows how TSEE response varies with the photon energy of the exciting UV radiation.

2. Response of undoped cotton

When irradiated, cotton does not exhibit any significant TSEE response; after very high doses (≈ 500 Gy), two weak peaks appear, but their intensities are incomparable with those produced by alumina doping.

In the case of TL emission the situation is somewhat more complicated: optical emission (continuous spectrum), that is not necessarily related to TL, but due to burning, may occur. This phenomenon has been confirmed (Figure 9) by eliminating adsorbed oxygen from the cotton by different techniques. The 120°C and 175°C peaks are not very radiosensitive.

These results led to the conclusion that it is necessary to load the cotton with alumina to obtain exploitable results. In practice, it is nevertheless necessary to make a compromise between the detection threshold sought, the grain size of the alumina powder employed and the tactile comfort of the resulting textile fabric. A carefully conceived procedure developed in collaboration with the "Centre de Recherche Textile de Mullhouse" (CRTM) enabled alumina to be incorporated into a suitable cotton textile fabric, while retaining its TSEE and TL properties.

3. Dosimetric studies of aluminized fabrics

These investigations were motivated by the question of whether alumina incorporated in textile fabrics behaved in the same way as the raw material. It was discovered that it behaved similarly, but that certain parameters such as the thermal sensitivity of the substrate, the transparence of the adhesive binder, burning phenomenon, desorbed gases, etc.... modified to some extent the response. Measurements were carried out on samples in the form of 18 mm diameter disks.

3.1. Exoelectron emission

Figure 10 shows the relative displacement of the TSEE peak of an alumina sensitized fabric and raw alumina for a 5 - 20 μm grain size. Figure 11 shows how the TSEE response varies for a fabric loaded with different surface densities of alumina. A surface density of between 8 and 20 grammes per square meter apparently gives the best results with a detection threshold of 1 cGy. It is also possible to use phototransfer techniques to make several successive measurements on the same sample; in spite of these factors the TSEE is not considered to be a very promising technique in this field.

3.2. Thermoluminescence

Measurements were carried out in a nitrogen atmosphere after having desorbed oxygen from the air in order to eliminate the response of the fabric substrate; the substrate response cannot be eliminated in an oxygen atmosphere. Figure 12 shows the TL curve obtained for aluminized cotton at positive temperatures (the inexistence of peaks A and B should be noted). The X-ray sensitivity increases with the surface density of the textile fabric: 0.025 nA per Gy without any alumina to 13 nA per Gy for a density of 38 grammes per square meter. The sensitivity also increases with grain size: a fourfold increase in sensitivity occurs when the grain size increases from 5 - 20 μm to 44 μm.

Figure 13 shows the response of an aluminized sample (20 grammes per square meter, 44μm) as a function of the gamma ray dose delivered by a Co-60 source. A satisfactory linearity has been obtained: correlation coefficient of 0.99.

3.3. Thermally induced fading

A greater amount of thermal fading occurs with TSEE (Figure 14) than with TL (Figure 15). This is a surprising result as the TSEE peak is deeper than the TL peak. After 15 days the fast decay component disappears and the signal remains stable over a period of several months (65% of residual signal with TSEE emission and 80% with TL emission).

3.4. Optically induced fading

Whereas thermal fading is not very problematic, this is not the case for optically induced fading related to well known phototransfer mechanisms in alumumina. When exposed to direct sunlight (over a period of 10 days) or to a UV source ($E > 4$ eV) (for a period of 10 minutes), a very troublesome loss in TL signal occurs (Figure 16), only 30% of the initial signal remaining. This phenomenon is much more pronounced with TSEE, more than 95% of the signal disappearing. This behaviour prevents TSEE being used.

When an accident has occurred one of two techniques can be used to overcome this difficulty :

- immediately putting the piece of fabric to be measured in the dark,

- accelerate the fading with an artificial irradiation (exposure to a xenotest lamp for a period of about 10 hours) in order to displace the measurement point to a constant value on the fading curve.

3.5. Other influencing parameters

Other parameters can alter the dosimetric signal, the most significant of these being :

- air humidity; this parameter can be neglected after dehydration,

- creasing/crumpling; this parameter can be neglected after a certain period of time,

- washing ; this parameter is by far the one to which the greatest amount of attention should be given: it should be noted that the most recent binders developed satisfy CEI washing standards i.e. 50 soda washes at 95°C or chlorinated washes at 75°C with a loss of less than 50% of the alumina content. An a posteriori calibration is therefore necessary: this can be done either by adding doses or after a first measurement has been made.

4. Conclusions

The studies undertaken have now reached a terminal stage as, an acceptable formulation exists for the adhesive binder to be employed: this formulation satisfies mechanical, tactile, optical, thermal and washing constraints. Furthermore, fast readout techniques applicable to both TL and TSEE measurements (uncertainty of ±10% for each individual measurement) can be completed by chemically extracting the alumina, the powder thus obtained being read in the same way as conventional dosimetric powders. The detection threshold can be reduced to a few cGy.

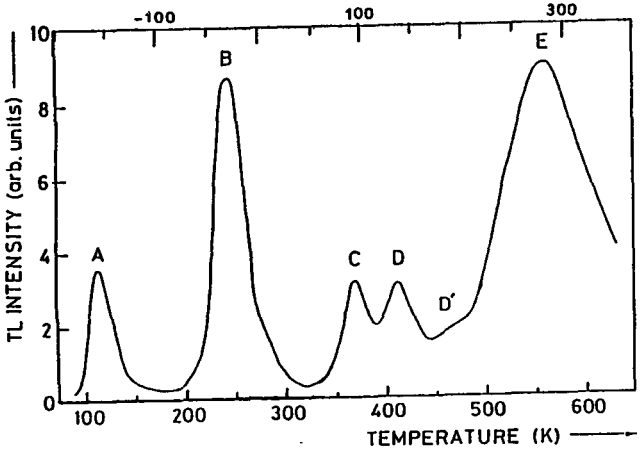

Figure 1 : Al_2O_3 TL glow curves.

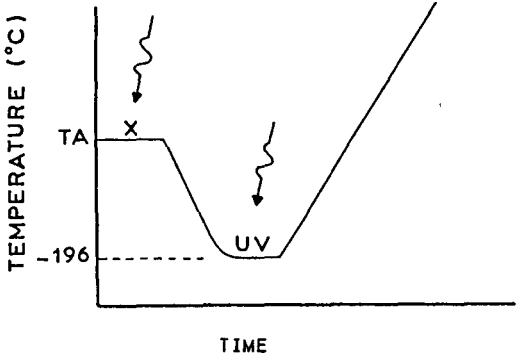

Figure 3 : U.V. photo-induction TL procedure.

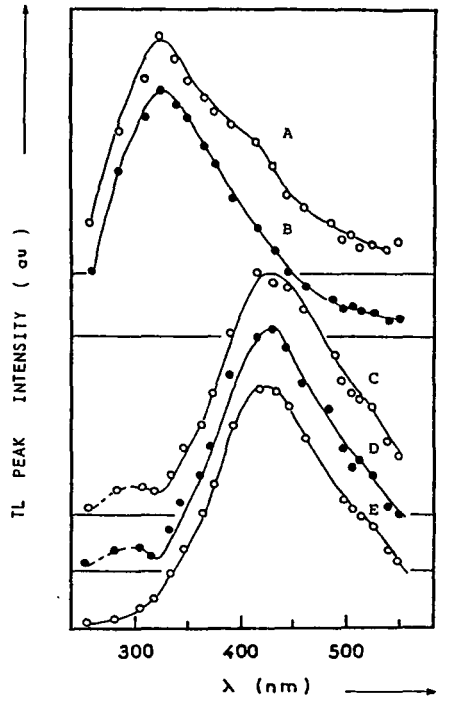

Figure 2 : Al_2O_3 TL peak emission spectra.

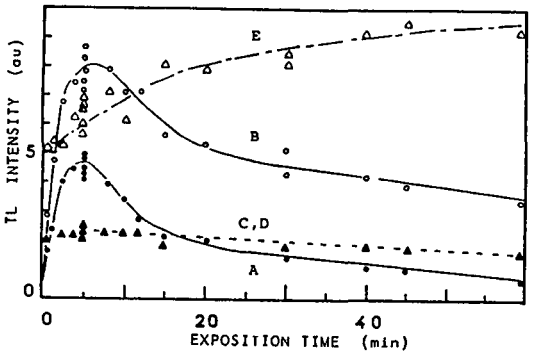

Figure 4 : Optical fading of main P.I.T.L peaks.

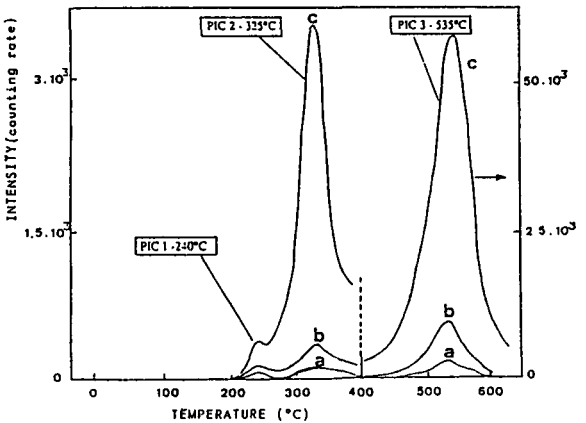

Figure 6 : Al_2O_3 TSEE response after constant U.V. energetic fluence excitation (a) 496 eV (b) 5.39 eV (c) 6 eV.

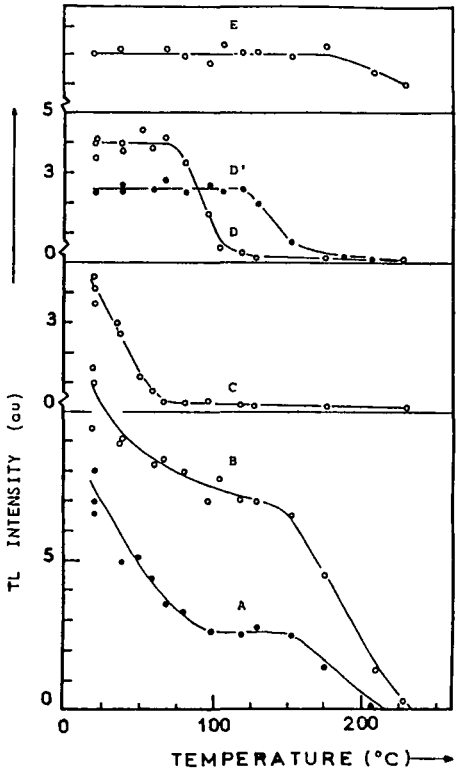

Figure 5 : Thermal annealing of P.I.T.L and TL peaks.

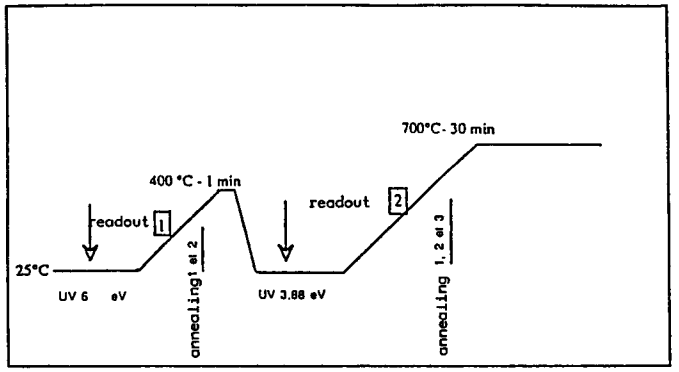

Figure 7 : Experimental procedure use in EETS U.V. phototransfert.

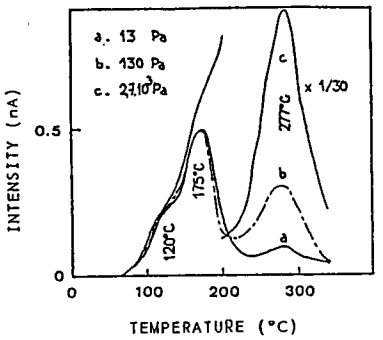

Figure 9 : TL glow curves obtained under N_2 atmosphere after different vaccum levels.

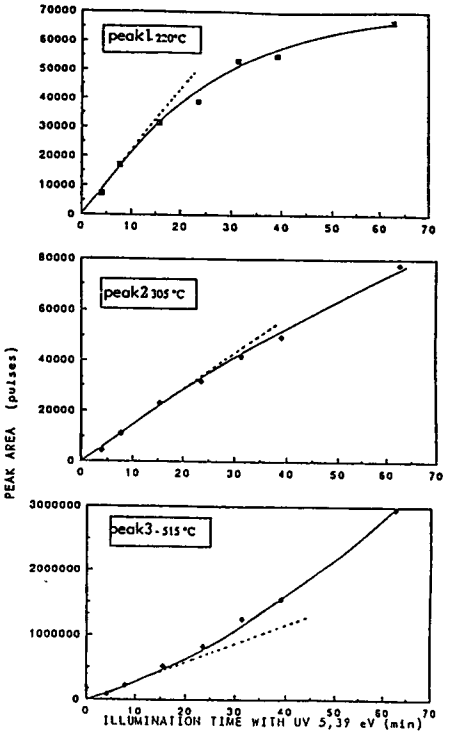

Figure 8 : TSEE response from (5-20 µm) Al_2O_3 versus U.V. excitation time.

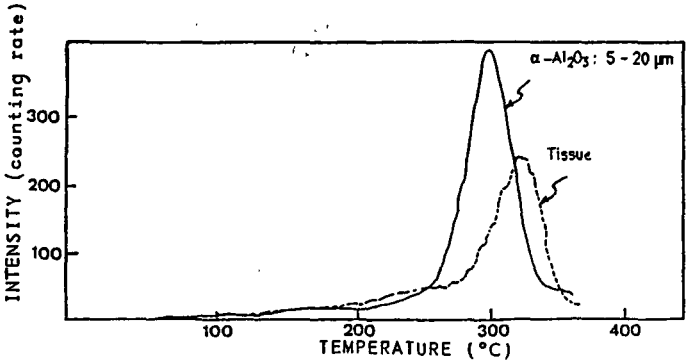

Figure 10 : Comparison between TSEE and TL glow curves for Al_2O_3 loaded fabrics.

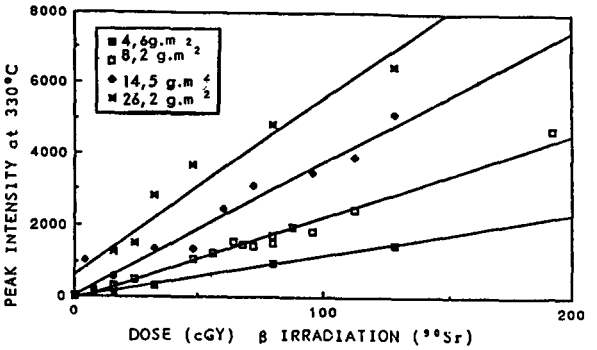

Figure 11 : TSEE response of different Al_2O_3 loaded fabrics versus beta dose.

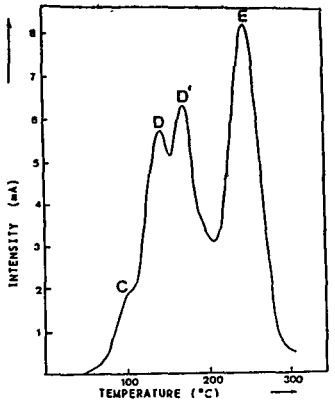

Figure 12 : TL glow curve of 8.2 gm^{-2} Al_2O_3 loaded fabrics.

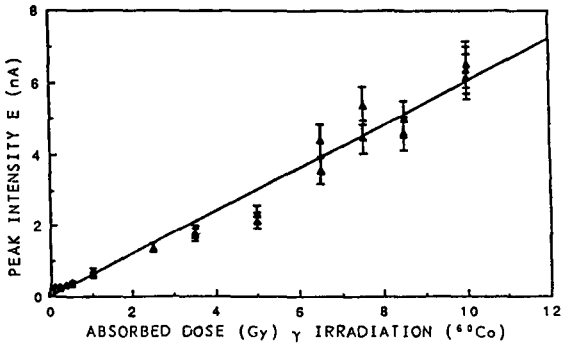

Figure 13 : TL response versus dose for 44 µm Al_2O_3 loaded fabrics.

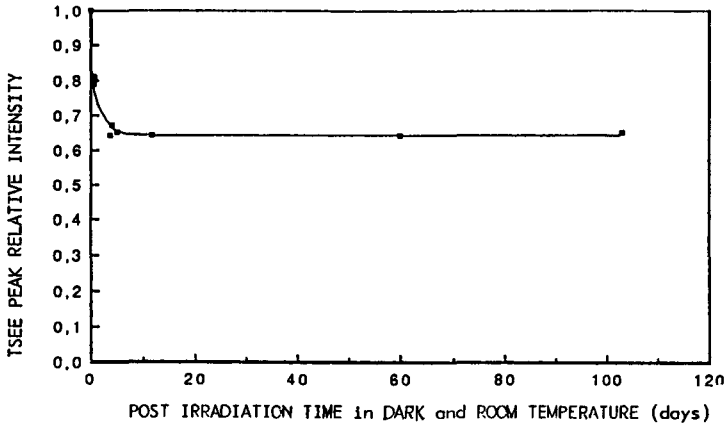

Figure 14 : TSEE thermal fading for 8.2 gm^{-2} Al_2O_3 loaded fabrics.

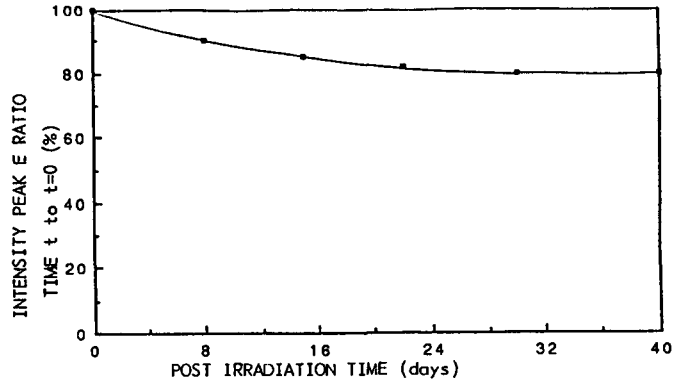

Figure 15 : TL thermal fading for 44 μm Al_2O_3 loaded fabrics.

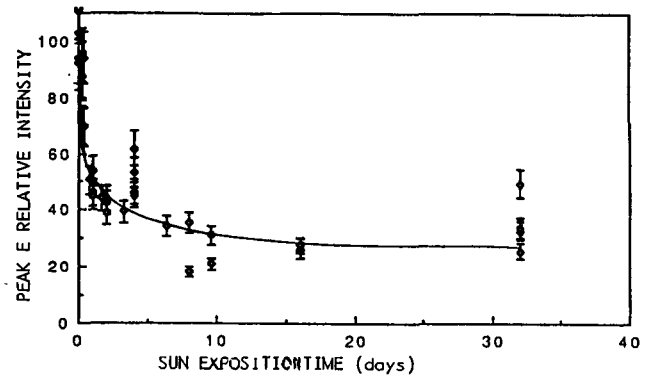

Figure 16 : Optical fading versus time in standard XENOTEST 450 conditions.

IV. Other research group(s) collaborating actively on this project [name(s) and address(es)]:

Laboratoire d'Emission Electronique et de Luminescence Universite de Nice,
Parc Valrose, 06000 Nice - F -
Laboratoire de physico-chimie des matériaux
Ecole Nationale des Mines de St Etienne
F - 42000 St Etienne
Centre de Recherche Textile de Mulhouse (CRTM)
185 rue de l'Illberg
F - 68200 Mulhouse

V. Publications:

D. LAPRAZ, P. IACCONI, Y. SAYADI, P, KELLER, J. BARTHE and G. PORTAL
"Some thermoluminescence properties of an α-Al_2O_3 sample. Sensitization effects".
Physica Status Solide a, 108, (1988) pp 783-794.

Y. SAYADI
Etude et caractérisation d'un phénomène de TL photo-induite dans l'alumine α. Application à la dosimétrie des rayonnements ionisants.
Thèse de doctorat Toulouse, Juillet (1988), n° 326.

P. IACCONI, M.F. ALESSANDRI-FRACCARO, D. LAPRAZ and M. PETEL:
"Thermostimulated exoelectronic emission of alpha alumina excited by ultra violet radiation".
9th International Symposium on Exoelectron Emission and Applications. WROCLAW Pologne, October 3-8 (1988).

P. IACCONI, D. LAPRAZ, M. F. ALESSANDRI and D. ADDI
"Phototransferred thermoluminescence and exoemission in alpha alumine".
9th Solid State Dosimetry, Vienna, Nov. 6-10, (1989).
(à paraitre dans Rad. Prot. Dos.).

D. LAPRAZ, P. IACCONI, M.F. ALESSANDRI, J. BARTHE and G. PORTAL
"Dosimetric characteristics of specially prepared clothing material".
9th Solid State Dosimetry, Vienne, Nov. 6-10, (1989).
(à paraitre dans Rad. Prot. Dos.).

Title of the project no.: 3

Dosimetry on natural and synthetic fabrice by ESR.

Head(s) of project:

J. BARTHE, F. BERMANN

Scientific staff:

R. CHUITON

I. Objectives of the project:

The general objective of the work is to develop a method to determine the doses received by a person not wearing a dosemeter.

Doses are evaluated using a method based on Electon Spin Resonance (ESR). This technique has the following advantages :

- it is non destructive,
- the information contained can be read and re-read as many times as desired,
- many textile polymers give ESR signals,

II. Objectives for the reporting period:

During this last year of studies, emphasis has been given to defining and optimizing practical procedures involved when employing the method. Various textile fabrics were studied, and several different treatments were tried to reduce fading effects.

A synthesis of the different aspects of the work already carried out was made in order to discover points that had not received attention and the parts of the work that remained to be completed.

III. Progress achieved:

1. EXPERIMENTAL EQUIPMENT

A commercially available BRUKER spectrometer : ER 200, operating in the X band (9 to 10 GHz) was used for the experiments. A microcomputer controlled device was used to rotate samples in the resonant cavity ; other complementary functions assured by the system are as follows :

- digitization of spectra,
- accumulation/substraction,
- angular servocontrol of the sample,
- rapid rotation during measurements.

1.1 - Sample rotation

The sample holder was designed to rotate the sample during measurements in order to reduce effects due to anisotropy through an averaging process.

Figure (1) shows how the signal varies with different speeds of rotation. The frequenes stated in the diagrams correspond to the control frequencies of the step by step motor (3200 steps per revolution). The best compromise is 10 kHz i.e. 3 revolutions per second.

1.2 - Textile fabrics studied

These studies are aimed at developing a method to measure the doses received by a person accidentally exposed to ionizing radiation. Studies began with cotton as it is the basic fiber from which laboratory coats were first made. It should be noted that the polyester fibers, which are by far the most important constituents of modern clothing do not exhibit any radiosensitivity.

In addition to the cotton fabrics studied, textiles made from polypropylene, wool, linen, thermovyl and even some glass and quartz fibers have been studied.

1.3 - Preparation of samples

Two pricipal difficulties were encountered :

- the variation of the signal with the orientation of the sample in the resonant cavity,
- a strong absorbtion of the microwave frequency signal due to water absorbed by the sample from the atmosphere air.

The first difficulty was greatly attenuated by rotating the sample in the cavity (paragraph 1.1.).

The second difficulty was partially overcome by dehydrating the fabric for a period of at least one hour at 40°C under vacuum. The fabric is then maintained for 10 minutes in a dry nitrogen or argon atmosphere at a pressure in excess of 1 atmosphere. The fabric is then pelletized into small cylinders in a hydraulic press with a pressure of 2 kilobars. The isotropy of the sample is considerably increased in this way ; the signal is also increased as the density of the sample is much higher ; at the same time the resitance of the sample to external perturbations (air, humidity) is augmented by slowing down the diffusion of gas from the surrounding atmosphere into the sample.

1.4 - Irradiation conditions

Fabrics were generally irradiated before being dehydrated and compressed so as to simulate real irradiation conditions.

Irradiations were performed with either a Co-60 or a Cs-137 source; dose rates ranged from 1 to 6 Gy per minute.

2. IRRADIATION EFFECTS

The following figures show the variations in amplitude and the modifications in the shapes of the ESR spectra of some of the fabrics studied. Examining these specta reveals that only fabrics made from cotton (Figure 2) or polypropylene (Figure 3) are sufficiently radiosensitive to be suitable for dosimetric purposes. Wool (Figure 4), linen (Figure 5) and

thermovyl (Figure 6) [commercial name] exhibit intense spectra ; however, these spectra do not depend on the dose received until very high doses are reached (several Gray) ; detailed studies of these fabrics will not therefore be pursued.

2.1 - Cotton

The dosimetric information obtained from the ESR spectra observed for these materials is due to the density of the free radicals produced as a result of the irradiation. Irradiation therefore results in an increase in the amplitude of the corresponding ESR spectra (Figure 2). It is for convenience and simplicity that the peak to trough ESR amplitude is employed as the measurement parameter instead of another parameter proportional to the free radical density as long as the shapes of the spectra do not vary, these two parameters are proportional one to another. The relationship between the ESR amplitude and the dose is linear over a region extending from a few Grays up to 10.000 Gy.

Beyond this region saturation sets in because the number of radicals destroyed by the radiation approaches the number generated.

At very low dose values a minimum ESR signal corresponding to the intrinsic free radical density of the cotton appears. Doses are determined by subtracting the ESR signal corresponding to non irradiated cotton from the signal corresponding to irradiated cotton. This limits the minimum detection threshold, in the most favorable case, to about 1 Gy.

2.2 - Polypropylene (PP)

The PP used in the textile industry is chiefly of a type having an isotactic structure ; such a structure ensures the mechanical and tactile qualities required.

The number of free radicals produced in PP by γ radiation and the shapes of the corresponding spectra depend on both the temperature during irradiation and during measurements. The presence of oxygen during irradiation leads to the formation of many different types of radicals, the most predominant of which, are of the peroxide type; the ESR spectra of peroxide radicals exhibit a characteristic asymmetic singlet (Figure 3).

As with cotton, the dosimetric information is related to the free radical density (density of peroxide radicals). The relationship between the ESR signal and dose (Figure 8) is linear between a few Grays (value beneath which the background noise signal dominates), saturation beginning to occur for doses of about 0.1 MGy.

3. TEMPERATURE EFFECTS

Irradiated textile fabrics generally exhibit a slow but progressive decay in their ESR signal with time, termed "fading". In general, the evolution in time of the corresponding signal diminishes with temperature; at liquid nitrogen temperature, the ESR signal remains stable. Signal decay accelerates at elevated temperatures. However, when a certain temperature threshold is reached, heat produces new radicals leading to an increase rather than a decrease in the corresponding signal.

3.1 - Fading at room temperature

Figure 9 shows how the room temperature fading of cotton varies over a period of 15 days. A fast decay in the signal is observed during the first 10 hours followed by a slower, or, in some cases, negligible decay. A more detailed analysis shows that the decay kinetics of the fast component increase with dose ; however for the slow component, decay is dose independent.

Similar phenomena occur for PP, the decay of which, however, appears to be more regular, presenting only a single component (Figure 10).

3.2 - Fading at elevated temperatures

These studies were undertaken in the hope of uncovering reversible temperature induced phenomena enabling the initial signal (prior to irradiation) to be determined.

In order to do this, a stepwise recombination model has been exploited. Figures 11 and 12 show respectively how the ESR spectra of cotton varies with temperature and also how the corresponding amplitude varies between room temperature and 205°C over approximately 1 hour intervals.

Similar phenomena occur with PP, but in this case, the minimum signal observed (Figure 13) corresponds to the intrinsic PP signal before irradiation. It is remarked that the phenomena is totally reversible and as long as the temperature does not exceed 100°C, the irradiation-signal erasing cycle remaining unchanged. Advantage has been taken of this phenomenon to evaluate pre-irradiation background signals.

Figure 14 shows the evolution of ESR spectra using this procedure:

a) initial background,
b) after irradiation (100 Gy),
c) after heating,
d) after being left 1 hour in the laboratory,
e) after being reheated.

4. Data processing

As stated above, dosimetric information is deduced from the difference between the peak to trough amplitude of the first derivative. A certain systematic error, however, affects the results when the background noise is poorly estimated. In order to overcome this difficulty, several methods have been developed which have not unfortunately led to a significant increase in accuracy.

a) analysis using Fourier transform techniques.

The Fourier frequency spectrum corresponding to the background noise of the sample is identified and then subtracted from the Fourier spectrum of the irradiated sample. A double integration in frequency space is then employed to determine the number of resonant radicals. The results obtained have led to a slight improvement in accuracy ; measurement time is, however much longer (4096 points are digitized) and the calculations necessary involve functions that are not always convergent.

b) analysis by interpolation.

A pre-existing catalogue of ESR spectra corresponding to the fabric being studied is employed. A fractional weighting method associated with a least squares analysis applied to the totality of the ESR spectra is used to determine an average proportionality factor. This method is very consistent for reference ESR spectra close to those of the fabric studied.

5. Conclusion

This method of dosimetry provides a useful tool for determining doses in the case of an accidental exposure to gamma irradiation, if the exposed individual is wearing clothing by a suitable nature :

1) stabilization of the irradiation induced signal prior to measurements,
2) cleaning with EDTA, (used to eliminate metallic compounds),
3) dehydration under vacuum,
4) saturation with nitrogen at high pressure,
5) very high pressure pelletizing,
6) dose measurement,
7) sensitivity measurements by adding doses,
8) dose measurement after heating (background noise).

Although the performance, that can be obtained with ESR measurements on textile fabrics, is insufficient to envisage applications in routine personnel dosimetry ; the method is certainly applicable to accident dosimetry where higher doses are involved. The exploitation of the results obtained from clothing covering the entire body can be used to provide information that is very useful to the medical practitioner treating the irradiated person.

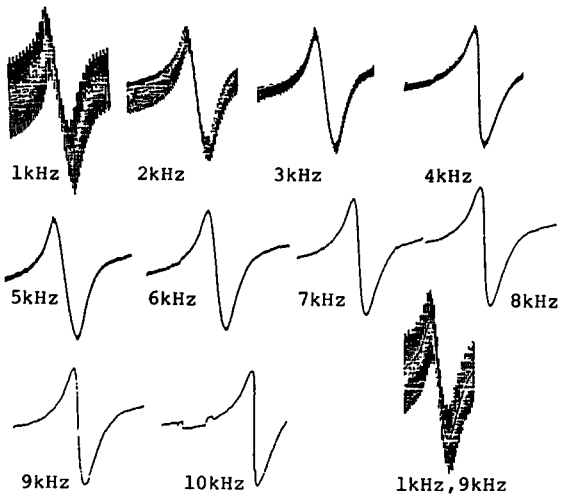

Figure 1 : Rotation speed influence on ESR response (3.2 kHz correspond to 1 rps).

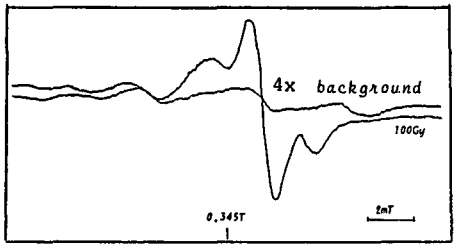

Figure 2 : ESR spectrum of cotton fabric.

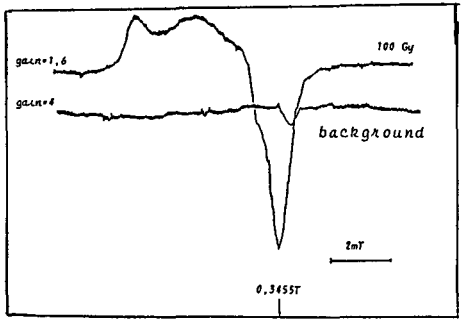

Figure 3 : ESR spectrum of PP fabric.

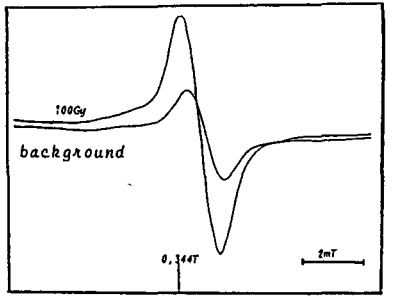

Figure 4 : ESR spectrum of wool fabric.

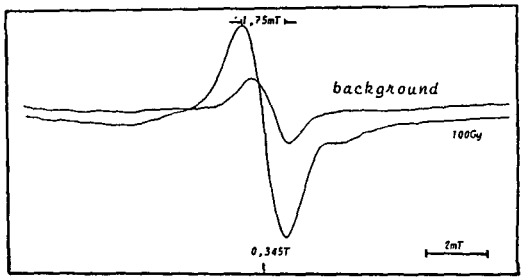

Figure 5 : ESR spectrum of linen fabric.

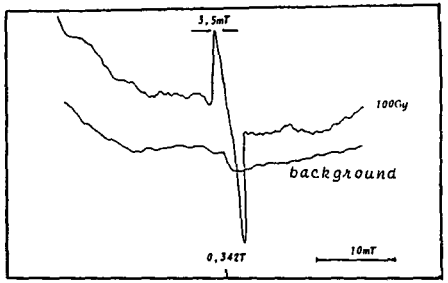

Figure 6 : ESR spectrum of thermoyl fabric.

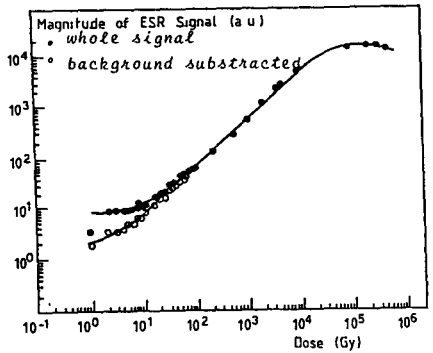

Figure 7 : Cotton ESR response versus dose.

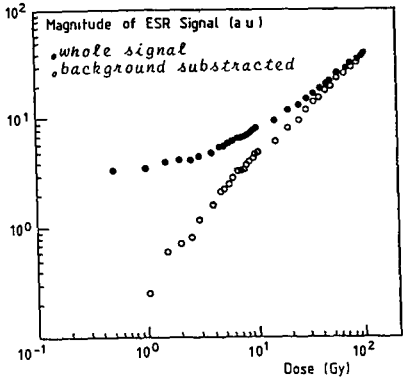

Figure 8 : PP ESR response versus dose.

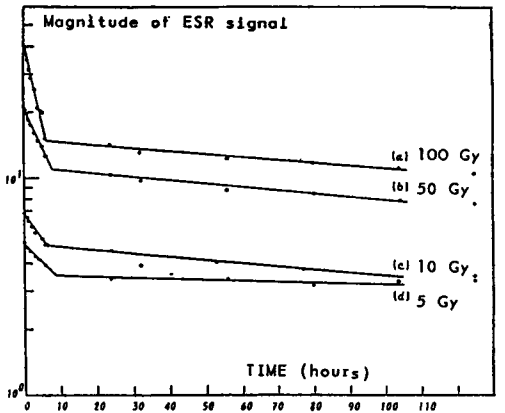

Figure 9 : Cotton fading at room temperature.

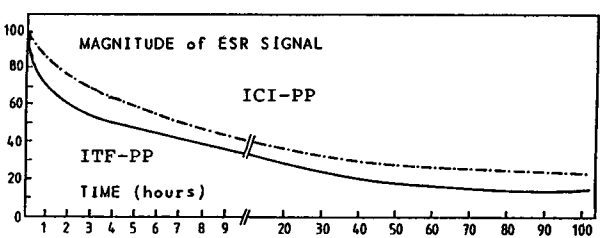

Figure 10 : PP fading at room temperature.

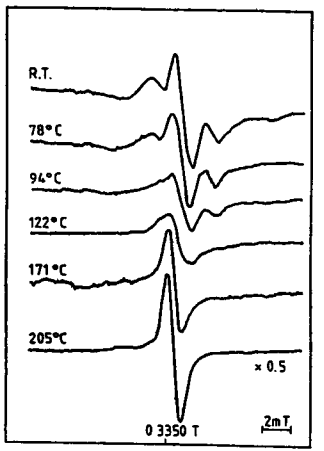

Figure 11 : Cotton ESR spectrum at different temperatures.

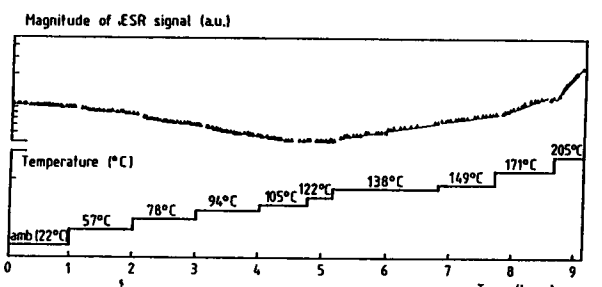

Figure 12 : Cotton ESR stepwise response.

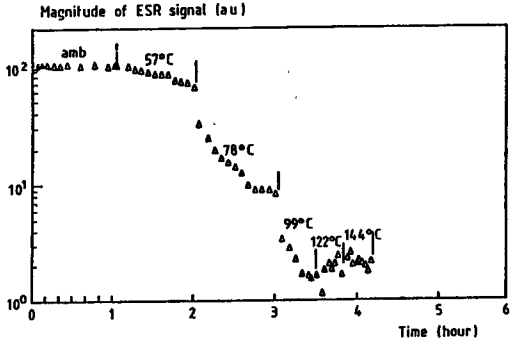

Figure 13 : PP ESR stepwise response.

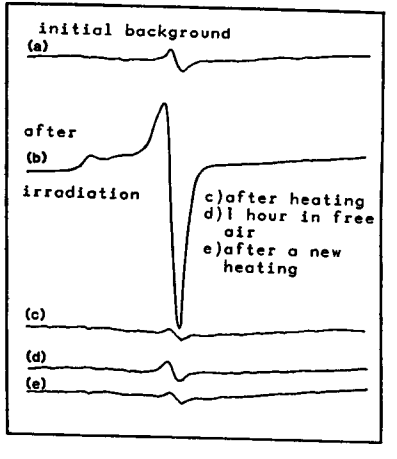

Figure 14 : Irradiation and thermal reversible cycle for PP.

IV. Other research group(s) collaborating actively on this project [name(s) and address(es)]:

Institut Textile de France
BP N°60
69132 ECULLY Cedex - France

V. Publications:

V. KAMENOPOULOU
"Accidental Gamma Irradiation Dosimetry using Clothing".
Proc. of the VII Int. Conf. or Sol. State Dosimetry.
Rad. Prot. Dosim. 17 (1/4) (1986) pp. 185-188.

V. KAMENOPOULOU
"Propriétés Dosimétriques des fibres textiles : Application à la dosimétrie, par résonance paramagnétique électronique, d'un accident d'irradiation gamma".
Thèse de doctorat, n° 176, Toulouse, Septembre (1987).

V. KAMENOPOULOU, B. CATOIRE et J. BARTHE
"Résonance paramagnétique électronique des fibres textiles coton et propylène = application à la dosimétrie d'un accident d'ionisation gamma".
Radioprotection, GEDIM 1988, Vol. 23, n° 3, pp 277-289.

J. BARTHE, V. KAMENOPOULOU, B. CATOIRE and G. PORTAL
"Dose evaluation from textile fibers. A post determination of initial ESR signal".
2nd Int. Symp. On ESR Dosimetry and Applications.
Munich/Neuherberg October 10-13 (1988).

J. BARTHE, V. KAMENOPOULOU, B. CATOIRE, F. BERMANN et G. PORTAL

"Résonance paramagnétique de textiles irradiés : application à la dosimétrie des rayonnements ionisants".

1°Journées Européennes d'Application de la RPE, Lyon 10-11 Janv. 90 (à paraître).

Title of the project no.: 4

Realization of an "operational" spectrometry unit for neutrons.

Head(s) of project:

J.L. CHARTIER

Scientific staff:

F. POSNY - C. ITIE - G. AUDOIN

I. Objectives of the project:

The "operational" spectrometry unit should be able to ensure the characterization of neutron fields encountered in radiation protection. For such measurements, the spectrometric system must have some essential qualities (good energy resolution, quasi-isotropic angular response, discrimination between neutrons and photons...) which have been approched as closely as possible by the use of two spherical gas-filled proportional counters (type SP2) and one liquid scintillator probe (type NE213).

II. Objectives for the reporting period:

The work carried out on this project during 5 years can be summarized as follows :

- choice and study of marketed detectors with qualities close to the required ones,
- realization of the associated electronic lines able to discriminate between neutrons and photons,
- adaptation of existing unfolding codes to our system on a microcomputer in order to keep the spectrometry unit transportable and "operational",
- measurements of wide spectra from 20 keV to 20 MeV.

III. Progress achieved:

III.1 - Introduction

The objective of the project was to study and realize an "operational" spectrometry system, that should be able to ensure the spectrometry of neutron fields met in actual radiation protection situations (occupational areas of nuclear power facilities, fuel cycle plants, research areas...).

This system represents a compromise between the different existing techniques :

- high resolution spectrometry techniques used in specialized laboratories on reference facilities,
- "multidetector" techniques leading to a simplified evaluation of the spectral distribution.

Moreover, the encountered radiation fields generally present a broad and complex energy distribution (from thermal neutron energies to 20 MeV), an anisotropic angular distribution and spurious photon radiations. Therefore, the spectral characterization of such fields requires the use of detectors with isotropic (or quasi-isotropic) angular response, good energy resolution ($\simeq$ 10%), sufficient sensitivity and the possibility to discriminate between neutrons and photons. Proton recoil detectors approach these essential qualities.

This choice led us to consider the following points :

- use of several detectors to cover a wide energy range : 20 keV to 20 MeV,
- realization of an associated measurement equipment able to discriminate between neutrons and photons,
- development of computer codes allowing to obtain the information required quickly after the measurements.

The spectrometry unit must also be reliable and transportable.

III.2 - Chronological events

1985 : . Realization of a preliminary spectrometry system associating :
- a small orthocylindrical (1/2" x 1/2") liquid scintillator (NE213),
- several cylindrical gas-filled proportional counters available at the CEA.

. Bibliographical research among the computer codes running on microcomputers ; choice of a differentiation unfolding method for the scintillator (based on TOM's code) and a differential matrix unfolding method for the counters (based on SPEC4 code).

. International market prospection to provide us with proton recoil proportional counters of spherical geometry : the only manufacturer was LND (USA).

1986 : . Determination of the LND'S spherical counter characteristics with monoenergetic neutron beams (Bruyères-le-Châtel and PTB facilities) : disappointing results (bad energy resolution, poor efficiency...) due to modifications of manufacturing criteria by the LND company.

. Study of the discrimination possibilities between detected neutrons and photons : "rise time" differentiation method for proportional counters, "decay time" method for the NE213 scintillator ; comparison and choice of the electronic elements.

1987 : . Purchase of two spherical gas-filled proportional counters (type SP2) from Winfrith laboratory : the former filled with hydrogen (3 bars), the latter filled with methane (5 bars), both with traces of ^{3}He for calibration purposes.

. Determination of the counter characteristics (response functions, efficiency, energy resolution) in monoenergetic neutron beams (Bruyères-le-Châtel) : encouraging results.

. Test of the whole spectrometry system in wide spectra at Cadarache (3 detectors + 2 electronic lines + 2 unfolding codes).

. New unfolding code (MATXUF) for the NE213 scintillator and verification of its associated electronic line at the BIPM facility (14.65 MeV neutrons).

1988 : . Introduction of the counter experimental data in the unfolding code (efficiency, energy resolution, response function shape correction factors) and check of the simplifying assumptions in the calcula- tions.

. Measurement of the two wide spectral distributions available at CEN Cadarache.

. Results presented at the 7th International Conference on Radiation Shielding held in Bournemouth.

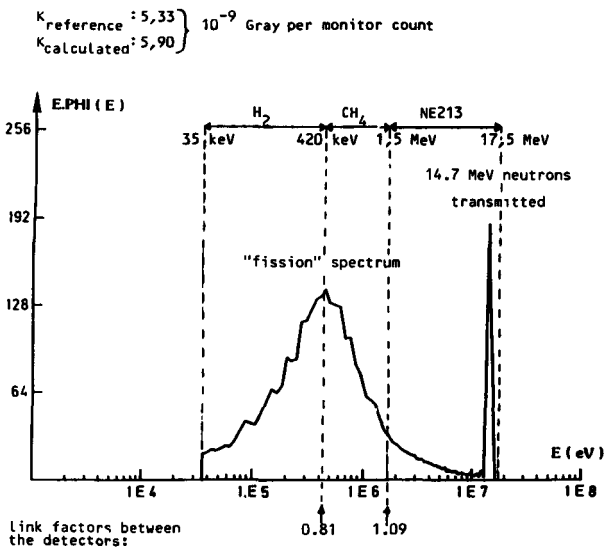

CONFIGURATION N°1: 14.7 MeV + ^{238}U

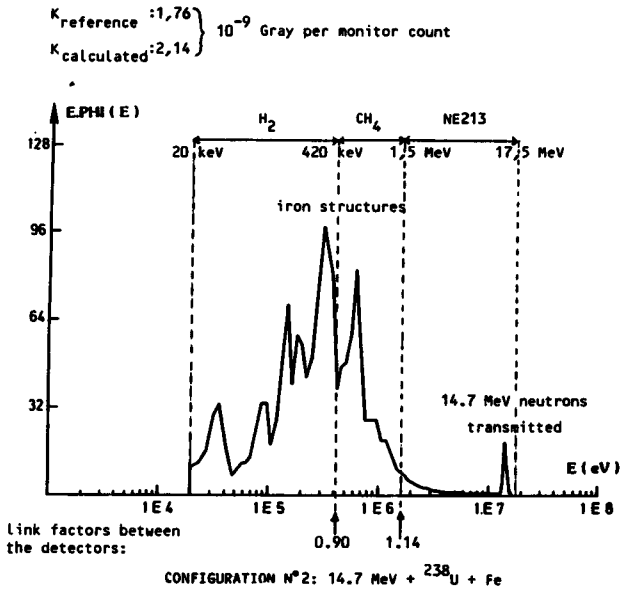

1989 : . The measurement of the spectral distribution of a calibrated Am-Be source was carried out at the begining of the year. In order to reduce the photon contribution, a 1mm thick lead shield was placed around the source. The results are given in the figure below :

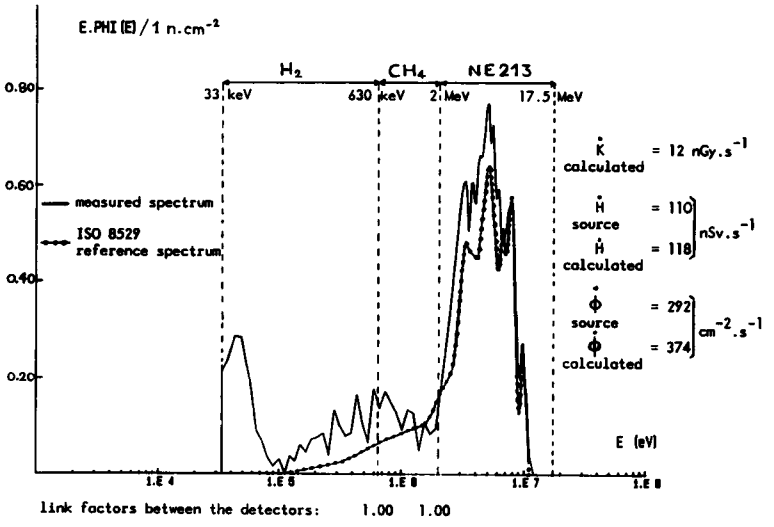

The dosimetric quantities $\dot{\Phi}$ and $\dot{H}$ calculated from the measured spectrum are compared with those deduced from the source calibration. The discrepancy between the results is relatively high, especially for the fluence rate : overestimation of 28%, 15% being due to energies below 100 keV. The component below 100 keV (not present in the ISO 8529 reference spectrum) takes place in the region where the hydrogen-filled counter is sensitive to photons. In spite of the lead shield and an estimation of the "high energy" photon contribution, it is not possible presently to decide whether no photons are recorded ; only the discrimination process could bring a definitive conclusion. Complementary measurements have to be done.

Some unexpected low values in the scintillator efficiency curve in the 2-3 MeV region led us to verify the influence of the target backing material for the T(p,n)^{3}He reaction with the Van-de-Graaf accelerator at Bruyères-le-Châtel. Parasitic (p,n) reactions were observed with copper backing, which modified the response function shape followed by an efficiency underestimation. Gold backing targets will now be used to avoid this parasitic contribution.

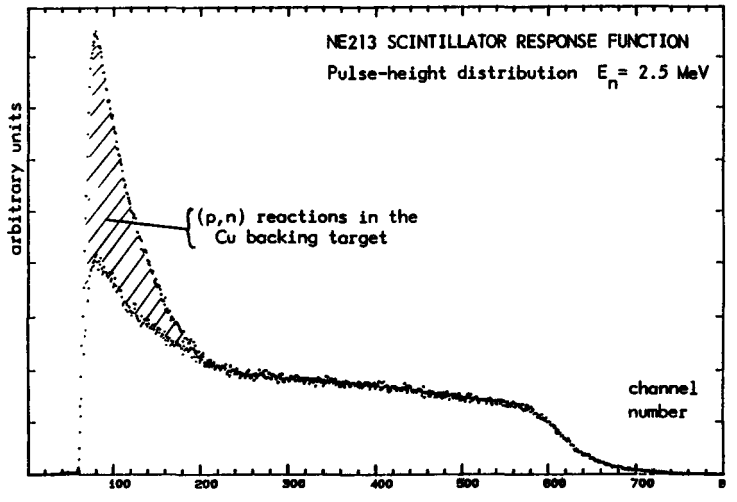

The study of the high energy neutron effect on the two spherical counters has begun with the 14.65 MeV neutron beam of the BIPM. The results are in progress.

In 1989 we had also to work on the measurement line maintenance. Currently marketed substitutes to out-of-date units had to be found:

- NE213 scintillators : two new ones have been purchased and mounted, they are under operating test,

- counter preamplifiers : the Winfrith Laboratory provided us with a preamplifer especially well-adapted to hydrogen-filled counters ; a home-made preamplifier is now available for the methane-filled counter,

- the multichannel analyser is being replaced by a microcomputer able to ensure data processing as well.

All these devices have been purchased but have to be put on line.

IV - Conclusion

The developments achieved in this project have allowed us to validate the choice of the spherical proton recoil proportional counters whose main characteristics (linear energy response, efficiency, energy resolution) have been determined. These experimental parameters have been included in the unfolding code. The counters associated with a NE213 scintillator have led to the realization of a spectrometry system able to cover an energy range from 20 keV to 20 MeV. However this unit needs further studies to become "operational" as defined in the introduction.

The results presented in this report suggest some comments on the use of such a spectrometry system for radiation protection purposes. The dosimetric quantity values deduced from the experimental spectra are fairly satisfying (in spite of a systematic overestimation of about 10%)

but the lowest energy analyzed is limited to 20 keV, or to 100 keV if any discrimination between neutrons and photons is performed. There is thus a lack of information between thermal neutron energies and the lower limit. A new orientation could be to associate to this spectrometry system a multisphere technique (already used by our laboratory) that should give results in this energy range. In spite of its poor energy resolution, the method could be efficient considering the spectral distributions encountered in radiation protection and the constant and low value of the quality factor value below 20 or 100 keV.

The overall neutron sensitivity of the spectrometry system is mainly limited by the spherical proportional counters. Calculations using the experimental response functions over the energy range covered by the counters have shown that the spectrometry system is expected to measure neutron spectra at dose-equivalent rates of about 50 $\mu Sv.h^{-1}$ and upwards. As the number of recorded pulses per unit of dose-equivalent rate is strongly dependent on the type of spectrum, and therefore on the fluence-to-dose-equivalent conversion factor, extensive experimental studies have to be carried out in order to specify this lowest limit in practical cases of radiation protection.

IV. Other research group(s) collaborating actively on this project [name(s) and address(es)]:

Dr. KLEIN - Dr. KNAUF
Neutron Metrology - Group 7.2
P.T.B.
3300 BRAUNSCHWEIG (FRG)

V. Publications:

M. BUXEROLLE, J.L. CHARTIER, J. KURKDJIAN, R. MEDIONI, M. MASSOUTIE, F. POSNY, E. DE MATOS and M. SUEUR
Experimental simulation of neutron spectra for the calibrating of radiation protection devices - (Sixth Symposium on Neutron Dosimetry - Munich 1987)
Radiation Protection dosimetry Vol 23 1-4 (1988).

J.L. CHARTIER, F. POSNY, R. MEDIONI and M. SUEUR
Experimental simulation and characterisation of neutron spectra for calibrating radiation protection devices.
7th International conference on radiation shielding
(12-16 Septembre 1988) Bournemouth (U.K).

Etude de deux systèmes spectrométriques pour les neutrons
Rapport de synthèse de la convention de recherche BNM N°87 2 46 0021
Mai 1988.

Title of the project no.: 5

Study and realization of an individual dosimeter based on photographic emulsions.

Head(s) of project:

G. PORTAL

Scientific staff:

Ph. BLANCHARD

I. Objectives of the project:

Study and realization of an individual neutron dosimeter based on photographic emulsions.

Replacement of the microscopic track counting method for nuclear emulsions by two methods based on the determination of the amount of silver present in an emulsion as a result of (n.p.) reaction :

- Neutrons activation
- X ray fluorescence detection.

II. Objectives for the reporting period:

- Construction of experimental devices.
- Evaluation of the efficiency of the neutron activation method.
- Evaluation of the efficiency of the X-ray fluorescence method.
- Reduction of background to lower detection threshold when these methods are used.

III. Progress achieved:

1. Methodology.

The technology proposed consists of macroscopically evaluating the amount of silver due to proton tracks induced by neutrons.

Two methods have been tested.

a) Activation method.

The emulsion is exposed in a reactor where the silver is activated.

The amount of silver present in the emulsion after processing is determined by β or γ counting.

b) X ray fluorescence method.

The emulsion is exposed to an X-ray beam. The X-ray emission due to silver is measured ; its intensity is proportional to the amount of silver in the emulsion.

Equipment has been constructed and tested ; standard samples have been used to evaluate the performance of these methods.

Processing conditions have been carefully studied to minimize :
- the chemical background of the emulsion.
- the signal due to mixed γ radiations.

2. Results.

An individual dosemeter consisting of various nuclear emulsions associated with a hydrogen converter has been studied.

The reduction of the chemical background of a blank sample has been studied extensively. Two methods were investigated : the use of chromium oxide and the use of steam induced oxidation. The first method was selected, the background noise being reduced by a factor of two.

Studies have also been conducted on n,γ discrimination. Two techniques were used : under-development by reducing development times ; the use of developers with variable oxido-reduction potentials (iron sulphate). The first method gave the most reproducible results, but discrimination was only enhanced by a factor of 30 percent.

To get better results a subtraction method was used ; the inconvenience, however of this technique is its inability to detect neutrons in the energy range 100 to 600 keV.

It was finally shown that, with the activation method, the threshold of detection for 2 MeV neutrons is about 0.5 mGy, a level that is sufficient for certain physical studies but insufficient for radiation protection. Results obtained with the X-ray fluorescence method were limited to a detection threshold of 5 mGy.

3. Discussion.

These results show that both methods can be used for high dose measurements but cannot be applied to individual dosimetry. It has been proposed to stop research in this field.

A thesis has been presented on this subject and published with reference to this contract : Thesis CRN/PN 87-33 N° 207 - Strasbourg.

Title of project No: 6

Area and Individual Dosimetry with proportional Counters

Head(s) of project:

J. BARTHE and M. PETEL

Scientific staff:

R. CHUITON and J.C. CHAPUIS

I - Objectives of the project:

The objectives of this work are multipurpose :

1/ to realize a new tissue equivalent plastic conducting material,
2/ to realize a large tissue equivalent counter (TEPC), which can be employed inside a rem-meter,
3/ to optimize by calculations and experiments, the ionization coefficients of the gaseous mixture, and, as a consequence, gaseous gain,
4/ to realize an individual dosemeter/ratemeter for dose equivalent measurements.

II - Objectives for the reporting period:

Measurements and calculations performed for the cylindrical or pseudo-spherical geometry used for the majority of counters, reveal the existence of inherent design deficiencies. Such counters are not suitable for use as individual dosemeters because of their size and also of the microphonic and mechanical effects that they manifest when used in this way. It was therefore decided to develop a field focusing multianode secondary elecron detecting system similar to the one designed and used for exoelectron detection (electron a few eV). The final objective of the work is the realization of a multicell counter based on this principle.

III. Progress achieved:

Various different phases of the research proposed are presented ; emphasis is given to the fact that, the first two phases have been realized, in spite of problems that have occurred in the industrial manufacturing stage.

1. Merlin Gerin tissue equivalent plastic

Figures 1 and 2 show how the theoretical equivalence of the material manufactured by Merlin Gerin (MG) compared to biological tissue ; the curves relate to neutrons and photons respectively. It is seen that this plastic is practically equivalent for neutrons, but possesses a better response for photons of low energy than Shonka plastic tissue equivalent material. Shonka plastic seems to be, however, easier to realize and mold.

2. Design and study of French counter

This counter was designed in close collaboration between the SIDR/FAR and Merlin Gerin and realized by Tinelli (MG). It is based on the following principles :

- an ortho-cylindrical geometry chosen because :
  - . such a geometry leads to a structure which is easy to construct from a mechanical point of view,
  - . it can be modelized easily,
  - . it possesses sufficient isotropy for radiation protection purposes.

- use of TE plastic from MG,

- use of an internal α source with a gravity effect shutter,

- separation and deactivation of adjoining volumes inside the confining envelope,

- circulation of a TE gas inside the volume of the counter ;

An operational counter will be constructed at a later date (internal diameter: 4 cm, cathode thickness: 5 mm, anode diameter: 25 μm, height: 4 cm.) Figure 3 shows a cross sectional view of the prototype counter constructed. Figure 4 shows the response of this counter to radiation from an Am-Be source.

Attention is drawn to the fact that this counter was observed to exhibit a non negligble sensitivity to beta particles from a Strontium-90 Yttrium-90 source. A certain microphonic sensitivity has also been observed.

3. Studies of gaseous gain in a cylindrical geometry

The absence of an ionization chamber regime at low voltages is an important feature of this counter, and is the result of a very intense electric field in the anode region. Consequently, an ionization regime with a collection efficiency of less than unity in the cathode region (partial recombination) coexists with a multiplication regime in the intense field region near to the anode.

This situation leads to serious difficulties in the experimental measurement of the source term, i.e. in determining the number of thermalized secondary electrons produced by the α particles.

Figure 6 shows the shape of the pulse spectra collected by the anode of the counter. The 1/2 energy peak corresponds to α particles having interacted with the anode wire.

Figure 7 shows the variations in pulse height (proportionnal to the gaseous gain value) as a function of the applied voltage.

Gaseous gain was investigated by varying the two main parameters i.e. gas pressure and the applied voltage on the anode. This procedure was repeated for several gas mixtures associated with different, but accurately known, transport parameters ; in this way calculation inaccuracies are minimized.

It has been observed (as clearly indicated in the previous report) that experimental estimations of gaseous gain are somewhat erroneous as a result of the simultaneous existence of two regimes, and because electrons in the intense field gradient zone cannot be considered to be in thermodynamic equilibrium. A further source of error will be revealed by a multineedle detection system.

4. Studies of multianode detection

In order two obtain the high sensitivity necessary for radiation protection, the surface area of the straight section must be made as large as possible. The multicell principle envisaged by H. Rossi has been adopted. Attention is drawn to the fact that the design of a system comprised of a large number of independent cells of this type is very complicated, difficult to realize and the cost prohibitive for individual detectors.

Preliminary work has involved the realization and study of a multianode system based on the multineedle detection system developed to detect exoelectrons emitted from a thermostimulated ionic crystal. Figure 8 is a schematic representation of the operating principles of such a system. Figure 9 shows the spectra obtained for an argon/methane mixture (50%) at a pressure of 100 torrs.

Because of the internal asymmetry of the electric field, collection effiency varies considerably with distance from the anode plane. The aim of this study is to define limiting values of the applied voltage and gas pressure consistent with operation in the proportional counter regime. A further aim of this study consists of characterizing the collection efficiency profile along the axis of symmetry of the system. The variable considered corresponds to the distance between the trajectory of the α particles emitted from the collimated source and the anode plane.

The following observations have been made :

1/ A critical voltage exists beyond which a selfsustained discharge regime dependent on the pressure and nature of the gas in the counter occurs ; this voltage increases with pressure and the proportion of methane in the argon/methane mixture (figure 9).

2/ The energy spectra of the pulses obtained shifts rapidly during the first few minutes of operation towards lower values, reaching a limiting value after a few hours. At the same time the amplitude of these pulses increases. This effect is attributed to the polymerization of the methane on the anodes; this phenomenon is not observed with argon and disappears after cleaning.

3/ The source term/anode plane distance greatly affects the shapes and energies of the spectra obtained. Integrated counts (area underneath the peaks) vary little with this distance, thus suggesting that the collection efficiency is practically constant. However, a considerable increase in pulse amplitude with distance takes place: a two-fold increase in amplitude occurs when the distance increaseses from 10 to 25 mm ; the pulses exhibit an exponential tail when the amplitude is very large (figure 10).

The way in which the spectra alter indicates that, under the conditions employed in these studies, multiplication occurs everywhere in the drift space. It is also possible to deduce the evolution of the integrated gain as a function of the distance between the source term and the anode plane. Intercomparison studies are currently underway, but the complex geometry of the electric field in the anode regions cannot, as yet be correctly represented.

5. Conclusions

The results obtained have led to a better comprehension of elementary phenomena coexisting in this type of proportional counter. The main problems related to the presence of an intense electric field in a methane atmosphere have been defined. The work performed in the framework of this contract has no permitted, as hoped, the completion of the studies undertaken in this field. A high priority is being given in our research program to these studies, which will be continued over the next few years.

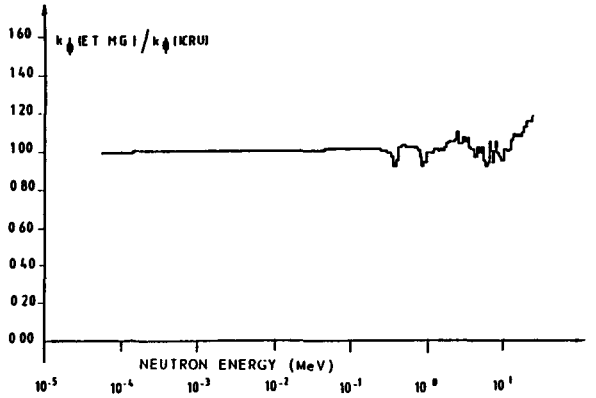

Figure 1 : Theoritical evaluation of the energy response of MG tissue equivalent material for neutrons

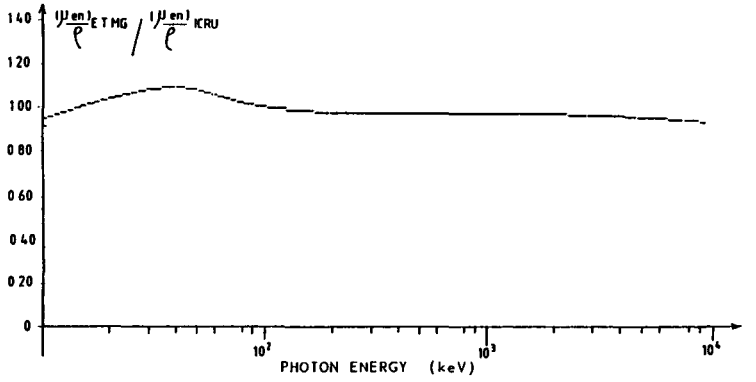

Figure 2 : Theoritical evaluation of the energy response of MG tissue equivalent material for photons.

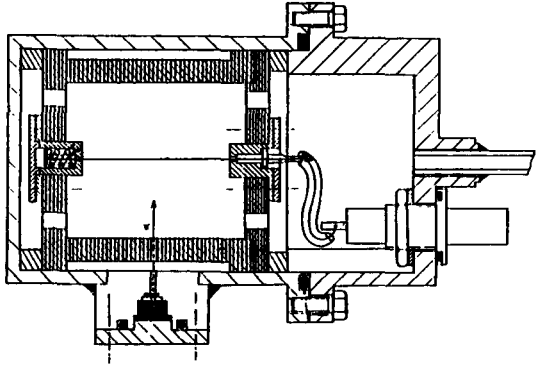

Figure 3 : Schematic view of MG1 proportional counter.

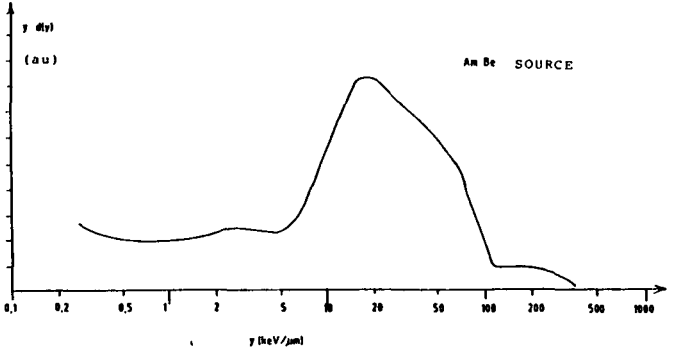

Figure 4 : Proportional counter response for an Am-Be neutron source.

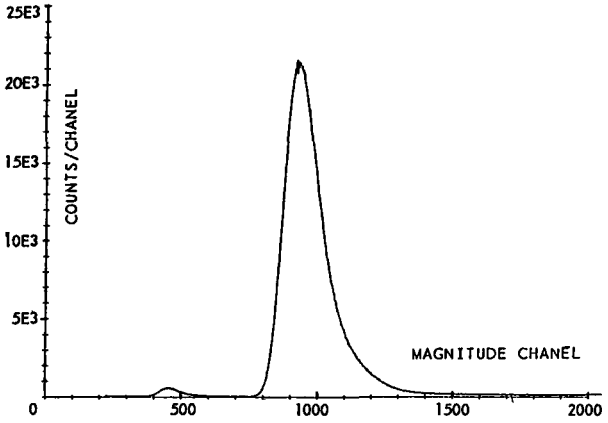

Figure 5 : Pulse distribution from an internal α source (MG1 counter).

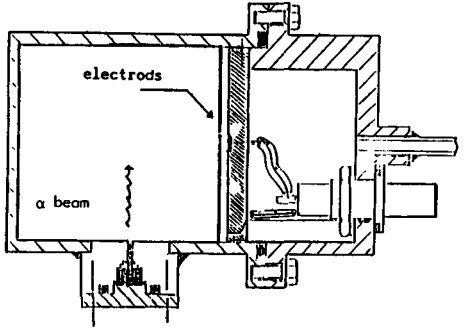

Figure 7 : Schematic view of multineedle proportional counter.

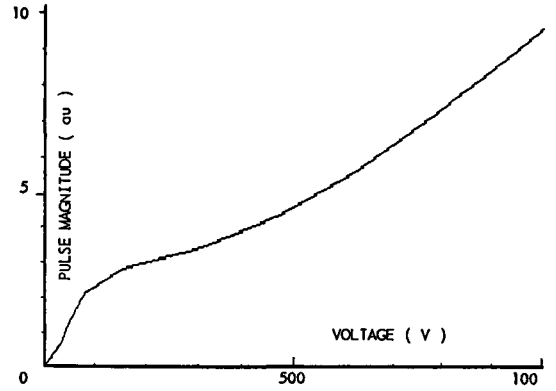

Figure 6 : Pulse magnitude versus applied voltage.

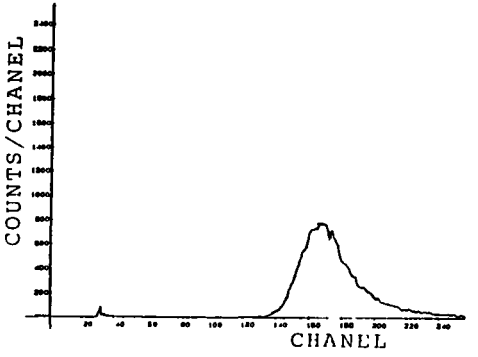

Figure 8 : Pulse distribution from an internal α source (MNPC).

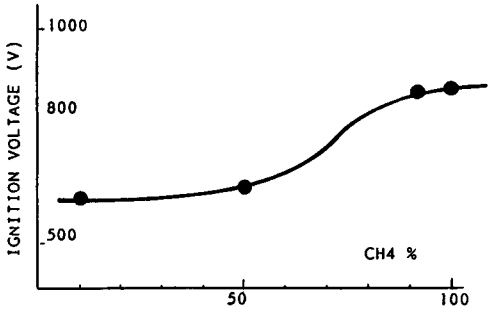

Figure 9 : Ignition voltage versus pressure for different Methan/argon gas mixtures.

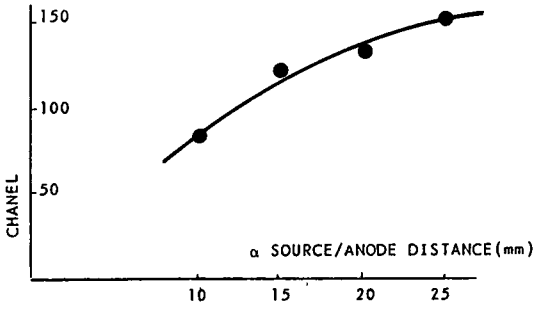

Figure 10 : Pulse magnitude evolution with α beam - anodic plan distance.

IV. Other research group(s) collaborating actively on this project [name(s) and address(es)]:

Groupe de recherche sur les décharges à faible intensité
Centre de Physique Atomique, Université P. Sabatier
31062 TOULOUSE Cedex - France -

V. Publications:

I. PEREZ
"Modélisation de la cinétique électronique et ionique dans un compteur proportionnel de type de Rossi".
Rapport de stage DEA Physique Radiologique, Toulouse, FRANCE (1987).

P. SEGUR, I. PEREZ, J.P. BOEUF and M.C. BORDAGE
"Microscopic Calculation of the gas gain in cylindrical proportional counters".
Workshop on the Implementation of Microdosimetric Techniques,
Schloss Elmau, October 18-20, FRG (1988).

P. SEGUR, I. PEREZ, J.P. BOEUF and J. BARTHE
"Modeling of the electron and ion kinetics in cylindrical proportional counters".
10th Symposium on Microdosimetry - Rome, May 21-26, 1989 (to be published).

P. TINELLI
"Etude et réalisation d'un détecteur microdosimétrique destiné à la radioprotection".
Doctorat de spécialité - Toulouse, 21 Novembre 1986.

RADIATION PROTECTION PROGRAMME
Final Report

Contractor:

Université Louis Pasteur
11, rue Humann
F-67085 Strasbourg Cédex

Contract no.: BI6-A-021-F

Head(s) of research team(s) [name(s) and address(es)]:

Dr. R.V. Rechenmann
LBRM - INSERM U.220
Université Louis Pasteur
11, rue Humann
F-67085 Strasbourg Cédex

Telephone number: 88-35.13.27

Title of the research contract:

Heavy charged particle track structure in tissuelike media, incidence on microdosimetric interpretations.

List of projects:

1. Heavy charged particle track structure in tissuelike media, incidence on microdosimetric interpretations.

Title of the project no.: BI6 - A - 021 - F

Heavy charged particle track structure in tissuelike media, incidence on microdosimetric interpretations.

Head(s) of project: R.V. Rechenmann

Scientific staff: R.V. Rechenmann
B. Senger
E. Wittendorp-Rechenmann

I. Objectives of the project:

The studies carried out in framework of the 1985-1989 Radiation Protection Programme dealt with track feature measurements along heavy charged particle (hcp) trajectories materialized in ionographic detectors, as well as their interpretation in terms of hcp interactions with dense matter.

During the reporting period emphasis has been laid on hcp range determinations, intergranular gap distributions along hcp trajectories, ionisation of molecules of radiobiological interest by protons and electrons, elastic scattering of low-energy electrons, as well as on the comparison of various formalisms describing the energy loss mechanisms by multi-dimensional graphical representations.

II. Objectives for the reporting period:

TRACK FEATURES RELATED TO THE INTERACTIONS OF CHARGED PARTICLES WITH TISSUELIKE MEDIA

1. Introduction

The present report summarizes the results obtained in the field of computerized track analysis, notably the design of modular, polyvalent opto-electronic image analysing assemblies with associated elaborate softwares, and their application to range determinations as well as to the intergranular gap distributions along materialized heavy charged particle (hcp) trajectories. A tentative preliminary interpretation of the latter phenomenon will be proposed.

The results obtained by the Double-Differential Cross-Section Mixed Treatment (DDCS-MT), developed in the Laboratory during preceding contract periods, has been extended to a large variety of molecules of radiobiologic interest. This approach has also been adapted in order to determine the ionisation induced by primary electrons. A relatively simple procedure has been developed for computing the elastic scattering of low- energy electrons, which is applicable to a large variety of targets within a relatively wide energy domain. Finally, computer-assisted 3- or 4- dimensional graphical representation modes have been designed in order to represent and to compare microdosimetric quantities obtained by means of available theoretical, empirical or semi-empirical expressions.

2. Interactive image analysis for track structure determinations

It shall be recalled that charged particle trajectories materialised in solid state nuclear track detectors, e.g. nuclear emulsions, contain an important quantity of information which can be quantified in terms of track parameters (Fig.1).

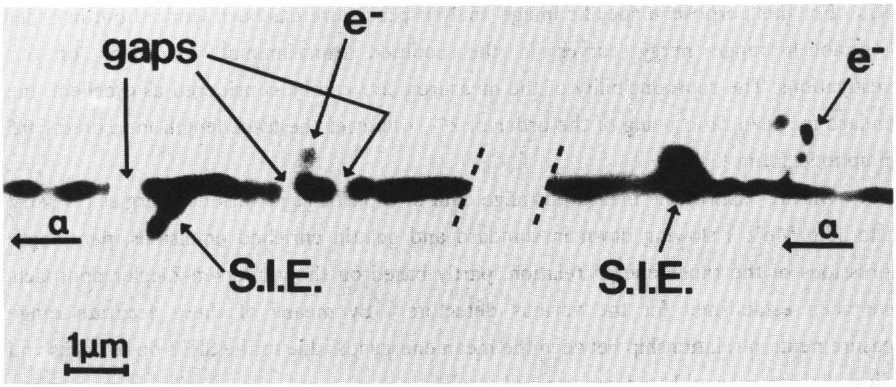

Fig. 1. Photomicrographs of various track features distributed along α-particle track segments recorded in Ilford L4 emulsion. S.I.E. = strong ionising event.

Numerous attempts to apply current image analysing systems, commercial or not, to the microscopic analysis of hcp track features yielded only partial success. During the contract period considered (1985-1989), a special effort has therefore been devoted to the

development of computer-assisted track structure analysis procedures. The small dimensions of the tracks, their complex morphological structure, which can hardly be categorised, as well as the necessity of performing multiparameter investigations on a large number of tracks (size > 1000) in order to attain high statistical precision, motivated the development of an interactive, modular track feature image analysis assembly. This system combines the advantages of high precision and reproducible visual microscopic measurements with automated data collection and treatment. For handling the different tasks related to the track structure analysis, elaborated data acquisition and evaluation computer codes have been designed.

These interactive track analysis procedures have actually been applied to hcp range measurements as well as to investigations concerning the distribution of "intergranular gaps" observed along α-particle trajectories recorded in nuclear emulsion.

3. Range determinations

In the evaluation of the damages induced in biological tissues by hcp's, the spatial extension of the interaction volume has to be taken into consideration, which is determined by the range of the primary particles as well as by the pathways of the ejected secondaries, especially the energetic recoils.

Determinations concerning the contribution of strong ionising events (SIE) to the energy loss of α-particles crossing ionographic detectors with a strong tissuelike component (51% up to 80% CNOH compound in volume) have been undertaken, in order to verify if the presence of SIE's has a significant influence on the first and second order moments of range of the primary, and eventually to establish a relationship between the mean energy loss due to the presence of SIE's along α-tracks and their radial spread [1].

For this purpose, a specific image analysis procedure has been worked out in order to establish range-energy curves in the codified experimental conditions of our investigations. The reproducibility of the measurements can be considered as excellent, the standard to mean ratio being of the order of 2%, whatever the track length measured (0.5 μm up to 92.5 μm).

On the basis of the measured range data of α-particles at various energies (4 MeV up to 13.6 MeV) slowing down in standard and gelatin enriched emulsions, parametric expressions of the range-energy relation, partly based on the Andersen-Ziegler approach, have been established for the various detectors . By means of these accurate range measurements, a relationship between the mean energy loss due to the SIE's on α-tracks and their radial spread could be demonstrated.

4. Intergranular "gap" distribution

Let us recall that intergranular gaps, which seemed to show a tendency to accumulate at particular α-particle energy intervals, have been detected along medium energy proton

and α-particle tracks recorded in highly sensitive emulsions [2]. A similar phenomenon had also been observed in dielectric substances [3,4].

In order to decide whether this feature can be effectively associated with energy loss mechanisms of heavy charged particles, this study has been resumed by applying an image analysing system (see section 1) to large samples (size : 1100) of 8.776-MeV α-particle tracks.

The results concerning the distribution of the intergranular gaps with length $\lambda > 0.1\mu m$ measured along 8.5-MeV α-particle tracks are represented in Fig. 2a. These data have been submitted to a detailed statistical analysis, notably by applying appropriate treatments, e.g. Kruskal-Wallis and independence tests, which both rejected, with a risk of being wrong much smaller than 1%, the hypothesis of an uniform distribution of the gaps in the domain of energy investigated. Furthermore, an intercomparison by means of both tests of the gap distributions within the 18 intervals constituting the histogram (Fig. 2a),

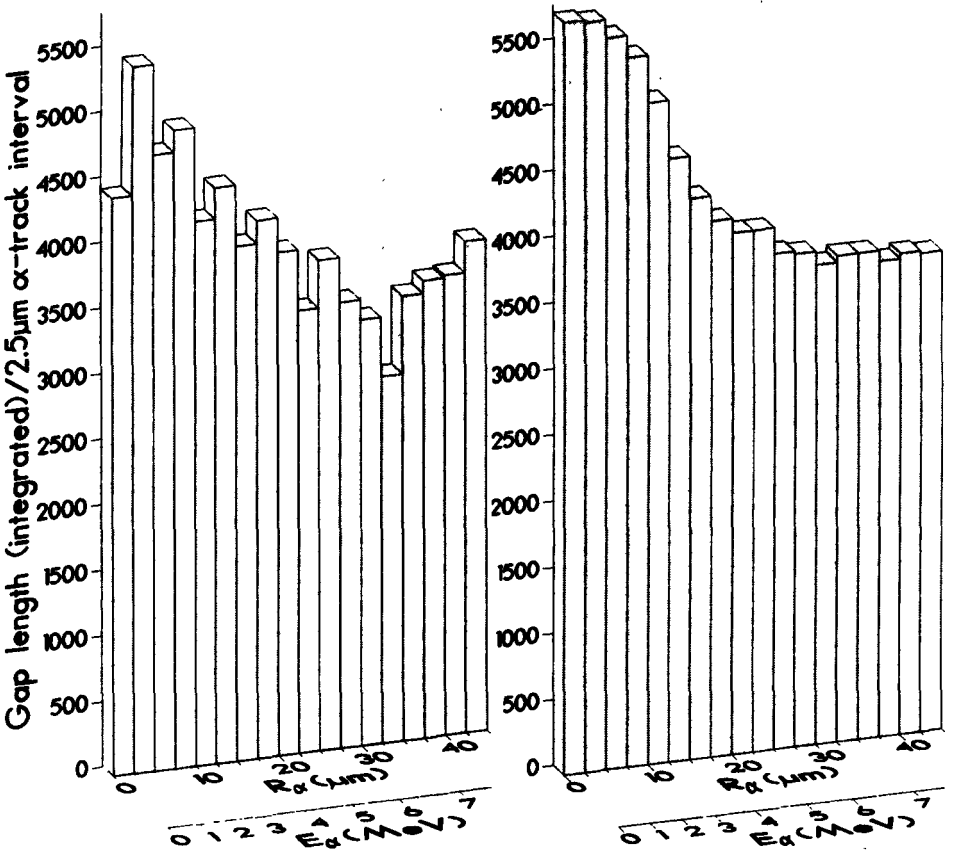

Fig. 2a *Fig. 2b*

Fig. 2. Intergranular gap length summed over 1100 α-tracks per 2.5μm primary track interval expressed in pixels (1 pixel = 0.01μm) plotted against α-particle residual range R_α or the corresponding energy E_α ; (a) experimental ; (b) calculated.

indicated that they differ significantly within a number of intervals. Thus, the highest gap frequency measured corresponds to the energy region of 0.7-1.5 MeV, and shows a strong contrast with the 7-MeV energy region characterised by a significantly lower gap frequency, which corresponds to a significantly stronger grain density (Fig. 2a) [5].

A tentative interpretation of the experimental observations has been undertaken in terms of spatial distributions of δ-rays around the incoming ion's path, by applying the DDCS-MT to the geometrical configuration of the AgBr microcrystals embedded in the gelatin matrix (Fig. 3). As far as the geometrical considerations are concerned, numerical simulations of the traversal of α-particles through the pattern of AgBr grains embedded in the CNOH compound of the photographic emulsion have been carried out by taking into account the various emulsion characteristics (silver halide concentration, stopping power of AgBr and gelatin, emulsion processing parameters, etc). Like expected, this approach resulted in a uniform gap distribution along the primary tracks. The experimental results had therefore to be described mainly in terms of physical, energy - depending mechanisms, namely the ionisation. The DDCS-MT has been applied for determining the production of δ-rays sticking out from the track core in order to evaluate the number of AgBr grains lying in the vicinity of the primaries' trajectories and therefore liable to participate to the track formation. At this preliminary state of our modelling, it could already be shown that the overall agreement with the experimental data is satisfactory in shape as well as in magnitude. Fig. 2b represents the calculated histogram of the total intergranular gap length summed over 1100 α-tracks per 2.5μm track interval as a function of the residual range (or energy) of the α-particles. At the actual state of our calculation, the simple model of interpretation proposed by us indicates that the observed phenomenon may be interpreted,

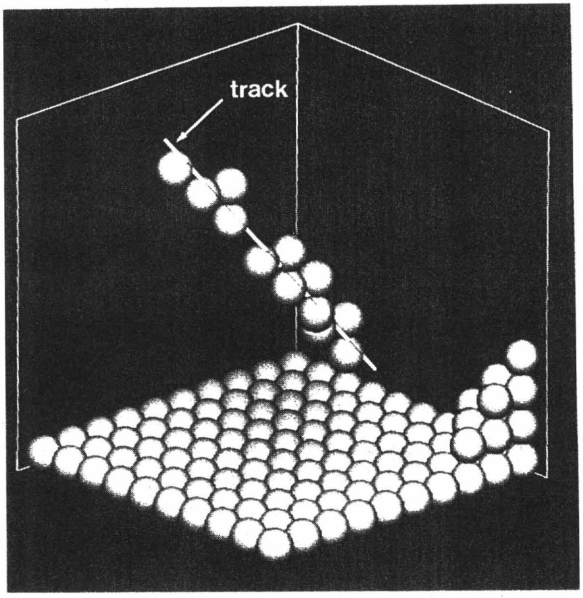

Fig. 3. 3-dimensional computer simulated schematic representation of the unprocessed AgBr microcristals (spheres) traversed by an α-particle (straight line), showing the track segments alternatively situated in (-----) and outside (——) the silver bromide grains.

at least partly, in terms of spatial ionisation patterns giving rise to the non-random destructive effects of corpuscular radiation, notably in tissuelike media.

5. Ionisation of molecules by protons

During the preceding contract period, a formalism was developed for the computation of double-differential ionisation cross-sections (DDCS) in the case of atoms, molecules and composite media irradiated by heavy charged particles (6-8). This approach, called DDCS-Mixed Treatment (DDCS-MT), has been applied to the determination of DDCS for a large variety of molecules of radiobiological interest (NH_3, CH_3NH_2, N_2, O_2, CO_2) which completes the study already devoted to H_2O and CH_4. The binding energy and the effective charge of each of the electrons constituting the electronic cloud of the molecule had been taken into account. Fig. 4 provides an example of the possibilities of the method elaborated. It can be seen that the calculated values reproduce satisfactorily the measured data over the entire angular domain, if one excepts the smaller values of the ejection energy T, where the experimental and calculated cross-sections diverge ; this effect may be due as well to the influence of the approximations introduced in the formalism as to the growing measurement difficulties [10].

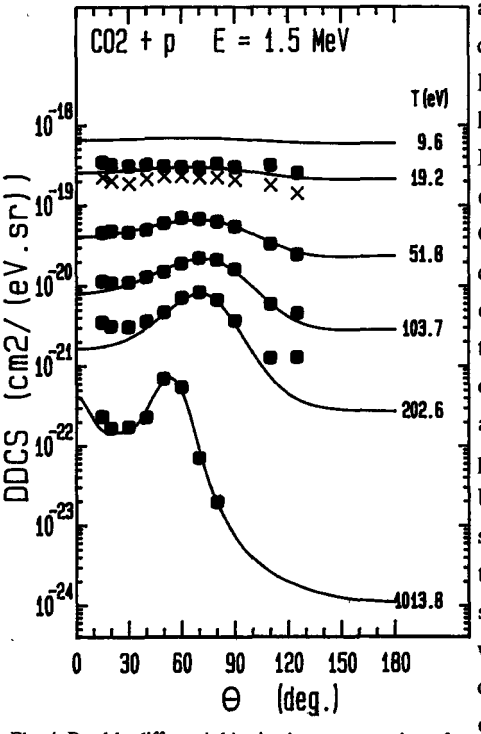

Fig. 4. Double-differential ionisation cross-section of carbon dioxide by 1.5-MeV protons, as a function of ejection angle and energy Θ and T. —— : calculated; ■ (x for T = 19.2 eV) : experimental values [9].

6. Ionisation induced by primary electrons

In order to quantify as precisely as possible the role of the interactions of the secondary electrons set in motion during the slowing-down of hcp's or primary electrons, it seemed interesting to try to extend the applicability of the DDCS-MT to the case of incident electrons [11]. An exchange factor [12] has been introduced in the DDCS-expression, which deviates mostly from unity when both emerging electrons have nearly the same velocity.

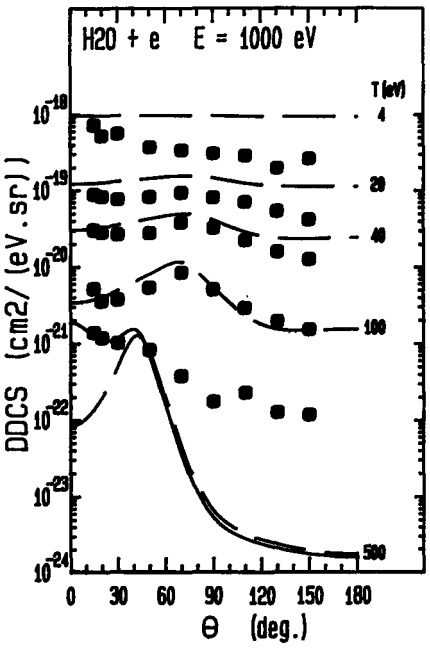

Fig. 5. Double-differential ionisation cross-section of water vapour bombarded by 1000-eV electrons, as a function of ejection angle Θ and ejection energy T. —— : present calculations without exchange factor ; —— : present calculations with exchange factor ; ■ : experimental values [13].

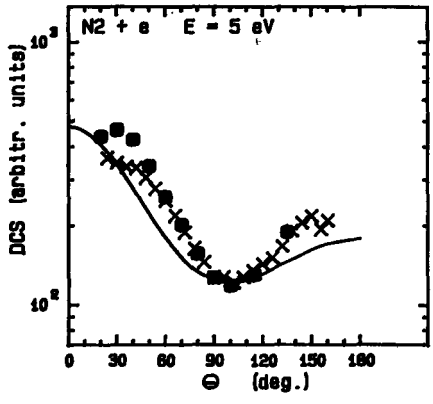

Fig. 6. Differential cross-section for the elastic scattering of electrons with energy E = 5 eV by molecular nitrogen, as a function of the scattering angle Θ. —— : present semi-empirical formalism; experimental : x [15], ■ [16].

As far as the description of the initial state of the target was concerned, each molecular orbital was breaked up into atomic components. It can be seen on Fig. 5 that, for relatively fast electrons, the agreement between calculated and measured data is reasonably good, if one excepts the ejection angles $\Theta \gtrsim 70°$ at ejection energy T = 500 eV where a strong discrepancy appears, partially attributable to O_K-Auger electrons not included in our computations.

7. Elastic scattering of low-energy electrons

Although the elastic scattering of the electrons does not lead to significant energy depositions in the traversed medium, this interaction influences the deposits by changing the direction of motion of the projectiles, all the more that their energy is small. Emphasis was therefore placed on the incoming electron energy region E < 200 eV. The aim of this study was to propose an approach, applicable to a large variety of targets and the widest possible energy domain. Two formulas have thus been developed, describing on the one hand the scattering differential cross-section (DCS), and on the other hand the scattering cross-section (CS) deduced from the preceding by integration over the scattering

angle Θ. Both formulas are parametric analytical functions, with parameters depending on the energy of the incoming electron. The parameters entering the DCS-expression were determined for various energies, and afterwards smoothed by simple functions of E [14]. Fig. 6 represents the calculated DCS, based on the parametric formula and the smoothed parameter values, which prove to be in good agreement with two sets of experimental DCS.

8. Multi-dimensional graphical representations

It is interesting from the microdosimetrical point of view to compare formalisms describing the energy loss mechanisms, proposed by various authors. Thus, multi-dimensional graphical representations appear as one of the most powerful methods for comparing various approaches aimed at the description of the ionisation cross-sections available in the li-

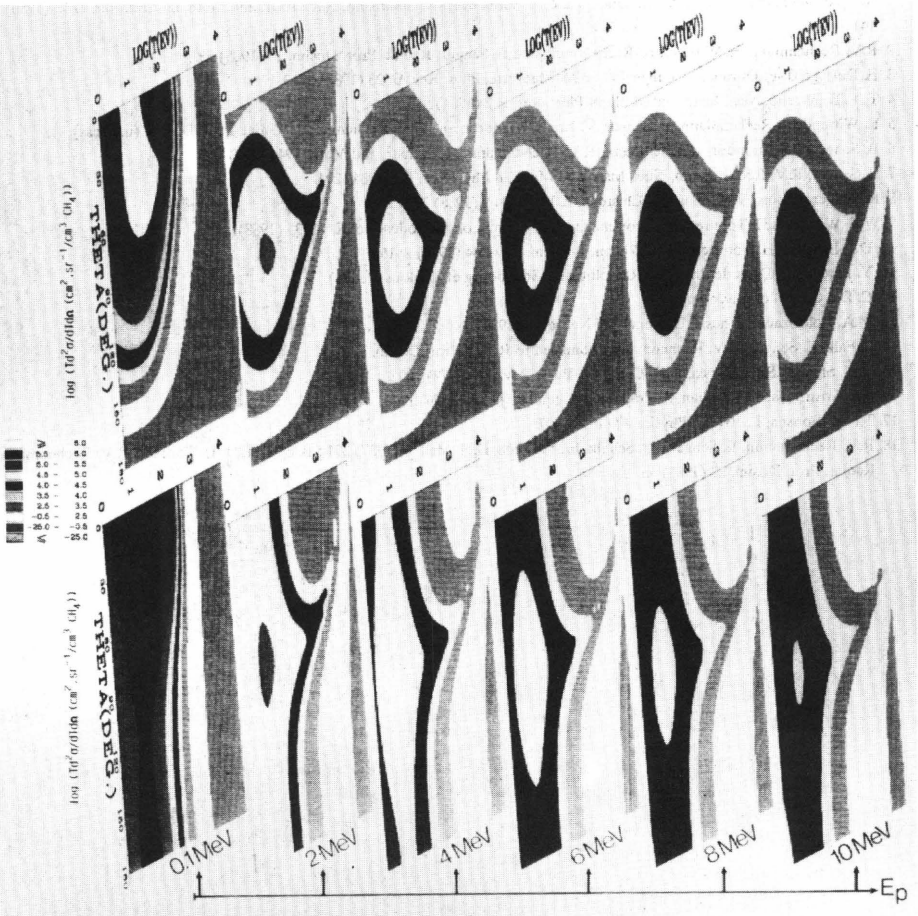

Fig. 7. Four-dimensional representation of TxDDCS as a function of the energy E of the incident α-particle, the ejection energy and angle of the ejected electron, T and Θ. The grey-level is correlated to the value of TxDDCS.

terature, notably the Binary Encounter Approximation (BEA) [17]. To this end a set of computer codes has been elaborated, which allowed to represent the microdosimetric consequences of the choice of a cross-section expression for the ionisation induced by hcp's.

As can be seen on Fig. 7, the distribution of the energy deposited around the hcp's trajectory varies strongly from one approach to the other. For instance, in the case of water vapour traversed by α-particles, some stricking differences between the DDCS-MT and the DDCS-BEA could be revealed, which would be more difficultly apprehended by more conventional means [18].

References

1. R.V. Rechenmann, B. Senger, J.B. Sanders and E. Wittendorp-Rechenmann, Nucl. Instr. and Meth. in Phys. Res. B 13 (1986) 141.
2. R.V. Rechenmann, E. Wittendorp-Rechenmann and B. Senger, Radiat. Prot. Dosim. 13 (1985) 53.
3. E. Dartyge, J.-P. Duraud, Y. Langevin and M. Maurette, Phys. Rev. B. 23 (1981) 5213.
4. T.A. Tombrello, Nucl. Instr. and Meth. in Phys. Res. B 2 (1984) 555.
5. E. Wittendorp-Rechenmann, B. Senger, V. Koziel-Vigneron and R.V. Rechenmann, Radiat. Prot. Dosim. (in press).
6. B. Senger, E. Wittendorp-Rechenmann, R.V. Rechenmann, Nucl. Instr. and Meth. 194 (1982) 437.
7. B. Senger, R.V. Rechenmann, Nucl. Instr. and Meth. in Phys. Res. B2 (1984) 204.
8. B. Senger, Atoms, Molecules and Clusters (Z. Phys. D) 9 (1988) 79.
9. W.E. Wilson, L.H. Toburen, priv. comm. and VIIth Symp. on Microdos., vol. I, p. 435 (1988).
10. D.J. Lynch, L.H. Toburen, W.E. Wilson, J. Chem. Phys. 64 (1976) 2616.
11. Y. Pétégnieff, DEA de Physique Radiologique, Strasbourg et Toulouse (1988).
12. C. Dal Cappello, priv. comm.
13. M.A. Bolorizadeh, Thesis, University of Nebraska (1984).
14. S. Falk, B. Senger, R.V. Rechenmann, submitted to Radiat.Prot. Dosim.
15. T.W. Shyn, R.S. Storlarski, G.R. Carignan, Phys. Rev. A6 (1972) 1002.
16. S.K. Srivastava, A. Chutjian, S. Trajmar, J. Chem. Phys. 64 (1976) 1340.
17. T.F.M. Bonsen, L. Vriens, Physica 47 (1970) 307.
18. R.V. Rechenmann, B. Senger, Ph. Schalk, Innov. Tech. Biol. Med. 8 (1987) 391 ; B. Senger, J.-L. Vonesch, R.V. Rechenmann, Radiat. Prot. Dosim. 23 (1988) 53.

IV. Other research group(s) collaborating actively on this project [name(s) and address(es)]:

- Fom-Institute for Atomic and Molecular Physics, Amsterdam (The Netherlands) (Dr. J.B. SANDERS).

- Laboratoire "Physique Moléculaire et Collisions", C.M.S.R., Université de Metz (Pr. Cl. TAVARD).

- Unité n° 311 de l'I.N.S.E.R.M., centre Régional de Transfusion Sanguine, Strasbourg (Pr. J.-P. CAZENAVE).

V. PUBLICATIONS 1985-1989

PART I

B. SENGER and R.V. RECHENMANN.
A calculated approach to the ionization of low-Z molecules by heavy charged particles.
Vth Symp. on Neutron Dosimetry. EUR. 9762 (1985) Vol. I, 265-273. Ed. H. Schraube, G. Burger and J. Booz.

R.V. RECHENMANN, E. WITTENDORP-RECHENMANN and B. SENGER.
Production by medium energy α particles of strong ionizing events in composite tissuelike media.
Vth Symp. on Neutron Dosimetry. EUR 9762 (1985) Vol. II, 845-853. Ed. H. Schraube, G. Burger and J. Booz.

R.V. RECHENMANN, E. WITTENDORP-RECHENMANN, B. SENGER.
Various aspects of heavy charged particle track structures in nuclear emulsion : A starting point for the description of track patterns in tissuelike media.
Radiat. Prot. Dosim. 13 (1985) 53-59.

R.V. RECHENMANN, B. SENGER, J.B. SANDERS, E. WITTENDORP-RECHENMANN.
Recent developments in the study of strong ionizing events distributed along α tracks ($E_\alpha < 13.6$ MeV) recorded in dense media.
Nucl. Instr. and Meth. in Phys. Res. B 13 (1986) 141-145.

B. SENGER et C. DAL CAPPELLO.
Sections efficaces doublement différentielles d'ionisation d'atomes et de molécules par des particules chargées lourdes. - I. Application à l'hélium.
11ème Colloque sur la Physique des Collisions Atomiques et Electroniques (Metz, juin 1986), Vol. I, 144-145.

R.V. RECHENMANN, B. SENGER, Ph. SCHALK.
Représentations multidimensionnelles assistées par ordinateur de sections efficaces d'ionisation par des particules α d'énergies moyennes traversant des milieux tissulaires.
Innov. Tech. Biol. Med. 8 (1987) 391-400.

B. SENGER, E. WITTENDORP-RECHENMANN, R.V. RECHENMANN.
Sections efficaces doublement différentielles d'ionisation par des particules chargées lourdes.
Actes des journées d'études:"Collisions (e,2e) et problèmes connexes"(RCP N° 784 - CNRS) Paris, décembre 1986 ; ed. Cl. Tavard (Université de Metz, 1987) 28-32.

E. WITTENDORP-RECHENMANN, J.-L. VONESCH, R.V. RECHENMANN, C. KLEIN-SOYER and J.-P. CAZENAVE.
Development of a computer-assisted methodology combined with a specific autoradiographic method. Application to the study of human endothelial cell regeneration.
Innov. Tech. Biol. Med. 9 (1988) 17-28.

S. FALK, B. SENGER et R.V. RECHENMANN.
Diffusion des électrons produits au cours de l'ionisation de molécules par des particules chargées lourdes.
Actes des journées d'études:"Collisions (e,2e) et problèmes connexes"(RCP N° 784 - CNRS) Paris, décembre 1987 ; ed. Cl. Tavard (Université de Metz, 1988) 23-28.

B. SENGER.
Calculated molecular double-differential cross-sections for ionisation under proton impact.
Atoms, Molecules and Clusters (Z. Phys. D) 9 (1988) 79 -89.

S. FALK, B. SENGER et R.V. RECHENMANN.
Diffusion élastique d'électrons de faible énergie par des molécules d'intérêt radiobiologique.
12ème Colloque sur la Physique des Collisions Atomiques et Electroniques (Caen, 1988) Vol. I, 83-84.

E. WITTENDORP-RECHENMANN, J.-L. VONESCH, V. KOZIEL-VIGNERON and R.V. RECHENMANN.
Modular interactive opto-electronic system for track structure analysis.
Radiat. Prot. Dosim. 23 (1988) 199-202.

B. SENGER, J.-L. VONESCH and R.V. RECHENMANN.
Application of computer-assisted multi-dimensional graphics in microdosimetry : ionisation of methane by 0-10 MeV protons.
Radiat. Prot. Dosim. 23 (1988) 53-56.

C. KLEIN-SOYER, A. BERETZ, J.P. CAZENAVE, E. WITTENDORP-RECHENMANN, J.-L. VONESCH, R.V. RECHENMANN, F. DRIOT and J.-P. MAFFRAND.
Repair process of a mechanical lesion of irradiated endothelial cells (EC) : Modulations by standard heparin (Hep) alone or in association with acidic fibroblast growth factor (aFGF).
Vth Int. Symp. on the Biology of Vascular Endothelial Cell (Toronto, Canada 1988).

Y. PETEGNIEF, B. SENGER et R.V. RECHENMANN.
Formalisme de sections efficaces différentielles d'ionisation de H_2O par des électrons de 100 à 1000 eV.
Actes des journées d'études : "Collisions (e,2e) et problèmes connexes" (RCP N° 784 - CNRS) Paris, décembre 1988 ; ed. Cl. Tavard (Université de Metz, 1989) 63-64.

B. SENGER, E. WITTENDORP-RECHENMANN and R.V. RECHENMANN.
Ionisation cross-sections for heavy charged particles traversing tissuelike media.
Proc. of "EULIMA Workshop on the potential value of light ion beam therapy" (Nice, 1988) ; ed. P. Chauvel and A. Wambersie (1989) 357-368.

Ph. SCHALK, G.N. LAMBROU et R.V. RECHENMANN.
A computer-based method for multidimensionnal representations and assessment of visual field data.
Innov. Tech. Biol. Med. 10 (1989) 115-126.

E. WITTENDORP-RECHENMANN, C. DEMANGEAT, M. FINCK and S. LEVY.
A fast, high efficiency microautoradiographic procedure for the localization of -decaying radionuclides - Case of indium-111.
Eur. J. Nucl. Med. 15 (1989) Abstract 711.

E. WITTENDORP-RECHENMANN, B. SENGER, V. KOZIEL-VIGNERON and R.V. RECHENMANN.
The distribution of intergranular gaps along α tracks recorded in ionographic emulsion.
(Radiat. Prot. Dosim, in press).

B. SENGER, S. FALK and R.V. RECHENMANN.
Semi-empirical expressions describing the elastic scattering of slow electrons by molecules.
(submitted to Radiat. Prot. Dosim).

PART II

J.-L. VONESCH : "Mise au point d'un ensemble de logiciels spécifiques de saisie et de traitements de données en vue de l'analyse d'images ionographiques à l'aide d'une chaîne de mesure opto-électronique semi-automatique".
Rapport de stage de D.E.S.T.U. option I.E.A. (Informatique, Electronique, Automatisme), Institut de Promotion Supérieur du Travail, Université Louis Pasteur, Strasbourg, 1986.

D. ADDI : "Relation parcours-énergie de particules α d'énergies moyennes (E_α < 13.6 MeV) dans des milieux tissulaires. Cas des émulsions ionographiques à 68 % et 80 % de composante CNOH en volume".
Rapport de stage de D.E.A. de Physique Radiologique, Université Louis Pasteur, Strasbourg, et Université Paul Sabatier, Toulouse, 1987.

S. FALK : "Diffusion élastique d'électrons (1 eV - 200 eV) par des molécules d'intérêt radiobiologique - Contribution à la modélisation de la structure des traces de particules chargées".
Thèse de l'Université Louis Pasteur (mention "Sciences"), Strasbourg, 1988.

B. DACOURI : "Mise au point d'une méthode ionographique à haute efficacité pour la détection et la localisation de radioéléments émetteurs β - . Premiers résultats dans le cas de l'indium-111".
Rapport de stage de D.E.A. de Physique Radiologique, Université Louis Pasteur, Strasbourg, et Université Paul Sabatier, Toulouse, 1988.

Y. PETEGNIEF : "Contribution à l'extension aux électrons primaires d'une expression permettant de déterminer la distribution spatiale des électrons δ dans les milieux tissulaires".
Rapport de stage de D.E.A. de Physique Radiologique,Université Louis Pasteur, Strasbourg, et Université Paul Sabatier, Toulouse, 1988.

M. FINCK : "Détection autoradiographique de radioéléments utilisés en Médecine Nucléaire - Cas de l'Indium-111.
Rapport de stage de D.E.A. "Effets biologiques des radiations ionisantes et Radiopathologie", Université Louis Pasteur, Strasbourg, et Universités Paris XII, XI et V et I.N.S.T.N., Paris, 1989.

J.-L. VONESCH : "Mise au point de systèmes opto-électroniques interactifs d'analyse de l'image ionographique - Applications microdosimétriques et autoradiographique".
Diplôme de Recherche Spécialisée de l'Université Louis Pasteur, Strasbourg, 1989.

RADIATION PROTECTION PROGRAMME

Progress Report

1989

Contractor:

Inst.Nat.de Physique des Particules
et Physique Nucléaire (IN2P3)
20, rue Berbier du Mets
F-75013 Paris

Contract no.: BI6-A-304-F

Head(s) of research team(s) [name(s) and address(es)]:

Dr. P. Siffert
Ctre de Recherches Nucléaires
Laboratoires PHASE
23, rue du Loess, BP 20
F-67037 Strasbourg Cedex

Telephone number: 88286543

Title of the research contract:

Development of an universal personal dosimeter using semiconductor sensors for mixed radiation fields.

List of projects:

1. Development of an universal personal dosimeter using semiconductor sensors for mixed radiation fields.

Title of the project no.: BI6 - A - 304 F

Development of an universal personal dosimeter using semiconductor sensors for mixed fields.

Head(s) of project:

SIFFERT Paul

Centre de Recherches Nucléaires, Laboratoire PHASE

23, rue du LOESS - BP 20, F-67037 STRASBOURG CEDEX (France)

Scientific staff:

SIFFERT Paul

JUNG Monique

TEISSIER Claude

I. Objectives of the project:

The general objective of this project is to develop in close collaboration with a series of european laboratories, a high sensitivity dosemetric system using optimalized semiconductor detectors, able to give a dose response as close as possible to the tissue equivalent, once in a mixed radiation field of both γ-rays and fast and thermal neutrons.

II. Objectives for the reporting period:

The general goal of this research programme is focused towards two major directions : development of a series of semiconductor sensors optimalized for γ-rays and both thermal and fast neutrons, in their response which has to be as close as possible to tissue equivalent ; development of a pocket sized dosemeter integrating these sensors together with a microprocessor giving the various contributions to the dosis.

In this first period, we have focused our activities towards 3 directions : computer simulation of the filters associated with various types of semiconductor detectors based on Si and CdTe, both for γ-rays and neutrons ; development of a large number of Si and CdTe detectors.

III. Progress achieved:

1. Methodology

To fullfill the 3 activity domains mentionned above, Monte Carlo codes have been developed in the laboratory to simulate the response of the various types of sensors associated with filters of different nature and tacking also into account the electronic pulse handling.

Several possibilities have been identified to reach a flat dose response as a function of energy, for the various types of radiations considered.

Furthermore, a large number of detectors have been prepared starting from various types of silicon (resistivity, lifetime of carriers, thickness) and cadmium telluride ; these detectors have been dispatched to the other partners.

2. Results

For gamma-rays in the studied regions from 20 keV to 1,5 MeV, the optimal Sn and Al filter thicknesses have been determined as well as those of the polyethylen used as fast neutron converter in the energy range from 1 MeV to 15 MeV.

For the experimental part, the read-out prototype is finished and allows to display the measured doses for the 3 channels, gamma, fast and thermal neutrons.

3. Discussion

It is clear that a good sensitivity can be obtained for the gamma detection in the frame of the international requirements for a gamma energy of above 100 keV and that an improvement could be possible towards measurements of lower energy by associating at least 2 or 3 Sn filters. For the fast neutron channel, the dose response could also be flatted with an association of 2 different thicknesses of polyethylen. In that case, it would be necessary to associate several of our prototypes

envisageable for an area dosemetric system.

The first experimental measurements performed by our partners show the great sensitivity of the material used for manufacturing the sensors on the response which is measured. This confirms that the Monte Carlo code developed is well adapted for this application. Detailled investigations we performed ourself on a specific device have shown that good agreement can be reached by our model.

The present status of our electronic set-up development indicates that a pocket sized dosemeter can be realized both for gamma - rays and neutrons (thermal and fast) with the possibility to display and to numerize the contribution of each type of radiation to the total dosis. This is an interesting progress in personal dosemetry in mixed fields.

IV. Objectives for the next reporting period:

The electronic set-up incorporating the microprocessor associated with the three types of detectors used (γ-rays, n and n_{th}) has to be finished and tested by incorporating the experimental results obtained on our detectors by our partners.

V. Other research group(s) collaborating actively on this project [name(s) and address(es)]:

1. Institute of Physics, University of Aarhus
   DK - 6000 AARHUS C (Denmark) (Prof. E. Uggerhøj)
2. Physikalisch Technische Bundesanstalt, Postfach 3345
   D - 3300 BRAUNSCHWEIGH (F.R.G.) (H.M. Kramer)
3. Institute of Physics, Rome University "La Sapienza", P. le. A. Moro 2,
   I - 00185 ROMA (Italy) (Prof. C. Furetta)
4. CERN, Div. TIS, CH - 1211 GENEVE 23 (Switzerland) (K. Goebel)
5. CNRS, Service Central de la Sécurité, 15 Quai Anatole FRANCE
   F - 75700 PARIS (France) (C. Teissier)

VI. Publications:

Theoretical Cs-137 gamma-ray detection sensitivity curves calculated for silicon sensor devices

M. JUNG, C. TEISSIER and P. SIFFERT

Submitted to the 7th Symposium on Radiation Measurements and Applications (Ann Arbor, Michigan (USA), May 21-24, 1990).

RADIATION PROTECTION PROGRAMME

Progress Report

1989

Contractor:

Institute of Physics
University of Aarhus
Ny Munkegade
DK-8000 Aarhus

Contract no.: BI6-A-303-DK

Head(s) of research team(s) [name(s) and address(es)]:

Prof. E. Uggerhøj
Institute of Physics
University of Aarhus
Ny Munkegade
DK-6000 Aarhus

Telephone number: 06-128899

Title of the research contract:

Development of an universal personal dosimeter using semiconductor sensors for mixed radiation fields.

List of projects:

1. Development of an universal personal dosimeter using semiconductor sensors for mixed radiation fields.

Title of the project no.:
BI6-A-303-DK

Development of an universal personal dosimeter using semiconductor sensors for mixed radiation fields.

Head(s) of project:

Professor E. Uggerhøj
Institute of Physics
Aarhus University
Ny Munkegade, DK-8000 Aarhus C

Scientific staff:

N. Hertel
E. Uggerhøj

I. Objectives of the project:

The objective of the program is to develop a pocket sized dosimeter which would give a flat energy response (when normalized to ^{137}Cs), a response that compares with the most recent ICRP recommandations. The dosimeter will be composed of silicon detectors and the associated electronics, especially designed to give the dose reading by appropriate weighting of the various radiation contributions to the field.

The mixed radiations field is composed of the following:
X- and gamma rays, thermal neutrons, epithermal neutrons up to 1 MeV and 1 to 15 MeV fast neutrons.

II. Objectives for the reporting period:

At the Institute of Physics, Aarhus University, Denmark, a Danish center for synchrotron radiation is under construction (see enclosed Newsletter).

The center includes a 100 MeV electron accelerator (race-track microtron) and a 0.6 GeV storage ring for the production of synchrotron radiation. The microtron is used both as an injector for the storage ring, and for the production of short-lived radioactive isotopes for use in nuclear medicine.

The contribution to the project from the Aarhus group consists of detailed tests of the proposed personal dosimeter in a radiation environment with a wide range of radiation types and energies.

III. Progress achieved:

The most intense source of high energy radiation in the above mentioned SR-facility is the microtron. Calculations and experiences from other machines of a similar nature leads to expected radiation doses inside the shielding of the order of 25 Sv/h for gamma radiation and 5 Sv/h for neutrons, so measurements of radiation levels ranging from these high levels to background levels will be possible.

The center will be used both for fundamental research in physics, chemistry, and biomedical sciences, and for industrial research and development.

Since the center will act as a service facility, most users come from outside the Institute of Physics. In a case like this, rigid safety procedures are demanded, and accurate and dependable systems able give precise values for both short- and long term doses are necessary.

Unfortunately, the money for this DK-contract was delayed one year (contract signed here June 1988 - first money arrived June 21, 1989). This meant that the necessary highly sensitive, wide range tissue equivalent radiation detectors for evaluation of actual radiation doses were not available here until the end of 1989. In order to remedy this problem we made an arrangement with the Swedish Synchrotron Radiation (SR) Laboratory in Lund. Here they have a SR facility like the Aarhus one, and the injector is also a 100 MeV race-track Microtron (see Newsletter). A radiation survey around the Microtron was made as a collaboration between the radiation protection group at CERN, The Max-Lab. and the Institute of Physics, Aarhus University. In the following the measurements are described.

Measurements of the radiation dose rate around a 100 MeV race-track microtron.

Measurements have been made of radiation dose rates in the vicinity of the 100 MeV race-track microtron at MAX-lab in Lund, Sweden. The measurements determined the intensities of both neutrons and gamma rays, as well as the angular dependence of the radiation.

In order to create worst case conditions, the electron beam was allowed to hit a 2.5 mm thick stainless steel plate at an angle of 45 deg. Radiation emerging from the point of collision was detected at a distance of 1m at angles between 0 and 90 deg.

All measurements were performed with the machine running at typical conditions. These are:

Electron energy:	100 MeV
Peak current:	20 mA
Pulse width:	1 μs
Repetition rate:	10 Hz

This corresponds to a 100 MeV DC beam with a current of 200 nA. The beam power is about 20 W. The power lost in the target is estimated to be zw.

The MAX microtron is situated in the basement of the building, surrounded with shielding walls consisting of 3 meters of sand. Entrance to the room is via a 2 meter thick, concrete door. Radiation doses outside the room are less than 25 μSv/h at all points. All measurements reported in the following were conducted inside the room.

Measurements of gamma dose rate were done using 1 cc EGG and 3 liter PTW air filled chambers, while the neutron dose rates were made with a REMION chamber, a Boron Chamber and a fission counter. Using this equipment, gamma radiation doses were found to vary between 43.1 and 1.0 Sv/h when going from 19 to 90 deg with respect to the beam direction. The neutron dose rates varied between 7.9 and 1.7 Sv/h.

The radiation survey has served to show what types and intensities of radiation can be expected in the vicinity of a race-track microtron, and it has indicated which types of monitoring equipment would be useful for routine monitoring of levels during routine use.

IV. Objectives for the next reporting period:

The Microtron radiation survey showed that a SR-facility with its mixed radiation field of varying intensity is ideal for a final test of the personal dosimeter. In the coming period the Aarhus group will test the final protypes produced and pre-tested by the other laboratories joining the project.

V. Other research group(s) collaborating actively on this project [name(s) and address(es)]:

FRANCE

CENTRE DE RECHERCHES NUCLAIRES
Laboratoire PHASE
P. SIFFERT
F-67037 STRASBOURG CEDEX
phone 88 28 65 43

C.N.R.S.
Service Central de Sécurité
C. TEISSIER
F-75007 PARIS
phone 88 28 63 21

GERMANY

PHYSIKALISCH TECHNISCHE BUNDESANSTALT
Postfach 3345
H.M. KRAMER
D-3300 BRAUNSCHWEIG
phone (0531) 5926410

ITALY

INSTITUTE OF PHYSICS
ROME UNIVERSITY "La Sapienza"
P.le.A.Moro 2
I-00185 ROMA
C. FURETTA
phone (00396) 4976459

CERN

Div. TIS
K. GOEBEL
CH-1211 GENEVE 23
phone (022) 83 21 59

VI. Publications:

None.

RADIATION PROTECTION PROGRAMME
Final Report

Contractor:

University of St.Andrews
College Gate
St.Andrews
GB Fife KY16 9AJ

Contract no.: BI6-A-024-UK

Head(s) of research team(s) [name(s) and address(es)]:

Dr. D.E. Watt
Dept.of Physics and Astronomy
University of St.Andrews
North Haugh
GB St.Andrews, Fife KY16 9SS

Telephone number: 334-75851

Title of the research contract:

Specification and measurement of radiation effectiveness.

List of projects:

1. Specification and measurement of radiation effectiveness.

Title of the project no.:

Specification and measurement of radiation effectiveness.

Head(s) of project:

Dr D E Watt

Scientific staff:

D E Watt, C Z Chen, L A Kadiri, E B Saion and A-R S Younis.

I. Objectives of the project:

To design and develop a microdosimeter which would be capable of selectively measuring the energy event spectrum from neutrons of intermediate energy in the presence of faster neutrons and gamma rays. The spectral information can be processed in a microchip to yield the quality factor and dose-equivalent of the intermediate energy neutrons. In pursuing these objectives, it was bourne in mind that energy event spectra may not necessarily be the most appropriate quantity for specification of radiation effectiveness. Consequently a parallel objective was the development of a model for quantification of biological effectiveness.

II. Objectives for the reporting period:

As above.

III. Progress achieved:

A new type of cylindrical microdosimeter was successfully developed and tested for the selective measurement of radiation quality and dose equivalent of intermediate energy neutrons in the presence of a mixed field of photons and faster neutrons. A number of technical difficulties had to be overcome and are detailed below. In parallel with the instrumental development, work on a new theoretical model for the specification of radiation effectiveness led to new concepts on the mechanism of radiation action. Progress in that area led, in turn, to the formation of a unified theory of biological effectiveness which is independent of radiation type and which makes possible the realisation of a universal system of radiation dosimetry. On the basis of these results proposals were made for a completely new generation of instruments for absolute dosimetry.

1. Technical developments and results on microdosimetry instrumentations

1.1 *Principles of the Method*

A coaxial double cylindrical proportional counter was designed and constructed for microdosimetry of intermediate energy neutrons in mixed fields. The inner and outer counters were separated by a thin, electrically conducting, polycarbon foil which was selected to have thickness equivalent to the range of the maximum energy of recoil that could be generated by the intermediate neutron energy of interest. Thus charged particle equilibrium is established for neutrons less than or equal to that energy. Unwanted contributions to the energy event spectrum, from higher energy (fast) neutrons which interact in either the inner or outer counters, can be vetoed by appropriate anti-coincidence techniques. A correction must be applied to allow for low energy recoils generated by fast neutrons and which fall within the energy band of interest. The correction factor is estimated to an adequate degree of accuracy either by calculation, using the method described below, or by deduction from the recorded coincidence and anti-coincidence events. Selection of the upper neutron energy limit is achieved by an appropriate choice of inner-wall thickness. Good discrimination is also expected against energy deposition events by electrons generated by the associated gamma ray field as these electrons usually have sufficient range to activate the coincidence system.

1.2 *Theoretical quantities*

To assist with the instrument design and development various established theoretical quantities had to be calculated: initial and equilibrium spectra of charged particles generated by neutrons, Monte-Carlo calculations of mean free path randomness (μ randomness) and internal source randomness (i randomness)[1]. In addition new theory was developed to enable calculation of event spectra in a co-axial double cylindrical tissue-equivalent proportional counter when operated in coincidence and anti-coincidence mode. Results are presented in No 21 of the publication list. New calculations were also made of the linear primary ionisation spectra or neutrons for the detector in both operational modes to assist with the interpretation of biological effects in terms of the observed interaction spectra. This latter arose because of interesting developments in a parallel study of the fundamental physical quantities though to be predominantly responsible for damage by heavy charged particles. The size of the radiosensitive sites were shown to be about 2 nanometers and intimately associated with the DNA. Details are given in Section 2 below.

1.3 *Theoretical correction factors for unwanted events from fast neutrons*

Corrections for the recoils, generated by fast neutrons interacting in the dividing wall, and contributing to the intermediate energy neutron region of interest were evaluated for simulated tissue diameters of 0.5, 1.0 and 3.0 micron and for fast neutron energies ranging from 500 keV to 5.0 MeV. As may be expected the event spectra are dominated by starters and stoppers. Crossers become important at higher neutron energies and small diameters. Starters and stoppers are important at lower energy deposition, whilst crossers dominate at higher energy depositions. Analysis of the results show that the correction factor attributed to the dividing wall is less than 12, 10 and 5%, in the presence of an equal dose of 1.0 MeV fast neutrons, to intermediate energy neutrons at simulated tissue diameters of 0.5, 1.0 and 3.0 μm respectively. The correction factor for 500 keV neutrons is less than that of 1 MeV neutrons because the events are dominated by starters which increase as the tissue diameter increases. Also

the correction factor for neutrons of energy > 1 MeV is less than that of 1 MeV neutrons since the starters decrease as the neutron energy increases. Detailed spectra are given in reference 21 of the publication list.

1.4 *Preparation of dividing wall*

TE self-supporting conducting film is a vital component of the co-axial double cylindrical TEPC, being used as a common dividing wall between the inner and outer counters. The film, in effect, determines the neutron energy band relevant to the recorded microdose spectrum and should have a thickness equivalent to the maximum range of protons generated by neutrons in the energy range of interest in tissue (about 1 μm for 100 keV neutrons and 30 μm for 1.2 MeV neutrons). Commercial A-150 TE plastic granules were further ground to a fine powder and the necessary amount determined by weighing. Best results were obtained using a custom-designed moulding press with optically flat steel jaws, and with an internal heating facility. To get good uniform films, strict temperature control was necessary (200°C) and a hydraulic pressure of 20 tons was optimal. A release agent (dimethyl polysiloxane) was required to free the films without causing structural damage. Film thicknesses were determined by weighing. Uniformity, measured by an alpha particle energy loss technique, was better than 7% on the thinnest films.

1.5 *Counter construction*

The final tissue equivalent counter was developed on the basis of experience gained with two prototype counters constructed from aluminium. Details of the design are given in publication 2. The internal electron amplification of the inner and outer counters were measured at various mean chord lengths and applied voltages to optimise the performance.

Field trials were carried out under mixed field conditions at the Scottish Universities Research and Reactor Centre, East Kilbride on their UTR-300 nuclear reactor. Microdose spectra were also determined for ^{252}Cf spontaneous fission neutrons and $^{241}Am/Be$ neutrons. Good discrimination

was achieved against fast neutrons, to the extent predicted. Also, the anti-coincidence system enabled much of the gamma-ray background to be vetoed. This latter property of the detector proved very useful in separating the contributions from events due to heavy charged particles and to fast electrons. Spectra with anti-coincidence are dominated by slow protons and electrons. Their mean lineal energies are higher than those of spectra without anti-coincidence. The quality factor and dose equivalent for spectra with anti-coincidence are higher than the spectra without anti-coincidence revealing the importance of intermediate energy neutrons in mixed fields. The quality factor and the corresponding dose equivalent corrected for saturation of lineal energy corresponding to 2 nm of ionisation spacing is consistently higher than those derived from the absorbed dose-based formulae. This latter procedure was carried out in view of the new findings on the mechanisms of radiation action detailed in section 2 below.

In conclusion, the new detector was successfully completed. It was found to have a number of features which constitute improvements over ordinary microdosimeters. For example, the device is able to examine spectra in energy bands below any arbitrary selectable threshold neutron energy. The anti-coincidence facility provides a means of differentiating between insiders and crossers whether they are generated by photons or neutrons and which could overcome one of the main disadvantages of the conventional spherical microdosimeters (they erroneously treat short-track events). Good discrimination is achieved against long-range particle background which will be of particular benefit in the study of low-intensity break-up reaction kinetics.

2. Theoretical studies on mechanisms of radiation action for the absolute specification of radiation effect and universal dosimetry

Re-examination of a wide range of published data on survival of mammalian cells, mutation induction and chromosome aberrations in terms of basic physical parameters led unequivocally to the conclusion that delta ray effects around heavy particle tracks play only a minor rôle in the induction of radiation effects. Contrary to current thought, it was concluded that damage is optimum when the

mean free path for primary ionisation along the tracks penetrating the cell nucleus matches the mean chord length (~ 2 nm) through a DNA segment. The biological effect is determined by the number of a correlated pair of events and is independent of energy deposition. Consequently, a fundamental challenge is presented to the use of the concepts of absorbed dose for the quantification of radiation effect!

On the basis of these findings a semi-theoretical model was constructed with the object of developing a unified theory of radiation action for application in fundamental dosimetry. The model could cope adequately with dose rate and repair effects for any radiation type. From the information obtained the feasibility of designing the response of dosimetry instruments for measurement of absolute biological effectiveness was discussed in a number of publications. The model proved useful in providing an interpretation of some unusual biological phenomena such as the inverse dose-rate effect and the action of incorporated auger electron emitters. New research is proposed on the development of instrumentation to simulate the response of the DNA to ionising radiation. Such instrumentation would constitute a universal dosimeter for the measurement of absolute biological effectiveness.

IV. Other research group(s) collaborating actively on this project [name(s) and address(es)]:

Dr P Colautti, INFN, Legnaro (Padova), Italy.

V. Publications:

1. Biophysical Mechanisms of Damage by Fast Ions to Mammalian Cells *in vitro* , R J Cannell and D E Watt, Phys Med Biol 30:255-258:1985.

2. Saturation Values of Lineal Energy in Microdosimetry: Quality Factor, I A M Al-Affan and D E Watt, Radiat Protet Dos 11:(11):65-68:1985.

3. Identification of Biophysical Mechanisms of Damage by Ionising Radiation, D E Watt, I A M Al-Affan, C Z Chen and G E Thomas, 9th Symposium on Microdosimetry, Toulouse, May 1985, Radiat Protect Dosim 13:No1-4: 285-294:1985.

4. Biophysical Mechanisms of Radiation Damage to Mammalian Cells by x and γ-rays, C Z Chen and D E Watt, Int J Radiat Biol 49:(1):131-142:1986.

5. Physical Mechanism for Inactivation of Metallo-enzymes by Characteristic X-rays, H H Jawad and D E Watt, Int J Radiat Biol 50:665-674:1986.

6. Determination of Quality Factors by Microdosimetry, I A M Al-Affan and D E Watt, 3rd Int Symp on Radiation Physica, Ferrara, Italy, Sept 1985: Nucl Inst and Methods in Physics A255:338-340:1987.

7. Some Current Advances in Biophysial Applications of Ionising Radiation for Health Preservation, D E Watt, 3rd Int Radiation Physics Symposium, Ferrara, Italy, Sept 1985: Nucl Inst and Methods in Physics A255:298-305:1987.

8. Physical Mechanism for Inactivation of Metallo-Enzymes: Response to Corresponsdence from Goodhead and Nikjoo, D E Watt and A-R S Younis, Int J Radiat Biol 52:657-658:1987.

9. Microdosimetry of Intermediate Energy Neutrons in Fast Neutron Fields, E B Saion and D E Watt, Radiat Protect Dos 23:No 1/4:265-268:1988.

10. Absolute biological effectiveness of neutrons and photons, D E Watt, Radiat Protect Dosim 23:(1/4):63-67:1988.

11. On absolute biological effectiveness and unified dosimetry, D E Watt, J Radiol Protect 9:(1):33-49:1989.

12. Model predictions and analysis of enhanced biological effectiveness at low dose rates, D E Watt, C E Sykes and A-R S Younis, Nucl Instr and Methods in Phys Res, 1989.

13. Towards a unified system for expression of biological damage by ionising radiations, D E Watt, C Z Chen, L A Kadiri and A-R S Younis, in health effects of low-dose ionising radiation - recent advances and their implications, BNES, London 11-14 May 1987: Paper 6:37-42:1988.

14. On the quality of radionuclides incorporated into mammalian cells, A-R S Younis and D E Watt, Phys Med Biol (in press), 1989.

15. An approach towards a unified theory of damage to mammalian cells by ionising radiation, D E Watt, Radiat Protect Dosim 1989, 27:(2):73-84:1989.

16. An approach to unified dosimetry for assessment of radiation effect, D E Watt, Paper B21-2V, 8th Int Congr on Radiat Res, July 19-24 1987. Taylor and Fancis 1988, Eds: Fielden, Fowler, Hendry and Scott.

17. Interpretation of the increase in the frequency of neoplastic transformations observed for some ionising radiations at low dose rates, C E Sykes and D E Watt, Inter J Radiat Biol, 55:(6):925-942:1989.

18. Interpretation of damage to mammalian cells, E Coli and bacteriophages by incorporated radionuclides for prolonged irradiation, A-R S Younis and D E Watt, Radiat Protect Dosim 1990.

19. Physical quantification of the biological effectiveness of ionising radiations, D E Watt and L A Kadiri, Int J of Quantum Chemistry, 1990.

20. A co-axial double cylindrical TEPC for the microdosimetry of selected energy bands in mixed fields of faster neutrons, E B Saion, D E Watt, B W East and P Colautti, Radiat Protect Dosim, 1990.

21. On microdosimetry of neutrons of selectable energy in mixed (n) fields, E B Saion, PhD thesis, University of St Andrews, Arpil 1989.

22. The quality of ionising radiations emitted by radionuclides incorporated into mammalian cells, A-R S Younis and D E Watt, Phys Med Biol 34:No 7:821-834:1989.

23. Biophysical damage in metallo-enzymes in mixed (n, γ) fields, A-R S Younis, PhD thesis, University of St Andrews, June 1989.

24. REPORT: Stopping Cross-sections, Mass Stopping Powers and Ranges in 30 Elements for Alpha Particles (1 keV to 100 MeV), D E Watt. Prepared for the International Committee on Radiation Units and Measurements, 7910 Woodmont Avenue, Bethesda, Maryland 20814, USA, April 1988.

RADIATION PROTECTION PROGRAMME
Final Report

Contractor: Contract no.: BI6-A-026-UK

European Radiation Dosimetry Group
EURADOS/CENDOS
Radiobiological Institute TNO
P.O.Box 5815
NL-2280 HV Rijswijk

Head(s) of research team(s) [name(s) and address(es)]:

Dr. J.A. Dennis
Chairman of EURADOS
NRPB
Chilton, Didcot
GB Oxon OX11 ORQ

Telephone number: 235/831600/2221

Title of the research contract:

Collaboration on research and development concerned with the methodology and data of radiation dosimetry.

List of projects:

1. Development and implementation of microdosimetric instruments and methods for radiation protection.
2. Skin dosimetry and surface contamination monitoring.
3. Application of thermoluminescence to routine personal dosimetry.
4. Dissemination and development of computer programs for dosimetric problems. ('Numerical dosimetry')
5. Basic physical data and characteristics of radiation protection instrumentation.
6. Assessment of internal dose.

Title of the project no.:

1. Development and Implementation of Microdosimetric Instruments and for Radiation Protection

Head(s) of project:

H G Menzel

Scientific staff:

A A Edwards, J Booz, G Dietze, G H Hartmann, L Lindborg, A Marchetto, V D Nguyen, H Paretzke, T Schmitz, H Schuhmacher

I. Objectives of the project:

The development of dose equivalent meters based on microdosimetric techniques for use in area monitoring, individual monitoring and as transfer instruments.

II. Objectives for the reporting period:

To analyse the results of the second part of the intercomparison of dose equivalent meters based on microdosimetric techniques and to prepare a report based on this intercomparison. To prepare a report summarising both parts of the intercomparison and providing conclusions and recommendations. To organise, together with CEC and GSF, Neuherberg a Workshop on Implementation of Dose Equivalent Meters Based on Microdosimetric Techniques in Radiation Protection at Schloss Elmau (FRG), October 18-20 1988. To continue energy deposition calculations for neutron radiation, (benchmark calculations, development of reference code) and calculations for the response of TEPC to photons.

III. Progress achieved:

The work within this project was focused on the development of survey instruments for radiation protection dosimetry based on tissue equivalent proportional counters (TEPC) and experimental and theoretical investigations of their dose equivalent response to neutron and gamma radiation. At the beginning of the reporting period several of the groups participating in this project finalised the development of prototype TEPC area monitors which were then used in common investigations, above all in a two-part intercomparison in neutron and photon reference fields jointly organised by Physikalisch-Technishe Bundesanstalt (PTB) and EURADOS. At the end of the reporting period the original task of this Working Committee was considered to be largely completed and its existence has therefore been discontinued. The progress achieved during this period is documented in four reports and in the proceedings of a Workshop, by the existence of at least two commercially available TEPC area monitors and by the steadily increasing use of these instruments in practice, for example, in nuclear industries, at physical and medical accelerators and in space radiation dosimetry.

The main activity of the Committee was to prepare, organise and evaluate the intercomparison of TEPC prototype area monitors and to publish the results in reports. The technical problems encountered in the development of the complex laboratory measurement technique used in conventional experimental microdosimetry into portable and sufficiently simple instruments to be operated also by non-specialists were solved individually by different groups. The investigation of physical aspects of dose equivalent measurements with TEPCs for neutrons and mixed radiations, however, was carried out in close collaboration, mainly within the intercomparison. The intercomparison was a research activity rather than a technical intercomparison.

Seven European laboratories participated in this activity. Measurements were carried out with monoenergetic neutrons with the nominal energies of thermal neutrons, 24.5 keV, 73 keV, 144 keV, 570 keV, 1.2 MeV, 2.5 MeV, 5.0 MeV and 14.8 MeV. In addition, a D_2O moderated ^{252}Cf source and a ^{60}Co gamma ray source were used. This large range of neutron energies and the use of a mixed radiation field with a broad neutron energy spectrum provided sufficient basis for assessing the properties of TEPC area monitors for all operational

conditions of practical interest. The results were given by the participants in terms of dose equivalent and absorbed dose rates, photon a neutron dose componoents and quality factors. A detailed analysis of the results was carried out which took account of the geometrical properties of the different detectors used and of the different evaluation procedures applied. The interpretation of the results was much facilitated by the microdosimetric spectra provided by some of the systems. The comparison of spectra measured by different systems, for example, enable the effects of primary fluence attenuation and thermalisation in the detector wall to be identified. Details of the intercomparison, the results and their interpretation can be found in the reports given in the list of publications.

The main conclusions drawn were:

- All TEPC based area dosemeters are in principle able to determine ambient dose equivalents in photon, neutron and mixed radiation fields.
- The systems are able to determine a mean quality factor of an unknown neutron/photon field. In monoenergetic neutron fields with energies below 500 keV the measured factor decreased more strongly with decreasing neutron energy than the theoretical quality factor.
- The ambient dose equivalent response decreases in monoenergetic neutron fields with decreasing neutron energy. In the neutron energy range investigated the response varied by a factor of 0 to 20 for the different participating systems. The main reasons for the differences in response between various systems are differences in wall thickness and simulated diameter.
- The analysis of the energy dependence of the quality factor response has shown that the decrease in dose equivalent response is in equal parts due to the deterioration of the TEPC as a LET spectrometer and to differences in radiation transport processes in the detector wall and the ICRU sphere.
- The dose equivalent responses of the different systems for the broad neutron energy spectrum of the 252Cf (D_2O) radiation are in much better agreement than for monoenergetic neutrons.

- The energy dependence of the dose equivalent responses of the TEPC dosemeters is opposite to that of moderator based systems. The response of these decreases with increasing energy.
- The sensitivity of TEPC area dosemeters depends in a complex way on the radiation field and the counter geometry. This is due to the fact that the statistical uncertainty depends on pulse rate as well as on the pulse height distribution. However, by choosing the appropriate detector size and wall thickness TEPCs can be made sufficiently sensitive for all operational conditions of practical interest. In particular, the sensitivity can be made as high as that of conventional moderator-based dosemeters.
- The results of the measurements document the excellent diagnostic properties of the TEPC based area dosemeters. They are expected to be especially useful in unknown radiation fields. The interpretation of measured data is facilitated if microdosimetric spectra are provided.
- Several of the prototype instruments are suitable for operational health physics applications.
- The conventional calibration procedures in terms of lineal energy or absorbed dose leads to a calibration in terms of kerma. Calibration in a neutron beam in terms of ambient dose equivalent improves the accuracy. The application of a correction factor to conventionally calibrated counters appears to be a reasonable alternative.
- The decrease of dose equivalent response with decreasing neutron energy will be less pronounced if sufficiently large TEPCs could be built which operate adequately at simulated diameters of 1 μm or less.
- For 24 kev neutrons and probably for neutrons of even lower energy the dose equivalent response can be improved by increasing the wall thickness. Increase of the wall thickness alone, however, is not sufficient to improve the overall dose equivalent response. The increase of the total mass of the counter wall by increasing the size of the counter appears to have an effect similar to increasing the wall thickness.

- The dose equivalent response of the variance technique can be improved by a decrease of the simulated diameter (at present 4.5 μm) and by using a modified algorithm for the evaluation of the quality factor.
- Further improvements of the dose equivalent response appear possible by modifying counter geometry, counter materials and evaluation procedure.

Jointly with the Commission of the European Communities and GSF, Munich, EURADOS organised a Workshop on "Implementation of Dose Equivalent Meters Based on Microdosimetric Techniques in Radiation Protection" at Schloss Elmau (FRG), 18-20 October 1988, where the results of the intercomparison were presented and discussed in detail. The Workshop attracted some 50 scientists working in different fields of radiation protection research and health physics. The proceedings of the Workshop have been published in the journal of Radiation Protection Dosimetry.

There are an increasing number of reports, mainly by laboratories collaborating within the Committee, on the use of TEPC area monitors in mixed radiation fields encountered in practice. Results have been reported for measurements at nuclear power plants, in nuclear fuel processing industries and at medical and physical accelerators. More recently, first results of measurements inside a spacecraft have been reported showing the suitability to provide relevant information also for the very complex radiation fields encountered in space.

Studies of the potential suitability of TEPC instruments in individual monitoring and as transfer instruments have also been performed. Although the dose equivalent response would be excellent the use in personal monitoring appeared to be not viable, mainly because of the high cost of such instruments. More detailed analysis of technical and physical aspects was therefore postponed. However, in providing the possibility of field calibrations for neutron energy dependent personal dosemeters (eg, albedo dosemeters) the TEPC can be indirectly useful for individual monitoring. The Committee concluded that the TEPC could be used as a standard instrument to cross-calibrate neutron beams and may

be useful in the context of the implementation of the ICRU operational quantities.

Other work performed within the project included the use and further development of energy deposition calculations for neutrons (in collaboration with J J Coyne, USA and with members of Working Committee 4) and the development of a computer code to convert photon fluence to energy deposition spectra in small volumes. Together with TEPC measurements for monoenergetic photons over a wide range of energies the latter calculations will be very valuable for the understanding of the TEPC response to photons.

Although the original task of the Committee is largely completed there are still scientifically interesting problems of practical relevance to be solved. Many of these will be studied within projects of individual research groups. It is expected, that the collaboration on these topics will be stimulated within new EURADOS working committees.

IV. Other research group(s) collaborating actively on this project [name(s) and address(es)]:

University Saarland, Homburg (Saar)
NRPB, Chilton
AERE, Harwell
PTB, Braunschweig
CEN, Grenoble
NIRP, Stockholm
CEN, Fontenay-aux-Roses
GSF, Neuherberg
KFA, Jülich
DKFZ, Heidelberg
PSI, Villigen (CH)
University of Leeds

V. Publications:

Menzel, H G
Practical Implementation of Microdosimetric Counters in Radiation Protection, Proc. 5th Symp. Neutron Dosimetry, EUR 9762, 287-305 (1985)

Dietze, G, Booz, J, Edwards, A A, Guldbakke, S, Kluge, H, Leroux, J B, Lindborg, L, Menzel, H G, Nguyen, V D, Schmitz, Th, Schumacher, H
Intercomparison of Dose Equivalent Meters Based on Microdosimetric Techniques, Radiat. Prot. Dosim. 23, 227-234 (1988)

Dietze, G, Edwards, A A, Guldbakke, S, Kluge H, Leroux, J B, Lindborg, L, Menzel H G, Nguyen, V D, Schmitz, Th, Schumacher, H
Investigation of Radiation Protection Instruments Based on Tissue Equivalent Proportional Counters. Results of an EURADOS Intercomparison, Commission of the European Communities, EUR 11867 (EN), Luxembourg, (1988)

Menzel, H G, Lindborg, L, Schmitz, Th, Schuhmacher, H, Waker, A J
Intercomparison of Dose Equivalent Meters Based on Microdosimetric Techniques: Detailed Analysis and Conclusions. Radiat. Prot. Dosim. 29, 55-68 (1989)

Menzel, H G, Paretzke, H G, Booz, J (eds.)
Implementation of Dose-Equivalent Meters Based on Microdosimetric Techniques in Radiation Protection, Proceedings of a Workshop, Radiat. Prot. Dosim. 29 (1989) (EUR 12188)

Publications on EURADOS-PTB Intercomparison prepared by PTB:

Dietze, G, Guldbakke, S, Kluge, H, Schmitz, Th
Intercomparison of Radiation Protection Instruments Based on Microdosimetric Principles, PTB Report ND-29 (1986)

Alberts, W G, Dietze, G, Guldbakke, S, Kluge, H, Schuhmacher, H
Radiation Protection Instruments Based on Tissue Equivalent Proportional Counters: Part II of an International Intercomparison. Report PTB-FMRB-117, Braunschweig (1988)

Alberts, W G, Dietze, G, Guldbakke, S, Kluge, H, Schumacher, H
International Intercomparison of TEPC Systems Used for Radiation Protection. Radiat. Prot. Dosim. 29, 47-53 (1989)

Title of the project no.:

2. Skin Dosimetry and Surface Contamination Monitoring

Head(s) of project:

P Christensen

Scientific staff:

J Böhm, T O Marshall, M Charles, J Patau, Y Herbaut, E Piesch, J R Harvey, D Regulla, M Heinzlemann, M J Rossiter, H Julius, H G Paretzke

I. Objectives of the project:

The evaluation of exposures to beta and low energy photon radiations and the development of appropriate techniques and methods for their measurement.

II. Objectives for the reporting period:

To finish the preparation of a review document on dose rate meters for skin dose measurements. To continue the use of computer codes to evaluate dose data for exposures to beta and low energy photon radiation. To continue the study of the importance of problems of skin dosimetry and surface contamination monitoring. To perform benchmark intercomparison of cumputational methods for beta radiation dosimetry. To continue comparative measurements of dose rates from ^{147}Pm sources carried out at different laboratories. To continue the evaluation of the biological effectiveness of low-penetrating radiations in co-operation with EULEP. To co-operate with Directorate General XII in the planning and organisation of a workshop on skin dosimetry and surface contamination monitoring.

III. Progress achieved:

The work within this project has focussed on improvements in the dosimetry of radiations of low penetrating power into the body and in particular on the dosimetry relevant to the assessment of the radiation hazards to the skin. Early in the reporting period a successful Workshop on the Dosimetry of Beta Particles and Low Energy X-rays was organised by the Commission, the Institute de Protection et de Sureté Nucleaire, CEA, that was co-sponsored by EURADOS-CENDOS and the US Dept. of Energy. Theoretical and practical studies on aspects of beta-ray dosimetry have been carried out and the practical problem areas in occupational situations have been identified. An important aspect has been the intercomparison of beta-ray sources between the primary national laboratories in an effort to harmonise standards of measurement for these radiations. All these aspects are reflected in the latest reports below.

Measurements have been performed at PTB of dose rates from an extended, 6 cm diameter, $^{90}Sr/^{90}Y$ source using an extrapolation chamber, in connection with a benchmark experiment testing the validity of computer programs for determining dose rates from beta sources. Absorbed dose rates to tissue have been determined for different tissue depths and angles of incidence of the radiation at various distances from the source. The $^{90}Sr/^{90}Y$ source is now available for interchanging between other laboratories for performing comparative measurements. computer programs for determining absorbed dose rates in a Perspex phantom exposed in the beta radiation field from the source taking into account both the electrons emitted directly from the source and those backscattered from the source holder have been developed at CPA. The experimental and calculated results from the experiment will be evaluated and reported in 1990.

Results from comparative measurements, using extrapolation chambers, of dose rates from four, equal 4 cm x 4 cm, ^{147}Pm sources at different laboratories (NRPB, PTB, Fontenay-aux-Roses and Risø) have been evaluated and various uncertainty sources have been identified. In particular difficulties have been identified in defining correction factors related to variations in the environmental conditions, eg,

temperature, pressure and relative humidity. The intercomparisons are planned to finish and a final report on the results to be prepared in 1990. The study of extrapolation chambers for dosimetry of beta and low-energy photon radiations is expected to continue in the form of a research project supported by the CEC Radiation Protection Programme 1990-1991.

The problem of localised skin exposure from radioactive particulates has found increasing interest in radiation protection as a substantial number of skin contaminations with isolated particualtes occur in the working areas of many PWR reactors in US. The most common radionuclide is ^{60}Co which originates predominantly through neutron activation of steel corrosion particulates. In cases of potential skin exposure from particulates the need arises for calculation of the skin dose. To investigate and improve the reliability of computer codes for the assessment of skin dose rates from the range of radioactive particulates associated with nuclear reactors and reprocessing plants operations a co-ordinated research programme (CEGB, CEN, CPA) comparing calculated data with experimental values has been planned. The project involves measurement of skin dose rates from a range of ^{690}Co particulates of various sizes produced by neutron activation and development of appropriate computer codes. The project is expected to get financial support through the CEC Radiation Protection Programme 1990-1991.

The results from investigations of the importance of weakly penetrating radiations in German nuclear plants show that exposure to very high dose rates (up to 2 Sv h^{-1}) from beta radiation fields may occur. The ratio of beta dose rate to photon dose rate is varying significantly from one working area to another at the workplace. Typically, ratios from 1:1 to 10:1 were measured in Germany nuclear power plants, however, in some cases values of up to 40:1 were found. A broad spectrum of energies from both low and high energy beta rays and low energy photons (K-capture radiation) may be involved in exposure to weakly penetrating radaitions at workplaces in the nuclear industry.

The collaboration with EULEP in evaluating data on biological effectiveness of low-penetrating radiations and depth of sensitive

layers in the skin has continued. A Task Group set up by ICRP to deal with these problems has prepared a report for the ICRP Main Committee for consideration for the coming ICRP recommendations. The report has been presented at a recent EULEP seminar and will appear in the proceedings from this seminar.

The work on a review document on dose-rate meters for skin dose measurements will be finished in 1990.

Plans for arranging a workshop on "Skin Dosimetry" in Dublin during spring 1991 have been initially discussed with Nuclear Energy Board, Dublin and DG XII, CEC, Brussels.

IV. Other research group(s) collaborating actively on this project [name(s) and address(es)]:

RNL, Riso	NRPB Chilton
PTB, Braunschweig	SPEE/LMR, Grenoble
GSF, Neuherberg	CEGB, Berkeley
CEN, Grenoble	RSO TNO, Arnhem
KFA, Julich	KFZ, Karlsruhe
NPL, Teddington	CPA, Toulouse

V. Publications:

1. Heinzelmann, M, Beitag der ß-Strahlung zur Dosis in Deutschen Kernkraftwerken, Report Jül-2260 (1989).

2. Rohloff, F and Heinzelmann, M, Absorbed Dose Rate Due to K-Radiation. Radiat. Prot. Dosim. 27, 193-196 (1989).

3. Charles, M W, Hopewell, J W, Wells, J and Coggle, J E. Recent Trends in Radiobiology of Skin and Repercussions for Dose Limitation and Personal Dosimetry, 1989. In: Proceedings of the Fourth Int. Symp. on Radiation Protection. Institute of Physics Publishing Ltd., Bristol.

4. Charles, M. The biological basis of radiation protection criteria for superficial, low penetrating radiation exposure. Rad. Prot. Dosim. 14, 79-90 (1986).

5. Christensen, P, Herbaut, Y, Marshall, T O. Personal monitoring for external sources of beta and low energy radiations. Rad. Prot. Dosim. 28, 241-260 (1987).

6. Christensen, P, Bohm, J, Francis, T M. Measurement of absorbed dose to tissue in a slab phantom for beta radiation incident at various angles. In: Body Dosimetry Fifth Information Seminar on the Radiation Protection Dosemeter Intercomparison Programme. Bologna, 25-27 May 1987, pp.39-75. Luxembourg, 1988 (EUR 11363EM).

Title of the project no.:

3. Application of Thermoluminescence to Routine Personal Dosimetry

Head(s) of project:

J R Harvey

Scientific staff:

J R Barthe, J Böhm, G Busuoli, P Christensen, K E Duftschmid, H W Julius, U Lauterbach, M Marshall, T O Marshall, M Oberhofer, D Regulla

I. Objectives of the project:

Study and resolution of problems encountered in the application of thermoluminescence dosimetry techniques in individual and environmental monitoring

II. Objectives for the reporting period:

The project terminated in 1987.

III. Progress achieved:

This group was formed to disseminate information on the effective and efficient use of thermoluminescent techniques for individual dosimetry. This objective was met by the preparation of four reviews and the organisation of a workshop. The workshop took place at the Joint Research Centre, Ispra and was attended by 26 delegates from ten nations. The reviews were presented at the 8th International Conference on Solid State Dosimetry held in Oxford in 1986 and published in the proceedings of that conference. The different publications of the group were published individually in the journal Radiation Protection Dosimetry and together as a special EURADOS-CENDOS publication on Aspects of Individual Monitoring.

IV. Other research group(s) collaborating actively on this project [name(s) and address(es)]:

CEGB Berkeley
ENEA, Bologna
OFZS, Seibersdorf
PTB, Braunschweig
NRPB, Chilton
GSF Neuherberg
CEA Fontenay-aux-Roses
RNL, Risø
RSO TNO, Arnhem
AERE, Harwell
CEC JRC, Ispra

V. Publications:

- Marshall, T O, Christensen, P, Julius, H W, Smith, J W. The relative merits of discriminating and non-discriminating dosemeters. Rad. Prot. Dosim. 14, 5-10 (1986).
- Harvey, J R, Gibson, J A B. A survey of personnel monitoring in European countries. Rad. Prot. Dosim. 14, 11-15 (1986).
- Driscoll, C M H, Barthe, J R, Oberhofer, M, Busuoli, G, Hickman, C. Annealing procedures for commonly used radiothermoluminescent materials. Rad. Prot. Dosim. 14, 17-32 (1986).
- Duftschmid, K E, Lauterbach, U, Pattison, R J. Comparison of most widely used automated TLD readout systems. Rad. Prot. Dosim. 14, 33-39 (1986).
- Gibson, J A B. The relative tissue kerma sensitivity of thermoluminescent materials to neutrons. Rad. Prot. Dosim. 15, 253-266 (1986).
- Barthe, J R, Böhm, J, Christensen, P, Driscoll, C M H, Harvey, J R, Julius, H W, Marshall, M, Marshall, T O, Oberhofer, M. Report on a Workshop on the Application of Thermoluminescence Dosimetry to Large Scale Individual Monitoring, ISPRA, 11-13 SEPT. 1985. Rad. Prot. Dosim. 18, 47-61 (1987).
- Christensen, P, Herbaut, Y, Marshall, T O. Personal monitoring for external sources of beta and low-energy photon radiations. Rad. Prot. Dosim. 18, 241-260 (1987).

Title of the project no.:

4. Dissemination and Development of Computer Programs for Dosimetric Problems ('Numerical Dosimetry')

Head(s) of project:

B R L Siebert

Scientific staff:

M Buxerolle, J L Chartier, D Jones, B Grosswendt, G-F Gualdrini, C Perks, G Hehn, D J Thomas, A J Wittmann, G Burger (Sponsor), A Alevra (Consultant)

I. Objectives of the project:

To disseminate information about computer programs developed (in Europe and America) for dosimetric and shielding problems by collecting information about existing programs and where necessary testing and evaluating them.

II. Objectives for the reporting period:

1. Report on the intercomparison of unfolding codes for Bonner spheres measurement.
2. Benchmark study on response functions for Bonner spheres.
3. Numerical study of external radiation dose from Cs ground contamination.
4. Definition and implementation of benchmark problems for photon and electron transport.

III. Progress achieved:

The work of this group has concentrated for most of the period in understanding the differences between different computation codes in the calculation of neutron spectra from radioactive sources used for calibration purposes. The reasons for the differences are now understood. Progress was also made in resolving difficulties in the codes used in conjunction with the Bonner sphere type of neutron spectrometer. Towards the end of the period attention was turned towards the problem of calculating the doses arising from the ground deposition of radioactivity from the Chernobyl accident. More recently the problems of accurately specifying the detail and variation of the geometry of the human body and its organs for accurate dosimetry have begun to be discussed. This will be an important topic in the next few years.

The Bonner sphere unfolding intercomparison has concentrated on the unfolding problem ignoring response function uncertainties by assuming these responses were known precisely. It was a 'blind' intercomparison, in that no spectral information was available beforehand, except for the energies of any monoenergetic components. In all, 12 sets of solutions were presented from 8 different participants. A detailed report on the work is now in print (c.f.ref. 2)

The benchmark study on response functions for Bonner spheres concentrated on a particular set of a spherical ^{3}He detector at the centre of moderating polyethylene spheres of different sizes. Two different densities (0.92 and 0.95 gcm^{-3}) were considered. First results are now available from four different authors using ANISN, MCNP, MCBEND and own codes. ANISN has the advantage of needing negligible computing times and the disadvantage of being restricted to spherical geometry. The other codes employed are full scale Monte Carlo codes and therefore long running programs. They, however, allow other geometries (eg, cylindrical counters) and the detailed study of resonance effects, which at higher neutron energies are quite important for larger spheres. In the thermal region discrepancies have been found which may be due to the use of different data. Further work and a detailed intercomparison with experimental data is underway.

Two authors contributed to the numerical study of external radiation dose from Cs ground contamination. In calculations for a number of isotopes an agreement of about 2% was found. In addition, more detailed calculations of organ doses some differences have been found. Some of these may be due to interpretational rather than calculational problems. this, once again, demonstrated the need of agreed upon phantoms for external and internal dosimetry (see below).

Two authors agreed on a benchmark problem for photon and electron transport at interfaces. They study the influence of the air gap in a calorimeter. One author uses EGS and the other author his own code. The main problem in this work is the extreme long computing time needed for achieving acceptable uncertainties.

The analytic code from Coyne and Caswell (NIST, Gaithersburg), which allows the energy deposition by secondary charged particles to be computed analytically is now available within Europe. An authorised version can be obtained from PTB.

In order to meet the increasing need for standardising phantoms for external and internal dosimetry a sub-group has been founded. First discussions of this sub-group concentrated on the shortcomings of the MIRD phantom and proposed the use of a voxel phantom. The MIRD phantom is essentially a standard for the mass and volume of man and his organs. It does not represent the range of human sizes and it does not include a representation of the form or age of organs. Its chemical composition is not specified and it is not representative of children. A better approach to providing a phantom may be in terms of a voxel model where the body is represented in terms of voxels each of which has a number which identifies its position and says what it is made of. The main problem with this approach, however, is seen with the considerable computer storage needed and possibly slow access times. Some voxel phantoms are already being studied, eg, at GSF.

IV. Other research group(s) collaborating actively on this project [name(s) and address(es)]:

AERE, Harwell
CEN, Cadarache
GSF, Munich
NPL, Teddington
PTB, Braunschweig
CEA, Fontenay-aux-Roses
ENEA, Bologna,
IKE, Stuttgart
NRPB, Chilton

V. Publications:

1. Siebert, B R L, Morhart, A: A Proposed Procedure for Standardising the Relationship Between the Directional Dose Equivalent and Neutron Fluence. Radiat. Prot. Dosim. 28, pp.47-51 (1989).

2. Alevra, A V, Siebert, B R L, Aroua, A, Buxerolle, M, Greccescu, M, Matzke, M, Mourges, M, Perks, C A, Schraube, H, Thomas, D J, Zabarowski, H L: Unfolding Bonner Sphere Data: A European Intercomparison of Computer Codes. Laborbericht PTB-7-21-1990-1 (Braunschweig, 1990).

Title of the project no.:

5. Basic Physical Data and Characteristics of Radiation Protection Instrumentation

Head(s) of project:

J J Broerse, J R Harvey, K G Harrison

Scientific staff:

1. Ionization Chambers: H J Brede, J J Broerse, G Dietze, S Guldbakke, V D Huynh, V E Lewis, D R Schlegel-Bickman, H Schraube, U J Schrewe, J Zoetelief. 2. Track-Etch Detectors: D T Bartlett, J-L Decossas, K G Harrison, R A Hollnagel, J R Harvey, L Lembo, R Medioni, E Piesch, H Schraube, L Tommasino, J-C Varielle, G Zapparoli.

I. Objectives of the project:

The collection and evaluation of physical data relevant to the assessment of the biological effects of ionizing radiations and to the assessment of occupational and environmental exposures of the population of the European Communities.

II. Objectives for the reporting period:

1. The data obtained from the Mg/Ar ionisation chamber studies performed in 1988 at PTB, Braunschweig, will be analysed and further measurements undertaken to resolve an anomalous wall attenuation effect. Results of a recent BIPM intercomparison will be analysed for differences in k_u values. The need for further experimental work will be examined possibly using a 14.7 MeV neutron field at NPL. The results of the past work will be published.

2. A joint irradiation of track-etch detectors will be carried out with participating laboratories from Europe and North America. Attempts will be made to pool information on available plastics for track-etch detection with an emphasis on quality control, background, ageing and environmental effects.

III Progress Achieved

This group has had two major strands of interest. The first has been the use of ionisation chambers for use in the accurate dosimetry of mixed radiations, primarily in biological experiments. This has led to the recognition of some systematic uncertainties in measurements made with these instruments and progress towards their resolution. The second has been with the use of the detection of tracks produced by densely ionising particles in plastics as a method of individual dosimetry for neutron radiations. This has been marked by entirely successful joint irradiations of different types of dosimeters, including prototypes, in conjunction with groups from North America. This work has led to faster progress in identifying methods for dealing with the technical problems of this form of dosimetry. More recently attention has turned to the possibility of using electronic detectors for the dosimetry of neutron radiations as described below.

1. Ionisation chamber studies:

Measurements of relative neutron senstivities, k_U, of the Mg/Ar chambers of the same design from five of the centres involved in this work performed at PTB for four neutron fields in January/February 1988 were evaluated further.

Additional measurements were made on wall correction factors, k_{wall}, of Mg/Ar and tissue equivalent (TE) ionisation chambers. From measurements by different groups for 15 and 19 MeV neutrons, K_{wall}-factors of Exradin T2 tissue equivalent ionisation chambers show agreement whereas for Exradin M2 Mg/Ar ionisiation chambers differences are observed, possibly related to differences in the photon component in the different mixed fields. A new evaluation of the 19 MeV spectrum, resulted in a 10 per cent increase in the k_T value. A second draft of a paper on measurement of k_U-values of argon-filled magnesium ionisation chambers is available and will be submitted soon for publication.

The main results formulated in the paper are:

- The k_u-values obtained for the individual Mg/Ar chambers in these studies for four neutron fields are of the highest attainable accuracy to date, which should be adequate for mixed field dosimetry.

There are, however, several problems that have been identified, but not solved:

- It is not clear why the response of a Mg/Ar chamber increases with increasing wall thickness in the 8 and 15 MeV neutron fields. This effect was not observed in previous attenuation measurements at these energies. It may affect the measured absolute k_u-values, and therefore deserves further investigation.
- Two types of behaviour were observed regarding the polarity effect as a function of energy. One chamber (serial number M2-121) displayed a polarity effect that was nearly independent of neutron energy while for the other three chambers this difference was larger and more variable.
- There appeared to be two pairs of chambers with different mean k_u-values. There is agreement between all four chambers only at 19 MeV. There is no clear correlation between this effect and the polarity effect, and therefore it could be due to a separate cause altogether. One possibility is that of surface contamination of the shell and/or collector either by chemical corrosion or by traces of chemicals such as adhesives used in the manufac ture.

Main conclusions are:

- The differences observed tend to confirm suspicions that Mg/Ar chambers used in previous comparisons of dose measurements may have had different k_u-values. Three of the chambers used in this work were employed in a comparison at NPL (Lewis, 1985) using 14.6 MeV neutrons, and the trend observed there is the same direction as that observed here. However, exact comparison is not possible since two of the devices were repaired in the meantime. The data of the more recent comparison organised by BIPM (Huynh, 1988) are more relevant to the present work and enable direct estimates to be made of the difference between the

14.8 MeV k_U-values of several M2 chambers with that of BIPM (M2-139). The largest difference, that with the NPL chamber (M2-119), is close to that observed here. Three other chambers have k_U-values only slightly higher than that of the chamber M2-139, and would therefore seem to belong to the same group.

- Users are advised to use both positive and negative polarity bias to take the mean result. If their chambers are used for fields with relatively low energies (less than 19 MeV), they are further advised to compare the responses with either a GM counter or a Mg/Ar chamber that has been used in a standard field in order to select an appropriate set of k_U-values.

2. **Track-etch detectors:**

Activities have been in three areas.

(a) Intercomparisons of etch and electro-chemical etch procedures and operational experiences. This has taken the form of one- or two-day meetings about once a year at which each delegate gives a presentation followed by discussion. The 1989 meeting took place at ENEA Bologna, 20-22 June.

(b) Joint neutron irradiations have been undertaken on three occasions. The latest was in late 1988/early 1989. Dosemeters were sent by post to the irradiation laboratories at PTB, GSF and PSI. Dosemeters were irradiated at energies of 0.075, 0.144, 0.57, 5.3, 14.8 and 27.8 MeV and with Cf-252 neutrons. The 27.8 MeV irradiation was a new energy to these intercomparisons and was made available by the Paul Scherrer Institut, Switzerland. As with the other joint irradiations, the results from the participating laboratories will be reported in a joint publication, on this occasion to be co-ordinated by GSF. These joint irradiations have proved to be very popular since they are a source of well calibrated neutrons over a wide energy range which allow assessment of individual systems and intercomparisons of systems from Europe, USA and Canada.

(c) A joint study has been made of the background characteristics of etch plastic from various sources. Background measurements from seven laboratories were combined in a standard format and published, together with conclusions and recommendations in an ENEA report: "Results of a survey of backgrounds of etched track neutron dosimeters organised by Eurados-Cendos in 1988" edited by L Lembo, Report PAS-FIBI-DOS (89) 1. A further study of the background and sensitivity characteristics of track-etch materials from a number of manufacturers was initiated at the 1989 committee meeting.

Electronic Neutron Dosemeter Group:

This group had a preliminary meeting in association with the track-etch group on June 22 at ENEA, Bologna. Basic physical requirements and characteristics of available detectors were discussed and it was concluded that a detector was feasible in principle. The committee encouraged work in the field, particularly attempts to attain detectors with thinner depletion layers so as to reduce the lower energy threshold of neutron detection.

IV. Other research group(s) collaborating actively on this project [name(s) and address(es)]:

BIPM, Paris
GSF, Neuherberg
PTB, Braunschweig
NPL, Teddington
TNO, Rijswijk
AERE, Harwell
NRPB, Chilton
CEA, Fontenay-aux-Roses
CEGB, Berkeley
ENEA, Bologna
ENEA, Rome
KfK, Karlsruhe
Limoges University

V. Publications:

Zoetelief, J, Schlegal-Bickmann, D, Schraube, H, Dietze, G. Characteristics of Mg/Ar ionization chambers used as gamma-ray dosimeters in mixed neutron fields. Phys. Med. Biol. 32, 1339-1352. (1986).

Piesch, E. Neutron irradiations of proton-sensitive track etch detectors: Results of the Joint European/USA/Canadian irradiations. KfK 4305. Eurados-Cendos Report 198701. (1987).

Neutron Irradiations of Proton Sensitive Track Detectors: Results of a Joint Irradiation Organized by CENDOS. Ed. K G Harrison, AERE Harwell Report AERE-R11926 (1985).

Title of the project no.:

6. Assessment of Internal Dose

Head(s) of project:

J A B Gibson

Scientific staff:

Full members: P J Darley, Miss F A Fry, K Henrichs, E Iranzo, R Kunkel, J Piechowski, R Roth, E Sollet, H Schieferdecker

EULEP Representative: D M Taylor Visiting Representative: C Wernli

Correspon. Members: U Baverstam, C Hurtgen, C Melandri, E Rampa, R L Kathren, S Suga, R G Thomas

I. Objectives of the project:

Preparation of guidance on the interpretation of monitoring data relating to internal exposures of radiation workers and the implementation of ICRP recommendations on this topic within Europe. The objective will be achieved by the pooling and exchange of information and in comparing operational experience.

II. Objectives for the reporting period:

To continue a programme of work to: develop computer models for excretion analysis; interpret data from air sampling, bioassay and in-vivo monitoring; establish availability of autopsy data; consider compatibility of dose records; exchange information.

Detailed objectives are:

(i) preparation of a research programme proposal on stable isotope metabolic studies for the 1990-1994 Euratom RP Programme;
(ii) establish the basis of a European Internal Dosimetry Registry; with access to appropriate models, autopsy data and other biological data; by discussion with EURADOS-CENDOS, EULEP, COGEMA and individual representatives of countries in the European Community;
(iii) consider the implications of the new ICRP lung and GI tract models on internal dose assessments;
(iv) co-ordinate intercomparisons between the UK and COGEMA;
(v) discuss the areas of possible co-operation with EULEP through Workshops; Registry, Intercomparisons and Models;
(vi) organise a Workshop on Internal Dose Assessment in FRG in 1990.

III. Progress achieved:

This group was formed towards the end of the reporting period, but is making rapid progress towards the provision of comprehensive European databases for internal dosimetry. This is an important topic which has hitherto lacked a specifically European dimension.

The Working Group 6 had met twice during the year, in Paris in April and in Chilton, UK in November. The committee has been strengthened by representatives from Spain, Switzerland and EULEP. At each meeting, progress in individual laboratories was reviewed and details of contract proposals was arranged. Two submissions for contracts were made. A research proposal for stable isotope metabolic studies was accepted. A second proposal to establish registries of dose assessments, autopsy data and models was not accepted as a research contract but is expected to be the subject of a study contract to determine feasibility of setting up the registries.

The working group had suggested that the metabolic studies should include stable isotopes of Ba, Ce, Co, Te, Mo and Sr and that the intestinal absorption fraction (f_1) was the metabolic parameter of prime concern. Both adults and children would be included in the study.

The study proposal for the registries is intended to cover collaboration between all CEC countries. Confidentiality of the database will be of paramount importance to avoid the identification of personal information. The format will be modelled on the Uranium and Transuranium Registries in the USA so that derived information can be exchanged. The aim is to provide improved information for internal dose assessments for all purposes. As a first step, the working group organised an inter-comparison of dose assessments including acute intakes of: ^{90}Sr and ^{137}Cs by inhalation; ^{32}P by injection; a wound contaminated by plutonium; inhalation of a mixed-actinide nitrate aerosol; and the chronic inhalation of plutonium-239 over 10 years. Initial assessment of the results at a meeting in November 1989 gave promising agreement and, after review, the data will be published without identifying the laboratories.

Members of the committee had considered the implications of the new ICRP lung model published at Versailles in 1988 and found that the

extretion pattern predicted did not agree with that observed in practice. This observation has resulted in modifications to the proposed model C.

Representatives of COGEMA and CEN, Cadarache attended the working group's April meeting in Paris and described existing intercomparisons on the measurement of radionuclides in biological materials. This group had operated informally under the auspices of the CEA but had become more formalised recently in order to standardise monitoring procedures and protocols. Also, there was an informal international collaboration on intercomparison of in-vivo monitors organised through the IAEA. Thus, it was not necessary for the EURADOS-CENDOS Working Group to arrange collaboration in these two areas which are vital to internal dosimetry.

Full collaboration with EULEP has been established with reciprocal representation arrangements between EULEP and EURADOS-CENDOS and any possible overlap would be carefully controlled.

The proposed workshop on internal dose assessment in 1990/91 would be broadened to consider the feasibility of establishing the registries.

IV. Other research group(s) collaborating actively on this project [name(s) and address(es)]:

UKAEA, Harwell, UK
NRPB, Chilton, UK
CEA/IPSN, Fontenay-aux-Roses, France
GSF, Neuherberg, FRG
ENEA-DISP/ARA Rome, Italy
CIEMAT (PRYMA), Madrid, Spain
US DOE, Washington, USA
PSI, Villigen, Switzerland
Nat. Inst. of Radn. Prot., Stokholm Sweden
EULEP Cttee. on Int. Dosimetry & Standardisation, KfK, Karlsruhe, FRG
CEGB Berkeley, UK
Univ. of Saarland, Homburg (Saar), FRG
GSF, Frankfurt, FRG
KfK, Karlsruhe, FRG
AMYS, Madrid, Spain
Hanford Env. Hlth. Found., USA
CEN/SCK, Mol, Belgium
JAERI, Tokai-mura, Japan
Swiss Federal Inst. for Reactor Research, Switzerland

V. Publications:

A Birchall. Uncertainty in bioassay determination of plutonium intakes. NRPB-M207 (in press).

A Birchall and A C James. A Microcomputer algorithm for solving first order compartmental models involving recycling. Health Physics 56, 857-868 (1989).

R K Bull and J A B Gibson. Experiences at Harwell in estimating intakes of actinides. Radiation Protection - Theory and Practice, 4th Int. Symp. Malvern, pp.215-218 (1989).

A Espinosa, C E Iranzo, A Bellido and E Iranzo. Aplicación de un modelo metabolico teorico para calculo de dosis a partir de datos experimentales de beoeliminación de plutonio. III Congress Nacional de Protección Radiólogica. Valencia, pp.813-825 (1989).

E Etherington, M R Bailey, M D Dorrian and a Hodgson. A study of the biokinetics of intravenously administered yttrium-88 in man. Proc. 4th Int. Symp. of the Society for Radiological Protection, pp.455-448 (1989).

J A B Gibson and R K Bull. Dose Assessment from Bioassay and Body Monitoring Measurements: Practical Experience. Workshop on Biological Assessment of Occupational Exposure to Actinides, Versailles, France, 1988. Rad. Protect. Dosim. 26, pp.271-277 (1989).

C E Iranzo, A Espinosa, A Bellido and E Iranzo. Factores de contractión suelo-planta para plutonium y su applicación en la evaluación de dosis. III Congreso Nacional de Protección Radiólogica. Valencia, pp.801-812 (1989).

R L Kathren. The United States Transuranium and Uranium Registries: Overview and recent progress. Workshop on Biological Assessment of Occupational Exposure to Actinides, Versailles, France, 1988. Rad. Protect. Dosim. 26, pp.323-330 (1989).

D Nosske, H D Roedler and H Schieferdecker. Fecal Excretion Measurements of the Accidental Plutonium-239 Inhalation - Interpretation by Modifying Lung Model Parameters. Workshop on Biological Assessment of Occupational Exposure to Actinides, Versailles, France, 1988. Rad. Prot. Dosim. 26, pp.293-296 (1989).

J Piechowski, et al. Model and practical information concerning the radiotoxicological assessment of a wound contaminated by plutonium. Workshop on Biological Assessment of Occupational Exposure to Actinides, Versailles, France, 1988. Rad. Prot. Dosim. 26, pp.265-270 (1989).

H Schieferdecker. Methoden zur Ermittlung der Korperdosis bei Inkerporation von Plutonium, In: L J Hacke, A Kaul, R Neider4, H Ruhle (Ed): Kompendium der Sommerschule Strahlenschutz, H Hoffman Verlag, Berlin-Nachtrag, 11 Seiten, pp.1-11 (1989).

H Schieferdecker. Dosimétrie en cas de contamination radioactive interne (Ubersetzung des Vortrags: Dosimetry in a case of radioactive internal contamination). EUR 11370 FR, Actes du Séminaire "Problémes de'intervention médicale á mettre en oeuvre en cas de surexposition aux rayonnements ionisants", Luxembourge, 19-21 février (1986), Radioprotection No.39, pp.180-200 (1989).

H Schieferdecker, H Dilger and H Doerfel. Practical Experience accumulated at the Karlsruhe Nuclear Research Centre in detecting incorporated plutonium. Workshop on Biological Assessment of Occupational Exposure to Actinides, Versailles, France, 1988. Rad. Prot. Dosim. 26, pp.177-182 (1989).

H Schieferdecker, R Sommer-Ballat. Health Physics and Safety Control Gmelin Handbook of Inorganic Chemistry (8th Ed) Th Thorium. Suppl. A5 Analysis Biology. Springer Verlag, Berlin, pp.238-264 (1989).

D M Taylor. The metabolism of plutonium and related elements: ICRP Publication 48. Workshop on Biological Assessment of Occupational Exposure to Actinides, Versailles, France, 1988. Rad. Prot. Dosim. 26, pp.123-135 (1989).

RADIATION PROTECTION PROGRAMME
Final Report

Contractor:

International Commission on
Radiation Units and Measurements
ICRU
7910 Woodmont Avenue, Suite 800
USA Bethesda, MD 20814

Contract no.: BI6-A-027-US

Head(s) of research team(s) [name(s) and address(es)]:

Prof. A. Allisy
Intern. Commission on Rad.
Units and Measurements, ICRU
7910 Woodmont Ave, Suite 800
USA Bethesda, MD 20814

Telephone number: 301-657-26.52

Title of the research contract:

Quantities, units and measurement techniques for ionizing radiation.

List of projects:

1. Quantities, units and measurement techniques for ionizing radiation.

Title of the project no.:

1. Quantities, Units and Measurement Techniques for Ionizing Radiation

Head(s) of project:

Professor Andre Allisy

Scientific staff:

I. Objectives of the project:

The development of internationally acceptable recommendations regarding:

(1) Quantities and units of radiation and radioactivity,

(2) Procedures suitable for the measurement and application of these quantities in clinical radiology and radiobiology,

(3) Physical data needed in the application of these procedures, the use of which tends to assure uniformity in reporting.

The ICRU also considers and makes recommendations in the field of radiation protection.

II. Objectives for the reporting period:

Completion of work (publication) of ICRU reports on: (1) the basis for quantities used in determination of dose equivalent from external radiation sources, (2) tissue substitutes and (3) physics aspects of clinical neutron dosimetry.

III. Progress achieved:

During the period 1985-1989 the ICRU published several reports of major significance to those concerned with radiation protection problems. In addition, drafting work was completed on other reports, with some about to enter the ICRU's review process. Further, work continued on the preparation of other important reports, and several new efforts were initiated aimed at the preparation of ICRU recommendations on topics of importance to those responsible for radiation protection activities.

The new reports published included the following:

(1) ICRU Report 38, Dose and Volume Specification for Reporting Intracavitary Therapy in Gynecology

(2) ICRU Report 39, Determination of Dose Equivalents Resulting from External Radiation Sources

(3) ICRU Report 40, The Quality Factor in Radiation Protection

(4) ICRU Report 41, Modulation Transfer Function of Screen-Film Systems

(5) ICRU Report 42, Use of Computers in External Beam Radiotherapy Procedures with High-Energy Photons and Electrons

(6) ICRU Report 43, Determination of Dose Equivalents from External Radiation Sources--Part II

(7) ICRU Report 44, Tissue Substitutes in Radiation Dosimetry and Measurement

(8) ICRU Report 45, Clinical Neutron Dosimetry -- Part 1: Determination of Absorbed Dose in a Patient Treated by External Beams of Fast Neutrons

Of particular significance in connection with radiation protection concerns are ICRU Reports 39, 40, 43 and 44 which provide recommendations of direct relevance to radiation protection activities. They provide the basis for quantities appropriate for assessing radiation exposure, the definition of the quantities, guidance on quality factor and data on tissue substitutes useful in assessing radiation exposure.

A report, "Supplemental Information on Tissue Substitutes in Radiation Dosimetry and Measurement" was reviewed by the ICRU at its most recent meeting. The report was approved and will be published as ICRU Report 46. The preparation of the printer's manuscript is now underway.

The drafting work on a number of other ICRU reports is essentially complete and they are expected to enter the ICRU's review process soon. Included in this group are reports on:

(1) measurement of dose equivalent

(2) stopping powers for protons and alpha particles

During the current contract period considerable progress was made on the development of reports treating the following topics:

(1) absorbed dose standards for photon irradiation and their dissemination

(2) dose specification for reporting external beam therapy with photons and electrons

(3) dose specification for reporting interstitial therapy

(4) fundamental quantities and units

(5) performance assessment in digital representation of images

(6) phantoms for therapy, diagnosis and protection

(7) quality assurance in external beam therapy procedures

(8) statistical methods used in particle counting

(9) stopping powers for heavy ions

A number of new programs were initiated during the current contract period. Some of these have already advanced to the stage where they are cited in the discussion above. Others that are in the early stages of development include those concerned with the following topics:

(1) proton therapy

(2) secondary electron spectra resulting from charged particle interactions

(3) clinical dosimetry for neutrons: specification of beam quality

(4) in situ gamma spectrometry in the environment

(5) hyperthermia

Currently under study are potential new activities relating to the following topics: (1) measurements for operational health physics, (2) spectrometry with semiconductors, (3) dosimetry and calibration of beta-ray ophthalmic applicators, (4) dosimetry for astronauts, (5) measurement of radionuclide concentrations in environmental samples, (6) retrospective dosimetry of humans and materials, (7) high powered synchotron x-ray sources, (8) small electron storage rings, and (9) whole body counting.

IV. Other research group(s) collaborating actively on this project [name(s) and address(es)]:

V. Publications:

ICRU Report 38, Dose and Volume Specification for Reporting Intracavitary Therapy in Gynecology

ICRU Report 39, Determination of Dose Equivalents Resulting from External Radiation Sources

ICRU Report 40, The Quality Factor in Radiation Protection

ICRU Report 41, Modulation Transfer Function of Screen-Film Systems

ICRU Report 42, Use of Computers in External Beam Radiotherapy Procedures with High-Energy Photons and Electrons

ICRU Report 43, Determination of Dose Equivalents from External Radiation Sources--Part II

ICRU Report 44, Tissue Substitutes in Radiation Dosimetry and Measurement

ICRU Report 45, Clinical Neutron Dosimetry -- Part 1: Determination of Absorbed Dose in a Patient Treated by External Beams of Fast Neutrons

RADIATION PROTECTION PROGRAMME
Final Report

Contractor:

Contract no.: BI6-A-217-US

ICRU - International Commission on
Radiation Units and Measurements
7910 Woodmont Avenue, Suite 800
USA Bethesda, MD 20814

Head(s) of research team(s) [name(s) and address(es)]:

Prof. A. Allisy
Intern. Commission on Rad.
Units and Measurements, ICRU
7910 Woodmont Ave, Suite 800
USA Bethesda, MD 20814

Telephone number: 301-657-26.52

Title of the research contract:

Environmental monitoring needs connected with nuclear reactor accidents.

List of projects:

1. Environmental monitoring needs connected with nuclear reactor accidents.

Title of the project no.:

1. Environmental Monitoring Needs Connected with Nuclear Reactor Accidents

Head(s) of project:

Professor Andre Allisy

Scientific staff:

I. Objectives of the project:

The development of internationally acceptable recommendations regarding the practical aspects of measuring dose equivalent, including environmental monitoring related to nuclear reactor accidents.

II. Objectives for the reporting period:

Completion of the drafting work and submission of the draft report to the ICRU for review.

III. Progress achieved:

The ICRU Report Committee responsible for the drafting work on an ICRU report on measurement of dose equivalent made considerable progress on the preparation of the report. The document is to be based on, and utilize concepts explicated in previously published ICRU recommendations, particularly those set out in ICRU Report 39, Determination of Dose Equivalents Resulting from External Radiation Sources, and ICRU Report 43, Determination of Dose Equivalents from External Radiation Sources--Part 2.

A draft report was formulated which consisted of major sections treating the following topics: the basis of measurements, characteristics of instruments, calibrations, and the impact of new operational quantities on the design of future instrumentation. This draft was submitted to the ICRU for action. Review by the ICRU identified the need for substantial modification of the draft report on the basis of the guidance formulated by the ICRU. This guidance emphasized the need to treat problems of instrumentation and calibration and to focus on the problem of measurement of the dose equivalent from x and gamma radiation.

The Report Committee has begun the task of revising the draft report. It is expected that work on this draft can be completed quickly so that the revised version can be submitted to the ICRU for action.

The revised version of the report initially gives the background on Dose Equivalent, Effective Dose Equivalent and the Operational Quantities. It then explains that this report is restricted to external photons and electrons because of current uncertainties relating to Q. Next the report treats general principles of measurement of the dose equivalent and defines instrument response, discusses accuracy requirements and then deals with operational quantities, defining such terms as penetration, expansion, alignment and isodirectional. There follows a somewhat abbreviated definition of the operational quantities. The principal part of the report, then discusses general characteristics and requirements. These include area survey instruments for strongly and weakly penetrating radiations and individual dosimeters for these two types. This is followed by a discussion of instrument types and their application in measurement of photons and electrons.

The types are: ionization chamber, proportional counters, geiger-muller counters, scintillation detectors, semiconductor detectors, photographic film, thermoluminescent dosimeters, thermally stimulated exoelectron emission detectors and photoluminescent detectors. A brief section of the report then covers calibrations, treating calibration procedures for environmental and personal dosimeters. An important item relates to the choice of phantoms for the calibration of individual dosimeters. Treated next is the impact of new operational quantities on the design of future instrumentation. This is a brief discussion of the applicability of current instrumentation for the measurement of operational quantities and consideration of desirable instruments or the development of new types. An appendix provides a listing of conversion factors which are provided in the form of tables as well as graphs.

III B

VERHALTEN UND KONTROLLE DER RADIONUKLIDE IN DER UMWELT

BEHAVIOUR AND CONTROL OF RADIONUCLIDES IN THE ENVIRONMENT

COMPORTEMENT ET CONTROLE DES RADIONUCLEIDES DANS L'ENVIRONNEMENT

RADIATION PROTECTION PROGRAMME
Final Report

Contractor:

Risø National Laboratory
DK-4000 Roskilde

Contract no.: BI6-B-030-DK

Head(s) of research team(s) [name(s) and address(es)]:

Dr A. Aarkrog
Health Physics Department
RISØ National Laboratory
DK-4000 Roskilde

Telephone number: 02/37.12.12

Title of the research contract:

Behaviour of long-lived radionuclides in terrestrial and marine (North Atlantic Region) environments.

List of projects:

1. Terrestrial environment : Dynamic models of the human foodchain and determination of less wellknown long-lived radionuclides.
2. Marine environment : Experimental studies (turnover of radionuclides in bioindicators), field studies (North Atlantic region - Baltic sea), and Thule studies.

Title of the project no.: BI6-B-030-DK.1

Terrestrial environment a) dynamic models of the human food chain and b) determination of less well-known long-lived radionuclides.

Head(s) of project:

Dr. Sven Poul Nielsen (a), Dr. Elis Holm (b), Univ. of Lund, Sweden.

Scientific staff:

Mrs. Mette Øhlenschlæger (a)
Dr. Lars Bøtter-Jensen (b)
Dr. Qing Jiang Chen (b)

I. Objectives of the project:

a) To test available dynamic models, (e.g. NRPB) using the Danish/Nordic fallout data bank, to simplify these models if warranted, to investigate the influence of changes on agricultural practice, which have taken place in the last 25-30 years on the models, and to see if such an influence could be dealt with in future modelling. The perspective of an EEC fallout data bank will also be considered.

b) To develop counting equipment and analytical methods for determining and measuring less well-known long-lived radionuclides in low concentrations in environmental samples.

II. Objectives for the reporting period:

III. Progress achieved:

a) **Dynamic models**

1. Methodology

After the Chernobyl accident in 1986 a large amount of data has been collected on the transfer of radioactive material in the environment. These data are very useful for modelling purposes because they in contrast to the data from the weapons-test fallout are due to a contamination event of short duration. The data thus permit the time response of the environmental systems to be recorded, which is of great importance for dynamic modelling. Consequently, the use of previous fallout data has been de-emphasized.

The initial version of the dynamic model for ^{137}Cs was implemented via the TAMDYN model-simulation code. The TAMDYN code was later replaced with the TIME-ZERO system since the latter provides a more flexible and user-friendly modelling environment. All of the results in the following are derived from models implemented with the TIME-ZERO system.

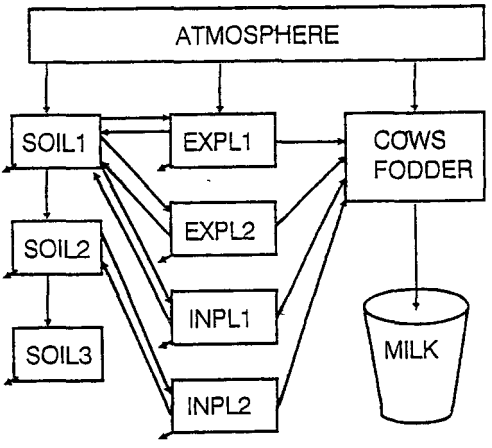

Figure 1. Schematic box structure of the iodine model.

The schematic iodine-model structure is shown in Fig. 1. The model comprises an atmospheric compartment, three soil compartments, and four grass compartments. The basic structure of the soil and grass compartments is similar to that used in the Farmland model developed by the National Radiological Protection Board.

The daily intakes of radioiodine by the cows are calculated from the fodder composition where the pasture component represents the major intake of radioiodine when the cows are not stabled. The intake also includes the inhalation pathway calculated from the breathing rate and the atmospheric concentrations. The milk concentrations are calculated from a simple multiplicative factor that accounts for the fraction of the daily intake of radioiodine by the cow that appears in each litre of milk.

The model dynamics uses a time step of one day, and as inputs to the model, atmospheric concentrations of ^{131}I are used together with data on precipitation and fodder composition, all given on a daily basis. The atmospheric iodine is assumed to comprise an

elemental fraction, a particulate fraction and an organic fraction. The deposition processes are modelled by dry deposition velocities and volumetric washout ratios that are different for each fraction.

The fraction of the total deposition that is retained initially on vegetation is modelled using a constant interception factor at a value of 0.3. The grass yield is assumed to be 0.14 kg dw m^{-2}. A weathering half-life of 10 days is used to account for the field-loss of initially retained iodine on the grass surfaces. When the cow is on a full grass diet the daily intake is 22 kg dry weight. The concentration of iodine in the milk is calculated from the daily intake using a factor of 0.001 Bq l^{-1} per Bq d^{-1}.

The schematic structure of the cesium model is shown in Figure 2. The pathways between the different compartments are indicated. The air, soil and plant compartments, all refer to an area of 1 m^2. The size of the time step is one day.

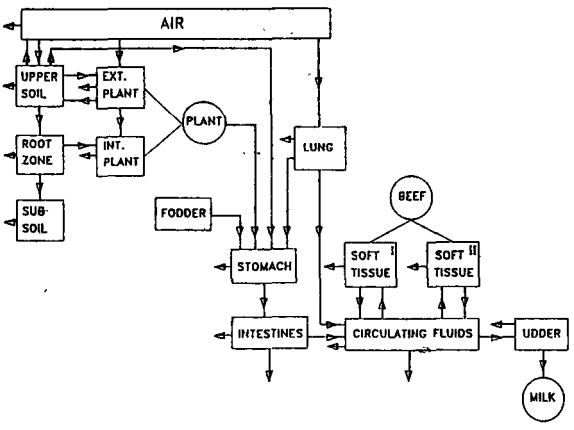

Figure 2. Schematic box structure of the cesium model.

The inputs to the model are the daily ^{137}Cs concentrations in the air after an accidental release. In order to calculate the wet deposition, average values for Danish precipitation are used; however, when data from the Chernobyl accident are used as input to the model, the actual amount of daily rain in 1986 is included in the model.

The deposition is partitioned between the soil and pasture using a common foliar interception factor of 0.3. The pasture growth rate is calculated from experiments made by the National Institute of Animal Science, Denmark and provides for the above-ground biomass and dilution of the concentration of ^{137}Cs in the grass during the growing season. The loss of ^{137}Cs from the surface of the grass to the soil is described by two weathering constants.

Three soil compartments are used in order to account for the intensive cultivation of the Danish soil. Resuspension of contaminated particles and soil ingestion by the livestock removes activity from the surface of the soil. Thus, an upper soil compartment of 1 cm thickness is considered. Plant uptake via roots is described by an expression similar to that used in the Pathway model. The effect of ploughing is simulated by converting the inventories of the external and internal parts of the plant

into the root zone compartment.

The cows diet specified in the model is based on the Danish agricultural practice. The cow model used here is based on a model previously published and adjusted to Danish conditions.

In areas of intensive agricultural farming, such as Denmark, changes of agricultural practices often occur by changing crop varieties in order to optimize the yield. The influence of such changes was studied by investigating the contamination potentials of barley varieties to direct as well indirect contamination. Direct contamination was studied from samples collected after the harvest in 1986, and indirect contamination was studied from pot experiments carried out in 1988.

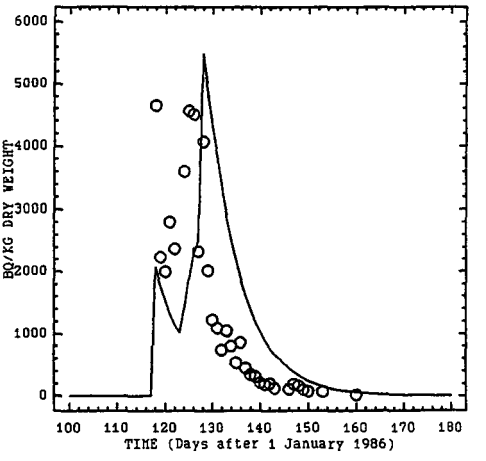

Figure 3. Predicted and measured levels of ^{131}I in grass at Roskilde after the Chernobyl accident (Bq kg^{-1} dry weight).

2. Results

The models were used to simulate the contamination of ^{131}I and ^{137}Cs of the Roskilde area in Denmark after the Chernobyl accident. Daily averages of measured levels of ^{131}I and ^{137}Cs in the air were used as input values. Since only the particulate fraction was measured, the following assumption was made of the iodine composition: 30% particulate, 30% elemental and 40% organic.

The predictions of the ^{131}I levels in grass are shown in Fig. 3 together with the observed levels. The predicted maximum level and the predicted time-integrated value are in relatively good agreement with the

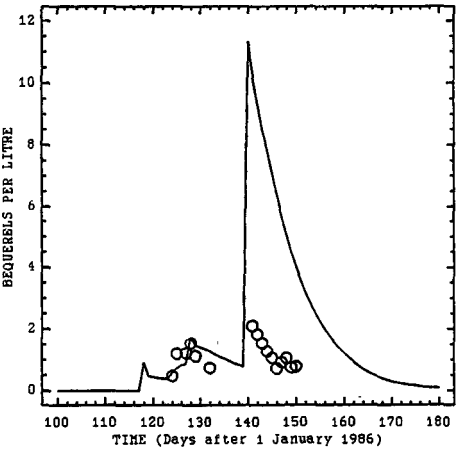

Figure 4. Predicted and measured levels of ^{131}I in milk collected near Roskilde after the Chernobyl accident (Bq l^{-1}).

observations giving predicted-to-observed (P/O) ratios of 1.2 and 1.3, respectively. However, the dynamic time variation of the predictions appears to be significantly out of phase in comparison with the observations, which shows that the deposition is inadequately simulated by the model. Considerable uncertainty is associated with the assumptions of a constant iodine fractionation, where higher levels of elemental iodine in the initial phase could account for the higher grass levels in this period. The model predictions of the milk levels are shown in Fig. 4 together with the observed values. The predicted milk levels from the stabling period are in good agreement with the observations, but when the cows are sent to pasture, the model significantly overestimates the milk levels (P/O = 5.7). This is caused mainly by the overestimate of the grass levels during the same period (P/O = 3.8).

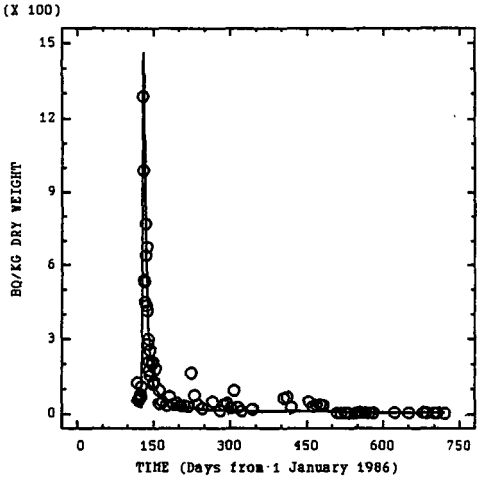

Figure 5. Cesium-137 in grass at Risø. Predicted and measured concentrations.

The levels in grass, milk and beef predicted by the cesium model are shown in Figs. 5-7 and the measured levels are given in comparison. The model predictions seem to be in good agreement with the measured levels. The cesium model was furthermore used to demonstrate the influence of the season following a release at different times of the year. Atmospheric contamination with cesium during winter thus causes significantly lower levels in foodstuffs compared to contamination during summer. In addition the effects of applying countermeasures (eg. increasing the stabling period) were investigated. The results of the investigation of the contamination potential of

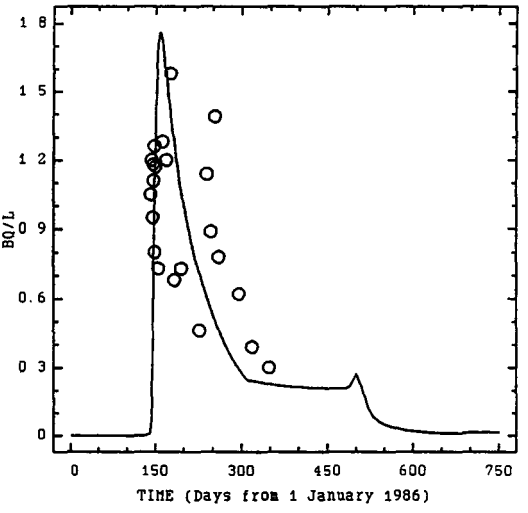

Figure 6. Cesium-137 in milk at Risø. Predicted and measured concentrations.

barley varieties demonstrate significant differences for both direct and indirect contamination. The ratios of the results for the barley varieties with the highest contamination potentials to those with the lowest contamination potentials range up to a factor of about two.

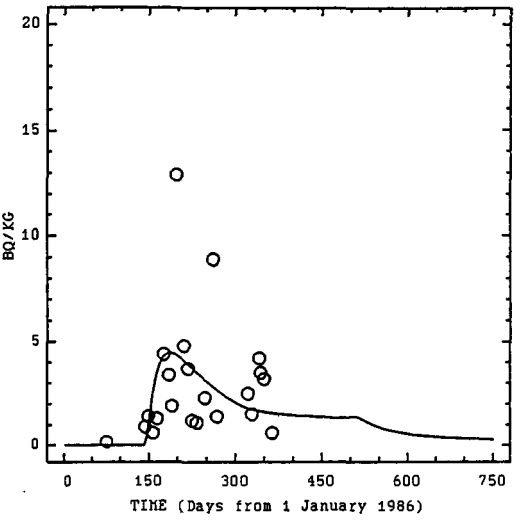

Figure 7. Cesium-137 in beef near Risø. Predicted and measured concentrations.

3. Discussion

The two models developed to simulate the transfer of radioactive iodine and cesium through the grass-cow-milk pathway are useful for radiological assessments of accidental releases to the atmosphere. The predictive accuracy of the models appears to be within a factor of two when compared with Chernobyl data from Denmark. However, the transfer of radioiodine from the atmosphere to the ground is more uncertain due to the chemical speciation of this element, since in particular elemental iodine dominates the deposition process. The cesium model includes features to account for the seasonal variations of the growth of vegetation which is of significance for the accuracy of the predictions including the long-term consequences.

The United Nations Scientific Committee on the Effects of Atomic Radiation (UNSCEAR) reports for their steady-state models transfer factors for ^{131}I and ^{137}Cs from total deposition to milk of 0.23 and 2.1 Bq d l^{-1} per Bq m^{-2}, respectively. The corresponding values for the dynamic models are 0.33 and 1.5 Bq d l^{-1} per Bq m^{-2},which also are within a factor of two compared with the above.

The investigation of the influence of changes on agricultural practice demonstrate significant differences between barley varieties for direct as well as indirect contamination of radiocesium. However, from a modelling view point these differences appear less significant considering the predictive accuracy of dynamic models in the case of accidental releases. The experience from the Chernobyl fallout shows a variability of the transfer from the atmosphere to the food stuffs in excess of a factor of two due to meteorological, seasonal and other site-specific conditions. The significance of the differences found between the barley varieties is that they indicate cost-effective means of reducing the radiological consequences after a nuclear accident.

b) Determination of less well-known long-lived radionuclides.

Methodology and results

Plutonium-241

Plutonium-241 (14.4 y) is the precursor of ^{241}Am (433 y) and ^{237}Np ($2.1x10^6$ y). A radiochemical procedure was developed for determining ^{241}Pu in environmental samples by measuring the ^{241}Am built up in plutonium originally electrodeposited on stainless steel discs.

Briefly described, the plutonium and built-up americium are leached from the stainless steel disc with HNO_3 and americium is separated from Fe, Ni and other actinides by anion exchange using mineral acids and methanol.

The method was applied to samples contaminated from different sources. The $^{241}Pu/^{239+240}Pu$ activity ratio characterize the source term and this ratio could be ranked for the following sources: Chernobyl accident > nuclear fuel reprocessing plants > nuclear weapons tests > nuclear weapons accidents.

Nickel-63 and nickel-59

A method was developed for the determination of ^{63}Ni (100 y) in environmental samples. Briefly described, nickel is extracted as dimethyl glyoxime by chloroform and electroplated onto copper. The radiochemical yield is determined by absorption measurements of stable nickel.

Nickel-63 is measured by either beta spectrometry using solid state ion-implanted detectors or by windowless anticoincidence shielded Geiger-Müller gas-flow counting. The minimum detectable activity was 8 and 1 mBq at 3000 min counting time for the two measurement systems, respectively.

The method was applied to samples (Fucus vesiculosus) collected at different distances from a nuclear power plant showing that ^{63}Ni has a similar distribution with distance from the plant as ^{60}Co.

It has not been possible to detect ^{59}Ni ($7.5x10^3$ y) which decays by electron capture. The activity ratio $^{59}Ni/^{63}Ni$ is expected to be only in the order of 1%.

Technetium-99

Technetium-99 ($2.1x10^5$ y) acts as an excellent tracer for water movements. However, the specific activity is low and large volumes are required for the analysis. We therefore developed a method for measurements of ^{99}Tc in large volume water samples.

The method is based on reduction of technetium to the +4 oxidation state with potassium disulfite followed by hydroxide precipitation. Further purification of technetium is done by precipitation of carbonates and hydroxides keeping technetium in the +7 oxidation state. Technetium(+7) is extracted with TBP. The radiochemical yield is determined with ^{99m}Tc and ^{99}Tc is measured by GM anticoincidence gas-flow counting.

The method allowed sequential separation from Pu, Am, Cs and was applied on samples from the Mediterranean, the Irish Sea, the North Sea, the Rhone river and also rain water.

After the Chernobyl accident it was noticed that the samples counted for ^{99}Tc contained impurities of ^{103}Ru, ^{106}Ru and ^{110m}Ag. The above mentioned analytical method did apparently not efficiently decontaminate for these radionuclides. Therefore a new method was developed to ensure that the Chernobyl accident did not pertubate the marine radiotracer studies, where ^{99}Tc probably now due to radiocesium fallout is the only usable tracer. The decontamination of $^{103,106}Ru$ from large volume (200-400 litres) seawater samples was achieved by repeated evaporation of RuO_4 from 0.1 N H_2SO_4 at 100°C, followed by extraction of TcO_4^- into 5% TIOA-xylene at controlled valence. Silver-110m was precipitated as AgCl. An average overall radiochemical yield of 70% was found for technetium. Decontamination factors were between $3x10^5$ and $2x10^7$ for Ru and $2x10^5$ for Ag. A new method to determine ^{99}Tc in seaweed by wet-ashing and simple extraction with 5% TIOA-xylene was also developed.

New beta multicounter systems for low-level measurements of ^{99}Tc in environmental samples were developed. Special efforts were directed towards reducing the counter backgrounds by using guard counters that work in anticoincidence with the sample counters. It was thus possible to reduce the counter backgrounds below 0.2 counts per minute resulting in lower limits of detection of 2 mBq of ^{99}Tc in the sample for 24 hours counting time.

Neptunium-237

A radiochemical procedure followed by alpha spectrometry was developed for the determination of ^{237}Np in large volume samples of sea water (up to 1800 litres). The analytical procedure is based on precipitation of hydroxides followed by anion exchange, fluoride precipitation and extraction with TTA. As radiochemical yield determinant ^{239}Np obtained from ^{243}Am is used. The major problem is to obtain satisfactory decontamination from ^{234}U having the same alpha energy. Sequential separation with Pu is possible.

The method was applied to samples from the North, the Norwegian, the Barents and the Greenland Seas showing decreasing concentrations from 4-10 mBq m^{-3} in the North Sea to 0.4-1 mBq m^{-3} in the Barents and the Greenland Seas.

Beta spectrometry

Silicon surface-barrier detectors, normally used for alpha spectrometry, have been applied for beta spectrometry and low-level measurements of pure beta particle emitters. General characteristics and performance of the detectors were investigated as well as effects of cooling.

The system has shown to be especially useful for quality control of measurements of pure beta-particle emitters such as ^{99}Tc and ^{63}Ni when the samples had been counted previously by conventional gas-flow beta counting. However, ion-implanted detectors are superior to surface-barrier detectors due to smaller leakage currents.

IV. Other group(s) collaborating actively on this project [name(s) and address(es)]:

Department of Radiation Physics
University of Lund
University Hospital
S-221 85 Lund
SWEDEN

V. Publications:

Ballestra, S., Barci, G., Holm, E., Lopez, J., Gastaud, J. Measurement of Technetium-99 in large volume water samples. J. Radioanal. Nucl. Chem., 115, p.51; 1987.

Bøtter-Jensen, L. and Nielsen, S. P. Beta multicounter systems for low-level measurements of environmental samples. Proceedings of the XVth Regional Congress of IRPA, Visby, Gotland, Sweden, 10-14 September, 1989.

Chen, Q. J., Aarkrog, A., Dahlgaard, H., Nielsen, S. P., Jensen, H. L., Bruun, J., Pedersen, A. H., Mandrup., K. Determination of ^{99}Tc in Environmental Samples by Anion Exchange. Risø-M-2739; 1988.

Chen, Q. J., Aarkrog, A., Dahlgaard, H., Nielsen, S. P., Dick, H., Mandrup, K. Determination of Technetium-99 in Environmental Samples by Solvent Extraction at Controlled Valence. Risø-M-2671; 1988.

Chen, Q. J., Nielsen, S. P., Aarkrog, A. Preparation of thin alpha sources by electrospraying for efficiency calibration purposes. J. Radioanal. Nucl. Chem. Letters, 135, No. 2, p. 117-123; 1989.

Chen, Q. J., Aarkrog, A., Dahlgaard, H., Nielsen, S. P., Holm, E., Dick, H., Mandrup, K. Determination of technetium-99 in environmental samples by solvent extraction at controlled valence. J. Radioanal. Nucl. Chem. Articles, 131, No. 1, p. 171-187; 1989.

Chen, Q. J., Dahlgaard, H., Hansen, H. J. M., Aarkrog, A. Determination of ^{99}Tc in environmental samples by anion exchange and liquid-liquid extraction at controlled valency. Accepted for publication in Analytica Chimica Acta.

Holm, E., Aarkrog, A., Ballestra, S. Determination of ^{237}Np in large volume samples of sea water. J. Radioanal. Nucl. Chem., 115, p.5; 1987.

Holm, E., Rioseco, J., Ballestra, S., Wilmet, F. Beta spectrometry with surface barrier detectors. The Science of the Total Environment, 69, p.61; 1988.

Holm, E. Determination of ^{241}Pu in environmental samples by a radiochemical procedure. Environmental International, 14, p. 363; 1988.

Holm, E., Rioseco, J., Ballestra, S., Walton, A. Radiochemical measurements of ^{99}Tc: Sources and environmental levels. J. Radioanal. Nucl. Chem., 123, p. 167; 1988.

Holm, E., Rioseco, J., Ballestra, S., Lopez, J. J., Fallout deposition of Actinides in Monaco and in Denmark following the Chernobyl accident. In: 4th Int. Symp. of Radioecology of Cadarache 14-18 March 1988.

Holm, E., Gastaud, J., Origione, B., Aarkrog, A., Dahlgaard, H., Smith, J. N. Chemical partitioning of plutonium and americium in sediments from the Thule region (Greenland). In: Radionuclides: A tool for oceanography. Elsevier Appl. Sci. Publ., p. 351; 1989.

Holm, E., Origioni, B., Vas, D., Petterson, H., Rioseco, J., Nilsson, U. ^{63}Ni: Radiochemical separation and measurement with ion implanted silicon detector. J. Radioanal. Nucl. Chem. (in press).

Kanyar, B., Fülöp, N., Keszthelyi, Z., Nielsen, S. P., Aarkrog, A. Model of the radionuclide transport through the terrestrial foodchains, including seasonal effects and countermeasures. Submitted for publication in Computers and Mathematics with Application, 1988.

Nielsen, S. P. and Kanyar, B., Simulation of ^{137}Cs contamination in Denmark from Chernobyl. 5th Nordic Radioecology Seminar, Rättvik, Sweden, 22-26 August 1988.

Nielsen, S. P. Modelling the transfer of ^{131}I to Danish milk after the Chernobyl accident. Proceedings of the XVth Regional Congress of IRPA, Visby, Gotland, Sweden, 10-14 September, 1989.

Nielsen, S. P. and Øhlenschlæger, M., Dynamic models for the transfer of ^{131}I and ^{137}Cs in the grass-cow-milk food chain. Risø-M-2848. To be published, 1990.

Øhlenschlæger, M. Dynamic modelling of ^{137}Cs contamination in Denmark. Proceedings of the XVth Regional Congress of IRPA, Visby, Gotland, Sweden, 10-14 September, 1989.

Title of the project no.: BI6-B-030-DK.2

Marine environment: a) Experimental studies (turnover of radionuclides in bioindicators), b) Field studies (North Atlantic region - Baltic Sea), and c) Thule studies.

Head(s) of project:

Dr. Henning Dahlgaard (a), Dr. Asker Aarkrog (b,c).

Scientific staff:

Dr. Sven Poul Nielsen, Dr. Elis Holm, Dr. Heinz Hansen, Dr. Qingjiang Chen.

I. Objectives of the project:

a) To improve knowledge on the turnover of radionuclides in the two most widely used bioindicator organisms in coastal waters: Fucus vesiculosus and Mytilus edulis under field comparable conditions. b) To study the dispersion of waterborne pollution in the northern North Atlantic by means of radioactive tracers discharged from nuclear facilities and to set up models for this dispersion. c) To follow the behaviour of Pu and Am in the benthic environment at Thule, Greenland. The results of this study may be implemented to waste disposal problems.

II. Objectives for the reporting period:

III. Progress achieved:

a. Experimental studies

1. Methodology

Multielement radioisotope tracer techniques with gamma- and alpha-emitters were used. Isotopes of Mn, Co, Zn, Ag, Tc, Ru, Cs, Ce, Eu, Np, Pu(IV), Pu(VI), Am and Cm were used.

Mussels, Mytilus edulis, or seaweed, Fucus vesiculosus, were allowed to accumulate the different radionuclides in the laboratory for 4-5 days before they were brought back to their environment. The amount of carrier added with the radionuclides was kept as low as possible in order to keep the metal concentrations at a natural low level. After being contaminated, the mussels were placed in small net bags which were suspended in the water column. Brances of young Fucus vesiculosus plants were fixed on pieces of string and tied up between the framework of a wellbox suspended in the water allowing adequate water movements. The plants grew during the whole experimental period of 1.5 year.

2. Results & discussion

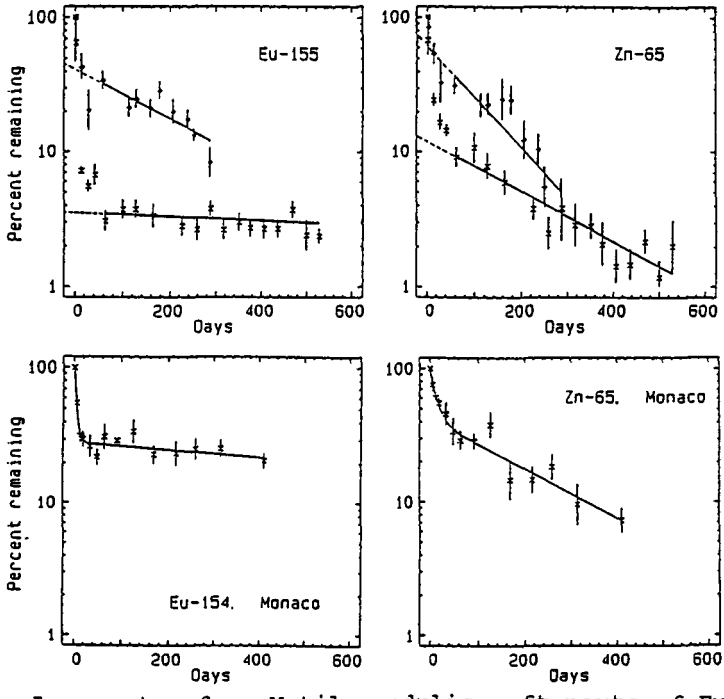

Figure 1. Loss rates from Mytilus edulis soft parts of Europium and Zinc in two Baltic (upper) and a Mediterranean experiment.

Element	N-Baltic Forsmark Nov. 83 - Aug. 84 Halflife days	Retention %	Central Baltic Oskarshamn June 85 - Dec. 86 Halflife days	Retention %	Mediterranean Monaco Dec. 87 - Jan. 89 Halflife days	Retention %
Manganese	90	33	212	1.50	-	-
Cobalt	79	77	287	4.3	203	24
Zinc	67	77	158	11.9	162	41
Technetium	∞	12	-	-	-	-
Ruthenium	-	-	-	-	162	39
Silver	45	36	∞	0.97	97	6.9
Cesium	-	-	78	0.07	18	18
Cerium	134	28	∞	0.73	-	-
Europium	137	45	∞	3.6	∞	29
Neptunium	133	82	-	-	-	-
Plutonium(IV)	98	71	∞	1.3	408	18
Plutonium(VI)	-	-	∞	4.9	-	-
Americium	141	44	-	-	∞	23
Curium	-	-	∞	2.9	∞	27

Table 1. Comparison of half lives (excluding growth dilution) and retention of slow compartment in two Baltic and a Mediterranean loss experiment with Mytilus edulis soft parts.

Table 1 and Figure 1 gives results from 2 Baltic and a Mediterranean loss experiment with Mytilus. For most elements it is seen that a slow compartment of substantial halflife exists. However, some interesting differences between the two Baltic experiments appear. In general the half lives are longer and the retention smaller in the Oskarshamn experiment, and for the Forsmark experiment loss rates could be correlated with season, whereas that was not the case in the Oskarshamn experiment. The difference between the Baltic experiments are too large to give a significant difference between loss in the Baltic and in the Mediterranean. If this result is generally valid it indicates, that large variations can occur in bioindicator results without direct correlation to environmental parameters as salinity, temperature and food conditions.

A 1.5 year loss experiment with Fucus vesiculosus at Oskarshamn (parallel with the Mytilus experiment) showed irreversible binding of 10% of the accumulated Mn, Co, Zn and Ag, 5% of the Pu and 1-2% for Ce, Eu and Cm. Furthermore the experiment showed a high degree of mobility (translocation) of Cs and Ag in the Fucus plants.

Generally, results from the long term loss experiments with Mytilus and Fucus indicate that for most elements studied, the growth rate is apparently more important for the concentration factor and for the bioindicator time integration, than is the actual loss of elements from the slow compartments. This effect is caused by dilution of pollutants present in the bioindicators by new growth.

These results are utilized in a model describing the accumulation and loss of radionuclides in Fucus as a function of month of discharge and month of sampling. The validity of the model has been verified on an independent set of data on corrosion products in Fucus near a Swedish nuclear power plant.

b. Field Data & Models

1. Methodology

During the period samples have been obtained from 8 major cruises: In april 1985 a collection of seaweed, mussels and seawater took place along the Channel coast in cooperation with French scientists. The discharges from La Hague, France were by means of bioindicators followed over a distance of 1200 km. In the summer of 1985 there was furthermore a cruise to the Fram Strait with F/S Polarstern, 1986 was perturbated by the Chernobyl accident, nevertheless samples of seawater were collected by F/S Walter Herwig in the East Greenland Current, and a major German-Scandinavian sampling of seawater and sediments from the Baltic Sea was carried out on board F/S Gauss in the autumn of 1986. In June 1987 seawater samples were collected from F/S Polarstern in the northern Greenland Sea and another set of samples from the southern part was obtained in Sept. from the Icelandic ship Bjarni Sämundson; in 1988 a number of deepwater samples were obtained on board the same ship. In the beginning of 1988 the German Hydrographic Institute in Hamburg collected seawater samples from the North Sea, the Channel and the Irish Sea for ^{99}Tc analysis.

Beside of these 8 cruises samples have regularily been obtained through R/V Dana from the Ministery of Fisheries, R/V Adolf Jensen from The Greenland Fisheries and Environmental Research Institute and from R/V Gunnar Thorsen from the Ministery of Environment, Denmark. Any marine environmental programme is dependent on the possibility of getting shipping opportunity. The costs of this project would have been about an order of magnitude higher if shipping opportunities had not been free.

2 Results

2.1 The English Channel

The authorized discharges of radionuclides from the reprocessing plant at Cap de la Hague in France have been used for tracing the water masses from the central part of the English Channel to the German Bight where the Jutland Current starts. In a joint French-Swedish-Danish effort samples were collected from the Europen and British sides of the Channel coast in the first half of 1985. The samples consisted of brown algae (mostly Fucus vesiculosus) and a number of seawater samples. The seaweed was analysed for ^{40}K, ^{60}Co, ^{90}Sr, ^{99}Tc, ^{106}Ru, ^{125}Sb, ^{134}Cs, ^{137}Cs, ^{238}Pu, ^{239,240}Pu and ^{241}Am. Sr-90 and ^{99}Tc were determined in the seawater. From the mutual determinations of seaweed and seawater the observed ratios between bioindicator and water were calculated. Furthermore, the ratios of the radionuclide concentrations in the various species were estimated. From this it was possible to normalize all seaweed data to Fucus vesiculosus concentrations. These concentrations were then related to the sea distance from

Cap de la Hague, and over a distance of more than one thousand kilometers the following regressions were found: Bq ^{99}Tc kg^{-1}dry weight = 19000 km$^{-0.7}$Y ^{60}Co: 2000 km^{-1}; ^{106}Ru: 300 km$^{-0.6}$ and ^{239,240}Pu: 3 km$^{-0.6}$. Hence the activity decreased approximately in inverse proportion to the distance or square root of the distance from the source. Similar distance relations have earlier been observed in British coastal waters for discharges from Sellafield in the UK.

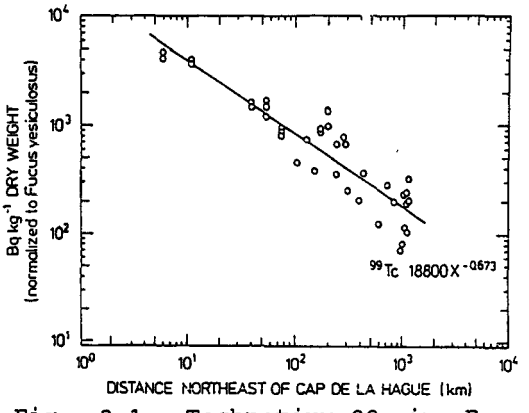

Fig. 2.1. Technetium-99 in Fucus between La Hague and Denmark.

2.2.1 Arctic waters - Technetium-99

Technetium-99 can be used to trace the effluents from the reprocessing of nuclear fuel in Western Europe to East Greenland waters and from here up along the West Greenland coast to Thule in North Greenland, i.e. over a distance of approximately 10000 km with the currents.

Furthermore it has been demonstrated that the transfer factor from Sellafield in the U.K. to the coastal waters around Greenland is on the order of 0.1-1 Bq m^{-3} (PBq a^{-1})$^{-1}$. This factor has been determined from ^{99}Tc measurements in Fucus vesiculosus/disticus as well as from ^{134}Cs measurements of surface seawater samples.

From the appearance of enhanced ^{99}Tc levels in fucoids collected since the 1960s along Greenland and in the Danish Straits, the transit time from Sellafield to East Greenland was found to be approximately seven years. This corresponds to an earlier estimate based upon ^{134}Cs and ^{137}Cs seawater data.

Finally, the unreported annual discharges of ^{99}Tc from Sellafield in the period 1970-77 has been estimated to be approximately 40 TBq.

2.2.2 Arctic waters - Cesium-137 and Strontium-90

Figure 2.2.2 and Table 2.2.2 show the mean ^{90}Sr and ^{137}Cs concentrations in surface sea water collected in 5° latitude bands in the coastal waters around Greenland in 1987.

The figure shows that the input of ^{137}Cs as well as of ^{90}Sr appears in the Fram Strait (in the northeast). In the case of ^{137}Cs, there are 3 sources to the enhanced levels in the northeastern

Greenland waters: 1) global fallout in the Arctic Ocean, 2) discharges from Sellafield, which have reached these waters with the Norwegian and West Spitbergen Currents, and 3) fallout in the NE Atlantic from the Chernobyl accident. In the case of ^{90}Sr, the main source is global fallout. From observations in the East Greenland Current made in earlier years, the global fallout backgrounds in 1987 may be estimated. This is done by extrapolation of the exponential decreasing concentrations measured at Danmarkshavn, Angmagssalik and Prins Christians Sund. In the Arctic water (from the East Greenland Current) we estimate 3.9 Bq ^{137}Cs m^{-3} and 3.3 Bq ^{90}Sr m^{-3}. In a similar way, the background levels in the NE Atlantic Ocean may be estimated from Faroese observations as 2.5 Bq ^{137}Cs m^{-3} and 1.75 Bq ^{90}Sr m^{-3}. From Fig. 2.2.2 it appears that the ^{137}Cs and ^{90}Sr concentrations observed along the west coast of Greenland are between the above estimates for Arctic and Atlantic water.

	Bq m^{-3} ±1 S.D. (N) west of 0°					
	West Greenland			East Greenland		
Latitude band	^{90}Sr	^{137}Cs	$^{137}Cs/^{90}Sr$	^{90}Sr	^{137}Cs	$^{137}Cs/^{90}Sr$
60-65	2.8±0.29 (3)	4.7±0.07 (2)	1.68±0.18	1.64 (1)	12.6 (1)	
65-70	2.3±0.22(18)	4.2±0.43(18)	1.83±0.26	2.6±0.97 (8)	5.5±1.76 (8)	2.12±1.04
70-75	2.2±0.35 (8)	3.3±0.47 (8)	1.50±0.32	3.0±1.14(17)	7.2±1.17(17)	2.40±0.99
75-80	2.5±0.14 (2)	3.0±0.21 (2)	1.20±0.11	3.9±0.65 (9)	8.7±1.32(10)	2.23±0.50

Table 2.2.2 Strontium-90 and cesium-137 mean concentration in surface sea water with salinities ≥ 30o/oo in 5° latitude bands collected around Greenland in 1987

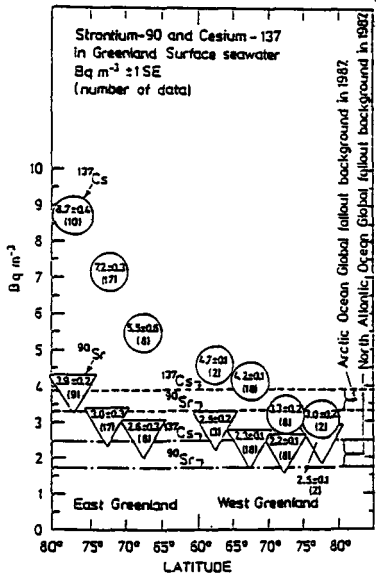

Fig. 2.2.2. Strontium-90 and cesium-137 in Greenland surface sea water (Unit: Bq m^{-3} ± 1 S.E. (n)). All data are west of 0°. Salinities below 30o/oo are excluded.

2.3 Technetium-99 in the Baltic Sea

Figure 2.3 shows the distribution of ^{99}Tc in the Baltic Sea. Samples from the Cattegat contained about 1-2 Bq ^{99}Tc m^{-3}, as expected from earlier studies. In the Baltic Sea the levels drop below 0.1 Bq m^{-3}. If the ^{99}Tc was from Chernobyl the highest levels would have been expected in the surface water, as observed for ^{137}Cs; instead, the ^{99}Tc concentrations in the Baltic Proper and the Bothnian Sea were generally higher below the halocline (at ~50m) than above. This is in accordance with expectations if the principal source of ^{99}Tc in the Baltic Sea is liquid discharge from reprocessing operations in western Europe. This would be mixed with North Sea water of high salinity entering the Baltic Sea through the Danish Straits as a bottom current.

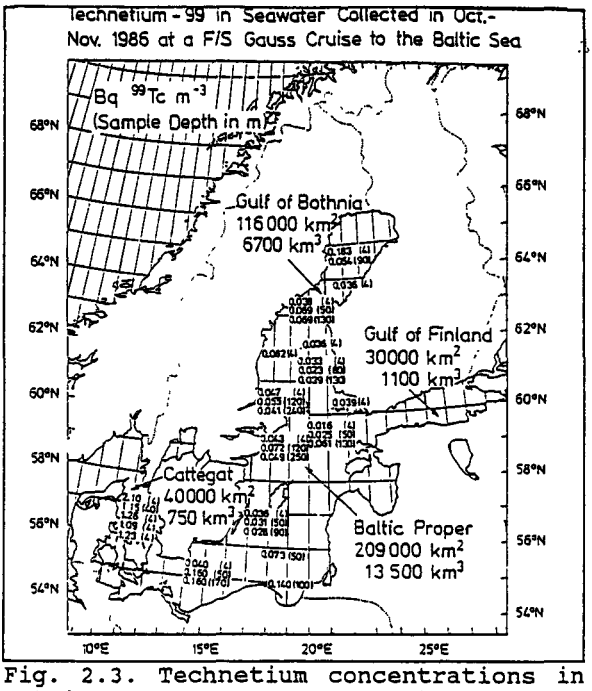

Fig. 2.3. Technetium concentrations in Baltic seawater collected in October-November 1986.

If the Chernobyl accident had contributed significant amounts of ^{99}Tc to the Baltic Sea, a correlation between the amounts of radiocesium and ^{99}Tc would have been expected in the seawater samples. But even the samples with the highest ^{137}Cs concentrations (500-1,000 Bq m^{-3}) showed no correlation between radiocesium and ^{99}Tc. As the K_d value for Tc in coastal waters is 30 times lower than that of Cs it is unlikely that Tc should have sedimented relative to Cs and thus have given rise to an underestimate of Chernobyl-derived radiocesium.

2.4 Inventories of Marine Antropogenic Radioactivity

The estimated inventories in the North Atlantic are at present (1989):

150 PBq ^{137}Cs from global fallout
30 PBq ^{137}Cs from nuclear reprocessing
20 PBq ^{137}Cs from the Chernobyl accident
100 PBq ^{90}Sr from global fallout
5 PBq ^{90}Sr from nuclear reprocessing and
3 PBq $^{239,240}Pu$ from global fallout

The mean residence time in the upper mixed layer of the North Atlantic is 25 years, and the present relaxation length for global fallout is about 1.2 km.

The concentrations of global fallout are significantly higher in the Arctic Ocean than in the remaining part of the North Atlantic (apart from the Baltic Sea). The highest concentrations from nuclear reprocessing are observed in the marginal seas of northwestern Europe.

The Baltic Sea contained the highest radiocesium concentrations after the Chernobyl accident.

2.5 Dose estimates from marine pathways due to the Chernobyl accident

Tables 2.5.1-2.5.2 show the time integrated concentrations of radiocesium and the corresponding collective effective dose equivalent commitments (CEDEC) based upon deposition data and seawater concentrations measured since the Chernobyl accident in the North Atlantic Region. Table 2.5.3 shows CEDEC calculated from the revised version of a NRPB model developed during the programme period (cf. references).

Fig. 2.5 shows the vertical mixing of the Chernobyl debris in the Cattegat. From May to August the mixture is complete (10-20 m depth). The figure also shows how highly contaminated water from the central Baltic Sea appears in the western Baltic about 1 year after the deposition.

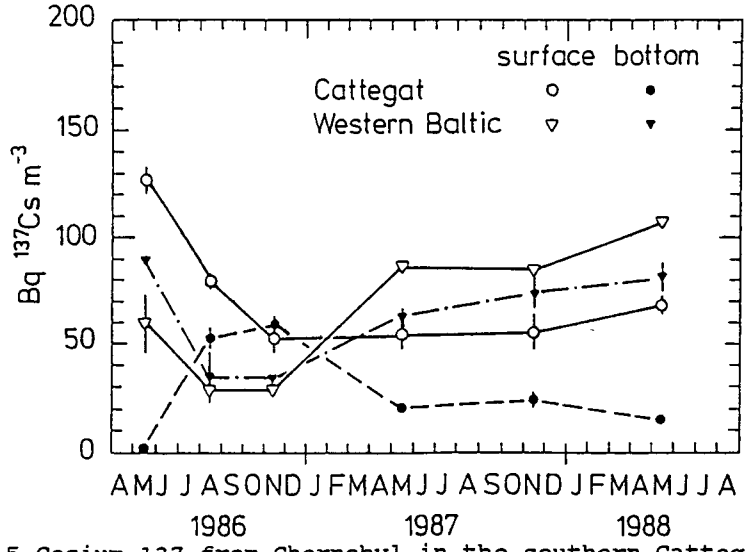

Fig. 2.5 Cesium-137 from Chernobyl in the southern Cattegat and the western Baltic Sea 1986-1988.

Area	^{137}Cs	^{134}Cs
2: Baltic Sea	4300	280
3: Danish Straits	1300	46
1: North Sea and Skagerak	110	14
4: North-East Atlantic, 60-70° N	44	2
5: Irish and Scottish Waters	61	15
6: North-East Atlantic, 40-60° N	3	0,01

Table 2.5.1. Time integrated concentrations of radiocaesium from the Chernobyl accident (Bq y m^{-3}).

Area	^{137}Cs	^{134}Cs
2: Baltic Sea	2200	280
3: Danish Straits	213	28
1: North Sea and Skagerak	38	12
4: North-East Atlantic, 60-70° N	41	8
5: Irish and Scottish Waters	25	7
6: North-East Atlantic, 40-60° N	1	0
Total	~ 2500	~ 340

Table 2.5.2. CEDEC applying measured data (man Sv).

Area	^{137}Cs	^{134}Cs
2: Baltic Sea	3600	310
3: Danish Straits	160	7
1: North Sea and Skagerak	83	14
4: North-East Atlantic, 60-70° N	44	3
5: Irish and Scottish Waters	34	11
6: North-East Atlantic, 40-60° N	1	0
Total	~ 3900	~ 350

Table 2.5.3. CEDEC applying the revised NRPB model (man Sv).

3. Discussion

The project was initiated during the former programme period (1980-1984), when the UK reprocessing plant, Sellafield was a major source to radioactive contamination of the North Atlantic region. Since the middle of the seventeeth the liquid discharges from Sellafield have been reduced by orders of magnitude for the important radionuclides, first of all Cesium-137. The Chernobyl accident introduced fresh amounts of Cs-137 and Cs-134 to the North-Atlantic and a distinction between the various sources (global fallout, nuclear reprocessing and Chernobyl) became difficult, which perturbated the use of radiocesium as a marine tracer. Furtunately another tracer has become available: Technetium-99 with a halflife of 2.1×10^5 yrs is mainly comming from reprocessing in La Hague and Sellafield. The production from Chernobyl was, as demonstrated under this project negligible. Formerly Tc-99 was mainly measured by means of bioindicators (Fucoids), but a new analytical technique has made large volume water determinations feasible. The Studies of Tc-99 in Arctic water masses contributes through their inclusion in the Greenland Sea Projects (GSP) and the World Ocean Circulation Experiment (WOCE) to the important studies of Meteorology and Oceanography in the Arctic region. The project has reconfirmed that the doses from marine pathways in general are orders of magnitude lower than those received from the terrestrial environment.

c. Thule studies

1. Methodology

Throughout the years the collection of samples in the Thule area has been carried out from ships. The last expedition in 1984 was on board the Canadian CSS Baffin. The scheduled expedition for 1989 has been postphoned due to lack of shipping opportunities. (The funding does not permit to hire a ship). The samples collected during the project, which stated in 1968 (after the socalled B-52 accident, when an aircraft carrying nuclear weapons crashed off Thule Air Base) have been analysed for plutonium and americium by radiochemical methods, which have been currently improved. These methods have recently been developed also to comprise urine analysis. A major effort has been a retrospective analysis of urine samples from those Danes actively involved in the post accident activities in Thule.

2. Results

The calculated inventories of $^{239,240}Pu$ were 0.98 TBq in 1974, 1.21 TBq in 1979, and 1.38 TBq in 1984. These estimates were not significantly different. The most recent value is preferred because it includes more samples than any of the other ones, although the earlier sampling grids have not underestimated the Pu inventory significantly. There have, thus, not been seen any tendency toward particularly high Pu sedimentation at the deep stations. The distance from the point of impact is more important than the depth of the station.

The mean $^{241}Am/^{239,240}Pu$ ratio in the sediments collected in 1984 was 0.13. An anova (analysis of variance) showed no significant difference in the ratio among locations, and between sampling years (1979 and 1984). However, the variation as a function of sampling depth was probably significant (P ~ 95%). The ratio increased with sampling depth. In the top sediment layers the ratio was, thus, approximately 0.10, while in the deeper layers it was 0.15. This may be influenced by the fact that global fallout becomes relatively more important in the deeper layers, and as the $^{241}Am/^{239,240}Pu$ is higher in global fallout than in Thule debris we may expect an increase with depth.

The mean $^{238}Pu/^{239,240}Pu$ in sediments was 0.018 in 1984, which is not significantly different from the ratio of 0.017 observed in 1979. An anova showed no significant difference in the ratio for the various locations and sediment layers.

From the above ratios and the inventory estimate of $^{239,240}Pu$ the inventories of ^{241}Am and ^{238}Pu at Thule were estimated at 0.18 TBq and 0.025 TBq, respectively.

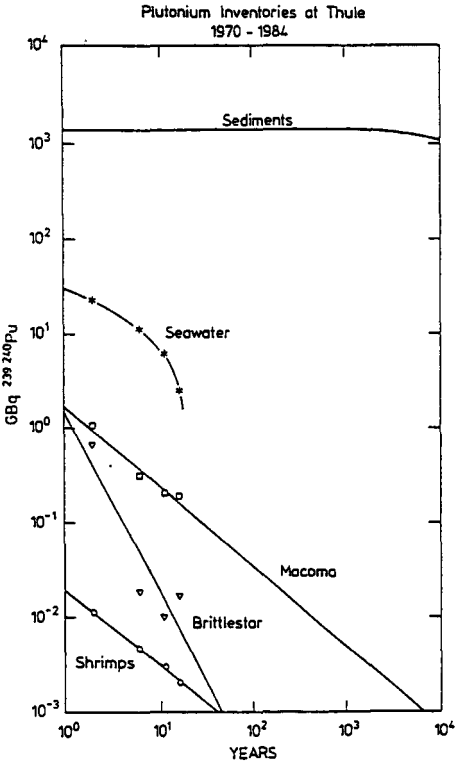

Fig. 1. $^{239,240}Pu$ inventories in environmental samples collected at Thule 1970-1984. Within the contaminated area (3.25×10^{9} m^2) the fresh weight biomass of shrimps was 0.11×10^{9} kg, of brittle star: 0.062×10^{9} kg, and of Macoma: flesh: 0.32×10^{9} kg, and shell: 0.26×10^{9} kg. The seawater mass was 3×10^{14} kg and the mass (dry weight) of the 0-15 cm sediment layer was 3×10^{11} kg. The abscissa is the time in years since the accident in 1968.

Fig. 1 shows the time variation in the plutonium inventories in the various sample types collected at Thule since 1968.

From these inventory estimates it is possible to estimate the transfer factors to biota for plutonium deposited in sediments.

For the Macoma community at Thule the transfer factor became: 0.027 Bq pr Bq yr^{-1}, i.e. if a source annually release 1 Bq $^{239,240}Pu$ to the sediments at Thule the Macoma community will at equilibrium contain 0.027 Bq $^{239,240}Pu$.

In case of brittle stars the transfer factor became: 2×10^{-6}Bq per Bq $yr^{-1}$and for shrimps: 0.5×10^{-3}Bq per Bq yr^{-1}.

3. Discussion

The biomass of shrimps at Thule is 0.035 kg m^{-2}, and the total mass of shrimps at the contaminated area (3.25×10^{9} m^{2}) is 0.11×10^{9} kg. The dose commitment to a member of the critical group consuming 20 kg of shrimps per year would be $20\times4.20\times0.05\times5/2\times10^{5}$ Sv=0.1 mSv, or 10% at one year's background exposure. The dose from ^{210}Po in the shrimps would amount to 0.2 mSv [5] in 50 years.

IV. Other research group(s) collaborating actively on this project:

N.S. Fisher, Brookhaven Nat. Lab., USA
Manuella Notter, SNV, Sweden
P. Guegueniat, CEA, France
C. Nolan and S.W. Fowler, IAEA, Monaco
A.D. Bettencourt, L.N.E.T.I., Portugal
Elis Holm, IAEA, Monaco
Gordon Christensen, IFE, Norway
John Smith, Bedford Inst. of Oceanography, Canada
Albert van Weers, ECN Netherlands Energy Research Foundation, Holland.
Hartmut Nies, Deutsches Hydrographisches Institut, Hamburg

V. Publications:

Aarkog A., Boelskifte S., Buch E., Christensen G., Dahlgaard H., Hallstadius L., Hansen H., Holm E., Mattsson S. and Meide A.. Environmental radioactivity in the North Atlantic region. The Faroe Islands and Greenland included. 1983. Risø-R-510. Risø National Laboratory (1984).

Aarkrog Asker, Dahlgaard Henning, Hansen Heinz, Holm Elis, Hallstadius Lars, Rioseco J. and Christensen Gordon. Radioactive tracer studies in the surface waters of the northern North Atlantic including the Greenland, Norwegian and Barents Seas. Reprint from Rit Fiskideildar 9: 37-42 (1985).

Aarkrog A., Boelskifte S., Bøtter-Jensen L., Dahlgaard H., Hansen Heinz and Nielsen S.P. Environmental Radioactivity in Denmark in 1985. Risø-R-540. Risø National Laboratory (1987).

Aarkrog A., Boelskifte S., Buch E., Christensen G.C., Dahlgaard H., Hallstadius L., Hansen H., Holm E. and Rioseco J. Environmental Radioactivity in the North Atlantic Region, The Faroe Islands and Greenland included. 1985. Risø-R-541. Risø National Laboratory (1987).

Aarkrog A., Boelskifte S., Dahlgaard H., Duniec S., Hallstadius L., Holm E. and Smith J.N. Technetium-99 and Cesium-134 as Long Distance Tracers in Arctic Waters. Estuarine, Coastal and Shelf Science 637-647 (1987).

Aarkrog A., Boelskifte S., Dahlgaard H., Duniec S., Holm E. and Smith J.N. Studies of Transuranics in an Arctic Environment. Journal of Radioanalytical and Nuclear Chemistry, Articles 39-50 (1987).

Aarkrog A., Bøtter-Jensen L., Chen Qing Jiang, Dahlgaard H., Hansen Heinz J.M., Holm Elis, Lauridsen Bente, Nielsen S.P. and Hansen-Søgaard. J. Environmental Radioactivity in Denmark in 1986. Risø-R-549 p. 274 (1988).

Aarkrog A. Studies of Chernobyl debris in Denmark. Environmental International Vol. 14, pp. 149-155 (1988).

Aarkrog A., Carlsson L., Chen Q.J., Dahlgaard H., Holm E., Huynh-Ngoc L., Jensen L.H., Nielsen S.P. & Nies H. Origin of technetium-99 and its use as a marine tracer. Nature Vol. 335, No.6188, pp. 338-340 22. September (1988).

Boelskifte S. The Application of Fucus vesiculosus as a Bioindicator of ^{60}Co Concentrations in the Danish Straits. J. Environ. Radioactivity 2, 215-227 (1985).

Chen Qing Jiang, Aarkrog Asker, Dahlgaard Henning, Nielsen Sven P., Jensen H.L., Bruun Jette, Pedersen Anna Holm, Mandrup Karen. Determination of ^{99}Tc in Environmental Samples by Anion Exchange. Risø-M-2739 p. 21 (1988).

Chen Jing Jiang, Aarkrog A., Dahlgaard Henning, Nielsen Svend P., Dick Nielle, Mandrup Karen. Determination of Technetium-99 in Environmental Samples by Solvent Extraction at Controlled Valence. Risø-M-2671 p. 31 (1988).

Dahlgaard Hnning. Effects of season and temperature on long-term in situ loss rates of Pu, Am, Np, Eu, Ce, Ag, Tc, Zn, Co and Mn in a Baltic Mytilus edulis population. Mar. Ecol. Prog. Ser., Vol. 33, 157-165 (1986).

Dahlgaard H., Aarkrog A., Hallstadius L., Holm E. and Rioseco J. Radiocaesium transport from the Irish Sea via the North Sea and the Norwegian Coastal Current to East Greenland. Rapp. P.-v. Reun. Cons. int. Explor. Mer 186: 70-79 (1986).

Dahlgaard Henning. Radionuclide Loss Rates from Baltic Mytilus edulis. Proc. Int. Conf. Heavy Metals in the Environment. Geneva Sept., 263-268 (1989).

Hallstadius L., Aarkrog A., Dahlgaard H., Holm E., Boelskifte S., Duniec S. and Persson B. Plutonium and Americium in Arctic Waters, the North Sea and Scottish and Irish Coastal Zones. J. Environ. Radioactivity 4, 11-30 (1986).

Hallstadius Lars, Garcia-Montano Estrella, Nilsson Ulf and Boelskifte Søren. An Improved and Validated Dispersion Model for the North Sea and Adjacent Waters. Journal of Environmental Radioactivity 261-274 (1987).

Holm E., Aarkrog A., Ballestra S. and Dahlgaard H. Origin and isotopic ratios of plutonium in the Barents and Greenland Seas, Earth and Planetary Science Letters 79, 27-32 (19869.

Holm E., Rioseco J., Aarkrog A., Dahlgaard H., Hallstadius L., Bjurmn B., Hedvall R. Technetium-99 in Algae from Temperate and Arctic Waters of the North Atlantic. In: Technetium in the Environment p. 53, CEC, Elsevier Appl. Sci. Publ. (1986).

Holm E., Aarkrog A., Ballestra S., Lopez J.J. Fallout deposition of Actinides in Monaco and in Denmark following the Chernobyl accident. IV Int. Symp. of Radioecology of Cadarache 14-18 March 1988.

Holm E., Rioseco J., Ballestra S., Walton A. Radiochemical measurements of ^{99}Tc: Sources and environmental levels. J. of radioanalytical and Nucl. Chem. 123, 167-179 (1988).

Holm E., Rioseco J., Ballestra S., Walton A. Radiochemical measurements of ^{99}Tc: Sources and environmental levels. J. of Radioanal. and Nucl. Chem., 123, p. 167 (1988).

Holm E., Aarkrog A., Ballestra S., Lopez J.J. Fallout deposition of actinides in Monaco and Denmark following the Chernobyl accident. In: Impact des accidents d'origine nucleaire sur l'environment. 4th International Symposium of Radioecology, Cadarache, France p. A-22 (1988).

Holm E., Gastaud J., Origioni B., Aarkrog A., Dahlgaard H., Smith J.N. Chemical partitioning of plutonium and americium in sediments from the Thule region (Greenland). In: Radionuclides: A tool for oceanography. Elsevier Appl. Sci. Publ. p. 351 (1989).

Kanyàr B. and Nielsen S.P. Users Guide for the Program TAMDYN. Risø-M-2741 (1988).

Nielsen S.P. and Kanyàr B. Simulation of ^{137}Cs contamination in Denmark from Chernobyl. 5th Nordic Radioecology Seminar, Rättvik, Sweden 22-26 August (1988).

RADIATION PROTECTION PROGRAMME

Progress Report

1989

Contractor: Contract no.: BI6-B-293-GR

GREEK ATOMIC ENERGY COMMISSION
N.R.C.P.S. "DEMOKRITOS"
Aghia Paraskevi
GR - 153 10 Attica

Head(s) of research team(s) [name(s) and address(es)]:

Dr. C. Apostolakis/ Dr. E.P. Papanicolaou
Lab. of Soils and Plant Nutrition
Greek Atomic Energy Commission
Aghia Paraskevi
GR - 153 10 Attica

Telephone number: 00-30-1-6511212

Title of the research contract:

Behaviour of long-lived radionuclides in soil-plant systems of the mediterranean region

List of projects:

1. **Behaviour of long-lived radionuclides in soil-plant systems of the mediterranean region**

Title of the project no.: B16-B-293-GR

Behaviour of long-lived radionuclides in soil-plant systems of the mediterranean region:

Head(s) of project:

Dr. C. Apostolakis/Dr. E. Papanicolaou
Lab. of Soils and Plant Nutrition
Greek Atomic Energy Commission
GR-153 10 Aghia Paraskevi, Attica

Scientific staff:

Institute of Biology	Institute of Nuclear Technology
C. Nobeli (Ms)	M.Bartzis
V. Skarlou (Ms)	P. Kritidis
	J. Papazoglou

I. Objectives of the project:

The objectives of the project, as approved, refer to the selection of regions in Greece with a high degree of contamination and sampling of the main soil types - in various depths - and of the cultivated or indigenous plants grown on them. Determination of the physicochemical parameters of the soil samples and the radionuclides concentration in the soil and plant samples. Greenhouse experimentation with selected soil types and main agricultural crops to establish uptake rates, and laboratory studies to investigate translocation of radionuclides within undisturbed soil columns. Correlation of climatic, analytical and experimental data and calculation of transfer factors from soil to plants and various products.

II. Objectives for the reporting period:

For the reporting period (July 1st - December 31st, 1989) the following were completed according to the targets set:

1. Continuation and completion of physical, chemical and radio-analyses for a part of the collected soil and plant samples.
2. Completion of harvesting, counting of soil and plant samples, calculation of transfer factors and correlation with soil properties for the greenhouse pot experiment with ^{85}Sr (1/2 life 64 days).
3. Establishment of the greenhouse experiment with cerium.
4. Preparatory work for the laboratory experiment on the translocation of radionuclides in undisturbed soil columns.
5. Preparation of a compartment model for long term contamination of perennial plant products based on experimental observations.

III. Progress achieved:

Physical, chemical and radio-analyses continued for a number of the collected in the field soil and plant samples while the samples of the greenhouse ^{85}Sr experiment were further processed and counted. Preparation of soils for the greenhouse experiment with ^{141}Ce and addition of the radionuclide for the incubation period and also preliminary analyses for the soil samples corresponding to the undisturbed columns for the laboratory experiment was completed. Processing of the radiocesium contamination data for fruit trees was performed by the collaborating in the project group of the University of Thessaloniki for establishing a compartment model for long term contamination of perennial plant products.

1. Methodology

For the presently reported period the physical and chemical characteristics such as texture, organic matter, calcium carbonate content, pH, cation exchange capacity and extractable cations were determined in soil samples from 32 sites (two depths). For this purpose generally accepted methods were used (Methods of Soil Analysis, ASA, Black C.A. Editor in Chief, 1965).

During the same period the determination of ^{137}Cs, ^{134}Cs and ^{40}K was continued in the soil and plant samples of previous field sampling periods thus completing the determination for 26 soil samples in two depths and 10 soil samples in one depth. Simultaneously same type of determinations were completed on alfalfa (22 samples) and wheat (16 samples).

In another aspect of the project the soil and plant samples from the greenhouse ^{85}Sr-experiment were prepared (as described in the previous report and counted (A total of 240 soil samples and approximately 400 plant parts).

For the determination of the radioelements an HpGe detector was used with relative efficiency 20-22% with respect to NaI (Tl) 3x3 in. crystal and energy resolution 1.9 KeV at the 1332.5 peak of ^{60}Co and proper shielding and geometry of the container.

In the preparatory phase for the laboratory undisturbed soil column experiment, the soil samples (19) corresponding to the 5 sites of the columns were submitted to a series of analyses using generally accepted methods as mentioned previously.

The commonly used procedure for greenhouse experiments was followed in the preparation of the soils for the ^{141}Ce-pot experiment. A total number of 120 pots was prepared according to the experimental plan for 5 soils x 4 plants x 6 replications.

The collaborating in the project group at the University of Thessaloniki utilized the accumulated, during the previous years, data based on experimental observations to prepare a compartment model for predicting various conditions occurring in leaves and fruits of selected apricot trees.

2. Results and Discussion

The data for the physical and chemical characteristics of the soil samples analysed during the reporting period indicate as to texture a group of sites with soils varying from loam to heavier textures, pH values ranging from 5.2 to 8.0, organic matter content from 2.0 to 3.2%, extractable (ammonium acetate)-K from 70 to 593 ppm with most values between 117 and 359 ppm and cation exchange capacity from 9 to 50 meq/100 g soil.

The radio-analyses of the soil and plant samples indicate in the case of the surface soil samples a contamination with ^{137}Cs ranging from 23 to 215 Bq/kg soil with most values between 42 to 139 Bq/kg. In the case of radioanalyses of soil samples taken in two depths the contamination of the 20-50 cm layer ranges between 3% and 50% of the surface value with values in the lower layer being higher in a few cases. Upon the completion of the project these last cases will have to be considered in a more detailed manner and in an overall correlation with the soil and environmental variables.

Plant samples indicate a contamination with ^{137}Cs for alfalfa which in the overall values is higher than wheat ranging from 1.5 to 26.6 Bq/kg as compared to from 0 to 9.2 Bq/kg for wheat. In the case of varying plant samples from the same soil sites alfalfa contamination with ^{137}Cs is higher than wheat but the differences are not great although the small number of plant pairs for the present samples does not permit the establishment of any trends.

From the greenhouse experiment with ^{85}Sr the obtained data concerning the transfer factors (concentration ratio, CR) of different crops and plant parts under various soil conditions are presented in the following table.

Crop	plant part	CR
Wheat	seed	0.034-1.39
"	straw	1.02-21.27
Alfalfa	hay 1st cut	2.77-23.23
"	" 2nd "	2.66-12.50
"	" 3rd "	3.49-10.78
Lettuce	plant material	1.74-17.18
Radish	root (edible part)	1.63-11.71
"	plant material	4.27-16.27
Beans	green beans (edible part)	0.26-8.51
"	plant material	4.16-28.38
Cucumber	edible part (fruit)	0.42-2.95
"	plant material	7.62-36.49

It is evident from these data that the values of concentration ratio of each crop or plant part show great differences in the different soils. In certain instances these values reach 40 fold differences (wheat seed).

These transfer factors were correlated with certain soil properties. Highly significant correlations were noticed thus far, between concentration ratio on one hand and pH (average r=-0.89 with C.V.=6.74%) as well as cation exchange capacity (average r=-0.84 with C.V.=11.9%) on the other.

Transfer factors calculated on the basis of the counted plant ^{85}Sr, assuming that soil ^{85}Sr was equal to total ^{85}Sr per pot minus plant ^{85}Sr, were as good as those based on counted ^{85}Sr in soil and plant samples.

In all of the cases where edible parts are separated, the transfer factor was found to be much lower than that of the remaining plant material, a fact that is of significant practical importance.

In the preliminary phase for the laboratory undisturbed soil column experiment the obtained data from the soil sample analyses indicate a wide variability of soil characteristics. Upon completion of the translocation experiment information may be obtained on the influence of soil properties on the behaviour of cesium in different soil types.

The greenhouse experiment in relation to the study of factors influencing cerium uptake was prepared according to the experimental plan and ^{141}Ce was added to the pots at the rate of about 0.23 mCi/pot. The soils were brought to field capacity and were left to stand for a period of one month before sowing the selected for the study plants.

The collaborating in the project group at the University of Thessaloniki utilizing the data accumulated previously is proposing a compartment model for long term contamination of perennial plant products based on experimental observations. The model predicts

(a) Exponentially declining contamination levels for fruits and leaves.

(b) A biological half life of the contamination of the crops of the order of 0.7 y.

(c) Total accumulated rejection of radiocesium over all years following deposition, to be one order of magnitude smaller than the inventory in the tree.

(d) Root uptake may be neglected not only for the first few years following deposition, but also for the long term contamination. Thus, contamination levels may be described by a single exponential term.

IV. Objectives for the next reporting period:

1. Continuation of physical, chemical and radio-analysis of the collected soil and plant samples.
2. Completion of greenhouse study on the transfer factors of ^{141}cerium.
3. Laboratory experiment of translocation of radionuclides in undisturbed soil columns.
4. Correlation of the overall data.

V. Other research group(s) collaborating actively on this project [name(s) and address(es)]:

Prof. M. Antonopoulos-Domis
Prof. A. Clouvas
School of Engineering
Aristotelian University of
Thessaloniki, Thessaloniki, GR

Prof. A. Gagianas
Agronomy Department
Aristotelian University of
Thessaloniki, Thessaloniki, GR

VI. Publications:

Compartment Model for Long Term Contamination Prediction
in Deciduous Fruit Trees after a Nuclear Accident.
M. Antonopoulos-Domis, A. Clouvas, A. Gagianas
Submitted for Publication to Health Physics.

RADIATION PROTECTION PROGRAMME
Final Report

Contractor:

Contract no.: BI6-B-032-UK

Imperial College of Science
and Technology
Exhibition Road
GB-London SW7 2AZ

Head(s) of research team(s) [name(s) and address(es)]:

Dr. J.N.B. Bell
Pure and Applied Biology Dept.
Imperial College Reactor Centre
Silwood Park
GB-Ascot, Berkshire SL5 7PY

Miss M.J. Minski
Imperial College Reactor Centre
Silwood Park, Buckhurst Road
GB-Ascot, Berkshire, SL5 7TE

Telephone number: 0990/23.911

Title of the research contract:

Time-dependent transfer of radionuclides from atmosphere and soil to crops, following simulated reactor accidents.

List of projects:

1. Time-dependent transfer of radionuclides from atmosphere and soil to crops, following simulated reactor accidents.

Title of the project no.:

Time-dependent transfer of radionuclides from atmosphere and soil to crops, following simulated reactor accidents.
B16-032-UK

Head(s) of project:

Prof. J.N.B. Bell
Department of Biology
Imperial College, Silwood Park
Ascot, Berkshire, SL5 7PY, U.K.

Miss M.J. Minski
Imperial College Reactor Centre
Silwood Park, Buckhurst Road
Ascot, Berkshire, SL5 7TE, U.K.

Scientific staff:

Mrs. E. Goodyear (Grade 3 technician)
Mr. W.R.C. Munro (Research Student)

I. Objectives of the project:

To further the understanding of the factors affecting uptake and subsequent retention of radioactive aerosols on aerial plant parts, and elucidate the relative importance of soil-plant and air-plant pathways for selected radionuclides on the ultimate collective dose to man. To determine the effect of temporal changes in the availability of radionuclides in the soil on uptake into crops.

II. Objectives for the reporting period:

Continuation of lysimeter studies with cabbage, with sequential harvests up to maturity. Estimation of changes in the exchangeable; total Cs ratio in experimental soils from all harvests throughout the programme. Measurement of contribution of soil resuspension to contamination of aerial plant parts, using Ti as a tracer. Dual-isotope experiment with cabbage in the wind-tunnel, followed by assessment of the fate of the foliar and soil applied Cs up to maturity.

III. Progress achieved:

1. Methodology

Over the project period as a whole, methodology has been centred around the wind-tunnel, production of labelled aerosols, and the system of lysimeters. Considerable effort has been put into improvements and modifications of the wind-tunnel, so that its aerodynamic characteristics are well defined and administration of aerosols to the air-flow results in an acceptably uniform concentration of aerosols above crop canopies in the working section. Concurrently, a technique has been developed for the production of 5μ diameter silica aerosols, labelled with a range of tracers, including ^{133}Cs which can be measured by neutron activation analysis. Experiments have been performed with ^{133}Cs contamination of the foliage of oil-seed rape and cabbage, using labelled aerosols. Two runs were performed, using ^{133}Cs-labelled silica (low availability) and solid $^{133}CsCl$ (high availability), to compare the influence of physico-chemical form on isotope behaviour. Immediately following contamination, ^{137}Cs was applied to the soil, and the plants transferred to the field, where half the crop was exposed and the other half placed underneath an open sided clear cover to eliminate precipitation. Sequential harvests were then taken of the crops up to maturity, with different plant organs being analysed for ^{133}Cs and ^{137}Cs by neutron activation analysis and γ-spectrometry to determine the behaviour of contaminants from atmospheric deposition and soil uptake, respectively. This part of the study was restricted to Cs, as Ru, Ce, and Sb stable isotopes suitable for aerial application were not available.

The lysimeter study was designed to determine the influence of freshly applied radionuclides compared with the same elements applied four years earlier which would have "aged" in the soil. Isotopes of Ce, Ru and Sb were not applied at the start of this project to the lysimeters which contained four major soil types characteristic of the principal wheat growing area of the EC, since it was not possible to compare their behaviour with that of radioisotopes of the same elements applied at an earlier date, as radioactive decay of the latter had reduced their radioactivity below detectable levels. Thus the comparison of "old" and "fresh" applications was restricted to ^{137}Cs (old) and ^{134}Cs (fresh). Winter wheat, oil-seed rape and cabbage were grown on three soils with sequential harvesting to maturity, followed by counting of all radioisotopes and estimation of the contribution of soil resuspension to contamination of aerosol parts, using Ti (measured by neutron activation analysis) as a soil tracer. In each case, half of each lysimeter was subjected to simulated ploughing by digging over to 20 cm depth, while the other half was subjected to minimal tillage. The migration of the radionuclides within the soil was measured on cores taken at the end of the experiment.

2. Results

Transfer factors for ^{134}Cs and ^{137}Cs to winter wheat growing on loam, silty loam and silty clay are shown in Tables 1, 2 and 3, respectively. Ploughing reduced uptake of both isotopes by up to 76% overall on all three soil types. However, in the case of the loam, this pattern was reversed for stem, leaf, chaff and grain at maturity and a similar trend occurred for grain only on silty loam. A notable result is the lower transfer factors recorded on all three soils for the ^{134}Cs than for the ^{137}Cs which had been applied four years later. The transfer factors to grain at the final harvest were consistently around half those to the stems for all soil types, irrespective of date of Cs application or tillage treatment. Transfer factors were generally greater for both ^{134}Cs and ^{137}Cs for loam > silty clay > silty loam.

Table 1

Soil-to-plant transfer factors for winter wheat grown on loam

		^{134}Cs				^{137}Cs			
		Ploughed		Minimum tillage		Ploughed		Minimum tillage	
		Mean	Standard error	Mean	Standard error	Mean	Standard error	Mean	Standard error
Harvest 1	stem	1.24E-02 ±	2.90E-03	6.25E-02 ±	2.72E-02	2.92E-02 ±	6.50E-02	1.47E-01 ±	6.15E-02
(174 days)	leaf	2.46E-02 ±	7.57E-03	1.85E-01 ±	3.14E-02	8.10E-03 ±	2.36E-03	3.74E-02 ±	6.00E-03
Harvest 3	stem	3.70E-03 ±	3.64E-04	2.76E-03 ±	2.62E-05	1.18E-02 ±	1.16E-03	1.01E-02 ±	1.58E-04
(293 days)	leaf	4.88E-03 ±	6.69E-04	3.03E-03 ±	5.38E-04	1.63E-02 ±	1.59E-03	1.32E-02 ±	2.37E-03
	chaff	4.53E-03 ±	6.17E-04	3.06E-03 ±	5.69E-04	1.48E-02 ±	1.70E-03	1.13E-02 ±	2.11E-03
	grain	2.24E-03 ±	3.45E-04	8.37E-04 ±	2.01E-04	6.87E-03 ±	9.47E-04	3.07E-03 ±	7.71E-04

Table 2

Soil-to-plant transfer factors for winter wheat grown on silty loam

		^{134}Cs				^{137}Cs			
		Ploughed		Minimum tillage		Ploughed		Minimum tillage	
		Mean	Standard error	Mean	Standard error	Mean	Standard error	Mean	Standard error
Harvest 1	stem	9.33E-04 ±	4.36E-04	2.24E-03 ±	5.51E-04	1.24E-03 ±	1.09E-03	5.42E-03 ±	1.58E-03
(174 days)	leaf	1.74E-03 ±	2.40E-04	1.25E-02 ±	6.73E-03	8.41E-04 ±	1.45E-04	4.47E-03 ±	2.52E-03
Harvest 3	stem	n/a	n/a	5.42E-04 ±	1.44E-04	n/a	n/a	2.34E-03 ±	6.85E-04
(293 days)	leaf	2.10E-03 ±	6.03E-04	2.14E-03 ±	8.25E-04	7.24E-03 ±	1.83E-03	8.27E-03 ±	2.52E-03
	chaff	3.50E-04 ±	7.34E-05	9.78E-04 ±	1.91E-04	2.11E-03 ±	7.56E-04	5.61E-03 ±	2.00E-03
	grain	8.68E-04 ±	5.04E-04	2.67E-04 ±	4.98E-05	3.44E-03 ±	2.05E-03	1.01E-03 ±	1.73E-04

Table 3

Soil-to-plant transfer factors for winter wheat grown on silty clay

		^{134}Cs				^{137}Cs			
		Ploughed		Minimum tillage		Ploughed		Minimum tillage	
		Mean	Standard error	Mean	Standard error	Mean	Standard error	Mean	Standard error
Harvest 1	stem	2.25E-03 ±	1.82E-04	5.79E-03 ±	8.19E-03	4.85E-03 ±	2.13E-03	1.12E-02 ±	2.46E-03
(174 days)	leaf	4.84E-03 ±	1.75E-03	1.11E-02 ±	2.26E-03	1.24E-03 ±	3.52E-04	2.63E-03 ±	6.03E-04
Harvest 3	stem	1.12E-03 ±	2.97E-04	1.52E-03 ±	6.89E-04	4.78E-03 ±	1.27E-03	5.49E-03 ±	2.04E-03
(293 days)	leaf	1.26E-03 ±	5.92E-04	2.86E-03 ±	7.11E-04	4.30E-04 ±	1.73E-03	8.40E-03 ±	1.61E-03
	chaff	9.38E-04 ±	1.66E-04	1.41E-03 ±	3.94E-04	3.42E-03 ±	4.26E-04	5.19E-03 ±	1.44E-03
	grain	4.09E-04 ±	4.46E-05	4.77E-04 ±	1.27E-04	1.37E-03 ±	1.22E-04	1.61E-03 ±	3.79E-04

Transfer factors for ^{134}Cs and ^{137}Cs to cabbage on loam and silty loam are shown in Tables 4 and 5, and can be compared with the values obtained for this species growing on silty clay (Eutric gleysol), which were reported in the 1988 Interim Report. Overall there was again a trend for the "aged" Cs to show a greater uptake than the freshly applied ^{134}Cs on all three soil types, reflecting the results obtained for the winter wheat. Ploughing had a consistent effect in reducing Cs uptake into all plant parts, irrespective of the duration of the isotopes in the soil.

Table 4

Soil-to-plant transfer factors for savoy cabbage grown on loam

		^{134}Cs				^{137}Cs			
		Ploughed		Minimum tillage		Ploughed		Minimum tillage	
		Mean	Standard error	Mean	Standard error	Mean	Standard error	Mean	Standard error
Harvest 1	stem	2.69E-02 ±	5.02E-03	5.00E-02 ±	4.64E-03	6.58E-02 ±	1.35E-02	1.06E-01 ±	1.25E-02
(43 days)	leaf	4.00E-02 ±	3.43E-03	8.06E-02 ±	1.39E-02	9.40E-02 ±	1.02E-02	1.54E-01 ±	2.79E-02
Harvest 2	stem	5.79E-03 ±	9.89E-04	1.15E-02 ±	1.24E-03	1.65E-02 ±	2.97E-03	2.87E-02 ±	3.69E-03
(62 days)	inner leaf	1.56e-02 ±	8.01e-03	4.86E-03 ±	n/a	4.06E-02 ±	2.06E-02	9.14E-03 ±	n/a
	outer leaf	5.86E-03 ±	4.14E-03	2.66E-02 ±	3.49E-03	1.42E-02 ±	1.00E-01	5.89E-02 ±	5.90E-03
Harvest 3	stem	1.04E-02 ±	1.45E-03	1.86E-02 ±	2.18E-02	2.58E-02 ±	3.09E-03	3.84E-02 ±	3.21E-03
(134 days)	inner leaf	1.43E-02 ±	2.22E-03	2.55E-02 ±	3.44E-03	3.21E-02 ±	4.09E-03	4.80E-02 ±	3.61E-03
	outer leaf	1.82E-02 ±	7.35E-03	6.45E-02 ±	1.15E-02	4.36E-02 ±	1.72E-02	1.32E-01 ±	1.97E-02
Harvest 4	stem	9.21E-03 ±	1.05E-03	1.00E-03 ±	2.86E-03	2.13E-02 ±	1.92E-03	2.07E-02 ±	4.55E-03
(188 days)	inner leaf	1.20E-02 ±	1.42E-03	2.02E-02 ±	9.11E-03	2.67E-02 ±	2.67E-03	4.10E-02 ±	1.73E-02
	outer leaf	n/a	n/a	n/a	n/a	n/a	n/a	n/a	n/a

Table 5 Soil-to-plant transfer factors for savoy cabbage grown on silty loam

		^{134}Cs				^{137}Cs			
		Ploughed		Minimum tillage		Ploughed		Minimum tillage	
		Mean	Standard error	Mean	Standard error	Mean	Standard error	Mean	Standard error
Harvest 1	stem	3.00E-03 ±	3.27E-04	1.22E-02 ±	6.99E-03	1.13E-02 ±	6.76E-03	2.16E-02 ±	1.19E-02
(43 days)	leaf	7.85E-03 ±	2.74E-03	1.85E-02 ±	8.97E-03	2.73E-02 ±	1.37E-02	3.47E-02 ±	1.74E-02
Harvest 2	stem	1.69E-03 ±	2.19E-04	2.70E-03 ±	1.18E-03	5.23E-03 ±	3.58E-04	6.56E-03 ±	2.86E-03
(62 days)	inner leaf	1.57E-03 ±	1.04E-03	3.02E-03 ±	2.33E-03	4.99E-03 ±	2.93E-03	6.08E-04 ±	5.27E-04
	outer leaf	3.38E-03 ±	2.24E-04	6.13E-03 ±	1.31E-03	1.02E-02 ±	1.69E-03	1.13E-02 ±	2.11E-03
Harvest 3	stem	1.47E-03 ±	1.68E-04	2.86E-03 ±	9.25E-04	3.053-03 ±	3.33E-04	6.19E-03 ±	1.51E-03
(134 days)	inner leaf	2.41E-03 ±	3.40E-04	3.73E-03 ±	5.88E-05	4.31E-03 ±	2.91E-04	6.95E-03 ±	5.03E-04
	outer leaf	3.46E-03 ±	5.84E-04	2.77E-02 ±	2.69E-03	7.27E-03 ±	1.14E-03	5.50E-02 ±	7.48E-03
Harvest 4	stem	1.75E-03 ±	2.10E-04	3.10E-03 ±	1.67E-03	5.47E-03 ±	3.10E-04	8.66E-03 ±	4.61E-03
(188 days)	inner leaf	2.81E-03 ±	1.94E-04	3.99E-03 ±	7.09E-04	5.76E-03 ±	3.11E-04	7.73E-03 ±	1.22E-03
	outer leaf	1.71E-02 ±	4.55E-03	4.67E-02 ±	1.60E-02	1.00E-02 ±	1.87E-03	1.09E-01 ±	2.90E-02

Titanium analyses of aerial parts of wheat and cabbage failed to reveal any detectable levels of this element, indicating minimal contamination by soil splash.

Distribution of ^{134}Cs and ^{137}Cs in the loam and silty clay soils is shown in Figures 1-4. Overall, the ploughed soils showed a relatively uniform distribution of both isotopes with depth, indicating uniform mixing, except for the 20-25 cm samples where the corer had probably penetrated into the unploughed zone. Surprisingly, in the unploughed soils, both ^{134}Cs and ^{137}Cs showed generally similar patterns, with a rapid fall to 15 cm depth, above which 80-90% of the isotopes were contained.

Since the 1988 Interim Report, a complete analysis has been performed for the measurements of ^{133}Cs and ^{137}Cs on the wind-tunnel contaminated oil-seed rape plants, following their transfer to exposed and covered conditions in the field. The final harvest at 108 days after contamination showed no significant further field loss of foliar applied Cs under either set of conditions, although the exponential downward trend appeared to continue; fitting an exponential curve to data for all harvests gave $T_{1/2}$ of 11.8 and 19.9 days for exposed and covered plants, respectively. The transfer factors for ^{134}Cs from the soil confirmed the generally higher transfer factor under covered conditions.

Table 6

Deposition velocities for low & high availability Cs, $cm.s^{-1}$

	1988 (low availability)	1989 (high availability)
Vg Plant	0.18	0.19
Vg Soil	0.16	0.15
Vg Canopy	0.34	0.34
Vg Inner Leaves	-	0.02
Vg Outer Leaves	-	0.16

Figure 1 - Depth profile of caesium 134 in loam soil

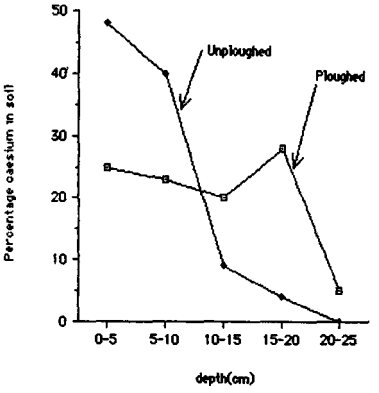

Figure 2 - Depth profile of caesium 137 in loam soil

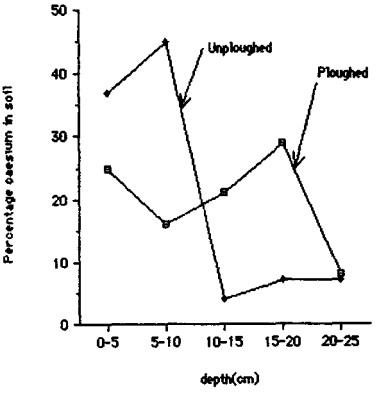

Figure 3 - Depth profile of caesium 134 in silty clay soil

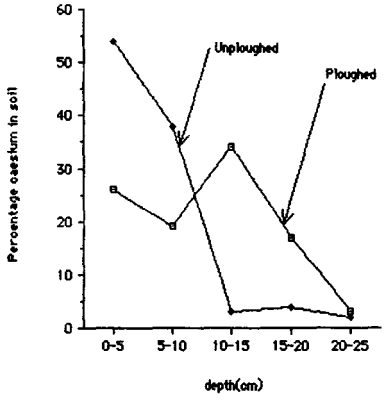

Figure 4 - Depth profile of caesium 137 in silty clay soil

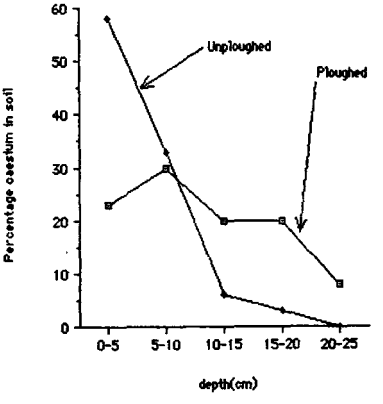

The values for deposition velocities were very similar for the two types of caesium aerosol i.e. low or high availability. Values were higher for the exposed plant than covered (see Table 6).

The field loss for cabbage after application of high availability Cs under exposed and covered conditions is shown in Figures 5 and 6 for different plant parts. The inner leaves and stem show similar losses under both conditions but the exposed leaves show a more rapid loss initially compared with the covered ones. Using an exponential fit for the outer leaves gave $T_{1/2}$ of 12 days for the covered and 9.5 days for the exposed.

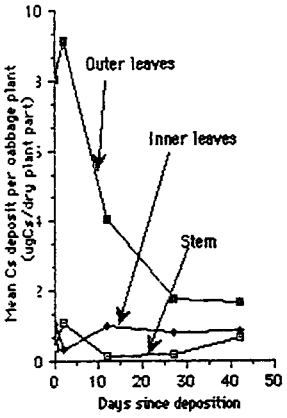

Fig. 5 - Field loss of solid caesium aerosol from cabbage under covered conditions.

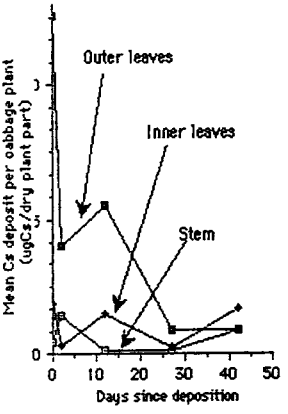

Fig. 6 - Field loss of solid caesium aerosol from cabbage under exposed conditions.

Figure 7 shows the soil-to-plant transfer factors after transfer of the cabbage contaminated by foliar deposition of high availability Cs. In all cases there is an increase in transfer factors over the first 25 days and generally the covered plants have higher values than the exposed.

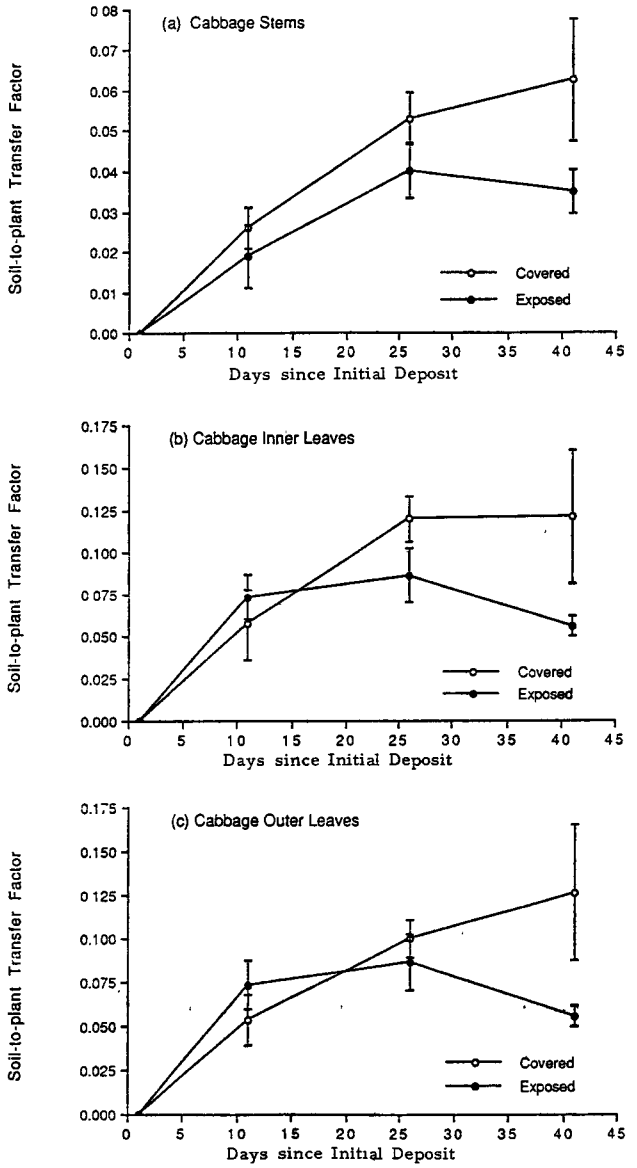

Fig. 7 Soil-to-plant transfer factor for cabbage on silty loam under exposed and covered conditions.

3. Discussion

The project has illustrated the value of dual isotope experiments in separating out the contribution of direct atmospheric deposition of Cs onto aerial parts of crops compared with uptake via the roots. This offers the opportunity of extended work using the dual isotope technique for wet deposition studies.

An important finding is the marked effect in most cases of ploughing in reducing uptake of Cs 'into the crops' compared with minimal tillage. The dilution of the radionuclide within the upper parts of the plough-layer where maximum uptake of ions into the roots takes place is clearly shown by the uniform distribution found in the soil core analyses. However, the reversal in the effect of ploughing observed for wheat grain in plants growing on the two loam type soils indicates that other mechanisms are influencing potential human dose. This requires further investigation, as it suggests that in the two loam soils the physico-chemical speciation of the Cs may be in a form which results in increased mobility within the plant. The occurrence of this phenomenon in both "aged" and "fresh" Cs suggests that any such change in speciation must be relatively rapid followed by the isotopes remaining in a form with a similar level of mobility. The lower transfer to grain than to wheat stems is consistent with previous studies at Imperial College and elsewhere (Grogan et al., 1987).

The most unexpected result of the project was the consistently higher transfer factors found for Cs uptake into all species from all soils when the isotope had been present for 4 years longer than the "freshly" applied ^{134}Cs. This questions the common assumption that fixation of Cs occurs rapidly in mineral soils. Other work at Imperial College (Adams et al., 1988) has shown marked annual cyclical changes in the availability of Chernobyl-derived Cs in three British arable mineral soils. The factors responsible for these unexpected patterns of availability merit further investigation, including the role of microbial activity. Neither ^{134}Cs nor ^{137}Cs appeared to be resuspended from the soil and deposited onto aerial parts of the crops to any extent, as the Ti analyses of foliage were below the detection limit. However, the influence of weather conditions on soil splash and subsequent removal of resuspended soil from plant shoots is poorly quantified, but likely to result in variable degrees of contamination over the course of a growing season (Bell et al., 1988). A comparison of the profiles of the "aged" and "fresh" Cs in unploughed soils shows a surprisingly similar pattern for the two isotopes. This suggests an initial rapid movement downwards, followed by some degree of fixation and a more detailed examination of this on a temporal basis might provide some explanation of the unexpected behaviour of the "aged" and "freshly" applied isotopes.

The wind tunnel experiments showed very similar velocity deposition values for Cs in two aerosols of very different physico-chemical form, to two different crop species. This indicates the importance of particle size (5μ in both cases) in controlling deposition and interception of radioactive material from the atmosphere, irrespective of the chemical form. In the case of cabbage, the inner leaves are well protected from aerosol contamination, with optimistic implications for dose. The patterns of field loss from the different species, including weathering half lives, are consistent with those reported elsewhere (Jayasekera et al., 1989).

In all experiments, soil to plant transfer for radiocaesium is reduced when the crop is protected from precipitation by a transparent cover. This effect occurs in cabbage in all organs analysed, with a markedly consistent temporal pattern of variation in all cases : thus the internal barriers which reduce Cs movement to edible parts of wheat plants do

not appear to operate in cabbage, although a study of translocation to reproductive organs in the latter case would be necessary in order to make such studies comparable for analogous plant part organs. The effect of removal of precipitation in Cs uptake via the roots confirms other work at Imperial College with wheat (Mitchell, 1990). It raises the possibility of rainfall patterns having a marked effect on soil to plant transfer of Cs, and the importance of carrying out controlled studies on climatic influences in radioecology, these having been largely neglected up to the present.

IV. Other research group(s) collaborating actively on this project [name(s) and address(es)]:

None

V. Publications:

1 Grogan, H.A., Mitchell, N.G., Minski, M.J., Bell, J.N.B.
Pollutant transport and fate in ecosystems. Ecological Aspects of Radionuclide Releases. 353-370 Blackwell (1987).

2. Bell, J.N.B., Minski, M.J.
Plant uptake of radionuclides. Soil Use and Management. 43(3), 76-84 (1988).

3. Jayasekera, P.N., Leese-Weller, R.J., Watterson, J.D., ApSimon, H.M., Bell, J.N.B., Goddard, A.J.H., Minski, M.J., Taylor-Russell, A.J.
Aerosoal contaminating activable tracers for deposition studies. Aerosols - their generation, behavious and application. 3rd Annual Conference Aerosol Society (1989).

4. Mitchell, N.G. - Ph.D. Thesis (1990).

RADIATION PROTECTION PROGRAMME
Final Report

Contractor:

Contract no.: BI6-B-033-D

Lehrgebiet Strahlenschutz in der
Kerntechnik der Rhein.Westfälissch.
Technischen Hochschule Aachen
Templergraben 55
D-5100 Aachen

Head(s) of research team(s) [name(s) and address(es)]:

Prof. Dr. H. Bonka
Lehrgebiet Strahlenschutz in der
Kerntechnik der RWTH Aachen
Templergraben 55
D-5100 Aachen

Telephone number: 0241/80.54.40

Title of the research contract:

Improvement of models for the calculation of the dry deposit of radionuclides and radioiodine bound to aerosol particles.

List of projects:

1. Measurement of the influence of the height on the diffusion coefficients of the turbulence both in the field and in a windtunnel.

Title of the project no.:

1. Measurement of the influence of the height on the diffusion coefficients of the turbulence both in the field and in a wind tunnel.

Head(s) of project:

Univ.-Prof. Dr. H. Bonka
Lehrgebiet Strahlenschutz in der
Kerntechnik der RWTH Aachen

Scientific staff:

Dr.-Ing. H.-G. Horn
Dipl.-Ing. R. Kreh

I. Objectives of the project:

Measurement of the vertical distribution of wind velocity and eddy diffusion-coefficient in and above different kinds of vegetation (field and wind tunnel experiments). Use of this results for the calculation of the deposition velocity.

II. Objectives for the reporting period:

- Completion of a wind tunnel to measure the deposition velocity
- Installation of an anemometrie-system to measure the wind velocity in and above different kinds of vegetation in field.
- Installation of an anemometrie-system to measure the three-dimensional eddy-flow in and above different kinds of vegetation. Developement of a computer code to calculate the eddy-diffusion coefficient.

1 Einleitung

Seit Einführung der Ablagerungsgeschwindigkeit zur Berechnung der abgelagerten Aktivität wurden eine Reihe von Experimenten zur Bestimmung der Ablagerungsgeschwindigkeit für aerosolgebundene und gasförmige Radionuklide an Vegetation durchgeführt. Da es nicht möglich ist, diese für alle notwendigen Parameter wie den aerodynamischen Teilchendurchmesser, die Windgeschwindigkeit, die Vegetationsart und -höhe usw. zu messen, ist es zweckmäßig, den vollständigen Datensatz letztlich zu berechnen. Die wichtigsten Größen zu ihrer Berechnung sind der Aktivitätskonzentrations- sowie der Windgeschwindigkeitsverlauf innerhalb der Vegetation, der Abscheidegrad an der Vegetation in Abhängigkeit von der Windgeschwindigkeit und die angeströmte Vegetationsfläche pro Einheitsbodenfläche. Soll die Aktivitätskonzentration in der Luft im Bereich der Vegetation nach der Diffusionstheorie berechnet werden, wird außerdem der turbulente Austauschkoeffizient innerhalb und oberhalb der Vegetation benötigt. Frühere Arbeiten /Bo 84/, /Ho 88/ ergaben, daß vor allem die Windgeschwindigkeit und der turbulente Austauschkoeffizient innerhalb der Vegetation nicht ausreichend bekannt sind. Aus diesem Grunde werden diese beiden Größen in der vorliegenden Arbeit näher untersucht.

2 Berechnung der Ablagerungsgeschwindigkeit

Werden an Aerosolteilchen gebundene radioaktive Stoffe durch turbulenten Austausch oder durch Sedimentation in Bodennähe oder in die Nähe der Vegetation gebracht, können sie dort abgeschieden werden. Die abgelagerte Aktivität pro Zeit- und Flächeneinheit ist proportional der Aktivitätskonzentration in der Vegetation. Da sie nur schwer angebbar ist, ist es üblich, die pro Zeiteinheit abgelagerte Aktivität auf die Aktivitätskonzentration in der Höhe 1 m oberhalb der Vegetation zu beziehen:

$$\dot{A} = C(z = 1\ m) \cdot v_d \tag{1}$$

Der Proportionalitätsfaktor hat die Dimension einer Geschwindigkeit und wird aus diesem Grunde Ablagerungsgeschwindigkeit genannt. Beträgt die Aktivitätskonzentration in der Höhe z innerhalb der Vegetation C(z), so ist die an der Vegetation pro Zeit und Flächeneinheit des Bodens abgelagerte Aktivität

$$\dot{A}_{Veg} = \int_0^h C(z) \cdot \bar{u}(z) \cdot E_{Veg}(z) \frac{F_{Veg}}{h} dz \tag{2}$$

$\bar{u}$: *Windgeschwindigkeit*

E_{Veg} : *Abscheidegrad für Aerosolteilchen oder Gase/Ho 88/*

F_{Veg} : *strömungsorthogonale Projektionsfläche pro Flächeneinheit des Bodens*

Mit der Aktivitätskonzentration in 1 m Höhe oberhalb der Vegetation und $\dot{A}_{Veg}$ nach Gleichung (2) kann $v_{d,Veg}$ für die Vegetation nach Gleichung (1) berechnet werden.

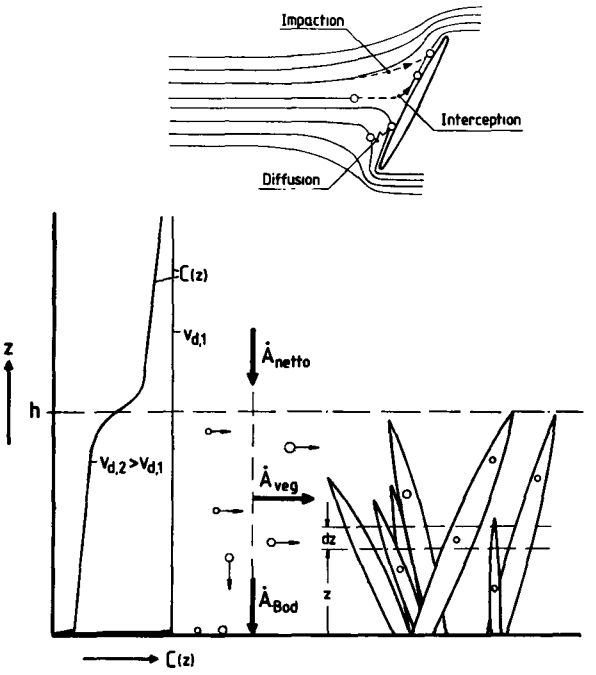

Abb. 1: Schematische Darstellung des Modells zur Berechnung der trockenen Ablagerung der an Aerosolteilchen gebundenen Aktivität

3 Aktivitätskonzentration in Höhe der Vegetation

Es gibt zwei Wege zur Berechnung der Aktivitätskonzentration in der Luft innerhalb und oberhalb der Vegetation, die Diffusionstheorie und die Monte–Carlo–Methode. In beiden Fällen wird angenommen, daß die Aerosolteilchen trägheitslos der Luftbewegung folgen.

3.1 Diffusionstheorie

Nach der Diffusionstheorie ergibt sich für die Bilanz an einem Volumenelement oberhalb der Vegetation

$$\frac{\partial C}{\partial t} = -\vec{v}\nabla C + \frac{\partial}{\partial x}K_x\frac{\partial C}{\partial x} + \frac{\partial}{\partial y}K_y\frac{\partial C}{\partial y} + \frac{\partial}{\partial z}\left[(K_z + D_{Br})\frac{\partial C}{\partial z} + C \cdot v_s\right] \qquad (3)$$

und innerhalb der Vegetation

$$\frac{\partial C}{\partial t} = -\vec{v}\nabla C + \frac{\partial}{\partial x}K_x\frac{\partial C}{\partial x} + \frac{\partial}{\partial y}K_y\frac{\partial C}{\partial y} + \frac{\partial}{\partial z}\left[(K_z + D_{Br})\frac{\partial C}{\partial z} + C \cdot v_s\right] - C \cdot \bar{u} \cdot E \cdot \frac{F_{Veg}}{h} \qquad (4)$$

Für die Berechnung der Ablagerungsgeschwindigkeit ist es ausreichend genau, den Transport der Teilchen einige Meter oberhalb der Vegetation und innerhalb der Vegetation eindimensional zu beschreiben. Der Nettoaktivitätsstrom durch turbulenten Transport, Brownsche Diffusion und Fallgeschwindigkeit ist dann in der Höhe z oberhalb der Vegetation

$$\dot{A}_{netto}(z) = \frac{\partial C(z)}{\partial z} \cdot [K_z(z) + D_{Br}] + C(z) \cdot v_s \qquad (5)$$

und innerhalb der Vegetation

$$\dot{A}_{netto}(z) = \frac{\partial C(z)}{\partial z} \cdot [K_z(z) + D_{Br}] + C(z) \cdot v_s - C(z) \cdot \bar{u}(z) \cdot E \cdot \frac{F_{Veg}}{h} \cdot dz \qquad (6)$$

In diesen Gleichungen ist K_z der turbulente Austauschkoeffizient, der in Analogie zur Brownschen Diffusion auch als turbulenter Diffusionskoeffizient bezeichnet werden kann. D_{Br} ist der Brownsche Diffusionskoeffizient und v_s die Fallgeschwindigkeit der Aerosolteilchen. Gleichung (6) enthält aufgrund der Abscheidung von Teilchen an der Vegetation einen Verlustterm wie in Gleichung (2).

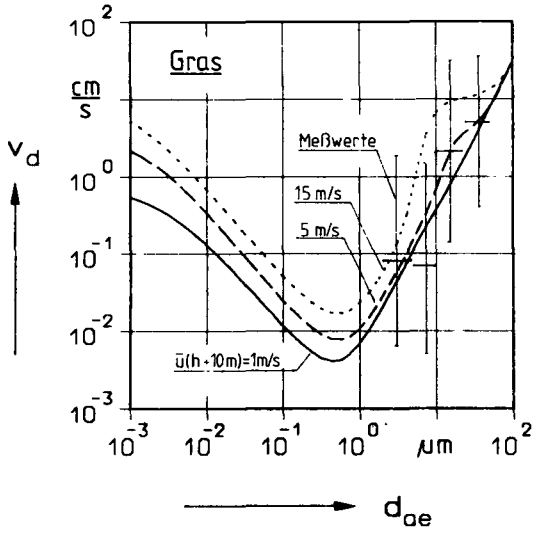

Abb. 2: Berechnete Ablagerungsgeschwindigkeit auf Gras als Funktion des aerodynamischen Teilchendurchmessers sowie Mittelwerte und Schwankungsbereich veröffentlichter Meßwerte /Ho 88/

Zur Berechnung von C(z) nach Gleichung (5) und (6) wurde ein FORTRAN-Rechenprogramm erstellt. Bei Angabe von K_z und $\bar{u}$ in Abhängigkeit von der Höhe, D_{Br} sowie E in Abhängigkeit von $\bar{u}$ kann C in der Höhe 1 m oberhalb der Vegetation und $\dot{A}_{Veg}$ nach Gleichung (2) berechnet werden. Die Ablagerungsgeschwindigkeit ergibt sich nach Gleichung (1) aus diesen beiden Größen. Abbildung 2 enthält einige Rechenergebnisse.

3.2 Die Monte–Carlo–Methode

Die Monte–Carlo–Methode ist ein zweiter Weg zur Berechnung der Aktivitätskonzentration innerhalb und oberhalb der Vegetation. Dabei geht man von der Modellvorstellung aus, daß an einem bestimmten festen Ort Teilchen in die Atmosphäre freigesetzt werden, deren Weg verfolgt wird. Die Bewegung wird durch einen dreidimensionalen Geschwindigkeitsvektor

$$\vec{v} = \bar{\vec{v}} + \vec{v'} \tag{7}$$

beschrieben, der sich aus dem advektiven Teil $\bar{\vec{v}}$ und einer fluktuierenden Größe $\vec{v'}$ zusammensetzt. Die Simulation des turbulenten Austausches geschieht dabei nur über den fluktuierenden Anteil des Geschwindigkeitsvektors. Für die Rechnung wird angenommen, daß dieser sich durch eine korrelierte und eine zufällige Komponente darstellen läßt.

$$\vec{v'}_{i(t)} = \vec{v'}_{i(t-\xi)} \cdot R_{i(\xi)} + v''_{i(t)} \quad (i = x, y, z) \tag{8}$$

Dabei ist der sogenannte Autokorrelationskoeffizient $R_{(\xi)}$, siehe Gleichung (14), ein Maß dafür, wie stark sich ein Teilchen an seine letzte turbulente Geschwindigkeit 'erinnert'. Eine Bestimmung des Autokorrelationskoeffizienten kann nur empirisch über umfangreiche Fluktuationsmessungen erfolgen. Der zufällige Anteil $\vec{v''}$ wird für jedes Teilchen zu jedem Zeitschritt mittels eines Zufallgenerators neu 'ausgewürfelt'. Über die Endpositionen der Teilchen nach einer bestimmten Ausbreitungszeit kann die Konzentration an jedem Ort angegeben werden. Die Abscheidung an der Vegetation wird auch bei Anwendung der Monte–Carlo–Methode mit Hilfe von Gleichung (2) berechnet.

Im Rahmen dieser Arbeit wurde ein FORTRAN–Rechenprogramm entwickelt, das eine Berechnung der Ablagerungsgeschwindigkeit gestattet. Dabei sollte nicht die atmosphärische Ausbreitung der Teilchen, sondern deren Weg in der Vegetation im Vordergrund stehen. Die ersten Ergebnisse waren recht erfolgreich.

4 Windgeschwindigkeit innerhalb und oberhalb des Bewuchses

4.1 Pflanzen

Die Windgeschwindigkeitsverteilung oberhalb der Vegetation wurde in zahlreichen Arbeiten gemessen. Die Messungen innerhalb der Vegetation erwiesen sich bei den theoretischen Arbeiten zur Ablagerungsgeschwindigkeit /Bo 83/, /Bo 84/, /Ho 88/ als nicht ausreichend. Aus diesem Grunde wurden die Windgeschwindigkeitsprofile innerhalb und oberhalb der Vegetation für Gras, Weizen–, Gerste– und Maisbestände detailliert gemessen. Die Meßeinrichtung, siehe Abbildung 3, bestand aus 3 NTC–Anemometern — zur Messung des Windprofils in und oberhalb des Bewuchses — und einem Schalenkreuzanemometer zur Messung der mittleren Windgeschwindigkeit in 5 m Höhe über dem Boden.

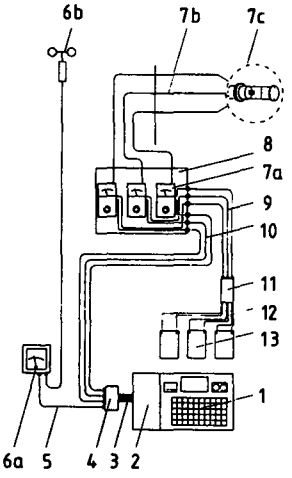

1	Rechner zur Datenerfassung
2	Analog/Digital-Wandler
3,4	Interface für die Anemometer
5	Signalleitung, Schalenkreuz
6 a,b	Schalenkreuzanemometer
7 a	NTC-Meßbrücke
7 b	NTC-Sondenträger
7 c	NTC-Anemometersonde (3 Stück)
8	Schutzgehäuse
9	NTC-Stromversorgungsleitungen
10	NTC-Signalleitungen
11-13	Stromversorgung

Abb. 3: Meßeinrichtung zur Windgeschwindigkeitsmessung /St 87/

Die so gefundenen Windgeschwindigkeitsprofile wurden durch eine logarithmische Funktion entsprechend der Theorie von Prandtl für adiabatische Schichtung

$$\bar{u}_{(z)} = \frac{u_*}{\kappa} ln \frac{z-d}{z_o} \tag{9}$$

angepaßt, siehe Abbildung 4.

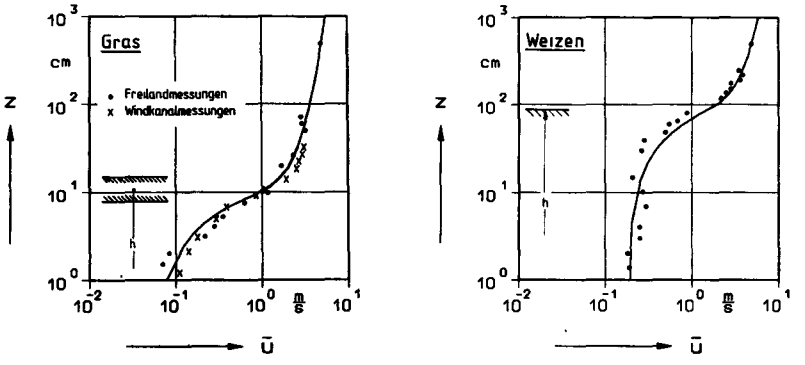

Abb. 4: Gemessene mittlere Windgeschwindigkeiten innerhalb und oberhalb von Gras und Weizen und Approximation nach Gleichung (9) und (10)

$$\bar{u}_{(z)} = \bar{u}_{(h)} exp[a(\frac{z}{h} - 1)] \tag{10}$$

Innerhalb der Vegetation läßt sich das Geschwindigkeitsprofil durch einen exponentiellen Ansatz, siehe /Ku 82/, annähern. Mit Hilfe der Messungen konnte der Pro-

filkoeffizient a, siehe Gleichung (10), ermittelt werden. Er ist in der Tabelle 1 für vier verschiedene Pflanzen und mittlere Windgeschwindigkeiten zusammengefaßt.

Vegetation	Nach Freilandversuchen ermittelte Parameter									Für die Modellrechnung abgeleitete Parameter		
	d/h und z_0/h bei verschiedenen Windgeschwindigkeiten in 5m Höhe											
	u=1,7m/s	2,3	2,5	3,0	3,3	4,0	5,0	6,0	a	d/h, z_0/h		a
Gras	d/h	0,00	0,30	0,00	0,30	0,00	0,30	0,30	0,30	2,3	d/h*	0,68	2,687
h=8-15cm	z_0/h		0,20		0,20		0,20	0,13	0,10		z_0/h*	0,10	
Weizen	d/h	0,75		0,75		0,75	0,70	0,70	0,65	2,0	d/h	0,65	2,191
h=90cm	z_0/h	0,05		0,10		0,10	0,10	0,10	0,15		z_0/h	0,095	
Gerste	d/h	0,75		0,70		0,70	0,70	0,60	0,55	2,4	d/h	0,57	2,506
h=100cm	z_0/h	0,07		0,10		0,10	0,10	0,17	0,25		z_0/h	0,17	
Mais	d/h		0,70		0,70		0,70	0,70	0,70	2,6	d/h	0,70	2,522
h=200cm	z_0/h		0,05		0,05		0,05	0,06	0,07		z_0/h	0,08	

*: h in der Modellrechnung = 10 cm

Tab. 1: Nach Freilandversuchen ermittelte und für Ablagerungsrechnungen abgeleitete Parameter

4.2 Baumbestand

Zur Berechnung der Ablagerungsgeschwindigkeit für Baumbestand wird gegenwärtig mit der gleichen Meßeinrichtung wie in Abbildung 3 die Windgeschwindigkeit in lockerem Baumbestand gemessen. Die Höhe der Laubbäume beträgt etwa 8 m. Als Bezugsgeschwindigkeit wird die in 10 m Höhe über dem Boden gewählt. Durch umfangreiche Messungen über die Höhe des Baumstammes und in den unteren Kronenbereich hinein konnte der Windgeschwindigkeitsverlauf bezogen auf die Windgeschwindigkeit in 10 m Höhe über dem Boden ermittelt werden. Es wurde eine Approximationsfunktion aus den Meßergebnissen abgeleitet. Die Messungen sollen in diesem Jahr auf den Kronenbereich zur Berechnung der Ablagerungsgeschwindigkeit in lockerem Baumbestand fortgesetzt werden.

4.3 Windkanal

Parallel zu den Freilandmessungen wurden Messungen in Modellgras bestehend aus Messingstreifen durchgeführt. Die Meßstrecke hat einen Querschnitt von etwa 0,4 m x 0,4 m und ist 2,8 m lang. In dem Windkanal sollen Ablagerungsmessungen bei reproduzierbaren Randbedingungen durchgeführt werden. Als Aerosolteilchen werden fluoreszierende Latexpartikel verwendet. Die Windgeschwindigkeit innerhalb und oberhalb des Modellgrases wurde mit einer Hitzdrahtsonde gemessen. Die hierbei gefundenen Meßergebnisse sind in Abbildung 4 links zusammen mit den Freilandergebnissen eingezeichnet.

5 Messungen mit dem 3–Draht–Anemometersystem

Zur Bestimmung des turbulenten Austauschkoeffizienten K_i (i = x, y, z) ist die Kenntnis der Windgeschwindigkeitsfluktuation v'$_i$ notwendig. Es ist möglich über die turbulente Energie den Austauschkoeffizienten K_i für homogene, stationäre Turbulenz /Br 78/ zu bestimmen /La 83/:

$$K_i = \overline{(v_i')^2} \cdot T_i^L \tag{11}$$

T_i^L, die sogenannte Langrange–Zeit, ist definiert als das Integral über die Autokorrelationsfunktion:

$$T_i^L := \int_0^\infty R_{i(\xi)} d\xi \tag{12}$$

mit

$$R_{i(\xi)} = \frac{\overline{v_i'(x_0, t_0) \cdot v_i'(x_1, t_1)}}{\overline{(v_i'(x_0, t_0))^2}} \qquad und \quad \xi = t_1 - t_0 \tag{13}$$

Eine ausführliche Ableitung findet sich in /Mo 71/.

Zur Messung der turbulenten Geschwindigkeitsanteile des Windfeldes werden Systeme benötigt, die einerseits eine geringe Trägheit besitzen, d.h. in der Lage sind, auch hohe Frequenzen darstellen zu können, und andererseits geringe Abmessungen aufweisen, um eine hohe örtliche Auflösung zu erreichen (kleines Meßvolumen). Deshalb wurde ein Meßsystem mit einer triaxialen Hitzfilmanemometersonde aufgebaut, siehe Abbildung 5. Die höchsten damit noch auflösbaren Frequenzen betragen etwa 30 kHz.

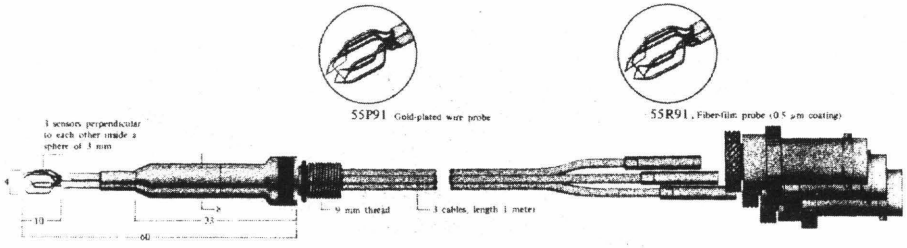

Abb. 5: Darstellung der 3–Draht–Sonde

Im Betrieb werden die Drähte auf eine konstante Temperatur aufgeheizt. Das Ausgangssignal der Sonde durchläuft einen Meßverstärker, an den sich ein Linearisator anschließt, der für jeden Sondendraht einzeln abgestimmt werden muß. Für die vorliegenden Versuchsbedingungen wurde der Linearisator an einen Meßbereich von 0,2 m/s bis 5 m/s Windgeschwindigkeit angepaßt. Das linearisierte analoge Signal wurde über einen Analog–Digital–Wandler von einem 8–bit Z80–Computer aufgenommen und gespeichert. Hierzu wurde ein Assembler–Programm zur schnellen Datenaufnahme entwickelt, um die von der Sonde gelieferten, hohen Meßfrequenzen ausnutzen zu können.

Dabei stellte sich allerdings das Problem, das dieser ältere Computertyp zwar in der Lage war, die enormen Datenmengen aufzunehmen, aber nicht mehr speichertechnisch oder rechnerisch in sinnvollen Zeiträumen zu bearbeiten. Aus diesem Grunde wurde ein neues System angeschafft, mit dem die Messungen auch im Freien leichter durchgeführt werden können.

Abb. 6: Flußdiagramm der Meßstrecke

Durch einen Abgleich der Meßstrecke mußte vor Einsatz der Sonde der funktionale Zusammenhang zwischen effektiver Kühlgeschwindigkeit und Linearisatorausgangsspannung ermittelt werden.

Ein weiterer wichtiger Schritt war die geometrische Kalibrierung der Sonde, d.h. die Bestimmung der Richtungsabhängigkeit der effektiven Kühlgeschwindigkeit vom momentanen Geschwindigkeitsvektor. v_{eff} wird aus den in Abbildung 7 dargestellten Komponenten berechnet zu:

$$v_{eff,i}^2 = v_{n,i}^2 + k_i^2 \cdot v_{t,i}^2 + h_i^2 \cdot v_{b,i}^2 \qquad (14)$$

$v_{n,i}$ = *Hauptnormalkomponente der Anströmgeschwindigkeit für den Sensor i*

$v_{t,i}$ = *Tangentialkomponente der Anströmgeschwindigkeit für den Sensor i*

$v_{b,i}$ = *Binormalkomponente der Anströmgeschwindigkeit für den Sensor i*

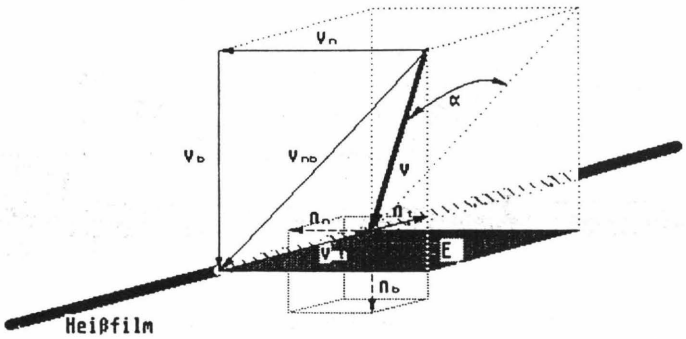

Abb. 7: Geschwindigkeitskomponenten am Heißfilm

Die Empfindlichkeitskoeffizienten für den Sensor i, k_i und h_i, wurden über die Methode des kleinsten Fehlerquadratminimums bestimmt. Hierzu wurde die effektive Kühlgeschwindigkeit im ersten Schritt unter Vorgabe von k_i und h_i berechnet. Im zweiten Schritt wird sie bei gleicher Vorgabe der Empfindlichkeitskoeffizienten gemessen, wobei das Ziel war, die optimalen k_i und h_i für bestimmte Anströmungen der Sonde zu finden /Ob 87/.

Sowohl für die Kalibrierung als auch für die endgültige Bestimmung des Geschwindigkeitsvektors aus den Linearisatorausgangssignalen wurden FORTRAN–Programme erstellt. Bei Testläufen zeigte sich, daß bei der Bestimmung des Windgeschwindigkeitsvektors noch numerische Probleme existieren, die in der eindeutigen Bestimmung des absoluten Fehlerquadratminimums liegen. Da hier von dem eingesetzten Programm mehrere lokale Minima gefunden wurden, war die Zuordnung einer bestimmten Richtung und Geschwindigkeit bisher nicht möglich. Dieses Problem wird im Augenblick bearbeitet.

Kurz nach Abschluß der Kalibrierung trat ein Defekt an der Sonde auf, der eine längere Reparaturzeit zur Folge hatte. Nach der Reparatur mußte der gesamte Kalibriervorgang wiederholt werden. Aus diesem Grunde konnten die Messungen mit der 3–Draht–Sonde lange Zeit nicht durchgeführt werden. Erst in den letzten Wochen konnten Messungen, unterstützt durch ein neues Computersystem, durchgeführt werden. Aufgrund der Probleme mit der Meßwertverarbeitung konnten die Austauschkoeffizienten in der Vegetation bisher nicht bestimmt werden. Die erstellte Einrichtung ist nun aber so weit entwickelt, daß im Sommer Meßungen durchgeführt werden können.

6 Literaturverzeichnis

/Ac 78/ Acrivlellis, M.
Auswertung von Hitzdrahtmessungen mehrdimensionaler Strömungen beliebiger Turbulenzintensität
Strömungsmechanik und Strömungsmaschinen, 25/78

/Bo 83/ Bonka, H.; Horn, M.
Review on the dry and wet deposition of aerosol particles
Proceedings, CEC Seminar on The Transfer of Radioactive Materials in the Terrestrial Environment Subsequent to an Accidental Release to Atmosphere, Dublin, 11.-15.4.1983
CEC, Luxemburg, V/3004/83-EN,FR,DE, 1983

/Bo 84/ Bonka,H; Horn, M.; Horn, H.-G.; Küppers, J.; Hattingen, Th.; Maqua, M.
Zum Transport von an Aerosolteilchen gebundenen Radionukliden in die Vegetation nach Emission aus kerntechnischen Anlagen
Forschungsbericht an den Bundsminister des Innern, Aachen, 1984

/Br 78/ Bradshaw, P.
Introduction
aus: Turbulence, Editor: Bradshaw, Topics in Applied Physics 12
Springer Verlag, Berlin, Heidelberg, 1978

/Ho 88/ Horn, H.-G.; Maqua, M.; Bonka, H.
Nasse und trockene Ablagerung radioaktiver Stoffe auf die Vegetation und den Erdboden
Deutsche Bibliothek, BMU–1988–195, 1988

/Ku 82/ Kurata, K.
Theoretische Untersuchung der Turbulenz innerhalb eines Pflanzenbestandes
Berichte des Instituts für Meteorologie und Klimatologie der Universität Hannover, ISSN 0440–2820, Hannover 1982

/La 83/ Lautenschlager, M.
Parametrisierung der turbulenten Diffusion in der Atmosphäre unter Benutzung der turbulenten Energiegleichung(en)
GKSS–Forschungszentrum Geesthacht GmbH, Geesthacht 1983

/Mo 71/ Monin, A.S.; Yaglom, A.M.
Statistical Fluid Mechanics
Vol. 1+2, MIT Press, 1971

/Ob 87/ Oberschachtsiek, D.
Zur Untersuchung turbulenter Strömungsfelder im Hinblick auf die Berechnung des Transports von radioaktiven Aerosolen
Diplomarbeit, Lehrgebiet Strahlenschutz in der Kerntechnik, RWTH-Aachen, 1987

/St 87/ Struth, St.
Windmessungen in und oberhalb verschiedener Vegetationarten: Vergleich von gemessenen Windprofilen mit berechneten Profilansätzen
Studienarbeit, Lehrgebiet Strahlenschutz in der Kerntechnik, RWTH-Aachen, 1987

IV. Other research group(s) collaborating actively on this project [name(s) and address(es)]:

V. Publications:

Horn, H.-G.; Maqua, M.; Bonka, H.
Nasse und trockene Ablagerung radioaktiver Stoffe auf die Vegetation und den Erdboden
Deutsche Bibliothek, BMU-1988-195, 1988

RADIATION PROTECTION PROGRAMME
Final Report

Contractor: Contract no.: BI6-B-041-D

Niedersächsisches Institut
für Radioökologie
Herrenhäuser Strasse 2
D-3000 Hannover 21

Head(s) of research team(s) [name(s) and address(es)]:

Dr. C. Bunnenberg
Niedersächsisches Institut
für Radioökologie
Herrenhäuser Strasse 2
D-3000 Hannover 21

Telephone number: 762.26.05

Title of the research contract:

Transfer of radionuclides in the food chain.

List of projects:

1.Dynamic environmental cycling of HTO/HT/OBT (experimental studies and modelling).
2. Accumulation and long-term transfer of iodine-129 in the food chain, in human thyroid glands and in waters of waste deposits.

Title of the project no.: 1

Dynamic environmental cycling or HTO/HT/OBT
(Experimental studies and modelling)

A: HTO transfer in the atmosphere-soil system;
B: HT deposition, conversion and reemission as HTO.

Head(s) of project:

Dr. C. Bunnenberg

Scientific staff:

Dr.C.Bunnenberg
Dr.J.Feinhals (until Sept.88)
B.Wiener (until Apr.88)
M. Täschner (starting Feb.87)
K. Schubert (starting Apr.89)

I. Objectives of the project:

A. Transfer of HTO from atmosphere to soil under consideration of atmospheric and soil physical parameters affecting the deposition of HTO by condensation and molecular exchange. Investigations on exchange processes and isotopic effects during diffusion of HTO and H_2O on soils with regard to tritium accumulation in soil.

B. Studies on the physical conditions influencing the deposition velocity of HT on soils and conversion to HTO and OBT. Reemission of HTO from soils after HT-releases from nuclear facilities. Development of a mathematical model describing the cycling of tritium in the atmosphere-soil system.

II. Objectives for the reporting period:

A. Laboratory experiments to complete the parameterization of HTO deposition towards a mathematical model. Analysis and description of HTO profiles in soil as a result of deposition processes.

B. Laboratory experiments with the soil column/wind tunnel set-up to determine the effects of meteorological and soil physical parameters on HTO reemission rates.

III. Progress achieved:
Introduction

In view of the increasing rates of tritium production and emission from fission and reprocessing facilities but especially of those expected from experimental fusion reactors and tritium handling plants, five European Laboratories experienced in tritium research have joined in a coordinated tritium project on the "Dynamic Environmental Cycling of HTO/HT/OBT" to study and model tritium behaviour in the environmental compartments from atmospheric releases of HT and HTO to its organic and inorganic appearance in plant and animal products meant for human consumption. The aim of the research is to parameterize and model environmental tritium processes, in order to feed a complete computer code on tritium burden to man from HT and HTO emissions.

In the frame of this joint project NIR concentrated on two subtopics:

A. HTO transfer in the atmosphere-soil system

B. HT deposition, conversion and reemission as HTO.

The investigations were carried out in laboratory experiments under controlled conditions to evaluate the effects of single parameters. The laboratory findings could be verified and extended and the mathematical models could be validated through the participation in the two HT field experiments performed in France [Dje 88] and Canada [Bur 88].

A. HTO transfer in the atmosphere - soil system

1. Methodology

On the basis of preceding investigations, the transfer of HTO from atmosphere to soil by vapour exchange or condensa-

tion was found to be an effective process for soil contamination after atmospheric releases of HTO. In order to quantify and parameterize this mechanism as to its contribution to the tritium burden of the downwind sector of an HTO source, a great number of soil column experiments with attached model atmospheres were performed simulating different soil physical and meteorological conditions in a controlled, successive manner. After exposure to HTO-labeled air, the soil columns were disassembled in single layers, to evaluate total deposits and single-layer contents of HTO and H_2O.

Two approaches were followed to model HTO transfer from air to soil:

1) Correlation of the HTO deposit B_{HTO} [$Bq \cdot m^{-2}$] to the total vapour deposit N [$kg \cdot m^{-2}$] by defining the "specific activity ratio" k:

$$k = \frac{B_{HTO}}{N \cdot C^a_{HTO}}, \qquad (1)$$

which is the ratio between the specific activity of the vapour deposit B_{HTO}/N [$Bq \cdot kg^{-1}$] and that of the air humidity C^a_{HTO} [$Bq \cdot kg^{-1}$]. This procedure is applicable for mean estimates of HTO deposition, when H_2O condensation rates are available and k can be derived from local meteorological measurements.

2) Application of the "deposition velocity" concept, which states that the deposition velocity of HTO, v_{HTO} [$m \cdot s^{-1}$], is correlated to the HTO concentration gradient at the air-soil interface, dC_{HTO} / dz [$Bq \cdot m^{-4}$]:

$$v_{HTO} \sim \frac{dC_{HTO}}{dz} \qquad (2)$$

This procedure is suggested, when momentary deposition rates are needed, eg, in case of an accidental release.

Consequently, the laboratory experiments were evaluated to find dependencies of k in Equ.(1) and of the proportionality factors in Equ.(2) on easily accessible environmental parameters, in order to develop an HTO deposition model for incorporation into tritium dose computer codes.

2. Results

Laboratory and field experiments showed that the HTO/H_2O ratio of the vapour deposit may be higher than that of the atmospheric humidity, which is in agreement with the theoretical understanding of gas transport between two compartments. For originally tritium-free soils values up to k=8 were found, depending on soil moisture and soil type. Detailed analyses yield a simple approximation equation for k:

$$k \approx \frac{m^a}{m^a - m^s} \quad , \tag{3}$$

where m^a [wt.%] is the soil moisture at the beginning of the deposition process and m^s [wt.%] is the soil moisture that would be in equilibrium with the air humidity. It was found that k remains constant during a deposition process with steady HTO resupply (continuous release), as all environmental parameters act on HTO and H_2O deposition in the same way.

Evaluation of the soil column experiments with respect to the deposition velocity concept and incorporation of relationships derived from wind tunnel experiments give a full description of the HTO deposition velocity:

$$v_{HTO} = - \frac{D_{HTO}}{C_{HTO}} \cdot \frac{dC_{HTO}}{dz} \cdot \sqrt{\frac{a+u}{u_1}} \tag{4}$$

with the effective HTO diffusion coefficient in soil D_{HTO} [$m^2 \cdot s^{-1}$], the linear diffusion velocity in air, $a=1.5 \cdot 10^{-3}$ $m \cdot s^{-1}$, the windspeed u [$m \cdot s^{-1}$] and the normalized windspeed,

$u_1 = 1 m \cdot s^{-1}$. For a particular deposition process under constant environmental conditions the HTO deposition velocity decreases with time t proportionally to $1/\sqrt{t}$, which is due to the decrease of the concentration gradient during deposition.

The two HTO deposition concepts have been proved consistent, expressed by the validated relation:

$$v_{HTO} = k \cdot v_{H_2O} \qquad (5)$$

It was also clarified that the higher specific activity of the vapour deposit relative to that of the atmospheric humidity, ie, $k > 1$, is not the consequence of an isotopic effect but the result of molecular exchange between two compartments. Therefore, it can not be called accumulation in the strict sense.

The final objective of HTO deposition investigations refers to the evaluation and mathematical description of HTO profiles in soils exposed to an HTO plume. With the boundary conditions of originally uncontaminated, relatively dry soil and steady resupply of HTO by air movement Fick's second law can be solved by an error function, describing the HTO concentration in soil, C^s_{HTO} [$Bq \cdot kg^{-1}$], at any depth z [m] and time t [s]:

$$C^s_{HTO}(z,t) = C^s_{HTO}(z=0) \cdot erfc\left(\frac{z}{2 \cdot \sqrt{D_{HTO} \cdot t}} \right) \qquad (6)$$

with $$erfc\left(\frac{z}{2 \cdot \sqrt{D_{HTO} \cdot t}} \right) = 1 - \frac{2}{\pi} \cdot \int_0^{z/(2 \cdot \sqrt{D_{HTO} \cdot t})} \exp(-t'^2) \cdot dt'.$$

Validation of the theoretical approach of Equ.(6) by the experimental data is demonstrated in Fig. 1 for different exposure times.

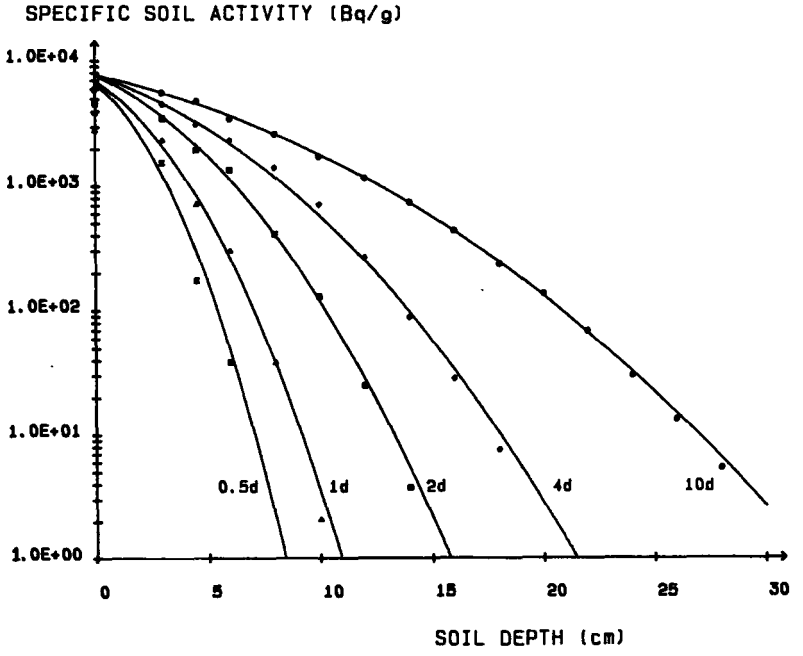

Fig.1: Experimental and respective theoretical HTO profiles in loess soil as a result of different exposure times to air-HTO.

3. Discussion

Successive investigations on single-parameter effects on HTO deposition to soil have provided a full understanding and mathematical modelling of the process itself and the resulting HTO profiles in soil on the basis of environmental input data. The specific activity ratio and the deposition velocity approaches have been found consistent, so that either model can be applied according to the input data available or to the HTO release situation under consideration.

The mathematical descriptions have been combined into a computer sub-code, which can be integrated into dynamic tritium dose codes to improve predictions on tritium burden from HTO emissions by including the HTO dry deposition pathway air-soil.

B: HT deposition, conversion and reemission as HTO

1. Methodology

Emissions of elementary tritium (eg, HT) are mainly expected from fusion reactors and associated tritium handling facilities. Common modelling practice to assume those emissions totally as HTO greatly misestimates radiation burden, as HT is about 10^4 times less radiotoxic than HTO, and transport mechanisms of the two chemical forms in the ecosphere differ greatly. Therefore, laboratory experiments with soil columns exposed to HT-labelled air and HT field releases have been performed to investigate the fate of HT in the environment. Main objectives were the HT deposition to soil and its conversion to HTO and organically bound tritium (OBT) by biochemical reactions within the soil matrix and its subsequent reemission as HTO from the soil back to the atmosphere.

For modelling, an HT deposition velocity v_{HT} [$m \cdot s^{-1}$] is defined, correlating the time-integrated HT concentration in air, $\bar{C}_{HT}$ [$Bq \cdot s \cdot m^{-3}$], to the tritium deposition B [$Bq \cdot m^{-2}$] during integration time:

$$B = v_{HT} \cdot \bar{C}_{HT} \qquad (7)$$

This formulation merges HT transport from reference height to soil, diffusion into soil and biochemical conversion into the one quantity v_{HT}, which hides the complexity of the processes occurring, but eases experimental determination and mathematical description.

A simple approach to describe the apparent reemission of HTO is based on the assumption of an exponential decrease of soil-HTO with time:

$$B(t) = B(t_0) \cdot \exp[-r \cdot (t-t_0)] \qquad (8)$$

The emission rate r [s^{-1} or $\%\cdot h^{-1}$] represents the net HTO loss rate, which is approximately the fraction of the momentary soil-HTO lost per hour. Unlike v_{HT}, r is expected to depend on windspeed. Therefore, a wind-tunnel has been installed for additional laboratory experiments with tritium labelled soil columns.

2. Results

HT deposition experiments with soil columns have demonstrated a characteristic dependency of v_{HT} on soil pore volume and moisture content with maximum values in the middle range [Bun 86]. At lower moisture contents the biological vitality for tritium conversion and hence v_{HT} is reduced, while at high moisture contents the reduction results from limited HT and oxygen diffusivity in the soil. This dependency could be verified by exposing soil columns to the HT plume in the French field experiment.

HT deposition velocity evaluations with natural soils in the HT field experiments yielded values ranging from $1.7\cdot10^{-4}$ to $2.7\cdot10^{-4}$ $m\cdot s^{-1}$ (France) and from $0.8\cdot10^{-4}$ to $7.1\cdot10^{-4}$ $m\cdot s^{-1}$ (Canada), the greater range in Canada resulting from differing soil types across the experimental area. It was also found that with freshly disturbed soil v_{HT} may be lower by more than one order of magnitude. This effect is attributed to the fact that soil disturbance upsets the established microbiological profile transferring less efficient HT oxidizing bacteria populations to the top soil layers responsible for HT conversion.

Because of higher diffusivity of HT compared to HTO in soils, HT deposition leads to deeper tritium penetration and hence improved availability to plant roots. For soils homogeneous with respect to pore volume and HT oxidizing ability a

profile of soil-HTO, C^b_{HTO} [Bq·m^{-3}], is expected, which decreases exponentially with depth z [cm]. This was verified by soil columns exposed to the HT plume in the French experiment, as shown in Fig. 2. Deviations from the theoretical curves in the top layers result from the fact that the soil had dried out between exposure and arrival of the plume. As this is generally the case during daytime, maximum HTO contents occur in a deeper layer under natural conditions.

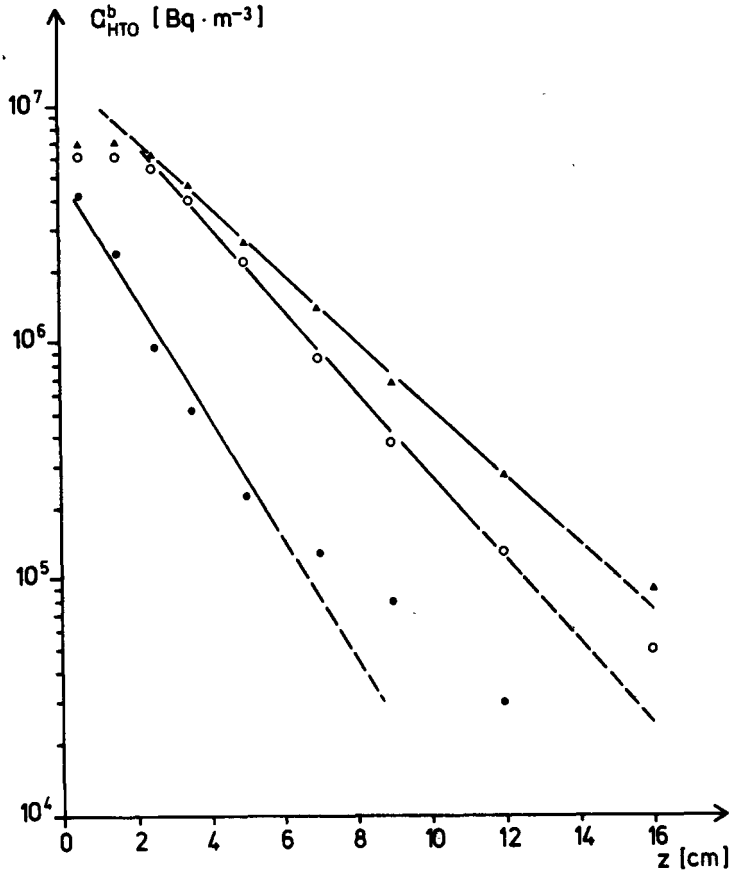

Fig. 2: Semi-log plots of soil-HTO profiles in the homogenized loess soil columns exposed to a short-duration HT plume. Curves from left to right with increasing pore volume, ie, decreasing soil moisture.

The soil-OBT fraction found from short-term HT deposition was always below 1 % of the activity applied. Unlike HTO, OBT does not participate in diffusion or reemission processes.

The complexity of the HTO reemission from soils back to the atmosphere was demonstrated by measurements during the two HT field releases and preliminary wind-tunnel experiments. While long-term evaluations in the order of weeks verified the exponential decrease of soil-HTO according to Eq. (8) with a reemission rate of 1 $\%\cdot h^{-1}$ or less under steady weather conditions, analyses on an hourly basis showed values up to more than 10 $\%\cdot h^{-1}$ with characteristic fluctuations of high values during daytime and low rates at night. Low windspeeds, high air-HTO contents, dew formation and rain events could be identified as important factors suppressing reemission. The wind tunnel experiments showed the great influence of the shape of the soil-HTO profile on reemission rates. It was also found that reemitted HTO can be redeposited to soil, when it is carried over less contaminated surfaces, and reemission and redeposition may even occur simultaneously depending on the momentary soil-HTO content giving rise to concentration gradients to the ground level air directed upwards or downwards, respectively.

3. Discussion

Soil column, field release and preliminary wind tunnel experiments contributed significant information to the understanding of HT deposition to soils, biochemical conversion and reemission as HTO and to the modelling of these processes. However there is still a lack of proven formulae to describe HTO reemission from soil back to the atmosphere on the basis of meteorological and soil physical parameters. The reemission rate is a key quantity especially with respect to inhalation doses immediately after accidental HT emissions, as the main

dose contribution arises from the HTO reemission plume originating from the surface of the deposition sector of the primary HT plume. Therefore, the detailed investigations on the parameterization of reemission will be continued with soil columns attached to a wind tunnel, which is capable of simulating all environmental parameters found to affect this process. This investigation will be performed under Contract No. BI6*/0345-D(AM) in 1990/91.

In view of the development of fusion and associated tritium handling technologies, it is an important task, but also a unique opportunity of radiation protection, to improve the knowledge on tritium behaviour in the environment with respect to dose consequences of HT and HTO emissions before the first reactor goes into operation, as radiation protection aspects can be recognized in the facility design, establishing a high degree of passive safety.

References

[Dje 88] Djerassi, H., Lesigne, B., (Eds.):
Environmental Tritium Behaviour - French Experiment.
Report for NET Contract No. 85-07 GSA (1988).

[Bur 88] Burnham, C.D., Brown, R.M., Ogram, G.L., Spencer, F.S. :
An Overview of Experiments at Chalk River on HT Dispersion in the Environment.
Fusion Technol. 14, 2, Part 2 B (1988).

[Bun 86] Bunnenberg, C., Feinhals, J., Wiener, B.:
Differences in the Behaviour of HTO and H_2O in Soil after Condensation from Atmosphere and Conversion of HT to HTO and OBT in Soil Relative to Moisture Content and Pore Volume.
Rad. Prot. Dos. 16 (1986).

IV. Other research group(s) collaborating actively on this project [name(s) and address(es)]:

Y. Belot, CEA/CEN Cadarache, France
H. Förstel, KFA Jülich, FRG
R. Kirchmann, C. Vandecasteele, CEN/SCK Mol, Belgium
J. van den Hoek, LBU Wageningen, The Netherlands

HT Field Experiments:

R. Brown, AECL Chalk River, Canada
S. Diabate, KfK Karlsruhe, FRG
O. Edlund, Studsvik Nuclear, Sweden
H. Nogushi, JAERI Tokai Mura, Japan
G. Ogram, F. Spencer, Ontario Hydro Toronto, Canada

V. Publications:

Journals

1. Bunnenberg, C., Feinhals, J., Wiener, B.:
Differences in the Behaviour of HTO and H_2O in Soil after Condensation from the Atmosphere and Conversion of HT to HTO and OBT in Soil Relative to Moisture Content and Pore Volume.
Rad. Prot. Dos. 16 (1986) 83-87

2. Feinhals, J., Bunnenberg, C.:
Laboratory Investigations of HTO Deposition to Soils.
Fusion Technol. 14 No. 2, Part 2B (1988) 1253-1257

3. Täschner, M., Wiener, B., Bunnenberg, C.:
HT Dispersion and Deposition in Soil after Experimental Releases of Tritiated Hydrogen.
Fusion Technol. 14 No. 2, Part 2B (1988) 1264-1269

4. Wiener, B., Täschner, M., Bunnenberg, C.:
HTO Reemission from Soil after HT Deposition and Dose Consequences.
Fusion Technol. 14 No. 2, Part 2B (1988) 1247-1253

5. Täschner, M., Bunnenberg, C.:
Plume Dispersion and Deposition Processes of Tracer Gas and Aerosols in Short-Distance Field Experiments.
Proc. IV. Int. Symp. on "The Impact of Nuclear Origin Accidents on Environment", Cadarache, Vol. 1 (1988).

Theses, Internal Reports

1. Wiener, B.:
Untersuchung zur Umsetzung von HT nach Emission aus kerntechnischen Anlagen.
M. Thesis, University of Hannover (1985).

2. Feinhals, J.:
HTO-Deposition durch Gasaustausch im System Atmosphäre-Boden.
Ph.D. Thesis, University of Hannover (1988).

3. Bunnenberg, C., Wiener, B., Täschner, M.:
NIR-Results of the French HT Field Experiment.
In: Environmental Tritium Behaviour - French Experiment.
Djerassi, H., Lesigne, B. (Eds.), CEA Report for NET Contract No. 85-07 GSA (1988).

4. Wiener, B., Täschner, M., Bunnenberg, C.:
NIR-Results of the Canadian HT Field Experiment. Appendix to: Ogram, G.L: The Canadian HT Dispersion Experiment at Chalk River - June 1987.
Summary Report CFFTP-G-88027 (1988).

5. Täschner, M., Bunnenberg, C., Edlund, O., Gulden, W.:
Maximum Permissible Amount of Accidentally Released HT Derived from the 1986 French Experiment to Meet Dose Limits for Public Exposure.
Report to ITER, No. ITER-IL-SA-4-9-79 (1989).

6.- 17. Bunnenberg, C., Feinhals, J., Schubert, K., Täschner, M., Wiener, B.:
In: "Annual Reports of the Lower Saxony Institute for Radioecology".
NIR Reports 1984/ 85/ 86/ 87/ 88/ 89.

Title of the project no.: 2

Accumulation and long-term transfer of iodine-129 in the food chain, in human thyroid glands and in waters of waste deposits.

Head(s) of project:

Dr. J. Handl

Scientific staff:

Dr. J. Handl
Dr. D. Jakob

I. Objectives of the project:

Investigations on the long-term translocation of I-129 in soils, its transfer from soil to plant and along the food chain: pasture-cow-milk-thyroid gland.

Inventory of I-129 and I-127 in human thyroids to examine the long-term development of the isotopic ratio I-129/I-127 in the food chain. Studies on I-129 and I-127 contents in waters of selected areas. Extensive balance analyses of I-127 in its natural circulation (rain, surface and groundwaters) and in special isolated areas (salt formations). Investigations on the effects of enhanced I-127 concentrations from natural or man-made sources on the accumulation of I-129.

II. Objectives for the reporting period:

Investigations on the translocation of I-129 in the soil of three experimental areas and transfer to plants.

Investigations on water samples of different origin to examine the dependency of I-129 concentrations on I-127 contents.

Inventory of I-129 and I-127 in human and animal thyroids especially with regard to areas strongly contaminated with the Chernobyl-fallout.

III. Progress achieved:

Introduction

The natural production of iodine-129, mainly by spontaneous fission of uranium and by cosmic ray interactions with xenon, and its extremely long half-life of $1.6 \cdot 10^7$ y has led to the pre-atomic I-129/I-127 ratio level of about 10^{-13}. Due to nuclear weapons testing and releases of I-129 from reprocessing plants and fuel storage facilities the isotopic ratio has increased to a present value of about 10^{-8}. In view of expected further increases of this level and the fact that iodine is accumulated in thyroid glands, it is considered very important:

1. to monitor I-129 levels in environmental compartments relevant for human exposure and in thyroid glands as natural iodine collectors and
2. to investigate the environmental behaviour of I-129 with respect to its transfer into and along the food chain to man.

It is the aim to closely follow the development of environmental levels of I-129 for prediction purposes and to identify processes relevant for radiation burden. Because of the long half-life the investigations have to be designed and performed on a long-term basis, to improve estimation accuracy for future situations.

In this frame of tasks four sub-topics have been treated during the contract period concerning I-129 inventory in thyroids, long-term translocation in soils, transfer to vegetation and along the food-chain as well as levels around potential deposit sites.

A. Inventory of I-129 in human and animal thyroids

1. Methodology

In order to monitor background levels of iodine-129, human thyroid glands have been collected in different areas without nuclear facilities in Lower Saxony (FRG) since 1979, and they have been investigated for I-129 and I-127 contents. Thyroids were removed during autopsy from selected individuals, who had not suffered from thyroid deseases nor had received any respective therapy. To determine I-129 and I-127 contents, whole organs have been processed for analysis.

2. Results and discussion

Values of the I-129 concentrations in human thyroids analyzed between 1979 and 1984 ranged from 8 to 137 $\mu Bq \cdot g^{-1}$ f.w. corresponding to I-129/I-127 atom ratios between $8 \cdot 10^{-9}$ and $2.5 \cdot 10^{-8}$ [1,2]. Human thyroids taken during the first three years following the reactor accident in Chernobyl exhibit concentrations of I-129 between 16 and 92 $\mu Bq \cdot g^{-1}$ f.w., and they show no significant differences in comparison with the ones of the pre-accident period. In order to determine the I-129 levels in thyroids from areas strongly contaminated with the Chernobyl fallout, five thyroids taken from reindeers in the Wilhelmina area (Sweden) were examined for I-129 content (Table 1). This area belongs to the most seriously contaminated regions outside the USSR. The organs show I-129/I-127 ratios more than one order of magnitude higher than the present worldwide I-129/I-127 level of about 10^{-8}. As a possible origin of the observed increase of the I-129 level the influence of some other fallouts (eg, the long-term radioactive pollution produced by the reprocessing plant Sellafield) should be, indeed, taken into account.

Table 1: Iodine-129 in reindeer thyroid glands taken from the Wilhelmina area (Sweden) in 1988

Fresh weight [g]	I-127 concentration [mg·g^{-1} f.w.]	I-129 concentration [mBq·g^{-1} f.w.]	I-129/I-127 atom ratio
4.5	3.0 ± 0.3	3.9 ± 0.6	(2.2 ± 0.3)·10^{-7}
4.0	1.3 ± 0.1	3.1 ± 0.3	(3.9 ± 0.5)·10^{-7}
1.5	0.9 ± 0.1	1.9 ± 0.2	(3.7 ± 0.4)·10^{-7}
3.8	3.2 ± 0.6	7 ± 1	(3.8 ± 0.6)·10^{-7}
4.0	2.3 ± 0.2	5.4 ± 0.6	(3.9 ± 0.4)·10^{-7}

In order to obtain information concerning the I-129 accumulation on the southern hemisphere human and bovine thyroids were collected in the Valdivia area (Chile) during 1985 and 1986. Three human thyroids and one bovine thyroid analyzed for I-129 are listed in Table 2.

Table 2: Iodine-129 in human and bovine thyroid glands taken from the Valdivia area (Chile) in 1985/86.

Fresh weight [g]	I-127 concentration [mg·g^{-1} f.w.]	I-129 concentration [μBq·g^{-1} f.w.]	I-129/I-127 atom ratio
	a) Human thyroids		
14.2	0.8 ± 0.1	9 ± 1	(2.0 ± 0.2)·10^{-9}
17.7	0.42 ± 0.05	29 ± 4	(1.1 ± 0.1)·10^{-8}
12.4	0.32 ± 0.04	3.0 ± 0.4	(1.5 ± 0.2)·10^{-9}
	b) Bovine thyroid		
26.9	1.2 ± 0.1	7.4 ± 0.9	(10 ± 1)·10^{-10}

They show a mean value of the I-129/I-127 ratio of $4 \cdot 10^{-9}$, which is by about the factor 3 lower than the atom ratio reported for different parts of the U.S.A., Japan and Europe [3]. It confirms that the transport of I-129 from the northern into the southern hemisphere proceeds very slowly.

B. Translocation of iodine-129 in soil and its long-term transfer from soil to vegetation

1. Methodology

The translocation of I-129 within the soil and its long-term transfer from soil to plant have been investigated using two experimental areas with different soil properties. The first one is an undisturbed soil column (surface area: 2,5 m^2, depth: 1,5 m) with a sandy soil of high humus content, the second one is a pasture (surface area: 200 m^2) with an allochtone soil on a river bank. The surface of the soil column was simultaneously contaminated with I-129 and sown with grass in April 1982, the pasture was contaminated in August 1984. After application of I-129, plant samples were harvested during each of the following growth seasons. The soil samples were taken from the monolith and the pasture in 5-cm and 10-cm steps to a depth of 50 cm and 100 cm, respectively.

2. Results and discussion

The I-129 profiles in both experimental soils exhibit great differences in the distribution of radioiodine. They show that the radioiodine migrates very slowly in the soil monolith and relatively fast in the allochtone soil of the pasture. Fig. 1 shows the translocation of radioiodine in the

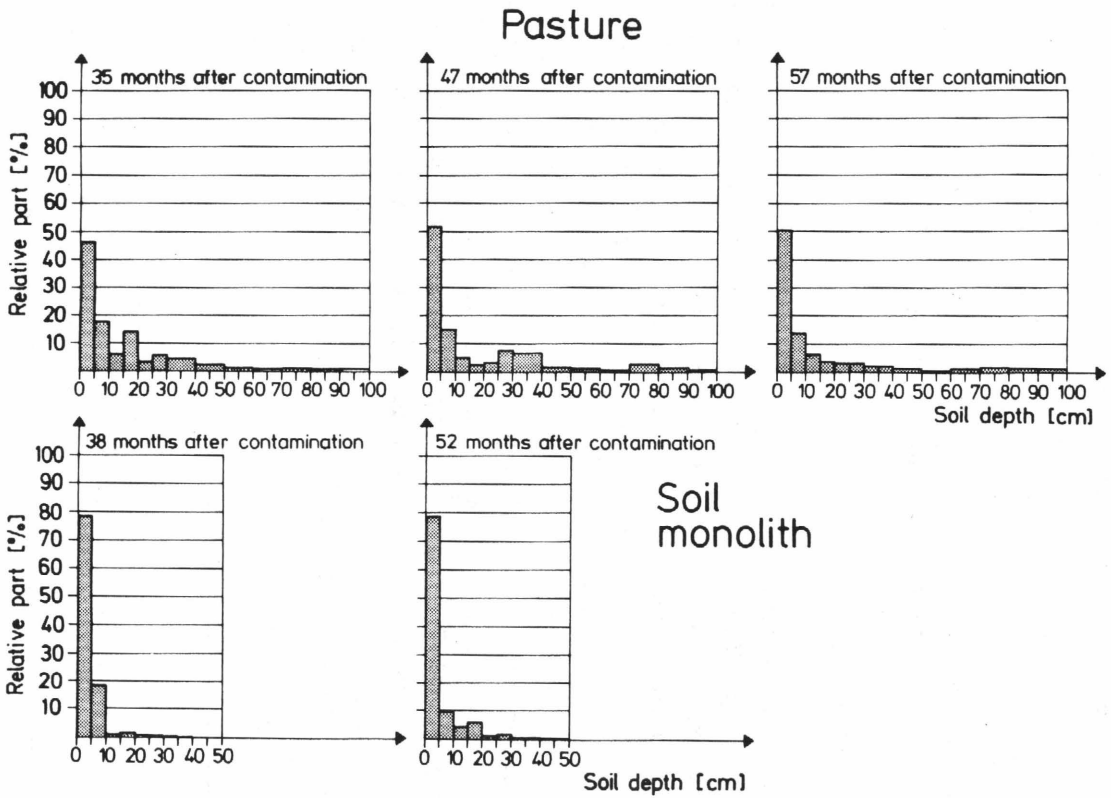

Fig. 1: Distributions of I-129 in a pasture (allochthone soil on a river bank) and in a soil monolith (sandy soil of high humus content).

soil of the column and the pasture at different times after surface contamination. After about 4.5 years, 88 % (monolith) and 66 % (pasture) of the total I-129 activity were found in the top soil layer of 10 cm, the main rooting zone of pasture grass.

For modelling of the plant availability of nuclides it is assumed that the concentration in the root zone decreases exponentially with time. Evaluation of the measurements yields residence half-lives of 250 and 64 months and delay constants of $1 \cdot 10^{-9}$ and $4 \cdot 10^{-9}$ s^{-1} for the monolith and the pasture, respectively. Apart from the different soil specific parameters, there is evidence that the main reason for the higher mobility of radioiodine in the pasture soil is associated with a chemical conversion under the temporary anaerobic soil conditions at higher water levels extending from the nearby river. The depth distribution of stable iodine was found rather homogeneous in both soils with mean values of 3.5 mg (monolith) and 4.5 mgI-127$\cdot kg^{-1}$ d.w. (pasture).

Transfer factors plant/soil (dry weight basis) obtained from the experimental areas between 1985 and 1989 are listed in Table 3. Whereas the monolith shows values of $2.6 \cdot 10^{-3}$ and $2.2 \cdot 10^{-3}$ corresponding with times of 38 and 52 months after contamination, respectively, transfer factors obtained from the pasture 35, 47 and 57 months after contamination range between $1.3 \cdot 10^{-2}$ and $6.3 \cdot 10^{-2}$. As the transfer of stable iodine shows significantly higher mean values in both soils of 1.0 (monolith) and 0.3 (pasture), the distribution of radioiodine in the soil proves to be a very important factor in soil-plant transfer, as it determines the geometric availability of iodine compounds to plants.

Table 3: Transfer factors vegetation/soil (dry weight basis) for I-129 and I-127 related to the upper 10-cm soil layer of the soil monolith and the pasture.

Year collected	Time after contamination [months]	TRANSFER FACTOR VEGETATION/SOIL I-129	I-127
		Soil monolith	
		Date of contamination: 04/02/1982	
1985	38	$(2.6 \pm 0.2) \cdot 10^{-3}$	1.2 ± 0.1
1986	52	$(2.2 \pm 0.2) \cdot 10^{-3}$	0.8 ± 0.1
1989	86	in preparation	
		Pasture	
		Date of contamination: 08/30/1984)	
1985	9	$(1.2 \pm 0.1) \cdot 10^{-1}$	0.40 ± 0.03
1986	23	$(4.0 \pm 0.3) \cdot 10^{-2}$	0.45 ± 0.05
1987	35	$(1.3 \pm 0.1) \cdot 10^{-2}$	0.44 ± 0.05
1988	47	$(2.6 \pm 0.3) \cdot 10^{-2}$	0.28 ± 0.03
1989	57	$(6.3 \pm 0.6) \cdot 10^{-2}$	0.20 ± 0.02

C. Long-term transfer of I-129 along the food chain

1. Methodology

In a feeding experiment with a dairy cow the transfer of I-129 from grass to milk, to cow meat and to pig thyroid via the cow's milk was followed after constant doses of I-129 in the pasture grass had been administered for a period of 53 days. In the experiment the cow was confined to a metabolism stall. Pasture grass contaminated with I-129 via roots was used as labeled feed.

Three kg of the I-129 labeled milk collected daily were fed to a pig to simulate the transfer of I-129 into the human

thyroid. With regard to the physiological similarity between pigs and humans the assay yields information about the radioactive burden on the human thyroid gland when drinking I-129 contaminated milk.

At the end of the feeding period the animals were slaughtered, in order the determine the specific activity of I-129 in various butcher cuts of the cow and in the thyroid gland of the pig.

2. Results and discussion

The time course of the I-129 amounts secreted daily by the cow into the milk exhibited relatively constant levels during the whole experimental period. The average value of the transfer factor milk/feed evaluated from the I-129 concentrations in the milk and from the constant I-129 intake was found to be $2.4 \cdot 10^{-3}$ $d \cdot kg^{-1}$.

Additionally the transfer of the stable iodine was followed during the experiment. The average value of the transfer factor milk/feed for I-127 was $5.9 \cdot 10^{-3}$ $d \cdot kg^{-1}$.

Transfer factors pig thyroid/milk and pig thyroid/cow feed of I-129 exhibited values of 1.2 and $8.7 \cdot 10^{-3}$, respectively.

Transfer factors meat/feed obtained for 9 muscle parts ranged from $7.3 \cdot 10^{-3}$ (forerib) to $5.4 \cdot 10^{-2}$ (best rib)) with a mean value of $3.8 \cdot 10^{-2}$ $d \cdot kg^{-1}$ f.w. Three organs examined, ie, liver, kidneys and thyroid, demonstrated very different transfer factors of $7.3 \cdot 10^{-3}$, $3 \cdot 10^{-4}$ and 4.4 $d \cdot kg^{-1}$ f.w., respectively. The very low value for kidney was probably caused by a high metabolism occurring in this organ.

The mean value of the transfer factor milk/feed of $2.4 \cdot 10^{-3}$ $d \cdot kg^{-1}$ is in good accordance with the value of $2.6 \cdot 10^{-3}$ $d \cdot kg^{-1}$ obtained for I-131 from the Chernobyl fallout during a feeding assay with 10 dairy cows carried out in May 1986 [4]. The results show a similar transfer feed-milk for radioiodine whether superficially contaminated by fallout or incorporated into plants by root uptake.

D. Inventory of I-129 and I-127 in waters from potential repository sites.

For environmental monitoring and licensing purposes I-129 and I-127 levels in water samples from sites envisaged for nuclear waste deposits were investigated. 12 surface water samples from ponds, wells and industrial reservoirs as well as 6 highly saline water samples from underground saline areas were analyzed for the iodine isotopes. The I-129 content found in the surface water samples ranged from 5 to 30 $\mu Bq \cdot l^{-1}$. Concentrations of I-127 were between 20 $\mu g \cdot l^{-1}$ (ponds, wells) and 600 $\mu g \cdot l^{-1}$ (industrial pools).

All underground water samples had an unusually high concentration of I-127 between 3.4 and 21 $mg \cdot l^{-1}$. As those samples have not been subject to direct anthropogenic influences, this is obviously the result of earlier geological processes (ie, sedimentation of iodine from sea water). Only with two samples originating from less isolated water I-129 could be detected, probably due to a long-term mixing with percolating rain water. No clear dependency of the I-129 concentration on the I-127 content could be observed.

References

[1] Handl J.:
Investigations on the accumulation of iodine-129 in vegetation, milk and human thyroid glands in the vicinity of nuclear facilities.
Radiation Protection Programme, Prog. Rep. 1980-1984 Vol. I, p. 589, CEC, Brüssel.

[2] Handl, J.:
Accumulation and long-term transfer of iodine-129 in the food chain, in human thyroid glands and in waters of waste deposits.
Radiation Protection Programme, 1985 Vol. I, p. 334, CEC, Brüssel.

[3] Handl, J., Pfau, A., Huth, F.W.:
Measurements of I-129 in human and bovine thyroids in Europe - Transfer of I-129 into the food chain.
Health Physics, Vol. 58, in press.

[4] Handl, J., Pfau, A.:
Feed-milk transfer of fission products following the Chernobyl accident.
Atomkernenergie-Kerntechnik, Vol. 49, p. 171-173, 1987.

IV. Other research group(s) collaborating actively on this project [name(s) and address(es)]:

D. Smidt, F.-W. Huth, A. Pfau,
Institut für Tierzucht und Tierverhalten der FAL Mariensee, FRG.

A. Georgii,
Pathologisches Institut der Medizinischen Hochschule Hannover, FRG.

V. Publications:

Journals

1. Handl, J. , Pfau, A.:
Feed-milk transfer of fission products following the Chernobyl accident.
Atomkernenergie-Kerntechnik, 49 (1987) 171-173.

2. Handl, J., Pfau, A.:
Long-term transfer of I-129 into the food chain.
The Science of the Total Environment, 85 (1989) 245-252.

3. Handl, J., Pfau, A., Huth, F.W.:
Measurements of I-129 in human and bovine thyroids in Europe - Transfer of I-129 into the food chain.
Health Physics, 58, in press.

Internal Reports

1. Handl, J., Pfau, A.:
Bestandsaufnahme und Transfer von I-129 in der Nahrungskette und Spaltprodukt-Transfer auf dem Weide-Kuh-Milch-Pfad nach dem Tschernobyl-Unfall.
NIR-Report, No. 2/86, 40 pp.

2. Handl, J., Pfau, A.:
Long-term transfer of I-129 into the food chain.
CEC Workshop on "The Transfer of Radionuclides to Livestock", Oxford, September 5-8, 1988.

3. Handl, J.:
Translocation of I-129 in soils of different properties and long-term transfer of I-129 from soil to vegetation.
IUR Workshop at Handeck, Grimsel, Switzerland, 23.-26.5. 1989.

4. Handl, J.:
Aktivierungsanalytische Bestimmung von I-129 und ihre Anwendung bei der Untersuchung des Langzeitverhaltens von I-129 in der Biosphäre.
14. Seminar "Aktivierungsanalyse", Hannover 10./11.Oktober 1989.

5. Handl, J.:
Annual Reports of the Lower Saxony Institute for Radioecology, NIR-Reports, 1984/85/86/87/88/89.

RADIATION PROTECTION PROGRAMME
Final Report

Contractor: Contract no.: BI6-B-194-UK

Associated Nuclear Services
Eastleigh House
60 East Street
GB- Epsom, Surrey KT17 1HA

Head(s) of research team(s) [name(s) and address(es)]:

Dr. P.J. Coughtrey
Biological Sciences Group
Associated Nuclear Services
Eastleigh House, 60 East Street
GB- Epsom, Surrey KT17 1HA

Telephone number: 40531

Title of the research contract:

Experimental programme to support the development of dynamic models describing carbon-14 (and other B-emitters) in soil-plant-animal systems.

List of projects:

1. Experimental programme to support the development of dynamic models describing carbon-14 (and other B-emitters) in soil-plant-animal systems.

Title of the project no.:

Experimental studies to support the development of dynamic models describing C-14 behaviour in soil-plant-animal systems

Head(s) of project:

Dr. P.J. Coughtrey

Scientific staff:

Mrs. J.A. Kirton
Mr. N.G. Mitchell
Mr. C.J. Beetham

I. Objectives of the project:

To improve knowledge on the behaviour of low energy β-emitters, particularly C-14, in soil-plant-animal systems in order to provide a basis for models used in radiological assessments.

II. Objectives for the reporting period:

As above.

III. Progress achieved:

1 INTRODUCTION

C-14 is a long-lived ($T_{\frac{1}{2}}$ ~5700 a) β-emitter released from gas and water-cooled reactors and from nuclear fuel reprocessing plants. C-14 has been shown to be much the greatest contributor to collective dose from nuclear facilities and also contributes significantly to doses to critical groups. It is also present in solid wastes and is important in the context of disposal of these wastes.

Carbon is a ubiquitous element, essential for biological systems. Understanding of the behaviour of C-14 in the environment therefore depends on a knowledge of the global carbon cycle which involves processes operating on timescales of a few hours to several thousands of years. Equilibrium may not be reached between C-14 entering a system and carbon already present in that system because of the operation of biological processes which serve to concentrate and retain carbon over long timescales. Typically, the behaviour of C-14 has been modelled using a 'specific activity' approach with the inherent assumption that the ratio of C-14 to stable carbon in various environmental compartments is a constant. This assumption is unlikely to be correct for discharges of C-14 occurring over short timescales, especially when inputs are not constant with time.

The experimental studies summarised here were designed to test whether or not typical land plants could obtain any part of their carbon requirements from soil and thereby test and refine mathematical models used to assess C-14 transport following waste disposal on land. Full results and discussion are presented in ANS Report No. 740-R2 (May 1989).

2 METHODOLOGY

2.1 Solution culture studies

A number of experiments were undertaken to test the design and operation of culture experiments in which plants could be exposed to C-14 as bicarbonate via full Hoaglands solution in sealed systems allowing complete analysis of C-14 inputs and outputs. The systems involved independent control of the solution to which roots were exposed as well as monitoring of air surrounding shoots isolated from the solution chamber. Experiments were undertaken in controlled environment chambers using various levels of replication, exposure regimes, and timescales (up to 48 h). Control systems were also included to test whether C-14 was lost to the local environment and to isolate the effects of any such losses of C-14 distribution in experimental systems.

2.2 Soil transfer studies

A number of experiments were undertaken in which C-14 was administered as bicarbonate to soil-plant systems in glasshouse conditions. These involved the use of a split-pot technique with one half of each pot contaminated and the other half acting as a control. Soil below plant shoots was sealed to allow sampling of the air immediately above the soil on a continuous basis. C-14 was injected at different levels within the soil profile and its final distribution within soil and plant fractions analysed after destructive harvests at periods of 9.4 h to 75 d after C-14 administration.

2.3 Field measurements

Preliminary sampling of vegetation was undertaken in September 1988 near to the CEGB installation at Trawsfynydd, N.Wales. Samples were taken from an area of rough grazing and included bulk, unsorted, vegetation, as well as individual plant species.

2.4 Analytical techniques

To overcome difficulties in the separation of C-14 from biological samples, a wet digestion technique weas developed for experimental studies using chromic acid in an enclosed vessel and collection of C-14 in a sodium hydroxide/sodium carbonate mixture via diffusion. Some plant samples from the culture solution experiments were subjected to an ethanol extraction to remove sugars, ammino acids and some polysaccharides, followed by a perchloric acid extraction to remove non-structural polysaccharides. C-14 extracted from soil and plant samples was trasnferred to a xylene-based micellar scintillator and was assayed by liquid scintillation methods.

Field samples were analysed for C-14 via dry combustion using methods developed by the Isotope Measurements Laboratory at the UK Atomic Energy Authority Research Establishment, Harwell.

3 RESULTS

3.1 Culture solution studies

In preliminary studies, 0.15 to 0.38% of administered C-14 was taken up by *Lolium perenne* over a 72 h period. Concentration ratios of C-14 in shoots to initial solution were in the range 0.62-1.4. Approximately 32% of C-14 in the plants was present in shoots.

The second series of studies used a more complex arrangement to account for the disposition of administered C-14. 0.2 to 0.5% of administered C-14 was present in *Lolium perenne* at 42 h post-administration. Of this, 51 to 62% was present in shoots. Approximately 2% of administered C-14 escaped from the solution chamber to the top chamber, presumably via plant uptake and subsequent respiration, or as organic compounds such as ethylene. Concentration ratios in shoots relative to solution ranged from 17-42. Of administered C-14, approximately 20% could not be readily accounted for and was assumed to have been present in association with bowl surfaces, waxes and pipework.

A further series of experiments with additional controls showed that 0.29 to 1.0% of administered C-14 was present in *L.perenne* at 48 h post-administration. Of this, 61 to 84% was present in shoots. Results for control systems raised doubts concerning the effectiveness of the seals between top and bottom chambers though it was considered unlikely, given the conditions of the experiment, that C-14 could have escaped from the system. Overall recovery of C-14 in the control system excluding plants was 97% of that administered. In systems containing plants the overall recovery was 58 to 87% of that administered.

3.2 Soil transfer studies

Preliminary studies indicated that *L.perenne* could obtain C-14 added as bicarbonate to a loam soil via root uptake, and demonstrated that total uptakes were 0.5 to 15% of that present in soil over periods of 21 to 95 d post administration.

Subsequent experiments using the split-pot systems and a sealed soil chamber showed an initially high C-14 concentration in shoots of plants grown in the contaminated soil and a subsequent rapid decline due to growth dilution and loss of C-14 to atmosphere. The rate of loss of administered C-14 was $\sim$1.4% d^{-1}. C-14 lost from treated pots was fixed by plants in the uncontaminated sections and subsequently translocated to roots. Additional experiments over various timescales demonstrated that up to 50% of administered C-14 could have been taken up by roots, with results varying between experiments as a function of design, period from exposure to harvest, state of growth at administration and rate of growth.

3.3 Field measurements

C-14 was readily detectable in the plant samples assayed. Gross specific activities in the range 0.310 to 0.355 Bq C-14/g were similar to those reported for vegetable samples in 1983 and 1984 at sites near to the Hinkley Point installations in S.W.England. Net

specific activities in the range ∿14 to 18 Bq C-14/kg C were similar to those reported for vegetation samples at 5.7 km distance from the BNFL Sellafield works. There was considerable variation in specific activity between species with highest values recorded for the soft rush, *Juncus effusus*, and lowest values recorded for a moss, *Polytrichum commune*.

4 DISCUSSION

Solution culture experiments demonstrated that C-14 applied to soil as bicarbonate is taken up the roots of *Lolium perenne* and translocated to shoots. The results obtained were in general accord with published literature for other plant species grown in culture solution but generally under less controlled conditions.

The final soil transfer experiment resulted in an almost total recovery of administered C-14. Though relatively high root uptake fractions had been indicated by earlier experiments, the final experiment indicated that <1% of originally administered C-14 was removed by root uptake within a few hours of administration. However, the soil conditions lead to a rapid loss of administered C-14 to atmosphere immediately above the soil surface and, over longer time periods (days to weeks), estimates of root uptake were subject to increasing uncertainty due to redistribution via the shoots to the open atmosphere.

Results of the soil experiments could not be explained on the basis of a specific activity model, even assuming that a relatively high fraction of the plant's activity was derived direct from soil. The implication of root uptake of C-14 is that the specific activity of above-ground plant material may not directly reflect that of the surrounding atmosphere. In field conditions these effects could be particularly marked after the passage of a pulse of C-14 leading to a more prolonged increase in soil specific activity relative to atmosphere, or in long-term contamination situations with a gradual decline

in atmospheric concentrations such that specific activity in soil lags behind that of atmosphere.

In field inverstigations of C-14 levels around nuclear installations, several authors have attributed variations in C-14 specific activity of different crops and vegetation to differences in their growth and development relative to patterns of C-14 exposure. The variations between individual plant species found in the current field sampling could either be attributed to different stages of growth, or to differences in uptake from the soil C-14 pool. In this respect, low specific activity in *P.commune* (which obtains the majority of its nutrients from atmosphere) compared with *Juncus effusus* (which has a very well developed rhizome system and a high degree of aerenchyma tissue) is of particular interest. No published information appears to be available on the behaviour of C-14 in vegetation and soils typical of semi-natural systems in the UK. Recycling of C-14 between soils and vegetation might be expected to be most efficient in such systems.

5 CONCLUSIONS

Methods have been developed in which C-14 added as bicarbonate to enclosed systems can be traced from solution to roots, roots to shoots, and shoots to atmosphere. Experimental studies with solution culture and soil systems in both laboratory and glasshouse conditions provide categorical evidence that small quantities of C-14 can be absorbed by plant roots and translocated to shoots. Though the quantities involved are small relative to carbon fixed by photosynthesis, they are sufficient to demonstrate that standard specific activity models used to assess the behaviour of C-14 in soil-plant systemns will not be appropriate to short-term releases to atmosphere or to conditions when C-14 is supplied to soil rather than to atmosphere. Preliminary field sampling around an operating nuclear installation has indicated that specific activities in native plant species are not constant, possibly as a result of differential uptake from soils.

IV. Other research group(s) collaborating actively on this project [name(s) and address(es)]:

University of Bristol, Department of Botany,
Woodland Road,
Bristol,
BS8 1UG.

University of Surrey, Department of Chemistry,
Guildford,
Surrey.

V. Publications:

Coughtrey, P.J., Nancarrow, D.J. and Jackson, D.J. (1980). Extraction of C-14 from biological samples by wet oxidation. Commun. Soil Sci. Plant Anal. 17:393-399.

Coughtrey, P.J., Jones, C.H., Kirton, J.A. and Crabtree, D.F. (1987). Models for assessing transfer of radionuclides through terrestrial agricultral systems to man. In: The Cycling of Long-lived Radionuclides in the Biosphere: Observations and Models. CEC, Luxembourg.

Kirton, J.A., Mitchell, N.G. and Beetham, C.J. (1989). Experimental studies to support the development of dynamic models describing C-14 behaviour in soil-plant-animal systems. ANS Report No. 740-R2. Associated Nuclear Services Ltd., Epsom, May 1989.

RADIATION PROTECTION PROGRAMME
Final Report

Contractor: Contract no.: BI6-B-035-B

Katholieke Universiteit Leuven
KUL
Naamsestraat 22
B-3000 Leuven

Head(s) of research team(s) [name(s) and address(es)]:

Prof A. Cremers
Centrum voor Oppervlaktescheikunde
en Colloïdale Scheikunde, K.U.L.
Kardinaal Mercierlaan 92
B-3030 Leuven (Heverlee)

Telephone number: 016/22.09.31

Title of the research contract:

Dynamics of radionuclide chemistry in soils and sediments.

List of projects:

1. Dynamics of radionuclide chemistry in soils and sediments.

Title of the project no.:

Dynamics of Radionuclide Chemistry in Soils and Sediments

Head(s) of project:

Prof.A.CREMERS

Scientific staff:

A. MAES, J. DE BRABANDERE, P. DE PRETER, F. VAN ELEWIJCK, J. TITS, L. SWEECK, E. VALCKE, J. WAUTERS

I. Objectives of the project:

The main objective of the project is a physico-chemical and mechanistic study of the geochemical behaviour of radionuclides in natural systems such as soils and sediments. The chief emphasis of the work is on the geochemical phase associations of radionuclides and dynamic aspects of radionuclide interception and remobilization processes. The various factors which are being considered are the geochemical characterization, physicho-chemical conditions and microbiological effects

II. Objectives for the reporting period:

The project is concerned with the study of the behaviour of the radionuclides of technetium, europium, strontium, zinc and caesium. During the early phases of the project, the main attention was focussed on Tc and Eu. During the 1987-89 period, the chief emphasis was on Sr,Zn and Cs. On an overall basis, the most intense efforts have been directed at the study of the environmental behaviour of radiocaesium for which a quantitative insight has been gained into the retention mechanistics and for which reliable tools have been developed for predicting its solid/liquid distribution behaviour in soils and sediments.

III. Progress achieved:

CAESIUM

Current views

There is a general consensus that the single most important factor, governing radiocaesium retention in soils and sediments, is the property of micaceous clays to preferentially retain alkali ions of low hydration. The specific sites, responsible for this process are localized at the interlayer-edge zones of the clay crystals: the so-called frayed edge sites (F.E.S.). Due to the lack of quantitative insight into this specific interception process and the nature of potentially competitive cations, it has so far not been possible to make predictions on solid/liquid distribution coefficients (K_D-values) of radiocaesium in terrestrial and aquatic systems. In the course of this project, some significant methodological developments have taken place allowing K_D-predictions to be made on the basis of readily measurable properties of the systems. Below, these new predictions are described and applied to a broad range of soils and sediments.

Methodology and theoretical background

The principle of the method is based on the use of the cationic silver-thiourea (AgTU) complex as a masking agent for the non-specific sites. AgTU shows and exceedingly high selectivity for the regular exchange sites in clay and organic matter and is excluded -on the basis of a combination of steric and poor selectivity reasons- from the F.E.S. pool. Thus, when operating in a suitably high background concentration of AgTU (.015 to .020M), it is possible to quantitatively characterize the capacity of and the Cs-selectivity pattern in the F.E.S.. *Figure 1* shows some typical examples of caesium sorption isotherms in the F.E.S.. Sorption data are corrected for a small interception of caesium in the non-specific sites, as explained in various papers in the literature list. In addition, the same procedure can be used for measuring the Cs-to-K selectivity pattern in the F.E.S.

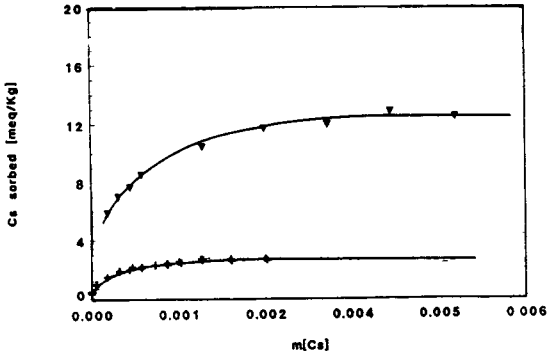

figure 1
Cs sorption isotherms in the F.E.S.-sites of illite(▼), Boom clay(+), and illite-smectite(□) in the presence of AgTU .015N (illite and Boom clay) or AgTU .02N (illite-smectite)

Figure 2 shows some examples of the composition dependence of the (logarithm of) Cs-to-K selectivity coefficient, as obtained from Cs sorption in the presence of .015 M AgTU and .01M KCl. The K_c value, defined with respect to the capacity of the F.E.S. pool has the form

$$K_c^{FES}(Cs/K) = \frac{Z_{Cs} \cdot m_K}{Z_K \cdot m_{Cs}} \qquad (1)$$

in which Z refers to the fractional ion occupancy in the F.E.S. and m to the ionic concentration in the liquid phase. Examination of this figure shows that: (a) K_c decreases with increasing Cs loadings, i.e. the F.E.S. group is heterogeneous; (b) the ln K_c value at zero Cs-loading approaches a value of about 7 to 8. The composition dependence of K_c can accurately be described in terms of a model comprising three kinds of sites two of which are extremely selective for Cs (ln K_c=9 and 12) and which represent about 5% of the F.E.S. capacity. Exactly the same selectivity behaviour has been found in a broad range of soils and sediments.

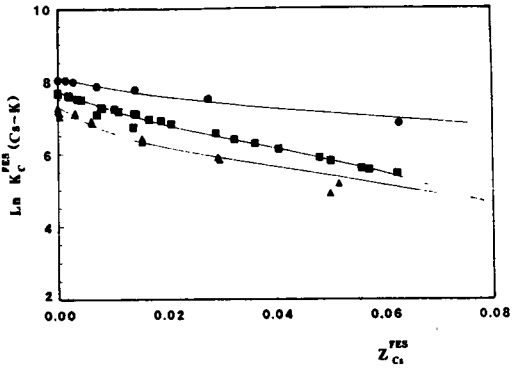

figure 2.
Composition dependence of ln K_c^{FES}(Cs/K) for the frayed edge sites of illite(▲), illite-smectite(●) and Boom clay(■). KCl and AgTU concentrations are .01N and .015N respectively.

This procedure, although useful for characterizing the properties of the specific sites, is rather laborious and not appropriate for routine practice. Moreover, in substrates of very low abundance of F.E.S., i.e. the real problem scenarios in case of a nuclear accident, the method is not sensitive enough to quantify the F.E.S. pool. In the final stages of the project, a more sensitive and expedient procedure has been developed, leading to the measurement of the product of the F.E.S. capacity and the trace Cs-to-K selectivity coefficient in the F.E.S., i.e. a quantity allowing to make predictions in geochemical substrates. The quantitative relation (see list of papers for details) has the form

$$K_D^*(Cs) = \frac{K_c^*(Cs/K)[FES]}{m_K} \qquad (2)$$

in which $K_D^*(Cs)$ is the trace K_D value of Cs, [FES] the capacity of the F.E.S.pool and $K_c^*(Cs/K)$ the trace Cs-to-K selectivity coefficient (i.e. at homoionic K-saturation in the F.E.S.). Eqn(2) expresses the fact that $K_D(Cs)$ mirrors the K_D value of K (between F.E.S. and the liquid phase), amplified by some characteristic selectivity factor. Eqn(2) predicts that the $K_D(Cs).m_K$ product should be constant and equal to the $[FES].K_c(Cs/K)$ product. This was tested for a broad range of substrates and some representative results are shown in *figure 3*. It is apparent that well-defined plateau values are obtained, corresponding to the $K_c(Cs/K).[FES]$ product. At lower K-concentrations (keeping AgTU constant at .015M) the $K_D(Cs).m_K$ product decreases somewhat, indicating that AgTU has (partial) access to the F.E.S., thereby displacing K, and of course radiocaesium.

The plateau values can be defined as specific radiocaesium interception potentials and are further represented by the symbol $[K_n(Cs).m_K]$.

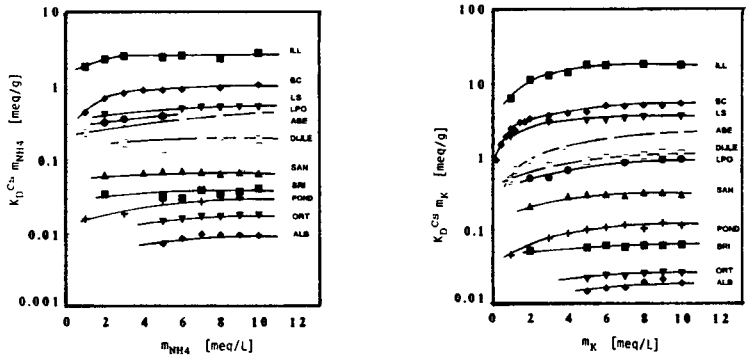

Figure 3. Dependence of $K_D(Cs).m_K$ and $K_D(Cs).m_N$ on K and NH_4 solution concentration in (top to bottom): illite, Boom clay, loam soil, diatomaecious sediment (lac Pavin, oxic),acid brown earth, Dijle river sediment, crushed sandstone, crushed clay brick, freshwater pond sediment, orthoclase and albite.

The K-ion is however not the only potentially competitive ion, NH_4 being the most likely candidate in view of its similar value in ion size. The NH_4 analog of eqn(2) has the form

$$K_D^*(Cs) = \frac{K_c^*(Cs/N).[FES]}{m_N} \qquad (3)$$

in which N is used as a shorthand symbol for NH_4. *Figure 3* shows that similarly well-defined plateau values are obtained i.e. $[K_D(Cs).m_N]$; moreover, a comparison of both sets of data of figure 3 clearly shows that, for any given substrate $[K_D(Cs).m_K]$ values are significantly higher than $[K_D(Cs).m_N]$. From eqn(2) and (3) it is readily obvious that the ratio $[K_D(Cs).m_K]/[K_D(Cs).m_N]$ can be identified with the N-to-K selectivity coefficient in the specific sites $K_c^*(N/K)$. Consequently, NH_4-ions are more competitive with radiocaesium than K, a finding which is discussed in some detail in section 3. In conclusion, it is of importance to develop some predictive equation for a mixed scenario in which both K- and NH_4-ions are present in the system. Taking a linear combination of eqn(2) and (3) it can be shown that $K_D(Cs)$ can be expressed by the equation

$$K_D(Cs) = \frac{[K_D(Cs).m_K]}{K_c(N/K)\ m_N + m_K} \qquad (4)$$

Taking the reciprocal of eqn(4) allows to identify the limiting forms of this expression

$$\frac{1}{K_D(Cs)} = \frac{m_N}{[K_D(Cs).m_N]} + \frac{m_K}{[K_D(Cs).m_K]} \qquad (5)$$

This equation is submitted to an experimental test in section 3.

Results and discussion

- Reference micaceous clays

A comprehensive study was carried out on four micaceous clay minerals (illite, illite-smectite mixed layer, sericite and muscovite). For all clays, the composition dependence of the Cs-selectivity pattern in the F.E.S. can be described in terms of a 3-site model involving two extremely selective sites as described above. Moreover, the NH_4-to-K selectivity coefficient varied in the range of 4 to 7, thus providing a characteristic fingerprint for the action of micaceous clays.

- Agricultural soils

Twelve soils of widely varying texture (sandy,loam,clay) were characterized in terms of F.E.S. capacity, trace caesium selectivity pattern, $[K_D(Cs).m_K]$ and $[K_D(Cs).m_N]$ values. The following results were obtained: (a) F.E.S. values varied in the range of 1 to 4 meq/kg, corresponding to a range of 1 to 3% of overall cation exchange capacity; (b) trace Cs-to-K selectivity coefficients are about 7 ($\ln K_c$); (c) the NH_4-to-K selectivity coefficient in the specific sites varies in the range of 4 to 7. These findings clearly demonstrate quantitatively the action of micaceous clays and demonstrates the higher competitivity of NH_4 over K.

- Freshwater sediments

The methods described above were applied to a broad series of freshwater sediments (lacustrine, river) of varying origin. The findings were in every respect similar to these obtained on soils and micaceous clays: F.E.S. values amount to a few percent of C.E.C. values; the trace $\ln K_c(Cs/K)$ value is near 6-7 and the $K_c(N/K)$ in the specific sites vary in a range of 4-6.

-Estuarine sediments

Twelve sediments originating from or near the Loire estuary were included in this study, textures varying from extremely sandy to very clayey. F.E.S. values, trace Cs-to-K selectivity coefficients in the F.E.S. and NH_4-to-K selectivity coefficients were very similar to these reported above. Moreover, it was demonstrated that at high concentrations, sodium ions become competitive with potassium ions, the K-to-Na selectivity in the F.E.S. amounting to values in the range of 50-100. It was furthermore demonstrated that Ca and Mg are very poorly competitive with potassium, even at a ten-fold excess, and play only a very secondary role on the solid/liquid distribution behaviour of radiocaesium. Reliable predictions of $K_D(Cs)$ can be made on the basis of solid phase characterization and seawater compositions.

-Upland soils

Eight soils originating from Cumbria were included in this study. These soils are characterized by high C.E.C. values (in the range of 24 to 100 meq/100g) and organic matter contents in the range of 25-90%. F.E.S. values cannot be measured in these soils but well defined but very low plateau values were obtained for $[K_D(Cs).m_K]$ and $[K_D(Cs).m_N]$. As expected their ratios varied in the range of 4.5 to 6.2, demonstrating the presence of micaceous clays. Furthermore, it was demonstrated that these soils are characterized by relatively high NH_4 levels, as could be expected from their poor drainage properties. It is demonstrated that for organic matter contents below 50%, $K_D(Cs)$ is essentially ruled by the specific sites and the K and NH_4 levels in the liquid phase. At organic matter

contents in the range of 80-90% (peat) the solid/liquid distribution behaviour is essentially ruled by the organic matter exchange sites and the K and NH_4 status of the soils.

Predictive tests

In view of the very coherent behaviour observed in regard to radiocaesium sorption in the set of substrates studied, a series of $K_D(Cs)$ measurements was made in a number of systems for various K and NH_4 scenarios, and the results compared with predictions based on eqn(4) and solid phase characterizations i.e. $[K_D(Cs).m_K]$ and $[K_D(Cs).m_N]$. The results are summarized in Table I, showing details on experimental scenarios and a comparison of measured and predicted $K_D(Cs)$ values.

Table I. Comparison of experimental and predicted $K_D(Cs)$ (eqn 4) obtained on illite, loam soil, acid brown earth, freshwater pond sediment, Po river sediment, Dijle river sediment.

Substrate	K	NH_4	$\log K_D^{Cs}$-exp.	Log K_D^{Cs}-pred.
Ill	1.00	1.00	3.14	3.26
LS	.21	.03	3.98	3.93
ABE (a)	.63	.23	3.07	2.97
(b)	.22	.27	3.18	3.11
POND (a)	.13		3.06	2.96
(b)	.13	.10	2.42	2.35
PO (a)	.062	.016	3.97	3.83
(b)	.059	.023	3.80	3.74
DYL (a)	.142	.044	3.54	3.46
(b)	.142	.196	3.09	2.96

K_D^{Cs} values are obtained by a batch procedure, using high speed centrifugation for phase separation and Cs^{137} monitoring of the supernatants. The following conditions apply (ionic concentrations expressed in meq/L in brackets)

- ILL: Exhaustive presaturation with a mixture of KCl (1), NH_4Cl (1), $CaCl_2$ (8); K_D measurement at sol./liq. ratio of 1/50.
- LS: One time dispersion in demin. water at sol./liq. ratio of 1/10.
- ABE: One time dispersion in 10^{-3} M KCl (a) and demin. water (b) at sol./liq. ratio of 1/10.
- POND: Exhaustive preaturation with a mixture of KCl (.13), NaCl (.76), $CaCl_2$ (4.37), $MgCl_2$ (.38) without (a) and with (b) NH_4Cl (0.1) at sol./liq. ratio of 1/20.
- DYL: One time equilibration with a mixture of KCl (0.14), NaCl (1.21), $CaCl_2$ (4.15), $MgCl_2$ (.87) without (a) and with (b) NH_4Cl (.16) at sol./liq. ratio of 1/20.
- PO: One time equilibration with a mixture of KCl (0.059), NaCl (.33), $CaCl_2$ (1.97), $MgCl_2$ (.66) without (a) and with (b) NH_4Cl (.011) at sol./liq. ratio of 1/20.

The ionic compositions used for POND, DYL and PO are representative for the compositions of these water bodies. K in the liquid phase is measured by atomic absorption and NH_4 is measured by a modified Berthelot reaction (Krom, 1980).

It is sufficiently evident that the agreement is quite good, demonstrating in fact that we are now in a position to predict rather reliably $K_D(Cs)$ on the basis of readily measurable properties of the

system. Moreover, the findings presented warrant practical considerations: (a) the significant effect of NH_4-ions on radiocaesium displacement provides a quantitative indication for the remobilization of radiocaesium from anoxic sediments; (b) the use of NH_4-fertilizers should be avoided in radiocaesium contaminated soils; (c) poor soil drainage characteristics are liable to enhance radiocaesium availability; (d) apparently slow kinetics based on K_D(Cs) measurements involving the use of river waters containing significant NH_4 levels may be caused by NH_4-to-NO_3 conversions during the experiments.

STRONTIUM

In contrast to caesium, the sorption behaviour of radiostrontium is generally not controlled by specific effects but by reversible ion exchange processes involving the regular ion exchange complex (clays, humics). In view of the well-known fact that only minor selectivity differences are encountered among alkaline earth cations, one may expect that the solid/liquid distribution coefficient of radiostrontium will be a close reflection of the overall K_D value of the bivalent ions (Ca and Mg) in the system. In particular, we may expect

$$K_D(Sr) = K_D(M) \cdot K_c(Sr/M) \qquad (6)$$

in which $K_D(M)$ refers to the overall K_D value of the two bivalent ions in the system and $K_c(Sr/M)$ to the Sr-to-M selectivity coefficient in the exchange complex. Eqn(6) has the same format as eqn(2), applied to the overall exchange complex, except for the fact that the amplification factor $K_c(Sr/M)$ is near unity.

This working hypothesis was tested for a set of 3 agricultural soils (sandy,loam,clay) and eight upland soils from Cumbria (discussed in the section on caesium). For the first set, $K_D(Sr)$ measurements (duplicate) were measured in distilled water dispersions at solid/liquid ratios of resp. 1/20, 1/10, 1/5 and 1/2. For all scenarios, exchangeable levels of Ca+Mg and their equilibrium concentrations in solution were measured. The statistical average (24 measurements) of the ratios $K_D(Sr)/K_D(M) = .97(\pm.41)$, a result which is in excellent agreement with expectations based on eqn(6). Similar results were obtained in the case of the Cumbrian soils. Table II shows a summary of the results.

Table II. A comparison of $K_D(Sr)$ and $K_D(Ca+Mg)$ in eight Cumbrian soils; disperion in 10^{-3}M KCl solutions in solid/liquid ratios of 1/20. Data are averages of duplicate measurements

Soils	$K_D(Sr)$	$K_D(Ca+Mg)$	$K_D(Sr)/K_D(Ca+Mg)$
Acid brown earth-1	260	179	1.45
Acid brown earth-2	123	74	1.66
Podzolized brown earth	202	150	1.35
Peaty gley	617	302	2.04
Peat ranker-1	377	218	1.73
Peat ranker-2	648	234	2.77
Deep peat	763	753	1.01
Improved peat ranker	641	621	1.03

The overall statistical average of the $K_D(Sr)/K_D(M)$ ratio is 1.63(±.54), again a result which agrees reasonably well with predictions based on eqn(6). Consequently, it would appear that $K_D(Sr)$ could be reasonably well predicted on the basis of the Ca,Mg status in the solid and liquid phase of the system. Whether this conclusion holds for field conditions remains to be confirmed by measurements under conditions approximating those prevailing in the field (low water content).

TECHNETIUM

Field and laboratory observations have demonstrated that technetium, when introduced as TcO_4^- in soils or sediments gradually shifts towards immobilized, solid-state associated forms, as evidenced by the low aqueous extraction yields. The necessary condition for such a process is the existence of reducing conditions, either in the bulk of the system (sediments) or in localized niches, commonly occurring in otherwise oxic soils, as generated by microbiological action.

A systematic study was carried out on the effect of a reducing environment (induced by either microbiological or physico-chemical means) on the dynamics of the behaviour of Tc in soils and sediments. Special efforts were directed towards identifying the forms and reactivity of the Tc-compounds generated in the process. The key features of the results can be briefly summarized as follows: (a) the reductive immobilization of Tc is a fairly rapid process which is generally completed within a few days, provided redox conditions are adequate; (b) the effect of microbiological action is essentially indirect through the generation of reducing conditions; (c) the bulk fraction of Tc is being scavenged in humic acid complexes; (d) the reductive complexation process proceeds at a significantly higher rate than the reoxidation process; (e) the reoxidation of reduced Tc forms is a heterogeneous process, that can be described in terms of an array of first order rate processes characterized by half-life values ranging from a few days up to four months; (f) Once technetium has been scavenged into some reduced form, it is characterized by a pronounced loss of reactivity, i.e. a very restricted rate of interchange among immobilized Tc-forms; (g) the TcO_4^- species appears to be the only one which is plant available; (h) the plant uptake of Tc from soils is describable in terms of the effective TcO_4^- level in the soil solution and the uptake behaviour, as studied in hydroponic systems; (i) alternating redox conditons lead to the formation of less readily oxidizable Tc-forms.

On the basis of these findings, a fairly coherent picture has emerged for the behaviour of Tc in soils and sediments, enabling the formulation of a working hypothesis for its long-term behaviour in environmental systems. A clear distinction has to be made between (a) systems which are permanently reducing and (b) those which are subjected to alternating redox regimes. For the first category (e.g. sediments), provided the pH-redox regime is adequate, Tc will be permanently scavenged in reduced forms, its bioavailability and geochemical mobility being radically curtailed in the process. Such a process is expected to be a matter of days. For the second category, the situation is somewhat more complex. In view of the fact that the rates of reduction significantly exceed the rates of reoxidation, some steady shift of Tc is bound to occur towards reduced (complexed) forms, as is in fact observed in field conditions. Moreover, on the basis of the wide range or reoxidation rates of reduced

Tc-forms, it can be predicted that, in alternating redox regimes, the most readily oxidizable Tc forms will preferentially decay into TcO_4^- which, upon a return to reducing conditions, will be redistributed among easily and poorly reoxidizable forms. A a result, cyclic changes in redox conditions are bound to lead to shifts of Tc into more refractory, i.e. highly oxidation-resistant forms. At some stage, the system can be expected to evolve towards some (soil textural and climate dependent) steady state corresponding to a condition of dynamic equilibrium between the sizes of the two Tc-pools and their respective decay rates. The aging process of Tc in soils therefore evolves towards a characteristic fraction, remaining available as TcO_4^-. In conclusion, a systematic study on the kinetics of Tc-uptake in hydroponic systems and soils has demonstrated that the soil-to-plant transfer process can quantitatively be interpreted in terms of the effective TcO_4 levels in the interstitial soil solution and TcO_4 uptake kinetics from nutrient solutions.

EUROPIUM

The main objective of this programme is the assessment of the geochemical phase association of europium in soils and sediments. In the early stages considerable efforts were directed towards improving methodologies for quantifying the binding strength of europium to humic acids (HA) and oxides. In particular, the experimental study of the binding of radionuclides by humic acids requires methodologies for measuring the nature and the capacities of the functional groups aund Eu-HA stability constants. The following methodological developments have taken place in the course of this project.

Titrimetric HA characterization

Acidimetric titrations were carried out on a series of HA's of different origin, making use of an automated and completely informatized titration system at the chemistry department of Glasgow University and currently set-up at the Leuven laboratory. The procedure allows the identification of various functional groups by plotting the titration data differentially in terms of the pH change per unit added base or acid. In general, two to three peaks, corresponding to different functional groups can be identified. A thorough theoretical investigation demonstrated that the polyelectrolyte behaviour can be accounted for by considering the Gibbs-Donnan model for polyelectrolyte systems. It follows from this approach that dissociation constants, obtained at high ionic strengths, are very close approximations of the intrinsic dissociation constants because neither electrostatic potential nor Donnan potential effects occur under such conditions.

Complexing capacity of HA

A new method has been developed for measuring the functional group capacity of HA, either in a mixed sediment or soil or a very dilute HA extract. The method is based on the strong coagulating effect of cobalti-hexammine (Cohex) on HA: the addition of an amount of Cohex, equivalent to the functional group capacity leads to quantitative HA coagulation. Analysis of the pH-dependence of the functional group capacity, obtained by using Co-60 labelling, clearly demonstrates the occurrence of the two functional groups (carboxylic, phenolic): the capacity of the COOH-groups,

obtained by this method, agrees with the result obtained by the classical Ca-acetate method. Charge densities and acid dissociation constants obtained by this procedure agree almost perfectly with results obtained by titration techniques under conditions of high ionic strength.

Europium-HA stability constants

A new procedure has been developed for obtaining the Eu-HA stability constants in slightly alkaline conditions, a scenario common for most sediments. This procedure was applied to a variety of humic acids from different origin and at ionic strength of .01 and .1. It was demonstrated that Eu-HA complexes of well-defined 1-1 stoechiometry were formed, characterized by stability constants in a rather narrow range of 13 to 14 for log K at pH 9. Classical ion exchange procedures were used for obtaining Eu-HA stability constants at near-neutral (pH 6) conditions. Again for the various HA samples studied a rather narrow range of log K (7 to 8) was found, irrespective of the origin. These results allow to predict that, in many environmental scenarios, typical for surface waters and sediments, Eu will occur chiefly as a Eu-HA complex.

ZINC

The behaviour of zinc, which is representative for a number of activation elements, was studied in regard to its geochemical phase association with the different subphases in soil systems. In the long run, such study paves the way to a better understanding of the mechanisms which determine the in situ soil solution concentration of free metal ion, available for plants. The main emphasis in this study is on the partitioning of zinc between oxides and soil organic matter and the relative importance of processes such as ion exchange, complexation and specific sorption as retention mechanisms. The main components addressed in this study are the organic matter enriched B-2h horizon of a podzolic soil, a humic acid extract of this horizon and goethite, a model oxide.

Examination of acid-base properties of metal-oxides (goethite) shows that their dependence on ionic strength is quite similar to that observed with humic materials. This observation opens possibilities to compare acid-base characteristics and complexation properties of different subphases in soils and sediments and to estimate their relative importance for metal complexation.

Comparison of overall apparent equilibrium binding constants and of overall proton release/metal cation adsorbed ratios indicate a greater affinity of zinc cations for the podzol soil and a higher number of protons released per metal cation adsorbed for the goethite system.

Masking the negative charge on the podzol sample with cobaltihexammine, followed by adsorption of Zn^{2+}, demonstrates that this last cation can adsorb on the podzol sample both as inner sphere and outer sphere complex. On the goethite sample on the contrary, below the zero point of charge (8.5), only inner-sphere complex formation can occur because no positive charge can occur below this pH. The fact that the presence of cobaltihexamine has no effect at all on the adsorption behaviour of Zn^{2+} proves this.

The adsorption behaviour of Zn^{2+} on mixed systems of goethite and podzol can be described reasonably well by an adapted multiple site adsorption model. The results show that the partitioning of zinc between the two phases was strongly dependent on pH and on the oxide-organic matter ratio, as illustrated in figure 4. The model used can not fully describe the adsorption behaviour of the metal cation, probably due to complex formation with dissolved organic ligands and their interactions with the oxide surface.

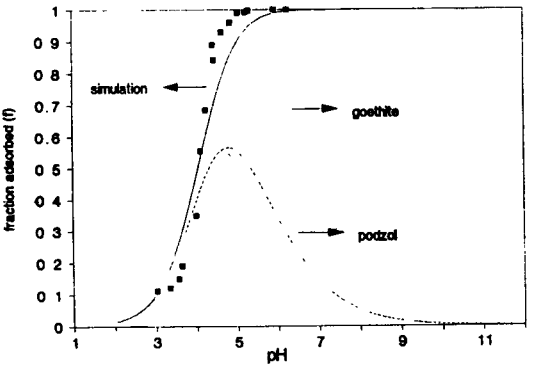

figure 4. Simulation of the Zn^{2+} adsorption edge on a mixed system with an oxide-podzol ratio of 1/4. Both simulation of total adsorption and simulation of the partition between oxide and podzol phases are shown.

IV. Other research group(s) collaborating actively on this project [name(s) and address(es)]:

- Laboratoire de Biochimie et de Radiochimie (J.Pieri), Université de Nantes, France
- Harwell Laboratory, Environmental & Medical Sciences Div. (J.Sandalls), Harwell Laboratory, United Kingdom.
- Unité de Physiologie Végétale (C.Myttenaere), Université Catholique de Louvain.

V. Publications:

1. Publications in scientific journals

- MAES A. and CREMERS A. Radionuclide sorption in soils and sediments: oxide organic matter competition in: "Speciation of Fission and Activation Products in the Environment" (eds. R.A.Bulman and J.R.Cooper). *Elsevier Appl.Sci.Publ.* 1986, 93-100
- CREMERS A. and MAES A. Radionuclide Partitioning in Environmental System. A critical analysis, in "Application of Distribution Coefficients to Radiological Assessment Models" (eds. T.H.Sibley and C.Myttenaere). *Elsevier Appl.Sci.Publ.* 1986, 4-14.
- STALMANS M., DE KEIJZER S., MAES,A. and CREMERS A. Europium Organic Matter Associations in a Campine Podzol, in "Application of Distribution Coefficients to Radiological Assessment Models" (eds. T.H.Sibley and C.Myttenaere) *Elsevier Appl.Sci.Publ.* 1986, 111-119.
- VAN LOON L., DESMET G., CREMERS A. The uptake of TcO_4 by plants: A Mathematical Description. *Health Physics*, 1989, 57, 309-314.
- CREMERS A., ELSEN A., DE PRETER P and MAES A. Quantitative analysis of radiocaesium retention in soils. *Nature*, 1988, 335, 247-249.
- MAES A., DE BRABANDERE J. and CREMERS A. A Modified Schubert Method for the measurement of the stability of Europium Humic Acid Complexes in Alkaline Conditions. *Radiochimica Acta* 1988, 44/45, 51-57.
- MAES A., VAN ELEWIJCK F., VANCLUYSEN J., TITS J. and CREMERS A. Cobaltihexammine as an index cation for measuring the cation exchange capacity of humic acids. Lecture notes in *Earth Sciences*, 1990 (in press).
- MAES A. and CREMERS A. Assessment of the capacity for complexation in natural organic matter. Proc. Int. Symp. Fertilization and the Environment, 1990 (in press).
- TITS J., BIGARE H., MAES A. and CREMERS A. The behaviour of Zinc in mixed oxide-podzol Bh-systems. Proc.Int.Symp. Fertilization and the Environment, 1990 (in press).
- MAES A., DE BRABANDERE J. and CREMERS A. Complexation of Eu^{3+} with humic substances. *Radiochimica Acta*, 1990 (in press).

- DE PRETER P., LUYTEN S. and CREMERS A. Specific sorption of poorly hydrated cations in clay Minerals: A quantitative Analysis. *Clay Minerals*, 1990 (in press).
- DE PRETER P., VAN LOON L., MAES A. and CREMERS A. Solid/liquid distribution of radiocaesium in Boom Clay: A quantitative Interpretation. *Radiochimica Acta*, 1990 (in press).
- SWEECK L., WAUTERS J., VALCKE E. and CREMERS A. The specific interception potential of soils for radiocaesium. Proc. Int. Workshop: The transfer of Radionuclides in Natural and Semi-Natural Environments. *Elsevier Appl.Sci.Publ.*,1990 (in press).
- CREMERS A., ELSEN A., VALCKE E., WAUTERS J., SANDALLS F.J. and GAUDERN S.L. The sensitivity of upland soils to radiocaesium contamination. Proc. Int. Workshop: The transfer of Radionuclides in Natural and Semi-Natural Environments. *Elsevier Appl.Sci.Publ.*,1990 (in press).

2. Conference abstracts

- STALMANS A., MAES A. and CREMERS A. Technetium-organic matter associations in soils: Methodological Aspects. Int.Workshop on the Behaviour of Technetium in Terrestrial and Aquatic Environments. Seattle 1986.
- STALMANS A., MAES A. and CREMERS A. The fate of technetium in soils and sediments: A physico-chemical approach. Int.Workshop on the Behaviour of Technetium in Terrestrial and Aquatic Environments. Seattle 1986.
- MAES A., HENRION P., DE BRABANDERE J. and CREMERS A. Europium-humic acid complexes in reducing conditions. Int. Conf.Chemistry and Migration Behaviour of Actinides and Fission Products in the Geosphere. Munich 1987.
- CREMERS A., ELSEN A. and MAES A. Solid/liquid distribution of radiocaesium and radiostrontium under in situ conditions. IVth Int.Symp.Radioecology, Cadarache, 1988.

3. Theses

Doctoral

- STALMANS M. The behaviour of technetium in the environment. Physicochemical aspects. 1986.
- VAN LOON L. Kinetic aspects of the soil-to-plant transfer of technetium. 1986.
- DE BRABANDERE J. Humic acid complexation of Europium in Boom clay. 1989.
- DE PRETER P. Radiocaesium interception in environmental substrates: a quantifying analysis. 1990 (in press).
- TITS J. Geochemical association of zinc in soils. 1990 (in press).

Master

- DE BRABANDERE J. & VAN ELEWIJCK F.; De invloed van mikro-organismen op yhet fysico-chemisch gedrag van technetium. 1985.
- CLAESSEN F. Methode ter bepaling van transitiemetaalspeciatie in bodems en sedimenten. 1985.
- STERCKX D. Studie van de fysicochemische faktoren die de distributie van technetium en europium in een podzolbodem bepalen. 1986.
- BIGARE H. Modelsystemen in de bepaling van de zink-speciatie in bodems. 1988.
- CLERCX N. Hoog selektief sorptiegedrag van cesium op referentie-mineralen. 1988.
- VAN LAER G. De "in situ" distributie van radionukliden in bodems. 1988.
- VERCAMBRE F. De interaktie van technetium met verschillende organische stoffrakties van podzol en Boomse klei. 1988.
- LUYTEN S. Kwantitatieve karakterisatie van hoog selektieve cesium sorptie sites. 1989.
- POLLAERT J. De kwantitatieve interpretatie van radiocesium distributie in rivier- en estuarium sedimenten. 1989.
- VALCKE E. & WAUTERS J. Radiocesiumretentie in bodems en sedimenten. Een kwantitatieve interpretatie. 1989.
- VAN HEMELRIJCK M. Studie van de adsorptiemechanismen van Zn^{2+} op de podzol B_{2h} horizont. 1989.

RADIATION PROTECTION PROGRAMME
Final Report

Contractor:

Contract no.: BI6-B-218-IRL

Nuclear Energy Board
3 Clonskeagh Square
Clonskeagh Road
IRL- Dublin 14

Head(s) of research team(s) [name(s) and address(es)]:

Dr. J.D. Cunningham
Nuclear Energy Board
3 Clonskeagh Square
Clonskeagh Road
IRL- Dublin 14

Telephone number: (1) 69.77.66

Title of the research contract:

Assessment of the radioactivity levels in Irish soils and their transfer into agricultural produce as a result of the Chernobyl accident.

List of projects:

1. Assessment of the radioactivity levels in Irish soils and their transfer into agricultural produce as a result of the Chernobyl accident.

Title of the project no.: B16-B-218-IRL

Assessment of the Radiocaesium Levels in Irish Soils and their Transfer to Crops

Head(s) of project: Dr Geraldine Mac Neill

Scientific staff: Dr Geraldine Mac Neill
Mr Jarlath Duffy
Dr John O'Grady

I. Objectives of the project:

The presence of radioactive contamination after the Chernobyl accident provided an opportunity to study the transfer of radiocaesium from different types of Irish soils into various crops.

The principal objectives of the research project were to study the levels of radiocaesium in Irish soils and to estimate soil to plant concentrations ratios for various types of agricultural produce. Factors influencing the transfer process were studied by considering the behaviour of deposited radionuclides in different soils and through a detailed examination of the soil characteristics.

II. Objectives for the reporting period:

(i) To complete radiometric and chemical analysis of soil and crop samples collected during 1988

(ii) To prepare a final report

III. Progress achieved:

1. PROJECT DESCRIPTION

A total of eleven farm sites were selected for sampling. The locations of the sites were chosen so that the principal soils used for agricultural purposes in Ireland were represented. These sites provided as wide a range as possible of texture, moisture regime and parent material characteristics. Where possible, the sites were located in areas which had suffered high deposition following the Chernobyl accident. A final selection criterion was that common agricultural produce should be available at all sites.

The soil types at the selected sites included Brown Earths, Grey Brown Podzolics, Gleys, Peat and Brown Podzolics.

1.1 Sampling Procedure

The samples collected included soil and grass from permanent pasture land, soil from tillage land and also samples of the crops grown there. With regard to the latter, it was decided to concentrate on three main types - wheat, barley and potatoes. These were expected to be widely available and this would enable comparison of results from different locations. Some additional vegetable samples were collected where available, particularly in areas which concentrated on vegetable rather than cereal production.

Sampling was carried out between spring and autumn of each year. Sampling of soil from pasture and tillage land was carried out twice yearly. Samples of grass were taken simultaneously with an additional sampling round for grass in the intervening period. Crops were sampled just prior to harvest.

Soil from the pasture land was taken using 4 corers of decreasing diameters, one for each of the depths 0-5cm, 5-10cm, 10-15cm and 15-30cm. The cores were taken at 25 points scattered over an area of approximately $10^4 m^2$ and bulked to form 4 samples one for each depth. The soil was then oven dried at 35°C and sieved to 2mm.

Sampling of tillage land was carried out using a single 0-20cm corer. This depth was selected to correspond with the ploughing depth in most areas. A total of 20 cores was taken from an area of approximately $10^4 m^2$. Sample preparation was as for the pasture soil.

Grass samples were cut from a height of approximately 5cm above the ground using a shears. The grass was then air dried at 20°C for 5 days, then oven dried at 40°C, milled and sieved to 1mm mesh.

Cereal samples were taken, a few days before they were due to be harvested, from 1mX20cm plots scattered over an area of approximately $10^4 m^2$. The samples were then air dried before being thrashed. No further sample preparation took place.

Potato samples were collected at the time of harvest. The potatoes were scrubbed clean and then oven dried at 105°C. They were then ground using a laboratory blender to ensure homogeneity for gamma spectrometry.

1.2 Methods of Analysis

Soil samples from the first sampling round were analysed for particle size, cation exchange capacity, pH, total carbon content, exchangeable cations and total potassium, using standard methods. All of these tests with the exception of those for percentage clay and carbon were repeated on the second round samples. The specific activities of all soil and crop samples were measured using gamma spectrometry.

2. RESULTS OF ANALYSIS

All gamma spectrometric analysis results have been backdated to the 3rd May 1986. This was done to facilitate data handling and also to allow comparison of samples from successive years. The computation of concentration ratios will not be affected by this approach. All measurements of specific activities refer to dried weight of samples and are quoted at the 95% confidence level.

2.1 Pasture Soil

Pasture soil was sampled in the spring and autumn of 1987 and 1988. Comparison of data from the four sampling rounds shows that there has been very little downward migration of caesium. In October 1988 (the final sampling round of the project), between 63 and 95% of the Chernobyl deposited caesium was still retained in the upper 5cm of soil at the various sites and in fact greater than 90% of the Chernobyl caesium was still within the 0-10cm layer at that time. Based on the known ratio of Chernobyl Cs-137 to Cs-134, the amount of pre-Chernobyl Cs-137 in the soil can be calculated. The mean Chernobyl caesium-137 activity concentration in pasture soils as a function of depth in 1987 and 1988 at a typical site is shown in Figure 1. Pre-Chernobyl caesium-137 is shown in Figure 2.

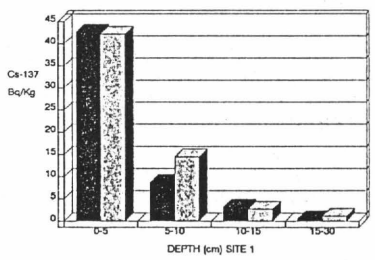

Fig 1. Mean Chernobyl Cs-137 in pasture soils as a function of depth in 1987 and 1988

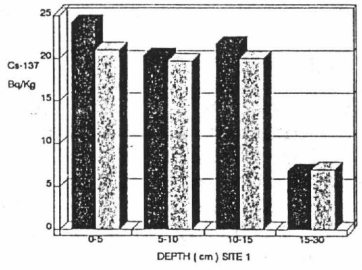

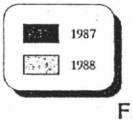

Fig 2. Mean Pre-Chernobyl Cs-137 in pasture soils as a function of depth in 1987 and 1988

It would appear that there has been very little migration beyond a depth of 15cm because at most sites more than 70% of the caesium from weapons fallout is still contained within the 0-15cm layer.

The measurements on pasture soil can be used to estimate the deposition per unit area of Chernobyl caesium at the eleven sites. Calculated values for 1987 ranged from 771Bq/m² to 4714Bq/m². This is an underestimate of deposition because it does not include a contribution from the material that was rejected during the sample preparation process. After sieving to 2mm the remaining soil can be as little as 43% by weight of the original sample.

Activity concentrations of potassium-40 in the 0-5cm layer for 1987 and 1988 ranged from 54 Bq/kg at site 8 (a peat soil) up to 661 Bq/kg at site 1 (a clay loam soil). The results show that there was little variation over the four sampling rounds.

2.2 Tillage Soil

Over the two year sampling period there were a number of changes in the sampling areas because of crop rotation by farmers. Where possible the new sampling area was selected to be close to the old one. Because of this change in sampling location, it is difficult to compare activity concentrations in soils from successive years. In general the greatest variation between 1987 and 1988 measurements was seen where the sampling area had been changed. The variations in unchanged sites did not show any obvious trends and were probably due to the uneven mixing of Chernobyl deposited nuclides in tilled soil.

2.3 Grass Samples

Levels of Cs-137 in grass ranged from 2.0 Bq/kg to 82.5 Bq/kg in 1987 and from 1.2 Bq/kg to 26.1 Bq/kg in 1988. Cs-134 levels were approx half those of Cs-137.

In 1987 there seemed to be a general trend of decreasing activity concentration between the first and third sampling rounds with the exception of sites 1 and 8. At these sites the levels decreased between the first and second rounds but then increased in the third round to a level higher than the first.

Measurements from the second sampling round showed no obvious pattern relative to either the first or third sampling round. The absence of a definite pattern in activity concentration between sampling rounds may be partly due to the stage of growth of grass at different sites which varied as a result of different grazing patterns.

Any trends in 1988 were even less evident than in the previous year. At most sites levels of caesium were higher in the third sampling round than the first. Second round values showed no definite pattern. Comparing measurements from 1987 and 1988, levels from the spring sampling round in 1988 were

significantly (by a factor of between 4.5 and 13) lower than those observed in the corresponding 1987 sampling round. There was one exception to this and that was site 1 where levels were similar in the two rounds. Site 1 was somewhat unusual as in the second year of sampling (1988) the pasture had been grazed by sheep. This meant that the grass was very short at the time of sampling and may not be directly comparable to that obtained at other sites.

Comparing activity concentrations from the autumn sampling rounds of the two years, we see that at eight sites levels were lower in 1988 than in 1987. However, the difference observed was not as great as for the first sampling rounds of each year with most 1987 autumn values being less than a factor of 2.5 greater than the 1988 values. Site 8 was the exception here with the 1987 values being approx. 5 times that of the 1988 measurements.

Comparing the two summer sampling rounds a similar pattern is seen with eight of the eleven sites having lower values in 1988 than 1987.

Potassium analysis was carried out on the 1987 grass samples in order to assist in the determination of the stage of growth. It was thought that this might explain the lack of any significant trends between sampling periods.

2.4 Grain Samples

In 1987 the Cs-137 activity concentrations ranged from 0.11 Bq/kg to 0.41 Bq/kg. The corresponding range in 1988 was between 0.17 Bq/kg and 0.35 Bq/kg. In general the levels of Cs-134 were below the limits of detection. Because the activity concentrations of both Cs-137 and Cs-134 were relatively low the associated errors are large. This makes comparison between successive years or between different sites almost meaningless. It also means that any attempt at correlating activity concentrations with soil parameters is unlikely to yield any useful result.

At site 5 samples of oats were collected because there was no wheat grown in that area. In 1987 the measured activity concentration of Cs-137 was 0.51 $\pm$ 0.20 Bq/kg and in 1988 the measured value was 0.43 $\pm$ 0.20 Bq/kg.

Specific activities of K-40 in grain ranged from 110 Bq/kg to 180 Bq/kg for barley and from 100 to 210 Bq/kg for wheat.

2.5 Potatoes.

Activity concentrations of Cs-137 in potatoes in 1987 ranged from 0.57 up to 3.5 Bq/kg. The 1988 values were between 0.1 and 3.8 Bq/kg. The highest value in samples from both years were seen at site 8 where the soil is peat.

Measured Cs-134 values ranged from 0.31 to 2.5 Bq/kg, but for many samples the levels were below the limits of detection.

The K-40 levels ranged from 472 to 835 Bq/kg with site 2 (clay loam) having the highest value both years.

2.6 Vegetables

Site 8, a peat soil, although not suitable for cereal production was highly suitable for the cultivation of vegetables. For this reason some additional vegetable samples were taken at this site. In addition to potatoes, samples of carrots, onions and parsnips were collected. The highest specific activity of Cs-137 observed in vegetables was in a carrot sample collected in September 1987 which had 55±5 Bq/kg. Relatively high concentrations were also observed in parsnips collected in February 1988. This sample contained 36.9±1.8 Bq/kg of Cs-137. Carrots sampled at this time, from the same plot, were found to contain 31.2±2.2 Bq/kg.

3. CALCULATION OF CONCENTRATION RATIOS

Concentrations ratios have been calculated at each site for all of the individual sampling rounds and plant types. The concentration ratio (CR) is defined as the ratio of activity concentration in the dried plant matter to that in the soil. For tillage crops the soil specific activity is that which was measured in the 0-20cm layer. For pasture, the 0-5cm layer was used.

In the case of grass, three Cs-137 CR values were calculated for each site in 1987 and 1988 corresponding to the three sampling rounds in each year. As soil was only collected in the first and third sampling round each year, the mid season value was calculated using an average soil activity concentration based on the other two rounds. CR values for Cs-134 and K-40 were calculated in a similar manner.

Concentration ratios for the tillage crops were calculated in the following way. Soil activity concentrations for Cs-137, Cs-134 and K-40 were averaged over the two sampling rounds. These values of Cs-137, Cs-134 and K-40, one each for 1987 and another for 1988, were then used with the measured plant specific activity from each year to compute the CR values. Because of the low activity concentrations observed in tillage crops, the errors associated with the CR values are large. In fact in many cases the Cs-134 in the plant was below the minimum detectable limit.

3.1 Concentration Ratios in Grass

In the first sampling round in 1987 values for the Cs-137 CR ranged from .033 to .49. The range in the corresponding round in 1988 was from .016 to .076. Final round values in 1987 were between .05 and .21 and in 1988 ranged from .021 to .11. Concentration ratios of Cs-137 in grass for May 1987 and May 1988 are shown in Figures 3 and 4.

Fig 3. Concentration ratios of Cs-137 in grass for May 1987

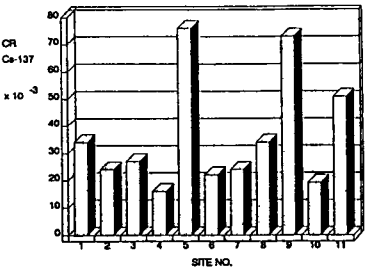

Fig 4. Concentration ratios of Cs-137 in grass for May 1988

Comparing the CR values for Cs-137 in the first and third sampling rounds of 1987, there seems to be a general trend towards lower values in the latter. Exceptions to this were site 8 (a peat soil) where the CR in the third round was higher than the first and site 1 where the CR did not vary much over the three sampling rounds. In 1988, however, most of the third round CR values were higher than those in the first. Some sites showed very little variation over the three sampling rounds.

As observed previously when considering the activity concentrations in grass, there was no apparent trend for second round values relative to either the first or third round.

Comparing CR values in the first round of 1988 to those observed in 1987 the 1988 values are seen to be lower with the exception of site 1 where the CR did not change. A similar pattern was seen at most sites when the third sampling rounds from the 2 years were compared although the decrease was less marked. An examination of soil activity concentrations over the two years shows that the decrease in transfer was unlikely to be due to caesium depletion. This might suggest that the Chernobyl deposited caesium had become less available with time leading to reduced transfer. However it is possible that the decrease between 1987 and 1988 was merely a fluctuation due to climatic or other effects. If this is the case then a longer term study over a number of years would be needed to show the real pattern of uptake.

Examining the range of values observed over the two years shows quite large variations in CR values between different sites. Site 5 (a heavy wet clay loam soil) generally shows the highest value of CR. Sites 8 (peat) and 9 (loam) also tend to have higher than average values.

CR values for K-40 have also been computed for grass. In 1987 these ranged from 0.26 up to 19, although most of the values lay between 1 and 6. In 1988 the CR values ranged from 1.24 up to 18.5. Site 8 had the highest values both years although the actual activity concentration of K-40 in the grass from site 8 was in fact comparable to that found at other sites.

3.2 Concentration Ratios for Grain

Concentration ratios for Cs-137 in wheat were generally less than .01 in 1987 and 1988. At most sites the Cs-134 in grain was below the limits of detection which meant that only upper limits could be set on the CR values (in general <.02).

Values for the Cs-137 CR for barley in 1987 were similar to those for wheat with a maximum value of .015 $\pm$ .004. The highest value in 1988 was .011 $\pm$ .006. Again only upper limits could be set on the Cs-134 CR values (in general <.03).

At site 5 oats were collected in place of wheat and Cs-137 CR values were calculated to have been .017 $\pm$ .007 in 1987 and .014 $\pm$ .007 in 1988.

CR values for K-40 have also been calculated for all grain samples. Values for wheat over the two years ranged from 0.16 up to .66. For barley the range was between 0.19 and 1.04. The highest value was observed at site 3 (a loam soil) in 1987. The following year the CR was 0.59 $\pm$ .06 at this site.

3.3 Concentration Ratios For Potatoes

In 1987 concentration ratios for Cs-137 in potatoes ranged from .017 to .07. The range in 1988 was between .005 and .067. There was no obvious decrease in CR values in 1988 compared to 1987. Again errors were large because of the low activity concentration in the plant. In most cases only upper limits could be set on Cs-134 CR values.

CR values for K-40 have also been calculated. In 1987 they ranged from 1.26 to 23 with the highest value being observed at site 8. In 1988 the range was between 0.93 and 5.9. Again site 8 had the highest value. Although the CR for site 8 in 1987 was almost an order of magnitude higher than other sites, the K-40 concentration in the plant was comparable to that observed at other sites.

3.4 Concentration Ratios for Vegetables From Peat Soil at Site 8

Concentration ratios have been calculated for vegetables sampled at site 8. For Cs-137, the highest value (.74 $\pm$ .07) was found for carrots in 1987. Carrots sampled in a different plot in February 1988 also showed a high CR value (.37 $\pm$ .03). Parsnips sampled at the same time and on the same soil showed a CR of .43 $\pm$ .02. However carrots sampled later that year (1988) from a different plot showed a CR of .03 $\pm$ .01. It may be worth noting that the K_{ex} in the soil from which these carrots were sampled was approx twice that found at the

other carrot plots. Similarly, the potatoes which also had somewhat lower CR values (.07 in 1987 and .04 in 1988) came from soil with relatively high K_{ex}.

Onions sampled in 1988 showed a low transfer of Cs-137 to the plant with a CR of <.01.

CR values for K-40 in carrots ranged from 26 $\pm$ 10 to 63 $\pm$ 46. This indicates less variation in potassium transfer than in caesium transfer for these samples.

K-40 CR values for other vegetable samples ranged from 5.9 $\pm$ 0.9 (potatoes 1988) to 27 $\pm$ 4 (parsnips 1988).

4 RESULTS OF STATISTICAL ANALYSIS

4.1 Comparison of Grass Concentration Ratios

The Cs-134 and Cs-137 concentration ratios for grass in 1987 and 1988 were compared in an attempt to identify any difference in availability between Chernobyl and weapons caesium.

The CR values from all three sampling rounds in 1987 and 1988 were converted to normal ranks using the method of Blom and an analysis of variance then applied to the ranked data. No significant difference was found between the Cs-134 and Cs-137 concentration ratios. We may then conclude that either there is no difference in availability between Chernobyl and weapons caesium or that the study has produced insufficient data to disclose a difference if one exists.

4.2 Correlation of Concentration Ratios With soil Parameters

Linear regression analysis has been used to try and identify any factors which may influence the transfer process. The CR values computed for grass have been used along with the measured soil parameters. Both simple and multiple regression techniques have been used.

For grass, because the soil parameters were measured only at the time of the first and third sampling round each year, only the CR values corresponding to these rounds have been used in the regression analysis. This means that there are two sets of Cs-137 CR values from each year. Simple regression has been used to try and correlate the Cs-137 CR values with each of the following parameters in turn: K_{ex}, pH, %carbon, Na_{ex} and CEC. There is no evidence of a consistent relationship between the CR and any one of these parameters. However, looking at the 1987 results in isolation the Cs-137 CR seems to be negatively correlated with soil pH (relationship significant at the 5% level for the first round and at the 10% level in the next round). The 1988 CR values do not support this result. This would suggest that although pH does seem to influence uptake, there are other factors which must be taken into consideration. It would appear that these factors tend to mask the effect of pH in 1988.

Multiple regression was used to try and correlate CR with various combinations of the soil parameters. Again no results consistent over the two years were obtained.

Linear regression was also used to try and correlate the first round (1987) CR with the final round (1987) CR and similarly for 1988. This was done to see if there was some kind of temporal variation of the CR which would follow a similar pattern at all of the eleven sites. However, no correlation was found. Similarly an attempt to correlate the Cs-137 CR of each round with the corresponding K-40 CR was unsuccessful. It had been thought that perhaps the caesium transfer might follow that of potassium.

Potassium analysis had been carried out on the grass from 1987 in order to try and determine stage of growth of the samples. It was thought that this might explain the lack of any apparent trends between the second round and either the first or third round of each year. Regression of the Cs-137 CR with the potassium in the grass showed a negative relationship for all three rounds in 1987 (significant at the 5% level for the first two rounds and at the 20% level for the final round, correlation coefficients=.69, .61 and .43 respectively).

Linear regression of the K-40 CR from the first round in 1987 on the K-40 CR from the final round in 1987 produced a correlation coefficient of 0.98 and significant T values. Similar results were found in 1988. The linear relationship with a slope that is not unity and a non zero intercept may suggest a seasonal variation in the K-40 transfer process which follows a similar pattern at the different sites. Regression of K-40 CR values with soil potassium (both exchangeable and total available) produced no significant relationships.

Because of the low activity concentrations measured in tillage crops, particularly grain, in many cases only upper limits could be set on the CR values. For this reason regression analysis has only been carried out on the CR values computed for Cs-137 in potatoes. A negative correlation with pH (correlation coefficient =.68, regression coefficients significant at the 5% level) was found in 1988. This relationship had not been observed in 1987. No other significant relationships were found using either simple of multiple regression.

5. CONCLUSIONS

There are a number of conclusions that may be drawn from the results of this project :

It would appear that there has been limited downward migration of recently deposited caesium. In October 1988 more than 90% of caesium of Chernobyl origin was still retained in the 0-10cm layer of undisturbed soil. Measurements on specific activity of soil have also shown that in general more than 70%

of weapons deposited caesium is still contained within the upper 15cm of soil.

Based on the measured soil concentration of Cs-137, conservative estimates of Chernobyl deposition have been made. Calculated values, backdated to the date of deposition, range from 771Bq/m² to 4714Bq/m² of Cs-137.

In 1987 concentration ratios for Cs-137 in grass ranged from .033 to .49. The range in 1988 was between .021 and .11. In an investigation of the influence of soil parameters on transfer, a negative correlation with pH was observed in 1987. No other soil parameters were positively identified as influencing transfer. Comparison of Cs-137 and Cs-134 concentration ratios for grass failed to identify any significant differences between the two. There is therefore no evidence of a difference in uptake between pre- and post-Chernobyl deposited caesium.

Concentration ratios for Cs-137 in wheat and barley were generally less than .02 in 1987 and 1988. Concentration ratios for K-40 in these crops ranged from .16 to 1.04.

Concentration ratios were estimated for Cs-137 in vegetables grown in peat soil. The relatively high values observed (.37 to .74) may be due to the high organic content of the soil at this site or alternately may be due to the absence of clay minerals in the soil.
Some anomalous results for vegetables which showed somewhat lower CR values for Cs-137 (.03 to .07) may be explained in terms of higher levels of K_{ex} observed in the soil in which these vegetables were grown. The high concentration ratios observed at this site make it deserving of further study.

In conclusion the project has succeeded in evaluating concentration ratios for a range of crops grown in Irish soils. This had not previously been done. It has highlighted certain soil parameters (pH,K_{ex} and organic matter) which appear to influence transfer in certain conditions. Finally it has identified areas which may benefit from further work.

RADIATION PROTECTION PROGRAMME
Final Report

Contractor:

Comitato Nazionale per la Ricerca e
lo Sviluppo dell'Energia Nucleare e
delle Energie Alternative, ENEA
Viale Regina Margherita 125
I-00198 Roma

Contract no.: BI6-B-034-I

Head(s) of research team(s) [name(s) and address(es)]:

Dr. V. Damiani
Centro St.Amb.Mar., ENEA
Santa Teresa
Casella Postale 316
I-19100 La Spezia (SP)

Telephone number: 187/53.61.11

Title of the research contract:

Laboratory and field research on long-lived radionuclides in the marine environment.

List of projects:

1. Behaviour of Tc and Se in the marine environment.
2. Mechanisms involved in accumulation of transuranium in some compartments of the marine environment.
3. Descriptive models for circulation of radionuclides and transfer of radionuclides in the marine food chain.

Title of the project no.: 1

BEHAVIOUR OF Tc AND Se IN THE MARINE ENVIRONMENT

Head(s) of project: FROM 1985 - 1986: DR.G.ZURLINI

Scientific staff: FROM 1985 - 1987: Dr.PERONI, Dr.BIANCHI, Dr.ZURLINI, Dr.CANNARSA, Dr.ZATTERA, Dr.SCOPPA, Dr.SCHULTE, C.PAPUCCI
FROM 1987 - 1989: Dr.DELFANTI, Dr.SCHULTE, C.PAPUCCI

I. Objectives of the project:

A better knowledge on the environmental behaviour of long-lived radionuclides is necessary for the implementation of recent recommendations of ICRP, in particular for the assessment of collective dose committments deriving from operations, such as programmed or accidental releases from nuclear plants and radioactive waste disposal, where transuranium nuclides and other long-lived radionuclides (Tc-99, I-129, Se-79, etc.) may represent an important contribution to the radiological impact on man.

II. Objectives for the reporting period:

- separation and identification of different chemical forms of Tc, including complexes with naturally occurring ligands and sulphur containing aminoacids
- experiments in closed systems to elucidate mechanisms responsible for immobilization of Tc in anoxic sediments
- remobilization of Tc and Se from sediments by "bioturbation" considering different species of bottom-dwelling organisms
- macro- and microdistribution of Tc and Se in benthic fish utilizing autoradiographic methods
- bioavailability and metabolic aspects of inorganic and organic compounds of Se in selected marine organisms
- role of zooplankton in vertical transport processes of radionuclides in the water column
- analysis of Tc-99 in biological matrices from the Mediterranean.

III. Progress achieved:

1. METHODOLOGY

According to the research topics covered during the reporting period the methods used varied considerably from biotechnology, experimental approaches in aquaria to field studies. Therefore, the specific methodology applied for the achievement of results in the various research fields will proceed the different reports of results.

2. RESULTS

2.1. Separation and identification of different chemical forms, including complexes with naturally occurring ligands and sulphur containing aminoacids.

Anion exchange HPLC has been utilized for rapid separation of pertechnetate from complexed and reduced chemical forms of technetium. Experiments with commercial humic and fulvic acids from different sources have shown that under pH and Eh conditions occurring in most natural waters they don't bind neither adsorb pertechnetate. On the other hand, it is well known that in the presence of reducing agents or in anoxic situations there is formation of stable complexes of technetium with soil organic matter. Thus, it is clear that transformation of pertechnetate to a lower oxidation state is the preliminary step required for complexation of technetium by such naturally occurring ligands.
Studies on the reactions between pertechnetate and small biological molecules containing sulphydryl groups have been performed utilizing spectrophotometric and chromatographic techniques. Although in acid solution pertechnetate is rapidly reduced and complexed in the presence of excess cysteine, the reaction becomes very slow when the pH is increased.
The tripeptide glutathione (-glutamylcysteinylglicine) which represents the most important source of SH-groups in the cell, may react very slowly with pertechnetate.

The results obtained led to the conclusion that both cysteine and glutathione should not have a significant role in the metabolism of trace amounts of pertechnetate.

2.2. Experiments in closed systems to elucidate the mechanism responsible for immobilization of technetium in anoxic conditions.

The behaviour of soluble heptavalent Tc in the presence of an autoclaved marine sediment (1.64% of organic carbon, 1.98% of inorganic carbon and 0.11% of total nitrogen) has been studied at different, artificially-induced Eh values under laboratory conditions.

Initially, 25% of the soluble Tc was linked to the particulate phase at a potential of - 50 mv, while 78% of Tc disappeared from solution at a potential of - 137 mv. When positive values of Eh were restored, about 30% of the Tc which had linked to

the sediment was made again soluble. A low decrease of soluble Tc from 0.9 to 5.1% was observed in the control sediment kept in oxidized conditions (Eh equal to +312 mv) The Tc which remained in solution was heptavalent, whereas the not soluble form was tetravalent. These results point out the main role of bacteria in Tc fixation to sediments, as their metabolism bring about Eh reduction.

2.3.Remobilization of technetium from sediments by "bioturbation" considering different species of bottom-dwelling organisms

Efforts have been made to evaluate the importance of different bottom-dwelling benthic species with respect to biologically mediated processes of remobilization of Tc from sediments. So far, there is little information if anoxic sediments represent an ultimate sink for the relative high amount of Tc remaining fixed or if a remobilization of Tc may occur over longer time scales by biological activities in the sediment known as "bioturbation". In this context different benthic bottom-dwelling species were considered on the basis of their importance in reworking of sediments.

Two polychaete species were used having different feeding habits which may be important to the distribution and fate of radionuclides in sediments. Nereis sp., a surface deposit feeder, may be especially important in vertical transport processes from the surface to deeper sediment layers, while Marphysa bellii, a subsurface feeder, may play an important role in the remobilization and recycling of radionuclides from sediment to the water column.

The worms were kept in tubes having 25cm sediment depths with an overlaying water volume of 50ml which was sampled daily and checked for released radioactivity. The results showed a steady release of radioactivity from the sediment to the water. On the average 0.26-0.36% of the total Tc-95m present were remobilized per day in relation to the polychaete biomass present. After 49 days the overall percentages of Tc-95m removed were 13.89%, 18.13% and 13.07% for tube 1,2, and 3 respectively, while in the same period the blank without worm lost only 4.36% of the total Tc which correspond to 0.089% per day.
The radioactivity content of Tc-95m in the interstitial water was found to be only 0.15-0.21% of the total Tc present in the sediment. Thus, it can be assumed that at the beginning of the experiment all Tc was bound to the sediment. The lost radioactivty from the blank may be explained by diffusion processes in the upper sediment layers and reoxidation in the water column.
At day 28 of the experiment tube 4 received one specimen of Marphysa bellii (2.57g) which removed only 2.21% of total Tc-95m in 20 days, i.e. 0.11% per day. This low value may be due to the lower physiological activity of this polychaete compared to Nereis. However, concentration factors (CF) calculated at the end of the 49 days period showed a medium value in Nereis of CF 13.5+-4.6 while Marphysa reached a CF of

80.6. This higher CF may result from direct uptake of Tc-95m from the sediment since Marphysa ingests very often sediment and produces fecal pellets consisting totally of sediment grains.
Transfer factors (TF) of Tc-95m from sediments to worms were low and confirmed data from the literature. Nereis showed medium values of TF 0.25 while in Marphysa the TF was about four times higher, i.e. TF 1.112 confirming a higher sediment bound nutrition than in Nereis sp..
So far, the results of the laboratory experiments let presume that in areas of high polychaete population densities where Tc results bound in the upper 20 cm of the sediment, a considerable amount of the radionuclide may be remobilized by the biological activities of the infauna.
In the case of Selenium, aliquots of sediment were spiked with 144.3kBq of 75-Se-methionine, 85.5 kBq of 75-Selenite, and 91.6kBq of 75-Selenate under strict anoxic conditions and filled into tubes, one pair for each 75-Selenium form (3.2 cm; 35cm length; 8cm2 surface) of which half of them received specimens of the polychaete worm Marphysa bellii.
After 73 days, only very small fractions of the radioactivity of the different Se-forms were remobilized from the sediments by the worms and realesed to the water column and/or subsequentely to the air where they were trapped by active carbon.
Total remobilized fractions of radioactivity from Se-methionine, selenite and selenate contamined sediments amounted to 9.57; 6.61; and 6.13%, respectively. Of these percentages parts of 4.8; 3.1; and 3.3% were lost to the water, while the blanks without the worms' activity loss only between 0.62 - 0.73% of the total radioactivity present in the sediments, probably by diffusion processes. All blanks showed a distinct reoxidized sediment zone of 7 mm depth at the end of the experiment.
In all three experimental sets volatile forms could be detected and trapped on active carbon (Se-Met: 1.22; Selenite: 0.66; and Selenate: 0.79%). The contents of the different Se-forms in the sediment-dwelling worms were surprisingly low; only 2.92; 2.67; and 1.93% of the initial Se-methioline, selenite, and selenate, respectively, were accumulated in the polychaetes.
At the end of the experiment the sediments contained still 70-86% of the initial radioactivity according to the Se-forms. After centrifugation the radioactivity in interstitial waters of the sediment samples varied between 0.05-0.25% of the initial activity thus, it can be assumed that at the beginning of the experiment all radioactivity was bound to the sediment. Interstitial water contents of the sediment varied on a weight/weight basis from 17.7 to 21% in the presence of worms and from 36.1-37.6% in the blanks, demonstrating clearly the effectiveness of the biological activity of the polychaetes in strongly compacting superficial sediments.

Comparing the results to those of experiments made with Tc-95m under similar conditions it can be concluded that Se-forms are far more tightly bound to sediments than pertechnetate and consequently, their remobilization and recycling to the water column is a much slower process.

2.4.Macro- and micro-distribution of Tc and Se in benthic fish utilizing autoradiographic methods

Further results on the macro- and micro-distribution of Tc in Gobius sp. have been achieved using the long-lived isotope Tc-99 and autoradiographic methods. Fish accumulated Tc either from food (polychaetes) after Tc-uptake from water (~110Bq/l) or from polychaetes receiving an aliquot of Tc-99 injected into the body cavity (10 ul, containing 370 kBq). The fish were fed daily with radioactive worms (Tc-uptake form water) for more than two months while fish receiving freshly contaminated worms (Tc-injection) were sacrified after three days when digestion was completed. All specimens were embedded in methyl-cellulose at -70 C and then sectioned (50-100 um) with a cryomicrotome at -20 C. The slices were exposed to KODAK X-OMAT AR Films (XAR-5) for some months.

The results obtained showed no differences in accumulation sites in the fish body between the two accumulation modes of Tc-99 by the organisms. These results confirmed also previous observations obtained in the same fish species using the gamma-emitter Tc-95m. Althought Tc-95m-images were sufficiently clear, exposures to Tc-99 resulted in better images of Tc-distributions in the fish.

After the relative short exposure time to Tc-99, considerable amounts of this isotope were incorporated into bony structures (fin rays, scales i.e. whole body surface, cartilage of the head and vertebrae). The far most amounts of TC-99 were still in the small intestine while the large intestine was little less contaminated. Liver, kindneys, and gills occupied the next grade showing similar quantities of Tc-99 accumulated. In sagittal cuts along the vertebral column the nervous system (brain, medulla) showed clearly higher technetium levels than 0.089% per day. the liver. The same holds for the retina of the eyes and the lenses. As in previous experiences no technetium traces could be detected, also after very long exposure times (9 months), in muscle tissues; thus the most important edible part of the fish remained uncontaminated.

2.5.Bioavailability and metabolic aspects of inorganic and organic compounds of Se in selected marine organisms

The kinetics of accumlation and loss of Se-75 have been studied in the benthic crustacean Palaemon elegans using seleno-L-methionine marked with Se-75. The seleno-amino acid was chosen because in marine surface waters selenium is predominantly present as organic compounds such as amino acids and peptides of low molecular weight.
The accumulation of 75-Se-L-methionine from water (370kBq/101) by the shrimp was followed for 25 days using two groups of 30 specimens each.
After 25 days of accumulation no equilibrium was reached by the shrimp and accumulation continued linearily. At the end of the accumulation phase 10 individuals were dissected and the organ distribution determined. The concentration factor of the whole organism had reached a value of more than 400. Most of the radioactivity was found in the hepatopancreas with a CF of

about 4000 followed by gills (CF 1300) and stomach (CF 800).
The release of 75-Se-methionine by the shrimp was observed for 59 days. At regular time intervals five specimens were dissected and the distribution of the radioactivity determined in the various organs and tissues. The release kinetic of selenium by the shrimp was characterized by three distinct phases: a fast phase, responsible for the elimina- tion of about 30% of the body burden of Se-75 fixed in the hepatopancreas and stomach, a medium phase which represents 52% of the total Se-75 and regards most of the remaining organs and a slow phase eliminating 18% of the total radioactivity localized in muscle tissues. The biological half-lives of 75-Se-methionine in the three compartments have been calculated to 2.3 days (digestive system), 15.4 days (remaining organs and tissues), and 138.6 days (muscle tissue).
About 90% of the 75-Se-methionine have been found in proteins (precipitation by Trichloroacetic acid) while the remainder was present as selenoamino acids or peptides. Thus, one can assume that 75-Se-L-methionine is incorporated into proteins and substitutes the essential amino acid L-methionine.
During the experiments high mortalities could be observed in the shirmp which were attributed to the chemical toxicity of L-seleno-methionine, highly accumulated in some organs (digestive system) although the initial concentration in the water was extremely low (1nM).
These results require further studies for a better evaluation of the behaviour of organic compounds of selenium in the aquatic environment considering its bioavailability and transfer through the food chain as well as the determination of toxic levels for most sensitive species.

2.6. Role of zooplankton in vertical transport processes of radionuclides in the water column.

As reported in the last year, following the Chernobyl accident, measurements of radioactive fallout in selected marine samples revealed peak concentrations of Chernobyl radionulclides in Ligurian Sea surface waters on day 4th and 5th of May 1986. After three weeks of contact with seawater only 2% of Cs-137 and 5% of Ru-103 present in the water column were in the particulate form and could be trapped on 0.45 um filters i.e. the radionuclide was adsorbed to particulate matter and then subjected to sinking processes finnaly reaching the sediment surface.
In this context we intended to study the role of zooplankton populations in enhancing the vertical transport processes of radionuclides via fecal pellets and their carcasses. Therefore, zooplankton has been sampled throughout the year bi-monthly in front of the La Spezia Gulf by means of a high-speed plankton sampler (7 knots), using plankton nets of 180 um mesh. Samples were fixed in formalin for further gamma spectometry and biological sorting.
Gamma spectrometry measurements of zooplankton samples from July 1986 indicated clearly the presence of considerable amounts (59.5; 30.0; 90.2 Bq/Kg) of the respective radioisotopes Cs-137, Cs-134, and Ru-103, the latter ones originating from the Chernobyl accident.

2.7.Analysis of Tc-99 in biological matrices from the Mediterranean

The long-lived radionuclide Tc-99 may enter the geo-biosphere via different routes. Sources of Tc-99 to the environment are natural decay processes, fallout from nuclear weapon testing, uranium enrichment facilities, and discharge of effluents from nuclear fuel reprocessing plants (accidental and/or programmed). Decay of the short-lived isomer Tc-99m, utilized for labelling radiopharmaceuticals, contributes only to a negligible extent to the amounts of Tc-99 present in the environment. However, the most important potential source of technetium is presented by radioactive waste disposal activities. In the Mediterranean technetium originates mainly from fallout, thus environmental concentrations of Tc-99 in different biological matrices may be found quite low.
Nevertheless, efforts were made to determine low Tc-concentrations in environmental samples using very highly efficient low-level beta-multicounter system consisting partly of a gas flow counter unit which incorporates five individual Geiger-Muller sample counter elements and a guard counter reducing drastically background radiation and resulting in a counting efficiency for Tc-99 of 42%.
During the reporting period various methods of the literature have been studied and tested for application to radiochemical preparation and analysis of different environmental and biological matrices. In the meantime samples have been collected from various sites along the Ligurian coast which are ready for radiochemical analysis of their Tc-99 content.

3) DISCUSSION

Most of the objectives foreseen for the reporting period have been reached and successfully concluded. Results on Tc- and Se-behaviour in anoxic sediments showed high affinities of these radioisotopes to particulate matter and weak remobilization by bioturbation caused by bottom-dwelling organisms. Selenium forms were more strongly bound to anoxic sediments than technetium.

In tissues and organs of benthic fish Tc-accumulation especially in the muscle was negligible, thus Tc-contamination of fish muscle will not present a hazard for man's health.

With respect to the role of zooplankton in vertical transport of radio- nuclides in the water column still further research is needed in order to sufficiently quantify the processes according to seasons and water depths. First results are encouraging for the evaluation of biologically meadiated transports of radioisotopes in the water column from surface waters to the deep ocean and to bottom sediments.

Finally, analysis of Tc-99 contents in biological matrices of the Mediderranean have been commenced only partly, and therefore, these studies wait for completion.

4) BIBLIOGRAPHY

ELECTROCHEMICAL BEHAVIOUR OF PERTECHNETATE AT THE RING-DISK ROTATING ELECTRODE. Scoppa P., Secondini A.; J. Nucl. Med. Appl. Sci., 29(3), 211-212, 1985.

SOURCES AND BEHAVIOUR OF TECHNETIUM IN THE ENVIRONMENT. Schulte E.H., Scoppa P.; Abstr. Intern. Workshop on "Environmental Chemistry", Algarve (Portugal), 12-13 April 1985.

ENVIRONMENTAL CHEMISTRY OF TECHNETIUM. Scoppa P., Secondini A.; Proceedings 2nd Intern. Symposium on "Technetium in Chemistry and Nuclear Medicine", Piazzola sul Brenta, 9-11 Settembre 1985.

SOURCES AND BEHAVIOUR OF TECHNETIUM IN THE ENVIRONMENT. Schulte E.H., Scoppa P.; The Science of Total Environment; 64, 163-179, 1987.

ENVIRONMENTAL BEHAVIOUR OF TECHNETIUM. Scoppa P., Myttenaere C., Secondini A.; Abstracts 7th Intern. Symposium on Environmental Biogeo- chemistry, p. 79, 1985.

TRASFERIMENTO DEI RADIONUCLIDI NELL'AMBIENTE IDRICO E SUA INFLUENZA SULL'ECOSISTEMA. Myttenaere C., Scoppa P.; Atti del Convegno "Inquinamento idrico e conservazione dell'ecosistema", Vico Equense 22-23 Febbraio 1988 (in stampa).

INCORPORAZIONE DI L-SELENOMETIONINA NEL GAMBERO PALAEMON ELEGANS. Scoppa P., Secondini A., Schulte E.H.; Atti della 18a Riunione Generale della Societ Italiana di Nutrizione Umana, n.192, 198S.

IL TECNEZIO: UN ELEMENTO ARTIFICIALE PRESENTE IN QUANTITA' CRESCENTI NELL'AMBIENTE. Scoppa P.; Boll. Assoc. Ital. Protez. Rad., LZ(64/65), 1-10, 1985.

COMPORTAMENTO DEL SELENIO NELL'AMBIENTE MARINO. Scoppa P., Secondini A.; Atti del XXIV Congresso Nazionale dell'Assoc. Ital. Protez. Rad., Torino 15-18 Ottobre 1985.

METODO RAPIDO PER LA DETERMINAZIONE DELLA CARICA ENERGETICA ADENILICA NEGLI ORGANISMI MARINI. Viarengo A., Secondini A., Scoppa P., Orunesu M.; Riassunti del 31x Congresso della Societa Italiana di Biochimica, Simposio sulla Biochimica Marina - Sez. Hl, 1985.

EFFETTI DEL RAME E DEL CADMIO SULL'ATTIVITA' MITOCONDRIALE E SULLA CARICA ENERGETICA ADENILICA DELLE CELLULE DELLA GHIANDOLA DIGESTIVA DI MITILI. Viarengo A., Secondini A., Scoppa P., Moore M.N., Orunesu M.; Atti della 54a Assemblea Generale della Societa' Italiana di Biologia Sperimentale, n. 135, 1985.

LE ORIGINI DEL TECNEZIO PRESENTE NELL'AMBIENTE. Scoppa P.; In: Il comportamento ambientale del tecnezio, S. Teresa 12/12/1984, ENEA-AIRP, Eds. G. Queirazza, A. Cigna, 13-30 (1986).

TRASFERIMENTO DEL TECNEZIO ATTRAVERSO LE CATENE ALIMENTARI. E.H. Schulte, In: Il comportamento ambientale del tecnezio, S. Teresa 12/12/1984, Eds. G. Queirazza, A. Cigna, 109-130 (1986).

CARATTERISTICHE DEL FALLOUT DA cHERNOBYL NELL'AMBIENTE MARINO COSTIERO ITALIANO. Delfanti R. and C. Papucci; Proceedings of the III Conv. Naz. SITE, Siena 21-25/10/1986; in press.

E.H. SCHULTE, P. SCOPPA, A. SECONDINI - Biokinetics of Selenium in the benthic shrimp Palaemon elegans; C.I.E.S.M., Athens 17-22/10/1988

E.H. SCHULTE - Remobilization of technetium form sediments by polychaetes at the sediment-water interface, C.I.E.S.M, Athens 17-22/10/1G88

R. DELFANTI, C. PAPUCCI - Characteristics of Chernobyl fallout in the Italian coastal marine environment. Proceedings of the Internation Conference on Environmental Radioactivity in the Mediterranean Area, Sociedad Nuclear Espanola, Barcelona, 489-502, 1988.

Title of the project no.: 2

MECHANISMS INVOLVED IN ACCUMULATION OF TRANSURANIUM NUCLIDES IN SOME COMPARTMENTS OF THE MARINE ENVIRONMENT.

Head of project: R. DELFANTI

Scientific staff: R. BONIFORTI, R. DELFANTI, I. NICCOLAI, C. PAPUCCI, C. PERONI, E. SCHULTE, A. ZATTERA.

I. Objectives of the project:

A better knowledge on the environmental behaviour of transuranium nuclides is necessary for the implementation of recent recommendations of ICRP, in particular for the assessment of collective dose commitments deriving from operations, such as programmed or accidental releases from nuclear plants and radioactive wastes disposal, where long-lived radionuclides may represent an important contribution to the radiological impact on man. In addition, transuranium nuclides can be used as tracers for a better comprehension of the sedimentological processes in the marine environment.

II. Objectives for the reporting period

- Field studies for the characterization of the study areas (La Spezia Gulf/Ligurian Sea, Gaeta Gulf/Tyrrhenian Sea, Taranto Gulf/Ionian Sea);
- analysis of the horizontal and vertical distributions of Pu-239,240 and Cs-137 in riverine and marine shelf sediments;
- evaluation of the inventories of Pu-239,240;
- role of mixing and sedimentation processes in Pu redistribution in coastal marine sediments;
- Plutonium distributions and inventories in slope and canyon sediments.
- Plutonium levels and vertical distributions in deep sea sediments.
- role of mixing, sedimentation and transport processes in Plutonium accumulation in slope, canyon, and deep-sea sediments.

III. Progress achieved:

1. METHODOLOGY

With the aim to identify, trace and quantify some of the environmental processes that may affect the fate of transuranium nuclides in the marine environment, studies on plutonium distribution in sediments have been carried out both in coastal and deep-sea environments.

Along the Italian coasts, three areas have been selected:
- La Spezia Area (Ligurian Sea), under the influence of the Magra river, which supplies a limited input of both water and suspended sediment. Suspended particles are transported by the prevailing currents in a north westerly direction into the Gulf of La Spezia and the Ligurian Sea, where small streams and direct runoff from the rugged cliffs add only limited amounts of particulate matter.
- Gaeta Area (Tyrrhenian Sea), under the influence of the rivers Garigliano and Volturno. Both rivers drain a volcanic basin and supply a considerable input of suspended material to the sea.
- Western Taranto Gulf (Ionian Sea), characterized by the presence of several minor rivers that transport to the sea a large amount of terrigenous material. The study area extends eastward to the Taranto Valley, a NW-SE canyon that reaches a depth of 2200 m. The head of the Valley is made up of smaller canyons which cut the shelf in the NW part of the Taranto Gulf. The terrigenous material from the shelf accumulate in the Valley, at the narrow base of a steep slope where various channels converge.

Deep-sea sediments were collected in 1984 and 1985 during the METEOR 69 and ESOPE (Etude des Sediments Oceaniques par PEnetration) cruises in the following Atlantic areas:
- Nordostatlantisches Monitoring Programme (NOAMP) Area
- Present NEA Dumpsite
- Great Meteor East (GME)
- Southern Nares Abyssal Plain (SNAP)

The sampling points were selected in order to be representative of different sedimentary regimes (abyssal hills, abyssal plains, fault areas).

The sampling was carried out by a modified Reineck corer or, in the last two atlantic areas, by a SIPAN corer with subsequent subsampling with a core barrel. The inner diameter of the cores was 20 cm, to avoid shortening during sampling.
The cores were sectioned directly onboard into slices 1 cm thick. Selected sections of each core were analyzed for Pu-239,240, Cs-137 and, for deep sea sediments, for C-14.

Pu-239,240 were separated from the matrix by a double anion exchange radiochemical procedure followed by electroplating in NH4SO4 and alfa spectrometry.

Cs-137 was determined by non-destructive gamma spectrometry.

C-14 measurements were carried out using a benzene liquid scintillation counting method.

2. RESULTS AND DISCUSSION

2.1. Shallow water environment

2.1.1.La Spezia and Gaeta Areas

In the La Spezia and Gaeta regions, Plutonium concentrations in marine surface sediments (0.2 to 1.8 Bq.kg-1 d.w.) are 10-15 times higher than in adjacent river sediments and are highly correlated with sediment porosities. Pu-239,240 inventories in sediments (30-350 Bq.m-2) decrease with increasing water depth and sediment grain size, and are higher than the average input from fallout in the bathimetric belt between -50 and -100 m and inside the gulfs, in relation with the higher sedimentation of fine particles exported by the rivers.

The inventory differences between shallow and deep water marine environments can be understood because Plutonium is removed from seawater in primarily hydrous Fe and Mn coatings on particles, both inorganic and biogenic. The few particles present in the open sea are transported downward only slowly resulting in low inventories of Pu in deep water sediments. Zooplankton fecal pellets provide an important transport pathway in this environment. In shallow water, on the other hand, higher primary productivity, greater runoff from land and resuspension of sediments near the sea floor, due to physical or biological processes, provide greater concentrations of particles and thus enhanced removal of Pu from the water.

Similarly, the inventory differences among the cores considered for this study can be explained by the concentrations of particles. Samples collected at the same water depth showed decreasing inventories with increasing sediment grain size and distance from the river(s) mouth. However, at higher water depths, low inventories were measured also in fine grained sediments. The lower particle concentrations at higher water depths would provide only diminished effectiveness in removing Pu from seawater.

Sedimentation rates ranging between 0.5 and 1.5 cm.y-1 were estimated from the penetration depth of Pu-239,240 and Cs-137 into the sediments, and from radionuclide subsurface maxima observed in the vertical profiles.

For a better evaluation of this parameter, Pb-210 was also determined in two cores collected from the two areas. The use of the vertical profiles of both Pu-239,240 and Pb-210 allowed the calculation of the sedimentation and

mixing rates at the two sampling stations. A time dependent sedimentation-mixing model was used, based on a mass balance equation. The shape of radionuclide vertical profiles indicated, at both sites, low mixing rates. It was assumed a constant flux of Pb-210 and a Pu-239,240 input function proportional to 90-Sr deposition. The mixing coefficient was assumed to be constant along the sediment column. In this way, sedimentation rates of 0.50 and 0.45 cm.y-1 and mixing coefficients of 0.25 and 0.50 cm2.y-1 were calculated for the La Spezia and Gaeta cores respectively. The shape and width of the Plutonium subsurface peaks and the 210-Pb vertical profiles were well described by the model, but the computed Pu-239,240 activities in the upper sediment layers were lower than the experimental values.
A higher mixing coefficient (in the order of 5 cm2.y-1) could better simulate Plutonium profiles, but Pb-210 vertical distribution indicated, in both cases, low mixing rates.
A possible explanation is that particle supply by river runoff has increased the Plutonium flux to the sediments with respect to the sole plutonium supply from atmospheric fallout. In fact, at both sites Pu-239,240 inventories (La Spezia Gulf:130 Bq.m-2; Gaeta Gulf: 255 Bq.m-2) are much higher than the cumulative fallout deposition (82 Bq.m-2) at these latitudes.

2.1.2.Gulf of Taranto

In the Taranto Gulf three sediment cores were collected on the continental shelf and along the slope of the Taranto Valley at water depth ranging between -130m and -800 m.

Pu-239,240 and Cs-137 are still detectable down to 32 cm for the shallower cores and to 24 cm for the deepest one.

In the cores collected along the slope of the canyon, maximum 137-Cs activities (14 Bq.kg-1 d.w.) were found in the first centimeter of the cores. The highest Pu-239,240 activities (in the order of 1 Bq.kg-1 d.w.) were determined in the 3 to 5 cm depth interval.
The vertical distributions of Plutonium and Cesium show similar patterns below the first 2-3 cm of sediment. At the sediment-water interface, the ratio Pu-239,240/Cs-137 is generally lower than in the deeper sediment layers, probably due to the deposition of Chernobyl Cs-137.
Chernobyl contribution is particularly evident in the core collected at 450 m water depth, where the ratio Pu-239,240/Cs-137 is 0.02 in the first 2 cm and 0.06 along the core.

In both cases the radionuclide vertical profiles can be due either to mixing or to sedimentation and to a variable combination of the two. For each profile, only a maximum rate for a single process can be set, if the rate of the other process is considered negligible. From fallout radionuclides penetration into the sediment column, a maximum sedimentation rate of about 0.5 cm.y-1 can be estimated, even if the vertical profiles seem to indicate a prevailing influence of mixing phenomena.

In the core collected on the continental shelf, Cs-137 and Pu-239,240 are still detectable in the deepest layer of the core (32 cm). The ratio Pu-239,240/Cs-137 decreases with depth into the sediment. The presence of Chernobyl 137-Cs can be hypothesized down to about 20 cm, where the ratio becomes relatively constant (0.07-0.08) and much lower than in the surface layer (0.03).

The inventory of Pu-239,240 in the deepest core is 90 Bq.m-2. For the other two samples the inventories are > 123 Bq.m-2 (shelf) and > 160 Bq.m-2 (slope). All of the calculated inventories are higher than the cumulative fallout deposition at these latitudes (82 Bq.m-2).

The high Plutonium inventory in shelf is likely related to the deposition of fine particles exported by the rivers; for the other cores, sediment transport along the slope and mixing phenomena inside the canyon can also be responsible of the enhanced scavenging of Plutonium from seawater.

2.2. Deep sea sediments.

2.2.1.Geochronology with C-14

For the characterization of the North-Atlantic areas, the vertical profiles of 14-C were analyzed. The use of a box-model allowed the calculation of the sedimentation rates (SR), the age of the particles arriving at the sediment surface (To) and the age of the mixed layer (Tml).

Station	Water depth (m)	T ml (y)	T 0 (y)	SR (cm.ky-1)
NOAMP/Hill	4060	4665	1343	1.61
NOAMP/Talus	4520	2593	515	3.69
NEA Dumpsite/Plain	4710	2835	488	2.53
GME/Hill	5265	5422	509	1.08

The 14-C vertical distributions in most of the cores indicate a continuous uniform sedimentation regime during the last 10,000 years. The sedimentation rates were strongly influenced by the geometry of the sea-bottom and by the contribution of the eroded material from adjacent areas.

Some evidence of horizontal influx has been recorded, as shown by the differences between the ages of the particles arriving at NOAMP/Hill and Talus, probably due to erosion processes.

As the GME sampling point was below the lysocline, the lower value of the sedimentation rate and age of the mixed layer are probably related to dissolution of the foraminifera within the sediment and subsequent reduction of sediment volume.

2.2.2.Plutonium vertical profiles and inventories

In NARES sediments Pu is only detectable in the first 1-2 cm.
In this area, very low Pu activities (0.05-0.13 Bq.kg-1 d.w.) were found in the surface layer of the cores. The large variability in Pu surface activities is probably due to different spatial deposition and not uniform biological activity in sediments.

In both NOAMP samples Plutonium activity in surface sediments reaches maximum values of about 40 dpm.kg-1 d.w., while in the NEA Dumpsite and in GME maximum Plutonium concentrations are in the order of 20 dpm.kg-1 d.w.

Plutonium penetration in sediments ranges between 6 and 10 cm.
The vertical distributions of Pu-239,240 in deep-sea sediments have been used for the description of the mixing phenomena taking place at the sediment-water interface.
In general, the concentration of these radionuclides is highest near the surface, and decreases downward into the sediments for several centimeters. Radionuclides penetration into the deep sediment layers, solely by pore water diffusion, is slow. Since from the time in which plutonium has been introduced in the atmosphere by nuclear tests, a neglegible sedimentation in deep-sea environments occurred, the retrieval of this radionuclide into the sediment depth must be related to particle mixing processes on short time scale.
Plutonium penetration in sediments can be used as an indication of the thickness of the mixed layer, and, under certain conditions, a simple diffusion equation, that fits Pu vertical profiles, can be used for the calculation of the rate at which mixing occurs.
The thicknesses of the mixed layer in sediments from the Dumpsite, NOAMP and GME areas, calculated from Pu penetration and from the layer of constant C-14 age, range from 6 to 10 cm.
In NARES samples, Pu-239,240 concentration drops to near zero values by 1 to 2 cm, and a mixing coefficient could not be calculated.
For the NOAMP station, a mixing coefficient 0.2 cm2.y-1 was determined.
Plutonium vertical profiles in the cores collected in the dumpsite and GME areas show a subsurface maximum. In these cases, living organisms probably do not transport sediment particles in a random manner over short distances into the sediment, as required by the diffusion model, but a different mechanism, that leads to the transport of surface material to preferential depths, is prevailing.

For the description of the mixing characteristics at these sites a model has been used that simulates the transport of surface, radionuclide-rich material to a fixed depth into the sediment by benthic organisms or an equivalent mechanism. By this model, a mixing coefficient of 0.1 cm2.y-1 with a tranport rate of 0.1 y-1 was calculated for the GME sample.

The Plutonium inventory calculated for the dumpsite area (14 Bq.m-2) is comparable to those found for the NOAMP and GME hill stations (12 Bq.m-2 and 9 Bq.m-2 respectively) which are 13-20% of the total fallout delivery at the corresponding latitudes. A higher inventory (25 Bq.m-2, 36% of Pu delivery) was found in a NOAMP station located at the foot of an abyssal hill. In the SNAP area Plutonium inventories (0.3-1.1 Bq.m-2) are only 1-3% of the fallout deposition. In general, Plutonium inventories are strongly related to primary production. This factor can explain the low inventories calculated in the oligotrophic SNAP area, but for understanding the differences between the two samples collected from the top and the foot of the same abyssal hill (NOAMP samples), it is necessary to consider different processes. 14-C measurements indicate undisturbed sedimentation (3.6 cm.ky-1) in the sample at the foot of the hill, with a mixed layer of 6-8 cm thickness. The sample collected at the top of the hill shows, on the contrary, a disturbed sedimentary record and higher 14-C age of the mixed layer. A possible mechanism leading to the unusual high inventory at the foot of the hill could be the transport of surficial eroded material downslope the abyssal hill, increasing Plutonium deposition at the foot.

IV. Other research group(s) collaborating actively on this project [name(s) and address(es)]:

Dr. L. Scarpina; AIRP (Italian Association for Radiation Protection). Bologna, Italy.

V. Publications:

Delfanti R. & Papucci C. (1986) - Il comportamento dei transuranici nell'ambiente marino costiero. Acqua e aria 6/86, 625-630.

Delfanti R., Papucci C. (1986) - Distribuzione verticale ed inventari del Pu-239,240 nei sedimenti dei Golfi di Gaeta e La Spezia: contributi del Garigliano e del Magra. In A. Delle Site e G.Santori eds: Problematiche ambientali e radiotossicologiche relative ad elementi transuranici, ENEA, Roma, 121-132.

Papucci C., Delfanti R. (1986) - Distribuzioni verticali ed inventari di Pu-239,240 in sedimenti superficiali dell'Atlantico Nord-orientale. Presented at VI Convegno Nazionale sull'attivita' di ricerca nei settori della radiochimica, chimica nucleare, delle radiazioni e dei radioelementi. Bologna, June 18-20.

Papucci,C. & Delfanti,R. (1987) - Distributions of Pu-239,240 and 14-C in North-East Atlantic sediments. In: Guary et al. eds, Radioactivity: a tool for Oceanography. Elsevier, London, 442.

Delfanti,R., Buffoni,G., Papucci,C. and Paganin,G. (1988) - Determination of recent sedimentation rates in the Tyrrhenian Sea using 210-Pb and Pu-239,240. Ibid.

Papucci,C. & Delfanti,R. (1988) - Evaluation of particle mixing depth and rates in Atlantic surface sediments using Pu-239,240 vertical profiles. ESOPE cruise Report, JRC Ispra. In press.

Papucci, C. & Delfanti, R. (1988) - C-14 and Pu-239,240 as tracers of sedimentation and mixing processes in North-East Atlantic sediments. In: Interim Oceanographic Description of the North-East Atlantic site for the disposal of low-level radioactive waste. OECD/NEA, Paris, in press.

Delfanti, R., Fiore, V., Lavarello, O. & Papucci, C. (1988) - Environmental Radioactivity along the Italian Coasts. In: Proceedings of the "International Conference on environmental radioactivity in the Mediterranean area. Sociedad Nuclear Espanola, Barcelona, 371-386.

Delfanti R., Papucci C., Scarpina L. (1989) - Distribuzioni di Pu-239,240 e Cs-137 nei sedimenti del Golfo di Taranto. In: Atti del VII Convegno Nazionale sull'attivita' di ricerca nei settori della Radiochimica e della Chimica Nucleare, delle radiazioni e dei radioelementi. Pavia, May 3-5. In Press.

Title of the project no.: 3

DESCRIPTIVE MODEL FOR:
A) CIRCULATION OF RADIONUCLIDES IN THE MARINE ENVIRONMENTS
B) TRANSFER OF RADIONUCLIDES IN THE MARINE FOOD CHAINS RELEVANT TO MAN

Head(s) of project:

Dr. G.C. BOERI
ENEA-DISP
Via Vitaliano Brancati, 48
I-00144 Roma

Scientific staff:

M. BELLI, M. BLASI, F. DE GUARRINI, R. GIACOMELLI, M. MARINARO, G. MATTASSI, M. NOCENTE, U. SANSONE, P. SPEZZANO, G. VENTURA

I. Objectives of the project:

Validations of existing theoretical models for representing dispersion and transfer process in the marine environment and in food chain leading to man.
Field studies in lagoon environments have been carried out with the objectives to correlate levels of radionuclides concentrations coming from Chernobyl fallout in biotic and abiotic matrices and to describe the geobiochemical cycling in the brackish environment.

II. Objectives for the reporting period:

- Selection of a multi-compartimental box model to predict the distribution of radionuclides, carried from rivers and tidal currents, into the Marano and Grado lagoon (Northeastern part of Adriatic sea).

- Experimental studies to define distribution of radionuclides concentrations in the lagoon.

III. Progress achieved:

1. Introduction

ENEA-DISP, the Italian Directorate for Nuclear Safety and Health Protection, supervises environmental impact assessment of nuclear power plants in both the licensing and operational phases.
Following the accident at the nuclear power plant in Chernobyl, ENEA-DISP was charged by Government, of coordinating national environmental radioactivity surveillance and has contributed to the study of the radiological situations in different Italian regions. In fact, after the Chernobyl cloud passage, some regional authorities asked for radiological campaigns to be carried out on their territories, or in particular locations, characterized by higher radioactivity levels.
In the Friuli-Venezia Giulia region, located in the north-eastern part of Italy, a generalized heavier fall-out was experienced (Cs-137 deposition ranging from 20 to 40 kBq/m^2), due to the effect of the orography on the intensity of rainfall phenomena, combined with the trajectories followed by the contamined cloud. Afterwards, when the situation, from radiological protection point of view was defined, the Friuli-Venezia Giulia Region has been adopted as a large natural laboratory in which, using radionuclides such as Cs-134 and Cs-137, terrestrial, freshwater and saltwater ecosystems dynamics can be studied in an adequate number of years. ENEA-DISP and the Regional Centre for Agricultural Experimentation of the Friuli-Venezia Giulia Region (C.R.S.A.), have therefore developed a multiyear radioecological research programme, with the main aim of the validation of transfer models for radionuclides within the environment.
The activities described in this project, related to the circulation of radionuclides in the aquatic environment, are part of the planned researches in this region of Italy. Attention was focused on the Marano and Grado lagoon, (northern part of the Adriatic Sea) because these environments are the last reception basins of materials coming from rill erosion of inland soils (Figure 1).

Description of the study area

The lagoon under study is bounded on the west side, by the Tagliamento river delta and on the east side by the Isonzo river delta. It has an area of 16000 ha and it is 32 km long and 5 km wide.
The Tagliamento river (170 km in length and with an average flow rate of 92 $m^3\ s^{-1}$) and the Isonzo river (140 km and 170 $m^3\ s^{-1}$) flow directly into the sea. Their bassins, respectively of 2840 km^2 and 3340 km^2, collect most of their water from the western alpine higlands (2000 mm

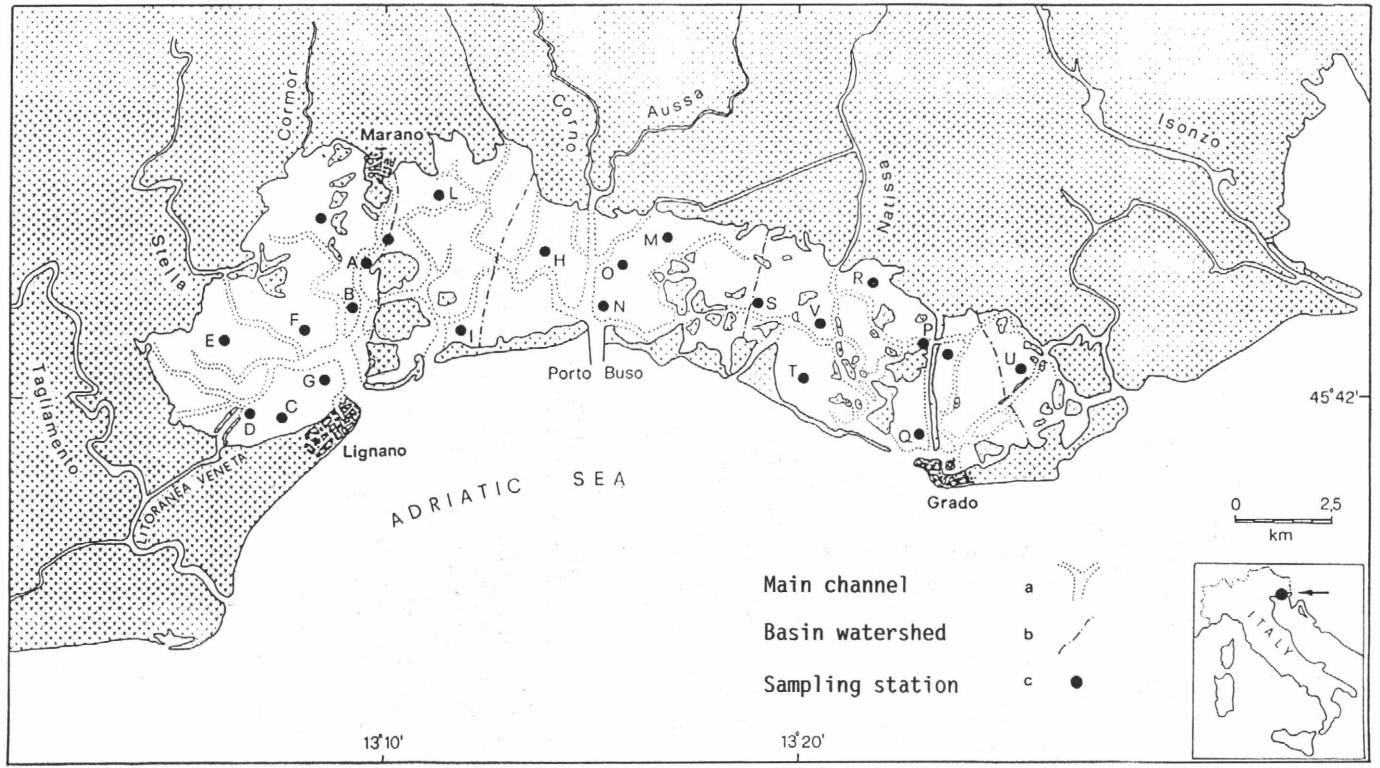

Fig. 1 - Marano and Grado lagoons: location of sampling stations

average annual rainfall).
The rivers Stella, Cormor and Natissa flow directly into the lagoon (average total flow rate 70 m^3 s^{-1}, more than half of which is provided by the Stella river).
Typical morphological features such as cheniers, (i.e. series of elongated islands separating the lagoon from the sea), tidal flats, marshes, channels, lagoon mouths and characteristics coastlines can be found in the lagoon environment.
The tidal fluctuation ranges between 10 cm to 120 cm, and the waters flow essentially through a network of channels that grow in depth towards the lagoon mouths (1 m inland and 10 m at the mouths).
In the Marano and Grado lagoon silt and clay particles carried by the water flow are sedimented mainly on tidal flats.
This process can be disturbed by exceptional events such as sea-storms, strong winds, and others. These events strongly influence hydrodynamic and sedimentation processes, dispersing and resuspending a variable amount of sedimented particles (350 mg l^{-1} of suspended solids were measured during a wind storm).

2. Methodology

The literature seems to show that a multi-compartimental box model is useful to predict the behaviour of radionuclides within an aquatic environment with high spatial variability of the environmental characteristics. Therefore for this study has been selected the model DRAM (Distribution of Radioactive material in Marine ecosystem). This multi-compartimental box model has been developed by the Italian Electricity Board (ENEL) to predict the distribution and the radiological consequences of radionuclides discharged from a nuclear power plant in the sea.
The Marano and Grado lagoon box structure is based on the sediment chemico-physical characteristics. Each box is subdivided in four compartiments: column water, suspended particles, "active sediment" and pore-water.
The partitioning of radionuclides between suspended particles and water is decribed by a distribution coefficient (Kd).
The thickness of the "active sediment" is based on estimated sediment mixing depths and rates .
The water circulation is determined by a hydrodinanic model of the lagoon. Particles in the water boxes are allowed to move laterally with the water, but the movement in the box is only vertical.

To define the box structures of Marano and Grado Lagoon, activities started in spring 1987 and were aimed at collecting data to define the characteristics of the lagoon environment and the distribution of radionuclides in sediments and in biotic components. With this aims 30 sampling stations were located in high accumulation areas

such as tidal flats and swamps. To describe the radionuclides distribution, in the water and in the suspended solids of the lagoon-sea exchange water and of the surface water, 4 sampling stations were located in the rivers and in the main mouth of the lagoon.

3. Results

Tables 1 and 2 report the results of analyses of water and suspended solids. These data indicate that Caesium in surface water is mainly associated to suspended solids. The specific activity of the solids carried by the Stella River is slightly higher than the activity in the Isonzo and Tagliamento Rivers. Caesium is mainly adsorbed on particles > 10 μ (Table 2).

	RIVERS			LAGOON	
	TAGLIAMENTO	STELLA	ISONZO	HIGH TIDE	LOW TIDE
pH	7.9	8.2	8.1	8.5	8.5
SUSPENDED SOLIDS (mg/l)	57	14	10	8	11
Cs-137 IN SUSPENDED SOLIDS (Bq/m^3 of water)	8.31±0.81	5.60 ± 0.74	2.14 ± 0.29	1.04 ± 0.34	1.40 ± 0.34
Cs-137 IN SOLUTION (Bq/m^3 of water)	0.47	0.77	0.39 ± 0.29	4.57 ± 1.00	4.21 ± 0.69
SPECIFIC ACTIVITY OF SUSPENDED SOLIDS (Bq/t of particolate)	1.4×10^5	4.0×10^5	2.1×10^5	1.3×10^5	1.3×10^5

Tab. 1 - Results of analyses on suspended solids

GRAIN SIZE μ	RIVERS			LAGOON	
	TAGLIAMENTO	STELLA	ISONZO	HIGH TIDE	LOW TIDE
10	7.51±0.77	3.03±0.51	1.74±0.25	0.79±0.27	0.63±0.18
3÷10	0.80±0.27	0.97±0.32	0.40±0.16	0.53	0.29±0.18
1÷ 3	0.59	0.82±0.31	0.34	0.60	0.13±0.11
0.6÷1	0.67	0.78±0.31	0.36	0.25±0.20	0.35±0.18

Tab. 2 - Cs-137 in suspended solids (Bq/m^3 of water)

S	Cs-134	Cs-137	K-40	EH	C	FT	MT	CT	FS	MS	OM	CA
	Bq/kg			mV	%							
A	5.3	20.8	329	-187	17	15	23	28	14	3	2.58	1.52
B	4.9	18.1	354	-117	16	14	22	41	5	1	5.19	3.00
C	5.0	19.6	304	- 20	16	11	18	31	23	1	1.85	1.09
D	10.7	34.2	210	-287	13	7	8	11	58	3	1.12	0.66
E	7.4	27.6	350	-323	21	17	35	21	6	1	3.90	2.30
F	15.5	53.0	408	-361	16	13	35	27	9	1	3.10	1.83
G	1.2	4.2	102	- 36	3	2	3	4	55	33	0.41	0.24
H	3.5	14.1	222	-132	18	9	16	34	22	1	1.92	1.13
I	3.4	11.7	180	- 58	19	6	9	17	47	2	1.25	0.75
L	4.3	16.7	325	-327	23	12	24	36	6	1	2.44	1.44
M	4.1	17.3	371	-152	18	15	27	32	7	1	3.90	2.30
N	4.6	14.4	431	- 58	16	8	16	37	8	10	4.90	2.90
O	3.7	18.1	357	-142	22	10	22	36	9	1	4.00	2,40
P	8.9	35.3	419	.	26	15	18	16	18	7	2.44	1.44
Q	4.4	14.3	185	- 89	9	5	16	19	41	10	1.78	1.05
R	4.3	21.7	508	-130	19	11	28	33	5	2	3.60	2.14
S	7.7	27.0	384	-166	20	10	26	34	9	1	1.90	1.17
T	4.6	18.6	340	-150	19	8	16	32	17	6	3.90	2.30
U	7.8	32.6	281	-129	19	9	17	45	8	1	1.58	0.93
V	8.4	27.0	420	-156	23	8	21	36	9	1	3.97	2.34

S = sampling station; EH = redox potential; C = clay
FT = fine silt; MT = medium silt; CT = coarse silt;
FS = fine sand; MS = medium sand; OM = organic matter;
CA = organic Carbon
Tab. 3 - Principal variables data

Table 3 report the results of analyses carried out on lagoon sediments. Statistical methods were applied to correlate sediment grain-saize spectrum with Cs-137, Cs-134, K-40, organic Carbon and Redox potential.

The Pearson correlation method allowed to point out the following Cs-137 and Cs-134 behaviour:
1) an inverse correlation with EH (r=-0.7);
2) a direct correlation (0.4 ≤ r ≤ 0.5) with medium and fine silt (20-6 μ) and consequently an inverse correlation with grain sizes larger than 60 μ (r=-0.5 with sand).
These different correlations relate to the different environments where sedimentation took place. In the lagoon inner area, into which rivers flow, low EH values and fine contaminated sediments are present. On the contrary in sandy bottom sediments, where EH is higher, Caesium concentrations are lower.
K-40 shows the best direct correlations with grain size fractions lower than 60 μ (0.6 ≤ r ≤ 0.7) and with organic matter (r=0.8)> The poor correlation with Caesium highlights a contamination unhomogeneity within the lagoon since even K-40 levels and sediments classes are the same, Cs-137 and Cs-134 levels vary widely.

Cs-137 concentration in aquatic plants (Table 4) ranges from 10 to 20 Bq/kg of dry matter. Such concentrations are directly correlated to those found in sediments. Cs-137 concentration in algae varies from 7 to 18 Bq/kg of dry matter; the maximum value has been recorded in the sample collected near the "litoranea veneta" chanel. A sample of periphyton coming from the Cormor river mouth area shows the highest value (36 Bq/kg d.m.).

Tab. 4

Caesium concentrations in algae, aquatic and terrestrial plants

S = Sampling station
AP = Aquatic plant
AL = Algae
PT = Terrestrial plant

S	Cs-134	Cs-137	
	Bq/kg		
A	5.5	19.0	AP
D	5.7	19.0	AL
F	2.2	7.6	AL
F	2.4	6.7	AL
H	10.0	36.0	AL
H	1.0	5.5	TP
D	1.0	7.2	TP
I	1.9	10.5	AP
Q	3.4	19.3	AP
U	5.1	20.7	AP
U	2.9	10.1	TP

Cs-137 concentrations measured in benthos and nekton are rather uniform (from 1 to 3 Bq/kg of fresh matter). In table 5 Cs-134 and Cs-137 average values are reported.

SPECIES	OBSERV	Cs-134 Bq/kg	STD	Cs-137 Bq/kg	STD
Atherina boyeri	6	0.45	0.16	0.88	0.21
Mullet	6	0.60	0.43	0.10	0.64
Gudgeon	5	0.53	0.27	1.09	0.31
Aphanius fascic.	5	0.49	0.29	1.00	0.41
Flatfish	6	0.59	0.23	1.38	0.79
Crab	6	0.60	0.34	1.30	0.30
Crayfish	6	0.58	0.29	1.38	0.34
Mussel	6	0.41	0.20	1.07	0.46

OBSERV = Number of observations
STD = Standard deviation

Tab. 5 - Fish: Cs-134 and Cs-137 mean concentrations

4. Conclusions

The research activity undertaken to characterize the estuary and lagoon environments in Friuli-Venezia Giulia region, is part of a larger radioecological investigation program promoted to improve the knowledge of radionuclides dynamics in the natural environment.
In this project attention was pointed mainly to define terrigenous contributions from rivers to lagoon and the hydrological and sedimentological parameters. The goal is to provide more precise informations about sediment deposition rates and redistribution operated by benthic organism.
The results obtained from the first years of activities lead to the following observations:

- the assessed radioactive fall-out on the lagoon hinterland was 1 kBq/m^3. Within the lagoon similar values have been found only in minimum sedimentation area;
- lagoon radioactive contamination is attributable to suspended particles carried from hills and mountains by the rivers;

- the Tagliamento and Isonzo rivers, that flow directly into the sea, carry terrigenous sediments that are subsequently drawn into the lagoon where also detritus carried by Cormor river and by the "litoranea veneta" channel accumulates;
- in the eastern portion of the lagoon only a small amount of sediments accumulation is evident;
- in superficial water Caesium are associated mostly to suspended particles with diameter larger than 10 μ. A similar remark is valid for sediments, where maximum correlation exists between Caesium and 0-20 μ grain size class.

IV. Other research group(s) collaborating actively on this project [name(s) and address(es)]:

SERVIZIO DI FISICA SANITARIA - USL 1 "TRIESTINA"
Via della Pietà, 19 - 34129 TRIESTE - ITALY

SETTORE IGIENE PUBBLICA - USL 8 "BASSA FRIULANA"
Stabilimento Ospedaliero - 33053 LATISANA (UD) - ITALY

ENEA-COMB
13040 SALUGGIA (VC) - ITALY

V. Publications:

1. **L. Guzzi, G. Queirazza (1986) - Progetto R.E.M. - ENEL, Direzione Studi e Ricerche, Centro di Ricerca Termica e Nucleare, Servizio Ambiente (E6/01/86/MI).**

2. **G. Ventura et al. (1988) - Radioecological research in northern Adriatic Lagoon: Activities and first - ENEA DISP (Doc. ENEA-DISP-ARA-SCA(1988)10).**

RADIATION PROTECTION PROGRAMME
Final Report

Contractor:

Univ. Catholique de Louvain
Halles Universitaires
Place de l'Université 1
B-1348 Louvain-la-Neuve

Contract no.: BI6-B-042-B

Head(s) of research team(s) [name(s) and address(es)]:

Prof J. Decallonne
Unité de Microbiologie
U.C.L.
Place Croix du Sud 2
B-1348 Louvain-la-Neuve

Telephone number: 010/47.36.72

Title of the research contract:

Description of the interactions and processes that are involved in Tc-99 movement and cycling.

List of projects:

1. Modelling of Technetium movement in soil
2. Study of the biogeochemical cycle of Tc-99 ; uncertainties associated with predictions

Title of the project no.: 1

Modeling of Technetium movement in soil.

Head(s) of project:

Prof. J. Decallonne.

Scientific staff:

Prof. J. Decallonne and Dr. C.N. Chiang.

I. Objectives of the project:

The first part of the project was to investigate the possibility of quantitatively predicting the movement of pertechnetate in soils and stream.

The second part of the project was to investigate the possibility of quantitatively predicting the effect of Tc-99 as pertechnetate on microorganisms.

Later work will consist to fit together the two submodels, in order to describe quantitatively the movement of pertechnetate through soils and streams, as influenced by microoganisms.

II. Objectives for the reporting period:

From 1985 to 1989 research activities were developed along two lines to meet the objectives of the project.

Firstly, the study of bacterial growth as influenced by pertechnetate at different concentrations. Complementary to this approach, the search and identification of bacterial strains with properties of reducing and/or accumulating Tc-99 were undertaken.

Secondly, in order to describe quantitatively the movement of Tc-99 as pertechnetate through soils, the calibration of experimental method to study its sorption to soils was investigated.

III. Progress achieved:

I. Methodology :

I-1. Study of Bacterial growth :

- Numerical methods :

The main objective of these methods is to obtain a quantitative relationship between the growth rate of micro-organisms and the concentration of Tc-99, added as pertechnetate to the growth media.

The growth rate of a micro-organism is defined by an equation of the type : $dn/dt = K(t).n$ (1)

where K is the growth rate, t is the time, and n is the biomass of microorganisms, expressed either in dry weight of cells or actual number of cells per unit volume.

The analytical representation of growth may be obtained by using the so-called logistic curve which has the following form :

$$n = K/(1 + \exp(a_0 + a_1.t)) \quad (2)$$

To improve the fit of this curve to the sigmoid shaped growth curve, the first degree polynomial in equation (2) can be replaced by a third or even a fifth degree polynomial. Thus, the improved form of logistic curve is obtained as :

$$n = K/1 + \exp(F(t)) \quad (3)$$

where F(t) is a third or fifth degree polynomial. Once the fit of equation (3) to growth data is obtained satisfactorily, by adjusting the the coefficients of the polynomial, the specific growth rate K can be calculated at any value of time using the equation :

$$(1/n)(dn/dt) = (n/K - 1).\ F(t) \quad (4)$$

If desired the time, after inoculation, may be replaced by t - L, where L is an estimate of the lag phase of the growth. Its value can be adjusted by the programme of calculation.

- Microbiological methods :

The objectives of these methods are : to study the bacterial growth as influenced by the pertechnetate concentrations, and to search and identify the bacteria able to accumulate and/or reduce the pertechnetate.

To study the influence of pertechnetate on bacterial growth, the method developed by Van de Casteels & al. (1982)- Environmental migration of long lived radionuclides, p.275, 1982, I.A.E.A.-was adapted out using the same strain of Azotobacter chroococcum. Ammonium pertechnetate was added to give final concentrations of 10^{-8}, 10^{-7}, 10^{-6}, 10^{-5}, 10^{-4}, and 10^{-3} M in the growth medium. The addition occured at the start of the culture i.e. at the inoculation time of the medium. The inoculum consistently used is an exponentially growing culture of Azotobater. Bacterial growth was measured by using a Coulter counter for counting the growing number of cells, from time zero to 80 hours or more, in average periodes of 4 to 10 hours.

To search and identify bacteria strains with properties of reducing and/or accumulating Tc-99, soil suspensions from long term Tc contaminated lysimeters, were inoculated to three media namely : Plate Count agar, Tryptic Soy Broth, and Lactobacillus Broth according to De Man, Rogosa and Sharpe (MRS). Inoculated media were incubated at 37 and 25°C. Once the growth was obvious, the most reprentative colonies were isolated for identification, using a procedure developed in this laboratory. (Maissin et al., 1987).

Experimental observations include microscopy check of the isolates for their purity, their morphology their motility and their staining, along with an effort to select spores forming strains. To achieve a rapid and accurate identification for bacillus isolates, a matrix of results, from tests in the API 20E and API 50CHB strips was used (Logan and Berkeley, 1984), totalizing 60 chemical tests. These tests were supplemented with gas chromathography analysis of bacterial cell-hydrolysates, for their specific fatty acids compasition. (Kaneda, 1977).

In addition to these identification tests, autoradiographic technique has been used to detect bacteria able to accumulate Tc-99. The procedure can be outlined as follows : bacteria are grown in medium enriched with Tc-99 (10^{-6} M), up to a population of 10^7 cells/ml. Then an agar film of washed bacteria, obtained on an haematometer (Thoma cell), is contact exposed with an appropriate film (Hyper film-3H, Amersham code RPN 12) during 3 weeks at -40°C.

I-2. Tc-99 sorption to soils :

The objectives of this study are to adjust soil conditions governing Tc-99 sorption and thereby permit the comparison of sorption data accross different soils.

The soil water content which affects soils microbial activity and redox conditions, and the organic matter content which increases Tc complexation, have been found the most important among the factors affecting Tc-99 sorption.(Henrot, 1988- PhD thesis presented at University of Tennessee. Knoxville). Therefore, our attention was focused on the development of a technique which can achieve comparable moisture conditions in different soil types.

The methodology developed can be summarized as follow : Selected soil samples, representing a range of soil textures and organic matter contents, were collected in the plough layer (0-20cm) and sieved (2mm) after air drying to constant weight. Ten-g samples were mixed with sand in small columns of 20 cm high and 2 cm in diameter. The appropriate amounts of sand added to each soil type, to achieve the desired moisture conditions, were calculated following Lueking and Schepers (1986)- Soil Sci. Soc. Am. J., 50: 1370-1373.-, adjusting their original sand and organic matter contents. The soil-sand columns were first leached with a saline solution, free of organic component, then incubated at 25°C for two weeks, in order to re-activate the microbial activity. Then, a solution of Tc-99 as NH_4-pertechnetate (925 Bq/ml) was added, in excess, to the soil-sand mixture and exposed for one hour to allow a thorough diffusion in the column. Prior to incubation, excess of both solutions, saline and Tc-99, are vacuum extracted with a suction of 80 kpa. until the desired moisture conditions are reached. For the soil types under study, two conditions were selected : 90 % of water filled porosity (WFP) for the so called aerobic condition and 120 % of WFP for the anaerobic condition. Separated determinations of bulk density (p_b) and particule density (p_s) of the soil-sand mixture allowed the calculations of the porosity and the water filled porosity, following :

$$\text{porosity} = 1 - p_b/p_s \quad \text{and} \quad \text{WFP} = w \times p_b/\text{porosity}.$$

w = gravimetric water content.

Control of water content was carried out by weighing the columns after each suction and during the incubation. After chosen period of time, 0, 1, 2, 3,....7 days, a set of columns, representing each soil type at the two moisture conditions were leached with 50 ml of $CaCl_2$ (0.01 M), in increments of 10 ml. Tc-99 activity was measured in the leachates by liquid scintillation counting.

II. Results :

II-1. Bacterial growth :

Typical growth curves of A. chroococcum, as influenced by Tc-99 concentrations, are shown in figure 1. for 0, 10^{-4} and 10^{-6} M. Effect of higher concentration (10^{-3} M)is not reported here since it causes an immediate inhibition of the growth. Continuous lines represent the non linear adjustment of the "improved" logistic curve to the experimental points. As it can be seen the fit was good enough, so that the calculations of instantaneous values of the growth rate can be done for the respective concentrations of Tc-99.

The most interesting fact which can be extracted from close examination of these resulting curves is : adding Tc-99, as NH_4-pertechnetate, at the onset of bacterial growth causes an increase in the growth rate. The concentration of 10^{-4} M was found to have the maximal effect. After this initial stimulation, the growth rate may fall below the control or the general average of the growth rate at all concentrations, as depicted in figure 2.

II-2. Search and identification of baterial strains :

From soil sampled in the long-term contaminated lysimeters, ten strains of aerobic bacteria, with sporulation ability, were isolated and subjected to identification tests.

They are mostly long rod shaped and gram positive Bacillus, among them Bacillus *thuringiensis*, B. *cereus*, B. *anthracis* and B. *mycoides* can be considered as correctely identified. These results obtained through biochemical tests were confirmed by the comparison of their fatty acids composition with control strains, using gas chromatography and cells acid hydrolysates. Figure 3 presents the typical gas chromatogram of methylated fatty acids for B. *cereus* and B. *thuringiensis*.

II-3. Sorption of Tc-99 to the soils :

Two soils representative of the silty soil types from central Belgium were studied for their ability to adsorp Tc-99.

Their main difference is in organic matter content, consequence of their respective pH value. For the first soil, Habay-la-Vieille sampled in the Ardennes, the pH value is 5.1, and its organic matter content is 4.5 %; while for the second soil, sampled at Beauvechin in the Brabant, its pH is 6.9 with 1.9 % as organic matter content.

Figure 4 shows the Tc-99 sorption to these soils versus time. The calculations of the sorption rate constant, assuming that the sorption obeys to a first order kinetics, through logarithmic plot of the data give the following table :

Figure 1 Adjustment of the logistic curve to growth data.

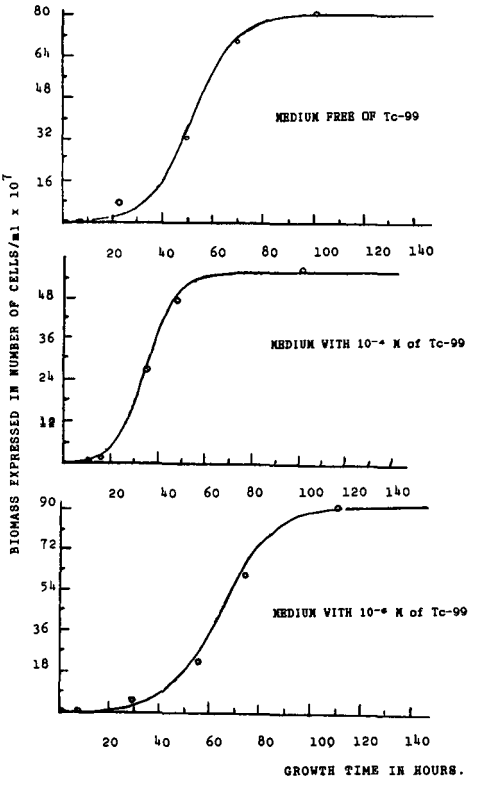

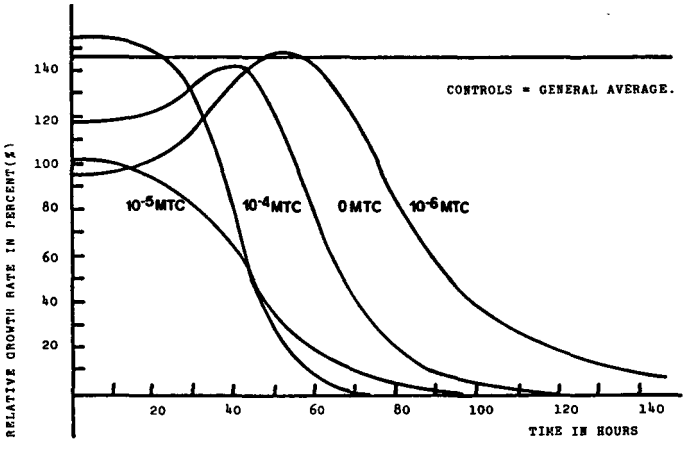

Figure 2. Growth rate variations at different Tc-99 concentrations. Each growth rate is related to the general average of growth rate at all concentrations.

Figure 3 Chromatogram of methylated fatty acids from bacterial cells hydrolysate. Identification of B. *thuringiensis* and B. *cereus*.

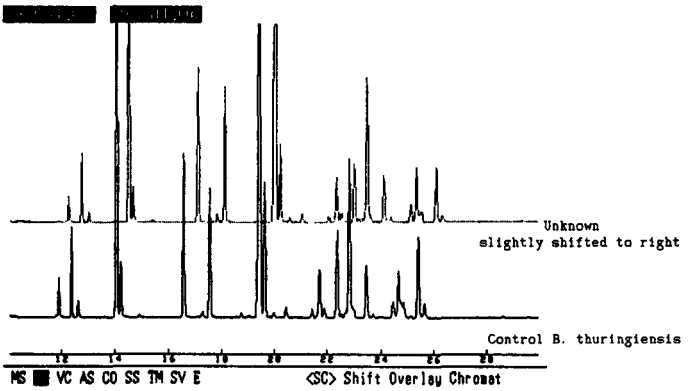

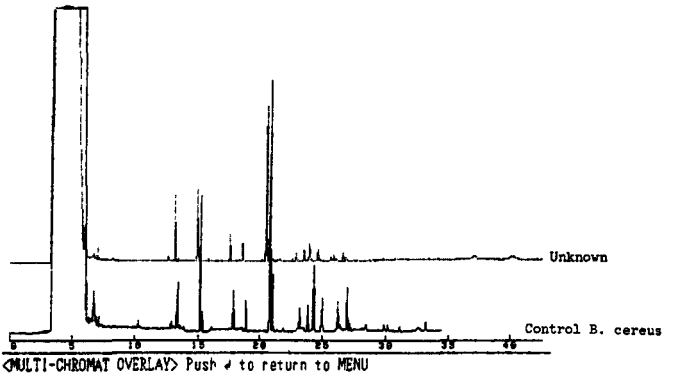

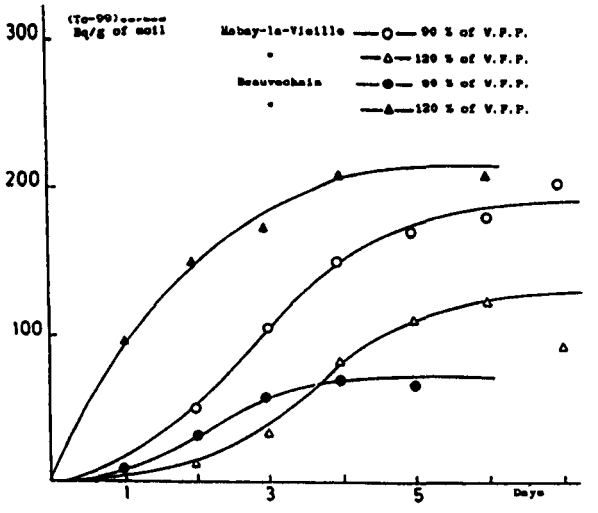

Figure 4. Time course of Tc-99 sorption to the soils.

Incubation conditions	S.R(1) Habay(H)	S.R(1) Beauvechain(B)	H.T(2) H	H.T(2) B	Maximun Sorption H	Maximun Sorption B
WFP = 90 %	0.1	0.37	7	2	202	68
= 120	0.6	0.14	1	5	120	204

(1) = sorption rate constant in day^{-1}.
(2) = half reaction time in days.

In the first soil, under so called aerobic condition, the adsorption rate of Tc-99 is rather low but the maximun adsorbed is high. While in anaerobic condition the adsorption rate is high, eventhough the maximun amount adsorbed is low. For the second soil, a quiet opposite figure is found i.e for aerobic condition, the rate constant value is high and the maximun sorption is low. Whereas in anaerobic condition, the rate of sorption is low but the quantity adsorbed, at the end of experiment, is important and comparable to the highest maximun found in the first soil. An explanation of these differences, in terms of sorption rate and concentrations of Tc-99 sorbed to the soils, can be found in the difference of their organic matter. This point will be discussed in the next part of the report.

III. Discussions :

III-1. Bacteria growth study :

This part of the project was to investigate the possibility of quantitatively describing bacterial growth, as influenced by Tc-99 concentration.

To meet this objective, a numerical method has been developed along with more improved experimental techniques.

Thereby, we have found that the fit between experimental results and the "improved" logistic curve is as good as reported formerly -Progress Report 1985- However an important fact should be pointed out : in most cases, the simple logistic curve was sufficient to describe the growth data.

This result may be due to the use of more elaborate methods to control the growth of bacteria i.e. a Coulter counter for counting the cells during the growth instead of turbitimetric measurements; consistent inoculation of the growth medium with exponentially growing cultures and addition of pertechnetate with the inoculum. Moreover, the possible artefacts alluded to previously seems to be excluded, since the same results have been found, supplemented by a more accurate description of the effect of lower concentrations of Tc-99.

The resulting calculation of instantaneous values of the growth rate, for different Tc-99 concentrations, has corroborated a former observation namely the stimulation of the growth rate at 10^{-4} M. This intriguing microbial reaction to pertechnetate has been found twice.

III-2. Search and identification of bactrial strains :

The procedure developed for bacterial strains identification is dicdated by the need to increase our knowledge of bacteria, able to accumulate and/or reduce the Tc-99 as TcO_4^-.

If our attention has been focused specially on the aerobic strains, it is due to the indications of their ability to accumulate Tc-99 found in the long term contaminated lysimeters soils - See Report of project n°2, "Tc speciation in soil".-and through small columns experiments, under aerobic conditions.

The autoradiographic method developed simultaneously should normally help to select the most efficient strains, in terms of their ability to transform the Tc-99. However, the lack of precision in the repeated preparations, so far, does not allow further interpretations.

For the time being, the gas chromatography technique represents a performing tool to confirm the chemical tests. It is found less time consuming and it reduces the uncertainties in the identification procedure. However, to conclude correctly about the ability of the strains to accumulate and/or reduce the TcO_4^-, specific tests or experiments (Henrot, 1988) should be performed.

III-3. Sorption of Tc-99 to the soils :

The results presented in precedent table are apparently contradictory. However, once the 2 soils are compared to each other, the main observation is the more important amounts of Tc-99 sorbed in the first soil, under both conditions.

The initial organic matter content can be an explanation to the difference found in their Tc-99 sorption : as reported by Henrot- See project n°2-, Tc sorption to the soil can be equated to Tc complexation by the soil organic matter. This effect is enhance when the soil is maintained at an anaerobic state. In our experiments, this last condition is met when the water filled porosity is higher than 100 %. Thus, the sorbed Tc concentration, for the second soil, is closer to the result obtained in the first soil, eventhough its organic content is much lower.

Small columns used here represent an inexpensive and time-efficient technique to standardize and document soil moisture conditions in the study of Tc sorption process. Simple addition of appropiate amount of sand can lead to establishment of desired moisture conditions during incubation studies. Standardization of the technique in terms of amendment-to-soil ratio and water content during incubation will result in more accurate and reliable estimates of Tc-99 sorption.

IV. Other research group(s) collaborating actively on this project [name(s) and address(es)]:

Prof. Myttenaere : Université Catholique de Louvain. Belgium.
Prof. Cremers A. : Katoliek Universiteit Leuven. Belgium.
Prof. Pieri J. : Université de Nantes. France.
Oak Ridge National Laboratory-ORNL : Dr. Auerbach, Hoffman, Blaybock USA

V. Publications:

Title of the project no.:

STUDY OF THE BIOCHEMICAL CYCLE OF TC-99.
UNCERTAINTIES ASSOCIATED WITH PREDICTION.

Head(s) of project: Prof. C. MYTTENAERE

Scientific staff: COGNEAU, M., DEHUT, J.P., SOMBRE, L., THIRY, Y., VANDECASTEELE, C.M.*, van der STEGEN de SCHRIECK, J.

I. Objectives of the project: The main objectives of the project were to :

- Reduce the uncertainty which affected the Tc behaviour in the terrestrial environment.
- Initiate works on post-Chernobyl problems and particularly on the contamination of forests which has raised important questions in case of accidental atmospheric releases.

II. Objectives for the reporting period: The following works were carried on in 1989.

- Technetium-99
  Study on the long term availability of Tc deposited on soil in the open lysimeters (validation of the model); final analysis of the collected data.
- Study of the availability of bioincorporated Tc final analysis of the collected data.
- Study of the absorption and retention of deposited Tc on spruces.
- Study of the absorption and retention of deposited Cs on spruces and of thermo-generated Cs deposited on a soil collected in a spruce forest.

* Scientific collaboration

III. Progress achieved:

1. INTRODUCTION

- Technetium may enter the environment as a result of nuclear weapons testing, the nuclear fuel cycle and pharmaceutical use. Tc-99 (2.15 x 105y) provided the impetus for the evaluation of its environmental behaviour and effects and it has been recognized that Tc-99 should be given consideration in nuclear fuel cycle assessments when there is recycling in uranium fuel. In case of release it initial likely form in the environment is TCO_4^-. Under that form it had to be mobile and available to biota. Intensive studies began in the framework of 1985-1989 Radiation Protection Programme to more precisely define the mechanisms controlling its mobility in the environment and to understand the phenomena observed which were in contradiction with the behaviour of its released chemical form. A summary of the results obtained by our laboratory is given here below.

- Forests may accumulate pollutants released in the atmosphere. The very high filtering capacity of these natural ecosystems is strongly dependant on the physico-chemical properties of the pollutants and on the metereological conditions prevailing during the deposition. (Accumulation during dry periods and leaching by rains). It thus seems important to know if forests may be considered as a sink or as source of the retained radioactivity. Our works have thus considered the behaviour of Cs-137 deposited on forest canopies.

2. BEHAVIOUR OF TC IN TERRESTRIAL ECOSYSTEMS

2.1 Long-term behaviour of Tc in agricultural soil

The accuracy of the assessment of the human risk associated with the releases of Tc-99 required a good understan-

ding of its behaviour in soil which governs its further accumulation by plants. Considerable uncertainties was associated with the transfer of Tc from soil to plants. In order to reduce these uncertainties four lysimeters were installed in an open field exposed to natural climatic conditions.

The lysimeters were sown with a grass pasture and contaminated on the soil surface by Tc-99. The successive harvests of forage were collected before and after an additionnal contamination. Vegetation and soil samples were analyzed for their Tc content and chemical speciation. Results obtained have given a clear indication that the soil to plant transfer varies with time. A two compartments model was built up and fits very well with the experimental data. The values estimated for λ_{s1} range from $1.24\ 10^{-2}$ to $1.36\ 10^{-2}$ d^{-1} (T1/2 eff = 55.9 to 51.0 d with a mean value of 53.8 ± 2.1 d).

This removal constant is only valid for about 70% of the deposited Tc while 30% is removed with a very long effective half-time ranging from 15.7 to 52.8 y with a mean value of 30 ± 15.9 Y (λ_{s2} ranges from $3.6\ 10^{-5}$ to $1.21\ 10^{-4}$ d^{-1}).

Immediately after the deposit the plant to soil concentration ratios are very high (about 400); they decrease to six three years after the contamination. The aging effect can be explained in one way by the progressive decrease of the amount of Tc present in the p low layer, the modifications of the chemical forms of the Tc remaining in the soil and to its removal by exportation of harvested material.

* VANDECASTEELE, C.M., DEHUT, J.P., VAN LAER, S., DEPRINS, D. and MYTTENAERE, C., Long term availability of Tc deposited on soil after accidental releases, Health Physics, 57, 2, p. 247-54 (1989).

2.2 Tc Speciation in soil

The long term behaviour of Tc in soil is in agreement with the chemical determination (sequential extractions of the Tc of the samples collected in the lysimeters in equilibrium conditions).

These extractions have shown that in these conditions:

- the total activity decreases with depth (more than 50% of the total activity were in the first 5cm layer).

- the Tc extracted by water represents only a very low percentage of the total activity (± 3% of the total Tc).

- the bound Tc is the most important fraction for the different depths (55% bound to organic substrates, 33% bound to sesquioxides; 9% removed by ashing and acid digestion).

The chemical forms of Tc were also isolated after having incorporated contaminated litter in the soil. The following results (in% of the total activity) were obtained after 900 days:

	Harches leaves	Poplar leaves
Solvent	Soluble and exchangeable forms	
Water	7	10
Grigg buffer	10	15
	Tc bound to the organic matter	
Pyrophosphate	30	26
H_2O_2 + NaClO	53	49

* VANDECASTEELE, C.M., GARTEN, , C.T., VAN BRUWAENE, R., JANSSENS, J., KIRCHMANN, R. and MYTTENAERE, C., Chemical speciation of technetium in soil and plants, Impact on soil-plant-animal transfer, in Speciation of fission and

activation products in the environment, Ed. Bulman, R.A. and Cooper, J.R., Elsevier Appl. Sc. Publ;, p. 368-81 (1986).

2.3 Influence of the microbial activity of the soil on the bioavailability of Tc

Bioaccumulation and chemical modification of TcO_4^- by aerobically and anaerobically soil bacteria and by pure cultures of sulfate-reducing bacteria were studied. Aerobically grown bacteria had no effect on TcO_4^-: they did not accumulate Tc nor modify its chemical form. Anaerobically grown bacteria exhibited high bioaccumulation and reduced TcO_4^-, enabling its association with organics of the growing medium.

Sulfate-reducing bacteria efficiently removed Tc and promoted its association with organics.

A soil horizon which is poor in organic matter and has a low bacterial population has a low portion potential for Tc. On the contrary a soil horizon which is richer in organic matter sorbs Tc (Tc is used by anaerobic bacteria and then conplexed with the carboxyl groups of the organic matter). When oxigen is present in the soil, there is an equilibrium between reduction complexation and oxidation of Tc that determines the partitioning of Tc between sorbed Tc and TcO_4^-. Sorbed Tc is partially released from the Tc-organic matter complexes when the soil air-dries. Consequently, Tc behaviour in soil is a dynamic process determined primarily by soil type and fluctuations in soil water content.

* HENROT, J., Behaviour of technetium in soil: sorption-desorption processes. A dissertation presented for the Doctor of Philosophy Degree, The University of Tennessee, Knoxville,(1988).

* HENROT, J., Bioaccumulation and chemical modification of Tc by soil bacteria, Health Physics, 57.2, p. 239-45 (1989).

2.4 Biological mechanisms responsible of Tc-99 absorption by annual plants and animals

Tc which is absorbed by plants (the absorption kinetics established in water culture for irrigated rice, revealed two phases - diffusion in the apparent free spaces - transfer in the cells and translocation) is translocated as TcO_4^- and is reduced in the leaf cells. The reduction power of the leaves and their metabolism (production of ligands) condition the Tc fixation in green material. Very few Tc is redistributed in the plant and the transfer factor varies with the light intensity and cultural methods. More details on the physiological mechanisms which are responsible of the Tc reduction in plant cells were given by other CEC contractors.

40% of Tc biologically incorporated in corn leaves via root uptake is present in plant tissue in forms that are not readily extractable except by boiling 2M NaOH. The bound form of Tc in the leaves appear to be mostly Tc complexes with proteins and polysaccharides of the plant cell walls.

Chromatography of the cell cytosol demonstrated that Tc was associated with molecules in the MW range of peptides (1500-5000 daltons) as well as with smaller molecules and some larger molecules. About half of the Tc in the cell cytosol co-chromatographed with TcO_4^-.

In rice field, in the case of a contamination of the irrigated water during the entire cycle at a concentration of 1 KBq l^{-1} the activity recovered in the grains is about 800 Bq kg^{-1} DW (180 Bq kg^{-1} DW in the caryopses). In the absence of contamination of the water during the next cultivation the transfer from soil to grain will give rise to a contamination level of the seeds of about 22 Bq kg^{-1} DW. The contribution of bio-incorporated Tc (green manure) to the contamination paddy does not seem to be critical.

Tc concentration in different organs of monogastric mammals was lower for bioincorporartd Tc than for I.V. injection, reflecting a lower gastrointestinal absorption in the case of Tc metabolized by plants. The most contaminated tissues were thyroid, hair kidneys liver and skin. In polygastric animals (suffolk sheep) the results obtained (in collaboration with the CEN/SCK) demonstrate an important influence of the rumen microflora which modify the Tc chemical form.

Transfer factors have been calculated for TcO_4^- from contaminated water and Tc bioincorporated in Azolla to young ducks. to that end animals were fed with contaminated fresh Azolla material. Feas were collected and ducks were sacrified. No other food was given during the treatment. Transfer factors are on order of magnitude lower than for food than between water and the different organs. Feathers may be considered as the best indicators of the contamination level of the animal.

* MYTTENAERE, C., VANDECASTEELE, C.M., ROUCOUX, P., LIETART, E.A., ITCHERT, A. and MOUSNY, J.M., Processus biologiques responsables de l'accumulation du Tc-99 par les végétaux, in Technetium in the environment, Ed. Desmet, G. and Myttenaere, C., Elsevier Appl. Sc. Publ., p. 281-94 (1986).

* GARTEN, C.T., MYTTENAERE, C., VANDECASTEELE, C.M., KIRCHMANN, R. and VAN BRUWAENE, R., Chemical form of technetium in corn (Zea mays) and the gastrointestinal absorption of plant-incorporated Tc by laboratory rats, in Technetium in the environment, Ed. Desmet, G. and Myttenaere, C., p. 319-332 (1986).

* VANDECASTEELE, C.M., GARTEN, C.T., VAN BRUWAENE, R., JANSSENS, J., KIRCHMANN, R. and MYTTENAERE, C., Chemical speciation of technetium in soil and plants: Impact on soil-plant-animal transfer, in speciation of fission and activation products in the environments, Elsevier Appl. Sc. Publ., p. 368-81 (1986).

* VANDECASTEELE, C.M., CAPOT, F., DEHUT, J.P., MOUSNY, J.M. and MYTTENAERE, C., Technetium fate in irrigated rice fields. The cycling of long-lived radionuclides in the

biosphere: observations and models, CCE-CIEMAT Proceedings, 15-19 September 1986, II (1986).

* DEHUT, J.P., VAN HOVE, C., VANDECASTEELE, C.M. and MYTTENAERE, C., Technetium cycle in the environement: Redistribution of Tc bioincorporated in *Azolla* sp. within the different compartments of terrestrial ecosystem, The cycling of long-lived radionuclides in the biosphere: observations and models, CCE - CIEMAT Proceedings, 15-19 September 1986, II (1986).

2.5 Influence of technetium on the nitrogenase activity

The toxicity of Tc to N_2 fixing organisms varies with quality of the medium; In absence of combined N Tc is much more toxic to these organisms. Nitrogenase activity is thus influenced by Tc and in case of environmental contamination may inhibit the N_2 fixation. The cause of the inhibition is not a substitution of Mo by Tc because Tc is bound in a non specific way on the proteins. It thus seems that the mechanism relay upon a reduction of Tc by the electrons and a lack of electrons for the nitrogenase activity.

* VANDECASTEELE, C.M., HENROT, J., PIERI, J.M., MYTTENAERE, C., COGNEAU, M. and VAN HOVE, C., Interaction entre technetium et molybdene dans l'inhibition de la nitrogenase d'Azotobacter chroococcum, in Technetium in the environment, Ed. Desmet, G. and Myttenaere, C., Elsevier Appl. Sc. Publ., p. 385-96 (1985).

* VANDECASTEELE, C.M., Influence du technetium sur la nitrogenase d'Azotobacter, Thèse UCL, 169pp (1987).

2.6 Transfer of bioincorporated Tc

The effective removal rate of radiopollutants from contaminated soil usually has been estimated by considering only the radioactive decay constant. Results obtained for Tc-99 showed that phenomena other than radioactive decay may be of importance in soil depletion and that uptake by plants as well as mechanisms affecting the availabilty must be taken into account. Results obtained in minilysimeters have shown

that an important part of the recycled bioincorprated Tc is immediatly and highly available to plants. Transfer factors obtained for grass indicate that bioincorporated Tc represents a real source of contamination; they are of the same order of magnitude as those observed for TcO_4^- deposited in soil.

The model which may be applied to grass, describing the increasing and decreasing phases of transfer factors was constructed as a mixture (i.e. a weighted sum) of a negative exponantiel and of the essential part (i.e. The Kernel) of a distribution avoiding the constraints of integration. A good agreement was obtained between the model and the experimental points. In case of incorporation of trees leaves in the soil (poplar and harche) a very important fraction of the plant material is directly available ($T_{1/2}$ 23 days for harche and 48 days for poplar leaves). The transfer factors obtained after 900 days decrease ($T_{1/2}$ 10 years for harches and $T_{1/2}$ 8 years for poplars) and reach about 20. Biodegradation phenomenas are slower for trees leaves than for grass and the mathematical model applied to the litter corresponds to a double negative exponentiel.

$$FT(t)=\alpha_1 e^{-\lambda_1 t} + \alpha_2 e^{-\lambda_2 t}$$

To summarize, it may be said that the use of the plant material or its incineration have to be taken into account in environmental transfer models for technetium.

* DEHUT, J.P., FONSNY, K. and MYTTENAERE, C., Bioavailability of Tc incorporated in plant material, Health Physics, 57, 2, p. 263-7 (1989).

2.7 Deposition of Tc on tree canopy surfaces

The expression for the concentration in plants due to direct deposition is given by a formula which takes into account besides other parameters the interception by the bio-

mass (interception fraction r), the translocation and the effective removal constants. Different experiments of direct contamination have been conducted during the five years contract.

- Picea trees (8 years old) have been contaminated by spraying a mixture of Tc-99 and Tc-95m on the pertechnetate form. it has been shown that the contamination of needles was clearly related to their situation in the tree and not to their age; a rain may export more than 50% of the radioactivity deposited. The study of the distribution of the radioactivity in the needles showed that the waxy coating of the needles plays a very important role in the Tc retention.

- Ray-grass was cultivated in containers covered with perforated plate avoiding any contamination of the soil. Grass was wet contaminated and cut after 14 days. The interception factors r measured the day after the contamination are situated between 0,040 and 0,046 which are lower values than those published in the litterature (0,079 to 0,17).

The radioactivity measured for the second cut (45 days after the contamination) does not decrease (translocation of the activity entrapped by the plant base), phenomena which does not allow to calculate a Tw value (ecological half-time).

AUVRAY, F., DEHUT, J.P. and MYTTENAERE, C., Interception and retention of technetium by herbaceous vegetation, Arch. int. Physiol. Biochem., 94, 3, p. 35 (1986).

XXX, Etude des perturbations de la nutrition minérale des épicéas par les pollutions atmosphériques, 25.11.86 - 12.87, Ministère Région Wallonne (1988).

2.8 Behaviour of Tc in forest ecosystems

Soil from spruce forests are very poor and the surface layer is very rich in organic matter. Samples of spruce soils

were collected in a Belgian forest (Vielsalm) and horizons were separated. Lysimeters were filled with three different soil horizons (holorganic-O level; hemiorganic-Ah level; mineral BW level). Soils were contaminated homogeneously with Tc-99 (TcO_4^-).

Young spruces were transplanted before the formation of 89 needles. After two months of growth in the different media the following conclusions may be drawn:

- The contamination levels of needles are clearly higher in mineral soil than in the organic one. (Contrary to what was observed for Cs^+: Bioavailability of Tc is higher in mineral soil than in soil rich in organic matter).

- The younger needles are the richest in Tc and the difference observed is more important in a mineral soil in which Tc is more available.

- The accumulation of Tc with time is again more important for a soil in which the bioavailability is higher.

The calculation of the concentration factors have shown that they were much more higher for a mineral soil; nevertheless the differences observed are partly due to the density of the different layers of soil investigated. Such a result draws again the attention on the validity of the CR concept.

3. BEHAVIOUR OF CS IN FOREST ECOSYSTEMS

3.1 Roles of direct and indirect contamination in the Cs-137 transfer in a coniferous ecosystems

In 1988 and 1989 the study 2.8 was extended to non grass type plants (coniferous ecosystems) and to another isotope (Cs-137) which have raised very important radioecological questions after the Tchernobyl accident.

8 years spruces were transplanted in open lysimeters. Before transplantation Cs-134 thermo-generated aerosols were deposited on the trees and the surface layer of the soil was contaminated in Cs-137.

The experiment is in course and the result will be published in the framework of the nex contract (Prof. Ronneau - Prof. Minski - CEC) It must be already mentionned that :

- the measurement of Cs-134 (Chernobyl like aerosols) which was deposited on the needles before transplanting is difficult; most of it has been quickly washed-off by rains. (The technique has to be reviewed in relation to the cultural conditions).

- The Cs-137 deposited on the soil is now fixed in the surface layers (first two cm) and very few or no Cs-137 is found in the percolates.

- Transplanting of the tree is followed by a recovering time during which trees do absorb very few nutrients and during which roots development is very low (That fact underlines the necessity to programme long term experiments).

- Some Cs-137 may be already measured in the 99 needles but it is to soon to calculate realistic transfer factors (they now

are of the order of 0,02 for dry weight needles 89 dry weight soil).

- The density of the different layers in a forest soil being very different and the developement of roots by unit of volume being different the concept of the CR for forest trees has to be rediscussed.

* DESMET, G., MYTTENAERE, C., Considerations of the role of natural ecosystems in the eventual contamination of man and his environment, J. Env; Radioactivity, 6, p. 197-202 (1988).

* RAYYES, A.A., RONNEAU, C., APERS, D. and MYTTENAERE, C., Ecological behaviour of thermo-generated cesium aerosols. Doklady Academic Naouk, UK SSR, 8, p. 76-9 (1988).

* SOMBRE, L., VAN HOUCHE, M., RONNEAU, C., LAMBOTTE, J.M. and MYTTENAERE, C., Transfer of radioceasium in forest ecosystems resulting from a nuclear accident, Workshop The transfer of radionuclides in natural and semi-natural environements, ENEA, DISP, CRSA, CEC, Udine, 11-15 September (1989).

RADIATION PROTECTION PROGRAMME
Final Report

Contractor:

United Kingdom Atomic Energy
Authority, UKAEA
Charles II Street 11
GB- London SW1Y 4QP

Contract no.: BI6-B-046-UK

Head(s) of research team(s) [name(s) and address(es)]:

Dr R.G. Derwent
Env.& Med. Sciences Div.
AERE
Harwell, Didcot
GB- Oxon OX11 ORA

Telephone number: 0235/241.41

Title of the research contract:

Distribution and transfer of radionuclides in terrestrial and sea environments.

List of projects:

1. Comparison of radionuclide deposition to vegetation
2. Comparative study of soil to plant transfer of Neptunium, Plutonium, Americium and Curium
3. Exchange of radionuclides between the sea and atmosphere.

Title of the project no: 1

Comparison of radionuclide deposition to vegetation

Head(s) of project:

Dr R G Derwent

Scientific staff: P A Cawse
S J Baker
P Burton
B Sykes

I. Objectives of the project:

The objectives are to examine the influence of geography and climate on the current concentrations of Sr-90, Am-241, Pu and gamma-emitters including Cs-134 and Cs-137 in atmospheric deposition, in soil and in vegetation, and to apply these 'baseline' data to parallel studies in the environment of nuclear installations. The continuous measurements allow seasonal effects to be established and sea to land transfer of actinides at coastal locations to be assessed. An associated collaborative study has been made in France by CEN Cadarache, extending southwards to 44°N (see Figure 1), for comparison with the measurements in Gt. Britain which extend northwards to 58°N.

Soon after the project started, the Chernobyl accident at the end of April 1986 introduced a further objective, namely to assess the transfer of fallout radiocaesium and Sr-90 to soil and vegetation.

II. Objectives for the reporting period:

(a) to maintain the sampling programme for atmospheric deposition and vegetation until mid-1989 according to the established schedule, and to continue with the analysis of gamma-emitters and actinides. The fate of Cs-134 and Cs-137 derived from Chernobyl fallout will continue to be followed.

(b) to derive an inventory of radionuclide deposition to soil and vegetation, including seasonal (summer/winter) comparisons, and to examine the site specific differences, and the climatic influence.

(c) to collaborate with CEN Cadarache on progress of the measurements and interpretation of results.

III. Progress achieved:

1. Methodology

The routine collection of total (wet and dry) deposition, ryegrass and lucerne was started in 1985/86 at field plots in Gt. Britain for comparison of radionuclide concentrations with France (Fig. 1 and Table 1). The experimental plots were located both near to and distant from nuclear installations. The final harvest of vegetation was made at the end of May 1989. Ryegrass and lucerne were selected as test species to examine the differences in retention of airborne particulates containing radionuclides by narrow-leaved and broad-leaved foliage, in addition to examination of differences in root uptake. The root systems of these crops are in contrast, with ryegrass being fibrous-rooted whereas lucerne is tap-rooted, penetrates to greater soil depth and is drought resistant. The deposition collector at each plot was changed when vegetation was sampled to provide quantitative data on interception by foliage of the atmospheric input inventory of radionuclides. A standard fertiliser treatment was applied to the grass which received N-P-K in March and N only in July. Lucerne received P-K fertiliser in March and again in autumn. The soil pH is kept at pH 6.5 minimum by addition of calcium carbonate.

Soil sampling and analysis was made at the start of the project in 1985/86 and again after the Chernobyl accident in April 1986. Over the period autumn 1987/spring 1988, soil profiles were sampled from permanent grassland at each field plot location to assess the migration of Cs-134 and Cs-137 to 0.5 metres by analysis of soil from 12 depth intervals.

2. Results and Discussion

(a) Radionuclides in soil

Concentrations of radionuclides in soil at the field plots in Gt. Britain and France (Table 2) show increases near some of the nuclear sites relative to distant (control) locations at each latitude. However, reference to generalised derived limits (GDL's) for radionuclides in mixed soil indicates that the maximum soil concentrations recorded are (except for Cs-137) only a very small percentage of the GDL ie Sr-90: 1.9%, Pu-239+240: 0.6% and Am-241: 0.2%. For Cs-137, the maximum concentration is 16% of the GDL, elevated by Chernobyl fallout. In the case of actinides, the sea to land transfer of plutonium and americium in marine aerosols may be partly responsible for observed increases in soil concentrations, in addition to deposition of airborne particulate originating from operations at nuclear installations.

The accumulated deposition of radionuclides in soil at control sites varied according to rainfall, for example at Corfe and S. Brent (Fig. 2) as a result of rainout and washout of nuclear weapons debris over the years. However, in the case of Sr-90, the sites with highest rainfall (Bala and S. Brent) showed little accumulation, owing to enchanced leaching of this radionuclide from the 0-30 cm layer.

For Cs-137, the Chernobyl fallout was insignificant below latitude 53^{o}N, but at Huna and Bala it contributed 54% and 45% respectively to the total Cs-137 present. The influence of latitude on the accumulated deposition of Pu-239+240, which is relatively non-mobile in soil, is evident if the British and French data from control plots is normalised to average annual rainfall (Table 3).

Measurements in 1987 of radiocaesium in soil profiles close to field plot locations showed that in N. Wales, Cumbria and Scotland the concentrations of Cs-137 in surface layers (0-4 cm depth) of permanent grassland soils near to nuclear installations were in the range 96-390 Bq/kg compared with 36-210 Bq/kg at distant locations. Figure 3 shows the

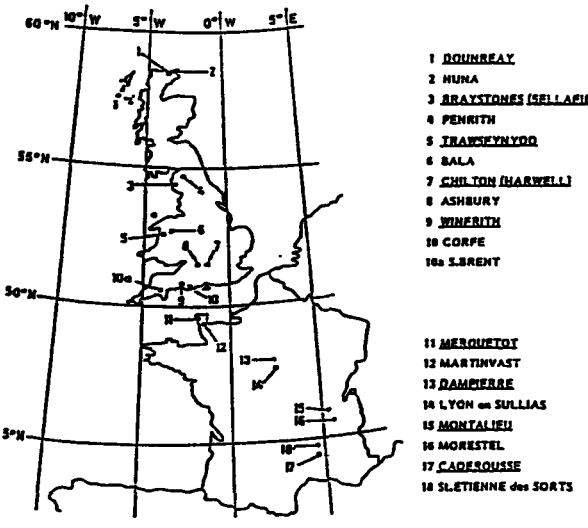

—— Underline denotes that plot is located at or very near to nuclear installation. The remainder are distant.

FIG.1 LOCATION OF FIELD PLOTS FOR MEASUREMENTS OF RADIONUCLIDES IN DEPOSITION AND VEGETATION

TABLE 1 FIELD PLOTS NEAR TO AND DISTANT FROM NUCLEAR INSTALLATIONS IN GT. BRITAIN AND FRANCE

Site No.	Locations in Gt. Britain	Latitude (approx)	Average Annual Rainfall (mm)	Altitude (m)	Distance from Sea (km)
1	DOUNREAY (on-site)	58°N	900	15	0.3
2	HUNA	58°N	780	10	0.3
3	BRAYSTONES (near Sellafield)	55°N	1040	15	1.1
4	PENRITH	55°N	880	137	41
5	TRAWSFYNYDD	53°N	1700	215	15
6	BALA	53°N	1300	95	39
7	CHILTON (Harwell, on-site)	52°N	590	130	94
8	ASHBURY	52°N	750	195	90
9	WINFRITH (on-site)	51°N	880	30	0.9
10	CORFE	51°N	810	15	0.6
10a	S.BRENT	51°N	2070	116	16
	Locations in France				
11	MERQUETOT (La Hague west)	50°N	1000	100	1.2
12	MARTINVAST (" " east)	50 N	1000	70	7
13	DAMPIERRE (north)	48°N	650	140	330
14	LION en SULLIAS (Dampierre south)	48°N	650	130	320
15	MONTALIEU (Creys Malville, s.west)	46°N	1000	200	280
16	MORESTEL (" " s.east)	46°N	1000	230	260
17	CADEROUSSE (Marcoule south)	44°N	820	30	80
18	ST. ETIENNE des SORTS (" north)	44°N	820	30	90

Note (i) For map locations of sites, see Figure 1.
(ii) Odd numbers denote sites near to nuclear installations.
Even numbers denote sites distant from nuclear installations.
(iii) Soil description: Gt. Britain
Site No. 1 Non-calcareous gley, 2 Peaty gley, 3 Brown earth,
4 Stagnogley, 5 Cambic stagnogley, 6 Brown Podzolic soil,
7 Rendzina, 8 Rendzina, 9 Humo-ferric podzol,
10 Gley podzol, 10a Brown earth.

TABLE 2

CONCENTRATIONS OF RADIONUCLIDES IN FIELD PLOT SOILS, SAMPLED POST-CHERNOBYL

Site No.	Field plot	Bq/kg 0-15cm depth Cs-134	Cs-137	Bq/kg, 0-30cm depth Pu-238	Pu-239 +240	Am-241	Sr-90
	Locations in Britain						
1	DOUNREAY	15.2	175	0.43	5.6	1.5	2.0
2	HUNA	20	62	0.016	0.33	0.23	5.4
3	BRAYSTONES	39	113	0.18	2.6	1.3	7.4
4	PENRITH	1.9	21	0.024	0.20	0.076	3.7
5	TRAWSFYNYDD	17.1	92	0.022	0.46	0.12	2.6
6	BALA	18.6	69	0.018	0.39	0.12	2.3
7	CHILTON	0.4	17.8	0.018	0.24	0.12	3.6
8	ASHBURY	0.4	8.9	<0.01	0.17	0.11	2.8
9	WINFRITH	<0.3	21	<0.01	0.25	0.038	3.5
10	CORFE	<0.3	15.8	<0.01	0.24	0.072	<0.2
10a	S.BRENT	<0.7	38	0.030	0.57	0.17	0.82
	Locations in France						Not Analysed
11	MERQUETOT	<0.5	10.0	0.012	0.28	0.13	
12	MARTINVAST	<0.5	14.9	0.027	0.29	0.18	
13	DAMPIERRE	<0.5	8.2	0.014	0.13	0.04	
14	LION en SULLIAS	<0.5	11.6	<0.01	0.17	0.09	
15	MONTALIEU	8.7	33	<0.01	0.21	0.14	
16	MORESTEL	11.2	43	0.041	0.38	0.17	
17	CADEROUSSE	3.2	21	0.015	0.48	0.19	
18	ST. ETIENNE des SORTS	4.1	19	0.026	0.67	0.27	

Note (i) Odd numbers denote sites near to nuclear installations.
Even numbers denote sites distant from nuclear installations.
(ii) All results are decay-corrected to 3 May 1986.

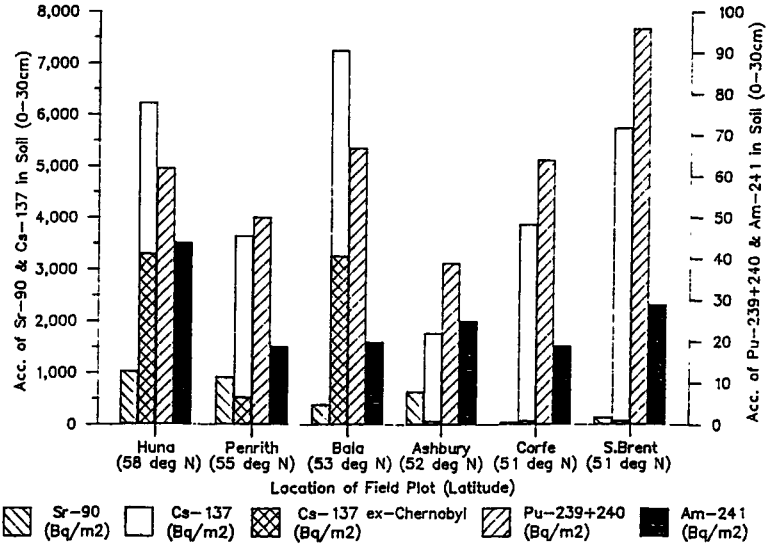

FIG.2 ACCUMULATION OF RADIONUCLIDES IN FIELD PLOT SOILS TO 30 cm DEPTH AT CONTROL SITES

TABLE 3 INFLUENCE OF LATITUDE ON ACCUMULATION OF PLUTONIUM-239+240 IN SOIL AT CONTROL SITES IN GT BRITAIN AND FRANCE

Site No.	Locations	Latitude	Pu-239+240 to 30cm depth Bq/m^2/1000mm rainfall
2	HUNA	58°N	79
4	PENRITH	55°N	57
6	BALA	53°N	52
8	ASHBURY	52°N	52
10	CORFE	51°N	79
10a	S.BRENT	51°N	46
12	MARTINVAST	50°N	110
14	LION EN SULLIAS	48°N	110
16	MORESTAL	46°N	151
18	ST ETIENNE DES SORTS	44°N	360

Note: average annual rainfall is listed in Table 1

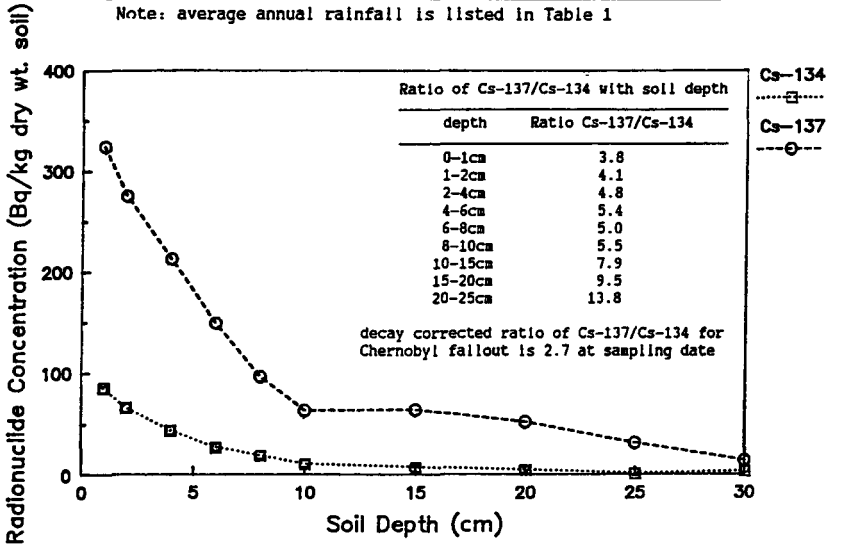

FIG.3 DEPTH PROFILE DISTRIBUTION OF ^{134}Cs AND ^{137}Cs IN SOIL FROM PERMANENT GRASSLAND AT BRAYSTONES CUMBRIA (NOVEMBER 1987)

depth distribution of radiocaesium at Braystones (near Sellafield) Cumbria. The ratios of $^{137}/^{134}$Cs increased with depth at both nuclear and distant sites owing to pre-Chernobyl deposition of ^{137}Cs. Surface soil concentrations of ^{137}Cs were an order of magnitude greater than found below 8 to 10 cm depth, both at nuclear and distant locations.

(b) Radionuclides in atmospheric deposition

The average annual total (wet + dry) atmospheric deposition of radionuclides at the field plots in Gt. Britain is listed in Table 4, together with measurements of Na and Ti which indicate the relative importance of sea spray aerosol and soil dust respectively. There was enhanced deposition of actinides near to the nuclear installations at Dounreay and Braystones (near Sellafield Works). At these sites, low ratios of summer/winter deposition of actinides were observed, and an increase of 4 to 8-fold in Na deposition over-winter suggests that marine

TABLE 4 AVERAGE ANNUAL ATMOSPHERIC DEPOSITION OF RADIONUCLIDES, SODIUM AND TITANIUM AT FIELDS PLOTS IN GT BRITAIN

Location of Field Plot	Average Annual Atmospheric Deposition of Radionuclides, Bq/m^2/yr, June 1986 - May 1989					
	Cs-137	Pu-239+240	Am-241	Sr-90	Na(g/m^2)	Ti(mg/m^2)
DOUNREAY	65	0.45 (0.7)	0.35 (0.8)	9.0 (2.9)	61 (0.12)	21 (0.60)
HUNA	54	0.062	0.027	2.6 (2.3)	41 (0.13)	12 (0.25)
BRAYSTONES	225 (5.9)	3.8 (0.3)	4.1 (0.4)	6.0 (0.2)	20 (0.25)	18 (1.4)
PENRITH	<40	0.077	0.1 (0.5)	2.3 (3.4)	2.7 (0.22)	44 (0.97)
TRAWSFYNYDD	71 (1.4)	0.069	0.043	2.7 (1.5)	8.1 (0.15)	47 (0.62)
BALA	33	<0.03	0.037	8.6 (20)	2.8 (0.24)	14 (0.54)
CHILTON	<6	0.078	0.061	0.8 (1.0)	1.4 (0.18)	33 (0.45)
ASHBURY	<14	0.047	0.026	1.7 (3.3)	2.3 (0.21)	83 (0.36)
WINFRITH	<9	0.046	<0.04	2.9 (4.9)	3.0 (0.18)	13 (0.56)
CORFE	<18	0.028	<0.03	0.6	4.7 (0.16)	37 (3.3)
S.BRENT	<13	0.049	<0.03	1.5	7.9 (0.24)	23 (0.69)

Notes: (i) Underline denotes that plot is at or near to nuclear installation
(ii) Sr-90 analysis was only undertaken during the period June 1986 to May 1987
(iii) Figures in parentheses indicate the average ratio of Summer/Winter atmospheric deposition
(iv) Results for Pu-239+240 and Am-241 at Dounreay and Huna are based on data from 1986 and 1987

aerosol is mainly responsible for this transfer mechanism which is recognised by separate studies of the coastal region in W. Cumbria (Pattenden et al. 1983). The annual average deposition of Na is an order of magnitude greater at the three coastal plots than at inland locations. In general, the atmospheric deposition of Ti followed the same seasonal pattern.

The relatively high ratios of summer/winter deposition of Sr-90 at some northerly plots (Table 4) indicated a contribution from Chernobyl fallout and a separate post-Chernobyl survey in N. Wales confirms this (Cawse et al. 1988).

Scanning electron microscopy was used to examine particulate matter present in rainwater and on leaves of ryegrass and lucerne. Three main groups of particles were found, namely spherical (1 to 10 μm diameter), angular (5 to 15 μm) and aggregate (16 to 50 μm). In rainwater samples collected in winter 1987/88 and in summer 1988 the number of particles in the range 1 to 10 μm diameter varied from 0.4 to 1.2 x 10^9/litre at the 19 plots in Gt. Britain and France, of which <3% were present in the 5 to 10 μm diameter size range. At 9 plots, particles were most numerous in the winter period ending May 1988. However, the association of particles with radionuclides is unknown.

TABLE 5 RADIONUCLIDES IN WET AND DRY DEPOSITION AFTER THE CHERNOBYL REACTOR ACCIDENT

Location of Field Plot	Bq/m^2 deposited in collection period Sept. 1985 to May 1986			
	Cs-137	Cs-134	Ru-103	Sr-90
DOUNREAY	2900	1500	2300	4.1
HUNA	2400	1250	2900	3.0
BRAYSTONES	5900	3300	7800	196
PENRITH	170	95	500	6.5
WINFRITH	100	51	<100	0.30
CORFE	84	43	<190	0.55
S.BRENT	55	28	<780	0.87

Note: Other plots, including those in France, were started post-Chernobyl

In Gt. Britain, deposition collectors at 7 field plots were installed in autumn 1985, therefore samples in May 1986 revealed Chernobyl fallout and up to 5900 Bq Cs-137/m^2 and 196 Bq Sr-90/m^2 were recorded, together with Ru-103 (Table 5). Over the following collection period, when all British and French sites were in operation, radiocaesium fallout decreased with latitude and was minimal below latitude 53°N (Cawse and Colle, 1988).

(c) Vegetation analysis

The average annual concentrations of radionuclides recorded in harvests of ryegrass are listed in Table 6 for both Gt. Britain and France. Elevated concentrations of Cs-137 in herbage from northerly locations in Gt. Britain showed the response to Chernobyl fallout in accordance with data from rainwater analysis (Table 4). Lucerne harvests in the first year of the Chernobyl accident contained less radiocaesium than ryegrass which is attributed to the deeper rooting nature of lucerne, less liable to uptake of fallout in surface soil (Cawse and Colle, 1988). The trend in radiocaesium concentrations in ryegrass after the Chernobyl accident showed a decrease of 2 orders of magnitude over one year (Fig. 4) comparable with the trend in total deposition: decreases in Sr-90 were also recorded.

Sr-90 levels in lucerne from control plots were from 11 to 43 Bq/kg and generally exceeded those found in ryegrass by ~80%, in agreement with the reported difference in soil to plant transfer factors (IUR/RIVM, 1987). Actinide concentrations in herbage increased by an order of magnitude at Dounreay and Braystones although levels near other nuclear installations in Gt. Brtain and in France were similar to herbage from control plots or below the analytical limits of detection (Table 6).

TABLE 6 AVERAGE ANNUAL CONCENTRATIONS OF RADIONUCLIDES IN RYEGRASS FROM FIELD PLOTS IN GT.BRITAIN AND FRANCE

Location of Field Plot	Average Annual Concentration, Bq/kg dry wt, June 1986 to May 1988 Cs-137	Pu-239+240	Am-241	Sr-90
CONTROL SITES, GT BRITAIN				
HUNA	10.8 (2.3)	<0.03	<0.03	7 (1.0)
PENRITH	4.9 (3.6)	<0.03	<0.06	17 (3.6)
BALA	3.7 (3.2)	<0.03	<0.05	26 (0.5)
ASHBURY	<1	<0.03	<0.03	4.8 (3.0)
CORFE	<1	<0.03	<0.05	19 (0.5)
SOUTH BRENT	3.7 (3.0)	<0.03	<0.04	16 (3.9)
NUCLEAR SITES, GT BRITAIN				
DOUNREAY	18.2 (2.8)	0.16 (1.8)	0.073 (2.5)	29 (0.7)
BRAYSTONES	42.4 (4.0)	0.30 (2.4)	0.31 (4.5)	22 (1.2)
TRAWSFYNYDD	5.7 (2.7)	<0.04	<0.04	24 (1.6)
CHILTON	<1	<0.04	<0.04	15 (10.4)
WINFRITH	4.6 (4.2)	<0.04	<0.04	24 (1.0)
CONTROL SITES, FRANCE				
MARTINVAST	<2	<0.02	0.021 (2.3)	
LION EN SULLIAS	<2	<0.02	<0.02	
MORESTEL	3.6 (2.6)	<0.02	<0.02	
ST. ETIENNE DES SORTS	2.5 (5.4)	<0.02	<0.02	
NUCLEAR SITES, FRANCE				
MERQUETOT	2.4 (1.7)	0.031 (1.4)	0.027 (1.7)	
DAMPIERRE	<2	<0.02	<0.02	
MONTALIEU	2.7 (1.6)	<0.02	<0.02	
CADEROUSSE	2.8 (1.6)	0.023 (1.3)	0.024 (2.2)	

Notes: (i) Sr-90 analysis of ryegrass was restricted to the period June 1986 to May 1987

(ii) Figures in parentheses indicate the average ratio of Summer/Winter concentrations

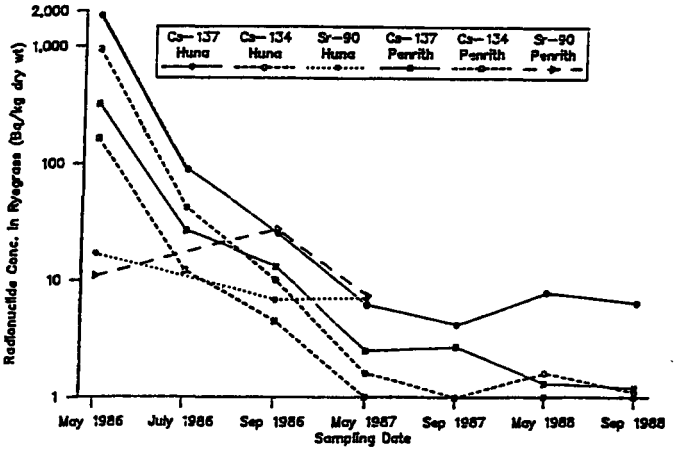

FIG.4 CONCENTRATIONS OF Cs-134, Cs-137 AND Sr-90 IN RYEGRASS AT HUNA AND PENRITH FIELD PLOTS (MAY 1986 TO SEPTEMBER 1988)

At the coastal plots situated at Dounreay and Braystones, a seasonal increase up to 5-fold in Pu-239+240 and Am-241 concentrations in herbage occurred in the summer growth period (June to September) compared with over-winter growth (October to May): this is opposite to the seasonal pattern of atmospheric deposition and has been observed in separate studies at other field plots near the coast in W. Cumbria. It is attributed to greater interception and retention by foliage of actinides transferred to land by the marine aerosol. A similar increase was recorded at the two coastal plots in France (Table 6). The increase in ratios of summer/winter concentrations of Sr-90 and Cs-137 in ryegrass at some plots (Table 6) is mainly attributed to inputs of Chernobyl fallout in the first summer growth period and/or resuspension of soil dust in dry regions of southern France.

The data obtained by continuous operation of field plots provides an inventory of radionuclide deposition and removal by harvest. Concentrations in herbage may be related to deposition rates by deriving the normalised specific activity. For example at Chilton field plot, in summer 1986:

Radionuclide: Pu-239+240		Ryegrass	Lucerne	
Yield** dry matter	kg m^{-2}	0.26	0.11	**newly
Concentration	Bq kg^{-1}	0.054	0.031	established
Removal by harvest	Bq m^{-2}	0.014	0.0034	vegetation
Soil pool to 30 cm	Bq m^{-2}	63		
Atmospheric input,	Bq m^{-2}	0.015 from June-September 1986.		
Crop removal of -				
Atmospheric input	%	93.3	22.7	
Soil pool to 30 cm	%	0.02	0.005	
NSA: m^2 days kg^{-1}		42	24	

$$\text{NSA} = \frac{\text{Bq/kg in herbage}}{\text{Bq/day/m}^2 \text{ in deposition}}$$

The above results show very efficient retention by ryegrass of plutonium in atmospheric deposition, but lucerne contained less and gave a lower yield since it was newly established.

The importance of direct deposition of airborne radionuclides to foliage was assessed by analysis of herbage from the sub-plots of standard soil placed within the main plot area. A comparison of data (Fig. 5) clearly shows the influence of some nuclear installations by increases up to an order of magnitude in Pu-239+240 and Am-241 in ryegrass compared with the control plots at the same latitude. Similar data was obtained from lucerne.

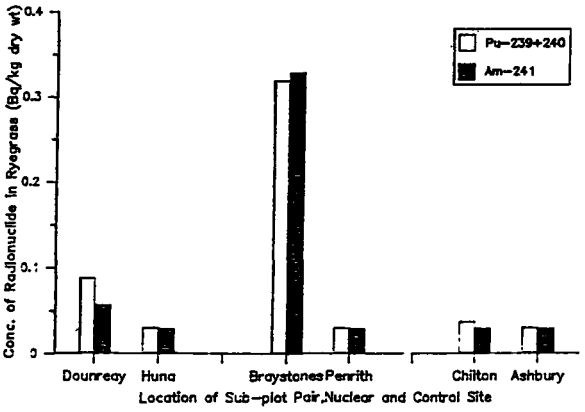

FIG.5 AVERAGE ANNUAL CONCENTRATIONS OF Pu-239+240 AND Am-241 IN RYEGRASS FROM SUB-PLOTS AT NUCLEAR AND CONTROL SITES (MAY 1986 TO MAY 1988)

Soil to plant transfer factors for actinides, derived from the average annual soil (30 cm depth) and herbage concentrations at the control field plots were <0.1 for Pu-239+240 and <0.3 for Am-241. Transfer factors for Sr-90 and Cs-137 were increased by Chernobyl inputs to foliage. The transfer factors for herbage from plots near to some nuclear installations were also elevated owing to direct deposition and retention of actinides by foliage, as demonstrated by the sub-plots data (Fig. 5).

(d) Generalised Derived Limits

Comparison of the maximum concentrations of radionuclides recorded in herbage with generalised derived limits (GDL's) proposed by the National Radiological Protection Board (NRPB) (Haywood, 1987,) shows the following:

Radionuclide	Max. Concn.* Bq/kg dry wt.		GDL Bq/kg dry wt.	% GDL	
	Ryegrass	Lucerne		Ryegrass	Lucerne
Sr-90	29	106	2000	1.5	5.3
Cs-137	120	36	800	15	4.5

*for an individual harvest, Summer 1986.

No GDL is proposed for plutonium or Am-241 in herbage since it is considered that there is little transfer to man via the cow-to-milk pathway. Haywood (1987) advises that environmental measurements exceeding ~25% of the GDL for each radionuclide and material analysed require more detailed study of the critical group doses. Clearly, none of the herbage measurements attain this level. However, at the end of May 1986, Cs-137 was present in ryegrass at 1850 to 2700 Bq/kg dry weight at northerly plots in Gt. Britain (Fig. 4), well in excess of the GDL at 800 Bq/kg. The maximum concentration of Sr-90 in May 1986 was 52 Bq/kg at Braystones, which is 2.6% of the GDL.

3. Conclusions

The results have provided a time series of data that reveals both seasonal differences and variation in concentrations of radiocaesium, strontium-90 and actinides in environmental media at nuclear and distant sites in Gt. Britain and France, and variation according to latitude and rainfall. Chernobyl fallout remains highly concentrated in surface soil layers. At some plots near nuclear sites, interception and retention of Pu and Am-241 by foliage is the main transfer pathway leading to elevated concentrations in herbage. Inventories of radionuclide deposition and removal by herbage together with information on accumulations of radionuclides in soil have contributed to understanding the relative importance of soil to plant transfer and direct deposition of radionuclides to foliage.

The collaborative project between Harwell Laboratory and CEN Cadarache has supported the Radiation Protection Programme of the CEC by providing more detailed information on the behaviour of radionuclides in the terrestrial environment and the impact of nuclear installations. It has also recorded effects of the Chernobyl accident. The study has established that currently, generalised derived limits for radiological protection are not exceeded in soil and vegetation.

4. Acknowledgements

In addition to support from the CEC, this study was supported in Gt. Britain by the Ministry of Agriculture, Food Sciences Division and in France by the Commissariat A l'Energie Atomique. The assistance of staff at Harwell and CEN Cadarache is gratefully acknowledged.

References

CAWSE, P.A. & BAKER, S.J. (1988). A post-Chernobyl survey of radionuclides in Wales, August-October 1986. AERE Harwell Report R-12828, HMSO, London.

CAWSE, P.A. & COLLE, C. (1988). Comparison of radionuclide deposition to soil and vegetation. D76-D89, In Impact des Accidents D'Origine Nucleaire sur l'Environnement, Vol. 1, Proc. 4th Int. Symposium Radioecology, CEN Cadarache, 14-18 March 1988.

HAYWOOD, S.M. (1987). Revised generalised derived limits for radioisotopes of strontium, iodine, caesium, plutonium, americium and curium. NRPB Report GS8, Chilton, Oxon.

IUR/RIVM. (1987) 5th report of the Workgroup on Soil to Plant Transfer Factors. RIVM, Bilthoven, The Netherlands.

PATTENDEN, N.J., CAMBRAY, R.S. and EAKINS, J.D. (1983). Radionuclide transfer processes from sea to land. Ecological Aspects of Radionuclide Release, Special Publicn. No. 3, British Ecological Society, Blackwell, Oxford.

IV. Other research group(s) collaborating actively on this project [name(s) and address(es)]

Centre d'Etudes Nucleaires de Cadarache, Service d'Etudes et de Recherches sur l'Environnement: Chef, A. Grauby, BP No. 1, 13108, Saint-Paul-lez-Durance, France.

Collaboration is made with A. Grauby, J. Delmas and C. Colle. Discussion took place with CEN Cadarache in September 1989 and January 1990 during exchange visits.

V. Publications:

CAWSE, P.A. and COLLE, C. (1988). Comparison of radionuclide deposition to soil and vegetation. In, Proceedings of the 4th International Symposium on Radioecology, Volume 1, D-76 to D89, Cadarache, France, March 1988.

Title of the project no: 2

Comparative study of soil to plant transfer of Neptunium, Plutonium, Americium and Curium.

Head(s) of project:

Dr R G Derwent

Scientific staff: P A Cawse
S J Baker
P Burton
B Sykes

I. Objectives of the project:

In a collaborative project with CEN Cadarache, the objectives were to provide improved data on soil to plant transfer of actinides following contamination of different soil types that occur in Gt. Britain and in France. The effect of ageing in soil of actinides was also determined with respect to plant uptake and the distribution of actinides in soil compartments. This information was needed to improve the accuracy of radiation dose estimates to man from the ingestion pathway.

II. Objectives for the reporting period:

Analysis of vegetation samples collected in 1988 will be completed for comparison with previous results. Further samples of ryegrass and lettuce will be grown in 1989, the lettuce being re-sown in Spring. Soil samples will be taken after the final harvest to assess the distribution of Np-237 and Am-241 in soil fractions. Studies on Cm-244 uptake will continue for 3 years until mid-1990 according to the established experimental programme and results will be discussed with CEN Cadarache.

III. Progress achieved:

1. Methodology

The collaborative project between Harwell Laboratory and CEN Cadarache was started in July 1986, with the application of Np-237 and Am-241 tracers in nitrate form to containers each holding 15 kg dry weight of soil. The soil types used were an organic (fen) soil, a brown earth (neutral, from the Sellafield area), an acidic brown earth and a brown calcareous soil. Their properties are listed in Table 1.

The tracer concentrations in soil were Np-237: 7.4 kBq/kg and Am-241: 18.5 kBq/kg dry weight. In Gt. Britain, Cm-244 was also used at a concentration of 18.5 kBq/kg, applied to the organic soil and neutral brown earth only. Studies with the neutral brown earth were only carried out in Britain: this soil contained 19 Bq Pu-239+240/kg dry weight, without tracer addition being necessary.

To examine soil to plant transfer of actinides, ryegrass and lettuce were used as test plants in Gt. Britain while in France other crops were examined, namely haricot bean, radish and lucerne. Ryegrass was harvested over summer and winter seasons, to examine the effect of ageing on uptake of actinides from soil. All samples of vegetation were ashed at 450°C for analysis.

In Gt. Britain, the effect of soil amendments on uptake of actinides by ryegrass was also examined. Sewage sludge was mixed with the organic soil and the neutral brown earth at 6.4% on a soil dry weight basis (sludge contained 3.7% total nitrogen) for comparison with untreated soil. The organic soil was also sterilised by treatment with 50 KGy of gamma-radiation in an industrial Co-60 irradiation facility before the addition of Np, Am and Cm tracers and cultivation of ryegrass.

In France, soils were fractionated after crop cultivations and ageing, using methods previously applied in separate studies of Np-237 and Am-241 in the water soluble, exchangeable, organic and chelated forms (Colle and Morello, 1986).

TABLE 1 BASIC SOIL PROPERTIES

TYPE OF SOIL	Origin	pH in water	pH in $CaCl_2$/KCl	Organic carbon %	Cation exchange capacity meq/100 g	Texture* Clay %	Silt %	Sand %
Organic soil (Fen)	Norfolk England	6.9	$CaCl_2$ 6.6	24.1	122.0	46	23	31
Brown earth (Sellafield)	Cumbria England	7.0	$CaCl_2$ 6.8	1.8	10.0	11	19	70
Brown acidic (Sol acide)	La Hague France	5.8	KCl 5.3	1.1	14.3	11	47	42
Brown calcareous (Sol calcaire)	Cadarache France	8.1	KCl 7.6	0.7	9.8	7	51	42

*soil texture results are expressed on a peroxidised oven dry soil basis

2. Results

The results have shown differences in soil to plant transfer of actinides according to:

i) Soil type, sterility and amendment with organic (sewage) sludge
ii) Radionuclide
iii) Vegetation type
iv) Ageing ie. temporal changes in uptake by ryegrass.

The transfer factors obtained for the test plants grown in different soils are shown in Figures 1, 2 and 3 for the three actinides. There was relatively high uptake by ryegrass of Np-237 and Am-241 from acid brown earth compared with the other soils ie. it was two orders of magnitude greater than with organic (fen) soil. Intermediate transfer factors were recorded for ryegrass grown in brown calcareous soil and Sellafield brown earth which have the highest pH values (Table 1). It is clear that the uptake of Np-237 exceeded soil to plant transfer of Am-241 and Cm-244 by an order of magnitude.

With the experiment on uptake of Cm-244 by ryegrass, the organic soil gave lower transfer factors than brown earth (Fig. 3). Lettuce showed a transfer factor of 2.0×10^{-4} for Cm-244 in the organic soil, which was higher than the average transfer factor of 9.8×10^{-5} for ryegrass.

Relatively low transfer factors for Np-237 and Am-241 uptake by haricot bean are attributed to prevention of translocation to the seed by the placental barrier: this was demonstrated by analysis of leaf tissues and the detailed results of all measurements on crops have been reported separately (Cawse and Colle, 1989).

In experiments in France with lucerne, the highest transfer factors again occurred in the acid brown earth compared with soils of higher pH (Figs. 1 & 2).

The 'expected values' for soil to plant transfer factors listed in the International Union of Radioecologists data bank (IUR/RIVM, 1987) have been compared with the present series of measurements. For Np-237 (Fig. 1) the IUR data for fodder is close to the maximum values we have found, although no expected values are listed for vegetables. For Am-241, the IUR data for vegetables is an order of magnitude greater than the results shown in Fig. 2, but for grass the 'expected values' for transfer factors are an order of magnitude less than given by ryegrass grown in acid brown earth.

In the case of Cm-244, no 'expected values' for soil to plant transfer are listed by the IUR. It is almost certain that an increase in uptake would be found in acid soils. In fact, Pimpl (1988) has reported transfer factors of 2.2×10^{-3} for grass in an acid sandy soil of pH 4.9 ($CaCl_2$) compared with 7.5×10^{-4} in gley soil at pH 5.4 ($CaCl_2$).

The total removal of tracers in the course of ryegrass harvests from July 1986 to May 1988 was 322 Bq Np-237 and 14 Bq Am-241 from the acidic brown earth, compared with only 4.6 Bq Np-237 and 0.44 Bq Am-241 from the organic soil.

Measurements of plutonium uptake by ryegrass grown in neutral brown earth soil gave a transfer factor of <0.003 which was not altered by the addition of sewage sludge, and showed no temporal change that would reflect an increase in availability on ageing: as a result, no further experiments were made.

The temporal changes in seasonal concentrations of Cm-244 in ryegrass grown in the organic (fen) soil and in neutral brown earth (Sellafield soil) were less than for the other actinides and this feature may be associated with the occurrence of more oxidation states for Np and Am in aqueous (soil) solution.

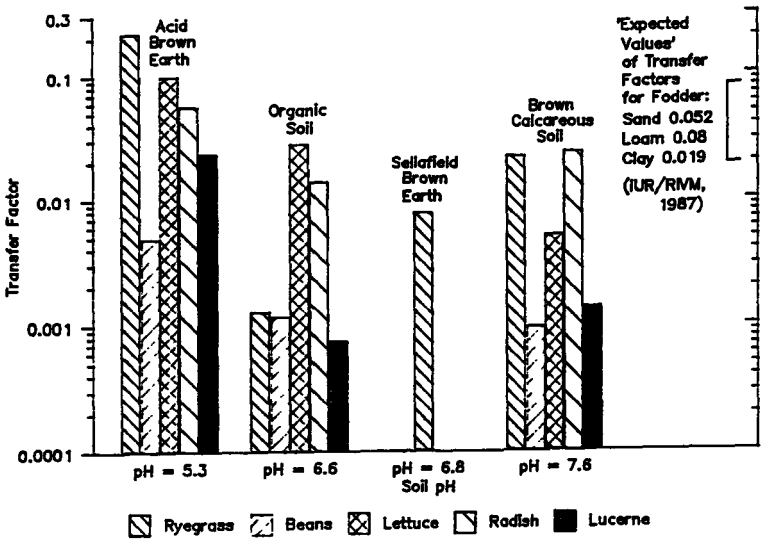

FIG.1 SOIL TO PLANT TRANSFER OF Np-237 BY DIFFERENT CROPS IN RELATION TO SOIL pH

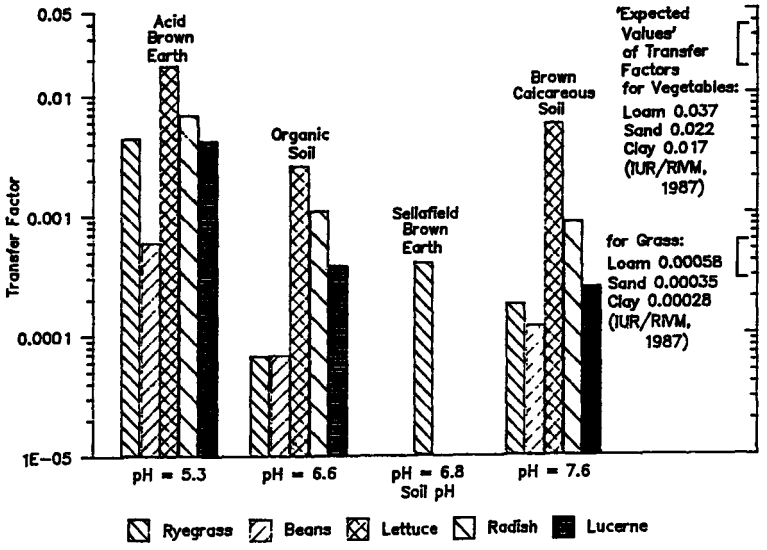

FIG.2 SOIL TO PLANT TRANSFER OF Am-241 BY DIFFERENT CROPS IN RELATION TO SOIL pH

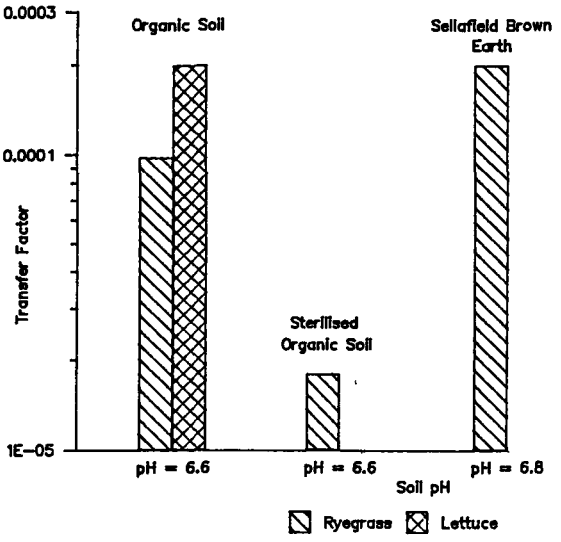

FIG.3 SOIL TO PLANT TRANSFER OF Cm-244 BY RYEGRASS AND LETTUCE

The seasonal variation and differences in concentrations of Am-241 grown in organic (fen) soil and in Sellafield soil (neutral brown earth) are shown in Fig. 4. An ageing effect was very clear in the brown earth, but this feature was not observed for Np-237 which showed an increase of 3-fold in the winter 1987/88 ryegrass harvest compared with concentrations in the previous season.

Application of sewage sludge to acidic brown earth increased uptake of Am-241 by ryegrass up to 4 fold, and up to an order of magnitude when added to the organic soil. In the case of Np-237, although initial harvests (in 1987) from organic soil gave order of magnitude increases in uptake by ryegrass in response to sewage addition, this was not sustained. On average, Cm-244 uptake by ryegrass showed the least response to application of sewage sludge, but when the individual seasonal data was examined a decreasing trend was evident.

The gamma-sterilisation of organic (fen) soil prior to addition of Cm-244 and cultivation of ryegrass resulted in decreased uptake (Fig. 4), and a similar effect was also obtained with Np-237. This may indicate suppression of micro-organisms associated with the root rhizosphere that normally enhance nutrient uptake. However, no similar response was found for Am-241 uptake in sterilised soil, which may imply that physico-chemical processes rather than root rhizosphere activity mainly control Am-241 uptake by roots. Soil sterility could not be maintained over the long term because although growth containers were in a glasshouse they remained open to the atmosphere and re-establishment of the microflora would gradually take place (Cawse, 1975). However, the effect of soil sterilisation on uptake of Cm-244 does persist for at least three seasons (Fig. 5).

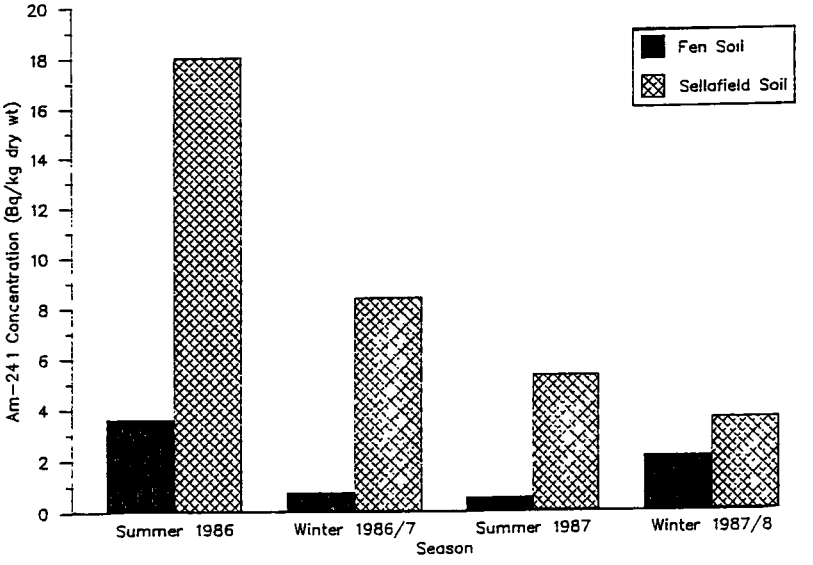

FIG.4 SEASONAL VARIATION IN THE UPTAKE OF Am-241 BY RYEGRASS GROWN IN DIFFERENT SOILS

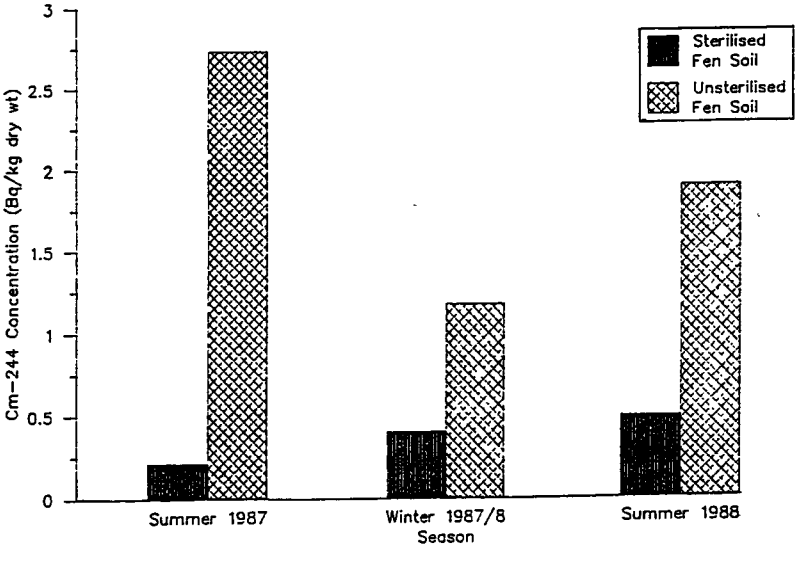

FIG.5 SEASONAL VARIATION IN THE UPTAKE OF Cm-244 BY RYEGRASS GROWN IN STERILISED AND UNSTERILISED FEN SOIL

The application by CEN Cadarache of soil extraction procedures (Colle and Morello, 1986) after crops were grown has established that an order of magnitude more Np-237 than Am-241 is contained in the water-soluble, exchangeable (with ammonium acetate) and organo-metallic fractions of the acid brown earth, brown calcareous soil and organic (fen) soil. As noted in the present series of experiments, Np-237 shows greater availability to the test crops than Am-241 (Figs. 1 & 2). Further results from these extraction procedures are described in the associated collaborative CEN contract no. B16-B-037-F.

3. Conclusions

The soil to plant transfer of Np-237, Am-241 and Cm-244 has been shown to be greatly influenced by soil type and amendment. The observation that acid brown earth enhances the uptake of actinides by ryegrass at a pH value (in water) of 5.8, ie only slightly acid, suggests that much higher transfer factors would be found in more acid soils with pH from 4.0 to 5.5. In fact, the National Soil Inventory of the Soil Survey of England and Wales has established that 38.2% of the land area has pH below 5.5.

In view of the reduction in soil to plant transfer of Np-237 and Cm-244 after soil sterilisation, the influence of soil microbial activity on root uptake of actinides requires investigation, particularly in relation to additions of organic fertilisers to soil.

The collaborative project between Harwell laboratory and CEN Cadarache has supported the Radiation Protection Programme of the CEC by providing information on the transfer of actinides to crop plants, where few data have been previously reported, and will improve assessment of the food chain transfer to man following an accidental release.

4. Acknowledgements

In addition to support from the CEC, this study was supported in Gt. Britain by the Ministry of Agriculture, Food Sciences Division and in France by the Commissariat A l'Energie Atomique. The assistance of staff at Harwell and CEN Cadarache is gratefully acknowledged.

References

CAWSE, P.A. and COLLE, C. (1989). Variability in soil to plant transfer of neptunium, americium and curium. In, 6th Report of the IUR Workgroup on Soil to Plant Transfer Factors, 22-29, Guttanen, Switzerland, May 1989. RIVM Bilthoven, The Netherlands.

CAWSE, P.A. (1975). The microbiology and biochemistry of irradiated soils, Chapter 5 In Soil Biochemistry Vol. 3, edit. A.D. McLaren & E.A. Paul, Marcel Dekker, New York.

COLLE, C. and MORELLO, M. (1986). Behaviour of neptunium in the terrestrial environment, 1-12, Session 2, In The Cycling of Long-Lived Radionuclides in the Biosphere: Observations and Models, Vol. 1, Proc. CEC Seminar, 15-19 September 1986, Madrid.

IUR/RIVM (1987). 5th Report of the Workgroup on Soil-to-Plant Transfer Factors, Egham, UK. 14-16 April 1987, RIVM Bilthoven, The Netherlands.

PIMPL, M. (1988). Untersuchungen zum Boden/Pflanzen-Transfer von Np-237,, Pu-238, Am-241 und Cm-244. Report 4452, Kernforschungszentrum Karlsruhe, GmbH.

IV. Other research group(s) collaborating actively on this project [name(s) and address(es)]

Centre d'Etudes Nucleaires de Cadarache, Service d'Etudes et de Recherches sur l'Environnement: Chef, A. Grauby, BP No. 1, 13108, Saint-Paul-lez Durance, France.

Collaboration was made with A. Grauby, J. Delmas and C. Colle. Experimental data for uptake by other crops of Np-237 and Am-241 has been obtained by CEN Cadarache using the same soil types and is compared with Harwell data which is complementary.

V. Publications:

CAWSE, P.A. and COLLE, C. (1989). Variability in soil to plant transfer of neptunium, americium and curium. In, 6th Report of the IUR Working Group on Soil-to-Plant Transfer Factors, 22-29, Guttanen, Switzerland, May 1989. RIVM Bilthoven, The Netherlands.

Title of the project no: 3

Exchange of radionuclides between sea and atmosphere

Head(s) of project:

W.A. McKay

Scientific staff: M.I. Walker
J. Cloke

I. Objectives of the project:

To investigate the mechanisms by which artificial radionuclides in the sea can be converted into aerosol in the atmosphere above the sea surface, and to study this aerosol as it is transferred to land. The present project is concerned with laboratory and field studies in roughly equal proportions, the associated project from France deals mainly with laboratory studies.

II. Objectives for the reporting period:

1. Develop a working system (The Harwell Bubble Burst Aerosol Sampler) for generating and collecting marine aerosol in order to test the hypotheses that
i) actinides are enriched in the marine aerosol generated by bubble bursting.
ii) particulate material in seawater is the vector for the actinides in marine aerosol.

2. Design and carry out a series of field and laboratory experiments to gain a greater understanding of
i) The characteristics of aerosol blown onshore (the size distribution, production rate and particulate content of the seaspray).
ii) the importance of organic material in seawater on aerosol flux and the enrichment of particulates.

Objectives 1 and 2 (ii) have been carried out in collaboration with the University of East Anglia.

III. Progress achieved:

1. The Harwell Bubble Burst Aerosol Sampler

The generation of marine sea-salt aerosol is generally attributed to bubble-bursting at the sea-surface. This process has been investigated in experiments performed in offshore Irish Sea waters using equipment developed as part of contract BIO-B-333-81-UK and further modified during the existing contract.

The equipment consists of an artifical bubble source and a high volume aerosol sampler (Fig. 1). Bubbles are generated by forcing air through a glass sinter held beneath the seawater surface, the droplets produced when the bubbles burst are sampled by the high-volume air sampler drawing the droplets ($\leq$ 25 μm diameter at 80% humidity) onto a Whatman filter located about 30 cm above the sea surface.

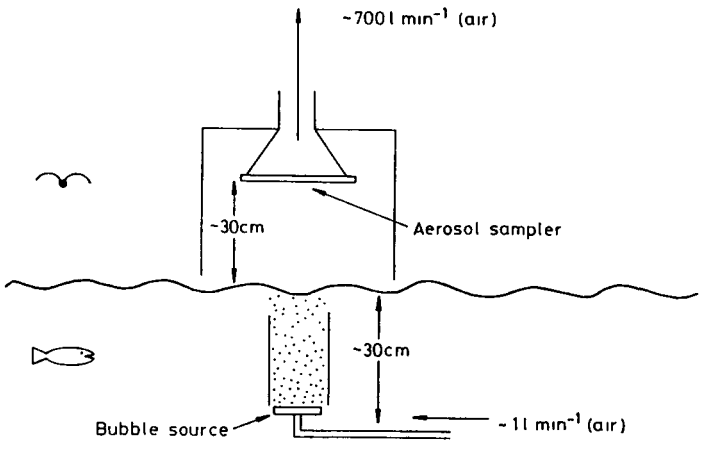

Figure 1. Bubble-Burst Aerosol Sampler

This equipment was used in the Irish Sea, close to the discharge outfall of the Sellafield nuclear reprocessing plant in Cumbria, on several occasions. The aerosol was found to be enriched in plutonium and americium by factors of between 30 and 700 over their concentrations in seawater. No enrichment of caesium-137, a nuclide which is mainly associated with the dissolved phase in seawater, was observed. Stable aluminium (a natural tracer of fine grained sediment) was also determined and gave aerosol enrichment factors comparable with the actinides giving strong support to the hypothesis that the particulate material in seawater is the vector for the actinides in marine aerosol.

The most likely mechanism of particulate enrichment in the aerosol is the scavenging of particulate by rising bubbles, which burst at the surface to produce particulate-rich droplets.

2.i) The Characteristics of Aerosol Blown Onshore

In developing a quantitative understanding of the transfer of radionuclides from sea to air to land, the onshore flux and droplet size of the sea spray at different wind speeds is required. In addition, since a significant amount of the actinide activity is likely to be associated with sediment particles, the sediment content of the aerosol needs also to be determined.

In-situ size and concentration measurements of seaspray were carried out using a LISATEK phase doppler instrument developed at Harwell (Livesley et al, 1989). The instrument contains a 25 mW Helium Neon laser with beam splitting optics which allow two coherent laser beams to be focussed in the open air; the intersection region of area ~0.2 mm^2 represents an isokinetic probe. When a particle passes through the probe volume an interference pattern is formed by the scattered light with the spatial frequency of the fringe pattern inversely proportional to the particle diameter. Every particle between about 3 and 100 μm diameter passing through the probe volume is counted and a representative number (on average ~40%) sized. The probe volume was set up normal to the wind direction and about 1-1.5 m above the beach. Typically, data sets of 30 minutes duration were taken, with the distance of the instrument to the surf zone being recorded at the start and end of each run.

For the collection of a representative sample of sea spray for stable-element analysis, a high volume air-sampler was used. This draws air through a 21 x 23 cm exposed area of Whatman 41 filter at a nominal rate of ~2 m^3 min^{-1}, giving a face velocity of 0.8 m s^{-1}. Inlet cones, which allowed the inlet velocity to be adjusted to a value close to that of ambient wind were fitted in front of the filter when necessary. The largest (inlet area = 111 cm^2) allowed isokinetic sampling at a nominal 3 m s^{-1}, with others for 6 (55.5 cm^2), 9 (37 cm^2) and 12 m s^{-1} (28 cm^2) winds. For intermediate wind speeds, the cone approximating closest to the measured wind speed was used.

In the collection of size-separated aerosol samples for stable element analysis, the same criterion of aiming to maintain isokinetic conditions was applied. A portable perspex wind tunnel was constructed, with a cross section of 40 x 40 cm (ie 1600 cm^2) and a fan operating of 1800 m^3 h^{-1} giving isokinetic sampling in winds speeds of ~3.5 m s^{-1}. At this wind speed the stopping distance of a 100 μm diameter unit density particle (around the upper limit of seaspray droplets) would be 6 cm, small compared to the cross-section of the tunnel. Sampling equipment was set 35 cm from the tunnel inlet, allowing a settling time of 0.1 cm seconds; in this time a 100 μm drop would fall only 3 cm, thus there is no droplet shaddow from the tunnel roof at the sampling point. The tunnel is shown in cross-section in Fig. 2. Inlet cones to the wind tunnel allowed isokinetic sampling to be maintained at 1.0 m s^{-1}, 3.5 m s^{-1} (no cone), 7.5 m s^{-1} and 12.5 m s^{-1}.

Inside the wind tunnel, particles in the sub-10 μm range were collected in a Sierra 236-high volume cascade impactor. In order to sample isokinetically a cone was attached to the first stage to produce an inlet velocity matching that inside the tunel. Whilst particles >10 μm will collect on stage 1 of the cascade impactor, the upper cut off size is unknown and an alternative technique was also used based upon the inertial impaction of particles onto cylindrical collectors. For the impaction of particles upon a cylinder to be 50% efficient, it must have a Stokes number of 1.7.

The Stokes number (Stk) is a measure of the impaction efficiency of particles onto a surface, and is related to the stopping distance of a particle (S_o) and the diameter of the obstacle (d_o).

$$Stk = S_o/d_o.$$

Particle diameters corresponding to calculate relaxation times can be deduced from nomographs.

Metal rods of 4 different diameters are suspended from the wind tunnel roof. The rod diameter, together with the cut-off particle diameters, at 3.5 m s^{-1}, are given below.

Rod diameter d_o (mm)	Relaxation time τ (μs)	Cut-off particle diameter (μm)
3	728	~15
12	3084	~33
32	7710	~50
44	10782	~60

The cylinder with the smallest diameter should collect more seaspray than the next largest and so on, since the collection efficiency for all particles increases with decreasing diameter ie large radius rods will collect large particles but few smaller ones whereas small diameter rods will collect large and small particles. The volume of air intercepted by each rod is the product of projected rod area (height x diameter), wind speed past the rod and sampling duration. The air concentration of sea-spray as determined using the narrowest rods should in theory be less than that determined on the first stage of the cascade impactor, since the impactor should collect all particles that the rods do plus particles of 8-15 μm diameter.

For rods ≥12 mm diameter, the rods were made of stainless steel while those of 3 mm were tungsten. This allowed concentrated nitric acid to be used as a washing agent to remove collected particles, with minimal dissolution of the rod and contamination (except possibly from iron). Distilled water runs off the rods, due to the presence of organic matter collected with the spray, without removing much of the material on the rods. Nitric acid oxidises the organic matter on the rods and improves the spray removal efficiency.

The results are still being analysed, but clearly indicate:

i) a strong dependence of sea spray concentration with wind speed,
ii) a decrease of about two orders of magnitude in the concentration of large spray drops (>10 μm diameter) as the edge of the water recedes from 13 m to 200 m from the instruments (Fig. 3),
iii) a major fraction of aerosol mass associated with particles greater than 50 μm diameter,
iv) a large enrichment of inorganic particulate in all samples of seaspray.

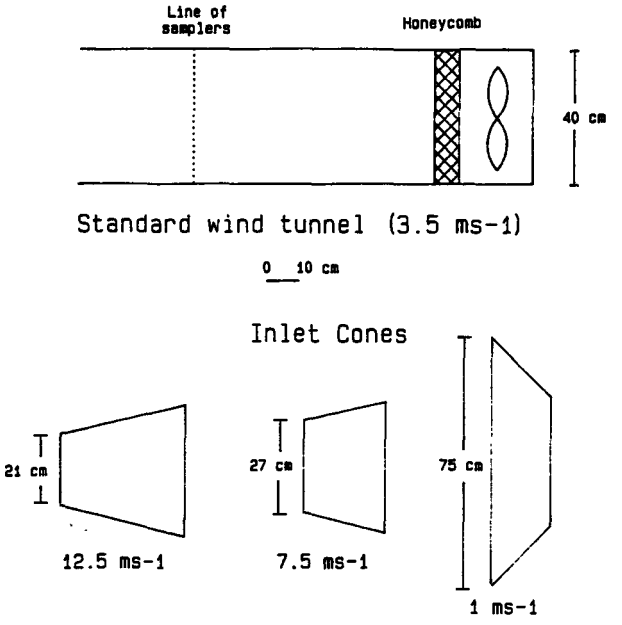

Fig. 2 Outline of wind tunnel and inlet cones

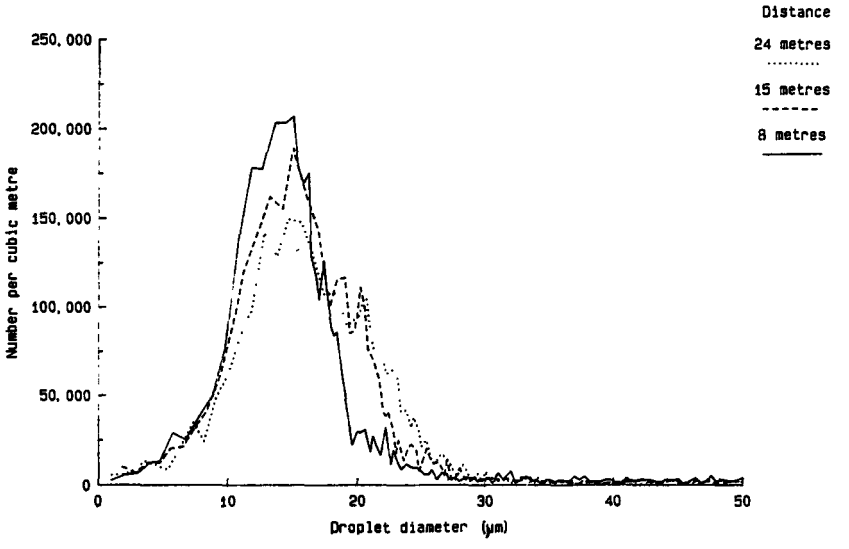

Fig. 3 Variation in droplet concentration with distance from surf zone

2.ii) The importance of organic material in seawater on aerosol flux and particulate enrichment

A periodicity in the on-land rate of transfer of sea spray associated actinide activity has been observed on the Cumbrian coast with a broad peak around the third quarter and a deep trough during the first quarter of the year (Pattenden et al, 1989). This phenomenum is not readily explained by gross changes in shore-line seawater concentrations or flux of sea spray.

Marine organic matter decreases the surface tension and reduces the dissolution rate of smaller bubbles (Blanchard, 1983), thus possibly increasing the specific surface area and relative carrying capacity for particulate material. The bubble rise velocity is also decreased by adsorbed organic matter (Scott, 1987), allowing a greater period of time for particulate to be scavenged. It is thus reasonable to hypothesise that variations in marine organics could influence aerosol flux and particulate enrichment.

The purpose of part of the programme was to determine the seasonality of organics, measured as dissolved organic carbon (DOC) and surfactant activity, in UK coastal waters, and try to quantify their effect on the generation and inorganic particulate enrichment of sea-salt aerosol under controlled laboratory conditions.

Although a seasonal trend in aerosol flux was seen, this did not correlate directly with surfactant activity or DOC concentrations. In contrast the enrichment factor for 3 μm spherical particles in aerosol appeared to be more directly correlated with surfactant activity and also varied with seawater particulate loading. The maximum enrichment factors were about a factor of three lower than those reported by Pattenden et al (1989). This may be a laboratory artefact resulting from the depletion of organics and particulate by bubbling, compared with continual replenishment in the environment. Whilst these results are preliminary they do suggest that seasonal variations in the enrichment of Pu and Am in sea spray on the Cumbrian coast may be partly due to changes in the surfactant activity and inorganic particulate loading in the surf zone.

References

BLANCHARD, D.C. (1983). The production, distribution and bacterial enrichment of the sea-salt aerosol. In Air-Sea Exchange of Gases and Particles, P.S. Liss and W.G.N. Slinn, eds, p407-454, D. Reidel.

LIVESLEY, D.M., MARLIN, S.R., DRAIN, L.E. and YEOMAN, M.L. (1989). Particle sizing using the phase-doppler technique: resolution limits and application to non-spherical particles. AERE R13388.

PATTENDEN, N.J., CAMBRAY, R.S. and PLAYFORD, K. (1989). Studies in Environmental Radioactivity Part 16. Trends in radionuclide concentrations in coastal airborne and deposited materials, 1978-87. AERE-R12617, HMSO.

SCOTT, J.C. (1987). The effect of organic films on water surface motions. In Oceanic Whitecaps and Their Role in Air-Sea Exchange Processes, eds, E.C. Monahan and G. MacNiocaill, pp.159-165.

IV. **Other research group(s) who have collaborated actively on this project [name(s) and address(es)]**

Professor P S Liss
School of Environmental Sciences
University of East Anglia
Norwich
NR4 7TJ
England

Dr Y Belot
Commissariat a l'Energie Atomique
Department d'Etudes et de
Recherches en Securite
Boite Postale 6
92260 Fontenay-aux-Roses
France

V. **Publications:**

(1) CLOKE, J., McKAY, W.A. and LISS, P.S. (1990). A laboratory study into the flux and enrichment of particulate material in sea-salt aerosol. Meeting on "Aerosols: their generation, behaviour and applications". The Aerosol Society, 4th Annual Conference, 9-11th April 1990.

(2) McKAY, W.A., PATTENDEN, N.J. and CAMBRAY, R.S. (1988). Some of the processes involved in the transfer of plutonium and americium from sea to land. Seminar on "The cycling of long-lived radionuclides in the biosphere: observations and models". 15-19 September 1986, Vol. 2. CEC.

(3) McKAY, W.A., WALKER, M.I. and SZWEDA, C. (1989). Studies of environmental radioactivity in Cumbria, Part 19. Possible influence of tributyl phosphate on aerosol generation in Cumbrian coastal waters. AERE R13468, HMSO, UK.

(4) WALKER, M.I., McKAY, W.A., PATTENDEN, N.J. and LISS, P.S. (1986). Actinide enrichment in marine aerosols. Nature 323, 141-143.

(5) WALKER, M.I. (1989). The sea to air transfer of radionuclides, Ph.D. University of East Anglia.

(6) WALKER, M.I. and LISS, P.S. (1989). Mechanisms of the sea-air exchange of radionuclides. Department of the Environment, RW 89080, UK.

VI. **Benefits to CEC**

This research programme should help reassure the population of the community that the environmental consequences of the nuclear power programme are being studied and the risks assessed. The project is soundly based scientifically and should contribute to the understanding of the transfer of pollutants from sea-to-air-to-land throughout the community.

RADIATION PROTECTION PROGRAMME
Final Report

Contractor:

Netherlands Institute
for Sea Research
P.O. Box 59
NL-1790 AB Den Burg

Contract no.: BI6-B-199-NL

Head(s) of research team(s) [name(s) and address(es)]:

Dr. E.K. Duursma
Netherlands Institute
for Sea Research
P.O. Box 59
NL-1790 AB Den Burg

Telephone number: 02220-19541

Title of the research contract:

Biological investigation in relation to the deep sea dumping of low level radioactive waste.

List of projects:

1. **Biological investigation in relation to the deep sea dumping of low level radioactive waste.**

Title of the project no.:

Biological investigation of the NEA-dumpsite in relation to the deep sea dumping of low level radioactive waste.

Head(s) of project:

Dr. H.J. Lindeboom
Dr. E.K. Duursma
Drs. M.S.S. Lavaleye

Scientific staff:

Drs. M.S.S. Lavaleye

I. Objectives of the project:

1. To indentify possible biological processes that influence the transport of radionuclides after their eventual release from the waste canisters at the NEA-dumpsite. To this purpose a thorough knowledge of the benthic fauna and the deep-sea foodweb is necessary. These topics will be studied at the dumpsite and also along a transect northward of the site.

2. To see if there is a transport of radionuclides from the waste canisters to organisms. For this purpose analysis of radionuclides in the megafauna collected at the site will be carried out.

II. Objectives for the reporting period: 1 Dec. 1987 - 1 Dec. 1989

- Participate in three expeditions to the NEA-dumpsite and surroundings, to collect bottomfauna for biological research and radionuclide analyses.
- Doing the research and writing a report.
- Preparing the megabenthic material for radionuclide analyses at the I.L.M.R.

Reporting period ended in 1989. But still for 1990 the following objectives are scheduled:
1. Some additional research on the macro- and megabenthos.
2. Radionuclide analyses of megafauna by I.L.M.R.
3. Publishing a final report in which these additional data will be incorporated.

III. Progress achieved:

1. Methodology

During 3 expeditions in 1988 and 1989 sedimentsamples, for meio- and macrofaunal research, and megafauna samples for radionuclide analyses were taken in and around the NEA-dumpsite in the N.E. Atlantic (fig.1). The waterdepth of all stations was between 4500 and 4750m, except for one trawlstation at 4000m. The sediment samples were collected with a Scrippsboxcorer (with a box surface of 2500cm^2), a cilinderboxcorer (NIOZ-design, with a boxsurface of 790cm^2) and a multiple corer. The last apparatus, collects very undisturbed samples of sediment together with the near-bottom water in 12 perspex cores with each a sample surface of 30cm^2. The methods used for extracting and further handling the meio- and macrofauna is described in Rutgers van der Loeff and Lavaleye (1986). Special attention was paid to the Foraminifera. During the Meteor cruise 10 Scrippsboxcore samples were taken as close as possible at the same spot (sta.233), to study the small scale distribution of the macro- and large meiofauna (>0.5mm). These samples were cut horizontally into several slices in the following way: 0-3, 3-10, 10-20, 20-30cm and remaining part.

2. Results and discussion

2.1 Meiofauna

2.1.1 General

The results of the meiofauna research do not differ very much with the findings of the DORA project (see Rutgers van der Loeff & Lavaleye,1986). The densities for Nematoda are high and this animal group is an important component of the whole meiofauna. But, in contrast with the DORA project data, the Nematoda are equaled or even dominated in density by the benthic living Foraminifera. This difference between the NAZORG and DORA project in data of more or less the same deepsea area can be explained by the fact that now more attention was paid to the sediment residue of the samples after treatment with the elutriation method. So, not only the larger light-weight, which stayed behind in the residue in spite of elutriation, were picked out, but the whole heap of mostly empty pelagic Foraminifera shells was carefully examined. Most of the living benthic Foraminifera were tiny shelled, alike those figured by Gooday (1986a, fig.11). Soft shelled specimens, belonging to the Allogromiina and Saccamminidae (Gooday,1986b) were present as a minority. No doubts about the living state of these creatures were raised, as the shells were mostly clear as glass and the content well and darkly coloured with rose bengal. For large Foraminifera , which formed only a small part of the total, this is different, and sometimes it is only possible to affirm their living state by breaking them up. The high densities of Foraminifera, always more than 500/10cm^2 and a maximum of 1852/10cm^2 in a subcore of sta. 31M2, support the idea of Gooday (1986). He concludes, based on his own study and that of Schafer & Cole (1982), that living benthic Foraminifera are almost always underestimated in benthic deep-sea studies. The mean biomass (15.7mg dry/m^2 for the upper 6cm sediment layer) of the Nematoda from the subcores of the boxcores of station 31,32 and 34 is very similar to that of the DORA project (14.4mg dry/m^2 for the whole sediment column). But multiple cores and sta.33 give higher figures.

In general most meiofauna is found in the upper centimetres. As a mean 90, 92 and 85% of the total number of respectively Nematoda, Copepoda + nauplii, and Foraminifera of the 6cm deep subcores are found in the upper 3 centimetre. The vertical distribution of these animals does not vary much between the 3 different apparati.

2.1.2 Comparison between multiple and box-corers

Although it is difficult to get samples from almost the same spot at tse bottom of the deepsea and the positions of the multiplecorer samples differ considerable with those of the Scrippsboxcores of the same stations, the differences in meiofauna densities between samples of these two apparati (sta.31,32 and 34) are striking and confirm the hypothesis that the multiple corer would be more efficient to catch meiofauna in the deepsea as the boxcorer. The abundance of Nematoda, but especially for Copepoda and nauplii are much higher in the multiple core samples. For Foraminifera this is much less clear. An explanation can be that the Scrippscorer has a larger bow effect, because of which light weight animals living at the surface of the bottom can be pushed away. Harpacticoida Copepoda and nauplii, presumed to be relatively good swimmers, might enlarge this effect by taking off from the sediment into the water column, because of disturbance by the bow wave. Another point of loss of animals in boxcores is a winnowing effect during hauling in from the bottom, if the lid(s) are not closed securely. A third point is that because of the bumping of the core frame against the ships hide during hauling on board, the water above the sediment sample is mostly muddy and has for the greater part to be drained off, before adequate subcoring is possibe. Of course, in this procedure animals, which are stirred up, will be lost.
The above mentioned 3 explanations of the difference in efficiency of the 2 apparati, all suppose a loss of animals that live very close to the surface. So if these explanations are true, one expects (an artificial) shift in the vertical distribution of the meiofauna in the samples. In a boxcore sample the percentage of animals living in the deeper layer (3-6cm) should than be greater than in the multiple core samples. However, this is not affirmed by the data for vertical distribution of Nematoda, Copepoda, naupli and Foraminifera.
At sta.33 and 34 a cilindrical boxcorer (NIOZ design) was used instead of the lost Scrippscorer. This corer samples a smaller surface (790 i.o 2500cm^2) and has a much better closing device. Because of this, it was expected that its efficiency to sample meiofauna would be close to that of a multiple corer. Its a pity that we have no samples from the multiple corer from sta.33, but the meiofauna data for sta.34 for the 2 apparati are very close, and point that the above mentioned expectation can very well be true.

2.1.3 Comparison of the transect stations

As already seen above multiple and different boxcorers are not equal efficient samplers, so the data derived from the different corers have to be dealed with seperately. The four stations, at the from the dumpsite northwards directed transect, show a slight decrease to the north in the amounts of Nematoda, when looked at the multiple core data. This trend is also shown in the Nematoda biomass. But the differences are small and can also be found between stations of the dumpsite of the DORA project and not much value has to be paid to it. If the boxcore data are compared no trend is visible between sta. 31, 32 and 34. However, station 33 is totally different. Its Nematoda density is very high, and when corrected for depth reaches a figure of

1008 per $10cm^2$, which is even higher than the record density found in the much shallower station 15 of the DORA project. Even more surprising is its Nematoda biomass, which with a value of $58.07mg/m^2$, is more than three times higher as all other data from the NAZORG as well as the DORA project. Even the Multiple core samples did not show such a high biomass and are at least two times smaller. This station jumps out not only because of the high density and biomass of Nematoda, but also because Foraminifera, Copepoda, naupli and small Polychaeta all have a relatively high density. For the time being we do not have an explanation for these high figures, but we can learn from it that the dumpsite, which does not seem to be very poor in meiofauna, is certainly not the richest deepsea area.

2.2 Macrofauna

2.2.1 General

The mean density for Metazoa (115.5 per m^2) is very close to the findings of the DORA project (124 per m^2). Foraminifera have the highest density. Within the metazoan groups the Polychaeta very clearly dominate with $32.3/m^2$, followed at distance by Porifera, Echinoidea, Sipunculida and Bivalvia and the other less important groups. In biomass, however the Sipunculida, which claim almost 41% of the total macrofauna biomass, are more important than the 31% of Polychaeta. During the DORA project this same feature was found. The other animal groups are all of much less importance. Tunicata (8%), Scaphopoda (7%), Holothuroidea (4%) and Echinoidea (2%) still make out a reasonable part of the biomass. In total macrofauna biomass the transect stations have a much higher mean (160.8, sd=129.0) as the DORA project results (79.9). The study of the vertical distribution shows that the largest number as well as most of the biomass of the macrobenthos is found in the upper 10 centimetres. Combined with the DORA project findings it is concluded, that the abundance of macrofauna is the largest in the upper 3cm and the biomass has its peak in the 3 to 10 cm layer.
In the large meiofauna fraction (>0.5mm and <1mm) the Foraminifera are becoming abundant (1300 per m^2) and form without any concurrence the main component of the total number of animals. The density of the Metazoa is much less with 405 per m^2, but this figure is fairly close to the figure of 366, which was found during the DORA-project. Polychaeta are the most abundant of the Metazoa with a density of 126 per m^2 and are followed by Isopoda (39.4), Bivalvia (35.8), Nematoda (22), Ostracoda (19) and Tanaidacea (18). The biomass is dominated, without any doubt by the Polychaeta with 49% (Table 10). Isopoda (9.1%), large Foraminifera especially Allogromiina (6.8%), Sipunculida (3%), Porifera (2.6%) and Holothuroidea (2.6%) are the other important groups. The 3 most important groups are the same and form an almost exact part of the biomass as was found during the DORA project, where it was 44, 8.5 and 6.3% respectively. The mean biomass ($21mg/m^2$, sd=9) is somewhat higher than the DORA project figure.

2.2.2 Small-scale distribution of macro- and large meiofauna

The range of the macrofauna density in the 4 Scrippsboxcores at sta.233 is 92 to 168 per m^2, with a mean of 116, sd=35,9. The animal groups with a relatively high density are present in all (Foraminifera, Polychaeta, Isopoda and Amphipoda) or in 3 out of 4 cores (Bivalvia, Sipunculida, Tanaidacea, Echinoidea and Tunicata). So there is also a reasonable similarity between the 4 boxcores in composition of the macrofauna. The mean density of metazoan animals is

almost the same as that of the 4 transect stations and it therefore seems justified to use these data also for those transect stations. Besides, all stations have about the same depth and very close physical properties.
The large meiofauna density (range 292 to 804 per m^2) of the 4 boxcores of the same station, have a mean of 541 per m^2, with standard deviation 218.7. So here is a lot more small scale patchiness. The composition of this fauna, however, shows a large similarity between the cores. All the groups, that have an important density, are present in all boxes (Foraminifera, Polychaeta, Nematoda, Isopoda, Tanaidacea, Copepoda and Ostracoda). From these data it is clear that differences between the transect stations must be very great, before it can be conluded that there are realy differences between areas and that these are not caused by the small scale patchiness.

2.2.3 Comparison between the different transect stations

An eye-catching feature, when comparing the 4 transect station at the composition of the macrobenthos, is the missing of all crustacean groups in station 33 and 34. Crustacea have smaller sizes in these two station and this group is only found in the meiofauna. On the other hand representatives of the irregulaire Echinoidea were discovered in these 2 stations. These relative large animals were not found in station 31 and 32, and also never in any of the DORA stations. The mean density of the 4 stations is 115.5 per m^2, with standard deviation of 54.7. From a comparison with the density data (mean 116, sd = 35.9) from the 4 Meteor boxcores of one station, it can be concluded that there is a larger difference between the stations as between boxcores from the same station. Then it is possible to defend that sta.32 is relative poor in macrobenthos and sta.33 very rich. This is very similar what is shown by the data for meiofauna. Here Nematoda and Copepoda + nauplii have a low density in station 32. This does not count for Foraminifera and Polychaeta. In sta.33 all important meiofauna groups are more or equal abundant as the other stations.
The composition of the large meiofauna (>0.5mm and <1mm) does not show major shanges between the stations. Again, the same as with the macrofauna, Echinoidea are only found in sta.33 and 34. The mean of the density of the large meiofauna is 405,1 per m^2, with a standard deviation of 173.2. This is less than the mean for the 4 cores of the same station: 541 per m^2, sd = 218.7. In percentage of the mean, the standard deviation is almost the same (40 and 43%) for both data sets, so it is concluded that patchiness on the small scale can be as large as differences between the stations. Therefore conclusion from differences between the transect stations do not have much value, but again the same trend is visible. Station 32 has the lowest abundance of large meiofauna and station 33 is the richest.
The macrofauna biomass for the transect stations gives a more or less similar picture as for the density. Station 33 is without doubt the most important station. This is caused by a fairly large Sipunculida. The stations 32 and 34 are relatively poor and sta.31, which is situated in the dumping area, is fairly rich. Compared with former data of the dumpsite and surrouding area (Rutgers van der Loeff & Lavaleye,1986), the biomass of sta. 31 is a lot higher, 172.7mg/m^2 against 84.7mg/m^2, but it falls just within the range of these DORA project data. Boxcore 34b2 is atypical, because Polychaeta and Sipunculida do not form the major part of the biomass. Instead Tunicata and Scaphopoda replace these taxa as the major components of biomass.
In the large meiofauna biomass the general trend, as seen above in the

densities and biomass of the macro- and smaller meiofauna, cannot been discovered clearly in the 4 transect stations. Station 34 is not exactly poor, but lost the first place to sta.31. But sta.32 is together with sta.34 indeed relatively poor. Again boxcore 34b2 is atypical in the composition of the biomass, because of the relatively high figure for Isopoda.

3. Radionuclide analyses

Radionuclide analyse of sediment, near bottom water and megabenthos at and near the NEA dumpsite for low-level radioactive waste (abstract);

by Noshkin,V., M.Rutgers van der Loeff & M.Lavaleye

3.1 Introduction

During the DORA-I (1982) and DORA-II (1984) expeditions sediment samples with boxcores, near-bottom water with a rosette-sampler and megabenthos with a 3.5m Agassiz trawl were collected at several stations at and near the NEA dumpsite for low-level radioactive waste in the N.E.Atlantic deep-sea. The sampling procedure and the exact positions of the stations is described in Rutgers van der Loeff & Lavaleye (1986). The samples were analised by gamma spectrometry and afterwards by chemical methods for plutonium radionuclides. These analyses were carried out by the first author at the Lawrence Livermore National Laboratory.

3.2 Results and discussion

3.2.1 Sediment

The concentrations of $^{239+240}Pu$ in the upper centimetre of the sediment of the boxcore samples, collected within the dumpsite, have a mean value of 0.38mBq/g. This figure is not different from global fallout levels in sediments, which have been measured in the N.E.Atlantic at depths greater than 4100m (Noshkin, 1986). The mean percentage of the total alpha activity due to ^{238}Pu at all measured stations within the dumpsite is 6% $\pm$3, which is almost equal to the mean fallout value of 7% $\pm$3 measured in sediments from outside the dumpsite. From the gamma spectrometry analyses and the above mentioned concentrations of the plutonium radionuclides, it is concluded, that the disposal of packaged radioactive waste has not led to area wide contamination of the sedimentary environment with waste related plutonium or other gamma radionuclides.

3.2.2 Near-bottom water

The measured concentrations of $^{239+240}Pu$ in the water, within 3 to 20m above the bottom, range from 4 to 243 µBq/l. The highest concentrations were usually associated with a high ^{238}Pu alpha activity. The percentage of total plutonium alpha activity due to ^{238}Pu (12-26%) is larger than that measured in the sediment (see above). The highest concentrations were measured in the western and northern part of the dumpsite (station 12, 13 and 28). Concerns over possible contamination during sampling procedures was eliminated, when the samples of the second DORA expedition confirmed the high levels

found in samples of the first expedition. There is no evidence that the surplus of radionuclides in the near-bottom water can be supplied by labelled surface water sinking from somewhere in the Atlantic to the dumpsite. Moreover there is a sharp increase in the median concentration if water was measured from below a depth of 20m above the bottom instead of water from higher above the bottom. This indicates that there must be an additional source near the sediment-water interface. That these high bottom water concentrations result from a unique remobilisation process of fallout plutonium with settling phases at the sediment-water interface does not seem right. First because at several stations no elevated levels were found, and we do not see any reasons why the above mentioned process would not work evenly over the entire area. And secondly, this unknown process should than release fallout ^{238}Pu at a faster rate than $^{239+240}Pu$, which is not confirmed by any research so far. So the only remaining obvious reason for the near-bottom clouds of elevated levels of plutonium is that the origin must be the disposed low-level radioactive waste canisters, which were dumped here in the past (see introduction). In this case one would expect also elevated levels of ^{137}Cs in the water samples, because ^{137}Cs is to be thought associated with the waste. This was not found, but there is a vague trend that the concentrations in the 0-10m interval above the bottom are higher (0.70mBq/l) than those in the 10-50m interval (0.47). So this also points to some near-bottom source.

3.2.3 Megabenthos

At station 28 one of the benthic organisms, a large deposit feeding Holothuria, showed elevated levels of ^{238}Pu (37%) and $^{239+240}Pu$ (156fCi/g dry) in the gut contents. The ^{137}Cs level (260fCi/g dry) was also higher in this gut content than the mean concentrations in the analised surface sediment from station 28 (40fCi/g dry). It seems clear that this seacucumber must have derived waste contamination from a bottom source, as the animal feeds on the upper sediment layer. Other animals from this and other stations did not show any evidence of excess plutonium or caesium radionuclides in the gut content or body tissue. So, the contaminated area must be very localised. It is therefore supposed that the sediment around some ruptured waste canisters derive contamination through leakage from these drums. But as most of the plutonium is dissolved and the adsorption rate is low because of the low particle concentrations in the water, most of the plutonium radionuclides will stay in the water and than can be easily dispersed by bottom currents over a greater area.

4. Foodweb

Most benthic animals in the deep-sea are direct or indirect dependent on the foodrain from the photic zone. Particle concentrations in the water are small, so obligate suspension feeders are thought to be absent or very scarce. Carnivores are relativey never very abundant in an ecosystem and scavengers are not likely to be common, because of the scarce food. So it is thought that most animals are depositfeeding. Information about the trophic levels of deepsea animals has to be derived indirectly by body morphology, study of the gut content and extrapolation from feeding habits of related, shallow water organisms. The most important animal groups in density and biomass will be treated here.

Foraminifera have a much higher density in the deep-sea as thought before. The biomas however seems not easy to assess and no data are give in this study. The animals in this area are mostly hard-shelled, but in a minority soft-shelled Foraminifera, with or without aglutinated particles are also present. All are thought to have pseudopodia, very thin protoplasmic threads, which can extend 2 to 3 times the diameter of the shell (Murray,1979). Food can be picked up from the sediment by these pseudopodia, and is transported by protoplasmic streams to the aperture of the shell. In some shallow water species an upstanding network of speudopodia is formed, which makes suspension feeding possible. Food can consist of algae (including diatoms), organic detritus and bacteria. Large Foraminifera can predate on other forams and metazoans, like small crustaceans. For a part the digestion can take place outside the shell. For obvious reasons the feeding habits of deep-sea Foraminifera are not known, but there are no clear reasons why these should differ very much from shallow water species. Suspension feeding does not seem very profitable and by the fact that still a fair amount of the Foraminifera live below 3cm, it is concluded that most are deposit feeders.

Nematoda. From a study of the mouth parts of Nematoda from the dumpsite, it is known that depositfeeders account for almost 70% of the total.biomass of Nematoda (Rutgers van der Loeff & Lavaleye, 1986).

Sipunculida. These relative large animals have a relative low, but even density in the dumpsite area. At the transect stations the density is 10 per m^2 and during the DORA project 9 animals per square meter were found. The group is, however, important because of its biomass. It claims 41% (DORA project 28%) of the total macrofauna biomass. These animals are without doubt depositfeeders and have the long very coiled intestine always full with sediment.

Polychaeta. These annelids are the most abundant metazoans of the macrofauna as well as the large meiofauna (>0.5mm and <1mm) of the dumpsite and are also very important in biomass. Of the macrofauna biomass 31% are Polychaeta and for the large meiofauna this almost 50%. It is a pity that most specimens are broken by the sieving procedures, which makes a study of these animals not very easy. Many of the animals and the fragments still had fair amounts of sediment in the guts. Few carnivores, recognizable by strong jaws, have been found. So there is no doubt that most are deposit feeding.

5. Conclusions

1. Relative richness of the benthic fauna of the dumpsite. The meiofauna of the dumpsite and its surroundings seemed to be fairly rich in comparison with other deepsea studies in the East Atlantic (Rutgers van der Loeff & Lavaleye,1986: table 4.2). For the macrofauna this was difficult to assess, as all sorts of different screensizes were used in other deep-sea studies in the Atlantic (Rutgers van der Loeff & Lavaleye, 1986: table 4.19). From a comparison of the NAZORG transect stations, it is now concluded that the dumpsite is not very special within the hilly deepsea area southwest of the Porcupine Abyssal Plain (fig.1). It is surely not the richest area, as sta.33

has a much higher benthos density and biomass.

2. Foodweb. As benthic deep-sea animals are almost all direct or indirectly dependent on the rain of foodparticles from the photic zone, it is not surprising that most of the benthos is deposit feeding.

3. Radionuclide analyses (by Noshkin, Rutgers van der Loeff & Lavaleye). From radionuclide measurements in and around the dumpsite it is concluded that bottom sediment was contaminated only very locally, around ruptured waste canisters. No elevated levels were found in the sediment samples, but the gut content of a seacucumber had abnormal highlevels of plutonium and caesium radionuclides. The near-bottom water was at several stations contaminated with plutonium, of which the dumped waste had to be the source. This water will spread relatively quick over large areas because of the currents and concentrations of the contaminants will be diluted.

4. Radiation and benthos. The dumpsite animals can come in close contact with waste radionuclides, especially depositfeeders, when eating contaminated sediment. However, this chance is relatively small as sediments are contaminated only very locally. Besides, the one seacucumber with elevated levels in its gut content did not have abnormal levels in his body tissue.

5. The multiple corer is more efficient in sampling meiofauna quantitatively than a Scrippsboxcorer. The loss of animals in the Scrippsboxcorer seems to be caused by the larger bow effect, a winnowing effect during hieving and loss during subsampling on board. However, it is strange that this is not confirmed by an artificial shift in the vertical distribution of meiofauna, in advantage of the deeper layer in a boxcore sample.

6. The small-scale distribution of macro- and large meiofauna is very patchy, and it is therefore difficult to assess the density and biomass of these groups by only one or two boxcores.

7. The view of Gooday (1986), that living benthic Foraminifera in deep-sea sediments are much more abundant than most previous studies have stated, is supported here by the results of this still deeper region.

6. Literature

Dickson, R.R., 1983. The 'topographic study'. Chapter 5B in: P.A. Gurbutt & R.R. Dickson (eds.) - Interim oceanographic description of tho North-East Atlantic site for the disposal of low-level radioactive waste. NEA/OECD,Paris.

Dickson, R.R. & W.J. Gould, 1983. The flow field. Chapter 5A in: P.A. Gurbutt & R.R. Dickson (eds.) - Interim oceanographic description of tho North-East Atlantic site for the disposal of low-level radioactive waste. NEA/OECD,Paris.

Dickson, R.R., P.A. Gurbutt & P.J. Kershaw (eds.), 1986. Interim oceanographic description of tho North-East Atlantic site for the disposal of low-level radioactive waste. Vol.2. NEA/OECD,Paris.

Durance, J.A., 1983. Historical hydrochemistry in and around the site. Chapter 7 in: Interim oceanographic description of tho North-East Atlantic site for the disposal of low-level radioactive waste. NEA/OECD,Paris.

Gooday, A.J., 1986a. Meiofaunal foraminiferans from the bathyal Porcupine Seabight (north-east Atlantic): size structure, standing stock, taxonomic composition, species diversity and vertical distribution in the sediment. Deep-sea Research 33 (10): 1345-1373.

Gooday, J.A., 1986b. Soft-shelled Foraminifera in meiofaunal samples from the bathyal northeast Atlantic. Sarsia 71 (3-4): 275-288.

Kershaw, P.J., J.N. Smith & V.E.Noshkin, 1986. Bioturbation. Chapter 6.2 in: Interim oceanographic description of tho North-East Atlantic site for the disposal of low-level radioactive waste. Vol.2. NEA/OECD,Paris.

NEA, 1980. Review of the continued suitability of the dumping site for radioactive waste in the North-East Atlantic. OECD,Paris.

NEA, 1985. Review of the continued suitability of the dumping site for radioactive waste in the North-East Atlantic. OECD,Paris.

Noshkin, V.E., 1986. Plutonium in northeast Atlantic sediments. in: Dickson, R.R., P.A. Gurbutt & P.J. Kershaw (eds.). Interim oceanographic description of the North-East Atlantic site for the disposal of low-level radioactive waste. Vol.2. NEA/OECD,Paris.

Nyffeler, F. & W. Simmons (eds.), 1988. Interim oceanographic description of tho North-East Atlantic site for the disposal of low-level radioactive waste. Vol.3. NEA/OECD,Paris.

Rutgers van der Loeff, M.M. & M.S.S. Lavaleye, 1984. Geochemical and biological research at the NEA dumpsite for low-level radioactive waste. Neth. Inst. for Sea Res. int. rept. 1984-2.

Rutgers van der Loeff, M.M. & M.S.S. Lavaleye, 1986. Sediments, fauna and the dispersal of radionuclides at the N.E. Atlantic dumpsite for low-level radioactive waste. Report of the Dutch DORA program. Neth. Inst. for Sea Research, Texel.

IV. Other research group(s) collaborating actively on this project [name(s) and address(es)]:

- Coordinated Research and Surveillance Programme (CRESP), coordinated by the Nuclear Energy Agency (NEA).
- Institut fur Hydrobiologie und Fischereiwissenschaft (IHF), Hamburg.
- Rijks Museum voor Natuurlijke Historie (RMNH). Leiden.
- International Laboratory of Marine Radioactivity (ILMR), Monaco.

V. Publications:

- Rutgers van der Loeff, M.M. & M.S.S. Lavaleye, 1986. Sediments, fauna and the dispersal of radionuclides at the N.E. Atlantic dumpsite for low-level radioactive waste. (Report of the Dutch Dora programm).

- Lavaleye, M.S.S., 1989. Benthos at a transect from the N.E. Atlantic dumpsite for low-level radioactive waste to the north (with some radionuclide concentration data). Report of the Dutch NAZORG project. Interim internal report NIOZ.

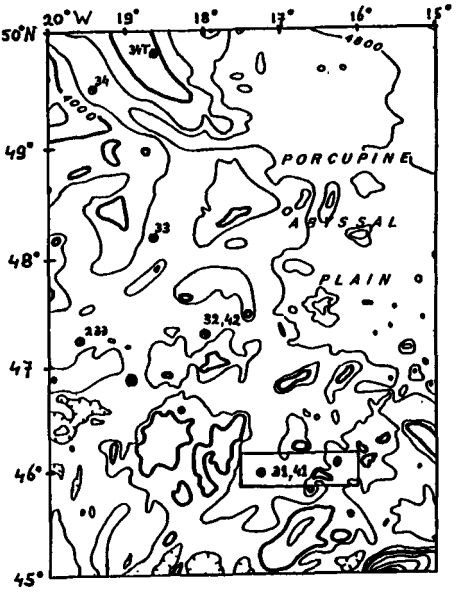

Fig.1. Map with the dumpsite (rectangle) and the stations of the NAZORG and METEOR expeditions indicated. The thick lines are 4000m bathymetric isolines.

RADIATION PROTECTION PROGRAMME
Final Report

Contractor:

Contract no.: BI6-B-036-NL

Rijksinstitut voor Volksgezondheid
en Milieuhygiëne, RIVM
P.O. Box 1
NL-3720 BA Bilthoven

Head(s) of research team(s) [name(s) and address(es)]:

Dr. M.J. Frissel
Laboratory for Radiation Research
R.I.V.M.
P.O. Box 1
NL-3720 BA Bilthoven

Telephone number: 030/74.25.15

Title of the research contract:

Countermeasures to the uptake of radionuclides from soils by food crops ; the long-term availability of radionuclides.

List of projects:

1. The long-term soil-to-plant transfer in the field, basic research long-term availability, and countermeasures to reduce soil-to-plant uptake with emphasis on practicability.

Title of the project no.:

Countermeasures to the uptake of radionuclides from soils by food crops; the long-term availability of radionuclides.

1. The long-term soil-to-plant transfer in the field, basic research long-term availability, and countermeasures to reduce soil-to-plant uptake with emphasis on practicability

Head(s) of project:

J.F. Lembrechts

Scientific staff:

G.M. Desmet, M.J. Frissel, H.W. Köster, J.F. Lembrechts, L.R. Van Loon, J.F. Stoutjesdijk

I. Objectives of the project:

The first topic, 'lysimeter experiments on counter measures', focussed on obtaining field data on possibilities to decrease uptake of radionuclides by plants by means of different agricultural techniques, such as soil amendment with stable elements. In addition to the determination of soil-to-plant transfer factors (TF's) an evaluation was made of the effects of the counter measures on bio-availability by studying the soil liquid phase. Attention was particularly given to Sr-90, a considerable fraction of which is present in the soil liquid phase.

The objective of the second part, on 'soil-to-grass transfer', was a study of the influence of meteorological factors on transfer over a longer period of time on one single crop, and to compare it to the long-term influence of soil related parameters. The choice of a perennial pasture for this study is evident as it allowed of seasonal cuts.

The goal of the third topic, 'uptake, distribution and metabolism of technetium in plants', was to describe absorption and incorporation of TcO_4^- by plants with a mechanistic model, involving growth medium as well as plant parameters. The fourth one, 'special studies on the soil-soil solution-plant relationship', concerned another specialized study on uptake mechanisms and bioavailability, supporting the pragmatic first part of this project. The experiments concerned the behaviour of Sr, Zn, Co and Cs. The latter two parts focussed on the effect of soil solution composition on radionuclide uptake.

II . Progress achieved:

METHODOLOGY

(1) Lysimeter experiments on counter measures.

Experiments were conducted under field conditions in 24 lysimeters described in earlier reports and publications [e.g. 23]. Three kinds of soil were represented : a clay (4 plots), sandy loam (12 plots) and a sandy soil (8 plots). The upper 20 cm layer of soil was homogeneously contaminated with Co-57/60, Cs-134/137, Mn-54, Sr-85/90 and Zn-65. Over a period of 4 years (1986-1989) beans (Phaseolus vulgaris L.) of which the pods were analysed, were grown in spring time and spinach (Spinacia oleracea L.) in autumn. The remedial measures applied were omission of the recommended fertilization and application of lime, organic matter or stable Zn and Mn. They were applied individually, on one or two containers per soil type. For the first period of three years the level and frequency of application are given elsewhere [18]. In 1989 the limed containers were amended with 4000 kg/ha of $Ca(OH)_2$. The concentration of each of the nuclides was measured in the homogenized, dried soil and plant samples. The interstitial soil liquid phase was regularly isolated and analysed for a number of chemical characteristics [18]. For parts (1) and (2) of the project the transfer factor (TF) is defined as the ratio of the concentration in the plant to that in the upper 20 cm layer of soil (both on a dry weight basis).

(2) Soil-to-grass transfer : a long-term lysimeter experiment.

Experiments were conducted under field conditions on 2 plots (1 m^2 in size) with a sandy loam and on 2 plots with a sandy soil. In 1981 Co-60, Cs-137, Mn-54, Sr-90 and Zn-65 were applied at levels between 2 and 4 $MBq.m^{-2}$. In 2 containers the upper 5 cm was contaminated in the other 2 the upper 15 cm. Three weeks later grass was sown. Dominant species in the grass mixture were Lolium, Phleum and Festuca. Between 1981 and 1988 28 harvests were analysed. The concentration of each radionuclide was measured in the dried and homogenized soil and plant samples [17].

(3) Uptake, distribution and metabolism of technetium in plants.

Seedlings of Spinacia oleracea L. were grown under controlled conditions [14, 27], for 2 to 4 weeks, on differently modified Hoagland-Arnon nutrient solutions and on different soils [27], labeled with NH_4TcO_4.

Whole shoots or separate leaves of different age were digested with HNO_3/H_2O_2 before analysing the total Tc content by liquid scintillation counting. Gel filtration chromatographic techniques were used to separate unmetabolized TcO_4^- and Tc-labeled organic complexes in organelle free extracts of labeled spinach plants or leaves [10]. Suspensions of isolated chloroplasts, chloroplast fragments or enzymes were used to study the relation between photosynthetic activity and TcO_4^- reduction [13].

For parts (3) and (4) of the project the TF is defined as the ratio of the concentration in fresh plant material to that in the nutrient solution or in the soil liquid phase. The soil solution was isolated by means of an immiscible displacement method.

(4) Special studies on the soil-soil solution-plant relationship.

Seedlings of Lactuca sativa L. cv. Ysbergsla were grown under controlled conditions for 2 to 5 weeks, on pots filled with a sandy loam or a sandy soil (1 kg/pot) or on modified Hoagland-Arnon nutrient solutions. Uptake of Co-57, Cs-134, Sr-85 and Zn-65 were studied as a function of e.g. fertilization, of soil moisture or organic matter content or of

liming. Radionuclide content and some chemical characteristics of the nutrient solution and of the soil liquid phase were regularly measured during the growth period.

RESULTS AND DISCUSSION

(1) Lysimeter experiments on counter measures.

The soil solution composition varied widely throughout the growing period. The specific effects of the counter measures were, however, clearly visible on the sandy and loamy soil, but not on the clay soil (table 1). Application of Zn and Mn, for example, enhanced their concentration in the soil solution whereas liming reduced their concentration as well as the Sr-90/Ca ratio. Changes induced by measures which were applied only once or twice, persisted during subsequent growing periods.

TF's of different nuclides of the same element were pooled because they were of the same order of magnitude and varied similarly. Significant and almost systematic, i.e. for all elements, fluctuations in TF were observed throughout the years. TF's, for example, halved in 1987 as compared to 1986.

TABLE 1 : Averages for some characteristics of the soil solution, subdivided according to type of soil and counter measure, over the period 07/1986-07/1989 (N = number of measurements; <DL = below the detection limit; Cond. = conductivity).

Soil	N	pH	Cond.	K	Mg	Ca	NO_3	Zn	Mn	Bq ^{90}Sr / mg Ca
			($mS.cm^{-1}$)			($mg.L^{-1}$)				
CLAY										
all	36	7.5	1.2	34	34	244	315	0.04	<DL	2.4
controle	18	7.6	1.2	29	31	237	302	0.04	<DL	3.1
org. mat.	9	7.4	1.1	38	34	208	290	0.04	<DL	1.4
Zn + Mn	9	7.4	1.2	41	39	294	367	0.04	0.01	1.8
LOAM										
all	110	6.7	0.8	36	27	161	245	0.11	0.01	4.0
controle	56	6.8	0.8	32	25	157	241	0.08	0.01	4.8
lime	9	7.7	0.9	30	22	235	282	0.07	0.01	2.8
org. mat.	18	6.2	0.9	57	33	154	242	0.14	0.01	2.4
Zn + Mn	18	6.2	0.8	41	33	185	239	0.27	0.03	4.3
unfertil.	9	7.1	0.5	15	11	85	246	0.02	0.01	3.4
SAND										
all	74	5.6	0.9	87	45	104	242	1.15	0.82	9.0
controle	38	5.5	0.9	92	49	95	230	1.21	0.41	11.4
lime	9	6.5	1.0	84	45	157	294	0.37	0.09	2.9
org. mat.	9	5.8	1.0	102	54	116	182	0.47	0.24	1.8
Zn + Mn	9	5.4	1.1	112	56	107	277	2.93	4.48	13.2
unfertil.	9	5.5	0.5	32	11	72	260	0.59	0.07	8.3

TABLE 2 : means and standard error of TF's subdivided according to plant, soil type and counter measure (period : 1986-1989). Data are expressed as a fraction of the TF on controle containers. The number of measurements is given between brackets.

	Co	Sr	Cs	Mn	Zn
BEANS					
CLAY					
controle	1.00±0.25(11)	1.00±0.34(10)	1.00±0.63(11)	1.00±0.51 (6)	1.00±0.18 (6)
org. mat.	0.74±0.29 (7)	0.67±0.23 (5)	0.49±0.22 (8)	0.70±0.30 (4)	0.87±0.32 (4)
Zn + Mn	0.55±0.05 (4)	0.67±0.14 (3)	0.46±0.17 (4)	0.51±0.18 (2)	0.21±0.05 (2)
LOAM					
controle	1.00±0.17(48)	1.00±0.23(36)	1.00±0.33(47)	1.00±0.28(24)	1.00±0.30(24)
lime	1.17±0.13 (8)	0.77±0.10 (6)	0.97±0.37 (8)	0.81±0.09 (4)	0.79±0.24 (4)
org. mat.	0.75±0.30(16)	0.56±0.19(12)	0.56±0.21(16)	1.02±0.37 (8)	0.91±0.29 (8)
Zn + Mn	0.70±0.25(16)	1.01±0.20(12)	0.96±0.30(16)	0.49±0.11 (8)	0.60±0.11 (8)
unfertil.	1.14±0.19 (8)	1.01±0.17 (6)	1.57±0.32 (8)	1.01±0.21 (4)	0.68±0.07 (4)
SAND					
controle	1.00±0.31(32)	1.00±0.31(24)	1.00±0.42(32)	1.00±0.30(16)	1.00±0.35(16)
lime	0.70±0,34 (8)	0.61±0.18 (6)	0.83±0.34 (8)	0.44±0.20 (4)	0.36±0.13 (4)
org. mat.	1.16±1.15 (8)	0.42±0.12 (6)	0.74±0.53 (8)	1.16±0.57 (4)	0.65±0.20 (4)
Zn + Mn	1.17±1.01 (8)	1.02±0.28 (6)	1.55±0.51 (8)	0.62±0.43 (4)	1.07±0.25 (4)
unfertil.	0.87±0.27 (8)	1.09±0.34 (6)	1.18±0.58 (8)	0.73±0.42 (4)	1.00±0.29 (4)
SPINACH					
CLAY					
controle	1.00±0.42(16)	1.00±0.11(12)	1.00±0.40(16)	1.00±0.28 (8)	1.00±0.30 (8)
org. mat.	0.67±0.35 (8)	0.82±0.27 (6)	0.69±0.28 (8)	0.60±0.22 (4)	1.02±0.23 (4)
Zn + Mn	0.87±0.52 (8)	0.98±0.17 (6)	0.78±0.29 (8)	0.62±0.34 (4)	0.56±0.50 (4)
LOAM					
controle	1.00±0.57(48)	1.00±0.29(36)	1.00±0.83(48)	1.00±0.31(24)	1.00±0.46(24)
lime	0.82±0.17 (8)	0.70±0.12 (6)	0.81±0.21 (8)	0.71±0.07 (4)	0.57±0.07 (4)
org. mat.	0.89±0.50(16)	0.69±0.18(12)	0.82±0.72(16)	0.95±0.21 (8)	1.05±0.28 (8)
Zn + Mn	0.75±0.21(16)	1.02±0.24(12)	0.77±0.28(16)	0.68±0.12 (8)	0.81±0.21 (8)
unfertil.	0.93±0.28 (8)	1.06±0.11 (6)	0.86±0.34 (8)	0.91±0.18 (4)	0.70±0.07 (4)
SAND					
controle	1.00±0.38(32)	1.00±0.26(22)	1.00±0.26(32)	1.00±0.45(15)	1.00±0.37(16)
lime	0.77±0.20 (8)	0.97±0.33 (5)	0.84±0.26 (8)	0.71±0.31 (4)	0.70±0.33 (4)
org. mat.	0.70±0.08 (8)	0.63±0.10 (6)	0.65±0.11 (8)	1.16±0.08 (4)	0.93±0.06 (4)
Zn + Mn	0.85±0.29 (8)	1.31±0.18 (6)	1.04±0.26 (8)	0.87±0.42 (4)	0.80±0.20 (4)
unfertil.	0.86±0.19 (8)	1.35±0.23 (6)	0.91±0.17 (8)	0.78±0.27 (4)	1.05±0.33 (4)

In most cases the mean TF on containers treated with one of the remedial measures was lower (by up to 70 %) than the TF on controle containers (table 2). Results obtained in 1989 confirmed the observations of previous years [18].

The TF's of Sr, Mn and Zn were most affected by liming, though the effect was less convincing than expected on the basis of observed shifts in soil solution composition. The organic matter applied reduced transfer of (Co), Cs and Sr and sometimes slightly enhanced that of Mn and Zn.

The effect of organic matter on the uptake of Sr may be due to the lime which was added at the same time. A lower nutritional status tended to result in higher transfer factors. Dilution of Mn-54 and Zn-65 with stable isotopes reduced their TF, although not consistently. The plant specific relationship between the bioavailable concentration of an element and the uptake rate may in part explain the frequently observed non-linearity of the effect of a counter measure.

The TF's were furthermore evaluated by the IUR working group on soil-to-plant transfer factors [2, 3, 7].

(2) Soil-to-grass transfer : a long-term lysimeter experiment.

For all 5 elements transfer to grass was significantly higher on sand as compared to loam, the difference being most marked for the elements with the lowest TF, Co-60 and Cs-137. TF's were higher in case of a surface contamination as compared to a plough layer contamination, which suggests the depth of feeding of grass to be smaller than the depth of the plough layer contamination. The difference was more significant for the loamy soil since root penetration is smallest on the soil with the highest density and water holding capacity (table 3). Plant concentrations were more variable on loam than on sand. The largest fluctuations were furthermore observed for Co-60 and Cs-137. For all elements their was a significant overlap between the concentration ranges (table 4) on different sites or soils.

No seasonal cycle could be observed in the fluctuations of the transfer factor throughout the experimental period. The ageing phenomenon, if present, was restricted to the very first period of the experiment but subsequently overshadowed by changes induced by other parameters

TABLE 3 : mean soil-to-grass transfer factor for 5 nuclides, subdivided according to soil type and thickness of the contaminated layer (PLC = plough layer contamination, SC = surface contamination, df = degrees of freedom).

	Co-60	Cs-137	Mn-54	Sr-90	Zn-65
Loam	0.019	0.014	0.39	1.17	0.76
Sand	0.077 #	0.101 #	0.97 #	2.08 #	1.30 #
df	55	55	51	54	41
PLC Loam	0.015	0.011	0.37	1.07	0.76
SC Loam	0.024 **	0.017 *	0.43 *	1.27 **	0.76
df	27	27	27	27	20
PLC Sand	0.058	0.098	0.87	2.13	1.24
SC Sand	0.102 **	0.105	1.05 **	2.03	1.36
df	27	27	23	26	20

*, **, # Difference significant at P<0.05, P<0.01, P<0.001

TABLE 4 : concentration ranges measured in grass grown on sand and loam, expressed as [maximum]/[minimum].

	Co-60	Cs-137	Mn-54	Sr-90	Zn-65
Loam	59	50	3.6	6.8	7.4
Sand	33	14	6.6	5.2	3.3

(fig. 1). The plant concentration of most nuclides went up and down in a comparable way on lysimeters filled with the same soil. Fluctuations on sites with different soils were positively though less convincingly correlated. Comparable fluctuations in transfer on different plots or soils suggest climatic factors to be of importance. These factors affect growth and nutrient uptake, as was apparent from the correlated variation in the plant concentration of different nuclides. Possible effects of seasonal changes in species composition of the vegetation were not studied. No reproducible overall effects of fertilization were observed.

The strikingly coincident, extreme fluctuations for Cs and Co, which are chemically very different and hardly absorbed by the roots, suggest that external contamination by adhering soil may have distorted observed transfer data for these radioelements. Arguments in favour and against this hypothesis are discussed elsewhere [17]. The smaller fluctuations in transfer for more intensively accumulated elements, Mn, Sr and Zn, are assumed to be related to climatic and seasonal influences upon the nutritional requirements of the standing crop.

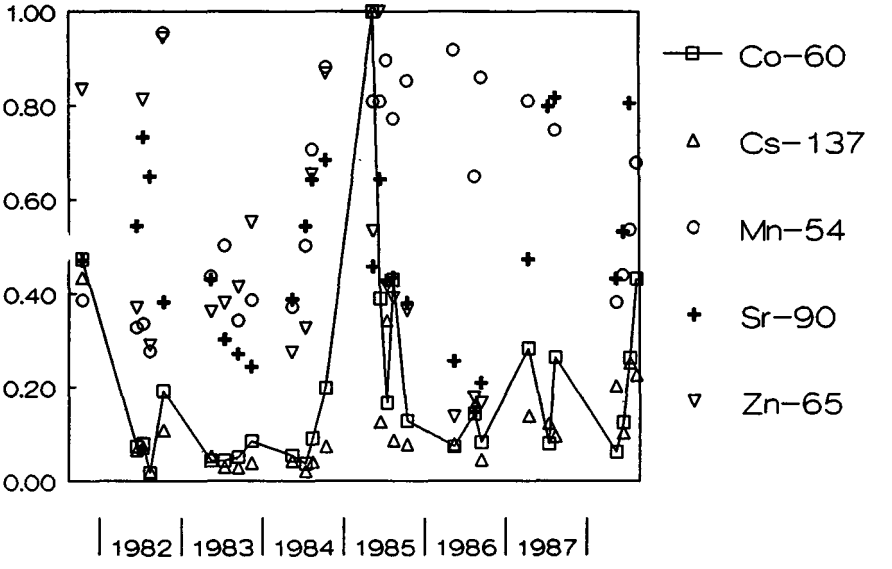

FIGURE 1 : evolution of the concentration of 5 different nuclides in grass grown on loam with a surface contamination. Results are expressed as a fraction of the maximum concentration measured during the experimental period.

(3) Uptake, distribution and metabolism of technetium in plants.

TcO_4^- uptake from nutrient solutions, as measured at various stages of the exponential growth phase, was shown to be a first order rate process in which rate values change with plant age. On the basis of gel filtration chromatographic analysis of Tc in plant homogenates two Tc classes could be demonstrated : TcO_4^- and labelled organic compounds [10, 11]. For a given composition of the nutrient solution the plant/medium ratio of TcO_4^- levels reached a constant an characteristic value after about two days, this value remaining about constant throughout the further growth period of 15 days. TcO_4^- decays in the plant into reduced

forms, a process providing the driving force for further TcO_4^- influx, consistent with a steady state level of the plant/medium ratio of TcO_4^-. Within a growing plant, however, young physiologically active leaves incorporated more Tc than old full-grown ones, the former producing more labelled compounds of high molecular mass [12, 14].

The resulting model [28], describing the concentration of Tc in exponentially growing plants ($[Tc]_{pl}$) in terms of the relative plant growth rate (RGR), the metabolic conversion of TcO_4^- in the leaves (b, k) and the ratio of the TcO_4^--concentration in the leaves and in the nutrient solution (K), is expressed by the formula :

$$[Tc]_{pl} = K[TcO_4^-]_{out}\left[1+\frac{k}{RGR}(1-e^{-RGRt})+\frac{b}{RGR^2}e^{-RGRt}(e^{RGRt}(RGRt-1)+1)\right]$$

where t = time.

In case of changing levels of TcO_4^- in the nutrient medium, a weighted mean concentration concept had to be introduced in order to account for the fact that the bulk fraction of Tc is taken up in the final growth stages [27]. The uptake pattern is furthermore clearly affected by the nutrient medium composition. It is most sensitive to the nitrate level, especially in the low concentration range (fig. 2). The equilibrium ratio K appeared to be affected by the nitrate level, whereas the transformation rate was not. Arguments were advanced to show that this effect is a purely metabolic one and not connected with competitive effects in the classical sense [27]. Reduced forms of Tc were shown not to be taken up to any significant extent, leaving TcO_4^- as the only bioavailable species [24, 26].

By monitoring the effective TcO_4^- and NO_3^- levels in the soil solution, using the immiscible displacement method, uptake of Tc by spinach

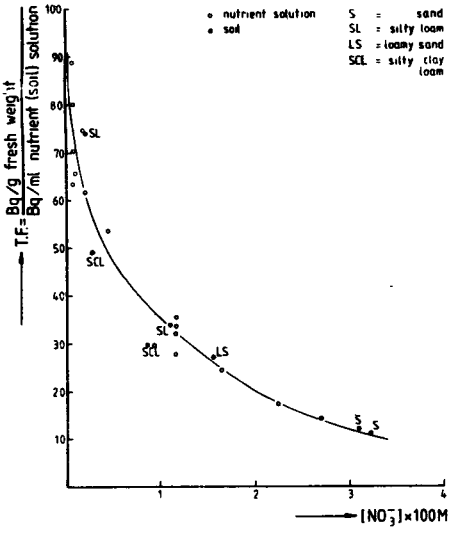

FIGURE 2 : relation between the nitrate concentration in the growth medium (nutrient solution or soil) and the transfer factor of TcO_4^-.

grown on soil was shown to be consistent with the observations made on hydroponic systems (fig. 2). The overall uptake could be predicted on the basis of the TcO_4^- and nitrate levels in the soil liquid phase.

The driving force of accumulation and incorporation of TcO_4^- was studied in detail [13]. TcO_4^- was shown to be reduced in illuminated suspensions of isolated, broken spinach chloroplasts. Reduction is proportional to the chlorophyll content of the mixtures. A competitive inhibition of TcO_4^- reduction by $NADP^+$ suggests both to be competing substrates of the electron transport chain (fig. 3).

The leakage of electrons towards TcO_4^- comprises only a minor fraction of the generated, reducing power. The process of reduction itself cannot cause the noxious effect of Tc on plants and N_2-reducing organisms. Thus, toxicity must be due to complexation reactions of activated, reduced Tc with vital biochemicals, which proceed disconnectedly from the photosynthetic reduction. Since the labeling pattern depends on the spectrum of potential ligands, it will be typical for each plant species. The oxidation state of Tc in reaction products of the in vitro experiments was +V. Based on a restricted number of experiments, thiol compounds were supposed to scavenge photosynthetically reduced Tc [16].

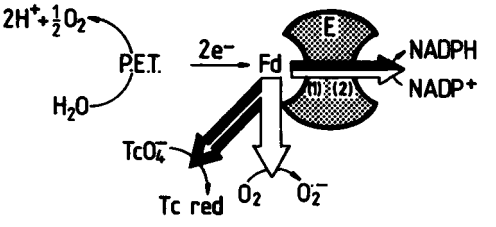

FIGURE 3 : model on the photosynthetic reduction of TcO_4^- (PET = photosynthetic electron transport; E = ferredoxine/NADP-reductase, (1) = binding site for ferredoxine, (2) = binding site for pyridine nucleotides; white pathways = aerobic conditions; black pathways = anaerobic conditions).

(4) Special studies on the soil-soil solution-plant relationship.

Because of the mutual relationship between strontium and calcium, uptake and availability of both elements were always measured at the same time. Transfer of Sr-85 to plants growing on nutrient solutions was dominated by the Ca/Sr ratio. Varying the concentration of other nutrients had minor effects. The uptake rate of Ca by lettuce was concentration independent within the concentration range studied. Actions and practices inducing comparable changes in both the Sr- and Ca-level of the soil solution will not change the Ca/Sr ratio and thus will have minor effects on the uptake rate. The TF was futhermore shown to decrease as a function of plant age.

Experiments on soils concerned influences of NPK-fertilizer and of moisture content, which affect the nutritional status of the soil solution concentration as a whole. Since these factors do not change the Ca/Sr ratio and increased levels of other nutrients cause only a slight decrease in Ca/Sr uptake, the observed changes in the Sr-85 content of the plant were rather limited. The soil matrix and liming determine the

ratio between Sr and Ca in the soil solution and consequently the transfer factor. Of more importance, however, was the observation that the uptake pattern of Sr-85 by lettuce from soils was consistent with that from hydroponic systems (fig. 4), i.e. : (1) transfer factors based on the concentration of the soil liquid phase (Bq per g fresh plant / Bq per ml soil solution) are of the order of magnitude of those measured on nutrient solutions, which roughly have a comparable chemical composition, and (2) in both systems changes in relevant variables induce comparable effects.

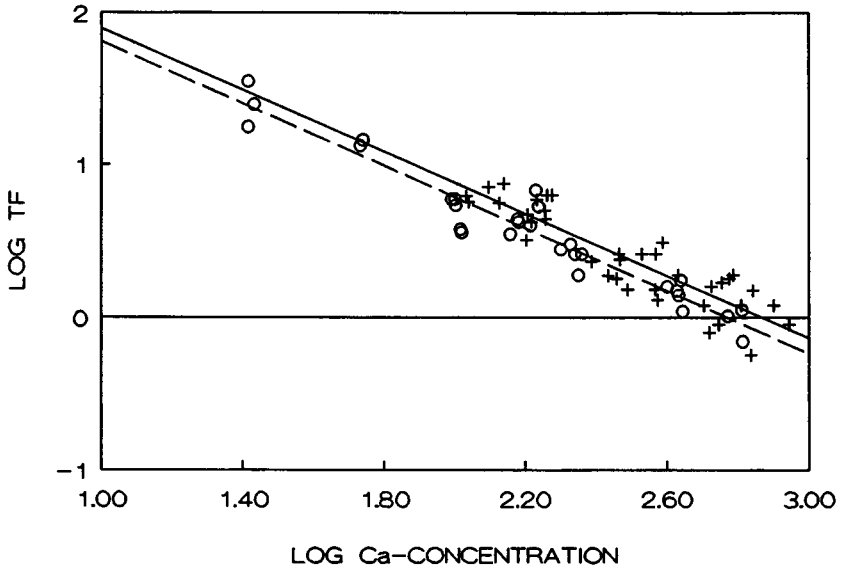

FIGURE 4 : transfer factor of Sr-85 from soil (+———+) or nutrient solution (0-----0) to lettuce as a function of he Ca-concentration of the nutrient solution (Y= -1.02X + 2.84, r= 0.966, N= 30) or of the soil liquid phase (Y= -1.01X + 2.91, r= 0.888, N= 37).

Liming was observed to reduce the availability of zinc in the soil solution. The transfer factor, based on the soil solution concentration, however, remained constant. The efficiency of the uptake process thus was not affected [15]. Amendments such as liming and addition of organic matter strongly affected the availability of cobalt as well as the uptake efficiency. An increased concentration in the soil liquid phase was associated with a lower transfer factor. The number of measurements for each of the simulated agricultural practices, however, was to small to relate changes in both patterns to any specific aspect of the soil solution chemical composition [15]. The uptake pattern of caesium from nutrient solutions and from soils showed to be more complex and is subject of further investigations.

The growing root system was, however, also shown to drastically change complexation of micronutrients and nuclides in the soil solution [20, 21]. In order to discern these effects of root-derived material from those of native soil organic matter plants were grown in a $^{14}CO_2$-labelled atmosphere. For Co, Zn and Mn the existence of complexation phenomena in the rhizosphere of maize and wheat was demonstrated.

CONCLUSIONS

(1) The application of soil amendments induced some obvious changes in soil-to-plant transfer factor (TF). However, the broad applicability of the investigated counter measures and the predictability of their effect seem questionable because of the complexity of the changes induced and because of an often seemingly specific effect for a given combination of soil, plant and nuclide. Observed differences in TF between the three types of soil were comparable to or smaller than those between the two plant species, even though the chemical and structural characteristics of the soils are quite diverse. The effects of an aspecific, chemical amendment, such as the application of organic matter, thus will often be small even when changing the overall nature of a soil. This means that in buffered agricultural systems there may be as much scope for producing uncontaminated crops by selecting plant species as by changing the composition of the soil.

(2) As a result of the long-term study of soil-to-grass TF's, effects of seasonal and meteorological conditions, as compared to those of soil related parameters, could be evaluated. The resemblance between the fluctuations of the TF's at various sites and a sometimes striking contrast between successive years clearly indicated variations in weather conditions to be an important cause of variation. Weather conditions affect active uptake (as for Sr-90) and external contamination (of importance for Co-60 and Cs-137). They cause fluctuations in the concentration of radionuclides in plants which mask the effect of their progressive fixation by the soil. These patterns are assumed not to be unique for periodically amended pastures but to be representative for all grazed, perennial vegetations.

(3) Conclusions from the study on transfer of technetium are a) that uptake, translocation and incorporation of TcO_4^-, the sole plant-available chemical form, proceed via (pseudo) first order kinetics, b) that uptake and as a result the transfer factor are age-dependent, c) that TcO_4^- is most probably reduced by the photosynthetic electron transport chain, d) that the spectrum of complexes produced depends on plant species and plant age, e) that uptake is most sensitive to nitrate and f) that the uptake behaviour from soils is entirely consistent with the observations made in hydroponic systems. As a result a mathematical model could be developed describing transfer on the basis of straightforward soil chemical and plant physiological principles.

(4) The experimental set-up and techniques developed to study the uptake of Tc by plants proved to be useful tools to accurately analyse and describe the relation between the soil, the soil liquid and the plant root. Experiments on the uptake of Sr and preliminary investigations with Zn, Co (and Cs) corroborated this point of view. It can be concluded that reliable interpretations of soil-to-plant transfer of radionuclides as well as of the effect of agricultural counter measures, may be based on a separate study of the effect of soil properties on availability on the one hand and of the uptake from solutions on the other hand.

IV. Other research group(s) collaborating actively on this project [name(s) and address(es)]:

K.U.L., Lab. voor Colloïdale Scheikunde, Leuven, Belgium (Prof. Dr. Ir. A. Cremers)
S.C.K./C.E.N., Radionuclide Metabolism Section, Mol, Belgium (Prof. Dr. O. Vanderborght)
N.R.P.B., Biology Dept., Chilton, Didcot, England (Dr. A. Nisbet)

V. Publications:

[1] DESMET G.M. -- Relevance of the study of technetium. Accumulation and speciation in plants. In : Technetium in the environment, G.M. Desmet and C. Myttenaere, eds., Elsevier Appl. Sci. Publ., London, 1986, 189-195

[2] FRISSEL M.J. -- Significance of cycling of elements in ecosystems and its import on radioecology. Proc. of a CEC/CIEMAT Workshop on Cycling of long-lived radionuclides in the biosphere : observations and models, Madrid, 860915, CEC, Luxembourg, 1987, Part II, 12p.

[3] FRISSEL M.J. and KOSTER J. -- Soil-to-plant transfer factors of radionuclides. Expected values and uncertainties. A summary of available data. Vth Report of the workgroup on soil-to-plant transfer factors of the IUR, Bilthoven, The Netherlands, 1987, 2-25

[4] FRISSEL M.J., STOUTJESDIJK J.F., KOOLWIJK A.C. and KÖSTER H.W. -- The Cs-137 contamination of soils in the Netherlands and its consequences for the contamination of crop products. Netherl. J. Agric. Sci. **35**, 1987, 339 - 346.

[5] FRISSEL M.J. and KOSTER J. -- The IUR project on soil-to-plant transfer factors of radionuclides : expected values and uncertainties. In : Reliability of radioactive transfer models, G.M. Desmet, Ed. Elsevier, London, 1988, 151-158

[6] FRISSEL M.J., KEVERLING BUISMAN A.S., STOUTE J.R.D., MATTERN F.C.M. and DROST R.M.S. -- The availability of deposited Cs-137 to man. Proc. of the IVth Int. Symp. on Radioecology of Cadarache, 880314. CEA/DERS, Cadarache, Part I, 1988, F 51-58

[7] FRISSEL M.J. and KOSTER J. -- Uncertainties of predicted soil-to-plant transfer factors because of averaging the impact of space, time, local conditions and crop variety. Proc. on "Experiences with radioecological assessment models, comparisons between predictions and observations", 861105, Neuherberg, FRG. BGA/ISH, Neuherberg, 1989, ISH-Heft 128, 16-27

[8] KÖSTER H.W., KEEN A., PENNDERS R.M.J., BANNINK D.W. and DE WINKEL J.H. -- Linear regression models for the natural radioactivity (U-238, Th-232 and K-40) in Dutch soils : a key to anomalies. Radiat. Prot. Dosim., 24, 1988, 63-68.

[9] KÖSTER H.W. -- The Chernobyl contamination of grass and milk in the Netherlands, validation of the transfer coefficient Fm for Cs. In Proc. on "Experiences with radioecological assessment models, comparisons between predictions and observations", 861105, Neuherberg, FRG. BGA/ISH, Neuherberg, 1989, ISH-Heft 128, 94-100

[10] LEMBRECHTS J.F., DESMET G.M. and OVERBEEK H. -- Molecular mass distribution of technetium complexes in spinach leaves. Environ. Exp. Bot. **25**, 1985, 355-360

[11] LEMBRECHTS J.F. and DESMET G.M. -- Effects of leaf ageing on the distribution and metabolism of technetium-99 in Spinacia oleracea L. Environ. Exp. Bot. **25**, 1985, 361-368

[12] LEMBRECHTS J.F. and DESMET G.M. -- Accumulation Tc-bio-organic complexes in spinach plants in relation to growth. In : Technetium in the environment, G.M. Desmet and C. Myttenaere, eds., Elsevier Appl. Sci. Publ., London, 1986, 295-300

[13] LEMBRECHTS J.F. and DESMET G.M. -- Light dependent reduction of pertechnetate by broken chloroplasts. Plant Physiol. **81**, 1986, 1003-1007

[14] LEMBRECHTS J.F. -- Technetium-99 in Spinacia oleracea L. Ph.D. Thesis, Universitaire Instelling Antwerpen, Biology Dept., Antwerp, Belgium, 1986, 131p.

[15] LEMBRECHTS J.F., VAN LOON L.R., VAN GINKEL J.H. and DESMET G.M. -- Interpretation of soil-to-plant transfer on the basis of soil solution chemical composition. Proc. of the IVth Int. Symp. on Radioecology of Cadarache, 880314. Part I, 1988, D 169-178.

[16] LEMBRECHTS J.F. and DESMET G.M. -- Reaction mechanisms responsible for the transformation of pertechnetate in photoautotrophic organisms. Health Phys. **57**, 1989, 255-262

[17] LEMBRECHTS J.F., STOUTJESDIJK J.F., VAN GINKEL J.H. and NOORDIJK H. -- Soil-to-grass transfer of radionuclides : local variations and fluctuations as a function of time. Proc. of a CEC/ENEA-DISP/CRSA Workshop on The transfer of radionuclides in natural and semi-natural environments, Udine, Italy, 890911. In press.

[18] LEMBRECHTS J.F., VAN GINKEL J.H., DE WINKEL J.H. and STOUTJESDIJK J.F. -- The effect of some agricultural techniques on soil-to-plant transfer of radionuclides under field conditions. Proc. Int. Symp. on Environmental contamination following a major nuclear accident, Vienna, Austria, 891016. In press.

[19] LEMBRECHTS J.F., VAN GINKEL J.H. and DESMET G.M. -- Comparative study on the uptake of strontium-85 from nutrient solutions and potted soils by lettuce. Plant and Soil, submitted for publication

[20] MERCKX R., VAN GINKEL J.H., SINNAEVE J. and CREMERS A. -- Plant induced changes in the rhizosphere of maize and wheat. Part I. Production and turnover of root derived naterial in the rhizosphere of maize and wheat. Plant and Soil **96**, 1986, 85-93

[21] MERCKX R., VAN GINKEL J.H., SINNAEVE J. and CREMERS A. -- Plant induced changes in the rhizosphere of maize and wheat. Part II. Chelation of cobalt, zinc and manganese in the rhizosphere of maize and wheat. Plant and Soil **96**, 1986, 95-107

[22] NISBET A.F. and LEMBRECHTS J.F. -- The dynamics of radionuclide behaviour in soil solution with special reference to the application of countermeasures. Proc. of a CEC/ENEA-DISP/CRSA Workshop on The transfer of radionuclides in natural and semi-natural environments, Udine, Italy, 890911. In press

[23] STOUTJESDIJK J,F., VAN GINKEL J.H. and PENNDERS R.M.J. -- Determination of soil-plant transfer factors and measures to influence the uptake of radionuclides. Vth Report of the workgroup on soil-to-plant transfer factors of the IUR, Bilthoven, The Netherlands, 1987, 26-37

[24] VAN LOON L.R., DESMET G.M. and CREMERS A. -- The influence of the chemical form of technetium on its uptake by plants. In : Speciation of fission and activation products in the environment, R.A. Bulman and J.R. Cooper, eds., Elsevier Appl. Sci. Publ., London, 1986, 352-360

[25] VAN LOON L.R., STALMANS M., MAES A., CREMERS A. and COGNEAU M. -- Soil-humic acid complexes of technetium : synthesis and characterization. In : Technetium in the environment, G.M. Desmet and C. Myttenaere, eds., Elsevier Appl. Sci. Publ., London, 1986, 143-153

[26] VAN LOON L.R. and LEMBRECHTS J.F. -- Speciation of technetium in plants grown on substrates which contained different chemical forms of technetium. In : Technetium in the environment, G.M. Desmet and C. Myttenaere, eds., Elsevier Appl. Sci. Publ., London, 1986, 301-306

[27] VAN LOON L.R. -- Kinetic aspects of the soil-to-plant transfer of technetium. Dissertationes de Agricultura No 150. Ph.D. Thesis, Katholieke Universiteit Leuven, Leuven, Belgium, 1986, 145 p.

[28] VAN LOON L.R., DESMET G.M. and CREMERS A. -- The uptake of pertechnetate by plants : a mathematical description. Health Phys. **57**, 1989, 309-314

RADIATION PROTECTION PROGRAMME
Final Report

Contractor:

Laboratorio Nacional de Engenharia
e Tecnologia Industrial (LNETI)
DPSR - Azinnhaga dos Lameiros
Estrada do Paço do Lumiar
P-1699 Lisboa

Contract no.: BI6-B-198-P

Head(s) of research team(s) [name(s) and address(es)]:

Dr J.P. Galvào
DPSR
LNETI
Estrada Nacional 10
P-2685 Sacavém

Telephone number: (1)255.49.81

Title of the research contract:

Behaviour of radionuclides and model development in aquatic ecosystems.

List of projects:

1. Radioecology of river ecosystems
2. Behaviour of radionuclides in the marine environment.

Title of the project no.: 1

Radioecology of River Ecosystems

Head(s) of project:

M.Carolina Vaz Carreiro

L.Canelas, as leader of the contribution from DCEA/UNL

Scientific staff:

M.C.Vaz Carreiro
M.J.Madruga
M.M.Sequeira
J.A.Corisco
L.Canelas (DCEA/UNL)
A.Brogueira
M.M.Brito

I. Objectives of the project:

The objective of this project is to obtain a better knowledge on the behaviour of radionuclides potentially released into the river Tejo and on the modalities of transfer in the river ecosystems. It covers the radiological survey of the river and radioecological experiments on a simplified trophic chain from the Fratel dam, with the aim of establishing an experimental biological transfer model.

Implementation of a mathematical simulation model for predicting radionuclides dispersion and transport along river Tejo.

II. Objectives for the reporting period:

1. Prossecution of the physico-chemical characterization of the water, chemical characterization of the biota and sediments, and also the mineralogical characterization of these ones; qualitative knowledge of the phytocenoses and of the icthyofauna, and a lymnological study.

2. Experiments concerning the Co-60 transfer in a simplified trophic chain from Fratel dam and its behaviour in water-sediments interactions, were intended to begin.

3. First simulations for radioisotopes using the capacity of the installed model to simulate one non-conservative parameter. Implementation of a specific mathematical model for radionuclides simulation.

III. Progress achieved:

A. GENERAL HYDROLOGICAL CHARACTERISTICS OF THE RIVER AND SAMPLING STATIONS

The Tejo River has its origin in Spain. Out of its 1.1×10^3 km length, only 230 km lie in Portugal, 43 km of it serving as frontier between both countries. Tejo hydrographic basin covers an area of about 8.1×10^4 km^2, of which 2.5×10^4 km^2 are within Portugal. The year-average volume flow of the river is 450 m^3 s^{-1}, with extreme mean values of 90 and 1000 m^3 s^{-1}.

There are several dams mainly for hydroelectric power, the most important at Cedillo in Spain (near the border) and at Fratel and Belver in Portugal. These dams do not have sediment discharges. In Spain there are three nuclear power plants: Trillo and Jose Cabrera upstrean NE of Madrid, and Almaraz, about 120 km from the border.

The hydrological regime of the Tejo River is greatly dependent on the dams exploitation, and may change, in short periods of time, with the release flows. So, during Summer, the flow may go down to 10 m^3 s^{-1}. This is very important for the implementation of the hydrodynamic model, bacause, in some sections of the river, the draining channels may change due to the appearing of sand banks. On the other hand, during the same period of time and for simulation purposes, the area between dams could be considered as a lake.

Therefore it became extremely important to gather local specific input data.

It should be noticed that a paper factory exists at Vila Velha de Rodão discharging its effluents into the river.

i) Fratel dam

This dam spreads out between Portas de Rodão (near Vila Velha de Rodão) and the confluence of Ocreza River, with 36 km of length, an area of 5.8 km^2 and a volume of 93×10^6 m^3; the maximum depth (500 m far from the breakwater) is 31 m. The surface/volume ratio is evaluated at 0.056 m^{-1}, which seems to be rather low. This is important, because in lakes the ^{137}Cs radioactivity in fish, through direct deposition, increases with this ratio.

The hydraulic regime of the dam, with periodic water discharges (following the rises), determines a low retention time, which may prevent an important transfer of the ^{137}Cs radioactivity onto the sediments.

The Fratel dam lies in a zone mainly constituted by metamorphic and sedi-

mentary rocks. The cultures nearby are mainly olive-groves and pine-woods and some others where organic and chemical fertilizers are used. Some reports point out high levels of phosphorous and nitrogen in this dam.

ii) Vila Nova da Barquinha

This sampling station is located after the confluence of Tejo River with its tributary, the Zêzere River, which contributs with an input of about 100 $m^3 s^{-1}$ (average), so being the cause of an important dilution effect. The flow rate in this location ranges between 48 and 80 cm s^{-1}.

iii) Valada do Ribatejo

At this location there is a water captation and treatment facility for supplying Lisbon with water. The flow rate is identical to that one at Barquinha, 36 to 74 cm s^{-1}.

B. RADIOECOLOGICAL CHARACTERIZATION OF THREE SAMPLING STATIONS IN TEJO RIVER

1. METHODOLOGY

1.1. Ecological Characterization

Physico-chemical parameters in water, sediments hydrophytes and fish were determined, Carreiro (1990), Reis et al. (1988), Freitas et al. (1989), Carreiro et al. (1989). Studies of structure and dynamics of the Planktonic communities, Oliveira et al. (1989) of the aquatic and river bank Phytocenosis, Moreira et al (1989), of Fish, Almaça et al. (1989) and of Macroinvertebrates, Capela et al. (1989) were carried out.

1.2. Radioactivity Measurements

The river water is filtered through 0.45 µm and follows radiochemical analysis for ^{137}Cs, ^{90}Sr and ^{3}H as described in Sequeira et al. (1989). ^{137}Cs is measured by Ge (Li) gamma spectrometry; ^{90}Sr is measured by beta counting; ^{3}H is measured by liquid scintillation spectrometry, preceded by electrolytical enrichment. Sediments are dried and, fish and plants are incinerated. All these samples are also measured by Ge (Li) gamma spectrometry.

2. RESULTS

2.1. Ecological Characterization

All the available results are reported in the documents referred in paragraph 1.1.

2.2. Radioactivity Measurements

Results are reported in Sequeira et al. (1989, 1990) and summarized in Tables 1 to 3. All the mean values presented are geometric means with the maximum value of the standard deviation.

3. DISCUSSION

3.1 Ecological Characterization

From the available data, the following points should be emphasized:

i) The K^+ concentration in water is higher than usually in freshwaters. Taking into account a possible radioactive cesium contamination, its concentration in biota or in sediments may be reduced by the chemical competition with potassium.

ii) The sediments constitution is mainly made of SiO_2, while the $Al_2 O_3$ content is low. This may have an effect in reducing the sediments contamination.

iii) In what concerns the Phytoplankton, considering that the Bacillariophyceae are the dominant species and that they present a high sedimentation rate, in the case of a radioactive contamination, they might play an important role. At Fratel they would be more important during Winter and Spring, when they dominate in the water column, while during Summer and Autumn, Cycnophyceae and Chlorophyceae are also abundant.

iv) Concerning the Zooplankton, the Cladocera are one of the most abundant groups at every sampling station, and they may be important in the case of a radioactive contamination, as they are filter feeding organisms. At Fratel there are large filtering species like Daphnia hyalina and along the river other small filtering Cladocera, like Bosminidae and Chydoridae; these two families feed on detritus and as their remains are not very soluble in water, they undergo a sedimentation.

v) The most abundant species of hydrophytes are: Potamogetum crispus, Myriophyllum spicatum and Ceratophyllum demersum. However, while the last one is a free floating species the other two are rooted, and therefore they may undergo a radioactive contamination not only directly from the water but also through the sediments.

vi) The most abundant fish species are: at Fratel Lepomis gibbosus (Centrarchidae), followed by Chondrostoma polylepis polylepis and Gobio gobio (both Cyprinidae); at Barquinha Ch. polylepis, which is always present, and at Valada Barbus bocagei (Cyprinidae). All are omnivorous, however Ch. polylepis feeds mainly on macro and microalgae and, therefore they may be more quickly contaminated, specially if the radioactive contamination would happen in Spring time, with the great algae bloom.

3.2 Radioactivity Measurements

A significant increase of the artificial radionuclides, ^{137}Cs and ^{3}H, in water was noticed during 1987, Table 1. The concentrations decreased again, until the normal situation, along 1988-89, Table 1, except for ^{3}H which shows again a rise during 1989.

The radioactivity measured in rainwater at Fratel, during 1987-89, is approximately constant, with a range of values from 0.3 ± 0.1 to 1.6 ± 0.3 Bq l^{-1}.

The ratio $^{137}Cs/^{90}Sr$, usually ranged between 1.06 and 1.82, with a mean value of 1.36, accordingly to values attributable to the fallout from nuclear test explosions. During 1987 this ratio was completly upset, reaching a maximum value of 35 in March at Fratel.

Table 1 - Artificial radionuclides concentration in Tejo River water

Years	Sampling location	Dissolved material (0.45 µm)		
		^{137}Cs mBq.l^{-1}	^{90}Sr mBq.l^{-1}	^{3}H Bq.l^{-1}
1986	Rodão	1.4 ± 0.5	2.1 ± 0.7	2.3 ± 0.2
1987	Rodão	9.0 ± 4.9	2.9 ± 0.7	7.0 ± 2.2
	Fratel	6.3 ± 2.1	2.4 ± 0.6	6.7 ± 1.5
	Barquinha	9.3 ± 4.9	3.2 ± 1.9	4.5 ± 0.6
	Válada	5.6 ± 5.1	2.9 ± 1.4	5.1 ± 3.6
1988	Rodão	1.7 ± 0.4	1.4 ± 0.3	2.1 ± 0.3
	Fratel	1.4 ± 0.4	2.8 ± 0.5	2.3 ± 0.3
	Barquinha	1.3 ± 0.3	3.0 ± 1.0	1.5 ± 0.2
	Valada	0.9 ± 0.3	1.8 ± 0.9	1.1 ± 0.1
1989	Rodão	1.5 ± 0.3	0.8 ± 0.2	14 ± 3
	Fratel	1.5 ± 0.7	1.5 ± 0.3	13 ± 1
	Barquinha	2.3 ± 0.4	1.7 ± 0.2	11 ± 3
	Valada	1.0 ± 0.2	1.4 ± 0.3	10 ± 3

Table 2 - ^{137}Cs concentration in Tejo River sediments

Years	Sampling location	^{137}Cs Bq.kg^{-1}		^{137}Cs / Al_2O_3 Bq.kg^{-1}	
		Sediment Total	Fraction < 212 µm	Sediment Total	Fraction < 212 µm
1987	Rodão	2.7 ± 0.5	3.1 ± 0.6	0.030	0.034
	Fratel	4.0 ± 2.2	4.8 ± 3.1	0.038	0.045
	Barquinha	≤ 2	2.8 ± 1.2	---	---
	Valada	≤ 2	2.9 ± 1.2	---	---
1988	Rodão	3.8 ± 0.6	7.6 ± 1.5	0.042	0.083
	Fratel	5.4 ± 2.5	7.2 ± 4.7	0.056	0.075
	Barquinha	≤ 2	5.5 ± 4.7	---	0.073
	Valada	2.4 ± 0.6	3.7 ± 3.1	0.039	0.060
1989	Rodão	5.4 ± 1.1	5.2 ± 0.9	0.059	0.057
	Fratel	3.3 ± 1.5	6.0 ± 2.8	0.033	0.059
	Barquinha	1.8 ± 0.2	2.6 ± 0.9	0.025	0.036
	Valada	1.5 ± 0.3	2.6 ± 1.7	0.023	0.040

In what concerns the sediments, it can be noticed that there was a small increase in the ^{137}Cs concentrations, during 1988-89, but mainly in 1988, noticed by the greater number of significative values in comparison with preceding years, Table 2 .

In Table 3 the columns concerning the aquatic macrophytes, show values that are usually similar. However, at Rodão there is also a greater abundance of significative values in 1988, mainly during the second half of the year, showing a mean value of 5.1 ± 0.7 Bq kg^{-1}(d.w.).

It is interesting to notice that in 1988 the cosmic ^{7}Be was detected in almost all the samples,while in preceeding years this only sporadically happened. Nevertheless, this difference may be due to the use of a new Ge (Li) detector with a higher efficiency.

The values of ^{137}Cs concentration in fish, Table 3, are scarce (due to difficulties in fishing). Most of them are under the detection limit. However, this data concern the whole fish. Therefore, it might be assumed that ^{137}Cs concentrations would be slightly higher if only the muscle was concerned. The relationship between the radioactivity in the whole fish and in the muscle is now being studied.

Accordingly to the above considerations concerning the water data, it might be assumed that the increased artificial radioactivity is neither due to

old bomb fallout, nor to Chernobyl fallout. Actually, no ^{134}Cs was present. So it is probably due to the operation of the Spanish nuclear power plants upstream the Tejo River, although no abnormal discharge has been reported.

Table 3 - Artificial radionuclides in Fish and Aquatic Macrophytes from Tejo River

Years	Sampling location	Concentration in Fish Bq.kg^{-1} (f.w.)	Concentration in Hydrophytes Bq.kg^{-1} (d.w.)	
		^{137}Cs	^{137}Cs	^{7}Be
1987	Rodão	0.06 ± 0.02	2.0 ± 0.5	---
	Fratel	≤ 0.05 *	1.7 ± 0.2	36 ± 18
	Barquinha	0.07 ± 0.03	1.5 ± 0.5	94 ± 14 *
	Valada	≤ 0.05 *	---	---
1988	Rodão	0.16 ± 0.08	4.6 ± 0.9	126 ± 40
	Fratel	0.12 ± 0.07	1.8 ± 0.5	24 ± 8
	Barquinha	0.17 ± 0.05	2.2 ± 0.5	---
	Valada	≤ 0.05 *	---	---
1989	Rodão	0.08 ± 0.03	1.6 ± 0.3	36 ± 12
	Fratel	0.08 ± 0.01	1.4 ± 0.2	19 ± 10
	Barquinha	0.08 ± 0.02	1.5 ± 0.5	41 ± 8
	Valada	0.12 ± 0.08	≤ 1	35 ± 5 *

* only one value

C. EXPERIMENTAL STUDIES OF ARTIFICIAL RADIONCULIDES TRANSFER IN A FRESHWATER TROPHIC CHAIN AND IN SEDIMENTS

1. METHODOLOGY

This study was performed considering the following trophic chain: Selenastrum capricornutum Printz (cl.Chlorophyceae), Daphnia magna Straus (cl. Crustacea) and Tinca tinca Linnaeus (cl.Osteichtyes, fam.Cyprinidae) in Fratel dam water.

The experiments concerning the water-sediments interaction, were carried out with sediments and water from Fratel dam. ^{134}Cs and ^{60}Co have been used in all the experiments and the detection system consists on a well-type NaI(Tl) detector connected to a multichannel analyser. The detector size is 4"x4" and the well is 1 1/4" diameter and 2 1/2" deep.

2. RESULTS

Results concerning the ^{134}Cs in the simplified trophic chain were acompli-

Table 4 - Experimental results for ^{134}Cs in a simplified trophic chain

Species	Contamination pathway	Experiments	
		uptake	loss
Selenastrum capricornutum		$CF = (1.6 \pm 0.16)\ 10^3$	$R_{(t)} = 77\ e^{-45t} + 20\ e^{-1.3t}$
Daphnia magna	water	$CF_{(t)} = 59\ (1 - e^{-0.29t})$	$R_{(t)} = 14\ e^{-6.2t} + 86\ e^{-0.43t}$
	S.capricornutum	$TF_{(t)} = 5.1\ (1 - e^{-0.25t})$	$R_{(t)} = 100\ e^{-0.41t}$
Tinca tinca	water	$CF_{(t)} = 0.58\ t^{-0.78}$ (t= 32 d)	$R_{(t)} = 25\ e^{-0.10t} + 75\ e^{-0.008t}$
	D.magna	$TF_{(t)} = 0.012\ t^{0.80}$ (t= 41 d)	$R_{(t)} = 91\ e^{-0.018t}$

shed by both pathways (water and food) and are reported in Corisco and Carreiro (a, b, c).

In what concerns the ^{60}Co and same trophic chain, the results are still delayed due to an equipment failure and, on the other hand, some previous studies on the physico-chemical forms had to be performed. As soon as the experiments are finished, they will be published with reference to this contract.

The water sediments interaction results concerning the ^{134}Cs are reported in Madruga et al. (1988), and those concerning the ^{60}Co, in Madruga and Carreiro (1990).

3. DISCUSSION

The study of the trophic chain allowed the evaluation of the ^{134}Cs transfer from Fratel water to a fish, through mathematical expressions, extrapolated from the experimental results. An analytical approach of the transfer from one compartment to another is obtained, showing the relative importance of the two pathways (water and food). In both cases, daphnids and fishes, the water is the main pathway. In what concerns the microalgae, Selenastrum capricornutum, it revealed a high accumulation.

Table 5 - Some results concerning sediments and water from Fratel dam (sediment concentration in water 1 mg/ml)

Radionuclide	Experiments	
	Adsorption	Desorption
^{134}Cs	$K_d = 1091 + 271 \ln t$	$R_{(t)} = 28.4\ e^{-37t} + 33.8\ e^{-0.90t} + 34.9\ e^{-0.096t}$
^{60}Co	$K_d = 1012 + 281 \ln t$	$R_{(t)} = 49.4\ e^{-0.58t} + 46.3\ e^{-0.014t}$

The excretion processes are very important, as they avoid the increase, or at least big increases, from one trophic level to the other, so avoiding biomagnification.

The water-sediments experiments with ^{134}Cs showed that at the studied sediment concentration range, the K_ds increased together with the sediment concentration. No explanation was found, but is seems that this happens also with other sediments, as reported at the Symposium of Radioecology (Cadarache) where this paper was presented. The compartmental analysis study allow the conclusion that, in both adsorption and desorption experiments, the mechanisms are similar and should concerns the chemisorbed layer, the crystal surface and the crystal interior of the sediment components.

In what concerns the K_ds and transfer factors, there is a good agreement between laboratory experiments and field studies.

In the ^{60}Co experiments, at the sediment concentration range studied and for the same initial radioactivity, the K_ds decreased with the increase of the sediment concentration, probably because the sediments, at low concentrations, serve as a nucleation site for the precipitation of the ^{60}Co. In this case also, the compartmental analysis study leads to the conclusion that, in both adsorption and desorption experiments, the mechanisms are similar and reversible, concerning very likely the chemisorbed layer and the crystal surface of the mineral sediment components.

In the identification of the ^{60}Co physico-chemical forms, the observed evolution from cationic to anionic and neuter forms, is due to the presence of the sediment, which might originate a chloride complex formation. However, the cationic forms are still predominant.

D. MODELLING

1. METHODOLOGY

Study of hydrological and hydraulic parameters of Tejo River.

Due to large variability of dam discharges a complementary field work was carried out:

Measurements of water velocity in several stretches;
Deepness measurements in different profiles and sections of the river;
Width measurements in some sections of the river;
Collecting of discharged flows data, registered at Castelo de Bode (Zêzere), Fratel and Belver dams, in time periods related to experimental determinations.

Detailed statistic treatment on flows released from Cedillo, Fratel, Belver and Castelo de Bode dams.

Implementation, development, and application of a model which includes: a hydrodynamic model for flows and water levels prediction, as well as a model for prediction of radionuclides concentration, as a result of potential releases from the Almaraz nuclear power plant.

2. RESULTS

The hydrodynamic model envolves the capacity of simulating discharges from Spain (Cedillo dam) and discharges from Fratel and Belver and dynamic simulation of flows, velocities and water levels in those systems.

It is also prepared to simulate at the same time the free flowing characteristics of the river after Belver dam,till the tidal area of influence of the estuary.

The model has been tested and is operating properly.

The water quality model envolves capacity of dynamic simulation of radionuclide concentrations in water and sediment and envolves mechanism of decay, adsorption,settling and sedimentation.

Efforts to get information from Spanish authorities concerning the complete charactirization of source term related to a potential accident at the Almaraz nuclear power plant, and releases from Cedillo, are underway and will allow in a near future simulation of realistic scenarios with the

developed simulation models.

3. DISCUSSION

Taking into account the referred particular hydraulic and hydrological characteristics of the Tejo River, a great effort was put in carrying out measurements and assembling the values in a data bank. Relations among different parameters were established and a comprehensive knowledge of the actual hydrodynamics of the river was obtained.

The linkage of the hydrodynamic model for radionuclides simulation is now being accomplished, and as soon as results become available, they will be published with reference to this project.

FINAL NOTE

It may be considered that the general objectives of the project were reasonably achieved.

IV. Other research group(s) collaborating actively on this project [name(s) and address(es)]:

Departamento de Ciências e Engenharia do Ambiente, Faculdade de Ciências e Tecnologia, Universidade Nova de Lisboa (DCEA/UNL)

V. Publications:

[1] - Carreiro, M.C.V. (1990)
Ecological Study of Tree Sampling Stations in Tejo River
LNETI/DPSR-B-Nº 4 (III Series)

[2] - Reis, M.F., Freitas, M.C., Carreiro, M.C.Vaz, Martinho, E. (1988)
Análise Multielementar de peixes e Água do Rio Tejo pela Técnica de Análise por Activação com Neutrões
1ª Conferência Nacional sobre a Qualidade do Ambiente, 22-24 Fevereiro 1988, Aveiro, Portugal

[3] - Freitas, M.C., Carreiro, M.C.Vaz, Reis, M.F., Martinho, E. (1988)
Determination of the Level of some Heavy Metals in an Aquatic Ecosystem by Instrumental Neutron Activation Analyses
Environmental Technology Letters, vol.9, pp. 969-976

[4] - Carreiro, M.C.Vaz, Reis, M.F., Freitas, M.C., Martinho, E. (1989)
Concentration of Heavy Metals in Ecosystems of Tagus River determined by INAA
Proceedings of the International Conference on Heavy Metals in the Environment, 12-15 September, 1989, Geneva, Switzerland, pp. 643-646

[5] - Oliveira, M.R.Leal, Monteiro, M.T. and Coutinho, M.T. Pereira (1989)
Estudo da Estrutura Dinâmica das Comunidades Planctónicas do Rio Tejo, nos troços de Fratel, Barquinha e Valada
INIP, Relatórios Técnicos e Científicos nº 11, 1989

[6] - Moreira, I.S., Cardoso, M.T.F. (1989)
Estudo das Fitocenoses Litorais do Rio Tejo em três Locais Seleccionados
Instituto Superior de Agronomia

[7] - Almaça, C., Collares-Pereira, M.J., Coelho, M.M. (1989)
Relatório do Estudo da Fauna Ictiológica do Rio Tejo
Faculdade de Ciências

[8] - Capela, R.A., Serrano, A.R.M. (1989)
Relatório sobre o Estudo de Macroinvertebrados em alguns troços do Rio Tejo
Faculdade de Ciências

[9] - Sequeira, M.M.A., Carreiro, M.C.Vaz, Bettencourt, A.O. (1989)
Controlo Radiológico do Rio Tejo, 1987 a 1988
LNETI/DPSR - B - nº 110

[10] - Sequeira, M.M., Carreiro, M.C.V., Bettencourt, A.O.
Controlo da Radioactividade do Rio Tejo,1989
(to be published as LNETI Report, in 1990)

[11]a - Corisco, J.A.G., Carreiro, M.C.V.
Étude Expérimentale sur l'Accumulation et le Rétention du ^{134}Cs par une Microalgue Planctonique, Selenastrum capricornutum Printz
(accepted to be published in Revue des Sciences de l'Eau)

[12]b - Corisco, J.A.G., Carreiro, M.C.V.
Direct and Food Chain Uptake and Loss of ^{134}Cs by Daphnia magna Straus (Crustacea, Cladocera)
(to be submitted)

[13]c - Corisco, J.A.G., Carreiro, M,C.V.
Study of the Uptake and Loss of Cs-134 by Tinca tinca Linnaeus (Teleostei, Cyprinidae) through the Water and the Food Chain
(to be submitted)

[14] - Madruga, M.J.B., Carreiro, M.C.V., Bettencourt, A.O.
Experimental Study of the Cs-134 Behaviour in Freshwater, Sediments
Proceedings of the IVth International Symposium of Radioecology, 14-18 March, 1988, Cadarache, France, pp.C-51

[15] - Madruga, M.J., Carreiro, M.C.V.
Experimental Studies of Co-60 Behaviour in Tejo River Sediments
(to be presented at the 5th International Symposium on the Interactions between Sediments and Water, Uppsala, Sweden, August, 1990)

Title of the project no.: 2

BEHAVIOUR OF RADIONUCLIDES IN THE MARINE ENVIRONMENT

Head(s) of project: A. O. Bettencourt

Scientific staff: A. O. Bettencourt
F. P. Carvalho
M. D. T. Elias
G. C. Ferrador

I. Objectives of the project: Study of the distribution and behaviour of the more significant natural and artificial radionuclides in the marine environment and of their respective contribution to the radiation doses to humans and to marine biota.

Evaluation of the field concentration factors of artificial and natural alpha emitters for deep-sea fish and for common sea-food from coastal areas, significant in the diet of the Portuguese population.

II. Objectives for the reporting period: Analyses of some marine biota samples for the determination of U, Ra and Th isotopes, in order to compare the radiation doses due to these radionuclides, with those arising from ^{210}Po and ^{210}Pb.

Analyses of transuranics in sea water to allow the calculation of the field concentration factors in deep-sea fish.

Study of the transfer of the main natural alpha-emitters to man, and assessment of doses through the consumption of sea-food, due to both the natural and the artificial alpha emitters.

III. Progress achieved:

1. METHODOLOGY

Fish and other marine biota samples have been collected along the Portuguese coast and off the Madeira Archipel. A special attention was given to the black scabbard fish (Aphanopus carbo), which lives at depths of 600 to 1200 m and is very significant in the diet of the Madeira population. Since recently, it is also being fished south of Lisbon.

1.1. Natural alpha emitters

Naturally-occurring alpha emitter analyses were performed through radiochemical separation procedures followed by isotope plating and alpha spectrometry. Briefly, samples were dissolved in mineral acids, after spiking with standard activities of appropriate tracers (^{232}U, ^{229}Th, ^{224}Ra and ^{209}Po). Radiochemical separations (Bojanowski et al, 1983, Carvalho, 1988 a, b) were achieved from chloride solution of samples through elution by anionic/ /cationic resin columns.

Sample sizes were 20-50 L for sea-water, and 10-50 g (wet weight) for ^{210}Po and 100-500 g for other alpha emitters in biological materials.

1.2. Artificial radionuclides

Transuranics have been analyzed, in samples of 1-2 kg of fish or 200 L of water, using the technique described by Ballestra et al (1978), with some adaptations. Radioactive tracers of ^{236}Pu, ^{243}Am and ^{244}Cm are added, and Pu and Am are separated by ion exchange chromatography, solvent extraction with HDEPH and electroplating.

Radioactivity measurements of all alpha emitters, both artificial and natural, were accomplished by alpha-spectrometry with surface-barrier detectors. ^{137}Cs has been analyzed either by direct gamma spectrometry on ashes, or by beta counting after radiochemical separation and precipitation with chloroplatinic acid.

In general, the quality of the methods has been tested by participation in the intercomparison exercises organized by the International Atomic Energy Agency (IAEA).

1.3. Dose assessment

Absorbed radiation dose rates and dose equivalent rates to marine biota have been computed, taking into account the measured concentrations and the assumptions reported in Carvalho (1988).

The individual committed effective dose equivalent, to a critical group of the population, due to the consumption of fish, was calculated for natural and artificial radionuclides, taking into account the average of the measured concentrations, appropriate dose factors (Camplin & Aarkrog, 1989), and a fish consumption rate of 70 $kg.a^{-1}$.

2. RESULTS

2.1. Natural alpha emitters

^{210}Po in surface waters off the Portuguese coast (Iberian basin) and off Madeira island is generally present in lower concentration than its precursor ^{210}Pb. The Po/Pb ratio in unfiltered sea water is 0.7 ± 0.3 (Table I). However, in coastal waters, both the ^{210}Po and ^{210}Pb concentrations and the particulate fraction of these nuclides is more variable, and Po/Pb ratios greater than unity were measured. Most part of ^{210}Po and ^{210}Pb are in dissolved form. For the entire water column in the ocean, ^{210}Po and ^{210}Pb are close to radioactive equilibrium.

Table I: ^{210}Po and ^{210}Pb concentration in surface sea water samples from different regions. ($mBq.L^{-1}$)

		Particulate (>0.45 µm)		Total	
		^{210}Pb	^{210}Po	^{210}Pb	^{210}Po
COASTAL:	surf zone	0.14 ± 0.02	0.83 ± 0.08	1.10 ± 0.04	1.91 ± 0.09
(Portugal)	" "	0.45 ± 0.02	1.71 ± 0.06	1.35 ± 0.04	2.98 ± 0.08
	5 mil. off	0.09 ± 0.02	0.85 ± 0.03	2.36 ± 0.16	2.55 ± 0.08
	" " "	0.38 ± 0.01	0.44 ± 0.01	2.67 ± 0.18	2.18 ± 0.08
OCEANIC:	n = 7	-	-	2.1 ± 0.6	1.5 ± 0.2
(Iberian basin)	n = 10	0.07 ± 0.06	-	2.1 ± 0.7	-
OCEANIC: (off Madeira)	n = 4	0.53 ± 0.25	0.52 ± 0.20	2.87 ± 0.54	2.10 ± 0.61

Uranium in the sea water is in the soluble phase. The concentrations of ^{238}U and ^{234}U in the sea is noticeably constant, both at the surface and with water depth. The average concentration of ^{238}U is 39.0 ± 1.5 $mBq.L^{-1}$ and $^{234}U/^{238}U$ is 1.15 ± 0.03, in a series of sea water sampling stations in the Iberian basin.

Thorium is less abundant in sea water. No attempt was made to measure ^{234}Th, a pure beta emitter. ^{232}Th concentrations are about 1 $\mu Bq.L^{-1}$, about 3 $\mu Bq.L^{-1}$ for ^{230}Th and about 10 $\mu Bq.L^{-1}$ for ^{228}Th.

Radium in the sea water is essentially in the dissolved form. Apparently, its concentration in shallow waters seems to be affected by river discharges. In the open ocean, ^{226}Ra surface concentration is about 1 (0.9-1.2) $mBq.L^{-1}$. However the ^{226}Ra vertical profile in the water column differs from those of U and Po, because the main ^{226}Ra source is the sea floor by redissolution from sediments.

Most of the effort in analyzing marine biota was put into the analysis of ^{210}Po and ^{210}Pb. Table II, summarizes results presented and discussed in detail elsewhere (Carvalho, 1988 a, b). It is clear that ^{210}Po is accumulated to high levels in most of marine organisms, and specially concentrated in some tissues as shrimp hepatopancreas, fish liver, and fish gonad. ^{210}Po concentrations in fish muscle varies between 2 and 21 $Bq.kg^{-1}$ for common edible species as sardines, maeckerel and tuna. However,some species display lower ^{210}Po concentrations in muscle tissue, as Aphanopus carbo (0.2 $Bq.kg^{-1}$), while others display extremely high ^{210}Po levels as the mesopelagic hatchet fish (980 $Bq.kg^{-1}$ in a whole body basis). There is no clear relationship between ^{210}Po concentrations in fish tissues and the depth or area in which they inhabit. ^{210}Po in fish seems to be dependent mainly upon food chain transfer.

Several common sea food were analyzed, among other samples, for the different natural alpha emitters concentrations in muscle, Table III. In all species, ^{210}Po is always present at the highest concentration, representing 80% or more of the total alpha activity, while the activity concentration of Th isotopes is the lowest.

2.2. Artificial radionuclides

The detailed results of $^{239+240}Pu$, ^{241}Am, and ^{137}Cs, in fish muscle, are reported in Ferrador et al (1990). Very low concentrations of $^{239+240}Pu$ and ^{241}Am were generally detected. The arithmetic means of measured concentrations are 0.4 $mBq.kg^{-1}$ for $^{239+240}Pu$, 0.3 $mBq.kg^{-1}$ for ^{241}Am, and 0.44 $Bq.kg^{-1}$ for ^{137}Cs.

These concentrations correspond to typical values due to fallout deposition in this region of the Atlantic (NEA, 1983; NEA, 1985; Camplin & Aarkrog, 1989). They are also consistent with our previous determinations, since 1979 (Bettencourt et al, 1988). Furthermore, no influence from the Chernobyl

Table II: Activity concentrations of ^{210}Po (Bq.kg^{-1} wet wt) in marine fish. Mean concentration and range in several species or concentration ± 1 SD in a single specimen analyzed. Only typical adult specimens were analyzed.

	^{210}Po			
	Muscle	Liver	Gonads	Skeleton
Epipelagic teleosts				
Clupeid and others[a]	7(1.8-21)	391(67-939)	40(11-94)	30(7-92)
Scomberesox saurus	231±20 (Muscle + skeleton)		1214±44 (Viscera)	
Tuna[b]	5(3-8)	288(278-297)	–	20(5-51)
Ruvettus pretiosus	0.7±0.02	36±2	8±0.5	5±0.3
Makaira nigricans	0.40±0.02	354±28	–	4.6±0.2
Mesopelagic teleosts				
Strict mesopelagic[c]	2.6(1.6-3.7)	552(258-845)	405(57-753)	186(163-208)
Hygophum hygomi	758±30 (Whole-body)			
Bathypelagic teleosts				
Aphanopus carbo	0.2(0.08-0.3)	6(1.1-14)	11(2-32)	2(1.3-5.0)
Benthodesmus simonyi	3.0±0.1	31±1	30±1	4.4±0.2
Demersal teleosts[d]	3(0.5-6.7)	12(4-18)	27(2.5-52)	6(3-10)
Elasmobranchs[e]	0.7(0.2-1.7)	8(0.3-32)	2(0.2-4.5)	6(1-11)

[a] *Sardina pilchardus, Scomber japonicus, S. scombrus, Trachurus trachurus, T. picturatus, Belone belone.*
[b] *Thunnus albacares, T. obesus, T. alalunga, E. (Katsuwonus) pelamis.*
[c] *Rouleina maderensis, Chiasmodon niger.*
[d] *Merluccius merluccius, Phycis blennioides, Mora mora, Synaphobranchus kaupi, Alepocephalus bairdii, A. rostratus.*
[e] *Raja undulata, Scyliorhinus canicula, Etmopterus pusillus, Deania calceus, Centroscymnus coelolepis, Centrophorus squamosus.*

Table III: Natural occurring alpha emitter concentrations in marine samples (mBq.kg^{-1} wet wt). All samples were made up with the edible part (muscle tissue)

	^{238}U	^{234}U	^{232}Th	^{230}Th	^{228}Th	^{226}Ra	^{210}Po
Filtered Sea water (average values)	39 ± 1.5	45 ± 1.7	$1x10^{-3}$	$3x10^{-3}$	$10x10^{-3}$	1±0.2	1.5
Tuna (alalunga)	2.8 ± 0.2	2.8 ± 0.2	0.3 ± 0.1	0.9 ± 0.3	741 ± 13	$6x10^2$	$5x10^3$
Blue-. marlin	8.5 ± 0.9	9.6 ± 0.9	0.17 ± 0.03	0.51 ± 0.07	5.05 ± 0.02	$5x10^2$	$1.5x10^2$
Sardines	24 ± 2	25 ± 2	2.9 ± 5.8	19 ± 17	588 ± 70	$4x10^2$	$1x10^5$
Black scabbard	3.6 ± 0.5	5.2 ± 0.6	0.66 ± 0.08	6.7 ± 0.5	22.5 ± 0.5	-	$1x10^3$
Rattail fish	21 ± 3	27 ± 3	1.7 ± 0.2	15 ± 1	80 ± 1	-	$3x10^2$
Squid	7.3 ± 0.5	7.2 ± 0.5	0.5 ± 0.1	2.1 ± 0.4	588 ± 14	-	-
Mussels and other molluscs	660 ± 268	786 ± 351	-	-	-	-	$1x10^5$

accident in the ^{137}Cs concentrations was detected in fish from these regions.

All the values above the detection limits, obtained from 1979 to 1989, have been statistically treated, taking into account both the depth at which the different species live, and their feeding habits. At these very low levels, it is difficult to draw conclusions from the available data. It is however very clear that the Aphanopus carbo (a bathypelagic species) has much lower concentrations for these three radionuclides than most of the other species that we have analyzed, except for the bathybentic Alepocephalus baiirdi. For a comparison of the concentrations observed for the different species fish that were analized, we have grouped them into 3 categories: Bathypelagic (comprising only the Aphanopus carbo), Bentopelagic & Bathybentic (Lepidopus caudatus, Alepocephalus baiirdi, and others), and Oceanic Pelagic (Sphyraena sphyraena, tuna, and others) (Table IV).

Table IV: Concentrations of $^{239+240}Pu$, ^{241}Am, and ^{137}Cs, in fish muscle

CATEGORY		$^{239+240}Pu$ mBq.kg^{-1}	^{241}Am mBq.kg^{-1}	^{137}Cs Bq.kg^{-1}
Bathypelagic	g.m.	0.076$\pm$0.017	0.25$\pm$0.04	0.34$\pm$0.05
	range	(0.03-0.13)	(0.16-0.44)	(0.11-1.02)
	N	10	6	14
Bathybentic & Bentopelagic	g.m.	0.72$\pm$0.25	0.58$\pm$0.22	0.62$\pm$0.11
	range	(0.14-4.2)	(0.15-3.1)	(0.27-1.7)
	N	14	10	13
Pelagic oceanic	g.m.	0.94$\pm$0.68	1.24$\pm$0.16	0.48$\pm$0.10
	range	(0.2 -2.2)	(1.1 -1.4)	(0.26-0.79)
	N	4	2	5

g.m.: geometric mean $\pm$ upper S.D. of the g.m.;
N = number of considered values

Results from sea water analysis will be soon published elsewhere in detail (Bettencourt et al, in prep.). Higher concentrations of $^{239+240}Pu$ and ^{241}Am are observed at a depth of around 1000 m than in surface waters (Table V). The results obtained in 1988/1989 are consistent with previous ones obtained in 1982/1983 in the same region of the North-East Atlantic (Bettencourt et al 1986), and also with the values reported in the literature (Camplin &

Aarkrog 1989, NEA 1983, among others).

Table V: Mean artificial radioactivity in Portuguese Oceanic waters (1982/83 and 1988/89).

Sample		$^{239+240}Pu$ mBq.m^{-3}	^{241}Am mBq.m^{-3}	^{137}Cs Bq.m^{-3}
SURFACE	g.m.	9.95$^{\pm}$1.67	1.4$^{\pm}$0.6	3.20$^{\pm}$0.40
	range	(6 - 13)	(1 - 2)	(2.05-3.94)
	N	5	2	5
DEPTH	g.m.	27.3$^{\pm}$1.3	5.65$^{\pm}$0.35	2.06$^{\pm}$0.07
	range	(26 -30)	(5 - 6)	(2.0 -2.13)
	N	3	3	2

g.m.: geometric mean $^{\pm}$ upper S.D. of the g.m.;
N = number of considered values

It should be noticed that, while the blackscabbard fish (Aphanopus carbo) shows lower concentrations than the shallow water fishes, the Pu and Am concentrations are higher in its habitat than at the surface.

Using the geometric means given in Table IV (recalculated without the values for Alepocephalus bairdi) and in Table V, we have calculated the concentration factors (CF) for these radionuclides. However, for the ^{241}Am concentration in shallow waters, we have used a value of 3 mBq.m^{-3}, more consistent with the available data from the literature and with the assumed Am/Pu ratio of 0.3 for fallout. The computed CFs are presented, and compared with the recommended values, in Table VI. Most of the calculated values are within the range of the recommended ones. However, for shallow water fish, we have calculated concentration factors for ^{241}Am up to 4 x 10^2, while the range reported by IAEA (1985) for this radionuclide is 0.5 to 2 x 10^2. On the other hand, it should be noticed that we have found significantly lower concentration factors for the Aphanopus carbo, both for Pu and Am, than for most of the other species (Table VI).

In some fish samples we have separately analyzed the muscle, and several other tissues, for the transuranics. Although most of the results were below the detection limits, it would seem that there is no significant difference between the muscle and the bone + skin + remainders, but a higher concentration of Pu and Am was observed in the gonads (Beetencourt et al, in prep.).

Table VI: Calculated concentration factors for Fish.

CATEGORY	$^{239+240}Pu$	^{241}Am	^{137}Cs
Bathypelagic (Aphanopus carbo)	2.8	44	105
Bathybentic & Bentopelagic (without Alepocephalus baiirdi)	78	230	205
Pelagic oceanic	95	400	139
IAEA/TRS Nº 247:			
Recommended values:	40	50	100
Range:	(0.5-100)	(0.5-200)	(10-300)

2.3. Dose assessment

Absorbed radiation doses in fish come from internally accumulated nuclides and external radiation sources. External sources, as cosmic radiation, dissolved ^{40}K in sea water and natural nuclides in bottom sediments, give, however, lower contribution than internally accumulated ^{210}Po (Carvalho, 1988).

Due to the variable ^{210}Po concentrations in fish tissues, also the contribution of this nuclide to the absorbed radiation dose varies accordingly. Considering for instance, the common sardine, the ^{210}Po contribution for the absorbed dose rate is always the most important in every tissue. Dose equivalent rates due to ^{210}Po alone can be so high as 0.3 $Sv.a^{-1}$ in sardine liver and 5.$Sv.a^{-1}$ in intestinal walls.

Figure 1 presents the relative contribution of ^{210}Po, as well as the contribution from other nuclides, for the overall absorbed radiation doses in two different cases among marine fish.

The committed effective dose equivalent to man, arising from the consumption of fish containing an average of the measured levels for these radionuclides has been calculated, and the results are presented in Table VII. It can be seen that ^{210}Po accounts for about 98% (in any case > 90%) for this dose. If calculated separately for the Aphanopus carbo, what could be interesting due to its commercial and dietary importance for the Madeira's population, the partial and total doses would be relatively lower than those presented hereafter.

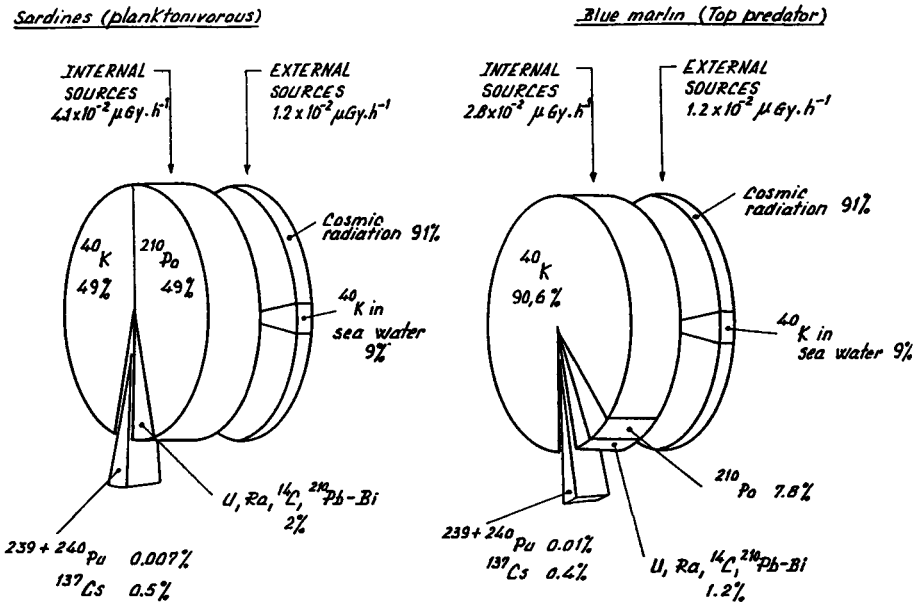

Figure 1: Absorbed radiation doses in fish (muscle tissue)

Table VII: Committed dose equivalents to man due to the consumption of fish.

	^{239}Pu	^{241}Am	^{137}Cs	^{210}Po	other natural alpha emitters
µSv/a	5 E-2	6 E-2	5 E-1	5 E+2	1 E+1
%	0.01	0.01	0.1	98	1.9

3. DISCUSSION

The objectives proposed for this project have been achieved. Throughout this study, new data was obtained which is relevant for the knowledge on the radionuclides behaviour in the marine environment and, mostly, for the assessement of the Portuguese population exposure through the ingestion of sea foods.

The most relevant data can be summarized as follows:

- The Aphanopus carbo (black scabbard), an important fish in the diet of the Portuguese population from the Madeira Archipel, shows quiet lower concentrations of ^{210}Po, $^{239+240}Pu$, ^{241}Am, and ^{137}Cs, than most of the other spe-

cies. This might be explained by the trophic chain level.

- The concentration factors (CF) for Cs, and specially for the transuranics are much lower for this species than for others. In particular, the low CF for Pu (2.8) is noticeable. On the other hand, concerning Am, we have found CFs for the other species of the order or even higher than the maximum values referred in the literature (IAEA, 1985).

- Marine biota exposure to radioactivity have been shown to arise mainly from the high unsupported ^{210}Po levels concentrated in internal tissues.

- At present, the highest dose to man arising through the consumption of sea food and due to artificial radionuclides present in the marine environment is attributable to ^{137}Cs. However, this dose is orders of magnitude lower than the dose due to the naturally-occurring alpha emitters, in particular to ^{210}Po.

IV. Other research group(s) collaborating actively on this project [name(s) and address(es)]:

Concerning oceanographic sampling, the Instituto Hidrográfico was actively involved in collaborating with this Project. In fish sampling at Madeira, we had the collaboration of the Direcção Regional das Pescas of Madeira. Thanks are due to both Institutes for their collaboration.

V. Publications:

Bettencourt, A. O., Elias M. D. T., Ferrador, G. (1988). Vigilância radiológica do meio marinho relacionada com a imersão de resíduos radioactivos no Oceano Atlântico Nordeste.

In: Proceedings do II Congresso Geral de Energia Nuclear, Rio de Janeiro, 1988, Vol. 3, pp. 425-436

LNETI/DPSR-B-Nº 2 (III Série), 1989

Bettencourt, A. O., Ferrador G. C., Elias M. D. T. (in prep.). Plutonium--239 + 240, Americium-241, and Cesium-137, in fish and waters off the Portuguese coast (1979-1989).

To be submitted

Carvalho, F. P. (1988, a). Polonium-210 in marine organisms: a wide range of natural radiation dose domains.

Radiat. Protect. Dosimetry, Vol. 24, pp. 113-117

Carvalho, F. P. (1988, b). A sequential extraction technique for ^{210}Pb, ^{210}Bi, ^{210}Po analysis in environmental materials (in Portuguese). VI Conferência Nacional de Física, 26-29 Spt., Aveiro, Portugal.

Carvalho, F. P. (1988). Polonium-210 in marine fish.

Rapp. Comm. Int. Mer Médit., Vol. 31(2), pg. 246

Ferrador, G., Bordalo Costa M. M., Elias M. D. T. (1990). Determinação de ^{239}Pu, ^{241}Am e ^{137}Cs em músculo de peixe.

LNETI/DPSR-B-Nº 3 (III Série), 1990

REFERENCES

Ballestra S., Holm E., Fukai R. (1978). Determination of transuranic elements in marine environmental samples.
In: Proc. Symp. Determination of Radionuclides in Environmental and Biological Materials, paper Nº 15

Bojanowski R., Fukai R., Ballestra S., Asari H. (1983). Determination of natural radioactive elements in marine environmental materials by ion-exchange and alpha spectrometry.
In: Symp. on the Determination of Radionuclides in Environmental and Biological Materials, London, April 1983

Bettencourt A. O., Bordalo Costa M. M., Carvalho F. P., Ferrador G., Alberto G. (1986). Measurement of long-lived radionuclides in the Atlantic related to radioactive wastes deep-sea disposal.
In: IAEA - TECDOC - 368, pp. 137-143, Vienna 1986

Campling W. C. & Aarkrog A. (1989). Radioactivity in North European waters: Report of Working Group II of CEC Project MARINA
Fisheries Research Data Report Nº 20, Fisheries Laboratory Lowestoft, 1989

International Atomic Energy Agency (1985). Sediment K_{ds} and Concentration Factors for radionuclides in the marine environment.
IAEA, Technical Report Series Nº 247, Vienna 1985

Nuclear Energy Agency (1983). État des connaissances oceanographiques relatives au site d'immersion de déchets radioactifs de faible activité dans l'Atlantique Nord-Est, pg. 91
NEA/OECD

Nuclear Energy Agency (1985). Review of the continued suitability of the dumping site for radioactive waste in the North-East Atlantic, pg. 81
NEA/OECD

RADIATION PROTECTION PROGRAMME
Final Report

Contractor:

Commissariat à l'Energie
Atomique, CEA
CEN de Cadarache
B.P. n° 1
F-13115 Saint-Paul-lez-Durance

Contract no.: BI6-B-037-F

Head(s) of research team(s) [name(s) and address(es)]:

Dr A. Grauby
SERE-DERS
CEA-CEN de Cadarache
B.P. n° 1
F-13115 Saint-Paul-lez-Durance

Telephone number: 42/25.73.25

Title of the research contract:

Behaviour of radionuclides in marine, freshwater and terrestrial environments.

List of projects:

1. Behaviour of Neptunium in marine ecosystem
2. Exchange of radionuclides between sea and atmosphere
3. Radioecology of continental waters
4. Radium transfer in fresh water ecosystem
5. Cycling of tritium
6. Radiological impact of radionuclides accidentally released
7. Comparative study of soil to plant transfer of Np, Pu and Am
8. Radionuclides deposition on vegetation and soils

Title of the project no.: 1

BEHAVIOUR OF NEPTUNIUM IN MARINE ECOSYSTEM

Head(s) of project:

Dr. GRAUBY

Dr. GUEGUENIAT

Scientific staff:

P. GERMAIN, R. GANDON. Th. LEROY

I. Objectives of the project:

Les données relatives aux transferts du neptunium vers les sédiments et les organismes aquatiques sont très rares. Or quelques travaux montrent la présence de ^{237}Np dans l'environnement marin. Puis ^{237}Np sera l'un des constituants majeurs, à long terme, des déchets eventuellement stockés en mer. De plus, par certains aspects physicochimiques, Np s'écarte des autres transuraniens, ce qui implique à son sujet des études spécifiques. Aussi, il est nécessaire de développer la connaissance des transferts (physicochimie, définitions des voies de transfert, cinétiques de fixation et de perte, organotropisme, définition de bioindicateurs, détermination des FC et kd...) dans le milieu marin. Les études sont menées selon deux approches : l'une *in situ*, l'autre expérimentale.

II. Objectives for the reporting period:

III. Progress achieved:

1 - Distribution du neptunium 237 le long des côtes de la Manche

Dans le cadre du comportement du neptunium dans les écosystèmes marins, nous avons dosé, lors des années précédentes, ^{237}Np, par activation neutronique, chez des espèces prélevées dans le nord Cotentin, à Goury, près de l'émissaire de l'usine de la Hague (1) (2). Il est évidemment intéressant de connaître la distribution spatiale de cet élément le long des côtes de la Manche. Pour ce faire, nous nous sommes référés aux études précitées (1) et (2), lesquelles ont permis de dégager des espèces indicatrices : les algues rouges *Corallina officinalis*, *Chondrus crispus*, les mollusques *Patella sp.* et *Gibbula umbilicalis*. Du fait de la facilité de prélèvement et d'une présence abondante sur tout le littoral, le choix, pour étudier la distribution dans l'espace de ^{237}Np, s'est porté sur *Patella sp.* Les études précédentes ont indiqué des potentialités de fixation des chairs supérieures ou égales à celles des coquilles, aussi nous avons dosé ^{237}Np essentiellement dans les chairs.

Les échantillons ont été prélevés en mars 1987 dans les stations signalées sur la figure 1. Les mesures ont été effectuées en utilisant l'analyse par activation neutronique après traitement radiochimique. Les résultats sont présentés sur le tableau 1.

Les teneurs en ^{237}Np sont très faibles, ainsi dans les chairs les niveaux sont inférieurs à 2 mBq kg^{-1} frais, et légèrement plus faibles que ceux enregistrés dans les coquilles. Les chairs ne montrent donc pas une potentialité de fixation supérieure à celle de la coquille contrairement à ce qui fut observé précédemment en 1984 et 1986 (1) (2). Ces différences sont peut-être dues à l'échantillonnage, à des faits éthologiques liés à la nourriture, à la physiologie de l'espèce au temps de contact plus long entre eau de mer et coquille pour les individus prélevés en 1987.

Les niveaux les plus élevés sont enregistrés à la station la plus proche de l'émissaire, Goury (n° 4). Vers le sud, les niveaux décroissent surtout entre la station du Rozel (n° 3, 23 kms) et Carteret (n° 2, 35 kms). Vers l'est, les niveaux décroissent à partir de Goury, et nous remarquons qu'à une distance équivalente (23 à 40 kms) les teneurs vers l'est sont inférieures à celles observées au Rozel. Ces distributions sont conformes à celles d'émetteurs γ, ^{106}Ru-Rh et ^{60}Co chez les *Fucus*, et obéissent essentiellement aux caractéristiques hydrodynamiques complexes de cette région (3). Toutefois, par rapport aux émetteurs γ, le niveau du ^{237}Np est nettement inférieur au

Rozel par rapport à Goury. Des études complémentaires seront nécessaires pour vérifier et expliquer ces tendances.

Le neptonium 237 n'est plus décelé dans les chairs de patelles à 100 kms au sud du point de rejet de l'usine de la Hague, et à l'est, les niveaux sont très faibles dès la rade de Cherbourg (20 kms).

2 - Transferts du neptunium vers les crustacés et les poissons :

Nous avons défini une classification des groupes zoologiques correspondant à un ordre décroissant des possibilités de fixation du ^{237}Np (2) : algues rouges, spongiaires, tuniciers > annelides, mollusques herbivores > lichen, algues brunes, mollusques carnivores, crustacés > poissons.

Des résultats *in situ* du ^{237}Np chez les crustacés et les poissons, prélevés près de l'émissaire de l'usine de la Hague, sont consignés dans le tableau 2.

Chez les crustacés, la capacité de fixation du ^{237}Np étant en fait associé au contenu viscéral.

Quelques expériences ont été menées au laboratoire afin de compléter les données sur les transferts du ^{237}Np chez les crustacés et les poissons.

L'isotope ^{239}Np a été utilisé. Cet élément possède une période physique très courte (2, 35 jours), mais il est intéressant car il permet d'obtenir des informations sur l'organotropisme. Il a été préparé selon le protocole décrit dans (4).

- Tout d'abord des crustacés décapodes, des homards, ont été marqués par l'ingestion de moules (2 repas pris à 24 heures d'intervalle ; ^{239}Np était injecté dans les moules). Après 48 heures de jeûne, une dissection a permis de constater que 35% de l'activité, introduite se trouvaient dans l'hépatopancréas, et 17% dans l'estomac le reste étant rejeté dans les fécés.

Les résultats *in situ*, les expériences en laboratoire, quoique limitées, laissent supposer que le tractus digestif joue un rôle prépondérant dans la fixation du neptunium par les parties molles du homard, comme ceci fut montré pour ^{241}Am (5).

- Quant aux poissons, les transferts eau-animaux ont été étudiés à l'aide du bar, *Dicentrarchus labrax*, aisément obtenu à partir d'une écloserie, espèce bien connue sur le plan éthologique, et qui présente un grand intérêt alimentaire. Les bars ont été placés par 3 (individus de 10 g) dans des bacs avec 15 l d'eau de mer filtrée et marquée par ^{239}Np, l'eau étant renouvelée quotidiennement ; lors du changement les bars étaient nourris d'artémia non contaminés. Après 7 jours de

marquage, les bars on été disséqués. Les transferts sont très faibles, le marquage ne concernant pratiquement que les parties externes, traduisant ainsi une simple adsorption, les nageoires pelviennes étant les plus marquées (rapport activité g^{-1} animal/activité ml^{-1} eau de mer est de l'ordre de 3 pour les nageoires, 0,7 pour la peau, 0,4 pour les branchies.

3 - Comparaison du comportement du neptunium avec les autres éléments transuraniens :

Nous avons montré que le neptunium existait dans l'eau de mer principalement à l'état d'oxydation V, alors que l'américium est à l'état III et le plutonium présente plusieurs états : III, IV, V et VI, la forme V étant cependant prédominante dans l'eau de mer (4). On ne peut pas toutefois exclure pour Np l'existence de complexes anioniques ou neutres, et des formes particulaires (4).

Comme les autres actinides, le neptunium se fixe sur les sédiments. Cependant les valeurs des kd sont généralement plus faibles ($3 * 10^2$ à $7 * 10^3$) que celles du plutonium et de l'américium (de l'ordre de 10^4 - 10^6) (4). La fraction carbonatée des sédiments joue un rôle important dans le transfert du Np à partir de l'eau de mer.

En ce qui concerne la biodisponibilité des éléments transuraniens, des expériences ont indiqué des capacités de fixation du neptunium chez des espèces (annélides, mollusques) inférieures à celles du plutonium et de l'américium (1) (4). *In situ*, nous avons noté dans le Cotentin, à Goury, des teneurs en Np inférieures à celles du Pu et Am (1). Dans le tableau III, nous complétons ces données en dosant le neptunium et le plutonium dans des espèces (algues, annélides, mollusques) prélevés en 1986 à Goury. Les niveaux du ^{237}Np sont nettement inférieures à ceux des $^{239\text{-}240}Pu$ et ^{238}Pu. Ces résultats reflètent les différences dans les quantités rejetées mais aussi une biodisponibilité du Np plus faible que celle des isotopes du Pu. Les rapports $^{237}Np/^{239\_240}Pu$ sont compris entre $3{,}6.10^{-3}$ et 0,12 pour les espèces étudiées. Ils sont en général différents de ceux des retombées atmosphériques, $3{,}6.10^{-3}$ dans les retombées elles mêmes, $2{,}7.10^{-3}$ dans les lichens (6). Les rapports de ces radioéléments sont également différents de ceux dus à une autre usine de retraitement, Windscale, à la fin des années 1970, 3 à $4 * 10^{-4}$ dans des sédiments et des algues (6), et pour Pentreath et Harvey (7), rapport $^{239\text{-}240}Pu/^{237}Np$ compris entre 180 et 2000 chez des algues et des animaux, soit nettement supérieurs à ceux de Goury, < 100, à une exception près *Fucus serratus*. Ceci traduit des différences quantitatives dans les rejets des transuraniens entre les deux usines, pour les époques considérées.

BIBLIOGRAPHIE

1. P. Germain, P. Guéguéniat, S. May, G. Pinte. Measurement of Transuranic Elements, chiefly ^{237}Np (by neutron Activation Analysis), in the Physical and biological Compartments of the French Shore of the English Channel. J. Environ. Radioactivity, 5, (1987) 319-331.

2. P. Germain, G. Pinte. Neptunium 237 in the marine environment. Determination in animal and plant species in the english channel : biological indicators and trophic relationships. Jour of Radioanalytical and Nuclear Chemistry (en cours).

3. P. Germain, Y. Baron, M. Masson, D. Calmet. Répartition de deux traceurs radioactifs (^{106}Ru-Rh, ^{60}Co) chez deux espèces indicatrices (*Fucus serratus*, L., *Mytilus edulis*, L.) le long du littoral français de la Manche. Radionuclides : A tool for oceanography, P., Pentreath, R.J. Elsevier Applied Science Publishers, pp. 312-320. 1988.

4. P. Germain, R. Gandon, M. Masson, P. Guéguéniat. Experimental Sutdies of the Transfer of Neptunium from Sea Water to Sediments and Organisms (Annelids and Mollusc) J. Environ. Radioactivity 5 (1987) 37-55.

5. P. Miramand, P. Germain, J.P. Trilles. Histo-autoradiographic localisation of americium (^{241}Am) in tissues of European lobster *Homarus gammarus* and edible crab *Canoor pagurus* after uptake from labelled sea water. Mar Ecol. Prog. Ser. 52, pp. 217-225, 1989.

6. Holm, E. Release of ^{237}Np to the environment. Measurements of marine samples contaminated by different sources. In impacts of radionuclide releases into the marine environment, 155-160, Vienna, IAEA, 1981.

7. Pentreath, R.J., Harvey, B.R. The presence of ^{237}Np in the Irish Sea. Mar Ecol. Prog. Ser., 6, 243-247, 1981.

Echantillon Date et lieu de prélèvement	PS/PF	mBq Kg^{-1} frais
Granville (- 95 km) 26/03/1987		
- chair	0,19	< 0,39
- coquille	0,88	0,27 ± 0,04
Carteret (- 35 km) 25/3/1987		
- chair	0,14	0,14 ± 0,03
Le Rozel (- 23 km) 25/03/1987		
- chair	0,16	0,41 ± 0,08
Goury (+ 5 km) 24/03/1987		
- chair	0,17	1,33 ± 0,26
- coquille	0,94	5,38 ± 0,97
Rade de Cherbourg (28 km) 24/03/1987		
- chair	0,17	0,09 ± 0,02
Fermanville (40 km) 26/03/1987		
- chair	0,13	< 0,13
St Vaast la Hougue (70 km) 25/03/1987		
- chair	0,16	0,07 ± 0,01
- coquille	0,87	1,22 ± 0,24

Tableau I

Niveau du ^{237}Np dans Palella sp. le long des côtes de la Manche (erreur relative 2σ)

(km) distance entre la station et l'émissaire de l'usine de la Hague.

Echantillon Date et lieu de prélèvement	PS/PF	mBq Kg^{-1} frais
CRUSTACES DECAPODES		
Carcinus maenas (a) Goury - 30/01/1986		
- carapace	0,83	4,8 ± 0,9
- hépatopancréas	0,21	1,6 ± 0,3
- chair	0,16	0,2 ± 0,1
- branchies	0,08	0,6 ± 0,2
Cancer pagurus (a) Goury - 12/03/1986		
- carapace	0,73	1,1 ± 0,3
- hépatopancréas	0,22	0,8 ± 0,2
- chair	0,18	0,2 ± 0,1
- branchies	0,12	0,6 ± 0,1
POISSONS LITTORAUX		
Blennius pholis (a) Goury - 30/01/1986		
- chair	0,19	< 0,3
- peau	0,12	< 0,3
- branchies	0,17	< 1,3
- foie	0,06	< 0,2
- nageoires	0,15	< 0,4
- viscères	0,09	1,2 ± 0,2
- arêtes	0,20	< 1,6
Laburs bergylta Goury - 27/04/1986		
- chair	0,20	< 0,06

Tableau II

Niveaux du ^{237}Np dans des crustacés décapodes et des poissons littoraux prélevés à Goury (erreur relative 2σ)
(a) d'après [2]

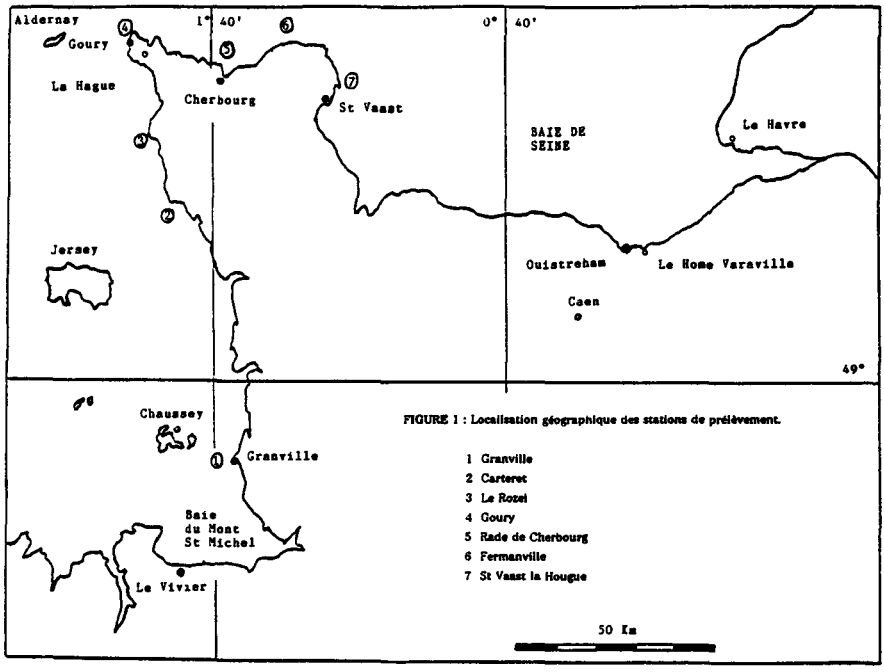

FIGURE 1 : Localisation géographique des stations de prélèvement.

1 Granville
2 Carteret
3 Le Rozel
4 Goury
5 Rade de Cherbourg
6 Fermanville
7 St Vaast la Hougue

Sample	dry/wet weight	$^{239+240}Pu$	^{238}Pu	^{237}Np	$^{237}Np/^{239+240}Pu$	$^{239+240}Pu/^{237}$
		mBq kg^{-1} wet weight				
Fucus serratus 27/01/86	0,14	278 ± 30	300 ± 30	1.0 ± 0.2	0.0036 ± 0.0008	278 ± 63
Corallina officinalis 27/01/86	0.38	529 ± 52	474 ± 48	64.3 ± 12.9	0.12 ± 0.03	8.2 ± 1.8
Porphyra umbilicalis 29/01/86	0.12	62.9 ± 7.4	22.2 ± 3.7	1.3 ± 0.3	0.02 ± 0.005	48.4 ± 12.5
Arenicola marina 5/02/86	0.15	89 ± 11	33 ± 7	5.9 ± 1.2	0.07 ± 0.02	15.1 ± 3.6
Patella vulgata - flesh 28/01/86	0.15	70 ± 7	52 ± 7	3.9 ± 0.8	0.06 ± 0.01	17.9 ± 4.1
Patella vulgata - shell 28/01/86	0.94	81 ± 15	67 ± 15	2.7 ± 0.5	0.03 ± 0.008	30.0 ± 7.9
					Fallout 0.0036 Lichen 0.0027 (E. Holm 1981) [6]	180 - 2000 algae and anim (Pentreath-Har 1981) [7]

Tableau III

Niveaux du ^{237}Np, du $^{239+240}Pu$ et du ^{238}Pu dans des échantillons marins prélevés à Goury près de la Hague (erreur relative 2σ).

Title of the project No 2 :
Echange de radionucleides entre la surface de la mer et l' aerosol atmospherique : etude experimentale des mecanismes de transfert

Head(s) of project and scientific staff :
C. Caput, D. Gauthier et Y. Belot
DERS / SERE, Centre d'Etudes Nucléaires, BP6, 92265 Fontenay aux Roses Cedex, France

1. Objectives of the project:
Etude en laboratoire des mécanismes par lesquels les radionucléides artificiels contenus dans la mer sont convertis en aérosols dans l'atmosphère. Les paramètre à étudier sont les caractéristiques du bullage, le rôle des particules en suspension dans l'eau de mer et le rôle de la matière organique.

III. Progress achieved:

1) Résultats acquis au cours des années précédentes

La production d'embruns à la surface de l'océan est une source significative d'éléments et de composés à l'état de trace dans l'atmosphère marine. Les embruns sont de minuscules gouttelettes qui résultent principalement de l'éclatement de bulles d'air à la surface de la mer (Blanchard 1983). La composition des gouttelettes d'embruns en constituants majeurs est généralement identique à celle de l'eau de mer, mais il apparaît de plus en plus évident que leur composition en constituants à l'état de trace est tout à fait différente. Il a été constaté en particulier que les embruns étaient beaucoup plus riches en transuraniens que l'eau de mer dont ils proviennent et nous avons pu reproduire cet enrichissement en laboratoire au moyen d'un dispositif de bullage (Belot et al. 1982). Ce dispositif a pu être utilisé pour comparer les enrichissements en américum, cobalt, zinc et manganèse radioactifs, toutes choses étant égales par ailleurs. Il nous est apparu que l'enrichissement augmentait avec l'affinité du radionucléides pour les particules solides contenues dans l'eau de mer. L'américium qui se trouve presqu'entièrement sous forme particulaire était le plus enrichi, alors que le cobalt presqu'entièrement soluble était le moins enrichi, les autres radionucléides occupant des positions intermédiaires en fonction de leur affinité pour les particules solides de l'eau de mer. Ce résultat nous suggère que l'enrichissement observé correspondrait en fait à un enrichissement en particules, et que tout élément ou substance lié aux particules de l'eau de mer se concentrerait dans les embruns.Cette hypothèse est renforcée par des expériences antérieures, effectuées en laboratoire, qui montrent qu'un certain nombre de substances particulaires à l'état de trace sont beaucoup plus abondantes dans les gouttelettes des embruns que dans l'eau de mer elle-même (Wallace and Duce 1978a,b, Hoffmann and Duce 1976, Blanchard et al 1981). Nous nous sommes donc engagé dans une étude sur l'accumulation dans les gouttelettes des embruns des particules naturellement présentes dans l'eau de mer, et sur les facteurs qui régissent cette accumulation.

2) Une méthode nouvelle d'étude de l'accumulation dans les embruns de particules initialement présentes dans l'eau de mer

Nous avons tout d'abord tenté de voir si la taille des particules et leur concentration dans l'eau pouvait jouer un rôle dans le processus d'accumulation que nous voulions étudier. Il n'était pas possible de travailler sur les particules qui se trouvent naturellement dans l'eau de mer, car elles sont difficiles à caractériser, et de plus, leur granularité, leur concentration et même leur nature peuvent varier d'un échantillon à l'autre, de sorte qu'il est très difficile de contrôler les conditions expérimentales.

Il importait alors de remplacer les particules naturelles par des particules synthétiques aussi proches que possible des particules naturelles, mais dont on puisse faire varier aisé-

ment la taille et la concentration. Il fallait préparer des échantillons d'eau de mer qui contiennent une quantité stable et connue de particules monodispersées. La principale difficulté était que des suspensions de particules monodispersées dans l'eau de mer produisent des agrégats de particules par le mécanisme de flocculation. La vitesse de flocculation est fortement augmentée par la force ionique de l'eau de mer, de sorte qu'il est généralement impossible d'éviter la formation d'agrégats et de maintenir en suspension un nombre stable de particules monodispersées pendant le temps nécessaire pour les expérimentations. La seule manière de pallier cette difficulté était d'utiliser des particules de polystyrène enduites de protéines qui résistent à la coagulation même dans des solutions dont la concentration en chlorure de sodium est comparable à celle de l'eau de mer (Van der Scheer et al 1978). Nous pensons que les particules ainsi enrobées peuvent être utilisées comme modèles des particules naturellement présentes dans l'eau de mer, car il a été montré que les particules naturelles étaient également enrobées de matière organique.

Les études expérimentales sur l'enrichissement des embruns en matière particulaire consistaient à faire éclater des bulles à la surface d'un échantillon d'eau de mer contenant des particules enrobées, à mesurer la concentration de ces particules dans les embruns et dans l'eau de mer dont les embruns étaient issus. Chaque échantillon d'eau de mer contenait de 1 à 10 mg de particules fluorescentes monodispersées (Fluoresbrite, Polysciences Inc.) qui avaient été préalablement enrobées de protéine par trempage des particules dans 15 ml d'une solution contenant 1,5 mg d'albumine de sérum bovin (BSA). L'échantillon d'eau de mer était placé dans le dispositif de bullage déjà utilisé et décrit par ailleurs (Belot et al 1982, Guichard et Lamauve 1988). Dans ce dispositif, un échantillon d'eau de mer de 1 L environ était placé dans une cuve dont le fond était constitué par une membrane poreuse hydrophobe en téflon de 25 cm de diamètre dont la dimension moyenne des pores était 10 µm, à travers laquelle on injectait de l'air à un débit de 0,3 L/min. Les embruns formés par éclatement des bulles à la surface de l'eau de mer étaient collectés sur filtre, puis mis en suspension dans de l'eau par agitation dans un bain à ultra-sons. Les particules de polystyrène et le sodium entraînés par les embruns étaient analysés respectivement par fluorimétrie et par potentiométrie au moyen d'une électrode spécifique. Le coefficient d'enrichissement était défini de manière classique comme le rapport de la concentration des particules dans l'eau des embruns, à la concentration des particules dans l'eau de mer.

3) Résultats des expériences d'enrichissement

Des mesures de granularité au moyen d'un granulomètre à rayon laser ont tout d'abord été effectuées sur des suspensions de particules enrobées de protéines préparées selon le protocole décrit plus haut. Ces mesures nous ont montré que l'on pouvait obtenir une suspension parfaitement stable de particules monodispersées dans de l'eau de mer, pour des

particules dans la gamme 0,1-6 µm et une concentration en particules de 1 à 10 mg/L. Ces suspensions ont été utilisées pour des expériences de bullage effectuées selon le protocole décrit précédemment. Les conditions de bullage étaient sensiblement identiques dans toutes les expériences et entraînaient la formation de bulles de 2 mm environ qui, arrivées en surface, grossissaient par coalescence et atteignaient une taille de 10 à 20 mm avant d'éclater.

La figure 1 donne le coefficient d'enrichissement en fonction du diamètre des particules pour des concentrationes massiques de ces particules égales à 10 mg/L et 1 mg/L, pour un volume d'échantillon de 1 L et opour une épaisseur d'eau de 5 cm. On voit sur ces figures que le coefficient d'enrichissement augmente lorsque la taille des particules et leur concentration dans l'eau de mer diminue. Le coefficient maximum obtenu est $2,5\ 10^3$ pour des particules de diamètre compris entre 0,1 et 1 µm et une concentration de 1 mg/L. Il n'est plus que $1,5\ 10^2$ pour des particules de 6,8 µm et une concentration de 10 mg/L. Dans quelques essais, les gouttellettes des embruns ont été séparées en classe granulométriques au moyen d'un impacteur d'Andersen. Il apparaît que l'enrichissement des gouttelettes d'embruns est le même quelle que soit la taille des gouttelettes.

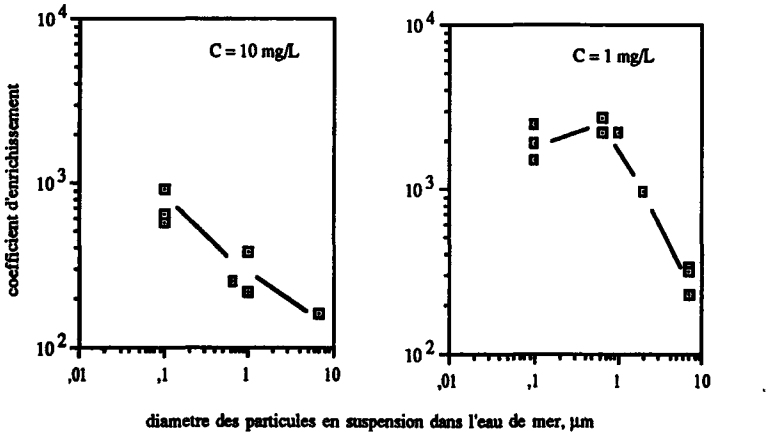

Fig. 1: Coefficient d'enrichissement des embruns en fonction du diamètre des particules en suspension pour deux concentrations de particules (10 mg/L et 1 mg/L)

4) Discussion et conclusions

Nous avons montré que des bulles de 10 à 20 mm produisaient en éclatant des gouttelettes (film drops) qui sont beaucoup plus riches en particules solides que l'eau de mer dont elles sont issues. Le rapport des concentrations peut atteindre 3 ordres de grandeur, pour des particules de diamètre compris entre 0,1 et 1 μm et pour des concentrations relativement faibles (1mg/L). Il peut être d'un ordre de grandeur plus faible pour des particules plus grosses et des concentrations plus élevées.

Des questions se posent sur la représentativité des bulles qui sont produites par le dispositif expérimental utilisé en laboratoire, ainsi que sur la représentativité des particules artificielles utilisées pour simuler les particules naturelles de l'eau de mer. Les bulles observées dans le dispositif expérimental à la surface de l'eau de mer sont des bulles de taille relativement grande qui résultent de l'accrétion de bulles plus petites. Elles ne sont représentatives que d'une partie des bulles produites à la surface de la mer. De telles bulles produisent des microgouttelettes appelées "film drops" par éclatement du film mince d'eau qui les recouvre. Ces gouttelettes diffèrent de gouttelettes appelées "jet drops" qui sont produites par éclatement de bulles plus petites. On ne sait pas encore de façon certaine si les microgouttelettes des embruns naturels proviennent principalement des "film drops" ou des "jet drops", mais néanmoins on pense que les "film drops" pourraient jouer un rôle essentiel (Blanchard 1983).

Les particules artificielles que nous avons utilisées comme modèles sont des particules de polystyrène portant des groupement carboxyle et enduites d'albumine. Ces particules représentent vraisemblablement assez bien les particules naturelles de l'eau de mer qui sont elles aussi enduites de matière organique (Hunter 1977), mais des études complémentaires seraient nécessaires pour s'assurer de la similitude et voir comment elle peut varier avec la protéine utilisée.

Les études de base que nous avons engagées sur l'entraînement des particules de l'eau de mer par les bulles et la concentration de ces particules dans les microgouttelettes qui résultent de l'éclatement des bulles dans l'atmosphère, se sont révélées plus difficiles que prévues. Parmi les sources de difficulté, nous avons rencontré au départ la quasi impossibilité d'avoir des échantillons d'eau de mer reproductibles et bien caractérisés. Nous avons alors essayé de remplacer les particules naturelles de l'eau de mer par des particules artificielles, et nous avons du adopter des particules enduites de protéine pour éviter le phénomène de coagulation des particules. La méthode retenue semble intéressante et pourrait servir de base pour des études plus approfondies. Compte tenu du temps passé à résoudre les difficultés fondamentales d'une telle expérimentation, nous n'avons pas pu aller aussi loin que souhaité dans l'étude des processus. Néanmoins nous avons pu établir qu'il était

possible d'observer un enrichissement important en particules de microgouttelettes produites par éclatement de bulles de 10 à 20 mm de diamètre. Le coefficient d'enrichissement peut dans certianes conditions atteindre de valeurs de 2000 à 3000, qui correspondent assez bien avec les facteurs d'enrichissement observés par ailleurs pour des substances à l'état de trace qui sont dans l'eau de mer sous forme particulaire.

5) References

Belot Y., Caput C. and Gauthier D. (1982) "Transfer of americium from sea water to atmosphere by bubble bursting" *Atmospheric Environment* **16**, 1463-1466.

Blanchard D.C.(1983) " The production, distribution and bacterial enrichment of the sea-salt aerosol" in *Air-sea Exchange of Gases and Particles* (P.S. Liss and W.G.N. Slinn eds.) Boston : Reidel, 407-454.

Blanchard D.C., Syzdek L. D. and Weber M.E. (1981) " Bubble scavenging of bacteria in freshwater quickly produces bacterial enrichment in airborne drops" *Limnol. Oceanogr.* **26**, 961-964.

Guichard J.C. and Lamauve M. (1988) "The laboratory production of the bubbling fraction of the marine aerosol - Application to polluted seawater" *Atmospheric Environment* **22**, 1835-1838.

Hoffman E.J. and Duce R.A. (1976) "Factors influencing the organic carbon content of marine aerosols : a laboratory study" *J. geophys; Res.* **81**, 3667-3670.

Hunter K.A. (1977) "Chemistry of the sea surface microlayer" Ph. D. Thesis University of East Anglia.

Van der Scheer A., Tanke M.A. and Smolders C. A. (1978) " Influence of adsorbed proproteins on the stability of polystyrene latex particles" *Faraday Discuss. Chem. Soc.* **65**, 264-287.

Wallace G.T., Jr. and Duce R.A. (1978a) "Transport of particulate organic matter by bubles in marine waters" *Limnol. Oceanogr.* **23**, 1155-1167.

Wallace G.T., Jr. and Duce R.A. (1978b) " Open-ocean transport of particulate trace metals by bubbles" *Deep-Sea Res.* **25**, 827-835.

V. Publications:

C. Caput, D. Gauthier and Y. Belot (1990) "On factors affecting the transport of particulate trace constituents from ocean to atmosphere" (en cours)

Title of the project no.:3 RADIOECOLOGY OF CONTINENTAL WATERS

(Etude comparée des eaux continentales du bassin de la Meuse et du bassin du Rhône)

Head(s) of project: FOULQUIER L. , GRAUBY A.

Scientific staff: LAMBRECHTS A. , BAUDIN J.P. , CHARMASSON S.
CALMET D. , GONTIER G. , NUCHO R. , REMILLET J.N.
DIMEGLIO Y.

I. Objectives of the project:

- Etudier la radioécologie du bassin Rhôdanien et de son débouché en Méditerranée par des prélèvements réguliers d'eau, de sédiments, de végétaux aquatiques et de poissons.

- Evaluer l'impact des installations nucléaires.

- Etudier les mécanismes de transfert du ^{60}Co dans un écosystème expérimental d'eau douce simplifié. Modéliser ces transferts afin de pouvoir interpréter les résultats obtenus *in situ*.

II. Objectives for the reporting period:

- Effectuer des campagnes de prélèvements sur le Rhône et en bord de mer afin d'établir un bilan comparatif de l'impact de Tchernobyl et de celui des installations nucléaires.

- Les modalités du transfert du ^{60}Co ont été étudiées dans un écosystème expérimental comportant de l'eau, du sédiment, une algue planctonique (*Scenedesmus obliquus*), un mollusque gastéropode (*Lymnaea stagnalis*), un crustacé benthique (*Gammarus pulex*), des larves limicoles d'insectes (*Chironomus sp.*) et un poisson omnivore (*Cyprinus carpio*).

III. Progress achieved:

ETUDE DE BASSIN RHODANIEN.

Sur 300 km de cours, le Rhône est équipé de 6 sites nucléaires regroupant 17 réacteurs de puissance, une usine d'enrichissement du combustible (Pierrelatte) et une usine de retraitement du combustible irradié (Marcoule). Ces différentes installations rejettent, après contrôle, des effluents liquides dont la radioactivité s'ajoute à celle, encore visible, des retombées des essais nucléaires atmosphériques (1956-1963) ou, à partir de 1986, à celle de l'accident de Tchernobyl.

L'étude radioécologique du fleuve permet d'apprécier l'impact de ces différents termes sources.

La radioactivité naturelle présente dans tous les compartiments du fleuve est due principalement au ^{40}K, aux 14 éléments en équilibre de la famille de l'uranium et aux 10 éléments de la famille du thorium, auxquels s'ajoutent parfois le ^{7}Be et le ^{210}Pb. La radioactivité naturelle totale est stable sur l'ensemble du fleuve :

- 1 $Bq.l^{-1}$ dans l'eau,
- 2300 $Bq.kg^{-1}$ sec dans le sédiment,
- 1780 $Bq.kg^{-1}$ sec dans les macrophytes immergées,
- 2270 $Bq.kg^{-1}$ sec dans les bryophytes immergées,
- 110 $Bq.kg^{-1}$ frais dans les poissons.

La radioactivité artificielle est due à l'impact de différentes sources de contamination :

- Impact des retombées atmosphériques : dans la zone allant du lac Léman à Creys-Malville, soumise aux seules retombées des essais atmosphériques, le ^{137}Cs est visible dans tous les compartiments du milieu avec environ 10 $Bq.kg^{-1}$ sec dans les sédiments, 6 $Bq.kg^{-1}$ sec dans les végétaux aquatiques et 0,4 $Bq.kg^{-1}$ frais dans les poissons. Le ^{90}Sr est mesuré dans les poissons (1,5 $Bq.kg^{-1}$ frais).

- Impact des effluents des centrales nucléaires : les analyses radioactives des échantillons prélevés dans la zone allant de Creys à Marcoule, mettent en évidence la présence d'une douzaine de radionucléides (Tableau 1). Les végétaux confirment leur qualité de radioindicateurs. Bien que d'un niveau plus faible, la radioactivité des poissons reflète la composition des effluents des centrales.
La radioactivité artificielle -hors tritium- des compartiments de cette zone du Rhône reste de 10 à 50 fois inférieure à leur radioactivité naturelle.

- Impact des effluents de l'usine de retraitement du combustible irradié de Marcoule : dans la zone du Rhône soumise aux effluents de l'usine de retraitement du combustible irradié de nouveaux radionucléides apparaissent et ceux qui existaient en amont de l'usine augmentent de façon significative (tableau 2). Après 30 années de fonctionnement de l'usine, la radioactivité artificielle des compartiments du fleuve, mesurée en aval de Marcoule reste inférieure ou de l'ordre de grandeur de la radioactivité naturelle.

- Impact de l'accident de Tchernobyl (26 avril 1986). Sept radionucléides ont été mis en évidence, de façon significative dans le Rhône : ^{132}Te, ^{131}I, ^{103},^{106}Ru, ^{134}, ^{137}Cs et ^{110m}Ag. Globalement le niveau de la radioactivité, de l'eau, du sédiment, des végétaux et des poissons du fleuve a augmenté rapidement. Les nucléides à période courte (^{132}Te et ^{131}I) ont disparu dès la mi-mai. Pour les autres, le processus a été lent.

C'est dans le haut-Rhône que l'impact de Tchernobyl a été le plus important et le plus visible du fait de l'absence d'installation nucléaire (tableau 3). La radioactivité artificielle mesurée en mai 1986 est de l'ordre de grandeur de celle que l'on mesurait antérieurement en aval de Marcoule.

Les végétaux aquatiques sont bien les meilleurs indicateurs de la contamination radioactive du milieu. La radioactivité des poissons est faible et n'a aucune incidence, d'un point de vue sanitaire, sur les populations riveraines qui les consomment. Dans les zones équipées d'installations nucléaires, on observe une augmentation des concentrations en radiocésium, la présence plus fréquente du ^{110m}Ag et du ^{106}Ru et l'apparition du ^{103}Ru. La radioactivité provenant de Tchernobyl est venue se cumuler avec celle des effluents rejetés par les installations.

Après mai 1986 on constate la décroissance de la radioactivité dans tous les compartimentes du fleuve. La vitesse d'élimination dépend d'une part de la période physique des radionucléides et d'autre part de la nature des compartiments (la période biologique des organismes) et des zones du fleuve. Le ruthénium 103 disparait en quelques semaines, le ruthénium 106 reste visible plusieurs mois dans les végétaux. A la fin de 1988 seuls des césiums 134 et 137 sont encore présents. Les périodes effectives mesurées dans les poissons prélevés dans le haut-Rhône sont de 230 jours pour le ^{134}Cs et 260 jours pour le ^{137}Cs.

ETUDES EN MEDITERRANEE.

Un réseau de 22 stations réparties entre St Cyprien et l'embouchure du Var a été échantillonné durant les années 1986, 1987 et 1988. Une phanérogames, *Posidonia oceanica*, des algues (*Ulva sp., Cystoseira sp., Codium sp., Corallina sp., Lithophyllum sp.,*), des mollusques (*Mytilus sp., Tapes decussatus* et *Ostrea edulis*) et un échinoderme (*Holothuria sp.*) ont été prélevés. Sept stations de ce réseau, situées de part et d'autre de l'embouchure rhodanienne ont été sélectionnées pour un suivi mensuel du bio-indicateur , *Mytilus sp.* Deux autres indicateurs, *Ulva sp.*, à Carteau et à Tamaris (Toulon) ainsi que *Tapes decussatus* à Carteau ont été régulièrement prélevés. Une base de données a été constituée à partir de 1988.

Les nombreuses mesures réalisées sur le littoral méditérranéen de part et d'autres de l'embouchure du Rhône, avant et après l'accident de Tchernobyl ont montré que la plupart des bio-indicateurs (phaéophycées, mollusques), répondent rapidement à l'introduction de radionucléides dans le milieu marin. Leur étude permet une bonne évaluation des zones soumises à ces apports, et ce aussi bien en situation accidentelle (Tchernobyl) qu'en situation normale (rejets contrôlés d'origine industrielle) (tableau 4, 5 et 6). Si seuls les ^{106}Ru et ^{137}Cs sont présents continuellement sur les stations proches de l'embouchure, d'autres radionucléides (^{103}Ru, ^{110m}Ag, ^{129m}Te, etc...) sont apparus, lors de l'accident de Tchernobyl, sur l'ensemble du bassin nord-occidental. Deux zones ont plus particulièrement été concernées :

- la région Est du littoral méditérranéen, exempte auparavant de rejets d'origine industrielle et sur laquelle les retombées ont été les plus importantes.

- l'Ouest de l'embouchure du Rhône, soumis habituellement aux situations de rejets contrôlés des installations industrielles situées sur le fleuve et qui a été, en outre, soumis aux radionucléides provenant de Tchernobyl par apports directs et par lessivage du bassin versant du fleuve.

La mesure des radionucléides sur le littoral méditérranéen français nord-occidental a permis de préciser l'impact du Rhône sur les stations du golfe du Lion.

Hors situation accidentelle, et pour des niveaux très faibles, il a été possible de correler les variations saisonnières de radioactivité dans un bio-indicateur, *Mytilus sp.*, aux fluctuations des principaux paramètres hydrobiologiques. En effet, l'apparition d'un bloom planctonique au printemps conduit à une augmentation des teneurs en ^{106}Ru et en ^{137}Cs dans la chair du mollusque.

L'extraction du tritium dans la matière organique de différents échantillons nous a permis d'établir des premières mesures de cet élément sur la zone prodeltaïque rhodanienne et le Golfe de Fos. Ces mesures, avec celles des émetteurs gamma, ont montré que des filtreurs comme *Mytilus sp.*, favorisent les transferts de radioactivité vers le fond par l'intermédiaire des phénomènes de biodéposition. Ainsi les biodépots prélevés dans le golfe de Fos contiennent 10000 fois plus de ^{137}Cs et 500 fois plus de tritium que les eaux prélevées dans la même zone. Les populations de bivalves filtreurs retiennent donc une partie du flux particulaire riche en plancton, pour produire de la biomasse concentrée issue des premiers maillons de la chaîne trophique.

L'intervention des organismes filtreurs dans les transferts de matières dans la colonne d'eau et les phénomènes de bioturbation au niveau du sédiment déterminent des mécanismes de redistribution de radioactivité dans le milieu marin qui peuvent être importants et sont actuellement mal déterminés. Les expérimentations utilisant des traceurs radioactifs et l'étude des milieux à haute productivité biologique, comme la zone de production mytilicole de Carteau, sont à même de nous procurer, dans l'avenir, des outils très performants pour mieux comprendre et mieux prévoir le devenir des radionucléides dans le milieu marin.

ETUDES EXPERIMENTALES.

Les différents transferts du ^{60}Co étudiés sont représentés dans la figure 1, qui comporte également les valeurs les plus significatives des facteurs de concentration (FC), des facteurs de transfert (FT) et des périodes biologiques (Tb). A côté de ces données, quelques constatations et conclusions peuvent être succintement dégager des nombreuses expériences réalisées.

La fixation de ^{60}Co par *Scenedesmus obliquus* a été étudiée dans diverses situations expérimentales afin d'évaluer l'influence de plusieurs paramètres tels que l'âge des cultures, l'état physiologique des cellules, le temps de contact, la concentration du milieu en cobalt stable et la périodicité de l'apport du radionucléide. Le facteur de concentration du ^{60}Co est étroitement lié à ces paramètres et la valeur maximale obtenue est de 4.10^4 en fonction du poids sec. La fixation du ^{60}Co par les algues est due essentiellement à des phénomènes passifs. Elle résulte initialement d'une adsorption du radionucléide sur les membranes, puis d'une diffusion intracellulaire. L'élimination du ^{60}Co par des algues contaminées, placées dans du milieu inactif, se présente comme un processus exponentiel biphasique traduisant l'existence de deux périodes biologiques du radioélément. La première ($0,6<Tb_1<6h$) correspond à la désorption du ^{60}Co adsorbé et la seconde ($30<Tb_2<116h$) à la perte de la fraction absorbée. De 80 à 90 % du radionucléide fixé sont éliminés, pourcentages qui mettent en évidence le caractère labile de la liaison entre le ^{60}Co et les cellules.

En ce qui concerne les gammares (Crustacé amphipode) et les larves de chironome (Diptère), l'ensemble des transferts étudiés démontre la prédominance du phytoplancton par rapport à l'eau et au sédiment dans la

bioaccumulation du ^{60}Co. Mais les facteurs de transfert restent très faibles, si bien que, même à long terme, il ne peut se produire de bioamplification du radionucléide lors de son transfert entre les algues et ces deux organismes. Cette impossibilité est encore renforcée par le fait que les gammares et les larves de chironomes éliminent très rapidement le ^{60}Co accumulé, quelle que soit la voie d'absorption. Cette rapide décontamination traduit une très faible assimilation du radionucléide ingéré avec les cellules algales.

Contrairement à ce qui est généralement observé pour les phénomènes biologiques, le facteur de concentration du ^{60}Co par *Cyprinus carpio* est très peu influencé par le facteur thermique. Ainsi, sa valeur maximale passe de 3,5 à 6 pour des températures variant de 8 à 25°C. L'étude comparative de l'accumulation du ^{60}Co en fonction du vecteur de la contamination, démontre que la contribution de la voie directe représente environ 75% dans la contamination de la carpe et qu'il y a addition du radionucléide accumulé par les voies directe et trophique.

En ce qui concerne l'absorption par la voie digestive, il faut souligner que le type de nourriture contaminée ingérée influe nettement sur la quantité de ^{60}Co accumulée. Par exemple, le facteur de rétention est 5 fois plus élevé lorsque le radionucléide est absorbé avec des gammares que lorsqu'il est absorbé avec des tissus mous de limnées (Mollusque gastéropode). L'élimination du ^{60}Co accumulé est également lié à ce paramètre ce qui se traduit par un taux de rétention proportionnel au facteur de transfert. La voie d'absorption préalable du radionucléide influe aussi très nettement sur la décontamination de la carpe. Ainsi, la période biologique longue (Tb2) du radiocobalt est de 35 ou 87 jours selon que l'accumulation soit due à un transfert trophique ou direct.

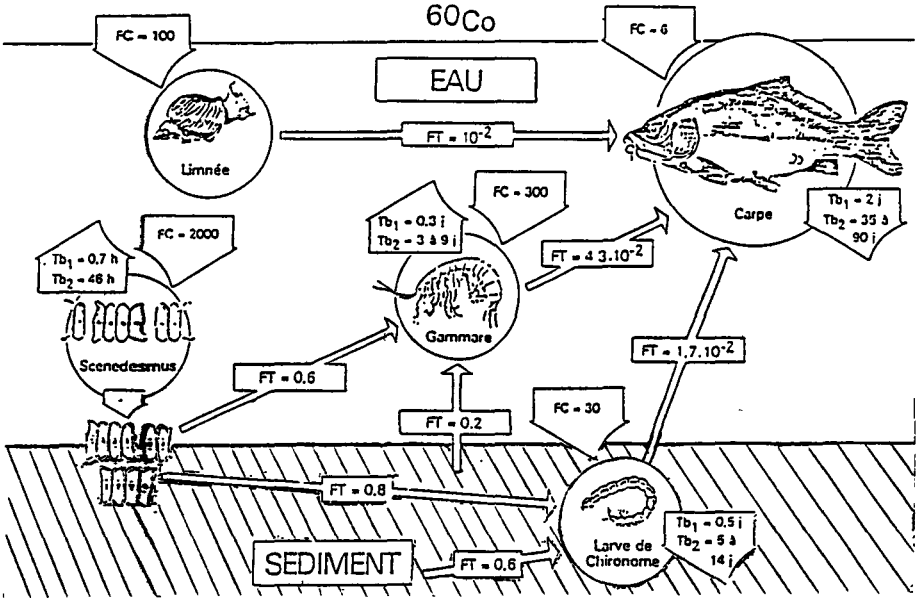

Fig. 1 - Représentation schématique de l'écosystème expérimental utilisé pour l'étude des transferts du ^{60}Co en eau douce et évaluation des principaux paramètres radioécologiques.

Tableau 1. Radioactivité artificielle des divers compartiments du Rhône de Creys à Marcoule.

Nucléides	eau Bq/l	sédiments Bq/kg sec	phanérogrames immergées Bq/kg sec	bryophytes Bq/kg sec	poissons Bq/kg sec
Ag 110m		3,0 ± 1,8 (6)	3,5 (1)		0,1 à 0,8 (4)
Co 57			8,5 ± 19,5 (6)		0,1 à 0,4 (2)
Co 58	LD à 0,004 (2)	5,4 ± 4,0 (5)	165 ± 207 (24)	48 à 296 (2)	16 ± 15 (35)
Co 60	LD à 0,007 (2)	4,1 ± 2,9 (13)	35,7 ± 41,9 (23)	16 à 22 (2)	2,3 ± 1,9 (57)
Cs 134		1,6 ± 1,0 (5)	1,7 (1)	8,8 (1)	0,4 ± 0,1 (78)
Cs 137	LD à 0,008 (2)	15,2 ± 6,9 (16)	5,1 ± 2,0 (25)	12 à 24 (2)	1,1 ± 1 (326)
Mn 54			42 ± 49 (14)	10 à 15 (2)	2 ± 2 (19)
Ru+Rh 106		95 (1)	71 (1)		1 à 8 (3)
Zn 65					0,4 à 20 (13)
Zr 95			10 à 62 (3)		0,1 à 1 (3)
Sr 90	LD à 0,04 (2)		5,4 ± 5,3 (4)		1,6 ± 0,5 (45)
H 3		5960 ± 3400 (11)	85 ± 76 (4)		20 à 1320 (12)

Tableau 2. Radioactivité artificielle des divers compartiments du Rhône en aval de Marcoule.

Nucléides	eau Bq/l	sédiments Bq/kg sec	phanérogrames immergées Bq/kg sec	poissons Bq/kg sec
Ag 110m		7,2 ± 2,3 (14)	5,3 ± 2,9 (9)	0,28 (1)
Am 214	LD (7)	14,9 1 3,7 (11)	5,1 ± 3,0 (5)	0,1 (1)
Ce+Pr 144	0,5 ± 1 (12)	139 ± 28 (16)	77 ± 19 (23)	0,3 à 5,7 (4)
Co 57	LD (4)	1 (2)	0,3 à 14 (6)	
Co 58	0,01 ± 0,003 (43)	5,7 ± 1,5 (8)	139 ± 86 (27)	0,06 à 0,35 (2)
Co 60	0,01 ± 0,003 (39)	6,8 ± 1,6 (17)	51 ± 32	1,9 ± 3,4 (18)
Cs 134	0,01 ± 0,003 (63)	58 ± 16 (19)	47 ± 17 (29)	2,3 ± 0,4 (97)
Cs 137	0,03 ± 0,006 (100)	403 ± 114 (20)	245 ± 18 (31)	11,5 1 2,2 (136)
Mn 54	0,01 ± 0,003 (43)	34 ± 12 (15)	204 ± 85 (31)	1,9 ± 2,1 (21)
Ru 103	LD (7)			0,15 à 4,8 (2)
Ru+Rh 106	0,45 ± 0,09 (100)	368 ± 100 (18)	765 ± 211 (30)	1,5 à 26 (6)
Sb 125	0,05 ± 0,02 (86)	13,2 ± 6,1 (12)	13,8 ± 7,6 (16)	
%				4,5 (1)
Zr 95		7 (1)	4,2 à 59 (3)	
Sr 90	0,04 ± 0,007 (11)		7,6 ± 1,2 (11)	1,5 ± 0,3 (55)
H 3	19,3 ± 2,8 (20)	12,3 ± 6,1 (4)	126 ± 47 (8)	148 ± 24 (21)
Pu 238		LD (1)	0,9 ± 0,5 (7)	LD à 0,03 (4)
Pu 239+240		0,7 (1)	2,4 ± 1,4 (10)	0,05 ± 0,04 (11)

Tableau 3. Radioactivité artificielle des divers compartiments du Haut-Rhône en mai 1986.

Nucléides	sédiments Bq/kg sec	phanérogrames immergées Bq/kg sec	poissons Bq/kg sec	
Cs 134	122 (1)	192 (1)	4,2 ± 1,6 (14)	2,3 ± 0,4 (97)
Cs 137	240 (1)	389 (1)	8,8 ± 1,6 (14)	11,5 ± 2,2 (136)
Ru 103	160 (1)	594 (1)	2,1 ± 1,4 (6)	0,15 ± 4,8 (2)
Ru+Rh 106	120 (1)	385 (1)		1,5 à 26 (6)

Dans ces tableaux les valeurs moyennes sont suivies de leurs écarts statistiques calculés, pour une probabilité de 95% par la formule t.s/√n où t est la variable de Stundent, s est l'écart-type population et n est le nombre de mesures (indiqué entre parenthèses).

Tableau 4. Teneurs moyennes de la chair de moule et Longueur Totale (LT) des coquilles.
x ± s X (NM = Non Mesuré) *1 litre d'eau de combustion

STATIONS	LT mm	^{40}K Bq/kg sec	^{137}Cs Bq/kg sec	^{106}Ru Bq/kg sec	Nb Ech	Période	Tritium Bq/l *1 12 éch. (1986)
Port Camargue	54,4 ± 7,5	217 ± 35	1,6 ± 1,3	37,1 ± 28,0	16	26/04/86-22/09/87	NM
Stes Maries	49,3 ± 5,8	229 ± 46	4,5 ± 4,7	101,8 ± 47,4	20	16/12/86-20/09/87	NM
Faraman	44,2 ± 5,6	215 ± 59	8,8 ± 13,9	158,1 ± 79,0	27	16/12/86-23/03/88	79,3 ± 70
Carteau	59,1 ± 6,5	235 ± 42	1,3 ± 1,1	32,3 ± 25,6	22	21/01/86-17/11/87	28,9 ± 37
Fos	52,6 ± 6,5	212 ± 33	2,5 ± 4,0	46,8 ± 39,3	19	06/02/86-16/11/87	NM
Ponteau	47,3 ± 5,8	207 ± 39	1,5 ± 1,7	45,3 ± 33,4	23	16/12/85-17/11/87	52,0 ± 50

Tableau 5 Mesure des émetteurs gamma dans Mytilus sp. (novembre 1986).
Valeurs d'encadrement = erreurs de comptage (± 10).

Mytilus sp. Bq/kg sec	^{40}K	^{137}Cs	^{106}Ru	^{103}Ru	^{110m}Ag	^{134}Cs	Date
Port Camargue	210 ± 40	<0,8	12 ± 3	<2	<1	<1	11/11/86
Stes Maries	270 ± 51	2 ± 1	72 ± 9	<2	1 ± 0,3	<1	11/11/86
Faraman	240 ± 50	1,6 ± 0,8	130 ± 30	4 ± 1	<2	1 ± 0,3	10/11/86
Port-St-Louis	220 ± 60	1,7 ± 0,9	38 ± 8	<2	<1	<1	10/11/86
Carteau	205 ± 60	0,6 ± 0,3	15 ± 3	<3	<1	<1	10/11/86
Fos	210 ± 50	1,1 ± 0,8	24 ± 6	<3	<2	<1	10/11/86
Ponteau	230 ± 150	1,6 ± 0,8	27 ± 5	<3	<2	<1	09/11/86
Tamaris	210 ± 50	<0,5	13 ± 4	<1	<1	<1	24/11/86
St Raphaël	220 ± 20	0,8 ± 0,5	25 ± 8	<3	2,8 ± 0,9	<1	08/11/86
Antibes	230 ± 50	1,6 ± 0,9	62 ± 9	13 ± 2	1,7 ± 0,5	1,2 ± 0,3	07/11/86
Cannes	210 ± 60	1,2 ± 0,9	31 ± 8	8 ± 2	1,6 ± 0,5	<2	07/11/86
St Laurent	220 ± 44	0,8 ± 0,5	25 ± 8	<3	2,8 ± 0,9	<1	06/11/86

Tableau 6 Radioéléments artificiels mesurés sur différents végétaux marins à la station de Villefranche.
Valeurs d'encadrement = erreurs de comptage (± 10) (01.06.1986).

Bq/kg sec	^{103}Ru	^{106}Ru	^{110m}Ag	^{134}Cs	^{137}Cs	^{144}Ce	^{141}Ce	^{131}I
CHLOROPHYCEAE Codium dichotoma	440 ± 20	180 ± 20	22 ± 3	10 ± 1	19 ± 3	42 ± 4	31 ± 3	1150 ± 130
PHAEOPHYCEAE Cystoseira stricta	970 ± 50	410 ± 50	36 ± 4	7 ± 1	16 ± 3	26 ± 3	11 ± 2	380 ± 70
Dictyopteris membranacea	1100 ± 300	430 ± 20	89 ± 7	18 ± 2	39 ± 7	85 ± 8	65 ± 6	720 ± 150
RHODOPHYCEAE Sphaeroccocus coronopifolius	700 ± 50	330 ± 30	27 ± 4	7 ± 1	12 ± 4	55 ± 8	55 ± 7	26000 ± 500
PHANEROGAMES Posidonia oceanica	600 ± 30	270 ± 20	57 ± 7	7 ± 1	16 ± 4	130 ± 15	100 ± 10	690 ± 120

IV. Other research group(s) collaborating actively on this project [name(s) and address(es)]:

- CEN-SCK-Mol (Dr. R. Kirchman)
- Université catholique de Louvain (Drs. S. Mittenaere & L. Sombré)
- Département de botanique de l'université de Liège. (Dr. Bourdon-Meurisse)
- Département de modélisation mathématique de l'université de Liège (Dr. Smitz).
- Discussion avec le LNETI au Portugal (Dr. Bettancourt & Vaz-Carreiro).

V. Publications:

ETUDE DU BASSIN RHODANIEN.

FOULQUIER L. , DESCAMPS B. & BAUDIN-JAULENT Y. (1985). Mesure et interprétation des teneurs en radionucléides des poissons du Haut-Rhône français. *Verh. Internat. Verein. Limnol. 22 : 2470-2475.*

FOULQUIER L. & PALLY M. (1984). Données radioécologiques sur les sédiments du Bas-Rhône. *Revue française des Sciences de l'eau, 3 : 259-277.*

FOULQUIER L. , LAMBRECHTS A. & PALLY M. (1986). Qualitative and quantitative evaluation of long half-life radionuclides in the sediments, plants and fish of the Rhône river. *Seminar on the cycling of long-lived radionuclides in the biosphere : observation and models. Madrid, 15-19 september 1986* : 40 p.

LAMBRECHTS A. & FOULQUIER L. (1987). Radioecology of the Rhône basin : Data on the fish of the Rhône (1974-1984). *J. Environ. Radioactivity,* 5 : 105-121.

FOULQUIER L. , LAMBRECHTS A. & PALLY M. (1987). Impact radioécologique d'une usine de retraitement de combustibles nucléaires sur un fleuve, le Rhône. *Proceed. of an Intern. Conf. on nuclear fuel reprocessing and waste management. Recod 87. Paris, 23-27 août 1987* : 1063-1070.

LAMBRECHTS A. , FOULQUIER L. & PALLY M. (1988). Etude comparée de l'impact radioécologique des installations nucléaires et de l'accident de Tchernobyl sur le fleuve Rhône. *IVème Symposium international de radioécologie de Cadarache. Impact des accidents d'origine nucléaire sur l'environnement. 14-18 mars 1988* : C39-C50.

FOULQUIER L. , GRAUBY A. , LAMBRECHTS A. & PALLY M. (1988). Le concept de retour d'expérience en radioécologie, application au cas d'un fleuve à forte implantation nucléaire : le Rhône. *Proceed. of 7th Intern. Congress of the IRPA. Sydney, 10-17 april 1988. Vol II* : 633-636.

FOULQUIER L. , DESCAMPS B. , LAMBRECHTS A. & PALLY M. (1989). Analyse et évolution de l'impact de l'accident de Tchernobyl sur le fleuve Rhône. *24th congress of the international Association of Theoretical and applied limnology. August 13-19 1989. Munich FRG.* (sous presse)

LAMBRECHTS A. , FOULQUIER L. & PALLY M. (1989). Méthodes d'évaluation de l'impact radioécologique de l'accident de Tchernobyl sur le fleuve Rhône. *Colloque international sur la contamination de l'environnement à la suite d'un accident nucléaire majeur. AIEA-SM-306, Vienne, Autriche, 16-20 octobre 1989.* (en cours de publication).

ETUDES EN MEDITERRANEE.

D. CALMET, S. CHARMASSON, G. GONTIER, M.L. DABURON. (1988). "The impact of Chernobyl fallout on *Mytilus sp.* collected from the french coast. IV symposium international de radioécologie, Cadarache, 14-18 mars 1988.

G. GONTIER, M. SACHER, C. GRENZ, D. CALMET. (1989). "Mussel watch" dans la zone littorale marine rhodanienne et influence du filtre biologique sur les échanges de radioactivité entre les constituants du milieu marin. Congrés de limnologie et d'océanographie. Marseille, 26-29 juin 1989.

D. CALMET, S. CHARMASSON, G. GONTIER, A. MEISNEZ, C.F. BOUDOURESQUE, (soumis, Journal Environmental Radioactivity). "Spatio-temporal variations of radionuclides in the Mediterranean seagrass *Posidonia oceanica* after Chernobyl radioactive fallout.

G. GONTIER, M. SACHER, C. GRENZ, D. CALMET, (soumis, Hydrobiologia), "Role of *Mytilus sp.* in radionuclide transfer between the water colum and sediments."

ETUDES EN LABORATOIRE.

FRITSCH A.F. (1985). Etude expérimentale de l'accumulation et de l'élimination du cobalt 60 par *Cyprinus carpio* L. Evaluation de la contribution respective des voies directe et trophique dans la radiocontamination ; influence du facteur thermique. *Thèse de Docteur Ingénieur, Université Aix-Marseille II- Rapport CEA-R-5326* : 114 p.

NUCHO R. & BAUDIN J.P. (1986). Données expérimentales sur la rétention du ^{60}Co par une algue planctonique, *Scenedesmus obliquus*. Influence de la température et de la photopériode. Sciences de l'eau, 5 (4) : 361-376.

BAUDIN J.P. & FRITSCH A.F. (1987). Retention of ingested ^{60}Co by a freshwater fish. *Water, Air, and Soil Pollution,* 36 : 207-217.

BAUDIN J.P. , RAMBAUD A. , FOULQUIER L. & BAUDIN J.P. (1988). Bioaccumulation du ^{60}Co par une algue planctonique, *Scenedesmus obliquus* Türps. (kütz). Influence du stage de développement de la culture sur la fixation du radionucléide. *Acta Oecologica ; Oecologia Applicata,* 9 (2) : 111-125.

BAUDIN J.P. & FRITSCH A.F. (1988). Influence de la température sur l'accumulation par la voie directe du ^{60}Co chez un poisson dulçaquicole. *Revue des Sciences de l'eau,* 1 (4) : 387-402.

BAUDIN J.P. & FRITSCH A.F. (1989). Relative contribution of food and water in the accumulation of ^{60}Co by a freshwater fish. Water Research, 23 (7) : 817-823.

NUCHO R. (1989). Modalités de la fixation et de la désorption du ^{60}Co par *Scenedesmus obliquus* et transfert du radioélément vers deux organismes benthiques. *Thèse de Doctorat en Sciences Biologiques de l'Université de Montpellier I- Rapport CEA-R-5496* : 309 p.

NUCHO R. & BAUDIN J.P. (1989). Accumulation du ^{60}Co par *Scenedesmus obliquus*. Modalités et contribution relative de l'absorption et de l'adsorption du radionucléide. *Rapport C.E.A.-R-5485* : 26 p.

NUCHO R. & BAUDIN J.P. ^{60}Co retention by a freshwater planktonic alga, *Scenedesmus obliquus*. *Environmental Pollution*, 62 : 265-279.

BAUDIN J.P. , FRITSCH A.F. & GEORGES J. Influence of labelled food type on the accumulation and retention of ^{60}Co by a freshwater fish, *Cyprinus carpio*. *Water, air, and Soil Pollution* (in progress).

Title of the project no.4 B 16 - B - 137 F

Behaviour of radionuclides in marine, freshwater and terrestrial environments.
Modalités de transfert du radium dans un écosystème aquatique d'eau douce. Etudes expérimentales en laboratoire contrôlé et études de terrain dans l'environnement d'un site minier.

Head(s) of project:

GRAUBY, A. et FOULQUIER, L.

Scientific staff:

DESCAMPS, B., BRUNO, V., BAUDIN-JAULENT, Y. REMILLET, JN.

I. Objectives of the project:

Ce projet vise à définir les risques radiologiques encourus par les populations de la Communauté Européenne du fait de l'extraction et du traitement du minerai d'uranium. Le programme est limité aux aspects liés à la radioécologie des eaux continentales. Le ^{226}Ra est le radionucléide étudié en priorité, expérimentalement, mais pour les études de terrain on s'intéresse aussi aux autres éléments de la famille de ^{238}U et en particulier au ^{210}Pb.

II. Objectives for the reporting period:

Durant ce contrat deux aspects ont été abordés :
- une étude expérimentale du site du Forez, un site minier en arrêt d'exploitation ;
- une étude expérimentale visant à modéliser le transfert du ^{226}Ra dans un écosystème aquatique simplifié intégrant l'eau, le sédiment et différents maillons biologiques aboutissant à un poisson carnassier, la truite.

Les échanges à étudier, qu'ils soient directs (à partir de l'eau et du sédiment) ou trophiques (entre deux maillons successifs) sont représentés dans la figure ci-contre.

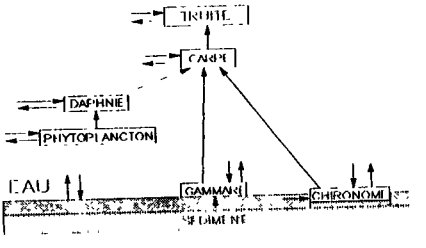

III. Progress achieved:

III.1 METHODOLOGIE

A. Le site minier du Forez

L'étude de radioécologie de ce site, en arrêt d'exploitation depuis 1980, s'est portée essentiellement sur le lac de 20 ha recouvrant le stockage des 20 millions de m^3 de résidus d'exploitation. Nous avons déterminé, en particulier pour le ^{226}Ra, les facteurs de concentration (FC) "globaux" pour les différentes espèces de poissons présentes et les FC "directs" obtenus grâce à la réalisation d'une expérience "cages flottantes". Ce FC "direct" ne prend en compte que les échanges eau-branchies des poissons alors que le FC "global" intégre aussi la vie trophique, c'est à dire les différents maillons de la chaîne alimentaire aboutissant aux poissons.

B. Le programme de recherches expérimentales

Dans le but d'expliquer les différences observées entre les deux types de FC il est nécessaire de réaliser toute une série d'expériences de laboratoire mettant en jeu les différents maillons intermédiaires entre le milieu physique et le poisson. Pour le ^{226}Ra ces expériences nécessitent un laboratoire approprié, spécialement construit à cet effet ; en effet le gaz radon (^{222}Rn), descendant du ^{226}Ra, implique un local en dépression par rapport à l'extérieur et des boites à gant, elles-mêmes en dépression par rapport au local. Le programme de recherches a été présenté en page précédente.

Il est à noter que le comptage du ^{226}Ra présente le désavantage d'imposer un temps de mise en équilibre radioactif de 15 jours ; ceci retarde notablement la vitesse de réalisation des expériences elles-mêmes.

III.2 RESULTATS

A. Le site minier du Forez

Les résultats sur ce lac, concerné par des résidus miniers solides, font suite à ceux obtenus pendant 5 ans sur l'environnement aquatique immédiat du site minier de Lodéve (1)(2) ; l'étude de ce site ayant débuté dès sa mise en exploitation en 1981. Deux résultats importants se dégagent de la comparaison de ces deux études radioécologiques in situ.

- Les FC "globaux" obtenus pour les poissons dans le lac du Forez sont supérieurs à ceux obtenus dans la rivière concernée (la Lergue) par le complexe minier de Lodève. Dans le premier cas ils varient de 160 à 1 200 selon l'espèce et dans le deuxième cas de 50 à 150. En espace clos il y aurait donc des différences de régimes alimentaires suffisamment importantes pour modifier sensiblement le FC "global" pour ce ^{226}Ra.

- Les FC "globaux" sont toujours supérieurs aux FC "directs", qu'ils soient obtenus en laboratoire (3) ou in situ , comme au Forez lors de l'expérience "cages flottantes". En effet, ces derniers ne dépassent pas la valeur de 10.

Un autre résultat peut être également mis en exergue : si les muscles des poissons représentent 40-50 % en masse ils représentent moins de 10 % en activité.

B. Le programme de recherches expérimentales

Les échanges vers la carpe

Pour la contamination de la carpe par voie directe (eau → branchies) le FC obtenu en fonction du temps atteint une valeur de 5 après 60 jours. L'exploitation mathématique des résultats (courbe ci-dessous) prévoit un FC de 6,7 après un an d'expérience. (4)

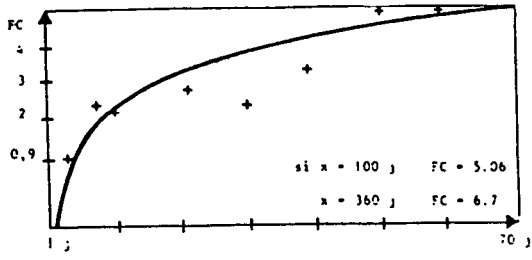

Courbe logarithmique

$Y = -0,72 + 1,2 \log X$

$R = 0,84$

Pour la contamination par voie trophique (ingestion de gammares préalablement contaminés) on a calculé aprés 3, 7, 10, 20 et 30 repas l'évolution du Facteur de Transfert (FT), définit comme le rapport entre la concentration de l'organisme prédateur et la concentration de l'organisme proie (en $Bq.kg^{-1}$ frais). Ce FT passe de 11 10^{-3} après 3 repas à 3 10^{-3} après 30 repas. Ce résultat laisse à penser qu'il ne peut pas y avoir bioamplification par cette seule voie de contamination.

La décontamination, réalisée après une contamination par voie directe, par l'analyse du facteur de rétention, aboutit à la formule suivante :

$$Y = (21\ e^{-0,137\ t}) + (79\ e^{-10^{-3}\ t})$$

d'où l'on tire Tb1 = 5 jours (période biologique courte)
Tb2 = 700 jours (période biologique longue)

On retiendra qu'après 10 jours de décontamination il reste encore 80 % du radium et que celui-ci s'éliminera avec une période de 700 jours.

L'étude de la répartition tissulaire confirme ce qui a été dit en III.2.A et indique aussi que le squelette n'est pas, contrairement à l'idée très répandue, un organe particulier de fixation du radium.

L'échange eau-algue (Scenedesmus obliquus)

L'influence du niveau de contamination de l'eau a été étudiée en testant 360, 3 600 et 36 000 $Bq.l^{-1}$. L'allure des courbes pour le Facteur de concentration (exprimé en fonction du poids sec) et les valeurs absolues sont comparables (figure page suivante). La valeur à retenir est un FC voisin de 10 000 à l'équilibre. (5)

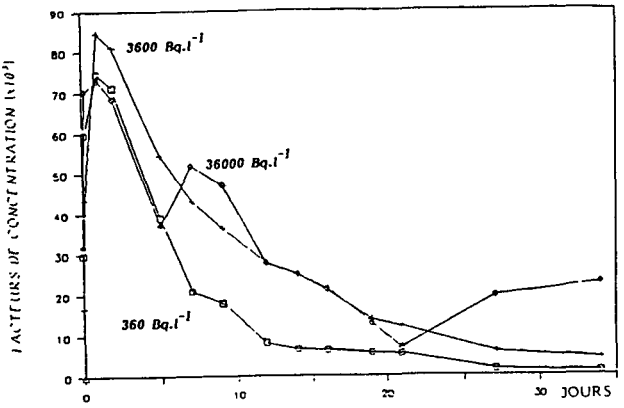

Evolution du facteur de concentration des algues, en fonction du poids sec, pour 3 concentrations en radium du milieu.

Facteur de concentration de l'algue Scenedesmus obliquus : pour 3 niveaux de concentration de l'eau en ^{226}Ra.
(Facteur de concentration exprimé en fonction du poids sec)

Pour tester des stades de développement différents de la culture on a fait varier le moment de la contamination :

- contamination au démarrage de la culture Co
- contamination durant la phase exponentielle rapide C5
- contamination durant la phase exponentielle lente C12
- contamination en phase stationnaire C24

Deux types de courbes apparaissent pour ce qui concerne l'évolution du FC en fonction du temps (figure ci-dessous).Pour les cultures CO et C5 la configuration est du même type que la figure présentée précédemment ; pour les cultures C12 et C25 il n'y a pas de phase exponentielle rapide mais seulement une lente montée, aboutissant d'ailleurs au bout de 16 jours à la même valeur (autour de 15 000).

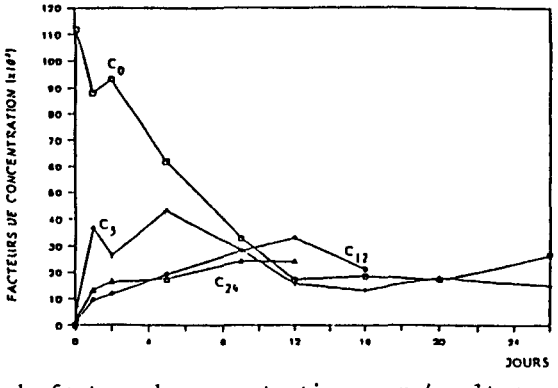

Evolution du facteur de concentration pour 4 cultures contaminées à différents stades de leur développement.

L'échange eau - daphnie

L'évolution du FC en fonction du temps pour le transfert eau-daphnie est de type exponentiel ; l'analyse des données aboutit à l'équation (en tenant compte du poids frais) :

$$Y = 55,7\ (1 - e^{-0,3t}) + 12,38\ (1 - e^{-8,24\ t})$$

La valeur d'équilibre (68) étant obtenu après 10 jours de contamination. Les résultats par le transfert algue-daphnie sont en cours d'exploitation.

L'échange eau - gammare

On obtient pour cet échange les paramètres suivants (poids frais) :

$$Y = 123,65\ (1 - e^{-0,257t}) + 7,1\ (1 - e^{-1,65t})$$

FC d'équilibre = 130
Temps d'équilibre = 29 jours

La décontamination de ces gammares aboutit à déterminer les deux périodes biologiques : 0,17 jour et 47 jours.

L'échange sédiment - gammare

La formule obtenue (poids frais) est :

$$Y = 1,5\ (1 - e^{-0,16t}) + 0,275\ (1 - e^{-0,47t})$$

L'échange eau - chironome (larve d'insecte vivant dans le sédiment)

Les paramètres suivants sont à retenir :

$$Y = 6\ (1 - e^{-0,8t}) + 15,7\ (1 - e^{-1,6t})$$

FC d'équilibre = 21
Temps d'équilibre = 4 jours

Les transferts sédiment-chironome et chironome-carpe sont réalisés et les résultats analytiques en cours de traitement.

Pour le dernier maillon, la truite, les trois ultimes expériences sont en cours de réalisation : il s'agit :

- de la contamination par voie directe (eau ➡ branchie)
- de la décontamination
- du transfert trophique carpe - truite.

III.3 INTERET GENERAL

L'ensemble de ces recherches expérimentales fera l'objet, en juin 1990, d'une thèse de Doctorat en Génie Civil ; elle sera intitulée : "Essai de modélisation du transfert du ^{226}Ra dans un écosystème simplifié d'eau douce". Elle devrait contribuer à expliquer les différences de niveaux de concentration, et de facteurs de concentration, constatées in situ en fonction du lieu (lac, au Forez ; rivière, pour le site de Lodève).

IV. Other research group(s) collaborating actively on this project [name(s) and address(es)]:

- Section de Radioécologie Physique du SERE par l'intermédiaire de ses deux entités métrologie : le LMEI à Orsay et l'antenne de Cadarache (M. PICAT).
- Service de Protection et d'Instrumentation Nucléaire du DPT à Fontenay-aux-Roses (M. ZETTWOOG).

V. Publications:

(1) B. DESCAMPS et Y. BAUDIN-JAULENT ; 1986. Tranfer of radium 226 to fish in the aquatic environment of a french mining complex : assessment of radiation dose to man. Seminar on the cycling of long-lived radionuclides in the biosphere -Observations and models. Madrid 15-19 Septembre 1986.

(2) B. DESCAMPS et Y. BAUDIN-JAULENT ; 1987. Etude radioécologique du complexe minier de Lodève (France) 1981-1985. Rapport CEA, R-5409, 98 pages.

(3) C. OTDJIAN ; 1987. Etude expérimentale de l'accumulation et de l'élimination du radium 226 par Cyprinus carpio (L). DEA Chimie de l'Environnement et Santé, présenté devant l'Université de Provence Aix-Marseille I en septembre 1987. 82 pages.

(4) C. MICHEL ; 1988. Le radium 226. Etude bibliographique sur l'incidence radioécologique aquatique. Etude expérimentale sur la contamination des carpes par une eau de lixiviation chargée en radium. Thèse Vétérinaire. Toulouse (juillet 1988).

(5) V. BRUNO, J-Y. GAL et B. DESCAMPS ; 1989. Etude de la fixation du ^{226}Ra par une algue phytoplanctonique, Scenedesmus obliquus. Elément d'explication du rôle primordial de la chaîne alimentaire dans la contamination des poissons. Radioprotection, 24, 2 : 99-108.

Title of project no 5 :
Transfert aux plantes du tritium contenu dans l'hydrogene, le methane et autres molecules tritiées

Head(s) of project and scientific staff:
Y. Belot, C. Caput et H Camus
DERS / SERE, Centre d'Etudes Nucléaires,
BP6, 92265 Fontenay aux Roses Cedex, France

1. Objectives of the project:
Le but du travail est d'étudier la dynamique de captation et de rétention par les plantes de l'hydrogène tritié, du méthane tritié et des molécules tritiées les plus importantes qui peuvent en dériver, en relation avec les paramètres climatiques et physiologiques et la composition de l'atmosphère. Le travail comporte des expériences de laboratoire et de terrain ainsi que des tentatives de modélisation.

III. Progress achieved:

1) Etude en chambre expérimentale de l'absorption de l'hydrogène tritié par la partie aérienne des végétaux

Des expériences réalisées dans plusieurs laboratoires ont montré que l'absorption de l'hydrogène tritié par les feuilles des plantes, si elle existe, est très faible. Dans le présent travail, nous avons repris des expériences pour essayer de mesurer tout effet d'oxydation ou d'incorporation, même minime, qui pourrait se produire lorsque de l'hydrogène tritié arrive au contact des feuilles des plantes. Pour cela, nous avons effectué des essais d'exposition de la partie aérienne des végétaux, en évitant toute interférence du sol, et en utilisant de l'hydrogène qui avait été préalablement purifié et contenait seulement des traces infimes d'eau tritiée.

Les essais ont été réalisés sur des plants de tournesol (*Helianthus annua L.*) âgés de 3 semaines environ et placés dans une chambre permettant d'isoler la partie aérienne du végétal et d'éviter toute contamination du sol. La chambre était balayée par un flux d'air d'humidité relative comprise entre 90 et 95 pourcent, de concentration en hydrogène tritié égale à $1,81 \times 10^6$ Bq / m^3 et de concentration en eau tritiée résiduelle égale à 3,17 Bq / m^3. Le rapport de la concentration d'eau tritiée à celle d'hydrogène tritié était ainsi de $1,75 \times 10^{-6}$. La durée de chaque exposition était de 3 heures environ.

Nous avons observé sur une dizaine d'expériences que la concentration en eau tritiée de l'air de balayage n'était pas modifiée par la présence de la plante. Par ailleurs, la concentration du tritium dans l'eau des feuilles était égale à 70-80 pourcent de la concentration résiduelle de tritium dans la vapeur d'eau de la chambre. Cette concentration était celle que l'on peut observer lorsque des feuilles sont exposées uniquement à de la vapeur d'eau tritiée. Ceci prouve qu'il n'y a pas d'oxydation mesurable de l'hydrogène tritié au niveau des feuilles. Par ailleurs, la matière organique des feuilles ne contenait pas de tritium en quantité mesurable, en dépit de la concentration relativement élevée de l'hydrogène tritié dans la chambre d'exposition. Ce dernier résultat indique que l'incorporation directe de l'hydrogène tritié dans la matière organique du végétal est certainement très faible, voire même inexistante.

2) Etude sur le terrain de l'absorption de l'hydrogène tritié par le sol et du transfert du tritium entre les sol et la végétation

Si l'hydrogène tritié ne peut pas être oxydé et absorbé au niveau de la partie aérienne des végétaux, en revanche il a été montré que l'hydrogène tritié pouvait être oxydé au niveau du sol et que l'eau tritiée formée pouvait être ensuite transférée aux plantes enracinées dans le sol. Nous avons réalisé des expériences de terrain au cours desquelles des petites

portions de sol en place, éventuellement couvertes de végétation, étaient exposées de manière contrôlée à des concentrations connues d'hydrogène tritié. Au cours de ces expériences, le sol et la végétation étaient exposés à de l'hydrogène tritié pendant 15 minutes, en utilisant une chambre à fond ouvert posée sur le sol. La vitesse de dépôt était calculée à partir de la vitesse de décroissance de la concentration du tritium à l'intérieur de la chambre. Lorsque l'hydrogène tritié contenu dans la chambre était complètement déposé, la chambre était alors balayée à un débit suffisamment élevé pour simuler de façon appropriée les conditions qui existent normalement entre la surface du sol et l'atmosphère libre. La concentration d'eau tritiée dans l'air de balayage était mesurée, toutes les heures le premier jour, puis chaque jour pendant deux semaines.

En utilisant cette méthode, nous avons effectué deux expériences comparatives sur sol nu et sur le même sol couvert d'herbe. Nous avons obtenu pour la vitesse de dépôt de l'hydrogène tritié sur le sol une valeur de 0,036 cm/s dans le cas d'un sol nu et de 0,023 cm/s dans le cas d'un sol couvert d'herbe. Ces valeurs ne sont pas très différentes des valeurs que nous avons obtenues par ailleurs sur prairie permanente à Mol (0,009 et 0,017 cm/s), et sur du blé en herbe à Cadarache (0,031 et 0,054 cm/s). La présence de végétaux ne semble pas jouer un rôle déterminant dans l'oxydation de l'hydrogène tritié à la surface du sol. La concentration du tritium dans l'eau des feuilles des plantes est liée à la concentration du tritium dans l'eau des couches superficielles du sol. Le transfert du tritium aux tissus végétaux se fait exclusivement par oxydation de l'hydrogène tritié à la surface du sol et par transport à l'intérieur de la plante de l'eau tritiée ainsi produite.

Le taux de réemission, défini comme la fraction du tritium reémise dans l'atmosphère par unité de temps, varie en particulier avec la couverture du sol. Pour le sol nu, le taux de réémission mesuré dans les expériences ci-dessus était initialement de 4 pourcent par heure, une heure plus tard il tombait à moins de 1 pourcent par heure, puis diminuait par la suite de plus en plus lentement au fur et à mesure de l'écoulement du temps. Dans le cas du sol couvert d'herbe, la valeur initiale était de 0,8 pourcent par heure, puis décroissait ensuite exponentiellement avec une demi-vie de 2,5 jours environ. Ces taux de réémission obtenus expérimentalement ont été comparés à ceux que l'on a pu obtenir par modélisation théorique du phénomène de transport du tritium dans le système sol-atmosphère. Le modèle est composé d'un système d'équations différentielles linéaires qui décrit la diffusoion de HTO à l'intérieur du sol, et son échange avec la vapeur d'eau non marquée de l'atmosphère. Le modèle donne des résultats en bon accord avec les résultats expérimentaux.

3) Etude en chambre expérimentale de l'absorption du méthane tritié par la partie aérienne des végétaux

Des expériences antérieures semblaient indiquer que l'incorporation du méthane tritié dans la matière organique de plantes était relativement importante. Pour vérifier et préciser ces résultats nous avons effectué des expériences en laboratoire pour étudier l'incorporation du méthane dans la partie aérienne des végétaux.

Les essais ont été effectués sur des plants individuels de tournesol âgés de quelques semaines et pacés dans une chambre à circulation permettant d'exposer la partie aérienne du végétal sans exposer le sol dans lequel la plante était enracinée. La chambre était balayée par un flux d'air d'humidité relative 90 à 95 pourcent, et de concentration en méthane tritié $2{,}2 \times 10^7$ Bq/m^3. Le méthane tritié utilisé était purifié par passage à travers une colonne de tamis moléculaire. Après 3 heures d'exposition, on mesurait le tritium dans l'eau libre des feuilles et l'eau de combustion de leur matière organique. Une dizaine d'expériences ont été effectuées portant chacune sur une plante individuelle. La vitesse de dépôt sur les feuilles a toujours été inférieure à 10^{-6} cm/s, valeurs beaucoup plus faible que ne le laissaient présager les expériences antérieures.

4) Etude en chambre expérimentale de l'absorption du formaldéhyde par la partie aérienne des végétaux

A l'occasion de travaux antérieurs, nous avions pu observer que l'activité spécifique de l'eau de combustion de la matière organique des plantes était fréquemment beaucoup plus élevée que l'activité spécifique de leur eau libre. Cette observation nous a conduit à penser que le cycle du tritium était imparfaitement connu, et que les plantes pouvaient assimiler à partir de l'atmosphère des molécules tritiées autres que l'eau tritiée. Parmi les molécules candidates se trouvaient en bonne place l'hydrogène tritié et le méthane tritié qui sont à l'état de traces dans l'atmosphère, mais ont des activités spécifiques beaucoup plus élevées que la vapeur d'eau. Or, comme nous l'avons vu plus haut, nous n'avons pu mettre en évidence aucune assimilation appréciable de l'hydrogène ou du méthane tritiés. Restaient quelques autres molécules simples qui pouvaient être formées par conversion de l'hydrogène tritié ou du méthane tritié au contact de l'air, telles que le formaldéhyde, l'acide formique ou le méthanol. De ces trois molécules le formaldéhyde était la plus abondante dans l'atmosphère. Compte tenu de sa solubilité dans l'eau et de sa réactivité, cette molécule pouvait être un des maillons manquants dans le cycle du tritium et particulièrement dans le transfert du tritium entre l'atmosphère et la matière organique des végétaux.

Des essais préliminaires d'incorporation du formaldéhyde dans les plantes furent lancés en 1987, en utilisant pour des raisons de disponibilité, du formaldéhyde marqué au ^{14}C, étant donné que le tritium lié à l'atome de carbone suit, au moins dans un premier temps, le même chemin que lui. Des essais ont été effectués sur des plants de tournesol, dont la partie aérienne a été exposée pendant 3 heures, à un flux d'air contenant 10^5 Bq/m^3 de formaldéhyde marqué, correspondant à une concentration de formaldéhyde d'environ 2 microgramme par m^3 d'air. La vitesse de d'incorporation du formaldéhyde dans la matière organique des feuilles a été déterminée sur 5 plants individuels. Elle était de 0,2 cm/s pour des plantes ayant leurs stomates pleinement ouverts et diminuait proportionnellement à la conductance stomatique, ce qui prouve que les stomates sont la voie d'entrée du formaldéhyde gazeux dans les plantes.

Au cours de l'année 1988, nous avons cherché à connaître les mécanismes par lesquels le formaldéhyde se fixait sur la matière organique des végétaux. Ce travail a été réalisé en collaboration avec un laboratoire de chimie biologique de l'Institut National de la Recherche Agronomique. Les expériences réalisées ont consisté à marquer des plants de tournesol par du ^{14}C-formaldéhyde puis a déterminer par des méthodes classiques de biochimie les composés dans lesquels le ^{14}C était incorporé. Le marquage des plantes a été réalisé en exposant leur partie aérienne à un flux d'air contenant 10^5 Bq/m^3 de formaldéhyde radioactif et 2 μg/m^3 d'entraîneur stable pendant une durée de 3 heures. Après un laps de temps variable les feuilles exposées ont ensuite été coupées, fixées dans l'azote liquide et lyophilisées avant d'être analysées. L'extraction des petites molécules marquées a été réalisée en utilisant utilisant de l'éthanol à 50 % selon le protocole de Schürman (1969). Cet extrait a été soumis à une séparation bidimensionnelle qui consiste en une électrophorèse sur couche mince suivie d'une double chromatographie.La détection des produits marqués a été faite par autoradiographie. Les composés marqués ont été récupérés par grattage de la couche mince puis tansférés dans des fioles de comptage pour détermination quantitative de leur radioactivité.

La répartition de la radioactivité entre l'extrait alcoolique et le résidu d'extraction varie suivant les échantillons. La fraction extractible constituée de petites molécules est en moyenne de 44 %, alors que la fraction résiduelle constituée majoritairement de protéines membranaires est de 56 %. Les cartes métaboliques obtenues sur les extraits alcooliques par séparation bidimensionnelle révèlent 4 groupes de taches radioactives.Un premier groupe de faible importance (1-2 %) correspond aux substances qui n'ont pas migré. Un deuxième groupe (2-10 %) correspond à une substance qui migre exclusivement par chromatographie et qui a été identifiée comme du formaldéhyde libre. Un troisième goupe (6-8 %) est vraisemblement constitué par du glycolate et du glycérate marqués. Le quatrième groupe le plus important (80-90 %) a été identifié comme étant formés par des produits d'addition du formaldéhyde et des acides aminés c'est-à-dire les produits de la forme CH_2= N

- R - COOH. Nous avons montré que ces composés d'addition pouvaient être révélés chimiquement par le réactif habituel des acides aminés, que leur comportement en chromatographie était le même que celui de acides aminés, mais que leur comportement en électrophorèse était différent (moindre migration).

Le formaldéhyde capté par les plantes après une exposition de quelques heures et un temps d'attente de 24 heures au maximum, se trouve fixé sur des composés solubles (principalement des acides aminés) ou sur des composés insolubles (probablement des protéines membranaires). La présence d'une petite proportion d'acides organiques marqués, glycolate et glycérate, semble indiquer un début de métabolisation. Pour vérifier cette hypothèse il conviendrait de réaliser des expériences plus longues.

5) Détermination du formaldéhyde tritié dans les effluents des installations nucléaires et dans l'atmosphère

Comme le formaldéhyde tritié est très soluble dans l'eau, on le recueille dans une solution aqueuse contenant un peu de formaldéhyde stable qui sert d'entraîneur. Cette solution est ensuite filtrée soigneusement pour éliminer toute particule radioactive qui aurait pu être collectée en même temps que les composés gazeux. Le formaldéhyde stable et le formaldéhyde tritié échantillonné sont précipités par la dimethylcyclohexane dione, appelée encore dimedon, qui forme avec le formaldéhyde un dérivé dimérique constitué de deux unités de dimédon liées par un pont méthylène. Ce dérivé dimérique précipite de manière optimale en milieu légèrement acide. Le solide cristallin obtenu est séparé par filtration puis brûlé sous un courant d'oxygène. Le contenu en tritium de l'eau de combustion et par conséquent de l'échantillon est déterminé par comptage en scintillation liquide.

Des essais préliminaires ont été réalisés en 1989 pour qualifier la procédure de séparation du formaldéhyde tritié. Des essais à blanc ont d'abord été effectués sur des solutions deau tritiée ne contenant pas de formaldéhyde tritié, ils ont montré que la quantité de tritium échangeable entraînée par le précipité, dans les conditions opératoires utilisées, était extrêmement faible et représentait moins de 0,001 pourcent de l'activité contenue dans la solution où le précipité avait été formé. Par ailleurs, il a été montré qu'il n'y avait pas d'échange possible entre le formaldéhyde stable de la solution absorbante et l'hydrogène tritié qui passe à travers cette solution au moment du prélèvement. La méthode mise au point a été utilisée pour déterminer le rapport du formaldéhyde tritié à l'eau tritiée dans les effluents gazeux d'une installation affectée au tritium. Nous avons trouvé des rapports compris entre 0,1 et 2 pourcent environ pour 27 échantillons répartis de manière aléatoire sur une période de deux mois environ.

Il est maintenant prévu d'effectuer la détermination du formaldéhyde tritié dans la chemi-

née d'autres installations, et aussi dans des boites à gants affectées à diverses opérations, de manière à identifier les processus qui pourraient être responsables de la production de cette molécule tritiée. Des études sont à poursuivre sur le transfert du formaldéhyde tritié aux végétaux et aux animaux, et son incidence radiologique sur les personnes exposées.

V. Publications:

Y. Belot, C. Caput, D. Gauthier, J. Guenot : "Distribution of organically bound tritium in plant samples exposed to fallout only", *Workshop Environmental and Human Risks of Tritium* , Karlsrühe, 17-19 Février 1986.

Y. Belot (1986) : "Tritium in plants, a review", *Workshop on the environmental and human risks of tritium* , Karlsrühe, 17-19 Février 1986.

Y. Belot, H. Clerc, J. Guenot, H. Djerassi and W. Gulden : "Assessment of the environmental impact of a tritium gas release", *Fusion Workshop* , Culham, Novembre 1986.

W. Gulden, J. Guenot, H. Clerc and H. Djerassi : "Experimental determination of the kinetic conversion rate of gaseous tritium into HTO", *Seminar on Fusion Technology,* Avignon , Octobre 1986.

J. Guenot, C. Caput, Y. Belot and H. Djerassi: "Oxydation of tritiated hydrogen at soil surface, experimentation and modeling", *Seminar on the cycle of long-lived radionuclides in the biosphere: observations and models* , Madrid, 15-19 September 1986.

Y. Belot, J. Guenot and C. Caput: "Emission to atmosphere of tritiated water formed at soil surface by oxidation of HT", 3d Topical meeting, Tritium Technology in fission, fusion and isotopic applications, Toronto, 1-6 Mai 1988. and *Fusion Technology* 1988, **14**,1231-1234.

Ph. Paillard, JP Calando, H. Clerc, R. Gros and Y. Belot: "Tritium release experiment in France: Results concerning HT / HTO conversion in the air and soil" *Fusion technology* 1988, **14**, 1226-1230.

Girard F., Jolivet P. et Belot Y. "Fixation et assimilation de ^{14}C-formaldéhyde gazeux par des feuilles de tournesol" *C.R. Acad. Sci. Paris* t.309, série III, 447-452, 1989

Belot Y. and Zettwoog P. "Tritium environmental risk in future fusion reactors" *Seminar on Safety, Environmental Impact and Economic Prospects of Nuclear Fusion* , Erice, Italy, August 6-12, 1989.

Title of the project no.: 6

Impact des radionucléides relâchés en conditions accidentelles

Head(s) of project:

HUGON J.

Scientific staff:

MAUBERT H.
ROUSSEL - DEBET S.

I. Objectives of the project:

Devenir dans l'environnement des produits de fission rejetés en cas d'accident.

II. Objectives for the reporting period:

Compte Rendu final

III. Progress achieved:

En cas d'accident de réacteur, une partie du coeur (combustibles + produits de fission) est volatisée et se répand dans l'atmosphère sous forme d'aérosols qui vont se déposer sur le sol et la végétation à des distances qui peuvent être très importantes. Lors de leur transfert dans l'atmosphère les particules composant l'aérosol peuvent subir des transformations physiques et/ou chimiques. Ce qui peut agir sur leur évolution ultérieur au niveau du sol et des végétaux avant d'arriver à la chaine trophique de l'homme.

Dans ce cadre nous avons étudié :

- la production d'aérosols de forme physiques et chimiques différente,
- l'évolution de ces aérosols au niveau du sol en fonction des différents types de sols et de conditions atmosphériques différentes,
- leur comportement au niveau foliaire et racinaire

De plus l'accident de Tchernobyl survenu en avril 1986 ayant fourni des aérosols typiques permettant d'étudier le comportement réel des radioéléments, le suivi des dépôts dans le sud Est de la France a été entrepris.

1. METHODOLOGIE :

1.1. MODE DE CONTAMINATION DES SOLS ET DES VEGETAUX :

Le radioisotope choisi a été le ^{134}Cs. Trois modes de contamination ont été testés :

- pulvérisation d'une solution de chlorure, iodure, carbonate, bicarbonate ou hydroxyde de Césium,
- production d'aérosols sec obtenus à partir des mêmes solutions, par un générateur à ultrason suivi d'un assécheur,
- production d'aérosols à l'aide d'un four à haute température. Dans ce cas le traceur est introduit par une pastille d'uranium dopée sur ^{134}Cs.

  La température du four est réglable et programmable de 500 à 2200°C. L'analyse par spéctroscopie électronique montre que l'aérosol formé est constitué de particules d'UO_2 autour de laquelle est aglutinée une couche enrichie en césium.

1.2. SUIVI IN SITU DE LA CONTAMINATION :

L'écosystème étudié est situé dans les Alpes du Sud de la France dans une zone comprise entre 1500 et 2500 mètres d'altitudes.

L'aire étudiée est couverte d'une forêt de conifères, d'alpages et dans la partie la plus haute de barres rocheuses. L'aire comprend également deux lacs et est drainée par le torrent du Cavelet.

Des échantillons d'eau, de sols, de sédiments et de végétation ont été collectés régulièrement de 1986 à 1989. La radioactivité par spectrométrie et par mesures β a été mesurée sur tous les échantillons et l'on s'est particulièrement intéressé à ^{110m}Ag, $^{106}Ru+Rh$, ^{134}Cs, ^{137}Cs et ^{125}Sb.

2. RESULTATS :

2.1. Les expériences réalisées avec des aérosols de sels solubles de Césium ont montré que les coefficients d'interception par les plantes varient avec :

- la forme chimique du sel de Césium,
- le type de végétal : haricot avec port horizontal des feuilles-herbe,
- le type de dépôt pour un même végétal.

Le tableau suivant montre les variations :

		Cs I	Cs Cl	$Cs_2 CO_3$
haricot	aérosol	32%2	90%	-
	pluie	-	-	-
herbe	aérosol	138%	-	-
	pluie	4%	-	8%
conifère	pluie	80%	-	-

TABLEAU 1 : Coefficient d'interception en %.

Dans le cas de l'herbe, les différences observées en fonction du type de dépôt peuvent s'expliquer sachant que dans le cas de la pluie, l'eau ruisselle sur

les feuilles et contamine principalement le sol, ce qui n'est pas le cas pour les aérosols.

Les différences entre l'herbe et les haricots pour une même contamination par aérosols peuvent s'expliquer par la différence de surfaces spécifiques des deux végétaux ; pour $1m^2$ de sol, la sufrace totale du végétal est supérieure pour l'herbe que pour le haricot.

Dans le cas d'aérosols, la forme chimique du dépôt peut influencer la contamination si les feuilles des végétaux ont un pot horizontal ; la différence le poids moléculaires et donc de poids des particules peut expliquer ce phénomène sachant que les faces supérieures et inférieures des feuilles sont contaminées.

Dans le cas de la pluie, les différences observées entre les conifères (80%) et l'herbe (4%) s'expliquent par la morphologie des écailles de Chamaecyparis, qui sont de bien meilleurs pièges pour l'eau de pluie que l'herbe.

2.2. LES EXPERIENCES REALISEES SUR DES EPINARDS ET DES EPICEAS AVEC DES AEROSOLS PRODUIT PAR LE GENERATEUR D'AEROSOLS INSOLUBLES ONT MONTRE QUE :

2.2.1. Pour des épinards contaminés à l'aide d'aérosols secs en l'absence de pluviolessivées, la contamination est due principalement à la croissance, c'est ce que montre le tableau n°2.

Date	Contamination en cpm/g sec	Poids sec en g
08/06	20 701 ± 3 289	0,615 ± 0,096
13/06	15 282 ± 2 137	1,042 ± 0,167
20/06	8 468 ± 2 619	1,268 ± 0,350

TABLEAU 2 : Etude de la radiocontamination en Cs-134 des plantes d'épinard au cours du temps pour des plantes non pluviolessivées.

La demi-vie écologique du césium s'avère être dans ces conditions de l'ordre de 10 jours, valeur proche de la valeur acceptée dans les modèles de transfert.

Le pluviolessivage 1 fois par semaine enlève plus de la moitié de la teneur en Césium dans la 1er semaine. L'importance de cette réduction ne varie guère ensuite avec le temps.

2.2.2. En ce qui concerne les conifères, trois épicéas de huit ans environ ont été soumis à une contamination sèche et un épicéa d'âge identique a été traité à l'aide d'une pluie enrichie en aérosols marqués. Un échantillonnage de rameaux et d'aiguilles selon l'âge et la position sur l'arbre a permis d'étudier la distribution du Cs-134 déposé.

On a pu ainsi mettre en évidence que :

- Le pouvoir d'interception des épicéas est très élevé (de l'ordre de 80%).

- Pour un dépôt sec de Cs-134 et en conditions de non turbulence, les épicéas sont contaminés de manière uniforme. La contamination par unité de poids d'aiguilles est fonction de la surface offerte au radiopolluant.

- La contamination des épicéas par une pluie contaminée est responsable d'un gradient de radioactivité (du haut vers le bas et de l'extérieur vers l'intérieur du l'arbre). L'efficacité de la contamination est moindre que par dépôt d'aérosols.

- En conditions normales de champ, le pluviolessivage est responsable d'une contamination rapide des arbres contaminés ; les travaux ultérieurs permettront d'évaluer la quantité retenue ainsi que la translocation du Cs-134 fixé par les aiguilles.

- La radioactivité déposée sur les aiguilles est aisément extraite par des lavages successifs à l'eau de pluie (confirmation de la conclusion précédente). Le radiocésium extrait est lié aux particules recouvrant la surface des aiguilles. L'origine et le rôle de celles-ci en radiocontamination demeurent à préciser.

- Pour des plantes annuelles, la croissance seule est responsable d'une demi-vie écologique de l'ordre de 10 jours ; le pluviolessivage des plantes annuelles contaminées est également responsable d'une décontamination importante.

3. COMPORTEMENT DANS LES SOLS ET RELATION SOL-PLANTS :

3.1. COMPORTEMENT DANS LES SOLS :

Dans une première expérience, on a déterminé les fractions échangeables et hudrosolubles du sol par quatre formes chimiques du Césium (CsI, CsOM, $CsMCO_3$, Cs_2CO_3).

Aucune variation significative n'a pu être observée entre les différentes formes chimiques. On observe un léger accroissement de la fraction "non échangeables" en fonction du vieillissement, cet effet est favorisée par l'humidification du sol.

Dans une deuxième expérience on a déterminé les fractions hydrosolubles et échangeables des différentes formes chimiques du Césium en fonction des caractéristiques du sol et ce pour 4 sols types européens décrit dans le tableau 3 ci-après.

Type	Origine	Matière organique %	Argile %	pH	C.E.C. m éq/100g
FEN	Emmen (NL)	23,3	3,0	4,5	46
Podzol	Hanovre (D)	7,9	4,2	5,2	17
Rendzine	Allonville (F)	3,9	12,7	7,3	21
Terra Fusca	Barri (F)	2,9	56,5	7,0	28

Aucune différence significative n'est observée en fonction des formes chimiques. En fonction du type de sol, c'est le sol le plus riche en argile (Terra-Fusca) qui a la fraction non échangeable la plus élevée. C'est sur le podzol, sol pauvre en argile et moyennement riche en matière organique que la fraction non échangeable est la plus faible.

3.2. RELATION SOL PLANTES :

Le facteur de transfert sol-plante est influencé :

- par un nombre de paramètres aussi important que ceux qui caractérisent un sol et son climat,
- par les pratiques culturales,

- par les caractéristiques physiologiques des mécanismes de transport sol-racinaire.

Il existe cependant un paramètre qui conditionne l'ensemble de tous les autes, c'est la solubilité de l'élément. De façon conventionnelle, la somme des formes solubles et échangeables d'un élément représente la quantité de l'élément potentiellement disponible à la plante.

Les facteurs des transferts (Poids frais d'herbe/poids de sol sec) ont été mesurés par les 4 types de sols et les 4 formes chimiques du Césium précédent citées.

Les facteurs de transfert varient avec les caractéristiques du sol dans un rapport de 1 à 100. Sur sol riche en argile (terra fusca), le transfert est voisin de 0,01. Sur podzol, sol où le pourcentage des formes échangeable et hydrosolubles est le plus élevé, le facteur de transfert est voisin de 1 excepté pour l'iodure du Cs.

Le transfert du Césium est fonction du type de sol : sur le Fen, il est le plus élevé pour le CsOH ; sur le podzol il est le plus faible pour CsI, sur le Rendzine il est le plus faible pour le Cs_2Co_3.

Si on exprime le rapport entre la teneur en césium du végétal et la concentration en césiump soluble et échangeable du sol on obtient le facteur d'assimilation.

La variation globale du facteur d'assimilation est réduite de plus de la moitié par rapport à celle du facteur de transfert, mais les différences observées au tableau A.3.1. sont confirmées et non diminuées. C'est une combinaison des caractéristiques du sol et de la forme chimique qui agit sur son transfert dans l'herbe.

- Sous la forme de CsOH, le Cs est le plus assimilable pour le Fen et le Podzol (les deux sols les plus riches en matière organique, les plus pauvres en argile et aux pH les plus bas).

- Sur rendzine, c'est sous la forme de CsI que le Césium est le plus assimilable et sous forme de Cs_2CO_3 qu'il l'est le moins (sol relativement riche en argile et pauver en matière organique).

- Sur Podzol c'est sous la forme de CsI que le césium dans le sol influence son transfert dans le végétal, mais que les caractéristiques du sols modifient beaucoup plus cet effet.

4. SUIVI DES DEPOTS CONSECUTIFS A L'ACCIDENT DE TCHERNOBYL DANS LE SUD EST DE LA FRANCE :

Dans l'espace on constate une grande variabilité de l'intensité des dépôts. Les conditions géographiques et climatiques sont à l'origine de cette variabilité. Les évaluations à l'échelle régionale ne mettent pas en évidence la diversité des conséquences et ne permettent pas la prise en compte des dépassements éventuels des niveaux maximaux admissibles localement au cours de la période initiale.

L'observation de ces situations locales exceptionnelles est d'un grand intérêt pour la compréhension des mécanismes à l'origine du dépôt et l'évaluation d'une éventuelle remise en circulation;

Deux périodes sont à considérer dans le déroulement de l'impact :

- La période initiale avec des évolutions rapides avant qu'il y ait équilibre avec le milieu.
- La période ultérieure après incorporation dans les compartiments du milieu qui ont la propriété de fixer les éléments radioactifs. Au cours de cette période, le déroulement se fait selon un cycle sédimentaire long.

Au cours de la période initiale les Césium et surtout les ruthénium présentent une mobilité plus grande que celle qui a été mise en évidence jusqu'a présent en laboratoire : on constate en effet une certaine mobilité dans les sols avec les pluies de début Mai 86, un entraînement jusqu'aux organismes vivants et aux sédiments des cours d'eau, enfin une accumulation dans les organismes vivants cotiers (moules) toujours en mai. L'entraînement immédiat d'une fraction des dépôts par le ruissellement jusqu'au milieu marin est certain.

La dynamique de l'incorporation dans le milieu vivant dépend du mode de vie, du radioélément, du milieu. Les concentrations maximums ont été atteintes dès les premiers prélèvements (22 mai 1986 pour les moules). Cette plus grande mobilité dans le milieu physique et cette disponibilité pour le milieu vivant au cours de la période initiale est peut-être le fait de formes particulières des Ruthénium et des Césium dispersés par l'accident.

Le cycle ultérieur où n'intervient pratiquement que le Cs, dans le milieu naturel, est principalement sédimentaire. La quasi totalité des Césiums est accumulée dans les premiers centimètres des sols et des sédiments, ces

compartiments du milieu jouant un rôle épurateur. Le milieu vivant, notamment les plantes, est peu affecté par cette accumulation.

L'entraînement par lessivage et ruissellement semble peu important globalement mais l'action des fortes pluies sur les dépôts de césium dans les couches organiques des forêts ou des prairies en pente, provoque des accumulations dans les points bas. Les cycles sédimentaires ont des périodes beaucoup plus longues

5. DISCUSSION :

Les facteurs d'interception par les parties aériennes des conifères des aérosols fabriqués à l'aide de nos dispositif et des aérosols en provenance de Tchernobyl sont très voisins (de l'ordre de 80%).

Ils semblent donc que nous disposions d'un équipement de simulation approprié à l'étude des accidents tout au moins pour les problèmes de contamination directe des végétaux.

Il y aurait lieu de vérifier cette identité de comportement dans les sols et sur le plan du transfert sol-plante. En effet les résultats obtenus dans une autre étude financée par la CEE sur la spéciation chimique des radionucléides donnant des résultats comparatifs entre aérosols Cs Cl et aérosols complexes montrent des différences significatives ; la forme complexe étant plus mobile que la forme saline.

Dans ce cas la moindre réactivité était trouvée également au niveau de l'absorption racinaire de cultures de radis pour lesquelles les facteurs de transfert racinaires étaient 3 fois plus faibles dans le cas du césium de Tchernobyl que dans le cas du Cs Cl.

L'étude des retombées dans le bassin du Var a permis de mettre en évidence un certain nombre de phénomènes :

- Les dépôts sont très hétérogènes en fonction de la répartition des pluies et des caractéristiques de ruissellement des terrains rencontrés.

- Des demies-vies effectives sur les végétaux entrant dans la chaîne alimentaire ont pu être calculées. Elles varient de 5 jours pour les légumes feuilles à plusieurs dizaines de jours pour les arbres fruitiers.

- Les prélèvements effectués en forêt ont confirmé le grand pouvoir de rétention de ces écosystèmes.

La modélisation des conséquences et le calcul de l'exposition due à l'ingestion de produits locaux pendant l'année qui a suivi le dépôt montrent que

- L'impact sanitaire de l'accident dans la région étudiée est extrêmement limité, l'équivalent de dose efficace étant de 0,2 mSv.

- L'essentiel de cette valeur est due en premier lieu aux isotopes 137 et 134 du césium via les produits d'origine animale et en second lieu à l'iode 131 via les produits laitiers. Les isotopes du ruthénium n'interviennent que pour une part négligeable.

En conclusion générale ce travail montre qu'il y aurait intérêt à améliorer nos connaissances sur les transferts de la radioactivité aux produits d'origine animale et à entreprendre dans les années qui viennent des travaux dans ce sens.

PUBLICATIONS :

[1] - Impact radiologique des radionucléides relâchés en conditions accidentelles. Rapport DERS/SERE/SReA n° 86/28 - Octobre 1986.

[2] - H. MAUBERT - A. GRAUBY - V. PONZETTO
Comparaison des prévisions de deux modèles radioécologiques avec des mesures réelles. Athènes Octobre 1987.

[3] - C. RONNEAU - E. FAGNIART - K. FONSNY - P. ANDRE - C. MYTTENAERE A. DEBAUCHE - J.M. LAMBOTTE - H. MAUBERT
Contamination des écosystèmes forestiers par le césium IVème Symposium international de radioécologie de CADARACHE. Mars 1988.

[4] - H. MAUBERT - S. ROUSSEL - R. LION
Les dépôts radioactifs consécutifs à l'accident de Tchernobyl dans le bassin du VAR.
IVème Symposium international de radioécologie de CADARACHE. Mars 1988

[5] - H. MAUBERT - F. DURET - C. COMBES - S. ROUSSEL
Behaviour of the radionuclides deposited after the Tchernobyl accident in a mountain ecosystem of the french southern alps. Workshop on the Transfer of Radionuclides in Natural and Semi-natural Environments. Udine Septembre 1989.

[6] - C. RONNEAU - H. MAUBERT
Etude du dépôts sur épicéas et épinards d'aérosols enrichis en ^{134}Cs.
Novembre 89.

[7] - H. MAUBERT - S. ROUSSEL - C. COMBES - F. DURET
Evaluation des données sur le transfert des radionucléides dans la chaîne alimentaire.
Spéciation chimique des Radionucléides. Septembre 88.

Title of the project no.: 7 : **Comparaison de la distribution et du transfert des radionucléides dans l'environnement terrestre en France et en Grande Bretagne. Etude du transfert sol-plante du neptunium et de l'américium.**

Head(s) of project:

A.GRAUBY

Scientific staff:

J.DELMAS
C.COLLE

I. Objectives of the project:

Ce programme réalisé en collaboration avec le centre d'études nucléaires de HARWELL (contrat B16-B-046-UK) a été développé selon deux thèmes principaux :
Thème 1 : Etude des dépôts sur le sol et la végétation des radionucléides (Cs,Pu,Am) issus des retombées atmosphériques dans l'environnement des installations nucléaires et dans le milieu naturel en fonction de différents situations géographiques et climatiques.
Thème 2 : Etude comparée du transfert sol-plante des actinides en fonction du type de végétal et du type de sol. Evaluation de la disponibilité de ces radioéléments dans les sols.

II. Objectives for the reporting period:

Dans le cadre des objectifs du thème 1 des prélèvements d'échantillons de végétaux (luzerne et ray-grass), d'eau de pluie et de sol ont eu lieu périodiquement sur des parcelles implantées dasn le milieu naturel ou à proximité d'installations nucléaires. Ils ont été analysés pour déterminer les concentrations en Cs, Pu et Am.

En ce qui concerne le thème 2 la détermination des facteurs de transfert sol-plante a été réalisé pour le neptunium et l'américium pour cinq sortes de végétaux et trois types de sol.

III. Progress achieved:

I) METHODOLOGIE

THEME 1

L'étude des dépots sur le sol et la végétation a été réalisée à partir de dix-neuf parcelles implantées dans le milieu naturel en France et en Grande Bretagne sous diverses latitudes (44° N à 58° N) et possédant des caractéristiques climatiques différentes (figure 1 et tableau 1).

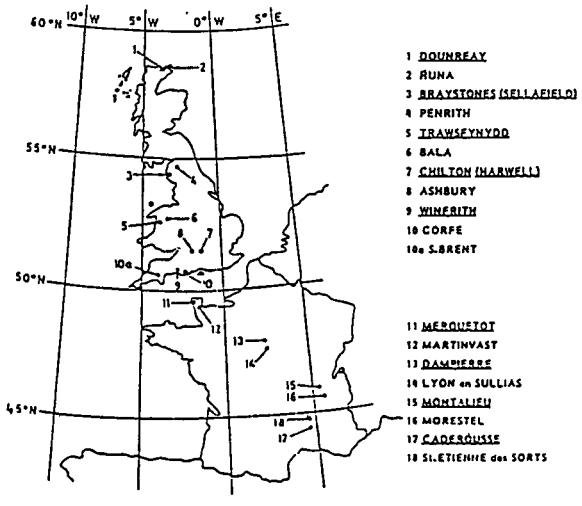

FIGURE 1: Localisation des parcelles pour l'étude des dépots des radionucléides en Grande Bretagne et en France.Les noms soulignés indiquent les parcelles situées sous l'influence directe d'une installation nucléaire.

	SITES	LATITUDE	PLUVIOMETRIE MOYENNE ANNUELLE (mm)	ALTITUDE (m)	DISTANCE A LA MER (Km)
1	DOUNREAY	58°N	900	15	0,3
2	HUNA	58°N	780	10	0,3
3	BRAYSTONES	55°N	1040	15	1,1
4	PENRITH	55°N	880	137	41
5	TRAWSFYNYDD	53°N	1700	215	15
6	BALA	53°N	1300	95	39
7	CHILTON	52°N	590	130	94
8	ASHBURY	52°N	750	195	90
9	WINFRITH	51°N	880	30	0,9
10	CORFE	51°N	810	15	0,6
10a	S.BRENT	51°N	2070	116	16
11	MERQUETOT	50°N	1000	100	1,2
12	MARTINVAST	50°N	1000	70	7
13	DAMPIERRE	48°N	650	140	330
14	LION EN SULLIAS	48°N	650	130	320
15	MONTALIEU	46°N	1000	200	280
16	MORESTEL	46°N	1000	230	260
17	CADEROUSSE	44°N	820	30	80
18	ST ETIENNE DES SORTS	44°N	820	30	90

TABLEAU 1: Principales caractéristiques géographiques et climatiques des lieux d'implantation des parcelles en Grande Bretagne et en France.

Neuf de ces parcelles ont été mises en place dans l'environnement de neuf installations nucléaires, les dix autres ont été disposées dans les mêmes situations géographiques et climatiques mais dans des endroits isolés de l'influence directe de ces installations.

Chacune de ces parcelles a été délimitée par une cloture (8x8m) et comportait trois dispositifs expérimentaux différents :

- une partie du sol indigène a été utilisé pour cultiver du ray-grass et de la luzerne. Ces végétaux ont été récoltés plusieurs fois chaque année et les différentes récoltes ont été groupées par période de six mois (été - automne et hiver - printemps). Ces échantillons semestriels ont été analysés pour déterminer les concentrations en césium, plutonium et américium.
- au centre de la parcelle, un bac témoin (2x2x0,3m) a été mis en place avec un sol standard pour l'ensemble des sites dans chacun des deux pays. Des cultures de ray-grass et de luzerne y ont été implantées et leurs récoltes ont été effectuées selon les m^emes modalités que précédemment.
- un dispositif de collecte des eaux de pluie afin de recueillir les précipitations semestrielle dans le but de mesurer les dépôts de radionucléides d'origine atmosphérique.

THEME 2

L'étude comparée du transfert sol-plante du neptunium et de l'américium a été réalisée à l'aide de cultures de salades, radis, haricots et luzernes à partir de trois types de sol (acide, calcaire et organique) dont les principales caractéristiques sont indiquées dans le tableau 2. Les bacs de culture utilisés contenaient 15 Kg de sol sec et leur contamination a été faite à l'aide de 7,4 KBq/Kg de sol pour le neptunium et de 18,5 KBq/Kg de sol pour l'américium. Ces radioéléments étaient sous forme nitrate et ils ont été mélangés au sol de façon homogène.

La détermination de la disponibilité de ces deux nucléides dans les sols est intervenue quatre années aprés la contamination par la mise en oeuvre d'extractions successives à l'aide de quatre réactifs différents: eau distillée, solution d'acétate d'ammonium 1N, mélange d'une solution d'hydroxyde de sodium (0,1N) et d'une solution de pyrophosphate de sodium (0,1N), et solution d'acétate de cuivre 0,1N. L'action de ces réactifs a permis de définir les formes hydrosolubles, échangeables, organiques et chélatées pour le neptunium et l'américium dans les trois types de sol.

Type de sol	Origine	pH à l'eau	pH dans le CaCl2/KCl	Matière organique(%)	Capacité d'échange meq/100g	Granulométrie		
						Argiles (%)	Limons (%)	Sables (%)
ORGANIQUE	Norfolk (G.B)	6,9	6,6	24,1	122,0	46	23	31
ACIDE	La Hague (F)	5,8	5,3	1,1	14,3	11	47	42
CALCAIRE	Cadarache (F)	8,1	7,6	0,7	9,8	7	51	42

TABLEAU 2 : Principales caractéristiques physico-chimiques des sols étudiés

II) RESULTATS, DISCUSSION.

THEME 1

1 - Mesure du dépôt des radionucléides dans les sols.

Ces mesures ont été réalisées sur l'ensemble des sites au moment de la mise en place de l'expérimentation afin de chiffrer l'accumulation des radionucléides qui avait eu lieu au cours du temps par le fait des retombées des essais nucléaires aériens et plus récemment à cause des dépôts issus de l'accident de Chernobyl, ces derniers étant identifiés à partir du césium 134. A propos de ces derniers la figure 2 montre les différences qui ont été observées dans le cas du césium 137 sur les sites de référence en fonction de la latitude. Il ressort une différence d'un ordre de grandeur entre les valeurs mesurées lorsqu'on passe de la latitude 58° N à celle 44° N. La raison en est probablement dûe à des conditions climatiques particulières au cours de l'été 1986 dans les zones considérées : abondance des précipitations, intensité et durée des pluies.

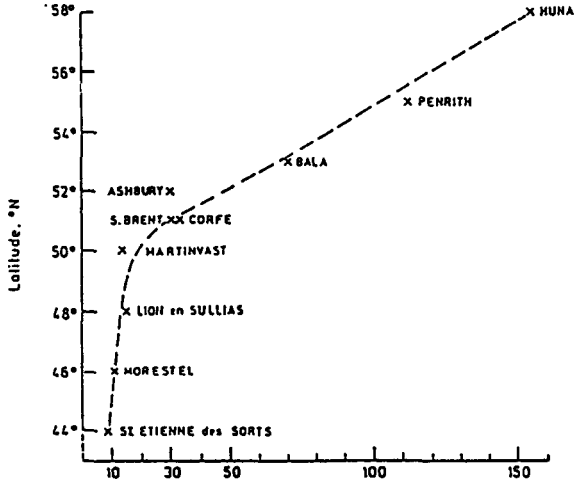

FIGURE 2 : Influence de la latitude sur les quantités de césium 137 (Becquerels par mètre carré) déposées sur les sols des sites de référence en Grande Bretagne et en France de juin 1986 à mai 1987.

La figure 3 représente les concentrations en radionucléides mesurées dans les sols des sites proches des installations nucléaires. Pour trois de ces sites (A, B et C) les valeurs en césium sont de cinq à dix fois supérieures à celles observées pour les sites de contrôle à la même latitude. Ces différences pourraient être attribuées à l'influence directe des installations nucléaires. Dans le cas du plutonium et de l'américium les deux sites A et B se singularisent avec des concentrations supérieures d'un ordre de grandeur à celles mesurées par ailleurs.

Pour expliquer ce fait il convient de remarquer que ces deux sites sont en situation côtière et donc soumis au dépôt d'embruns marins en même temps qu'à l'influence directe des installations nucléaires. Par ailleurs ces dernières ne semblent pas avoir marqué de façon significative les sols des autres sites.

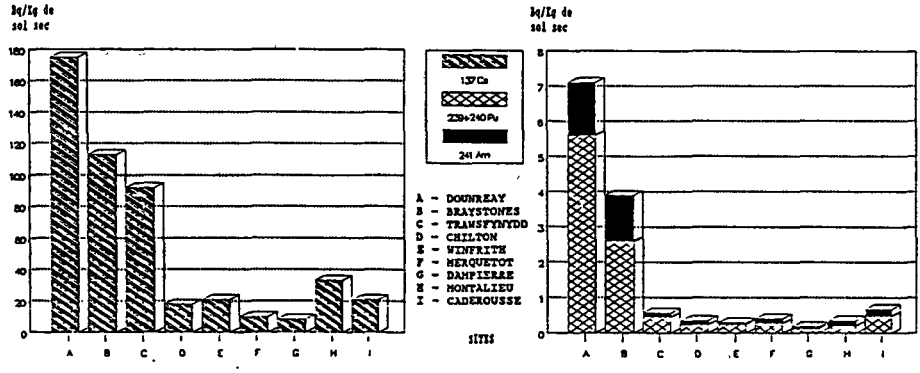

FIGURE 3: Concentrations en radionucléides des sols provenant des sites proches des installations nucléaires. Les valeurs indiquent la concentration moyenne de la couche 0-15 cm pour le césium et de la couche 0-30 cm pour le plutonium et l'américium.

2 - Mesure des dépôts d'origine atmosphérique.

Les résultats des mesures réalisées sont portées dans le tableau 3 qui regroupent les dépôts moyens annuels collectés sur l'ensemble des sites français pour les périodes d'hiver (janvier à juin) et d'été (juillet à décembre). Ces mesures rendent compte à la fois des dépôts secs (poussières) et des dépôts contenus dans l'eau de pluie durant trois années consécutives.

Ces valeurs font apparaître un effet saisonnier sur l'importance des concentrations des différents radionucléides analysés en liaison avec les conditions climatiques spécifiques à chaque site, ces dépôts étant plus importants l'hiver que l'été. Ce phénomène est plus accentué dans les cas des sites implantés dans les régions les plus au sud pour lesquelles le déséquilibre de la pluviométrie entre l'hiver et l'été est le plus grand.

	Cs-137 (Bq/m²)		Pu-239+240 (Bq/m²)		Am-241 (Bq/m²)		Na (g/m²)	
	HIVER	ETE	HIVER	ETE	HIVER	ETE	HIVER	ETE
MERQUETOT	9,7	3,4	0,039	0,026	0,031	0,019	29,0	17,5
MARTINVAST	9,4	4,4	0,024	0,020	0,038	0,016	13,4	12,5
DAMPIERRE	7,7	3,9	0,019	0,013	0,020	0,012	0,8	0,4
LION EN SULLIAS	6,7	5,9	0,019	<0,01	0,010	<0,01	0,9	0,3
MONTALIEU	5,7	6,3	0,020	<0,01	0,016	<0,01	0,6	0,2
MORESTEL	4,9	4,0	0,026	<0,01	0,014	<0,01	0,7	0,3
CADEROUSSE	3,5	<2	0,039	<0,01	0,034	<0,01	0,6	0,2
ST ETIENNE DES SORTS	4,2	<2	0,033	0,016	0,019	<0,01	0,6	0,2

Tableau 3 : Moyenne saisonnière (hiver et été) des dépôts d'origine atmosphérique receuillis sur l'ensemble des sites en France du mois de juin 1986 au mois de juillet 1989.

Les résultats des analyses de sodium rendent compte de l'influence marine et des possibilités de dépôts d'embruns sur les sols. Pour les sites français étudiés ce cas se limite aux deux parcelles établies le plus au nord. La comparaison entre les dépôts de césium, plutonium et américium touchant les sites nucléaires et ceux touchant les sites de référence qui leur sont associés ne fait pas apparaître de différence significative entre les niveaux d'activité mesurés.

3 - Mesure des concentrations en radionucléides de la végétation.

Le tableau 4 regroupe l'ensemble des données obtenues pour les cultures de ray-gras sur l'ensemble des sites en Grande Bretagne et en France, ainsi que le rapport entre les valeurs mesurées l'été et celles mesurées l'hiver. Dans tous les cas où ce rapport a pu être calculé, il apparaît qu'il existe un effet saisonnier marqué sur l'importance du transfert global des radionucléides par les plantes (transfert sol-plante augmenté de la rétention foliaire des dépôts atmosphériques. Ce rapport montre une rétention plus importante des éléments durant la période estivale.

	Cs 137	Pu 239+240	Am 241
SITES DE REFERENCE			
HUNA	10,8 (2,3)	<0,03	<0,03
PENRITH	4,9 (3,6)	<0,03	<0,06
BALA	3,7 (3,2)	<0,03	<0,05
ASHBURY	< 1	<0,03	<0,03
CORFE	< 1	<0,03	<0,05
S.BRENT	3,7 (3,0)	<0,03	<0,04
MARTINVAST	< 2	<0,02	0,021 (2,3)
LION EN SULLIAS	< 2	<0,02	<0,02
MORESTEL	3,6 (2,6)	<0,02	<0,02
ST ETIENNE DES SORTS	2,5 (5,4)	<0,02	<0,02
SITES NUCLEAIRES			
DOUNREAY	18,2 (2,8)	0,16 (1,8)	0,073 (2,5)
BRAYSTONES	42,4 (4,0)	0,30 (2,4)	0,31 (4,5)
TRAWSFYNYDD	5,7 (2,7)	<0,04	<0,04
CHILTON	< 1	<0,04	<0,04
WINFRITH	4,6 (4,2)	<0,04	<0,04
MERQUETOT	2,4 (1,7)	0,031 (1,4)	0,027 (1,7)
DAMPIERRE	< 2	<0,02	<0,02
MONTALIEU	2,7 (1,6)	<0,02	<0,02
CADEROUSSE	2,8 (1,6)	0,023 (1,3)	0,024 (2,2)

TABLEAU 4 : Concentrations moyennes annuelles (Bq/Kg de matière sèche) des radionucléides dans les récoltes de ray-grass effectuées de juin 1986 à mai 1988 sur les parcelles des sites de référence et des sites nucléaires.(Les chiffres entre parenthèses indiquent le rapport entre les concentrations mesurées en été et celles mesurées en hiver).

Pour les sites les plus au nord les valeurs élevées en césium 137 s'expliquent par l'impact des retombées de Chernobyl. Leur effet a été direct à cause des dépôts foliaires pour les premières récoltes en 1986 mais il a continué à être ressenti au cours de la saison suivante à cause des transferts par voie racinaire. Cet effet secondaire a été plus remarqué pour le ray-grass que pour la luzerne du fait que cette dernière plante a un enracinement profond donc hors d'atteinte des dépôts situés à la surface des sols. L'ensemble des récoltes de ray-grass et de luzerne effectué sur les autres sites n'a pas été marqué significativement par l'accident de Chernobyl.

Les analyses des actinides montrent des teneurs élevées en plutonium et en américium dans les récoltes de ray-grass en provenance des deux sites nucléaires localisés aux latitudes les plus élevées contrairement à tous les autres. Une observation identique a été faite sur les cultures de luzerne issues de ces mêmes zones.

THEME 2

1 - Etude des transferts sol-plante du neptunium et de l'américium.

Les valeurs des facteurs de transfert obtenues au cours de cette expérimentation sont indiquées dans les figures 4 et 5 pour les parties des végétaux qui entrent directement dans l'alimentation humaine ou animale. Quant au tableau 5 il regroupe les données relatives aux feuilles de radis et de haricot.

Cette représentation fait apparaître l'influence du type de sol et du type de végétal sur l'absorption par voie racinaire du neptunium 237 et de l'américium 241.

Influence du sol.

Pour l'ensemble des espèces et pour chacun des deux actinides les transferts sont supérieurs de un à deux ordres de grandeur sur le sol acide par comparaison avec les deux autres types de sols, exception faite pour les racines de radis où cet écart est plus atténué surtout pour le neptunium. Dans le cas du ray-grass et pour les deux nucléides l'importance des transferts suit un ordre décroissant lorsqu'on passe du sol acide au sol calcaire puis au sol organique. Le même phénomène apparaît pour le transfert de l'américium à la salade et au haricot. Toutefois d'une manière générale les différences de comportement des actinides entre le sol calcaire et le sol organique semblent plutôt dues au type de végétal qu'au type de sol.

Influence de l'espèce végétale.

Indépendamment de tous les autres paramètres c'est dans les fruits de haricot que l'on observe les transferts les plus faibles avec des différences de un à deux ordres de grandeur en dessous des valeurs observées pour les autres espèces. Il s'agit là d'un phénomène dont les causes sont d'origine physiologique (rôle de la barrière placentaire).

Si l'on met à part le cas des fruits de haricot il est à remarquer que c'est sur le sol acide où les différences entre les facteurs de transfert sont les plus faibles et ceci quel que soit le radioélément.

Influence du radioélément.

Elle apparait de façon évidente quel que soit le sol ou le végétal pris en considération : les transferts sol-plante du neptunium 237 sont de dix à cent fois supérieurs à ceux de l'américium 241.

FACTEUR de TRANSFERT

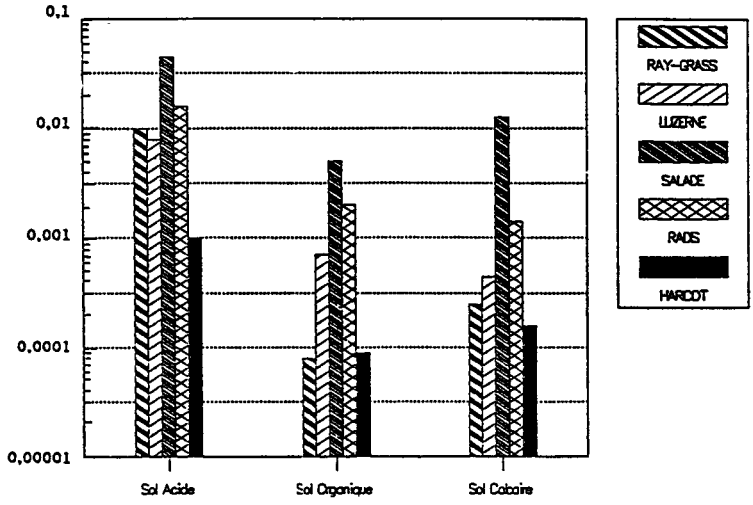

FIGURE 4 : Facteurs de transfert sol-plante de l'américium 241 pour trois types de sol et différentes espèces végétales.

FACTEUR de TRANSFERT

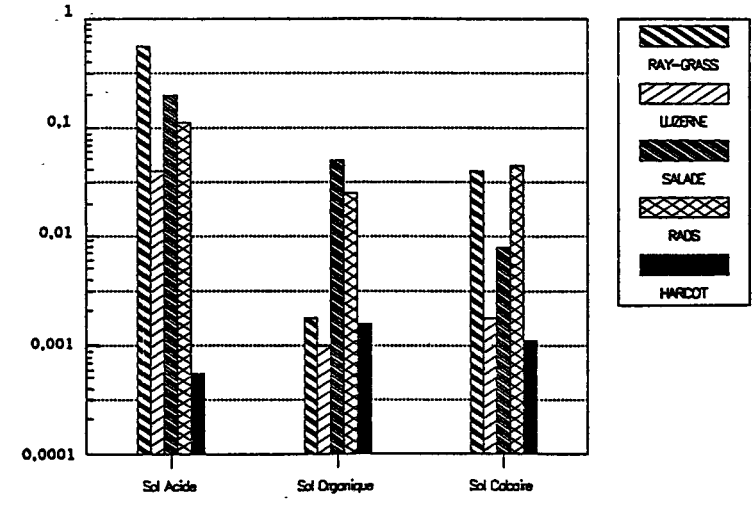

FIGURE 5 : Facteurs de transfert sol-plante du neptunium 237 pour trois types de sol et différentes espèces végétales.

TYPE DE VEGETAL	TYPE DE SOL	237 Np	241 Am
RADIS:(feuilles)	Sol acide	4,2E-01	9,1E-02
	Sol calcaire	3,8E-02	1,0E-02
	Sol organique	9,4E-03	1,7E-02
HARICOT:(feuilles + tiges)	Sol acide	2,2E-02	4,4E-03
	Sol calcaire	6,3E-03	7,3E-04
	Sol organique	8,1E-03	1,4E-03

TABLEAU 5 : Facteurs de transfert sol-plante du neptunium 237 et de l'américium 241 à partir des trois types de sol et pour les feuilles de radis et de haricot

2 - Evaluation de la biodisponibilité du neptunium et de l'américium dans les trois types de sol étudiés.

A la fin de l'expérimentation sur la détermination des facteurs de transfert sol-plante qui a duré quatre ans, des prélèvements de sol ont été réalisés dans les bacs de culture. La technique des extractions successives décrites précédemment dans la méthodologie a été apliquée à ces échantillons ce qui a permis de définir la distribution des différentes formes physico-chimiques sous lesquelles se trouvaient les deux radionucléides présents dans les trois types de sol. Les fractions hydrosolubles, échangeables, organiques et chélatées ont été mesurées directement dans les solutions d'extraction. La fraction appelée résidu représente la quantité de radioélément qui n'a pu être extraite par les procédés employés et elle a été évaluée par différence entre la mesure de la concentration totale de chacun des deux actinides dans les sols et la somme des quatre fractions définies précédemment. Les figures 6 et 7 relatent les résultats de ces investigations. L'analyse des données permet dans une certaine mesure de renseigner sur le niveau de biodisponibilité de l'élément dans un sol. En effet on peut considérer qu'en cumulant les parties hydrosolubles et échangeables on obtient une bonne estimation de ce qui est facilement disponible pour les végétaux. Parallelement la somme des formes organiques et chélatées renseigne sur l'importance des quantités de l'élément associées à la matière organique ou aux complexes organométalliques du sol. Ces formes représentent des états non directement disponibles pour les plantes mais qui peuvent le devenir au cours du temps en fonction de leur dégradation éventuelle.

Plusieurs remarques se dégagent des résultats obtenus:

- la majeure partie de l'américium se présente sous une forme non extractible par les réactifs utilisés: de 83% dans le sol acide à 92% dans le sol organique. La somme des fractions hydrosolubles et échangeables ne dépasse pas 2% quel soit le type de sol. Quant aux complexes organiques ils représentent environ 4% de la totalité du radioélément dans les trois cas. En ce qui concerne les formes chélatées elles varient de 11% dans le sol acide à 11% dans le sol organique.

– le cas du neptunium est nettement différent. Tout d'abord il est à remarquer que la quasi totalité du radioélément a pu être extraite du sol organique alors que cette proportion a été de 52% sur le sol acide et de 24% sur le sol calcaire. La somme des formes hydrosolubles et échangeables dans les trois sols montre qu'elle suit l'ordre décroissant : sol acide (19%) sol organique (9%) sol calcaire (6%).

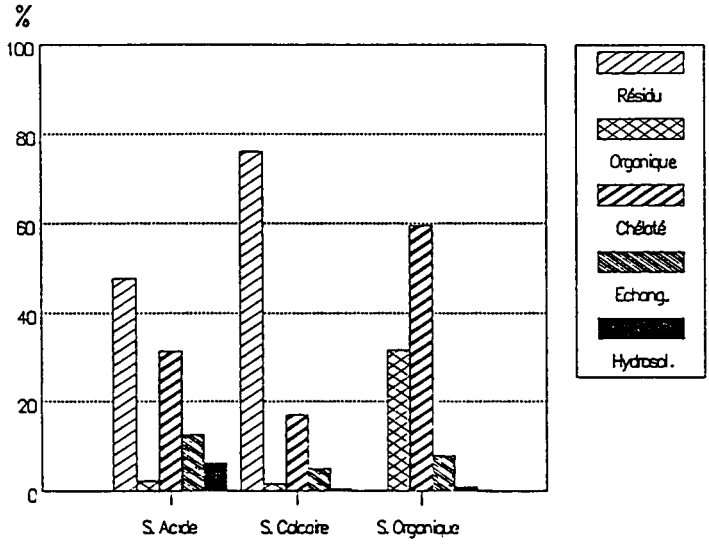

FIGURE 7 : Distribution des différentes formes physico-chimiques du neptunium 237 dans les trois types de sol étudiés.

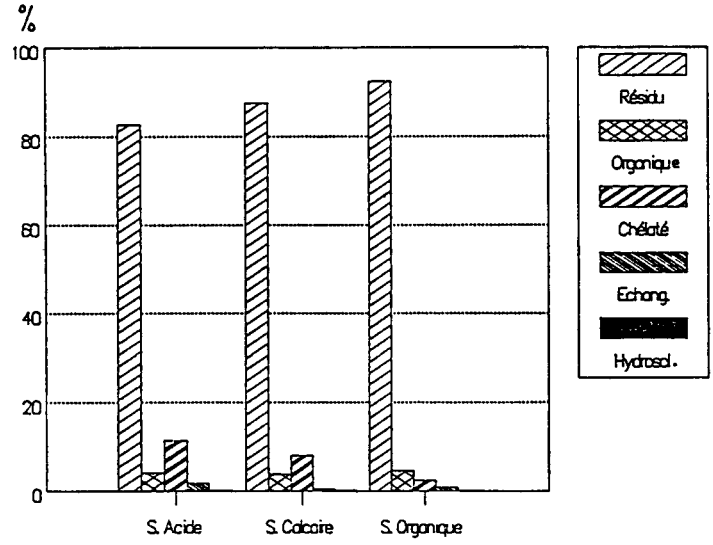

FIGURE 6 : Distribution des différentes formes physico-chimiques de l'américium 241 dans les trois types de sol étudiés.

La mise en parallèle de ces résultats et des valeurs expérimentales relatives aux facteurs de transfert sol-plante montre une bonne corrélation entre le niveau de disponibilité qui est évalué à partir de la somme des fractions hydrosolubles et échangeables et l'importance de l'absorption racinaire par les végétaux du radioélément à partir d'un sol donné. D'autre part l'ensemble de cette étude montre que le pH du sol a une influence capitale sur le transfert sol-plante des actinides et du neptunium en particulier. Le sol étudié ici, bien que modérément acide (pH=5,8) a induit des transferts dix à cent fois supérieurs à ceux provenant des sols alcalins. Il est donc permis de penser que pour des sols plus acides ces différences pourraient être plus accentuées.

IV. Other research group(s) collaborating actively on this project [name(s) and address(es)]:

Centre de recherches d'Harwell (GB) : Environmental and Medical Sciences Division. Notre collaboration s'effectue avec Monsieur P.A.CAWSE.

Remarque : la rédaction du rapport final effectué par chacun des deux partenaires résulte d'une mise en commun des différents résultats obtenus individuellement dans chaque pays respectif.

V. Publications:

P.A. CAWSE, C.COLLE . Comparison of radionuclide deposition to soil and vegetation. Actes du IVème Symposium International de Radioécologie de Cadarache, 14 - 18 mars 1988, Tome 1, D75-D89.

P.A. CAWSE, C.COLLE. Variability in soil to plant transfert of neptunium, américium and curium. VIth report of the working group soil-to-plant transfert factors , may 24-26 1989. RIVM, Bilthoven, THE NETHERLANDS.

Title of the project no.: **8 : Dépot des radionucléides sur le sol et la végétation.**

Head(s) of project:

A.GRAUBY

Scientific staff:

J.DELMAS
C.COLLE

I. Objectives of the project:

Ce programme de recherche réalisé en collaboration avec le Centre de Radioagronomie de Jülich (RFA) a trois objectifs principaux:

1 - Déterminer l'influence de l'apport dans le sol de césium ou de cobalt stable sur l'absorption racinaire par les végétaux des radionucléides correspondants.

2 - Comparer les transferts aux plantes du césium et du cobalt dans le cas d'une contamination chronique du sol et dans le cas d'une contamination accidentelle touchant le sol ou la végétation à divers stades végétatifs.

3 - Etudier les possibilités de réduire les transerts par voie racinaire résultant d'une contamination accidentelle en utilisant des techniques culturales particulières.

II. Objectives for the reporting period:

Au cours des cinq années pendant lesquelles ce programme a été développé,les trois objectifs indiqués précedemment ont été atteints.

III. Progress achieved:

I – METHODOLOGIE

Ce programme a été réalisé à partir d'un dispositif expérimental constitué de seize lysimètres (surface : 0,25m2, profondeur : 0,6m) placé à l'air libre en conditions climatiques naturelles. Ils ont été remplis à l'aide de 200 kg d'un sol brun calcaire prélevé dans la région de Cadarache et dont les principales propriétés physico-chimiques sont les suivantes : pH(H20) = 8.1, matière organique = 0,7%, capacité totale d'échange = 9,8 méq/100g, argiles = 7%, limons = 51% et sables = 42%.

Afin de permettre l'utilisation de ce dispositif pour l'étude de l'ensemble des paramètres énumérés dans les objectifs cités plus haut et dans le but de pouvoir opérer des comparaisons rigoureuses quant à leur influence respective sur les niveaux de transfert, deux couples de radionucléides ont été utilisés :

- le premier couple (césium 137 et cobalt 60) a été employé pour l'étude des transferts sol-plante dans le cadre de la simulation d'une contamination des sols résultant des dépôts de nucléides issus des rejets chroniques des installations nucléaires. Cette contamination a été effectuée en mélangeant les radioéléments de façon homogène aux trente premiers centimètres du sol, ce qui correspond à la profondeur moyenne des labours. Elle a eu lieu deux mois avant le début de la mise en culture de manière à permettre la mise à l'équilibre des radioéléments dans le sol.

7500 KBq de césium 137 et de Cobalt 60 ont été respectivement distribués dans chacun des lysimètres. Cette contamination a été également combinée à une application de l'élément stable correspondant à chaque nucléide apporté, ceci pour huit lysimètres dans le cas du cobalt et de huit autres pour le césium. Les quantités d'éléments stables apportées ont été de 50 et de 10 mg/Kg de sol respectivement pour le cobalt et le césium.

Cinq types de végétaux ont été testés dans cette première partie de l'expérimentation : blé, orge, carotte, salade et haricot.

- le deuxième couple (césium 134 et cobalt 57) a été utilisé pour simuler le dépôt sur le sol ou la végétation de nucléides issus de rejets accidentels. Cette simulation a été effectuée sur les lysimètres précédents et les contaminations ont eu lieu selon les deux modalités suivantes : d'une part sur les parties aériennes des végétaux soit en une seule fois (quatre lysimètres) soit fractionnée en trois fois au cours du cycle végétatif (quatre lysimètres) et d'autre part uniquement sur le sol soit en une seule fois (quatre lysimètres) soit fractionnée en trois fois au cours du cycle végétatif (quatre lysimètres).

Quel que soit le mode de contamination du sol ou de la végétation les activités mises en oeuvre pour chacun des deux radionucléides ont été de 7500 KBq par lysimètre. Cette simulation de contamination accidentelle a porté sur des cultures de blé et de carottes, mais pour cette dernière plante l'apport des radionucléides n'a eu lieu qu'en une seule fois sur le sol ou la végétation. Dans le cas du blé le dépôt des radioisotopes sur les organes aériens a toujours été fait au plus tard avant le début de l'épiaison.

A la suite de ces travaux trois techniques culturales ont été appliquées sur les lysimètres dont le sol avait reçu en surface la contamination de type accidentel :

* un labour superficiel touchant les 10 cm de surface
* un labour normal sur 30 cm de profondeur
* un labour profond qui a porté à 50 cm la couche du sol qui avait reçu les radioéléments.

Du blé et de la luzerne ont été plantés sur les sols ainsi préparés.

II - RESULTATS

1 - Détermination des facteurs de transfert sol-plante du césium et du cobalt pour différentes cultures. Etude de l'influence de la concentration du sol en césium et cobalt stable sur l'absorption racinaire par les végétaux du césium 137 et du cobalt 60.

Les facteurs de transfert sol-plante (calculés par rapport à la matière sèche obtenus au cours de cette première partie de l'expérimentation sont regroupés dans le tableau 1.

		Facteur de transfert du cobalt 60		Facteur de transfert du césium 137	
		Sol sans apport de Co stable	Sol avec apport de Co stable	Sol sans apport de Cs stable	Sol avec apport de Cs stable
BLE	Paille	9,6E-03	7,3E-02	7,3E-03	8,8E-02
	Grain	7,2E-03	3,0E-02	4,2E-03	6,1E-02
ORGE	Paille	9,4E-03	6,9E-02	7,1E-03	9,0E-02
	Grain	7,3E-03	2,9E-02	4,0E-03	6,4E-02
SALADE	Feuilles	6,5E-02	1,2E-01	5,4E-02	3,1E-01
HARICOT	Feuilles	5,1E-02	1,4E-01	3,2E-02	5,3E-01
	Fruits	1,2E-02	8,2E-02	1,7E-02	2,9E-01
CAROTTE	Feuilles	4,6E-02	9,1E-02	7,6E-02	5,8E-01
	Racines	4,7E-02	2,1E-01	6,4E-02	5,3E-01

TABLEAU 1 : Influence de l'apport de cobalt et de césium stables sur le transfert sol-plante du cobalt 60 et du césium 137 pour différents végétaux.

Les cultures des cinq types de végétaux testés se sont déroulées au cours d'une année et demi. La contamination du sol ayant eu lieu au mois de janvier 1985, du blé et de l'orge de printemps ont été semés au mois de mars. La récolte de ces deux céréales est intervenue au mois de juillet, ce qui a permis de faire se succéder sur les lysimètres pour le reste de l'année 1985, des cultures de salades, de haricots et de carottes, ces dernières ayant été cueillies au début de 1986.

2 – Comparaison des transferts aux végétaux du césium et du cobalt entre les cas d'une contamination chronique du sol et d'une contamination accidentelle touchant le sol ou la végétation à divers stades de développement des plantes.

Cette étude s'est déroulée de 1986 à 1987 avec deux végétaux : blé et carotte. Les résultats obtenus sont portés dans le tableau 2 où les valeurs indiquées sont celles des concentrations en césium et cobalt mesurées dans les organes comestibles (grain pour le blé et racine pour la carotte). L'apport des radionucléides dans le cadre de la simulation de la contamination accidentelle a été réalisée pour le sol juste aprés le semis dans le cas de l'apport unique et en cours de végétation pour le cas des apports fractionnés.

		Blé Grain Bq/Kg sec		Carotte Racine Bq/Kg sec	
		Césium	Cobalt	Césium	Cobalt
Sol contaminé à la suite d'un dépôt mélangé de façon homogène aux trente premiers centimètres du sol.		1,2	0,8	5,7	3,6
Dépôt à la surface du sol.	Apport unique	8,0	1,8	106,0	98,0
	Apport fractionné en trois fois	7,0	1,4		
Dépôt sur les organes aériens des plantes.	Apport unique	500,0	325,0	5336,0	3542,0
	Apport fractionné en trois fois	475,0	340,0		

TABLEAU 2 : Influence du mode d'apport des radioéléments sur le transfert du césium 137 et du cobalt 60 au blé et à la carotte.

3 – Etude des possibilités de réduction du transfert sol–plante par l'application de différents types de labours à des sols ayant reçu une contamination accidentelle en surface.

Les lysimètres ayant reçu le dépôt de type accidentel à la surface du sol ont subi les différentes sortes de labour au cours de l'hiver 1987. La façon d'opérer a consisté à retirer la couche de sol contaminé, à la mélanger dans la zone des 10 premiers centimètres en surface (travail superficiel du sol), ou bien à la disposer à 30 centimètres de profondeur (labour normal) ou encore à la placer à 50 centimètres de la surface (labour profond).

Sur les lysimètres ainsi traités un semis de blé a été mis en place au printemps 1988. La récolte ayant eu lieu au mois de juillet, une culture de luzerne lui a fait suite pour laquelle sept récoltes étalées sur douze mois ont pu se succéder jusqu'en 1989. Les concentrations en radionucléides mesurées dans les produits récoltés à l'issue de cette expérimentation sont indiquées dans le tableau 3. Ils sont relatifs au grain pour le blé et à l'ensemble tiges plus feuilles pour la luzerne. En outre pour cette dernière espèce les valeurs sont notées pour la première et la dernière récolte.

	TRANSFERT DU CESIUM 137		TRANSFERT DU COBALT 60	
	BLE GRAIN Bq/g sec	LUZERNE Bq/g sec	BLE GRAIN Bq/g sec	LUZERNE Bq/g sec
Sol contaminé de façon homogène sur trente centimètres	1,2	3,0	0,8	1,8
Sol contaminé par un dépôt en surface	8,0	13,2	1,8	6,1
Labour superficiel 10 centimètres.	3,3	10,4	2,6	8,0
Labour normal 30cm	0,7	Récolte n°1: 0,3 Récolte n°7: 1,8	0,5	Récolte n°1: 0,4 Récolte n°7: 2,2
Labour profond 50cm	0,04	Récolte n°1: 0,1 Récolte n°7: 0,5	0,1	Récolte n°1: 0,1 Récolte n°7: 1,2

TABLEAU 3 : Action comparée de trois types de labours sur le transfert du césium 137 et du cobalt 60 au blé et à la luzerne à partir de sols ayant reçu un dépot important de ces deux nucléides en surface.

III - DISCUSSION

L'analyse de l'ensemble des résultats obtenus au cours de cette expérimentation appelle les observations suivantes :

1 - L'importance des transferts par voie racinaire du radiocobalt et du radiocésium peuvent être modifiés de façon notable par l'incorporation au sol des isotopes stables correspondants. Dans le cas de notre expérience les apports de 50 mg/Kg de sol de cobalt et de 10 mg/Kg de sol de césium ont provoqué une augmentation des facteurs de transfert d'un ordre de grandeur environ (tableau 1).

2 - Les transferts sol-plante sont sensiblement plus importants s'ils résultent d'un apport des radionucléides à la surface du sol que s'ils sont issus d'une contamination équivalente mais incorporée d'une façon homogène dans la zone d'exploration des racines (tableau 2).

3 - Dans les conditions de cette expérimentation le fractionnement de l'apport des radionucléides sur le sol ou la végétation n'a pas modifié de façon significative le niveau de contamination des produits récoltés par rapport au résultat d'un apport unique (tableau 2).

4 - l'utilisation des labours apparaît comme étant une mesure efficace pour réduire les transferts sol-plante dans le cas où le sol a reçu en surface un dépôt important de césium ou de cobalt (tableau 3). Dans le cas de l'expérimentation sur les cultures de blé ce phénomène a certainement été amplifié par le fait que durant toute la durée du cycle végétatif les plantes ont reçu des irrigations fréquentes mais de faible intensité. Cette façon de procéder a contribué à favoriser le développement du système racinaire du blé prés de la surface et donc d'éviter qu'il n'aille prospecter la zone plus profonde où avaient été enfouis les radionucléides. Une façon de procéder similaire a été appliquée aux cultures de luzerne mais l'observation des résultats montre qu'au fil du temps la contamination des récoltes a augmenté. La raison est certainement due au fait que la luzerne qui est une palnte pluriannuelle a un système racinaire plus profond qui se développe tout au long de la durée de vie de la plante.

IV. Other research group(s) collaborating actively on this project [name(s) and address(es)]:

Institut de Recherches en Agronomie de Jülich (RFA).

Cette collaboration s'effectue avec Mrs. W.STEFFENS et W.MITTELSTAEDT.

V. Publications:

RADIATION PROTECTION PROGRAMME

Progress Report

1989

Contractor: Contract no.: BI6-B-325-F

Commissariat à l'Energie Atomique
CEA, CEN de Cadarche
B.P. n° 1
F - 13108 Saint-Paul-lez-Durance

Head(s) of research team(s) [name(s) and address(es)]:

Dr. A. Grauby
Département de Protection
CEN de Cadarache
B.P. 1
F- 13108 Saint-Paul-lez-Durance

Telephone number: 42.25.70.00

Title of the research contract:

Conséquences sur l'environnement d'un accident majeur sur centrale nucléaire: réhabilitation des sols et des surfaces (Programme RESSAC)

List of projects:

Conséquences sur l'environnement d'un accident majeur sur centrale nucléaire: réhabilitation des sols et des surfaces (Programme RESSAC)

Title of the project no: BI6-B-325-F

Conséquences sur l'environnement d'un accident majeur sur ceentrale nucléaire: Réhabilitaion des sols et des surfaces (programme RESSAC)

Head of project

Dr. André GRAUBY

Scientific staff

Henri MAUBERT
Philippe FACHE
Pierre RONGIER
André JOUVE
Michel MOUTIER
Michel HAMONIAUX
René ESCARIOT

Objective of the project

La mission du projet RESSAC est d'étudier les moyens techniques et leur mise en oeuvre pour une intervention dans les zones contaminées par un accident nucléaire majeur en vue de réhabiliter les surfaces pour les rendre à un usage normal. L'impact à court et long terme de l'accident doit être évalué, même dans les zones déjà soumises à réhabilitation. Cette prévision doit être basée sur la connaissance du comportement des radionucléides dans les sols et sur leurs transferts à la végétation en fonction du temps.

Ce contrat porte sur les essais globaux, c'est à dire la mise en oeuvre de lysimètres de grandes dimensions contaminés par un terme source représentatif d'un accident.

Objective for the reporting period

a. Concertation pour le choix des sols Européens pour les lysimètres.

b. Mise au point du prototype des lysimètres et démonstration de la faisabilité du prélèvement et des performances du système de régulation hydrique.

   Poursuite des travaux de qualification du générateur d'aérosols POLYR.

c. Avancement des études relatives au bâtiment et lancement des travaux.

Progress achieved

Point a.

La question du choix des sols a été évoquée en réunion du Comité Programme en Septembre 1989. Des rapports sur les méthodes utilisées en France et sur les sols choisis ont été distribués à tous les participants. Les organismes intéressés pour placer un lysimètre avec un sol choisi par eux dans le bâtiment RESSAC ont été invités à émettre des propositions. Une réunion dont le but est d'arrêter un choix est prévue pour le printemps 1990.

Point b.

La mise au point des lysimètres s'est faite par étapes. D'abord un prototype de 1000 mm de côté a d'abord été réalisé. Sur ce prototype on a testé le dispositif de régulation du potentiel hydrique. Le principe en est le suivant: Un tensiomètre est placé dans le champ près du lieu de prélèvement du lysimètre. Un autre tensiomètre est situé dans le lysimètre à une profondeur

équivalente. Les deux mesures du potentiel hydrique sont comparées et si une différence entre les deux valeurs est détectée une action sur la pression de l'eau dans le fond poreux du lysimètre est déclenchée de façon à rétablir l'égalité. Ce système travaille correctement (cf rapport joint), ce qui a montré la faisabilité de la régulation du potentiel hydrique.

Le prototype tête de série des lysimètres en grandeur définitive a été construit. Les dimensions du bloc de terre sont de 1800x1800x1400 mm. Un premier prélèvement a eu lieu sur les terrains du CEN de Cadarache. L'ensemble pèse 13 tonnes. Toutefois certaines limitations dans la qualité des terrains qui pourront être échantillonnés sont apparues: Il faut que les sols soient assez cohésifs pour que le bloc isolé par des tranchées ne s'écroule pas avant la mise en place de la cuve. Il faut d'autre part qu'il y ait relativement peu de pierres au niveau du fond du bloc, d'une part pour la faisabilité du découpage, d'autre part pour que le contact de la terre avec le fond poreux soit satisfaisant.

Ce lysimètre est en cours d'équipement pour vérifier le bon fonctionnement à cette échelle du dispositif de régulation hydrique.

Les travaux sur le générateur d'aérosols POLYR se sont poursuivis. L'émission des différents cops peut maintenant être considérée comme acceptable. En outre le procédé de transfert des aérosols vers les lysimètres a été modifié dans le sens d'un meilleur rendement.

Point c.

L'Avant Projet Définitif du bâtiment RESSAC a été accepté fin 1989. La construction devrait démarrer dans le premier trimestre de 1990 et les travaux dureront environ 18 mois. La réception des premiers lysimètres devrait pouvoir être réalisée à la fin de 1991.

Objective for the next reporting period

Une concertation avec nos collègues Européens devrait permettre de choisir un ensemble de sols devant être échantillonnés. En France 4 sites seront sélectionnés de façon à préparer les prélèvements.

Les performances du système de régulation du potentiel hydrique du lysimètre 1800 seront évaluées. Le coût et les conditions de la réalisation et du transport des lysimètres seront définis.

Une expérience de contamination d'herbe et de fourrages sera conduite en 1990. Ces matériaux contaminés seront fournis au centre nucléaire de MOL et à l'université de Piacenza.

La construction du bâtiment débutera et se poursuivra.

Other research group collaborating actively on this project

Dr. R. KIRCHMANN
Unité de Physique et de Chimie Analytique
Fac. des Sciences Agronom. de l'Etat
Avenue de la Faculté 8
B - 5800 Gembloux

Dr J. ROED
Health Physics Department
Riso National Laboratory
Postbox 49
DK - 4000 Roskilde

Publications

Internal reports:

M. MOUTIER; R. ESCARIOT; Conception, réalisation et essais de régulation de poteniel hydrique pour une maquette de lysimètre RESSAC (prototype 1000).

M. MOUTIER; Ph. FACHE; Les lysimètres RESSAC. Conception et contraintes de prélèvement. Sep. 1989.

P. RONGIER; Bilan des expériences POLYR. Déc. 1989

RADIATION PROTECTION PROGRAMME
Final Report

Contractor:

Natural Environment
Research Council
Polaris House
North Star Avenue
GB- Swindon SN2 1EU Wilts

Contract no.: BI6-B-038-UK

Head(s) of research team(s) [name(s) and address(es)]:

Dr E.I. Hamilton
Inst. Marine Env. Research
Prospect Place - The Hoe
GB- Plymouth Devon PL1 3DH

Telephone number: 0752/221.371

Title of the research contract:

The role of surfaces in the transport of radionuclides in the marine environment.

List of projects:

1. The role of surfaces in the transport of radionuclides in the marine environment.

Title of the project no.:

The role of surfaces in the transport of radionuclides in the marine environment.

Head(s) of project:

Dr. E.I.Hamilton,
1985-March 1989 Plymouth Marine Laboratory,Prospect Place,Plymouth,Devon PL1 3DH UK.
March 1989-December 1989 Phoenix Research Laboratory, Penglebe,Dunterton,Devon PL19 0QJ, UK.

Scientific staff:

1985-1986. Mr. R.J.Clifton, Miss H.E.Stevens
1986-1989. Mr. R.J.Clifton (until March 1989)
1989 Nil (since March 1989)

I. Objectives of the project:

Investigation and definition of the nature of important surfaces (physical,chemical and biological) which control the distribution of radionuclides in the marine environment. It is assumed that some surfaces are more suitable for the uptake of radionuclides than others; an objective is to identify the nature of such surfaces in relation to changes in redox state, pH and biological productivity in the retention, loss and recycling of radionuclides in estuaries,the near shore environment and the oceans.

II. Objectives for the reporting period:

Investigate the origins and properties of organoliths in order to evaluate their associations with radionuclides, especially alpha particle emitters.Examination of the composition of surface deposits to sediment grains by various microchemical methods. Process the Atlantic Ocean samples (n=320) in order to evaluate transfer of radionuclides from the ocean to nearshore waters and estuaries of the UK.To determine the process whereby radionuclides are transferred from surface waters to the deep ocean, ie the role of faecal debris and surfaces of detritus.Continue Chernobyl studies. Prepare a final report for the research project.

III. Progress achieved:

INTRODUCTION.

This contract has been concerned with the nature (physical,chemical and biological) of a variety of surfaces found in natural environments which are associated with radionuclides from natural and man made surfaces. Many radionuclides have a strong affinity towards such surfaces and they are important components in the transfer of radionuclides to man via food chains and inhalation. The prime objective of the research has been to determine whether or not any particular types of surface can provide a major route for transfer of radionuclides to man; also the extent to which changes, both short and long term (eg. 100-1000 years), in the availability of such surfaces are likely to influence the dose to man which is of direct concern to radiological protection.

From a consideration of classical concepts which have been developed in geochemistry, the partition of elements (and compounds) in natural systems, between solid and liquid phases, is related to such factors as ionic size, charge, ligand type and reactivity; for a solid it is an element's solid state chemistry which controls its behaviour in marine and terrestrial environments. The partition of elements (and compounds) between solids and liquids depends upon the nature and activity of surface ligands in terms of reflecting the composition of the solids, or the particular properties of their surface, eg. the presence of surface coatings; the dissolution of surface layers can lead to the formation of element depleted surfaces or the formation of surface precipitates by reaction between solid and liquid phases. Many surface deposits are in a state of disequilibrium; through the process of ageing structured crystalline forms can develop, for example the initial precipitation of amorphous silica, or calcium carbonate which with time undergoes crystallisation, eg amorphous calcium carbonate to aragonite to calcite. Ageing effects are important (eg for hydrated iron compounds). Initially the inorganic states are not pure ; in practice , in many environments, they interact with compounds in solution or become coated with organic material whose surface properties then control the subsequent surface exchange processes. Once fresh surfaces are exposed they provide sites for deposition of active biological species, eg bacteria, fungi and viruses. Biological metabolic processes are often very active in altering the nature of surface processes, ie the effect of biofilms. The surface of resistant minerals, such as quartz (often the most abundant mineral phase in sediments) can become etched through the action of various metabolic products . Redox changes effect ferrous-ferric reaction rates which can be significant at the air-water interface, or within particles which consist of inorganic debris encapsulated by decaying biogenic debris. In any natural system the most rapid changes take place at interfaces, eg air-water, water-solids where states of

disequilibrium exist. For systems which are cut-off from these extreme states the tendency is for some degree of equilibrium to be reached. In solid phases recrystallisation processes take place; those elements which are not accomodated tend to be excluded, eg in diagenetic processes. Therefore, because of the diversity of surfaces and surface processes in natural systems, this research project has placed emphasis upon attempting to identify the nature of naturally occuring surfaces, especially those which are associated with alpha emitters.

In relation to the original objectives of the research some changes in direction and emphasis have taken place, but not to the detriment of reaching the stated objectives. The changes are as follows:

a) Studies were implemented following Chernobyl in order to utilise the presence of radionuclides fallout associated with the surfaces of environmental materials.
b) The research was extended from estuaries and coastal waters to the open ocean in order provide a more comprehensive evaluation of the overall transfer processes. Perspectives concerning the relative radioactivity of natural sources of radiation, to those related to the nuclear industry was also studied. In relation to public concern it seems essential to understand more fully the contribution to dose from natural sources, over which there is often little control and then to compare them with the contribution received from man-made sources, eg see E.I.Hamilton,(1989), Terrestrial radiation-an overview. Radiat.Phys.Chem,34,pp 195-212.
c) In 1986 full time use of one member of the original research team was lost. In 1988, following the decision of the Natural Environment Research Council to identify environmental radioactivity as one of low priority, my post with the Plymouth Marine Laboratory was terminated. The CEC research was then transferred to the Phoenix Research Laboratory (PRL-founded in 1984) which only received the CEC contribution for 1989 , the rest being provided from resources of the PRL.

MATERIALS & METHODS. (see earlier reports for general methods)

The geographical areas studied were: Cumbria(NW England), which receives a variety of radionuclides derived from the reprocessing of nuclear fuels by British Nuclear Fuel plc,(BNF), Sellafield, Cumbria ,together with effluent containing uranium and daughter products from a nearby factory which manufacturers fertilisers. Special attention was paid to estuaries and coastal environments of the UK and the NE Atlantic Ocean. Materials (marine and terrestrial) studied included sediments, water, air particluates, fauna and flora. Particular studies included:
i) Extended use of the dielectric detector CR-39 for the quantitative evaluation of alpha particle emitters on surfaces. For purposes of comparison, measurements have been calculated in terms of alpha particles/cm2/sec-1 from thick sources, for exposures of between a few hours to 2.5 years

over which time fading of the etchable alpha track does not occur.Sources of background contamination were studied; GFC filters used for filtration of water samples have a background value of 3.0. E-5 alphas/cm2/s, compared with 2.0.E-6 for Millipore filters which prevents their use in these low background studies. The technique is used to determine the distribution of alpha emitters originating from conservative and non-conservative distributions associated with surfaces; to identify the position of hot particles on surfaces for subsequent removal for the analysis of individual alpha emitters by surface barrier spectrometry.

ii) A backscatter analyser was developed (4, 2mCi 242-Cm sources with a scattering angle of 174.5 degrees as used for the analysis of the surface of lunar sediments (see Turkevich et. al J.Geophys.Res. 72 (1967), 831-839.) This instrument has been used to identify the presence of C-N-O on the surface of sediments to a depth of 5-10 microns. Signals have also been obtained for the concentration of major elements such as Al,Si,Fe.Various problems have arisen in the manner of presenting the surface of the sample to the incident alpha beam as the depth to which alpha particles penetrate is only about 5 microns.

iii) High gradient magnetic separation techniques have been used to isolate hot particles together with various magnetic fractions from sediments. The technique offers the possibility of removing radioactive hot particles from technical effluents.

Preliminary studies have investigated the role of microbial metabolism in the formation of intracellular magnetic bodies (magnetite) and their role in bioreactor systems related to the removal of radionuclides from technical effluents and natural systems. Parallel studies, using sediment inoculations of micro magnetic spheres coated with a variety of surface materials, are proving to be valuable as probes in studying the composition of surfaces in relation to radionuclide uptake.

iv) A number of electrochemical techniques have been investigated to determine the concentration of uranium and related elements in small samples; overall the methods have not been useful for quantitative analysis, but have provided some data concerning the extent to which the elements are associated with organic bound substances.

v)Studies of element-radionuclide distributions in sediments by various sequential leaching methods have been abandoned. In brief, such methods have little value unless the distribution of the elements examined is known in relation to the composition of the sediment. Some studies showed that for bulk sediment no relation existed between the abundance of U,Pu,Am, Ce,Ru and Cs radionuclides and the concentrations of Fe,Mn. However, careful evaluation of the composition of the sediments clearly showed excellent correlations associated with 1-5micron Fe-Mn coatings on selected mineral phases . Because of the presence of macro components of iron and manganese debris, dissolution of such materials during sequential leaching totally swamps any association between Fe and Mn and radionuclides. Notwithstanding the use of Kd

factors in radionuclide monitoring and modelling, an extension of these studies has indicated a need to ignore the use of generalised global Kd values in furthering our understanding of the partition of radionuclides between liquid and solid phases in natural systems for specific geographical areas.

vi) An examination of surface area of various materials by the nitrogen method, and aqueous binding sites by protonation techniques, has shown that overall the surface area of estuarine and some marine sediments is not very large; surface area of unashed and ashed sediments decrease with depth; little change is observed for exchangable proton sites for either unashed or ashed sediment. However, failure to identify the nature of the variety of constituents of a sediment hinders the use of the methods. It has been shown that some minor phases have relatively high surface areas which are often associated with enhanced levels of radionuclides; some types of mineral debris are encapsulated in either ferruginous patinas or organic substances which then control uptake loss patterns of elements and radionuclides. Many of these materials are associated with seasonal changes, which in turn have been related to the observed seasonal differences in the uptake of a number of radionuclides by sediments.

vii) A major, albeit rather simple conclusion of this research is that unless far more attention is paid to what is being analysed, some bodies of data are in danger of being interpretated in relation to artifacts of methods and techniques rather than providing useful scientific information.

RESULTS & DISCUSSION.

The following examples illustrate some selected case histories in which the findings indicated above have been applied.

a) Studies in the Esk estuary Cumbria UK.

In an examination of large numbers of different sediments it was noted that despite considerable differences in their composition the relative abundance of most radionuclides remained constant, thus indicating the general labelling of surfaces according to an idealised Kd distribution control. Radioactive hot particles were quite distinct; some populations have been shown to consist of depleted uranium debris. In relation to the total alpha activity of the sediments the hot particles account for <10% of the total alpha activity, but there are some exceptions which are related to spatial and temporal factors. One common population of particles with enhanced concentrations of alpha activity covered a considerable range in size, eg from 1-2mm to <5microns MPD, but on the basis of surface alpha activity they were similar. During late 1987 until July 1989 new insitu sampling methods were deployed with the objective of carrying out separations in the field on fresh wet materials by various wet sieving and gravity separation techniques. For Esk silts these studies showed the presence of 0.5-2mm MPD particles which were concentrated in the low density phases of

sediment and for the time being they are called organoliths. The particles consist of average sediment coated with ,<5micron Fe-Mn deposits whose surface alpha activity is 10-100 times greater than the bulk activity which is similar to that for average sediment. The <65 micron fraction had the lowest surface alpha activity and the <500->106 micron fraction the highest levels of alpha activity- see Hamilton, Marine Pollution Bull, 20 (1989)587-589. Because of the high radioactivity of the coatings individual organoliths were analysed by direct surface-barrier alpha spectrometry or thin source preparations of the surface coatings which had been removed following treatment with dilute acids. The Pu/Am ratio varied between 0.3-3.0 indicating material of different age; some organoliths contain uranium and 210-Po. Sofar 820 organoliths have been examined and none are associated with discrete hot particles,ie the alpha radioactivity is diffuse. Various populations of particles have been observed; those which appear black have the highest,and those light brown in colour the lowest alpha particle activity. Although studies are still in progress the organoliths appear to be characteristic of the Esk and are believed to have an origin through mineralisation of small sections of protruding burrows of a locally abundant amphipod. The organoliths reflect processes involving redox changes which take place at the sediment-water interface proper. Their morphology and radioactivity appears to be related to seasonal changes-the highest abundance of particles occurs in late spring and the lowest in late winter. In relation to classical concepts of Kd (for the Esk silts) the derived Kd value is not related to general labelling of sediment surfaces, but rather the labelling of selected surfaces whose presence or absence will influence the overall Kd value. The mode of formation of organoliths is still under study together with their identification in other areas. If unique to the Esk a natural local origin seems remote; it is unlikely that they are related to the production of iron flocs when the BNF effluent enters the sea; it is possible that they may be related to waste product gypsum effluent from the fertiliser factory. Preliminary data for the isotopic composition of uranium, stable lead and rare earth element compositions are currently being considered in relation to the problem.

b) Radionuclide uptake , retention and loss by the common mussel.

This study has been described by Clifton et al Mar. Ecol. Prog. Ser. 54 (1989) 91-98. In brief, the radioactivity of total soft tissues of Mytilus edulis in animals from the Esk, Cumbria, which are contaminated with radionuclides from BNF,when transplanted to a area devoid of man-made radionuclides this resulted in an increase in the concentrations of 241Am in soft tissues over a period of 6 months. The transplant site contained relatively high concentrations of iron, copper, zinc and manganese (relative to the native Esk population) and provided conditions of stress which results in the dissolution of the inner nacreous

aragonite layer of the shell which provided the source for the 241-Am. Further studies showed that the rate of loss of radionuclides from the animal did not involve the induced presence of metallothioneins as a consequence of metal stress. Useful data were also obtained for the biological half-life of 241-Am,106-Ru and 137-Cs for actual versus theoretical derived values, based upon the steady state concentration of these isotopes. For soft tissues the time required to reach 80% of the steady state values for 241-Am, 239+240-Pu, 238-Pu 137-Cs and 106-Ru was 704,1644,557,90 and 606 days respectively. This data clearly identifies major problems when attempting to derive bioconcentration factors from short term laboratory experiments. The rate of uptake, and time to reach steady state conditions for radionuclides associated with shell was <60 days. An examination of alpha activity from Pu and Am in intracellular fluids for total soft tissue, kidney and digestive gland indicated that the major component was associated with the mitochrondria-nuclei fraction; uptake by lysosomes was less than that in the soluble cellular fraction. Research continues on the subcellular distribution of a number of radionuclides.

c) 210-Pb studies.

Polonium-210 has a very high affinity for surfaces; in an ongoing attempt to use polonium-210 concentrations for evaluating the relative ability of surfaces to absorb alpha emitting radionuclides , and some stable element analogues, the concentration and distribution of 210-Po in a variety of samples has been studied. Mussels from the Esk estuary Cumbria, and other populations (n=10), remote from sources of man made radionuclides, contain similar concentrations of 210-Po. Studies on total soft tissue, and 8 different organs and tissues, showed that the highest concentrations were associated with the kidney and pericardial gland; typical values (dry wt)are, total soft tissue 142Bg.kg, kidney 288Bq.kg and pericardial gland 668Bq.Kg which may be compared with concentrations of between 10-35Bq.Kg for estuarine sediments. The concentration of 210-Po on the surface of grass, lichens and moss within a 35km radius of BNF was similar to that found elsewhere in the UK, except near the fertiliser factory where they were related to the presence of solid phosphate ore dust on vegetation which contained c2000BkKg 210-Po and 130ppm U. Of more interest was the observation that samples of vegetation growing on coastal cliffs and in fields downwind of the factory contained significantly higher concentrations of 210-Po ; surface deposits of ore were absent. The effluent from the fertiliser factory passes via a pipeline into the NE Irish Sea just to the North of the BNF outlet.The effluent contains higher concentration of uranium and daughter products than are present in the BNF effluent and large amounts of waste-product gypsum containing 1100BgKg of 226-Ra which is fine grained and rapidly dissolves in seawater. Although still being investigated it is probable that as the gypsum dissolves , as it is transported in a southerly direction by inshore currents

radon-222 is released, together with particulate marine aerosol debris which is generated in the area and is enriched in 210-Po, and could provide a source for the 210-Po present on vegetation along the coastal strip. However, it should be noted that in the manufacturer of the fertiliser loss of 222-Rn and 210-Po via stack releases must occur, but within the study area deposition to the ground is not obvious. Various other stable and isotopic anomalies which are probably associated with the fertiliser factory rather than BNF continue to be studied.

It seems a reflection of the direction that radiological protection has developed that until quite recently many well known sources of radioactive materials present in the environment of natural origin have been neglected.

d) Uranium studies.

In relation to the 210-Po studies a comprehensive evaluation of the distribution of uranium in marine ecosystems has been initiated in relation to its association with surfaces. The overall objective is to account for the transfer of heavy radionuclides from the open ocean to nearshore waters in relation to the disposal of radioactive wastes to the sea and coastal waters.

i) In the coastal waters off Cumbria the presence of small quantities of depleted uranium and 236-U which can be leached from the surface of sediment debris, together with hot particles, indicates inputs from BNF. Although the well known relationship between dissolved uranium concentrations in seawater and salinity is confirmed, interest centres upon the 234U/238U ratios. Within the region nearshore waters can contain slightly excessive concentrations of dissolved uranium. Overall the tendency is towards an enrichment in 234U relative to 238U; maximum values of 1.387 for the 234U/238U ratio have been obtained which are not related to concentrations of dissolved uranium. The source of the excess uranium and 234U may not be related to BNF effluents, but rather inputs from the fertiliser factory. There is also an indication that perhaps an additional source of uranium may be derived from a factory at Springfields (South of the Esk) where uranium fuel elements and uranium hexafluoride are manufactured. The 234U/238U ratio is being used to evaluate the contribution of uranium from either terrestrial or marine sources.

ii) A slight enrichment in dissolved uranium is observed at the edge of the continental shelf and at the mouths of rivers, eg. Tamar (Devon), Thames and Rhine complex. Analysis of suspended particulates in seawater from 19 stations by the fission track and delayed neutron methods indicates normal values of between 0.9-2.9ppmU, but with values of between 5ppmU and 8ppmU off the Rhine and Thames respectively. In all filtered particulate matter the concentration (particles/litre seawater) of uranium in hot particles has been determined ; the highest numbers being found in parts of the Irish Sea and

the Dover Straits-Thames estuary region. Mean particle diameters (n=343) range from 4-70microns with maxima at 14, 24 35 and 42 microns. The mean concentration of uranium in individual hot particles for the various stations varies from 451ppmU to 24157ppmU. Apart from samples from the Irish Sea scanning electron microprobe studies of the particles indicate that most consist of small grains of zircon, and other naturally occuring radioactive minerals, which is compatible with the measured concentrations of uranium. The abundance and distribution of uranium minerals in the environment is important to radiological protection in providing a much firmer basis for evaluating exposure to man from radon. In one separate study trace amounts of reduced iron were floculated from filtered seawater; it was expected that no iron, beyond that in particulate form would be removed;in practice uranium was removed with the iron precipitate and the highest amounts were associated with samples from bays, estuaries and the mouth of rivers. This study is being continued in relation to speciation of uranium in natural waters.

d)The radioactivity of lakes.

The depositional history of radionuclides present in five Cumbrian lakes is being evaluated. The chronological sequence of deposition over the last 2000 years, at least, is well documented, hence suitable time markers are available against which deposition of radionuclides can be evaluated. This study has been started in order to provide information for the long term history of radionuclide deposition in relation to climatic and other changes of the region. Using CR-39 , radionuclide distributions in core profiles have been undertaken for insitu emplacement v laboratory exposures; good agreement has been obtained and effects related to the presence of radon and thoron emanation are insignificant. The BNF total alpha particle signal is preserved in sediments; BNF hot particles are absent , but they are found around the margins of the lakes, hence they do not survive transport to the bottom. Sedimentation rates of 1-2mmy are common for these lakes. I observe significant (higher and lower) changes in the deposition of alpha emitters since 1753 than occur today. Similarly, the concentration of uranium shows similar types of variability some of which may be related to changes in land use eg. differences in surface retention patterns, and climate. Of more interest is the possibility that because of changes in land use, linked to climatic change, the redox conditions of the watershed may have changed, hence altering the availability and speciation of radionuclides and elements. These valuable and unique bodies of data have a bearing upon the long term modelling of radionuclide behaviour in terrestrial and nearshore waters and estuaries are of some importance to radiological protection.

e) Chernobyl.

Thirteen radionuclides present in Chernobyl fallout have been examined in diverse natural systems, eg terrestrial, estuarine

marine and lake sediments, ombotrophic peats, air particluates,rain, grass, lichens, mosses,household dust, sheep thyroids and thymus. The Chernobyl cloud covered SW England and most features of deposition were similar to those found in Cumbria which received higher levels of fallout. At the time of the accident local scientific communities showed little interest in the use of the acute spike to study important natural processes, but more concerning potential hazards from the fallout. The presence of local surface mining of clay minerals,eg kaolinite from fluorine decomposed granite, appears to have resulted in local retention of Cs radionuclides. Trace amounts of 241-Am appear to have been deposited after the main deposition of debris.Overall the most interesting feature of the Chernobyl debris is its presistence on surface deposits via resuspension. This feature continues to be studied in high and lowland lakes of the area in order to evaluate resuspension features and washout factors. Albeit low, the deposition of Chernobyl debris throughout SW England should provide a valuable data base and highlight those areas within the region which are likely to be of concern should the region be subjected to fallout from any future accident. Apart from obtaining useful data relating to deposition of radionuclides on surfaces, of direct relevance to the CEC research, the studies have also identified the importance of variability in ground cover in relation to retention of radionuclides.

f) Open ocean studies.

A laboratory (PRL) together with the essential methodology has been developed for the study of low activity materials.CR-39 methodology has been quantified. Alpha particle emissions from samples from the NE Atlantic are mainly from 210-Po and 226-Ra.Studies are made on sediment, suspended particulates, biota (phytoplankton,zooplankton,Thaliacea, Crustacea and fish eg Myctophidae, Sternoptchiidae, Cyclothone etc.). Special attention is paid to gut contents and faecal debris, either by direct samping or following extrusion after incubation on board ship. Samples from the water column are collected from 5m to 3,000m together with bottom sediments. After two years of preliminary investigations most operational problems have been overcome. Some preliminary findings are :

i) For biota the gut contents usually contain 10E0-E3 more alpha activity than are found in muscle tissue. Highest concentrations of activity are found in the hepatopancreas of Crustacea and the livers of fish.
ii) Over a depth of 2500m the alpha activity of faecal debris in gut materials and faecal pellets during the period of maximum productivity, is a factor 10E2-E3 higher than three months later ; for both states the specific activity of faecal debris decreases with depth in the water column by a factor 4.
iii) Salps have median levels of alpha activity, but because of their abundance they are important in the transfer of radioactivity in the oceans; interest centres upon the region where seasonal mortality is high, ie extreme NE Atlantic.

Radiolaria , especially the Acantharia, contain 226-Ra; because of their forms they are easily recognised as free bodies or when present in faecal debris.
iv) 210-Po concentrations in many forms of biota are high; total concentrations in shrimps (dry wt) range from 2-20Bq.g dry wt for whole animals; values of 100->200Bq.g are found in the hepatopancreas of some crustaceans. For all samples of marine biota the distribution of alpha particles is diffuse and hot particles are not present.
v)Characteristics of the alpha particle activity of different types of seawater can be identified, eg. nephloid layers originating from the continental shelf have higher activity than surrounding water; deep inflow of Mediterranian water into the mid-Atlantic can be recognised and confirmed on the basis of salinity and carbon values.
vi) Sediments at 2000m water depth for post bloom times contained a 5-8cm layer of sediment which is totally mixed and contains high concentrations of 226-Ra and 210-Po relative to deeper layers.Within this deposit foraminifera tests concentrate at the surface ; these sediments show enhanced losses of 222Rn . On the basis of the radioactivity of the top c5cms of sediment when compared with deeper layers , very little of this activity remains to form part of the permanent sedimentary record.

An overall conclusion from this research is that in the open oceans radioactive alpha emitters are transferred to bottom sediments through transfer by an association with faecal debris; for near shore waters the main transport pathways are associated with resuspension of bottom sediments.

THE SIGNIFICANCE OF RESULTS TO THE RADIOLOGICAL PROTECTION PROGRAMME.

1. The bioavailability of radionuclides which are associated with particular,and geographicaly restricted regions, need to be evaluated in relation to transfer of radionuclides from the natural environment to man. The use of globaly derived Kd values need to be reconsidered for near source regions when radionuclides are associated with particular types of surfaces. The practical value of sequential leaching studies and short term laboratory measurements of bioconcentration factors has limitations in relation to the needs of radiological studies.

2. The concentration and distribution of naturally occuring radionuclides need to be compared with those which are derived from the nuclear industry for environmental states over the past 50 years and the next 500-1000 years, including the the possible effects of climatic change on availability of radionuclides

3. A new large scale use of alpha particle distributions in natural systems has been validated. Applications which are pertinent to radiological protection include spatial and temporal transfer of radionuclides over large distances and through diverse ecosystems in an economic manner.

IV. Other research group(s) collaborating actively on this project [name(s) and address(es)]:

Informal collaboration in the form of discussions and an exchange of ideas on matters relating to the research have been maintained throughout the contract period with: MAFF Directorate of Fisheries Research, Lowestoft, UK, namely Dr. R.J.Pentreath, Dr. Dr. D.S.Woodhead and Dr. P. J. Kershaw; CEC Joint Research Centre, Ispra (Varese) Italy, namely Dr. E. Sabbioni.

V. Publications:

Hamilton, E.I. (1986). Kd values:an assessment of field v laboratory measurements. In-Application of Distribution Coefficients to Radiological Assessment Models; eds. T.H. Sibley and C. Myttenaere. Elsevier Sci. Pub. Amsterdam, pp 35-59.

Hamilton, E.I. and R.J.Clifton (1986). Geobiological cycling of long-lived radionuclides: an overview. CEC Workshop, Madrid (in press)

Hamilton, E.I., Zou, B. and R.J.Clifton (1986). The Chernobyl accident-radionuclide fallout in SW England. Sci. Total Environ. 57, pp231-251.

Hamilton, E.I. The Periodic Table of the elements:geochemical and biochemical associations. In- Pollutant Transport and Fate in Ecosystems; Special Pub British Ecological Society, No.6; eds. P.J.Coughtrey, M.H.Martin and M.H.Unsworth. Blackwell Sci. Pub. Oxford.(1987), pp 5-33.

Hamilton, E.I.(1988) Geobiocoenosis: the chemical elements and relative abundances in biotic and abiotic systems. Sci. Total Environ. 71, pp253-267.

Clifton, R.J., Stevens,H.E. and E.I.Hamilton (1989). Uptake and depuration of 241-Am, 239+240-Pu, 238-Pu, 137-Cs and 106-Ru by Mytilus edulis under natural stress. Mar. Ecol. Prog. Ser. 54, pp 91-98.

Hamilton, E.I. (1989). Radionuclides and large particles in estuarine sediments. Mar. Poll. B. 20, pp 603-607

RADIATION PROTECTION PROGRAMME
Final Report

Contractor:

Nat. Environment Research Council
Polaris House, North Star Avenue
GB- SWINDON, Wiltshire, SN2 1EU

Contract no.: BI6-B-233-UK

Head(s) of research team(s) [name(s) and address(es)]:

Dr. O.W. Heal
Merlewood Research Station
Institute of Terrestrial Ecology
Grange-over-Sands
GB- Cumbria LA11 6JU

Telephone number: (04484) 2264

Title of the research contract:

The Relationship between Soil Organic Matter and the Actinide Elements

List of projects:

1. The Relationship between Soil Organic Matter and the Actinide Elements.

Title of the project no.:

SUMMARY REPORT: THE RELATIONSHIP BETWEEN SOIL ORGANIC MATTER AND THE ACTINIDE ELEMENTS

Head(s) of project:

F R LIVENS

Scientific staff:

D L SINGLETON

I. Objectives of the project:

Isolation, on a relatively large scale, of actinide-enriched organic matter fractions from a soil in which substantially elevated levels of the actinides occur.

Physico-chemical characterisation of these fractions by gel filtration, solvent extraction, ultrafiltration and other appropriate techniques.

II. Objectives for the reporting period:

To conclude the experimental work, to collate and interpret the results, to prepare a final report and papers.

1 Isolation of humic and fulvic acid fractions

Humic and fulvic acid fractions were isolated from a gley soil in which substantially elevated levels of plutonium and americium (5-10 kBq kg^{-1} dry wt $^{239,240}Pu$ and comparable ^{241}Am activities). The soil was extracted with alkali and the humic and fulvic acids separated by conventional precipitation, dialysis and freeze-drying procedures.

The actinide recoveries and the specific activities of the fractions isolated are presented in Tables 1 and 2.

Table 1: Plutonium balance calculation

Input	Bq	Recovered	Bq
600 g wet soil at 2860 Bq kg^{-1}	1720	12.4 g humic acid at 27400 Bq kg^{-1}	340
		5.4 g fulvic acid at 6860 Bq kg^{-1}	37
		40 l dialysable fulvic acid at 0.65 Bq l^{-1}	26
		Extract residue	1300
Total	1720		1703

Table 2: Americium balance calculation

Input	Bq	Recovered	Bq
600 g wet soil	1590	12.4 g humic acid at 18600 Bq kg^{-1}	230
		5.4 g fulvic acid at 6100 Bq kg^{-1}	33
		40 l dialysable fulvic acid at 1.05 Bq l^{-1}	42
		Extract residue	1270
Total	1590		1575

The proportions of plutonium and americium extracted are almost identical (23%) but their distribution between fractions is not (Figs 1 and 2). There are two possible explanations for the differing $^{239,240}Pu/^{241}Am$ ratios (1.48 in humic acid, 1.12 in fulvic acid and 0.62 in dialysable fulvic acid). One is that the plutonium and americium have been in the soil for different times and a gradual 'ageing' process within the soil has thus acted on the two elements for different periods. This, in turn, would imply that plutonium/americium discrimination occurs during the transport of contaminated material from the discharge point to the soil. The alternative explanation is that the observed differences reflect different reactions of plutonium and americium with humic materials.

Since the $^{238}Pu/^{239,240}Pu$ ratio in the Sellafield effluents has increased over time to a modern value of about 0.3, then 'pools' of different ages would be expected to have different $^{238}Pu/^{239,240}Pu$ ratios. Since the $^{238}Pu/^{239,240}Pu$ ratio is constant within error, at 0.24, in all the fractions, this suggests that the actinide content of the soil represents a single input, of uncertain duration, and the widely varying $^{239,240}Pu/^{241}Am$ ratios must reflect differences in the soil chemistry of the two elements.

2 Separation of humic and fulvic acids by gel filtration

A considerable amount of effort was devoted to improvement of the gel permeation procedures used in the preliminary studies (Livens *et al.*, 1987). Both Sephadex (Pharmacia) and Fractogel (Merck) media were evaluated under a variety of flow rates, pressures and column heights. The best separations were obtained on Sephadex G-100 for humic acid and G-50 for fulvic acid. Sorption to the gels is an insuperable problem, but can be minimised by careful control of flow rate and correct choice of gel. Nevertheless, 5% of the humic acid and 2% of the fulvic acid was irreversibly adsorbed.

After optimising the gel permeation method, good separations of both humic and fulvic acids were obtained (Figures 3 and 4). The specific activities of the fractions isolated are presented in Table 3.

Table 3: Fractions isolated by gel permeation chromatography

Fraction	% of sample	$^{239,240}Pu$ (Bq kg^{-1})	^{241}Am (Bq kg^{-1})
Humic acid (high mw)	43	39500	26400
Humic acid (low mw)	52	9480	10400
Fulvic acid (high mw)	57	7220	5380
Fulvic acid (low mw)	41	5520	7080

3 Solubility in organic solvents

The technique employed here is an extension of that developed by Vos *et al.* (1983), in which soils were treated with organic solvents, roughly in order of increasing polarity. There is much difficulty in the interpretation of such results, since inorganic soil components may also be dissolved. The application of this scheme to isolated organic fractions should, however, yield more easily interpreted results. Both humic and fulvic acids were extracted with a series of solvents in a Soxhlet apparatus.

The results are shown in Tables 4 and 5.

Table 4: Solubility of humic acid in Soxhlet extraction

Fraction	Wt %	% Pu	% Am
Hexane	2.0	0.05	0.04
Ether	<0.1	0.01	0.02
Ethyl acetate	<0.1	0.02	0.02
Methanol	32.0	4.50	4.60
Acetic acid	<0.1	0.40	0.40
Undissolved	66	95.10	94.90

Table 5: Solubility of Fulvic acid in Soxhlet extraction

Fraction	Wt %	% Pu	% Am
Hexane	0.3	0.02	0.01
Ether	<0.1	0.01	0.02
Ethyl acetate	<0.1	0.01	0.01
Methanol	2.4	1.1	1.0
Acetic acid	34	24.4	23.7
Undissolved	63	74.5	74.9

Only methanol and acetic acid dissolve significant amounts of sample material. Methanol is more effective at dissolving humic acid, but acetic acid dissolves a substantial part of the fulvic acid. The relative solubility of humic acid in methanol and acetic acid is a reflection of the chemical nature of the samples since reversal of the order of extraction has only a small effect on the distribution. Fulvic acid, on the other hand, is sensitive to the order of extraction. Extraction with acetic acid before methanol removes a large part of the methanol-soluble fraction as well.

These observations are in keeping with the known reactions of humic materials with organic solvents. The small amount of sample dissolved in the first three extractions reflects the low abundance of non-polar components, such as fats, waxes and resins, in the samples. This is not surprising, since the preparation procedures employed to isolate the humic materials will alter the lipid fraction by hydrolysis, esterification and saponification, rendering them water soluble. Thus, if this fraction does occur in the original soils, it is likely to be lost in the preparation and isolation procedures.

The methanol-soluble fraction of the humic acid corresponds to hymatomelanic acid. This has been interpreted as being a partially oxidised and hydrolysed humic fraction (Kononova, 1966), although there is some dispute as to whether it is formed in the soil or during extraction and fractionation. Chemically, hymatomelanic

acid fractions and their parent humic acids are similar in character. The acetic acid soluble fraction probably represents the products of acid hydrolysis. These are believed to arise from lignin impurities (Jakob *et al.*, 1963) and from hydrolysis of functional groups on the periphery of the aromatic 'core' of the molecule. The solubilisation of only a small part of the humic acid in acetic acid supports this view. Nevertheless, the solution of a significant, but minor, part of the actinide activity in acetic acid may represent leaching of metal ions in bridging or peripheral positions or in inorganic impurities such as oxides and clays.

The solubility pattern of fulvic acid also conforms to that seen by other workers. These are much more prone to acid hydrolysis than humic acids (Haworth, 1971; Schnitzer, 1972). In particular, total acidity and carboxylate concentrations decreased, accompanied by dissolution of much of the sample. The E_4/E_6 ratio (the ratio of the absorbances at 465 and 665 nm, often used as an index of molecular condensation) decreased on hydrolysis, suggesting that a more condensed structure was formed. This, together with the extensive dissolution of the sample, can be interpreted as a removal of functional groups held by hydrolysable links such as carboxylate or nitrogen-containing groups.

4 Separation of clay-humate aggregates

This procedure was developed by Lowe and Klinka (1981) and is based on the differential flocculation of large clay-organic aggregates and smaller organic species. The samples are dissolved, then the electrolyte concentration adjusted to precipitate the clay-humate particles, and they are separated by centrifugation. The results are presented in Table 6.

Table 6: Distribution of organic matter, Pu and Am between humate and clay-humate fractions

Fraction	Organic material (%)		$^{239,240}Pu$		^{241}Am
		%	Bq kg^{-1}	%	Bq kg^{-1}
Humate	82	47	15700	36	8200
Clay-humate	18	53	78900	64	64400

Clearly there is a substantial concentration of actinides into the clay-humate fraction, resulting in a very high specific activity. About half of the plutonioum is found in each fraction, whilst a rather greater proportion (about 2/3) of the americium is found in the clay-humate. There is again a discrimination between plutonium and americium. The humate fraction has a $^{239,240}Pu/^{241}Am$ ratio of 1.9, compared with 1.2 in the clay-humate.

The specific activities, element ratios and relative abundances of these fractions differ considerably from those of any humic fractions isolated by gel filtration. This suggests that the two procedures are not fractionating the samples in the same way, even though it might be expected that physical size of the clay-organic species would lead to their forming the 'high molecular weight' fraction in the gel filtration experiments. This may, in fact, be the case, but if it is, there is also a high molecular weight component of the humic acid which does not flocculate with the clay-organic fraction.

5 Summary

These experiments have shown that it is possible to isolate, from a contaminated soil, humic and fulvic fractions with specific

activities much greater than those in the soil from which they are derived. In particular, the humic acid fraction has activities four to five times higher. Humic and fulvic acids can each be separated into two fractions of differing nominal molecular weights using gel filtration chromatography. Plutonium and americium are not distributed uniformly throughout the fractions isolated, with the $^{239,240}Pu$ ratio decreasing in the order:

High m.w.humic > High m.w.fulvic > Low m.w. humic > Low m.w. fulvic

High humic acid is partially soluble in methanol (the hymatomelanic acid fraction), but relatively little actinide activity is associated with this component. No other organic solvents used dissolved significant amounts of sample material or extracted much actinide activity. A similar pattern is seen with fulvic acid for all solvents except acetic acid, which hydrolyses the sample, dissolving about 35% and extracts a significant quantity of plutonium and americium.

There is a pronounced concentration of the actinides into the 'clay-humate' fraction, isolated by flocculation, although the unflocculated fraction holds 35-50% of the total actinide inventory by virtue of its abundance. Neverthless, the 'clay-humate' fraction does not correspond to the high molecular weight humic fraction isolated by gel filtration.

This summary is based on a full account of this project which is available from the authors at Merlewood Research Station,

Grange-Over-Sands, Cumbria, LA11 6JU, England.

6 Acknowledgements

We would like to thank the staff of the chemistry section for their help with iron analysis and UV spectrometry and other colleagues at Merlewood for their advice. This project was partially funded under the CEC Radiation Protection Programme (Contract B16.0233.UK).

7 References

Haworth, R.D. (1971). The chemical nature of humic acid. Soil Sci, 111, 71-79.

Jakob, T., Dubach, P., Mehta, N.C. & Deuel, H. (1963). Decomposition of humic substances. III. Decomposition with alkali. Z. Pflanz. Bodenk., 102, 8-17.

Kononova, M.M. (1966). Soil Organic Matter. Pergamon Press.

Livens, F.R. & Singleton, D.L. (1989b). An evaluation of methods for the radiometric measurement of americium in environmental samples. Analyst, 114, 1097-1101.

Livens, F.R., Baxter, M.S. & Allen, S.E. (1987). Association of plutonium with soil organic matter. Soil Sci., 144, 24-28.

Vos, H.A., Williams, G.A. & Cooper,, M.B. (1983). The speciation of radionuclides in sediments and soils. Part II. Studies with a sequential organic extraction procedure. Australian Radiation Laboratory Report ARL/TR 058.

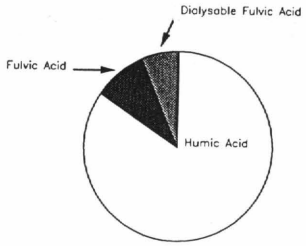

Fig. 1: Plutonium held in organic fractions

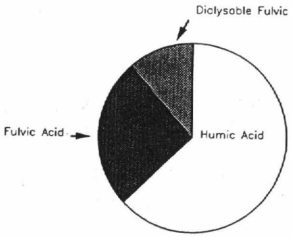

Fig. 2: Americium held in organic fractions

Fig. 3: Elution of humic acid and actinides from G−100

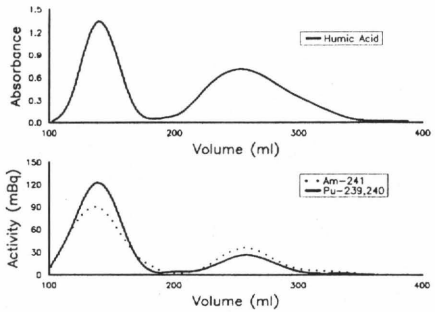

Fig. 4: Elution of fulvic acid and actinides from G−50

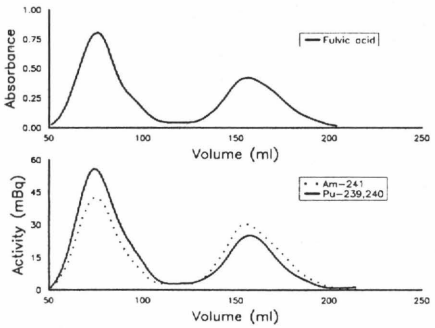

IV. Other research group(s) collaborating actively on this project [name(s) and address(es)]:

V. Publications:

F R LIVENS. Chemical Reactions of Metals with Humic Materials. Submitted to Science of the Total Environment.

F R LIVENS & D L SINGLETON. Plutonium and Americium in Soil Organic Matter. Submitted to J. Environmental Radioactivity.

RADIATION PROTECTION PROGRAMME
Final Report

Contractor:

University of Aberdeen
Regent Walk, Aberdeen
AB9 2UE Grampian, Scotland

Contract no.: BI6-B-318-UK

Head(s) of research team(s) [name(s) and address(es)]:

Dr. B. Heaton
Dept. of Bio-Medical Physics
University of Aberdeen
Regent Walk, Aberdeen
AB9 1FX GRAMPIAN, Scotland

Telephone number:

Title of the research contract:

The Dynamics of Caesium-137 from Chernobyl in Upland,Peat Moorland Ecosystems

List of projects:

1. The Dynamics of Caesium-137 from Chernobyl in Upland, Peat Moorland Ecosystems.

Title of the project no.: The Dynamics of Caesium -137 from Chernobyl in Upland, Peat Moorland Ecosystems.

Head(s) of project: Dr B. Heaton
Dr K. Killham

Scientific staff: University of Thessaloniki
Dr D. Veresoglou
University of Aberdeen
Mr R. Mitchell

I. **Objectives of the project:** To identify the mechanisms controlling the uptake/release of Caesium -137 from peat based soils. By using peat soils in Northern Scotland and Northern Greece a broad model can be prepared to cover a wide range of climatic conditions. In both areas field measurements will be used in conjunction with wide ranging laboratory experiments using intact peat/vegetation microcosms. In the latter experiments the controlled variation of different parameters will allow the effect of individual mechanisms to be identified.

II. **Objectives for the reporting period:** The field monitoring program in Northern Scotland was to be continued and a field monitoring program in the Fillipi basin in Northern Greece started. The soil characteristics of both areas were to be compared. Laboratory based experiments, using artificially contaminated peat/vegetation microcosms, were to be constructed and measurements made identifying the effect of animal waste, urea, climatic cycling and cropping rates on the release/uptake characteristics of the caesium -134 in the microcosms.

III. Progress achieved: Materials and Methods

a) Field monitoring.

Field techniques developed at Aberdeen for monitoring caesium movement in peat moorland systems were used in this study. Duplicate cores (in PVC tubes of 6.4cm diam., 40cm depth of peat/vegetation) were taken from four sites in the Northern Scotland and from six sites in the Phillipi peat basin of north eastern Greece. All sites were chosen with gradients of less than 1 in 20. The cores from the Scottish sites were taken from areas of perennial grass, largely Festuca ovina. Most were open moorland but one was from a walled enclosure. The cores from Greece were taken from arable fields and their headlands.

The cores were taken back to the laboratory, and frozen until sectioning was to be carried out. The cores were pushed out of the tube with a piston and cut into sections 10-15 mm thick with an electrically-driven sectioning knife. A scalpel was employed to assist in the cutting of roots and fibrous vegetation in order to minimise distortion of the core section. Each sample was left in a stream of air at room temperature to dry.

The peat samples from each section was mixed and compressed into containers. The radionuclide contents were analysed using an Ortec Intrinsic Germanium Coaxial Detector and efficiency calibrations carried out using N.P.L. trace radionuclide standards. Radionuclide concentrations were corrected to give the values at time of sample collection.

Grass and vegetation was cut from the area immediately above each core. Oven-dry weights of peat cores were determined to obtain bulk densities. All activities were subsequently expressed on a unit volume basis in order to facilitate comparison of caesium distribution at different sites.

b) The Laboratory Microcosm Study.

Peat cores (7.5cm diam; 50cm depth) sampled from close to Aberdeen were brought back to the laboratory. The vegetation (above and below ground) was removed prior to seeding with

Festuca ovina, a perennial grass of common occurrence on peat moorlands. Once the grass sward was established, caesium-134 was applied in solution (CsCl) at a rate equivalent to 50kBqm^{-2}. This is approximately one order of magnitude greater than was deposited on northern Scotland as a result of Chernobyl. The solution was applied by nebuliser to simulate a rainfall event using techniques developed in Aberdeen. After application of caesium, a number of treatments were applied to the cores to attempt to identify factors affecting caesium mobility: 1) Application of sheep dung at a rate equivalent to a low and high grazing density. The dung was homogenised and the low and high treatments corresponded to a total N application of 0.09 and0.18 g N m^{-2} respectively. A control, where distilled water was added in the same volume as the dung, was also included; 2) Application of urea at low and high rates, corresponding to the same N applications as the dung treatments: 3) Freeze (-8^{o}C)/thaw of the cores involving a single freeze/thaw cycle at the onset of the experiment, and 5 cycles, one every 10 days for the first 50 days of the experiment; 4) Cropping of grass to 1 cm ata low rate (every 10 days), at a high rate (every 5 days), and at control rate (every 25 days). Apart from the cropping experiment, all cores were cropped every 25 days. All cores were watered gravimetrically to their original water potentials at 10 day intervals over a total period of 100 days.

Sectioning of the peat cores and sample preparation for subsequent analysis of caesium was carried out as described for the field cores. Counting was carried out on a NaI well counter.

RESULTS

Although pre-Chernobyl Cs-137 levels in the profile were only known for one site the Cs-134/Cs-137 ratio was used to calculate the Chernobyl derived Cs-137 for the other sites. An initial ratio of 2 was assumed with subsequent corrections being applied to take into account the Cs-134 decay. On one site in Northern Scotland a contribution from wind blown

caesium-137 from waste sea discharges was possible.

Some important physiochemical and biological properties of one of the Scottish and Greek peat samples are shown in Table 1. These data illustrate the acid, base-poor status of the Scottish blanket peats and the high base status of the near neutral Greek basin peats. The Greek peats also have a much higher mineral content.

TABLE 1.

Properties of the Scottish and Greek Peats.

Scotland	Greece
Uncultivated	Cultivated
Blanket Peat	Sedge Peat
Oligotrophic, base poor,	Eutrophic, base rich,
percentage base saturation.	percentage base saturation.
27.3%	64.29%
Cation exchange capacity	Cation exchange capacity
19.19 meq/100g	29.17 meq/100g
pH: 3.07	pH: 5.7
Organic Matter Content:68.49%	Organic Matter Content: 17.36%
Available ammonium:0.24meq/100g	Available ammonium:1.32meq/100g
" potassium:1.604meq/100g	" potassium:2.32meq/100g
" nitrate: 0.0102meq/100g	" nitrate: 2.32meq/100g
Water content: 79.6%	Water content: 61.43%
Bulk Density: 22.78 mg/cm^3	Bulk Density: 56.33 mg/cm^3
Rooting Density: 52.28mg/g soil	
Soil/Animals: 83 mite/kg	Soil/Animals: 22nematodes/kg
8 springtails/kg	6 enchytraeids/kg
4 enchytraeids/kg	2 spiders/kg

Radiochemical analysis of the peat cores sampled from Northern Scotland revealed a clear pattern in terms of caesium distribution. Much of the Chernobyl-derived caesium-137 remained in the top 10 cm of the peat and in the vegetation (Figure 1) sampled from Carbreck, Sutherland. Similar patterns were also found for the three other sites in Northern Scotland (Data not shown.) Of the original Chernobyl deposition, it was estimated that approximately 73% has remained in the top 10 cm of the peat profile at these sites.

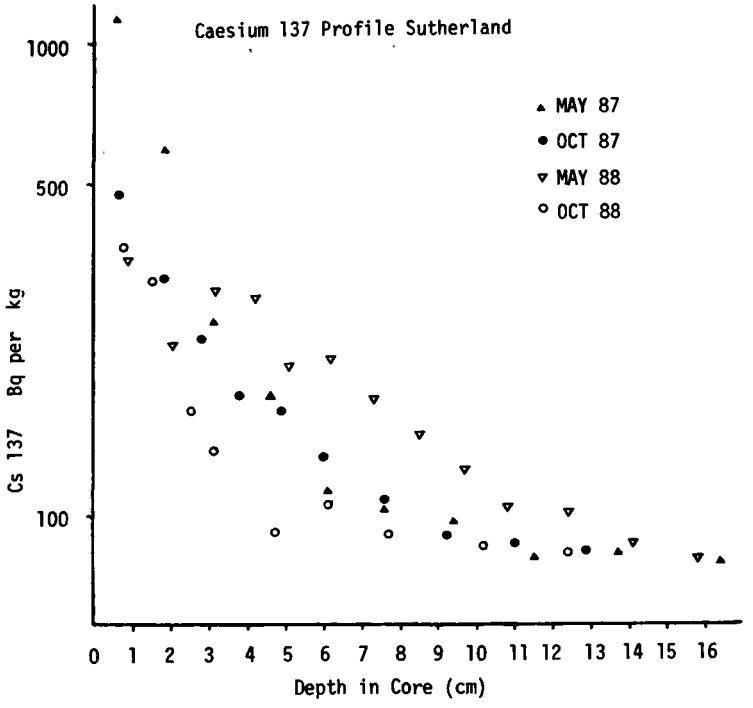

Figure 1.

Analysis of peat cores sampled from the Phillipi basin of north east Greece demonstrates a similar pattern of volume distribution of caesium to that of Northern Scotland. Approximately 78% of the Chernobyl derived caesium was detected in the top 10 cm although little was detected in the vegetation(fig2)

Whether the caesium lost from the peat samples of Greece and Scotland was removed as plant offtake or was leached beyond the rooting depth is uncertain as no samples of vegetation or peat were taken during the year following Chernobyl.

To provide some preliminary indication of the factors most likely to mediate the cycling of caesium in the Scottish peat moorlands, simple correlation tests were carried out between caesium distribution data and certain key plant/soil parameters (Table 2.) These tests showed strong correlations between caesium distribution and both rooting density and the population density of soil animals.

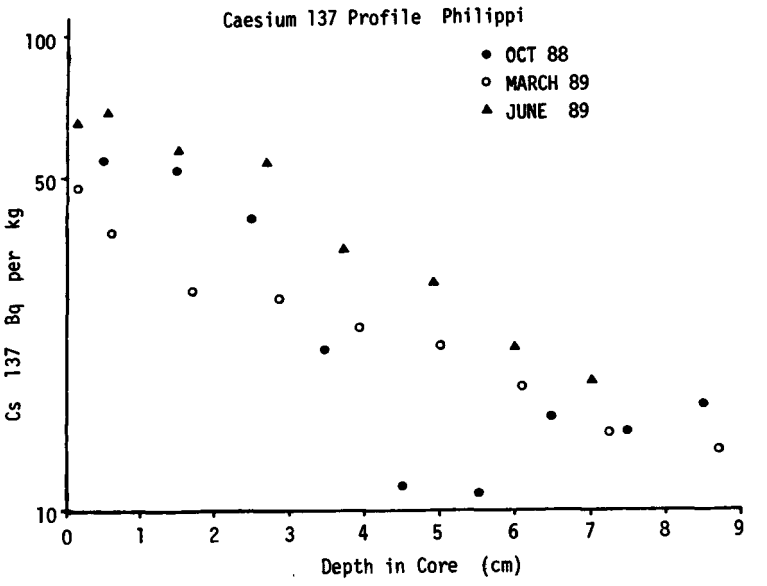

Figure 2.

TABLE 2.

Correlation coefficients (r^2) between caesium activity per unit volume of peat and a number of physicochemical and biological properties.

Property	r^2
pH	0.777
% Organic matter	0.092
Cation exchange capacity	0.106
% Base saturation	0.561
Available ammonium	0.403
Available nitrate	0.050
Available potassium	0.587
Root Density	0.948
Soil animal population density	0.952

DISCUSSION

The high transfer ratios of caesium from soils to roots, particularly for ericaceous species, is the probable reason for the strong relationship between root density and caesium distribution. The relative rapid turnover of root systems

however makes the identification of live and dead roots difficult. Clearly vegetation, through its capacity of root uptake of caesium (and its analogues such as potassium) will play an important role in caesium retention/cycling in peats. Mycorrhizal root infection, enabling greater scavenging for scarcely available nutrients, may also result in enhanced caesium offtake by plants.

A relationship between soil animal and caesium distribution is likely since both microbial and faunal populations of soils will regulate the turnover of organic matter, releasing nutrients as well as caesium. Once in soil solution, these nutrients will become available for both plant uptake and leaching, this being encouraged by channels formed by faunal burrowing. The soil microbial (and faunal) population can also immobilise caesium for later release. The lack of release of caesium into the alfalfa growing on the Fillipi peat is undoubtedly due to the trapping effect of the small amount of clay present in the mineral content.

Further identification of factors involved in caesium cycling in Scottish peats was provided by the laboratory microcosm experiment. Caesium offtake was significantly ($P < 0.05$) increased relative to controls by application of dung at low rates and of urea at low and high rates (Figure 3). A single freeze-thaw cycle significantly increased caesium offtake, although multiple cycles reduced offtake, probably as a result of damage to the F. ovina. The interval of cropping also had a significant influence on caesium offtake of Festuca, a 5-day interval increasing offtake, probably due to stimulation of the rooting system, but a 10-day interval causing no significant difference from controls. Profile distribution patterns of caesium in the peat cores confirmed markedly greater retention in the surface layers of the cores where offtake was greatest. Data of caesium discharge in core leachates confirmed greater losses from cores with lower caesium offtake.

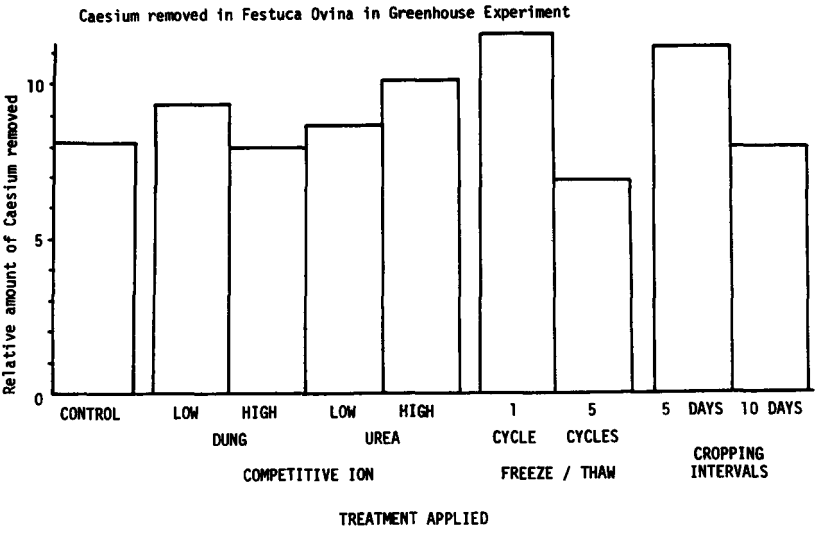

Figure 3.

CONCLUSIONS

This study has identified retention/cycling of caesium in Scottish upland peats and retention of caesium from Greek basin peats. The clay component of the mineral fraction of the Greek peats is probably responsible for profile retention of caesium. Plant rooting density and soil animal activity appear to be important agents of caesium cycling in Scottish peats. A competitive ion effect from ammonium through animal excretion, disruption of organic matter through freeze/thaw, and intensity of cropping (which affects root activity) may be important controls of caesium mobility. Further research is now needed to more closely characterise these mechanisms of caesium mobility/retention in peats.

IV. Other research group(s) collaborating actively on this project [name(s) and address(es)]:

V. Publications: Heaton B., Killham K., Mitchell R., Veresoglou D., Caesium Dynamics in the Peats and Associated Vegetation of Northern Greece and Northern Scotland. In proceedings of CEC workshop The Transfer of Radionuclides in Natural and Semi-natural Environments. Editor G. Desmet to be published in 1990.

RADIATION PROTECTION PROGRAMME
Final Report

Contractor: Contract no.: BI6-B-039-D

Biologische Anstalt Helgoland
Notkestrasse 31
D-2000 Hamburg 52

Head(s) of research team(s) [name(s) and address(es)]:

Dr. M. Hoppenheit
Laboratorium Sülldorf
Biologische Anstalt Helgoland
Wüstland 2
D-2000 Hamburg 55

Telephone number: 040/87.10.26

Title of the research contract:

Speciation and availability of Am in tidal water.

List of projects:

1. Reexamination of the concept 'concentration factor' for actinides and redefinition of the term taking into consideration the physical-chemical states of these radioelements.

Title of the project no.: [1]

Überprüfung des Konzeptes des Konzentrationsfaktors für Actiniden und Neudefinition des Begriffs unter Berücksichtigung der physikalisch-chemischen Zustände der Elemente.

Head(s) of project:

M. Hoppenheit

Scientific staff:

H. Herrmann

I. Objectives of the project:

Es wird erwartet, daß der Transport und die Bioverfügbarkeit der Actiniden durch starke Wechselwirkung mit partikulärer Substanz beeinflußt werden. Suspendierte Substanz ist von überragender Bedeutung besonders in Tidengebieten und Ästuarien. Untersuchungen, die die stark fluktuierenden chemischen und physikalischen Bedingungen im Küstenwasser simulieren, sollen mehr Einsicht in die chemischen Prozesse gewähren, die die Speziierung und Bioverfügbarkeit von ^{241}Am beeinflussen.

II. Objectives for the reporting period:

Der Einfluß folgender Faktoren auf die Speziierung von Am und seine Akkumulation in Crustaceen wurde untersucht: 1. Einfluß physikalischer und chemischer Faktoren, 1.1 pH, 1.2 Salinität, 1.3 Konkurrenz mit Seewasserionen (Ca^{2+}-Ionen), 1.4 Komplexierung mit organischem Material (Citronensäure), 1,5 Bindung an Schwebstoffe/Sediment (Tonmineralplättchen ϕ 0,1 µm), 2. Einfluß physiologischer Faktoren, 2.1 Fütterung, 2.2 Häutung, 2.3 Transport durch isolierte Kiemen

III. Progress achieved:

1. Methodology

Die Am-Aufnahme aus wäßrigem Medium und seine anschließende Abgabe erfolgte semistatisch (täglicher Wechsel des Versuchsmediums) über jeweils 7 Tage.
Als Versuchsmedien wurden folgende Seewasserverdünnungen (Am-Konzentration 0,6 mol dm^{-3}) verwendet (S = Salzgehalt):
S = 10/pH 8; S = 10/pH 6; S = 1,1/pH 8; S = 1,1/pH 8/Ca^{2+}-Zusatz (Gesamt-Ca-Gehalt 118 mg kg^{-1}, entsprechend S = 10); S = 1,1/pH 8/Citronensäure-Zusatz (100 mg kg^{-1}); S = 1,1/pH 8/Tonmineral-Zusatz (Montmorillonit M40, Teilchendurchmesser < 0,1 µm, 100 mg kg^{-1}); S = 10/pH 8/gefütterte Tiere (d.h., daß die Tiere während des Versuchs unkontaminiert gefüttert wurden).
Für Filtrationen (Cellulosenitratfilter, Porengröße 0,1 bzw. 0,01 µm) wurden vor und nach den Tierversuchen Wasserproben entnommen.
Versuchstiere waren erwachsene Männchen des euryhalinen Amphipoden Gammarus duebeni duebeni (5 - 7 Tiere pro Versuchsmedium).

Alle Versuche zur Am-Aufnahme aus kontaminiertem Futter sind semistatisch mit je 5 Tieren im Versuchsmedium S = 10/pH 8 durchgeführt worden. Gefüttert wurde mit kontaminierten Algenstücken von Enteromorpha.

Versuche mit den isolierten Kiemen 6 - 8 der Strandkrabbe Carcinus maenas wurden zusammen mit der Arbeitsgruppe Dr. Siebers, Biologische Anstalt Helgoland, durchgeführt (siehe Siebers, D., Winkler, A., Lucu, C., Thedens, G. & Weichart, D., 1985. Mar. Biol. 87, 185 - 192). Als Badmedien für die Kiemen wurden folgende Versuchsmedien gewählt (Am-Konzentration 103,9 kBq dm^{-3}):
S = 15/pH 8; S = 15/pH 6; S = 15/pH 8/Citronensäure-Zusatz (100 mg kg^{-1}); S = 1,1/pH 6/Ca^{2+}-Zusatz (20,7 mg $CaCl_2$ kg^{-1}, erhöht die Leitfähigkeit von S = 1,1 auf die von S = 15).

2. Results

2.1 Exponentialfunktionen zur Beschreibung der Am-Aufnahme bzw. Abgabe, errechnet aus den Mittelwerten der Am-Konzentrationen in den Gammariden

Tab.1

Versuchs-bedingungen	e-Funktion für die Am-Aufnahme	e-Funktion für die Am-Abgabe
S=10 /pH 8	$y=4206-4224e^{-0,14x}$	$y=1295+63052e^{-0,56x}$
S=10 /pH 6	$y=2300-2254e^{-0,11x}$	$y= 801+25232e^{-0,57x}$
S=1,1/pH 8	$y=2932-2990e^{-0,15x}$	$y=1326+ 6884e^{-0,37x}$
S=1,1/pH 8/Ca	$y=5153-5223e^{-0,11x}$	$y=1682+24341e^{-0,45x}$
S=1,1/pH 8/Citrat	$y=1202-1210e^{-0,60x}$	$y= 124+23863e^{-0,86x}$
S=1,1/pH 8/M40	$y=1714-1688e^{-0,19x}$	$y= 923+41516e^{-0,68x}$
S=10 /pH 8/ gefütterte Tiere	$y=3826-3811e^{-0,12x}$	$y= 972+74879e^{-0,59x}$

Das Mittel der Variationskoeffizienten aller Versuche lag bei 28,9%; der Minimalwert war 16,1%, der Maximalwert 54,3%.

2.2 Bioakkumulationsfaktoren (BCF) aus kinetischen Parametern

Eine Auswertung der Daten nach der OECD-Testvorschrift 305 E (Bioakkumulation: Flow-through Fish Test) wurde von Dr. W. Butte und Dr. G.-P. Zauke, Universität Oldenburg, vorgenommen (siehe Butte, W., Willig, A., & Zauke, G.-P., 1985. Umweltforschungsplan des Bundesministers des Innern, Umweltchemikalien, Forschungsbericht: FKZ 106 02 024/04 und Zauke, G.-P., von Lemm, R., Meurs, H.-G., Todeskino, D., Bäumer, H.-P. & Butte, W., 1986. Umweltforschungsplan des Bundesministers des Innern, Wasser, Forschungsbericht: FKZ 102 05 209).

Tab.2

Versuchs-bedingungen	BCF	Geschw. konstante der Am-Aufnahme	Geschw. konstante der Am-Abgabe
S=10/pH 8	197±27	25,5±1,8	0,129±0,015
S=10/pH 6	140±25	12,6±0,9	0,090±0,014
S=1,1/pH 8	250±45	16,4±1,0	0,066±0,011
S=1,1/pH 8/Ca	295±42	24,5±1,4	0,083±0,011
S=1,1/pH 8/Citrat	16± 5	3,2±0,6	0,198±0,053
S=1,1/pH 8/M40	164±37	13,1±1,1	0,080±0,017
S=10/pH 8/ gefütterte Tiere	144±19	22,0±1,6	0,152±0,017

Für die Versuche mit S = 10/pH 8 , S = 1,1/pH 8 und S = 1,1/ pH 8/Ca ist die Kurvenanpassung gut, für die Versuche mit S = 10/pH 6, S = 1,1/pH 8/Citrat und S = 1,1/pH 8/M40 könnte ein Drei-Kompartment-Modell ein besseres Ergebnis liefern. Dabei muß beachtet werden, daß die Versuchsdurchführung nicht den OECD-Richtlinien entspricht, und die Dauer von Aufnahme- und Ausscheidungsphase korrekterweise hätte wesentlich länger sein müssen (für den Versuch in S = 10/ pH 8 z.B. ungefähr 17 Tage für die Aufnahme und 34 Tage für die Ausscheidung). Die errechnete Anpassung würde durch die höhere Anzahl an Meßpunkten sicher genauer werden.

2.3 Konzentrationsfaktoren (CF) aus Konzentration im Tier und Konzentration im wäßrigen Medium

Für die Am-Aufnahme-Daten der ersten Versuchswoche wurden die Konzentrationsfaktoren errechnet aus der Am-Konzentration pro kg Feuchtgewicht der Tiere (die Trockenmasse der Gammariden beträgt 26,5% ± 2,1 vom Feuchtgewicht) dividiert durch die mittlere eingesetzte Am-Konzentration pro dm^3 wäßriges Medium.
An den ersten zwei Aufnahmetagen sind die Kurven noch nicht deutlich getrennt, was an einer noch nicht genügenden Adaptation der Tiere an das Versuchsmedium liegen mag. Für den 7.

Aufnahmetag erhält man die größten CFs in den Medien mit S = 1,1/pH 8/Ca und S = 10/pH 8; sie sind nahezu identisch. Im Medium mit S = 1,1/pH 8 sind die Konzentrationsfaktoren niedriger, noch tiefer liegen sie bei S = 10/pH 6 und S = 1,1/pH 8/M40, wobei diese sehr ähnlich sind. Auffallend klein sind die CFs bei S = 1,1/pH 8/Citronensäure.

2.4 Häutungen

Pro Versuchsreihe häuteten sich 1 - 4 Tiere, vornehmlich in der ersten Versuchswoche (Aufnahmephase).
Die Am-Aufnahme der Tiere ist, im Vergleich mit der bei sich nicht häutenden Gammariden, vor der Häutung im allgemeinen etwas erhöht, bei S = 10/pH 6 sogar stark. Nach der Häutung nimmt die Am-Akkumulation bei S = 10/pH 6 und S = 1,1/pH 8 sehr stark zu, bei S = 10/pH 8 und S = 1,1/pH 8/Ca stark, bei S = 1,1/pH 8/M40 wenig und bei S = 1,1/pH 8/Citronensäure gar nicht.
Die Am-Abgabe gehäuteter Tiere an unkontaminiertes Wasser ist sehr gering, egal ob sich die Tiere in kontaminiertem oder unkontaminiertem Wasser gehäutet haben. (Ein nach der Häutung hochkontaminierte Gammaride aus S = 10/pH 6 wurde 7 Wochen in unkontaminiertem Wasser gleicher Beschaffenheit gehalten; er verlor in diesem Zeitraum 48,5 Bq von 1196,4 Bq, das sind 4,1% der akkumulierten Menge. Ein Tier, das sich kurz nach dem Umsetzen in unkontaminiertes Wasser bei S = 1,1/pH 8 gehäutet hat, verlor in den nachfolgenden 4 Wochen 11,6% von 109,7 Bq.) Leider konnte keines der Tiere ein zweites Mal zur Häutung gebracht werden.

2.5 Filtrationen

Zu allen Versuchen wurden Proben der kontaminierten Medien vor und nach den Tierversuchen abgenommen und über Membranfilter mit Porengrößen von 0,1 und 0,01 µm filtriert.
Der Einfluß von Salzgehalt (Leitfähigkeit), pH-Wert, Komplexierung und Bindung an Tonminerale auf die Filtrierbarkeit des eingesetzten Am läßt sich leicht feststellen. Aus den Lö-

sungen mit niedriger Leitfähigkeit läßt sich durch die beschriebenen Filtrationen mehr Am abtrennen als aus denen mit höherer (S = 1,1/pH 8, Leitf. 2,11 ± 0,04 mS cm^{-1}; S = 1,1/pH 8/Ca, Leitf. 2,63 ± 0,04 mS cm^{-1}; S = 10/pH 8, Leitf. 16,2 + 0,3 mS cm^{-1}). Die filtrierbare Am-Menge steigt mit sinkendem pH-Wert (S = 10/pH 6; S = 10/pH 8). Mit Citronensäure komplexiert läßt sich nahezu das gesamte Am filtrieren, nur noch minimale Am-Mengen bleiben nach Bindung an ein Tonmineral filtrierbar. Die Am-Gehalte der Filtrate der vor dem Einsetzen der Tiere entnommenen Proben ist nur bei den Versuchen in Wasser mit einem Salzgehalt von S = 10 stärker unterschiedlich zu denen nach dem Aufenthalt der Tiere genommenen. Die filtrierbare Am-Menge ist nach den Tierversuchen für die Medien mit einem Salzgehalt von S = 10 geringer, für die Medien mit einem Salzgehalt von S = 1,1 etwas höher als die vor den Tierversuchen. Der Unterschied in der filtrierbaren Am-Menge, der durch die Verwendung von Filtern mit verschiedener Porengröße (0,1 µm und 0,01 µm) zustande kommt, ist gering.

2.6 Fütterungsversuche

Bei allen Versuchen zur Am-Abgabe nach Fütterung mit kontaminierten Algen sank die Am-Konzentration im Tier im Lauf der ersten Tage nach der Nahrungsaufnahme drastisch ab, dann nur noch langsam bis zu einem geringen verbleibenden Endwert. Die Abnahmekurven aller Versuche mit kontaminiertem Futter lassen sich nicht durch eingliedrige Exponentialfunktionen beschreiben.

2.7 Versuche mit isolierten Kiemen (Carcinus maenas)

Bei allen Kiemenversuchen konnte kein Am-Transport durch die Kiemenmembran in die Hämolymphe festgestellt werden. Keine der gemessenen Proben zeigte nennenswerte Abweichungen von der Untergrundaktivität. Selbst bei einem über längere Zeit durchgeführten Versuch bei S = 15/pH 6 (insgesmt 77 min., Annahme: Am^{3+} wird als "nacktes" Ion leichter durch Membranen

transportiert als gebundenes) sowie bei dem Versuch mit Seewasserlösung mit S = 1,1 und Ca^{2+}-Zusatz (Überlegung: Ca^{2+} fördert die Am-Aufnahme bei Gammariden) war keine Am-Aktivität in der Hämolymphe-Ersatzflüssigkeit nachzuweisen. Es bleibt zu bedenken, daß die Versuche zum Nachweis der Aufnahme sehr geringer Am-Mengen über die Kiemen eventuell nicht lange genug und mit zu geringer Probenzahl durchgeführt wurden.

3. Discussion

3.1 Die Am-Aufnahme durch Gammariden aus wäßriger Lösung ist pH-abhängig und im alkalischen Medium höher als im sauren (S = 10/pH 8, S = 10/pH 6). Bei beiden pH-Werten findet die Am-Anreicherung hauptsächlich auf der Cuticula der Tiere statt. Die Bioakkumulation läßt sich bei pH 8 gut durch ein Zwei-Kompartment-Modell beschreiben; bei pH 6 ist die Anpassung nicht gut.
Bei S = 10/pH 8 ist der vorherrschende Mechanismus wohl die physikalische Adsorption von $Am(OH)(CO_3)$ auf der Tieroberfläche. Bei S = 10/pH 6 scheint die Adsorption verschiedener geladener Am-Spezies vorzuliegen. Da im sauren Medium außerdem eine Decalcifizierung der Cuticula stattfindet, ist eine Gegenreaktion des Tieres durch einen vermehrten Carbonat-Stoffwechsel denkbar.
Die Am-Aufnahme ist vor und nach einer Häutung bei beiden pH-Werten erhöht, im sauren Medium sogar sehr viel stärker als im Häutungsintervall. Der fest gebundene Anteil an Am, der auch nach einer Häutung im Tier verbleibt, kann durch das Trinken des Tieres von der Umgebungsflüssigkeit aufgenommen worden sein.

3.2 Die Am-Aufnahme der Gammariden ist vom Salzgehalt der Brackwasserlösung abhängig, und zwar ist sie höher bei höherem Salzgehalt (S = 10/pH 8, S =1,1/pH 8). Die Bioakkumula-

tion läßt sich bei beiden Salzgehalten gut durch ein Zwei-Kompartment-Modell beschreiben. Für beide Salzgehalte wird als dominierender Mechanismus die Adsorption von $Am(OH)(CO_3)$ angenommen, die aufgrund der höheren Carbonatkonzentration im Wasser bei S = 10 höher ausfällt. Bei niedrigem Salzgehalt wird weniger des aufgenommenen Am mit der Exuvie abgegeben als bei höherem Salzgehalt. Dies kann durch eine verstärkte Resorption der Cuticula bei Tieren erklärt werden, die in Wasser mit geringem Ca-Gehalt leben. Die Am-Aufnahme nach der Häutung ist in Seewasser mit geringem Salzgehalt ebenfalls sehr viel stärker als in dem mit höherem.

3.3 Die Ca^{2+}-Konzentration der Brackwasserlösungen beeinflußt die Am-Aufnahme durch die Gammariden dahingehend, daß ein höherer Ca-Gehalt die Am-Aufnahme fördert (S = 10/pH 8; S = 1,1/pH 8/Ca; S = 1,1/pH 8). Die Akkumulation in Brackwasser von S = 1,1/pH 8 läßt sich gut durch ein Zwei-Kompartment-Modell beschreiben, wobei die Am-Aufnahme vom Ca^{2+}-Gehalt, die Am-Abgabe vom Gesamt-Salzgehalt der Lösung abhängt. Der Anteil des sich auf der Cuticula befindenden Am ist generell sehr hoch. Verantwortlich gemacht werden für diese hohe Am-Adsorption können folgende Einflüsse:
a. Der Carbonatgehalt der Lösung mit S = 1,1/pH 8 wird durch den Ca^{2+}-Zusatz erhöht.
b. Die Struktur der wäßrigen Lösung wird beeinflußt. Die Am-haltigen Kolloide scheinen weniger stabil zu sein und stärker zur Adsorption zu neigen.
c. Das physiologische Verhalten des Tieres wird durch das veränderte Ionenverhältnis im Wasser beeinflußt.
Nach einer Häutung entspricht die erhöhte Am-Adsorption der bei Brackwasser mit S = 10/pH 8 vorliegenden, also der mit gleichem Ca^{2+}-Gehalt.

3.4 Die Am-Aufnahme der Gammariden wird durch Zusatz von Citronensäure stark herabgesetzt. Die Akkumulation kann durch ein Zwei-Kompartment-Modell nur unzureichend beschrieben werden. Das aufgenommene Am befindet sich zum größten Teil auf der Exuvie. Am liegt hauptsächlich als $Am(cit)_2^{3-}$ vor

und wird als negativ geladene Spezies nicht adsorbiert. Selbst nach einer Häutung tritt keine Erhöhung der Am-Aufnahme ein.

3.5 Die Am-Aufnahme der Gammariden ist in Gegenwart von Tonmineralien herabgesetzt, allerdings nicht so stark wie durch Zusatz von Citronensäure. Die Akkumulation wird durch das Zwei-Kompartment-Modell nur unzureichend beschrieben. Das aufgenommene Am wird nur zur Hälfte auf der Exuvie gefunden. Es ist möglich, daß sich sehr kleine Teilchen der Tonmineralschwebstoffe, an denen das Am adsorbiert bzw. präzipitiert ist, an die Tieroberfläche anlagern. Größere Partikel werden vielleicht auch gefressen.

3.6 Ein Vergleich der Am-Aufnahme und Abgabe aus wäßriger Phase (S = 10/pH 8) bei gefütterten und ungefütterten Tieren zeigt, daß die gefütterten Gammariden weniger Am akkumulieren als die ungefütterten (Student's t-Test zeigt Signifikanz für den Unterschied der Am-Konzentrationen in den Tieren am 7. Tag der Aufnahmephase), der Verlauf von Am-Aufnahme bzw. Abnahme bei beiden Versuchen aber nahezu identisch ist. Die physiologisch größere Aktivität gefütterter Tiere scheint dekontaminierende Wirkung zu haben.

3.7 Die Am-Abgabe bei Aufnahme aus der wäßrigen Phase erfolgt bei ähnlich großer Kontamination erheblich langsamer als die bei Aufnahme aus kontaminiertem Futter. Die Bindung von Am an das Exoskelett der Gammariden scheint stärker zu sein als die an inneres Gewebe.

3.8 Am wird nicht über die Kiemen aufgenommen.

4. Abstract

4.1 Am wird von euryhalinen Krebsen nicht durch die Kiemen aufgenommen.
4.2 Die Am-Aufnahme über den Magen-Darm-Trakt ist gering. Über 90% des mit dem Futter aufgenommenen Am wird innerhalb kürzester Zeit wieder ausgeschieden; aus der Umgebungsflüssigkeit durch Trinken aufgenommenes ionales Am kann stärker im Tier gebunden werden.
4.3 Die Am-Aufnahme über die Cuticula der Crustaceen hängt stark von der Speziierung des Am ab und kann sehr hoch sein. Sie ist hauptsächlich von pH-Wert und der ionalen Zusammensetzung des Seewassers abhängig
sowie von seinem Gehalt an organischen Komplexbildnern. Bei pH 8 und hohem Ca^{2+}-Gehalt ist die Am-Adsorption groß; es handelt sich wohl hauptsächlich um die "physikalische" Adsorption von neutralem $Am(OH)(CO_3)$. Bei pH 8 und Zusatz von Citronensäure findet kaum Am-Adsorption statt; Am liegt überwiegend als $Am(cit)_2^{3-}$gelöst vor.
4.4 Eine Häutung der Crustaceen in Am-haltigem Wasser kann die Am-Aufnahme stark beeinflussen. Bei verstärkter Aufnahme von Wasser über den Magen-Darm-Trakt führt ein aktiver Einbau in die neu zu bildende Cuticula bei geringem Ca^{2+}-Gehalt der Seewasserlösung bzw. niedrigem pH zu einer vergleichsweise extrem hohen Am-Akkumulation im Tier, die äußerst persistent ist.

Da der Hauptaufnahmeweg für Am bei Euphausiaceen nicht über kontaminierte Nahrung, sondern über die wäßrige Phase führt (siehe Fisher N.S., Bjerregaard, P. & Fowler, S.W., 1983. Mar. Biol. 75, 261 - 268), und die Stabilität von Carbonato-, Hydroxo-, Citrat- und Humat-Komplexen ähnlich groß ist (siehe Kim, J.I., 1986. In: Handbook on the Physics and Chemistry of the Actinides; Hrsg. von A.J. Freeman und C. Keller, Elsevier Science Publishers B. V., Chapter 8) kann eine Am-Akkumulation durch Adsorption anorganischer Am-Spezies nicht vernachlässigt werden, zumal, wenn diese durch physiologische Aktivitäten der Tiere noch drastisch erhöht werden kann.

IV. Other research group(s) collaborating actively on this project [name(s) and address(es)]:

Dr. D. Siebers und Mitarbeiter (Biologische Anstalt Helgoland), Dr. G.-P. Zauke und Dr. W. Butte (Universität Oldenburg), Prof. Dr. O. Vanderborght und Mitarbeiter (Radionuclide Metabolism Section, SCK/CEN, Mol, Belgien).

V. Publications:

RADIATION PROTECTION PROGRAMME

Progress Report

1989

Contractor: Contract no.: BI6-B-327-B

Fac.des Sciences Agronom. de l'Etat
Passage des Déportés 2
B - 5800 Gembloux

Head(s) of research team(s) [name(s) and address(es)]:

Dr. R. Kirchmann
Unité de Physique et Chimie Physique
Fac. des Sciences Agronom. de l'Etat
Avenue de la Faculté 8
B - 5800 Gembloux

Telephone number: 081/611576

Title of the research contract:

Study of the transfer of accidentally released radionuclides in agricultural products with the aim of developing appropriate countermeasures

List of projects:

Study of the transfer of accidentally released radionuclides in agricultural products with the aim of developing appropriate countermeasures

Title of the project no.:

B16-B-327-B

Study of the transfer of accidentally released radionuclides in agricultural products with the aim of developing appropriate countermeasures.

Head(s) of project: Dr. R.Kirchmann & Prof. J.Deltour
Unité de Radioécologie
Fac.Sci.Agronomiques de l'Etat
Avenue de la Faculté, 8
B-5800 GEMBLOUX
Tel.:081/62.24.97 or 62.24.95

Scientific staff: O.Burton & C.Chalmagne

I. Objectives of the project:

The objective of the study is to define the countermeasures to be applied in order to improve the radiological quality of agricultural products after a major nuclear accident at a NPP (PWR type).

In order to reach this goal, one should consider two main phases :

1) identification of sensitive soils and agricultural products in the near and intermediate fields;
2) experimental research to define the parameters and the methods to reduce the transfers along the soil-plant-animal foodchain and to investigate the possible use of industrial processes to reduce the level of radioactivity in the end-products of the plant and animal production.

II. Objectives for the reporting period:

- Realization of a general survey, around the relevant NPP, of the soils types and of agricultural production. This survey is performed in the framework of a contract with the Ministery of Public Health "Service de Protection contre les Radiations Ionisantes" (S.P.R.I.).
- Identification of the "sensitive" soils and crops, in relation with the major radionuclides of concern (Cs, Sr, Ru) (databank, statistics, field sampling).

III. Progress achieved:

1. Methodology.

The identification of the sensitive soils and crops from the radio-ecological point of view lies on the confrontation on the one hand of the results of the soils and agricultural products surveys, and on the other hand of the soil-to-plant transfer factors.

Theses surveys were realized on the belgian territory, in a radius of 15 km around the NPP of Tihange, Chooz, Doel. For each of them, it was proceeded as follows.

a) The soils classification requires the knowledge of the parameters that influence the transfer of radionuclides from soils to plants .
The most important of them (texture, hydric conditions, presence of lime), as far as agricultural ecosystems are concerned, are taken into account in the Belgian Soil Map published by I.G.N.
So, gathering the cartographic units, six soil types, based on these three parameters, were retained :
- sandy soils
- stony loamy soils
- loamy soils (loess)
- clayey soils
- calcareous stony loamy soils
- hydromorphic soils.

A coloured map (scale 1:50,000) shows the localisation of these six classes of soils.

b) The question of the agricultural products was achieved according to two ways.
The first one is a statistic one. It was carried out by counting in each commune around the relevant sites, the areas devoted to specific crops (grass, cereals, root crops, fodder, ...) as well as the cattle (cows, pigs, fowls, sheeps). The original documents are provided by agricultural statistics of the belgian I.N.S.
The second one was performed by using remote sensing (Landsat image) which allowed to localize the agricultural areas but also to compare these ones with the soil map produced at the same scale.

c) That stage allows the determination , in each point around the NPP, of the soil-plant association. Then the superposition with transfer factors was made, in function of the qualitative and quantitative results of the surveys.

The transfer factors values used were provided by the data bank worked out by the IUR's Working group on soil-to-plant transfer factors.

2. Results

For the three nuclear sites, we have identified the sensitive soils and crops for Cs and Sr. These results are given in the attached report. The most important result is that for Cs like for Sr, permanent pastures appear to be the critical pathway in the soil-plant foodchain, because of both their abundance in the country and their high transfer factor values.
Furthermore, in the case of Cs, special attention has to be drawn on potatoes cultivated on sandy and loamy soils.

3. Discusssion.

The objectives planned for the reporting period were reached and a practical knowledge of the environment of the NPP was gained; the radioecological sensitivity of the soil-to-plant transfer has been identified. The results obtained have to be validated :

- by experiments on selected pastures to study the behaviour of radionuclides from the PWR simulated source-term in soil-to-plant transfer;
- by experiments on the plant-to-animal transfer of the relevant radionuclides (Cr, Sr, Ru) with the simulated source-term built in Cadarache.

IV. Objectives for the next reporting period :

In the framework of the RESSAC programme, a close cooperation is foreseen with CEN/SERE of Cadarache and CEN/SCK of Mol. An experiment on permanent pasture (critical pathway) is designed to estimate the transfer factors from soil (MAT) to grass and from grass to milk, for radionuclides of biological importance released in case of a nuclear accident (Cs, Sr, Ru). The transfer of the radionuclides released as aerosols (by a simulated PWR source-term) will be compared with that of solutions of well known chemical form , in order to realize a comparative assessment of the bioavailability of theses two different source-terms. These aerosols and solutions will be produced at Cadarache; the soils (MAT horizon) will be sampled in the surroundings of the NPP of Chooz. The soil-plant experiment will be carried out at Gembloux and the plant-animal experiment will be carried out at the experimental farm of the CEN/SCK of Mol.

V. Other research group(s) collaborating actively on this project [name(s) and address(es)] :

C.E.N. Cadarache I.P.S.N./S.E.R.E.
Laboratoire d'études d'impacts
F. 13108 Saint-Paul-Lez-Durance
FRANCE

C.E.N./S.C.K Département de Radioprotection
Boeretang 200
B - 2400 Mol
BELGIUM

VI. Publications :

- Rapport d'avancement S.P.R.I.-C.C.E. (01/01-31/12/1989).

RADIATION PROTECTION PROGRAMME
Final Report

Contractor:

The University of Dublin
Trinity College
IRL- Dublin 2

Contract no.: BI6-B-043-IRL

Head(s) of research team(s) [name(s) and address(es)]:

Dr. I.R. McAulay
Dept. of Pure and Applied Physics
Trinity College
IRL- Dublin 2

Telephone number: 77.29.41

Title of the research contract:

Radioactivity in the sea and food in Ireland.

List of projects:

1. Reduction of radioactivity in Irish Sea subsequent to changes at Sellafield Reprocessing Plant.
2. Radioactivity in foodstuffs produced in Republic of Ireland.

Title of the project no.:
1 of contract BI6-B-043-IRL Reduction of radioactivity in the Irish Sea consequent to changes at the Sellafield Reprocessing Plant.

Head(s) of project: Dr I R McAulay
Department of Pure & Applied Physics
Trinity College
IRL - Dublin 2.

Scientific staff: Miss A Hayes, (Part-time)
Department of Pure & Applied Physics
Trinity College
Dublin 2.

I. Objectives of the project:

The discharges of radioactive isotopes from Sellafield were to be assessed for their effect at the Irish Coast by measurements on samples of seaweed and seawater from the eastern coast of Ireland. The effect of new plant coming into operation at Sellafield was to be determined and data obtained for use in appropriate models.

II. Objectives for the reporting period:

Sampling at the selected stations was continued during 1989. The levels of 134-caesium wer determined using longer counting times but proved to have fallen so far as to be too low for accurate measurement. Seasonal variation in 137 caesium levels was continued. Fish samples from inshore waters were measured and an estimate made of the committed collective lose to the Irish population. The results are being prepared for publication.

III. Progress achieved:

METHODOLOGY

The discharge of radioactive isotopes from the fuel reprocessing plant at Sellafield results in a distribution of the isotopes concerned throughout the Irish sea and, in particular, at the east coast of Ireland. The objective of this project was to assess the effect of new and more efficient equipment coming into operation on Sellafield by measurement of the radioactive isotopes of caesium present is seaweed and water collected along the east coast of Ireland. During the final year of the project, measurement of the caesium content in fish landed at Irish ports from the Irish Sea would enable an assessment of the population dose equivalent in Ireland resulting from the Sellafield discharges.

Samples of focus vesiculosus were collected at four sampling points along the east coast of Ireland at intervals of 6-8 weeks. Seawater was collected at one of the sampling points (no. 2) several times per year.

The location of the sampling points is shown in Fig 1.

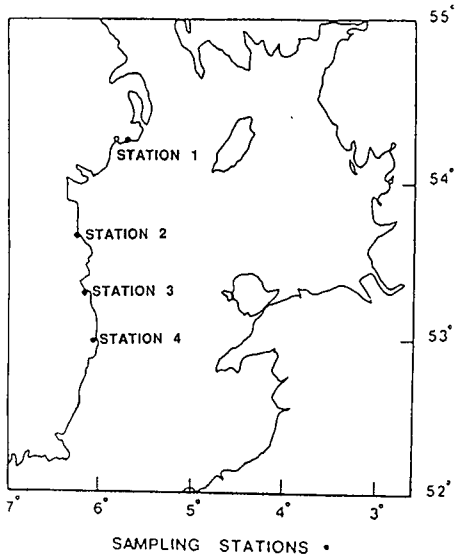

FIG 1

The seaweed samples were prepared by oven drying for 12-16 hours and then powdered by means of an electric grinder. It was found that there was some variability in the percentage dry weight of the original samples (ranging from 16% to 23% in most cases) resulting from this treatment and the results given below have been normalised to a dry weight of 20%.

The seawater were acidified at collection, pre-filtered, and then passed through an ion exchange resin specific to caesium. Fish samples were oven dried and then reduced to powder by an electric grinder.

The samples were measured using a high resolution semiconductor system. The counting times used were in most cases greater than 50,000 seconds which was sufficient to give a minimum detectable level of approximately 0.5 Bq per kilogram of sample weight.

The sampling time was reduced for some samples collected after fallout from the Chernobyl accident because of the much higher caesium levels found in these samples. For the water samples, the limit of detection corresponded to about 1 millibecquerel per litre of sample.

RESULTS

The results are shown in tables 1, 2, and 3 for the isotopes of caesium in seaweed and seawater.

TABLE 1

Mean values for 137-caesium in fucus seaweed. (Bq/kg, normalised to dry weight 20%).

	Station 1	Station 2	Station 3	Station 4
1984	114	120	90	70
1985	85	78	65	46
1986 (Pre-Chernobyl)	50	43	35	--
1986 (After-Chernobyl)	67	89	45	33
1987	42	48	33	25
1988	26	31	21	15
1989	20	28	19	16

TABLE 2

Mean values for 134-caesium in fucus seaweed. (Bq/kg, normalised to dry weight 20%).

	Station 1	Station 2	Station 3	Station 4
1984	4	3	3	2
1985	3	2	NM	NM
1986 (Pre-Chernobyl)	NM	NM	ND	--
1986 (After-Chernobyl)	11	21	8.1	5.6
1987	2.8	3.5	1.9	1.4
1988	1.1	1.2	NM	ND
1989	ND	ND	ND	ND

ND = not detected NM = detected but not measurable as error > 50%.

TABLE 3

Mean values for caesium isotopes in seawater samples collected in station 3. (mBq per litre).

	137-caesium	134-caesium
1985	310	Not Measured
1986	210	17
1987	130	10.4
1988	90	3.6
1989	79	1.9

The uncertainties in the above tables due to the standard deviations in the statistical means is 10-20% for the 137-Cs figures in table 1; 20-40% for the figures in table 2 and 10% for the 137-Cs figures in table 3.

Table 4 shows the BNFL figures for discharges from Sellafield during the relevant period.

TABLE 4

Reported discharges of caesium-137 from Sellafield to the Irish Sea. 1980-88.

Year	137-Cs discharged (TBq).
1980	3000
1981	2400
1982	2000
1983	1200
1984	434
1985	325
1986	18
1987	12
1988	13

DISCUSSION

The figures clearly show a reduction by a factor of about five in the caesium isotopes reaching the Irish coast from Sellafield over the contract period. This reduction was interrupted temporarily by the effect of Chernobyl fallout. The impact of the Chernobyl fallout was quite marked on seaweed as heavy rain at the Irish Coast during the passage of the fallout cloud resulted in direct uptake by the seaweed from rainfall and from land runoff.

The effect on seawater was not directly detectable in 137-caesium levels, but a perceptible increase in 134-caesium levels was found. This is in excellent accord with the measured 137 Cs/134 Cs ratio of 1.9 found in Chernobyl fallout by rainfall and other measurements in Ireland.

It can be seen from the figures that caesium from the Chernobyl fallout had fallen below detectable limits by 1988, rather less than two years after the accident.

On the basis that the ratio of 137 Cs to 134 Cs in the Sellafield discharges is about 14, it would appear that from 1984 to 1986 the age of the caesium at the Irish coast is about $2\frac{1}{2}$ years.

The M.A.F.F. compartment model of the Irish Sea suggests that the transit time of Sellafield discharges to the Irish coast is about one year. However, the ratio of the caesium isotopes in seaweed in the vicinity of Sellafield was about 20 in 1985, due to the presence of "older" caesium in the coastal water which mixes with the caesium in the discharges. A transit time of about one year from Sellafield to the Irish coast is therefore in good agreement with the results obtained in this study.

Before the fallout from the Chernobyl accident affected the result, it had been observed that the figures obtained for caesium in seaweed appeared to follow an annual cycle with higher values being obtained for samples

collected in the months April to August each year. This pattern was confirmed for the values obtained in seaweed in 1988 and 1989. However, such patterns do not appear in the seawater measurements and could not be established for potassium levels in seaweed. It is therefore believed that there is either an increased uptake of caesium during the late spring and summer months or else there is some other biological factor affecting the results but not yet identified.

Overall, the figures obtained in this study are in good agreement with expectation from the reduced discharges from Sellafield as reported by British Nuclear Fuels Ltd. It is confirmed that measurements on seaweed exhibit less variability than direct measurements on fish. However, a seasonal variation of caesium levels in seaweed does occur and this implies that measurements should be made on samples taken regularly at the same site and the annual average used as a long term indicator for variation in level.

RADIATION DOSES TO THE IRISH POPULATION AS A RESULT OF CAESIUM LEVELS IN THE IRISH SEA.

Previous calculations from measurements in this laboratory indicated a committed collective dose equivalent to the Irish population of 2 man-sievert in 1981 (Ref 1) and of 0.7 man-sievert in 1986 (Ref 2).

A series of measurements on 81 white fish samples landed at Irish ports during 1988 were made and the average value of 137-Cs of 6.5 Bq/kg wet weight found in 1981 suggest that the committed collective dose to the Irish population from eating fish from the Irish sea calcualted on the same basis as previously was less than 0.2 man-sievert for 1988. Similar calculations for a member of a critical group eating 200 g of fish per day lead to an annual dose of 7 μSv/y for such an individual in 1988. This compares with the recommended ICRP dose limit of 100 μSv/y for individual members of the public. Diret measurements on fish therefore confirm reasonably well the reduction in dose which can be inferred from mean values of caesium isotopes found in seaweed.

However, the values of 134 caesium now existing in seaweed and water at the Irish coast preclude its accurate measurement unless large volume sampls and very long counting times are used. It is therefore doubtful that much further scientific information could be obtained by continued monitoring. Any sudden input pulse due to an accidental discharge at Sellafield could however be reliably and accurately detected at the Irish coast after the appropriate transit time.

It may be concluded that the results of this project have been broadly achieved and that the unanticipated effect of the Chernobyl accident provided confirmatory data for conclusions drawn from the data resulting from the Sellafield discharges.

REFERENCES:

Ref 1 McAulay and Doyle. Radiocaesium levels in Irish sea fish and the resulting dose to the population of the Irish Republic. Health Physics: 8, 3, 333-337.

Ref 2 McAulay and Pollard. Fucus Vesiculosus as an indicator for caesium isotopes in Irish Coastal waters. Radionuclides: A tool for Ocenaography. Ed J C Guary, P Guegueniat and R J Peutreath, Elsevier.

IV. Other research group(s) collaborating actively on this project [name(s) and address(es)]:

Mr J Cunningham
Nuclear Energy Board
3 Clonskeagh Square
Clonskeagh Road
Dublin 14
Ireland

Dr P Mitchell
Department of Physics
University College
National University of Ireland
Dublin 4
Ireland

Dr N Mitchell
Fisheries Radiobiological Laboratory
Lowestoft
Suffolk
United Kingdom

Dr A Aarkrog
Risø National Laboratory
DK-4000 ROSKILDE
Denmark

V. Publications:

McAulay & Pollard, Fucus Vesiculosus as an indicator for caesium isotopes in Irish Coastal waters. Radionuclides: A tool for Oceanography pp 304-311. Ed. J C Guary, P Guegueniat and R J Pentreath, Elsevier.

Title of the project no.:

Number 2 of contract B16-B-043-IRL. Radioactivity in foodstuffs produced in the Republic of Ireland.

Head(s) of project:

Dr I R McAulay
Department of Pure & Applied Physics
Trinity College
IRL - Dublin 2.

Scientific staff:

Mr Diarmuid Moran
Miss Annette Hayes
Department of Pure & Applied Physics
Trinity College
Dublin 2.

I. Objectives of the project:

To identify the natural and artificial radioactive isotopes present in agricultural produce in the Republic of Ireland and to assess the collective dose resulting from their consumption. To investigate the paths by which artificial radio isotopes progress through the food chain and identify the sources of the isotopes where possible. To compare the data obtained with similar studies elsewhere.

II. Objectives for the reporting period:

Final sampling to be completed at the ten selected agricultural sites with particular emphasis on the translocation of caesium isotopes through the soil column. Further studies to be made of radioactivity levels in vegetable and other agricultural produce. Further measurements to be made on uptake of caesium by plants in areas of poor quality soils. Further efforts to be made to establish committed collective dose equivalents from agricultural produce obtained from different regions.

III. Progress achieved:

METHODOLOGY

The original aim of this project was to investigate the levels of artificial and natural radioactive substances in soils in the Republic of Ireland and to investigate their passage through the foodchain and the radiation dose resulting from their ultimate consumption by man. The Chernobyl accident, which occurred a little over one year after the start of the project, resulted in the deposition of considerable amounts of artificial radio-isotopes on the soil throughout Ireland. In the case of 137-caesium, this deposition ranged up to 20 kBq m^{-2} in some areas. However, the accurately determined value for the ratio of 137-caesium in the Chernobyl fallout enabled a clear distinction to be made between the behaviour of fallout from weapons testing (which contains no 134-caesium) and that from the Chernobyl accident.

Samples of soils were taken at each of the ten selected farm sites at regular intervals, dried, crushed and their radioactivity measured using high resolution gamma ray spectrometry.

Soil samples on undisturbed pasture land were taken by using a corer driven into the ground at 12 locations within an area of about 10,000 m^2 at each site. The samples were divided into slices of 5 cm thickness and these were aggregated for each level. Soil samples from cultivated land were taken at a comparable number of locations within a field but consisted of an aggregate of samples taken to ploughing depth.

The distribution of natural radioactivity over the country was determined by measurements made on 106 samples of topsoil (0-5 cm) taken randomly over the land area of the Republic of Ireland. Radium and thorium series and 40-potassium levels were determined again by use of high resolution gamma ray spectrometry.

A series of milk powder samples were obtained for the period of the project after the Chernobyl accident and these were analysed for caesium isotopes using above techniques. The last component of the project involved the collection of heather and soil samples from a number of areas where the soil quality was known to be poor and where the predominant utilisation for agricultural purposes was by the grazing of sheep. Analysis of these samples was carried out in the same way as for the samples taken at farms.

RESULTS

The ten sites selected for study of good agricultural land are shown on the outline map (with 100 km grid square) in fig 1.

FIG. 1

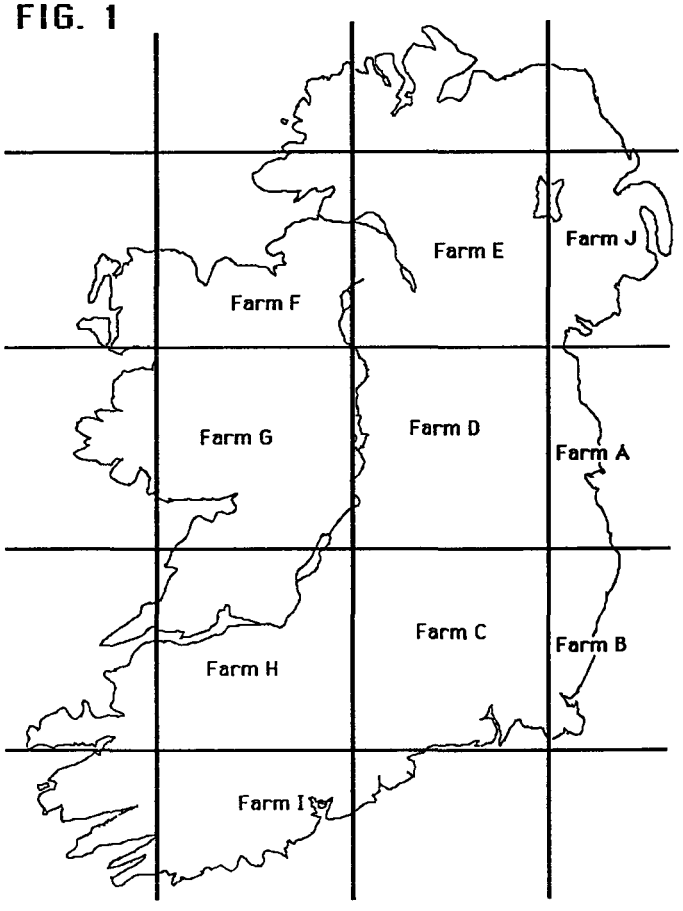

Samples taken at regular intervals at each of these sites from 1986 to 1989 have shown that, for undisturbed soils, a slow downward movement of the caesium fallout from the Chernobyl accident has occurred. This has been the case at all sites and is exemplified by the results from Farm G which are shown in table 1, as 137-Caesium concentration in soil at different levels on the indicated sampling dates. The figures are corrected to activities on 1 May 1986 and are calculated from measured 134-Cs activities assuming a 137-Caesium to 134-Caesium ratio of 1.92 in the Chernobyl fallout.

TABLE 1

Farm G	**137-Cs (Bq/kg) with 90% confidence limits**				
Depth					
0-5 cm	110 ± 4	82 ± 3	82 ± 3	81 ± 3	76 ± 3
5-10 cm	3 ± 0.7	7.4 ± 0.6	14.7 ± 1.2	14.1 ± 1.2	20 ± 1.6
10-15 cm	0.7 ± 0.3	2.4 ± 0.5	2.8 ± 0.4	2.4 ± 0.5	4.7 ± 0.6
15-20 cm	0.3 ± 0.2	1.4 ± 0.6	1.7 ± 0.5	1.0 ± 0.4	1.7 ± 0.7
20-25 cm	1.4 ± 0.4	0.6 ± 0.3	0.4 ± 0.2	0.4 ± 0.2	1.7 ± 0.7
>25 cm	NM	NM	NM	NM	1.0 ± 0.4

The values of Chernobyl 137-Cs concentrations in soil at the first and last sampling rounds (first round spring 1987; last round spring 1989) are shown for all farms in Table 2. The confidence limits are not detailed in the table but are comparable to those given in Table 1. Values corrected to 1st May 1986.

TABLE 2: Part 1

Depth	**Farm A**		**Farm B**	
	1st round	**Last round**	**1st round**	**last round**
0-5 cm	76	67	26	22
5-10 cm	7	8	2.2	3.6
10-15 cm	2	1.8	0.5	0.6
15-20 cm	NM	0.8	0.5	0.6
20-25 cm	NM	NM	NM	NM
>25 cm	NM	NM	NM	NM

NM = indicates not measurable

TABLE 2: Part 2

Depth	Farm C 1st round	Farm C Last round	Farm D 1st round	Farm D last round
0-5 cm	99	89	88	82
5-10 cm	9.5	23	3.7	9.3
10-15 cm	0.6	4.0	0.9	1.9
15-20 cm	NM	NM	NM	0.5
20-25 cm	NM	NM	NM	0.3
> 25 cm	NM	NM	NM	NM

NM = indicates not measurable

TABLE 2: Part 3

Depth	Farm E 1st round	Farm E Last round	Farm F 1st round	Farm F last round
0-5 cm	127	83	157	22
5-10 cm	4.9	19	7.3	3.6
10-15 cm	0.3	3.6	0.5	0.6
15-20 cm	0.4	0.9	0.5	0.6
20-25 cm	NM	0.5	NM	NM
> 25 cm	NM	NM	NM	NM

NM = indicates not measurable

TABLE 2: Part 4

Depth	Farm G 1st round	Farm G Last round	Farm H 1st round	Farm H last round
0-5 cm	110	76	66	49
5-10 cm	3.1	20	3.3	14
10-15 cm	0.7	4.7	0.4	2.5
15-20 cm	0.3	1.7	0.7	0.8
20-25 cm	1.4	1.7	0.5	0.4
> 25 cm	NM	1.0	NM	0.3

NM = indicates not measurable

TABLE 2: Part 5

Depth	Farm I 1st round	Farm I Last round	Farm J 1st round	Farm J last round
0-5 cm	163	112	130	91
5-10 cm	12.6	17	5.2	14
10-15 cm	4.7	3.6	0.7	1.7
15-20 cm	NM	1.0	NM	NM
20-25 cm	NM	0.4	NM	NM
> 25 cm	NM	0.3	NM	NM

NM = indicates not measurable

137-caesium was also present at all sites as a result of weapons testing in earlier decades. This had penetrated through the soil to a greater depth and was generally a few tens of Bq/kg down to a depth of 15-20 cms. The readings given in the tables above may be slightly effected by smearing which can take place during sampling with corer tubes and values of less than 2 Bq/kg are probably not reliable.

Most of the vegetable and grain crops grown in Ireland are from the regions represented by farm sites A, B, C, D, and J. The remaining sites are typical pasture farmland with very little crop cultivation. However, vegetable and grain samples were obtained at or near each of the sites sampled, though in several cases only a narrow range of samples could be taken. It was found that in all cases the transfer due to the Chernobyl accident was either undetectable or extremely low, with concentration ratios below 0.01 at the most. In view of the experimental uncertainties in such measurements, the results are not quoted in this summary report.

Transfer of caesium fallout to milk powder.

Because of the importance of the pathway to man via dairy produce of radioactive caesium fallout onto pastureland, it was decided to sample milk powder produced in a single area at regular intervals and to analyse the powder for 137-Cs and 134-Cs. With the co-operation of a milk products factory regular powder samples were obtained and analysed for the three years beginning in January 1987.

The results are shown in Table 3, the figures being in Bq/kg of powder averaged over each quarter of the year's production. The errors quoted are the statistical standard deviations of the means. The measurement errors were small, typically 5% at 50 Bq/kg and with a detection limit of about 0.5 Bq/kg for each isotope in each measurement. The values are as at the measurement date and are not corrected for decay.

Table 3

137-Cs and 134-Cs in milk powder, Bq/kg.
Average values for each quarter.

1987,	137-Cs	134-Cs	No. of samples
1st quarter	81 ± 17	32 ± 7	8
2nd quarter	12 ± 14	4.4 ± 5.5	40
3rd quarter	3.8 ± 0.9	1.2 ± 0.4	25
4th quarter	3.1 ± 1.1	<1	18

1988,	137-Cs	134-Cs	No. of samples
1st quarter	5.3 ± 1.3	< 1.5	11
2nd quarter	2.7 ± 1.3	<1	37
3rd quarter	2.4 ± 0.8	<1	54
4th quarter	2.6 ± 0.9	<1	23

1989,	137-Cs	134-Cs	No. of samples
1st quarter	2.1 ± 17	NM	33
2nd quarter	<2	NM	55
3rd quarter	<2	NM	51
4th quarter	<2	NM	29

These figures will represent approximately ten times the corresponding activity present in liquid milk.

The steep drop between the concentrations found in the first and second quarters of 1987 is attributed to the widespread use of stored fodder from 1986. The use of stored fodder decreases during April each year as animals go out on pasture which also accounts for the high standard deviations found for measurements made during the second quarter of 1987. The slight increase in activities found during the first quarter of 1988 is similarly attributed to animals being fed with some silage or fodder stored since 1986. Apart from these features there has been a steady decline in the Chernobyl fallout present in milk products as established by direct measurement. Corresponding levels in liquid milk would be difficult to measure with existing equipment and direct measurement of activities in grass would not be possible.

Transfer of caesium isotopes through the food chain from poor quality soils.

In Ireland there are many areas, usually at more than 300 m or so above sea level, which consist of rocky soil with a high peat content. Much of the vegetation in such areas is of heather and the regions are used for grazing by sheep apart from in the winter months. It has previously been established in this project that high concentrations of caesium (several hundred Bq/kg) had been found in honey produced by bees which had fed in such upland heather covered areas. Unfortunately, the honey production from such areas has been low in recent years due to poor summers and factors affecting the health of bees, and it was not possible to obtain sufficient numbers of honey samples to follow up this effect.

During 1988 and 1989, studies were carried out at a small number of upland poor quality soil sites used for sheep grazing. The results of this survey found that there was a high transfer of caesium from soil to plants of the species Calluna vulgaris. The measured activity concentrations were such as to enable a distinction to be made between old caesium resulting from weapons test fallout and the more recent fallout resulting from the Chernobyl accident. It was found that the Chernobyl caesium was more efficiently taken up by the heather plants than the older form. Concentration of ratios of plant to soil activities for caesium on a dry weight basis were found to exceed one in some cases and the Chernobyl fallout caesium was concentrated two to three times more efficiently by the heather plants than the older form. The results from the 1988 measurements on poor quality soils have been published (Ref 1) and further publication is expected for more recent data.

Natural radioactivity in soil in the Republic of Ireland.

Measurements of the activity concentration of uranium series, thorium series, and 40-K isotopes were made on samples of soil taken at 110 sites throughout the Republic of Ireland. The results of this survey have been published (Ref 2) and led to the identification of several areas in which higher than average levels of uranium series activity exist in topsoil. These areas correlate well with areas identified by Dr J P McLaughlin of University College, Dublin, as being associated with higher than average levels of radon in the domestic environment (Ref 3).

In the context of the present project, it must be pointed out that all the areas identified as being associated with high activity concentrations of uranium or radium are in regions of the country which are not involved in crop production to any significant degree. This fact, together with the difficulty of measuring uranium series isotopes using only gamma ray spectrometry, meant that relatively few samples of crops were subjected to analysis and, of these, none showed measurable levels of natural radioactivity other than 40 K.

DISCUSSION

The results obtained in the section of the project relating to caesium isotopes in the human foodchain have established that there is a very slow translocation through good quality undisturbed agricultural soil. The concentration ratios for crops to soil are very low (less than 0.01) and it was not therefore possible to establish committed collective doses to the Irish population in years subsequent to that of the Chernobyl accident and resulting from it. However, it can be concluded that individual doses resulting from average levels of crop consumption are not likely to exceed one or two microsievert per annum.

The situation in upland areas of poor quality soil is more complex. The high mobility of caesium in such soils and its transfer to sheep via heather and other plants means that levels of caesium isotopes will be found in sheepmeat for many years to come at up to some hundreds to thousands of Bq/kg.

The behaviour of caesium in sheep was not studied as part of this project, but a report by the Nuclear Energy Board of Ireland (Ref) has indicated that the caesium levels in sheepmeat decrease relatively quickly if the sheep are returned to grazing on good quality pasture for some weeks before slaughter.

The measurements on milk powder indicate that detectable levels of radioactive caesium persist in this foodstuff for some years after an accidental deposition on soil at some thousands of Bq/m^2. However, the low levels of activity present in grass and in liquid milk precluded a detailed study of the processes in this project.

The section of the project dealing with levels of natural radioactivity present in soil has proved to be potentially the most interesting. The path to man via the foodchain does not appear to be significant as regards the regions of interest in the Republic of Ireland.

However, the apparent correspondence of high areas of uranium series isotopes in soil with areas in which high domestic levels of radon have been measured leads to the possibility of using soil activity levels as a predictor for radon in the domestic environment and the workplace.

In view of the high doses associated with domestic radon (up to 80 mSv/y in some regions of the Republic of Ireland), this is by far the most important source of exposure of man to radiation.

In summary, most of the objectives aimed for in this project have been achieved. The main failures have been in the area of quantitative assessment of doses from various foodchain paths. This has been balanced by the confirmation of differences in the behaviour of "old" and "new" caesium in poor quality soils and by the linking of radon levels in the domestic environment with soil activity levels of uranium and radium, though it must be stressed that more work remains to be done to investigate this apparent association.

REFERENCES:

Ref 1 I R McAulay, P A Colgan and D Moran. Measurements on retention and transfer characteristics of radiocaesium from poor quality upland soils to heather and from heather to sheep. Science of the Total Environment. 85 (1989) 159-167.

Ref 2 I R McAulay and D Moran. Natural radioactivity in soil in the Republic of Ireland. Radiation Protection Dosimetry, Vol. 24, 47-49. (1988).

Ref 3 J P McLaughlin and P Wasiolek, Radon levels in Irish dwellings, Radiation Protection Dosimetry 24, 383, (1988).

Ref 4 P A Colgan and B J Scully, 1988 Sheep Monitoring Programme. Nuclear Energy Board, Dublin, 1989.

IV. Other research group(s) collaborating actively on this project [name(s) and address(es)]:

Dr J P McLaughlin
Department of Physics
University College
Dublin
Ireland

Dr R Kirchmann
CEN-SCK
Mol
Belgium

Dr P A Colgan
Nuclear Energy Board
3 Clonskeagh Square
Dublin 4
Ireland

V. Publications:

I R McAulay and D Moran. Natural Radioactivity in soil in the Republic of Ireland. Radiation Protection Dosimetry 24, 47-49, (1988).

I R McAulay and D Moran. Radiocaesium fallout in Ireland from the Chernobyl accident, Journal of Radiological Protection, 9, 29-32, (1989).

I R McAulay, P A Colgan and D Moran. Measurements on retention and transfer characteristics of radiocaesium from poor quality upland soils to heather and from heather to sheep. Science of the Total Environment. 85, 159-167, (1989).

RADIATION PROTECTION PROGRAMME
Final Report

Contractor:

C.I.E.M.A.T.
Avenida Complutense n° 22
E-28040 Madrid

Contract no.: BI6-B-195-E

Head(s) of research team(s) [name(s) and address(es)]:

Dr. F. Mingot Buades
Area de Protec.Radio.y Medi.Ambiente
C.I.E.M.A.T.
Avenida Complutense n° 22
E-28040 Madrid

Telephone number: 499.01.77

Title of the research contract:

Behaviour of plutonium and americium in the marine environment.

List of projects:

1. Plutonium, Americium and stable heavy metals in marine sediment. Study of the factors governing the transport from water to the sediments.

Title of the project no.:

PLUTONIUM,AMERICIUM AND STABLE HEAVY METALS IN MARINE SEDIMENT.STUDY OF THE FACTORS GOVERNING THE TRANSPORT FROM WATER TO THE SEDIMENT.

Head(s) of project:

E.IRANZO

Scientific staff:

C.Gascó,L.Romero,M.Deyá,E.Mingarro,P.Rivas,C.Rodriguez,J.Guerrero,A.Jornet,A.M.Lobo,

I. Objectives of the project:

-To study the processes controling the behaviour and distribution of radioactive and heavy metals pollutants in the marine environment of Southern coast of Spain including Palomares area.

-To determine $^{239}Pu+^{240}Pu$ and ^{241}Am inventories in the continental shelf,slope and deep ocean floor of this area.

-To examine the geochemistry of Pu,Am and heavy metals in the marine sediments and to study the processes that control the removal of Pu and Am from sea water to sediments.

II. Objectives for the reporting period:

1. Sampling of sediments cores.Pretreatment,porosity calculations, grain size composition.
2. Sampling of suspended matter.Seasonal variation of suspended particles population.
3. Distribution of $^{239}Pu+^{240}Pu$, ^{241}Am, ^{137}Cs, ^{210}Pb unsupported in selected cores from shelf,slope and deep ocean floor.
4. Inventories of $^{239}Pu+^{240}Pu$, ^{137}Cs and ^{241}Am in selected cores from shelf,slope and deep ocean floor.
5. Distribution of heavy metals fraction associated with hydrous Fe and Mn oxide coatings on the surfaces of sediment particles in selected cores of shelf, slope and deep ocean floor.
6. Chemical and mineralogical composition,petrography and chronology of sediments.

III. Progress achieved:

1. INTRODUCTION

The source of fallout radionuclides to the marine environment is atmospheric nuclear weapons testing which occured during the 1950s and early 1960s (1, 2, 3) Other sources are the discharges land to sea produced by reprocessing plants, the efluents releases from Nuclear Power Plants and the accidents.

The behaviour of radionuclides in sea water and, in particular, transuranides, has been studied in several sea-areas. In general, absorption fenomena produced by the presence of suspended matter, do that the transuranides go to the sediments and disappear of the water column. The radionuclides settled into the sediments can be removed and incorpored to the upper-layers by several processes as pH changes, ox-reduction reactions, bioturbation, complexing agents.

No large-scale compilation of Pu, Am and Cs distribution along the Western Mediterranean area has been published (4, 5, 6, 7, 8, 9, 10) In the IAEA-TECDOC 481 (11) the transuranides inventories in sediments have been infravalored as the concentration has been determined in deep sea. The shallow regions concentrate the highest quantities of radionuclides. This fenomena has been observed in our experimental work and in one of Papucci in Italian coast after Chernobyl accident.

The importance of sediments as a mayor repository for Pu introduced to the ocean has been frequently noted. The accidental release of transuranides, occured in 1966 in the coastal village of Palomares (Southern of Spain) provides an exceptional natural laboratory(26, 27, 28) that allows the experimental study of transuranics transference and to differ the transuranics contribution due to the accident from the fallout.

The main objetive of this study has been to determine the distribution of certain radionuclides and heavy metals in the area of Palomares, to compare this distribution in three depth regimenes and to study some factors governing the transport from water to the sediments.

2. METHODOLOGY

2.1 SAMPLING AND PRETREATMENT

2.1.1 Marine sediments sampling

The area choosen for the study was the southern coast of Spain, including the coastal area of Palomares, between Cape of Palos and Cape of Gata. Samples were collected at 50, 100, 200, 500 and 1000 m depth.

- Sediments were collected by a new desing box-corer (Papucci-Jennings), which allows to obtain cores up to 50 cm depth. Twenty five cores were taken in all and 30 surface sediments with a shipek-grab sampler. Their location is shown in progress reports.
- The samples were obtained by extruding each core in slides of 1 cm thick.

2.1.2 Suspended particles sampling.

Four seasonal sampling cruises (March, July, November of 1988 and February of 1989) were achived. The sampling network was established after knowledge of turbidity, salinity and temperature at each station. Twelve stations were established with 3-4 sampling levels. Samples of suspended matter were collected by 30 L Niskin bottles. Few hours later, water samples were filtered by a vacuum system, through preweighed 47 mm Nuclepore filters (45 µm pore size) and washed repeatedly with destilled water. Filters so obtained were dried at 50°C and weighed.

2.1.3 Pretreatment of the samples

Sediment samples were dried, and divided for different studies as follows.

a) An aliquot for chemical, mineralogical and petrographical studies
b) An aliquot for grain size analysis
c) The remaining sample was ball-milled and sieved trough 1 mm size, to obtain:
   - An aliquot for radionuclide analyses.
   - An aliquot for heavy metal analyses.

2.2 GEOCHEMISTRY PARAMETERS

2.2.1 **Chemical and mineralogical composition**

The chemical composition has been determined by Plasma and Atomic Absorption Spectrometry on dry sediment samples quartered by a Universal Channel Sampler.

The mineral composition has been calculated by the association grades between the chemical compounds.

2.2.2 **Petrography**

The petrographycal study has been carried out by optical microscopy in the size fraction > 63µm of surface sediments.The nature of the studied sediments,sands and limes no consolidated,has compeled to do the agregation and compaction with sinthetic resins.

2.2.3 **Grain size**

Fractional division of 63 µm particles, after leaching with water over a mesh of a prescribed size, was carried out by screening according to NLT 104/72 standards.

Particles smaller than 63 µm were analysed by counting of suspended particle in a COULTER TA II.

2.2.4 **Porosity and bulk dry density**

These data were calculated according to the formulas:

BDD = Dry weight/volume of trimmed section

$$\Phi \text{ (Porosity)} = \frac{1}{\frac{\text{Dry weight}}{2.5(\text{wet}_w - \text{dry}_w)} + 1}$$

And porosity data so obtained were fitted to this ecuation:

$$\Phi = (\Phi_o - \Phi_\infty)\, e^{(-\alpha z)} + \Phi_\infty$$

2.2.5 **Compaction corrected depth**

The compaction corrected depth at each core (Z′) is calculated by the equation:

$$Z' = Z + \int_0^z (\Phi_o - \Phi)/(1-\Phi_o)dz$$

where:

Φ_o = Porosity of sediment at the interface Z=0

Φ = Porosity at any depth

2.3 RADIOCHEMICAL PROCEDURES

2.3.1 **Plutonium-(239+240)**

The plutonium was separated from sediments using the Wong's procedure (12) with some modifications. The measurements were carried out by alpha spectrometry of the plutonium electroplated onto stainless steel discs by the Talvitie's procedure (13).

Plutonium-242 tracer is added to each sample to determine the recovery of the analysis.

2.3.2 **Americium-241**

Americium analysis are performed in the same matrix than plutonium. The americium fraction is purified by sequential separations according to the Holm's method (14). Americium was electroplated onto a stainless steel disc and counted by alpha spectrometry. Radiochemical yield was obtained by using ^{243}Am as tracer.

2.3.3 **Cesium-137**

^{137}Cs measurements are performed by gamma spectrometry using an intrisec Germanium detector and its associated system.

The accuracy of the methods was tested by analysing IAEA standard reference materials.

2.4 HEAVY METALS

Analysis of the heavy metals (Cr, Mn, Fe and Pb) associated with hydrous Fe and Mn oxide coatings on the sediments particles have been performed on 1g of sediment using the Rapin's (15) sequential extraction procedure.

International intercalibration exercises (ICES and MEDPOL II) confirm the accuracy of the data.

2.5 ADDITIONAL

2.5.1 **Chronology of sediments by ^{210}Pb**

The ^{210}Pb method has been applied to study the chronology of sediments.Total ^{210}Pb mesasurements are performed by gamma spectrometry with an intrisec Germanium detector. The supported ^{210}Pb is obtained by the measurement of ^{214}Pb.

Depending on the shape of unsupported ^{210}Pb profiles obtained ,different models (CRS constant rate of supply,CIC constant initial concentration) were applied (16, 17) using the Pu,Am and Cs profiles to check the suitability of each model.

2.5.2 **Inventories of radionuclides**

The inventory was obtained by the following equation:

$$\text{Inventory} = \sum_{i=o}^{n} a_i Dw_i / s_i$$

Where:

a_i = activity concentration of radionuclide

Dw_i = dry weight of each slide;

s_i = section of each slide.

3. RESULTS AND DISCUSSION

3.1 DESCRIPTION OF THE AREA

3.1.1 **Chemical and mineralogical composition**

The average composition from all the sampling sediments is mainly SiO_2 (35% ± 6σ) CaO (23% ± 4σ) CO_2 (20% ± 4σ)and Al_2O_3 (8% ± 2σ).The mineral compounds as it is shown by the association level are : Calcite 42%,Illite 29%, Quartz 24% and Dolomite 4%.

There are three groups in relation with the silica contents :Group 1 with contents of SiO_2 up to 48%,the second group with contents between 20% and 40% and the third group with a contents of silica less than 20%.

The highest contents of silicates correspond to the areas close to the mouths of Almanzora and Antax rivers.

The highest content of quartz defines the facies of the sediments nearest to the coast.

The highest contents of carbonates are at 100-200 m depth in the proximity area of the continental slope.

3.1.2 **Petrography**

A band of sand with high content of bioclastos exist along the coast at a distance of 4.5 Km and 100-200 m depth.The terrigenous sedimentation is predominant close to south of Almanzora,Antax and Aguas rivers.

The studied sediments constitute a facies silica-carbonated.Its alotoctonous or terrigenous component is constituted mainly by quartz,filosilicates,as illita ,and several accesories minerals which are the components of esquistes,micaceus granatiferus fragments,-cuarcites and volcanic rocks.The autoctonous component is constituted basically by carbonates that are the main components of the bioclastos and determine the content of the sand grained phase of the sediments.

3.1.3 **Grain size distribution**

There are three groups of grain size sediment composition:sand,silt and clay.The percentage of textural macrocomponents in the three depth regimenes are shown in the Table 8.-There is an enrichment of sand in the continental shelf, and clay predominates in deep sea.-The correlation of these composition parameters with depth has been studied.The linear correlation is good for clays:the contents of clay increase with the depth.More data of the distribution in the area are widely described in annual report CIEMAT-CEE 1.(1987)

3.1.4 **Porosity and Bulk dry density of sediments**

The porosity are between 0.567 (58 m depth) and 0.822 (800 m depth) and decreases exponentialy with depth due to compaction.This parameter is partially correlated with grain

size and sediments with the highest porosity should have a less size grain average composition.

More data of these parameters are summarized in annual reports.

3.1.5 **Sedimentation rate and chronology**

The sedimentation rates,in three depth regimenes,have been determined to investigate the depositional history of sediments, .The average sedimentation rates are the following:

	Core n°	Sed.rate $g.cm^{-2}.y^{-1}$	Location
Shelf	12	0.22	North Almanzora river
	31	0.26	South Almanzora river
	29	0.29	South Almanzora river
Slope	20	0.13	South Almanzora river
Deep	16	0.06	South Almanzora river

The sedimentation rate decreases as water depth increases, as expected, due to either the terrigenous input of the rivers or because of a higher concentration of particulate matter in the continental shelves.

The chronology of selected cores is shown in Table 10 .Additional comentaries are done in 3.2.1.2.

3.1.6 **Seasonal suspended particles**

The results obtained from the four samplings cruises are shortly shown in Table 1.

A decrease of population concentration has been observed with the distance to the coast in spring.In summer,the particles concentration decreases in shelf and slope,and increases in deep sea.

The higher bottom particles concentration in shelf than in deep-sea could explain a more effective scavening of radionuclides in Continental shelf.

Supporting data on temperature and salinity show a thermic regimen similar to the model described for Southern Mediterranean and a higher presence of Atlantic water in spring and autumn than in summer.

3.2 RADIONUCLIDES IN SEDIMENT

3.2.1 **Distribution**

3.2.1.1 Surface sediments

Plutonium and Americium concentration has been determined in the surface sediments.The results obtained are shown in Table 9. The Pu values are in the range of 5.2 Bq/Kg to 0.18 Bq/Kg in Continental shelf and 1.09 to 0.09 in deep-sea . The Am values are in the range 2,94 Bq/Kg and 0.39 Bq/kg.Diferences in distribution are related nor only with location but also with porosity . Papucci and Jennings (18, 19) stablished a correlation inter these parameters in surface sediments from Mediterranean sea, showing that sediments with higher porosity had more Pu concentration. There are several points located at south of Almanzora river mouth which have higher concentration than expected,this fact could confirm the contribution described in the following section.

3.2.1.2 Vertical distribution

The distribution of plutonium and americium has been determined in six sediment cores from continental shelf, four from slope and three from deep-sea.The distribution of cesium-137 has been also determined in selected cores.The results are shown in the Tables 4,5,6,7.

As is shown, there is higher transuranides concentration in sediments from continental shelves than in deep sea.Close to the coast,in estuarine environments,two opposite fenomena can occur: the removal,for the river water input,of radionuclides settled in sea sediment,and the scavenning more efective,by the suspended particles from the terrigenous input of the rivers.

The maximum Pu,Am and Cs concentration in core profiles do not appear at the same

deep layers. This could be a consequence of the decreasing sedimentation rate from shelf to deep sea.

Cores in continental shelf show Pu concentration reaching 16-22 cm deep-layer and only 8-10 cm deep-layer in slope and deep sea.The depth of radionuclide penetration into the sediment generally decreases as the water depth increases.The Pu and Am concentration detected in layers older than 1945,could be explained by the movility of Pu in the pore water or its preferential transport by a selective mixing process.

Buessler (20, 21, 22) analyzing the geochemistry of Pu fallout in three regimenes of North Atlantic observed that the depth of radionuclides penetration into the sediment generally decreases as the water depth increases as we have found .The shallowest core exhibits detectable Pu at least 35 cm and 10-15 cm only in 500 m depth.

The maximum Pu,Am and Cs concentration appear within the same period of time (1960--1965 Fallout peak)according with ^{210}Pb dating of sediment in each core (see Table 10)

In core 31,the nearest located at southern of Almanzora river mouth,a second peak of maximum Pu and Am concentration corresponding 74-78 period has been found by analyzing intermedium slides .This anomaly could be a consequence of the washing out of Palomares area by the Almanzora river during the flood which took place in october 1973.This hypothesis has been confirmed by the higher sedimentation rate and the grain size distribution in this core slide and also by the highest Pu and Am concentration in surface sediment located between Almanzora river mouth and the core 31.Besides,the petrographycal studies at this area shows that the sediment composition is mostly terrigenous.

Sediments and sedimentary particles have a substantial capacity to remove radionuclides from seawater.The area of terrigenous input of Almanzora river, shows an enhaced of Pu,Am concentration.This fenomena can be a consecuence either or the washing out by the river before mentioned or the more efective scavening of radionuclides by particulate matter. Data from core-dating, grain size of sediments, and the course of the local streams point to these theories.

3.2.2 Inventories

The inventories of plutonium,americium and cesium are expresed in Table 2 .The major trend is decreasing inventories of both Pu and Am with increasing water depth. In shallow regions, near the coast, the resuspension of fine grained material can act to enhace the scavening of particle reactive elements.This fact has been confirmed with our study of suspended particles in the area.The concentration of suspended particles at the interface water-sediment is higher in continental shelf than in deep-sea. This resuspension effect can be controlled by either biological or physical processes.Studies on benthic infauna at the area show that biogenic removal is higher in area close to the coast than in deeper sediment (23).This studies confirm the theory that biological sediment mixing processes modulate the removal of a number of elements including Pu,in coastal enviroments. In deeper waters, the effectiveness of boundary scavenging processes decreases since biological removal and transport via fecal pellets production is likely o become increasingly import.

The Pu and Am inventories in the sediment cores of Continental Shelf decrease from the Almanzora river mouth to the south.This fact could confirm the indicated contribution of the river.

3.3 HEAVY METALS IN SEDIMENTS

The results of the range of concentration in the three depth regimenes are summarized in the Table 3.

The distribution in shelf and slope is mostly homogenous and there is not peaks of maximun concentrations.Close to Portman, the maximun heavy metals concentration has been observed. This fact is due to the presence of a extraction minerals factory and the wastes contribution to the sea through the pipes which release the waste from mineral washing .In deep-sea ,the Mn distribution shows at 2-3 cm depth layer one peak with 1 thousand times higher concentration (24 , 25)

4.CONCLUSIONS

The following conclusions have been obtained:

1. The benthic infauna,suspended particles and sedimentation rate have been studied in the area of Vera Gulf.The benthic infauna shows variation in its distribution in three depth regimenes; more biological activity,biomass and higher density of biological communities exists closer to the coast.The content of suspended particles in the shallow area is higher than in slope and deep sea as well as the sedimentation rate.The knowledge of these factors is necessary to predict higher radionuclides concentrations into the sediments.Our determinations on Pu,Am and Cs have been confirmed this theory.It is concluded that shallow regions,due to its biogeochemical characteristics,shows the highest capacity to concentrate radionuclides into the sediments.
2. The radionuclides concentration decreases as water depth increases (the explanation of this fenomena are the factors before mentioned)and increases at the south of Almanzora river mouth,decreasing along the coast(this fact could be a better scavenning of radionuclides by the particulate matter coming from the river or an input which took place through the Almanzora river).
3. The radionuclides concentrations are similar to those found in others Mediterranean areas except in one small area located south of Almanzora river mouth.
4. In core 31,two peaks of maximum Pu and Am concentration but only one for Cs appear.This fact could explain an extra input of transuranides by the river as consequence of a flood which took place in 1973.In favor of this point of view is the fact that the Pu/Cs relation up to the river is 0.35 and down to the river is 1.2.
5. The radionuclides penetration into the sediment column decreases as water depth increases.
6. The heavy metals show a constant distribution in shelf and slope and an increment close to the area of a minerals treatment plant(Portman).The periodical input of radionuclides in to the coast is different that the one of heavy metals,this fact do that distribution of radionuclides in the sediments column presents differents profiles.The radionuclides distribution shows peaks due to the epoca of maximun fallout or extra input.Heavy metals do not present these peaks as the input have been constant.In deep sea,there are peaks,especially for Mn,in surface layers that could be explained by a preferential precipitation of Mn(in solution) in deep-sea.

5.REFERENCES

(1) Perkins R.W and Thomas C.W. (1980) Worldwide fallout in:Transuranic Elements in the Environment. W.C.Hanson ed.
(2) Hardy E.P et al. (1973) Global inventory and distribution of fallout plutonium. Nature 241,444-445
(3) Harley (1980) Plutonium in the environment a review.J.Radiation Res.21,83-104.
(4) Livingston H.D,Bowen V.T and Burke J.C (1976) Fallout Radionuclides in Mediterranean Sediments 16pp 25 Congress and Plenary Assembly of C.I.E.S.M Slipt,Yugoslavia 22 Oct 1976.
(5) Fukai R.,Ballestra S. and Thein M. (1980) Vertical distribution of transuranic Nuclides in the Eastern Mediterranean sea.p.79-87 in Proceeding of a technical committee meeting on the behaviour of transuranides in the aquatic environment and sediment water exchanges (IAEA and CEC).Ispra,Italy 24-28 March 1980.
(6) Bowen V.T (1979) Element Specific Redistribution in the Marine water column(Abstract from a workshop March 7-9,1979,Gaithesburg,Maryland;US-DOE,CONF 790382.
(7) Murray C.N and Fukai R. (1978) Measurements of ^{239}Pu + ^{240}Pu in the North Western Mediterranean . Estuarine Coastal Mar.Sci.6,145-151.
(8) Fukai R.,Holm E. and Ballestra S. (1979) Note on vertical distribution of plutonium and americium in the Mediterranean sea. Oceanol.Acta 2,129-132.
(9) Aakrog A.Worlwide (1988) Data on fluxes of $^{239,240}Pu$ and ^{238}Pu to the oceans. IAEA-TECDOC-481. pp 103-137.
(10) Whitehead N.E (1988) Inventory of ^{137}Cs and ^{90}Sr in the World's Oceans.IAEA-TECDOC-481-.pp 51-69.
(11) IAEA TECDOC 481 (1988) Inventories of selected radionuclides in the Oceans.
(12) Wong,K.M (1971) Radiochemical determination of Plutonium in sea water,sediments and marine organism.Anal.Chim.Acta 56,355-64

(13) Talvitie,N.A. (1972) Anal.Chem 44,280.
(14) Holm,E.Fukai,R and Ballestra S. (1979) A method for ion-exchange separation of low levels of americium in environmental matrices.Talanta 26,791-794.
(15) Rapin,F,et al. (—) Heavy metals in marine sediment phases determined by sequential chemical extraction and their interaction with interstitial water.Env.Tech.letters 4,387-396.
(16) Olfield,F and Appleby P (1984) Empirical testing of ^{210}Pb dating models for lake sediments.Lake sediments and environmental history.Haworth-Lund Ed.Leicester Univ.Press 93-124.
(17) P.G.Appleby and F.Oldfield (1978) The calculation of lead 210 assuming a constant rate of supply of unsupported ^{210}Pb to the sediment.Catena 5,1-8
(18) Papucci,C et al (1986) Il comportamento dei Transuranici nell'ambiente marino costiero.Acqua Aria 6.
(19) Jennings,D et al (1985) The distribution and inventory of fallout plutonium in sediments of the Ligurian sea near la Spezia.J.Environ.Radioactivity 2,293-310
(20) Buesseler,K et al. (1987) The geochemistry of fallout plutonium in the North Atlantic:I.A pore water study in shelf,slope and deep-sea sediments.Geochim et Coscochim Acta 51,2605-2622.
(21) Buesseler,K et al. (1987) The geochemistry of fallout pluonium in the North Atlantic:II $^{240}Pu/^{239}Pu$ ratios and their significance.Geochim et Coscochim Acta 51,2623-2637.
(22) Buesseler,K et al. (1985) $^{239,240}Pu$ and excess ^{210}Pb inventories along the shelf and slope of the northeast U.S.A.Earth and Planetary Science Letters 76,10-22.
(23) Alonso,A y López-Jamar,E (1989) Infauna bentónica de las costas de Almería.-Inf.Tec.Esp.Oceanogr(in press).
(24) Lyons,W et al. (1980) Trace metal fluxes to near shore Long Island Sound sediments.-Mar.Poll.Bull 11,157-161
(25) Lognathan,P et al. (1973) Sorption of Heavy metals ions by hidrous manganese oxide.Geochem et Cosmochim Acta 87,1277-1293.
(26) Iranzo,E et al. (1987) Air concentrations of ^{239}Pu and ^{240}Pu and potential radiation doses to persons living near Pu-contaminated areas in Palomares Spain. Health Physics 52,-453-461.
(27) Iranzo,E et al. (1987) Geochemical Distribution of Plutonium and Americium in Palomares Soil".Book:Cycling of Long-lived radionuclides in the Biosphere.Observations and models.-2,392-419.Spain.
(28) Iranzo,E et al (1988) Evaluation of remedial actions taken in an agricultural area contaminated by transuranides". .Book:Impact des Accidents d'origine nucleaire sur l'environment.2.Cadarache.FRANCE.ISBN:2-7272-0143-5.
(29) E,Iranzo.,L.Romero.,C.Gascó (1988) Temporal distribution of long-lived radionuclides in marine sediments at Southern Coast of Spain.Rapp.Comm.int.Mer Médit.,31,2 pag 245. Mónaco

6.TABLES

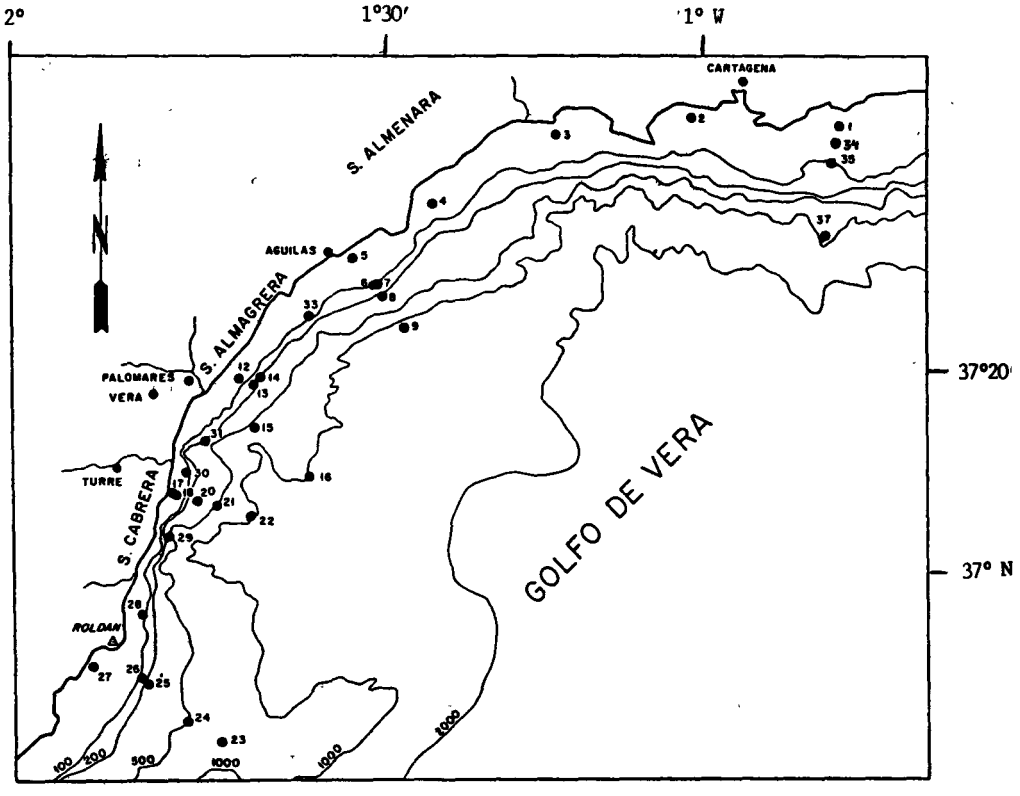

FIG 1 : SAMPLING AREA

TABLE 1 : REPRESENTATION OF AVERAGE CONCENTRATION OF SUSPENDED PARTICLES (mg/L) VERSUS SEASON.

		Depth Level (m)	>100	500	1000	Total
		Surface	0.41	0.32	0.21	0.31
	Spring	Interm	0.39	0.39	0.14	0.31
		Bottom	0.39	0.40	0.08	0.29
		Surface	0.30	0.22	0.35	0.29
S	Summer	Interm	0.27	0.23	0.26	0.25
E		Bottom	0.42	0.28	0.26	0.32
A		Surface	0.40	0.30	0.28	0.33
S	Autumn	Interm	0.61	0.18	0.09	0.29
O		Bottom	0.18	0.18	0.27	0.21
N		Surface	0.20	0.21	0.25	0.22
	Winter	Interm	0.27	0.16	0.14	0.19
		Bottom	0.22	0.18	0.18	0.19

TABLE 2 : INVENTORIES OF RADIONUCLIDES EXPRESED IN Bq/m^2 IN THREE DEPTH REGIMENES.

		#	SHELF	#	SLOPE	#	DEEP-SEA
		34	177	08	52		
		12	128	15	<0.5	16	43
R	Pu	31	529				
A		30	327				
D		18	254	20	78	22	18
I		29	252	24	3	23	17
O							
N		34	55	08	28		
U		12	60	15	12	16	25
C	Am	31	160				
L		30	80				
I		18	30	20	45	22	24
D		29	58	24	13		
E							
		12	442			16	94
	Cs	31	676				
		30	748				
		29	512	20	390		

TABLE 3 : RANGE OF CONCENTRATION OF HEAVY METALS EXPRESED IN $\mu g/g$ IN THREE DEPTH REGIMENES.

		#	SHELF	#	SLOPE	#	DEEP SEA
		12	60-70	08	70-260	16	10-5500
		18	66-120	15	64-75	22	50-1800
	Mn	29	65-67	20	60-66		
H		30	63-69	24	52-70		
E		31	65-81				
A		34	100-900				
V							
Y		12	19-31	08	6-20	16	5-37
		18	13-26	15	5-7	22	4-30
M	Pb	29	16-21	20	12-18		
E		30	14-21	24	3-10		
T		31	15-22				
A		34	50-400				
L							
S		12	1.5-2.8	08	1.0-2.1	16	1.3-1.6
		18	0.9-1.1	15	1.3-1.7	22	0.5-1.8
	Cr	29	0.9-1.1	20	0.9-1.3		
		30	0.9-1.1	24	1.2-1.6		
		31	1.2-1.5				
		34	1.8-2.5				

Core number

TABLE 4 : CONCENTRATION OF ^{239}Pu+^{240}Pu, ^{137}Cs AND ^{241}Am EXPRESED IN Bq/Kg d.w IN SEDIMENT CORE FROM CONTINENTAL SHELF,SLOPE AND DEEP SEA (error 1σ) VERSUS DEPTH IN CORE IN cm.

CORE 12 : 37° 16.4' N 01° 43.5' W (Depth 58 m)

SLIDE cm	CONCENTRATION (Bq/Kg) Pu	Cs	Am
0–1	1.33±0.10	5.1±0.4	0.59±0.07
1–2	1.39±0.07	5.5±0.4	0.66*
2–3	1.80±0.13	5.0±0.6	0.73±0.06
3–4	*1.33	4.6±0.7	0.62*
4–5	0.83±0.08	4.0±0.6	0.52±0.02
5–6	*0.67	2.2±0.5	0.43*
6–7	0.50±0.07	1.5±0.6	0.34±0.07
7–8	*0.33	1.9±0.5	———
8–9	0.17±0.02	1.0±0.6	———
9–10	*0.13	<LID	
10–11	*0.10		
11–12	0.07±0.02		
12–13	*0.05		
13–14	*0.03		
14–15	0.02±0.01		
17–18	———		

CORE 31 : 37° 10.7' N 01° 46.3' W (Depth 94 m)

SLIDE cm	CONCENTRATION (Bq/Kg) Pu	Cs	Am
0–1	3.02±0.13	4.8±0.9	0.94 ± 0.11
1–2	5.75±0.24	5.6±1.0	1.84 ± 0.09
2–3	3.27±0.12	6.6±1.0	1.83 ± 0.20
3–4	3.96±0.01	7.4±1.1	1.39 ± 0.09
4–5	4.38±0.18	6.7±0.9	1.96 ± 0.11
5–6	3.58±0.19	5.5±1.0	1.67*
6–7	2.80±0.12	4.0±0.9	1.38 ± 0.12
7–8	2.48±0.17	3.5±0.8	———
8–9	2.52±0.10	3.9±1.0	0.9*
9–10	*2.23	2.6±0.9	———
10–11	*1.9	2.0±0.9	———
11–12	1.67±0.08	1.7±1.0	———
12–13	*1.57	1.2±1.0	
13–14	*1.47	1.2±0.9	
14–15	1.35±0.13	1.1±0.9	
15–16	*1.30	<0.96	
16–17	*1.2		
17–18	1.18±0.10		
18–19	*0.90		
19–20	*0.67		
20–22.5	0.13±0.05		

CORE 20 : 37° 06.8' N 01° 47.5' W (Depth 200 m)

SLIDE cm	CONCENTRATION (Bq/Kg) Pu	Cs	Am
0–1	1.20±0.08	4.7±0.9	0.75±0.08
1–2	1.25±0.11	5.2±0.9	0.70*
2–3	1.20±0.08	5.1±0.9	0.65
3–4	1.07*	4.3±1.0	0.86*
4–5	0.95±0.07	2.5±0.9	1.07
5–6	0.75*	2.6±1.0	0.72*
6–7	0.55*	1.7±0.9	0.36
7–8	0.35*	2.0±0.9	0.24*
8–9	0.17±0.02	<1.5	0.13
9–10	0.11*	0.6±0.5	
10–11	0.06*	———	
11–12	0.037±0.01	<1.5	
12–13	———	———	
13–14	< 0.01	1.3±0.7	
15–16		<1.5	
17–19.5		<1.4	

CORE 16 : 37° 09.0' N 01° 36.8' W (Depth 1000 m)

SLIDE cm	CONCENTRATION (Bq/Kg) Pu	Cs	Am
0–1	1.75±0.04	8.1±1.3	L.I.D
1–2	1.69*	5.4±1.5	———
2–3	1.63±0.09	1.8±1.0	0.58±0.11
3–4	0.90*	<1.6	———
4–5	0.15±0.02	———	0.78±0.14
5–6	0.11	<1.0	———
6–7	0.08±0.01	———	———
7–8	0.50*	———	———
8–9	<0.01	———	———

TABLE 5 : CONCENTRATION OF ^{239}Pu+^{240}Pu, ^{137}Cs AND ^{241}Am EXPRESED IN Bq/Kg d.w IN SEDIMENT CORE FROM CONTINENTAL SHELF(error 1σ)VERSUS DEPTH IN CORE IN cm.

CORE 29 : 37° 04.4' N 01° 49.8' W (Depth 78 m)

SLIDE cm	CONCENTRATION (Bq/Kg) Pu	Cs	Am
0-1	1.22±0.10	3.2±1.1	0.68±0.06
1-2	*1.58	3.5±0.9	————
2-3	1.90±0.10	3.6±1.0	P.E.A
3-4	*1.75	4.3±0.9	————
4-5	1.60±0.08	3.9±1.1	0.74±0.17
5-6	*1.78	3.6±1.0	0.49*
6-7	1.95±0.17	4.3±1.1	0.23±0.05
7-8	*1.58	4.4±1.0	0.15*
8-9	1.22±0.07	3.2±1.0	0.06±0.01
9-10	*1.00	————	0.09*
10-11	*0.77	1.4±0.8	0.13*
11-12	0.57±0.05	————	0.16±0.03
12-13	*0.48	<1.4	————
13-14	*0.40	————	
14-15	0.32±0.05	<1.4	
15-16	*0.23	————	
16-17	*0.17	<1.6	
17-18	0.08±0.02		

CORE 30 : 37° 08.1' N 01° 48.5' W (Depth 64 m)

SLIDE cm	CONCENTRATION (Bq/Kg) Pu	Cs	Am
0-1	1.35±0.12	5.1±1.0	0.76±0.07
1-2	1.29±0.05	5.4±0.9	0.8*
2-3	1.82±0.15	5.0±1.1	0.84±0.09
3-4	*2.05	4.6±1.1	0.93*
4-5	2.33±0.20	5.2±1.0	1.02±0.09
5-6	*2.23	5.8±1.0	0.87*
6-7	2.12±0.15	7.2±1.0	0.73±0.2
7-8	*2.80	6.3±1.2	0.45*
8-9	3.58±0.27	————	P.E.A
9-10	*2.57	4.5±1.0	
10-11	*1.53	————	
11-12	0.45±0.03	2.5±1.1	
12-13	*0.37	————	
13-14	*0.30	<1.46	
14-15	0.20±0.03	————	
15-16	*0.10	<1.27	
17-18	————	<1.55	

*Interpolated activity
L.I.D Detection Limit
P.E.A Lost in analysis
Cs:error expresed in 2σ

TABLE 6 : CONCENTRATION OF $^{239}Pu+^{240}Pu$ AND ^{241}Am EXPRESSED IN Bq/Kg d.w IN SEDIMENT CORE FROM CONTINENTAL SHELF(error 1σ)VERSUS DEPTH IN CORE IN cm.

CORE 18 : 37° 07.0' N 01° 48.6' W (Depth 58 m)

SLIDE cm	CONCENTRATION (Bq/Kg) Pu	Am
0-1	1.67±0.10	0.84±0.19
1-2	*1.78	0.67*
2-3	1.88±0.22	0.50±0.14
3-4	*1.75	0.34*
4-5	1.62±0.17	P.E.A
5-6	*1.83	0.02*
6-7	2.07±0.23	P.E.A
7-8	*1.60	———
8-9	1.18±0.10	———
9-10	*1.13	
10-11	*1.10	
11-12	1.07±0.07	
12-13	*0.72	
13-14	*0.40	
14-15	0.08±0.02	
15-16	*0.08	
16-17	*0.08	
17-18	0.08±0.02	
18-19	*0.05	
19-20	*0.05	
20-21	0.05±0.02	
21-22	*0.07	
22-23	*0.08	
23-24	0.10±0.02	
26-28.5	————	

CORE 34 : 37° 33.6'N 00° 50.3'W (Depth 50 m)

SLIDE cm	CONCENTRATION (Bq/Kg) Pu	Am
0-1	1.47±0.10	P.E.A (0.6)
1-2	1.77±0.10	0.78
2-3	*1.75	0.87*
3-4	*1.73	1.0*
4-5	1.73±0.13	1.07±0.06
5-6	*1.80	0.8*
6-7	1.90±0.12	0.6*
7-8	*1.70	0.5*
8-9	1.48±0.07	0.43±0.08
9-10	*1.18	
10-11	*0.88	
11-12	0.60±0.08	
12-13	*0.48	
13-14	*0.37	
14-15	0.25±0.02	
15-16	*0.20	
16-17	*0.15	
17-18	0.10±0.2	
20-21	————	

TABLE 7 : CONCENTRATION OF $^{239}Pu+^{240}Pu$ AND ^{241}Am EXPRESED IN Bq/Kg d.w IN SEDIMENT CORE FROM SLOPE AND DEEP SEA (error 1σ) VERSUS DEPTH IN CORE IN cm.

CORE 08 : 37° 21.0′ N 01° 28.7′ W (Depth 450 m)

SLIDE cm	CONCENTRATION (Bq/Kg) Pu	Am
0–1	0.56±0.06	0.79 ± 0.08
1–2	0.47*	0.73*
2–3	0.39±0.05	0.67 ± 0.06
3–4	0.40*	0.58*
4–5	0.42*	0.49±0.05
5–6	0.44*	———
6–7	0.45±0.06	
7–8	0.67*	
8–9	0.91±0.09	
9–10	0.7*	
10–11	0.4*	
11–12	0.16±0.01	

CORE 24 : 36° 51.4′ N 01° 48.0′ W (Depth 500m)

SLIDE cm	CONCENTRATION (Bq/Kg) Pu	Am
0–1	0.19±0.03	0. 73±0.10
1–2	0.1*	0.54*
2–3	0.05±0.02	0.35±0.08
3–4	0.03	
4–5	<0.01	L.I.D
5–6	———	
		L.I.D

CORE 22 : 37° 05.5′ N 01° 42.0′ W (Depth 980 m)

SLIDE cm	CONCENTRATION (Bq/Kg) Pu	Am
0–1	0.65±0.06	P.E.A
1–2	0.51±0.08	
2–3	0.30±0.04	<L.I.D
3–4	0.23*	
4–5	0.15±0.03	0.70±0.08
5–6	0.11*	
6–7	0.08*	0.60±0.09
7–8	0.05*	
8–9	0.04±0.02	
9–10	———	

CORE 23 : 36° 50.2′ N 01° 43.7′ W (Depth 825m)

SLIDE cm	CONCENTRATION (Bq/Kg) Pu	Am
0–1	0.61±0.07	
1–2	0.74±0.13	
2–3	0.65±0.11	
3–4	0.55*	
4–5	0.20±0.05	

TABLE 8 : SURFACE SEDIMENTS.PERCENTAGE OF TEXTURAL MACROCOMPONENTS.

	STATION	SAND	SILT	CLAY
	01	18.5	73.2	8.3
C	02	16.6	79.2	4.3
O	03	29.4	67.0	3.6
N	04	74.8	23.2	2.0
T	05	30.5	62.9	6.6
I	06	44.9	48.2	6.9
N	07	88.9	8.8	2.2
E	12	40.2	55.3	4.6
N	13	77.6	18.9	3.4
T	14	66.2	31.4	2.4
A	17	84.8	13.4	1.8
L	18	18.0	77.2	4.5
	20	24.3	67.6	8.0
	25	36.2	57.0	6.9
S	26	67.7	27.6	4.6
H	27	26.5	69.4	4.1
E	28	45.5	49.5	4.9
L	29	16.1	76.8	7.1
F	30	20.8	74.1	5.0
	33	80.5	17.5	2.0
	35	36.3	52.4	11.3

	STATION	SAND	SILT	CLAY
S				
L	08	2.4	79.1	18.5
O	15	9.8	83.1	7.2
P	21	1.7	84.3	14.0
E	24	4.0	78.9	17.0

	STATION	SAND	SILT	CLAY
D	09	0.5	74.8	24.7
E	16	1.0	66.7	32.3
E	23	0.0	72.1	27.9
P	37	0.4	80.3	19.3

TABLE 9 : CONTENTS OF ^{239}Pu AND ^{240}PU IN SURFACE SEDIMENTS.CONCENTRATION EXPRESED IN Bq/Kg dry weight (error 1σ)

	STATION	ACTIVITY (Bq/Kg)
	01	1.55±0.15
	02	1.17±0.10
	03	0.92±0.08
C	05	1.12±0.07
O	06	0.77±0.07
N	07	0.18±0.03
T	10	0.43±0.07
I	11	5.22±0.32
N	12	1.80±0.13
E	13	0.48±0.07
N	17	0.38±0.05
T	18	1.72±0.17
A	20	0.73±0.10
L	25	0.72±0.07
	26	1.15±0.08
S	27	1.32±0.08
H	28	1.92±0.17
E	29	1.93±0.12
L	30	2.47±0.20
F	31	2.43±0.18
	33	0.67±0.08
	35	1.05±0.10

	STATION	ACTIVITY (Bq/Kg
S		
L		
O	16	0.43±0.05
P		
E	22	0.09±0.02
D	09	0.69±0.08
E		
P	21	1.09±0.07
P		

TABLE 10: RADIONUCLIDES CONCENTRATION AND THEIR CHRONOLOGY IN SELECTED CORES
(Concentration of 239Pu+240Pu, 241Am, AND 137Cs expresed in Bq/Kg dry weight, error 1σ for Pu and Am and 2σ for Cs and Pb)

	Nuclide Concentration			210Pb unsupp	Sed rate	Year
	Pu	Am	Cs	Bq/Kg	$g.cm^{-2}.y^{-1}$	
CORE 12						
0-1	1.33±0.10	0.59±0.07	5.1±0.4	47±7	0.28	1985
1-2	1.39±0.07	0.66*	5.5±0.4	33±6	0.31	1977
2-3	1.80±0.13	0.73±0.06	5.0±0.6	42±8	0.22	1973
3-4	1.33*	0.62*	4.6±0.7	43±8	0.18	1967
4-5	0.83±0.08	0.52±0.02	4.0±0.6	32±7	0.18	1958
5-6	0.67*	0.43*	2.2±0.5	28±8	0.15	1949
6-7	0.50±0.07	0.34±0.07	1.5±0.6	13±6	0.22	1935
7-8	0.33*	< 0.05	1.9±0.5	11±4	0.21	1928
8-9	0.17±0.02	———	1.0±0.6	8±2	0.22	1921
9-10	0.13*	———	<	13±4	0.11	1913
10-11	0.10*	———	———	15±5	0.06	1896
11-12	0.07±0.02	———	———	2±1	0.05	1827
12-13	0.05	———	———	———	———	———
13-14	0.02±0.01	———	———	———	———	———
CORE 31						
0-1	3.02±0.13	0.94±0.11	4.8±0.9	46±8	0.36	1982
1-2	5.75±0.24	1.84±0.09	5.6±1.0	46±9	0.33	1978
2-3	3.27±0.12	1.83±0.20	6.6±1.0	55±8	0.24	1974
3-4	3.96±0.01	1.39±0.09	7.4±1.1	57±9	0.20	1968
4-5	4.38±0.18	1.96±0.11	6.7±0.9	42±9	0.23	1963
5-6	3.58±0.19	1.67*	5.5±1.0	37±9	0.22	1956
6-7	2.80±0.12	1.38±0.12	4.0±0.9	25±9	0.27	1951
7-8	2.48±0.17	0.64±0.04	3.5±0.8	23±8	0.25	1945
8-9	2.52±0.10	0.9*	3.9±1.0	34±9	0.14	1935
9-10	2.23*	———	2.6±0.9	13±12	0.27	1931
10-11	1.97	0.3*	2.0±0.8	21±8	0.15	1921
11-12	1.67±0.08	0.1*	1.7±1.0	11±11	0.19	1914
12-13	1.57*	———	1.2±1.0	19±9	0.09	1898
13-14	1.47*	———	1.2±0.9	13±9	0.08	———
14-15	1.35±0.13	———	1.0±0.9	———	———	———
15-16	1.30*	———	———	———	———	———
16-17	1.23*	———	———	———	———	———
17-18	1.18±0.10	———	———	———	———	———
18-19	0.90	———	———	———	———	———
19-20	0.67*	———	———	———	———	———
22-22.5	0.13±0.05	———	———	———	———	———

*Interpolated activity

IV. Other research group(s) collaborating actively on this project [name(s) and address(es)]:

C.D.Jennings,Eckerd College,P.O.Box 12560,St Petersburg Fl.33733. USA.
M.M.Deyá.Instituto Oceanográfico de Baleares.Muelle de Poniente,sn.Apartado 291.07080 Palma de Mallorca.

V. Publications:

L.Romero and E.Iranzo."Informe de la campaña de muestreo de sedimentos marinos en el Sureste Español realizada en Abril del 1986" M2A/PM01/-/86.

C.Gascó"Pretratamiento y análisis de transuránidos en sedimentos marinos del sureste de España".M2A/PM02/-/86

L.Romero and C.Gascó"Distribución e inventario del plutonio en sedimentos marinos procedentes del Sureste Español"II Congreso Nacional de la Sociedad Española de Protección Radiológica".Toledo 4-6 Noviembre 1987.

L.Romero,C.Gascó and E. Iranzo."Estudio de la distribución temporal de radionucleidos de vida larga en sedimentos marinos del S.E español".International Conference on Environmental Radioactivity in the Mediterranean Area.Barcelona 10 a 13 de Mayo de 1988.

L.Romero,C.Gascó and E.Iranzo."Estudio de la deposición de radionucleidos de vida larga en sedimentos marinos del Sureste Español".XXII Reunión Bienal de la Real Sociedad Española de Quimica.Murcia 26-30 de Setiembre 1988.

L.Romero,C.Gascó and E.Iranzo."Temporal distribution of long-lived radionuclides in marine sediments at southern Coast of Spain".Rapp.Comm.int.Mer Medit,31,2(1988).Commission internationale pour L'exploration scientifique de la Mer Mediterranee.XXXI Congress.Athenes.(Grecia)

L.Romero,C.Gascó and E. Iranzo "Estudio de la deposición temporal de radionucleidos de vidad larga".Congreso de la SNE celebrado en Marbella.Octubre 1988.

L.Romero,C.Gascó,E.Iranzo,E.Mingarro and P.Ribas."Temporal distribution of Pu and Am in the marine environment of Southern Coast of Spain" REPORT CIEMAT-641.1989(in press).

RADIATION PROTECTION PROGRAMME
Final Report

Contractor: Contract no.: BI6-B-047-F

Université de Nantes
Laboratoire de Biochimie
et Radiobiochimie
Chemin de la Houssinière, 2
F-44072 Nantes Cedex

Head(s) of research team(s) [name(s) and address(es)]:

Prof. J. Pieri
Lab. de Biochimie et Radiobiochimie
Université de Nantes
Chemin de la Houssinière 2
F-44072 Nantes Cedex

Telephone number: 40/74.00.26

Title of the research contract:

Ligands of technetium and transfer.

List of projects:

1. Ligands of technetium and transfer.

Title of the project no.:

Subcellular ligands of technetium in living organisms.

Head(s) of project:

Professeur J. PIERI

Laboratoire de Biochimie et Radiobiochimie

Rue de la Houssinière, 2 - UNIVERSITE DE NANTES

F- 44072 NANTES Cedex 03

Scientific staff:

Pr. J. PIERI, F. GOUDARD

I. Objectives of the project:

Etude des ligands bioorganiques du Tc cytosolique

Etude des métabolites liant le Tc

Affinité du Tc selon le ligand (sites de fixation).

II. Objectives for the reporting period:

Etudier le devenir des différents ligands bioorganiques du technetium au niveau métabolique et leur élimination à l'échelon moléculaire ont été l'objectif des recherches envisagées.

L'analyse des complexes du Tc avec des macromolécules bioorganiques a été poursuivie.

Le passage du Tc par les systèmes biologiques a été examiné au niveau des surfaces biologiques (membranes), au niveau des organites chargés de la détoxification (lysosomes) et enfin au niveau soluble (protéines).

III. Progress achieved:

Transfert aux biota au niveau moléculaire.

Le technétium rejeté dans l'environnement a pour source principale l'utilisation de l'énergie nucléaire à des fins militaires et civiles. Dans les étapes du cycle du combustible, cette dispersion est observée au niveau de l'enrichissement et du retraitement.

Au niveau du sol comme au niveau marin, le Tc se présente sous forme anionique oxydée, TcO_4^- . En l'absence d'agents réducteurs puissants, cette forme chimique est très mobile.

Pour le maintien des fonctions essentielles à la vie, des systèmes sont présents pour contrôler les concentrations intracellulaires des métaux essentiels et de ceux qui ne le sont pas et pour les éliminer.

Du point de vue de la radioprotection , l'élucidation de ces voies métaboliques et la caractérisation des complexes radionucléides-molécules bioorganiques doivent aider à la compréhension de leur rétention et de leur stockage.

Des complexes du technétium avec des macromolécules bioorganiques de haut poids moléculaire (150 000) et de faibles poids moléculaire (10 000) avaient été mis en évidence lors d'études précédentes (Goudard et al , 1985). Une grande affinité pour la fraction de poids moléculaire 10 KD avait été décelée.

De façon à étudier ces ligands bioorganiques du Tc , une étude a été conduite chez Homarus gammarus qui concentre fortement ce radionucléide dans sa glande digestive (Facteur de concentration 15 000).

Les crustacés ont été contaminés par voie trophique par le laboratoire de Radioécologie marine de La Hague (CEA) . La contamination était obtenue par des moules marquées par du TcO_4^- (^{95m}Tc).

Nous avons fait une étude parallèle au niveau moléculaire des complexes macromolécules biologiques-radionucléides avec des homards marqués par voie trophique à l'Am-241 et nous avons ainsi comparé les voies métaboliques de ces deux radioéléments qui n'ont aucune fonction biochimique connue dans la cellule.

Un autre travail a été effectué pour comparaison sur la glande digestive du mollusque prosobranche Littorina littorea contaminé par l'eau marquée à l'Am-241 ainsi que chez le crustacé Astacus leptodactylus. Une étude similaire avec le Tc-99 n'a pas pu être poursuivie à cause d'un facteur de concentration inférieur à 10, résultat à rapprocher d'une étude effectuée par Masson chez Haliotis tuberculata où la voie trophique serait prépondérante chez les mollusques brouteurs (Masson et al. , 1986).

Méthodologie

Les glandes digestives sont disséquées et rapidement homogénéisées dans un milieu contenant essentiellement du Tris-HCL 20 mM pH 7,6 , 0,25 M de saccharose, 0,9 % de NaCl et des inhibiteurs des protéases (PMSF, leupeptine et pepstatine).

Les différentes fractions subcellulaires des glandes digestives sont séparées par centrifugation différentielle et purifiées sur gradient de densité (Galey et al. , 1986). Les protéines du cytosol (surnageant final) sont fractionnées par filtration sur gel (Séphacryl S300). Pour chacune des fractions obtenues, la radioactivité du Tc ou de l'Am et la densité optique à 280, 270, 250 nm ont été mesurées. Les métaux stables comme le Cd, Cu, Zn et fe sont dosés par spectrophotométrie d'absorption atomique.

Les ligands du Tc sont ensuite séparés par chromatographie sur échangeur d'ions.

La séparation des constituants des lysosomes, des membranes plasmiques et du cytosol solubles dans le SDS est effectuée par chromatographie sur gel.

Résultats et discussion

Le technétium est essentiellement associé aux constituants du cytosol ($\simeq$ 76 %) dans la glande digestive. Contrairement au transuranien accumulé dans les lysosomes (38 %) , cette fraction contient une faible proportion (12 %) de 95mTc.

La répartition du technétium après séparation du culot 12 000 g (14,4 % de la radioactivité globale) a été étudiée sur gradient de métrizamide. Les courbes de phosphatase acide et de cytochrome oxydase localisant les lysosomes et les mitochondries témoignent de la

bonne séparation des organites cellulaires.
Le ^{95m}Tc mesuré essentiellement dans les fractions de 1 à 7 (72 %) de densité moyenne 1.138 g/cm^3 est donc associé aux lysosomes . En revanche, l'Am-241 est clairement lié au matériel particulaire : un premier pic (25 % de l'activité correspond aux lysosomes de faible densité ; la plus grande partie de l'activité est distribuée tout le long du gradient en deux pics assez larges (30 et 36 %) selon un schéma observé pour les lysosomes secondaires et les corps résiduels qui ont des activités phosphatase acide faible.

Une fraction de très faible densité essentiellement constituée de lipides contient environ 6% du radionucléide.

La localisation du technétium étant essentiellement cytosolique. L'analyse plus détaillée de ses constituants a été réalisée par filtration sur gel (Fig. 1-a).

Le radionucléide ne se fixerait pas sur l'hémocyanine (B) synthétisée dans cette glande digestive (Senkbeil et Wriston, 1981) ni sur la ferritine (C) qui est un des ligands de l'américium.

Les ligands du technétium se retrouvent à 10 000 - 12 000 daltons (A) coélués avec du cuivre et du zinc (Fig. 1-b). Ces molécules possèdent des propriétés ioniques différentes et sont séparées sur résine échangeuse d'ions (DE 52, Watman) =

- 15 % du 95mTc déposés ne sont pas fixés par la cellulose.

- 51 % sont élués en deux pics distincts A et B par le gradient de concentration de Tris-Hcl 10mM-400 mM pH. 8,6.

Le reste du technétium est décroché par un gradient de Tris-Hcl 0,4 à 1 M pH. 8,6.

Chaque fraction technétiée est liée à des protéines contenant du cuivre (environ 4 atomes de cuivre par molécule). Des études sont en cours pour approfondir la nature de ces ligands et en particulier pour savoir s'il s'agit de métallothionéines vraies, protéines induites responsables de la détoxification des métaux lourds ou de "low molecular weight metal binding proteins" très souvent rencontrées chez ces animaux.

La grande spécificité de fixation du technétium à 10 000 - 12 000 D par rapport aux autres protéines solubles laisse supposer une grande affinité du Tc pour ces protéines. Ce fait avait déjà été

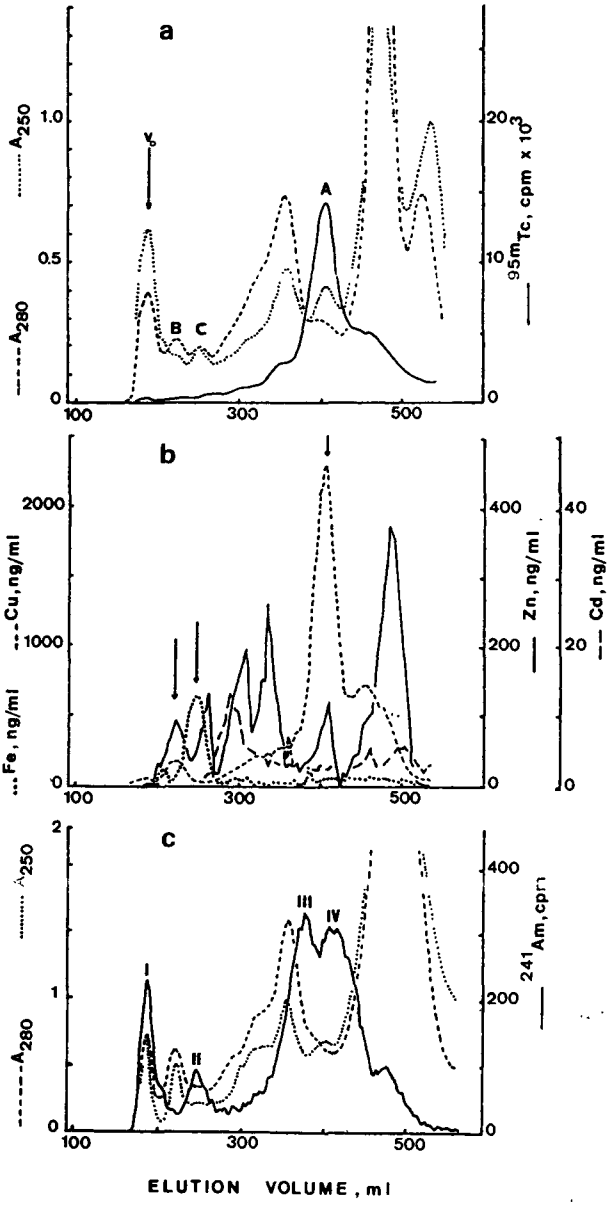

Fig. 1: Profils d'élution sur Séphacryl S300 de la fraction cytosol de Homarus gammarus contaminé par Tc-95m (a,b) et Am-241 (c).

observé lors d'expériences précédentes effectuées chez Marthasterias glacialis (Goudard et al. , 1985 ; Goudard, 1987).

Nos essais de contamination in vitro ont montré que la fixation cytosolique du Tc est de 0,3 % pour le pertechnétate et jusqu'à 56 % pour le Tc réduit selon la technique de Fowler (Fowler et al.,1980) On voit ainsi à l'échelon métabolique que la fixation du Tc dépend des transformations de sa forme physico-chimique (Cros, 1989).

Après élimination progressive du cuivre, le rapport % Tc/Do passe de 56 à 96 % . Le cuivre étant en général plus fortement accroché aux protéines qui le lient que d'autres métaux (Cd, Zn), la fixation possible du technétium dans les sites anioniques ne permet pas de prévoir une élimination rapide du radionucléide, sinon par le "turn-over" protéique.

Dans le surnageant final (cytosol), après chromatographie sur gel de Séphacryl S300 (Fig. 1-c) la courbe d'élution de l'Am-241 montre une large majorité du transuranien (67 %) élué en deux pics faiblement résolus (III et IV) correspondant à des protéines de PM apparent 21 000 et 10 000 daltons. Une étude est en cours pour préciser la liaison de l'Am sur ces protéines.

Nous avons montré qu'il se fixait aussi sur la ferritine (6,2 % (II) ce que l'on ne savait pas chez ces animaux marins.

Au niveau des surfaces biologiques comme les membranes cellulaires et le sac lysosomal, on s'aperçoit que le Tc se lie aux protéines de ces deux compartiments solubles dans le SDS à (85 % et 65 %).

Les complexes Tc-protéines (Fig. 2- a;b) constituent un ensemble de composés de masse molaire très différente , ce qui tendrait à prouver une grande facilité de fixation du métal à ce niveau, probablement dû à une forme physico-chimique particulière : des études sont en cours pour élucider ce point.

En revanche, l'Am-241 ne se fixe qu'à 32 et 24 % sur les ligands solubles de ces deux compartiments (Fig. 2-c;d). Il est remarquable de constater qu'il s'élue exclusivement avec des composés de haut poids moléculaire. Comme la fixation du radionucléide s' effectue essentiellement dans les vésicules hétérogènes constituant le culot mitochondries-lysosomes, il est très probable que son compartimentage dans la cellule est fait par la voie lysosomo-vacuolaire.

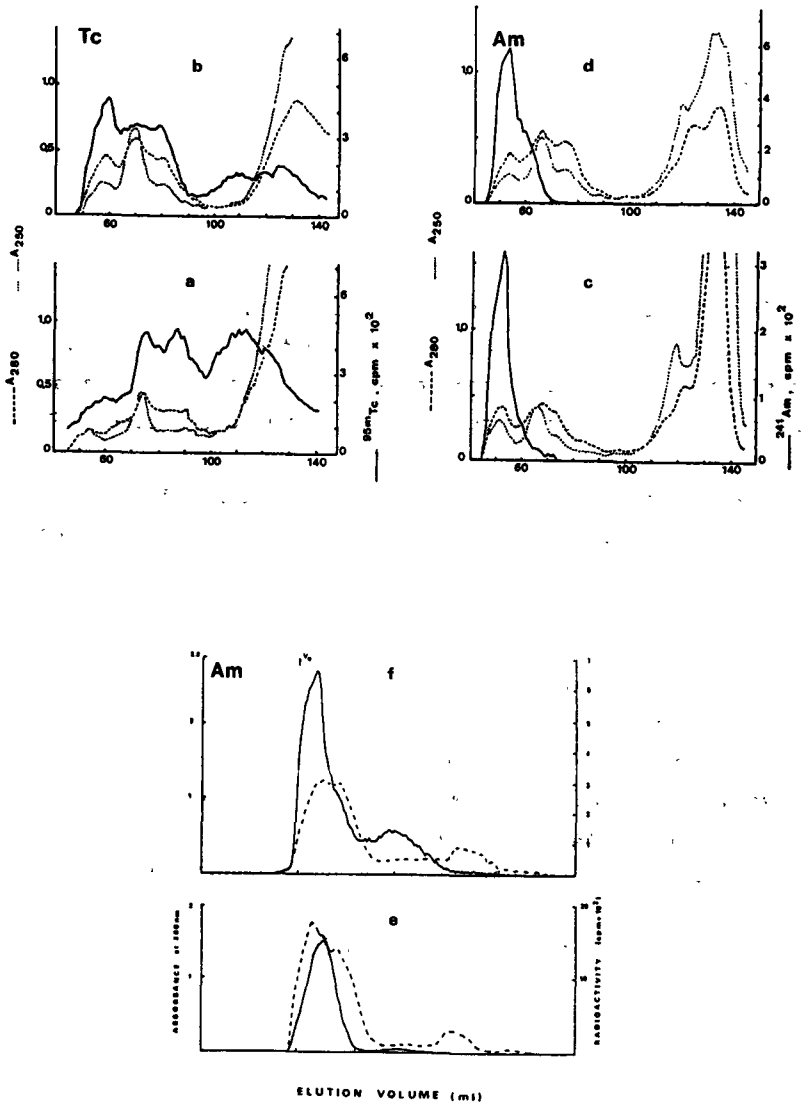

Fig. 2: Comparaison des ligands du Tc et de l'Am solubles dans le SDS chez Homarus gammarus (a,b et c,d) et chez Littorina l. (e,f).

Ce phénomène apparait être général comme nous l'avons mis en évidence chez Littorina littorea (Fig. 2- e et f) (Galey et al. , 1986). Il fut aussi montré chez les mammifères (Gruner et al. , 1981). Enfin, il faut noter que, chez le mollusque gastéropode Littorina littorea , l'accumulation de l'Am-241 dans les fractions lourdes est encore plus importante.

Des résultats allant dans le même sens avaient été obtenus chez Astacus leptodactylus où 27 % de l'Am-241 apparaissait lié aux molécules organiques solubles (13 % chez la littorine).

Enfin, nous avons pu montrer (extraction spécifique des granules ou corps résiduels ; microscopie électronique) que ce sont les lysosomes secondaires chez Littorina littorea qui présentent la radioactivité maxima.

Conclusion

Pour la radioprotection , il est important de connaître les transformations du pertechnétate entrant dans les chaines alimentaires et aussi son devenir quand il est inclus dans le métabolisme.

Le premier résultat obtenu est qu'il se lie préférentiellement à certaines macromolécules bioorganiques. Or le devenir de la radioactivité ingérée par les crustacés aurait pu être complexe du fait qu'il possède plusieurs états d'oxydation pouvant donner des formes chimiques variées. C'est au niveau des surfaces biologiques comme les membranes de la glande digestive que le Tc montre une grande disparité de liaison. Mais, au niveau cytosolique, à l'intérieur de la cellule les résultats de la chromatographie montre qu'il se trouve extrêmement localisé sur des ligands bioorganiques dont nous avons déterminé l'une des caractéristiques physiques (poids moléculaire) et chimiques (groupements chimiques). Ce n'était pas le cas dans les feuilles d'épinards (Desmet,1986). Tout ceci prouve la spécificité de la fixation. Les résultats sur le "binding" in vitro et sur la compétition entre métaux mettent en évidence que le Tc serait réduit par les mécanismes d'oxydo-réduction cellulaires et qu'il pourrait se fixer sur les sites d'acceptation du cuivre. On peut supposer que les animaux possédant un pouvoir réducteur élevé fixeront beaucoup le Tc.

Le passage du Tc par les systèmes bioorganiques donne donc naissance à des nouveaux complexes affectant sa forme physico-

chimique et sa biodisponibilité.

En effet, sa liaison avec les protéines à 10-12 000 D ferait dépendre sa détoxification du "turn-over" protéique et finalement de l'élimination lysosomale.

Par comparaison, l'américium pénétrant dans les cellules de la glande digestive se trouve au niveau membranaire localisé exclusivement dans des complexes de haut poids moléculaire. Dans la cellule digestive, il est très rapidement accumulé dans les organites entourés d'une membrane, puis excrété dans les fécès. On le retrouve aussi dans la ferritine, protéine non hémique du métabolisme du fer.

Ces résultats sont à mettre en parallèle avec ceux connus pour les métaux polluants capables de se substituer aux éléments-trace essentiels. Ces derniers sont transportés et stockés par des protéines. D'autres sont cloisonnés dans les organites, principalement les lysosomes.

Les mécanismes d'accumulation dans ces organites aboutissant parfois à la formation de granules ne sont pas définis. Mais il semblerait que les différentes voies métaboliques, à un moment donné, convergent et que les métaux soient finalement éliminés par les lysosomes ou les granules.

Ces différents types d'immobilisation des radionucléides par les ligands bioorganiques peuvent permettre de prévoir des rythmes d'élimination différents qui tiennent compte de "turn-over" protéiques différents.

Références

- CROS S. (1989)
DEA , Université de Nantes , 30 p.

- DESMET G. (1986)
In : Technetium in the Environment, DESMET G. and C. MYTTENAERE (Eds.) Elsevier Applied Science Publishers, LONDON and New-York, 189-195.

- FOWLER S.W. , BENAYOUN G., PARSI P., ESSA M.W.A. and SCHULTE E.H. (1981)
In : Impacts of radionuclide releases into the marine marine environnment. Vienna , IAEA , pp. 319-339.

- GALEY J. , F. GOUDARD , J. PIERI , P. GERMAIN and S.G. GEORGE (1986)
Comp. Biochem. Physiol. 85A, 333-340.

- GRUNER R. , A. SEIDEL and R. WINTER (1981)
Radiation Research 85, 367-379.

- GOUDARD F. , J. GALEY , J. PIERI , S.W. FOWLER , S. HEUSSNER and S. LA ROSA (1985)
Marine Biology 85, 43-50.

- GOUDARD F. (1987)
Thèse d'Etat de Sciences , Université de Nantes , 112 p.

- MASSON M. , G. APROSI and P. GERMAIN (1986)
In : Technetium in the Environment, DESMET G. and C. MYTTENAERE (Eds.) Elsevier Applied Science Publishers , LONDON and New-York , 251-264.

- SENKBEIL E.G. and WRISTON Jr.J.C. (1981)
Comp. Biochem. Physiol. 68B , 163-171.

IV. Other research group(s) collaborating actively on this project [name(s) and address(es)]:

Laboratorium voor colloïdchemie, Katholieke Universiteit, Leuven - Professeur A. CREMERS

Laboratoire de Radioécologie marine CEA. La Hague

V. Publications:

- 1 -

- J. GALEY, F. GOUDARD, J. PIERI, S.W. FOWLER and F.P. CARVALHO Tissue and subcellular distribution of ^{252}Cf and ^{241}Am in the seastar Marthasterias glacialis. Marine Biology 75, 253-259 (1983)

- F. GOUDARD, J.GALEY, J. PIERI, S.W. FOWLER, S.HEUSSNER and J. LA ROSA. Intracellular localization and binding of technetium-95m in the seastar Marthasterias glacialis. Marine Biology 85, 43-50 (1985).

- J. GALEY, F. GOUDARD, J. PIERI, P. GERMAIN and S.G. GEORGE ^{241}Am binding-components in the digestive gland cells of the marine prosobranch Littorina littorea . Comp. Biochem. Physiol. 85 A, 333-340 (1986).

- F. GOUDARD, J. GALEY, J. PIERI, M. MASSON and S.G. GEORGE. Localization of ^{95m}Tc and ^{241}Am subcellular binding ligands in the lobster (Homarus gammarus) in relation to some stable metals (Cu, Fe, Zn and Cd). Soumise à Comp. Biochem. Biophys.

- J. NIKODIC and J. PIERI. Sorption kinetics of 60-Co by main clay-type minerals present in estuaries. Concentration, pH, salinity and temperature effects on K_D values equilibrium dialysis application. In : Application of distribution coefficients to radiological assessement models. C.E.C. Elsevier Applied Science Publishers (1985).

- 2 -

- F. GOUDARD
  Contribution à l'étude du métabolisme des radionucléides ^{252}Cf, ^{241}Am et ^{95m}Tc.
  Thèse de Doctorat d'Etat de Sciences (1987) Faculté des Sciences et des Techniques de Nantes.

- S. CROS
  Complexe Technétium-Protéine.
  DEA (1989) Faculté des Sciences et des Techniques de Nantes.

- M.C. MILCENT
  Complexe Américium-Protéine.
  DEA (1989) Faculté des Sciences et des Techniques de Nantes.

RADIATION PROTECTION PROGRAMME

Progress Report

1989

Contractor: Contract no.: BI6-B-326-DK

Risø National Laboratory
DK - 4000 Roskilde

Head(s) of research team(s) [name(s) and address(es)]:

Mr. J. Roed
Health Physics Department
Risø National Laboratory
Postbox 49
DK - 4000 Roskilde

Telephone number: 02-371212

Title of the research contract:

Design and Development of a Skim and Burial Plough for Reclamation of Contaminated Land

List of projects:

Design and Development of a Skim and Burial Plough for Reclamation of Contaminated Land

Title of the project no.:
BI6-B-326-DK

Design and Development of a Skim and Burial Plough for Reclamation of Contaminated Land.

Head(s) of project:

Jørn Roed

Scientific staff:

H.L. Gjørup
Jørn Roed

I. Objectives of the project:

To design and develop a plough that can remove a contaminated top-layer of about 5 cm soil and bury it beneath some 50 cm soil without inverting the 5-50 cm horizon, in order to avoid less fertile subsoils to be brought to the surface and allow normal tilling procedure to be carried out without mixing the contaminated buried material with the ≈ 30 cm layer of tilled soil.

II. Objectives for the reporting period:

To try to modify a conventional plough so that it can skim-off the topmost 5 cm soil and place it beneath a non-inverted soil layer and if this is not feasible to try to design a new plough able to perform the procedure.

III. Progress achieved:

Methodology

In order to design the skim and burial plough some consultations with different experts about how to modify a conventional plough for this purpose has taken place.

On later consultations it was discussed whether or not ideas from the design group on how to construct a skim and burial plough could succeed.

Results

The discussion with the experts indicated that it was very difficult to imagine how conventional ploughs could be modified in order to act as skim and burial ploughs.

The design group then came up with three different ideas of how to design a skim and burial plough, and after discussion with different experts in the field one of the ideas were chosen to be the most promising.

Small scale models of the chosen design were built and presented to a plough factory. The factory accepted to try to build a plough after these ideas.

Discussion

The model of the new designed plough was well received by the design engineer at the plough factory, however, the plough seems to be a fairly heavy construction and nothing can yet be said about whether or not the plough will function after its intentions.

IV. Objectives for the next reporting period:

From the design status to develop and produce a prototype of the skim and burial plough, and then to perform some tests of the plough in the field.

V. Other research group(s) collaborating actively on this project [name(s) and address(es)]:

VI. Publications:

RADIATION PROTECTION PROGRAMME

Progress Report

1989

Contractor: Contract no.: BI6-B-329-I

Univ. Catt. del Sacro Cuore
Largo A. Gemelli, 1
I - 20123 Milano

Head(s) of research team(s) [name(s) and address(es)]:

Prof. S. Silva
Radioisotopes Laboratory
Facoltà di Agraria
Via Emilia Parmense 84
I - 29100 Piacenza

Telephone number: 0523/62600

Title of the research contract:

Chemical treatments to reduce the transfer of caesium radioisotopes to the human foodchain after a serious nuclear accident

List of projects:

Chemical treatments to reduce the transfer of caesium radioisotopes to the human foodchain after a serious nuclear accident

Title of the project no.:

Chemical treatments to reduce the transfer of caesium radioisotopes to the human foodchain after a serious nuclear accident

Head(s) of project:

Prof. S. Silva

Radioisotopes Laboratory - Facoltà di Agraria

Via Emilia Parmense, 84 29100 PIACENZA - Italy

Scientific staff:

S. Silva, V. Cappa, F. Carini, P. Bani, M. Montruccoli, P. Vazhapilly

I. Objectives of the project:

The project includes two distinct working departments (A and B) which have one aim: to produce a reduction of the transfer factors of radiocesium in plants, milk and meat.

Particularly the first department (A) studies the possibility to reduce the radiocesium transferred to the plant; the second department (B) studies the possibility to reduce the radiocesium in the milk and in the meat as a consequence of the feeding with contaminated fodder.

II. Objectives for the reporting period:

Dep. A: during the first year the methods have been got ready, particularly those concerning the contamination of plants in field by nebulization of radiocesium. Besides methods validity has been checked for the objectives to follow and the first data has been collected to value the utilized techniques.

Dep. B: with the researches carried out on sheep we wanted to evaluate the amount of radiocesium (^{134}Cs and ^{137}Cs) that, administered to the animals as contaminated lay, was excreted in feces and urine or accumulated in the organs,as well as the effect of feeding AFCF on their contamination level.

III. Progress achieved:

Department A:

1. Methodology

Three species of plants:winter barley, winter wheat and tomato were cultivated in open field. At the same time the equipment to contaminate the plants has got ready: a watery solution of cesium chloride holding Cs-134 was nebulized directly into a plexiglass box placed on the plant to treat. The box dimension varied according to the growing stage and the kind of plant. The attempt to produce dry aerosol by passage of this one through a column containing silica gel has failed owing to the high percentage of moisture inside the box due to the plant evapotranspiration.
The treatments were carried out on wheat at ripening and on tomato at turn of colour and at ripening. After every nebulization the plant was sprinkled directly with KCl solution at three different concentrations: 0-100-300 mg K/l. Three plots were treated for every potassium concentration. Activities of 306.7 and 575 KBq/m^2 were nebulized on the wheat (areas of 0.25 m^2) and on the tomato (areas of 0.40 m^2) respectively. The produce was harvested at ripening and was analysed with regard to Cs-134 and K-40 by a Ge(Li) semiconductor.

2. Results

The spraying carried out by increasing doses of potassium salts causes a lowering of the Cs-134/K-40 ratio(if compared with "zero" dose) only in the second series of tomato treatments. On the contrary, in the first series of tomato treatments and in the single series of wheat treatments, the amount of radiocesium retained by the plants (wheat grain and straw, tomato fruits) not treated with potassium is less than that one retained by the plant treated with potassium salts.

3. Discussion

The treatments were carried out in micro-environments (plexiglass boxes) where relative moisture amount achieved 100%, so as to affect the stomata opening and to preclude the possibility of an exchange between the sprayed potassium and the absorbed radiocesium.
In tomato fruits the presence of the box has caused a concentration of potassium amounts higher than those present without boxes; this fact also occurred for the treatment without potassium, pointing out a change in crop physiology.

Dep. B:METHODOLOGY

The research were carried out using hay contaminated by radiocaesium (^{134}Cs = 3,077 Bq/kg DM, ^{137}Cs = 11,103 Bq/kg DM) in consequence of the accident happened at Chernobyl. This roughage was fed to four lambs (already weaned, average body weight of 28 kg) as 55 g of dry matter/kg $BW^{0.75}$/day for 55 days. From the 28th day onwards, the four animals were kept in individual metabolic cages and, after a week for adaptation, two lambs were fed 0.32/head/day of Ammonium Iron (III) Hexacianoferrate (II) (AFCF). This product was equally divided in the two hay meals the animals received per day. Water was always available. The quantitative and individual collection of feces and urines started three days before the 1st AFCF administration and went on for three weeks; samples of them were analyzed for radiocaesium content. Another lamb from the same flock was fed during the experimental period a very low contaminated hay ($^{134+137}Cs$ = 143 Bq/kg DM).
At the end of the trial all the five lambs were slaugthered and the radiocontamination of their organs was measured.

RESULTS

Fecal radiocaesium excretion (related to the intake) was 96.05% in the treated (AFCF) couple and 78.49% in the other couple; urinary output was 1.61% and 11.9% respectively. AFCF appeared to be effective since the 1st day of its use. The figures of meat and organs contamination are shown in Tab. 1. Transfer coefficient of radiocaesium was as high as 3.4% in the AFCF lambs, 25.6% in the other two animals fed contaminated hay, and 42% in the fifth, "control" animal. Data in Tab. 1 emphasize that fall in Cs isotopes content, as a result of the AFCF treatment, was greater in liver, kidneys, testicles and heart (over 20 times less) respective to muscles (7 times) and gut (4 times) maybe as a consequence of more rapid turnover of caesium in the first group of organs. The high contamination measured in testicles should cause a certain amount of concern.

CONCLUSION

The chemical tested appeared to be effective against the accumulation of both ^{134}Cs and ^{137}Cs in the animal body. Moreover, it had a prompt effect. Transfer coefficient of Cs to the meat may not be a constant figure but it may depend on doses of radiocontaminants and on other factors.

TABLE 1

TREATMENT	RADIOACTIVE HAY	RADIOACTIVE HAY + A F C F	NON RADIOACTIVE HAY
MUSCLES	1399	11620	248
HEART	337	7112	143
LIVER	288	6635	96
KIDNEYS	818	17290	406
TESTICLES	622	12917	306
SMALL INTESTINE	195	756	28
LARGE INTESTINE	357	1699	87

IV. Objectives for the next reporting period:

Dep. A: in the second year, additional spraying trials will be carried out employing potassium salts at doses higher than the above one. Above all it will be taken care to allow plants to return to their normal water state before performing treatments with potassic salts. Besides it will be valued if inverting the sequence of treatments (before KCl, then CsCl) the contamination might be lower.

Dep B: following the results of the first trial, we want to carry out another similar research modifying the amount of the chemical already tested (AFCF) as well as using further substances, like bentonite and zeolite. In addition, similar researches will be carried out on lactating cows to check the effectiveness of these chemicals on the extent of the Cs transfer to milk.

V. Other research group(s) collaborating actively on this project [name(s) and address(es)]:

VI. Publications:

As regards the department A a paper on this research will be published on the "Annali della Facoltà di Agraria dell'Università Cattolica del Sacro Cuore" in 1990.

As regards the department B the results already achieved will appear on the Scientific Italian Association of Animal Production's review "Zootecnica e Nutrizione Animale", probably by the middle 1990.

RADIATION PROTECTION PROGRAMME
Final Report

Contractor:

National Radiological
Protection Board, NRPB
Chilton, Didcot
GB-Oxon, OX11 ORQ

Contract no.: BI6-B-048-UK

Head(s) of research team(s) [name(s) and address(es)]:

Dr. J.W. Stather
Biomedical Effects Dept.
NRPB
Chilton, Didcot
GB-Oxon OX11 ORQ

Dr. F A Fry
Environmental Measurements Dept.
NRPB
Chilton, Didcot
GB-Oxon OX11 ORQ

Telephone number: 0235/83.16.00

Title of the research contract:

Behaviour of radionuclides in the environment.

List of projects:

1. Soil-to-plant transfer factors for radionuclides.
2. The speciation of radionuclides in plants and foodstuffs and the influence of this on their gastrointestinal uptake.

Title of the project no.:

1

Soil-to-plant transfer of radionuclides

Head(s) of project:

Dr D S Popplewell

Scientific staff:

Dr A F Nisbet

I. Objectives of the project:

To investigate the dynamics and time dependent transfer of ^{239}Pu, ^{241}Am, ^{90}Sr and ^{137}Cs to food crops from soils of widely differing textural classes, representative of those found in the EEC.

II. Objectives for the reporting period:

(a) To complete the investigation into the effect of glyphosate on radionuclide uptake to crops.
(b) To complete the investigation into the time dependent transfer of radionuclides to crops.
(c) To continue work on the radionuclide composition of soil solution under field and lysimeter conditions to support plant uptake studies.

III. Progress achieved:

Methodology

(a) Glyphosate study

Glyphosate (n-phosphonomethyl glycine) is a broad spectrum herbicide widely used in lowland agriculture, forestry and improved upland pastures. Although its metal chelating properties are well established, its interaction with certain man-made radionuclides remains unknown. As chelators provide the carrier mechanism for replenishing depleted ions at the root surface, it is important to establish the effect, if any, of glyphosate on the root uptake of radionuclides. This is particularly relevant since a large proportion of foliarly applied glyphosate reaches the soil.

The current study (Nisbet and Shaw, 1989) was designed to investigate the effect of soil applications of glyphosate on radionuclide uptake to food crops grown in a range of soil types. Peas and carrots grown during 1987 in artificially contaminated loam, peat and sand soils with and without glyphosate (3 lha-1) have been analysed for ^{239}Pu, ^{241}Am, ^{90}Sr and ^{137}Cs. To complete this study supplementary laboratory batch equilibrium experiments have been conducted on the same three soil types to investigate the effects of glyphosate on radionuclide desorption from these soils. Representative samples of soil were taken from large lysimeters containing radio-contaminated loam, peat and sand. Soil solution was collected from porous ceramic cups installed in each lysimeter. The soils were then shaken with the appropriate soil solution with and without glyphosate in conical flasks overnight. The effect of glyphosate on the distribution of ^{239}Pu, ^{241}Am, ^{90}Sr and ^{137}Cs between solid and liquid phases was subsequently determined.

(b) Time dependent transfer study

Studies on the time dependent transfer of radionuclides from soils to plants are important for predicting consequences of release. It

cannot be assumed automatically that availability decreases with time. In fact, there is some evidence that plutonium uptake to plants increases with time.

The current study was designed to investigate the time dependent transfer of radionuclides to food crops growing in a range of soil types. Lysimeters containing loam, peat and sand soils were artificially contaminated with ^{239}Pu, ^{241}Am, ^{90}Sr and ^{137}Cs (as nitrates) in 1983. Since then crops of cabbage, barley and carrots have been grown in rotation in the lysimeters to determine changes in radionuclide availability with time. Radiochemical analysis of the 1988 spring barley crop from the lysimeter soils has been completed. Soil-to-plant concentration ratios have been calculated and compared with those for the 1986 spring barley crop. Spring cabbage and carrots harvested during 1989 are currently undergoing analysis. Radionuclide uptake to these crops will be compared to those grown in 1985 and 1986.

(c) Soil solution studies

Soil solution is the intermediary phase in soil-plant relationships. A disturbing feature of soil-plant transfer data is their variability. In order to assess radionuclide availability to crops more reliably it is essential that the mechanisms of radionuclide movement from soil to soil solution to plant root be as fully understood as possible. Any investigation into the soil-plant transfer of radionuclides should therefore include a comprehensive chemical analysis of soil solution.

The current investigation was designed to complement existing soil-plant transfer studies by providing more information on the activity concentrations of ^{239}Pu, ^{241}Am, ^{90}Sr and ^{137}Cs in soil solution extracted from field and lysimeter soils. Soil solution has been routinely collected from the greenhouse lysimeter soils and from reclaimed land and uplands in north west England throughout 1988 and 1989, using porous ceramic cups. Analysis for ^{239}Pu, ^{241}Am, ^{90}Sr and ^{137}Cs has been completed for 1988, and been related to plant uptake data where available.

Soil solution was also used as the basis for investigating the effects of various fertiliser treatments on radionuclide sorption/desorption in soils under lysimeter and laboratory conditions. This is because of the disturbances that soil-based countermeasures cause to soil:solution equilibria and radionuclide distribution between solid and liquid phases. As potassium and caesium are chemically very similar, much interest has been shown in the use of potassium as a possible soil-based countermeasure to reduce radiocaesium uptake to plants. Any changes in sorption/desorption of radiocaesium induced by potassium fertiliser treatments in lysimeter and field soils have been detected from the routine radiochemical analysis of soil solution. The effect of potassium was also investigated in the laboratory using a modified batch equilibrium technique (Nisbet, 1989) which involved shaking radio-contaminated soil and its associated soil solution with and without potassium.

Results

(a) Glyphosate Study

The most marked effect of the glyphosate treatment was on the uptake of ^{241}Am to crops grown in loam soil, by a factor of 3 in peas and a factor of 2 in carrot peel. Glyphosate had little effect on the uptake of any other radionuclides.

Treatment of the soil with glyphosate also affected the distribution of radionuclides in the liquid phase of loan, peat and sand soils. Shaking these soils and their associated soil solutions with the higher glyphosate application was found to increase the activity concentration of ^{241}Am in the liquid phase of loam and sand soils by factors of 10 and 1.5 respectively. ^{241}Am desorption also occurred in loam soils following standard applications of glyphosate. Glyphosate had no significant effect on the desorption of any other radionuclides.

(b) Time dependent transfer study

Soil-to-plant concentration ratios for ^{239}Pu, ^{241}Am, ^{90}Sr and ^{137}Cs in the 1988 spring barley crop have been compared with those for the

1986 crop in Table 1. Concentration ratios for ^{239}Pu, ^{241}Am and ^{90}Sr are all consistently lower in 1988 than 1986. Concentration ratios for ^{137}Cs in loam and sand showed no difference between years, whilst those for peat actually increased.

(c) Soil solution studies

The transfer of ^{90}Sr and ^{239}Pu along the soil-soil solution-plant pathway for barley grown in lysimeter soils is summarised in Table 2. The radionuclide content of barley and soil solution is considerably lower than in bulk soil, especially for ^{239}Pu. The activity concentrations of ^{239}Pu and ^{90}Sr have been ranked in ascending order for each phase according to soil type. ^{90}Sr uptake to barley was greatest from sand and this corresponds well with the activity concentrations of ^{90}Sr in the solution phase of sand rather than in bulk soil. Some information on calcium has been included as ^{90}Sr uptake is inversely proportional to solution phase calcium. No straightforward relationship emerged for ^{239}Pu uptake to barley.

The effect of potassium applications on ^{137}Cs activity in soil solution from lysimeter soils is shown in Figure 1. Application of potassium in September 1988 was followed by a concomitant rise in ^{137}Cs activity, which was most pronounced in loam and sand soils. These elevated radiocaesium levels were sustained for about four months. Concentrations of potassium in soil solution have also been plotted in Figure 1 for comparison. Potassium applications resulted in increased levels of potassium in soil solution in the order peat > sand >> loam.

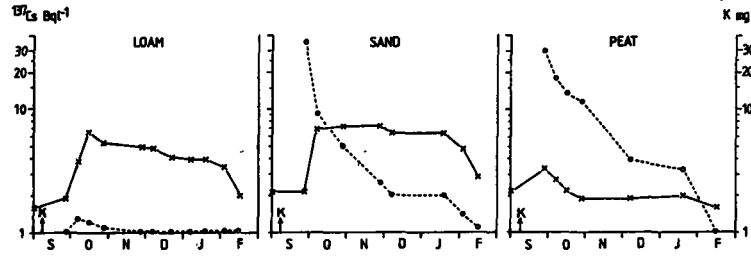

Figure 1. Dynamics of ^{137}Cs and K in soil solution following soil applications of potassium to lysimeter soils (o---o K; X——X ^{137}Cs).

TABLE 1

*TIME DEPENDENT TRANSFER OF ^{239}Pu, ^{214}Am, ^{90}Sr and ^{137}Cs TO BARLEY

^{239}Pu

	LOAM	PEAT	SAND
1986	3.2 + 0.48 E-5	9.8 + 1.20 E-6	2.2 + 0.27 E-5
1988	8.5 + 1.85 E-6	2.5 + 0.52 E-6	1.2 + 0.22 E-5

^{241}Am

	LOAM	PEAT	SAND
1986	3.5 + 0.39 E-5	1.2 + 0.11 E-5	3.5 + 0.30 E-5
1988	9.2 + 1.53 E-6	4.2 + 0.58 E-6	1.8 + 0.19 E-5

^{90}Sr

	LOAM	PEAT	SAND
1986	3.5 + 0.36 E-1	4.2 + 0.40 E-2	5.7 + 0.59 E-1
1988	2.3 + 0.23 E-1	2.4 + 0.23 E-2	3.7 + 0.38 E-1

^{137}Cs

	LOAM	PEAT	SAND
1986	1.4 + 0.14 E-3	6.0 + 0.51 E-2	2.2 + 0.13 E-3
1988	1.6 + 0.15 E-3	1.1 + 0.01 E-1	2.0 + 0.14 E-3

* Expressed as $\frac{Bqkg^{-1} \text{ DRY WEIGHT CROP}}{Bqkg^{-1} \text{ DRY WEIGHT SOIL}}$

TABLE 2

SOIL - SOIL SOLUTION - PLANT TRANSFER OF ^{90}Sr AND ^{239}Pu TO BARLEY FROM LYSIMETER SOILS

^{90}Sr

	LOAM	SAND	PEAT	
SOIL (Bq kg^{-1} dw)	1600	1700	8700	P>S>L
BARLEY (Bq kg^{-1} dw)	366	622	213	S>L>P
SOIL SOLUTION (Bq L^{-1})	30	75	10	S>L>P
		Ca in soil solution		P>L>S

^{239}Pu

	LOAM	SAND	PEAT	
SOIL (Bq Kg^{-1} dw)	1300	1600	3700	P>S>L
BARLEY (Bq Kg^{-1} dw)	0.01	0.02	0.01	S>L>P
SOIL SOLUTION (Bq L^{-1})	0.02	0.10	1.63	P>S>L

The results presented here illustrate three different conditions that can arise in the soil solution following treatment of the soil with potassium:

(1) ^{137}Cs increases but K remains low e.g. loam. Potassium displaces ^{137}Cs from the low selectivity exchange sites and becomes extensively sorbed, thereby increasing the soil solution concentration of ^{137}Cs but not K;

(2) ^{137}Cs increases and K also increases e.g. sand. Potassium displaces some ^{137}Cs from the low selectivity exchange sites, thereby increasing ^{137}Cs and K in the soil solution;

(3) ^{137}Cs remains constant and K increases e.g. peat. Potassium does not exchange for ^{137}Cs to any great extent, consequently only the potassium concentration increases in the soil solution.

Results showing the effect of potassium fertiliser on ^{137}Cs and ^{90}Sr desorption in lysimeter soils under batch equilibrium conditions are given in Table 3. Shaking radiolabelled soil and its associated soil solution with potassium was found to increase ^{137}Cs and ^{90}Sr concentrations in the liquid phase. This was most pronounced in loam and sand soils, thereby supporting the findings of the lysimeter study.

TABLE 3

EFFECT OF POTASSIUM FERTILISER ON ^{137}Cs and ^{90}Sr DESORPTION IN AGRICULTURAL SOILS USING A BATCH EQUILIBRIUM TECHNIQUE

	^{137}Cs ($mBql^{-1}$)	^{90}Sr ($mBql^{-1}$)
LOAM +K	2700	44400
LOAM -K	1300	30900
SAND +K	2400	31300
SAND -K	1300	23400
PEAT +K	1700	37400
PEAT -K	1200	24600

Discussion

(a) Glyphosate study

Greenhouse and laboratory experiments have shown that soil applications of glyphosate can affect the behaviour of certain radionuclides in soils and plants. The most marked effect of glyphosate was noted in loam soils where it increased ^{241}Am desorption from the solid phase and also increased ^{241}Am uptake to peas and carrot peel. It was postulated that the higher pH conditions of the loam favoured the formation of a stable Am-glyphosate complex which was more available for crop uptake than Am alone. Consequently, results from other radioecological soil-plant transfer studies that have inadvertently used glyphosate to remove weeds from field plots, lysimeters etc. should be interpreted with caution, especially if these studies involved di- or tri-valent radionuclides.

(b) Time dependent transfer studies

The transfer data for ^{239}Pu, ^{241}Am, and ^{137}Cs from loam and sand to barley grain were at the lower end of the expected range quoted by the International Union of Radioecologists for standard conditions (1987). The data for ^{90}Sr were at the upper end of this range. The consistent reduction in uptake of ^{239}Pu, ^{241}Am and ^{90}Sr to barley between 1986 and 1988 would seem to indicate a reduction in availability of these radionuclides with time. However, the possibility of different climatic factors influencing uptake between these two years cannot be ignored, neither can it be proven. There were no significant reductions in the uptake of ^{137}Cs from loam and sand soils to barley between the years, and the uptake from peat actually increased. This would seem to provide more evidence for the long term availability of radiocaesium in predominantly peaty soils.

(c) Soil solution studies

The radiochemical content of soil solution has generally provided a good indication of radionuclide availability to plants for ^{90}Sr and ^{137}Cs, but not for ^{239}Pu and ^{241}Am. To assess the relationship between

bioavailability and speciation of polyvalent radionuclides ultrafiltration has been used to separate soil solution into different size fractions. The results indicate that more than 75% of the ^{239}Pu in bulk soil solution from peat soils is associated with high molecular material, >1000D. As such it is probably unavailable to plant roots thereby explaining the low soil-to-plant transfer in peaty soil.

Lysimeter and laboratory studies have shown that soil applications of potassium at standard agricultural rates can cause a marked increase in the ^{137}Cs activity in loam and sand soils. This is thought to be due to the displacement of radiocaesium from some of the low selectivity exchange sites on the illite clay present in sand and loam. Any increase in the radiocaesium activity in soil solution can lead to enhanced uptake of this radionuclide by plants. Conversely, any increase in the potassium concentration in soil solution may be expected to suppress radiocaesium uptake. Application of potassium to the three soil types studied here might be expected to increase radiocaesium uptake to plants in loam soil, have little effect in the sand and, provided potassium was in excess, reduce radiocaesium uptake to plants in the peat.

Conclusions

(a) Glyphosate study

The uptake of ^{241}Am to vegetation growing on mineral soils of pH greater than 7 could be significantly increased by the application of herbicides containing glyphosate.

(b) Time dependent transfer study

The uptake of ^{239}Pu, ^{241}Am and ^{90}Sr to barley from the three principal agricultural soil types loam, peat and sand decreases with time after contamination. The uptake of ^{137}Cs may actually increase with time in predominantly peaty soils.

(c) Soil solution studies

Soil solution has proved to be a useful medium for studying the

transfer of radionuclides from soils to plants. Analysis of bulk soil solution does not always provide sufficient information, however. A comprehensive chemical analysis of soil solution is required, followed by more detailed speciation studies for polyvalent radionuclides.

Investigations of ^{137}Cs-K interactions in soil solution have highlighted the importance of soil type in influencing the effect of potassium on radiocaesium dynamics in soil-plant systems. A better understanding of ^{137}Cs-K interactions must be sought before the widespread use of potassium as a soil-based countermeasure.

Small scale laboratory batch equilibrium experiments using soil and its associated soil solution have provided an invaluable initial step in the practical evaluation of soil-based countermeasures.

Publications

Nisbet A F (1989) Investigation of Cs-K interactions in agricultural soils by soil solution analysis. In Report of the 6th IUR Working Group on Soil-to-Plant Transfer Factors, RIVM, Bilthoven, The Netherlands.

Nisbet A F and Shaw S (1989) Effects of the herbicide glyphosate on the uptake of ^{239}Pu and ^{241}Am to vegetation. In 'The Transfer of Radionuclides in Natural and Semi-Natural Environments.' Udine, Italy.

Nisbet A F and Lembrechts J F (1989) The dynamics of radionuclide behaviour in soil solution with special reference to the application of countermeasures. In 'The Transfer of Radionuclides in Natural and Semi-Natural Environments.' Udine, Italy.

Jackson D and Nisbet A F (1989) The effects of fertiliser treatment, soil pH and grazing on the transfer of radiocaesium to upland fell vegetation. In 'The Transfer of Radionuclides in Natural and Semi-Natural Environments.' Udine, Italy.

Title of the project no.: 2

The speciation of radionuclides in plants and foodstuffs and the influence of this on their gastrointestinal uptake.

Head(s) of project:

Dr D S Popplewell

Scientific staff:

Dr R A Bulman, Mr G J Ham, Dr J D Harrison, Dr G P L Naylor, Ms S L Prosser, Mr G Szabo.

I. Objectives of the project:

To investigate (i) the influence of chemical form on the availability for uptake of radionuclides into plants;

(ii) the chemical form of radionuclides in foodstuffs;

(iii) the effect of chemical form and other factors on gastrointestinal absorption in animals;

(iv) the gastrointestinal absorption of neptunium and curium in humans.

II. Objectives for the reporting period:

Methodology

(i) Speciation in soils

A salt marsh soil, radiolabelled by a natural process arising as result of a marine input of radioactivity from the nearby nuclear fuel reprocessing facility at Sellafield in West Cumbria, has been examined. As land such as this might someday be reclaimed for agricultural purposes, an investigation of this type of soil might permit predictions to be made about the chemical changes which transuranic radionuclides might undergo over a long time.

Separation procedures

In a continuation of earlier work (1), soil was separated into particles of 10 μm and subjected to heavy-liquid sink-float analysis. Fractions in the density range 2.7-3.3 and > 3.3 g ml^{-1} were further fractionated on a Franz isodynamic separator to produce paramagnetic materials. The physically separated fractions were in turn extracted with nitrilotriacetohydroxamic acid (NTAHA), an hydroxamic acid which bears some chemical similarity to the siderophores released by some plants and soil microorganisms to facilitate the mobilization of iron. Gel filtration demonstrated that the released radionulides were present as low molecular weight complexes. Investigation of the association of humic substances with isolated soil particles was made by Raman light illumination of the particles on a modified light microscope (2).

Electroultrafiltration has been evaluated for ability to release radionulides from soils.

Experiments have been done to see if the association of cerium with humic substances in an organic cerium-rich Hawaiian soil could be used to predict the nature of the association of transuranics with humic substances. N-methylmorpholine-N-oxide (NMMNO), used in earlier studies, (1), has been used to extract humic substances from the Hawaiian soil.

Two chemical extraction procedures employing derivatization of humic substances with trimethylchlorosilane and an alkylepoxide have been examined. As these derivatives are soluble in dimethylformamide they can be separated by non-aqueous gel permeation chromatography and the distribution of radionulides between the components determined.

Chemical immobilization of humic substances

The recognition that humic substances bind the transuranic cations has prompted detailed investigations into the nature of their interactions with humic substances. Chemical immobilization procedures have been used to produce chemically bound humic acid (CBHA) and chemically bound fulvic acid

(CBFA). These materials facilitate quicker and simpler methods of determining the conditions which control the uptake and release of the transuranic elements from humic substances.

(ii) Speciation in plants and foodstuffs

Phytic acid in juice expressed from potatoes is a potential binding agent for Pu (IV) in potatoes (3). New potato tubers were radiolabelled by injecting the parent tuber with ^{239}Pu(IV) and ^{241}Am(III) citrates. The speciation of the radionuclides was investigated by gel filtration on Sephadex G25 superfine.

By using a simulated digestion procedure which entailed the digestion of finely chopped boiled potatoes with pepsin for 2 hours at pH 2.0 at 37°C, followed by digestion with a preparation of pancreatin enzymes at pH 7.4 at 37°C for 2 hours, radionuclides could be released into solution.

Similar simulated digestion processes were used to see if low molecular weight complexes of radionulides would be formed on digestion of animal products containing radionulides such as ^{233}U(VI), ^{239}Pu(IV), and ^{241}Am(III). These radionuclides were biologically incoporated into liver and kidney by injecting the animals with the citrate forms of the radionuclides. In addition an investigation of the speciation of ^{239}Pu(IV) in simulated digests of ^{239}Pu-labelled lactoferrin was also conducted by radiolabelling lactoferrin with ^{239}Pu(IV).

Isotachophoresis (ITP) has been evaluated as an analytical aid for investigation of the speciation of the chemical forms of the cations of the transuranic elements, and niobium, an element whose chemistry is relatively poorly understood.

Results

(i) Speciation in soils

Determination of the distribution of ^{239}Pu and ^{241}Am in the physically separated soil particles of 10 μm diameter have shown a wide variation in the distribution of the radionuclides (Table 1). This variation in distribution must reflect the differences in affinities of the radionulide species for the surfaces of the particles. Attempts to demonstrate the presence of organic materials on the particles by Raman light microscopy failed (2).

The mobilization of ^{239}Pu and ^{241}Am from the particles by nitrilotriacetohydroxamic acid has demonstrated that siderophores, originating as extracellular products of soil microorganisms or as plant root exudates, could lead to the mobilization of these radionuclides from soil

particles and might represent the chemical forms which cross the plant root membrane.

The absence of any solublization of any forms of cerium from the Hawiaan soil by either NTAHA or by molten NMMNO indicates the presence of cerium in highly inert forms such as oxide or fluoride. This non-extractability of cerium might point to the fate of americium (III) in soil on a time scale approaching geological time (2).

Table 1

Density g ml^{-1}	^{239}Pu Bq g^{-1}	^{241}Am	% solubilization Fe	Pu	Am
<2.62	3.5 ± 0.4	0.61 ± 0.06	-	-	-
2.62-2.72	0.37 ± 0.03	0.006 ± 0.002	2.51	21.7	28.4
2.72-3.3					
paramagnetic	1.73 ± 0.5	0.21 ± 0.04	25.6	21.6	15.4
nonparamagnetic	1.33 ± 0.01	0.7 ± 0.07	-	16.4	14.3
<3.3					
paramagnetic	6.02 ± 0.8	2.7 ± 0.3	16.7	14.8	15.2
nonparamagnetic	3.51 ± 0.5	1.61 ± 0.1	25.3	26.3	21.4
Major organics+	2.43 ± 0.3	1.9 ± 0.2	22.3	19.6	18.4

+ plant debris

Extraction of humic substances from saltmarsh soil (^{239}Pu content Ca. 4 Bq/g) by alkylepoxidation of the humic substances mobilized only a small quantity of ^{239}Pu but, in contrast, trimethylsilylation mobilized about 60% (4). Low pressure non-aqueous gel filtration of the silylated extracts demonstrated the presence of two forms of ^{239}Pu in the isolate (Fig 1). From molecular weight determinations the material eluted in fractions 25, 40 and 44 have molecular weights of about 50, 2.5 and 1 kDa, respectively (5). Preliminary investigations demonstrate the to separation by high performance liquid chromatography (6).

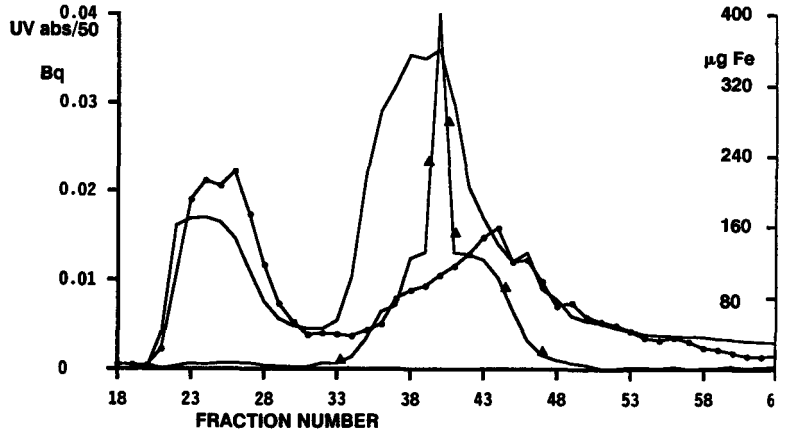

Fig 1. Elution profile of TMSi-humate from silica columns: Fe (▲—▲), ^{239}Pu (●-●) and UV absorption (o-o).

Investigations of the uptake of Pu (IV) and Am (III) by CBHA and CBFA from citrate and phosphate media indicate significantly different adsorption characteristics of Pu (IV) and Am (III) by humic and fulvic acids (Fig 2ab). (7). In aqueous solutions such as ground waters and soil solutions it would appear that humic acids will bind Pu (IV) and Am (III) and not fulvic acids. These materials will simplify investigations of the biogeochemistry of transuranic humates.

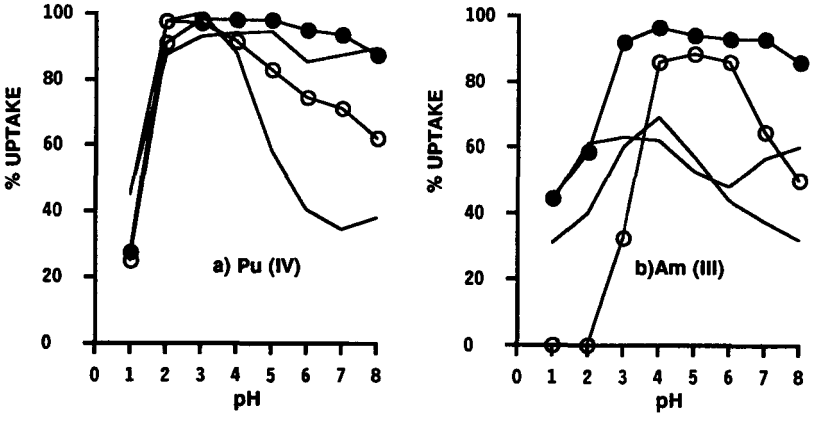

Figure 2ab. Adsorption, at 60 min, of Pu (Iv) and Am (III) by CBHA from phosphate (●-●) and citrate (—), and by CBFA from phosphate (o-o) and citrate (▲-▲).

(ii) Speciation in plants and foodstuffs

Gel filtration of the juice pressed from potatoes showed that ^{239}Pu was present as a phytate complex and as an uncharacterised complex. Whereas, the action of pepsin alone on finely divided boiled potatoes brought about the release of only 5% of the incorporated ^{239}Pu as a component with a molecular weight of about 3-9 kDa, both pepsin and pancreatin digestion released 70% of ^{239}Pu as an unknown low molecular weight complex.

Isotachophoretic analysis of non-active potato digest has demonstrated an unknown complexing agent. Unfortunately, a lack of standards has posed problems in characterizing it. From an examination of the phytase degradation products of myoinositolhexaphosphoric acid it does not appear to be a degradation of this hexaphosphate.

Examination of the distribution of the radionuclides in the supernatants obtained from the simulated digests of the animal tissues, lactoferrin and milk showed that low molecular weight complexes of these radionulides are not formed and, therefore, these animal products are highly unlikely to serve as sources of radionuclides for which there might be an enhanced f_1 value - a phenomenon normally ascribed to low molecular weight complexes.

Preparative isotachophoresis indicates the formation of ^{95}Nb (V) citrate on mixing a nitric acid solution of ^{95}Nb with citrate but only 50% of the ^{95}Nb migrated as the citrate. The remainder existed as a nm-migrating complex of 0.5 - 1 kDa (8). Isotachophoresis has also demonstrated the formation of only one form of Pu(IV) citrate (8).

(iii) The effect of chemical form and other factors on gastrointestinal absorption in animals

The gastrointestinal absorption of plutonium in a number of different chemical forms has been studied. Values of 5×10^{-5} to 10^{-4} were obtained for the absorption in fed hamsters of plutonium ingested in a single dose as Pu(IV) citrate, isocitrate, phytate, and malate complexes and Pu(III) ascorbate compared with $3 - 4 \times 10^{-5}$ for Pu(IV) nitrate. These chemical forms were studied because of their possible importance as soluble organic binding ligands in a wide variety of foodstuffs. The citrate has been the most widely studied complex of plutonium and is present in most food materials. The similar values of absorption obtained for these organic complexes of Pu suggest that it may be reasonable to take the range of results obtained for the citrate in different species, about 10^{-4} to 2×10^{-3}, as representative of soluble organically-bound Pu in a general diet.

Measurements have been made of the absorption of plutonium and americium by rats and hamsters fed potato powder containing these actinides. Labelled potatoes were obtained either by foliar application of activity or by injection of the original seed potato from which the plant was grown. For rats, the f_1 values obtained were about 10^{-3} for Pu and 1.5×10^{-3} for Am, independent of the method of labelling. Similar results were obtained for the uptake of Pu and Am from potato powder after in vitro mixing. For hamsters, absorption was greater with values of about $2 - 3 \times 10^{-3}$ for the uptake of both Pu and Am from in vivo and in vitro labelled potato.

The absorption of neptunium, plutonium and americium was measured in the common Marmoset (C. jacchus). Values of about 2×10^{-3} and 6×10^{-4} were obtained for the uptake of Pu and Am, respectively, administered as a mixture with potato powder. Values of 10^{-3} for Pu and 2×10^{-3} for Np, administered as the citrate complexes, were also obtained.

A comparison of the age-dependent absorption of Fe-59 and Co-57 in rats and guinea pigs has been carried out to determine the extent to which increased absorption in neonates continues beyond the suckling period for these elements. Based on comparisons of whole-body measurements at 14 days after either oral administration or intraperitoneal injection, the absorption of both iron and cobalt in one day-old rats was shown to be virtually complete. By the end of the suckling period at 20 days, absorption had fallen to about 0.7 for iron and about 0.8 for cobalt. Shortly after weaning at 30 days of age, absorption had decreased to about 0.25 for iron and about 0.35 for cobalt. Adult values were about 0.1 and 0.25, respectively. The absorption of both elements by guinea pigs was lower than for rats at all ages. Iron absorption decreased from about 0.25 in one day-old guinea pigs to about 0.1 at the end of the suckling period while cobalt absorption decreased from about 0.6 to 0.2 over the same period. The adult values were about 0.03 for both elements.

The results obtained for the absorption of iron and cobalt provide support for the f_1 values proposed by a Nuclear Energy Agency Expert Group (NEA, 1988). For both elements, the values proposed were 0.6 for the first year of life and 0.3 for children from one year and adults.

The absorption of Nb-95 ingested in milk by adult guinea pigs on a milk supplemented diet was about 8×10^{-3} and a value of 1.4×10^{-2} was obtained for guinea pigs fasted for 24 hours before and 2 hours after the oral administration of Nb-95 in a nitrate solution. The absorption in 2 day-old animals given Nb-95 citrate solution was estimated as 1.5×10^{-2}. These

results support the ICRP Publication 30 value of 10^{-2} for adults. They also support the use of an f_1 of 10^{-2} for niobium absorption from food by adults and children from one year of age and a value of 2×10^{-2} for infants in the first year of life (NEA, 1988).

(iv) The gastrointestinal absorption of neptunium and curium in humans

Of the higher actinides, only two studies, on Pu and Am, have been published on the measurement of the gastrointestinal transfer factor (f_1) in humans. We have carried out experiments to measure f_1 values in volunteers exposed to acceptably low radiation doses by using ^{239}Np and ^{242}Cm, the former a β- and γ-emitter with t ½ 2.35 d and the latter an α-emitter of t½ 163 d. The committed effective dose equivalent (CEDE) estimates for each volunteer receiving an intravenous injection and later an oral intake of a mixture of ^{239}Np and ^{242}Cm was about 400 μSv.

The experiments depend on the principle that actinides entering the blood stream from the gastrointestinal tract distribute in essentially the same way as actinides injected intravenously in soluble form. The first stage of the experiment measured the proportion of the intravenously injected actinide that was excreted in the urine over a given period. The second, or oral stage measured the urinary excretion and calculated the equivalence of the systemic burden of actinides using data from stage 1 of the work. The systemic burden in relation to the amount of the oral intake gave the gut transfer factor.

The mixture of radionuclides was administered at midday, intravenously by a physician, or in the oral experiments, self administered part-way through the midday meal. Total collections of urine were made for about 10 d, the maximum period over which it was possible to measure the ^{239}Np and ^{242}Cm in the 24 h urine samples. Each urine sample was spiked with ^{237}Np and ^{244}Cm tracers and Np and Cm were separated from the urine by radiochemical methods. For about 2 or 3 d after the administration of the two actinides it was possible to measure the ^{239}Np in the urine samples by direct γ ray-spectrometry. After the γ-spectrometric measurement, the urine sample was then subjected to radiochemical analysis.

Five volunteers were available for this experiment. Work with four volunteers has been completed and f_1 values are presented in the Table.

In proposing the fractional gut transfer factor of 10^{-3} for Np and Cm, ICRP said: "The use of the cautious value of 10^{-3} may not be considered appropriate in all situations if a different value more suitable to a specific situation can be justified, it should be employed." The f_1 values

Fractional gut transfer factors.

Volunteer	Np	Cm
JDH	(1.2 ± 0.1) x 10-4	(1.3 ± 0.1) x 10-4
DSP	(1.9 ± 0.1) x 10-4	(1.9 ± 0.2) x 10-4
BH	(2.3 ± 0.1) x 10-4	(1.1 ± 0.1) x 10-4
GJH	(1.8 ± 0.1) x 10-4	(0.95 ± 0.15) x 10-4

Mean f_1 values are: neptunium 1.9×10^{-4}, curium 1.3×10^{-4}

quoted above are derived from experiments on humans using Np(V) citrate and Cm(III) citrate. They are consistent and suggest that an f_1 value of about 2×10^{-4} might be appropriate for the ingestion by adults of Np and Cm with food.

Publications

An examination of new procedures for fractionation of plutonium- and americium-bearing sediments. R A Bulman, T E Johnson and A L Reed, Sci Total Environment 35, 239-250 (1984).

Investigations of interactions of transuranics and cerium with humates, R A Bulman, T E Johnson and S T Baker, Sci Total Environment 62, 213-218 (1987).

Phytate may influence the absorption of plutonium from food materials. J R Cooper and J D Harrison, Health Physics 43, 912 (1982).

Comparison and development of new extraction procedures for ^{239}Pu, Ca, Fe and Cu organic complexes in soils. G Szabo, R A Bulman, and A J Wedgwood, J Environ Radioactivity, in press.

Evaluation of new organic phase extraction procedures for studying the role of terrestrial humic substances in the speciation of iron and plutonium, R A Bulman, G Szabo and A J Wedgwood. To be published in Analytical Procedures for Studying the Speciation of the Elements, Springer Verlag 1990.

Size exclusion HPLC investigations of the speciation of some metals with soil organics extracted by in situ trimethylsilylation of soils. S L Prosser, G Szabo, R A Bulman and A J Wedgwood, Organic Geochem., submitted.

Investigations of the interaction of transuranic radionulides with humic and fulvic acids chemically immobilized on silica. G Szabo and R A Bulman. Presented at International Conference on Humic Substances in the Environment, Linkoping 1989; to be published in Lecture Notes in Earth Sciences, Springer Verlag, 1990.

Isotachophoretic investigations into the speciation of polyvalent cations. S L Prosser and R A Bulman. To be published in Analytical Procedures for Studying the Speciation of the Elements, Springer Verlag 1990.

Ingested actinides. J D Harrison. Radiol. Prot. Bull. 68, 22-24 (1986).

The absorption of ingested plutonium in newborn guinea-pigs. J A Bomford and J D Harrison. Health Physics. 51, 804-808 (1986).

The gastrointestinal absorption of organically-bound forms of plutonium in fed and fasted hamsters. J D Harrison, J R Cooper, J A Bomford and A J David. Int. J. Radiat. Biol. 50, 1083-1091 (1986).

Age-related factors in radionuclide metabolism and dosimetry. J D Harrison. Radiol. Prot. Bull. 82, 17-20 (1987).

The effect of ingested mass on plutonium absorption in the rat. J D Harrison and A J David. Health Physics 53, 187-189 (1987).

The gastrointestinal absorption of plutonium and americium in neonatal mammals. In: Age-related Factors in Radionuclide Metabolism and Dosimetry. J D Harrison, J A Bomford and A J David. Proc. CEC Workshop, Angers, France, Nov. 1986. pp.27-33.

Plutonium and americium uptake in rats fed with Cumbrian shellfish - Implications for estimates of dose to man. J D Harrison, H Smith and A J David. Sci. Total Environ. 68, 187-196 (1987).

Contributors to: Gastrointestinal absorption of selected radionuclides. A report by an NEA Expert Group. J D Harrison, R A Bulman. OECD, Paris (1988).

Gastrointestinal absorption of neptunium and curium in volunteers. J D Harrison, D S Popplewell, G Etherington and G J Ham Radiol. Prot. Bull. 93, 11-14 (1988).

The distribution of caesium-137, plutonium and americium in sheep. G J Ham, J D Harrison, D S Popplewell and E J C Curtis. Sci. of the Total Environ., 85, 235-244 (1989).

The absorption and intestinal retention of ingested radionuclides in neonatal mammals. G P L Naylor, J D Harrison and J W Haines. In: Radiation Protection - Theory and Practice. (E.P. Goldfinch, Ed.) Institute of Physics, Bristol. pp.451-454 (1989).

The measurement of the gastrointestinal absorption of neptunium-239 and curium-242 in humans. D S Popplewell, J D Harrison and G J Ham. In: Radiation Protection - Theory and Practice. (E P Goldfinch, Ed.) Institute of Physics, Bristol. pp.239-242 (1989).

The gastrointestinal absorption and retention of niobium in adult and newborn guinea pigs. J D Harrison, J W Haines and D S Popplewell. Int. J. Radiat. Biol. (in press).

Variability in dose per unit intake to adults, children and infants from ingestion of Pu-239. G M Kendall, A W Phipps and J D Harrison. Radiat. Prot. Dosim. (in press).

RADIATION PROTECTION PROGRAMME
Final Report

Contractor:

Contract no.: BI6-B-040-B

Centre d'Etude de l'Energie
Nucléaire, CEN/SCK
Rue Charles Lemaire 1
B-1160 Bruxelles

Head(s) of research team(s) [name(s) and address(es)]:

Dr. C. Vandecasteele
Département de Radio-
biologie, CEN/SCK
Boeretang 200
B-2400 Mol

Telephone number: 014/31.18.01

Title of the research contract:

Behaviour of radionuclides in terrestrial and freshwater environments.

List of projects:

1. Technetium behaviour and toxicity in mammals.
2. Comparative study of the radioecology of the continental water of the Meuse and Rhône basins.
3. Dynamic environmental cycling of HTO/HT/OBT. Experimental studies and modelling.

Title of the project no.: 1

Technetium behaviour and toxicity in mammals

Head(s) of project:

J. Vankerkom

Scientific staff:

C. Vandecasteele, M. Van Hees, K. Pollaris, M. Lambiet-Collier, J. Maisin, R. Kirchmann (advisor), G. Gerber (advisor)

I. Objectives of the project:

The project aims to define the uptake, metabolism and retention of technetium in mammals under different conditions of exposure. It also aims to determine the chemical and radiological effects of this long-lived radionuclide in developing and adult organisms in order to assess the risk of technetium uptake by man. The data obtained will allow to define realistic transfer factors to be used in mathematical models.

II. Objectives for the reporting period:

The objective of this five-years project was to improve our knowledge on the transfer of technetium to animals chosen as models for human (rat and pig) or as a link in the food-chain pathway to man (sheep).
The parameters of absorption, accumulation into organs and excretion, depending on the animal species and the chemical form administered had to be investigated into more detail. The toxic effects on the thyroid metabolism and the possible carcinogenicity of chronic oral administration of technetium had to be studied. Studies on the transfer to the foetus or to the new born of technetium administered to the dam during pregnancy and lactation were to be performed.

III. Progress achieved:

Technetium-99 is a long-lived radionuclide ($T_{1/2}$ = 2.12 x 10^5 y) produced during nuclear fission at a high yield (6%), comparable to that of Caesium and Strontium. Its high mobility in the environment and its high potential for biological uptake lead it to be considered as a potential hazard for man.
The efforts devoted during the previous decade to the study of the environmental behaviour of this element were mostly directed towards the behaviour of Tc in soil, its transfer from soil to plant and its behaviour in marine ecosystems ; only a limited number of reports have addressed its transfer and metabolism in terrestrial animals.
The results obtained in the various investigated fields converged on the conclusion that one of the most important parameters governing the transfer of Tc between the various compartments of the ecosystem or of the food chain was its chemical form. When dispersed into the environment this element may undergo a variety of chemical and biological transformations which profoundly modify its behaviour in soil, its transfer from soil to plant and could alter its absorption by mammals. This fact had been verified by preliminary experiments on rats given Tc as anionic oxidised form (TcO_4^-) or bioincorporated in algae and in maize leaves (see final report 80-84).
On the other hand, Tc accumulates to a large extent in the thyroid but large amounts of TcO_4^- (>15 µg/g) in food are needed to affect the metabolism of this gland (changes in iodine uptake and levels of thyroxin (T4) and triiodothyronine (T3) in blood) or to cause histological alterations of the thyroid structure. However, iodine might interfere with the metabolism of Tc and its concentration in the diet of experimental animals is generally much higher than in human diet, for which I-levels close to deficiency conditions can sometimes be approached.
Finally, negative effects of Tc at large doses (in the order of 50 µg/g food) had also been noticed regarding the fertility of adult rats.

A set of experiments conducted in the framework of this contract aimed to gather more information regarding the influence of the food processing in the gastro-intestinal tract of different mammal species and of the speciation of Tc on the accumulation and retention of this radioelement in animals. Other investigations aimed to study the toxical effect of Tc on the thyroid under conditions of I-deficiency, the possible carcinogenic effects on thyroid after long-term exposure and the effects on animal fertility. In parallel, information was to be obtained on the transfer to and the accumulation sites in the foetus from contaminated mothers.

I. Effect of animal species and chemical form.

In preliminary experiences, TcO_4^- had been intravenously injected in both rat and sheep and excretion had been followed over a 7 d period in order to determine the endogenous secretion from blood into the gastro-intestinal tract (GIT). The endogenous secretion, estimated as the fraction of the activity excreted with the faeces, amounted to about 31 % of the administered dose in rat and to about 70 % in sheep. The higher value obtained for sheep can be attributed to a different enterohepatic circulation in these two animal species and very probably to an important

recirculation of Tc secreted into the GIT by the way of saliva, since saliva has been reported to concentrate Tc by an order of magnitude compared to plasma and its production is very important in ruminants.

The influence of the chemical form of Tc on its absorption by mono- and polygastric mammals has been investigated by feeding rats and sheep with standard food contaminated with TcO_4^- in aqueous solution or with Tc bioincorporated into plant material (maize plants grown on nutrient solution contaminated by TcO_4^-). In rats given TcO_4^-, the cumulative excretion over a 7 d period was rather equally distributed between faeces and urine while much more activity was excreted in faeces (about 80 %) after feeding with bioincorporated Tc. This indicates that Tc accumulated into plant material is less readily absorbed through the intestinal barrier than the oxidised form.
In sheep, much more Tc was excreted in the faeces than in rats regardless of the Tc chemical form administered ; only a small fraction was eliminated in urine. The cumulative excretion over 7 d in urine amounted to about 2% in sheep given oral TcO_4^- and was still lower (less than 1 %) in animals given bioincorporated Tc, in agreement with the observations in rats. The much higher excretion of Tc in faeces in a ruminant animal compared to that observed in a monogastric mammal has to be correlated to a higher endogenous secretion as already shown and to the reducing conditions prevailing in the rumen of polygastric mammals which transform Tc into less available, low valence chemical forms.

The lower gastro-intestinal absorption of Tc bioincorporated into plant material compared to that of TcO_4^- was also reflected by the lower contamination levels (in Bq/g organ per MBq administered/kg animal body weight) measured in selected tissues of rats and sheep, 3 and 7 d after oral application (table 1).
Regardless of the treatment, highest activities per gramme of tissue occurred in the thyroid gland followed by the kidney ; however, skin, bone muscle and liver contributed a substantial part to the total body burden. The high concentration of Tc in wool and hair taken from the back of the two species (where external contamination is unlikely to occur) suggests that hair could be considered as a suitable indicator of bodily Tc contamination. Comparing the Tc contamination levels in the tissues of the two animal species, higher values are found in rat tissues than in the corresponding tissues from sheep, reflecting the lower gastro-intestinal absorption and the higher endogenous secretion in ruminants.

Excretion of Tc has been followed in the two animal species after administration of TcO_4^- or of Tc bound to maize. No statistical difference could be observed between the half-times of the various compartments identified in relation to the Tc chemical form administered. The total (combined urinary and faecal excretions) excretion in sheep was fitted to a sum of three exponential functions with respective half-times of 0.8, 6 and about 30 d ; the contribution of the long-lived components represents, however, less than 1 % of the administered dose. In rat, due to a limited collection period for excreta, only the parameters of the first compartment have been determined with a good reliability, the half-time has been estimated to 0.6 d ; however, the data showed that, at

least one other long-lived compartment with a metabolic half-time of more than 2 d was present.
The half-time parameters calculated for the excretion in both animal species are in good agreement with those estimated on the base of the retention of Tc accumulated in various organs. The removal of tissue Tc in sheep has been followed up to 90 d after dosing and has been fitted by a sum of two exponential functions respectively characterised by half-times of 5 d for the first component, irrespective of the tissue considered, and of approximately 20 d for kidney, 40 d for liver and 50 d or more for bone, muscle and skin. The retention of Tc in the organs of rats has been followed in an other experiment up to 140 d after the contamination phase. The data corresponding to the various tissues were best fitted to sums of at least two exponential functions (table I): the short-term compartment was characterised by a half-time of about 0.7 (± 0.3) d (ranging from 0.24 d in brain to 1.5 d in liver and the long-term compartment exhibited values of about 60 (± 27) d (with the lowest value for liver (25 d) and the highest for fat (122 d)). In kidneys and liver, a third compartment of intermediate half-time (respectively 3.6 and 2.5 d) could be estimated.

From these results it can be concluded that Tc is better assimilated by monogastric animals (including man) than by ruminants. In both animal types, bioincorporation of Tc reduces its gastro-intestinal absorption. Highest contamination levels are measured in the thyroid (critical organ), but high concentrations are also found in kidneys and liver. Hair also exhibits high Tc content and can be suggested to be used as a suitable indicator of body burden of Tc, even and especially in human.

ORGAN	FIRST COMPARTMENT		SECOND COMPARTMENT	
	CAPACITY Bq/g organ MBq/g food	HALF-TIME d	CAPACITY Bq/g organ MBq/g food	HALF-TIME d
Thyroid	4045.4 ± 295.3	0.74 ± 0.18	1249.4 ± 196.2	42 ± 15
Heart	6.8 ± 0.3	0.50 ± 0.11	1.1 ± 0.1	58 ± 21
Spleen	9.2 ± 0.7	0.51 ± 0.21	3.0 ± 0.4	59 ± 20
Kidneys	141.5 ± 1.6	1.03 ± 0.02	24.2 ± 1.4	30 ± 2
Liver	39.5 ± 0.2	0.82 ± 0.01	2.7 ± 0.1	25 ± 2
Pancreas	8.1 ± 0.2	0.51 ± 0.05	0.8 ± 0.1	60 ± 19
Lungs	15.1 ± 0.3	0.62 ± 0.05	1.0 ± 0.2	56 ± 24
Brain	1.3 ± 0.1	0.24 ± 1.28	0.3 ± 0.1	92 ± 58
Muscles	not available		0.6 ± 0.0	52 ± 6
Bones	10.3 ± 0.6	1.48 ± 0.26	2.9 ± 0.4	78 ± 28
Fat	4.9 ± 0.1	0.67 ± 0.03	1.2 ± 0.1	122 ± 46
Salivary gl.	10.5 ± 0.1	0.47 ± 0.08	1.2 ± 0.2	45 ± 16

Table 1. Parameters of excretion curves from selected organs of rats.

II. Toxical effects of Technetium.

The preferential accumulation of Tc in the thyroid and the high contamination level which can be reached in this organ let it be considered as a critical organ. Also the developing organism may be considered as critical because of its high radiosensitivity.

Earlier studies in rats conducted during the previous contractual period (80-84) had demonstrated that contamination of animals by Tc could affect both the metabolism of thyroid and the fertility ; these toxic effects were, however, only detectable at high Tc concentrations in the food (from 10 µg Tc/g food). However, Tc might compete with Iodine for thyroid uptake, and the human diet is usually much lower in I content than the normal diet fed to experimental animals (containing about 500 µg I/kg food) and may sometimes approach conditions of I-deficiencies.

Experiments were therefore performed on adult female rats kept on an I-deficient diet containing 60 µg I/kg food to which 20 µg I/kg food as KI has been added in some experiments. Tc as NH_4TcO_4 was added to the food to reach concentrations of 10 and 50 µg Tc/g food. The diet was started 2 weeks before mating.
Food intake in adult non-pregnant rats receiving a 60 µg I/g diet was slightly reduced compared to that in animals given a normal food ; food intake was further significantly lowered after the addition of 50 µg Tc/g food but not after that of 10 µg/g. In pregnant rats I-deficiency did not affect the normal increase in body weight during pregnancy compared to rats on I-rich diet, and only slightly diminished the characteristic peek of food intake during lactation. Addition of 10 µg Tc/g food did not give rise to a significant reduction of these parameters while a diet containing 50 µg Tc/g food prevented the characteristic increase of the body weight during pregnancy and of food intake during lactation.
Thyroid weight was slightly increased in rats fed an I-deficient diet for 5 weeks compared to those on normal food. The addition of 10 µg Tc/g in the food produced a more marked and significant increase of the thyroid weight. At 50 µg Tc/g food, the increase of the thyroid weight was, however, lower than at 10 µg Tc/g. Analysis of serum hormones indicated that Tc decreased of the serum levels of T3 and T4 in adult mothers when associated to an I-deficient food but not when given in a normal food. Uptake of radioactive iodine by thyroids of contaminated rats was also significantly reduced (75 % of the uptake in control groups) both for rats given normal food and rats kept on I-deficient diet.
Histological analyses were performed on the thyroid of rats kept on a normal or I-deficient diet supplemented with Tc (10 and 50 µg/g food). Six animals were examined in each group. The thyroids of rats given Tc in a normal diet displayed hypertrophy, with small follicles and reduced colloid. At certain sites, the epithelial lining was multicellular and showed high rates of proliferation. Some nuclei appeared to be enlarged and polymorphic ; a few ones were pyknotic. These alterations were more pronounced in animals exposed to the highest Tc level. The thyroids from the rats on an I-deficient diet showed the typical high epithelium and reduction of colloid ; those from rats further treated with Tc displayed changes similar to those reported for thyroids of animals on contaminated normal diet.

Finally, whereas I-deficiency and 10 µg Tc/g food did not significantly affect the size of the litter nor the weight of the total conceptus of the embryo and placenta at day 19 of pregnancy, 50 µg Tc/g food reduced these values markedly ; the effect on the foetus weight was more pronounced than that on the placenta. The observed reduction of the fertility has to be attributed to intra-uterine death of the embryos rather than to a decrease of the female fecundity : no significant differences were observed in the number of corporea lutea even after the highest amount of 50 µg Tc/g but a drastic reduction of live embryos was noticed after day 10 of pregnancy. There were also some excess mortality in the newborns from mothers on the high Tc diet and the surviving youngs showed a reduced growth rate.

These data allow to conclude that iodine deficiency only slightly influences the toxicity of Tc on the thyroid metabolism.
The toxicity (chemical and radiological) of Tc in rats appears to be small. Consequently, it seems unlikely that contamination levels in the environment would ever reach levels that could lead to serious non-stochastic effects, even in developing organisms.
However the results reported here above dealt with rather short-term exposure and the possible effect of long-term exposure to Tc on the thyroid carcinogenesis remained to be investigated.

This was studied on rats born from contaminated mothers and kept on contaminated food for more than 1 y. After successful mating, twenty-eight positive females were divided into two groups (treated and control). The rats from the treated group were fed contaminated food (10 µg Tc/g food). At weaning 56 young rats (28 males + 28 females) from each group were selected and the young rats were kept on the same contaminated food as their mothers. Moreover all young rats from both groups were given a goitrogen (propylthiouracyl 0.04%) in the drinking water until the age of 6 months in order to promote eventual transformed cells to form cancers. At the age of 8 months one third of the animals in each group have been slaughtered for microscopic examination of their thyroids. The remaining animals were maintained in the same conditions and were sacrificed 8 months later.
For both male and female rats at the age of 8 or 16 months, the total body weights were comparable in treated and control groups. Moreover Tc did not affect the growth of individual organs, except thyroid, between the two sacrifice times. The weight of thyroid was significantly higher in 8 months rats given Tc in food than in control ones. Such an hypertrophy had already been observed and reported after shorter periods of exposure. However, comparing the thyroid weight at the age of 8 m and 8 months later, those of control rats had increased markedly (by a factor 3 to 4) with time, while but a small, non significant increase was observed in treated rats. At the age of 16 months, the thyroid weight in treated rats was about twice lower than that of control rats. Histological analysis of crossed sections of the thyroid of rats from each group were performed.
The thyroid from control rats displayed a normal shape, with normal follicles dispersed in a layer of normal epithelial cells. Colloid were found in follicles. In a few thyroids some infammative changes could be discerned. All thyroids of Tc treated rats showed a slight hypertrophy and hyperplasia with disturbance of the normal structure. Inflammation

extended in some cases to the whole organ. There was a preponderance of stroma with a slight fibrosa. Many cell divisions as well as many hypertrophic and pyknotic cells could be seen. Some follicles were normal, containing little colloid ; others showed a partial destruction of the follicle epithelium with degenerated colloid and a few inflammatory cells. No tumor or adenoma was observed in treated or control rats after 8 months. Not all data are available for the 16 months exposure period, but some tumors were observed in treated as well as in control rats.

III. Transfer to the embryo.

Experiments were performed in order to study the transfer of Tc from the mother to the developing animal during gestation.
Tc was administered to pregnant female rats by intravenous injection or intubation in the stomach at day 15 or 18 of pregnancy. The animals were sacrificed 24 h later and foetuses as well as selected organs of the mother were taken for radioactivity measurements (table 2). The accumulation of Tc was much higher in the organs from the mother than in the foetus. Moreover the retention in foetus increased markedly (by a factor 6 to 15) between day 15 and day 18 of pregnancy.

TISSUE	day 15 of pregnancy		day 18 of pregnancy	
	I.V.	P.O.	I.V.	P.O.
kidneys	10.7 ± 0.7	6.5 ± 0.7	10.1 ± 0.4	10.0 ± 1.6
liver	7.1 ± 0.8	3.5 ± 0.6	5.2 ± 0.3	6.7 ± 1.2
foetus	0.003 ± 0.001	0.012 ± 0.002	0.046 ± 0.004	0.076 ± 0.015

Table 2. Tc content in selected maternal organs and foetuses in Bq/organ per kBq injected or given orally at day 15 or 18 of pregnancy. The animals were sacrificed 24 h after administration.

Distribution of Tc in the foetus has been investigated by autoradiography of 20 µm deep frozen cross sections of 21 d old foetuses taken from pregnant rats fed Tc contaminated food during the whole pregnancy (see photo). Tc is highly accumulated in the thyroid of the pups, but skin, stomach and placenta (not shown) appear as other sites of preferential accumulation. Activity measurements of dissected organs of the pups confirm these visual observations. The transfer coefficient for the whole foetus, calculated from its specific activity and the daily intake of the mother, amounted to 0.2 d/kg ; in comparison, the transfer coefficient for thyroid was higher than 0.8 (fetal thyroid is very small and could not be completely isolated from the trachea), that of stomach was 1.1 and that of skin and kidneys, about 0.7 and 0.3 respectively. Other tissues had lower transfer coefficient (0.2 for muscles, 0.2 for liver and 0.1 for lungs).

As a general conclusion, the toxicity (chemical and radiological) of Tc in mammals is small, even if animals are exposed in utero and for long period of time thereafter. The concentration levels used in these experiments were very high (10 ppm in the feeding stuffs) ; consequently, it seems unlikely that Tc concentration in the environment would ever reach levels that could lead to serious non-stochastic effects, even in developing organisms.

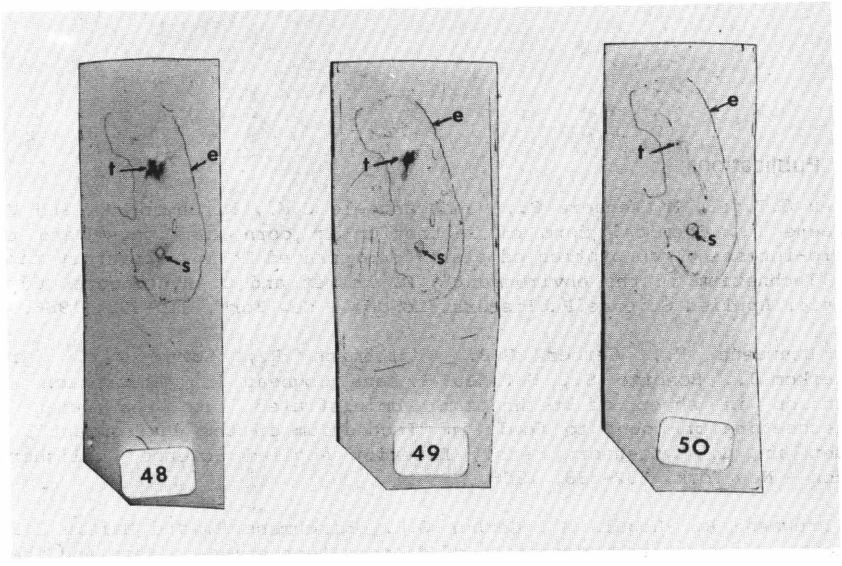

Localisation (autoradiography) of ^{95m}Tc in successive cross sections of 21 d old rat foetuses contaminated in utero.
t : thyroid ; e : skin ; s = stomach.

IV. Other research group(s) collaborating actively on this project [name(s) and address(es)]:

Laboratoire de Physiologie Végétale, Univ. Catholique de Louvain, LLN.
Laboratorium voor Colloïdale Scheikunde, Katholieke Univ. Leuven, Leuven.
Laboratoire de Biochimie, Univ. de Nantes, Nantes (France)

V. Publications:

Garten C.T.jr., Myttenaere C., Vandecasteele C.M., Kirchmann R. and Van Bruwaene R., Chemical form of Technetium in corn (Zea mays) and the gastro-intestinal absorption of plant incorporated Tc in laboratory rats, in "Technetium in the environment", G. Desmet and C. Myttenaere, eds., Elsevier Applied Science Publishers, London - New York, 319-332, 1986.

Van Bruwaene R., Gerber G.B., Kirchmann R., Garten C.T. jr., Vankerkom J., Bonotto S., Mathieu T. and Cogneau M., Absorption and retention in sheep of technetium administrated into the rumen as pertechnetate or bound to food, in "Technetium in the environment", G. Desmet and C. Myttenaere, eds., Elsevier Applied Science Publishers, London - New York, 332-338, 1986.

Van Bruwaene R., Hegela M., Gerber G.B., Kirchmann R. and Maisin J.R., Toxicity of long term application of dietary technetium to rats and their offspring, in "Technetium in the environment", G. Desmet and C. Myttenaere, eds., Elsevier Applied Science Publishers, London - New York, 371-396, 1986.

Vandecasteele C.M., Garten C.T. jr., Van Bruwaene R., Janssens J., Kirchmann R. and Myttenaere C., Chemical speciation of technetium in soil and plants : impact on the soil-plants : impact on the soil-plant-animal transfer, in "Speciation of fission and activation products in the environment", R.A. Bullman and J.R. Cooper, eds., Elsevier Applied Science Publishers, London - New York, 368-381, 1986.

Kirchmann R., Fagniart E., Van Hees M., Van Bruwaene R., Gerber G.B., Colard J. and Cogneau M., Experimental studies on technetium transfer to man, via the food chain, following a contamination of the soil surface, Proc. Int. Symp. on "Emergency planning and preparedness for nuclear facilities", Rome (Italy) November 4-8, 1985, IAEA-SM-280/34 P, IAEA, STI PUB 701 : 343-345, 1986.

Fagniart E., Vandecasteele C.M. and Kirchmann R., Variability in the soil-plant transfer factors of radionuclides observed in experimental fields, Proc. ESNA XVIth Annual Meeting, Warszawa (Poland), September 9-13, 1985, ESNA Newsletter, Working group environmental pollution, 22-35, 1986.

Vandecasteele C.M., "Influence du technetium sur la nitrogénase d' Azotobacter". Thèse de doctorat, Université Catholique de Louvain, Louvain-la-Neuve, 178 pp, 1987.

Vandecasteele C.M., F. Capot, J.-P. Dehut, J.-M. Mousny and C. Myttenaere,
"Technetium fate in irrigated rice field", Proc. Seminar on the "Cycling of long-lived radionuclides in the biosphere : observations and models", Madrid (E), September 15-19, 1986, CIEMAT, Vol 2 : 207-225, 1987.

Dehut J.-P., C. Van Hove, C.M. Vandecasteele and C. Myttenaere, "Technetium cycle in the environment : redistribution of bioincorporated Tc in Azolla sp. within the different compartment of a terrestrial ecosystem", Proc. Seminar on the "Cycling of long-lived radionuclides in the biosphere : observations and models", Madrid (E), September 25-19, 1986, CIEMAT, Vol 2 : 227-238, 1987.

Vandecasteele C.M., J.-P. Dehut, D. Deprins, S. Van Laere, F. Auvray and C. Myttenaere, Long-term availability of technetium deposited on soil after accidental releases, Health Phys., 57 (2) : 247-254, 1989.

Dehut J.-P., K. Fonsny, C.M. Vandecasteele, C. Myttenaere and M. Cogneau, Bioavailability of technetium incorporated in plant material, Health Phys., 57 (2) : 263-267, 1989.

Zeevaert Th., C.M. Vandecasteele and R. Kirchmann, Assessment of the dose to man from liquid releases of Tc-99, Health Phys., 57 (2) : 337-343, 1989.

Gerber G.B., M. Van Hees, C.T. Garten Jr., C.M. Vandecasteele, J. Vankerkom, R. Van Bruwaene, R. Kirchmann, J. Colard and M. Cogneau, Technetium absorption and turnover in monogastric and polygastric animals, Health Phys., 57 (2) : 315-319, 1989.

Gerber G.B., M. Hegela, J. Vankerkom, R. Kirchmann, J.R. Maisin and M. Lambiet-Collier, Toxicity of Tc-99 : can it represent a risk to man?, Health Phys., 57 (2) : 345-350, 1989.

Vandecasteele C.M., Th. Zeevaert and R. Kirchmann, Factors influencing the transfer of radionuclides in agricultural food chains, 3rd Int. Conf. on Anticarcinogenesis and Radiation Protection (3-ICARP), Dubrovnic, October 15-21, 1989, to be published.

Title of the project no.: 2

Comparative study of the radioecology of the continental water of the Meuse and Rhone basins : Partim the Meuse basin.

Head(s) of project:

C. Vandecasteele

Scientific staff:

J.R. Maisin, A. Leonard, P. Govaerts, E. Fagniart, E. Bonnijns, J.C. Micha, J.P. Descy, A. Gillet, R. Kirchmann, J. Lambinon, M. Meurice-Bourdon, C. Myttenaere, L. Sombré, Y. Thiry, J. Smitz, E. Everbecq, J. Remacle, F. Berhin, G. Beuken, H. Declercq-Versele, J.L. Havaux

I. Objectives of the project:

This project is part of a coordinated research programme involving the CEN/SCK (Mol-Belgium) associated to several Belgian laboratories and the CEN/CEA (Cadarache-France). The general objective of this programme is to gain a better understanding of the behaviour of radionuclides released into freshwater ecosystems and to gather a more accurate knowledge on their transfer to man through the food chains. The ultimate objective is to build a general transfer model in freshwater systems based on field measurements and observations, completed by laboratory experiments at various levels. Two waterway systems are investigated : the Meuse basin (Belgian contribution) and the Rhone basin (French contribution) ; the data and models obtained for both rivers will be compared.

II. Objectives for the reporting period:

- Creation of a data bank containing ecological and radioecological site specific data for the Meuse river (previously obtained data and new ones obtained in the framework of this contract).
- Determination of the transfer parameters for ^{134}Cs (and ^{60}Co) between the different compartments of a freshwater ecosystems.
- Modelling of the controlled experiments and development of a general model of the radionuclides transfer in an aquatic ecosystem.

III. Progress achieved:

1. Field studies :

Based on data obtained in the framework of the previous contracts, as well as on new ones gathered in the framework of this contract, a databank with the same structure as that available at the CEA-Cadarache has been created and a synthesis of the structure and functioning of the ecosystem "Meuse" has been realised, laying stress on the composition and dynamics of the phytoplankton population. A balance of the primary production in this system has been struck and translated into a model.

The characterisation of the aquatic food chain has been further developed by investigations on the alimentary regime of primary and secondary consumers. Three fish species representative of the Meuse fauna were regularly caught in the river and analysed for their stomachal contents.
The roach (Rutilus rutilus) can be classified as an omnivore with a marked herbivorous propensity. It feeds mostly on algae (Chlorophytae and Chrysophytae), but also on molluscs (Dreissena polymorpha and Bithynia tentaculata) and arthropods (dipterous).
The pike-perch (Stizostedion lucioperca) is a piscivorous fish. Its diet consists in small fishes, mostly bleaks (Alburnus alburnus), possibly due to its abundance, gudgeons (Gobio gobio), roaches (Rutilus rutilus), näslings (Chondrostoma nasus), breams (Abramis brama + Blicca bjoerkna) and chubs (Leuciscus cephalus) were occasionally found in pike-perch stomachs. The size of the preys ranges from 3.5 to 15.6 cm, but are most frequently of about 8-9 cm ; their weight varies between 2.45 and 29.7 g. The feed ratio, defined as the ratio between the weight of the stomach content and the body weight, ranges from 0.2 to 5.0%.
The perch (Perca fluviatilis) diet has been studied on 109 individuals whose size ranged from 7 to 30 cm. Chironomidae constitute the major fraction of its diet (54%). Crustaceans (Asellus, Gammarus and Corophium) represent 26% and Trichoptera, principally Cyrnus trimaculatus, account for 10% of the perch's feed. This fish also feeds on grups of Ephemerotera and Diptera and on smaller fishes (bleaks and chub) which represent 6% of its diet. The alimentary regime of the perch varies depending on their size. Perch smaller than 8 cm are essentially plancton-eaters (Cladocera and Copepods) ; small fishes are preyed upon by perches larger than 16 cm. The regime varies also depending on the season : it consists mainly in Cladocera, Chironomidae and Trichoptera in autumn while it is more diversified in spring and comprises invertebrates as well as fishes.

Sampling campaigns have been organised to collect, in various stations on the Meuse, aquatic plants and fishes (roach and perch) for radioactivity analysis. The selected stations were : Ham-sur-Meuse (Up-stream from Chooz), Waulsort and Annevoie (up-stream from Namur), Ampsin-Neuville (down-stream from the Tihange nuclear plant) and Monsin, Argenteau and Lanaye (down-stream from Liège).
In aquatic mosses collected in October 1987 between Ham-sur-Meuse and Monsin, highest concentrations of $^{58-60}Co$, $^{134-137}Cs$ and ^{54}Mn were found immediately down-stream from Tihange Nuclear plant ; radiocobalt and radiomanganese, but not radiocaesium, were still detectable at Monsin.

The evolution from 1984 to 1988 of the ^{137}Cs contamination levels measured in two of the fish species are presented in table 1. Because of the biological variability and the possible variations due to the sampling period (in relation with variations in the composition of the diet) it is uneasy to obtain a clear picture of the longitudinal evolution of the radiocontamination in fish ; however, it seems that the contamination levels are lower near Liège than in the higher parts of the river. A significant increase in the ^{137}Cs content of the fishes can be noticed from 1984 to 1987, most probably due to the environmental contamination after the Chernobyl accident ; the Cs levels decreased in the two next years but were still higher in 1988 than those measured in 1984.

Sampling period		09/84	04-05/87	06/88	10/88
Species	Station				
ROACH	Waulsort	-	5	-	-
	Annevoie	-	3.6	-	0.5
	Ampsin	0.71	2.8	1.3	2.3
	Argenteau	0.29	3.5	-	-
	Lanaye	0.19	-	-	0.6
PERCH	Waulsort	-	12.4	4.5	2.5
	Annevoie	-	7.5	-	-
	Ampsin	0.84	-	5.4	2.5
	Argenteau	1.26	-	-	-
	Lanaye	0.5	-	1.8	1.5

Table 1. ^{137}Cs content (Bq/kg) in two fish species collected at different station on the Meuse river between 1984 and 1988.

2. Laboratory studies :

2.1. Interactions with sediments

Fixation kinetic of radiocaesium by sediments collected from the Meuse has been investigated under hydro-dynamic conditions in an experimental model of a river section. 600 l water (Meuse water) was circulated by a pump (maximal flow rate of 10 l/s). The flow in the river section was made laminar by forcing the water through two honeycombs placed at the extremities of the simulated river section. The water contained in the whole system has been contaminated by the addition of 6 MBq of Cs-137 as

CsCl. Water samples and sediment cores were taken regularly for radioactivity measurements. Moreover, water samples were passed through 0.5 µm filters to separate suspended matters. It was observed that the contamination level in the filtrated water decreased progressively and reached an equilibrium value corresponding to 23% of the initial radioactivity. At this time 75% of the radiocaesium was accumulated in the bottom sediment and 2 to 3% were associated with the suspended matters (2.77 g/ml). The estimation of the distribution coefficients gave a Kd value of 400 l/kg for the bulk of the bottom sediments while the value for the suspended matters was about 100 times higher.

Exploratory investigations were also conducted to estimate the role of the bacterial flora, present in the water column or associated with sediments, on the behaviour of radiocaesium and radiocobalt in a river ecosystem and especially at the sediment level. These investigations will be carried on in the framework of the next CEC programme.

2.2. Transfer to the phytoplankton.

Algal strains (unicellular and colonial green algae and diatoms) were isolated from the Meuse water and determined. Bacteria associated with algae were isolated on appropriate media and tested for their resistance to antibiotics in order to produce for experiment purposes bacteria-free algal cultures. Preliminary studies have been conducted in order to define suitable culture conditions, as close as possible to the environmental conditions, and to determine the growth curves and the evolution of the morphological parameters under these conditions.
The uptake of ^{60}Co and ^{134}Cs by Cyclotella meneghiniana, a diatom representing an important fraction of the Meuse phytoplankton, and by mixed algal populations (total phytoplankton collected at the various seasons of the year) has been investigated using chloride forms or contaminated effluents from the three units of the Tihange nuclear plant. The uptake of both radionuclides by algae was very rapid and equilibrium was achieved within 24 h or less. The estimated transfer factors ranged from 10^3 to 10^4 and from $5\ 10^3$ to $1.3\ 10^4$ for Cs and Co respectively. The results were comparable regardless of the source of the radioisotopes introduced in the growth medium, commercially purchased chlorides or PWR effluents ; they suggest that radiocaesium and radiocobalt in the effluents of PWR nuclear plant are released as ionic forms or under chemical forms of similar availability for algae.

2.3. Transfer through the food chain.
Several experiences have been conducted under laboratory conditions in order to determine the kinetics and parameters of the transfer of radiocaesium in different links of a freshwater food chain. This food chain included a unicellular green alga (Scenedesmus obliquus), a mussel (Dreissena polymorpha), an omnivorous fish (Barbus barbus) and a carnivorous one (Perca fluviatilis).

The uptake kinetics of radiocaesium by freshwater organisms were fitted using a mathematical relation derived from the Mitscherlich's equation :

$$Y_t = M\ (1 - e^{-t/b})$$

where Y_t is the contamination level in the organism considered at time t,
M^t represents the steady state equilibrium concentration in the organism (reached when t = 3b/0.95) and
b is a parameter depending on the accumulation rate and is considered by several authors as an estimation of the biological half-time.

This equation was also used to analyse the changes with time of the concentration ratios (Y) between the organism considered and the radiocontaminated precursor ; in this case M represents the transfer factor.

2.3.a. Transfer water-alga-mussel

Uptake kinetics of radiocaesium by mussels from water (^{134}CsCl) or through the food chain (^{137}Cs labelled algae) were simultaneously investigated and the calculated concentration ratios (CR) were fitted using the here above described mathematical equation. The parameters estimated are given in table 2.

mussel fraction	^{134}Cs in water		^{137}Cs in algae*	
	M	b (h)	M	b (h)
flesh	230	26	148	23
shell	38	14	16	9
total	124	55	36	5

Table 2. Parameters of the equations fitting the evolution of the CR between mussels and water or algae. The CR were calculated as the ratio between activities in mussels (Bq/g DW) and activities in water (Bq/ml). * The radioactivity in algae was expressed per ml of water in which the algae were dispersed.

2.3.b. Decorporation from mussels.

Desorption kinetics were followed in mussels directly contaminated from water or from animals contaminated through their diet (labelled algae) and the ecological half-times were estimated. Radiocaesium was rapidly eliminated from the flesh of mussels contaminated from water : 37% of the radioactivity was excreted with a half-time of 9 h and 63% were retained with a longer half-time of 17 d. Radiocaesium excretion from mussels contaminated through the food chain was slower : if 20% of the accumulated activity was released with a half-time of 10 h, 80% of the flesh burden is retained for a much longer period (half-time of about 3.7 y).

2.3.c. Transfer water-mussel-fish.

Barbels were exposed to contaminated water (^{137}CsCl) and simultaneously were fed ^{134}Cs labelled flesh of mussels. The results showed that radiocaesium in barbels exposed to contaminated water reached an equilibrium concentration after about 9 months (b=89 d ; M=37 ml/g FW). When the fishes were fed contaminated mussels, the equilibrium concentration ratio between the fish and its feed amounted to about 6 g DW/g DW and was estimated to be reached after 3 y (b=350 d). This very long time needed to achieve equilibrium is most probably overestimated, since the biomass ratio between preys and carnivorous fishes in this experiment was much lower (0.03) than that observed under real conditions (0.7 to 0.8).
From these results it is possible to conclude that, if the food chain accounts for 2% of the fish contamination in the short-term, in the long-term, when equilibrium would have been reached in each compartment, 90% of the radiocaesium accumulated by the fish will have been provided by the food chain.

2.3.d. Transfer fish-carnivorous fish

The only radiocontamination pathway considered in this case was the food chain pathway. The equilibrium concentration ratio (1.5 g FW/g FW) was reached after 8 months (b=77 d). After 14 weeks feeding radiocaesium labelled preys (barbels), most of the activity was recovered in muscles of the perch (61% of the fish burden) ; the gastro-intestinal tract accounted for 9%, the skeleton, for 6% and the liver, for 1%.

3. Modelling :

Models of two different types have been developed : the first ones were built to describe processes and, especially, to simulate the experiments conducted under laboratory conditions ; the second one is a general model describing the behaviour of radionuclides in aquatic ecosystems (rivers or lakes). The general model integrates the first type sub-models.

3.1. Process models

Primary production in most aquatic ecosystems is mainly attributable to Phytoplankton. Thus, in order to gain a better knowledge of the dynamic of the food chain contamination, a deterministic model of the radiocontamination of phytoplankton has been elaborated. Figure 1 provides an example of the changes of the ^{137}Cs contamination and decontamination fluxes with time for a representative phytoplanktonic alga (Scenedesmus obliquus). Figure 2 presents the simulation of the contamination of this alga by ^{60}Co together with the experimental points. The transfer of ^{137}Cs to mussels has also been simulated considering a simple food chain (water-alga-mussel) (Figure 3) and has later been extended up to the fish level.

These process models, based on conservation equations for water, algal and animal biomasses and radionuclides, allow to stress the relative importance of the various phenomena involved in the transfer (adsorption,

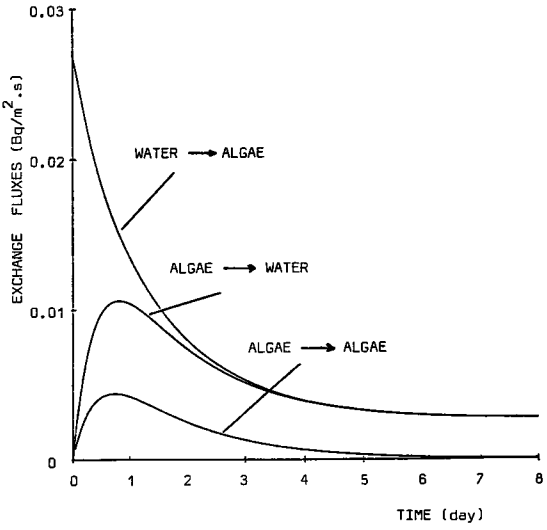

Fig.1. Simulation of the time evolution of the ^{137}Cs fluxes in water-alga system.

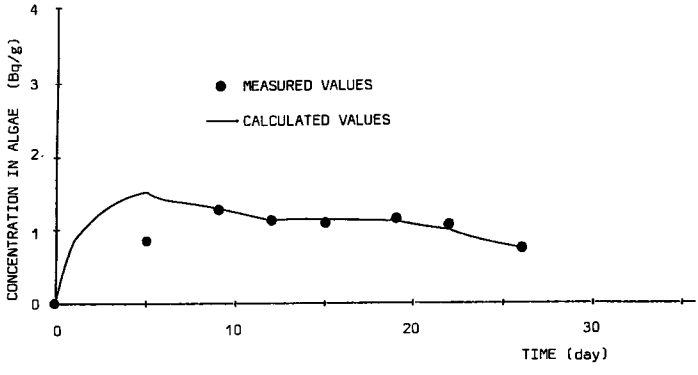

Fig.2. Comparison of the experimental data and model calculations for the transfer of ^{60}Co from water to phytoplankton.

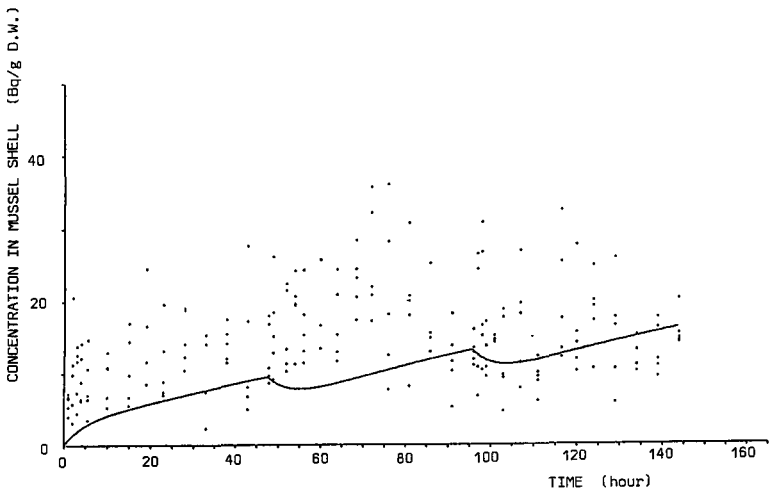

Fig.3. Simulation of the transfer of radiocaesium from water and radiolabelled algae to mussel. Comparison with the experimental data.

ingestion, decontamination). The results obtained show that the concentration ratio between water and algae, for example, at steady state equilibrium (defined as the concentration factors - CF) depends considerably on the experimental conditions. These simulations thus pointed out that the CF's do not allow the quantification of the phenomena involved and display only a very limited predictive capacity. On the contrary, a deterministic model may significantly improve the understanding of the processes involved.

3.2. General model.

Modelling of the transfers of radionuclides in an aquatic ecosystem needs, as a preliminary, an adequate knowledge of the hydro-dynamic characteristic of the system, including the transport of suspended matters and bottom sediments.
The general model that has been developed, proceeded in four successive stages :

- a hydro-dynamic sub-model represents and computes for any time and any location the flows, the water heights, the river cross-sections and the tensions on the bottom
- a sediment sub-model allows to calculate the concentrations in suspended solids in the water column (g/m^3) and the deposited sediment concentration (g/m^2)
- a radionuclide sub-model assesses the transport and distribution of the radioelements in water, sediments and suspended matter
- a radioecologic sub-model describes the food chain transfers and computes the amounts of radionuclides incorporated into the various biologic compartments as well as the fluxes between these compartments.

This model is a one-dimensional, non-stationary model. It has been applied to the Meuse river. Figures 4 and 5 present the changes with time of the concentrations of ^{137}Cs and ^{60}Co associated with the bottom sediments calculated by the model, taking into account the real releases into the river, and give, for comparison, the measured values. Figure 6 shows the evolution of the ^{137}Cs concentration in fish (typical carp of the Meuse) calculated by the model ; the calculated values, ranging from 10 to 30 Bq/kg fresh weight are in good agreement with the contamination values measured in fishes from the Meuse during the period considered (8 to 66 Bq/kg F.W.).

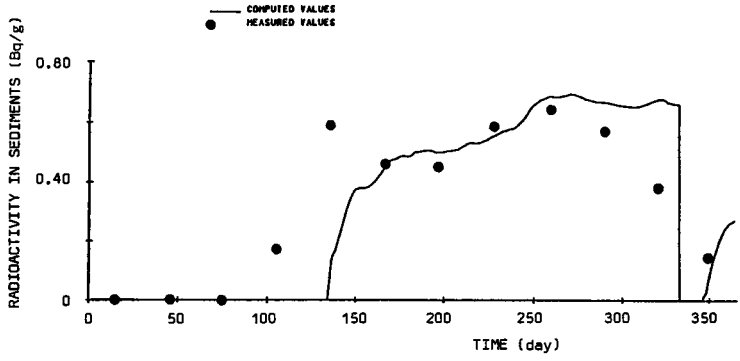

Fig.4. Simulation of the changes with time of the ^{137}Cs contamination level in bottom sediments of the Meuse at Hastière in 1975.

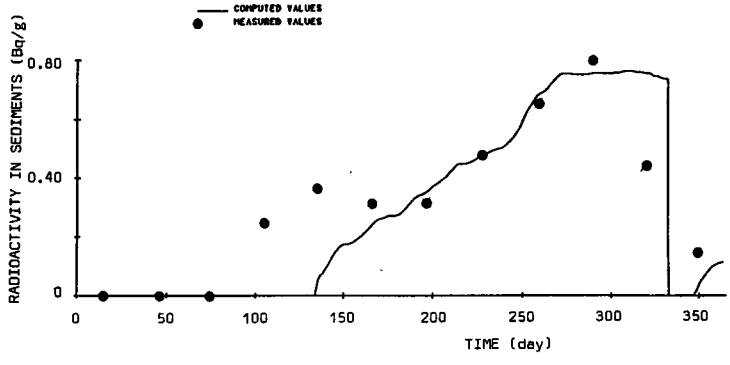

Fig.5. Simulation of the changes with time of the ^{60}Co contamination level in bottom sediments of the Meuse at Hastière in 1975.

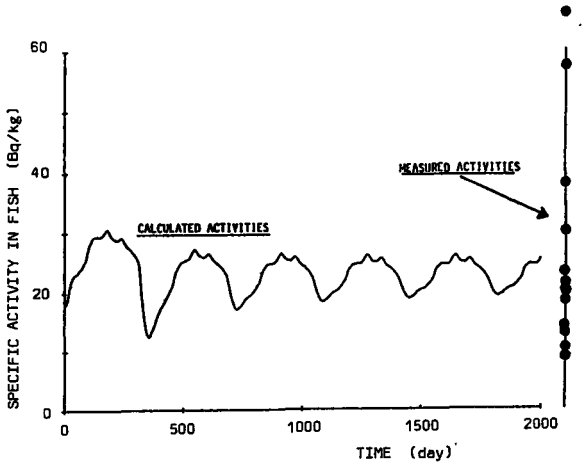

Fig.6. Simulation of the evolution of the ^{137}Cs concentration in fish (carp) at Hastière taking into account the real releases in the river Mesue from 1975. Comparison with in situ measurements over the same period.

This model is of general application and allows to estimate the relations between releases, water flows and contamination levels in the various compartments of the aquatic ecosystem. It works under non-stationary conditions corresponding to the real world.

An extended synthesis of the data and information gathered in the framework of the contract will be published in 1990.

IV. Other research group(s) collaborating actively on this project [name(s) and address(es)]:

- Unité d'Ecologie des Eaux Douces, Facultés Notre Dame de la Paix, Namur.
- Laboratoire de Physiologie Végétale, Univ. Catholique de Louvain, LLN.
- Laboratoire de Radioécologie, Univ. de Liège, Sart-Tilman (Liège).
- Unité de Modélisation Mathématique des Eaux Intérieures, Univ. de Liège, Sart-Tilman (Liège).
- Institut d'Hygiène et d'Epidémiologie, Bruxelles.
- The Centrale Nucléaire de Tihange (Intercom) collaborates actively to this project.
- Laboratoire d'Etude de la Pollution des Eaux, CEN-CEA Cadarache (France).

V. Publications:

Meurisse-Genin M., Reydams-Detollenaere A., Donatti O., Micha J.C., Caractéristiques biologiques de la crevette d'eau douce Atyaephyra desmaresti Millet dans la Meuse, Annals Limnol. 21, 2, 214-140, 1985.

Kirchmann R. (éd.), L'impact des rejets de la centrale nucléaire de Tihange (Belgique) sur l'écosystème Meuse : études in situ et recherches expérimentales pendant la période 1981-1984, BLG 573, Mol, 48 pp, 1985.

Debauche A. et Descy J.P., Radiological monitoring in the Belgian part of the river Meuse (1984) : results in the aquatic mosses. UIR, 8th annual meeting, Brussels, 1985.

Mouvet C., Descy J.P., Speciation of some heavy metals in the river Meuse : comparison between observed and calculated values, Proc. Symp. on the Belgian research on heavy metals cycling in the environment, Brussels 11-12 oct. 1985, D. Rondia Ed., 125-133, 1986.

Descy J.P., Qualité des eaux de la Meuse : évaluation en une de la réintroduction du saumon atlantique dans le bassin mosan, Proc. Colloque sul la Réintroduction du saumon atlantique dans le bassin de la Meuse, Service de la Pêche, Région Wallonne, mars 1985, p 49-63, 1986.

Smitz J.S. and E. Everbecq, Modelling the behaviour of radionuclides in the aquatic ecosystem, in The cycling of long-lived radionuclides in the biosphere : observations and models, Madrid, September 15-19, 1986, CIEMAT, Vol. I, 267-294, 1987.

CEN/SCK, Etude comparée de la radioécologie des eaux continentales des bassins mosan et rhodanien, contribution des laboratoires belges. Rapport technique d'avancement 1985, 158 pp., 1986.

Detollenaere A., Micha J.C., Impact des rejets thermiques de la centrale nucléaire de Tihange sur les poissons de la Meuse. Tib. Cebedeau, 516, 39, 9-26, 1986.

Meurisse-Genin M., Reydams-Detollenaere A., Stroot Ph. et Micha J.C., Les macroinvertébrés benthiques de la Meuse belge : bilan de cinq années de recherches (1980 à 1984). Arch. Hydrobiol., 109, 1, 67-88, 1986.

Galvez M. et Micha J.C., Introduction, extension et répartition du sandre en Belgique. Trib. Cebedeau, 521, 33-42, 1987.

Sombre L., Contribution à l'étude du transfert du radiocésium (^{134}Cs et ^{137}Cs) dans une chaîne alimentaire d'eau douce simplifiée : eau-algue verte (Scenedesmus obliquus) - mollusque filtreur (Dreissena polymorpha). Thèse de doctorat, Faculté des Sciences Saint Charles, Université de Provence (Aix-Marseille I), 146 pp, 1987.

CEN/SCK, Etude comparée de la radioécologie des eaux continentales des bassins mosan et rhodaniens, contribution des laboratoires belges. Rapport technique d'avancement 1986, 191 pp, 1987.

Gillet A. and Micha J.C., Biologie et radiocontamination de trois espèces animales (Dreissena polymorpha (P.), Rutilus rutilus (L.), et Perca fluviatilis (L.)) représentatives de différents maillons trophiques de l'écosystème Meuse, Ann. Assoc. Belge Radioprotection, 12 (2-3) : 139-156, 1987.

Descy J.P., Etudes écologiques de la Meuse en relation avec les rejets des centrales nucléaires, Ann. Assoc. Belge Radioprotection, 12 (2-3) : 127-138, 1987.

Sombré L., Carraro S. and C. Myttenaere, Transfert du Cs-134 dans une chaîne alimentaire d'eau douce simplifiée : eau - algue verte (Scenedesmus obliquus) - mollusque filtreur (Dreissena polymorpha), Ann. Assoc. Belge Radioprotection, 12 (2-3) : 205-230, 1987.

Sombré L., Carraro S. and C. Myttenaere, Contamination d'une algue verte d'eau douce (Scenedesmus obliquus) par des radionucléides typiques des rejets d'une centrale PWR : culture dans un turbidostat, Ann. Assoc. Belge Radioprotection, 12 (2-3) : 157-170, 1987.

Smitz J.S., Everbecq E. and Coméliau B., Modélisation du transfert du Cs-137 de l'eau vers le phytoplancton et simulation des expérimentations de laboratoire, Ann. Assoc. Belge Radioprotection, 12 (2-3) : 171-204, 1987.

Zeevaert Th, Fieuw G., Kirchmann R., Koch G. and Vandecasteele C.M., Assessment of the dose to man from the sediments of a river receiving radioactive effluents released by a waste treatment facility, Ann. Assoc. Belge Radioprotection, 12 (2-3) : 247-286, 1987.

Sombré L., L. Foulquier et C. Myttenaere, Simulation de la contamination d'un écosystème dulcicole par du radiocésium rejeté en conditions accidentelles, IVème Symp. Int. de Radioécologie de Cadarache sur l'"Impact des accidents d'origine nucléaire sur l'environnement", Cadarache, 14-18 mars 1988, CEA Cadarache, Tome 1 : C99-C106, 1988.

Sombré L., Essai de modélisation du transfert du radiocaesium (Cs-134 et Cs-137) dans une chaîne alimentaire d'eau douce simplifiée : eau-algue verte (Scenedesmus obliquus)-mollusque filtreur (Dreissena polymorpha)-poisson (Barbus barbus), Thèse de doctorat en Ecologie (Radiohydrobiologie), Faculté des Sciences Saint-Charles, Université de Provence, Aix-Marseille I, 152pp, 1988.

Smitz J.S. and E. Everbecq, Accidental releases of radionuclides in waterways, CEC Workshop on "Recent advances in reactor accident consequence assessment", Roma, 25-29 January 1988, Report EUR 11408/EN : 257-268, 1988.

CEN/SCK, Etude comparée de la radioécologie des eaux continentales des bassins mosan et rhodanien, contribution des laboratoires belges, Rapport Technique d'Avancement 1987, 132pp, 1989.

CEN/SCK, Etude comparée de la radioécologie des eaux continentales des bassins mosan et rhodanien, contribution des laboratoires belges, Rapport Technique d'Avancement 1988, in press.

Title of the project no.: 3

Dynamic environmental cycling of HTO/HT/OBT.
Experimental studies and modelling.

Head(s) of project:

S. Bonotto (Source term)
E. Fagniart (dynamic models in soil-plant systems)
C. Vandecasteele (Tritium and C-14 transfer in mammals)

Scientific staff:

J. Vankerkom, M. Van Hees, M. Meurice-Bourdon, H. De Clercq-Versele, J. Binet, R. Kirchmann (advisor), G. Gerber (advisor), M. Mergeay (advisor)

I. Objectives of the project:

The general objective of this project is to gain a better understanding of the environmental behaviour of tritium and carbon-14 by an integrated approach involving modellers and experimenters. Three aspects of the environmental cycle of tritium and carbon-14 will be considered :
- the source term : study on the formation and release of OBT by degradation of resins used for water purification in PWR and on the possible contribution of microorganisms to OBT formation,
- The modelling of H-3 and C-14 behaviour in a soil-plant system : laboratory and field experiments are planned to gather information on the physical and biological mechanisms of HT oxidation and incorporation by different plant species,
- the transfer of C-14 and tritium under various chemical forms to mammals (mono- and polygastric) is studied in order to predict the behaviour of tritium and C-14 labelled organic molecules in man.

II. Objectives for the reporting period:

Determination of the mechanisms of OBT production in the primary loop of a PWR. Study of the availability of these OBT forms.
Study under field and controlled conditions of the mechanisms involved in the incorporation of HT by plants.
Study on the transfer and metabolism of organically bound Tritium (OBT) and organically bound ^{14}C in mammals.

III. Progress achieved:

1. Source term :

As suggested in previous work, the organically bound tritium (OBT) revealed by biological tests, based on preferential uptake by the microalga Scenedesmus obliquus, in the liquid effluents of nuclear power plants of the PWR type might originate from :

1. Degradation of purification resins, originating tritiated organic molecules having a high specific activity ;
2. Biosynthetic activity of microorganisms growing on the purification resins and in the surrounding medium ;
3. Other unknown processes (as, for example, tritiation of organic matter introduced into the primary circuit with the unwashed purification resins or by other routine operations).

Indirect evidence that purification resins might be a source of organically bound tritium (OBT) was obtained by using an experimental device simulating the flow of water of the primary loop through a column containing the resins. Unirradiated (control) as well as gamma-irradiated (Co-60, 336 Gy) resins released organic matter, which became heavily tritiated when submitted to an external irradiation in the presence of tritiated water (HTO), thus producing OBT. However, the role of eventual microorganisms present in the primary loop, in the production mechanism of OBT could not be excluded by this experimental approach.

Consequently, it was of interest to know whether :

1. Microorganisms are introduced into the primary circuit with the purification resins ;
2. These microorganisms are capable of growing on the resins and/or in the surrounding liquid medium ;
3. They are able to produce tritiated organic molecules in the presence of tritiated water (HTO).

In a series of new experiments, the purification resins were shaked in a H_3BO_3 solution (10 g l^{-1}) and washed 5-6 times with sterile demineralized water. Nevertheless, they still contained few bacteria and some fungi. This finding demonstrated that microorganisms may be introduced into the primary circuit as contaminants of the purification resins. Once introduced in this stressful environment, they could survive if a substrate is available or eventually die. Theoretically, in both cases, because of the presence of HTO, their organic matter could undergo a more or less pronounced tritiation, thus originating OBT.

One of the microorganisms previously found in the primary cooling system of a nuclear reactor was submitted to various microbiological tests and recognized as a Rhodotorula. Its optimal growth occurs at 25-30° C, decreasing toward higher values. No development was observed at 42° C, a value which is only 2° C higher than the temperature (40° C) of the purification resins in operating PWR reactors. When a suspension of Rhodotorula (about 7 x 10^6 cells ml^{-1}) is introduced into the simulated circuit maintained at 40° C, the number of living cells circulating in the liquid medium decreases by 2-3 orders of magnitude (passing from 1 - 3 x 10^6 to 0.4 - 2 x 10^4 cells) in 7 days. These results were confirmed by using tritiated Rhodotorula suspensions, labeled by supplying the

cells with ^{3}H-Leucine (185.000 Bq ml^{-1}), during a period of 1 to 2 weeks. In the circulating medium, the appearance of some other microorganisms (Gram-) was noticed. These latter may originate from the resins, the circuit and/or the manipulations during the sampling of the medium for bacteriological analyses.

The decrease of Rhodotorula in the circulating medium does not correspond to a significant increase of healthy living cells, capable of producing colonies, at the level of the purification resins, which would function as filters. Consequently, the number of living Rhodotorula cells is really reduced, several factors being potentially responsible for this decrease :

1. Thermic stress (40° C), strongly reducing cell survival ;
2. Potential toxicity of the refrigerant, due to its chemical composition.
3. Lack of suitable substrates, preventing cell division and provoking a reduction of the total cell population ;
4. Competition between Rhodotorula and other microorganisms ;

The role of these factors may be checked experimentally.

The bacteriological investigations have clearly revealed that microorganisms may be introduced, mainly with the resins, in a simulated primary loop, where they remain alive and eventually develop as a function of time. All these microorganisms, in the presence of ^{3}H (mainly HTO), are probably capable of synthesizing tritiated organic molecules (OBT). This hypothesis was verified by culturing Rhodotorula cells in tritiated water (37000 Bq ml^{-1}) for 6 days and by analysing their tritium content by a microcombustion procedure. The results showed that tritium incorporation into the total organic matter of Rhodotorula increased linearly, as a function of time and of the HTO concentrations (0, 37, 370, 3700, 18500 and 37000 Bq ml^{-1}) in the culture medium. The maximal incorporation values observed ranged from 3400 to 5500 Bq g^{-1} dry matter.

In addition, the nature of the tritiated organic compounds synthesized by Rhodotorula cultures was investigated by analysing labeled (HTO) extracts by column chromatography. The chromatograms showed that most of the newly formed molecules had a relatively low molecular weight (< 10 kdaltons) (fig. 1).

In addition, parallel experiments, in which radioactive sodium bicarbonate ($NaH^{14}CO_3$) was used to label the culture, have revealed that an appreciable amount (up to 13 %) of organic matter is lost by Rhodotorula cells into the surrounding medium. However, the nature of the lost ^{14}C-labeled organic molecules was not determined. Consequently, when the ^{3}H-labeled cells die, at least part of their tritiated compounds enter the external medium.

In conclusion, indirect experimental evidence was obtained suggesting that both the purification resins and the contaminating microorganisms may be a source of tritiated organic molecules (OBT), which once released into the aquatic environment (liquid effluents) might be selectively incorporated by living organisms. It remains to be investigated whether some microorganisms can use the resins as a

substrate for their growth and thus provoke their degradation. This problem deserves further attention for its possible radioecological implications (formation of tritiated volatile compounds and leaching processes).

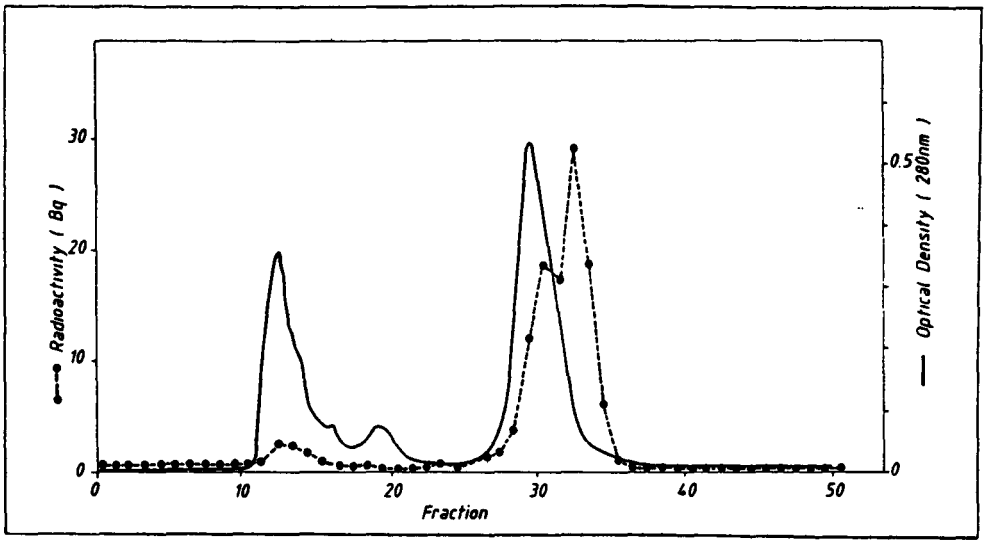

Fig. 1 : Column chromatography analysis of an extract of Rhodotorula cells supplied with HTO (37,000 Bq ml^{-1}) during 7 days, showing the presence of labeled organic molecules, which are separated into three peaks. Most of the newly synthesized compounds have a low molecular weight.

2. Dynamic models in soil-plant systems :

Tritium, dispersed into the environment from nuclear installations under two main chemical forms (elemental HT and tritiated water HTO), enters the biosphere and is incorporated into plants as tritiated water (HTO) and organically bound tritium (OBT). With respect to the consequences of ^{3}H releases on the human health, elementary tritium has generally been considered as less critical than tritiated water. Early studies were therefore focused on the transfer of ^{3}H released as HTO. In the last years, however, as the behaviour of HTO appeared to be well documented, interest shifted to investigations on the risks associated to HT releases, particularly in relation with future fusion reactor development.

2.1. Experimental study of tritium incorporation by plants exposed to HT or HTO under field conditions.

The contamination by tritium of plant products of agricultural importance was compared after exposure to elementary tritium or to tritium oxide (water vapour). Maize, potatoes and rye-grass grown under field conditions were exposed under plastic greenhouses to HT or HTO vapour during 4 h. HTO and OBT levels were measured in different tissues of the plants at various time interval up to 20 d after exposure. Core samples of bare soils were also collected and analysed for their HTO content in different layers.
The results obtained showed that HT diffuses deeper in the soil than HTO and is very efficiently oxidised into HTO that can later on be absorbed by the plant roots. The evolution pattern of HTO content in the various plant species was similar regardless of the tritium form provided : immediately after exposure, the HTO concentrations were higher than the OBT concentrations but fell more rapidly so that after 20 days, they decreased below the OBT levels. Leaves contained initially more HTO than stems but, with time, the ratio was reversed due to the contribution of the soil water activity.
After HTO exposure, OBT concentration in leaves of maize represented about 1/30 of the HTO concentration shortly after exposure ; it fell rapidly with a half-life in the order of 10 days. Stems contained initially less OBT than leaves but lost it more slowly. OBT concentration in potato leaves was initially higher compared to that of maize leaves but decreased with a shorter half-life than in the case of maize.
After HT exposure, OBT concentration in maize and potato leaves was about one fifth of that observed after exposure to an equal amount of tritium water vapour but changed very little with time. OBT concentration in potato stems and very markedly in tubers increased with time.

2.2. Study on the incorporation of tritium by plants exposed to HT under controlled conditions.

The question of whether plants only incorporate HTO produced by the oxidation of HT in the atmosphere or, more intensively, in soils or whether they are able to oxidise and metabolise HT by themselves was raised. To answer this question, different plant species, grown on nutrient solutions (in absence of any soil system), were exposed in a glove box to high HT concentrations (up to 40 MBq/l). Care was taken to avoid the presence of HTO as a contaminant in the HT gas injected by washing the tritiated gas with water prior to injection into the experimental system containing the plants (HTO concentration in the air was less than $5.\ 10^{-6}$ the concentration of HT). The rooting system of the plants was isolated from the atmosphere so that only the aerial parts were directly exposed to HT. The concentration and speciation of tritium in the confined atmosphere during exposure was continuously monitored by sampling the atmosphere of the glove box and discriminating between HT and HTO. The CO_2 concentration in the air was continuously monitored and periodically corrected in order to allow photosynthesis to proceed under physiological conditions. After exposure, the atmosphere of the glove box was replaced by uncontaminated air and the system was

open. The plants were removed from their nutrient solution, the roots were rinsed with water and the plants were put on a fresh nutrient solution. From that time, solutions and plants were sampled at regular intervals from 1 hour up to 21 days after the end of the exposure.
Immediately after exposure it was observed that most of the ^{3}H activity taken up by the plant was present as HTO ; less than 1% of the ^{3}H in the plant was present as OBT. The results also showed that the HTO content in the atmosphere of the glove box remained very low and could not explain the amount of ^{3}H incorporated by plants. HTO specific activities measured in the nutrient solution on which the plants were maintained during exposure were lower than those in the plant tissues. This observation demonstrate that HT is oxidised by the plant and suggests that an important fraction of the HTO produced is exudated by the roots into the nutrient solution.
One hour after exposure of maize plants, the HTO levels were higher in roots and stems than in leaves. In pea plants, the HTO concentrations measured in leaves and stem were comparable and up to 10 times higher than those in roots. This discrepancy between these two species can be explained by the existence in maize plants of gas conducting vessels, similar to those present in rice plants, that allow the diffusion of atmospheric gases up to the roots.
HTO concentrations in the various parts of the plants decreased rapidly with time due to transpiration of the plants. OBT in the plant organs increased to a maximum value in the hours following exposure as HTO is incorporated into organic molecules and decreased thereafter, mostly diluted by the growth of the plant. In pea plants, highest OBT activities were detected in the ^{3}H pods (storage organs).
Based on the total amount of ^{3}H in plants and nutrient solutions, the deposition velocity has been estimated to 0.5 and 1 10^{-6} m/s for pea and maize respectively, two orders of magnitude lower than the characteristics values obtained for soils.

In potato tubers exposed under the same conditions as maize and pea plants, the ratio between OBT (in Bq/g O.M.) and HTO (in Bq/ml) was of about 0.1 in each sample. Taking into account the proportions of tissue water and organic matter, OBT contributes to about 2% of the ^{3}H in the tuber. A gradient is observed for both HTO and OBT levels from the outer parts to the inner parts of the potatoes. By comparing the ^{3}H content in tubers exposed with or without epidermis (peeled or unpeeled), it was noticeable that the potato epidermis constitutes an important barrier to the diffusion of HT to the inner layers, but it is also obvious when comparing the potatoes parings exposed as so to the second parings of peeled potatoes and to the two successive parings of whole potatoes that oxidation of HT arises with a higher rate in the epidermis zone.

2.3. Transfer of ^{14}C to plants.

Beside the studies on the uptake of tritium by plants experiments were also conducted on the plant contamination by carbon-14.
In order to produce ^{14}C labelled forage for transfer experiments to ruminants, grass was exposed in October for 24 h to $^{14}CO_2$ (initial concentration of 2 kBq/l air) in a tightly closed plastic greenhouse. Absorption of total CO_2 was continuously monitored and stable CO_2 was

periodically injected into the greenhouse to compensate for photosynthesis. The concentration of ^{14}C in the plants immediately after exposure amounted to 10 kBq/g O.M. and decreased thereafter with a half-time of 47 d.
On another hand, the recycling to plants of ^{14}C incorporated into the soil as organic matter has also been investigated. ^{14}C labelled maize plants were composted or given to a cow. Compost and cow's faeces, sterilised or not, were incorporated into a soil on which various plant species were grown. Considering the transfer of ^{14}C from maize compost incorporated in soil, it was observed that the ^{14}C content depends on the plant species as well as on the organ considered : lettuce and cabbage show the highest transfer factors followed by potato, spinach and maize ; leaves are more contaminated than stems ; ^{14}C concentration in tuber, cob and grain is generally lower. The dilution factor shows that less than 5% of the carbon in the leaves originates from the soil and less than 2% of the tuber and grains is provided by the soil. Stems are intermediate. The total annual export of ^{14}C for each crop (taking into account the aerial part only) accounts for less than 1% of the soil activity. The transfer decreases from the first year to the third year. Transfer of ^{14}C from faeces incorporated into the soil is of the same order of magnitude than that obtained for compost. The presence of the ruminant digestive tract flora seems to enhance a little bit the transfer comparing sterilised and non sterilised faeces. Soil-to-plant transfer factors obtained with faeces and compost range from 2.7 to 5.10^{-3}.

2.4. Conclusion.

The data obtained indicate that environmental contaminations by HT releases may give rise to a substantial exposure of the populations through their food chains. The critical pathway appears to be the oxidation of HT in soils. HT gas, due to its high diffusibility, readily penetrates deeply into the soils and is converted very efficiently into HTO that is further taken up by plant roots. The easy penetration into the soil and the long retention after exposure to HT makes tritium available for longer period of time than after HTO exposure, leading to a longer lasting contamination. Direct oxidation of HT by the plants can be considered as negligible in regards of the oxidation processes in soils.
The incorporation of ^{14}C as CO_2 by the plants is much higher than that of ^{3}H as HT and HTO : at similar specific activity in the air incorporation of ^{14}C into plant organic matter is 300 times higher than for plants exposed to HTO (vapour) and 1200 times higher than in the case of HT.

3. Tritium and C-14 transfer in mammals :

In order to study the metabolism of organically bound tritium and ^{14}C in mammals both at the CEN/SCK, Mol and at the Landbouwhogeschool, Wageningen (Dr J. Van den Hoek), various contaminated food constituents were prepared at Mol. Contaminated plants have been obtained by growing rye-grass and potatoes on soils repeatedly sprayed with tritiated water or by exposing rye-grass and maize plants to $^{14}CO_2$ in plastic greenhouses. Tritiated algae were produced by growing these organisms in

nutrient solutions contaminated with HTO. Tritiated milk was obtained from cows given HTO in drinking water, milk was powdered and for some experiments separated into its main constituents.

3.1. Transfer of OBT to pig and progeny

The metabolism of OBT and transfer of ^{3}H to the progeny has been studied in a pregnant sow given for 84 d before delivery and 42 d during the lactation period a tritiated diet consisting in 41% milk powder (636 Bq/g), 2.3% dried algal hydrolysate (3087 Bq/g), 51% dried potato powder (481 Bq/g) and 5.7% minerals. As pregnancy progressed and during lactation, the amount of food had to be increased correspondingly (1.86 kg/d from -84 to -63 d before delivery, 2.06 kg/d until -38 d, 2.31 kg/d until -5 d, 3.01 kg/d until day 15 of lactation and 3.66 kg/d until day 41). In order to learn how much activity was transferred in utero or during the lactation period and how this activity was retained subsequently, 3 non-contaminated piglets from a control sow were transferred to the radioactive sow 3 days after delivery, 2 contaminated piglets were placed with the non-radioactive sow and 3 contaminated piglets were left with their contaminated dam. Shortly after birth and 24 d later, at weaning and some time after terminating radioactive feeding, piglets were sacrificed, and OBT and tissue free water tritium (TFWT) activity were determined in different tissues. Measurements were also taken in urine and faeces.

OBT activity (Bq/g OM) measured in tissue from the newborn was about once to twice that in the administered food and five times higher than the tritium oxide (Bq/ml) in tissues. OBT activity was highest in erythrocytes, heart and kidneys, and relatively lower in bone, liver and muscle (table 1). When piglets were maintained with their contaminated dam until weaning, the activity levels did not change markedly, except for an increase in liver, muscles and bones. Piglets born from a control sow and placed with a contaminated one during lactation attained about the same activity levels than those born from a contaminated sow and maintained with their dam until weaning ; this is not surprising considering the fact that almost 90% of the body weight at weaning is gained during the lactation period.

Following removal from radioactive contamination, activity levels in piglet tissues decreased due to metabolic excretion and dilution by growth. This occurs more rapidly for tissue free water tritium, with a biological half-time of 5 d in the new born and of 10 d in the weaned piglets (calculated from urine and tissue data) than for OBT. Loss of activity is more rapid in animals removed from tritium diet at birth than in those removed at weaning which display a slower relative growth rate. If changes in weight are taken into account, parenchymal organs, such as kidneys and liver, lose activity shortly after weaning at a half-time of about 10-20 d and later more slowly at a half-time of 20-50 d. Skin and muscles OBT has a half-time of 100 d and more. In nearly all tissues a second compartment of longer half-time (20 to 60 % of the total OBT pool) appears to be present but the too small number of animals available did not allow a reliable estimate.

OBT DURING	PREGNANCY			PREGNANCY + LACTATION				LACTATION		
AGE	1	24	42	1	40	61	145	43	64	148
Erythrocyte	1307	286	152	1307	1342	530	54	1220	442	43
Liver	626	73	21	626	1036	209	20	798	105	29
Kidneys	1178	102	33	1178	1201	265	25	982	179	37
Muscles	641	135	69	641	1040	668	69	791	342	81
Heart	1200	152	58	1200	1090	419	42	1045	290	45
Skin	840	98	27	840	845	463	80	842	342	104
Bone	634	111	67	634	844	278	23	937	305	43
Brain	924	351	188	924	935	574	127	744	363	100
HTO	195	nd	nd	195	270	3	nd	236	13	nd

Table 1: Specific activity (Bq/g per 10^3 Bq/g food) in organic matter and tissue free water of different organs of piglets from the various groups sacrificed at different ages. nd = not detected.

3.2. Transfer of different, specific chemical forms of OBT to rat.

Tritiated milk obtained from a lactating cow given HTO over a period of 30 d has been skimmed and the skimmed milk was powdered. Casein and lactose were separated from tritiated and uncontaminated skimmed milk powder. Tritiated fat has been separated from tritiated milk cream. Commercial butter will be used as uncontaminated fat. Each of the tritiated constituents (10% in weight of the mixed feed) together with the two uncontaminated others has been mixed with a standard food. This food was fed to rats (during 33 d to non-pregnant females and up to the end of lactation -during 57 d- in pregnant ones) in order to study the uptake, distribution and retention of tritium from proteins, sugars or fat of pregnant and non pregnant adult rats. Thereafter, excretion of ^3H and retention in various organs was followed over a period of 63 d after the end of the contamination.
The excretion pattern of ^3H in urine from non-pregnant rats and rats contaminated during pregnancy and lactation were comparable regardless of the source of OBT in food. The half-time of ^3H in urine was estimated at about 5 d for all treatments. The retention in the organs of adult rats has been estimated on the base of the OBT content in selected organs. In muscles, one compartment could be estimated : its half-time ranged from 36 to 44 d in rats contaminated during pregnancy and lactation and appeared to be slightly shorter in non-pregnant animals (23 to 29 d). For both groups of rats, the elimination half-time was highest after feeding with tritiated lactose. Tritium labelled lactose also was responsible of a longer retention of OBT in liver (most probably due to the glycogen metabolism) than tritiated fat and proteins. No significant differences between the various treatments were noticed regarding the retention of OBT in kidneys (half-time ranging from 11 to 24 d). The distribution between the various organs of the incorporated OBT was deeply affected by the nature of the tritiated precursor in food. Highest OBT activities (Bq/g O.M.) in organs of rats fed tritiated casein were found in liver, kidneys, blood, heart, spleen and lung and were equal or slightly lower to that in the food ; that of

fat was 10 times lower. After feeding tritiated lactose, the highest specific activity was found in liver (0.5 times that of food) ; in heart, spleen, kidney and muscles, it ranged from 10 to 20% of the specific activity in food and was even lower in fat. On the contrary, highest specific activity was found in fat after administration of tritiated milk fat, confirming that tritium labelled lipids undergo little dilution when they are converted into body lipids.

3.3. Transfer of organic ^{14}C to cow's milk.

Transfer of ^{14}C biologically incorporated in plant material (maize) to a lactating cow was also investigated. This experiment has been conducted at Mol in close collaboration with Dr J. Van Den Hoek from the Landbouwhogeschool in Wageningen (14-C determination in milk and its constituents). 53% of the administered activity (3900 Bq/day during 33 days) was excreted with the faeces, urine accounted for 2% and milk for 10% ; the remaining being incorporated in the animal body. Taking into account the weight of the animal and the total weight of milk production (13% dry matter) and its specific gravity (1.030 kg/l) it can be concluded that the milk production has priority in the body metabolism. An equilibrium is reached six days after the start of administration. The transfer coefficient for ^{14}C incorporated in maize to milk is estimated at $4.5\ 10^{-3}$ day/l. This value is 3 times lower than that previously obtained for ^{3}H given as OBT in food, but in the case of ^{14}C, all the radioactivity is present as organically bound carbon.

3.4. Conclusion.

The data presented here, together with other previously obtained, demonstrate that OBT given in food is more readily incorporated into tissue OBT than ^{3}H given as HTO. Moreover the distribution of the OBT in the body depends on the nature of the precursor in the feed : tritiated lipids are incorporated with practically no dilution in the fat while tritium from labelled proteins tends to accumulates into liver, kidneys, heart and other organs exhibiting high metabolic activities, and contaminated lactose gives rise to highest OBT content in liver. Estimates of the total tissue dose after OBT feeding indicate that after OBT feeding, OBT contributes about 5-10 times more to this dose than TFWT. However, at equilibrium, compared to the estimated dose delivered under conditions in which contamination arise from HTO in drinking water, the dose from OBT in food was only about 40 to 50% . Thus, under realistic conditions of water and OBT food intake, the total dose would probably not exceed more than 1.5 times that from HTO only. These calculations are not very meaningful with regard to possible biological damage. Most likely, the bulk of long-lived OBT is associated to relatively radioresistant tissues with low cell division rate such as bone, skin, muscles or brain and/or at extracellular locations (connective tissue, myeline, organic bone matrix) from where the low energy beta cannot irradiate cell nuclei ; although, some tissues might be at a risk if the tritium is close to radiosensitive sites (^{3}H associated with DNA in tissues with high cell proliferation).
The transfer of plant bioincorporated ^{14}C to cow's milk is 3 times lower than the transfer of OBT, but while an important fraction (80 to 90% of the total milk activity) of ^{3}H after OBT feeding in milk water, all ^{14}C

is present as organic molecules which will be transferred easily in the next links of the food chain. Moreover the physical half-life of ^{14}C is longer than that of ^{3}H and its beta particles are about 10 times more energetic than those of ^{3}H. Although the amounts of ^{14}C released from the applications of nuclear energy are much lower than those of ^{3}H, the above conclusions allow to consider ^{14}C as a potential hazard for human health.

IV. Other research group(s) collaborating actively on this project [name(s) and address(es)]:

Laboratorium voor Dieren Fysiologie, Landbouwhogeschool, Wageningen.
SERE-IPSN-DPS, CEA Fontenay-aux-Roses
Niedersäschsisches Institut für Radioökologie, Hannover
Institut für Radioagronomie, KFA Jülich
Zentralabt. Sicherheit, Radioökologie, KFK Karslruhe
Laboratoire de radioécologie, ULg Liège.

V. Publications:

Van Den Hoek J., Ten Have H.M.J., Gerber G.B., Kirchmann R., The transfer of tritium labeled organic material from grass into cow's milk, Radiation Research 103 : 105-113 (1985).

Bonotto S., Arapis G., Bosson M.C., Bossus A., Gerber G.B., Kirchmann R., Koch G., Nuyts G., Tritium distribution in marine and freshwater mussels fed with labelled microalgae, in Seminar on the Behaviour of Radionuclides in Estuaries, C.E.C., XII/380/85-EN, Luxembourg, pp. 267-286 (1985).

Kirchmann R., Gerber G.B., Fagniart E., Van Bruwaene R., Van Den Hoek J., Comparative studies on food chain pathways for tritium transfer to man following accidental exposure to tritium oxide, Proc. Int. Symp. on Emergency planning and preparedness for Nuclear facilities, Roma (Italy), November 4-8, 1985, IAEA-SM-280/35 p, IAEA STI PUB 701, 345-348, 1986.

Van Den Hoek J., Gerber G.B. and Kirchmann R., Similarities and differences in transfer of tritium and carbon-14 along the food chain, Proc. Int. Symp. on Emergency planning and preparedness for Nuclear facilities, Roma (Italy), November 4-8, 1985, IAEA-SM-280/61 p, IAEA STI PUB 701, 361-362, 1986.

Kirchmann R., Meurice-Bourdon M., Fagniart E., Binet J. and Bonotto S., Purification resins in reactor circuits as source for organic tritium, in Environmental and Human Risks of Tritium (G. Gerber, C. Myttenaere, H. Smith, Eds.), Radiation Protection Dosimetry, 16 (1-2) : 45-48, 1986.

Rocco P. and Kirchmann R., Source terms of tritium, in Environmental and Human Risks of Tritium (G. Gerber, C. Myttenaere and H. Smith, Eds., Radiation Protection Dosimetry, 16 (1-2) : 49, 1986.

Kirchmann R., Gerber G.B., Fagniart E., Vandecasteele C.M. and Van Hees M., Accidental release of elemental tritium gas and tritium oxide : models and in situ experiments on various plant species, in Environmental and Human Risks of Tritium (G. Gerber, C. Myttenaere and H. Smith, Eds., Radiation Protection Dosimetry, 16 (1-2) : 107-110, 1986.

Van Hees M., Gerber G.B., Kirchmann R., Vankerkom J. and Van Bruwaene R., Retention in young pigs of organically bound tritium given during pregnancy and lactation, in Environmental and Human Risks of Tritium (G. Gerber, C. Myttenaere and H. Smith, Eds., Radiation Protection Dosimetry, 16 (1-2) : 123-126, 1986.

Fagniart E., Van Hees M. and Kirchmann R., Study on the persistance of ^{14}C in an agricultural ecosystem ESNA XVIIth Annual Meeting, Hannover, September 14-19, 1986.

Kirchmann R., Study on the persistance of ^{14}C in an agricultural ecosystem. Progress Report IAEA coordinated Research Programme on "Carbon-14 from Nuclear Facilities" third meeting, San Carlos de Bariloche, November 24-28, 1986.

Vandecasteele C.M., Th Zeevaert and R. Kirchmann, Factors influencing the transfer of radionuclides in agricultural food chains, 3rd Int. Conf. on Anticarcinogenesis and Radiation Protection (3-ICARP), Dubrovnic, October 15-21, 1989, to be published.

RADIATION PROTECTION PROGRAMME
Final Report

Contractor:

Landbouwhogeschool
Agricultural University
Salverdaplein 10
NL- 6709 PJ Wageningen

Contract no.: BI6-B-051-NL

Head(s) of research team(s) [name(s) and address(es)]:

Dr. J. van den Hoek
Dept. Dierfysiologie
Landbouwhogeschool
Haarweg 10
NL- 6709 PJ Wageningen

Telephone number: 83703/83025

Title of the research contract:

Dynamic environmental cycling of HTO/HT/OBT. Experimental studies and modelling. Incorporation and metabolism of OBT, HT and Carbon 14 in mammals.

List of projects:

1. Dynamic environmental cycling of HTO/HT/OBT. Experimental studies and modelling. Incorporation and metabolism of OBT, HT and Carbon-14 in mammals.

Title of the project no.:

Dynamic environmental cycling of HTO/HT/OBT. Experimental studies and modelling. Incorporation and metabolism of OBT, HT and Carbon-14 in mammals.

Head(s) of project:

Dr. J. van den Hoek

Scientific staff:

Dr. J. van den Hoek, Ir. J.T.M. Koumans,
M.H.J. van den Hoek-ten Have, T.C. Viets, D. Vink

I. Objectives of the project:

Organically bound tritium (OBT) in foodstuffs may be incorporated directly into organic compounds of various organs and tissues of animals and man. The fraction of OBT which is incorporated, the residence time of the tritiated organic compounds and their location are important parameters for the determination of the radiation hazard of environmental tritium to man. It is an important objective of this project to obtain quantitative data for these parameters which are to be used in the model, developed to describe the kinetics of tritium in the human body. The extent of metabolization of tritium gaz (HT) will be investigated by direct introduction of HT into the animals. Also, the long-term behaviour of Carbon-14 will be studied in animals.

II. Objectives for the reporting period:

The metabolism of a tritiated protein (casein) was compared with that of the same protein labelled with C-14. This was done by introducing these labelled compounds directly into the abomasum of the lactating goat, and by determination of the tritium and carbon-14 content into newly synthesized organic milk components (milk casein and milk fat). These two substances may be considered representative of newly synthesized proteins and fats elsewhere in the body. Since the abomasum of the ruminant is quite comparable to the stomach of monogastric animals, the results observed in this experiment may be considered to reflect the situation in monogastric animals.

III. Progress achieved:

1. Methodology

Organically bound tritium (OBT) in the feed of cows and minigoats was obtained by spraying young growing grass with THO. After drying in order to evacuate THO completely, the resulting hay was fed to the experimental animals which had been equipped with fistules in either rumen or abomasum (4th stomach) or in both. The tritiated feed was administered daily in doses of about 9.5 μCi (351 kBq) for varying periods of time, e.g. during the entire pregnancy period of about 150 days and/or during the lactation period (80-220 days). After removal of the young, milk samples were taken daily at first and at regular intervals later. In a few cases, sampling was continued in two or three successive lactation periods. In another series of experiments, the young animals were left with their mothers after birth during the lactation period. OBT administration was discontinued at weaning, and animals were sacrificed at 0,7,21,48, 92,115,155,205,240,276 and 280 days.

Carbon-14 was incorporated into growing corn plants by exposing them to $^{14}CO_2$ for 8 hours. After harvest of the full-grown plants, the corn was cut, thoroughly mixed and fed to a lactating cow for a period of 33 days. The average daily activity ingested was about 105.6 μCi (391 kBq).

Tritium and carbon-14 levels were determined in organic milk constituents (milk casein, milk fat and milk sugar or lactose), in milk water and in organs and tissues of young animals by combustion of samples and subsequent liquid scintillation counting.

Casein, labelled with tritium or carbon-14 was obtained from milk of cows which had been given feed in which the organic fraction had been labelled with tritium or carbon-14. The casein was separated from the milk by conventional methods, freeze-dried and introduced directly into the abomasum of a lactating goat through a fistule. Milk samples of the animal were taken daily and processed as described above.

2. Results

The results are shown in Figure 1 and Tables 1-3.
Figure 1 shows tritium levels in various milk constituents of one of the goats during 190 days of lactation following 160 days of OBT feeding during pregnancy and during 10 days of lactation. Results of other animals are very similar to those presented in Figure 1.
Table 1 shows the decrease of tritium activity in some organic milk constituents from two goats and a cow, expressed as biological half-life values. These were obtained by carrying out non-linear regression analysis on tritium levels in organic milk components after cessation of tritium administration.
Table 2 shows the decrease of tritium activity in organs and tissues of young growing goats, expressed also as biological half-life values. The mothers of these animals were given daily organically bound tritium as hay during pregnancy and during about three months of lactation untill weaning of the young. Correction was made for the tritium dilution in organs and tissues as a result of new growth.
Table 3 shows the average carbon-14 levels in casein, milk fat and lactose during the period when plateau levels in milk were reached, e.g. day 6-day 33. As one would expect, these plateau levels in organic milk constituents were reached quite rapidly, and they showed a similar rapid decrease when the administration of carbon-14 labelled corn to the cow was discontinued. Pools of slow turnover became visible after a few weeks.

3. Discussion

The results presented in Figure 1 show that OBT from foodstuffs is incorporated directly into newly synthesized fat (milk fat) and milk protein (casein), and to a much lesser extent, in milk carbohydrates (lactose) during OBT feeding. A considerable fraction of ingested OBT is used for metabolic oxydation as reflected by the presence of tritium in body water. The relatively low incorporation of tritium in

newly synthesized carbohydrates as reflected by the low tritium values in lactose are probably typical for ruminant animals. During the fermentation processes of the feed in the forestomachs, digestible carbohydrates are almost completely broken down. It may be expected that higher levels of tritium will be found in newly synthesized carbohydrates in monogastric animals under similar experimental conditions as a result of the different digestion of carbohydrates in these animals. However, the synthesis of tritiated carbohydrates is likely to be of minor radiological importance.
As shown in Figure 1, tritium is incorporated continuously in casein and in milk fat after cessation of the administration of OBT to the lactating goat. The source of this ^{3}H is located probably in certain body deposits some of which turn over quite slowly. This is illustrated in Table 1. The biological half-life values for the slow components of casein and milk fat vary from 73 to 123 days in a cow and two goats. The agreement is quite remarkable, particularly because the cow received OBT for 28 days only. The values shown are probably averages of various pools with different turnovers. Pools with still longer half-lives probably exist. They may have a particular interest from a radiobiological standpoint.
Determination of tritium levels in various tissues of young and adult animals indicate that important OBT deposits are located in body fat and in muscular tissue. Analysis by column-chromatography has shown that, at steady state, more than 96% of bodyfat deposits consisted of tritiated triglycerides. After about one year, tritium levels of body fat of adult animals decreased to 29% of the levels at steady state, and to about 20% in muscular tissue.

Table 2 shows the decrease of OBT in young growing goats which had received OBT during pregnancy and during about three months of lactation via the mother. OBT administration was stopped at weaning.
Two animals were killed at weaning (t=0). The average tri-

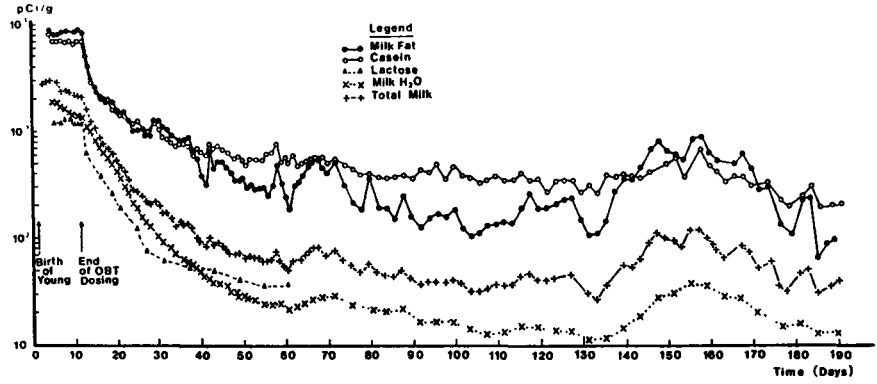

Fig 1: Tritium levels in various milk constituents and in whole milk of a miniature goat during a 190 day lactation period following 150 days of feeding of OBT.

	$T^{1/2}$ of Component (days)								
	1st			2nd			3rd		
	G44	G47	Cow	G44	G47	Cow	G44	G47	Cow
Casein	0.57±0.06	1.4±0.33	1.5±0.06	5.3±0.42	7.3±1.7	10.2±0.40	86.6± 8.3	122.7±62.4	82.0±2.3
Milk Fat	0.76±0.28	2.2±0.45	1.6±0.03	5.5±1.4	8.3±2.8	7.6±0.40	74.8±15.3	72.8±41.6	88.0±5.3
Lactose	4.9 ±1.4	–	5.1±0.11	32.6±6.9	–	34.4±4.4	–	–	–
Milk H_2O	4.2 ±0.07	5.7±0.10	5.0±0.03	39.5±12.7	–	–	76.2	214.8±97.0	67.7±8.0
Total Milk	1.7 ±0.21	3.0±1.3	1.6±0.12	8.3±0.7	6.4±1.1	5.1±0.12	69.3	173.3±83.2	68.0±3.5

Table 1: Biological half-life values for some milk components and whole milk in a lactating cow and two miniature goats (G44, G47).

tium levels in about 30 organs and tissues amounted to 5.05 πCi (187 Bq) and 4.80 πCi (178 Bq) per gram of dry matter respectively with a standard deviation of about 17%. Several fat tissues such as omentum, subcutaneous tissue and kidney fat, showed rather high levels, reflecting the high tritium content of milk fat during lactation. Generally speaking, a rather homogeneous tritiation of the body had occurred, amounting to about 0.05% of the daily dose per gram of dry tissue.

Since organs usually consist of several types of tissues, the half-life values given in Table 2, must be considered as averages. As shown in Table 2, the decrease of tritium in the organic material of some organs and tissues could be described more satisfactorily by two components than in others. The fast components in thymus, lymph glands, small intestine, testis, liver and kidney reflect the rapid turnover of organic material either as cells or as a result of metabolic cellular activity. These fast components also have the larger pool sizes. Intermediate half-life values are found in the various stomachs and the uterus. OBT, incorporated in heart muscle turns over more rapidly than that in skeletal muscle. The smooth involuntary muscle of the urinary bladder shows a still slower turnover of its organically bound tritium. It is interesting to see that the turnover in various body fat tissues is not the same. OBT decreases with a half-life of about 55 days in kidney fat, omentum and bone marrow, but nearly twice as slow in the fatty pad of mammary tissue.

The carbon-14 activity levels in Table 3 are expressed as concentration levels and as specific activities. The much higher ^{14}C levels in milk fat reflect the higher carbon content of fat as compared to that in casein and lactose. The specific activity (S.A.) value for lactose is rather high as compared to those in casein and lactose.

The transfer of carbon-14 from feed to cow's milk, expressed as the percentage of daily ingested carbon-14 which is secreted in one litre of milk, was as follows: 0.13% for casein,

Organ	$T_{\frac{1}{2}}$ (days)	Organ	$T_{\frac{1}{2}}$ (days)
Thymus	6 – 61	Rumen	122
Lymph gland	8 – 75	Omasum	160
Small intestine	10 – 107	Abomasum	111
Testis	12 – 279	Skeletal muscle	128
Liver	14 – 81	Heart muscle	80
Kidney	14 – 105	Uterus	106
Large intestine	15 – 137	Kidney fat	53
Lung	20 – 164	Omentum	54
Urinary bladder	21 – 518	Bone marrow	55
Brain	35 – 472	Subcutaneous tissue	78
Spleen	71	Mesentary tissue	84
Pancreas	91	Mammary fat	93
Lig. Nuchae	2711	Plasma	12
		Serum	12

Table 2: Turnover of OBT in various organs and tissues of youny growing goats, expressed as biological half lives of tritium.

	Carbon-14 Levels	
	pCi/g	S.A.
Casein	4076	7745
Milk Fat	6333	8423
Lactose	4185	9960

Table 3. Carbon-14 levels in casein, milk fat and lactose in cow's milk after continuous ingestion of carbon-14 labelled corn. The data are averages for the period of apparent steady state conditions (day 6 - day 33).

0.24% for milk fat and 0.18% for lactose.
Carbon-14 was being incorporated into casein and milk fat for at least one year after cessation of dosing. The levels in milk fat showed fairly large variatons, and an increased rate of mobilization of carbon-14 containing milk fat precursors from body reserves could be seen to occur regularly. It was particularly evident during the first six weeks of lactation after the birth of the calf. The carbon-14 levels in casein were decreasing much more regularly.
The results of regression analysis showed carbon-14 levels in organic milk constituents to decrease with two components. The half-life values for the first and rapid component were about 13 hours for lactose and about 24 hours for milk fat and casein. The long component had a half-life of about 100 days for casein and milk fat, and it was quite insignificant quantitatively for lactose. It can be concluded that only carbon-14 retention in protein and fat in the body merits attention from a radiobiological point of view.

In the final series of experiments, tritiated casein and casein labelled with carbon-14 were administered twice daily into the abomasum of a lactating goat. The tritium and carbon-14 levels in newly synthesized casein and fat from the milk of the goat reached plateau levels in a few days. After the administration of the labelled casein was discontinued, the decrease of tritium and carbon-14 activities in newly formed milk casein and milk fat was very fast and amounted to more than 50% within 24 hours. The half-life values are 0.60 and 0.79 days for the decrease of carbon-14 activity in milk fat and casein. The values for tritium decrease are 0.79 and 0.82 days in the same two components respectively. About 17% of the administered carbon-14 and about 22% of the administered tritium could be recuperated from newly formed milk casein and milk fat. On the basis of these preliminary experiments, it can be concluded that the metabolic behaviour of OBT and carbon-14, administered into the mammalian stomach incorporated into a well digestible protein, did not show any qualitatively significant differences.

IV. Other research group(s) collaborating actively on this project [name(s) and address(es)]:

Dr. G.B. Gerber, C.E.C., rue de la Loi, Brussels, Belgium
Ir. R. Kirchmann, Drs. C. van de Casteele, E. Fagniart,
Department of Radiobiology, S.C.K.-C.E.N., Mol, Belgium.

V. Publications:

1. Publications in Scientific Journals, Monographs, ...

- The transfer of Tritium-Labeled Organic Material from Grass into Cow's Milk.
  J. van den Hoek, M.H.J. ten Have, G.B. Gerber and R. Kirchmann.
  Radiation Research, 103, 1985, 105-113

- Similarities and Differences in the Transfer of Tritium and Carbon-14 along the Foodchain.
  J. van den Hoek, G.B. Gerber and R. Kirchmann.
  Paper presented at the International Symposium on Emergency Planning and Preparedness for Nuclear Facilities. Rome, 4-8 November 1985.

- Tritium Metabolism in Animals
  J. van den Hoek.
  Invited Paper Workshop "Environmental and Human Risk of Tritium",
  Karlsruhe, February 17th-19th 1986.
  Radiation Protection Dosimetry, 16, 1986, 117-121.

- The cycling of H-3 and C-14 in the biosphere: similarities and differences
  J. van den Hoek, G.B. Gerber, R. Kirchmann
  Paper presented at the Seminar on "Cycling of long-lived Radionuclides in the Biosphere: Observations and Models", C.E.C.-J.E.N., Madrid, September 15th-19th 1986, Book of Abstracts B5.

- Some aspects of carbon-14 metabolism in the animal organism.
  J. van den Hoek
  Paper presented at the Third Meeting of the IAEA Coordinated Research Programme on "Carbon-14 from Nuclear Facilities", San Carlos de Bariloche, November 24th-28th 1986.

- The transfer of Radionuclides to Domestic Animals
  J. van den Hoek
  Invited Paper on the International Scientific Seminar on Foodstuffs Intervention Levels following a Nuclear Accident, Luxemburg, 27-30 April 1987, EUR 11232. 373-380.

- European research on the transfer of radionuclides to animals, a historic perspective.
  J. van den Hoek
  Invited paper presented at the Workshop on "The Transfer of Radionuclides to Livestock", 5-8 September 1988, University of Oxford, U.K.

RADIATION PROTECTION PROGRAMME
Final Report

Contractor:

Institut Royal des Sciences
Naturelles de Belgique, IRSNB
Rue Vautier 29
B-1040 Bruxelles

Contract no.: BI6-B-049-B

Head(s) of research team(s) [name(s) and address(es)]:

Dr. D. van der Ben
Département Biologie
IRSNB
Rue Vautier 29
B-1040 Bruxelles

Telephone number: 648.04.75 X286

Title of the research contract:

Behaviour of technetium in the marine benthic environment. Experimental studies and modelling.

List of projects:

1. Studies of the technetium behaviour in sediments, sea water and marine organisms and elaboration of a mathematical model allowing to simulate the behaviour of technetium in marine environment of the Belgian coast.

Title of the project no.: 1

Studies of the technetium behaviour in sediments, sea water and marine organisms and elaboration of a mathematical model allowing to simulate the behaviour of technetium in marine environment of the Belgian coast.

Head(s) of project:

Prof. Dick van der Ben
Département Biologie, I.R.S.N.B., rue Vautier 29, B-1040 Bruxelles

Scientific staff:

S. Bonotto and C. Hurtgen (C.E.N.-S.C.K.), J.-M. Bouquegneau and C. Dopagne (U.Lg.), F. Auvray, F. Capot, M. Cogneau, J.-P. Dehut, K. Fonsny and L. Pignolet (U.C.L.), Z. Moureau and S. Wartel (I.R.S.N.B.)

I. Objectives of the project:

The main objectives of this pluridisciplinary project were the following :

1. Determination of the uptake and distribution of technetium in coastal marine organisms, including microorganisms, algae, molluscs and fishes.
2. Study of the fixation of technetium by coastal sediments.
3. Evaluation of the exchange of technetium between sea water, sediments and selected marine organisms.
4. Study of the transfer of technetium through simple experimental food chains.
5. Modelling of the behaviour of technetium in the marine benthic environment, by using data from both field investigations and laboratory experiments.

INTRODUCTION

The radioactive artificial element technetium may enter the environment from five principal sources : nuclear weapon tests, nuclear power plants, nuclear fuel reprocessing facilities, nuclear waste storage and pharmaceutical and medical uses. A significant part of the produced technetium will ultimately reach the oceans, where it will be diluted into the very large water mass. However, before final dilution, technetium might attain in some particular places (e.g. near liquid effluents release points) concentration levels allowing biological uptake and accumulation. The concentration of Tc-99 (T1/2 = 2.1 x 10^5 years) found in the Irish Sea was comprised between 14.8 and 74 mBq l^{-1}, whereas lower activities (3-19.3 mBq l^{-1}) were measured in the Channel. In normally oxygenated sea water, technetium is present as the oxyanion pertechnetate TcO_4^-, which is stable. When the sea water has a pH of 8 and a redox potential of around 0 volts, the heptavalent (+7) TcO_4^- can be reduced to the tetravalent (+4) TcO_2, which is insoluble.
Because of its long half-life, high solubility and mobility and chemical toxicity, studies on the behaviour of technetium in terrestrial and aquatic ecosystems were carried out in several countries.
For the duration of the contract (1.07.1985-31.12.1989), the five particpating laboratories worked together in a co-ordinate way, by combining field investigations along the Belgian coast with laboratory experiments, in order to obtain a more complete insight of the behaviour of technetium in the main constituents (water, sediments and biota) of the marine benthic environment. In this final report, the most significant results are briefly reported together with the relevant publications.

MATERIALS AND METHODS

The various materials and methods employed in this project were described in the published papers, reported in the list of references. Some marine animals (molluscs) and plants (brown algae) were regularly collected at four places (Nieuwpoort, Oostende, Blankenberge and Zeebrugge) along the Belgian coast (Fig.1). Fishes (Solia vulgaris) were caught near Nieuwpoort and sediments were taken in the coastal area.
It is to note that an important part of the experimental work was made possible thanks to the production of Tc-95m (a gamma-emitting isotope with a half-life of 61.2 days) in the cyclotron of Louvain-la-Neuve, by irradiating a Mo-source.

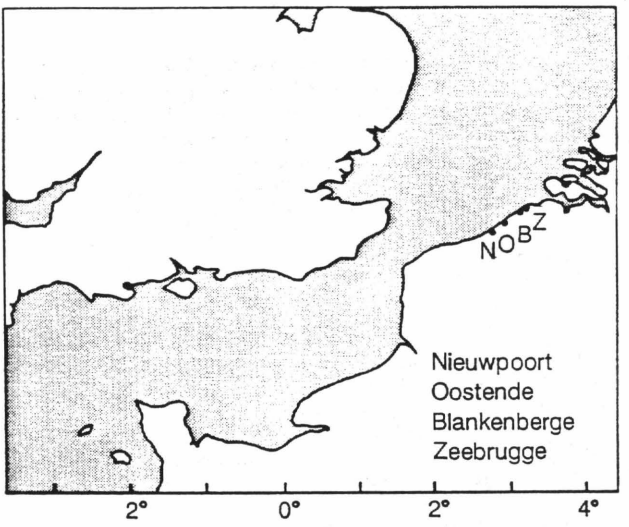

Fig.1.
Map of the area with the four places (Nieuwpoort, Oostende, Blankenberge and Zeebrugge) along the Belgian coast, where marine animals and plants were regularly collected.

RESULTS AND DISCUSSION

Sea water, sediments and microorganisms

It was found, by thin layer chromatography, that the predominant form of technetium in aerated sea water is TcO_4^-. Under reducing conditions, however, TcO_2 is formed.
Microorganisms play an important role in the fixation of technetium, both in the water column and in the sediments. Marine bacteria (Flavobacterium halmephilum, Moraxella sp., Planococcus sp. and a mixed population of anaerobes) from a coastal sediment were able to accumulate technetium, the concentration factors (CFs) being the highest during their stationary phase of growth. In the case of Planococcus, the CF attained the maximal value of 750 at low redox potential (Fig.2). A metabolic process seems responsible for Tc concentration by marine bacteria, in which it binds mainly to high molecular weight cellular constituents. Polysaccaride polymers, which were visualized with the scanning electron microscope (SEM) around the bacterial cells were suspected to bind technetium. However, direct experimental evidence in favour of this hypothesis could not yet be obtained.
Fixation of technetium occurred also in protozoa (Uronema marinum) and in microalgae, but their CFs were rather low.

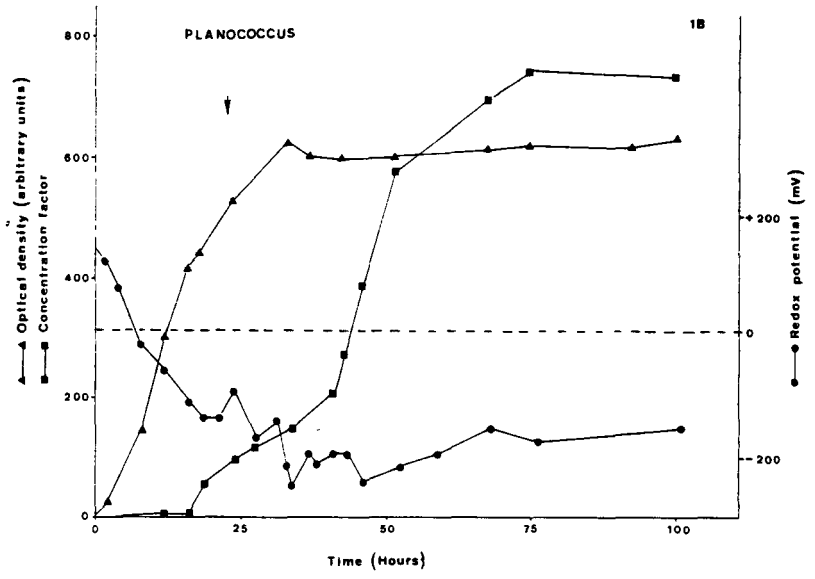

Fig.2.
Growth and concentration factor of technetium in the marine bacterium Planococcus sp., as a function of time and in relation to the redox potential. The arrow indicates the moment when aeration was stopped.

Algae

Radiochemical analyses have shown that the concentration of Tc-99 in the brown alga Fucus spiralis, growing along the Belgian coast, increased as a function of time (Fig.3), attaining CFs up to 5.1×10^4. This finding suggests that it may be used as a bioindicator for the level of radioactivity in the sea.
The mechanism of Tc-fixation by marine algae was investigated, under laboratory conditions, in the species Fucus serratus, F. spiralis and F. vesiculosus. Various experiments, under light, in darkness, at two different temperatures (4 and 20°C) and after heat-inactivation, suggested that the accumulation of technetium is a physiologically controlled process. This hypothesis is supported also by chromatographic analyses of algal extracts (F. serratus), in which the proportion of technetium bound to organic molecules was found to be higher under light than in darkness or at 4°C, and by autoradiography of whole plants labeled with Tc-95m.
The metabolism of technetium was studied in two marine green algae, Acetabularia acetabulum and Bryopsis hypnoides, which accumulate this radioelement. Column chromatography of labeled Acetabularia extracts showed that most of the technetium penetrated into the cells was bound to cellular compounds (Fig.4).

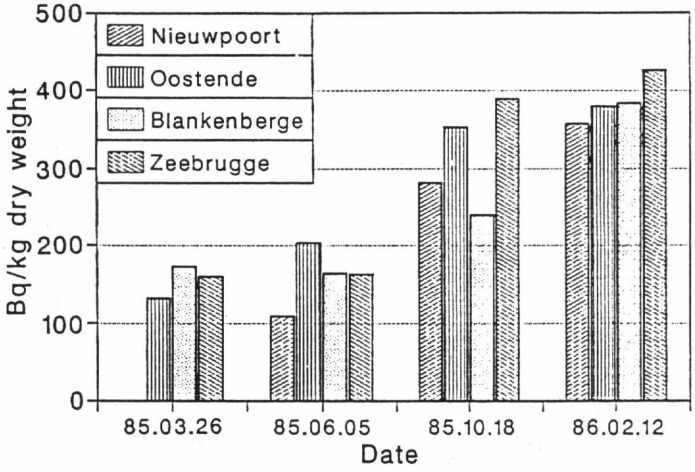

Fig.3.
Technetium-99 concentration in whole Fucus spiralis plants, collected at four places along the Belgian coast, as a function of time.

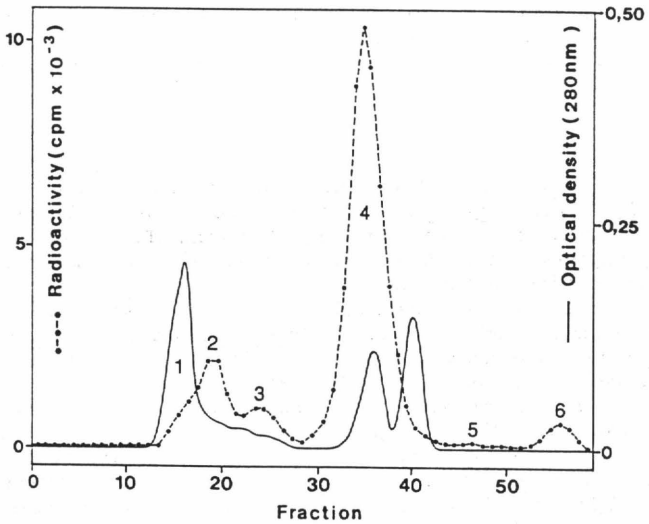

Fig.4.
Molecular sieving chromatography (Sephacryl S-200) of an extract (postmitochondrial supernatant) of Acetabularia, labeled during two weeks with Tc-95m. The numbers of the radioactive profile indicate respectively the binding of technetium to proteins (1, 2 and 3) and to low molecular weight organic molecules (4 and 5) and the presence of pertechnetate (6).

Mussels, food chains and modelling

Although the mussels show a low Tc-accumulation (CF for the whole animal < 3), they are of interest for at least three reasons : 1) they are filter-feeding marine animals, which collect indiscriminately radioactive and not radioactive particles, including different forms of micro-organisms (bacteria, protozoa and microalgae) ; 2) they are an important link in the marine food chain ; 3) they contribute significantly to the human diet, especially in the northern European countries. Radiochemical analyses of the soft parts of mussels (Mytilus edulis) regularly collected along the Belgian coast have shown that their technetium (Tc-99) content was low ($\leqslant$ 5 mBq g^{-1} dry).
When the mussels were supplied with Tc-95m (pertechnetate), the highest specific activity was found in their hepatopancreas. Extracts of this organ contained technetium bound to organic molecules (most probably proteins) as well as to pertechnetate (Fig.5.).

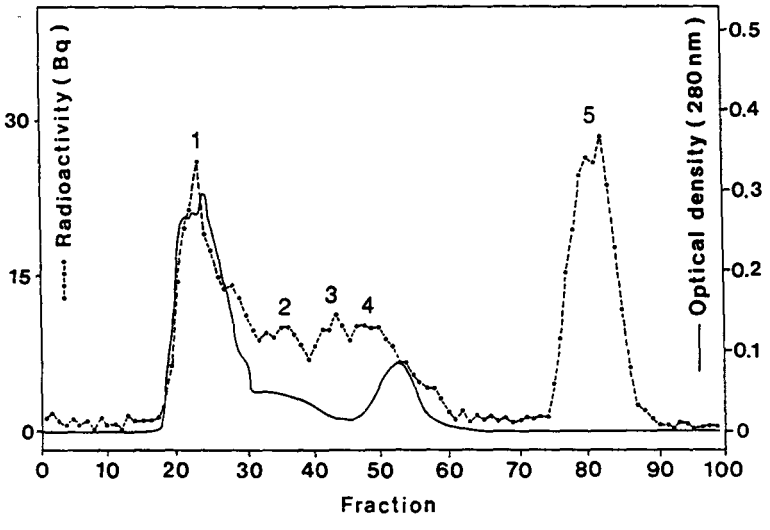

Fig.5.
Mytilus edulis : column chromatography (Sephacryl S-300) of an extract of hepatopancreas, showing the presence of Tc-95m bound to organic molecules (peaks 1, 2, 3 and 4) as well as to pertechnetate (peak 5).

In further work, in which, for modelling purposes, a simple experimental food chain (water-microalgae-molluscs) was employed, it was observed that technetium (Tc-99) uptake from contaminated food was much less important (8-20%) than from contaminated sea water (80-92%). Besides, the way in which Tc is eliminated by the mussels suggests the existence of two compartments : one (75% of the accumulated Tc), with a very short half-life of elimination (about one hour), and another with a half-life of about ten days. The energetic metabolism seems to have little influence on the contamination kinetics of the mussels.

In a second experimental food chain (water-sediment-mollusc-fish), several parameters were measured (water temperature, redox potential and concentrations of NH_4, NO_2 and NO_3) in order to elaborate a hydrodynamic model. After a treatment of 80 days, the CF of technetium in the mussels (whole animal) was of about 3, a value which confirms previous work. In the fish (Solia vulgaris), after 50 days, the following CFs were found : 3.5 (fish separated from the sediment by a net) ; 3.3 (fish in contact with the sediment) ; 4.8 (fish in contaminated water without sediment).

These results show that the presence of the sediment, for which a Kd of 100 was found (for the first cm), does not influence very much the CF of technetium in the fish. However, the sediment might constitute a reservoir, from which technetium may be lost under particular environmental conditions, thus becoming available to marine biota and entering the food chains. New research along this line would be worthy.

Publications:

S. BONOTTO, R. KIRCHMANN, J. VAN BAELEN, C. HURTGEN, M. COGNEAU, D. van der BEN, C. VERTHE and J.M. BOUQUEGNEAU
Behaviour of technetium in marine algae. In : Speciation of Fission and Activation Products in the Environment. R.A. Bulman and J.R. Cooper, eds., Elsevier, pp. 382-390 (1986).

B. MANIA, Z. MOUREAU, D. van der BEN, J. VAN BAELEN, C. VERTHE, J.M. BOUQUEGNEAU, M. COGNEAU, S. BONOTTO, C.M. VANDECASTEELE, L. PIGNOLET and C. MYTTENAERE
Technetium in marine micro-organisms. In : Technetium in the Environment, G. Desmet and C. Myttenaere, eds., Elsevier, pp. 229-244 (1986).

C. VERTHE, Z. MOUREAU, B. MANIA, J. VAN BAELEN, D. van der BEN, M. COGNEAU, C.M. VANDECASTEELE, J.M. BOUQUEGNEAU, C. MYTTENAERE and S. BONOTTO
Technetium in marine animals. In : Technetium in the Environment. G. Desmet and C. Myttenaere, eds., Elsevier, pp. 245-250 (1986).

S. BONOTTO, G. NUYTS, A. BOSSUS, F. CAPOT, M. COGNEAU and D. van der BEN
Autoradiographic localization of Tc-95m fixed under laboratory conditions by three macroalgae of the Belgian coast : Fucus spiralis, Porphyra sp. and Ulva lactuca. Rapp. Comm. int. Mer Médit., 30, 214 (1986).

F. CAPOT, A. BOSSUS, G. NUYTS, M. COGNEAU, D. van der BEN and S. BONOTTO
Labile binding of Tc-95m to proteins in the giant unicellular alga Acetabularia actabulum. Rapp. Comm. int. Mer Médit., 30, 215 (1986).

G. ARAPIS, S. BONOTTO, A. BOSSUS, G. NUYTS, G.B. GERBER, R. KIRCHMANN, J. COLARD, P. MATHOT and M. COGNEAU
Tritium and technetium uptake and distribution in three marine algae. Fourth International Ocean Disposal Symposium, Plymouth, England, 11-15 April 1983. In : Ocean Processes in Marine Pollution. Vol. 1 J.M. Capuzzo and D.R. Kester, eds., Robert E. Krieger Publ. Co, Malabar, Florida, pp. 133-144 (1987).

S. BONOTTO, D. van der BEN, F. CAPOT, J.M. BOUQUEGNEAU and M. COGNEAU
Technetium in coastal environments : Field observations and laboratory experiments. In : Metals in Coastal Environments of Latin America, U. Seeliger, L.D. de Lacerda and S.R. Patchineelam, eds., Springer-Verlag, Berlin, pp. 222-236 (1988).

S. BONOTTO, V. ROBBRECHT, G. NUYTS, M. COGNEAU and D. van der BEN
Uptake of technetium by marine algae. 1. Autoradiographic localization. Mar. Pollut. Bull., 19, 61-65 (1988).

S. BONOTTO and D. van der BEN
Uptake, distribution, metabolism and biological effects of technetium in marine algae. Giorn. Bot. Ital., 122, Suppl. 1, 132 (1988).

S. BONOTTO, H. FLOROU, M. COGNEAU, G. NUYTS, A. BOSSUS, V. ROBBRECHT and D. van der BEN
Factors affecting the uptake of ^{95m}Tc by the brown alga Fucus serratus. Arch. Int. Physiol. Biochim., 96, pp. 34 (1988).

S. BONOTTO, C. HURTGEN, D. van der BEN, J.M. BOUQUEGNEAU and M. COGNEAU
Study of the contamination of the Belgian coast by technetium. In : Environmental Contamination, A.A. Orio ed., CEP Consultants Ltd., Edinburgh, pp. 64-66 (1988).

H. FLOROU, M. COGNEAU, Z. MOUREAU, V. ROBBRECHT, D. van der BEN and S. BONOTTO
Incorporation of Tc-95m in the brown macroalgae Fucus serratus and Fucus spiralis under different experimental conditions. XXXIst Congress of I.C.S.E.M., Athens, 17-22 October, 1988. Rapp. Comm. int. Mer Médit., 31, 247 (1988).

C. HURTGEN, G. KOCH, D. van der BEN and S. BONOTTO
The determination of technetium-99 in the brown marine alga Fucus spiralis collected along the Belgian coast. The Science of the Total Environment, 70, 131-149 (1988).

M. LICOT, J.-M. BOUQUEGNEAU and C. DOPAGNE
Accumulation of technetium by Phaedactylum tricornutum BOHLIN in culture. Océanics, 14, 525-531 (1988).

D. van der BEN, M. COGNEAU, V. ROBBRECHT, G. NUYTS, A. BOSSUS, C. HURTGEN and S. BONOTTO
Uptake of technetium by marine algae. Report of the Marine Radioecology (MARECO) Working Group Meeting at Brugge, Belgium, June 13, 1989, International Union of Radioecologists (IUR), pp. 92-106 (1989).

L. PIGNOLET, F. AUVRAY, K. FONSNY, F. CAPOT and Z. MOUREAU
Role of various microorganisms on Tc behaviour in sediments. Health Physics, 57, 791-800, 1989.

D. van der BEN, M. COGNEAU, V. ROBBRECHT, G. NUYTS, A. BOSSUS, C. HURTGEN and S. BONOTTO
Factors influencing the uptake of technetium by the brown alga Fucus serratus. Mar. Pollut. Bull. (in press).

RADIATION PROTECTION PROGRAMME
Final Report

Contractor:

Studiecentrum voor
Kernenergie, SCK/CEN
Rue Charles Lemaire, 1
B-1160 Bruxelles

Contract no.: BI6-B-050-B

Head(s) of research team(s) [name(s) and address(es)]:

Prof. O. Vanderborght
Radionuclide Metabolism Section
SCK/CEN
Boeretang 200
B-2400 Mol

Telephone number: 014/31.18.01

Title of the research contract:

Bioavailability of transuranium nuclides in aquatic environments.

List of projects:

1. Biological availability of transuranics in aquatic ecosystems.
2. Speciation of transuranics in aquatic environments.

Title of the project no.: 1

Biological availability of transuranics in aquatic ecosystems : MICROBIAL ACTIVITY IN SEDIMENTS INFLUENCING MODERATELY BIOLOGICAL AVAILABILITY AND Kd OF 241-Am AND 244-Cm

Head(s) of project:

S. Van Puymbroeck, O. Vanderborght

Scientific staff:

I. Objectives of the project:

This project aims to identify the routes and kinetics of uptake of transuranics (americium and curium) in freshwater animals. The uptake and storage of curium and americium in various freshwater animals will be assessed. The role of the hepatopancreas in crustaceans (esp. Astacus leptodactylus) for uptake and storage will be studied, together with the subcellular distribution in target organs. Furthermore, the uptake process of both americium and curium via the gills in freshwater fish (e.g. Salmo gairdneri) will be studied. The project further aims to study the mode and kinetics of excretion of incorporated forms through the excretory system of the animals. In this way determination of turn-over rates will become possible.

II. Objectives for the reporting period:

Experiments with 241-Am and 244-Cm were set up to evaluate the difference in adsorption (= Kd) of these elements on sediments in the presence or absence of microorganisms (2,3,4,6). The potential role of microbial activity on the change in bioavailability of these transuranics for two indicator species was also examined.
Kd = radioactivity per gram wet sediment / radioactivity per gram water.
About 100 Kd-values and 50 CF were determined in 7 water-sediment systems for 241-Am and 244-Cm. "Flooding" of sandy acid sediments with sea water was also simulated for 241-Am ; and gave rise to the highest total amount of Am fixed in the tested organisms.

III. Progress achieved:

1. Methods

Kd values for 241-Am and 244-Cm were determined in sterile and non sterile sediment-surface water systems after a short (4 days) and a longer (4 weeks for 241-Am and 5 weeks for 244-Cm) period of contact. The Kd is defined as : radioactivity per g wet sediment/radioactivity per g water.

After this longer period of contact, the uptake of these isotopes by Gammarus pulex and Artemia salina was examined in the same systems. For sterilization gamma irradiation was chosen in order to change as little as possible (1) the physico-chemical parameters in the sediments and waters. To have conditions as closely comparable in the sterile and non-sterile sediments, both were gamma irradiated but in one half of the sediment-water systems sterility was maintained, while in the other sterility was broken by adding a small amount of fresh sediment to the bulk of irradiated sediment. In the experiment with 241Cm, we included a third series of flasks, not irradiated and only filled with fresh sediment and surface water, to look for differences due to the irradiation of the sediments. In the experiment with 241-Am we tested only coarse sand sediments : one from the Belgian coast (Knokke) and two from the northern part of Belgium (Turnhout), one of them from an acidified lake and the other from a neutral low land brooklet. We also combined the acid lake sediment with sea water to simulate the flooding of a continental contaminated area by the sea.
With 244-Cm we examined next to the two sandy sediment from the north of Belgium, one loamy sediment (20% clay and 47% silt), one loamy sand sediment (3.1% clay and 49% silt) and one clay sediment (41.9% clay and 55.5% silt) respectively from the river La Berwinne (18 km to the east of Liège) a brooklet in the valley of the river de Dender (46 km to the west of Brussels) and from a 200 m deep layer of Boomclay in Mol intended to bury radioactive wastes. The sediment and the surface water was mixed in a ratio of 1.2 g per 50 ml filtered (1.2 µm pore size) water. For the tests with 241-Am we used 250 ml erlemeyer glass flasks stoppered with hydrophobic cotton wool to contain the sediment water systems and for the tests with 244-Cm we irradiated in 250 ml polystyrene vessels for cell culture (Nunc, Denmark).
The flasks and their content (sediment + water) were for both tests sterilized by irradiation with 2.1 Megarad. The strong acid solutions of both isotopes (^{241}Am from Amersham in 3 N HNO_3 and 244-Cm from Harwell in 2 N HNO_3) were properly diluted, sterilized by filtration and immediately added in a volume of 1 ml to the irradiated flasks to obtain solutions of respectively 740 kBq and 92.5 kBq per liter. The original pH was restored by adding 0.1 N NaOH under sterile conditions. The flasks were constantly shaken (2).

The data presented are mean values of at least five duplications. The 95% P errors are not given in this synoptic report, but are mostly about ± 30% of the mean value for Kd (up to maximally 60%) ; these errors are about ± 60% for the CF (maximally 90%).

The Kd values were determined by measuring the residual activity in the filtered water by gammaspectrometry for 241-Am and by liquid scintillation for 244-Cm. For the filtration two pore sizes were used : 1.2 and 0.22 µm. Biological fixation was tested by putting during 4 days 5 freshwater crustacea Gammarus pulex or 10 adult Artemia salina in the sterile and non sterile sediment water systems. After four days the animals were rinsed with uncontaminated water and their radioactivity measured. The radioactivity was calculated per unit wet weight and compared with this of the water at the end of the experiment. The ratio of both radioactivities is called the concentration function (C.F.). Sterility and growth in the non sterile sediments was controlled by counting the aerobic heterotrophic bacterial colonies after plating an appropriate dilution of water on a nutrient agar (Difco nr 001) and growing at 28°C during 48 hours.

Results

241-Am

The results are given in the synoptic table 1.
For 241-Am (added as nitrate to sandy sediments only) low Kd values are found, two orders of magnitude lower than those reported by some other authors. They are comparable to those mentioned by Kepkay (1986) and obtained by Johnson (1980) (4,5). They vary between 500 and 8000 depending on the time of contact between sediment and water and the size of the pores of the filters used to filter the water. After 4 weeks the highest value (8000) is reached in the sea sediment with sea water and the lowest (1100) in the acid lake sediment with acid water (pH 4.1). Little or no difference between the values obtained with filters of 1.2 µm and .22 µm pore size are shown except for the brook sediment with brookwater. Here the value measured with the smallest pore size is double as high as this found with the larger pore size, probably due to the high particle formation of 241-Am in this water by neutral pH. Time influences the Kd values but especially this of sea sediment in sea water (with a factor more than ten), indicating the much slower reaching of an equilibrium in high salinity conditions. Sterility never influences the Kd value with a factor more than two, which means that at least for those coarse sand sediments microbial activity is of little importance in modelling studies. Also no profound effect of sterilisation of the sediments on the consequent uptake of 241-Am can be seen. For Artemia salina in the sea sediment + sea water a C.F. only twice as high is found in the non sterile solutions compared to the C.F. in the sterile systems. Also the radioactivity fixed per gram fresh weight differs with a factor two. With Gammarus pulex we obtain a C.F. 20 times higher in non sterile conditions than in sterile conditions although the animals take up the same amount of radioactivity under both conditions. This high difference in C.F. is due to the almost twenty times higher solubility (not mentioned in the table) of 241-Am in the sterile than in the non sterile brook water. For this system the concentration function depends also very strongly on the kind of filter we use to measure the Am in solution. With a 1.2 µm filter we obtain a solubility almost five to ten times higher than with a .22 µm filter and consequently a 5 to 10 times lower C.F. This illustrates how cautiously concentration functions needs to be handled.

^{241}Am	pH of water		INOCULATED Filter 1.2 Øµm	INOCULATED Filter 0.2 Øµm	STERILISED Filter 1.2 Øµm	STERILISED Filter 0.2 Øµm
Acid lake sandy	4,1	Kd 4 days	1600	1100	1100	1000
		Kd 4 weeks		1700		1100
		CF Gammarus	200		200	
		% Activity/g	13,6%		13%	
Neutral brook sandy	6,9	Kd 4 days	700	2000	1100	2000
		Kd 4 weeks		1900		4000
		CF Gammarus	1000	5000	60	800
		% Activity/g	6,3%		4,8%	
Sea sand + sea water	8,0	Kd 4 days	400	600	500	600
		Kd 4 weeks			6300	8000
		CF Artemia	1000		700	
		% Activity/g	20%		9,5%	
Sandy acid + sea water	8,0	Kd 4 days	500	600	500	600
		Kd 4 weeks		3600		1500
		CF Artemia	800		500	
		% Activity/g	31%		25%	

^{244}Cm	pH of water		INOCULATED Filter 1.2 Øµm	INOCULATED Filter 0.2 Øµm	STERILISED Filter 1.2 Øµm	STERILISED Filter 0.2 Øµm	FRESH SEDIMENT Filter 1.2 Øµm	FRESH SEDIMENT Filter 0.2 Øµm
Acid lake sandy	4,3	Kd 4 days	570	560	410	470	350	500
		Kd 4 weeks	520	850	500	1100	350	580
		CF Gammarus	100	160	70	140	60	100
		% Activity/g	10,1%		10,1%		9,4%	
Neutral brook sandy	5,6	Kd 4 days	460	1800	280	1050	340	1280
		Kd 4 weeks	1800	1300	430	400	1000	650
		CF Gammarus	90	70	15	14	41	27
		% Activity/g	2,8%		1,9%		3,4%	
Loamy sand	7,9	Kd 4 days	1670	3000	1600	2100	1800	2800
		Kd 4 weeks	2500	3900	2200	2700	4000	4500
		CF Gammarus	100	130	90	115	180	240
		% Activity/g	2,7%		2,1%		2,3%	
Loamy	7,1	Kd 4 days	1030	1850	270	940	1160	1900
		Kd 4 weeks	2210	3600	1120	1190	2500	4300
		CF Gammarus	50	90	28	29	80	130
		% Activity/g	1,2%		1,3%		1,9%	
Clay	7,2	Kd 4 days	4100	6200	1900	2900	3700	7000
		Kd 4 weeks	3200	5600	1300	1100	3200	6500
		CF Gammarus	65	110	23	23	60	120
		% Activity/g	1,1%		1,0%		1,0%	

Table I.

Effect of microbial sterility on Kd and CF for ^{241}Am and ^{244}Cm in different water-sediment systems and for two crustacean indicator species.

The % activity/g is calculated as the radionuclide content that would be found if 1 g of animal had been present in the system. The actual mean weight of the animals per vessel was about 0.10 g.

244-Cm

For 244-Cm, values comparable to those obtained for 241-Am are measured (7). After a stabilisation period of five weeks the highest values (7000) are measured in the non sterile clay sediments after filtration with the filters with the smallest pore size and the lowest (350) in the sandy acid lake and the sandy brook sediments after filtration with the filters with the larger pore size. After the longer period of contact the Kd values obtained for the sterile sediments almost do not differ with the pore size of the filters any more. For the non sterile systems, those obtained after filtration over filters with .22 µm pore size are higher (maximum two times for the clay sediments) than those calculated with the radioactivity measured after filtration over filters with 1.2 µm pore size. Time of contact too does not influence the Kd values measured for the acid lake and the clay sediments, where as for the loamy brook, the loamy sand and the sand brook sediments higher (maximum four times) Kd values are obtained after a five weeks stabilization period than after the short four days contact. These differences are more pronounced for those values measured after filtering over 1.2 µm pore size filters than those obtained with the filters with the smallest pore size, indicating that for those last mentioned sediments there are curium particles (pseudo colloids) formed measuring between 1.2 and .22 µm which need some time to settle down.
Sterilization too influences the Kd values very little in the sandy sediments, for these sediments the non sterile ones have at the most a Kd value twice as high as the sterile ones. In the two sediments with a higher clay content however the Kd values of non sterile sediments can be six times higher.
The composition and grain size of the sediments too do not influence the Kd value profoundly. Comparing the sterile sediments only, we see that the coarse sandy brook and acid lake sediments have two to six times lower Kd values than the other three, from which the clay sediment attains the highest Kd, whereas the other two notwithstanding their different clay content have comparable Kd values. Between the Kd values of the non sterile untreated fresh sediments and the irradiated inoculated non sterile sediments only minor differences exist with maximally a factor two in the sandy brook sediment. This can be explained by the differences in biological activity measured.
The uptake of curium by Gammarus pulex is the lowest in the loamy and the clay sediment. It is twice as high in the loamy sand and the sand brook sediment and nine times higher in the sand acid lake sediment. This pattern is not completely followed by the concentration functions. The C.F.'s are indeed the lowest in the loamy and clay sediments (30), but in the sandy brook sediment the uptake twice as high does not result in a two times higher C.F. as it does in the loamy sand brooklet. Particularly in the acid lake system the only two times higher C.F. in comparison with that measured in the neutral sandy brooklet does not correspond with the nine times higher uptake. It can be explained by the five times higher solubility of 244-Cm in the acid lake water than in the water of the brooklet.

Because for 241-Am only sandy sediments were examined we can only compare the uptake of both transuranics under these conditions. For these systems we can conclude that Gammarus pulex fixes comparable amounts of 241-Am and 244-Cm. This corresponds with the finding of P. Mizamonol, P. Germain and J.C. Anzur (1987) for bentic marine species.

General conclusions

The claim that microbial activity can profoundly change the behaviour of 241-Am and 244-Cm in sediments and water cannot be demonstrated for neither of the two isotopes in coarse sandy sediments. For sediments with a higher silt and particularly a higher clay content however larger differences in adsorption are obtained, up to six times more in the non sterile than in the sterile sediments.

Bioavailability is not seriously influenced by microbial activity. Gammarus pulex fixes quite similar quantities under sterile and non sterile conditions of these both transuranics. The CF of 241-Am were in these experiments about one order of magnitude higher than for 244-Cm.

The data demonstrate how experimental Kd and C.F. are to be used with caution in modelling and risk assessment studies. The physiological parameters of the organisms could well influence preponderantly their uptake of radionuclides.

References

1. Keulder, P.C. (University of Orange Free State, Bloemfontein) (1979) Sterilization of suspended sediments by gamma radiation. J. Limnol. Soc. South Africa ISSN, 0377-9688, V.5(2), p. 103-106.
2. Seymour, A.H., Nevissi, A., Schell, W.R., Sanchez, A. (1979) Distribution coefficients for radionuclides in aquatic environments. Development of methods and results for plutonium and americium in fresh and marine watersediment systems. Nureg/CR-0801, p. 39.
3. Effect of microbial biomass reduction by gamma-irradiation on the sorption of 137-Cs, 85-Sr, 139-Ce, 57-Co, 109-Cd, 65-Zn, 109-Ru, 95mTc and 131-I by soils. K. Bunzl and W. Schimmack (Nov. 1987), Springer Verlag.
4. Kepkay, P.E. (1986) Microbial binding of trace metals and radionuclides in sediments : results from an in situ dialysis technique. Journal Environ. Radioactivity 3, 85-102.
5. Johnson, H.M., Gillham, R.W. (1980) A review of selected radionuclide distribution coefficients of geology materials. Chalk River, Ontario, Atomic Energy of Canada (TA.901).
6. Wildung, R.E., Drucke, H. The relationship of microbial processes to the fate of transuranic elements in soil. Nevada Applied Ecology Group Symposium on the Dynamics of Transuranics in Terrestrial and Aquatic Environments, Gatlinburg, Tennessee, Oct. 5-7, 1976. BNWL-SA-5971.

7. Nakayama, S., Nelson, D.M. (1988) Comparison of distribution coefficients for americium and curium : effects of pH and naturally ocurring colloids. J. Environ. Radioactivity 8, 173-181.
8. Miramand, P., Germain, P., Arzur, J.C. (1987) Uptake of curium by five benthic marine species. Comparison with americium and plutonium. J. Environ. Radioactivity 5, 209-218.

IV. Other research group(s) collaborating actively on this project [name(s) and address(es)]:

Prof. K. Simkiss, Dept. of Zoology, University of Reading, Reading, U.K.

V. Publications:

Publications see list project 2.

Title of the project no.: 2

Speciation of transuranics in aquatic environments

Head(s) of project:

O. Vanderborght

Scientific staff:

O. Vanderborght
S. Van Puymbroeck
H. Witters

I. Objectives of the project:

Test the effect of the speciation of transuranics, on their biological fate.

II. Objectives for the reporting period:

Conclude on the speciation effects for biological models.

III. Progress achieved:
Methodology and results

Most of the research efforts of this contract period went to the bioavailability studies of curium and americium in freshwater animals, and the speciation of these radionuclides. The importance of those two transuranium radionuclides in the radioactive waste problem is evident from the fact that one ton of fission materials from a nuclear reactor contains about 70.000 Ci of curium-242 for one year after unloading and about 2000 Ci of curium-244 during 10 years. This makes curium the most prominent transuranium radionuclide after neptunium-239 and uranium-237. Americium-241 on the other hand becomes the most prominent radionuclide in the total transuranium radionuclide inventory one century after unloading.

The speciation of both curium-244 and americium-241 in different freshwater environments was studied experimentally. An important finding was the similarity of the behaviour of iron and americium in as far as the particulate formation, the formation of organically complexed forms and the adsorptive behaviour on biological surfaces is concerned. The binding of curium and americium in organic complexes is very much influenced by the presence of other complex forming metals. A striking decomplexation of americium from its humic acid complexes can be induced by the presence of aluminium in the water. Aluminium is known to be a major metal present when waters become acidified.

The biological fixation of americium and curium was experimentally checked in 9 different animal species : in Mollusca gastropoda (valvata species), in Crustacea isopoda (azellus species), in Insecta colleoptera, in Mollusca lamellibranchiata (sphirium), in Insecta colleoptera (hydrophyllus), in Herudinea (:the leach) and in three different fish species. The concentration factors ranged in this series of animals from a high 1000 to a low 2 with a mean of about 100. Because the Mollusca gastropoda and the Crustaceae showed the highest uptake of curium and americium, a more detailed study of the uptake physiology and of the organ distribution was done as well for curium as for americium in the snail Lymnaea stagnalis as in the crayfish Astaccus leptodactycus. The uptake of curium is decreased by a factor of 2 by the presence of organic acids, such as humic acids, in the water ; but the organ distribution remains the same with or without these organic acids. In the freshwater snail, curium is fixed three times more in the soft tissues of the animal than americium, the latter being mostly adsorbed on the shell. This higher uptake of curium in the soft and eadible tissues of the animal has to be taken into account when environmental limits of curium and americium are to be set. Notwithstanding this note of caution, it must be said that no such difference in uptake between americium and curium could be seen in the rainbow trout.

The subcellular distribution of americium after its uptake in the crayfish Astaccus leptodactylus was also studied. From this study, it seems that americium displays the characteristics of a class A metal. It is preferentially found in the lysosomal-mitochrondrial fraction of the hepatopancreas cells. This is in contrast with the class B metals, such as copper that is preferentially found in the cytoplasmatic fraction. The

blood clearance after intracardial injection follows a two component exponential curve with a half-life of 3 and of 27 hours, which is comparable with the half-life of calcium in this animal.
In rainbow trout (Salmo gairdneri) on the other hand, about 1/3 of the total Cm of the fish is fixed on the gills after an exposure of 1 week. The CF is 4 times higher in the gills than in liver and reaches about unity after thin weak exposure.

Discussion

To conclude, about 20 transfer functions and organ distributions were observed for different freshwater species in different conditions of complexation for Cm and Am. For modelling purposes, this study indicates a minor effect of speciation (giving rise to a decrease by a factor of $\pm$ 2 due to complexation) of Am and Cm ; and a slightly higher uptake of Cm. Gills and liver are most contaminated in fish for Am and Cm, the hepatopancreas in gastropods for Cm. Different animal species exhibit large differences in CF for Am and Cm, ranging from 1 to 1000 and stabilizing after 1 to 2 weeks ; the highest CF are found in some freshwater gastropods and crustacea.
The physiological status of the organisms is determined by both the internal status (endocrinology, development, feeding status, ...) and the external "multiple stress" factors (e.g. presence of other metals affecting the epithelial transport processes, pH and Ca affecting the membrane permeabilities, external stimulation by light and temperature). This physiological status could well be of more relevancy for the biological fixation of radionuclides in aquatic animals, than the speciation of the radionuclides themselves.

Fig.1.
In the freshwater snail Lymnaea stagnalis, the CF (concentration function = 244-Cm per g tissue/244-Cm per ml water) in the hepatopancreas is increasing steadily for 3 weeks, and is lowered by the presence of humic acids in the water. Most of the Cm fixed by the animals is found in the soft tissues, this contrasts with the tissue distribution of Am. Error bars indicate 95% P limits.

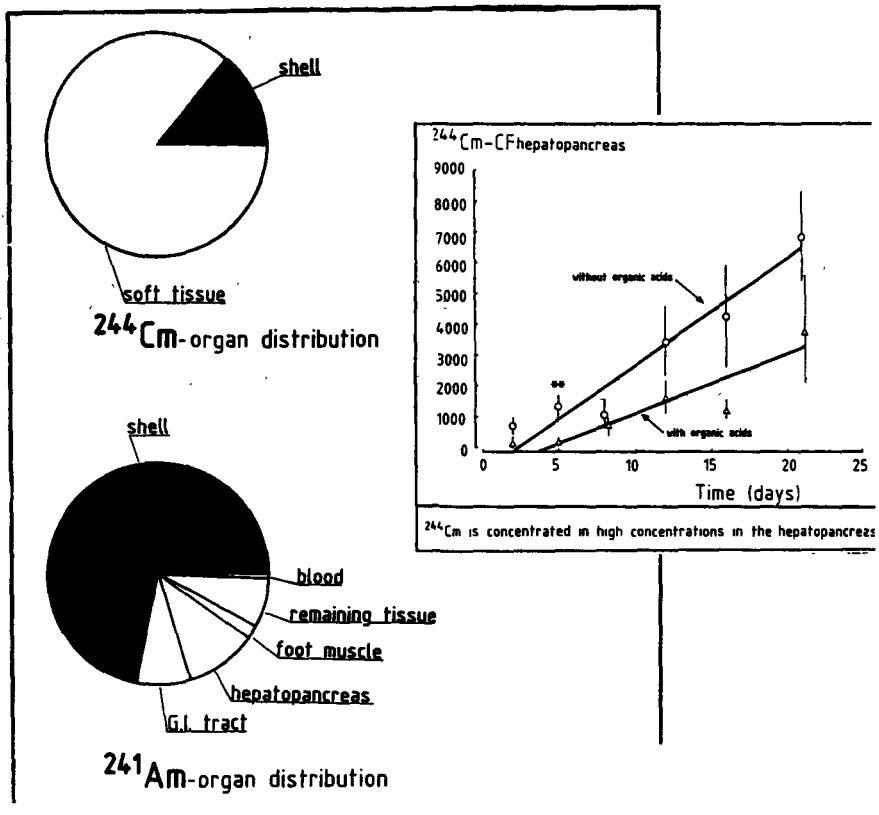

IV. Other research group(s) collaborating actively on this project [name(s) and address(es)]:

Dr. M. Hoppenheit, Biologische Anstalt Helgoland, Hamburg (Germany)

V. Publications:

Publications

Effect of aluminium and humic acid on the 241-Am adsorption on the exoskeleton of the crayfish Astacus leptodactylus Eschscholtz.
J. BIERKENS, J.H.D. VANGENECHTEN, S. VAN PUYMBROECK, O.L.J. VANDERBORGHT
Health Physics, 50 (2), 277-280 (1986).

Intubation of different chemical forms of americium-241 in crayfish Astacus leptodactylus.
J. BIERKENS, J.H.D. VANGENECHTEN, S. VAN PUYMBROECK, O. VANDERBORGHT
In : "Speciation of Fission Products in the Environment" ;
Editors R.A. Bulman & J.C. Cooper, Elsevier Applied Science Publishers, London, 1986, p. 286-293.

241-Amercium and 59-Iron speciation in natural surface waters and sorption onto crayfish exoskeleton.
J.H.D. VANGENECHTEN, N.A. CHUGHTAI, J. BIERKENS, O. VANDERBORGHT
J. Envtl. Radioactivity 5, 275-286 (1987).

Speciation and biological availability in freshwater : review.
O. VANDERBORGHT
In : "Speciation of Fission Products in the Environment" ;
Editors R.A. Bulman & J.C. Cooper, Elsevier Applied Science Publishers, London, 1986, p. 250-261.

Speciation and bioaccumulation of transuranic elements in the freshwater environment.
J. BIERKENS, O.L.J. VANDERBORGHT
In : "Speciation of Actinide Elements in the Environment", Editor R.A. Bulman - CRC Press Inc. Uniscience Books.

Curium-244 and americium-241 uptake in freshwater fish.
J.H.D. VANGENECHTEN, S. VAN PUYMBROECK, O.L.J. VANDERBORGHT
Toxicological and Environmental Chemistry, 19, 147-152 (1989).

Ecophysiology of acid stress in aquatic organisms.
Eds. H. WITTERS & O. VANDERBORGHT, Annls. Soc. R. Zool. Belg., 117 (suppl. 1) (1987), pp. 472.

Internal or external toxicity of aluminium in fish exposed to acid water.
H.E. WITTERS, J.H.D. VANGENECHTEN, S. VAN PUYMBROECK, O.L.J. VANDERBORGHT
In : Proc. International Symposium on Air Pollution and Ecosystems. P. Mathy (Ed.), Grenoble 1987, Commission of the European Communities, pp. 965-970, D. Reidel Publishing Company, Dordrecht (1988).

A microanalytical study of the gills of aluminium-exposed rainbow trout (Salmo gairdneri).
C. GOOSSENAERTS, R. VAN GRIEKEN, W. JACOB, H. WITTERS, O. VANDERBORGHT
Intern. J. Environ. Anal. Chem., 34, 227-237 (1988).

Laboratory studies on invertebrate survival and physiology in acid waters.
J.H.D. VANGENECHTEN, H. WITTERS, O.L.J. VANDERBORGHT
In : "Acid Toxicity and Aquatic Animals", Eds. R. Morris, D.J.A. Brown, E.W. Taylor and J.A. Brown. Society for Experimental Biology, Seminar Series. Cambridge University Press, Cambridge, pp. 153-169 (1989).

Nuclear winter : an update.
O.L.J. VANDERBORGHT
In : "The Nuclear Threat to Europe : Risk and Prescriptions", Proc. 2nd European Symposium, International Physicians for Prevention of Nuclear War, Madrid, October 1986.

The essential valuation of environmental monitoring is given by its biological relevance.
O.L.J. VANDERBORGHT
In : "Ecophysiology of Acid Stress in Aquatic Organisms", Eds. H. Witters & O. Vanderborght, Annls. Soc. R. Zool. Belg., 117 (suppl. 1), p. 3-4 (1987).

Abstracts

Uptake of americium-241 by the crayfish Astacus leptodactylus following intragastric and intracardial injection.
J. BIERKENS, J.H.D. VANGENECHTEN, S. VAN PUYMBROECK, O.L.J. VANDERBORGHT
Abstract in "Seminar on the cycling of long-lived radionuclides in the biosphere : observations and models". CEC/JEN, Madrid 1986.

Acid-base regulation and ion balance in acid-stressed channel catfish Ictalurus punctatus.
J.H.D. VANGENECHTEN, J.N. CAMERON
Abstract Prod. of the 8th Conference of the European Society for Comparative Physiology and Biochemistry, "Comparative Physiology of Environmental Adaptations", Strasbourg, 1986.

Licentiate theses (University of Antwerp)

ANNAERT Wim (1985)
Uptake and distribution of 241-americium in amphibians.

BOGAERTS Christine (1988)
Intraspecific differences in sensitivity for acidification in fishes.

Ph.D. theses (University of Antwerp)

BIERKENS Johan (1986)
Americium availability to freshwater organisms.

LEMBRECHTS Johan (1986)
Technetium speciation and mobility in a dicotyledon plant.

RADIATION PROTECTION PROGRAMME
Final Report

Contractor:

Union Internationale des
Radioécologistes, UIR
Association Internationale
Rue Cardinal Cardijn 5
B-4480 Oupeye

Contract no.: BI6-B-052-B

Head(s) of research team(s) [name(s) and address(es)]:

Dr. A. Aarkrog
IUR
Rue Cardinal Cardijn 5 - Bte 18
B-4480 Oupeye

Telephone number: 041/64.25.64

Title of the research contract:

Promotion of research and exchange of information in radioecology.

List of projects:

1. Intercomparison and harmonization of methodologies, identification of future objectives in radioecology, and training and exchange of scientists.

Title of the project no : 1.Intercomparaison and harmonization of methodologies, identification of future objectives in Radioecology, training and exchange of scientists.

Head(s) of project: Dr.A.AARKROG
Chairman of I.U.R.
rue Cardinal Cardijn,5,Bte 18
B-4480 OUPEYE BELGIUM

Scientific staff:
Working Group Leaders : H.Dahlgaard, L.Foulquier, M.Frissel, G.Linsley, C.Myttenaere, J.Van den Hoek

I.Objectives of the project:

To provide support for exchange of information, standardisation and development of experimental research in Radioecology with a view to protect Man from the harmful effects of radionuclides present in the environment.

To identify the specific needs of developing countries in the field of Radioecology.

To promote the formation of young scientists through participation to scientific meetings and visits to advanced laboratories.

II.Objectives for the reporting period:

a) The aim of the working group "Plant to Animal Transfer" is to establish reliable plant to animal transfer factors for various radionuclides, and to evaluate the importance of different parameters which may influence this transfer.
b) The aim of the working group "Soil-to-Plant Transfer Factors" is to derive reliable transfer factors of radionuclides for nuclear safety assessment studies.
c) The aim of the working group Marine Radioecology (MARECO) is to give scientists engaged in marine radioecology studies an opportunity to meet and exchange information and to co-operate on marine radioecological projects.
d) The WG "Radioecology of Continental Waters" aims to review the studies on the behaviour and transfer of radionuclides, particularly from the Nuclear fuel Cycle, in the freshwater ecosystems.

III. Progress achieved:

REPORT OF THE IUR WORKING GROUP "SOIL-TO-PLANT TRANSFER"
Working Group Leader: M.J.FRISSEL

I. Objectives

1. Exchange of information on soil-to-plant transfer of radionuclides and of Transfer Factors (TF-values) in particular, Promote international cooperation and avoiding of unwanted duplication of experiments.

2. Promote determination of TF-values with the aim to provide reliable estimates of TF-values and uncertainty ranges.

3. Promote determination of local and national variability because of differences in climate, management, etc.

II. Progress

Methodology: One of the actions of the Working Group aimed at (1) Standardization of the experimental determination methods and (2) Standardization of reporting results.

Ad (1) Standardization focussed on factors which may influence-unforseen-the uptake. Therefore guidelines were provided for items and minimum dimensions for fields, lysimeters and pots, realistic fertilization schemes, correct labeling of soils, etc., while maintaining rational agricultural management systems and conditions.

Ad (2) Information forms developed so that relevant information on experimental conditions - in combination with determined TF-values- could be included into a data bank. The investigators filled out the forms themselves, this stimulated them to determine the required additional details and avoided errors which may slip in when data are derived from literature by someone who cannot be familiar with all details of all experiments. No data were accepted from unknown investigators, investigators and their experimental methods had to be known by the working group; this procedure limits errors.

III. Results

At the end of 1989 participants of the working group collected the following number of entries (TF-values and experimental conditions):

Cs	2030 entries	Pu	680 entries	Other radionuclides	1900 entries
Sr	920 entries	Am	520 entries	Stable nuclides	260 entries
Co	780 entries	Np	460 entries	Special cases	250 entries

The TF-values were analysed in two ways: (1) Multilinear regression method. An advantage of such a method is that the input of all relevant parameters - if reported to the data bank - can be

determinded. A disavantage of the method is that the multidimensional grid, which in fact is used by the method, must be sufficiently filled with data. For obvious reasons this was not always the case. Only for logical combinations of soils, crops and climate experiments were carried out. For Cs, Sr and Pu sufficient data were available for a multi-linear regression analyses to determine estimates of expected TF-values and uncertainty ranges as function of the environmental conditions.
Important parameters which determine the TF-values are -besides the type of nuclide and crop- : type of soil, pH, time elapsed since a soil was contaminated, organic matter content of soil, depth of radionuclide and soil moisture content. Tables and equations were derived to allow estimates of expected TF-values as function of soil type, pH and time elapsed. For Am, Np, Cm, Co, Mn, Ni, Zn and a few other nuclides simpler statistical methods were applied to calculate mean values for the best estimate of expected TF-values and uncertainty ranges. Also for these nuclides tables for expected values and ranges were derived. The tables cover several pages -of compressed letter type- therefore no attempt has been made to report results within this report.

Discussion: At the end of this 5 year period it can be concluded that the Working Group has been very successful. More institutions participated than expected and also the number of TF-values determined was higher than expected. Because of this, numerous estimates of TF-values became available. The uncertainty of the estimated values was for the mean value of TF-values which cover yields of a few years, fiels and crops satisfactory, it is about a factor of two for many situations. The uncertainty of an estimate for one single harvest if often a factor of about 10 or 20 higher. This latter uncertainty can only be reduced by taking into account results of specific soil analyses. This outcome is somewhat embarrassing. For general assessment models this is usually of no concern because such models consider average situations.

Dissemination of results: the results of all determinations have been stored into a data bank. All these data were every two years reported in Reports of the Working Group. These Reports contained also the results of the multi-linear regression analyses and other statistical calculations. The results of the 1989 report (VIth Report of the Working Group) formed the base of a Technical Report to be published by the IAEA and CEC on Parameter Values for Radioecological Assessment Models. As already indicated the number of entries (transfer value plus environmental and experimental conditions) has increased to about 7700. This is an amount whch cannot be handled without modern ways of data processing. To promote further analysis of results, the Working Group decided to make the data available on diskettes. The content of the diskettes will in general be identical to the data reported in the VIth report of the Working Group. Although this is an open report, and the data are therefore available to everyone, the Working Group decided to ask investigators/institutions who reported data to the data bank, as well as the CEC for their agreement.

Collaboration of Research Groups (Providing Data).

Austria: Nat.Res.Center Seibersdorf; Belgium: EC, SCK/CEN, Univ.Cath.de Louvain; Brasil: CNEN; Canada: AECL; Cechoslovakia: Inst. of Radioecology; Denmark: Riso Nat.Lab.; France: CEA/DERS/SERE; FRG: Bundesanst. f. Milchforsc., Bayer.L.Bodenk., GSF, KFA Karlsruhe, KFA/IRA, Univ.Bremen, Univ.Hannover; Ireland: NEB; Italy: ENEA-DISP, Univ.del Sacro Cuore; Netherlands: RIVM; Sweden: Swedish Univ.of Agric.; UK.: Inst.Terrest.Ecology, Harwell Lab., Imperial Coll., Merlewood Res.St.,NRPB.; USA: New York Univ.; Yugoslavia: Jozef Stefan Inst.
Other groups participated without or not yet bringing in data. Examples are Assoc.Nucl.Services (UK), Bundesanst.f.Lebensmitteluntersuchung (Austria), Ontario Hydro (Canada) and NAGRA (Switserland).

Publications

1) IVth Report of the Working Group Soil-to-Plant Transfer Factors. Bilthoven, Netherlands, 1985.
2) Appendix to IVth Report of the Working Group Soil-to Plant Transfer Factors. Bilthoven, Netherlands, 1985.
3) Vth Report of the Working Group Soil-to-Plant Transfer Factors. Bilthoven, Netherlands, 1987.
4) VIth Report of the Working Group Soil-to-Plant Transfer Factors. Bilthoven, Netherlands, 1989.

Separately specified contributions in (1) :
5) Erikson,A. Plant uptake of Pu-238, Np-237 and Am-241 from four soils compared in a 9-year old lysimeter study.
6) Cawse, P.A. and Baker, S.J. Soil to Plant Transfer Factors for Am-241 and Additional data for Cs-137 and Pu-239+240.
7) Ham, G.J., Popplewell, D.S. and Shuttler, S.D. The uptake of Pu-239, Am-241 and Cs-137 into Cabbage and Potatoes.
8) Kirchmann, R. and Fagniart, E. Additional transfer data for Cs-134, Co-60 and Tc-99.
9) Linsalata, P. The pocos de Caldas plateau.

Separately specified contribution in (2):
10) Heisterkamp, S.H. and Koster J. Results of reanalysis of data from IUR-workshop on soil to plant transfer parameters.

Separately specified contributions in (3):
11) Stoutjesdijk, J.F. Ginkel, J.H. van, Pennders, R.M.J. Determination of soil-plant transfer factors and measures to influence the uptake of radionuclides.
12) Eriksson, A. and Rosen, K. Observations on the transfer of Cs-137 from soils to barley crops in Sweden after the Chernobyl fallout.
13) Cawse, P.A. and Baker, S.J. Atmospheric deposition of radionuclides and transfer to vegetation in Great Britain.
14) Juznic, K. On the transfer of radiostrontium from soil to plants
15) Kirchmann, R. and Fagniart, E. Transfer factor values observed in experimental field conditions and from Chernobyl fallout.

Separately specified contributions in (4):

16) Frissel, M.J. and Heisterkamp, S.H. Geometric mean Transfer values calculated with multi-linear regression analyses.
17) Frissel, M.J. and Bergeijk, K.E. van. Mean transfer values derived by simple statistical analyses.
18) Cawse, P.A. and Colle, C. Variability in Soil to Plant Transfer of neptunium, americium and curium.
19) Henrich, E. Radionuclide transfer investigations in Austria: an overview.
20) Juznic, K. On transfer of Sr-90 from soil to plants
21) Nisbet, A. Investigations of Cs-K interactions in agricultural soils by soil solution analyses.
22) Frissel, M.J. and Koster, J. Uncertainties of predicted soil-to-plant transfer factors because of averaging the impact of space, time local conditions and crop variety. 1989 ISH-Heft 128 p16-27, BGA-ISH Neuherberg, FRG.
23) Frissel, M.J. and Koster, J. The IUR project on Soil-to-Plant Transfer Factors of Radionuclides. Expected values and uncertainties. 1988 Elsevier Applied Science, London, p151-158.
24) Frissel, M.J. and Bergeijk, K.E. The impact of extreme environmental conditions, as occuring in natural ecosystems, on the soil-to-plant transfer of radionuclides. (in press) (Presented in Udine, 1989).

REPORT OF THE IUR WORKING GROUP "PLANT TO ANIMAL TRANSFER"

Working Group Leader: J.VAN DEN HOEK

I. Objectives

The aim of the Working Group "Plant to Animal Transfer" is to establish reliable plant-to-animal transfer factors for various radionuclides, and to evaluate the importance of different parameters which may influence this transfer.

II. Progress achieved.

Methodology.

The essential activity of the W.G. is the exchange of scientific experimental information between the scientists who participate in the activities of the W.G. during the three day meeting at the Institute or Organization hosting the meeting.
Since the W.G. is an IUR activity, interested scientists from a variety of countries, both inside and outside the European Community, are invited to join the W.G. activities. This approach has turned out to be very rewarding in the evaluation of the consequences of the Chernobyl contamination event which has affected also large areas of land outside the countries of the European Community.

Results and discussion.

The scientific work in the area of "Plant to Animal Transfer" has been greatly influenced by the contamination of agricultural,

semi-natural and natural ecosystems with Cs-137 and Cs-134 as a result of the Chernobyl accident. This has prompted a great variety of experimental work, aiming at investigating to what extent the behaviour of Cesium isotopes in plants and animals is influenced by many different parameters.
The importance of these parameters was discussed in detail during the second meeting of the W.G. in October 1987 in order to establish priorities for further experimental work.
The following parameters were identified:

- the initial interception of the deposited radionuclide by plants. This depends itself on various other factors such as the nature of the deposition (wet or dry), the growing season, the plant species, and others. The initial interception determines largely the fraction of the radionuclide which can be possibly retained, and which enters directly into the soil.

- the availability of the radionuclide in the soil which determines, through root uptake, contamination levels at a later stage. Type of soil and its physico-chemical characteristics, organic matter content from dead vegetable material and animal excreta deposited on the soil, are among the important parameters.

- the measurement of feed intake and the choice of plant species and other feedstuffs (mushrooms, berries) by grazing and free ranging animals is one of the high priority research subjects. It will make available accurate information on radionuclide intake by the animal which is necessary for establishing reliable figures for absorption percentages in the gastro-intestinal tract, for transfer to milk and meat and for other parameters.

- the influence of soil intake by animals on the intestinal absorption of Cesium and possibly other radionuclides. It is necessary to determine also for which animal species this factor is of importance.

- the importance of animal management practices. They may influence the retention of the deposited radionuclide on plants, the radionuclide intake by the animal as a result of different feeding methods such as stripgrazing, grazing on permanent pasture, cut grass fed at the stable and other methods.

- the differences in body levels between young and adult animals after intake of radionuclides, and in retention as expressed by biological half lives.

- the effectiveness of different remedial measures.

Since the October 1987 meeting, two international workshops were organized jointly by the European Commission and local organizations which had a direct relation to the subjects studied by the members of the Working Group. These were the Workshop in Oxford (U.K.) in September 1988, and the Workshop in Udine (Italy) in October 1989.

Therefore, it was decided to hold the next meeting of the W.G. in April 1990 in Neuherberg (FRG). The progress made will be discussed, particularly regarding the transfer of Cesium in plants and animals which has been studied extensively over the last years. The possibility will be considered to bring together in one publication the experimental results of different laboratories which have worked on the same or related subjects.

IV. Research Groups collaborating actively in the W.G. activities.

The following scientists collaborated actively in the activities of the Working Group:

Dr.C.Vandecasteele	Belgium
Miss M.Van Hees	"
Dr.P.J.Coughtrey	United Kingdom
Dr.F.Schönhofer	Austria
Dr.G.Pröhl	FRG
Dr.G.N.Kistner	"
Dr.G.Desmet	Belgium
Dr.E.Henrich	Austria
Dr.J.Handl	FRG
Mrs.Z.Jeran	Yugoslavia
Dr.P.Stegnar	"
Dr.K.J.Johanson	Sweden
Dr.J.Van den Hoek	The Netherlands
Dr.R.W.Mayes	United Kingdom
Dr.B.Wilkins	" "
Dr.B.J.Howard	United Kingdom
Mr.N.A.Beresford	" "

REPORT OF THE IUR WORKING GROUP "RADIOECOLOGY OF CONTINENTAL WATERS"
Working Group Leader: L.FOULQUIER

1. Objectives

The aim of the Working Group "Radioecology of Continental waters" is to search, to analyse and to circulate the informations dealing with the transfer in freshwater ecosystems of the radionuclides related with the Nuclear Fuel cycle.
This inventary of data will allow the assessment of the radioecological impact of the nuclear installations both in routine or accidental situations and the transfer of these radionuclides in the food chains.

2. Work performed

2.1. Method: the approach is based on the knowledge of the relevant laboratories in the field, the exchange of data (mailing and/or personal contacts) and their study in order to identify the evolution of the situation and the future needs.
Beyond these exchanges of data, the Working Group met three times: Brussels (24-27 September, 1985), Madrid (15-19 September, 1986) and Cadarache (14-19 March, 1988). The number of participants was respectively: 10 (6 countries), 13 (7 countries) and 34 (14

countries).

2.2. Results and discussion

The Working Group collected, through these exchanges, a great number of data on the radioecology of rivers and lakes, in particular following the Chernobyl accident.
The general conclusions are the following :
- there are few studies "site specific" which allow the evaluation of the kinetics of transfer in all the compartments of the aquatic ecosystem;
- the field studies are usually performed for a surveillance purpose and therefore are not always useful for the radioecological research;
- a great effort is still needed in the description of the sampling stations, the methods of sampling and of preparation, the technics of measurements and the expression of the results. Every Data Base must include the elements in order to allow an evaluation of the "quality" of the data available;
- their is a lack of data on radionuclides which need a radiochemical treatment before their measurement (89-90-Sr, 3-H, α-emitters particularly);
- laboratory experiments remain necessary to understand the mechanisms of transfer, i.e. the experimental data were very useful in the interpretation of the data observed on the 137-Cs fixation following the Chernobyl accident; these experiments were later largely validated by the field observations;
- it is clear that the rivers on one hand and the lakes on the other hand are two different ecological entities and that the transfer are ruled by different kinetics.

3. Laboratories and Scientists having participated to the WG activities.

SERE. Laboratoire de radioécologie des eaux continentales. (Mr.Foulquier)* Commissariat à l'énergie atomique. C.E.N. Cadarache.13108 St-Paul-Lez-Durance. France.
* Responsable du groupe de travail.

Benes,P. Department of Nuclear Chemistry. Technical University of Prague.Brehova 7,115 19 Praha 1 Tchéchoslovaquie.

LNETI. Departamento de proteccao e Seguranca radiologica. Estrada Nacional n°10. 2685 Sacavem.Portugal. Dr.A.Ortins de Bettencourt et C.Vaz Carreiro.

A.Cigna. c/o ENEA. I.13040 Saluggia Italie.

J.Hilton. Institute of Freshwater Ecology. The Ferry House Ambleside LA22 OLP Cumbria. United Kingdom.

R.Kirchmann et Mme Meurice M.
Laboratoire de Radioécologie. Université de Liège.Sart Tilman 4000 Liège Belgique.

J.Smitz. Laboratoire de Géophysique. Université de Liège. Sart Tilman, 4000 Liège Belgique.

C.Myttenaere, L.Sombré. Université Catholique de Louvain Place Croix du Sud, 4. 1348 Louvain-la-Neuve. Belgique.

Ormai,P. Packs Nuclear Power Plant. 7031 Packs P.O.Box 71 Hongrie.

Polikarpov, G.G. Institute of Biology of South Seas. Acad.of Sciences. 2, Prospekt Nakhimova, 335000 Sevastopol URSS.

Roy,J.C. Département de Chimie. Faculté des Sciences. Université Laval - Quebec, Canada.

Institute of Radioecology. Komenskeha. 0461 Kosice Tchéchoslovaquie.

Schönhofer, F. Bundesanstalt fur Lebensmittel untersuchung und forschung. Kinderspitalg 15, Postfach 15. Wien 1095, Autriche.

4. Publications.

N.B.: the publications mentioned hereafter are only those presented by the working Group Members to International Meetings.

Transfert des radionucléides en écosystème fluvial. Journée d'étude organisée à Mol le 19 Juin 1986 par le groupe mixte CEA-CEN-CCE "Radioécologie des eaux continentales". Annales de l'Association Belge de Radioprotection. Vol.12. N° 2-3, 2ème-3ème Trimestre 1987, 286 p.

FOULQUIER L.,LAMBRECHTS A.,and PALLY M. (1987). Qualitative and quantitative evaluation of long-life radionuclides in the sediments, plants and fish of the Rhône river. Proceeding of a seminar on the cycling of long-lived radionuclides in the biosphere: observations and models (Vol.2). Madrid, 15-19 september 1986. CCE and CIEMAT, 40 p.

DESCAMPS B. and BAUDIN-JAULENT Y. (1987). Transfer of radium-226 to fish in the aquatic environment of a french mining complex: assessment of radiation dose to man. Proceeding of a seminar on the cycling of long-lived radionuclides in the biosphere: observations and models (Vol.2). Madrid, 15-19 september 1986. CCE and CIEMAT, 17 p.

POLIKARPOV G.G. and LAZORENKO G.E. (1988). Experimental comparative study of accumulation and loss of the Black Sea and the lower Dnieper. IVème symposium International de Radioécologie, CEN.Cadarache France, 14-18 mars 1988.

POLIKARPOV G.G., TIMOSHCHUK V.I. and KULEBAKINA L.G. (1988). Decrease of 90-Sr concentrations in aquatic environment of the lower Dnieper in the Black sea direction. IV ème symposium International de Radioécologie, CEN Cadarache, 14-18 mars 1988.

LAMBRECHTS A., FOULQUIER L., and PALLY M. (1988). Etude comparée de l'impact radioécologique des installations nucléaires et de l'accident de Tchernobyl sur le fleuve Rhône. IV ème symposium International de Radioécologie, CEN Cadarache, 14-18 mars 1988.

VAZ CARREIRO M.C. and MADRUGA M.J. (1988). The experimental study of Cs-134 behaviour in freshwater sediments. IV ème symposium International de Radioécologie, CEN Cadarache, 14-18 mars 1988.

BENES P. (1988). Interaction of radionuclides with solid phase in the modelling of the migration of radionuclides in surface water. IV ème symposium International de Radioécologie, CEN Cadarache, 14-18 mars 1988.

DESCAMPS B. and BAUDIN-JAULENT Y;(1988). Evolution de l'impact radioécologique de l'accident de Tchernobyl dans trois rivières françaises. IV ème symposium International de Radioécologie,CEN Cadarache, 14-18 mars 1988.

FOULQUIER L. (1988). Evaluation de l'impact radioécologique de l'accident de Tchernobyl en France sur des écosystèmes aquatiques. IV ème symposium International de Radioécologie, CEN Cadarache, 14-18 mars,1988.

VANGENECHTEN J.H.D., VAN PUYMBROECK S. and VANDERBORGHT O.J.L. (1988). Curium-224 uptake in freshwater snails. IV ème symposium International de Radioécologie, CEN Cadarache, 14-18 mars 1988.

SOMBRE L., MYTTENAERE C. and FOULQUIER L.(1988). Simulation de la contamination d'un écosystème dulcicole par du césium rejeté en conditions accidentelles. IV ème syposium International de Radioécologie, CEN Cadarache, 14-18 mars 1988.

ZEEVAERT T., VANDECASTEELE C.R., VOLKAERT G. and KIRCHMANN R. (1988). Dose assessment and uncertainly with respect to liquid effluent discharges. In: Reliability of radioactive transfer model. Ed. by G.DESMET CEC. Elsevier applied Sciences. London and New-York, 355 p.

VAZ CARREIRO M.C. and SEQUEIRA M.M.A. (1988). 226-Ra and 228-Ac in a freshwater ecosystem. In Natural Radioactivity. Radiation protection dosimétrie. Proceeding of the fourth Internat.Symposium on the natural radiation environment held at Lisbon Portugal. December 7-11, 1987. Organised by CCE,LNETI.
Ed. A.O.de Bettencourt et coll. Conf. 871208 - Eur 11895. Published by nuclear technology publishing, vol.24, N° 1-4 1988, 559 p.

DESCAMPS B. and FOULQUIER L. (1988). Natural radioactivity in the

principal constituents of french river ecosystem. In Natural Radioactivity. Radiation protection dosimétrie. Proceeding of the fourth Internat.Symposium on the natural radiation environment held at Lisbon Portugal. Decemb. 7-11-1987. Organised by CCE, LNETI. Ed.A.O. de Bettancourt et coll. Conf. 871208 - Eur 11895. Published by nuclear technology publishing, vol.24, N° 1-4 1988, 559 p.

MARINE RADIOECOLOGY WORKING GROUP (MARECO)
(Working Group Leader : H.DAHLGAARD)

The Marine Radioecology working group (MARECO) was established June 1988 at an IUR meeting at Riso, Denmark. The first meeting of the working group was held in connection with the EC MARINA seminar, 13 June 1989 in Brugge, Belgium.

The following points of scientific interest, which were set up during the June 1988 meeting, were maintained:

1) Updating of CF and Kd reviews with new data and evaluation of effects of environmental parameters as e.g. salinity on CF and Kd. These data are essential for model calculations of e.g. transport of radiocesium to man.

2) Intercomparison exercise for sediment samplers. Furthermore results from earlier intercomparisons should be synthesized.

3) Comparison of techniques for sampling of suspended particulate radioactivity and effects of suspended particulates on transport and bioavailability of radionuclides.

4) Studies of Chernobyl debris in river-run-off and estuaries including suspended matter, seawater and sediments.

5) Studies of Tc and Pu under anoxic conditions in the sea.

6) Nuclear discharges used as oceanographis long distance tracers, e.g. in Artic waters.

7) Natural radionuclides, especially Po-210 in the marine environment and the effects of run-off from land.

8) Experimental Marine Radioecology including e.g. effects of environmental variables on turnover rates of radionuclides in biota.

9) Modelling of subprocesses, e.g. bioturbation or resuspension, to be applied in (large) marine radiological models.

Furthermore, it appeared that MARECO could play a role in putting up recommendations on the use of certain terms like CF and Kd and on the use of different bases of concentration (fresh weight, dry weight and ash weight).

There was a general interest for maintaining the MARECO working group as an informal, non-government, independent and truly scientific group of experts. A major task for the group will be to promote open international contacts beyond the restraints put up in most other marine radioactivity groups like e.g. the MARINA (that has now come to an end), other CEC groups, the NEA/CRESP and the IAEA CRP's. In this way we hope to be able to promote the exchange of experience and to improve international understanding and collaboration.

Publications:

Report of the Marine Radioecology (MARECO);Working group Meeting, Brugge, Belgium, June 13, 1989. International Union of Radioecologists, Oupeye, Belgium, 114 pp.

IUR ENVIRONMENTAL ASSESSMENT MODELLING WORKING GROUP

(1985 - 1989 Leader G.S.LINSLEY)

I. Objectives

To provide a forum for the exchange of information between environmental assessment modellers, to contribute to and support international projects on model testing and to promote projects in the field of environmental assessment modelling which require or benefit from international co-operation.

II. Progress

There have been two meetings of the working Group since it inception in 1985. The first meeting took place in Brussels at the time of the VIIIth Annual Meeting of the IUR, 23 - 27 September, 1985. Twenty one persons attended. The meeting included formal presentations on the international BIOMOVS model testing study, IAEA Modelling Activities, a UK National Assessment Model Comparison and an FRG/UK Assessment Model Comparison exercice, as well as short presentations on the work of each of the participants. From the general discussions which followed these presentation the following main points can be extracted:

- more effort is needed in evaluating/demonstrating the reliability of model predictions
- assessment modelling is an effective tool for establishing research priorities
- problems exist in communication between modellers and experimentalists

A positive recommandation from the Working Group was that the IUR should associate itself with international model validation studies such as the Swedish international study BIOMOVS and more recently the IAEA's VAMP study since this is one of the most effective international mechanisms for bringing about improvements in the quality of assessment modelling.

This recommendation was accepted by the IUR's General Council and subsequently the IUR Assessment Modelling Working Group has been represented at BIOMOVS and VAMP meetings. IUR has also provided some travel funding in support of IUR members who are key participants in the BIOMOVS study.
The second meeting of the Working Group took place in Athens in association with the CEC Workshop 5-9 October 1987. The main topic for discussion was the IAEA/IUR/CEC draft Handbook of Environmental Transfer Factors. Progress on this project was described and comments on the draft report were invited from members of the Working Group. This document provides a source of basic data for assessment modelling and is mainly the result of combining data from the USA with that of the IUR Soil-Plant Working Group;
The document has subsequently been revised taking into account amount of comments received from among others the IUR Environmental Assessment Working Group.
The revised version will be circulated again for comment in 1990. The review group for the document is made up of 4 members of IUR.
The Working Group also discussed relevant events which had occured following the Chernobyl Accident and progress in the BIOMOVS study was reported.
In the period 1985-1989, circular information letters were sent out to Working Group Members on the following topics: preliminary proposals for first Working Group Meeting (22/07/85), Report on first meeting (IUR Bulletin 1986), general information letter (activities forthcoming meetings (14/04/86), announcement letter for second WG meeting (01/07/87) and announcement of the IAEA model validation study (VAMP) (30/11/87).
At the CEC/IUR meeting in Madrid (18 September 1986) the Environmental Assessment Modelling Working Group Leader gave a presentation on Priorities for Radioecology from an assessment modelling viewpoint.

Summary of Progress

The Working Group was helped in the important task of providing for the exchange of information between environmental assessment modellers. More meetings of the Group would have been desirable but work pressure on members especially in the post-chernobyl period made this difficult to achieve. The Working Group has been effective in prompting the important international model validation studies BIOMOVS and VAMP and has provided financial help to key members to attend the meetings of BIOMOVS (4) and VAMP (3). Finally the Working Group has acted as a review body for the IAEA/IUR/CEC Handbook on Environmental Transfer Factors.

Members of the Working Group.

Amaral, E.C.S., Belot, Y., Benes, P., Desmet, G., Haristoy, D., Haywood, S., Hoffman, F.O., Kanyar, B., Kirchmann, R., König, L., Kourim, V., Luykx, F., McAulay, I.R., Moberg, L., Molinari, J., Myttenaere, C., Paschoa, A.S., Plsko, ., Pröhl, G., Smitz, J.S., Tveten, U., van Dorp, F., Walters, B., Wirth E., Zeevaert, Th.

RADIOECOLOGICAL ASSESSMENT WORKING GROUP.

Chairman: MYTTENAERE C.

Within the framework of the risk assessment Working Group, the IUR is formally associated with the VAMP programme of the IAEA (coordinated Research Programme: validation of Model Predictions). The possibilities for data acquisition and models testing were in fact recognized at the Post Accident review meeting held in Vienna in 1986. To that end the VAMP programme was created in view to:

- validate the existing models by using Post-Chernobyl data
- acquire data from affected countries (USSR, Eastern and Western European countries, other parts of the World)
- Produce reports on the current status.

The CRP is concerned with models and transfer data relevant to terrestrial, urban and aquatic environments. A validation exercise that considers pathways to populations is also included in the programme.

The first Research Co-ordination Meeting was held in May 1988 and questionnaires were sent out from each Working Group to Labs and Institutions early in 1989.
The responses were analysed by the Working Group Leaders in September 1989 and a Second Research Co-ordination Meeting organized in December 1989. As fas as the terrestrial Working Group is concerned (chaired by Myttenaere,C). The proposed method of proceeding was to acquire firstly all available data sets covering the issues: Forest ecosystems, Food Processing Losses, Seasonality and Resuspension Final Reports on these subjects will be discussed early in 1991.

Two new subjects were choosen for review during the december Meeting: - Agricultural counter-measures
- Radionuclide behaviour in wild Food sources.

Questionnaires will be prepared and reviewers will be appointed soon.
The summary of discussions on the different reports prepared by the reviewers of the different Working Groups will be published early in 1990 (Progress Report N°2 of the VAMP; Progress N°1 has been published in June 1988).

Europäische Gemeinschaften — Kommission
European Communities — Commission
Communautés européennes — Commission

EUR 13268 — Tätigkeitsbericht — Programm Strahlenschutz — 1985—1989
Progress report — Radiation protection programme — 1985-89
Rapport d'activité — Programme « radioprotection » — 1985-1989
Volume 1

Luxembourg: Office for Official Publications of the European Communities

1991 — X, 1 116 pp. — 16.2 x 22.9 cm

Radiation protection series

ISBN 92-826-2169-3

Kat./cat.: CD-NA-13268-3A-C

Preis in Luxemburg (ohne MwSt.):
Price (excluding VAT) in Luxembourg: ECU 69
Prix au Luxembourg, TVA exclue:

The final report of the 1985-89 radiation protection programme outlines the research work carried out during the whole contractual period under all contracts between the Commission of the European Communities and research groups in the Member States. More than 700 scientists collaborated on this programme.

Results of more than 440 projects are reported. They are grouped into six sectors: radiation dosimetry and its interpretation; behaviour and control of radionuclides in the environment; non-stochastic effects of ionizing radiation; radiation carcinogenesis; genetic effects of ionizing radiation; evaluation of radiation risks and optimization of protection.

Within the framework programme, the aim of this scientific research is to improve the conditions of life with respect to work and protection of man and his environment and to assure safe production of energy, i.e.:

(i) to improve methods necessary to protect workers and the population by updating the scientific basis for appropriate standards;
(ii) to prevent and counteract harmful effects of radiation;
(iii) to assess radiation risks and provide methods to cope with the consequences of radiation accidents.